ADVANCED THERAPIES FOR CARDIAC REGENERATION

EDITED BY: Valeria Chiono, Ipsita Roy, Monica Boffito, Irene Carmagnola and Susanna Sartori

PUBLISHED IN: Frontiers in Bioengineering and Biotechnology

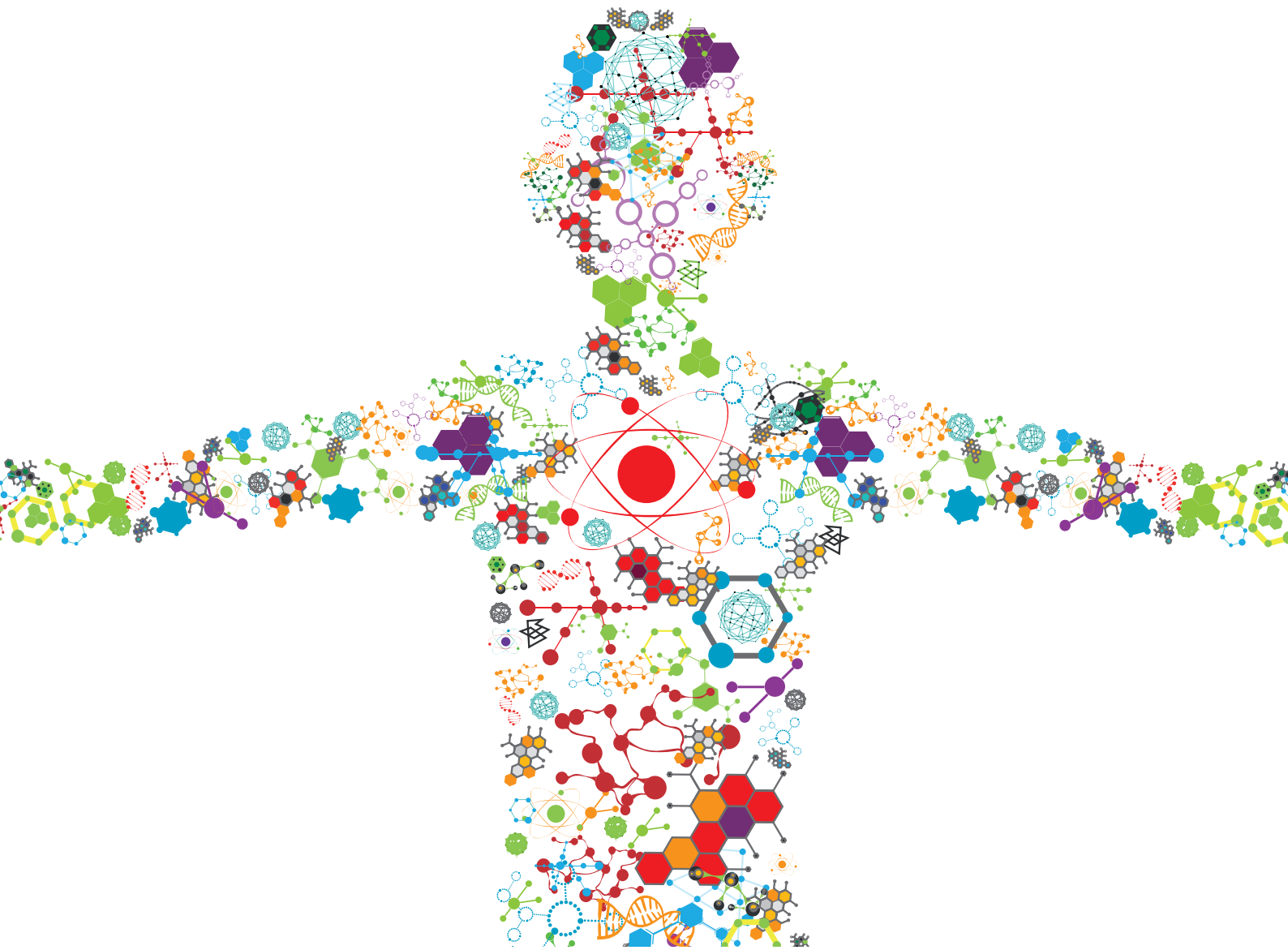

frontiers Research Topics

Frontiers eBook Copyright Statement

The copyright in the text of individual articles in this eBook is the property of their respective authors or their respective institutions or funders. The copyright in graphics and images within each article may be subject to copyright of other parties. In both cases this is subject to a license granted to Frontiers.

The compilation of articles constituting this eBook is the property of Frontiers.

Each article within this eBook, and the eBook itself, are published under the most recent version of the Creative Commons CC-BY licence. The version current at the date of publication of this eBook is CC-BY 4.0. If the CC-BY licence is updated, the licence granted by Frontiers is automatically updated to the new version.

When exercising any right under the CC-BY licence, Frontiers must be attributed as the original publisher of the article or eBook, as applicable.

Authors have the responsibility of ensuring that any graphics or other materials which are the property of others may be included in the CC-BY licence, but this should be checked before relying on the CC-BY licence to reproduce those materials. Any copyright notices relating to those materials must be complied with.

Copyright and source acknowledgement notices may not be removed and must be displayed in any copy, derivative work or partial copy which includes the elements in question.

All copyright, and all rights therein, are protected by national and international copyright laws. The above represents a summary only. For further information please read Frontiers' Conditions for Website Use and Copyright Statement, and the applicable CC-BY licence.

ISSN 1664-8714
ISBN 978-2-88966-695-9
DOI 10.3389/978-2-88966-695-9

About Frontiers

Frontiers is more than just an open-access publisher of scholarly articles: it is a pioneering approach to the world of academia, radically improving the way scholarly research is managed. The grand vision of Frontiers is a world where all people have an equal opportunity to seek, share and generate knowledge. Frontiers provides immediate and permanent online open access to all its publications, but this alone is not enough to realize our grand goals.

Frontiers Journal Series

The Frontiers Journal Series is a multi-tier and interdisciplinary set of open-access, online journals, promising a paradigm shift from the current review, selection and dissemination processes in academic publishing. All Frontiers journals are driven by researchers for researchers; therefore, they constitute a service to the scholarly community. At the same time, the Frontiers Journal Series operates on a revolutionary invention, the tiered publishing system, initially addressing specific communities of scholars, and gradually climbing up to broader public understanding, thus serving the interests of the lay society, too.

Dedication to Quality

Each Frontiers article is a landmark of the highest quality, thanks to genuinely collaborative interactions between authors and review editors, who include some of the world's best academicians. Research must be certified by peers before entering a stream of knowledge that may eventually reach the public - and shape society; therefore, Frontiers only applies the most rigorous and unbiased reviews.
Frontiers revolutionizes research publishing by freely delivering the most outstanding research, evaluated with no bias from both the academic and social point of view. By applying the most advanced information technologies, Frontiers is catapulting scholarly publishing into a new generation.

What are Frontiers Research Topics?

Frontiers Research Topics are very popular trademarks of the Frontiers Journals Series: they are collections of at least ten articles, all centered on a particular subject. With their unique mix of varied contributions from Original Research to Review Articles, Frontiers Research Topics unify the most influential researchers, the latest key findings and historical advances in a hot research area! Find out more on how to host your own Frontiers Research Topic or contribute to one as an author by contacting the Frontiers Editorial Office: frontiersin.org/about/contact

ADVANCED THERAPIES FOR CARDIAC REGENERATION

Topic Editors:
Valeria Chiono, Polytechnic University of Turin, Italy
Ipsita Roy, The University of Sheffield, United Kingdom
Monica Boffito, Politecnico di Torino, Italy
Irene Carmagnola, Politecnico di Torino, Italy
Susanna Sartori, Politecnico di Torino, Italy

The Research Topic is organized in the framework of the project BIORECAR (grant number: 772168; http://www.biorecar.polito.it/index.html)

Citation: Chiono, V., Roy, I., Boffito, M., Carmagnola, I., Sartori, S., eds. (2021). Advanced Therapies for Cardiac Regeneration. Lausanne: Frontiers Media SA. doi: 10.3389/978-2-88966-695-9

Table of Contents

05 ***Editorial: Advanced Therapies for Cardiac Regeneration***
Monica Boffito, Susanna Sartori, Ipsita Roy, Irene Carmagnola and Valeria Chiono

08 ***Small Caliber Compliant Vascular Grafts Based on Elastin-Like Recombinamers for* in situ *Tissue Engineering***
Alicia Fernández-Colino, Frederic Wolf, Stephan Rütten, Thomas Schmitz-Rode, Jose Carlos Rodríguez-Cabello, Stefan Jockenhoevel and Petra Mela

21 ***Inducing Endogenous Cardiac Regeneration: Can Biomaterials Connect the Dots?***
Assaf Bar and Smadar Cohen

40 ***Decellularized Human Dermal Matrix as a Biological Scaffold for Cardiac Repair and Regeneration***
Immacolata Belviso, Veronica Romano, Anna Maria Sacco, Giulia Ricci, Diana Massai, Marcella Cammarota, Angiolina Catizone, Chiara Schiraldi, Daria Nurzynska, Mara Terzini, Alessandra Aldieri, Gianpaolo Serino, Fabrizio Schonauer, Felice Sirico, Francesco D'Andrea, Stefania Montagnani, Franca Di Meglio and Clotilde Castaldo

58 ***MicroRNA Mediated Cardioprotection – Is There a Path to Clinical Translation?***
Timo Z. Nazari-Shafti, Vasileios Exarchos, Héctor Rodriguez Cetina Biefer, Nikola Cesarovic, Heike Meyborg, Volkmar Falk and Maximilian Y. Emmert

71 ***Engineering Immunomodulatory Biomaterials for Regenerating the Infarcted Myocardium***
Nora Bloise, Isobel Rountree, Collin Polucha, Giulia Montagna, Livia Visai, Kareen L. K. Coulombe and Fabiola Munarin

85 ***Combining Nanomaterials and Developmental Pathways to Design New Treatments for Cardiac Regeneration: The Pulsing Heart of Advanced Therapies***
Marco Cassani, Soraia Fernandes, Jan Vrbsky, Ece Ergir, Francesca Cavalieri and Giancarlo Forte

111 ***Alginate Formulations: Current Developments in the Race for Hydrogel-Based Cardiac Regeneration***
Giada Cattelan, Amparo Guerrero Gerbolés, Ruben Foresti, Peter P. Pramstaller, Alessandra Rossini, Michele Miragoli and Cristina Caffarra Malvezzi

127 ***Young at Heart: Combining Strategies to Rejuvenate Endogenous Mechanisms of Cardiac Repair***
Edoardo Maghin, Patrizia Garbati, Rodolfo Quarto, Martina Piccoli and Sveva Bollini

141 ***Blocking Extracellular Chaperones to Improve Cardiac Regeneration***
Laura Seclì, Matteo Sorge, Alessandro Morotti and Mara Brancaccio

149 ***Toward Cardiac Regeneration: Combination of Pluripotent Stem Cell-Based Therapies and Bioengineering Strategies***
Marta Mazzola and Elisa Di Pasquale

172 ***Molecular and Biomechanical Clues From Cardiac Tissue Decellularized Extracellular Matrix Drive Stromal Cell Plasticity***
Gabriel Romero Liguori, Tácia Tavares Aquinas Liguori, Sérgio Rodrigues de Moraes, Viktor Sinkunas, Vincenzo Terlizzi, Joris A. van Dongen, Prashant K. Sharma, Luiz Felipe Pinho Moreira and Martin Conrad Harmsen

191 ***MicroRNA-Mediated Direct Reprogramming of Human Adult Fibroblasts Toward Cardiac Phenotype***
C. Paoletti, C. Divieto, G. Tarricone, F. Di Meglio, D. Nurzynska and V. Chiono

200 ***Agrin-Mediated Cardiac Regeneration: Some Open Questions***
Maria Giulia Bigotti, Katie L. Skeffington, Ffion P. Jones, Massimo Caputo and Andrea Brancaccio

208 ***DMD Pluripotent Stem Cell Derived Cardiac Cells Recapitulate* in vitro *Human Cardiac Pathophysiology***
Sarka Jelinkova, Aleksandra Vilotic, Jan Pribyl, Franck Aimond, Anton Salykin, Ivana Acimovic, Martin Pesl, Guido Caluori, Simon Klimovic, Tomas Urban, Hana Dobrovolna, Vladimir Soska, Petr Skladal, Alain Lacampagne, Petr Dvorak, Albano C. Meli and Vladimir Rotrekl

227 ***Elastin-Based Materials: Promising Candidates for Cardiac Tissue Regeneration***
Israel Gonzalez de Torre, Matilde Alonso and Jose-Carlos Rodriguez-Cabello

247 ***Bioreactor Platform for Biomimetic Culture and* in situ *Monitoring of the Mechanical Response of* in vitro *Engineered Models of Cardiac Tissue***
Diana Massai, Giuseppe Pisani, Giuseppe Isu, Andres Rodriguez Ruiz, Giulia Cerino, Renato Galluzzi, Alessia Pisanu, Andrea Tonoli, Cristina Bignardi, Alberto L. Audenino, Anna Marsano and Umberto Morbiducci

261 ***Cells, Materials, and Fabrication Processes for Cardiac Tissue Engineering***
Pilar Montero, María Flandes-Iparraguirre, Saioa Musquiz, María Pérez Araluce, Daniel Plano, Carmen Sanmartín, Gorka Orive, Juan José Gavira, Felipe Prosper and Manuel M. Mazo

288 ***Cytocompatibility Evaluation of a Novel Series of PEG-Functionalized Lactide-Caprolactone Copolymer Biomaterials for Cardiovascular Applications***
Sandra Pacharra, Seán McMahon, Patrick Duffy, Pooja Basnett, Wenfa Yu, Sabine Seisel, Ulrik Stervbo, Nina Babel, Ipsita Roy, Richard Viebahn, Wenxin Wang and Jochen Salber

303 ***Biomaterials in Valvular Heart Diseases***
Bita Taghizadeh, Laleh Ghavami, Hossein Derakhshankhah, Ehsan Zangene, Mahdieh Razmi, Mehdi Jaymand, Payam Zarrintaj, Nosratollah Zarghami, Mahmoud Reza Jaafari, Matin Moallem Shahri, Adrineh Moghaddasian, Lobat Tayebi and Zhila Izadi

frontiers in Bioengineering and Biotechnology

EDITORIAL
published: 04 March 2021
doi: 10.3389/fbioe.2021.644076

Editorial: Advanced Therapies for Cardiac Regeneration

Monica Boffito [1], Susanna Sartori [1]*, Ipsita Roy [2]*, Irene Carmagnola [1]* and Valeria Chiono [1]**

[1] Department of Mechanical and Aerospace Engineering, Politecnico di Torino, Turin, Italy, [2] Department of Materials Science and Engineering, The University of Sheffield, Sheffield, United Kingdom

Keywords: cardiac tissue engineering, regenerative medicine, scaffolds, biomaterials, hydrogels, stem cells, reprogramming, physico-chemical stimuli

OPEN ACCESS

Edited and reviewed by:
Hasan Uludag,
University of Alberta, Canada

****Correspondence:***
Monica Boffito
monica.boffito@polito.it
Susanna Sartori
susanna.sartori@polito.it
Ipsita Roy
I.Roy@sheffield.ac.uk
Irene Carmagnola
irene.carmagnola@polito.it
Valeria Chiono
valeria.chiono@polito.it

Specialty section:
This article was submitted to Biomaterials, a section of the journal Frontiers in Bioengineering and Biotechnology

Received: *19 December 2020*
Accepted: *09 February 2021*
Published: *04 March 2021*

Citation:
Boffito M, Sartori S, Roy I, Carmagnola I and Chiono V (2021) Editorial: Advanced Therapies for Cardiac Regeneration. Front. Bioeng. Biotechnol. 9:644076. doi: 10.3389/fbioe.2021.644076

Editorial on the Research Topic

Advanced Therapies for Cardiac Regeneration

Cardiovascular diseases (CVDs) are the leading cause of death worldwide, accounting for ∼18 million deaths annually (WHO data). The term CVD gathers a group of different disorders involving the heart, its constituent structures, and the blood vessels. Among CVDs, coronary heart disease and stroke are responsible for four out of five CVD-related deaths, and one third of these deaths occur prematurely in people aged 70 or younger. The progressive or sudden obstruction of the coronary arteries is responsible for the onset of myocardial infarction which initiates a detrimental cascade of events finally leading to heart failure. More in detail, heart failure results from the continuous remodeling of the scar tissue replacing the beating heart muscle in the infarcted region, and represents a chronic condition in which the heart muscle progressively loses its ability to pump enough blood to fulfill the needs of all the body's compartments. Heart failure thus represents the main cause of morbidity and mortality of myocardial infarcted patients in the long term. Within this context, cardiac tissue engineering/regenerative medicine (TERM) strategies could arise as cutting-edge therapies in the management of myocardial infarcted patients, opening the way to the possibility to replace the damaged heart tissue and recover its functionality. Such an approach could effectively represent a valid alternative to the gold standard heart transplantation, encompassing all issues related to donor shortage and the need for life-long administration of immunosuppressive therapies. Among other common cardiovascular diseases, we also recall valve heart diseases and cardiomyopathies. It must be highlighted the strong associations existing between different cardiovascular diseases, such as coronary heart disease and valvular heart disease, cardiomyopathy and heart failure. This observation indicates that a multiple regenerative medicine approach, which considers different diseases, could be an effective strategy in the management of CVDs. The Research Topic "Advanced Therapies for Cardiac Regeneration" aims at presenting a series of articles summarizing the latest research updates on cardiac TERM approaches which combine cells, biomaterials, hydrogels, tissue engineered scaffolds/patches and physico-chemical stimuli to achieve the ultimate goal of regenerating the injured heart tissue. The issue is comprised of 19 peer-reviewed manuscripts (nine reviews, two perspectives, seven original research articles, and one Brief Research Report) derived from the many fields involved in the topic, namely (bio)materials science and engineering, biology, biotechnology, and biomedical engineering.

To better contextualize the Research Topic, the review by Montero et al. presents an in-depth overview of the specific characteristics of the myocardium that determine the needs and requirements cardiac TERM has to meet, with particular emphasis on heart tissue components, architecture and biophysical properties. The authors also briefly revise the key components required to design new cardiac TERM approaches, namely cells, materials, maturation stimuli, and scaffold fabrication techniques. Given the central role of biomaterials in the establishment

of cardiac TERM therapies, Bar and Cohen focus their review on the current application of biomaterials in the field of cardiac regeneration, mainly discussing their use as forming materials for nano-carriers and matrices for cardiac regeneration induced by biomolecule release, injectable hydrogels for cell delivery, and cardiac patches. Further and more detailed insight on the use of specific biomaterials in cardiac TERM are provided by Cattelan et al. and Gonzalez De Torre et al., with particular emphasis on their application as hydrogel constituents. Being three-dimensional highly hydrated networks showing mechanical properties similar to soft tissues, hydrogels hold great promise in cardiac TERM. Cattelan et al. elucidate the promising properties of alginate in cardiac regeneration strategies and the outcomes of clinical trials in which this material has been tested to treat myocardial infarcted patients. An additional demonstration of the suitability of this material for cardiac TERM is provided by Bloise et al. who develop alginate hydrogels for the controlled release of immunomodulatory and reparative cytokines (anti-inflammatory interleukins 4/6/13 and colony-stimulating factor) to direct immune cell fate and control the wound healing process in the ischemic heart. The therapeutic ability of the proposed treatment has been proved in rat models by macrophage polarization toward healing and the improved global cardiac functionality. Differently, Gonzalez De Torre et al. discuss on the potential of elastin-based biomaterials as constituents of hydrogel scaffolds, injectable systems, or complex devices (e.g., heart valves, stents) to treat CVD-affected patients. In this regard, Fernàndez-Colino et al. investigate the use of elastin-like recombinamers as forming materials of small caliber compliant vascular grafts. The authors describe material processing into macroporous three-dimensional structures favoring cell homing, extracellular matrix (ECM) deposition and endothelium development, while exhibiting non-thrombogenicity and elastic properties mimicking the native elastin. Graft textile components are finely designed to confer proper suture retention, long-term structural stability, burst strength and compliance. The proper selection of the biomaterials used as constituents of cardiac scaffolds/patches/devices or hydrogels thus represents the first step toward the engineering of successful regenerative strategies for the management of CVD-affected patients. Indeed, biomaterials strongly affect the possibility to provide the resulting devices with proper biological signals and physical stimuli to achieve the final goal of recovering the initial organ/tissue functionality. In this regard, Belviso et al. report on the potential of decellularized human skin as scaffold to restore the native ECM which plays a pivotal role in guiding heart compliance, cardiomyocyte maturation, and function. The authors argue that a dermal matrix could effectively represent a viable alternative biological scaffold in cardiac TERM, with the key advantages of being autologous, easily accessible, and cost-effective. On the other hand, decellularized organ-derived ECM (dECM) can also be exploited to design hydrogels, thus combining the ECM characteristic pro-regenerative properties with the possibility to shape the material according to specific requirements. Liguori et al. investigate the differences among dECM hydrogels prepared starting from cardiovascular tissues of different origin, namely left ventricle, mitral valve, and aorta. The authors demonstrate that the source of dECM plays a pivotal role in determining cell differentiation and vascular network formation, because of the different molecular and biomechanical cues provided to cells. For instance, ventricular dECM hydrogels exhibit more robust vascular network formation, while aorta-derived dECM drives adipose-derived stromal cell differentiation toward a myogenic phenotype in the absence of TGF-β1 supplement to the culture medium. The readers can also find a thorough survey on the use of decellularized cardiac ECM as biomaterial for cardiac TERM in the review by Maghin et al. Besides the physical stimuli provided by the designed cell-culture platforms through their architecture and their mechanical properties, the possibility to mechanically stimulate cellularized constructs by mimicking the native milieu also promotes the development and maturation of cardiac tissue analogs, as described by Massai et al. The authors develop an automated bioreactor platform for tuneable cyclic stretch of cellularized samples coupled with a specific set-up for the *in situ* monitoring of the mechanical response of *in vitro* engineered cardiac tissues. Another key form of stimulus playing a central role in cardiac regeneration is represented by biochemical cues, as thoroughly surveyed by Cassani et al. Particularly, the authors mainly gather their attention on the crucial need of specific carriers (e.g., nanoparticles) to deliver such biochemical cues, which would ensure an efficient delivery of the therapeutic cargo, inhibit its metabolic inactivation, and avoid potential side effects. According to a different approach, proper biochemical stimuli driving cardiac repair and regeneration can be also applied by cell-secreted soluble factors. The literature review by Maghin et al. reports on the therapeutic profiling of stem cell secretome, with regard to the cardio-active ability of cell-released extracellular vesicles, including exosomes carrying cardioprotective and regenerative RNA molecules. An in-depth analysis of the potential and the mechanisms of action of miRNAs as mediators of cardioprotection is provided by Nazari-Shafti et al. The authors highlight the crucial need to identify all miRNAs involved in cardioprotection and remodeling, as well as their composition and exact mechanism of action in view of their application in clinical practice. A class of miRNAs has also been reported to drive the direct reprogramming of fibroblasts into cardiomyocyte-like cells. In the perspective of a clinical translation of this approach, Paoletti et al. test the capability of miRcombo (i.e., a combination of four microRNA mimics) to guide the direct reprogramming of adult human cardiac fibroblasts into induced cardiomyocytes, as previously observed with murine fibroblasts. Other repair and regenerative strategies currently explored in literature target different aspects of the cascade initiated by myocardial insults. For instance, Seclì et al. concentrate on the different role exerted by chaperone proteins in the healthy and injured heart. In detail, in the healthy heart chaperone proteins contribute to the regulation of myocardial physiology, while under stress conditions or during cell damage events, they are secreted by myocardial cells and induce inflammation and cardiomyocyte apoptosis. Blocking chaperone activity has been already demonstrated to produce beneficial effects on heart function in preclinical models. Hence, combining the release of specific antibodies blocking extracellular chaperones with TERM approaches may represent a future

innovation to treat infarcted patients. Differently, Bigotti et al. discuss the possible exploitation of agrin as mediator of cardiac regeneration. Recently published works have demonstrated that agrin can promote heart regeneration in murine models through cardiomyocyte de-differentiation and proliferation. Moving from these data, the authors survey the currently available literature on this topic, and critically discuss on the potential clinical translation of agrin-based therapies.

Last but not least, a new chapter in the TERM field has been opened over the last two decades with the discovery of induced pluripotent stem cells (iPSCs). These cells offer the advantage of being of autologous origin, while retaining the proper characteristics of embryonic stem cells, thus completely overcoming both ethical issues and rejection risks. Mazzola and Di Pasquale provide an overview on the differentiation potential of iPSCs toward cardiomyocytes and their application in cell-based therapies, highlighting the typical drawbacks of such approaches in terms of poor cell retention and risks of occurrence of adverse effects (e.g., arrhythmias). A possible route to overcome these issues consists in combining the use of iPSCs with bioengineering technologies which can retain cells in the therapeutic target while favoring their phenotypical maturation and integration in the host tissue. iPSCs can also be successfully used as cell source in the establishment of cardiac tissue models. In addition, their autologous origin can be exploited to recapitulate *in vitro* human cardiac pathophysiology. In this regard, Jelinkova et al. report the design of an *in vitro* human model of the cardiac tissue of Duchenne muscular dystrophy (DMD)-affected patients. DMD is a severe genetic disorder associated with progressive dilated cardiomyopathy which culminates with heart failure onset, finally leading to patient death. The authors demonstrate that the designed cardiac models effectively recapitulate DMD-induced functional defects and cardiac wasting, thus offering a promising tool for a better understanding of DMD-associated cardiomyopathy and its treatment.

Finally, to complete our survey on the topic, Taghizadeh et al. exhaustively review the different types of biomaterials applied in the treatment of valvular heart diseases which represent another CVD with high incidence in developed countries, and in particular among the elderly. In the U.S. about 28,000 deaths are due to heart valve disease every year, with approx. the 60% of deaths due to disorders involving the aortic valve (data from the Centers for Disease Control and Prevention). Strict requirements in terms of material physico-chemical properties should also be fulfilled when vascular stents are engineered. Learning from a recent FDA report dealing with the adverse cardiac events and thrombosis observed at the 2-year follow-up on the first FDA-approved bioresorbable vascular stents, Pacharra et al. characterize a series of polyethylene glycol-functionalized poly-L-lactide-co-ε-caprolactone copolymers as a new generation of stent-forming materials, with improved cyto- and hemo-compatibility. As an outcome of the research work, the authors identify promising candidates for cardiovascular implant fabrication, with the additional advantage of being suitable for an easy translation of the synthesis procedure (a one-step synthesis strategy) toward industrial practice.

The reader can easily appreciate from the brief summaries of the contributions comprised in this issue that the addressed Research Topic is broad in nature and represents a still open question in the TERM field. The definition of regenerative approaches to fight the detrimental consequences of CVDs is still in its infancy. However, the cross-contamination of new ideas coming from complementary but not overlapping fields, as highlighted in the papers published within this issue, will likely lead in the future to the effective and successful repair and regeneration of injured myocardial tissue.

AUTHOR CONTRIBUTIONS

MB wrote the editorial, which was revised, proof-read, and approved by all authors.

FUNDING

This work has received funding from the European Research Council (ERC) under the European Union's Horizon 2020 research and innovation program (grant agreement No. 772168, BIORECAR, http://www.biorecar.polito.it/index.html).

Conflict of Interest: The authors declare that the research was conducted in the absence of any commercial or financial relationships that could be construed as a potential conflict of interest.

Copyright © 2021 Boffito, Sartori, Roy, Carmagnola and Chiono. This is an open-access article distributed under the terms of the Creative Commons Attribution License (CC BY). The use, distribution or reproduction in other forums is permitted, provided the original author(s) and the copyright owner(s) are credited and that the original publication in this journal is cited, in accordance with accepted academic practice. No use, distribution or reproduction is permitted which does not comply with these terms.

frontiers in Bioengineering and Biotechnology

ORIGINAL RESEARCH
published: 19 November 2019
doi: 10.3389/fbioe.2019.00340

Small Caliber Compliant Vascular Grafts Based on Elastin-Like Recombinamers for *in situ* Tissue Engineering

Alicia Fernández-Colino[1], Frederic Wolf[1], Stephan Rütten[2], Thomas Schmitz-Rode[3], Jose Carlos Rodríguez-Cabello[4], Stefan Jockenhoevel[1,5] and Petra Mela[1,6]**

[1] Department of Biohybrid & Medical Textiles (BioTex), AME-Institute of Applied Medical Engineering, Helmholtz Institute, RWTH Aachen University, Aachen, Germany, [2] Electron Microscopy Facility, Uniklinik RWTH Aachen, Aachen, Germany, [3] AME-Institute of Applied Medical Engineering, Helmholtz Institute, RWTH Aachen University, Aachen, Germany, [4] Bioforge Lab, University of Valladolid, CIBER-BBN, Valladolid, Spain, [5] AMIBM-Aachen-Maastricht-Institute for Biobased Materials, Maastricht University, Geleen, Netherlands, [6] Medical Materials and Implants, Department of Mechanical Engineering and Munich School of BioEngineering, Technical University of Munich, Garching, Germany

Vascular disease is a leading cause of death worldwide, but surgical options are restricted by the limited availability of autologous vessels, and the suboptimal performance of prosthetic vascular grafts. This is especially evident for coronary artery by-pass grafts, whose small caliber is associated with a high occlusion propensity. Despite the potential of tissue-engineered grafts, compliance mismatch, dilatation, thrombus formation, and the lack of functional elastin are still major limitations leading to graft failure. This calls for advanced materials and fabrication schemes to achieve improved control on the grafts' properties and performance. Here, bioinspired materials and technical textile components are combined to create biohybrid cell-free implants for endogenous tissue regeneration. Clickable elastin-like recombinamers are processed to form an open macroporous 3D architecture to favor cell ingrowth, while being endowed with the non-thrombogenicity and the elastic behavior of the native elastin. The textile components (i.e., warp-knitted and electrospun meshes) are designed to confer suture retention, long-term structural stability, burst strength, and compliance. Notably, by controlling the electrospun layer's thickness, the compliance can be modulated over a wide range of values encompassing those of native vessels. The grafts support cell ingrowth, extracellular matrix deposition and endothelium development *in vitro*. Overall, the fabrication strategy results in promising off-the-shelf hemocompatible vascular implants for *in situ* tissue engineering by addressing the known limitations of bioartificial vessel substitutes.

Keywords: biohybrid scaffolds, elastin-like recombinamers, textile technical components, vascular grafts, off-the-shelf implants

OPEN ACCESS

Edited by:
Valeria Chiono,
Polytechnic University of Turin, Italy

Reviewed by:
Chris A. Bashur,
Florida Institute of Technology,
United States
Vipuil Kishore,
Florida Institute of Technology,
United States

****Correspondence:***
Stefan Jockenhoevel
jockenhoevel@ame.rwth-aachen.de
Petra Mela
petra.mela@tum.de

Specialty section:
This article was submitted to Biomaterials, a section of the journal Frontiers in Bioengineering and Biotechnology

Received: *04 August 2019*
Accepted: *30 October 2019*
Published: *19 November 2019*

Citation:
Fernández-Colino A, Wolf F, Rütten S, Schmitz-Rode T, Rodríguez-Cabello JC, Jockenhoevel S and Mela P (2019) Small Caliber Compliant Vascular Grafts Based on Elastin-Like Recombinamers for in situ Tissue Engineering. Front. Bioeng. Biotechnol. 7:340. doi: 10.3389/fbioe.2019.00340

INTRODUCTION

Cardiovascular disease is the most common cause of death worldwide (Townsend et al., 2016). The progressive constriction and stiffening of the blood vessels requires, in complex conditions, bypass surgery (Townsend et al., 2016). Native autologous vein and artery segments remain the gold standard as grafts for this procedure, but they are not always available due to a previous harvest, anatomical variability or disease progression. Furthermore, the failure rate of saphenous vein grafts, the most widely used conduits for coronary artery bypass, reaches 25% during the first 12–18 months after surgery, clearly showing the need for better solutions (Hess et al., 2014). The synthetic vascular prostheses available today are made of expanded polytetrafluoroethylene (GORE-TEX®), poly(ethylene terephthalate) (Dacron) or polyurethane. These vascular prostheses lack the remodeling and growing capabilities of living tissues and are not suitable as small-diameter substitutes (<6 mm) because of poor blood compatibility and compliance mismatch that lead to thrombosis and intimal hyperplasia (Salacinski et al., 2001; Zilla et al., 2007).

Tissue engineering (TE) approaches have the potential to provide alternative solutions to current underachieving artificial replacements. Vascular TE strategies are increasingly moving from a classical to an *in situ* approach also known as directed endogenous regeneration. Here, cell-free scaffolds are implanted to be colonized and remodeled endogenously, resulting in autologous vessel substitutes (Wissing et al., 2017). Off-the-shelf availability, lower regulatory burden for clinical translation and no need for tissue harvest for cell isolation are major advantages of *in situ* TE with respect to the classical cell-based approach. On the other hand, this strategy places strong demands on the implant's material and fabrication method as the graft has to perform adequately upon implantation, which means it has to be able to withstand the systemic circulation, be hemocompatible, and provide a microenvironment suitable for cell infiltration and tissue generation (Billiet et al., 2012).

Electrospinning is a widely employed technique to obtain biodegradable grafts (Park et al., 2019), which has been in some cases combined with surface functionalization to promote endothelialization and improve hemocompatibility (Zhao et al., 2019). However, electrospun scaffolds typically suffer from poor cellular infiltration because of the dense fibrous network (Zhong et al., 2012). Salt leaching (Lee et al., 2011) and freeze drying (Sugiura et al., 2016) techniques have been used to create interconnected porous architectures which are advantageous in term of cellular colonization and matrix deposition. However, the initial poor mechanical properties of the porous scaffold might compromise a safe implantation (Lee et al., 2011). Despite encouraging results demonstrating the potential of *in situ* TE (Wissing et al., 2017), control over the properties of the developed grafts remains at best partial.

The development of vascular grafts that combine both the elasticity to allow an energy-efficient transmission of the pulsatile blood flow with the strength to withstand the blood pressure is particularly challenging, as burst strength and compliance are often inversely related (Sarkar et al., 2007). While compliance mismatch can lead to intimal hyperplasia, low patency and consequent graft failure (Abbott et al., 1987; Trubel et al., 1995; Ballyk et al., 1998; Salacinski et al., 2001; Kannan et al., 2005; Sarkar et al., 2006), compliance as endpoint in vascular graft design has been many times overlooked in the literature (Pashneh-Tala et al., 2015). Additionally, because of the variability of this property between different vessels, vascular TE should ideally aim at developing compliant vessel substitutes with mechanical properties tailored to the intended implantation site. The ability of cardiovascular structures to deform elastically with the pressure pulse is crucial to maintain their function over time and relies on the high percentage of elastin in the native vessel wall, accounting for 50% of the dry weight of major arteries (Rosenbloom et al., 1993). The lack of functional elastin synthesis by the cells is a major drawback of tissue-engineered vascular grafts (TEVGs), which results in aneurysm formation as a major failure mechanism (Wissing et al., 2017). This makes elastin and elastomeric materials highly attractive for the engineering of vessel substitutes.

Our approach is to develop a platform that enables an *ad-hoc* vascular fabrication according to the specific target by combining the elastic properties provided by the elastin-like recombinamers (ELRs) with the mechanical support of technical textile components. The ELRs are a family of artificial polymers bioinspired by the pentapeptide VPGVG present in the natural elastin (MacEwan and Chilkoti, 2010; Girotti et al., 2011). They are positioned midway between natural products and synthetic polymers, as they are engineered in a controlled and highly reproducible way while still maintaining inherent properties of the natural elastin such as elastic mechanical behavior, hemocompatibility, and bioactivity (Arias et al., 2014). The textile components consist of a warp knitted polyvinylidene fluoride (PVDF) mesh to confer suturability, long term stability and, in combination with an electrospun polycaprolactone (PCL) mesh, burst strength and tunable compliance.

Evaluation of the obtained biohybrid vascular grafts included burst strength, compliance, suture retention, cell infiltration, hemocompatibility, extracellular matrix (ECM) deposition, and endothelialization.

MATERIALS AND METHODS

Complement Convertase

Complement activation was measured using the Complement Convertase Kit (CCA, HaemoScan, Groningen, Netherlands), which follows the international standard ISO 10993/Part 4 to evaluate the biocompatibility of biomaterials and medical devices. The assay was performed according to the manufacturer's protocol. Briefly, 1 cm^2 samples of different materials (i.e., the click-ELR test material, and MS (medical steel) and PDMS (polydimethylsiloxane) reference materials provided with the kit as internal controls) were incubated first with plasma for 15 min, and then with a chromogenic C5 convertase substrate for 24 h. Cleavage of the substrate by C5 convertases present on the surface of the tested materials was quantified by measuring the optical density at 405 nm in a microplate reader (Infinite M200, Tecan).

Thrombogenicity

Blood (12 mL) was drawn from healthy volunteers and mixed with 3.2% sodium citrate using an S-Monovette CPDA1 device (Sarstedt, Germany) at a volumetric ratio of 1:9. Six mL of blood were centrifuged at 270 × *g* for 15 min while the other 6 mL were centrifuged at 2,000 × *g* for 15 min. The resulting supernatants were mixed at a volumetric ratio of 1:1 to obtain platelet-rich plasma (PRP). Each sample was placed in a 96-well plate, and 100 μL of PRP was added and incubated for 1 h at 37°C. The samples were then gently washed with PBS and fixed in 3% glutaraldehyde in 0.1 M Sorenson's buffer (pH 7.4) for SEM. Evaluation of platelet adhesion was carried out based on the SEM images by assessing images from three independent experiments, and for each experiment, three fields of 350 μm^2 each were analyzed.

Scaffold Fabrication

We used two ELRs, namely VKVx24 and HRGD6. VKVx24 is a structural recombinamer with no bioactive sequence, whereas HRGD6 is a recombinamer containing a RGD adhesion sequence (**Table 1**). The lysine residues of each ELR were chemically modified as previously reported (Gonzalez de Torre et al., 2014) to introduce cyclo-octyne and azide groups, resulting in VKVx24-cyclo-octyne and HRGD6-azide, respectively.

For the fabrication of the macroporous ELR-based scaffolds, we used the salt leaching/gas foaming technique that we recently developed (Fernandez-Colino et al., 2018). Briefly, each ELR component was dissolved to a concentration of 75 mg/mL in a 1:1 (v/v) mixture of PBS and ethanol. $NaHCO_3$ particles (diameter < 100 μm) were added to each ELR solution at a recombinamer/salt weight ratio of 1:10. Each preparation was loaded into a syringe, and injected into the mold using a dual chamber syringe applicator. The mold consisted of a gas-permeable outer silicone tube (inner diameter = 6.4 mm; Ismatec) and an inner metal cylinder (outer diameter = 3 mm) placed coaxially to the silicone tube. A PVDF mesh was positioned in the annular space between the cylinders. The mesh was produced at the Institute of Textile Engineering (Institut für Textiltechnik) of the RWTH Aachen University (Aachen, Germany). The space between cylinders was then filled with the ELR components. After incubating for 30 min at 37°C, the mold was removed, and the click-ELR scaffold was released and placed in 3 M citric acid for 30 min in an ultrasound bath (Martin et al., 2009). The scaffolds were washed with aqueous phosphate-buffered saline (PBS) to eliminate residual ethanol, salts and acid, and then they were enclosed in an outer PCL sheath by directly electrospinning on the graft. The PCL (GMP grade, Purasorb PC12, Corbion Purac Gorinchem, Netherlands) was dissolved at a concentration of 14% in a 1:3 (v/v) mixture of methanol and chloroform, which was infused through a 27-gauge needle at a constant flow rate of 3 mL/h. A voltage difference of 24 kV was applied between the needle and the collector, which were placed 18 cm apart. The temperature and the humidity were set at 32°C and 20%, respectively. Finally, the vascular grafts were sterilized by washing with 70% ethanol for 30 min and stored in fresh 70% ethanol overnight. The scaffolds were then incubated in PBS for 2 × 30 min and 1× 16 h.

TABLE 1 | The amino acid sequences of each recombinamer and the corresponding reactive groups used for click chemistry.

ELR	Amino acid sequence	Reactive group
VKVx24-c	MESLLPVGVPGVG[VPGKG(VPGVG)$_5$]$_{23}$ VPGKGVPGVGVPGVGVPGVGVPGV	Cyclo-octyne
HRGD6-a	MGSSHHHHHHSSGLVPRGSHMESLLP[(VPG IG)$_2$(VPGKG)(VPGIG)$_2$]$_2$AVTGRGDSPASS [(VPGIG)$_2$(VPGKG)(VPGIG)$_2$]$_2$	Azide

The reactive groups were incorporated by chemical modification of the lysine residues. VKVx24-c refers to VKVx24-cyclo-octyne and HRGD6-a to HRGD6-azide.

Scanning Electron Microscopy (SEM)

Samples were fixed in 3% glutaraldehyde in 0.1 M Sorenson's buffer (pH 7.4) at room temperature for 1 h. They were rinsed with 0.2 M sodium phosphate buffer (pH 7.39, Merk) and dehydrated in 30, 50, 70, and 90% acetone, and then three times in 100% acetone, for 10 min each. After critical point drying in CO_2, the samples were sputter-coated (Leica EM SC D500) with a 20 nm gold–palladium layer. Images were captured using an ESEM XL 30 FEG microscope (FEI, Philips, Eindhoven, Netherlands) with an acceleration voltage of 10 kV. The pore size was determined using ImageJ software by analyzing three different regions, with 50 measurements taken in each region. Some of the SEM images were colored with MountainsMap SEM software courtesy of Digital Surf, France.

Burst Strength

Burst strength values were measured in a custom-made burst strength chamber equipped with a pressure sensor (Jumo Midas pressure transmitter; JUMO GmbH & Co. KG) and a peristaltic pump (IPC Ismatec, IDEX Health & Science GmbH). Samples (n = 3) with areas of 1 cm^2 were placed in the burst chamber and exposed to increasing pressure by pumping PBS at a constant rate of 5 mL/min until the structural failure of the sample was detected as a sudden drop in the pressure recorded by LabVIEW (National Instruments). The highest pressure measured before failure was defined as the burst strength value.

Suture Retention

Suture retention strength was measured by inserting a 7–0 prolene suture 1 mm from the edge of each graft. The suture was fixed on the upper hook of a Z2.5 Zwick/Roell tensile tester (Zwick GmbH & CO. KG; Ulm; Germany) and the grafts were immobilized on the lower hook. The system was then strained at a speed of 50 mm/min (in accordance with ISO guidelines) to pull the suture away from the graft, and the required force was recorded. Three samples were measured for Elastingraft_eM, and six for the ElastinGraft_0.

Compliance and Stiffness Index

The vascular grafts were placed in a bioreactor system that comprised a custom-made chamber made of polyoxymethylene (POM; Licharz GmbH, Buchholz, Germany) with transparent poly(methyl methacrylate) (PMMA) sides and an optical micrometer [model LS-7030(M), Keyence Deutschland GmbH,

Neu-Isenburg, Germany] to measure the diameter of the vascular graft by emitting a parallel beam of green light to the graft and assessing its shadow. Additionally, the system featured silicone tubes (Ismatec), a flow sensor (SonoTT^{TM} Flowcomputer, em-tec GmbH), an adjustable resistance to control the flow within the system, a pressure sensor (Xtrans, Codan pvb Medical GmbH), and a small centrifugal pump (702-6882, RS components), which was controlled by a custom-developed control unit (Wolf et al., 2018).

The flow-loop was filled with phosphate buffer solution (Gibco, pH: 7.4). The mean pressure was created by a continuous flow generated by the centrifugal pump, in combination with an adjustable resistance. The pressure pulses (20/60, 30/70, 40/80, 50/90, 60/100, 70/110, 80/120, 90/130, and 110/150 mmHg) were created by modulation of the pulse-free flow, due to changing the constant input voltage, using a sinusoidal function. The values of pressures and corresponding graft diameters were recorded with a custom-developed LabVIEW program (LabVIEW 7.1; National Instruments). The average values of the compliance were estimated from such values, using the following equation

$$C = [((D_2 - D_1)/D_1) \times 10^4]/(P_2 - P_1)$$

where P_1 is the lowest internal pressure, P_2 is the highest internal pressure, D_1 is the diameter at the pressure P_1 and the D_2 is the diameter at the pressure P_2. Pressure–diameter measurements were also used to calculate the dimensionless stiffness index (Soletti et al., 2010):

$$\beta = \ln(P_2/P_1)/[(D_2 - D_1)/D_1]$$

Ultrasound Monitoring

The stretching and recoiling capability of the vascular grafts was also visualized with an ultrasound system, Vivid-I (S/N 3642VI General Electric), with a linear probe (8L-RS, General Electric).

Cell Isolation and Culture

Smooth muscle cells (SMCs) were isolated from the veins of human umbilical cords as previously described (Moreira et al., 2015). Briefly, the vein was washed with PBS (Gibco) before endothelial cells were removed using 1 mg/mL collagenase (Sigma) and the adventitia was stripped off. To isolate SMCs, the digested vein was minced into 1-mm rings and then bathed in Dulbecco's modified Eagle's medium (DMEM) supplemented with 10% FBS and 1% antibiotic/antimycotic solution (all reagents from Gibco). To obtain a sufficient cell number, the cells were serially passaged using 0.05% trypsin/0.02% EDTA (Gibco) and cultured at 95% humidity and 37°C in a 5% CO_2 atmosphere. SMC phenotype was verified by the presence of alpha-SMA positive cells and the absence of von Willebrand factor expression by immunocytochemistry. Cell passages 4–7 were used for all experiments. To study the interaction between the SMCs and the click-ELR vascular grafts, the ElastinGrafts were coaxially introduced in a silicone tube clamped at one end. One mL of the cell-suspension at 3×10^6 cells/mL was then introduced into the silicone tube and the other end was also clamped. The system was attached to a mandrel connected to the head of a roller pump (MCP Process; Ismatec), and rotated along the longitudinal axis for 6 h following a cycle of 20 s in rotation at 1 rpm and 200 s in static to allow cell attachment. The remaining cell suspension was then removed, and the graft was placed in fresh culture medium. Cell behavior and ECM deposition were investigated after 12 days of static culture by SEM and immunohistochemistry.

Endothelial progenitor cells (EPCs) were isolated from human adult peripheral blood mononuclear cells. Anticoagulated blood of healthy donors was carefully added to the separating solution Histo-Paque-1077 (Sigma-Aldrich, St. Louis, Missouri), and centrifuged at $400 \times g$ at room temperature for 30 min. The layer containing mononuclear cells was washed twice by gently mixing with PBS, and subsequent centrifuging at $250 \times g$ for 10 min. The cell pellet was resuspended with 15 mL of endothelial cell growth medium (Endothelial Cell Growth Medium MV2; PromoCell, Heidelberg, Germany), containing epidermal growth factor (5 ng/mL), basic fibroblast growth factor (10 ng/mL), insulin-like growth factor (20 ng/mL), vascular endothelial growth factor 165 (0.5 ng/mL), ascorbic acid (1 μg/mL), and hydrocoecisone (0.2 μg/mL), and transferred into T-75 culture flask pre-coated with human fibronectin (1 mg/cm^2, Sigma-Aldrich, St. Louis, MO). The cells were incubated at 37°C in a humidified atmosphere containing 5% CO_2. When EPCs colonies were formed, they were trypsinized [0.05% trypsin/0.02% ethylenediaminetetraacetic acid solution (Gibco, Karlsruhe, Germany)] and transferred to T-25 culture flask pre-coated with type I rat-tail collagen (5 mg/cm^2, BD Biosciences, San Jose, CA). When cells reached 70–80% of confluence, they were trypsinized and transferred into T-75 culture flasks. The phenotype of EPCs was corroborated by immunocytochemical staining for the markers vWF and CD31 and by flow cytometric analysis, which showed positive signals for the EC markers CD31 and CD144 and negative signals for the monocytic markers CD14 and CD45. Cells up to eight passages were used for all experiments.

To study the ability of the click-ELR grafts to support endothelialization, the scaffolds were incubated with a suspension of EPCs (3×10^6 cells/mL) while rotating at 1 rpm for 6 h as described for SMC seeding. Then, the scaffolds were cultured in static for 1 and 4 days and subsequent investigated by SEM and immunohistochemistry followed by confocal microscopy.

Immunohistochemistry

Native human umbilical cord and click-ELR scaffolds seeded with SMCs were fixed in Carnoy's solution and embedded in paraffin before sectioning. The sections were deparaffinized, non-specific sites were blocked and the cells permeabilized by incubating in 5% normal goat serum (NGS, Dako) in 0.1% Triton-PBS. The sections were incubated for 1 h at 37°C with the primary rabbit anti-collagen I antibody (R 1038, Acris) diluted 1:200. The sections were then incubated for 1 h at 37°C with a fluorescein-conjugated secondary antibody produced in rabbit (A11008, Molecular Probes) diluted 1:400. The native human umbilical cord served as a positive control. For negative controls, samples were incubated in diluent and the secondary antibody

only. Tissue sections were counterstained with 4′,6-diamidino-2-phenylindole (DAPI) nucleic acid stain (Molecular Probes). Samples were observed under a microscope equipped for epi-illumination (AxioObserver Z1, Carl Zeiss GmbH). Images were acquired using a digital camera (AxioCam MRm, Carl Zeiss GmbH). Click-ELR scaffolds seeded with EPCs were fixed with methanol-free formaldehyde (Roth, Karlsruhe, Germany) at 4% for 1 h at room temperature. Non-specific sites were blocked and the cells permeabilized by incubating in 5% normal goat serum (NGS, Dako) in 0.1% Triton-PBS. The samples were incubated overnight at 4°C with the primary mouse anti-CD31 antibody (P8590, Sigma) diluted 1:100. The samples were then incubated for 1 h at room temperature with AlexaFluor 594 anti-mouse antibody produced in goat (A11005, Invitrogen) diluted 1:400. Images were acquired using a Zeiss LSM 710 confocal laser scanning microscope.

Statistical Analysis

Differences between three or more groups were assessed using one-way ANOVA with Tukey's *post-hoc* test. Statistical difference between two groups was evaluated by the Student's *t*-test. A significance level $p = 0.05$ was set for all the tests. In the figures, statistical significance is denoted as * for p-value ≤ 0.05, ** for p-value ≤ 0.01, *** for p-value ≤ 0.001.

RESULTS AND DISCUSSION

In vitro Hemocompatibility Testing

The concept of ready-to-use vascular grafts implies the absence of any *in vitro* seeding of the device prior implantation. Such device will be in direct contact with blood before a native endothelium covers its surface, and consequently, the first requirement that the base material has to meet is to be hemocompatible. Therefore, we first evaluated the hemocompatibility of the ELRs by assessing the activation of the complement system. For this purpose, we used a complement convertase assay that complies with the international standard ISO 10993/Part 4. Results and given thresholds to evaluate the activation are indicated in **Figure 1A**. The ELR hydrogels behaved as a complement non-activating biomaterial (<0.06 OD/24 h/cm^2), giving the lowest value among all the tested materials (i.e., MS and PDMS).

The reaction of blood components to the presence of ELR was further studied by performing a thrombogenicity test. A high number of activated and adherent platelets were present on the GORE-TEX® and fibrin control after 1 h of PRP contact, whereas minimal platelet adhesion was detected on the surface of the ELR-samples (**Figure 1B**). Moreover, the platelets on the GORE-TEX® and fibrin samples presented either extended pseudopodia (colored in salmon **Figure 1C**iv,vi) or "fried egg" morphology (colored in gold in **Figure 1C**iv,vi), indicative of activated and highly activated states, respectively (**Figure 1C**), whereas the few platelets on the ELR samples presented a rounded morphology, with few pseudopodia (correlated with a lower activation state) (Goodman et al., 1989; Sorrentino et al., 2016). These results agree with previous studies which propose elastin and elastin-like polymers as excellent candidates for the fabrication of blood-contacting materials (Ito et al., 1998; Woodhouse et al., 2004; Jordan et al., 2007; de Torre et al., 2015) and support the use of ELRs for the fabrication of vascular grafts as cell-free implants which will be in direct contact with the blood before endothelialization.

Fabrication of the Click-ELR Vascular Grafts (ElastinGrafts)

Vessel substitutes were fabricated as schematically shown in **Figure 2**. Microscopic inspection of the ElastinGrafts revealed that (i) a highly porous structure was obtained throughout the whole construct, with a mean pore size of 33 μm, which has been indicated as adequate for the interaction with smooth muscle cells (SMCs) (Lee et al., 2011); (ii) the textile was well embedded within the ELR (**Figure 2B**iii) without any gaps in between the mesh pores (**Supplementary Figure 1**); and (iii) a fibrillar sheath enclosed the vascular graft (**Figure 2C**). The scaffold structure determines both the mechanical performance and the cell behavior of the implant (e.g., cell ingrowth and ECM formation), and ultimately its overall success. The porous microstructure should provide a template for cell ingrowth, whereas the textile reinforcement and the electrospun sheath should provide adequate mechanical properties. These aspects were addressed in the next set of experiments.

Mechanical Characterization

A vessel substitute *in vivo* must withstand the pulsatile blood pressure and flow, and must display enough strength to provide a safe implantation, while maintaining the capability of recoiling after stretching. To confirm whether our fabrication approach achieved an implantable device, we carried out burst strength, compliance and suture retention tests.

The burst strength of the vascular grafts was proportional to the PCL-sheath thickness, as shown in **Figure 3a**, and ranged from 436 ± 76 mmHg (ElastinGraft_0, **Figure 2**vii) to 2181 ± 37 mmHg (ElastinGraft_eL, **Figure 2**vii), which approximates the value of human saphenous vein (2250 mmHg) (Sarkar et al., 2006). Notably, all grafts displayed adequate strength (4–12 times the physiological pressure of 120 mmHg) for implantation. Historically, vascular engineering has aimed at developing vessel conduits that overmatch the values of native vessels (L'Heureux et al., 2006; Zhang et al., 2006; Drilling et al., 2009; McAllister et al., 2009). These supraphysiological burst strengths are normally the result of a long bioreactor conditioning phase producing dense tissues mainly composed of collagen and lacking elastin. However, there is an increasing number of studies showing that vascular grafts with a less mature matrix and featuring burst strength values lower than those displayed by target native vessels are still adequate for a safe implantation *in vivo* (Koch et al., 2010; Lee et al., 2011; Fukunishi et al., 2016; von Bornstadt et al., 2018) while favoring a more extensive *in situ* remodeling. The necessity of evaluating the burst pressure is indicated in the ISO guidelines 7198, but no target burst pressure values are given, and the question on which threshold pressure is required for a safe implantation remains open.

Matching compliance is of key importance to avoid hemodynamic flow changes across anastomosis, which have

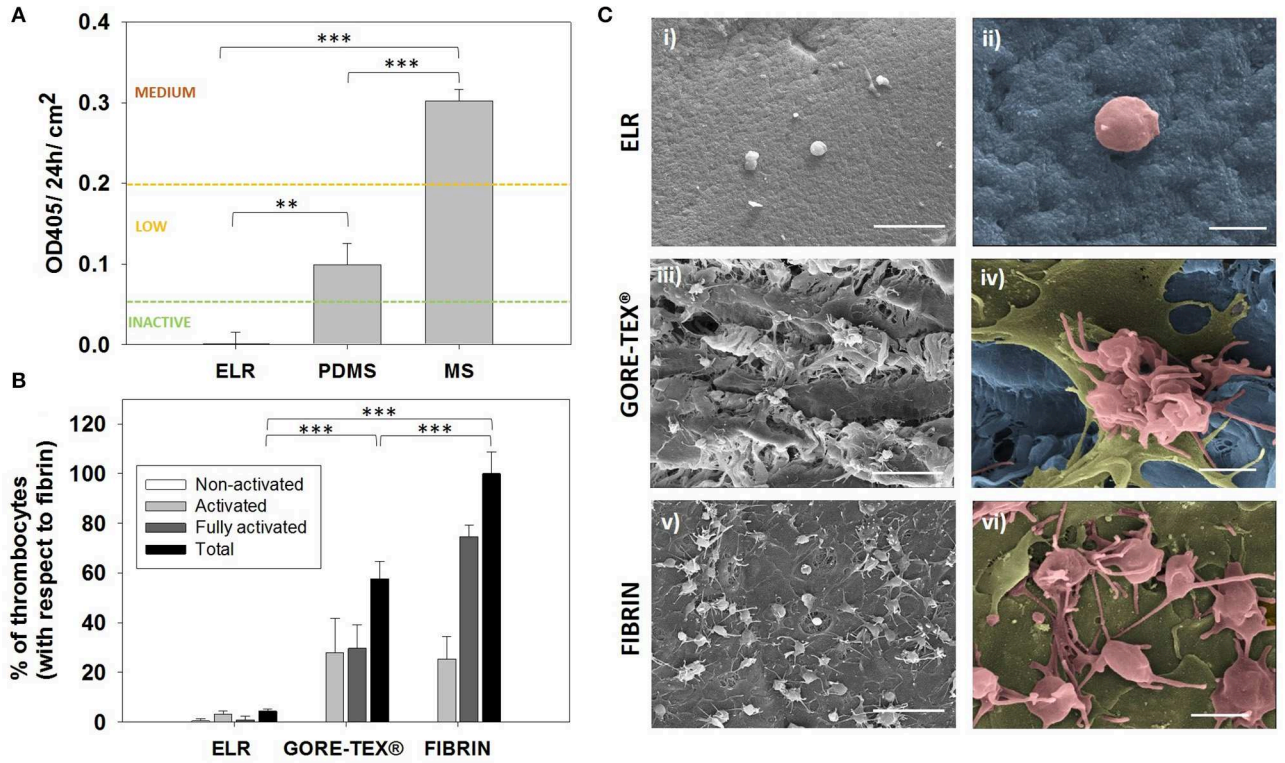

FIGURE 1 | Hemocompatibility assessment. **(A)** Hemocompatibility of ELR-gels assessed using the C5 complement convertase activity. Control materials used for comparison: medical steel (MS) and polydimethylsiloxane (PDMS). **(B)** Evaluation of adhered platelets based on SEM images. Results are plotted as the mean of three different experiments ± standard deviation. **(C)** SEM images of (i,ii) ELR hydrogel, (iii,iv) GORE-TEX®, and (v,vi) fibrin-gel after 1 h in contact with platelet rich plasma. Activated and fully activated platelets were covering fibrin and GORE-TEX® surfaces, while ELR surfaces presented minimal platelet adhesion. In the images ii, iv and vi, the ELR and GORE-TEX® scaffolds were colored in blue, the platelets with a spread morphology in gold and the more rounded platelets in salmon. Scale bars: (i,iii,v): 10 μm; (ii,iv,vi) 2 μm.

been associated with intimal hyperplasia, low patency, and consequent graft failure (Abbott et al., 1987; Trubel et al., 1995; Ballyk et al., 1998; Salacinski et al., 2001; Sarkar et al., 2006). Besides these effects at the graft site, the compliance miss-match can also lead to deleterious effects on the cardiac function. For example, the ascending aorta replacement with non-compliant grafts can result in aortic valve insufficiency and left ventricular hypertrophy (Spadaccio et al., 2016). The dynamic compliances of the vascular grafts at different pressure ranges are summarized in **Figure 3**. All the ElastinGrafts, except the ElastinGraft-eL, displayed higher compliances values than the commercially available grafts made of Dacron (1.9 ± 0.3% $mmHg^{-1} \times 10^{-2}$) and ePTFE (1.6 ± 0.2% $mmHg^{-1} \times 10^{-2}$) (Salacinski et al., 2001), which evidences the potential for energy-efficient transmission of the pulsatile flow provided by their elastic structure. Notably, the ElastinGraft_eM (4.11% $mmHg^{-1} \times 10^{-2}$) compares well with the compliance of human arteries [4.5–6.2% $mmHg^{-1} \times 10^{-2}$ (L'Heureux et al., 2006)] in the 80–120 mmHg range.

Importantly, the arterial tissue is anisotropic, that is, it does not obey Hook's law in response to cyclical blood pressure changes. As such, the relationship between the intraluminal pressure and the degree of radial deformation is not linear. The increased compliance found at lower physiological pressures is of key importance to preserve the pulsatile energy in situations of hemorrhagic shock (systolic blood pressure <90 mmHg) (Salacinski et al., 2001). However, this anisotropy is not displayed by prosthetic grafts, which typically present a constant compliance regardless the pressure, and they may, therefore, compromise patient-safety in case of a response of shock. The ElastinGrafts were able to recapitulate this anisotropic behavior, presumably because of the elastin-like structure, and specifically the ElastinGraft_eM mirrored the values of the native artery in the whole range of mean pressures tested (**Figure 3e** and **Supplementary Video 1**). The stiffness of the vascular grafts was also analyzed by calculating the β-index, which is a parameter less dependent on blood pressure (Mackenzie et al., 2002) and, therefore, facilitates the comparison among the performance of different grafts reported in the literature. The β-index of all but the ElastinGraft-eL was much lower than that of the human saphenous vein (45 ± 12.5) (Zhang et al., 2017) and Dacron (67.8 ± 32.3) (Tai et al., 2000), and importantly, the ElastinGraft_eM's β-index (24.6 ± 0.64) matched that of the femoral artery (23.7 ± 0.8) (Emoto et al., 1998).

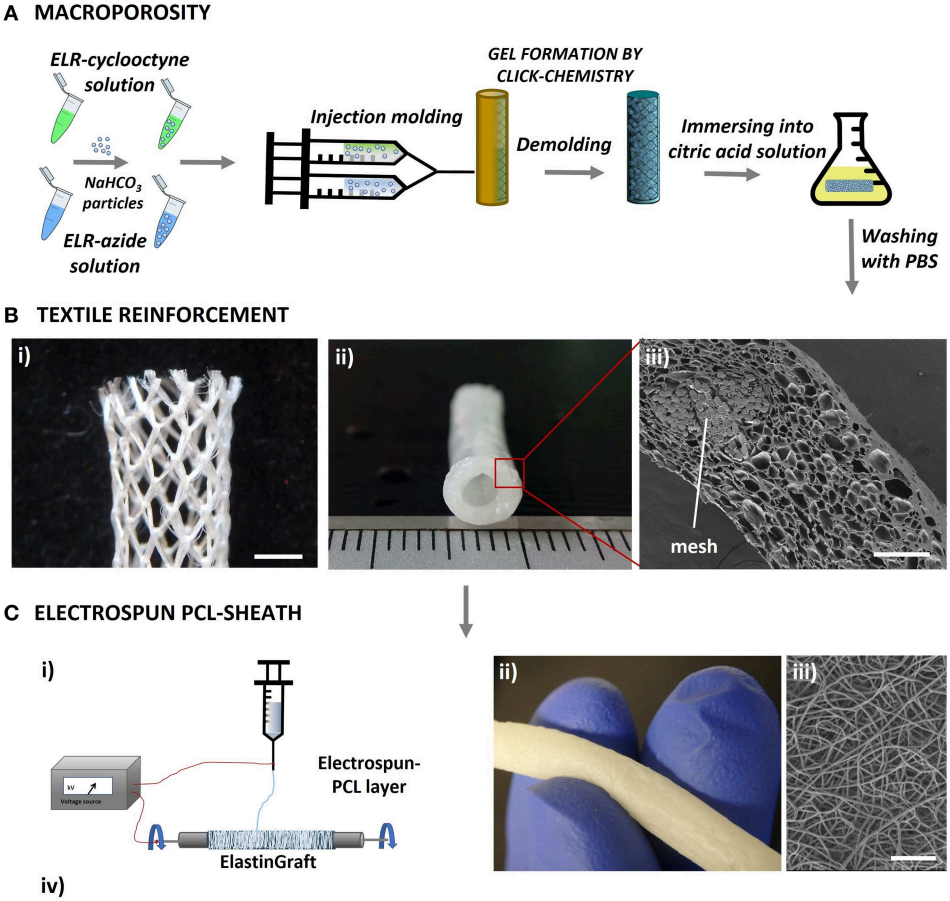

	PCL sheath thickness (µm)
ElastinGraft_0	0
ElastinGraft_eS	10 ± 4
ElastinGraft_eM	30 ± 6
ElastinGraft_eL	232 ± 26

FIGURE 2 | Biofabrication scheme of the ElastinGrafts: textile-reinforced macroporous vascular grafts based on ELRs. **(A)** Procedure used to obtain the macroporous click-ELR vascular graft. **(B)** Images of the textile-reinforced macroporous vascular graft: (i) PVDF-textile reinforcement to provide mechanical strength. (ii) Elastin graft. (iii) Cross-sectional SEM image of the macroporous ELR-vascular graft. **(C)** Electrospun PCL-sheath. (i) Sketch of the electrospinning procedure. (ii) Macroscopic image of the ElastinGraft enclosed with a PCL-sheath. (iii) SEM images of the electrospun sheath around the ELR-scaffold. (iv) Different versions of the ElastinGrafts differing in the thickness of the electrospun PCL-sheath. Specifically, "0" refers to "no e-spun layer"; "eS" to "the smallest thickness of the e-spun layer," "eM" to "the intermediate thickness of the e-spun layer" and "eL" to "the largest thickness of the e-layer." Scale bars: **(B)** (i) 2 mm; (iii) 200 µm; **(C)** (iii) 50 µm.

The compliance of the ElastinGrafts can be tuned over a wide range of values encompassing those of native vessels, as shown in **Figure 3**. The mechanical properties of the implant can, therefore, be tailored in a vessel specific manner. Considering that later steps in the vascular grafts' evaluation will inevitably involve animal trials, the possibility of tuning the compliance accordingly to that of the target animal vessel may result in a more accurate evaluation of its performance. For example, the native carotid artery of the sheep, which is a broadly used implantation model for vessel evaluation, has a compliance of approximately 12–14% (Fukunishi et al., 2016), which compares better with our ElastinGraft_0 (9.6% $mmHg^{-1} \times 10^{-2}$) than with the ElastinGraft_eM (4.11% $mmHg^{-1} \times 10^{-2}$). Whether the initial compliance should match that of the target vessel is, however, an open question that only further *in vivo* testing can elucidate as the *in situ* remodeling of the graft after implantation may result in changes in the mechanical properties. Collagen deposition, for example, may lead to an increase in the stiffness of the graft and to a concomitant decrease in the compliance (Uchida et al., 1989; Zilla et al., 2007; Fukunishi

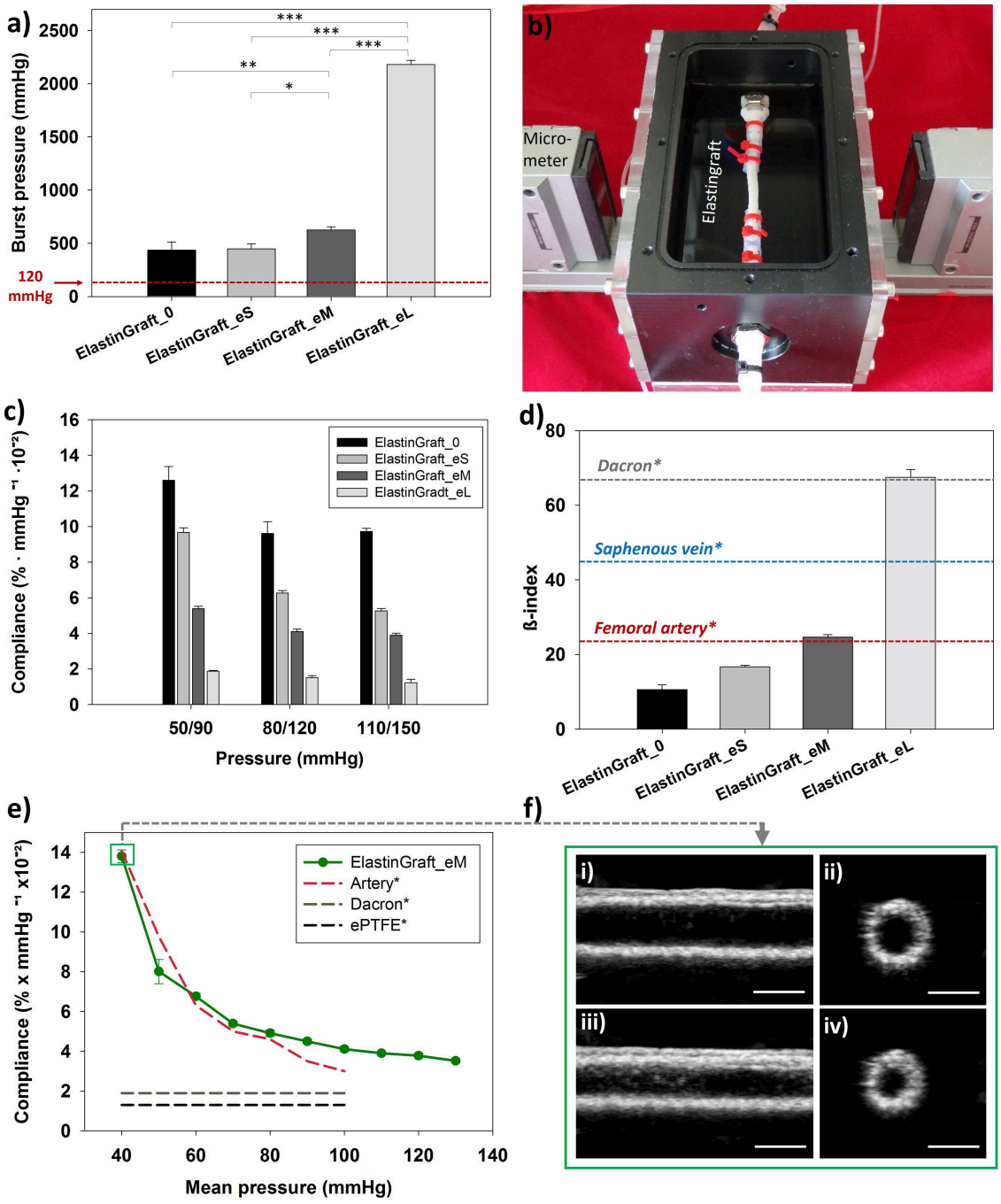

FIGURE 3 | Mechanical characterization of the ElastinGrafts. **(a)** Burst strength. **(b)** Vascular graft chamber used for assessing the compliance. **(c)** Compliances of the different ElastinGrafts at low (50–90 mmHg), normal (80–120 mmHg), and high pressure (110–150 mmHg). **(d)** Comparison of stiffness (β-index) between the ElastinGrafts, native blood vessels [value of the human femoral artery taken from Emoto et al. (1998) and value of the human saphenous vein taken from Zhang et al. (2017)] and Dacron [value taken from Tai et al. (2000)]. Values taken from literature are marked with an asterisk (*). **(e)** Compliance-mean pressure curve for the ElastinGraft_eM, artery, Dacron, and ePTFE. The values from the human external iliac artery, Dacron and ePTFE were adapted from Tai et al. (2000), Sarkar et al. (2006). **(f)** Ultrasound images of the ElastinGraft_eM in the simulated systolic low pressure of 60 mmHg (i,ii) and diastolic low pressure of 20 mmHg (iii,iv). The complete videos for the low (20/60 and 50/90 mmHg), normal (80/120 mmHg), and higher pressure ranges (110/150 mmHg) are available as supporting information (**Supplementary Video S1**).

et al., 2016). Under such scenario, the use of implants with initial compliance values higher than those of the target vessels may be recommended. However, how the scaffold degradation can additionally influence the compliance by, for example, counterbalancing the increased collagen amount, belongs as well to the gap of knowledge that represents a challenging aspect of

the design of any implant based on the concept of endogenous tissue growth (Pashneh-Tala et al., 2015; Wissing et al., 2017). Nevertheless, the platform that we developed here enables to meet a desired compliance once defined as design endpoint (Ozolanta et al., 1998).

The suture retention force of the ElastinGraft_0 and the ElastinGraft_eM was 2.1 ± 1.4 and 2.8 ± 1.8 N, respectively. These values compare well with the human internal mammary arteries (1.4 N) and human saphenous veins (1.8 N) (Konig et al., 2009). The absence of statistical difference between both ElastinGrafts ($p > 0.05$) suggests that the PCL layer does not play a significant role in providing suture retention which is, therefore, attributable to the knitted mesh. The high standard deviation reflects the structure of the knit pattern of the PVDF mesh (**Figure 2B**). Overall, these results indicate that the newly developed grafts have a suture retention strength adequate for direct anastomosis (Wu et al., 2012). PVDF is one of the most popular polymers in textile biomedical engineering due to its processability, mechanical properties, biostability, and minimal tissue response (Klinge et al., 2002). The mechanical reinforcement provided by a knitted textile has been previously exploited in classically tissue-engineered cell-based vascular grafts implanted as arteriovenous shunts (Mertens et al., 2015) and as interpositional grafts in the systemic circulation of a large animal model (Koch et al., 2010; Wolf et al., 2019).

Cell Ingrowth and Extracellular Matrix Production

To determine whether the ElastinGrafts can support cell colonization and ECM deposition, we cultured them *in vitro* with SMCs. SEM and immunohistochemistry confirmed cell infiltration into the walls of the vascular grafts, and ECM deposition was shown after 12 days of static culture *in vitro* (**Figures 4**, **5**). Specifically, the SEM images revealed the presence of fibrillar structures attributable to the secreted ECM in most of the pores along the cross-section of the vascular graft wall (**Figure 4B**).

Immunohistochemistry revealed α-SMA positive-stained cells, which corroborated their SMC phenotype, besides the deposition of collagen I, collagen III, fibronectin and fibrillin I (**Figure 5**). Fibrillin I is an elastic matrix-forming protein, whose expression precedes that of elastin (Votteler et al., 2013) and guides elastogenesis (Mariko et al., 2011). There was also a positive signal for elastin, although it is not possible to assess whether this signal is solely attributed to elastin-like nature of the vascular graft, or to elastin newly secreted by the cells. The vast majority of the stained substrate has a smooth porous structure (**Supplementary Figure 2**, yellow asterisk), which fits with the appearance in the bright field of the elastin-like scaffold, and therefore, the elastin signal seems to correspond mainly to the ELR-scaffold. The intense fluorescence emission of the ELR can mask the signal from newly synthetized elastin, expected to be in lower amounts. The presence of small amounts of elastin cannot, therefore, be ruled out, and positive signal within the secreted ECM (indicated with arrows in the figure) seems to corroborate this (**Supplementary Figure 2**).

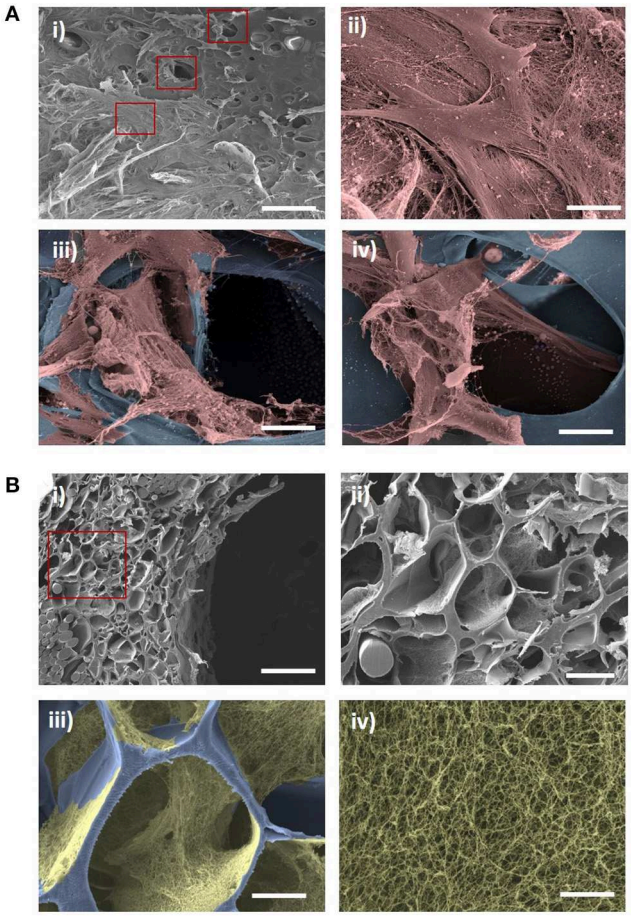

FIGURE 4 | SEM evaluation of cell ingrowth and ECM production after *in vitro* culture of the ElastinGrafts with SMCs. **(A)** Luminal surface of the ElastinGraft; (i) overview and (ii) detailed view of the SMCs covering the luminal surface of the graft. (iii,iv) Detailed views of SMCs infiltrating the scaffold. In images **(A)** (ii–iv) the ELR-scaffold was colored in blue and the SMCs in salmon. **(B)** (i,ii) Porous structure of ElastinGraft visualized at a cross-section. (iii) Representative pore covered with deposited ECM. (iv) Zoomed-in view of the fibrillar ECM. In the images **(B)** (iii,iv) the ELR-scaffold was colored in blue and the fibrillar ECM was colored in gold. Scale bars. **(A)** (i) 200 μm: **(B)** (ii–iv) 20 μm. **(B)** (i) 200 μm; (ii) 50 μm; (iii) 20 μm; (iv) 2 μm.

The presence of elastin (whether it is secreted or synthetic elastin) provides the basis for an adequate elastic response to pulsatile pressure. Despite the primordial role of the elastin in ensuring appropriate mechanical function of the vessels, the expression of mature elastin in arterial tissue engineering represents still a significant challenge (Patel et al., 2006; Lee et al., 2011). We circumvent here this problem by using the ELRs as a fabrication material of the grafts. Overall, these results confirmed that the fabricated ElastinGrafts can guide cell infiltration and tissue remodeling, resulting in vascular equivalents that emulate the composition of the native vessels.

The endothelium is the physiological and ideal blood-contacting surface, and additionally, it plays an important role in vascular biology, e.g., blood vessel tone, hemostasis,

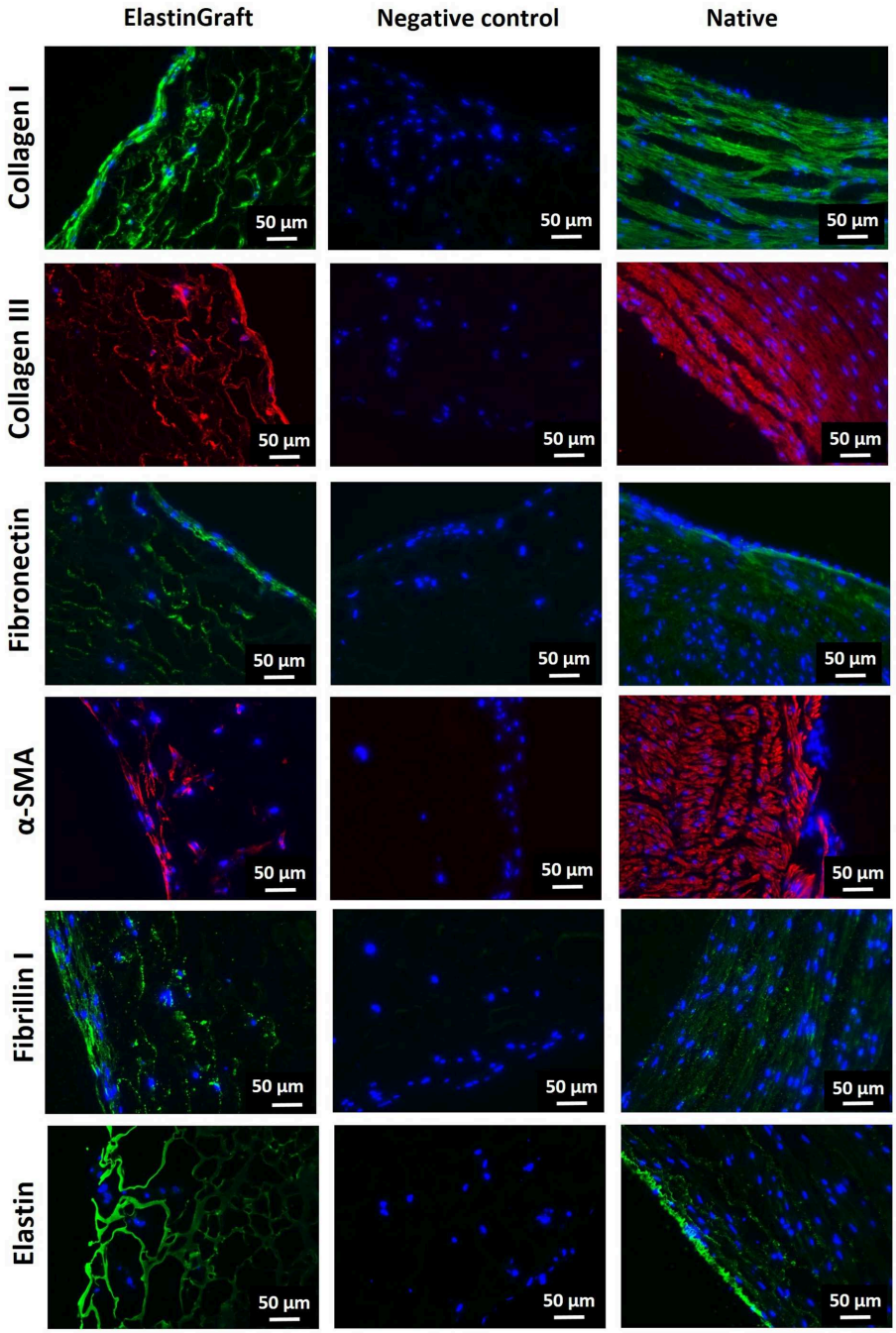

FIGURE 5 | Immunohistochemical evaluation of cell ingrowth and ECM production after *in vitro* culture of the ElastinGrafts with SMCs. Analysis of the ElastinGraft and a native human artery from the umbilical cord, showing staining for alpha-SMA, collagen I, collagen III, fibronectin, fibrillin I, and elastin. Negative controls (absence of the primary antibody) for all markers showed undetectable levels of staining.

neutrophil recruitment and hormone trafficking (Sandoo et al., 2010; Rajendran et al., 2013). Therefore, the ability of a vascular graft to support endothelialization is crucial for the success of the implant. While transanastomotic endothelialization in humans is restricted to the immediate perianastomotic region (Zilla et al., 2007; Talacua et al., 2015), circulating EPCs are increasingly recognized as important contributors to vascular prosthesis endothelialization, making them important mediators of implant compatibility (Yu et al., 2015; Melchiorri et al., 2016). In order to evaluate the ability of the ElastinGrafts to support endothelialization, we seeded them with EPCs from human peripheral blood. Endothelial cells attached to and spread on

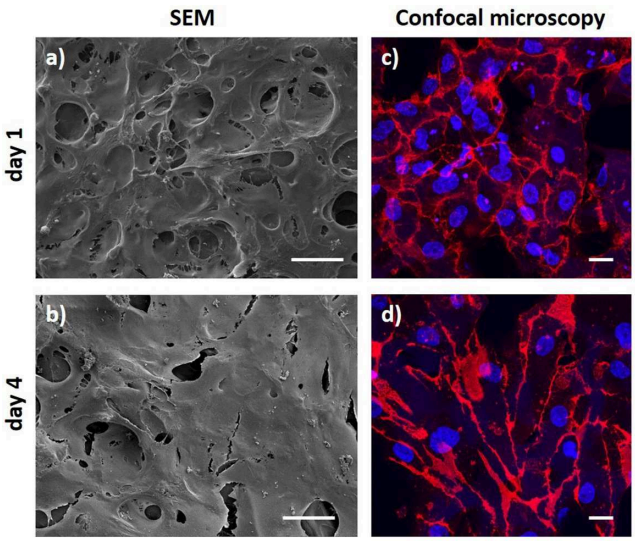

FIGURE 6 | Endothelial progenitor cell layer obtained after 1 day and 4 days of culture. **(a,b)** SEM images. **(c,d)** Confocal microscopy images after CD31 staining (red) with DAPI as nuclear counterstain (blue). Scale bars: **(a,b)** 50 μm; **(c,d)** 20 μm.

the surface of the ELR scaffolds (**Figure 6**), which agrees with the presence of the integrin-mediated adhesion epitope RGD in the ELR scaffold (**Table 1**). After 4 days, an increase in cell density on the implant was evident, and resulted in a confluent endothelial layer. Further analysis by CD31 immunostaining confirmed the endothelialization of the ELRs grafts (**Figures 6c,d**).

CONCLUSIONS

We fabricated small-caliber elastin-like vascular grafts featuring an open-porous structure while maintaining mechanical performance to withstand the arterial hemodynamic loads. Different from the clinically available prosthesis, the ElastinGrafts allow an energy-efficient transmission of pulsatile flow, and are able to match the compliance of a wide range of implantation targets. Moreover, the grafts promoted cell ingrowth and ECM deposition, which further supports their application as ready-to-use cell-free implants. Overall, these vascular grafts combine the reproducibility and off-the-shelf availability normally provided by synthetic grafts with the bioactivity, hemocompatibility and remodeling behavior of autografts, and represent a promising option for coronary artery by-pass surgery. The recombinant nature of the ELRs offers the potential to incorporate further biofunctionalities in an accurate and controlled manner, in order to tune the performance of the resulting grafts.

DATA AVAILABILITY STATEMENT

Data associated with this study is available upon request to the corresponding authors.

ETHICS STATEMENT

The umbilical cords were kindly provided by the Department of Gynecology at the University Hospital Aachen in accordance with the human subjects' approval of the ethics committee (EK 2067) upon written informed consent.

AUTHOR CONTRIBUTIONS

PM and AF-C designed the study and wrote the manuscript. AF-C and FW performed the experiments. SR characterized the samples by scanning electron microscopy. SJ, JR-C, and TS-R revised the manuscript. All authors approved the final version.

FUNDING

This work was funded by the Excellence Initiative of the German federal and state governments in the framework of the i3tm Rotational Position Program (2014-R4-01), the START-UP Program (StUpPD_330-18), and by the START-Program of the Medical Faculty of RWTH Aachen University (60/17). JR-C appreciates the funding from the European Commission (NMP-2014-646075), MINECO of the Spanish Government (PCIN-2015-010, MAT2016-78903-R), Junta de Castilla y León (VA317P18), and Centro en Red de Medicina Regenerativa y Terapia Celular de Castilla y León.

ACKNOWLEDGMENTS

The authors acknowledge the support of Prof. Dr. Müller-Newen, Sabrina Ernst, and the confocal microscopy facility, a core facility of the Interdisciplinary Center for Clinical Research (IZKF) Aachen within the Faculty of Medicine at RWTH Aachen University. We also acknowledge the Flow Cytometry Facility, a core facility of the Interdisciplinary Center for Clinical Research (IZKF) Aachen within the Faculty of Medicine at RWTH Aachen University.

SUPPLEMENTARY MATERIAL

The Supplementary Material for this article can be found online at: https://www.frontiersin.org/articles/10.3389/fbioe.2019.00340/full#supplementary-material

Supplementary Figure 1 | Structure of the ElastinGraft. **(a)** PVDF-mesh. **(b–d)** Macroscopic ElastinGraft images: the PVDF-mesh is fully embedded with the ELR scaffold. **(e)** SEM image of the cross-section of the ElastinGraft wall, showing the porous structure of the ELR (colored in green) completely embedding the PVDF-mesh (colored in purple with the software MountainsMap SEM software courtesy of Digital Surf, France).

Supplementary Figure 2 | Morphology of the ElastinGraft before and after cell seeding. **(a)** Microscopy images of paraffin-cuts of the ElastinGraft before seeding. The grafts present a porous structure and the wall of the pores show a smooth appearance. **(b)** Microscopy images of paraffin-cuts of the ElastinGraft 12 days after cell seeding and cultivation. Scale bars: **(a)** (i), **(b)** (i) and **(b)** (iii) 50 μm. **(a)** (ii), **(b)** (ii) and **(b)** (iv) 20 μm.

Supplementary Video 1 | Ultrasound video of the ElastinGraft_eM in the simulated low (20/60 and 50/90 mmHg), normal (80/120 mmHg), and high pressure ranges (110/150 mmHg). Scale bar 5 mm. File type MP4.

REFERENCES

Abbott, W. M., Megerman, J., Hasson, J. E., L'Italien, G., and Warnock, D. (1987). Effect of compliance mismatch on vascular graft patency. *J. Vasc. Surg.* 5, 376–382. doi: 10.1016/0741-5214(87)90148-0

Arias, F. J., Santos, M., Fernandez-Colino, A., Pinedo, G., and Girotti, A. (2014). Recent contributions of elastin-like recombinamers to biomedicine and nanotechnology. *Curr. Top. Med. Chem.* 14, 819–836. doi: 10.2174/1568026614660140118223412

Ballyk, P. D., Walsh, C., Butany, J., and Ojha, M. (1998). Compliance mismatch may promote graft-artery intimal hyperplasia by altering suture-line stresses. *J. Biomech.* 31, 229–237. doi: 10.1016/S0197-3975(97)00111-5

Billiet, T., Vandenhaute, M., Schelfhout, J., Van Vlierberghe, S., and Dubruel, P. (2012). A review of trends and limitations in hydrogel-rapid prototyping for tissue engineering. *Biomaterials* 33, 6020–6041. doi: 10.1016/j.biomaterials.2012.04.050

de Torre, I. G., Wolf, F., Santos, M., Rongen, L., Alonso, M., Jockenhoevel, S., et al. (2015). Elastin-like recombinamer-covered stents: Towards a fully biocompatible and non-thrombogenic device for cardiovascular diseases. *Acta Biomater.* 12, 146–155. doi: 10.1016/j.actbio.2014.10.029

Drilling, S., Gaumer, J., and Lannutti, J. (2009). Fabrication of burst pressure competent vascular grafts via electrospinning: effects of microstructure. *J. Biomed. Mater. Res. A* 88, 923–934. doi: 10.1002/jbm.a.31926

Emoto, M., Nishizawa, Y., Kawagishi, T., Maekawa, K., Hiura, Y., Kanda, H., et al. (1998). Stiffness indexes beta of the common carotid and femoral arteries are associated with insulin resistance in NIDDM. *Diabetes Care* 21, 1178–1182. doi: 10.2337/diacare.21.7.1178

Fernandez-Colino, A., Wolf, F., Keijdener, H., Rutten, S., Schmitz-Rode, T., Jockenhoevel, S., et al. (2018). Macroporous click-elastin-like hydrogels for tissue engineering applications. *Mater. Sci. Eng. C Mater. Biol. Appl.* 88, 140–147. doi: 10.1016/j.msec.2018.03.013

Fukunishi, T., Best, C. A., Sugiura, T., Shoji, T., Yi, T., Udelsman, B., et al. (2016). Tissue-engineered small diameter arterial vascular grafts from cell-free nanofiber PCL/chitosan scaffolds in a sheep model. *PLoS ONE* 11:e0158555. doi: 10.1371/journal.pone.0158555

Girotti, A., Fernández-Colino, A., López, I. M., Rodríguez-Cabello, J. C., and Arias, F. J. (2011). Elastin-like recombinamers: biosynthetic strategies and biotechnological applications. *Biotechnol. J.* 6, 1174–1186. doi: 10.1002/biot.201100116

Gonzalez de Torre, I., Santos, M., Quintanilla, L., Testera, A., Alonso, M., Rodriguez Cabello, J., et al. (2014). Elastin-like recombinamer catalyst-free click gels: characterization of poroelastic and intrinsic viscoelastic properties. *Acta Biomater.* 10, 2495–2505. doi: 10.1016/j.actbio.2014.02.006

Goodman, S. L., Grasel, T. G., Cooper, S. L., and Albrecht, R. (1989). Platelet shape change and cytoskeletal reorganization on polyurethaneureas. *J. Biomed. Mater. Res.* 23, 105–123. doi: 10.1002/jbm.820230109

Hess, C. N., Lopes, R. D., Gibson, C. M., Hager, R., Wojdyla, D. M., Englum, B. R., et al. (2014). Saphenous vein graft failure after coronary artery bypass surgery: insights from PREVENT IV. *Circulation* 130, 1445–1451. doi: 10.1161/CIRCULATIONAHA.113.008193

Ito, S., Ishimaru, S., and Wilson, S. E. (1998). Application of coacervated alpha-elastin to arterial prostheses for inhibition of anastomotic intimal hyperplasia. *ASAIO J.* 44, M501–505. doi: 10.1097/00002480-199809000-00036

Jordan, S. W., Haller, C. A., Sallach, R. E., Apkarian, R., Hanson, S. R., and Chaikof, E. L. (2007). The effect of a recombinant elastin-mimetic coating of an ePTFE prosthesis on acute thrombogenicity in a baboon arteriovenous shunt. *Biomaterials* 28, 1191–1197. doi: 10.1016/j.biomaterials.2006.09.048

Kannan, R. Y., Salacinski, H. J., Butler, P. E., Hamilton, G., and Seifalian, A. M. (2005). Current status of prosthetic bypass grafts: a review. *J. Biomed. Mater. Res. Part B Appl. Biomater.* 74, 570–581. doi: 10.1002/jbm.b.30247

Klinge, U., Klosterhalfen, B., Ottinger, A. P., Junge, K., and Schumpelick, V. (2002). PVDF as a new polymer for the construction of surgical meshes. *Biomaterials* 23, 3487–3493. doi: 10.1016/S0142-9612(02)00070-4

Koch, S., Flanagan, T. C., Sachweh, J. S., Tanios, F., Schnoering, H., Deichmann, T, et al. (2010). Fibrin-polylactide-based tissue-engineered vascular graft in the arterial circulation. *Biomaterials* 31, 4731–4739. doi: 10.1016/j.biomaterials.2010.02.051

Konig, G., McAllister, T. N., Dusserre, N., Garrido, S. A., Iyican, C., Marini, A., et al. (2009). Mechanical properties of completely autologous human tissue engineered blood vessels compared to human saphenous vein and mammary artery. *Biomaterials* 30, 1542–1550. doi: 10.1016/j.biomaterials.2008.11.011

Lee, K. W., Stolz, D. B., and Wang, Y. (2011). Substantial expression of mature elastin in arterial constructs. *Proc. Natl. Acad. Sci. U.S.A.* 108, 2705–2710. doi: 10.1073/pnas.1017834108

L'Heureux, N., Dusserre, N., Konig, G., Victor, B., Keire, P., Wight, T., et al. (2006). Human tissue engineered blood vessel for adult arterial revascularization. *Nat. Med.* 12, 361–365. doi: 10.1038/nm1364

MacEwan, S. R., and Chilkoti, A. (2010). Elastin-like polypeptides: biomedical applications of tunable biopolymers. *Biopolymers* 94, 60–77. doi: 10.1002/bip.21327

Mackenzie, I. S., Wilkinson, I. B., and Cockcroft, J. R. (2002). Assessment of arterial stiffness in clinical practice. *QJM* 95, 67–74. doi: 10.1093/qjmed/95.2.67

Mariko, B., Pezet, M., Escoubet, B., Bouillot, S., Andrieu, J. P., Starcher, B., et al. (2011). Fibrillin-1 genetic deficiency leads to pathological aging of arteries in mice. *J. Pathol.* 224, 33–44. doi: 10.1002/path.2840

Martin, L., Alonso, M., Girotti, A., Javier Arias, F., and Carlos Rodriguez-Cabello, J. (2009). Synthesis and characterization of macroporous thermosensitive hydrogels from recombinant elastin-like polymers. *Biomacromolecules* 10, 3015–3022. doi: 10.1021/bm900560a

McAllister, T. N., Maruszewski, M., Garrido, S. A., Wystrychowski, W., Dusserre, N., Marini, A., et al. (2009). Effectiveness of haemodialysis access with an autologous tissue-engineered vascular graft: a multicentre cohort study. *Lancet* 373, 1440–1446. doi: 10.1016/S0140-6736(09)60248-8

Melchiorri, A. J., Bracaglia, L. G., Kimerer, L. K., Hibino, N., and Fisher J. P. (2016). *In vitro* endothelialization of biodegradable vascular grafts via endothelial progenitor cell seeding and maturation in a tubular perfusion system bioreactor. *Tissue Eng. Part C Methods* 22, 663–670. doi: 10.1089/ten.tec.2015.0562

Mertens, M. E., Koch, S., Schuster, P., Wehner, J., Wu, Z., Gremse, F., et al. (2015). USPIO-labeled textile materials for non-invasive MR imaging of tissue-engineered vascular grafts. *Biomaterials* 39, 155–163. doi: 10.1016/j.biomaterials.2014.10.076

Moreira, R., Velz, T., Alves, N., Gesche, V. N., Malischewski, A., Schmitz-Rode, J., et al. (2015). Tissue-engineered heart valve with a tubular leaflet design for minimally invasive transcatheter implantation. *Tissue Eng. Part C* 21, 530–540. doi: 10.1089/ten.tec.2014.0214

Ozolanta, I., Tetere, G., Purinya, B., and Kasyanov, V. (1998). Changes in the mechanical properties, biochemical contents and wall structure of the human coronary arteries with age and sex. *Med. Eng. Phys.* 20, 523–533. doi: 10.1016/S1350-4533(98)00050-2

Park, S., Kim, J., Lee, M.-K., Park, C., Jung, H.-D., Kim, H.-E., et al. (2019). Fabrication of strong, bioactive vascular grafts with PCL/collagen and PCL/silica bilayers for small-diameter vascular applications. *Mater. Des.* 181:108079. doi: 10.1016/j.matdes.2019.108079

Pashneh-Tala, S., MacNeil, S., and Claeyssens, F. (2015). The tissue-engineered vascular graft-past, present, and future. *Tissue Eng. Part B Rev.* 22, 68–100. doi: 10.1089/ten.teb.2015.0100

Patel, A., Fine, B., Sandig, M., and Mequanint, K. (2006). Elastin biosynthesis: the missing link in tissue-engineered blood vessels. *Cardiovasc. Res.* 71, 40–49. doi: 10.1016/j.cardiores.2006.02.021

Rajendran, P., Rengarajan, T., Thangavel, J., Nishigaki, Y., Sakthisekaran, D., Sethi, G., et al. (2013). The vascular endothelium and human diseases. *Int. J. Biol. Sci.* 9, 1057–1069. doi: 10.7150/ijbs.7502

Rosenbloom, J., Abrams, W. R., and Mecham, R. (1993). Extracellular matrix 4: the elastic fiber. *FASEB J.* 7, 1208–1218. doi: 10.1096/fasebj.7.13.8405806

Salacinski, H. J., Goldner, S., Giudiceandrea, A., Hamilton, G., Seifalian, A. M., Edwards, A., et al. (2001). The mechanical behavior of vascular grafts: a review. *J. Biomater. Appl.* 15, 241–278. doi: 10.1106/NA5T-J57A-JTDD-FD04

Sandoo, A., van Zanten, J. J., Metsios, G. S., Carroll, D., and Kitas, G. D. (2010). The endothelium and its role in regulating vascular tone. *Open Cardiovasc. Med. J.* 4, 302–312. doi: 10.2174/1874192401004010302

Sarkar, S., Salacinski, H. J., Hamilton, G., and Seifalian, A. M. (2006). The mechanical properties of infrainguinal vascular bypass grafts: their role in influencing patency. *Eur. J. Vasc. Endovasc. Surg.* 31, 627–636. doi: 10.1016/j.ejvs.2006.01.006

Sarkar, S., Schmitz-Rixen, T., Hamilton, G., and Seifalian, A. M. (2007). Achieving the ideal properties for vascular bypass grafts using a tissue engineered approach: a review. *Med. Biol. Eng. Comput.* 45, 327–336. doi: 10.1007/s11517-007-0176-z

Soletti, L., Hong, Y., Guan, J., Stankus, J. J., El-Kurdi, M., Wagner, W. R., et al. (2010). A bilayered elastomeric scaffold for tissue engineering of small diameter vascular grafts. *Acta Biomater.* 6, 110–122. doi: 10.1016/j.actbio.2009.06.026

Sorrentino, S., Studt, J.-D., Horev, M., B., Medalia, O., and Sapra, K. (2016). Toward correlating structure and mechanics of platelets. *Cell Adh. Migr.* 10, 568–575. doi: 10.1080/19336918.2016.1173803

Spadaccio, C., Nappi, F., Al-Attar, N., Sutherland, F. W., Acar, C., Nenna, A., et al. (2016). Old myths, new concerns: the long-term effects of ascending aorta replacement with dacron grafts. Not all that glitters is gold. *J. Cardiovasc. Transl. Res.* 9, 334–342. doi: 10.1007/s12265-016-9699-8

Sugiura, T., Tara, S., Nakayama, H., Kurobe, H., Yi, T., Lee, Y.-U., et al. (2016). Novel bioresorbable vascular graft with sponge-type scaffold as a small-diameter arterial graft. *Ann. Thorac. Surg.* 102, 720–727. doi: 10.1016/j.athoracsur.2016.01.110

Tai, N. R., Salacinski, H. J., Edwards, A., Hamilton, G., and Seifalian, A. (2000). Compliance properties of conduits used in vascular reconstruction. *Br. J. Surg.* 87, 1516–1524. doi: 10.1046/j.1365-2168.2000.01566.x

Talacua, H., Smits, A. I., Muylaert, D. E., van Rijswijk, J., Vink, A., Verhaar, M. C., et al. (2015). *In situ* tissue engineering of functional small-diameter blood vessels by host circulating cells only. *Tissue Eng. Part A* 21, 2583–2594. doi: 10.1089/ten.tea.2015.0066

Townsend, N., Wilson, L., Bhatnagar, P., Wickramasinghe, K., Rayner, M., and Nichols, M. (2016). Cardiovascular disease in Europe: epidemiological update 2016. *Eur. Heart J.* 37, 3232–3245. doi: 10.1093/eurheartj/ehw334

Trubel, W., Schima, H., Moritz, A., Raderer, F., Windisch, A., Ullrich, R., et al. (1995). Compliance mismatch and formation of distal anastomotic intimal hyperplasia in externally stiffened and lumen-adapted venous grafts. *Eur. J. Vasc. Endovasc. Surg.* 10, 415–423. doi: 10.1016/S1078-5884(05)80163-7

Uchida, N., Emoto, H., Kambic, H., Harasaki, H., Chen, J. F., Hsu, S. H., et al. (1989). Compliance effect on patency of small diameter vascular grafts. *ASAIO Trans.* 35, 556–558. doi: 10.1097/00002480-198907000-00124

von Bornstadt, D., Wang, H., Paulsen, M. J., Goldstone, A. B., Eskandari, A., Thakore, A., et al. (2018). Rapid self-assembly of bioengineered cardiovascular bypass grafts from scaffold-stabilized, tubular bilevel cell sheets. *Circulation* 138, 2130–2144. doi: 10.1161/CIRCULATIONAHA.118.035231

Votteler, M., Berrio, D. A. C., Horke, A., Sabatier, L., Reinhardt, D., Nsair, A., et al. (2013). Elastogenesis at the onset of human cardiac valve development. *Development* 140, 2345–2353. doi: 10.1242/dev.093500

Wissing, T. B., Bonito, V., Bouten, C., V. C., and Smits, A. I. (2017). Biomaterial-driven *in situ* cardiovascular tissue engineering—a multi-disciplinary perspective. *NPJ Regenerat. Med.* 2:18. doi: 10.1038/s41536-017-0023-2

Wolf, F., Paefgen, V., Winz, O., Mertens, M., Koch, S., Gross-Weege, N., et al. (2019). MR and PET-CT monitoring of tissue-engineered vascular grafts in the ovine carotid artery. *Biomaterials* 216:119228. doi: 10.1016/j.biomaterials.2019.119228

Wolf, F., Rojas Gonzalez, D. M., Steinseifer, U., Obdenbusch, M., Herfs, W., Brecher, C., et al. (2018). VascuTrainer: a mobile and disposable bioreactor system for the conditioning of tissue-engineered vascular grafts. *Ann. Biomed. Eng.* 46, 616–626. doi: 10.1007/s10439-018-1977-y

Woodhouse, K. A., Klement, P., Chen, V., Gorbet, M. B., Keeley, F., Stahl, R., et al. (2004). Investigation of recombinant human elastin polypeptides as non-thrombogenic coatings. *Biomaterials* 25, 4543–4553. doi: 10.1016/j.biomaterials.2003.11.043

Wu, W., Allen, R. A., and Wang, Y. (2012). Fast degrading elastomer enables rapid remodeling of a cell-free synthetic graft into a neo-artery. *Nat. Med.* 18, 1148–1153. doi: 10.1038/nm.2821

Yu, Y., Wise, S. G., Michael, P. L., Bax, D., Yuen, G. S., Hiob, M. A., et al. (2015). Characterization of endothelial progenitor cell interactions with human tropoelastin. *PLoS ONE* 10:e0131101. doi: 10.1371/journal.pone.0131101

Zhang, L., Ao, Q., Wang, A., Lu, G., Kong, L., Gong, Y., et al. (2006). A sandwich tubular scaffold derived from chitosan for blood vessel tissue engineering. *J. Biomed. Mater. Res. A* 77, 277–284. doi: 10.1002/jbm.a.30614

Zhang, Y., Li, X. S., Guex, A. G., Liu, S., Muller, E., Malini, R. I., et al. (2017). A compliant and biomimetic three-layered vascular graft for small blood vessels. *Biofabrication* 9, 025010. doi: 10.1088/1758-5090/aa730a

Zhao, J., Bai, L., Ren, X. K., Guo, J., Xia, S., Zhang, W., et al. (2019). Co-immobilization of ACH11 antithrombotic peptide and CAG cell-adhesive peptide onto vascular grafts for improved hemocompatibility and endothelialization. *Acta Biomater.* 97, 344–359. doi: 10.1016/j.actbio.2019.07.057

Zhong, S., Zhang, Y., and Lim, C. T. (2012). Fabrication of large pores in electrospun nanofibrous scaffolds for cellular infiltration: a review. *Tissue Eng. Part B Rev.* 18, 77–87. doi: 10.1089/ten.teb.2011.0390

Zilla, P., Bezuidenhout, D., and Human, P. (2007). Prosthetic vascular grafts: wrong models, wrong questions and no healing. *Biomaterials* 28, 5009–5027. doi: 10.1016/j.biomaterials.2007.07.017

Conflict of Interest: The authors declare that the research was conducted in the absence of any commercial or financial relationships that could be construed as a potential conflict of interest.

Copyright © 2019 Fernández-Colino, Wolf, Rütten, Schmitz-Rode, Rodríguez-Cabello, Jockenhoevel and Mela. This is an open-access article distributed under the terms of the Creative Commons Attribution License (CC BY). The use, distribution or reproduction in other forums is permitted, provided the original author(s) and the copyright owner(s) are credited and that the original publication in this journal is cited, in accordance with accepted academic practice. No use, distribution or reproduction is permitted which does not comply with these terms.

frontiers in Bioengineering and Biotechnology

REVIEW
published: 27 February 2020
doi: 10.3389/fbioe.2020.00126

Inducing Endogenous Cardiac Regeneration: Can Biomaterials Connect the Dots?

Assaf Bar[1] *and Smadar Cohen*[1,2,3]*

[1] The Avram and Stella Goldstein-Goren Department of Biotechnology Engineering, Faculty of Engineering Sciences, Ben-Gurion University of the Negev, Beersheba, Israel, [2] Regenerative Medicine and Stem Cell Research Center, Ben-Gurion University of the Negev, Beersheba, Israel, [3] Ilse Katz Institute for Nanoscale Science and Technology, Ben-Gurion University of the Negev, Beersheba, Israel

Heart failure (HF) after myocardial infarction (MI) due to blockage of coronary arteries is a major public health issue. MI results in massive loss of cardiac muscle due to ischemia. Unfortunately, the adult mammalian myocardium presents a low regenerative potential, leading to two main responses to injury: fibrotic scar formation and hypertrophic remodeling. To date, complete heart transplantation remains the only clinical option to restore heart function. In the last two decades, tissue engineering has emerged as a promising approach to promote cardiac regeneration. Tissue engineering aims to target processes associated with MI, including cardiomyogenesis, modulation of extracellular matrix (ECM) remodeling, and fibrosis. Tissue engineering dogmas suggest the utilization and combination of two key components: bioactive molecules and biomaterials. This chapter will present current therapeutic applications of biomaterials in cardiac regeneration and the challenges still faced ahead. The following biomaterial-based approaches will be discussed: Nano-carriers for cardiac regeneration-inducing biomolecules; corresponding matrices for their controlled release; injectable hydrogels for cell delivery and cardiac patches. The concept of combining cardiac patches with controlled release matrices will be introduced, presenting a promising strategy to promote endogenous cardiac regeneration.

Keywords: biomaterials, cardiac patch, cardiac regeneration, drug delivery, myocardial infarction, tissue engineering

OPEN ACCESS

Edited by:
Monica Boffito,
Politecnico di Torino, Italy

Reviewed by:
Carmine Gentile,
University of Technology Sydney, Australia
Shayanti Mukherjee,
Hudson Institute of Medical Research, Australia
Sara Maria Giannitelli,
Campus Bio-Medico University, Italy

***Correspondence:**
Smadar Cohen
scohen@bgu.ac.il;
scohen@bgu.cc.il

Specialty section:
This article was submitted to Biomaterials, a section of the journal Frontiers in Bioengineering and Biotechnology

Received: *20 October 2019*
Accepted: *10 February 2020*
Published: *27 February 2020*

Citation:
Bar A and Cohen S (2020) Inducing Endogenous Cardiac Regeneration: Can Biomaterials Connect the Dots? Front. Bioeng. Biotechnol. 8:126. doi: 10.3389/fbioe.2020.00126

INTRODUCTION

Heart failure (HF) is a leading, growing public health problem, affecting millions of people worldwide (Laflamme and Murry, 2011). Most cases of HF are the result of a myocardial infarction (MI), defined as massive cardiac muscle death due to ischemia as a consequence of temporary or permanent blockage of blood supply to the myocardium, generally originated by thrombosis (Laflamme and Murry, 2005; Gaziano et al., 2010; Eng et al., 2014; Saleh and Ambrose, 2018). The cardiac cell death and blood vessel damage lead to extensive inflammatory responses followed by wound healing.

The human heart has only a modest capability to replace the damaged tissue and restore functionality after MI. Conversely, in the case of lower vertebrates, including some fish and amphibian species, regenerative capacity is retained throughout adult life without evidence of scarring (Matz et al., 1998; Poss et al., 2002; Cano-Martínez et al., 2010; Jopling et al., 2010). It was

also shown that neonatal mammalian hearts, including mice (Porrello et al., 2011, 2013), rats, and even humans (Haubner et al., 2016), can exhibit the ability to regenerate and functionally recover in several injury models, in a limited time window immediately after birth. Genetic fate mapping in zebrafish and neonatal mice revealed that endogenous heart repair was achieved by the proliferation of pre-existing cardiomyocytes (CMs), not by the mobilization of undifferentiated precursors (Jopling et al., 2010; Kikuchi et al., 2010). However, the human adult heart consists mostly of terminally differentiated CM, excluding a small subpopulation of cardiac stem cells involved in maintaining cellular homeostasis (Torella et al., 2006). In light of these differences, following injury the damaged portions are vastly replaced by a rigid, collagenous fibrotic scar to avoid cardiac rupture (Mercola et al., 2011; Ong et al., 2018). The outcome of the wound healing process is a mechanically inferior cardiac muscle, unable to function sufficiently and mostly followed by sequential HF. Other pathologies may also impair the heart's ability to function sufficiently and lead to HF, including valvular disease, hypertension, genetic cardiomyopathies, or aging, which cause slow functional cell loss over time.

Currently, the most common clinical intervention after MI resulting from blood vessel occlusion includes rapid re-perfusion to minimize CM death (Gerczuk and Kloner, 2012). Primary percutaneous coronary intervention (PCI) is the preferred procedure to treat narrowing or blockage of coronary arteries (stenosis). Nonetheless, a quick diagnosis (<90 min from first medical contact) of acute MI symptoms is required in order to make this strategy effective (Liem et al., 1998; Cannon et al., 2000). In the case of end-stage heart conditions, whole heart transplantation remains the only option for heart function regeneration. However, the insufficient number of donors (approximately 4000 patients on a waiting list in the US as of April 2018) and abundant post-transplantation complications limit the implementation of this strategy (Benjamin et al., 2019).

In this review, the intrinsic restraints behind endogenous cardiac regeneration following cardiac injury will be presented, defining five main target processes for therapeutic interventions. Next, cardiac regeneration strategies and limitations, namely cell-based therapies and exogenous administration of bioactive molecules will be discussed. Finally, the biomaterial-based tissue engineering approach will be introduced, focusing on current therapeutic applications of endogenous cardiac regeneration, remaining challenges and future perspectives.

Endogenous Cardiac Regeneration Limitations

The main obstacle on the way to recovery from myocardial injury is the poor endogenous regenerative capacity of the adult mammalian heart. Cardiac regeneration is limited mainly since the majority of adult CMs do not proliferate. Shortly after birth, the cardiac tissue mechanism of growth shifts from hyperplasia to hypertrophy, meaning cell enlargement (Foglia and Poss, 2016). A major aspect of this transition is that most CMs in the mammalian myocardium withdraw from the cell cycle and grow 30–40 times in mass (Li et al., 1996). Proliferating cell populations were found to present negligible turnover rates (<1% per year and decreasing with age) (Bergmann et al., 2015). Even though there are evidences for cardiac progenitor cells (CPCs) or stem cells (CSC) residing in the adult myocardium, these subpopulations are considered minuscule (approximately 1 cell per 13,000 myocytes) (Torella et al., 2006). Even though these cell populations were observed to increase dramatically in number after MI, almost 50% exhibited a senescent phenotype, incapable of cycling and differentiating (Urbanek et al., 2005). In addition, recruitment and activation of these cells is inadequate to lead to cardiac repair due to physical barriers and lack of appropriate signaling (Ruvinov et al., 2012). Overall, these attributes result in insufficient intrinsic regenerative potential, unable to compensate for the extensive loss of heart muscle cells.

Consequently, the adult myocardium responds to MI by two main mechanisms: (a) The formation of a fibrotic scar through a wound healing process and (b) hypertrophic remodeling of the surviving myocardium (Sutton and Sharpe, 2000; Eng et al., 2014). These structural changes markedly increase the mechanical stress on the ventricular wall and promote progressive contractile dysfunction, eventually leading to HF (Ruvinov et al., 2012).

Major Target Processes to Promote Cardiac Regeneration

Considering the poor intrinsic capability of the adult heart to properly regenerate, key hallmarks of adult heart post-MI must be overcome. Achieving effective cardiac regeneration should include tissue recovery following injury (meaning cell survival), overturn or attenuation of tissue remodeling and fibrosis, and myocardium renewal via formation of new myocardium and blood vessels. Therefore, the therapeutic strategy could target each or all the following five major processes associated with MI:

(a) Cardioprotection – prevention of resident CMs massive death (up to 1 billion cells) post-MI, by inhibition of apoptotic signaling pathways and/or induction of pro-survival signals (Garg et al., 2005; Abbate et al., 2006).
(b) Inflammation – in response to ischemia, necrotic CM signaling initiates a pro-inflammatory response, in order to remove remaining cell debris. The second phase includes an anti-inflammatory response, the purpose of which is to allow wound healing and scar formation. The shift between each of these responses is tightly regulated by multiple interactions between cellular myocardium components and the immune system. Manipulation of the time frames of the pro-/anti-inflammatory response after MI by changing the chemokine/cytokine profile or cellular responses may allow proper tissue repair to occur rather than the undesired results of an excessive inflammation, including cell death and scarring (Frangogiannis et al., 2002; Ong et al., 2018).
(c) Extracellular matrix (ECM) remodeling and cardiac fibrosis – attenuation of the fibrotic response, meaning ECM composition changes and scar formation, by altering pro-fibrotic signaling pathways. This includes inhibition of matrix metalloproteinases (MMPs) or changes in balance between MMPs and tissue residing inhibitors, in order to

slow down scarring in favor of desired tissue healing (Leask, 2007; Francis Stuart et al., 2016).

(d) Angiogenesis and vascularization – formation of new blood vessels to allow appropriate nutrient supply to the ischemic regions. This could be achieved by induction of pro-angiogenesis signals, including proteins, endothelial cell (EC) recruitment, and altering inflammation and scarring (Renault and Losordo, 2007).

(e) Cardiomyogenesis – To fully restore cardiac function, it is essential that the infarct zone will be replaced by regenerated myocardium, which could involve proliferation of CPCs/CSCs, proliferation of adult CMs via induction of cell-cycle re-entry, and/or exogenous transplantation of CMs/CPCs (Mohamed et al., 2018).

CARDIAC REGENERATION STRATEGIES AND CHALLENGES

Cell-Based Therapies

Several approaches to repair or replace injured cardiac tissue were suggested over the last two decades. One of them is the cell-based therapy, namely injection of a cell suspension. The concept is to use an engraftment of cardiac cells to reconstruct the lost muscle tissue. Injection of these suspended cells directly into the myocardium could attenuate myocardial deterioration and dysfunction.

This application requires the use of cell sources capable of yielding mature and functional CMs. Furthermore, the transplanted cells should be of autologous origin or immunotolerated by the host. Several cell sources were suggested for this purpose. CPCs/CSCs, assumed to naturally occupy the adult myocardium, are one subpopulation capable of self-renewal and differentiation. Yet, harvesting these cells requires their isolation from a myocardial biopsy, followed by cell expansion, thus limiting their availability for transplantation when treating acute MI (Torella et al., 2006).

In the last decade, human embryonic stem cells (hESCs) and induced pluripotent stem cells (iPSCs) have been considered the most attractive stem cell types as a source for *de novo*, mature CM production. Both cell types can be differentiated into CMs *in vitro* (Passier et al., 2005; Lian et al., 2013), while also having limitless cell division capability. Yet, both hESCs and iPSCs present some limitations. For instance, the origin of hESCs from blastocyst inner cell mass raises some ethical issues, along with a risk of eliciting an immune response due to their allogeneic nature (Barad et al., 2014). iPSCs are considered less immunogenic since these cells are derived from somatic cells, which potentially could be autologous to the patient. Another concern regarding the use of both types of these cells for transplantation is their pluripotency. Incomplete differentiation or ineffective isolation of the desired cell population could eventually lead to the formation of teratomas after transplantation (Nussbaum et al., 2007).

Nonetheless, this strategy alone presents very limited clinical impact due to low cell survival and retention rates inside the injected heart, resulting in only up to 10% of the delivered cells surviving 24 h after transplantation. Hence, to become clinically relevant, this kind of strategy demands the injection of an enormous number of cells (Menasché et al., 2014; Guo et al., 2017; Yanamandala et al., 2017). Besides cellular retention, cells injected within a suspension are lacking an optimal microenvironment, provided naturally by surrounding ECM. In order to reconstruct tissue organization and functionality, it is essential to supply the cells with appropriate mechanical support, topographical guidance, and proper biochemical signaling to allow desired tissue organization, differentiation, and maturation *in situ* (Frantz et al., 2010; Hubmacher and Apte, 2013; Frangogiannis, 2017).

On another note, the exact role of the injected cells in inducing cardiac regeneration is still not fully understood – do these cells act as a substitute at the injured portions of the myocardium, or perhaps, as some researchers suggest, injected cells mainly act in a paracrine manner, introducing secreted ECM and signaling molecules to surrounding host myocardium, a theory also known as "the paracrine hypothesis" (Menasché, 2008). Mesenchymal stem cell (MSC) therapy is a predominant example for this mechanism of action (Gnecchi et al., 2006; Wehman et al., 2016). MSCs, which present only limited ability to *trans*-differentiate into CMs *in vivo* (Silva et al., 2005), were shown to secret signaling molecules improving cell survival, modulating immune response, and even inducing angiogenesis (Pittenger and Martin, 2004; Thakker and Yang, 2014; Wehman et al., 2016). Although this approach was already examined in several clinical trials, evaluating different aspects of MSC delivery and their origin, it still presents major concerns limiting its efficacy. From the technical point of view, use of autologous MSCs requires their isolation and further expansion in order to be transplanted, which limits their applicability in an acute setting (Singh et al., 2016). Some clinical trials, but not all, have also highlighted safety issues, including the possibility of malignant tumor formation (Jeong et al., 2011) and paracrine proarrhythmic effects (Askar et al., 2013) post transplantation.

Recently, it was demonstrated in an ischemia mice model that the marginally improved heart function after stem cell therapy is mostly attributed to the induction of acute immune response rather than proliferation of transplanted or endogenous CMs. Vagnozzi et al. (2019) showed that the functional benefit underlying this strategy is inflammatory-based wound healing and attenuation of fibrosis, suggesting that the moderate improvement in cardiac function observed in the past corresponds better with the paracrine hypothesis.

Bioactive Molecules

Assuming the "paracrine effect" is the engine behind cardiac regeneration, an opposing strategy to cell injection is based on the administration of bioactive signaling molecules. Three main classes of secretory factors were identified to induce cardiac regeneration, covering most of the targets specified above: growth factors (GFs) (i.e. cytokines/chemokines), non-coding RNA (i.e. microRNAs (miRNAs) and small interference RNA), and extracellular vesicles (EVs) (i.e. microvesicles and exosomes).

Growth Factors

Growth factors are signaling molecules, mostly proteins, which were identified to participate in various cellular processes. For example, insulin-like GF 1 (IGF-1) was previously shown to delay cellular aging and promote cell survival, while also benefit angiogenesis (Torella et al., 2004). Vascular endothelial GF (VEGF) is another cardiac-regenerating inducer; it was demonstrated to improve viability of cardiac tissue and reduce infarct size post-MI in multiple animal models through pro-angiogenic and cardiomyogenic effects (Ferrarini et al., 2006; Janavel et al., 2006). Activation of the ERBB2/ERBB4 signaling pathway by neuregulin 1 (NRG1) administration has also shown regenerative potential, driven by induction of CM proliferation (Bersell et al., 2009; D'Uva et al., 2015).

Nevertheless, the effect of systemic/local administration of GFs was inconsistent in clinical trials, showing no beneficial effects (Simons et al., 2002; Abdel-Latif et al., 2008). This could be explained by an insufficient amount of the therapeutic molecules at the target site, obligating usage of higher dosage of GFs or, alternatively, the use of a proper delivery vehicle to overcome issues of fast elimination, low protein stability, and unspecific delivery (Ruvinov et al., 2011a). Another concern is the pleiotropic functions that most cytokines have, which further encourage the use of a delivery system for their local and scheduled administration.

MicroRNAs

MicroRNAs are short (∼22 nucleotides long), non-coding, single stranded RNAs. Most commonly, these RNA molecules are inhibitors of protein expression, by interacting with specific mRNA in the cytoplasm, subsequently leading to mRNA cleavage or repression of translation (Lai, 2002). Numerous studies have connected miRNAs and various cardiovascular diseases, showing that miRNA expression levels were altered in MI, cardiac hypertrophy, and HF. Therefore, over the last decade miRNAs have become a therapeutic target for treatment of cardiovascular diseases (Barwari et al., 2016). For instance, Eulalio et al. (2012) performed a functional screening study to identify which human miRNAs can promote CM proliferation at neonatal stages. Two of these miRNAs, miR-199a-3p and miR-590-3p, were further demonstrated to induce cardiac regeneration in an adult mouse MI model.

Besides CM proliferation, miRNAs were shown to affect other target processes associated with MI, including miR-21, which could modulate inflammation processes and reduce CM apoptosis (Dong et al., 2009; Essandoh et al., 2016). Inhibition of miRNAs is also a possibility as demonstrated by Montgomery et al. (2011). By subcutaneous delivery of an antisense oligonucleotide they were able to inhibit miR-208a in the heart, improving cardiac function. In a preclinical trial, a catheter-based administration of a miR-92a inhibitor significantly reduced infarct size, while also excreting cardioprotective, proangiogenic, and anti-inflammatory effects (Rabea et al., 2013).

Even though miRNAs are normally detected outside the cell in body fluids, circulating miRNAs are at risk to be cleaved by RNases in these biofluids. Moreover, the strong negative charge of soluble nucleic acids results in inadequate cellular uptake (Remaut et al., 2007). Hence, it is essential to use proper vehicles to deliver miRNA, keeping it stable and protected from degradation in the extracellular environment (Chistiakov et al., 2012). Safety issues are also a concern when applying constitutive expression of miRNAs, as in the case of adeno-associated virus (AAV) delivery. Such a delivery strategy presents the risk of unwanted pathologies, such as uncontrolled heart growth (Gabisonia et al., 2019) or undesired, off-target transfection (e.g. in the liver) (Lovric et al., 2012). Therefore, it is required for miRNA delivery to be time-limited and controlled.

Extracellular Vesicles

Extracellular vesicles are emerging, natural carriers that could potentially deliver miRNA. These are small, membrane-enclosed vesicles that are generated and secreted by living cells. One class of EVs are exosomes, classified as double-membraned vesicles that range between 30 and 150 nm in diameter (Das and Halushka, 2015). Exosome content usually includes proteins, mRNA and miRNA.

It has been well documented that exosomes are used for communication between cells (Simons and Raposo, 2009); prominent examples can be found in cancer cells (Webber et al., 2010; Costa-Silva et al., 2015) and in the cardiovascular system (Emanueli et al., 2015). More recently, exosomes secreted by different sources of stem cells were compared to assess their potential for inducing cardiac repair in a MI model. Analysis of miRNA repertoire in exosomes secreted by iPS-derived CMs and hESCs-CMs revealed that miRNA content included some miRNAs that are known to be cardioprotective (Lee et al., 2017).

Exosomes from other cell types originating from the cardiovascular system were also shown to have potential to improve cardiac repair. For instance, monocyte-derived exosomes were shown to affect migration of ECs via exosomal transfer of miR-150, promoting angiogenesis (Zhang et al., 2010), while CPCs were demonstrated to stimulate regeneration and improve cardiac function via secretion of exosomes (Ibrahim et al., 2014; El Harane et al., 2018). The MSCs secretome was also widely investigated for its therapeutic potential, as the experience with clinical trials demonstrated only limited effects of MSC transplantation. Administration of MSC-derived exosomes contributed to cell survival, reduced inflammation, and decreased oxidative stress *in vitro* and *in vivo* (Arslan et al., 2013; Ferguson et al., 2018). Another possibility is loading exosomes with specific cargo (Luan et al., 2017), enriching them with either drugs (Sun et al., 2010), proteins (Jung et al., 2018), or miRNAs (Zhang et al., 2016). This approach could be used to manipulate exosome cargo and turn them into therapeutic agents, to be internalized by target cells and deliver desired molecules for treating different pathologies in these cells.

Even though exosome-based delivery eases the uptake by target recipient cells and is not considered toxic, it is still lacking the ability of having a long-lasting effect. Much like cytokines, exosomes have a short half-life, due to a rapid cellular internalization rate, therefore narrowing their effect to a limited time window (Kishore and Khan, 2016).

BIOMATERIAL-BASED TISSUE ENGINEERING APPROACH

The challenges presented by both cell-based therapies and cardiac regenerating agent delivery have set the stage for the emergence of cardiac tissue engineering (CTE). In general, TE strategies suggest using biomaterials, mostly in combination with bioactive molecules and/or a cell source for regeneration (Lanza et al., 2014). The rich repertoire of natural and synthetic polymers TE application could utilize for cardiac TE and the relevant criteria for such application were already reviewed in details elsewhere (Griffith, 2002; Christman and Lee, 2006; Chen et al., 2008; Nelson et al., 2011; Reis et al., 2016), therefore will not be addressed in the current review. Nevertheless, in the context of CTE, biomaterials can give solutions for both cell-based therapies and applications involving bioactive molecules (**Figure 1**).

The traditional applications of TE destinate biomaterials the role of a three-dimensional scaffold for cell retention (Langer and Vacanti, 1993). Biomaterial-based scaffolds provide the cells with needed mechanical, topographical, and biochemical stimuli, acting as ECM replacement (Yang et al., 2001). On that basis, biomaterial scaffolds were investigated in a plethora of studies for *ex vivo* cell cultivation, reviewed in Freed et al. (1994) and Shachar and Cohen (2003). These ECM properties, mimicked by biomaterials, are also of great significance when applying cell-based therapies (Leor et al., 2000).

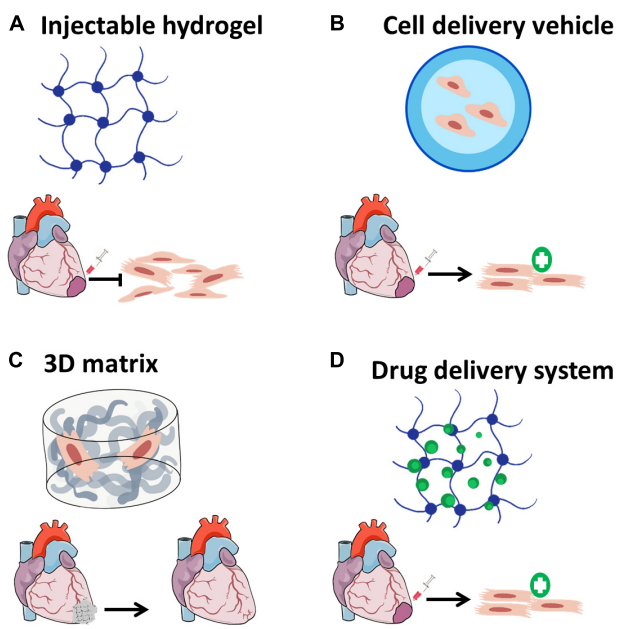

FIGURE 1 | Biomaterial-based applications for cardiac tissue engineering. **(A)** Biomaterials can be injected alone into the infarcted regions in order to attenuate scar formation, **(B)** cell-delivery using injectable hydrogels can improve cell retention and survival after transplantation; **(C)** three-dimensional matrices can be fabricated with or without cells, then implanted as cardiac patches to improve cardiac function; and **(D)** biomaterials designed to release drugs and bioactive molecules may induce cardiac regeneration in a sustained effective manner.

Biomaterials, in the form of injectable hydrogel scaffolds, can be used as a vehicle to deliver cells to the target infarct zone (Yost et al., 2004; Wei et al., 2008; Ruvinov and Cohen, 2016). In parallel, the hydrogel provides the cells with the missing anchoring positions and biophysical cues, this until the cells produce their own ECM, reconstruct their microenvironments and guide their reorganization into a 3D tissue *in situ* (Dvir et al., 2005; Hubmacher and Apte, 2013).

Moreover, hydrogels embody an additional, important benefit for CTE strategies, as their injection alone into the infarct zone also reduces wall stress (Laplace law) by thickening the scar (Dai et al., 2005; Landa et al., 2008; Tsur-Gang et al., 2009). Mechanically weak, natural biomaterials are the most investigated hydrogels for this application, including collagen (McLaughlin et al., 2019), alginate (Landa et al., 2008; Sabbah et al., 2013), hyaluronic acid (HA) (Rodell et al., 2016), and decellularized myocardial matrix (Seif-Naraghi et al., 2013). In the case of the latter, it was postulated that myocardial hydrogels also have effect at the transcription level, inducing regenerative processes following their injection (Wassenaar et al., 2016). The application of mechanically strong, fully synthetic biomaterials was also beneficial (Dobner et al., 2009; Matsumura et al., 2019). Several studies, including those conducted in large animal models of MI, have shown that injection of hydrogel was effective at preventing negative tissue remodeling and improving left ventricular function post-MI, as evident by reduction in the degree of interstitial fibrosis and thickening of infarcted wall (Dobner et al., 2009; Leor et al., 2009; Rodell et al., 2016).

Biomaterials are also commonly used for the purpose of drug delivery vehicles (Koseva et al., 2015; Roy and Sahoo, 2015; Ho et al., 2016). Various polymeric materials could be used to encapsulate or entrap bioactive molecules, forming small dimension-particles (microns to sub-nano scale). Such particles enable the delivery of soluble and insoluble bioactive molecules to their target site, increasing stability, elongating drug shelf life, improving drug safety, and specificity (Roy and Sahoo, 2015).

Drug delivery platforms could also be fabricated from biomaterials, as a standalone application or incorporated with delivery vehicles. Biomaterial mechanical properties could be designed and tailored using different fabrication methods and by chemical formulation and modifications (Tibbitt and Langer, 2017; Zadpoor and Malda, 2017). Therefore, such matrices could release drugs through various mechanisms, depending on their degradation/erosion rate, exogenous triggers, or environment conditioning (Wong and Choi, 2015). This idea is an expansion of the microenvironment mimicry concept. Neighboring cells in the natural microenvironment communicate with each other by paracrine pathways, mediated by secreted proteins, small RNA species, and EVs. The ECM also acts as a reservoir system of signaling molecules (Hynes, 2009; Hinz, 2015). Incorporation of proteins and protein-binding features into biomaterials could resemble another ECM function and elicit desired cellular responses, such as cell proliferation, migration, and differentiation. Therefore, biomaterials originated (Shapira et al., 2016) or inspired (Freeman et al., 2008) by ECM components and biomechanical properties are potential candidates to perform as sophisticated drug delivery systems for spatial–temporal

presentation and release of therapeutic agents, essential for endogenous tissue regeneration.

All these advantages are already implemented in biomaterial-based strategies meant to improve cardiac regeneration and restore functionality post cardiac injuries. In the following section, four main classes of biomaterial-based approaches will be reviewed: (a) bioactive nano-carriers; (b) hydrogel-assisted cell delivery, (c) cardiac patches, and (d) drug delivery platforms (**Figure 2** and **Table 1**).

THERAPEUTIC APPLICATIONS OF BIOMATERIALS IN CARDIAC REGENERATION

Nano-Carriers of Bioactive Molecules

Many efforts were invested to improve the delivery of regeneration inducing agents, mainly in the means of treatment safety, efficacy, and specificity. Nano-carriers can be generally divided into two classes: nanoparticles (NPs) and natural or bio-inspired biomolecule carriers.

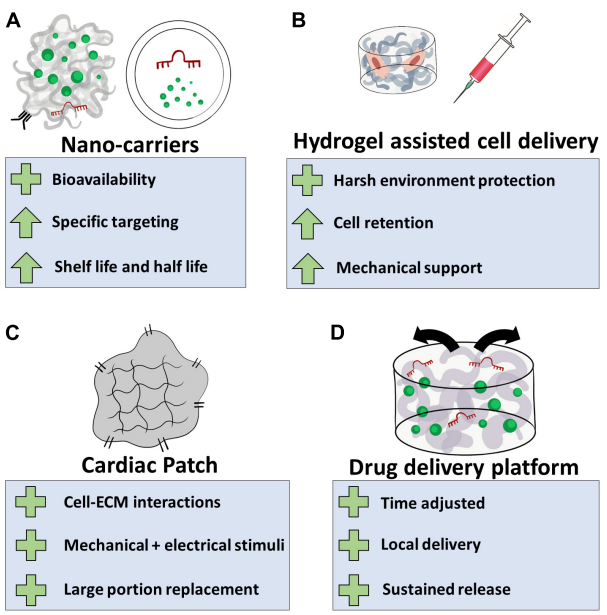

FIGURE 2 | Biomaterial-based applications for cardiac regeneration. **(A)** Natural or synthetic polymers can be used as nano-carriers for the delivery of cardiac inducing agents. This will assist their bioavailability, allow specific targeting to the infarcted region or destination cell population, and increase their half-life in the tissue, eventually improving treatment efficacy; **(B)** hydrogel systems can be utilized to protect transplanted cells from the hostile post-MI microenvironment. This strategy can improve cell retention and provide the transplanted cells and the infarcted tissue the mechanical support lost as a result of massive loss of muscle tissue; **(C)** biomaterials can be used to fabricate cellular or acellular cardiac patches, providing cell with ECM interactions, mechanical and electrical stimuli. Depending on their size and mechanical properties, cardiac patches can perform as temporary or permanent replacements for damaged tissue; **(D)** regeneration-inducing agents can be encapsulated or bound to biomaterial-based delivery platforms, allowing effective release of these agents in a spatial–temporal manner. Plus sign indicates benefits of the application, arrow indicates an attribute that improves.

Nanoparticles

Polymer-based NPs could come in many forms, including polymeric chains enveloping therapeutic drugs, polymer–macromolecule conjugates or drugs encapsulated in polymeric micelles (Duncan, 2003). These macromolecular structures are of great pharmaceutical importance when the delivered agent has a very short half-life in circulation, or its systemic delivery is accompanied with some cytotoxicity or undesired side effects (Roy and Sahoo, 2015). The advantages of such nano-carriers were demonstrated in the case of the antioxidant drug Puerarin (PUE), an FDA approved drug for various cardiovascular diseases, including MI (Liu et al., 2016). Dong et al. (2017) developed a micelle-forming polymeric vehicle, administered intravenously and modified with Arg–Gly–Asp (RGD) peptide to increase specificity to the ischemic region. The fabricated NPs were shown to improve PUE pharmaceutical properties, including a threefold increase in half life and drug absorbance, assessed by area under the curve (AUC). Moreover, this formulation was successful at reducing infarct size in a rat MI model, presenting an enhanced effect when RGD modification was added to its surface (Dong et al., 2017).

Nanoparticles were also shown to improve protein bioavailability and decrease their toxicity due to supraphysiological dosage (Vaishya et al., 2015). For example, affinity-binding alginate can form nano-scale polymer–protein complexes (Ruvinov et al., 2016). Sulfated alginate (AlgS) was previously demonstrated to interact with heparin-binding proteins with similar affinity to heparin (Freeman et al., 2008). Ruvinov et al. (2010) showed that AlgS can co-assemble with heparin-binding proteins to form injectable NPs that protect the proteins from degradation.

Nucleic acids delivered systemically (e.g. small RNA species, mRNA, and plasmid DNA) are subjected to fast elimination and/or degradation, while also facing difficulties to enter their target cells (Remaut et al., 2007; Jones et al., 2013). Even though viral vectors are effective for delivering these agents, their application also carries significant safety issues. Thus, non-viral vehicles have emerged as a promising alternative. One of the suggested strategies is using complexes of small RNA (i.e. small interference RNA and miRNA) and plasmid DNA with calcium ions, based on electrostatic interaction between them, resulting in the formation of mildly anionic NPs (Ruvinov et al., 2015; Goldshtein et al., 2019). When these components were mixed with alginate or hyaluronan sulfate, they also spontaneously assembled into NPs mediated by ion bridges (Korin et al., 2017). The incorporation of a polymeric material to the complex enabled the addition of surface features to the resulting NPs using chemical modifications, important for targeting. These NPs were tested in order to attenuate inflammatory response and promote cardiac regeneration in a small animal MI model. In this study, miR-21 mimic was delivered in these NPs, aiming to switch macrophage phenotype to a reparative one during the innate immune system response to MI (Bejerano et al., 2018). Following intravenous administration of the NPs delivering the

TABLE 1 | Summary of biomaterials-based applications, advantages, and limitations (selected studies).

Application	Biomaterial (formulation)	Delivered component	Animal model	Advantages	Limitations	Study
Hydrogel-assisted cell delivery	Alginate, chitosan/β-glycerophosphate (Hydrogel)	MSCs	Rat	• Cell retention↑ • Protection from harsh microenvironment • Mechanical support↑ • Tissue integration↑	• Requires large cell quantities • Limited nutrient supply • Electrical coupling with the host	Roche et al., 2014
	Chitosan (Hydrogel)	MSCs	Rat			Liu et al., 2012
	Fibrin (Hydrogel)	Skeletal myoblasts	Rat			Christman et al., 2004
	Gelatin (Hydrogel)	MSCs	Mouse			Gottipati et al., 2019
	RGD modified, self-assembling peptide (Hydrogel)	hESCs-CMs	Mouse			Ban et al., 2014
Bioactive nano-carriers	Alginate/hyaluronan sulfate (NPs)	HGF, IGF-1	Rat	• Half-life↑ • Drug absorbance↑ • Protection from degradation • Specificity and targeting↑ • Persistence and effect↑ • Invasiveness↓	• Requires high dosages • Cytotoxicity and immunogenic response • Undesired accumulation	Ruvinov et al., 2011b
	Alginate sulfate (NPs)	miR-21	Mouse			Bejerano et al., 2018
	Peptide modified, CSC-exosomes	miRNAs, proteins	Rat			Vandergriff et al., 2018
	mESC-exosomes	miRNAs, proteins	Mouse			Khan et al., 2015a
	Liposomes	miR-199a-3p, miR-590-3p	Adult mouse			Pierluigi et al., 2017
	RGD modified, PEGylated lipid (NPs)	Puerarin	Rat			Dong et al., 2017
	Peptide modified, PEGylated liposomes	–	Mouse			Dvir et al., 2011
	MMP-specific peptide – polynorbornene amphiphiles (NPs)	–	Rat			Nguyen et al., 2015
Cardiac patches	Alginate (Scaffold)	Fetal cardiac cells	Rat	• Cell retention↑ • Protection from harsh microenvironment • Mechanical support↑ • Provides complex 3D architecture • Cell fate guidance • Replacing large tissue portions	• Requires surgery • Immunogenic response • Limited nutrient supply • Electrical coupling through large areas	Leor et al., 2000
	RGD-/HBP-modified alginate (Scaffold)	hESCs-CMs	–			Sapir et al., 2011
	Decellularized cardiac ECM–gelatin composite (Scaffold)	CPCs	Rat			Bejleri et al., 2018
	Fibrin (Scaffold)	hESCs-cardiac progenitors	Human			Menasché et al., 2018
	Fibrinogen (Scaffold)	hiPSCs-CMs	Swine			Ling et al., 2018
	Chitosan–polyaniline composite (scaffold)	–	Rat			Kapnisi et al., 2018
	Polyurethane–ECM composite (Scaffold)	–	Rat			D'Amore et al., 2016

(Continued)

TABLE 1 | Continued

Application	Biomaterial (formulation)	Delivered component	Animal model	Advantages	Limitations	Study
	Fibrinogen (Scaffold)	hiPSCs-CMs	Swine			Ling et al., 2018
	Chitosan–polyaniline composite (scaffold)	–	Rat			Kapnisi et al., 2018
	Polyurethane–ECM composite (Scaffold)	–	Rat			D'Amore et al., 2016
	Porcine small intestine submucosa ECM (Scaffold)	–	Pig, ovine			Mewhort et al., 2016; Baker et al., 2019
Drug delivery platforms	Alginate-alginate sulfate (Hydrogel)	Cytokines	Rat	• Sustained drug release • Persistence and effect† • Protection from degradation • Local delivery • No cellular component required	• Biomaterial clearance • Immunogenic response • Inapplicable for chronic conditions	Ruvinov et al., 2011b
	Collagen (Hydrogel)	iPSC-CM-derived EVs	Rat			Liu et al., 2018
	Hyaluronic acid (Hydrogel)	miR-302/367 cluster	Rat			Wang et al., 2017
	PEG (Hydrogel)	Erythropoietin, iPSC-CMs	Rat			Chow et al., 2017

CMs, cardiomyocytes; MSCs, mesenchymal stem cells; ESCs, embryonic stem cells; iPSCs, induced pluripotent stem cells; EVs, extracellular vesicles; NPs, nanoparticles; ECM, extracellular matrix; HGF, hepatocyte growth factor; IGF-1, insulin-like growth factor.

miR-21 mimic, the particles were shown to target macrophages in the infarcted zone and change their phenotype, resulting in reduced cell apoptosis, fibrosis, and hypertrophy.

Bio-Inspired Carriers

The second class of nano-carriers utilizes natural existing delivery vehicles. One example for such carriers are liposomes, closed bilayer phospholipid systems, inspired by the cellular membrane. Liposomes have been investigated for over half a century, and have been applied in very sophisticated drug delivery systems for proteins and nucleic acids, reviewed in details by Allen and Cullis (2013). In a study looking for alternatives for the use of viral vectors for miRNA mimics delivery, Pierluigi et al. (2017) assessed the efficacy of different liposomes at inducing cardiac regeneration through CM proliferation mechanism. Since liposomes lack the intrinsic ability to specifically target the heart, they used a local, intracardiac injection to deliver the liposomes straight to the infarcted area, resulting in almost 40% reduction in infarct size.

Liposomes can be targeted to the infarcted region by conjugation of specific ligands overexpressed in infarcted hearts. Such strategy was demonstrated by Dvir et al. (2011), exploiting the change in angiotensin II type 1 (AT1) receptor expression levels after hypoxia to specifically target the MI zone. They modified PEGylated liposomes' surface by addition of a short peptide, similar on one end to angiotensin II (a ligand of AT1 receptor). Then, they showed that the NPs specifically accumulated in the left ventricular wall 7 days post-MI, but not in healthy hearts. These findings were of great significance, since they indicated not only successful targeting that increases treatment efficacy, but also passively target the heart in case of future HF (Dvir et al., 2011).

Hydrogel-Assisted Cell Delivery

Improvement of cell retention is one of the key requirements in cell-based therapies (Menasché, 2018). Biomaterials support the transplanted cells, protecting them from the harsh environment of the infarcted region. We were among the first groups to report on a successful implantation of cardiac cell-seeded porous alginate scaffolds into infarcted rat hearts. We found that the seeded fetal rat cardiac cells retained viability within the scaffolds and within 24 h formed multicellular beating cell clusters. Following implantation of the cellular constructs into the infarcted myocardium, some of the cells appeared to differentiate into mature myocardial fibers. The graft and surrounding area were populated with a large number of newly formed blood vessels, consequently leading to attenuation in LV dilatation and improved heart function (Leor et al., 2000). An additional group demonstrated this concept using an injectable fibrin scaffold for myoblast delivery into infarcted hearts. An examination of cell location 5 weeks post injection indicated that cells injected in hydrogel were still present in the infarcted region, compared to cells suspended in BSA, which were located solely at the border zone (Christman et al., 2004). Another study demonstrated that cell viability was improved following cell administration using alginate and chitosan/β-glycerophosphate hydrogels compared to saline, showing a superior 50–60% cell retention, 24 h post

transplantation (Roche et al., 2014). Since then, a variety of biomaterials and cell types were tested for cell delivery, reviewed elsewhere (O'Neill et al., 2016).

Hydrogel design criteria for cardiac cell delivery should include three key parameters: (a) mechanical stiffness of injected hydrogel; (b) physical and biochemical microenvironment suitable for encapsulated cells; and (c) duration of cell retention post transplantation. For hydrogels to withstand the mechanical demands required for myocardial applications, their stiffness modulus should be between 20 and 0.1 kPa (Reis et al., 2016). On the other hand, biomaterial elasticity could also have a role in stem cell fate determination, including differentiation (Engler et al., 2006). In case stem cells are delivered, it is mandatory to consider the use of a hydrogel system with mechanical properties resembling the myocardium in order to avoid differentiation into the wrong lineage.

Nevertheless, the microenvironment provided by the encapsulating matrix is also important in directing cell fate. Biochemical cues, including matrix-anchoring features, have a beneficial effect on cell survival and maturation. In a study aimed at enhancing engraftment of hESC-derived CMs, researchers developed a hydrogel system composed of self-assembling peptides, incorporated with RGD residue. This hydrogel not only increased cell retention in the infarcted heart, it also induced transplanted cells' maturation and integration with the host, evident by expression of mature phenotype and formation of gap junctions with host CMs (Ban et al., 2014).

The duration of cell survival post transplantation depends on the mechanism by which the delivered cells promote regeneration. If cell transplantation aims to replace damaged tissue (e.g. CPCs, ESCs/iPSCs derived CMs), the degradation profile should allow cell integration into host myocardium (>10 days). However, if transplanted cells act by a paracrine effect (e.g. stem cells), the biomaterial should support cell survival for enough time to be effective (Levit et al., 2013). For example, the efficacy of MSC-based therapy is dependent on the number of cells surviving after transplantation (Afzal et al., 2015). Therefore, efforts have been made in order to protect cells upon delivery, using hydrogels to encapsulate MSCs, protecting them for a prolonged time from the hostile microenvironment of the ischemic region, including reactive oxygen species (Liu et al., 2012), phagocytosis, and inflammation (Gottipati et al., 2019).

Cardiac Patches

Cellularized Patches

The holy grail of CTE is the fabrication of a fully developed, three-dimensional (3D) functioning heart tissue, developed *ex vivo* and ready for transplant. In the context of cardiac malfunction, such patches could be used to replace large portions of the injured heart (**Figure 3**; Liau et al., 2011; Zhang et al., 2013, Zhang J. et al., 2018). Many cardiac patch designs place emphasis on providing engrafted cells with the proper microenvironment for tissue development and maturation. Besides the 3D architecture biomaterial-based matrices provided to the cells, it is essential to provide the cells with necessary ECM–cell interactions. For instance, one group suggested to use decellularized ECM of porcine origin for the fabrication of injectable hydrogels and cardiac patches, successfully demonstrating encapsulation and culture of cardiac cells (Shevach et al., 2015). Others suggested a composite of ECM components with synthetic, fibrillary, and elastic polymers, beneficial mostly at slowing the progression of scar formation and promoting angiogenesis (D'Amore et al., 2016). Similar ECM biochemical cues can be artificially added to semi-synthetic polymers. Sapir et al. (2011) suggested the covalent binding of RGD and HBP peptides to macroporous alginate scaffolds, promoting the striation and muscle fiber structure similar to that of a mature cardiac tissue. These scaffolds were further tested for their ability to promote cardiac regeneration from hESC-derived CMs, exhibiting improved functionality (Hayoun-Neeman et al., 2019).

Besides biochemical cues, anisotropic features were also shown to promote better tissue organization (Prabhakaran et al., 2011; Khan et al., 2015b; Margolis et al., 2018). Since both cardiac muscle and blood vessels are considered direction-oriented tissue constructs, different fabrication methods, including electrospinning of nanofiber structures, were investigated for influencing scaffold topography (Lutolf and Hubbell, 2005). For instance, polyurethane scaffolds were electrospun into aligned fibrous scaffolds, improving differentiation of murine ESC into CMs (Parrag et al., 2012). A more sophisticated design used a hybrid scaffold, consisted of a network of conductive nanofibers and gelatin-based hydrogel, promoting aligned and elongated CM maturation (Wu et al., 2017). Recently, our group described a method of creating a magnetically aligned, 3D tissue culture matrix for tissue engineering comprised of three distinct classes of structural anisotropy – anisotropic topographic features in the sub-micron scale, the directionality of the pore shape, and increased anisotropic stiffness in the direction of the magnetic alignment. Because magnetic forces govern the alignment phenomenon in the scaffold, all the anisotropic features shared a unidirectional structure that can synergistically benefit cultured cells (Margolis et al., 2018).

The advances in cardiac patch research are not limited to the microenvironment scale. Cardiac patch designs have demonstrated improved cellular delivery rates and feasibility to achieve a clinically relevant cardiac graft in means of size and function (Riegler et al., 2015; Shadrin et al., 2017; Ling et al., 2018). 3D bio-printing has also emerged as a strategy to assemble complex structures (Fleischer et al., 2017; Bejleri et al., 2018; Lee et al., 2019).

Other studies offer the use of exogenous stimuli to improve cardiac maturation and tissue organization *ex vivo*. After application of mechanical and electrical stimuli, iPSC-derived CMs were successfully forced to maturation and increased tissue contractility (Ruan et al., 2016). Another approach suggested to use a magnetically responsive scaffold to induce mechanical stimulation, promoting ECs organization into blood vessels (Sapir et al., 2012).

Acellular Patches

Even though the presence of cells contributes to cardiac recovery (either directly or in a paracrine manner), the benefits of a cardiac patch are not limited to cellular components. To date,

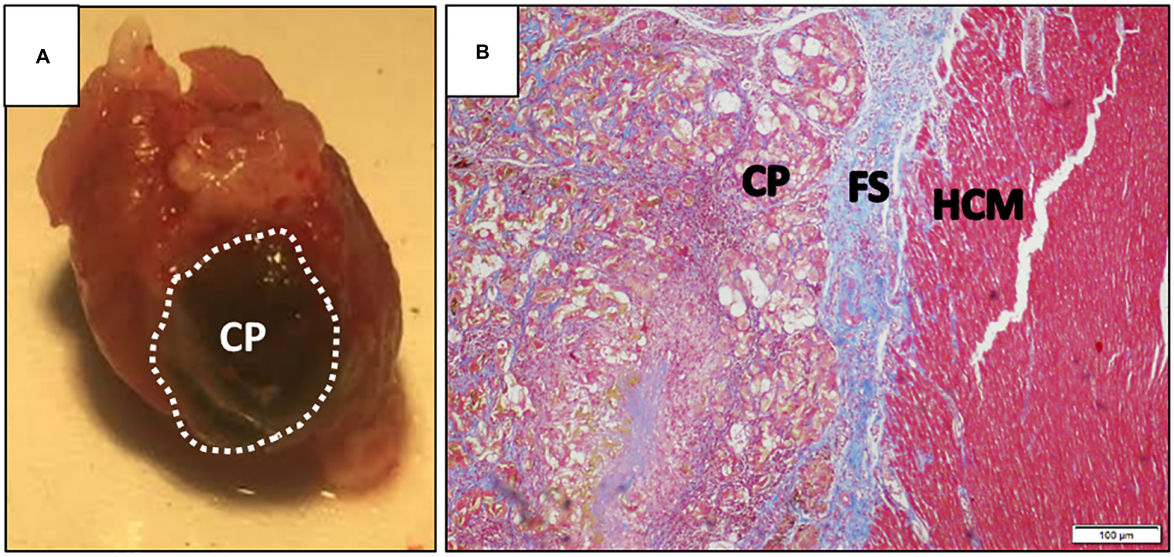

FIGURE 3 | Cardiac patch after explant. **(A)** Representative image of a dissected rat heart, 30 days post-implementation of an alginate cardiac patch. The cardiac patch consists of a macroporous alginate scaffold, incorporated with magnetic nanoparticles. The construct was seeded with human embryonic stem cell-derived cardiomyocytes, and cultivated for 24 h prior to implementation on top of an infarcted rat heart. Dashed line denotes cardiac patch borders; **(B)** photomicrograph of Masson's trichrome-stained section of the interface between implanted cardiac patch and host myocardium, 30 days post-transplantation. CP, cardiac patch; FS, fibrotic scar; HCM, host cardiac muscle. Scale bar is 100 μm. Images are courtesy of Mr. Edan Elovic.

the most investigated biomaterial used for acellular patches is decellularized ECM. Studies conducted in small (D'Amore et al., 2016) and large (Baker et al., 2019) animal models have revealed that ECM-based patches not only provide the infarcted tissue with mechanical support but also alter ventricular wall remodeling, demonstrated consistent conduction across the patch, and even promoted neovascularization. Decellularized ECM patches, originated from porcine small intestinal submucosa are already commercially available (CorMatrix®) (Mosala Nezhad et al., 2016). CorMatrix® patches remain flexible, exhibiting no calcification after 21 months post-implant; however, the formation of new CMs was not observed in these patches, suggesting this strategy mainly has a mechanical contribution (Nelson et al., 2016). Another kind of acellular patches is designated to withstand the mechanical demands of a contracting heart. To this end, a unique auxetic pattern design was applied, allowing the patch to be stretched in multiple directions simultaneously (Kapnisi et al., 2018). Using a chitosan–polyaniline composite to fabricate a conductive scaffold (Mawad et al., 2016), the auxetic patch remained intact and attached, while maintaining left ventricular mass, presumably as a result of reduced wall stress (Kapnisi et al., 2018). Further progress was recently achieved in applying acellular patches to restore cardiac function, as a first-in-man study was completed, demonstrating the feasibility of transendocardial injection of decellularized matrix (further discussed in the section "Clinical Trials of Biomaterial-Based Applications").

Challenges Facing Cardiac Patch Implementation

The successful implementation of cardiac patches as a therapeutic strategy still faces several hurdles. In order to truly restore cardiac function, the cardiac patches must assimilate with the surrounding myocardium at three levels: physical and biochemical continuity, electrophysiological communication, and nutrient supply (**Figure 4**).

Even though cardiac patches improve cell viability and retention, cells engrafted through such constructs or through intracardiac injection could still provoke an immunogenic response, which ultimately will lead to allograft rejection (Yanamandala et al., 2017). In addition, cardiac patch transplantation not accompanied with suppression of the host immune system will limit transplanted cell survival rate and therefore will result in failing integration (Malliaras et al., 2012).

It is also mandatory that designed scaffolds would be accessible for cell migration from areas close to the infarcted zones and allow the formation of blood vessels and nerves (Sachlos and Czernuszka, 2003; Muschler et al., 2004). Later, these networks must integrate properly with those of the host (Jackman et al., 2018).

To date, grafts still present inferior functionality, mainly in action potential conductivity (Wendel et al., 2013). Moreover, any graft transplanted would have to overcome the major restriction of integration. A graft not incorrectly integrated with the host heart tissue, both mechanically and electrically, could possibly lead to arrhythmia caused by unsynchronized electrophysiological signal transmission between the graft, the host myocardium, and the fibrotic interface in between (Chen et al., 2009). This problem was demonstrated in a study performed on primate hearts, using hESC-CM transplantation. Unlike smaller animal models, ventricular arrhythmias were observed consistently (Chong et al., 2014). This phenomenon could be related to the large distances the electrical and

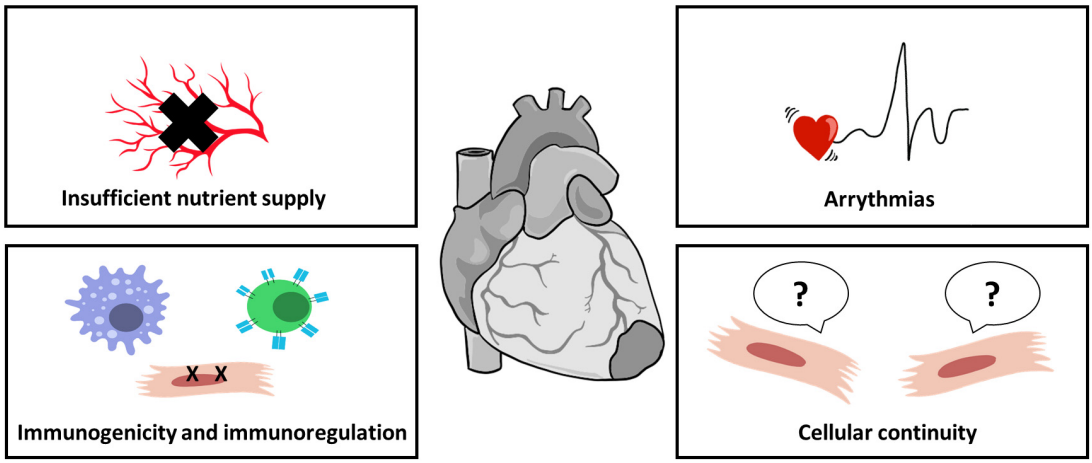

FIGURE 4 | Challenges in cardiac patch implementation. Cardiac patches must integrate properly with host myocardium to properly improve cardiac function. For cell-seeded patches, sufficient nutrient supply by blood vessels is crucial for cell survival; biomaterials, as foreign objects, induce immunogenic response immediately after their introduction, impairing integration and leading to patch rejection; improper electrical coupling of the patch with host myocardium may result in arrhythmias; and cellular continuum, translated into biomechanical integrity, is also important for patch assimilation.

mechanical signals must travel, decreasing conductivity. Even in small animal models, cardiac patches were shown to fail at electrically integrating with the host, mainly due to the presence of a fibrotic scar barrier (Jackman et al., 2018). Thus, cardiac patch designs must address these limitations to be clinically relevant. Future designs must take into consideration not only the patch's own functionality, but also its assimilation with host myocardium and synchronization over large distances.

Biomaterials, yet again, were recruited in order to overcome these hurdles. The main dogma suggests the use of porous scaffolds (Shapiro and Cohen, 1997; Dattola et al., 2019; Yang et al., 2019). Among previously mentioned advantages, such architecture also provides appropriate space and/or guiding routes for cells to penetrate the matrix. This principle could be exploited to dictate biomaterial degradation in a rate suitable for new tissue reconstruction (Bar et al., 2018). Nutrient supply and electrophysiological mediated integration could also be improved using smart biomaterial designs. For instance, VEGF containing scaffolds were designed to increase vascularization within the patch *in vivo* (Freeman and Cohen, 2009; Miyagi et al., 2011). Prevasularization of scaffolds was also suggested to improve mass transport into cardiac patches. To this end, ECM nanofibers and MSCs were used as a sheet designated to promote vascular constructs when co-cultured with ECs. They hypothesized that seeded MSCs will support the formation of microvessels and their structure through the secretion of angiogenic factors (Zhang L. et al., 2018). In order to improve electrical coupling, Shevach et al. (2014) suggested to decorate decellularized matrices with gold NPs and nanowires, presenting stronger contractile force and lowering excitation threshold.

Biomaterials were also suggested as an alternative for stitching. By using near-infrared (NIR)-stimulated gold nanowires incorporated within the scaffold, engineered tissue was positioned on the myocardium and successfully attached (Malki et al., 2018). Another scaffold design suggested the use of a microneedle array composed of poly(vinyl alcohol), integrated with CSCs encapsulated within fibrin hydrogel (Tang et al., 2018). The proposed design was strong enough to allow microneedle penetration into the ischemic region, while also enabling cell migration into the microneedle array acting mostly in a paracrine manner. Altogether, the overviewed approaches indicate that biomaterials, alongside smart scaffold designs could potentially lead to true functional integration with surrounding tissue.

Controlled Release Platforms

Platforms of controlled, sustained release are required for applications demanding local, time adjusted, and temporary delivery of bioactive molecules. Polymeric materials, capable of forming 2D and 3D matrices, have been superior candidates for this purpose for several decades (Langer and Peppas, 1981; Hubbell, 1999; O'Neill et al., 2016). Since endogenous cardiac regeneration strategies usually aim to act locally, delivery systems impregnated within injectable hydrogels and cardiac patches are very appealing.

Wang et al. (2017) illustrated the potential of a bioactive, injectable hydrogel to induce cardiac regeneration *in situ*. They developed an injectable hydrogel, based on high-affinity interactions between two oligosaccharides, modified with HA. This hydrogel system was capable of binding cholesterol with high affinity. For the application, miR-302 mimic, an identified CM proliferating inducer, was conjugated to cholesterol and mixed within the hydrogel. The resulting hydrogel exhibited a slow, sustained release profile over 3 weeks, thus demonstrating the potential to induce cardiac proliferation in the relatively long term. Indeed, they were able to show significant clonal expansion of CMs, following miR-302 releasing hydrogel injection into infarcted hearts of Confetti mice (Wang et al., 2017).

Injectable hydrogels were also used to improve cell survival and attenuate fibrotic responses immediately after MI. Ruvinov et al. (2011b) speculated that the release of two

GFs – IGF-1 (considered cardioprotective) and hepatocyte growth factor (HGF; considered anti-fibrotic) will improve cardiac regeneration by targeting two key processes in scar formation. They used injectable alginate hydrogel consisting of affinity-binding AlgS, capable of binding both GFs. The injection of the proposed hydrogel into infarcted rat hearts had positive effects: reduced myocyte apoptosis and induction of CM proliferation attenuated infarct expansion and reduced fibrosis (Ruvinov et al., 2011b).

Cell-free cardiac patches were also demonstrated to be effective at inducing endogenous cardiac regeneration, based on the "paracrine effect." It is quite acceptable that one of the mechanisms in which cell-based therapies improve cardiac regeneration is through the secretion of cardioprotective factors, signaling surrounding cells in the infarct area. In one study, the researchers hypothesized that EVs derived from iPS or iPS-CM would have a similar effect. Therefore, they isolated these EVs *in vitro* and analyzed their miRNA content, supporting their assumptions. However, as mentioned, EVs are rapidly consumed by recipient cells, therefore their effect is time limited. In order to increase treatment efficacy, the isolated EVs were encapsulated in a cell-free collagen hydrogel, serving as a patch. The collagen hydrogel allowed a prolonged release of EVs up to 7 days *in vivo*. When the patch was applied in a rat MI model, it was able to reduce scar formation and apoptosis of CMs, while also promoting recovery of contractile functions, without any signs for arrhythmias (Liu et al., 2018). This system's main strength is its independence on any cellular component, reducing issues of immunogenicity and concerns regarding cellular viability and retention.

CLINICAL TRIALS OF BIOMATERIAL-BASED APPLICATIONS

Applications involving the use of biomaterials for cardiac regeneration have already entered clinical trials. The IK-5001 device, an injectable, bio-absorbable alginate hydrogel [also known as bioabsorbable cardiac matrix (BCM)], was tested for its safety and effectiveness for prevention of left ventricular remodeling (Bellerophon BCM LLC, ClinicalTrials.gov identifier: NCT01226563). This trial was conducted in a randomized, double-blind, controlled setup, treating 303 patients worldwide. The interventional procedure included the injection of BCM into the infarct-related artery, 2–5 days after primary PCI. Safety endpoints for this research show no significant difference from saline injections; however, the BCM treatment did not reduce LV remodeling or major cardiovascular events after a 6-month follow-up. Among the reasons for this observation, the researchers specified the large infarct sizes selected (around 30% of LV area), in which remodeling could not possibly be prevented (Rao et al., 2016).

Another acellular, alginate hydrogel formulation examined in clinical trials is the Algisyl-LVR™ device (LoneStar Heart Inc., Laguna Hills, CA, United States). Algisyl-LVR™ was tested for its safety and efficacy in two separate clinical trials: One aimed to quantify its effect when combined with coronary artery bypass grafting (ClinicalTrials.gov identifier: NCT0084796) and the second its employment as a method of left ventricular augmentation and restoration to treat patients with advanced chronic HF (ClinicalTrials.gov identifier: NCT01311791). In both trials the treatment included an open-heart procedure, followed by 10–15 implant injections into the left ventricular heart muscle. The first clinical trial showed remarkable improvement in cardiac function, including elevated ejection fraction (from 32 ± 8 to 47 ± 17% after 3 months), decreased end-systolic and diastolic volumes, and an increase in average wall thickness compared with control saline injections (Lee et al., 2013). In the second, randomized and controlled study, known as the AUGMENT-HF trial, effectiveness of treatment was assessed. Seventy-eight patients with dilated cardiomyopathy were selected as treatment group, and exhibited significant improvement in exercise capacity and symptoms (elevated Peak VO_2 and longer distance in 6-min walk test) compared to control. However, these results should be considered with caution, as this trial was subjected to bias due to lack of blinding for the assignment of patients to the surgical procedure (Anker et al., 2015).

VentriGel™ (Ventrix, Inc., San Diego, CA, United States), an acellular, porcine-cardiac ECM hydrogel, was also examined in a recently published phase I clinical trial (ClinicalTrials.gov identifier: NCT02305602). In this study, researchers evaluated the safety and feasibility of VentriGel™. The hydrogel was delivered *trans*-endocardially within a time window between 60 days to 3 years since the first, large ST elevation MI. The outcomes of this first-in-man trial highlighted the safety and feasibility of this treatment, while also showing improvement in exercise capacity examined by a 6-min walk test, even though this study was not designed to test effectiveness of treatment (Traverse et al., 2019). Even though the collective results of clinical trials involving injection of hydrogels alone highlight the feasibility and safety of this method at improving cardiac function after MI, there is still no sufficient evidence for the capability of pristine hydrogels to promote endogenous cardiac regeneration by themselves.

CorMatrix® ECM cardiac patches, which recently received FDA approval, were tested in clinical trials (CorMatrix Cardiovascular, Inc., ClinicalTrials.gov identifier: NCT02887768), claimed to promote endogenous cardiac regeneration. Pre-clinical studies with CorMatrix® patches for epicardial infarct repair in a pig model supported this claim, presenting neovascularization in the interface between the infarct and the patch (Mewhort et al., 2016). Yet, in a study performed in children with congenital heart disease, there was no evidence for endogenous ingrowth of native cardiac muscle within 21 months (Nelson et al., 2016). At the present time point, clinical trials using CorMatrix patches have been designed to evaluate safety only rather than their effectiveness.

Recently, the results of a phase I clinical trial were published, determining the safety and efficacy of transplanting cardiac-committed progenitor cells derived from hESCs, using a fibrin cardiac patch (ClinicalTrials.gov identifier: NCT02057900). The fibrin cardiac patch, 20 cm^2 in size seeded with *ex vivo* differentiated cells, was inserted inside a "pocket" under the pericardium. The results of this trial mostly demonstrated the capability to produce highly purified hESC-derived cardiac

progenitor cells, without evidence of tumor formation or arrhythmias (Menasché et al., 2018). Although the feasibility to produce clinical-grade hESC-CM for transplantation was demonstrated, clinical trials assessing efficacy were not yet conducted.

CONCLUSION, LIMITATIONS, AND FUTURE PERSPECTIVES

Biomaterial-based strategies offer a wide range of solutions and additives to various cardiac regeneration therapeutic approaches, making them more and more effective and clinically relevant. Biomaterials may be utilized as a vehicle for efficient delivery of regeneration-inducing small molecules and/or cells, to act as matrix guiding cell maturation (*in vitro* and *in situ*), and perform as a platform for sustained drug delivery, achieving cardiac regeneration based on the paracrine effect hypothesis. The common principle behind the use of biomaterials is their ability to function as potential mediators between the therapeutic agents and their target, while also having beneficial influence on their own.

Even though biomaterials were already tested in clinical trials for their safety, showing encouraging results and implying improvement in cardiac function, there are still some findings in pre-clinical and clinical trials that should not be overlooked. The most important issue regards foreign body response of the host to biomaterials used as medical devices. An adverse immunogenic response is common to all the biomaterial applications discussed in this review. In general, when a biomaterial, either natural or synthetic, is in contact with host tissue, it induces a response of the innate immune system, and later the adaptive immune system. Degradation products of implanted biomaterials also activate immune system components. The development of an excessive inflammatory response might severely impair the efficacy of biomaterial applications, since the endpoint of this process is fibrotic encapsulation of the device, thus minimizing its surface interplay with the host tissue and if the device is a drug delivery system, the encapsulation would affect the release profile of the drug from the device (Mariani et al., 2019). Therefore, it is extremely important to evaluate host response when applying biomaterial-based strategies for cardiac regeneration, mostly due to the adverse inflammatory response following MI. Some of the presented strategies are more susceptible to fibrotic encapsulation, mostly those involving synthetic biomaterials or containing allogeneic cellular components, thus these attributes should be taken into consideration. A possible strategy to make cellular biomaterials more tolerated is the application of immunosuppressive agents combined within the therapeutic approach (Orr et al., 2016).

Even though biomaterials are already established members in many therapeutic approaches for cardiovascular diseases, such applications have not yet reached their full potential, as there is still more room for improvements in means of mechanical stability, tolerance to immunogenic host responses, and proper integration and functional improvement with biomaterial applications. For example, the greatest challenge cardiac patches are still facing is associated with their assimilation with host myocardium. Based on the success of biomaterials to perform as drug delivery platforms and construct a highly sophisticated cardiac patch design, it is also possible that biomaterials could be the answer for that issue as well, by combining the two. For instance, incorporation of a biomaterial-based drug delivery system within a fully developed cardiac patch, acting simultaneously to treat the harmful consequences of MI while also having the potential to restore cardiac function by improving integration with the remaining, healthy cardiac tissue. Since none of the applications can fully regenerate an entire new muscle by itself, this combination could have a synergistic effect on cardiac regeneration.

AUTHOR CONTRIBUTIONS

AB wrote the manuscript with inputs from SC.

FUNDING

AB gratefully acknowledges the BioTech Doctoral Fellowship from Kreitman School.

ACKNOWLEDGMENTS

The authors greatly thank Carmit Bar for the creative pictures. SC holds the Claire and Harold Oshry Professor Chair in Biotechnology.

REFERENCES

Abbate, A., Bussani, R., Amin, M. S., Vetrovec, G. W., and Baldi, A. (2006). Acute myocardial infarction and heart failure: role of apoptosis. *Int. J. Biochem. Cell Biol.* 38, 1834–1840. doi: 10.1016/j.biocel.2006.04.010

Abdel-Latif, A., Bolli, R., Zuba-Surma, E. K., Tleyjeh, I. M., Hornung, C. A., and Dawn, B. (2008). Granulocyte colony-stimulating factor therapy for cardiac repair after acute myocardial infarction: a systematic review and meta-analysis of randomized controlled trials. *Am. Heart J.* 156, 216–226.e9. doi: 10.1016/j.ahj.2008.03.024

Afzal, M. R., Samanta, A., Shah, Z. I., Jeevanantham, V., Abdel-Latif, A., Zuba-Surma, E. K., et al. (2015). Adult bone marrow cell therapy for ischemic heart disease: evidence and insights from randomized controlled trials. *Circ. Res.* 117, 558–575. doi: 10.1161/CIRCRESAHA.114.304792

Allen, T. M., and Cullis, P. R. (2013). Liposomal drug delivery systems: from concept to clinical applications. *Adv. Drug Deliv. Rev.* 65, 36–48. doi: 10.1016/j.addr.2012.09.037

Anker, S. D., Coats, A. J. S., Cristian, G., Dragomir, D., Pusineri, E., Piredda, M., et al. (2015). A prospective comparison of alginate-hydrogel with standard medical therapy to determine impact on functional capacity and clinical outcomes in patients with advanced heart failure (AUGMENT-HF trial). *Eur. Heart J.* 36, 2297–2309. doi: 10.1093/eurheartj/ehv259

Arslan, F., Lai, R. C., Smeets, M. B., Akeroyd, L., Choo, A., Aguor, E. N. E., et al. (2013). Mesenchymal stem cell-derived exosomes increase ATP levels, decrease oxidative stress and activate PI3K/Akt pathway to enhance myocardial viability

and prevent adverse remodeling after myocardial ischemia/reperfusion injury. *Stem Cell Res.* 10, 301–312. doi: 10.1016/j.scr.2013.01.002

Askar, S. F. A., Ramkisoensing, A. A., Atsma, D. E., Schalij, M. J., de Vries, A. A. F., and Pijnappels, D. A. (2013). Engraftment patterns of human adult mesenchymal stem cells expose electrotonic and paracrine proarrhythmic mechanisms in myocardial cell cultures. *Circ. Arrhythmia Electrophysiol.* 6, 380–391. doi: 10.1161/CIRCEP.111.000215

Baker, R. S., Zafar, F., Kimura, N., Knilans, T., Osinska, H., Robbins, J., et al. (2019). *In vivo* remodeling of an extracellular matrix cardiac patch in an ovine model. *Asaio J.* 65, 744–752. doi: 10.1097/MAT.0000000000000864

Ban, K., Park, H.-J., Kim, S., Andukuri, A., Cho, K.-W., Hwang, J. W., et al. (2014). Cell therapy with embryonic stem cell-derived cardiomyocytes encapsulated in injectable nanomatrix gel enhances cell engraftment and promotes cardiac repair. *ACS Nano* 8, 10815–10825. doi: 10.1021/nn504617g

Bar, A., Ruvinov, E., and Cohen, S. (2018). Live imaging flow bioreactor for the simulation of articular cartilage regeneration after treatment with bioactive hydrogel. *Biotechnol. Bioeng.* 115, 2205–2216. doi: 10.1002/bit.26736

Barad, L., Schick, R., Zeevi-Levin, N., Itskovitz-Eldor, J., and Binah, O. (2014). Human embryonic stem cells vs human induced pluripotent stem cells for cardiac repair. *Can. J. Cardiol.* 30, 1279–1287. doi: 10.1016/j.cjca.2014.06.023

Barwari, T., Joshi, A., and Mayr, M. (2016). MicroRNAs in cardiovascular disease. *J. Am. Coll. Cardiol.* 68, 2577–2584. doi: 10.1016/j.jacc.2016.09.945

Bejerano, T., Etzion, S., Elyagon, S., Etzion, Y., and Cohen, S. (2018). Nanoparticle delivery of miRNA-21 mimic to cardiac macrophages improves myocardial remodeling after myocardial infarction. *Nano Lett.* 18, 5885–5891. doi: 10.1021/acs.nanolett.8b02578

Bejleri, D., Streeter, B. W., Nachlas, A. L. Y., Brown, M. E., Gaetani, R., Christman, K. L., et al. (2018). A bioprinted cardiac patch composed of cardiac-specific extracellular matrix and progenitor cells for heart repair. *Adv. Healthc. Mater.* 7:1800672. doi: 10.1002/adhm.201800672

Benjamin, E. J., Muntner, P., and Bittencourt, M. S. (2019). Heart disease and stroke statistics-2019 update: a report From the American Heart Association. *Circulation* 139, e56–e528. doi: 10.1161/CIR.0000000000000659

Bergmann, O., Zdunek, S., Felker, A., Salehpour, M., Alkass, K., Bernard, S., et al. (2015). Dynamics of cell generation and turnover in the human heart. *Cell* 161, 1566–1575. doi: 10.1016/j.cell.2015.05.026

Bersell, K., Arab, S., Haring, B., and Kühn, B. (2009). Neuregulin1/ErbB4 signaling induces cardiomyocyte proliferation and repair of heart injury. *Cell* 138, 257–270. doi: 10.1016/j.cell.2009.04.060

Cannon, C. P., Gibson, C. M., Lambrew, C. T., Shoultz, D. A., Levy, D., French, W. J., et al. (2000). Relationship of symptom-onset-to-balloon time and door-to-balloon time with mortality in patients undergoing angioplasty for acute myocardial infarction. *JAMA* 283, 2941–2947.

Cano-Martínez, A., Vargas-González, A., Guarner-Lans, V., Prado-Zayago, E., Leon-Oleda, M., and Nieto-Lima, B. (2010). Functional and structural regeneration in the axolotl heart (*Ambystoma mexicanum*) after partial ventricular amputation. *Arch. Cardiol. Mex.* 80, 79–86.

Chen, H.-S. V., Kim, C., and Mercola, M. (2009). Electrophysiological challenges of cell-based myocardial repair. *Circulation* 120, 2496–2508. doi: 10.1161/circulationaha.107.751412

Chen, Q.-Z., Harding, S. E., Ali, N. N., Lyon, A. R., and Boccaccini, A. R. (2008). Biomaterials in cardiac tissue engineering: ten years of research survey. *Mater. Sci. Eng. R Rep.* 59, 1–37. doi: 10.1016/j.mser.2007.08.001

Chistiakov, D. A., Sobenin, I. A., and Orekhov, A. N. (2012). Strategies to deliver microRNAs as potential therapeutics in the treatment of cardiovascular pathology. *Drug Deliv.* 19, 392–405. doi: 10.3109/10717544.2012.738436

Chong, J. J. H., Yang, X., Don, C. W., Minami, E., Liu, Y.-W., Weyers, J. J., et al. (2014). Human embryonic-stem-cell-derived cardiomyocytes regenerate non-human primate hearts. *Nature* 510, 273–277. doi: 10.1038/nature13233

Chow, A., Stuckey, D. J., Kidher, E., Rocco, M., Jabbour, R. J., Mansfield, C. A., et al. (2017). Human induced pluripotent stem cell-derived cardiomyocyte encapsulating bioactive hydrogels improve rat heart function post myocardial infarction. *Stem Cell Rep.* 9, 1415–1422. doi: 10.1016/j.stemcr.2017.09.003

Christman, K. L., and Lee, R. J. (2006). Biomaterials for the treatment of myocardial infarction. *J. Am. Coll. Cardiol.* 48, 907–913. doi: 10.1016/j.jacc.2006.06.005

Christman, K. L., Vardanian, A. J., Fang, Q., Sievers, R. E., Fok, H. H., and Lee, R. J. (2004). Injectable fibrin scaffold improves cell transplant survival, reduces infarct expansion, and induces neovasculature formation in ischemic myocardium. *J. Am. Coll. Cardiol.* 44, 654–660. doi: 10.1016/j.jacc.2004.04.040

Costa-Silva, B., Aiello, N. M., Ocean, A. J., Singh, S., Zhang, H., Thakur, B. K., et al. (2015). Pancreatic cancer exosomes initiate pre-metastatic niche formation in the liver. *Nat. Cell Biol.* 17, 816–826.

Dai, W., Wold, L. E., Dow, J. S., and Kloner, R. A. (2005). Thickening of the infarcted wall by collagen injection improves left ventricular function in rats: a novel approach to preserve cardiac function after myocardial infarction. *J. Am. Coll. Cardiol.* 46, 714–719. doi: 10.1016/j.jacc.2005.04.056

D'Amore, A., Yoshizumi, T., Luketich, S. K., Wolf, M. T., Gu, X., Cammarata, M., et al. (2016). Bi-layered polyurethane – Extracellular matrix cardiac patch improves ischemic ventricular wall remodeling in a rat model. *Biomaterials* 107, 1–14. doi: 10.1016/j.biomaterials.2016.07.039

Das, S., and Halushka, M. K. (2015). Extracellular vesicle microRNA transfer in cardiovascular disease. *Cardiovasc. Pathol.* 24, 199–206. doi: 10.1016/j.carpath.2015.04.007

Dattola, E., Parrotta, E. I., Scalise, S., Perozziello, G., Limongi, T., Candeloro, P., et al. (2019). Development of 3D PVA scaffolds for cardiac tissue engineering and cell screening applications. *RSC Adv.* 9, 4246–4257. doi: 10.1039/c8ra08187e

Dobner, S., Bezuidenhout, D., Govender, P., Zilla, P., and Davies, N. (2009). A synthetic non-degradable polyethylene glycol hydrogel retards adverse post-infarct left ventricular remodeling. *J. Card. Fail.* 15, 629–636. doi: 10.1016/j.cardfail.2009.03.003

Dong, S., Cheng, Y., Yang, J., Li, J., Liu, X., Wang, X., et al. (2009). MicroRNA expression signature and the role of microRNA-21 in the early phase of acute myocardial infarction. *J. Biol. Chem.* 284, 29514–29525. doi: 10.1074/jbc.M109.027896

Dong, Z., Guo, J., Xing, X., Zhang, X., Du, Y., and Lu, Q. (2017). RGD modified and PEGylated lipid nanoparticles loaded with puerarin: formulation, characterization and protective effects on acute myocardial ischemia model. *Biomed. Pharmacother.* 89, 297–304. doi: 10.1016/j.biopha.2017.02.029

Duncan, R. (2003). The dawning era of polymer therapeutics. *Nat. Rev. Drug Discov.* 2, 347–360. doi: 10.1038/nrd1088

D'Uva, G., Aharonov, A., Lauriola, M., Kain, D., Yahalom-Ronen, Y., Carvalho, S., et al. (2015). ERBB2 triggers mammalian heart regeneration by promoting cardiomyocyte dedifferentiation and proliferation. *Nat. Cell Biol.* 17, 627–638. doi: 10.1038/ncb3149

Dvir, T., Bauer, M., Schroeder, A., Tsui, J. H., Anderson, D. G., Langer, R., et al. (2011). Nanoparticles targeting the infarcted heart. *Nano Lett.* 11, 4411–4414. doi: 10.1021/nl2025882

Dvir, T., Tsur-Gang, O., and Cohen, S. (2005). "Designer" scaffolds for tissue engineering and regeneration. *Isr. J. Chem.* 45, 487–494. doi: 10.1560/378J-XMB1-NAKF-YKQ1

El Harane, N., Kervadec, A., Bellamy, V., Pidial, L., Neametalla, H. J., Perier, M.-C., et al. (2018). Acellular therapeutic approach for heart failure: *in vitro* production of extracellular vesicles from human cardiovascular progenitors. *Eur. Heart J.* 39, 1835–1847. doi: 10.1093/eurheartj/ehy012

Emanueli, C., Shearn, A. I. U., Angelini, G. D., and Sahoo, S. (2015). Exosomes and exosomal miRNAs in cardiovascular protection and repair. *Vascul. Pharmacol.* 71, 24–30. doi: 10.1016/j.vph.2015.02.008

Eng, G., Lee, B. W., Radisic, M., and Vunjak-Novakovic, G. (2014). "Chapter 38 - Cardiac Tissue Engineering," in *Principles of Tissue Engeenering*, 4th Edn, eds R. Lanza, R. Langer, and J. Vacanti (Boston, MA: Academic Press), 771–792. doi: 10.1016/B978-0-12-398358-9.00038-0

Engler, A. J., Sen, S., Sweeney, H. L., and Discher, D. E. (2006). Matrix elasticity directs stem cell lineage specification. *Cell* 126, 677–689. doi: 10.1016/j.cell.2006.06.044

Essandoh, K., Li, Y., Huo, J., and Fan, G.-C. (2016). MiRNA-mediated macrophage polarization and its potential role in the regulation of inflammatory response. *Shock* 46, 122–131. doi: 10.1097/SHK.0000000000000604

Eulalio, A., Mano, M., Dal Ferro, M., Zentilin, L., Sinagra, G., Zacchigna, S., et al. (2012). Functional screening identifies miRNAs inducing cardiac regeneration. *Nature* 492, 376–381. doi: 10.1038/nature11739

Ferguson, S. W., Wang, J., Lee, C. J., Liu, M., Neelamegham, S., Canty, J. M., et al. (2018). The microRNA regulatory landscape of MSC-derived exosomes: a systems view. *Sci. Rep.* 8:1419. doi: 10.1038/s41598-018-19581-x

Ferrarini, M., Arsic, N., Recchia, F. A., Zentilin, L., Zacchigna, S., Xu, X., et al. (2006). Adeno-associated virus-mediated transduction of VEGF165 improves cardiac tissue viability and functional recovery after permanent coronary occlusion in conscious dogs. *Circ. Res.* 98, 954–961. doi: 10.1161/01.res.0000217342.83731.89

Fleischer, S., Feiner, R., and Dvir, T. (2017). Cutting-edge platforms in cardiac tissue engineering. *Curr. Opin. Biotechnol.* 47, 23–29. doi: 10.1016/j.copbio.2017.05.008

Foglia, M. J., and Poss, K. D. (2016). Building and re-building the heart by cardiomyocyte proliferation. *Development* 143, 729–740. doi: 10.1242/dev.132910

Francis Stuart, S. D., De Jesus, N. M., Lindsey, M. L., and Ripplinger, C. M. (2016). The crossroads of inflammation, fibrosis, and arrhythmia following myocardial infarction. *J. Mol. Cell. Cardiol.* 91, 114–122. doi: 10.1016/j.yjmcc.2015.12.024

Frangogiannis, N. G. (2017). The extracellular matrix in myocardial injury, repair, and remodeling. *J. Clin. Invest.* 127, 1600–1612. doi: 10.1172/JCI87491

Frangogiannis, N. G., Smith, C. W., and Entman, M. L. (2002). The inflammatory response in myocardial infarction. *Cardiovasc. Res.* 53, 31–47. doi: 10.1016/s0008-6363(01)00434-5

Frantz, C., Stewart, K. M., and Weaver, V. M. (2010). The extracellular matrix at a glance. *J. Cell Sci.* 123, 4195–4200. doi: 10.1242/jcs.023820

Freed, L. E., Vunjak-Novakovic, G., Biron, R. J., Eagles, D. B., Lesnoy, D. C., Barlow, S. K., et al. (1994). Biodegradable polymer scaffolds for tissue engineering. *Biotechnology* 12, 689–693. doi: 10.1038/nbt0794-689

Freeman, I., and Cohen, S. (2009). The influence of the sequential delivery of angiogenic factors from affinity-binding alginate scaffolds on vascularization. *Biomaterials* 30, 2122–2131. doi: 10.1016/j.biomaterials.2008.12.057

Freeman, I., Kedem, A., and Cohen, S. (2008). The effect of sulfation of alginate hydrogels on the specific binding and controlled release of heparin-binding proteins. *Biomaterials* 29, 3260–3268. doi: 10.1016/j.biomaterials.2008.04.025

Gabisonia, K., Prosdocimo, G., Aquaro, G. D., Carlucci, L., Zentilin, L., Secco, I., et al. (2019). MicroRNA therapy stimulates uncontrolled cardiac repair after myocardial infarction in pigs. *Nature* 569, 418–422. doi: 10.1038/s41586-019-1191-6

Garg, S., Narula, J., and Chandrashekhar, Y. (2005). Apoptosis and heart failure: clinical relevance and therapeutic target. *J. Mol. Cell. Cardiol.* 38, 73–79. doi: 10.1016/j.yjmcc.2004.11.006

Gaziano, T. A., Bitton, A., Anand, S., Abrahams-Gessel, S., and Murphy, A. (2010). Growing epidemic of coronary heart disease in low-and middle-income countries. *Curr. Probl. Cardiol.* 35, 72–115. doi: 10.1016/j.cpcardiol.2009.10.002

Gerczuk, P. Z., and Kloner, R. A. (2012). An update on cardioprotection. *J. Am. Coll. Cardiol.* 59, 969–978. doi: 10.1016/j.jacc.2011.07.054

Gnecchi, M., He, H., Noiseux, N., Liang, O. D., Zhang, L., Morello, F., et al. (2006). Evidence supporting paracrine hypothesis for Akt-modified mesenchymal stem cell-mediated cardiac protection and functional improvement. *FASEB J.* 20, 661–669. doi: 10.1096/fj.05-5211com

Goldshtein, M., Shamir, S., Vinogradov, E., Monsonego, A., and Cohen, S. (2019). Co-assembled Ca^{2+} alginate-sulfate nanoparticles for intracellular plasmid DNA delivery. *Mol. Ther. Nucleic Acids* 16, 378–390. doi: 10.1016/j.omtn.2019.03.006

Gottipati, A., Chelvarajan, L., Peng, H., Kong, R., Cahall, C. F., Li, C., et al. (2019). Gelatin based polymer cell coating improves bone marrow-derived cell retention in the heart after myocardial infarction. *Stem Cell Rev. Rep.* 15, 404–414. doi: 10.1007/s12015-018-9870-5

Griffith, L. G. (2002). Emerging design principles in biomaterials and scaffolds for tissue engineering. *Ann. N. Y. Acad. Sci.* 961, 83–95. doi: 10.1111/j.1749-6632.2002.tb03056.x

Guo, Y., Wysoczynski, M., Nong, Y., Tomlin, A., Zhu, X., Gumpert, A. M., et al. (2017). Repeated doses of cardiac mesenchymal cells are therapeutically superior to a single dose in mice with old myocardial infarction. *Basic Res. Cardiol.* 112:18. doi: 10.1007/s00395-017-0606-5

Haubner, B. J., Schneider, J., Schweigmann, U., Schuetz, T., Dichtl, W., Velik-Salchner, C., et al. (2016). Functional recovery of a human neonatal heart after severe myocardial infarction. *Circ. Res.* 118, 216–221. doi: 10.1161/CIRCRESAHA.115.307017

Hayoun-Neeman, D., Korover, N., Etzion, S., Ofir, R., Lichtenstein, R. G., and Cohen, S. (2019). Exploring peptide-functionalized alginate scaffolds for engineering cardiac tissue from human embryonic stem cell-derived cardiomyocytes in serum-free medium. *Polym. Adv. Technol.* 30, 2493–2505. doi: 10.1002/pat.4602

Hinz, B. (2015). The extracellular matrix and transforming growth factor-β1: tale of a strained relationship. *Matrix Biol.* 47, 54–65. doi: 10.1016/j.matbio.2015.05.006

Ho, W., Zhang, X.-Q., and Xu, X. (2016). Biomaterials in siRNA delivery: a comprehensive review. *Adv. Healthc. Mater.* 5, 2715–2731. doi: 10.1002/adhm.201600418

Hubbell, J. A. (1999). Bioactive biomaterials. *Curr. Opin. Biotechnol.* 10, 123–129. doi: 10.1016/S0958-1669(99)80021-4

Hubmacher, D., and Apte, S. S. (2013). The biology of the extracellular matrix: novel insights. *Curr. Opin. Rheumatol.* 25, 65–70. doi: 10.1097/BOR.0b013e32835b137b

Hynes, R. O. (2009). The extracellular matrix: not just pretty fibrils. *Science* 326, 1216–1219. doi: 10.1126/science.1176009

Ibrahim, A. G.-E., Cheng, K., and Marbán, E. (2014). Exosomes as critical agents of cardiac regeneration triggered by cell therapy. *Stem Cell Rep.* 2, 606–619. doi: 10.1016/j.stemcr.2014.04.006

Jackman, C. P., Ganapathi, A. M., Asfour, H., Qian, Y., Allen, B. W., Li, Y., et al. (2018). Engineered cardiac tissue patch maintains structural and electrical properties after epicardial implantation. *Biomaterials* 159, 48–58. doi: 10.1016/j.biomaterials.2018.01.002

Janavel, G. V., Crottogini, A., Meckert, P. C., Cuniberti, L., Mele, A., Papouchado, M., et al. (2006). Plasmid-mediated VEGF gene transfer induces cardiomyogenesis and reduces myocardial infarct size in sheep. *Gene Ther.* 13, 1133–1142. doi: 10.1038/sj.gt.3302708

Jeong, J.-O., Han, J. W., Kim, J.-M., Cho, H.-J., Park, C., Lee, N., et al. (2011). Malignant tumor formation after transplantation of short-term cultured bone marrow mesenchymal stem cells in experimental myocardial infarction and diabetic neuropathy. *Circ. Res.* 108, 1340–1347. doi: 10.1161/CIRCRESAHA.110.239848

Jones, C. H., Chen, C.-K., Ravikrishnan, A., Rane, S., and Pfeifer, B. A. (2013). Overcoming nonviral gene delivery barriers: perspective and future. *Mol. Pharm.* 10, 4082–4098. doi: 10.1021/mp400467x

Jopling, C., Sleep, E., Raya, M., Martí, M., Raya, A., and Izpisúa Belmonte, J. C. (2010). Zebrafish heart regeneration occurs by cardiomyocyte dedifferentiation and proliferation. *Nature* 464, 606–609. doi: 10.1038/nature08899

Jung, K. O., Jo, H., Yu, J. H., Gambhir, S. S., and Pratx, G. (2018). Development and MPI tracking of novel hypoxia-targeted theranostic exosomes. *Biomaterials* 177, 139–148. doi: 10.1016/j.biomaterials.2018.05.048

Kapnisi, M., Mansfield, C., Marijon, C., Guex, A. G., Perbellini, F., Bardi, I., et al. (2018). Auxetic cardiac patches with tunable mechanical and conductive properties toward treating myocardial infarction. *Adv. Funct. Mater.* 28:1800618. doi: 10.1002/adfm.201800618

Khan, M., Nickoloff, E., Abramova, T., Johnson, J., Verma, S. K., Krishnamurthy, P., et al. (2015a). Embryonic stem cell–derived exosomes promote endogenous repair mechanisms and enhance cardiac function following myocardial infarction. *Circ. Res.* 117, 52–64. doi: 10.1161/CIRCRESAHA.117.305990

Khan, M., Xu, Y., Hua, S., Johnson, J., Belevych, A., Janssen, P. M. L., et al. (2015b). Evaluation of changes in morphology and function of human induced pluripotent stem cell derived cardiomyocytes (HiPSC-CMs) cultured on an aligned-nanofiber cardiac patch. *PLoS One* 10:e0126338. doi: 10.1371/journal.pone.0126338

Kikuchi, K., Holdway, J. E., Werdich, A. A., Anderson, R. M., Fang, Y., Egnaczyk, G. F., et al. (2010). Primary contribution to zebrafish heart regeneration by gata4+ cardiomyocytes. *Nature* 464, 601–605. doi: 10.1038/nature08804

Kishore, R., and Khan, M. (2016). More than tiny sacks: stem cell exosomes as cell-free modality for cardiac repair. *Circ. Res.* 118, 330–343. doi: 10.1161/CIRCRESAHA.115.307654

Korin, E., Bejerano, T., and Cohen, S. (2017). GalNAc bio-functionalization of nanoparticles assembled by electrostatic interactions improves siRNA targeting to the liver. *J. Control. Release* 266, 310–320. doi: 10.1016/j.jconrel.2017.10.001

Koseva, N. S., Rydz, J., Stoyanova, E. V., and Mitova, V. A. (2015). "Chapter three - hybrid protein–synthetic polymer nanoparticles for drug delivery," in *Protein and Peptide Nanoparticles for Drug Delivery*, eds N. S. Koseva, J. Rydz, E. V. Stoyanova, and V. A. Mitova (Cambridge, MA: Academic Press), 93–119. doi: 10.1016/bs.apcsb.2014.12.003

Laflamme, M. A., and Murry, C. E. (2005). Regenerating the heart. *Nat. Biotechnol.* 23, 845–856. doi: 10.1038/nbt1117

Laflamme, M. A., and Murry, C. E. (2011). Heart regeneration. *Nature* 473, 326–335. doi: 10.1038/nature10147

Lai, E. C. (2002). Micro RNAs are complementary to 3' UTR sequence motifs that mediate negative post-transcriptional regulation. *Nat. Genet.* 30, 363–364. doi: 10.1038/ng865

Landa, N., Miller, L., Feinberg, M. S., Holbova, R., Shachar, M., Freeman, I., et al. (2008). Effect of injectable alginate implant on cardiac remodeling and function after recent and old infarcts in rat. *Circulation* 117, 1388–1396. doi: 10.1161/CIRCULATIONAHA.107.727420

Langer, R., and Vacanti, J. P. (1993). Tissue Engineering. *Science* 260, 920–926. doi: 10.1126/science.8493529

Langer, R. S., and Peppas, N. A. (1981). Present and future applications of biomaterials in controlled drug delivery systems. *Biomaterials* 2, 201–214. doi: 10.1016/0142-9612(81)90059-4

Lanza, R., Langer, R., and Vacanti, J. B. (2014). *Principles of Tissue Engineering*, 4th Edn. Boston, MA: Academic Press. doi: 10.1016/B978-0-12-398358-9.12001-4

Leask, A. (2007). TGFβ, cardiac fibroblasts, and the fibrotic response. *Cardiovasc. Res.* 74, 207–212. doi: 10.1016/j.cardiores.2006.07.012

Lee, A., Hudson, A. R., Shiwarski, D. J., Tashman, J. W., Hinton, T. J., Yerneni, S., et al. (2019). 3D bioprinting of collagen to rebuild components of the human heart. *Science* 365, 482–487. doi: 10.1126/science.aav9051

Lee, L. C., Wall, S. T., Klepach, D., Ge, L., Zhang, Z., Lee, R. J., et al. (2013). Algisyl-LVRTM with coronary artery bypass grafting reduces left ventricular wall stress and improves function in the failing human heart. *Int. J. Cardiol.* 168, 2022–2028. doi: 10.1016/j.ijcard.2013.01.003

Lee, W. H., Chen, W., Shao, N., Xiao, D., Qin, X., Baker, N., et al. (2017). Comparison of non-coding RNAs in exosomes and functional efficacy of human embryonic stem cell-versus induced pluripotent stem cell-derived cardiomyocytes. *Stem Cells* 35, 2138–2149. doi: 10.1002/stem.2669

Leor, J., Aboulafia-Etzion, S., Dar, A., Shapiro, L., Barbash, I. M., Battler, A., et al. (2000). Bioengineered cardiac grafts: a new approach to repair the infarcted myocardium? *Circulation* 102, Iii–56. doi: 10.1161/01.cir.102.suppl_3.iii-56

Leor, J., Tuvia, S., Guetta, V., Manczur, F., Castel, D., Willenz, U., et al. (2009). Intracoronary injection of in situ forming alginate hydrogel reverses left ventricular remodeling after myocardial infarction in swine. *J. Am. Coll. Cardiol.* 54, 1014–1023. doi: 10.1016/j.jacc.2009.06.010

Levit, R. D., Landázuri, N., Phelps, E. A., Brown, M. E., García, A. J., Davis, M. E., et al. (2013). Cellular encapsulation enhances cardiac repair. *J. Am. Heart Assoc.* 2:e000367. doi: 10.1161/JAHA.113.000367

Li, F., Wang, X., Capasso, J. M., and Gerdes, A. M. (1996). Rapid transition of cardiac myocytes from hyperplasia to hypertrophy during postnatal development. *J. Mol. Cell. Cardiol.* 28, 1737–1746. doi: 10.1006/jmcc.1996.0163

Lian, X., Zhang, J., Azarin, S. M., Zhu, K., Hazeltine, L. B., Bao, X., et al. (2013). Directed cardiomyocyte differentiation from human pluripotent stem cells by modulating Wnt/β-catenin signaling under fully defined conditions. *Nat. Protoc.* 8, 162–175. doi: 10.1038/nprot.2012.150

Liau, B., Christoforou, N., Leong, K. W., and Bursac, N. (2011). Pluripotent stem cell-derived cardiac tissue patch with advanced structure and function. *Biomaterials* 32, 9180–9187. doi: 10.1016/j.biomaterials.2011.08.050

Liem, A. L., van't Hof, A. W. J., Hoorntje, J. C. A., de Boer, M.-J., Suryapranata, H., and Zijlstra, F. (1998). Influence of treatment delay on infarct size and clinical outcome in patients with acute myocardial infarction treated with primary angioplasty. *J. Am. Coll. Cardiol.* 32, 629–633. doi: 10.1016/s0735-1097(98)00280-0

Ling, G., Gregorich, Z. R., Wuqiang, Z., Saidulu, M., Yasin, O., Xi, L., et al. (2018). Large cardiac muscle patches engineered from human induced-pluripotent stem cell–derived cardiac cells improve recovery from myocardial infarction in swine. *Circulation* 137, 1712–1730. doi: 10.1161/CIRCULATIONAHA.117.030785

Liu, B., Lee, B. W., Nakanishi, K., Villasante, A., Williamson, R., Metz, J., et al. (2018). Cardiac recovery via extended cell-free delivery of extracellular vesicles secreted by cardiomyocytes derived from induced pluripotent stem cells. *Nat. Biomed. Eng.* 2, 293–303. doi: 10.1038/s41551-018-0229-7

Liu, X., Ding, Y., Zhao, B., Liu, Y., Luo, S., Wu, J., et al. (2016). In vitro and in vivo evaluation of puerarin-loaded PEGylated mesoporous silica nanoparticles. *Drug Dev. Ind. Pharm.* 42, 2031–2037. doi: 10.1080/03639045.2016.1190742

Liu, Z., Wang, H., Wang, Y., Lin, Q., Yao, A., Cao, F., et al. (2012). The influence of chitosan hydrogel on stem cell engraftment, survival and homing in the ischemic myocardial microenvironment. *Biomaterials* 33, 3093–3106. doi: 10.1016/j.biomaterials.2011.12.044

Lovric, J., Mano, M., Zentilin, L., Eulalio, A., Zacchigna, S., and Giacca, M. (2012). Terminal differentiation of cardiac and skeletal myocytes induces permissivity to AAV transduction by relieving inhibition imposed by DNA damage response proteins. *Mol. Ther.* 20, 2087–2097. doi: 10.1038/mt.2012.144

Luan, X., Sansanaphongpricha, K., Myers, I., Chen, H., Yuan, H., and Sun, D. (2017). Engineering exosomes as refined biological nanoplatforms for drug delivery. *Acta Pharmacol. Sin.* 38, 754–763. doi: 10.1038/aps.2017.12

Lutolf, M. P., and Hubbell, J. A. (2005). Synthetic biomaterials as instructive extracellular microenvironments for morphogenesis in tissue engineering. *Nat. Biotechnol.* 23, 47–55. doi: 10.1038/nbt1055

Malki, M., Fleischer, S., Shapira, A., and Dvir, T. (2018). Gold nanorod-based engineered cardiac patch for suture-free engraftment by near IR. *Nano Lett.* 18, 4069–4073. doi: 10.1021/acs.nanolett.7b04924

Malliaras, K., Li, T.-S., Luthringer, D., Terrovitis, J., Cheng, K., Chakravarty, T., et al. (2012). Safety and efficacy of allogeneic cell therapy in infarcted rats transplanted with mismatched cardiosphere-derived cells. *Circulation* 125, 100–112. doi: 10.1161/CIRCULATIONAHA.111.042598

Margolis, G., Polyak, B., and Cohen, S. (2018). Magnetic induction of multiscale anisotropy in macroporous alginate scaffolds. *Nano Lett.* 18, 7314–7322. doi: 10.1021/acs.nanolett.8b03514

Mariani, E., Lisignoli, G., Borzì, R. M., and Pulsatelli, L. (2019). Biomaterials: foreign bodies or tuners for the immune response? *Int. J. Mol. Sci.* 20:E636. doi: 10.3390/ijms20030636

Matsumura, Y., Zhu, Y., Jiang, H., D'Amore, A., Luketich, S. K., Charwat, V., et al. (2019). Intramyocardial injection of a fully synthetic hydrogel attenuates left ventricular remodeling post myocardial infarction. *Biomaterials* 217:119289. doi: 10.1016/j.biomaterials.2019.119289

Matz, D. G., Oberpriller, J. O., and Oberpriller, J. C. (1998). Comparison of mitosis in binucleated and mononucleated newt cardiac myocytes. *Anat. Rec.* 251, 245–255. doi: 10.1002/(sici)1097-0185(199806)251:2<245::aid-ar14>3.0.co;2-o

Mawad, D., Mansfield, C., Lauto, A., Perbellini, F., Nelson, G. W., Tonkin, J., et al. (2016). A conducting polymer with enhanced electronic stability applied in cardiac models. *Sci. Adv.* 2:e1601007. doi: 10.1126/sciadv.1601007

McLaughlin, S., McNeill, B., Podrebarac, J., Hosoyama, K., Sedlakova, V., Cron, G., et al. (2019). Injectable human recombinant collagen matrices limit adverse remodeling and improve cardiac function after myocardial infarction. *Nat. Commun.* 10:4866. doi: 10.1038/s41467-019-12748-8

Menasché, P. (2008). Current status and future prospects for cell transplantation to prevent congestive heart failure. *Semin. Thorac. Cardiovasc. Surg.* 20, 131–137. doi: 10.1053/j.semtcvs.2008.03.001

Menasché, P. (2018). Cell therapy trials for heart regeneration—lessons learned and future directions. *Nat. Rev. Cardiol.* 15, 659–671. doi: 10.1038/s41569-018-0013-0

Menasché, P., Vanneaux, V., Fabreguettes, J.-R., Bel, A., Tosca, L., Garcia, S., et al. (2014). Towards a clinical use of human embryonic stem cell-derived cardiac progenitors: a translational experience. *Eur. Heart J.* 36, 743–750. doi: 10.1093/eurheartj/ehu192

Menasché, P., Vanneaux, V., Hagège, A., Bel, A., Cholley, B., Parouchev, A., et al. (2018). Transplantation of human embryonic stem cell–derived cardiovascular progenitors for severe ischemic left ventricular dysfunction. *J. Am. Coll. Cardiol.* 71, 429–438. doi: 10.1016/j.jacc.2017.11.047

Mercola, M., Ruiz-Lozano, P., and Schneider, M. D. (2011). Cardiac muscle regeneration: lessons from development. *Genes Dev.* 25, 299–309. doi: 10.1101/gad.2018411

Mewhort, H. E. M., Turnbull, J. D., Satriano, A., Chow, K., Flewitt, J. A., Andrei, A.-C., et al. (2016). Epicardial infarct repair with bioinductive extracellular matrix promotes vasculogenesis and myocardial recovery. *J. Hear. Lung Transplant.* 35, 661–670. doi: 10.1016/j.healun.2016.01.012

Miyagi, Y., Chiu, L. L. Y., Cimini, M., Weisel, R. D., Radisic, M., and Li, R.-K. (2011). Biodegradable collagen patch with covalently immobilized VEGF for myocardial repair. *Biomaterials* 32, 1280–1290. doi: 10.1016/j.biomaterials.2010.10.007

Mohamed, T. M. A., Ang, Y.-S., Radzinsky, E., Zhou, P., Huang, Y., Elfenbein, A., et al. (2018). Regulation of cell cycle to stimulate adult cardiomyocyte proliferation and cardiac regeneration. *Cell* 173, 104–116. doi: 10.1016/j.cell.2018.02.014

Montgomery, R. L., Hullinger, T. G., Semus, H. M., Dickinson, B. A., Seto, A. G., Lynch, J. M., et al. (2011). Therapeutic inhibition of miR-208a improves cardiac function and survival during heart failure. *Circulation* 124, 1537–1547. doi: 10.1161/CIRCULATIONAHA.111.030932

Mosala Nezhad, Z., Poncelet, A., de Kerchove, L., Gianello, P., Fervaille, C., and El Khoury, G. (2016). Small intestinal submucosa extracellular matrix (CorMatrix®) in cardiovascular surgery: a systematic review. *Interact. Cardiovasc. Thorac. Surg.* 22, 839–850. doi: 10.1093/icvts/ivw020

Muschler, G. F., Nakamoto, C., and Griffith, L. G. (2004). Engineering principles of clinical cell-based tissue engineering. *JBJS* 86, 1541–1558.

Nelson, D. M., Ma, Z., Fujimoto, K. L., Hashizume, R., and Wagner, W. R. (2011). Intra-myocardial biomaterial injection therapy in the treatment of heart failure: materials, outcomes and challenges. *Acta Biomater.* 7, 1–15. doi: 10.1016/j.actbio.2010.06.039

Nelson, J. S., Heider, A., Si, M.-S., and Ohye, R. G. (2016). Evaluation of explanted CorMatrix intracardiac patches in children with congenital heart disease. *Ann. Thorac. Surg.* 102, 1329–1335. doi: 10.1016/j.athoracsur.2016.03.086

Nguyen, M. M., Carlini, A. S., Chien, M., Sonnenberg, S., Luo, C., Braden, R. L., et al. (2015). Enzyme-responsive nanoparticles for targeted accumulation and prolonged retention in heart tissue after myocardial infarction. *Adv. Mater.* 27, 5547–5552. doi: 10.1002/adma.201502003

Nussbaum, J., Minami, E., Laflamme, M. A., Virag, J. A. I., Ware, C. B., Masino, A., et al. (2007). Transplantation of undifferentiated murine embryonic stem cells in the heart: teratoma formation and immune response. *FASEB J.* 21, 1345–1357. doi: 10.1096/fj.06-6769com

O'Neill, H. S., Gallagher, L. B., O'Sullivan, J., Whyte, W., Curley, C., Dolan, E., et al. (2016). Biomaterial-enhanced cell and drug delivery: lessons learned in the cardiac field and future perspectives. *Adv. Mater.* 28, 5648–5661. doi: 10.1002/adma.201505349

Ong, S.-B., Hernández-Reséndiz, S., Crespo-Avilan, G. E., Mukhametshina, R. T., Kwek, X.-Y., Cabrera-Fuentes, H. A., et al. (2018). Inflammation following acute myocardial infarction: multiple players, dynamic roles, and novel therapeutic opportunities. *Pharmacol. Ther.* 186, 73–87. doi: 10.1016/j.pharmthera.2018.01.001

Orr, S., Strominger, I., Eremenko, E., Vinogradov, E., Ruvinov, E., Monsonego, A., et al. (2016). TGF-β affinity-bound to a macroporous alginate scaffold generates local and peripheral immunotolerant responses and improves allocell transplantation. *Acta Biomater.* 45, 196–209. doi: 10.1016/j.actbio.2016.08.015

Parrag, I. C., Zandstra, P. W., and Woodhouse, K. A. (2012). Fiber alignment and coculture with fibroblasts improves the differentiated phenotype of murine embryonic stem cell-derived cardiomyocytes for cardiac tissue engineering. *Biotechnol. Bioeng.* 109, 813–822. doi: 10.1002/bit.23353

Passier, R., Oostwaard, D. W., Snapper, J., Kloots, J., Hassink, R. J., Kuijk, E., et al. (2005). Increased cardiomyocyte differentiation from human embryonic stem cells in serum-free cultures. *Stem Cells* 23, 772–780. doi: 10.1634/stemcells.2004-0184

Pierluigi, L., Giulia, P., Valentina, M., Gianfranco, S., Serena, Z., and Mauro, G. (2017). Single-dose intracardiac injection of pro-regenerative microRNAS improves cardiac function after myocardial infarction. *Circ. Res.* 120, 1298–1304. doi: 10.1161/CIRCRESAHA.116.309589

Pittenger, M. F., and Martin, B. J. (2004). Mesenchymal stem cells and their potential as cardiac therapeutics. *Circ. Res.* 95, 9–20. doi: 10.1161/01.RES.0000135902.99383.6f

Porrello, E. R., Mahmoud, A. I., Simpson, E., Hill, J. A., Richardson, J. A., Olson, E. N., et al. (2011). Transient regenerative potential of the neonatal mouse heart. *Science* 331, 1078–1080. doi: 10.1126/science.1200708

Porrello, E. R., Mahmoud, A. I., Simpson, E., Johnson, B. A., Grinsfelder, D., Canseco, D., et al. (2013). Regulation of neonatal and adult mammalian heart regeneration by the miR-15 family. *Proc. Natl. Acad. Sci. U.S.A.* 110, 187–192. doi: 10.1073/pnas.1208863110

Poss, K. D., Wilson, L. G., and Keating, M. T. (2002). Heart regeneration in zebrafish. *Science* 298, 2188–2190. doi: 10.1126/science.1077857

Prabhakaran, M. P., Kai, D., Ghasemi-Mobarakeh, L., and Ramakrishna, S. (2011). Electrospun biocomposite nanofibrous patch for cardiac tissue engineering. *Biomed. Mater.* 6:055001. doi: 10.1088/1748-6041/6/5/055001

Rabea, H., Daniela, P., Stefanie, Z., Ariane, F., Wira, H., Quan-Fu, X., et al. (2013). Inhibition of microRNA-92a protects against ischemia/reperfusion injury in a large-animal model. *Circulation* 128, 1066–1075. doi: 10.1161/CIRCULATIONAHA.113.001904

Rao, S. V., Zeymer, U., Douglas, P. S., Al-Khalidi, H., White, J. A., Liu, J., et al. (2016). Bioabsorbable intracoronary matrix for prevention of ventricular remodeling after myocardial infarction. *J. Am. Coll. Cardiol.* 68, 715–723. doi: 10.1016/j.jacc.2016.05.053

Reis, L. A., Chiu, L. L. Y., Feric, N., Fu, L., and Radisic, M. (2016). Biomaterials in myocardial tissue engineering. *J. Tissue Eng. Regen. Med.* 10, 11–28. doi: 10.1002/term.1944

Remaut, K., Sanders, N. N., De Geest, B. G., Braeckmans, K., Demeester, J., and De Smedt, S. C. (2007). Nucleic acid delivery: where material sciences and bio-sciences meet. *Mater. Sci. Eng. R Rep.* 58, 117–161. doi: 10.1016/j.mser.2007.06.001

Renault, M.-A., and Losordo, D. W. (2007). Therapeutic myocardial angiogenesis. *Microvasc. Res.* 74, 159–171. doi: 10.1016/j.mvr.2007.08.005

Riegler, J., Tiburcy, M., Ebert, A., Tzatzalos, E., Raaz, U., Abilez, O. J., et al. (2015). Human engineered heart muscles engraft and survive long term in a rodent myocardial infarction model. *Circ. Res.* 117, 720–730. doi: 10.1161/CIRCRESAHA.115.306985

Roche, E. T., Hastings, C. L., Lewin, S. A., Shvartsman, D. E., Brudno, Y., Vasilyev, N. V., et al. (2014). Comparison of biomaterial delivery vehicles for improving acute retention of stem cells in the infarcted heart. *Biomaterials* 35, 6850–6858. doi: 10.1016/j.biomaterials.2014.04.114

Rodell, C. B., Lee, M. E., Wang, H., Takebayashi, S., Takayama, T., Kawamura, T., et al. (2016). Injectable shear-thinning hydrogels for minimally invasive delivery to infarcted myocardium to limit left ventricular remodeling. *Circ. Cardiovasc. Interv.* 9:e004058.

Roy, S. M., and Sahoo, S. K. (2015). "Controlled drug delivery: polymeric biomaterials for," in *Encyclopedia of Biomedical Polymers and Polymeric Biomaterials*, Vol. 11, (Boca Raton, FL: CRC Press), 2135–2146. doi: 10.1081/e-ebpp-120050023

Ruan, J.-L., Tulloch, N. L., Razumova, M. V., Saiget, M., Muskheli, V., Pabon, L., et al. (2016). Mechanical stress conditioning and electrical stimulation promote contractility and force maturation of induced pluripotent stem cell-derived human cardiac tissue. *Circulation* 134, 1557–1567. doi: 10.1161/CIRCULATIONAHA.114.014998

Ruvinov, E., and Cohen, S. (2016). Alginate biomaterial for the treatment of myocardial infarction: progress, translational strategies, and clinical outlook. From ocean algae to patient bedside. *Adv. Drug Deliv. Rev.* 96, 54–76. doi: 10.1016/j.addr.2015.04.021

Ruvinov, E., Freeman, I., Fredo, R., and Cohen, S. (2016). Spontaneous coassembly of biologically active nanoparticles via affinity binding of heparin-binding proteins to alginate-sulfate. *Nano Lett.* 16, 883–888. doi: 10.1021/acs.nanolett.5b03598

Ruvinov, E., Harel-Adar, T., and Cohen, S. (2011a). Bioengineering the infarcted heart by applying bio-inspired materials. *J. Cardiovasc. Transl. Res.* 4, 559–574. doi: 10.1007/s12265-011-9288-9

Ruvinov, E., Kryukov, O., Forti, E., Korin, E., Goldstein, M., and Cohen, S. (2015). Calcium–siRNA nanocomplexes: what reversibility is all about. *J. Control. Release* 203, 150–160. doi: 10.1016/j.jconrel.2015.02.029

Ruvinov, E., Leor, J., and Cohen, S. (2010). The effects of controlled HGF delivery from an affinity-binding alginate biomaterial on angiogenesis and blood perfusion in a hindlimb ischemia model. *Biomaterials* 31, 4573–4582. doi: 10.1016/j.biomaterials.2010.02.026

Ruvinov, E., Leor, J., and Cohen, S. (2011b). The promotion of myocardial repair by the sequential delivery of IGF-1 and HGF from an injectable alginate biomaterial in a model of acute myocardial infarction. *Biomaterials* 32, 565–578. doi: 10.1016/j.biomaterials.2010.08.097

Ruvinov, E., Sapir, Y., and Cohen, S. (2012). Cardiac tissue engineering: principles, materials, and applications. *Synth. Lect. Tissue Eng.* 4, 1–200. doi: 10.2200/s00437ed1v01y201207tis009

Sabbah, H. N., Wang, M., Gupta, R. C., Rastogi, S., Ilsar, I., Sabbah, M. S., et al. (2013). Augmentation of left ventricular wall thickness with alginate

hydrogel implants improves left ventricular function and prevents progressive remodeling in dogs with chronic heart failure. *JACC Heart Fail.* 1, 252–258. doi: 10.1016/j.jchf.2013.02.006

Sachlos, E., and Czernuszka, J. T. (2003). Making tissue engineering scaffolds work. Review: the application of solid freeform fabrication technology to the production of tissue engineering scaffolds. *Eur. Cell. Mater.* 5, 39–40.

Saleh, M., and Ambrose, J. A. (2018). Understanding myocardial infarction. *F1000Res.* 7:F1000 Faculty Rev-1378. doi: 10.12688/f1000research.15096.1

Sapir, Y., Cohen, S., Friedman, G., and Polyak, B. (2012). The promotion of in vitro vessel-like organization of endothelial cells in magnetically responsive alginate scaffolds. *Biomaterials* 33, 4100–4109. doi: 10.1016/j.biomaterials.2012.02.037

Sapir, Y., Kryukov, O., and Cohen, S. (2011). Integration of multiple cell-matrix interactions into alginate scaffolds for promoting cardiac tissue regeneration. *Biomaterials* 32, 1838–1847. doi: 10.1016/j.biomaterials.2010.11.008

Seif-Naraghi, S. B., Singelyn, J. M., Salvatore, M. A., Osborn, K. G., Wang, J. J., Sampat, U., et al. (2013). Safety and efficacy of an injectable extracellular matrix hydrogel for treating myocardial infarction. *Sci. Transl. Med.* 5:173ra25. doi: 10.1126/scitranslmed.3005503

Shachar, M., and Cohen, S. (2003). Cardiac tissue engineering, ex-vivo: design principles in biomaterials and bioreactors. *Heart Fail. Rev.* 8, 271–276. doi: 10.1023/A:1024729919743

Shadrin, I. Y., Allen, B. W., Qian, Y., Jackman, C. P., Carlson, A. L., Juhas, M. E., et al. (2017). Cardiopatch platform enables maturation and scale-up of human pluripotent stem cell-derived engineered heart tissues. *Nat. Commun.* 8:1825. doi: 10.1038/s41467-017-01946-x

Shapira, A., Feiner, R., and Dvir, T. (2016). Composite biomaterial scaffolds for cardiac tissue engineering. *Int. Mater. Rev.* 61, 1–19. doi: 10.1179/1743280415y.0000000012

Shapiro, L., and Cohen, S. (1997). Novel alginate sponges for cell culture and transplantation. *Biomaterials* 18, 583–590. doi: 10.1016/S0142-9612(96)00181-0

Shevach, M., Fleischer, S., Shapira, A., and Dvir, T. (2014). Gold nanoparticle-decellularized matrix hybrids for cardiac tissue engineering. *Nano Lett.* 14, 5792–5796. doi: 10.1021/nl502673m

Shevach, M., Zax, R., Abrahamov, A., Fleischer, S., Shapira, A., and Dvir, T. (2015). Omentum ECM-based hydrogel as a platform for cardiac cell delivery. *Biomed. Mater.* 10:34106. doi: 10.1088/1748-6041/10/3/034106

Silva, G. V., Litovsky, S., Assad, J. A. R., Sousa, A. L. S., Martin, B. J., Vela, D., et al. (2005). Mesenchymal stem cells differentiate into an endothelial phenotype, enhance vascular density, and improve heart function in a canine chronic ischemia model. *Circulation* 111, 150–156. doi: 10.1161/01.CIR.0000151812.86142.45

Simons, M., Annex, B. H., Laham, R. J., Kleiman, N., Henry, T., Dauerman, H., et al. (2002). Pharmacological treatment of coronary artery disease with recombinant fibroblast growth factor-2: double-blind, randomized, controlled clinical trial. *Circulation* 105, 788–793. doi: 10.1161/hc0802.104407

Simons, M., and Raposo, G. (2009). Exosomes–vesicular carriers for intercellular communication. *Curr. Opin. Cell Biol.* 21, 575–581. doi: 10.1016/j.ceb.2009.03.007

Singh, A., Singh, A., and Sen, D. (2016). Mesenchymal stem cells in cardiac regeneration: a detailed progress report of the last 6 years (2010-2015). *Stem Cell Res. Ther.* 7:82. doi: 10.1186/s13287-016-0341-0

Sun, D., Zhuang, X., Xiang, X., Liu, Y., Zhang, S., Liu, C., et al. (2010). A novel nanoparticle drug delivery system: the anti-inflammatory activity of curcumin is enhanced when encapsulated in exosomes. *Mol. Ther.* 18, 1606–1614. doi: 10.1038/mt.2010.105

Sutton, M. G. S. J., and Sharpe, N. (2000). Left ventricular remodeling after myocardial infarction: pathophysiology and therapy. *Circulation* 101, 2981–2988. doi: 10.1161/01.cir.101.25.2981

Tang, J., Wang, J., Huang, K., Ye, Y., Su, T., Qiao, L., et al. (2018). Cardiac cell–integrated microneedle patch for treating myocardial infarction. *Sci. Adv.* 4:eaat9365. doi: 10.1126/sciadv.aat9365

Thakker, R., and Yang, P. (2014). Mesenchymal stem cell therapy for cardiac repair. *Curr. Treat. Options Cardiovasc. Med.* 16:323. doi: 10.1007/s11936-014-0323-4

Tibbitt, M. W., and Langer, R. (2017). Living biomaterials. *Acc Chem. Res.* 50, 508–513. doi: 10.1021/acs.accounts.6b00499

Torella, D., Ellison, G. M., Méndez-Ferrer, S., Ibanez, B., and Nadal-Ginard, B. (2006). Resident human cardiac stem cells: role in cardiac cellular homeostasis and potential for myocardial regeneration. *Nat. Rev. Cardiol.* 3, S8–S13.

Torella, D., Rota, M., Nurzynska, D., Musso, E., Monsen, A., Shiraishi, I., et al. (2004). Cardiac stem cell and myocyte aging, heart failure, and insulin-like growth factor-1 overexpression. *Circ. Res.* 94, 514–524. doi: 10.1161/01.res.0000117306.10142.50

Traverse, J. H., Henry, T. D., Dib, N., Patel, A. N., Pepine, C., Schaer, G. L., et al. (2019). First-in-man study of a cardiac extracellular matrix hydrogel in early and late myocardial infarction patients. *JACC Basic Transl. Sci.* 4, 659–669. doi: 10.1016/j.jacbts.2019.07.012

Tsur-Gang, O., Ruvinov, E., Landa, N., Holbova, R., Feinberg, M. S., Leor, J., et al. (2009). The effects of peptide-based modification of alginate on left ventricular remodeling and function after myocardial infarction. *Biomaterials* 30, 189–195. doi: 10.1016/j.biomaterials.2008.09.018

Urbanek, K., Torella, D., Sheikh, F., De Angelis, A., Nurzynska, D., Silvestri, F., et al. (2005). Myocardial regeneration by activation of multipotent cardiac stem cells in ischemic heart failure. *Proc. Natl. Acad. Sci. U.S.A.* 102, 8692–8697. doi: 10.1073/pnas.0500169102

Vagnozzi, R. J., Maillet, M., Sargent, M. A., Khalil, H., Johansen, A. K., Schwanekamp, J. A., et al. (2019). An acute immune response underlies the benefit of cardiac stem-cell therapy. *Nature* 577, 405–409. doi: 10.1038/s41586-019-1802-2

Vaishya, R. D., Mandal, A., Gokulgandhi, M., Patel, S., and Mitra, A. K. (2015). Reversible hydrophobic ion-paring complex strategy to minimize acylation of octreotide during long-term delivery from PLGA microparticles. *Int. J. Pharm.* 489, 237–245. doi: 10.1016/j.ijpharm.2015.04.075

Vandergriff, A., Huang, K., Shen, D., Hu, S., Hensley, M. T., Caranasos, T. G., et al. (2018). Targeting regenerative exosomes to myocardial infarction using cardiac homing peptide. *Theranostics* 8, 1869–1878. doi: 10.7150/thno.20524

Wang, L. L., Liu, Y., Chung, J. J., Wang, T., Gaffey, A. C., Lu, M., et al. (2017). Sustained miRNA delivery from an injectable hydrogel promotes cardiomyocyte proliferation and functional regeneration after ischaemic injury. *Nat. Biomed. Eng.* 1, 983–992. doi: 10.1038/s41551-017-0157-y

Wassenaar, J. W., Gaetani, R., Garcia, J. J., Braden, R. L., Luo, C. G., Huang, D., et al. (2016). Evidence for mechanisms underlying the functional benefits of a myocardial matrix hydrogel for post-MI treatment. *J. Am. Coll. Cardiol.* 67, 1074–1086. doi: 10.1016/j.jacc.2015.12.035

Webber, J., Steadman, R., Mason, M. D., Tabi, Z., and Clayton, A. (2010). Cancer exosomes trigger fibroblast to myofibroblast differentiation. *Cancer Res.* 70, 9621–9630. doi: 10.1158/0008-5472.CAN-10-1722

Wehman, B., Sharma, S., Pietris, N., Mishra, R., Siddiqui, O. T., Bigham, G., et al. (2016). Mesenchymal stem cells preserve neonatal right ventricular function in a porcine model of pressure overload. *Am. J. Physiol. Circ. Physiol.* 310, H1816–H1826. doi: 10.1152/ajpheart.00955.2015

Wei, H.-J., Chen, C.-H., Lee, W.-Y., Chiu, I., Hwang, S.-M., Lin, W.-W., et al. (2008). Bioengineered cardiac patch constructed from multilayered mesenchymal stem cells for myocardial repair. *Biomaterials* 29, 3547–3556. doi: 10.1016/j.biomaterials.2008.05.009

Wendel, J. S., Ye, L., Zhang, P., Tranquillo, R. T., and Zhang, J. J. (2013). Functional consequences of a tissue-engineered myocardial patch for cardiac repair in a rat infarct model. *Tissue Eng. Part A* 20, 1325–1335. doi: 10.1089/ten.tea.2013.0312

Wong, P. T., and Choi, S. K. (2015). Mechanisms of drug release in nanotherapeutic delivery systems. *Chem. Rev.* 115, 3388–3432. doi: 10.1021/cr5004634

Wu, Y., Wang, L., Guo, B., and Ma, P. X. (2017). Interwoven aligned conductive nanofiber yarn/hydrogel composite scaffolds for engineered 3d cardiac anisotropy. *ACS Nano* 11, 5646–5659. doi: 10.1021/acsnano.7b01062

Yanamandala, M., Zhu, W., Garry, D. J., Kamp, T. J., Hare, J. M., Jun, H., et al. (2017). Overcoming the roadblocks to cardiac cell therapy using tissue engineering. *J. Am. Coll. Cardiol.* 70, 766–775. doi: 10.1016/j.jacc.2017.06.012

Yang, H., Wei, L., Liu, C., Zhong, W., Li, B., Chen, Y., et al. (2019). Engineering human ventricular heart tissue based on macroporous iron oxide scaffolds. *Acta Biomater.* 88, 540–553. doi: 10.1016/j.actbio.2019.02.024

Yang, S., Leong, K.-F., Du, Z., and Chua, C.-K. (2001). The design of scaffolds for use in tissue engineering. Part I. Traditional factors. *Tissue Eng.* 7, 679–689. doi: 10.1089/107632701753337645

Yost, M. J., Baicu, C. F., Stonerock, C. E., Goodwin, R. L., Price, R. L., Davis, J. M., et al. (2004). A novel tubular scaffold for cardiovascular

tissue engineering. *Tissue Eng.* 10, 273–284. doi: 10.1089/10763270432279 1916

Zadpoor, A. A., and Malda, J. (2017). Additive manufacturing of biomaterials, tissues, and organs. *Ann. Biomed. Eng.* 45, 1–11. doi: 10.1007/s10439-016-17 19-y

Zhang, D., Lee, H., Zhu, Z., Minhas, J. K., and Jin, Y. (2016). Enrichment of selective miRNAs in exosomes and delivery of exosomal miRNAs *in vitro* and *in vivo*. *Am. J. Physiol. Circ. Physiol.* 312, L110–L121.

Zhang, D., Shadrin, I. Y., Lam, J., Xian, H.-Q., Snodgrass, H. R., and Bursac, N. (2013). Tissue-engineered cardiac patch for advanced functional maturation of human ESC-derived cardiomyocytes. *Biomaterials* 34, 5813–5820. doi: 10.1016/ j.biomaterials.2013.04.026

Zhang, J., Zhu, W., Radisic, M., and Vunjak-Novakovic, G. (2018). Can we engineer a human cardiac patch for therapy? *Circ. Res.* 123, 244–265. doi: 10.1161/ CIRCRESAHA.118.311213

Zhang, L., Qian, Z., Tahtinen, M., Qi, S., and Zhao, F. (2018). Prevascularization of natural nanofibrous extracellular matrix for engineering completely biological three-dimensional prevascularized tissues for diverse applications. *J. Tissue Eng. Regen. Med.* 12, e1325–e1336. doi: 10.1002/term. 2512

Zhang, Y., Liu, D., Chen, X., Li, J., Li, L., Bian, Z., et al. (2010). Secreted monocytic miR-150 enhances targeted endothelial cell migration. *Mol. Cell* 39, 133–144. doi: 10.1016/j.molcel.2010.06.010

Conflict of Interest: The authors declare that the research was conducted in the absence of any commercial or financial relationships that could be construed as a potential conflict of interest.

Copyright © 2020 Bar and Cohen. This is an open-access article distributed under the terms of the Creative Commons Attribution License (CC BY). The use, distribution or reproduction in other forums is permitted, provided the original author(s) and the copyright owner(s) are credited and that the original publication in this journal is cited, in accordance with accepted academic practice. No use, distribution or reproduction is permitted which does not comply with these terms.

frontiers in Bioengineering and Biotechnology

ORIGINAL RESEARCH
published: 20 March 2020
doi: 10.3389/fbioe.2020.00229

Decellularized Human Dermal Matrix as a Biological Scaffold for Cardiac Repair and Regeneration

Immacolata Belviso[1], Veronica Romano[1], Anna Maria Sacco[1], Giulia Ricci[2], Diana Massai[3], Marcella Cammarota[2], Angiolina Catizone[4], Chiara Schiraldi[2], Daria Nurzynska[1], Mara Terzini[3], Alessandra Aldieri[3], Gianpaolo Serino[3], Fabrizio Schonauer[1], Felice Sirico[1], Francesco D'Andrea[1], Stefania Montagnani[1], Franca Di Meglio[1] and Clotilde Castaldo[1]**

[1] Department of Public Health, University of Naples Federico II, Naples, Italy, [2] Department of Experimental Medicine, Università degli Studi della Campania Luigi Vanvitelli, Naples, Italy, [3] Department of Mechanical and Aerospace Engineering, Politecnico di Torino, Turin, Italy, [4] Department of Anatomy, Histology, Forensic-Medicine and Orthopedics, Sapienza University of Rome, Rome, Italy

OPEN ACCESS

Edited by:
Ipsita Roy,
The University of Sheffield,
United Kingdom

Reviewed by:
Sveva Bollini,
University of Genoa, Italy
Arnaud Scherberich,
University Hospital of Basel,
Switzerland

***Correspondence:**
Franca Di Meglio
franca.dimeglio@unina.it
Clotilde Castaldo
clotilde.castaldo@unina.it

Specialty section:
This article was submitted to Tissue Engineering and Regenerative Medicine, a section of the journal Frontiers in Bioengineering and Biotechnology

Received: 12 November 2019
Accepted: 05 March 2020
Published: 20 March 2020

Citation:
Belviso I, Romano V, Sacco AM, Ricci G, Massai D, Cammarota M, Catizone A, Schiraldi C, Nurzynska D, Terzini M, Aldieri A, Serino G, Schonauer F, Sirico F, D'Andrea F, Montagnani S, Di Meglio F and Castaldo C (2020) Decellularized Human Dermal Matrix as a Biological Scaffold for Cardiac Repair and Regeneration. Front. Bioeng. Biotechnol. 8:229. doi: 10.3389/fbioe.2020.00229

The complex and highly organized environment in which cells reside consists primarily of the extracellular matrix (ECM) that delivers biological signals and physical stimuli to resident cells. In the native myocardium, the ECM contributes to both heart compliance and cardiomyocyte maturation and function. Thus, myocardium regeneration cannot be accomplished if cardiac ECM is not restored. We hypothesize that decellularized human skin might make an easily accessible and viable alternate biological scaffold for cardiac tissue engineering (CTE). To test our hypothesis, we decellularized specimens of both human skin and human myocardium and analyzed and compared their composition by histological methods and quantitative assays. Decellularized dermal matrix was then cut into 600-μm-thick sections and either tested by uniaxial tensile stretching to characterize its mechanical behavior or used as three-dimensional scaffold to assess its capability to support regeneration by resident cardiac progenitor cells (hCPCs) *in vitro*. Histological and quantitative analyses of the dermal matrix provided evidence of both effective decellularization with preserved tissue architecture and retention of ECM proteins and growth factors typical of cardiac matrix. Further, the elastic modulus of the dermal matrix resulted comparable with that reported in literature for the human myocardium and, when tested *in vitro*, dermal matrix resulted a comfortable and protective substrate promoting and supporting hCPC engraftment, survival and cardiomyogenic potential. Our study provides compelling evidence that dermal matrix holds promise as a fully autologous and cost-effective biological scaffold for CTE.

Keywords: decellularized extracellular matrix, human dermal matrix, cardiac tissue engineering/regenerative medicine, human cardiac progenitor cells, biological scaffolds

INTRODUCTION

Accounting for more than 13% of all deaths, ischemic heart disease (IHD) is the single most common cause of death globally (GBD 2016 Causes of Death Collaborators, 2017). Although IHD is preventable by addressing behavioral risk factors such as tobacco use and harmful use of alcohol, unhealthy diet, physical inactivity, and obesity, it has remained the leading cause of

death for the last 16 years worldwide (GBD 2016 Risk Factors Collaborators, 2017). IHD is most commonly caused by the formation of a thrombus on a ruptured atherosclerotic plaque in the wall of a coronary artery. Blocking the blood flow, the clot prevents the supply of oxygen and nutrients to the myocardium fed by the involved vessel and leads to the ischemic death of cardiac myocytes. Since the heart has very limited regenerative ability, the reparative process that takes place after myocardial damage is characterized by the replacement of dead myocytes and the microenvironment they reside with non-compliant scar tissue. The complex and highly organized environment in which cells reside *in vivo* consists mostly of the extracellular matrix (ECM) that results from a tissue-specific combination of structural and functional proteins, polysaccharides and soluble factors (Brown and Badylak, 2014). The composition of the ECM and the exact spatial orientation of its components is responsible for both the biological signaling delivered to resident cells and the generation and transfer of mechanical forces to which cells are exposed (Frantz et al., 2010; Wade and Burdick, 2012). Therefore, the profound changes in the ventricular wall structure and mechanics caused by the ischemic damage impact upon cardiac function. Currently, the only effective therapeutic option capable of restoring the physiological heart function is heart transplant. However, due to organ donor shortage and to the high incidence of IHD, alternative strategies are urgently needed. Cardiac tissue engineering (CTE) aiming at developing three-dimensional myocardium-like scaffolds for therapeutic use by combining cells, synthetic or natural biomaterials, and biomimetic signals is rapidly emerging as the most promising alternative to heart transplant (Vunjak-Novakovic et al., 2010; Massai et al., 2013; Feric and Radisic, 2016; Stoppel et al., 2016; Fujita and Zimmermann, 2017; Weinberger et al., 2017; Madonna et al., 2019). Among biomaterials, decellularized tissues are emerging as the most promising scaffolds for regenerative medicine, due to their potential to provide natural biological cues (Yaling et al., 2016). However, the regenerative capability of the substrate depends not only on its chemical properties, but also on its ability to recapitulate the mechanical behavior of the native tissue, providing physical signals essential for mechanotransduction pathways (Huang et al., 2004; O'Brien, 2011). Specifically, in native myocardium, heart compliance and cardiomyocyte alignment and differentiation are strictly dependent on the elastic properties of the tissue. In particular, the content of elastin, the dominant mammalian elastic protein and the main component of elastic fibers (Kielty et al., 2002; Li et al., 2014), has been related to cardiac myocyte differentiation and maturation as it progressively increases in the developing mammalian heart, but then decreases soon after birth (Hanson et al., 2013; Thimm et al., 2015). Interestingly, elastin-based biomaterials have been developed and used to enhance tissue biocompatibility and promote stem cell differentiation (Celebi et al., 2012; Ozsvar et al., 2015). In this perspective, due to its remarkable intrinsic elasticity and to the anisotropic mechanical behavior (Terzini et al., 2016), the skin ECM might recapitulate, at least partially, the mechanical properties of the myocardium (Gilbert et al., 2007). Furthermore, while in the native myocardium elasticity is essentially conferred by the cardiomyocytes themselves (Jacot et al., 2010) and, thus, the decellularization process leads to scaffolds with poor mechanical properties, skin elasticity is provided by the ECM rather than by the resident cells and, then, the decellularization treatment is unlikely to cause loss of elasticity (Hoganson et al., 2010; Krieg and Aumailley, 2011). On this basis, we hypothesize that dermal decellularized ECM (d-ECM) may represent an innovative and viable alternate biological scaffold to restore myocardial microenvironment for future *in vitro* cardiac tissue production. To test our hypothesis, we collected specimens of adult human skin from patients undergoing abdominoplasty and prepared scaffolds of decellularized human skin (d-HuSk). The composition of d-HuSk and its potential to deliver biological signals comparable to that of the cardiac native matrix were evaluated by histochemistry and immunohistochemistry analyses and by specific quantitative assays. Additionally, uniaxial tensile tests were performed to mechanically characterize d-HuSk. Finally, 600-μm-thick sections of d-HuSk were seeded with resident human cardiac progenitor cells (hCPCs) to test their ability to ensure hCPC engraftment and survival and to support hCPC retention of the expression of markers specific for cardiac myocytes.

MATERIALS AND METHODS

Tissue Specimens

Skin specimens were obtained from patients undergoing abdominoplasty (n = 8, mean age 42.25 ± 7.94). Upon receipt, subcutaneous tissue was removed, and multiple samples were cut marking Langer's line orientation (Langer, 1978). Resulting specimens were then promptly processed for histological analysis or decellularization. Further, triplets of paired specimens weighting 20 mg each were collected for each patient for a comparative analysis between native and decellularized skin in terms of elastin and glycosaminoglycan (GAG) content, and the samples were snap frozen until use. Cardiac specimens were harvested from macroscopically uninjured areas of the left ventricle of explanted hearts of patients undergoing heart transplant (n = 10, mean age 49.5 ± 4.7) and snap-frozen or enzymatically digested to isolate hCPCs. Patients provided written informed consent and specimens were collected without patient identifiers, following protocols approved by the Hospital Ethical Committee and in conformity with the principles outlined in the Declaration of Helsinki.

Decellularization

Following the simple and effective protocol we recently described for the decellularization of human myocardial sections (Di Meglio et al., 2017), skin specimens and 600-μm-thick sections of human myocardium were incubated in decellularizing solution for 24 h. Decellularization of skin specimens was obtained by placing them in a beaker containing the decellularizing solution under constant stirring, while sections of human myocardium were decellularized (d-HuM) under constant agitation on an

orbital shaker. The solution was replaced every 8 h. During the decellularization of skin specimens, and more often after 16 h, the epidermis detached from the dermis and was removed. d-HuSk and d-HuM samples were then rinsed for 24 h in antibiotic solution and then for an additional 30 min in sterile bidistilled water. After decellularization, samples of d-HuSk were either fixed in formalin for paraffin embedding and histological analysis or stored at −80°C until use for molecular analysis and cryosectioning. Sections of d-HuM were either stored at 4°C in Ham's F12 medium (Sigma-Aldrich) supplemented with 10% FBS (Sigma-Aldrich), 5% horse serum (Sigma-Aldrich), 10 ng/ml basic fibroblast growth factor (bFGF) (Peprotech, Rocky Hill, NJ, United States), and 50 IU/ml penicillin G-streptomycin (Sigma-Aldrich) (F12K medium), or stored in dry conditions at −80°C until use.

Cryosectioning of Decellularized Dermal Matrix

As previously described for human myocardium (Di Meglio et al., 2017), frozen specimens of d-HuSk were mounted on a cryostat chuck using Tissue Freezing Medium (Leica Microsystems, Wetzlar, Germany) and sliced into 600-μm-thick sections by a Leica CM1950 cryostat (Leica Microsystems). Cryosections were collected in sterile cell culture dishes and stored at 4°C in the same medium described for d-HuM sections until use.

Quantitative Measurement of DNA Content

Genomic DNA (gDNA) was extracted from specimens of frozen native skin (n = 4) and d-HuSk (n = 6), using the AllPrep DNA/RNA Mini Kit (Qiagen, Hilden, Germany), according to the manufacturer's instructions. DNA concentration was determined by measuring the absorbance at 260 nm using a Nanodrop1000 (Thermo Scientific, Waltham, MA, United States) and the gDNA band was visualized with agarose electrophoresis. Data were averaged and expressed as the mean ng of DNA ± SEM per mg of dry tissue.

Histochemistry and Immunohistochemistry

Specimens of native skin (n = 8) and d-HuSk (n = 8) were fixed in 10% neutral-buffered formalin, dehydrated in a graded series of alcohols, embedded in paraffin, then sliced into serial 5-μm-thick sections. Following standard protocols, after rehydration sections were stained with Hematoxylin and Eosin to evaluate the effectiveness of decellularization, and with Paraldehyde fuchsin Gomori or Alcian blue to detect elastic fibers or GAGs, respectively, by specific staining kits (both from Bio-Optica, Milan, Italy). For the immunodetection of collagen, fibronectin, tenascin, and laminin, sections of d-HuSk were deparaffinized, rehydrated, and immunostained using indirect immunoperoxidase technique. The presence and localization of antigen · antibody complexes were revealed by the UltraVision LP Detection System HRP Polymer & DAB Plus Chromogen (Thermo Scientific, Waltham, MA, United States), as previously described (Di Meglio et al., 2017). Stained sections were evaluated and documented by at least three independent observers using a light microscope DM2000 Led (Leica Microsystems) equipped with an ICC50HD camera (Leica Microsystems).

Quantitative Measurement of Elastin

Elastin was extracted from paired specimens of native skin (n = 5) and d-HuSk (n = 5) and from frozen specimens of d-HuM (n = 5), weighting 20 mg each before decellularization. Following manufacturer's directions, elastin was extracted heating specimens at 100°C for three 1-h periods in 0.25 M oxalic acid. Tissue extracts were then assayed in the Fastin Elastin Assay quantitative dye-binding method (Biocolor, Ltd., Carrickfergus, United Kingdom), in accordance with manual provided by manufacturer. Briefly, samples were incubated with Elastin Precipitating Reagent to obtain the complete precipitation of α-elastin, to which Dye Reagent was then added. Elastin-Dye complexes that formed were treated with Dye Dissociation Reagent before proceeding with absorbance reading. All samples were tested in triplicate and the absorbance was read at 490 nm using the ELx800 Absorbance Microplate Reader (BioTek Instruments, Winooski, VT, United States), and analyzed with Microsoft Excel (Microsoft Corp., Redmond, WA, United States) to generate the calibration curve and calculate the final concentration of elastin for each absorbance reading. Data were averaged and expressed as the mean value ± SEM of μg of elastin per mg of dry tissue.

Quantitative Measurement of Sulfated GAGs (sGAGs)

As described for the Fastin Elastin Assay, frozen samples of 20 mg each of native skin (n = 5) and frozen samples of d-HuSk (n = 5) and d-HuM (n = 5) weighting 20 mg each before decellularization were assayed for the quantitative analysis of sGAG content in Blyscan Assay (Biocolor, Ltd.). All samples were tested in triplicate. Assay was performed according to previously published protocol (Di Meglio et al., 2017). Absorbance was read at 600 nm using the BioPhotometer (Eppendorf) and analyzed with Microsoft Excel (Microsoft Corp.) to generate the calibration curve and calculate the final concentration of sGAGs for each absorbance reading. Data were averaged and expressed as the mean value ± SEM of μg of sGAGs per mg of dry tissue.

Growth Factor Array

Frozen d-HuSk (n = 4) and d-HuM (n = 4) specimens were lysed as previously described (Di Meglio et al., 2017). Protein concentration was determined by a Bradford assay, and then 100 μg of each tissue lysate was assayed in the Human Growth Factor Array C1 (Raybiotech, Norcross, GA, United States). The assay and following analysis were performed as previously described (Di Meglio et al., 2017). Data were expressed as the mean ± SEM.

Mechanical Characterization

The mechanical behavior of d-HuSk was characterized by uniaxial tensile stretching. For three donors, 3 to 8 cryosections

were cut along and across the Langer's lines with a custom-made die cutter, and stored in 50 ml sterile plastic tubes in saline solution at 4°C. The specimens were measured by photogrammetry, using a digital camera (EOS 5D Mark II, Canon Inc., Tokyo, Japan), with an autofocus lens for macro photography (EF 100 mm f/2.8 Macro USM, Canon Inc.), mounted on a stand. The measuring process was performed by ImageJ software[1]. The average width of the specimens resulted in 4.80 ± 0.84 mm, while thickness, set during the cryosectioning, was assumed to be equal to 600 μm. To characterize the specimens in room-temperature and "wet-like" conditions, the plastic tubes were taken out of the fridge 1 h before the test, and each specimen was collected just before testing. Uniaxial tensile tests were carried out with a universal testing machine (QTest/10, MTS Systems Corporation, Eden Prairie, Minnesota, United States), and specimens were clamped in titanium grips with knurled-flat faces, specifically developed for preventing specimen slipping (TA Instruments, Inc., New Castle, DE, United States). The grips were placed at an initial distance of 5 mm, and the strain rate was set equal to 3.2% s^{-1} (Terzini et al., 2016). The results of uniaxial tensile tests were reported in terms of engineering stress and strain. The engineering stress σ was calculated as:

$$\sigma = \frac{F}{A_0}$$

where F is the recorded applied force, and A_0 is the original cross-sectional area of the specimen. The engineering strain ε, referred to the increasing distance between the grips, was expressed as:

$$\varepsilon = \frac{\Delta L}{L_0}$$

where ΔL is the change in length, and L_0 is the original length of the specimen. From the engineering stress-strain curves, the stiffness of the specimens was measured as the elastic modulus at increasing levels of strain. In particular, considering the human left ventricular longitudinal strain range (Kuznetsova et al., 2008), the elastic moduli at 10% ($E_{10\%}$) and 20% ($E_{20\%}$) of strain were computed as the stress-strain curve slope at 10 and 20% of strain, respectively. The average values of the measured elastic moduli were then compared with literature data on human myocardium (Jawad et al., 2007; Chen et al., 2008; Bouten et al., 2011; Sommer et al., 2015; Terzini et al., 2016). In addition, to assess the tissue rupture behavior, the ultimate tensile strength (UTS, i.e., the maximum stress achieved by the stress-strain curve) and the ultimate strain (ε_{UTS}, i.e., the strain at which the UTS occurs) were investigated. The method applied to extract UTS and ε_{UTS} is described in detail in Section "**Supplementary Material**" and **Supplementary Table S1**.

Cell Culture

To isolate hCPCs, myocardial specimens were dissected, minced, and enzymatically disaggregated as previously described (Nurzynska et al., 2013). Briefly, samples were digested with 0.25% trypsin and 0.1% collagenase (both from Sigma-Aldrich) and the obtained cell population was depleted of fibroblasts by incubation with anti-fibroblast MicroBeads (Miltenyi Biotec, Bergisch Gladbach, Germany), to magnetically label fibroblasts, and then loading cells onto a MACS column (Miltenyi Biotec) placed in the magnetic field of a MACS separator (Miltenyi Biotec) to retain labeled fibroblasts within the column and allow unlabeled cells to run through. Hence, hCPCs were purified from the negative cell fraction by positive selection with anti-human-CD117 MicroBeads. The so obtained hCPCs were then collected and used for repopulating d-HuSk and d-HuM to evaluate d-HuSk cytocompatibility and ability to support hCPC engraftment and differentiation potential.

In vitro Assay of Decellularized Dermal Matrix Biocompatibility

Six hundred-micrometer-thick cryosections of d-Husk (n = 3) were cut and placed on sterile 96-well culture plates, sterilized by exposure to ultraviolet radiation for 40 min, then rehydrated for 7 days with F12K medium in an incubator at 37°C with 5% CO_2. Successively, 5×10^4 hCPCs were seeded onto each d-HuSk bearing-well and cultured under standard static culture conditions using the same medium. Sterilized and rehydrated d-HuM (n = 3) sections were seeded and cultured in the same conditions and used as a reference. Beginning at 48 h after seeding, and then every day for 1 week, cell death rate was assessed using trypan blue exclusion assay following a previously described protocol with some modifications (Di Meglio et al., 2017). Specifically, every day cells were detached from a subset of wells in the multiwell plates by incubation with 0.25% trypsin-EDTA solution (Sigma-Aldrich) for 10 min. Detached cells were then stained with trypan blue stain (0.4% in PBS) (Lonza, Walkersville, MD, United States) for 2 min at room temperature and counted by three independent observers using a hemocytometer. Due to a damage of the plasma membrane, dead cells uptake the dye but are not capable of excluding it and stain blue. Alive cells, instead, exclude the dye and can be recognized among the dead blue cells as unstained cells. Therefore, such assay allows the computation of both cell death rate and cell viability. The percentage of dead cells and of alive cells over total cells for each time point was calculated and expressed as the mean percentages of the total number of cells ± SEM.

Scanning Electron Microscopy

Six hundred-micrometer -thick cryosections of d-HuSk placed in 35-mm culture dishes were sterilized, rehydrated and repopulated with 5×10^5 hCPCs as described above and cultured under standard culture conditions for 4 weeks. Surface ultrastructure was then studied by Scanning Electron Microscopy (SEM). Briefly, samples fixed in 10% neutral-buffered formalin were dehydrated with ascending ethanol series (30–100%), subjected to Critical Point Dryer (EMITECH K850), mounted on a stub and sputtered with platinum-palladium Denton Vacuum (DESK V). FESEM (Field-Emission SEM) Supra 40 (ZEISS;

[1]https://imagej.nih.gov/ij/download.html

EHT = 5.00 kV, WD = 22 mm, detector in lens) was used for observation.

Gene Expression Analysis

Total RNA was extracted from hCPCs cultured on d-HuSk (n = 4) and on d-HuM (n = 4) for 4 weeks. RNA was dissolved in RNase-free water, and the final concentration was determined using a Nanodrop 1000 spectrophotometer (Thermo Scientific). Then, 100 ng of RNA extracted from each sample was reverse transcribed into cDNA using a QuantiTect Reverse Transcription Kit (Qiagen) and gene expression analysis for genes specific for cardiac program, like *GATA4* and *TBX5*, and for cardiac myocytes, like *CX43*, *CX37*, *TBX3*, *TBX5*, *MEF2C*, *ACTC1*, *MYH7* (**Supplementary Table S4**) was performed by real-time PCR as previously described (Di Meglio et al., 2010). All samples were tested in triplicate with the housekeeping gene (*GAPDH*). Comparative quantification of target gene expression in the samples was performed based on the cycle threshold (Ct) normalized to the housekeeping gene.

Immunofluorescence

Immunofluorescence experiments were performed on hCPCs cultured on d-HuSk for 4 weeks using primary antibodies specific for actin (α-sarcomeric) (Sigma-Aldrich), Connexin-43 (Abcam, Cambridge, United Kingdom), desmin and dystrophin (Sigma-Aldrich) following a previously published protocol (Castaldo et al., 2013; Nurzynska et al., 2013). Microscopic analyses were performed with a Nikon Eclipse Ti-E Microscope DS-Qi2 by NIS Elements software (Nikon Instruments, Tokyo, Japan). The expression of cardiac myocyte differentiation markers was also analyzed by confocal microscopy. To this aim, formalin-fixed samples were permeabilized for 3 h with a permeabilizing solution containing 1% BSA and 0.1% Triton in PBS, then blocked with 5% donkey serum and incubated overnight with primary antibodies. Then samples were extensively washed with PBS and incubated for 90 min with a fluorescein-conjugated donkey anti-mouse (Jackson ImmunoResearch Europe). Rhodamin-conjugated phalloidin was used to detect F-actin while TO-PRO3 iodide fluorescent dye 642/661 (Invitrogen) was used for nuclear staining. As a negative control, the primary antibody was omitted. Microscopic analysis and digital microphotography was performed by a Leica Confocal Microscope (Laser Scanning TCS SP2 equipped with Kr/Ar and He/Ne lasers) performing optical spatial series with a step size of 2 μm.

Statistical Analysis

Statistical analysis was performed using GraphPad Prism version 5.00 for Windows (GraphPad Software, San Diego, CA, United States[2]). Data obtained from the growth factor array, trypan blue exclusion assay and qPCR were analyzed using t-test, while data obtained from the analyses of Elastin and GAG content were analyzed using one-way analysis of variance (ANOVA) with Tukey's post-test. Further, two-way ANOVA was adopted to determine how the response to uniaxial tensile tests was affected by the "donor" and the "orientation" factors. All experiments were performed in triplicate and all data were expressed as the mean ± SEM. A value of $p \leq 0.05$ was used to identify any statistically significant differences.

[2]www.graphpad.com

RESULTS

Evaluation of the Decellularization Procedure

The first obvious change that occurred with the decellularization was macroscopic, as with respect to the brownish color of native skin (**Figure 1A**) the d-HuSk samples turned completely white (**Figure 1B**). Hematoxylin and Eosin staining, and quantitative measurement of DNA content were then used to evaluate the effectiveness of decellularization. When compared with native skin (**Figure 1C**), the noticeable absence of nuclei in d-HuSk (**Figure 1D**) emerged from the histological analysis while the residual dsDNA content in d-HuSk, as measured by quantitative analysis, resulted as low as 7.50 ± 2.162 ng per mg of dry tissue (**Figures 1E,F**). Therefore, d-HuSk fulfilled the requirements proposed for the evaluation of the effectiveness of decellularization procedures, which include the absence of nuclei as revealed by histology and a content of dsDNA per mg of dry tissue below the set threshold of 50 ng (Crapo et al., 2011). An overall well-preserved organization of the dermal connective tissue in d-HuSk was also apparent at the histological analysis (**Figure 1D**).

Analysis of Decellularized Dermal Matrix Composition

Paraldehyde fuchsin Gomori staining and Alcian blue staining were used to evaluate the effects of the decellularization procedure on dermal architecture and to assess the retention and distribution of elastic fibers and GAGs in d-HuSk. Additionally, quantitative dye-binding assays were used to perform comparative analyses in elastin and GAG content between d-HuSk and native skin to confirm the effectiveness of decellularization in preserving matrix composition, and between d-HuSk and d-HuM to evaluate whether the content of the investigated components of the ECM in d-HuSk was comparable to that in cardiac matrix. Paraldehyde fuchsin Gomori staining clearly showed the presence of elastic fibers in native skin (**Figure 2A**) and in d-HuSk (**Figure 2B**), where the retention and distribution of elastic fibers resulted more obvious in the connective tissue surrounding well-preserved blood vessels (**Figure 2B**). Quantitative Fastin Elastin assay not only confirmed the presence of elastin in d-HuSk but also showed that elastin content did not differ significantly from that of native skin (34.205 ± 2.529 μg/mg of dry tissue in d-HuSk vs. 37.577 ± 2.561 μg/mg of dry tissue in native skin) (**Figure 2C**). Similarly, Alcian blue staining revealed the presence of GAGs in native skin (**Figure 2D**) and their retention in d-HuSk (**Figure 2E**), while quantitative Blyscan assay provided further confirmation of the effectiveness of decellularization procedure in producing a well-preserved

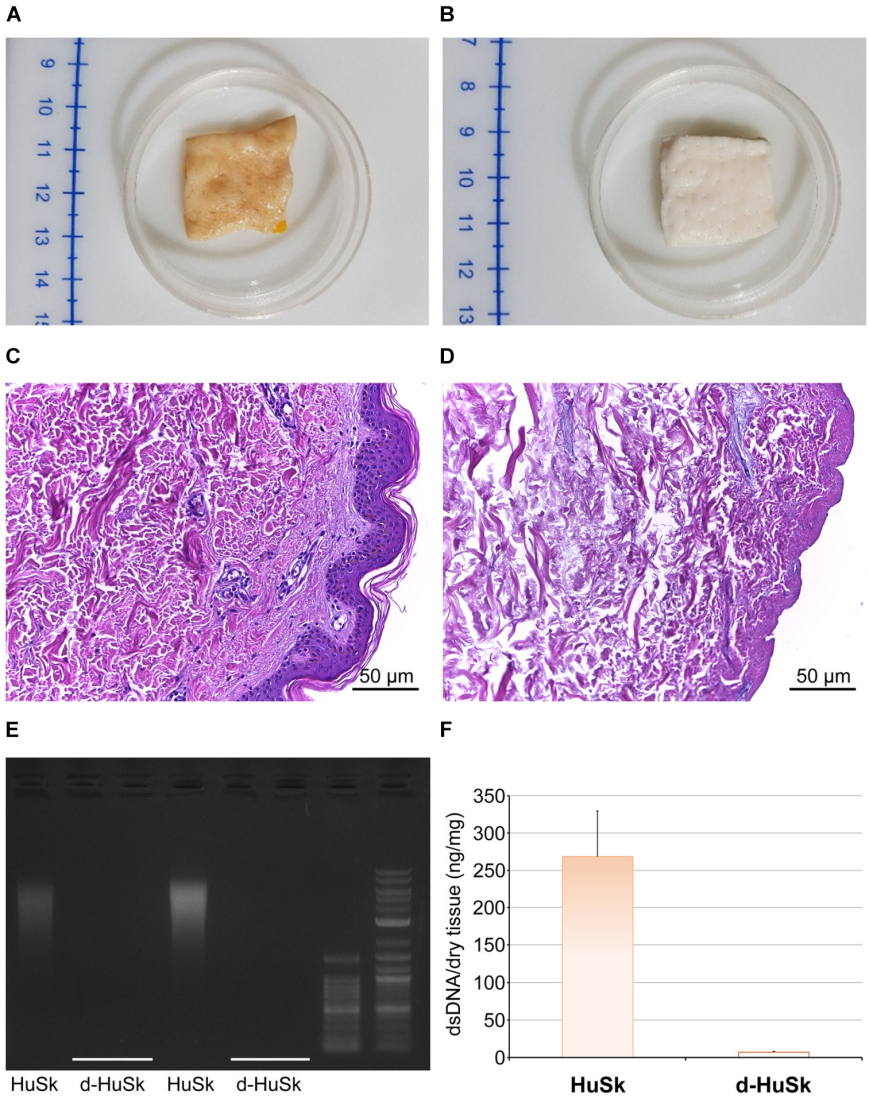

FIGURE 1 | Evaluation of the effectiveness of the decellularization procedure of adult human skin. Representative images of macroscopic examination of native human skin (HuSk) **(A)** and decellularized human skin (d-HuSk) **(B)** showing an obvious change in color after decellularization. Representative images of hematoxylin and eosin staining comparing HuSk **(C)** with d-HuSk **(D)** and showing the preserved tissue architecture and the absence of nuclei in d-HuSk (Scale bar: 50 µm). **(E)** Representative gel electrophoresis revealing an extremely low content of residual dsDNA in d-HuSk when compared with HuSk. **(F)** Quantification of dsDNA in d-HuSk showing a content well below that of HuSk and the proposed criterion of 50 ng.

dermal matrix containing amounts of GAGs that did not differ significantly from those of native skin (76.89 ± 14.22 µg/mg of dry tissue in d-HuSk vs. 100.70 ± 17.36 µg/mg of dry tissue in native skin) (**Figure 2F**). Conversely, while the elastin content of d-HuSk did not differ significantly from that of d-HuM (34.205 ± 2.529 µg/mg of dry tissue vs. 48.18 ± 9.629 µg/mg of dry tissue) (**Figure 3A**), quantitative analysis revealed in d-HuSk a significantly higher content of GAGs than in d-HuM (76.89 ± 14.220 µg/mg of dry tissue vs. 12.60 ± 2.30 µg/mg of dry tissue, $p \leq 0.001$) (**Figure 3B**).

To further evaluate the suitability of d-HuSk as substitute for cardiac ECM, we evaluated by immunohistochemistry the presence and localization in d-HuSk of structural and functional proteins that are components of both cardiac and dermal ECM. Immunohistochemical analysis revealed that d-HuSk contained ECM proteins of critical importance for myocardium development and maintenance like the types I, III, and IV collagens (**Figures 4A–C**), and the non-collagenous proteins fibronectin, laminin, and tenascin (**Figures 4D–F**). Types I and III (**Figures 4A,B**) collagens along with fibronectin and tenascin (**Figures 4D,F**) were scattered throughout the dermis, where type I collagen (**Figure 4A**) and fibronectin (**Figure 4D**) were visible as thicker bundles, while type III collagen (**Figure 4B**) and tenascin (**Figure 4F**) formed a delicate texture. Type IV collagen (**Figure 4C**) and laminin (**Figure 4E**) were localized mostly in the basement membrane of vessels, instead. Since the ECM is

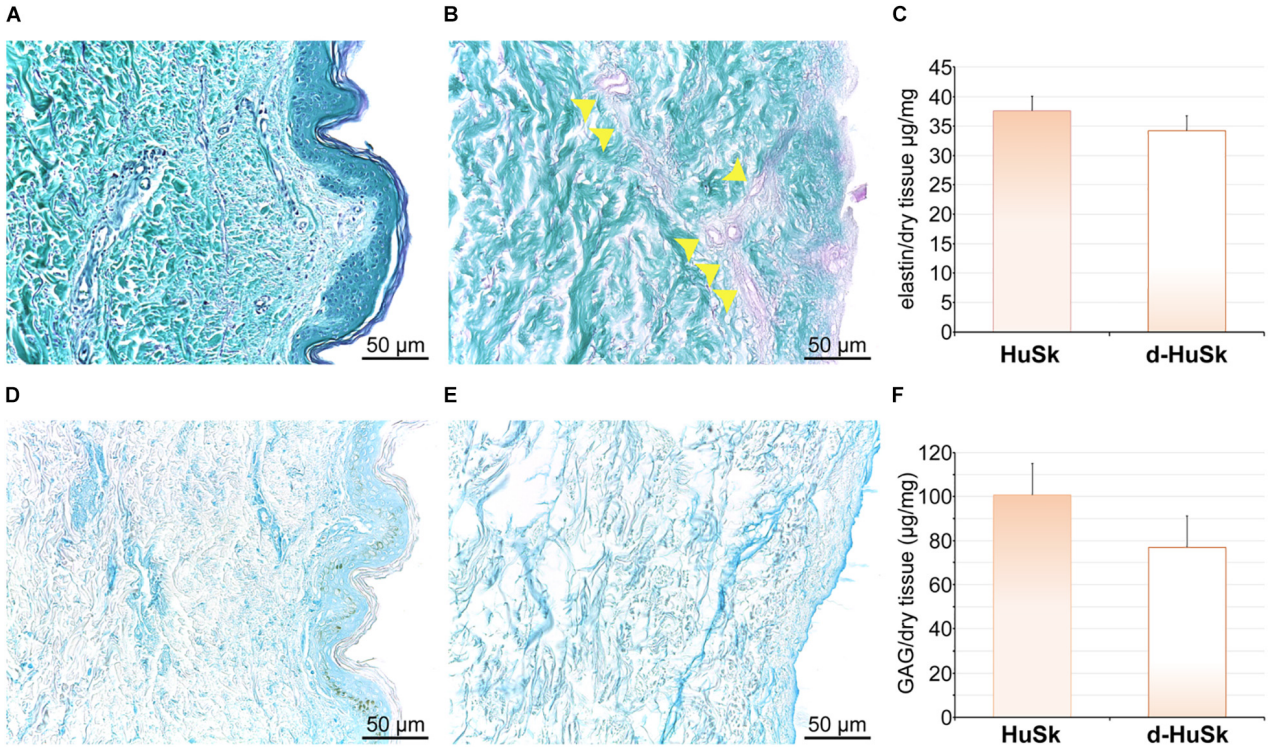

FIGURE 2 | Histochemical and quantitative analysis of elastin and GAG content in native human skin (HuSk) and in d-HuSk. Representative images of the histochemical analysis performed by Paraldehyde fuchsin Gomori staining showing the presence of elastic fibers in HuSk **(A)** and d-HuSk **(B)**. Patent blood vessels surrounded by abundant elastic fibers are apparent in d-HuSk (yellow arrowheads). **(C)** Quantification of elastin by specific dye-binding assay showing comparable content of elastin in d-HuSk and HuSk. Representative images of the histochemical analysis performed by Alcian Blue staining and showing by the light blue color the presence of GAGs in HuSk **(D)** and d-HuSk **(E)**. **(F)** Quantification of GAGs by specific dye-binding assay showing no statistically significant difference in content of GAGs in d-HuSk and HuSk. Scale bar is 50 µm.

known to function as storage for growth factors, we performed a comparative analysis of the growth factor profile of d-HuSk and d-HuM by protein array (**Figure 5**). The analysis revealed that the two matrices contained, to a large extent, the same growth factors, including hepatocyte growth factor (HGF), insulin-like growth factor (IGF), stem cell factor (SCF), platelet-derived growth factor (PDGF), and vascular endothelial growth factor (VEGF). Additionally, d-HuSk resulted enriched with growth factors that were virtually absent in d-HuM, like granulocyte-macrophage colony-stimulating factor (GMCSF) and transforming growth factor (TGF-beta), and contained significantly higher amount of growth factors like basic fibroblast growth factor (bFGF) and epidermal growth factor (EGF).

Mechanical Characterization

To investigate the d-HuSk mechanical behavior, uniaxial tensile tests were performed on d-HuSk specimens oriented along and across the Langer's lines. Focusing on the human left ventricular longitudinal strain range (Kuznetsova et al., 2008), specimens oriented along the Langer's lines presented, at 10% of strain, average elastic modulus $E_{10\%}$ values equal to 0.25 ± 0.13 MPa, and, at 20% of strain, average elastic modulus $E_{20\%}$ values equal to 0.42 ± 0.26 MPa (**Figures 6A,B**). These values were comparable both with that reported in literature for native human myocardium at the end of diastole (0.2–0.5 MPa, dotted lines in **Figures 6A,B**) (Jawad et al., 2007; Chen et al., 2008; Bouten et al., 2011), and with human myocardium elastic moduli values measured by Sommer et al. (2015) along (0.26 ± 0.06 MPa) and across (0.15 ± 0.06 MPa) the fibers, calculated as the slope of the mean equi-biaxial engineering stress-strain curves at 10% strain on human myocardial tissue samples from 26 subjects (gray-colored bands in **Figure 6A**, respectively). Measured $E_{10\%}$ and $E_{20\%}$ values of specimens oriented along the Langer's lines were higher (on average: +58.4% ± 12.1% for $E_{10\%}$; +69.9% ± 10.3% for $E_{20\%}$; $p < 0.0001$) than the average elastic moduli measured for the across-fiber specimens (0.12 ± 0.07 MPa for $E_{10\%}$, **Figure 6A**; 0.15 ± 0.09 MPa for $E_{20\%}$, **Figure 6B**). Moreover, specimens oriented along Langer's lines showed a higher rupture resistance in terms of ultimate tensile strength UTS (**Figure 6C**), although the ultimate strain ε_{UTS} values did not present significant differences (**Figure 6D**). The only exception was represented by specimens from the third donor, characterized by higher UTS values in across-fiber specimens, however, this discrepancy was not statistically significant. Variance analyses are reported in **Supplementary Tables S2**, **S3**. Both the "donor" and the "orientation" factors were significant when considered individually ($p < 0.05$), with the only exception of ε_{UTS} which did not show significant differences.

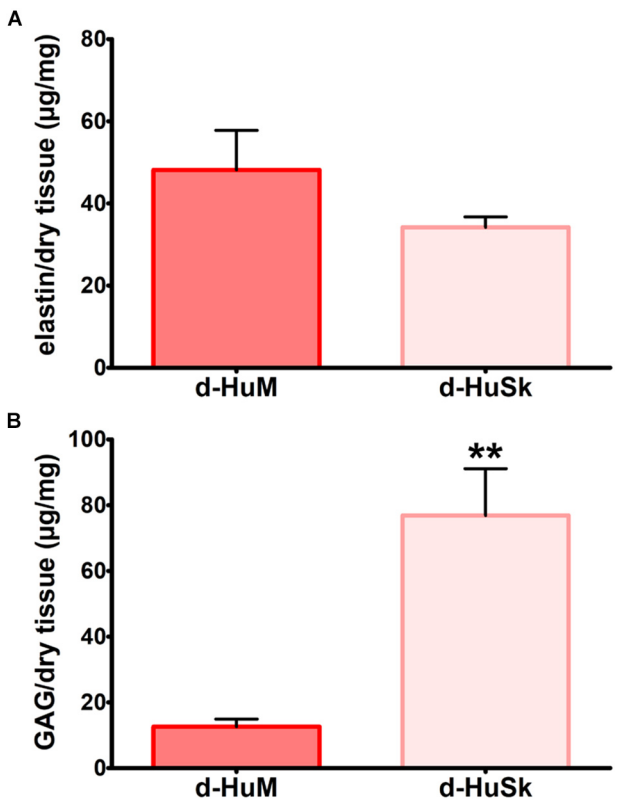

FIGURE 3 | Comparative analysis of the content of elastin and GAGs in decellularized human myocardium (d-HuM) and d-HuSk. Graphs comparing the content of elastin **(A)** and GAG **(B)** between d-HuM and d-HuSk evaluated by specific quantitative dye-binding assays. Double asterisks indicate very significant difference (**$p \leq 0.01$).

Effects of Decellularized Dermal Matrix on hCPCs *in vitro*

To evaluate the ability of d-HuSk to serve as a viable substitute for cardiac native microenvironment, we seeded and cultured hCPCs on d-HuSk and used as a reference hCPCs seeded and cultured on d-HuM in the same conditions. By binding the nuclear DNA, the DAPI staining showed the presence of hCPCs that engrafted onto d-HuSk (**Figure 7A**), while SEM analysis not only confirmed the engraftment of hCPCs on d-HuSk but also allowed to visualize the cell-to-cell contacts (**Figure 7B**) and to examine the cellular morphology. hCPCs engrafted on d-ECM appeared either as mesenchymal-like cells characterized by elongated irregular shape and multiple filopodia (**Figure 7C**) or as rectangular/polygonal-shaped cells resembling differentiating cardiomyocyte (**Figure 7D**).

Cell death rate and cell viability of hCPCs cultured on d-HuSK or on d-HuM were quantified using a trypan blue exclusion assay. The death rate of hCPCs measured 48 h after seeding did not differ significantly between d-HuM and d-HuSk (9.814 ± 1.792% and 9.112 ± 1.532%, respectively) and on both matrices the hCPC death rate dramatically decreased with time, till it reached values well below 1% of total cells, without any statistically significant differences between the two matrices (0.257 ± 0.107% on d-HuM and 0.253 ± 0.104% on d-HuSk). Obviously, cell viability had an inverted trend and increased with time on both d-HuM and d-HuSk. Specifically, the mean percentage of live cells was 90.186 ± 1.792% and 90.888 ± 1.792% after 48 h on d-HuM and d-HuSk, respectively, but increased up to 99.743 ± 0.107% and 99.747 ± 0.107% after 7 days on d-HuM and d-HuSk, respectively (**Figure 8**). Finally, to assess the suitability of d-HuSk to serve as a cardiogenic environment for hCPCs, we analyzed the expression of cardiac myocyte differentiation markers, again using as a reference the expression of the same markers in hCPCs cultured in the same conditions on d-HuM. Gene expression analysis showed that not only hCPCs cultured on d-HuSk for 4 weeks retained the expression of markers typical of cardiac myocytes, but the transcription of all investigated genes was also significantly up-regulated ($p \leq 0.05$) up to twofold in hCPCs cultured on d-HuSk (**Figure 9**). Moreover, the expression of cardiac myocyte specific markers by hCPCs engrafted onto d-HuSk was further evaluated by immunocytochemistry and the analyses at the fluorescence or confocal microscope showed the immunopositivity of hCPCs engrafted onto d-HuSk for the markers investigated. Clearly, the main cell population of hCPCs consisted of cells expressing alpha-sarcomeric actin and connexin-43 (**Figures 10A,B**), as well as desmin and dystrophin (**Figures 10C,D**) that are all markers of cardiac myocytes. The confocal microscope revealed as F-actin filaments distributed in approximately parallel rows, a pattern that suggests cardiomyocyte differentiation.

DISCUSSION

Projections show that by 2030 the prevalence of IHD will increase about 18% from 2013 estimates and almost 23.6 million people will die from CVDs, mainly from heart disease and stroke (Mozaffarian et al., 2016). Although not all coronary events are lethal, most of them lead to the formation of a permanent scar that, rather than merely be an inert region of the heart wall, holds the potential to complicate the clinical course by promoting reactive fibrosis in the uninjured myocardium (Schelbert et al., 2014). Indeed, reparative scar tissue, through pro-fibrotic signaling factors that induce transdifferentiation of fibroblast to myofibroblasts and ECM deposition (Frangogiannis, 2014; Talman and Ruskoaho, 2016), might eventually lead to heart failure. No current pharmacological therapy holds the potential to restore the histological integrity of the myocardium. Therefore, engineered cardiac tissue, developed through a combination of supporting scaffolds, cardiac specific cell lineages with regenerative ability, biological signals, such as growth factors and ECM components, and mechanical and electrical stimulation (Zimmermann et al., 2000; Radisic et al., 2004; Zhang et al., 2013; Tiburcy et al., 2017; Ronaldson-Bouchard et al., 2018), is rapidly and powerfully emerging as the only alternative therapeutic approach with the potential to accomplish the challenging task of reestablishing the structural, biomechanical and functional integrity of ischemic myocardium. Unquestionably, the best-performing scaffold in terms of both biological signaling

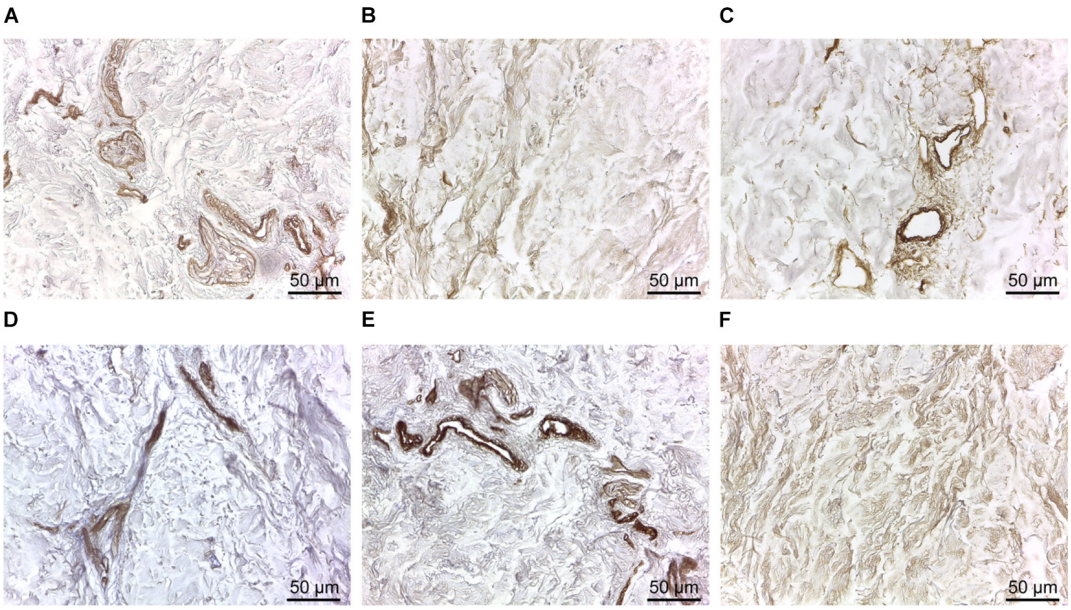

FIGURE 4 | Immunodetection of collagenous and non-collagenous ECM proteins in d-HuSk. Representative images of the immunohistochemical analysis showing the presence and localization in d-HuSk of type I **(A)**, type III **(B)**, and type IV **(C)** collagen, and of fibronectin **(D)**, laminin **(E)**, and tenascin **(F)**. Scale bar is 50 μm.

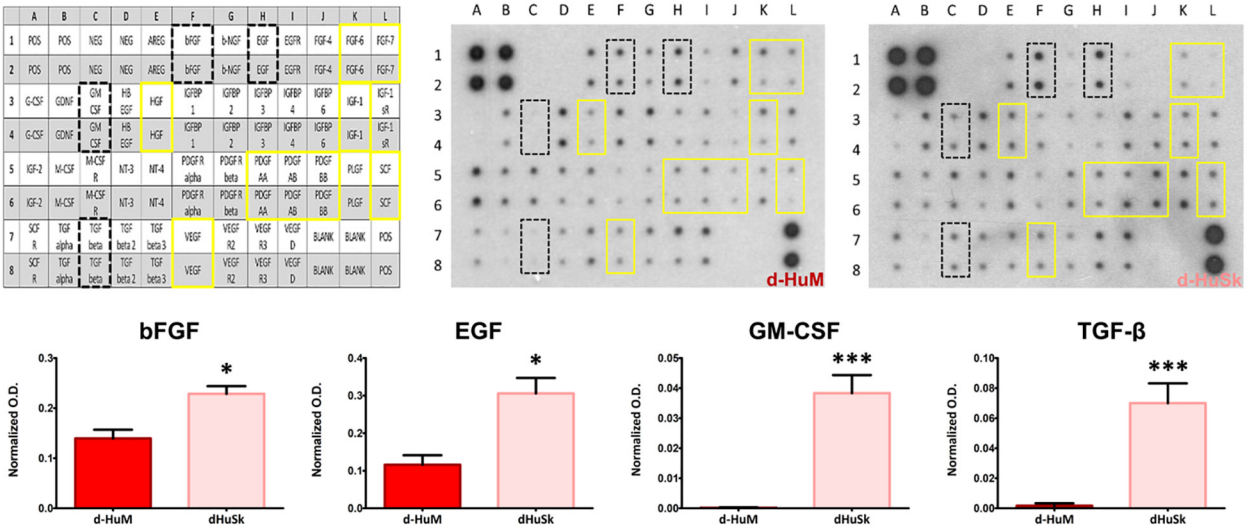

FIGURE 5 | Comparative analysis and quantification of growth factor content in d-HuM and d-HuSk. The representative images of the protein array membranes showed that nine of the targeted growth factors were present both in d-HuM and d-HuSk without any significant difference (yellow solid squares), while bFGF, EGF, GM-CSF, and TGF-beta (black dotted squares) were present at a significantly higher concentration in d-HuSk, as confirmed by the quantification shown by the graphs. In the upper left corner, the array map is shown as a reference. Asterisks were used to report significance in each comparison as follows: significant (*$p \leq 0.05$) and very significant (***$p \leq 0.001$). O.D.: optical density.

and compliance with cardiomyocyte contraction is the native cardiac ECM. However, even though such simple and obvious consideration has triggered in the last decade a multitude of studies aimed at obtaining biological scaffolds for CTE from native matrix through the decellularization of the myocardium (Moroni and Mirabella, 2014; Oberwallner et al., 2014), the dramatically unbalanced ratio between demand and availability of healthy human hearts has forced the search for alternative scaffolds. Needless to say, the ideal scaffold should recapitulate the composition and the mechanical properties of the native cardiac environment (Ye and Black, 2011). Additionally, biocompatibility and biodegradability are key requirements needed for a scaffold to be considered of clinical value and, not of secondary importance, any scaffold should be cost

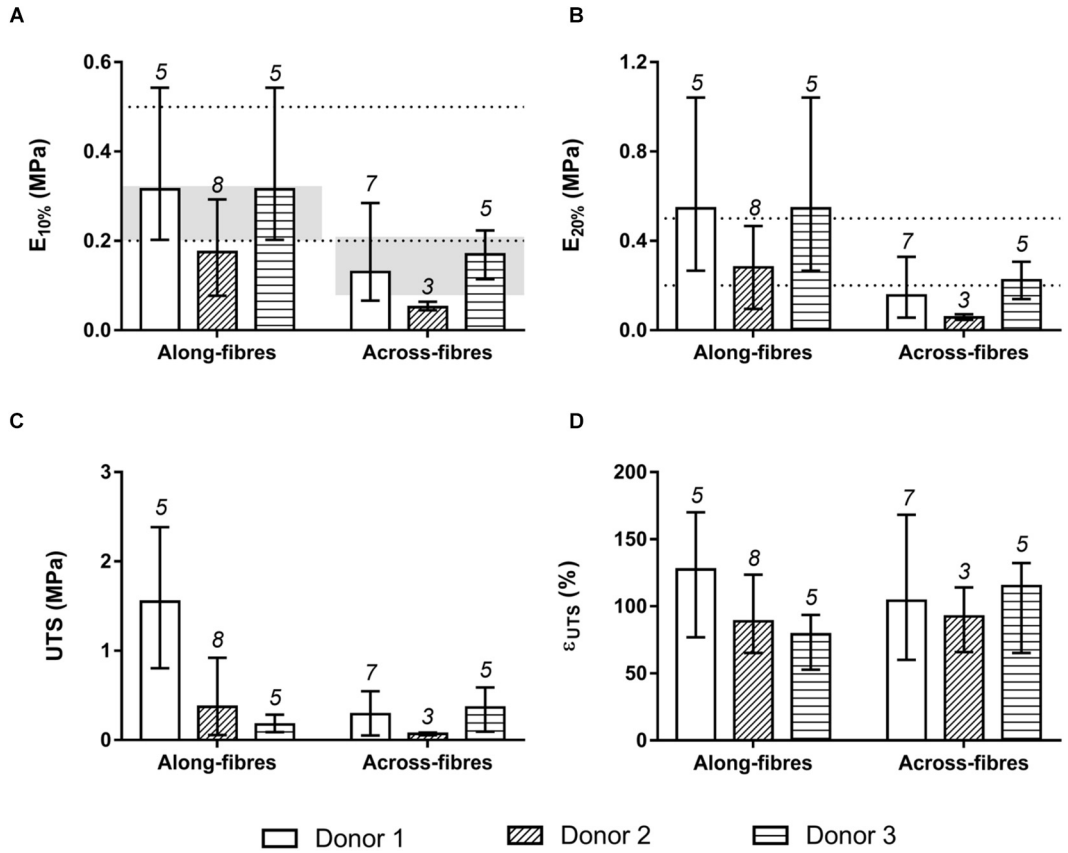

FIGURE 6 | Mechanical characterization by uniaxial tensile stretching of d-HuSk specimens oriented along and across the Langer's lines. **(A)** Average values and ranges of variation of elastic modulus $E_{10\%}$ measured at 10% of strain. The dotted lines delimit the range of elastic modulus values reported in literature for human myocardium at the end of diastole (0.2–0.5 MPa), while the gray-colored bands refer to human myocardium elastic moduli values calculated by Sommer et al. (2015) along and across the fibres. **(B)** Average values and ranges of variation of elastic modulus $E_{20\%}$ measured at 20% of strain. **(C)** Average values and ranges of variation of ultimate tensile strength UTS. **(D)** Average values and ranges of variation of ultimate strain ε_{UTS}.

effective to become commercially viable (O'Brien, 2011). Most of the aforementioned requisites needed for determining the suitability of scaffolds for CTE might be possessed by biological scaffolds produced by decellularization of tissues. However, to serve as substitute for the cardiac ECM the tissue/organ should have similarities with the cardiac environment and the decellularization process produce a thoroughly acellular scaffold without disrupting the ECM composition. Therefore, we explored the possibility of using d-HuSk as an autologous, cost effective and easily accessible scaffold for CTE and evaluated *in vitro* its capability to support resident CPC engraftment, survival and differentiation potential.

Following a recently described protocol for the decellularization of the adult human heart (Di Meglio et al., 2017), the adult human skin was easily and successfully decellularized to produce a scaffold that, being deprived of any nuclear remnants and residual dsDNA (**Figure 1**), met the criteria proposed to satisfy the intent of decellularization (Crapo et al., 2011). Nevertheless, although skin matrix consists of proteins that are also found in the cardiac matrix (Uitto et al., 1989; Lockhart et al., 2011) and is biocompatible by definition, thorough removal of resident cells is a necessary but not sufficient criterion to ensure safety and grant clinical use of d-HuSk. Indeed, the treatment with decellularizing detergents could cause biological impoverishment of the ECM, by disrupting crucial proteins of cardiac interstitium and removing soluble factors, and leave potentially harmful compounds that might impair scaffold recellularization and prevent its clinical use (Kawecki et al., 2018). Importantly, other than providing structural integrity and connecting muscle cells and blood vessels, the interstitial connective tissue of the myocardium is known to provide biological and mechanical cues that are responsible for directing stem cell fate (Ahmed and Ffrench-Constant, 2016) and cell behavior during cardiac development, adult myocardium maintenance and physiological response to pathological stimuli (Guilak et al., 2009; Gattazzo et al., 2014; Nakayama et al., 2014; Williams and Black, 2015). The investigated ECM components, namely collagens, elastin, GAGs, fibronectin, laminin, and tenascin, are the main structural and functional proteins of cardiac interstitial matrix (Li et al., 2018). The retention of these components in d-HuSk, as proved by histological and quantitative analyses (**Figures 2–4**), provides

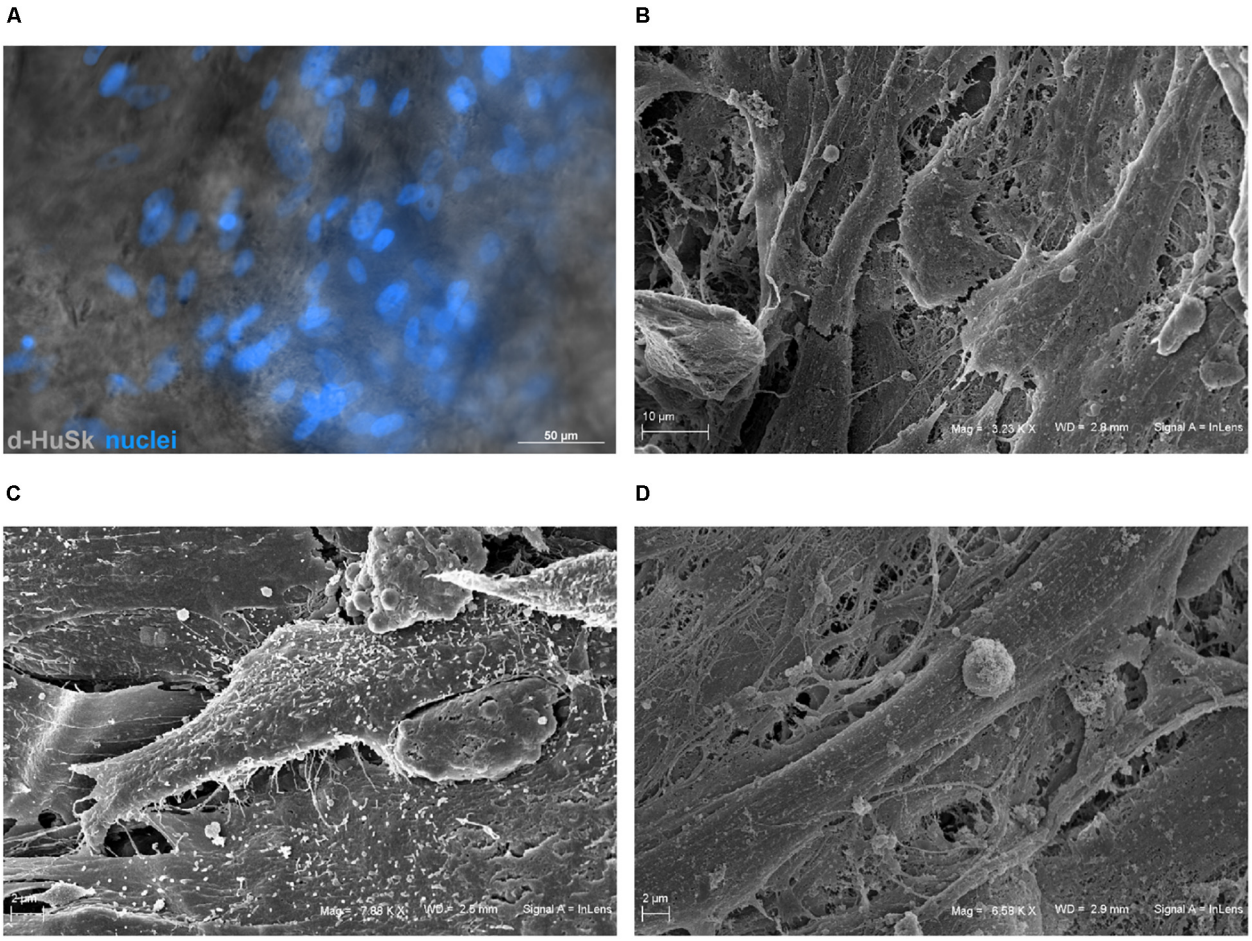

FIGURE 7 | Microscopic analysis of hCPCs engraftment on d-HuSk. **(A)** Representative image of fluorescence and phase contrast microscope analysis showing by the nuclear staining with DAPI the presence of hCPCs engrafted onto d-HuSk. Representative images of SEM analysis showing two hCPCs that contact each other **(B)**, one cell with elongated irregular shape characterized by multiple filopodia **(C)** and a cell with an elongated rectangular shape **(D)**. [Scale bar: 50 μm for **(A)**, 10 μm for **(B)**, and 2 μm for **(C,D)**].

evidence to substantiate the ability of d-HuSk to deliver a combination of structural support and biological signals that act in cardiac microenvironment. Specifically, the fibrillar collagens types I and III are the major ECM components of the cardiac embryonic and mature connective tissue network and, together with elastin that is the dominant mammalian elastic protein of the ECM and the main component of elastic fibers (Green et al., 2014), are responsible for conferring tensile strength, resilience and elasticity to the cardiac matrix (Borg et al., 1996). Additionally, they ensure proper myocyte alignment, acting as an adhesive substrate for adjoining myocytes in both developing and adult myocardium (Weber, 1989). Due to their significant water-binding capacity, also GAGs contribute to mechanical stabilization of tissues (Nimeskern et al., 2016) and, as major constituents of cardiac jelly, are implicated in the acquisition of trabeculated wall architecture and septation during cardiac development (Camenisch et al., 2000, 2002). Cardiac jelly is the primitive cardiac ECM that mechanically connects the inner endocardial layer and the outer myocardium layer of the tubular heart and that forms a thick viscoelastic layer that mechanically supports the valveless pumping function of the embryonic heart (Garita et al., 2011). GAGs control the hydration of the cardiac jelly generating turgor pressure that is involved in the remodeling process of the ventricular tube that initiates trabeculation and formation of cardiac chambers (Farouz et al., 2015; Männer and Yelbuz, 2019). Further important components of d-HuSk that are also crucial components of the cardiac matrix, since its earliest form as cardiac jelly, include the non-collagenous glycoproteins fibronectin and laminin. Fibronectin is a fibrillar protein whose significant influence over mechanical properties of the matrix and behavior of adhering cells has been extensively documented in embryonic and adult heart. The profound implication of fibronectin in mesodermal migration, adhesion and differentiation as well as in embryonic cardiomyocyte proliferation is testified by the cardiovascular defects that develop at later stages of embryogenesis in fibronectin deficient embryos and that are incompatible with life (Little and Rongish, 1995; Rienks et al., 2014; Williams and Black, 2015). Although

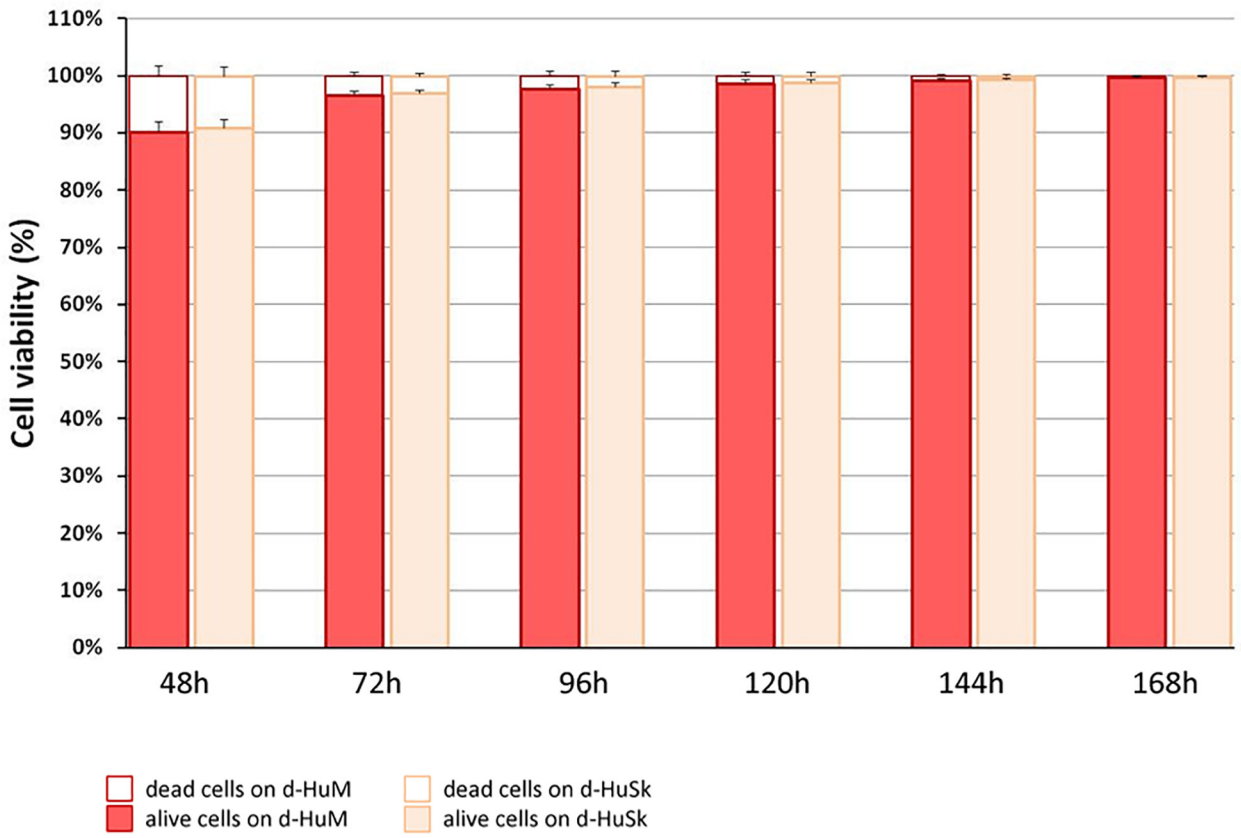

FIGURE 8 | Quantification of cell death rate and viability of hCPCs on d-HuM and d-HuSk. Mean death rate and mean viability of hCPCs cultured on d-HuSk or d-HuM, as measured by trypan blue exclusion assay. With time cell death rate dramatically decreased from around 9% to less than 1%, without any statistically significant differences between cells cultured on d-HuM or d-HuSk.

fibronectin decreases with developmental age, it is still required in the adult heart for providing structural support by linking the cardiac interstitium with the basement membranes of endothelial and muscle cells and for the reparative response following a myocardial infarction (Borg et al., 1984; Kim et al., 1999; Konstandin et al., 2013). Conversely, laminin expression is constant throughout life and, while heart organogenesis does not proceed in the absence of laminin, in the post-natal heart it is a major component of the basement membrane that surrounds mature cardiomyocytes and acts as an adhesive ligand (Castaldo et al., 2008). Furthermore, tenascin C is a matricellular protein highly but transiently expressed during the embryonic development of the heart that reappears in various pathological conditions. Its spatiotemporally restricted expression is critical to promote the differentiation of cardiomyocytes in the embryonic heart (Imanaka-Yoshida et al., 2003) and the recruitment of myofibroblasts in tissue remodeling during several heart diseases like myocardial infarction (Imanaka-Yoshida et al., 2014). It has also been reported that tenascin C is an elastic molecule that can be stretched to several times its resting length *in vitro* (Oberhauser et al., 1998; Marín et al., 2003) and contributes to tissue elasticity (Imanaka-Yoshida and Aoki, 2014). Additionally, other than holding the potential to provide cardiac-like biochemical cues, d-HuSk also has the added value of hosting very well preserved vessels, as shown by the histological analysis (**Figure 2**). Although its patency has yet to be verified, this residual vascular network can play a major role in the diffusion of nutrients that supports cell survival and differentiation.

However, along with the cardiac-like biochemical and structural behavior, the ideal scaffold for CTE should also recapitulate the resultant mechanical properties of the human healthy myocardium. Healthy myocardium is characterized by an anisotropic hierarchical structure and a non-linear viscoelastic mechanical behavior (Pislaru et al., 2014), for which both the cardiac matrix and mostly the cellular component are responsible. Elasticity, indeed, is an intrinsic property of cardiomyocytes largely conferred by sarcomere structure and critical for the contraction and relaxation during cardiac cycle (Janssen, 2010; Ait Mou et al., 2015). Obviously, muscle cells need a compliant matrix able to elastically deform during contraction-relaxation cycles (Hanson et al., 2013). Similarly, human skin reacts to loadings with a viscoelastic, anisotropic dual behavior, and it is characterized by a preferential collagen fiber orientation, referred to as Langer's lines (Langer, 1978). At low strain values, elastin fibers are responsible for skin

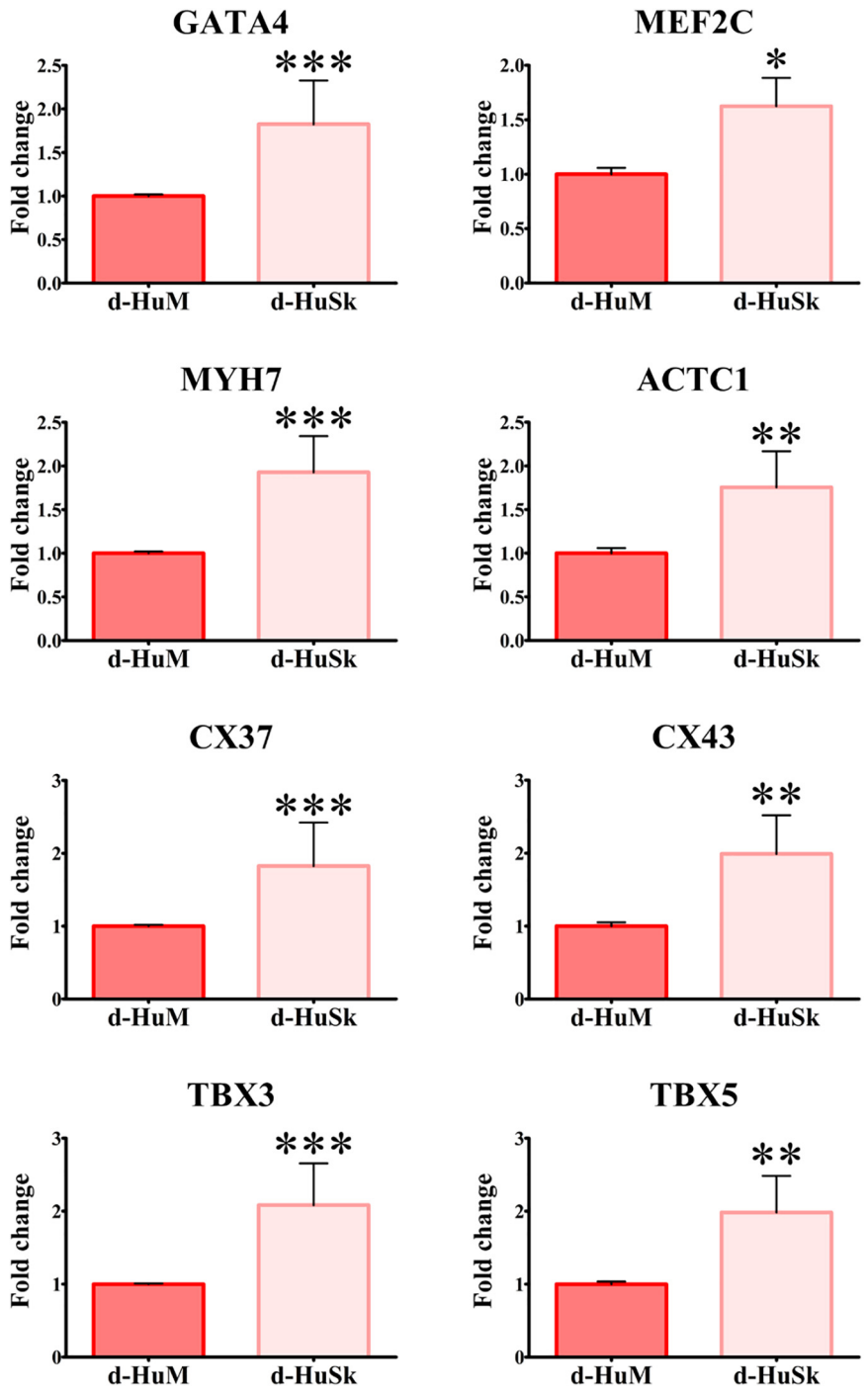

FIGURE 9 | Gene expression analysis of cardiac myocyte markers in hCPCs cultured on d-HuM and d-HuSk for 4 weeks. Real-time PCR analysis of the expression of genes characteristic of cardiac myocytes showing an upregulation of the transcription for all markers in hCPCs cultured on d-HuSk when compared with hCPCs cultured on d-HuM. Asterisks are indicators of the p value obtained in each comparison as follows: significant (*$p \leq 0.05$), very significant (**$p \leq 0.01$), and extremely significant (***$p \leq 0.001$).

mechanical behavior, whereas at large strains collagen fibers become dominant (Terzini et al., 2016). To investigate the mechanical performance of d-HuSk, we performed uniaxial tensile tests on d-HuSk specimens oriented along and across the Langer's lines. Applying a strain range typical of the human left ventricle (Kuznetsova et al., 2008), d-HuSk specimens oriented along the Langer's lines presented average elastic moduli $E_{10\%}$ and $E_{20\%}$ comparable with literature data on

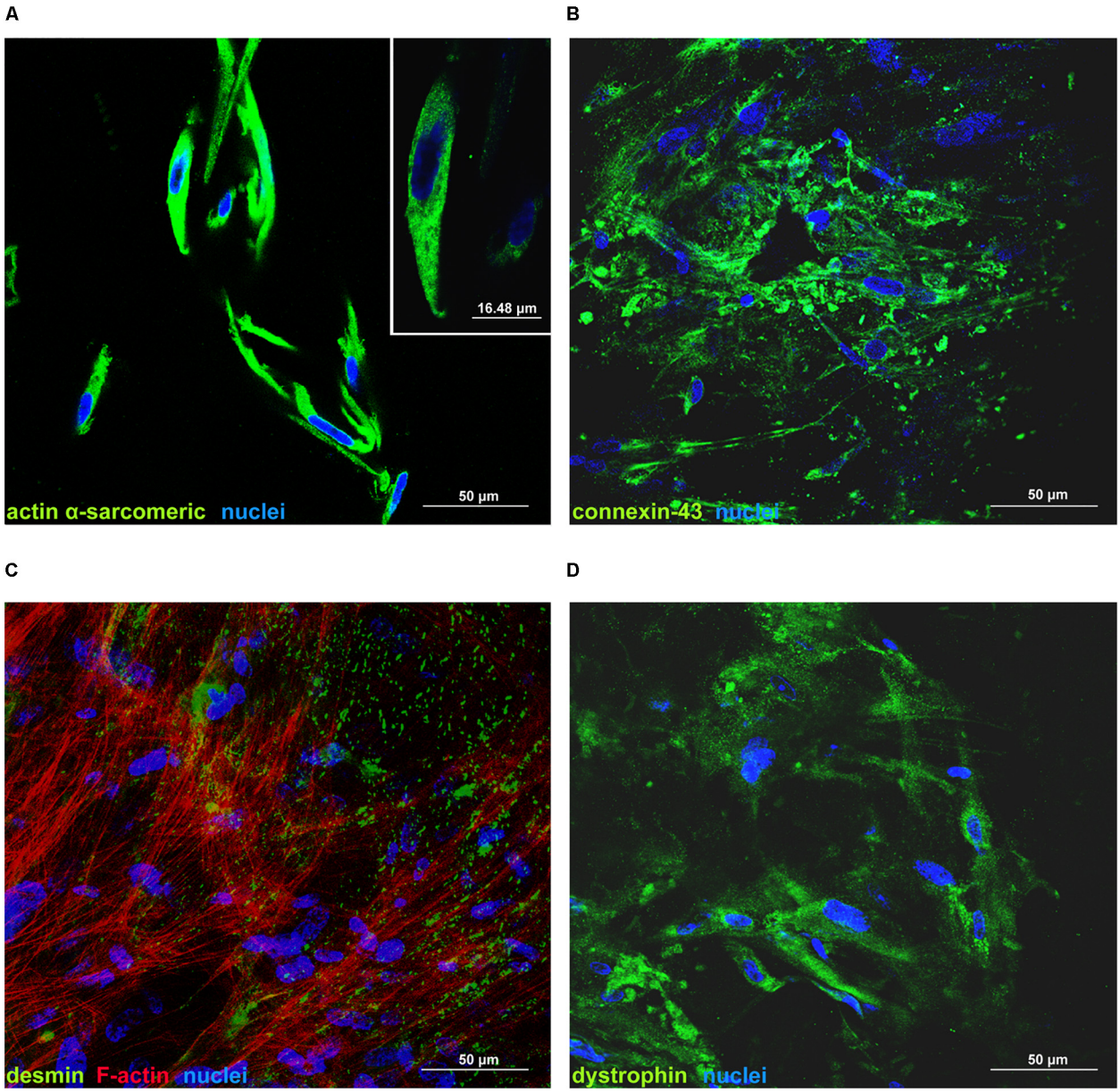

FIGURE 10 | Immunofluorescence analysis of the expression of cardiac myocyte markers by hCPCs cultured on d-HuSk for 4 weeks. Representative images of confocal microscopy analyses showing the immunopositivity and distribution of alpha-sarcomeric actin **(A)**, connexin-43 **(B)**, desmin along with F-actin **(C)**, and dystrophin **(D)** in hCPCs cultured on d-HuSk. The inset in **(A)** shows at higher magnification the expression of alpha-sarcomeric actin. (Scale bar: 50 µm in all pictures, 16.48 µm in the inset).

native human myocardium (Jawad et al., 2007; Chen et al., 2008; Bouten et al., 2011; Sommer et al., 2015), and higher than elastic moduli values measured for the across-fiber specimens (**Figure 6**). Mechanical characterization of d-HuSk confirms that skin elasticity is mostly provided by the ECM rather than by resident cells, and the d-HuSk elasticity guarantees a mechanical behavior suitable for CTE application. Moreover, d-HuSk presents directionally dependent anisotropic behavior depending on the ECM protein fiber network predominantly oriented along the Langer's lines (Demer and Yin, 1983) and similar with the structural organization of the myocardium (Gilbert et al., 2007).

Based on this intriguing resemblance between d-HuSk and cardiac ECM, it is tempting to speculate that d-HuSk might function as a scaffold to support and boost cardiac differentiation in a stem/progenitor cell-based cardiac regeneration approach. Nonetheless, to be considered suitable for regenerative medicine purposes, any scaffold must first be biocompatible (O'Brien, 2011). This implies that it must have the ability to attract cells and provide a comfortable environment capable to support

or promote cell adhesion and survival. Tests of *in vitro* recellularization of d-HuSk with hCPCs proved that d-HuSk provided an environment as effective and safe as the native cardiac matrix in that it supported engraftment (**Figure 7**) and survival (**Figure 8**) of hCPCs. Additionally, the positive effect of a biological scaffold loaded with signals that direct and control cardiac development and homeostasis on the expression of markers specific for cardiomyocytes by hCPCs was somehow predictable. It was yet astounding that the expression of markers specific for cardiomyocytes in hCPCs cultured on d-HuSk not only persisted, but resulted also up-regulated, when compared with that of the same cell population cultured on d-HuM in the same conditions (**Figures 9**, **10**). Such evidence, along with the morphology of cells observed at the SEM (**Figure 7**), supports the hypothesis that d-HuSk might constitute a myocardial-like environment that ensures the survival and sustains the differentiation of resident CPCs. Accordingly, when compared with d-HuM, d-HuSk also contained growth factors that are commonly stored in the native cardiac matrix, like HGF, IGF, SCF, PDGF, and VEGF, and was enriched with growth factors like bFGF, EGF, GM-CSF, and TGF-beta (**Figure 5**). These factors are involved in a variety of cardiac processes like cardiac development (Saetrum Opgaard and Wang, 2005; Deshwar et al., 2016), mobilization and proliferation of endothelial progenitor cells (Qiu et al., 2014), angiogenesis and neovascularization (Murakami and Simons, 2008; Beohar et al., 2010), cardiomyocyte proliferation and differentiation (Ma et al., 2017; Farzaneh et al., 2019), cardioprotection (Zhu et al., 2017), cardiac remodeling (Sala and Crepaldi, 2011), and repair (Vandervelde et al., 2005). Such abundance of growth factors in d-HuSk strengthens its suitability for CTE as a promising tool capable of providing alone two of the three pillars of tissue engineering (O'Brien, 2011), namely the scaffold and the signals, and whose potential to boost cardiac regeneration as stand-alone or cellularized scaffold is worth being further explored.

The presented work is affected by some limitations. Firstly, the biocompatibility of d-HuSk was evaluated exclusively *in vitro* and in static conditions. Nonetheless, the evidence that CPCs engrafted on a novel and more easily accessible biological scaffold of dermal ECM and retained their differentiation potential represents an important advance in CTE. Indeed, the use of d-HuSk overcomes problems related to the preparation of myocardial biological scaffolds and paves the way for *in vivo* studies that will provide more extensive insights into the clinical utility of d-HuSk. Moreover, to investigate the influence of cardiac-like cyclic stretch stimulation on the matrix and the developing construct, *in vitro* studies within a customized mechanical stretching bioreactor (Putame et al., 2019) are planned.

CONCLUSION

We developed a novel biological scaffold for cardiac regenerative medicine that we termed d-HuSk. Obtained from the adult human skin through a simple and effective decellularization procedure (Di Meglio et al., 2017), d-HuSk not only fulfilled the key requirements proposed for the evaluation of the effectiveness of decellularization, but also preserved the histological organization and composition of the native tissue, providing compelling evidence of a highly efficient decellularization method. Other than providing cell attachment sites ensuring cell adhesion, d-HuSk also retained well-preserved vessels that are critical to ensure diffusion of nutrients, thus addressing two serious problems that frequently affect the use of synthetic biomaterials. Furthermore, the biological nature of d-HuSk ensures a full biodegradability, making d-HuSk a powerful biomaterial. Indeed, a scaffold should be considered a temporary implant that provides support to cells that are, then, expected to replace it with a newly synthesized cardiac matrix. Based on evidence emerging from this work, d-HuSk is a myocardial matrix substitute characterized by myocardium-like biological and mechanical behavior that, despite its different anatomical site of origin, proved to be a suitable environment to support the engraftment, proliferation and differentiation potential of hCPC *in vitro*. If proven *in vivo*, such evidence could have a tremendous potential, as d-HuSk might be used as an autologous scaffold to promote and sustain cardiac regeneration by stem/progenitor cells. Finally, easy accessibility, cost-effective production and autologous origin are all additional groundbreaking features of d-HuSk. In fact, using d-HuSk as an auto-graft would imply transplanting a fully compatible scaffold capable of averting the immunological response and the risk of rejection that affect the heterologous and xenogeneic transplant or implant. Noticeably yet, it has been recently demonstrated that adult fibroblasts isolated from the abdominal skin can be reprogrammed with higher efficiency (Sacco et al., 2019) and that skin fibroblasts can be directly reprogrammed to cardiac mature cells (Cao et al., 2016). Therefore, the preparation of d-HuSk scaffolds holds the potential to eventually evolve into the development of a more complex therapeutic strategy aimed at constructing, with one single intervention of skin harvesting, a fully autologous engineered myocardium using cardiac direct reprogramming of fibroblast to restore the cellular compartment and the decellularized dermal ECM to replace the extracellular compartment.

DATA AVAILABILITY STATEMENT

All data supporting the findings of this study are available within the article and its **Supplementary Information**; source data for the figures in this study are available from the authors upon request.

ETHICS STATEMENT

This study was carried out following protocols approved by the Hospital Ethical Committee. Patients provided written informed consent in conformity with the principles outlined in the Declaration of Helsinki.

AUTHOR CONTRIBUTIONS

IB, VR, AS, GR, DM, SM, FD, and CC contributed conception and design of the study. IB, VR, AS, GR, MC, AC, CS, DN, FSi, FD, and CC conducted experiments and analyzed experimental data. DM, MT, AA, and GS performed mechanical characterization and analysis. CC wrote the first draft of the manuscript. GR, MC, DM, and MT wrote sections of the manuscript. FSc and FD'A provided the surgical specimens. All authors contributed to manuscript revision, read and approved the submitted version. IB, VR, and AS are equal contributors.

SUPPLEMENTARY MATERIAL

The Supplementary Material for this article can be found online at: https://www.frontiersin.org/articles/10.3389/fbioe.2020.00229/full#supplementary-material

REFERENCES

Ahmed, M., and Ffrench-Constant, C. (2016). Extracellular matrix regulation of stem cell behavior. *Curr. Stem Cell Rep.* 2, 197–206. doi: 10.1007/s40778-016-0056-2

Ait Mou, Y., Bollensdorff, C., Cazorla, O., Magdi, Y., and de Tombe, P. P. (2015). Exploring cardiac biophysical properties. *Glob. Cardiol. Sci. Pract.* 2015:10. doi: 10.5339/gcsp.2015.10

Beohar, N., Rapp, J., Pandya, S., and Losordo, D. W. (2010). Rebuilding the damaged heart: the potential of cytokines and growth factors in the treatment of ischemic heart disease. *J. Am. Coll. Cardiol.* 56, 1287–1297. doi: 10.1016/j.jacc.2010.05.039

Borg, T. K., Rubin, K., Carver, W., Samarel, A., and Terracio, L. (1996). The cell biology of the cardiac interstitium. *Trends Cardiovasc. Med.* 6, 65–70. doi: 10.1016/1050-1738(96)00005-9

Borg, T. K., Rubin, K., Lundgren, E., Borg, K., and Obrink, B. (1984). Recognition of extracellular matrix components by neonatal and adult cardiac myocytes. *Dev. Biol.* 104, 86–96. doi: 10.1016/0012-1606(84)90038-1

Bouten, C. V., Dankers, P. Y., Driessen-Mol, A., Pedron, S., Brizard, A. M., and Baaijens, F. P. (2011). Substrates for cardiovascular tissue engineering. *Adv. Drug Deliv. Rev.* 63, 221–241. doi: 10.1016/j.addr.2011.01.007

Brown, B. N., and Badylak, S. F. (2014). Extracellular matrix as an inductive scaffold for functional tissue reconstruction. *Transl. Res.* 163, 268–285. doi: 10.1016/j.trsl.2013.11.003

Camenisch, T. D., Schroeder, J. A., Bradley, J., Klewer, S. E., and McDonald, J. A. (2002). Heart-valve mesenchyme formation is dependent on hyaluronan-augmented activation of ErbB2-ErbB3 receptors. *Nat. Med.* 8, 850–855. doi: 10.1038/nm742

Camenisch, T. D., Spicer, A. P., Brehm-Gibson, T., Biesterfeldt, J., Augustine, M. L., Calabro, A. Jr., et al. (2000). Disruption of hyaluronan synthase-2 abrogates normal cardiac morphogenesis and hyaluronan-mediated transformation of epithelium to mesenchyme. *J. Clin. Invest.* 106, 349–360. doi: 10.1172/JCI10272

Cao, N., Huang, Y., Zheng, J., Spencer, C. I., Zhang, Y., Fu, J. D., et al. (2016). Conversion of human fibroblasts into functional cardiomyocytes by small molecules. *Science* 352, 1216–1220. doi: 10.1126/science.aaf1502

Castaldo, C., Di Meglio, F., Miraglia, R., Sacco, A. M., Romano, V., Bancone, C., et al. (2013). Cardiac fibroblast-derived extracellular matrix (biomatrix) as a model for the studies of cardiac primitive cell biological properties in normal and pathological adult human heart. *Biomed. Res. Int.* 2013, 352–370. doi: 10.1155/2013/352370

Castaldo, C., Di Meglio, F., Nurzynska, D., Romano, G., Maiello, C., Bancone, C., et al. (2008). CD117-positive cells in adult human heart are localized in the subepicardium, and their activation is associated with laminin-1 and alpha6 integrin expression. *Stem Cells* 26, 1723–1731. doi: 10.1634/stemcells.2007-0732

Celebi, B., Cloutier, M., Rabelo, R. B., Mantovani, D., and Bandiera, A. (2012). Human elastin-based recombinant biopolymers improve mesenchymal stem cell differentiation. *Macromol. Biosci.* 12, 1546–1554. doi: 10.1002/mabi.201200170

Chen, Q. Z., Bismarck, A., Hansen, U., Junaid, S., Tran, M. Q., Harding, S. E., et al. (2008). Characterisation of a soft elastomer poly (glycerol sebacate) designed to match the mechanical properties of myocardial tissue. *Biomaterials* 29, 47–57. doi: 10.1016/j.biomaterials.2007.09.010

Crapo, P. M., Gilbert, T. W., and Badylak, S. F. (2011). An overview of tissue and whole organ decellularization processes. *Biomaterials* 32, 3233–3243. doi: 10.1016/j.biomaterials.2011.01.057

Demer, L. L., and Yin, F. C. (1983). Passive biaxial mechanical properties of isolated canine myocardium. *J. Physiol.* 339, 615–630. doi: 10.1113/jphysiol.1983.sp014738

Deshwar, A. R., Chng, S. C., Ho, L., Reversade, B., and Scott, I. C. (2016). The Apelin receptor enhances Nodal/TGFβ signaling to ensure proper cardiac development. *Elife* 5:e13758. doi: 10.7554/eLife.13758

Di Meglio, F., Castaldo, C., Nurzynska, D., Romano, V., Miraglia, R., Bancone, C., et al. (2010). Epithelial-mesenchymal transition of epicardial mesothelium is a source of cardiac CD117-positive stem cells in adult human heart. *J. Mol. Cell. Cardiol.* 49, 719–727. doi: 10.1016/j.yjmcc.2010.05.013

Di Meglio, F., Nurzynska, D., Romano, V., Miraglia, R., Belviso, I., Sacco, A. M., et al. (2017). Optimization of human myocardium decellularization method for the construction of implantable patches. *Tissue Eng. Part C Methods* 23, 525–539. doi: 10.1089/ten.TEC.2017.0267

Farouz, Y., Chen, Y., Terzic, A., and Menasché, P. (2015). Concise review: growing hearts in the right place: on the design of biomimetic materials for cardiac stem cell differentiation. *Stem Cells* 33, 1021–1035. doi: 10.1002/stem.1929

Farzaneh, M., Rahimi, F., Alishahi, M., and Khoshnam, S. E. (2019). Paracrine mechanisms involved in mesenchymal stem cell differentiation into cardiomyocytes. *Curr. Stem Cell Res. Ther.* 14, 9–13. doi: 10.2174/1574888X13666180821160421

Feric, N. T., and Radisic, M. (2016). Maturing human pluripotent stem cell-derived cardiomyocytes in human engineered cardiac tissues. *Adv. Drug Deliv. Rev.* 96, 110–134. doi: 10.1016/j.addr.2015.04.019

Frangogiannis, N. G. (2014). The inflammatory response in myocardial injury, repair, and remodeling. *Nat. Rev. Cardiol.* 11, 255–265. doi: 10.1038/nrcardio.2014.28

Frantz, C., Stewart, K. M., and Weaver, V. M. (2010). The extracellular matrix at a glance. *J. Cell Sci.* 123, 4195–4200. doi: 10.1242/jcs.023820

Fujita, B., and Zimmermann, W. H. (2017). Myocardial tissue engineering for regenerative applications. *Curr. Cardiol. Rep.* 19:78. doi: 10.1007/s11886-017-0892-4

Garita, B., Jenkins, M. W., Han, M., Zhou, C., Vanauker, M., Rollins, A. M., et al. (2011). Blood flow dynamics of one cardiac cycle and relationship to mechanotransduction and trabeculation during heart looping. *Am. J. Physiol. Heart Circ. Physiol.* 300, H879–H891. doi: 10.1152/ajpheart.00433.2010

Gattazzo, F., Urciuolo, A., and Bonaldo, P. (2014). Extracellular matrix: a dynamic microenvironment for stem cell niche. *Biochim. Biophys. Acta* 1840, 2506–2519. doi: 10.1016/j.bbagen.2014.01.010

GBD 2016 Causes of Death Collaborators (2017). Global, regional, and national age-sex specific mortality for 264 causes of death, 1980-2016: a systematic analysis for the Global Burden of Disease Study 2016. *Lancet* 390, 1151–1210. doi: 10.1016/S0140-6736(17)32152-9

GBD 2016 Risk Factors Collaborators (2017). Global, regional, and national comparative risk assessment of 84 behavioural, environmental and occupational, and metabolic risks or clusters of risks, 1990-2016: a systematic analysis for the Global Burden of Disease Study 2016. *Lancet* 390, 1345–1422. doi: 10.1016/S0140-6736(17)32366-8

Gilbert, S. H., Benson, A. P., Li, P., and Holden, A. V. (2007). Regional localisation of left ventricular sheet structure: integration with current models of cardiac fibre, sheet and band structure Eur. *J. Cardiothorac. Surg.* 32, 231–249. doi: 10.1016/j.ejcts.2007.03.032

Green, E. M., Mansfield, J. C., Bell, J. S., and Winlove, C. P. (2014). The structure and micromechanics of elastic tissue. *Interface Focus* 4:20130058. doi: 10.1098/rsfs.2013.0058

Guilak, F., Cohen, D. M., Estes, B. T., Gimble, J. M., Liedtke, W., and Chen, C. S. (2009). Control of stem cell fate by physical interactions with the extracellular matrix. *Cell Stem Cell* 5, 17–26. doi: 10.1016/j.stem.2009.06.016

Hanson, K. P., Jung, J. P., Tran, Q. A., Hsu, S. P., Iida, R., Ajeti, V., et al. (2013). Spatial and temporal analysis of extracellular matrix proteins in the developing murine heart: a blueprint for regeneration. *Tissue Eng. Part A* 19, 1132–1143. doi: 10.1089/ten.TEA.2012.0316

Hoganson, D. M., O'Doherty, E. M., Owens, G. E., Harilal, D. O., Goldman, S. M., and Bowley, C. M. (2010). The retention of extracellular matrix proteins and angiogenic and mitogenic cytokines in a decellularized porcine dermis. *Biomaterials* 31, 6730–6737. doi: 10.1016/j.biomaterials.2010.05.019

Huang, H., Kamm, R. D., and Lee, R. T. (2004). Cell mechanics and mechanotransduction: pathways, probes, and physiology. *Am. J. Physiol. Cell Physiol.* 287, C1–C11. doi: 10.1152/ajpcell.00559.2003

Imanaka-Yoshida, K., and Aoki, H. (2014). Tenascin-C and mechanotransduction in the development and diseases of cardiovascular system. *Front. Physiol.* 5:283. doi: 10.3389/fphys.2014.00283

Imanaka-Yoshida, K., Matsumoto, K., Hara, M., Sakakura, T., and Yoshida, T. (2003). The dynamic expression of tenascin-C and tenascin-X during early heart development in the mouse. *Differentiation* 71, 291–298. doi: 10.1046/j.1432-0436.2003.7104506.x

Imanaka-Yoshida, K., Yoshida, T., and Miyagawa-Tomita, S. (2014). Tenascin-C in development and disease of blood vessels. *Anat. Rec. (Hoboken)* 297, 1747–1757. doi: 10.1002/ar.22985

Jacot, J. G., Martin, J. C., and Hunt, D. L. (2010). Mechanobiology of cardiomyocyte development. *J. Biomech.* 43, 93–98. doi: 10.1016/j.jbiomech.2009.09.014

Janssen, P. M. (2010). Kinetics of cardiac muscle contraction and relaxation are linked and determined by properties of the cardiac sarcomere. *Am. J. Physiol. Heart Circ. Physiol.* 299, H1092–H1099. doi: 10.1152/ajpheart.00417.2010

Jawad, H., Ali, N. N., Lyon, A. R., Chen, Q. Z., Harding, S. E., and Boccaccini, A. R. (2007). Myocardial tissue engineering: a review. *J. Tissue Eng. Regen. Med.* 1, 327–342. doi: 10.1002/term.46

Kawecki, M., Łabuś, W., Klama-Baryla, A., Kitala, D., Kraut, M., Glik, J., et al. (2018). A review of decellurization methods caused by an urgent need for quality control of cell-free extracellular matrix scaffolds and their role in regenerative medicine. *J. Biomed. Mater. Res. B Appl. Biomater.* 106, 909–923. doi: 10.1002/jbm.b.33865

Kielty, C. M., Sherratt, M. J., and Shuttleworth, C. A. (2002). Elastic fibres. *J. Cell Sci.* 115, 2817–2828.

Kim, H., Yoon, C. S., Kim, H., and Rah, B. (1999). Expression of extracellular matrix components fibronectin and laminin in the human fetal heart. *Cell Struct. Funct.* 24, 19–26. doi: 10.1247/csf.24.19

Konstandin, M. H., Toko, H., Gastelum, G. M., Quijada, P., De La Torre, A., Quintana, M., et al. (2013). Fibronectin is essential for reparative cardiac progenitor cell response after myocardial infarction. *Circ. Res.* 113, 115–125. doi: 10.1161/CIRCRESAHA.113.301152

Krieg, T., and Aumailley, M. (2011). The extracellular matrix of the dermis: flexible structures with dynamic functions. *Exp. Dermatol.* 20, 689–695. doi: 10.1111/j.1600-0625.2011.01313.x

Kuznetsova, T., Herbots, L., Richart, T., D'hooge, J., Thijs, L., Fagard, R. H., et al. (2008). Left ventricular strain and strain rate in a general population. *Eur. Heart J.* 29, 2014–2023. doi: 10.1093/eurheartj/ehn280

Langer, K. (1978). On the anatomy and physiology of the skin. *Br. J. Plast. Surg.* 31, 3–8. doi: 10.1016/0007-1226(78)90003-6

Li, L., Zhao, Q., and Kong, W. (2018). Extracellular matrix remodeling and cardiac fibrosis. *Matrix Biol.* 6, 490–506. doi: 10.1016/j.matbio.2018.01.013

Li, Y., Huang, G., Zhang, X., Wang, L., Du, Y., Lu, T. J., et al. (2014). Engineering cell alignment in vitro. *Biotechnol. Adv.* 32, 347–365. doi: 10.1016/j.biotechadv.2013.11.007

Little, C. D., and Rongish, B. J. (1995). The extracellular matrix during heart development. *Experientia* 51, 873–882. doi: 10.1007/bf01921738

Lockhart, M., Wirrig, E., Phelps, A., and Wessels, A. (2011). Extracellular matrix and heart development. *Birth Defects Res. A Clin. Mol. Teratol.* 91, 535–550. doi: 10.1002/bdra.20810

Ma, J., Zhao, Y., Sun, L., Sun, X., Zhao, X., Sun, X., et al. (2017). Exosomes derived from Akt-modified human umbilical cord mesenchymal stem cells improve cardiac regeneration and promote angiogenesis via activating platelet-derived growth factor D. *Stem Cells Transl. Med.* 6, 51–59. doi: 10.5966/sctm.2016-0038

Madonna, R., Van Laake, L. W., Botker, H. E., Davidson, S. M., De Caterina, R., Engel, F. B., et al. (2019). ESC working group on cellular biology of the heart: position paper for cardiovascular research: tissue engineering strategies combined with cell therapies for cardiac repair in ischaemic heart disease and heart failure. *Cardiovasc. Res.* 115, 488–500. doi: 10.1093/cvr/cvz010

Männer, J., and Yelbuz, T. M. (2019). Functional morphology of the cardiac jelly in the tubular heart of vertebrate embryos. *J. Cardiovasc. Dev. Dis.* 6:E12. doi: 10.3390/jcdd6010012

Marín, J. L., Muñiz, J., Huerta, M., and Trujillo, X. (2003). Folding-unfolding of FN-III domains in tenascin: an elastically coupled two-state system. *J. Biomech.* 36, 1733–1737. doi: 10.1016/s0021-9290(03)00172-6

Massai, D., Cerino, G., Gallo, D., Pennella, F., Deriu, M. A., Rodriguez, A., et al. (2013). Bioreactors as engineering support to treat cardiac muscle and vascular disease. *J. Healthc. Eng.* 4, 329–370. doi: 10.1260/2040-2295.4.3.329

Moroni, F., and Mirabella, T. (2014). Decellularized matrices for cardiovascular tissue engineering. *Am. J. Stem Cells* 3, 1–20.

Mozaffarian, D., Benjamin, E. J., Go, A. S., Arnett, D. K., Blaha, M. J., Cushman, M., et al. (2016). Heart disease and stroke statistics-2016 update: a report from the American Heart Association. *Circulation* 133, e38–e360. doi: 10.1161/CIR.0000000000000350

Murakami, M., and Simons, M. (2008). Fibroblast growth factor regulation of neovascularization. *Curr. Opin. Hematol.* 15, 215–220. doi: 10.1097/MOH.0b013e3282f97d98

Nakayama, K. H., Hou, L., and Huang, N. F. (2014). Role of extracellular matrix signaling cues in modulating cell fate commitment for cardiovascular tissue engineering. *Adv. Healthc. Mater.* 3, 628–641. doi: 10.1002/adhm.201300620

Nimeskern, L., Utomo, L., Lehtoviita, I., Fessel, G., Snedeker, J. G., van Osch, G. J., et al. (2016). Tissue composition regulates distinct viscoelastic responses in auricular and articular cartilage. *J. Biomech.* 49, 344–352. doi: 10.1016/j.jbiomech.2015.12.032

Nurzynska, D., Di Meglio, F., Romano, V., Miraglia, R., Sacco, A. M., Latino, F., et al. (2013). Cardiac primitive cells become committed to a cardiac fate in adult human heart with chronic ischemic disease but fail to acquire mature phenotype: genetic and phenotypic study. *Basic Res. Cardiol.* 108:320. doi: 10.1007/s00395-012-0320-2

Oberhauser, A. F., Marszalek, P. E., Erickson, H. P., and Fernandez, J. M. (1998). The molecular elasticity of the extracellular matrix protein tenascin. *Nature* 393, 181–185. doi: 10.1038/30270

Oberwallner, B., Brodarac, A., Choi, Y. H., Saric, T., Aniæ, P., Morawietz, L., et al. (2014). Preparation of cardiac extracellular matrix scaffolds by decellularization of human myocardium. *J. Biomed. Mater. Res. A* 102, 3263–3272. doi: 10.1002/jbma.35000

O'Brien, F. J. (2011). Biomaterials and scaffolds for tissue engineering. *Mat. Today* 14, 88–95. doi: 10.1016/S1369-7021(11)70058-X

Ozsvar, J., Mithieux, S. M., Wang, R., and Weiss, A. S. (2015). Elastin-based biomaterials and mesenchymal stem cells. *Biomater. Sci.* 3, 800–809. doi: 10.1039/C5BM00038F

Pislaru, C., Urban, M. W., Pislaru, S. V., Kinnick, R. R., and Greenleaf, J. F. (2014). Viscoelastic properties of normal and infarcted myocardium measured by a multifrequency shear wave method: comparison with pressure-segment length method. *Ultrasound Med. Biol.* 40, 1785–1795. doi: 10.1016/j.ultrasmedbio.2014.03.004

Putame, G., Terzini, M., Carbonaro, D., Pisani, G., Serino, G., Di Meglio, F., et al. (2019). Application of 3D printing technology for design and manufacturing of customized components for a mechanical stretching bioreactor. *J. Healthc. Eng.* 2019:3957931. doi: 10.1155/2019/3957931

Qiu, C., Xie, Q., Zhang, D., Chen, Q., Hu, J., and Xu, L. (2014). GM-CSF induces cyclin D1 expression and proliferation of endothelial progenitor cells via PI3K and MAPK signaling. *Cell Physiol. Biochem.* 33, 784–795. doi: 10.1159/000358652

Radisic, M., Park, H., Shing, H., Consi, T., Schoen, F. J., Langer, R., et al. (2004). Functional assembly of engineered myocardium by electrical stimulation of cardiac myocytes cultured on scaffolds. *Proc. Natl. Acad. Sci. U.S.A.* 101, 18129–18134. doi: 10.1073/pnas.0407817101

Rienks, M., Papageorgiou, A. P., Frangogiannis, N. G., and Heymans, S. (2014). Myocardial extracellular matrix an ever-changing and diverse entity. *Circ. Res.* 114, 872–888. doi: 10.1161/CIRCRESAHA.114.302533

Ronaldson-Bouchard, K., Ma, S. P., Yeager, K., Chen, T., Song, L., Sirabella, D., et al. (2018). Advanced maturation of human cardiac tissue grown from pluripotent stem cells. *Nature* 556, 239–243. doi: 10.1038/s41586-018-0016-3

Sacco, A. M., Belviso, I., Romano, V., Carfora, A., Schonauer, F., Nurzynska, D., et al. (2019). Diversity of dermal fibroblasts as major determinant of variability in cell reprogramming. *J. Cell. Mol. Med.* 23, 4256–4268. doi: 10.1111/jcmm.14316

Saetrum Opgaard, O., and Wang, P. H. (2005). IGF-1 is a matter of heart. *Growth Horm. IGF Res.* 15, 89–94. doi: 10.1016/j.ghir.2005.02.002

Sala, V., and Crepaldi, T. (2011). Novel therapy for myocardial infarction: can HGF/Met be beneficial? *Cell Mol. Life Sci.* 68, 1703–1717. doi: 10.1007/s00018-011-0633-6

Schelbert, E. B., Fonarow, G. C., Bonow, R. O., Butler, J., and Gheorghiade, M. (2014). Therapeutic targets in heart failure: refocusing on the myocardial interstitium. *J. Am. Coll. Cardiol.* 63, 2188–2198. doi: 10.1016/j.jacc.2014.01.068

Sommer, G., Schriefl, A. J., Andrä, M., Sacherer, M., Viertler, C., Wolinski, H., et al. (2015). Biomechanical properties and microstructure of human ventricular myocardium. *Acta Biomater.* 24, 172–192. doi: 10.1016/j.actbio.2015.06.031

Stoppel, W. L., Kaplan, D. L., and Black, L. D. III (2016). Electrical and mechanical stimulation of cardiac cells and tissue constructs. *Adv. Drug Deliv. Rev.* 96, 135–155. doi: 10.1016/j.addr.2015.07.009

Talman, V., and Ruskoaho, H. (2016). Cardiac fibrosis in myocardial infarction-from repair and remodeling to regeneration. *Cell Tissue Res.* 365, 563–581. doi: 10.1007/s00441-016-2431-9

Terzini, M., Bignardi, C., Castagnoli, C., Cambieri, I., Zanetti, E. M., and Audenino, A. L. (2016). Dermis mechanical behaviour after different cell removal treatments. *Med. Eng. Phys.* 38, 862–869. doi: 10.1016/j.medengphy.2016.02.012

Thimm, T. N., Squirrell, J. M., Liu, Y., Eliceiri, K. W., and Ogle, B. M. (2015). Endogenous optical signals reveal changes of elastin and collagen organization during differentiation of mouse embryonic stem cells. *Tissue Eng. Part C Methods* 21, 995–1004. doi: 10.1089/ten.TEC.2014.0699

Tiburcy, M., Hudson, J. E., Balfanz, P., Schlick, S., Meyer, T., Chang Liao, M. L., et al. (2017). Defined engineered human myocardium with advanced maturation for applications in heart failure modeling and repair. *Circulation* 135, 1832–1847. doi: 10.1161/CIRCULATIONAHA.116.024145

Uitto, J., Olsen, D. R., and Fazio, M. J. (1989). Extracellular matrix of the skin: 50 years of progress. *J. Invest. Dermatol.* 92, 61S–77S. doi: 10.1111/1523-1747.ep13075039

Vandervelde, S., van Luyn, M. J., Tio, R. A., and Harmsen, M. C. (2005). Signalling factors in stem cell-mediated repair of infarcted myocardium. *J. Mol. Cell. Cardiol.* 39, 363–376. doi: 10.1016/j.yjmcc.2005.05.012

Vunjak-Novakovic, G., Tandon, N., Godier, A., Maidhof, R., Marsano, A., Martens, T. P., et al. (2010). Challenges in cardiac tissue engineering. *Tissue Eng. Part B Rev.* 16, 169–187. doi: 10.1089/ten.TEB.2009.0352

Wade, R. J., and Burdick, J. A. (2012). Engineering ECM signals into biomaterials. *Mater. Today* 15, 454–459. doi: 10.1016/S1369-7021(12)70197-9

Weber, K. T. (1989). Cardiac interstitium in health and disease: the fibrillar collagen network. *J. Am. Coll. Cardiol.* 13, 1637–1652. doi: 10.1016/0735-1097(89)90360-4

Weinberger, F., Mannhardt, I., and Eschenhagen, T. (2017). Engineering cardiac muscle tissue: a maturating field of research. *Circ. Res.* 120, 1487–1500. doi: 10.1161/CIRCRESAHA.117.310738

Williams, C., and Black, L. D. (2015). "The role of extracellular matrix in cardiac development," in *Biomaterials for Cardiac Regeneration*, eds E. J. Suuronen and M. Ruel (Berlin: Springer International Publishing), 1–35. doi: 10.1007/978-3-319-10972-5_1

Yaling, Y., Ali, A., Yuqiang, D., and Jin, M. (2016). Decellularized scaffolds in regenerative medicine. *Oncotarget* 7, 58671–58683. doi: 10.18632/oncotarget.10945

Ye, K. Y., and Black, L. D. III (2011). Strategies for tissue engineering cardiac constructs to affect functional repair following myocardial infarction. *J. Cardiovasc. Transl. Res.* 4, 575–591. doi: 10.1007/s12265-011-9303-1

Zhang, D., Shadrin, I. Y., Lam, J., Xian, H. Q., Snodgrass, H. R., and Bursac, N. (2013). Tissue-engineered cardiac patch for advanced functional maturation of human ESC-derived cardiomyocytes. *Biomaterials* 34, 5813–5820. doi: 10.1016/j.biomaterials.2013.04.026

Zhu, H., Li, X., Yuan, M., Wan, W., Hu, M., Wang, X., et al. (2017). Intramyocardial delivery of bFGF with a biodegradable and thermosensitive hydrogel improves angiogenesis and cardio-protection in infarcted myocardium. *Exp. Ther. Med.* 14, 3609–3615. doi: 10.3892/etm.2017.5015

Zimmermann, W. H., Fink, C., Kralisch, D., Remmers, U., Weil, J., and Eschenhagen, T. (2000). Three-dimensional engineered heart tissue from neonatal rat cardiac myocytes. *Biotechnol. Bioeng.* 68, 106–114. doi: 10.1002/(SICI)1097-0290(20000405)68:1<106::AID-BIT13<3.0.CO;2-3

Conflict of Interest: The authors declare that the research was conducted in the absence of any commercial or financial relationships that could be construed as a potential conflict of interest.

Copyright © 2020 Belviso, Romano, Sacco, Ricci, Massai, Cammarota, Catizone, Schiraldi, Nurzynska, Terzini, Aldieri, Serino, Schonauer, Sirico, D'Andrea, Montagnani, Di Meglio and Castaldo. This is an open-access article distributed under the terms of the Creative Commons Attribution License (CC BY). The use, distribution or reproduction in other forums is permitted, provided the original author(s) and the copyright owner(s) are credited and that the original publication in this journal is cited, in accordance with accepted academic practice. No use, distribution or reproduction is permitted which does not comply with these terms.

frontiers in Bioengineering and Biotechnology

REVIEW
published: 20 March 2020
doi: 10.3389/fbioe.2020.00149

MicroRNA Mediated Cardioprotection – Is There a Path to Clinical Translation?

*Timo Z. Nazari-Shafti[1,2,3], Vasileios Exarchos[1,4], Héctor Rodriguez Cetina Biefer[1,5], Nikola Cesarovic[1,4], Heike Meyborg[1], Volkmar Falk[1,3,4,5] and Maximilian Y. Emmert[1,3,5,6,7]**

[1] Department for Cardiovascular and Thoracic Surgery, German Heart Center Berlin, Berlin, Germany, [2] Berlin Institute of Health, Berlin, Germany, [3] Deutsches Zentrum für Herz-und Kreislauferkrankungen, Berlin, Germany, [4] Department of Health Sciences and Technology, ETH Zürich, Zurich, Switzerland, [5] Clinic for Cardiovascular Surgery, Charité Universitätsmedizin Berlin, Berlin, Germany, [6] Institute for Regenerative Medicine, University of Zurich, Zurich, Switzerland, [7] Wyss Zurich, University of Zurich and ETH Zurich, Zurich, Switzerland

In the past 20 years, there have been several approaches to achieve cardioprotection or cardiac regeneration using a vast variety of cell therapies and remote ischemic pre-conditioning (RIPC). To date, substantial proof that either cell therapy or RIPC has the potential for clinically relevant cardiac repair or regeneration of cardiac tissue is still pending. Preclinical trials indicate that the secretome of cells *in situ* (during RIPC) as well as of transplanted cells may exhibit cardioprotective properties in the acute setting of cardiac injury. The secretome generally consists of cell-specific cytokines and extracellular vesicles (EVs) containing microRNAs (miRNAs). It is currently hypothesized that a subset of known miRNAs play a crucial part in the facilitation of cardioprotective effects. miRNAs are small non-coding RNA molecules that inhibit post-transcriptional translation of messenger RNAs (mRNAs) and play an important role in gene translation regulation. It is also known that one miRNAs usually targets multiple mRNAs. This makes predictability of pharmacokinetics and mechanism of action very difficult and could in part explain the inferior performance of various progenitor cells in clinical studies. Identification of miRNAs involved in cardioprotection and remodeling, the composition of miRNA profiles, and the exact mechanism of action are important to the design of future cell-based but also cell-free cardioprotective therapeutics. This review will give a description of miRNA with cardioprotective properties and a current overview on known mechanism of action and potential missing links. Additionally, we will give an outlook on the potential for clinical translation of miRNAs in the setting of myocardial infarction and heart failure.

Keywords: microRNA, extracellular vesicles, second generation cell therapies, translation, cardioprotection, secretome

OPEN ACCESS

Edited by:
Monica Boffito, Politecnico di Torino, Italy

Reviewed by:
Zoltan Varga, Semmelweis University, Hungary
Mara Brancaccio, University of Turin, Italy

Correspondence:
Maximilian Y. Emmert
Maximilian.Emmert@irem.uzh.ch; maximilian.emmert@uzh.ch

Specialty section:
This article was submitted to Biomaterials, a section of the journal Frontiers in Bioengineering and Biotechnology

Received: *21 October 2019*
Accepted: *13 February 2020*
Published: *20 March 2020*

Citation:
Nazari-Shafti TZ, Exarchos V, Rodriguez Cetina Biefer H, Cesarovic N, Meyborg H, Falk V and Emmert MY (2020) MicroRNA Mediated Cardioprotection – Is There a Path to Clinical Translation? Front. Bioeng. Biotechnol. 8:149. doi: 10.3389/fbioe.2020.00149

INTRODUCTION

Cardiovascular disease remains one of the most important challenges clinicians face today. Despite huge efforts in prevention and undeniable progress in acute and short-term survival, disease progression over long-term still burdens our health care system without a real curative approach. The reason: regenerative capacity of an adult human heart is quite limited due to the low turnover

rate of cardiomyocytes and lack of a sufficient pool of tissue resident progenitors (Tzahor and Poss, 2017). This renders the human heart very susceptible to any form of acute or chronic injury with a critical loss of cardiomyocytes or their function, ultimately leading to the clinical manifestation of heart failure. For these facts, cardiac medicine has been identified as a promising field for application of regeneration technologies. In the past 20 years, cell-based therapies have aimed to either induce '*de novo*' generation or stimulate tissue dormant progenitors to differentiate into mature cardiomyocytes (Behfar et al., 2014). The promising results from *in vitro* studies and pre-clinical trials have led to a large number of clinical trials that for the most part investigated the therapeutic effect of different bone marrow, adipose- or neonatal tissue derived progenitor cells (first generation cell therapy). With limited pre-clinical data available in hindsight, a rush into first clinical trials in the early and mid 2000s has largely failed to demonstrate any meaningful results for patients with cardiac disease. More recently, myocardium resident cardiac progenitor cells, iPSCs, and conditioned progenitor cells have also been investigated in that context (second generation cell therapy) (Cambria et al., 2017). However, they as well failed to reach respective primary endpoints in most clinical trials; that is to say reduction in scar size and stabilization or improvement of cardiac function (Moyé, 2014; Gyöngyösi et al., 2015). As a result, the idea of a regenerating heart has been abandoned by many scientists. Luckily, the failure of such clinical studies has also led to *post hoc* analyses of the mechanism of action by which various cell types exhibit cardioprotection in the injured heart. Today, there is consensus that paracrine mediators, released by transplanted cells upon injury signals, mediate protection and limit adverse myocardial remodeling (Madonna et al., 2019). There is evidence emerging, that mediators can limit the extend of cardiomyocyte loss during acute injury and positively impact adverse myocardial remodeling in the chronic setting. Within the past 10 years, microRNAs (miRNAs) have come into focus as the next generation "cell" therapy studies have demonstrated that the paracrine secretion of nano- and macrovesicles containing miRNAs are mainly responsible for the cardioprotective effect of cellular therapies. Preclinical trials were able to demonstrate that miRNAs or extracellular vesicles (EVs) containing miRNAs were capable to reproduce the cellular effects of cardioprotection (Behfar and Terzic, 2019; Madonna et al., 2019; Maring et al., 2019). Within the scope of this review, we intend to provide a general overview of the potential role of miRNAs in cardioprotection and elaborate on potential use of miRNAs as a therapeutic agent.

MICRO RNAs – ONE SHOE FITS ALL?

MicroRNAs play an important role in the inhibition of messenger RNA (mRNA) translation in the cytoplasm but have been also identified to regulate transcription in the nuclear compartment of mammalian cells (Bartel, 2004). The biosynthesis was long believed to be linear and universal for all miRNAs. However, recent functional studies demonstrated, that a multitude of alternate miRNA-specific biosynthesis pathways exist and that they require a plethora of regulatory mechanisms – many of which still need to be identified (Lee et al., 1993; Bartel, 2004) (**Figure 1**). miRNA are encoded within the entire genome and are usually arranged in clusters (Rodriguez et al., 2004). Most miRNA genes are located in the non-coding areas of the genome. In some cases, miRNAs are located within the introns of protein coding genes such as miR-103 which is located within in the intron of pantothenate kinase 1, 2, and 3 together with miR-107 (Rodriguez et al., 2004; Lin et al., 2006). miRNAs are transcribed by RNA Polymerases II and III into a primary miRNA (pri-miRNA). The pri-miRNA consists of a terminal loop region, a stem and two single-stranded flanking RNA regions up- and downstream of the hairpin (Cai et al., 2004; Lee et al., 2004). For the canonical pathway of miRNA maturation, the terminal single stranded RNA region is then spliced by the complex of Drosha and DGCR8 protein (DiGeorge critical region 8) (Lee et al., 2003). The DGCR8 protein has a binding and proof-reading domain that ensures the correct binding and identification of the cleavage site for the Drosha protein, a RNase III enzyme. For some miRNAs additional factors may be required for the correct splicing of the hairpin precursor (Guil and Cáceres, 2007; Davis et al., 2008; Michlewski et al., 2008) before the precursor miRNA (pre-miRNA) is transported from the nucleus into the cytoplasm by Exportin-5 (Yi et al., 2003). Exportin-5 not only acts as a transporter but also as an additional "proof-reader" only transporting correctly processed pre-miRNA (Zeng and Cullen, 2004). In the cytoplasm, the pre-miRNA – still consisting of the terminal loop and the double stranded stem – binds to the RNA-induced silencing complex (RISC) (Gregory et al., 2005). This protein complex contains RNase Dicer, double stranded RNA binding domain proteins (Tar RNA binding protein), PACT (protein activator of PKR), and Argonaute-2 (MacRae et al., 2008). The latter is the key component that mediates the miRNA inhibition of transcription of mRNAs (Diederichs and Haber, 2007). The terminal loop of pre-miRNAs is spliced off, whereas for some of the miRNAs both the guide and passenger strand can serve as individual mature miRNAs (Matranga et al., 2005). In general, the passenger strand is degraded after unwinding of the double stranded pre-miRNA by helicases (Leuschner et al., 2006). Similar to the processing of miRNAs in the nucleus some miRNAs are dependent on additional co-factors for maturation (Hutvágner et al., 2001; Diederichs et al., 2008). This highlights again, that miRNA biosynthesis is subject to an integrate regulatory machinery which we only just begin to understand. Upon maturation, miRNAs as part of the RISC complex either inhibit the translation of their target mRNA or they are packaged into EVs contained in multivesicular bodies to be released in the extracellular space (Turchinovich et al., 2012). The encapsulation of miRNAs does not happen at random and is also a highly regulated process (Turchinovich et al., 2012; Villarroya-Beltri et al., 2013). This allows for the dynamic response of cells in regard to which miRNAs are released upon microenvironmental cues. A study by Villarroya-Beltri et al. (2013) has shown that specific motifs within the sequence of miRNA determine their localization in either the cytoplasm or EVs. They have also identified heterogeneous

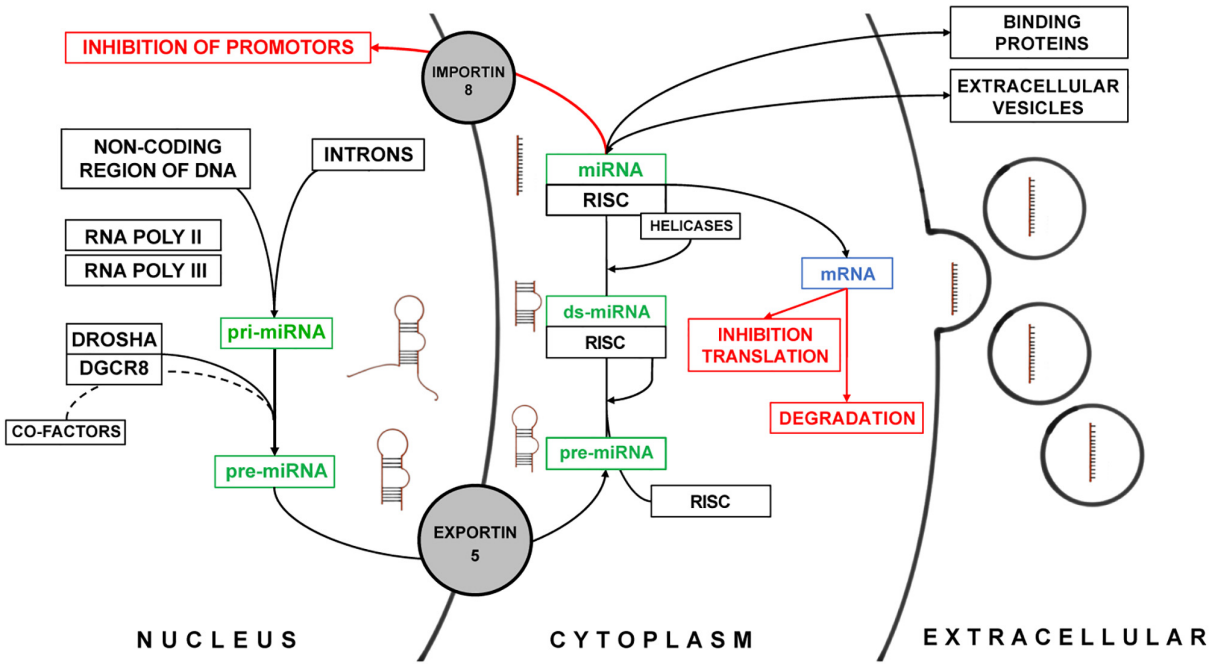

FIGURE 1 | Summary of the biosynthesis and the biological effect of miRNAs. The different stages of miRNA are schematically depicted next to the green description of miRNA. The biological effect of miRNAs is marked in red.

nuclear ribonucleoproteins such as hnRNPA2B1 and hnRNPA1 that specifically bind to these motifs and are also present in EVs. Independent of their origin, all miRNAs have in common to alter gene expression via inhibitory mechanisms of posttranscriptional modification of mRNAs. The mechanism of inhibition depends on the complementarity of the miRNA sequence to its target mRNA. miRNAs with high complementarity direct the RISC to the mRNA and initiate the degradation. Lower complementarity can lead to inhibition of ribosomal translation of the target mRNA. It is overall hypothesized that the specificity of miRNAs is determined by the quality and stability of base pairing to their respective targets. Furthermore, miRNAs have also been identified to perform transcriptional silencing by targeting promotor regions within the heterochromatin. The aforementioned regulation of biosynthesis, maturation, and biological effects of numerous miRNA can be influenced by changes in the cellular microenvironment in a non-linear manner – posing a major challenge for scientists to predict possible effects of miRNA *in vivo* (Lee et al., 1993; Liu B. et al., 2014).

CARDIOPROTECTIVE MIRNAs – A TWO-SIDED SWORD

For some time now, it has been hypothesized that factors released by cells under stress can induce a protective effect in neighboring or remote tissues (Kharbanda et al., 2002; Chen et al., 2008; Hausenloy et al., 2015). We now know that the key player in transmitting these signals are miRNAs. In the extracellular compartment, miRNAs are usually transported via EVs or binding proteins to protect them from degradation by nucleases (Li et al., 2012; Boon and Dimmeler, 2015). Similarly, the effect of therapeutic cell preparations exhibits their protective effect via the transmission of EVs loaded with miRNAs. Over the course of the past 10 years the sera of patients undergoing an ischemic event as well as the secretory profile of most cells utilized for cardioprotective purposes have been characterized (Baglio et al., 2015; Barile et al., 2016; Barile and Vassalli, 2017; Shao et al., 2017; Bellin et al., 2019). Each year, an increasing number of pathways are identified that either hint toward protection or damage of the myocardium (Barile et al., 2014, 2016; Gallet et al., 2016; Ciullo et al., 2019). Many functional studies have preceded these in-depth analyses of miRNA as cardioprotective agents, remote ischemic pre-conditioning (RIPC) being one of the most prominent examples (Kharbanda et al., 2002; Hausenloy et al., 2015). Here, a different organ or the heart itself is exposed to brief, non-fatal ischemia/reperfusion. Pre-clinical models show that RIPC can increase the survival of cardiomyocytes upon injury and positively impacts the myocardial remodeling (Konstantinov et al., 2005; Wei et al., 2011). In RIPC, circulating miRNA and EVs play an important role (Frey et al., 2018; Spannbauer et al., 2019). Even though circulating miRNAs and EVs have been identified as key mediators of that cardioprotective effect, it is a rather crude and a non-targeted therapeutic approach. Most when RIPC was investigated in clinical trials, none of the primary endpoints predicted by preclinical studies were met (Brevoord et al., 2012). Similar to experience from clinical trials investigating cell therapies, the exact mechanisms of action of RIPC were not fully understood and may explain the failed translation.

However, the data collected on miRNAs from these studies laid the groundwork for many functional studies investigating the cardioprotective effects of miRNAs.

In recent years, a plethora of mechanistical studies for the downstream effect of various miRNA were conducted. Here, miRNAs were either investigated as diagnostic markers or as potential targets for therapies (Barile et al., 2016). The in-depth analysis of regulation of the identified miRNAs and their downstream targets revealed that some miRNAs had contradictory effects in the myocardium (**Table 1**). Furthermore, to the best of our knowledge no study performed any concurrent analysis to identify potential targets that are not related to a cardioprotective effect. In this next section, we highlight a selection of miRNAs that have been associated with a cardioprotective potential but also bear the risk of adverse or off-target effects. Most of these miRNAs were identified either in EVs of therapeutic cell products or as biomarkers during acute and chronic myocardial injury. The knowledge of their exact mechanism of action is therefore highly recommended. The following miRNAs are only a small example of miRNAs that are commonly identified but not limited to their cardioprotective potential. The selection of miRNA should not be seen as a comprehensive summary of all known cardioprotective miRNAs which would be beyond the scope of this review. Others have provided more detailed lists of cardioprotective miRNAs (Varga et al., 2015; Wendt et al., 2018). The pre-clinical experience with the following miRNAs should highlight the potential and pitfalls we as scientist may face when designing therapeutic strategies with miRNAs.

MicroRNAs – The Good, the Bad, and the Ugly

Off-Target Effects of miRNAs

Especially studies investigating RIPC have identified clusters of cardioprotective miRNAs (Varga et al., 2015). In these studies as well as in those that used EVs, an undefined cocktail of miRNAs was systemically applied. In both cases, defining the mode of action is virtually impossible. Usually, hundreds of miRNAs can be identified in RIPC and even in EV preparations numerous miRNAs can be found, some of which taken by themselves have been identified as damaging to the myocardium. As an example, miR-665 has been identified in sera and serum exosomes of patients with heart failure (Li et al., 2016; Fan et al., 2019). MiR-665 directly targets the cannabinoid receptor 2 (CbR2) and adenylate kinase 1 (AK1) (Möhnle et al., 2014; Lin et al., 2019). In a rat heart Langendorff preparation, inhibition of CbR2 and AK1 leads to the upregulation of pro-apoptotic genes such as B cell lymphoma 2 (Bcl-2) and Bcl-2-associated X protein (Bax) and caspase-3 in H9c2 cells, a commonly used rat cardiomyocyte cell line (Yu et al., 2019). In a murine model of myocardial infarction, AAV9 transfection with miR-665 antisense miRNA led to improvement of cardiac function (Fan et al., 2018). Here, the group has identified glucagon-like peptide-1 receptor (GLP1R) as the target for miR-665. Inhibition of miR-665 expression led to increased cAMP signaling in the heart via the promotor GLP1R and reduced apoptotic events upon ischemia/reperfusion injury in the heart. Identification of harmful miRNAs like miRNA-665 in autologous exosome preparations from patients with heart failure could serve as quality markers and help prevent potential off-target effects. In some cases, off target effects or cardioprotective miRNAs have already been identified. miRNA-206, for example, has been associated with both cardioprotective, but also damaging effects upon overexpression (**Table 1**). Transcription of miR-206 can be induced via histamine release upon myocardial stress in mice (Ding et al., 2018). *In vitro*, miR-206 can prevent apoptosis in hypoxic conditions by targeting autophagy related protein 2 (ATG3) (Kong et al., 2019). In a murine model of acute myocardial infarction, this prevented ubiquitination of cytosomal proteins and apoptosis (Ding et al., 2018). By cardiac-specific overexpression of miR-206 is has been shown that forkhead box protein P1 induces hypertrophy of cardiomyocytes which during stress can prevent cardiomyocyte apoptosis (Yang et al., 2015). By inhibiting metalloproteinase inhibitor 3 (TIMP3), miR-206 has also been shown to attenuate cardiac fibrosis in the setting of chronic heart failure (Limana et al., 2011). However, two independent groups have also uncovered two mechanisms by which miR-206 increases the risk of cardiac arrhythmias. miR-206 targets connexin 43 (Cx43), an important component of gap junctions in the myocardium in a transgenic mouse model (Roell et al., 2007). Low expression of Cx43 has been associated with cardiac arrhythmias such as atrial fibrillation. Additionally, Wei et al. (2018) uncovered that miR-206 binds to GTP cyclohydrolase I (GCH1) in a canine model of atrial fibrillation (Afib). GCH1 is the rate limiting enzyme in *de novo* synthesis of tetrahydrobiopterin (BH4). Decreased expression of BH4 was associated with shortened refractory times in atrial cardiomyocytes in humans, which led to Afib (Wei et al., 2018). In this example, different groups were able to demonstrate a cardioprotective effect of miR-206. At the same time potential off target effects were uncovered that could impede the translation of important signal transduction proteins in the myocardium. These off-target effects were never investigated in the murine models that investigated the cardioprotective effects for this miRNA. It has also been shown that miRNA have species specific effects. A recently published large animal study demonstrated that the delivery of miR-199 via adenoviral transfer to the myocardium of pigs resulted in improved contractility and myocardial mass in the short term (Gabisonia et al., 2019). After 1 month, however, the pigs died of arrhythmias. Histological analysis revealed that the myocardium was infiltrated with proliferating cells displaying a poorly differentiated myoblastic phenotype. This off-target effect of miR-199 was not identified in small animal studies. Results like these raise the question whether results from murine models or even porcine models are really translatable into clinical applications without additional safeguards that can predict these off-target and adverse effects.

Neoangiogenesis – Good for Cardioprotection, Bad for Cancer Progression

Neoangiogenesis plays an important role in protecting the myocardium in the border zones from infarcts from myocardial

TABLE 1 | Summarizes a selection of miRNAs that have been identified with either a harmful or cardioprotective property in cardiovascular disease.

miRNA	Disease model	Releasing cell type	Experimental approach	Experimental model	Effect	Identified targets	Recipient cell	Off-target effects	PMID
miR-665	I/R	CM	Suppression of miR-665 via dexmedetomidine	Rat heart Langendorff preparation	Improved LVDP during reperfusion	AK1, Cbr2	Cardiac cells	Not investigated	31026731
	HF	–	I.m. injection with anti-sense miRNA plasmids	Rat model of HF	Improved LVEF, reduced CM apoptosis, improved Mc ultrastructure	GLP1R	Cardiac cells	Not investigated	30666648
	HF	Global	I.v. injection of rAAV miR-665 inhb.	Murine model of LV pressure overload	Improved LVEF, reduced fibrosis, improved vascularization	CD34	Global	Not investigated	30243022
	–	Human CM	*In vitro* gain and loss of function in human CM	Mechanistic model	–	Cbr1 and Cbr2	Human CM	–	25111814
miR-132	I/R	–	Loss of function *in vivo*, gain of function *in vitro*	Murine hind limb ischemia	Slower perfusion recovery, less collateralization, modulation of RAS-MAPK signaling	Rasa1 and Spred1	–	Not investigated	25016614
	Afib	–	*In vitro* loss and gain of function in CF	Mechanistic model	In human and dog with Afib decreased expr. miR-132 in atrium	CTGF	CF	–	28731126
	DCM	–	*In vitro* analysis of cardiac cell isolates from DCM rats, overexpression of miR-132	DCM rat model	Activation of PI3K/Akt pathway, CM apoptosis down	PTEN	–	–	30271437
	AMI	BM-MSCex electroporated with miR-132	I.m. injections with MSCex	Murine model of AMI	Increased LVEF, enhanced neovascularization in BZ	Rasa1	HUVECS	Not investigated	30216493
miR-132 + miR-126	DMap	–	Transfection of aortic rings with miR-132, miR-126	Endothelial sprouting in aortic rings under high glucose	Decreased EC apoptosis, improved endothelial sprouting	Spred1	HUVECS, Ecs	–	31179325
miR-210 + miR-132 + miR-146a-3p	AMI	CPCs	I.v. injection with CPCex rich in miR-210, miR-132, miR-146a-3p vs. Fibex	Murine model of AMI	Less CM apoptosis, enhanced angiogenesis in BZ, improved LVEF	EFNA3, PTP1b	–	Not investigated	28731126
miR-126	AMI	AT-MSCs overexpressing miR-126	I.m. injection of AT-MSCex	Murine model of AMI	Increased neoangiogenesis	Not investigated	–	Not investigated	29241208
miR-126-5p	Endothelial injury	–	KO of EC Dicer and rescue experiment with miR-126-5p transfection	CA injury	Endothelial Dicer processes pre-mir-126 into mir-126-3p (guide strand) and the passenger strand-5p. 5p is involved in dendothelial repair and proliferation by targeting the Notch1 inhibitor Delta-like homolog 1 (Dlk1)	Dlk1	ECs	Not investigated	30213595

(Continued)

TABLE 1 | Continued

miRNA	Disease model	Releasing cell type	Experimental approach	Experimental model	Effect	Identified targets	Recipient cell	Off-target effects	PMID
mir-210	AMI	–	Observational study	AMI in rats	Increased levels of miR-210	–	–	–	31596148
	AMI	BM-MSCs	BM-MSCs rich in miR-210 vs. BM-MSCs with miR-210 silencing	Murine model of myocardial infarction	Increase LVEF, increased neoangiogenesis	EFNA3	–	Not investigated	28249798
	I/R	BM-EPCs	BM-EPCs gain and loss of miR-210	Murine hind limb ischemia	With miR-210 improved perfusion recovery and collateralization	EFNA3	ECs	Not investigated	29908843
	I/R	–	Loss and gain of function	*In vitro* in H9c2 cells, mechanistic model		CXCR4	H9c2	–	29710553
mir-206	Afib		Lentiviral overexpression of miR-206 in PVFP	Canine model of Afib	Overexpression of miR-206 increased incidence of Afib	GCH1	–	Not investigated	29436714
	Afib	–	Overexpression of miR-206 in murine hearts	Transgenic mouse model	Overexpression led to decreased lifespan and arrhythmias	Cx43	–	Not investigated	30322759
	AMI	–	Cardiac specific expression of miR-206	Murine model of AMI	CM hypertrophy and increases survival under AMI	FBPP1	–	Not investigated	26333362
	HF	–	Increased expression of miR-206 via HMGB1	Murine model of AMI	Increased collagenolytic activity, decreases myocardial fibrosis	TIMP3	CF	Not investigated	21731608
	AMI	–	*In vitro* loss and gain of function, with *in vivo* confirmation	Murine model of AMI	Reduced CM apoptosis, improved LVEF	ATG3	H9c2	Not investigated	30551524
miR-206 + miR-216b	AMI	–	Via HDC gain and loss influence expression of miR-206, miR-216b	Murine model of AMI	Targets Atg13 and reduces autophagy upon hypoxia. miR-206 is induced via histamine	ATG3	–	Not investigated	29880830
miR-206 + miR-1	DMap	–	*In vitro* loss and gain of function	*In vitro* in H9c2 cells, mechanistic model	Increased CM apoptosis	Hsp60	H9c2	–	20655308
miR-146a	DCM	CF, CM	AAV9 mediated overexpression of miR146a *in vivo* and *in vitro*	Murine model of LV pressure overload	Decreased myocardial contractility	SUMO1	CM	Not investigated	30355233
	AMI	EPCs	EPC injection in BZ	AMI in rats	Downregulation of miR-146a and reduced CM apoptosis and increased VEGF expression	–	–	Not investigated	30344699
	–	–	Lentiviral overexpression of miR-146a in H92c	*In vitro* in H9c2 cells, mechanistic model	Increases MMP9, may reduce fibrosis in injured heart	FOS, AP1	CM	–	26112171
	Sepsis induced cardiac dysfunction	–	Transfection of mice with miR-146a, *in vitro* H9c2 and macrophages	Murine sepsis model	Attenuation of sepsis induced myocardial dysfunction	IRAK, TRAF6	H9c2, J774 macrophages		26048146

(Continued)

TABLE 1 | Continued

miRNA	Disease model	Releasing cell type	Experimental approach	Experimental model	Effect	Identified targets	Recipient cell	Off-target effects	PMID
	DoxDCM	CM	*In vitro* overexpression and suppression of miR-146a	*In vitro* in H9c2 cells, mechanistic model	Induction of cell death upon Dox treatment	ErbB4	H9c2	–	20495188
	AMI	AT-MSCs overexpressing miR-146a	I.m. injections of AT-MSCex native and overexpressing miR-146a	AMI in rats	Decreased CM apoptosis, decreased inflammation, decreased fibrosis	EGR1	H9c2	Not investigated	30362610
miR-146a-5p	DoxDCM	CPCs	CPCex rich in miR-146a-5p vs. Fibex	DoxDCM model in rats	Decreased CM apoptosis	Traf6, Smad4, Nox4, Mpo	–	Not investigated	31098627
miR-146a + miR-155	–	DC	Injection of endotoxin exposed mice with Dcex rich in miR-155 and miR-146a	Murine model of endotoxin inflammation	miR-146a attenuates inflammation, miR-155 increases inflammation	–	–	Not investigated	26084661
miR-22	AMI	–	AAV9 overexpression of miR-22	AMI in rats	Decreased CM apoptosis, decreases infarct size	CBP	–	Not investigated	24338162
	–	–	Overexpression of miR-22 in murine lungs, zebrafish and ECs *in vitro*	–		VEC	EC	Not investigated	28112401
	AMI, HF	–	Gain and loss study on miR-22	*In vitro* in CF, mechanistic model	Overexpression limits expression of Col1α1, Col3α1	TGFβR	CF	–	27997889
	AMI	–	Gain and loss study on miR-22	*In vitro* in rat CMs	Overexpression prevented autophagy and apoptosis in CMs	p38α	CM	–	
	AMI	–	I.m. injection of miR-22 inhib., loss and gain function *in vitro*	AMI in rats	Inhibition decreases infarct size, reduces CM apoptosis	Sirt1, PGC1α	H9c2	Not investigated	27174562
	DCM	–	miR-22 deficient mice and gain and loss function in H9c2	Murine model of left ventricular pressure over load	miR-22 suppression led to left ventricular dilation	PReBPb	H9c2	Not investigated	22570371
	DCM	–	Gain and loss of miR-22 in mice	Murine model of left ventricular pressure overload	Overexpression of miR-22 protected from DCM	Sirt1, Hdac4	–	Not investigated	23524588
	–	–	Gain and loss study in H9c2	*In vitro* in H9c2 cells, mechanistic model	Prevents the activation of NFkB/Caspase3 mediated apoptosis upon stress	p65	H9c2	–	30504734
	AMI	–	*In vitro* gain and loss study, *in vivo* miR-22 KO mice	Murine model of AMI	In miR-21 KO mice decreased survival, decreased LVEF, increased scar size	KBTBD7	Macrophages		29991775

(Continued)

TABLE 1 | Continued

miRNA	Disease model	Releasing cell type	Experimental approach	Experimental model	Effect	Identified targets	Recipient cell	Off-target effects	PMID
miR-21	AMI	–	AAV9 overexpression of miR-21	AMI in rats	Promotes cardiac fibroblast activation and CF to myofibroblast transformation (CMT)	Jagged1	–	Not investigated	29808534
	–				Targets PDCD4 to reduce apoptosis after HIF-1alpha activated expression of mir21				29170412
	AMI	–	*In vitro* in CF, *in vivo* induction of miR-21 via TGF-β1	Murine model of AMI	Increased fibrosis in the heart upon AMI	Smad7	CF	Not investigated	28817807
	–	–	Gain and loss study in H9c2 cells	*In vitro* in H9c2 cells, mechanistic model	Inhibits autophagy and apoptosis upon I/R partially via the Akt/mTOR pathway	–	H9c2	–	27680680
	–	–	Exposure of H9c2 cells with CPC derived EVs rich in miR-21	*In vitro* in H9c2 cells, mechanistic model	Targets PDCD4 when CDC derived exosomes are added to CMs	–	H9c2	–	27336721
	–	–	Gain and loss study in PBMCs	*In vitro* in human PBMCs, mechanistic model	Via targeting SMAD7, mir-21 can reduce the number of circulating Tregs	Smad7	Human Tregs	–	26383248
	–	–	Gain and loss study in H9c2 cells	*In vitro* in H9c2 cells, mechanistic model	Proof for a positive feedback loop between mir-21 and HIF-1alpha which reduces apoptosis upon hypoxia and stress	PTEN	H9c2	–	24983504
miR-21-5p	–	–	Gain and loss study in H9c2	*In vitro* in H9c2 cells, mechanistic model	Modulation of reliance on glycolytic or fatty acid oxidation in mitochondria	–	H9c2	–	30657727
	–	BM-MSCs	Exposure of H9c2 cells with BM-MSCex rich in miR-21a-5p	*In vitro* in H9c2 cells, mechanistic model	Reduction of CM apoptosis upon stress. This was identified in EVs from MSCs (miR-21a-5p).	PDCD4, PTEN, Peli1 an dFasL	H9c2	–	29698635

AAV, adeno-associated-virus; Afib, atrial fibrillation; AMI, acute myocardial infarction; AT-MSCex, AT-MSC exosomes; AT-MSCs, adipose tissue derived mesenchymal stem cells; BM-EPCs, bone marrow derived endothelial progenitor cells; BM-MSCex, BM-MSC exosomes; BM-MSCs, bone marrow derived mesenchymal stem cells; CF, cardiac fibroblast; CPCs, cardiac progenitor cells; DCex, dendritic cell exosomes; DCM, dilated cardiomyopathy; DCs, dendritic cells; DMap, diabetic myocardial microangiopathy; DoxDCM, doxorubicin induced dilated cardiomyopathy; ECs, endothelial cells; EPCs, endothelial progenitor cells; HF, heart failure; HUVECs, human umbilical vein endothelial cells; I/R, ischemia reperfusion.

remodeling. Therefore, many miRNAs such as miR-132, miR-126, and miR-210 have been investigated for their angiogenic potential (**Table 1**). The transcription of most of these miRNAs is dependent on the expression VEGF (Lei et al., 2015; Chodari et al., 2019). For instance, miR-132 expression is dependent in the promotor cAMP response element-binding protein as the transcription factor, which is induced by VEGF stimulation (Chodari et al., 2019). EVs from cardiac progenitor cells (CPCs) rich in miR-132 inhibit the translation of Ras GTPase activating protein (p120RasGAP) which promotes proliferation and sprouting of endothelial cells thus improving neovascularization *in vivo* and *in vitro* (Barile et al., 2014). In a murine model of acute myocardial infarction this led to improved left ventricular ejection fraction on a functional level and improved vascularization in the infarct border zone on a histological level (Barile et al., 2014). Similarly, EVs from adipose-derived mesenchymal stem cells (AT-MSCs) that overexpressed miR-126, also improved cardiac function and resulted in a denser microvasculature in the infarct border zone in rats (Luo et al., 2017). Functional studies have shown that miR-126 is highly depended on the activation of endothelial dicer RNA Polymerase III. Only the passenger strand miR-126-5p can bind to the Notch1 inhibitor Delta-like homolog 1 (Dlk1) (Zhou Z. et al., 2018). The notch signaling pathway is crucial to endothelial cell differentiation and endothelial sprouting (Mack and Iruela-Arispe, 2018). While there is no direct evidence linking the cardioprotective effect of miR-132 to cardiomyocytes, there is evidence that miR-132 can also reduce fibrosis in by targeting connective tissue growth factor (Zhang C.-J. et al., 2018). Furthermore, miR-132 has also been identified in a rat model of DCM to target phosphatase and tensin homolog (PTEN) (Ma et al., 2018). Suppression of PTEN activates the phosphoinositide 3-kinases/protein kinase B pathway (PI3K/Akt-pathway) which facilitates cardiomyocyte and endothelial proliferation alike (Zhang C.-J. et al., 2018). miR-210 has also been shown to promote angiogenesis in the myocardium (Mutharasan et al., 2011). In contrast to miR-126 and miR132, the expression of miR-210 depends on HIF-1alpha, which is also released under hypoxic stress (Barile et al., 2014). In both murine models of acute myocardial infarction and hind limb ischemia it has been shown that miR-210 encapsulated by EVs promotes angiogenesis in endothelial cells as well as suppresses apoptosis in cardiomyocytes by targeting Ephrin A3 (Barile et al., 2014; Wang et al., 2017; Besnier et al., 2018). While the upregulation or substitution of all aforementioned miRNAs are associated with a pro-angiogenic profile in the setting of myocardial infarction, they have also been identified in cancer biogenesis and metastasis formation. Also, in the field of cancer biology the data for these miRNAs is heterogeneous and in depending on cancer type they are both associated as a positive and negative prognostic marker. The heterogeneity of these results and their role in tumor progression could, however, pose an obstacle for their use as a cardioprotective agent. As a solution, patients susceptible to certain cancers that depend on overexpression of these miRNA need to be identified to prevent adverse effects from a hypothetical therapeutic miRNA.

How to Deal With Contradictory Results

miR-146a is part of a negative feedback loop in the canonical pathway of NFkB activation. miR-146a binds to the mRNA encoding for interleukin-1 receptor associated kinase 1 (IRAK1) and tumor necrosis factor receptor-associated receptor 6 (TRAF6). Both of this receptor bound factors are essential for the IL-1 and TNFalpha activation of NFkB (Fish and Cybulsky, 2015; Gao et al., 2015; Milano et al., 2019). As part of that negative feedback loop miR-146a is highly expressed in atherosclerotic plaques. However, the overexpression of this miRNA can also attenuate the inflammatory response as shown in gain and loss studies in ApoE deficient mice, where miRNA-146a plays an important part in the attenuation of atherosclerotic plaques (Fish and Cybulsky, 2015). In a rat model of AMI, EVs from AT-MSCs overexpressing miR-146a targeted the early growth response protein 1 in cardiomyocytes decreasing cardiomyocyte apoptosis, cardiac fibrosis and ultimately improving the heart function (Pan et al., 2019). Milano et al. (2019) demonstrated that the passenger strand miR-146a-5p reduced the inflammatory signaling pathways by directly targeting TRAF6, SMAD4, IRAK1, NADPH oxidase 4 (NOX4), and myeloperoxidase (MPO) in a model of doxorubicin/trastuzumab induced cardiomyopathy. Interestingly, another group showed that with treatment of doxorubicin alone an upregulation of miR146a occurs, targeting the receptor tyrosine-protein kinase erbB-4 (ErbB4). Here, a negative correlation between miR-146a and cardiac function was confirmed and explained by the suppression of the ErbB4 dependent neuregulin1/ErbB pathway, which is essential for adult cardiac function (Horie et al., 2010). It is, however, important to note that these results were only obtained from *in vitro* experiments. Both miR-21 and -22 have been associated with cardioprotective properties by reducing cardiomyocyte apoptosis and have been found in most EVs from therapeutic cell product isolates to date (Barile et al., 2016; Gallet et al., 2016). While there is evidence, that miR-22 also exhibits an anti-fibrotic effect during myocardial remodeling, overexpression of miR-21 is clearly associated with promoting cardiac fibrosis (**Table 1**). miR-21 directly targets jagged1 and SMAD7 in rat hearts when overexpressed via AAV9 (Zhou X.-L. et al., 2018). In the aforementioned experiment, jagged1 suppression activates cardiac fibroblast proliferation and facilitates cardiac fibroblast to myofibroblast transformation. In a murine model of AMI, suppression of SMAD7 via miR-21 led to an increased expression of Collagen 1 alpha, alpha-smooth muscle actin (alpha-SMA) and F-actin. In a similar model of AMI in rats, AVV9 mediated overexpression of miR-22 let to the inhibition of CBP-associated factor AP1 (Yang et al., 2014). Downregulation of this promotor leads to the activation of MMP9, which in turn can reduce cardiac fibrosis. Additionally, miR-22 binds to the mRNA coding for the TGFbeta receptor 1 (Hong et al., 2016). In mice, silencing of miR-22 led to increased expression of Collagen 1 alpha 1 and 3alpha1 and an overall increased amount of cardiac fibrosis after myocardial infarction. Regarding the anti-apoptotic effect of miR-22, there are contradictory results published to date. Gurha et al. (2012) and Du et al. (2016) both demonstrated that SIRT1 and PGC1alpha are both targeted by miR-22 in

cardiomyocytes. In both experiments, overexpression of miR-22 lead to increased cell death and reduction in myocardial mass whereas in the studies published by Huang et al. (2013) and Hong et al. (2016) cardiac mass increased upon miR-22 overexpression and ischemia/reperfusion injury. Huang et al. (2013) also demonstrate the targeting of SIRT1 but in their hands, cardiomyocyte hypertrophy was the predominant finding. Hong et al. (2016) demonstrated decreased apoptosis levels in the myocardium and linked that effect to the inhibition of CREB. For miR-21 the anti-apoptotic effects is shown more robustly between different research teams (**Table 1**). miR-21 expression is under direct control of HIF1alpha but can also influence the expression of HIF1alpha itself in a positive feedback loop (Liu Y. et al., 2014). The miRNA targets programmed cell death protein 4 (PCDP4) and reduces cell apoptosis upon hypoxic stress. This effect has been demonstrated with EVs containing high levels of miR-21 from different cell types such as CPCs and MSCs (Xiao et al., 2016; Luther et al., 2018). Both miR-21 and miR-22 exemplify the various outcomes that can be seen when working with miRNAs in pre-clinical models. Even within one species there are variations and sometime contradictory results that can be elaborated by other groups on both ends of the aisle. Especially miRNAs that can promote fibrosis can have severe and unwanted effects in the injured heart and may lead to increase in scar mass. Here, patient screening and good patient selection may help to prevent these contradictory results. This can only be achieved by understanding all pathways that can be altered by each respective miRNA and tools to identify patients that may be susceptible to treatments with certain miRNAs.

SUMMARY

The data that has been collected on miRNAs targeting cardioprotection so far exemplifies the importance of knowing the relevant targets of miRNAs, since introduction of foreign miRNAs via exosomal transfer or other clinical relevant approaches may have some severe side effects. In this context, it is also worth noting that all of the aforementioned miRNAs are also involved in tumor biology. Especially miRNAs that impact neoangiogenesis in myocardial repair are important factors in tumor angiogenesis as well. In addition, most of the mechanistical studies have focused on the interaction of one miRNA on multiple targets. Upon ischemia/reperfusion or transfer of exogenous EVs the interaction of numerous miRNAs on multiple potential targets needs to be taken into account. With current methods, experimental data usually depicts a single linear arm in a complex matrix of interactions between miRNAs, mRNAs and transcription factors. Our current understanding of these complex matrices is only rudimental at best. And it may also be one of the main reasons why none of the clinical trials with cell-based therapies or RIPC have delivered the expected results we anticipated from pre-clinical experience. As repeatedly highlighted by numerous experts in the field, understanding the pathways by which a single- or a collection of miRNAs in an exosome, facilitate cardioprotection will be crucial for successful clinical translation (Madonna et al., 2016, 2019; Behfar and Terzic, 2019). Combined effort of computational models and artificial intelligence in merging and interpreting the acquired data, might help us in the future to achieve this goal. Identifying such 'pathway' matrices will be detrimental in defining quality standards for therapeutic exosome or single miRNA-based products. The past experience from cell-based therapies have taught us that preclinical data in the field of cardiac regeneration or cardioprotection does not necessarily translate into therapeutic success in the clinical setting. Going forward, we will have to deepen our understanding of miRNA interactions by strengthen our efforts to collaborate with bioinformaticians for more sophisticated predictive algorithms.

AUTHOR CONTRIBUTIONS

TN-S and ME contributed to the conception and design of this review. VE, HR, and HM helped to organize the article database and supported the literature review. TN-S wrote the first draft of the manuscript. All authors contributed to manuscript revision, read and approved the submitted version.

FUNDING

TN-S is a participant in the BIH Charité Clinician Scientist Program funded by the Charité -Universitätsmedizin Berlin and the Berlin Institute of Health.

REFERENCES

Baglio, S. R., Rooijers, K., Koppers-Lalic, D., Verweij, F. J., Pérez Lanzón, M., Zini, N., et al. (2015). Human bone marrow- and adipose-mesenchymal stem cells secrete exosomes enriched in distinctive miRNA and tRNA species. *Stem Cell Res. Ther.* 6:127. doi: 10.1186/s13287-015-0116-z

Barile, L., Lionetti, V., Cervio, E., Matteucci, M., Gherghiceanu, M., Popescu, L. M., et al. (2014). Extracellular vesicles from human cardiac progenitor cells inhibit cardiomyocyte apoptosis and improve cardiac function after myocardial infarction. *Cardiovasc. Res.* 103, 530–541. doi: 10.1093/cvr/cvu167

Barile, L., Moccetti, T., Marbán, E., and Vassalli, G. (2016). Roles of exosomes in cardioprotection. *Eur. Heart J.* 38, 1372–1379. doi: 10.1093/eurheartj/ehw304

Barile, L., and Vassalli, G. (2017). Exosomes: therapy delivery tools and biomarkers of diseases. *Pharmacol. Ther.* 174, 63–78. doi: 10.1016/j.pharmthera.2017.02.020

Bartel, D. P. (2004). MicroRNAs: genomics, biogenesis, mechanism, and function. *Cell* 116, 281–297. doi: 10.1016/S0092-8674(04)00045-5

Behfar, A., Crespo-Diaz, R., Terzic, A., and Gersh, B. J. (2014). Cell therapy for cardiac repair–lessons from clinical trials. *Nat. Rev. Cardiol.* 11, 232–246. doi: 10.1038/nrcardio.2014.9

Behfar, A., and Terzic, A. (2019). Regeneration for all: an Odyssey in biotherapy. *Eur. Heart J.* 40, 1033–1035. doi: 10.1093/eurheartj/ehz095

Bellin, G., Gardin, C., Ferroni, L., Chachques, J., Rogante, M., Mitrečić, D., et al. (2019). Exosome in cardiovascular diseases: a complex world full of hope. *Cells* 8:166. doi: 10.3390/cells8020166

Besnier, M., Gasparino, S., Vono, R., Sangalli, E., Facoetti, A., Bollati, V., et al. (2018). miR-210 enhances the therapeutic potential of bone-marrow-derived circulating proangiogenic cells in the setting of limb ischemia. *Mol. Ther.* 26, 1694–1705. doi: 10.1016/j.ymthe.2018.06.003

Boon, R. A., and Dimmeler, S. (2015). MicroRNAs in myocardial infarction. *Nat. Rev. Cardiol.* 12, 135–142. doi: 10.1038/nrcardio.2014.207

Brevoord, D., Kranke, P., Kuijpers, M., Weber, N., Hollmann, M., and Preckel, B. (2012). Remote ischemic conditioning to protect against ischemia-reperfusion injury: a systematic review and meta-analysis. *PLoS One* 7:e42179. doi: 10.1371/journal.pone.0042179

Cai, X., Hagedorn, C. H., and Cullen, B. R. (2004). Human microRNAs are processed from capped, polyadenylated transcripts that can also function as mRNAs. *RNA* 10, 1957–1966. doi: 10.1261/rna.7135204

Cambria, E., Pasqualini, F. S., Wolint, P., Günter, J., Steiger, J., Bopp, A., et al. (2017). Translational cardiac stem cell therapy: advancing from first-generation to next-generation cell types. *npj Regen. Med.* 2:17. doi: 10.1038/s41536-017-0024-1

Chen, L., Tredget, E. E., Wu, P. Y. G., Wu, Y., and Wu, Y. (2008). Paracrine factors of mesenchymal stem cells recruit macrophages and endothelial lineage cells and enhance wound healing. *PLoS One* 3:e1886. doi: 10.1371/journal.pone.0001886

Chodari, L., Dariushnejad, H., and Ghorbanzadeh, V. (2019). Voluntary wheel running and testosterone replacement increases heart angiogenesis through miR-132 in castrated diabetic rats. *Physiol. Int.* 106, 48–58. doi: 10.1556/2060.106.2019.06

Ciullo, A., Biemmi, V., Milano, G., Bolis, S., Cervio, E., Fertig, E. T., et al. (2019). Exosomal expression of CXCR4 targets cardioprotective vesicles to myocardial infarction and improves outcome after systemic administration. *Int. J. Mol. Sci.* 20:468. doi: 10.3390/ijms20030468

Davis, B. N., Hilyard, A. C., Lagna, G., and Hata, A. (2008). SMAD proteins control DROSHA-mediated microRNA maturation. *Nature* 454, 56–61. doi: 10.1038/nature07086

Diederichs, S., and Haber, D. A. (2007). Dual role for argonautes in microRNA processing and posttranscriptional regulation of microRNA expression. *Cell* 131, 1097–1108. doi: 10.1016/j.cell.2007.10.032

Diederichs, S., Jung, S., Rothenberg, S. M., Smolen, G. A., Mlody, B. G., and Haber, D. A. (2008). Coexpression of Argonaute-2 enhances RNA interference toward perfect match binding sites. *Proc. Natl. Acad. Sci. U.S.A.* 105, 9284–9289. doi: 10.1073/pnas.0800803105

Ding, S., Abudupataer, M., Zhou, Z., Chen, J., Li, H., Xu, L., et al. (2018). Histamine deficiency aggravates cardiac injury through miR-206/216b-Atg13 axis-mediated autophagic-dependant apoptosis. *Cell Death Dis.* 9:694. doi: 10.1038/s41419-018-0723-6

Du, J.-K., Cong, B.-H., Yu, Q., Wang, H., Wang, L., Wang, C.-N., et al. (2016). Upregulation of microRNA-22 contributes to myocardial ischemia-reperfusion injury by interfering with the mitochondrial function. *Free Radic. Biol. Med.* 96, 406–417. doi: 10.1016/j.freeradbiomed.2016.05.006

Fan, J., Li, H., Nie, X., Yin, Z., Zhao, Y., Zhang, X., et al. (2018). MiR-665 aggravates heart failure via suppressing CD34-mediated coronary microvessel angiogenesis. *Aging (Albany NY)* 10, 2459–2479. doi: 10.18632/aging.101562

Fan, J., Zhang, X., Nie, X., Li, H., Yuan, S., Dai, B., et al., (2019). Nuclear miR-665 aggravates heart failure via suppressing phosphatase and tensin homolog transcription. *Sci. China Life Sci.* 1–13. doi: 10.1007/s11427-018-9515-1

Fish, J. E., and Cybulsky, M. I. (2015). ApoE attenuates atherosclerosis via miR-146a. *Circ. Res.* 117, 3–6. doi: 10.1161/CIRCRESAHA.115.306733

Frey, U. H., Klaassen, M., Ochsenfarth, C., Murke, F., Thielmann, M., Kottenberg, E., et al. (2018). Remote ischaemic preconditioning increases serum extracellular vesicle concentrations with altered micro−RNA signature in CABG patients. *Acta Anaesthesiol. Scand.* 63, 483–492. doi: 10.1111/aas.13296

Gabisonia, K., Prosdocimo, G., Aquaro, G. D., Carlucci, L., Zentilin, L., Secco, I., et al. (2019). MicroRNA therapy stimulates uncontrolled cardiac repair after myocardial infarction in pigs. *Nature* 569, 418–422. doi: 10.1038/s41586-019-1191-6

Gallet, R., Dawkins, J., Valle, J., Simsolo, E., de Couto, G., Middleton, R., et al. (2016). Exosomes secreted by cardiosphere-derived cells reduce scarring, attenuate adverse remodelling, and improve function in acute and chronic porcine myocardial infarction. *Eur. Heart J.* 38, 201–211. doi: 10.1093/eurheartj/ehw240

Gao, M., Wang, X., Zhang, X., Ha, T., Ma, H., Liu, L., et al. (2015). Attenuation of cardiac dysfunction in polymicrobial sepsis by MicroRNA-146a is mediated via targeting of IRAK1 and TRAF6 expression. *J. Immunol.* 195, 672–682. doi: 10.4049/jimmunol.1403155

Gregory, R. I., Chendrimada, T. P., Cooch, N., and Shiekhattar, R. (2005). Human RISC couples microRNA biogenesis and posttranscriptional gene silencing. *Cell* 123, 631–640. doi: 10.1016/j.cell.2005.10.022

Guil, S., and Cáceres, J. F. (2007). The multifunctional RNA-binding protein hnRNP A1 is required for processing of miR-18a. *Nat. Struct. Mol. Biol.* 14, 591–596. doi: 10.1038/nsmb1250

Gurha, P., Abreu-Goodger, C., Wang, T., Ramirez, M. O., Drumond, A. L., Van Dongen, S., et al. (2012). Targeted deletion of MicroRNA-22 promotes stress-induced cardiac dilation and contractile dysfunction. *Circulation* 125, 2751–2761. doi: 10.1161/CIRCULATIONAHA.111.044354

Gyöngyösi, M., Wojakowski, W., Lemarchand, P., Lunde, K., Tendera, M., Bartunek, J., et al. (2015). Meta-analysis of cell-based CaRdiac stUdiEs (ACCRUE) in patients with acute myocardial infarction based on individual patient data. *Circ. Res.* 116, 1346–1360. doi: 10.1161/CIRCRESAHA.116.304346

Hausenloy, D. J., Candilio, L., Evans, R., Ariti, C., Jenkins, D. P., Kolvekar, S., et al. (2015). Remote ischemic preconditioning and outcomes of cardiac surgery. *N. Engl. J. Med.* 373, 1408–1417. doi: 10.1056/NEJMoa1413534

Hong, Y., Cao, H., Wang, Q., Ye, J., Sui, L., Feng, J., et al. (2016). MiR-22 may suppress fibrogenesis by targeting TGFβR I in cardiac fibroblasts. *Cell. Physiol. Biochem.* 40, 1345–1353. doi: 10.1159/000453187

Horie, T., Ono, K., Nishi, H., Nagao, K., Kinoshita, M., Watanabe, S., et al. (2010). Acute doxorubicin cardiotoxicity is associated with miR-146a-induced inhibition of the neuregulin-ErbB pathway. *Cardiovasc. Res.* 87, 656–664. doi: 10.1093/cvr/cvq148

Huang, Z.-P., Chen, J., Seok, H. Y., Zhang, Z., Kataoka, M., Hu, X., et al. (2013). MicroRNA-22 regulates cardiac hypertrophy and remodeling in response to stress. *Circ. Res.* 112, 1234–1243. doi: 10.1161/CIRCRESAHA.112.300682

Hutvágner, G., McLachlan, J., Pasquinelli, A. E., Bálint, É, Tuschl, T., and Zamore, P. D. (2001). A cellular function for the RNA-interference enzyme dicer in the maturation of the let-7 small temporal RNA. *Science* 293, 834–838. doi: 10.1126/science.1062961

Kharbanda, R. K., Mortensen, U. M., White, P. A., Kristiansen, S. B., Schmidt, M. R., Hoschtitzky, J. A., et al. (2002). Transient limb ischemia induces remote ischemic preconditioning in vivo. *Circulation* 106, 2881–2883. doi: 10.1161/01.CIR.0000043806.51912.9B

Kong, F., Jin, J., Lv, X., Han, Y., Liang, X., Gao, Y., et al. (2019). Long noncoding RNA RMRP upregulation aggravates myocardial ischemia-reperfusion injury by sponging miR-206 to target ATG3 expression. *Biomed. Pharmacother.* 109, 716–725. doi: 10.1016/j.biopha.2018.10.079

Konstantinov, I. E., Arab, S., Li, J., Coles, J. G., Boscarino, C., Mori, A., et al. (2005). The remote ischemic preconditioning stimulus modifies gene expression in mouse myocardium. *J. Thorac. Cardiovasc. Surg.* 130, 1326–1332. doi: 10.1016/j.jtcvs.2005.03.050

Lee, R. C., Feinbaum, R. L., and Ambros, V. (1993). The *C. elegans* heterochronic gene lin-4 encodes small rnas with antisense complementarity to lin-14. *Cell* 75, 843–854. doi: 10.1016/0092-8674(93)90529-Y

Lee, Y., Ahn, C., Han, J., Choi, H., Kim, J., Yim, J., et al. (2003). The nuclear RNase III Drosha initiates microRNA processing. *Nature* 425, 415–419. doi: 10.1038/nature01957

Lee, Y., Kim, M., Han, J., Yeom, K. H., Lee, S., Baek, S. H., et al. (2004). MicroRNA genes are transcribed by RNA polymerase II. *EMBO J.* 23, 4051–4060. doi: 10.1038/sj.emboj.7600385

Lei, Z., van Mil, A., Brandt, M. M., Grundmann, S., Hoefer, I., Smits, M., et al. (2015). MicroRNA-132/212 family enhances arteriogenesis after hindlimb ischaemia through modulation of the Ras-MAPK pathway. *J. Cell. Mol. Med.* 19, 1994–2005. doi: 10.1111/jcmm.12586

Leuschner, P. J. F., Ameres, S. L., Kueng, S., and Martinez, J. (2006). Cleavage of the siRNA passenger strand during RISC assembly in human cells. *EMBO Rep.* 7, 314–320. doi: 10.1038/sj.embor.7400637

Li, H., Fan, J., Yin, Z., Wang, F., Chen, C., and Wang, D. W. (2016). Identification of cardiac-related circulating microRNA profile in human chronic heart failure. *Oncotarget* 7, 33–45. doi: 10.18632/ONCOTARGET.6631

Li, L., Zhu, D., Huang, L., Zhang, J., Bian, Z., Chen, X., et al. (2012). Argonaute 2 complexes selectively protect the circulating MicroRNAs in

cell-secreted microvesicles. *PLoS One* 7:e46957. doi: 10.1371/journal.pone.0046957

Limana, F., Esposito, G., D'Arcangelo, D., Di Carlo, A., Romani, S., Melillo, G., et al. (2011). HMGB1 attenuates cardiac remodelling in the failing heart via enhanced cardiac regeneration and miR-206-mediated inhibition of TIMP-3. *PLoS One* 6:e19845. doi: 10.1371/journal.pone.0019845

Lin, B., Feng, D. G., and Xu, J. (2019). microRNA-665 silencing improves cardiac function in rats with heart failure through activation of the cAMP signaling pathway. *J. Cell. Physiol.* 234, 13169–13181. doi: 10.1002/jcp.27987

Lin, S. L., Miller, J. D., and Ying, S. Y. (2006). Intronic microRNA (miRNA). *J. Biomed. Biotechnol* 2006:26818. doi: 10.1155/JBB/2006/26818

Liu, B., Li, J., and Cairns, M. J. (2014). Identifying miRNAs, targets and functions. *Brief. Bioinform.* 15, 1–19. doi: 10.1093/bib/bbs075

Liu, Y., Nie, H., Zhang, K., Ma, D., Yang, G., Zheng, Z., et al. (2014). A feedback regulatory loop between HIF-1α and miR-21 in response to hypoxia in cardiomyocytes. *FEBS Lett.* 588, 3137–3146. doi: 10.1016/j.febslet.2014.05.067

Luo, Q., Guo, D., Liu, G., Chen, G., Hang, M., and Jin, M. (2017). Exosomes from MiR-126-overexpressing Adscs Are therapeutic in relieving acute myocardial ischaemic injury. *Cell. Physiol. Biochem.* 44, 2105–2116. doi: 10.1159/000485949

Luther, K. M., Haar, L., McGuinness, M., Wang, Y., Lynch Iv, T. L., Phan, A., et al. (2018). Exosomal miR-21a-5p mediates cardioprotection by mesenchymal stem cells. *J. Mol. Cell. Cardiol.* 119, 125–137. doi: 10.1016/j.yjmcc.2018.04.012

Ma, T., Chen, Y., Chen, Y., Meng, Q., Sun, J., Shao, L., et al. (2018). MicroRNA-132, delivered by mesenchymal stem cell-derived exosomes, promote angiogenesis in myocardial infarction. *Stem Cells Int.* 2018:3290372. doi: 10.1155/2018/3290372

Mack, J. J., and Iruela-Arispe, M. L. (2018). NOTCH regulation of the endothelial cell phenotype. *Curr. Opin. Hematol.* 25, 212–218. doi: 10.1097/MOH.0000000000000425

MacRae, I. J., Ma, E., Zhou, M., Robinson, C. V., and Doudna, J. A. (2008). In vitro reconstitution of the human RISC-loading complex. *Proc. Natl. Acad. Sci. U.S.A.* 105, 512–517. doi: 10.1073/pnas.0710869105

Madonna, R., Van Laake, L. W., Botker, H. E., Davidson, S. M., De Caterina, R., Engel, F. B., et al. (2019). ESC working group on cellular biology of the heart: position paper for cardiovascular research: tissue engineering strategies combined with cell therapies for cardiac repair in ischaemic heart disease and heart failure. *Cardiovasc. Res.* 115, 488–500. doi: 10.1093/cvr/cvz010

Madonna, R., Van Laake, L. W., Davidson, S. M., Engel, F. B., Hausenloy, D. J., Lecour, S., et al. (2016). Position paper of the European society of cardiology working group cellular biology of the heart: cell-based therapies for myocardial repair and regeneration in ischemic heart disease and heart failure. *Eur. Heart J.* 37, 1789–1798. doi: 10.1093/eurheartj/ehw113

Maring, J. A., Lodder, K., Mol, E., Verhage, V., Wiesmeijer, K. C., Dingenouts, C. K. E., et al. (2019). Cardiac progenitor cell–derived extracellular vesicles reduce infarct size and associate with increased cardiovascular cell proliferation. *J. Cardiovasc. Transl. Res.* 12, 5–17. doi: 10.1007/s12265-018-9842-9

Matranga, C., Tomari, Y., Shin, C., Bartel, D. P., and Zamore, P. D. (2005). Passenger-strand cleavage facilitates assembly of siRNA into Ago2-containing RNAi enzyme complexes. *Cell* 123, 607–620. doi: 10.1016/j.cell.2005.08.044

Michlewski, G., Guil, S., Semple, C. A., and Cáceres, J. F. (2008). Posttranscriptional regulation of miRNAs harboring conserved terminal loops. *Mol. Cell* 32, 383–393. doi: 10.1016/j.molcel.2008.10.013

Milano, G., Biemmi, V., Lazzarini, E., Balbi, C., Ciullo, A., Bolis, S., et al. (2019). Intravenous administration of cardiac progenitor cell-derived exosomes protects against doxorubicin/trastuzumab-induced cardiac toxicity. *Cardiovasc. Res.* 116, 383–392. doi: 10.1093/cvr/cvz108

Möhnle, P., Schütz, S. V., Schmidt, M., Hinske, C., Hübner, M., Heyn, J., et al. (2014). MicroRNA-665 is involved in the regulation of the expression of the cardioprotective cannabinoid receptor CB2 in patients with severe heart failure. *Biochem. Biophys. Res. Commun.* 451, 516–521. doi: 10.1016/j.bbrc.2014.08.008

Moyé, L. (2014). DAMASCENE and meta-ecological research: a bridge too far. *Circ. Res.* 115, 484–487. doi: 10.1161/CIRCRESAHA.114.304767

Mutharasan, R. K., Nagpal, V., Ichikawa, Y., and Ardehali, H. (2011). microRNA-210 is upregulated in hypoxic cardiomyocytes through Akt- and p53-dependent pathways and exerts cytoprotective effects. *Am. J. Physiol. Circ. Physiol.* 301, H1519–H1530. doi: 10.1152/ajpheart.01080.2010

Pan, J., Alimujiang, M., Chen, Q., Shi, H., and Luo, X. (2019). Exosomes derived from miR-146a-modified adipose-derived stem cells attenuate acute myocardial infarction-induced myocardial damage via downregulation of early growth response factor 1. *J. Cell. Biochem.* 120, 4433–4443. doi: 10.1002/jcb.27731

Rodriguez, A., Griffiths-Jones, S., Ashurst, J. L., and Bradley, A. (2004). Identification of mammalian microRNA host genes and transcription units. *Genome Res.* 14, 1902–1910. doi: 10.1101/gr.2722704

Roell, W., Lewalter, T., Sasse, P., Tallini, Y. N., Choi, B.-R., Breitbach, M., et al. (2007). Engraftment of connexin 43-expressing cells prevents post-infarct arrhythmia. *Nature* 450, 819–824. doi: 10.1038/nature06321

Shao, L., Zhang, Y., Lan, B., Wang, J., Zhang, Z., Zhang, L., et al. (2017). MiRNA-sequence indicates that mesenchymal stem cells and exosomes have similar mechanism to enhance cardiac repair. *Biomed Res. Int.* 2017:4150705. doi: 10.1155/2017/4150705

Spannbauer, A., Traxler, D., Lukovic, D., Zlabinger, K., Winkler, J., Gugerell, A., et al. (2019). Effect of ischemic preconditioning and postconditioning on exosome-rich fraction microRNA levels, in relation with electrophysiological parameters and ventricular arrhythmia in experimental closed-chest reperfused myocardial infarction. *Int. J. Mol. Sci.* 20:2140. doi: 10.3390/ijms20092140

Turchinovich, A., Weiz, L., and Burwinkel, B. (2012). Extracellular miRNAs: the mystery of their origin and function. *Trends Biochem. Sci.* 37, 460–465. doi: 10.1016/j.tibs.2012.08.003

Tzahor, E., and Poss, K. D. (2017). Cardiac regeneration strategies: staying young at heart. *Science* 356, 1035–1039. doi: 10.1126/science.aam5894

Varga, Z. V., Giricz, Z., Bencsik, P., Madonna, R., Gyongyosi, M., Schulz, R., et al., (2015). Functional genomics of cardioprotection by ischemic conditioning and the influence of comorbid conditions: implications in target identification. *Curr. Drug Targets* 16, 904–911. doi: 10.2174/1389450116666150427154203

Villarroya-Beltri, C., Gutiérrez-Vázquez, C., Sánchez-Cabo, F., Pérez-Hernández, D., Vázquez, J., Martin-Cofreces, N., et al. (2013). Sumoylated hnRNPA2B1 controls the sorting of miRNAs into exosomes through binding to specific motifs. *Nat. Commun.* 4:2980. doi: 10.1038/ncomms3980

Wang, N., Chen, C., Yang, D., Liao, Q., Luo, H., Wang, X., et al. (2017). Mesenchymal stem cells-derived extracellular vesicles, via miR-210, improve infarcted cardiac function by promotion of angiogenesis. *Biochim. Biophys. Acta Mol. Basis Dis.* 1863, 2085–2092. doi: 10.1016/j.bbadis.2017.02.023

Wei, J., Zhang, Y., Li, Z., Wang, X., Chen, L., Du, J., et al. (2018). GCH1 attenuates cardiac autonomic nervous remodeling in canines with atrial-tachypacing via tetrahydrobiopterin pathway regulated by microRNA-206. *Pacing Clin. Electrophysiol.* 41, 459–471. doi: 10.1111/pace.13289

Wei, M., Xin, P., Li, S., Tao, J., Li, Y., Li, J., et al. (2011). Repeated remote ischemic postconditioning protects against adverse left ventricular remodeling and improves survival in a rat model of myocardial infarction. *Circ. Res.* 108, 1220–1225. doi: 10.1161/CIRCRESAHA.110.236190

Wendt, S., Goetzenich, A., Goettsch, C., Stoppe, C., Bleilevens, C., Kraemer, S., et al. (2018). Evaluation of the cardioprotective potential of extracellular vesicles – a systematic review and meta-analysis. *Sci. Rep.* 8:15702. doi: 10.1038/s41598-018-33862-5

Xiao, J., Pan, Y., Li, X. H., Yang, X. Y., Feng, Y. L., Tan, H. H., et al. (2016). Cardiac progenitor cell-derived exosomes prevent cardiomyocytes apoptosis through exosomal miR-21 by targeting PDCD4. *Cell Death Dis.* 7:e2277. doi: 10.1038/cddis.2016.181

Yang, J., Yang, J., Chen, L., Ding, J., Li, S., Wu, H., et al. (2014). MicroRNA-22 targeting CBP protects against myocardial ischemia-reperfusion injury through anti-apoptosis in rats. *Mol. Biol. Rep.* 41, 555–561. doi: 10.1007/s11033-013-2891-x

Yang, Y., Del Re, D. P., Nakano, N., Sciarretta, S., Zhai, P., Park, J., et al. (2015). miR-206 mediates YAP-induced cardiac hypertrophy and survival. *Circ. Res.* 117, 891–904. doi: 10.1161/CIRCRESAHA.115.306624

Yi, R., Qin, Y., Macara, I. G., and Cullen, B. R. (2003). Exportin-5 mediates the nuclear export of pre-microRNAs and short hairpin RNAs. *Genes Dev.* 17, 3011–3016. doi: 10.1101/gad.1158803

Yu, J., Yang, W., Wang, W., Wang, Z., Pu, Y., Chen, H., et al. (2019). Involvement of miR-665 in protection effect of dexmedetomidine against oxidative stress injury in myocardial cells via CB2 and CK1. *Biomed. Pharmacother.* 115:108894. doi: 10.1016/j.biopha.2019.108894

Zeng, Y., and Cullen, B. R. (2004). Structural requirements for pre-microRNA binding and nuclear export by Exportin 5. *Nucleic Acids Res.* 32, 4776–4785. doi: 10.1093/nar/gkh824

Zhang, C.-J., Huang, Y., Lu, J.-D., Lin, J., Ge, Z.-R., and Huang, H. (2018). Upregulated microRNA-132 rescues cardiac fibrosis and restores cardiocyte proliferation in dilated cardiomyopathy through the phosphatase and tensin homolog-mediated PI3K/Akt signal transduction pathway. *J. Cell. Biochem.* 120, 1232–1244. doi: 10.1002/jcb.27081

Zhou, X.-L., Xu, H., Liu, Z.-B., Wu, Q.-C., Zhu, R.-R., and Liu, J.-C. (2018). miR-21 promotes cardiac fibroblast-to-myofibroblast transformation and myocardial fibrosis by targeting Jagged1. *J. Cell. Mol. Med.* 22, 3816–3824. doi: 10.1111/jcmm.13654

Zhou, Z., Schober, A., and Nazari-Jahantigh, M. (2018). Dicer promotes endothelial recovery and limits lesion formation after vascular injury through miR-126-5p. *Int. J. Cardiol.* 273, 199–202. doi: 10.1016/j.ijcard.2018.09.006

Conflict of Interest: The authors declare that the research was conducted in the absence of any commercial or financial relationships that could be construed as a potential conflict of interest.

Copyright © 2020 Nazari-Shafti, Exarchos, Rodriguez Cetina Biefer, Cesarovic, Meyborg, Falk and Emmert. This is an open-access article distributed under the terms of the Creative Commons Attribution License (CC BY). The use, distribution or reproduction in other forums is permitted, provided the original author(s) and the copyright owner(s) are credited and that the original publication in this journal is cited, in accordance with accepted academic practice. No use, distribution or reproduction is permitted which does not comply with these terms.

frontiers in Bioengineering and Biotechnology

ORIGINAL RESEARCH
published: 07 April 2020
doi: 10.3389/fbioe.2020.00292

Engineering Immunomodulatory Biomaterials for Regenerating the Infarcted Myocardium

*Nora Bloise[1,2], Isobel Rountree[3], Collin Polucha[3], Giulia Montagna[1,4], Livia Visai[1,2], Kareen L. K. Coulombe[3] and Fabiola Munarin[3]**

[1] Department of Molecular Medicine, Center for Health Technologies (CHT), INSTM UdR of Pavia, University of Pavia, Pavia, Italy, [2] Department of Occupational Medicine, Toxicology and Environmental Risks, ICS Maugeri, IRCCS, Pavia, Italy, [3] Center for Biomedical Engineering, School of Engineering, Brown University, Providence, RI, United States, [4] Department of Electrical, Computer and Biomedical Engineering, Centre for Health Technologies (CHT), University of Pavia, Pavia, Italy

Coronary artery disease is a severe ischemic condition characterized by the reduction of blood flow in the arteries of the heart that results in the dysfunction and death of cardiac tissue. Despite research over several decades on how to reduce long-term complications and promote angiogenesis in the infarct, the medical field has yet to define effective treatments for inducing revascularization in the ischemic tissue. With this work, we have developed functional biomaterials for the controlled release of immunomodulatory cytokines to direct immune cell fate for controlling wound healing in the ischemic myocardium. The reparative effects of colony-stimulating factor (CSF-1), and anti-inflammatory interleukins 4/6/13 (IL4/6/13) have been evaluated *in vitro* and in a predictive *in vivo* model of ischemia (the skin flap model) to optimize a new immunomodulatory biomaterial that we use for treating infarcted rat hearts. Alginate hydrogels have been produced by internal gelation with calcium carbonate ($CaCO_3$) as carriers for the immunomodulatory cues, and their stability, degradation, rheological properties and release kinetics have been evaluated *in vitro*. CD14 positive human peripheral blood monocytes treated with the immunomodulatory biomaterials show polarization into pro-healing macrophage phenotypes. Unloaded and CSF-1/IL4 loaded alginate gel formulations have been implanted in skin flap ischemic wounds to test the safety and efficacy of the delivery system *in vivo*. Faster wound healing is observed with the new therapeutic treatment, compared to the wounds treated with the unloaded controls at day 14. The optimized therapy has been evaluated in a rat model of myocardial infarct (ischemia/reperfusion). Macrophage polarization toward healing phenotypes and global cardiac function measured with echocardiography and immunohistochemistry at 4 and 15 days demonstrate the therapeutic potential of the proposed immunomodulatory treatment in a clinically relevant infarct model.

Keywords: immune engineering, biomaterials, angiogenesis, revascularization, myocardial infarct, macrophages, cytokines

OPEN ACCESS

Edited by:
Susanna Sartori, Politecnico di Torino, Italy

Reviewed by:
Jochen Salber, University Hospital Bochum GmbH, Germany
Stephanie K. Seidlits, University of California, Los Angeles, United States

***Correspondence:**
Fabiola Munarin
fabiola_munarin@brown.edu

Specialty section:
This article was submitted to Biomaterials, a section of the journal Frontiers in Bioengineering and Biotechnology

Received: *19 December 2019*
Accepted: *19 March 2020*
Published: *07 April 2020*

Citation:
Bloise N, Rountree I, Polucha C, Montagna G, Visai L, Coulombe KLK and Munarin F (2020) Engineering Immunomodulatory Biomaterials for Regenerating the Infarcted Myocardium. Front. Bioeng. Biotechnol. 8:292. doi: 10.3389/fbioe.2020.00292

INTRODUCTION

Ischemic heart disease, or myocardial infarction (MI), is the leading cause of death globally, causing 1.8 million deaths per year in Europe (40% of all deaths) and 647000 deaths per year (25% of all deaths) in the United States (Wilkins et al., 2017; Benjamin et al., 2019). MI is typically caused by the formation of atherosclerotic plaques that occlude a coronary artery, resulting in

cardiomyocyte death due to insufficient oxygen perfusion (Shimokawa and Yasuda, 2008; Frank et al., 2012). Despite decades of research, treatments for improving vascularization of the infarcted myocardium are still needed, and bioengineering approaches are starting to emerge (Kellar et al., 2005; Dvir et al., 2009; Fleischer et al., 2017). Recent studies have demonstrated the crucial role of reparative macrophage phenotypes for initiating angiogenesis and reparative processes in the heart and in other tissues of the body (Godwin et al., 2013; Aurora et al., 2014; Cattin et al., 2015). Cardiomyocyte death following an ischemic injury triggers the innate immune response, and a plethora of immune cells, including leukocytes, monocytes and macrophages, are rapidly recruited and activated in the injured site (Sica and Mantovani, 2012). In this early inflammatory phase, monocytes are polarized into pro-inflammatory subtypes that secrete inflammatory chemokines and are responsible for the phagocytosis of apoptotic cells and debris. After the acute inflammatory phase, a subpopulation of reparative macrophages initiates the healing process by secreting pro-angiogenic growth factors such as vascular endothelial growth factor-α (VEGF-α), platelet-derived growth factor (PDGF), transforming growth factor-β (TGF-β) and insulin-like growth factor-1 (IGF-1) (Sica and Mantovani, 2012; Butoi et al., 2016; Hesketh et al., 2017) to stimulate endothelial cell morphogenesis and activation (Kalucka et al., 2017). Macrophages are extremely diverse and plastic cells, and their phenotypic subset is determined by environmental signals (Murray, 2017). Beyond the pro-inflammatory and pro-healing subtypes, there is a continuum of functional states, with some macrophages displaying characteristics of both classically defined phenotypes (Mosser and Edwards, 2008). In the infarcted myocardium, the controlled recruitment and activation of monocytes and macrophages is required for orchestrating tissue repair and neoangiogenesis to limit excessive scarring and fibrosis (Frangogiannis, 2018; Swirski and Nahrendorf, 2018). Unbalanced or impaired activation of the cells of the immune system after myocardial ischemia results in maladaptive ventricular dilatation, systolic or diastolic dysfunction and myocardial stiffness (Frangogiannis, 2014).

With this study, we aim at exploiting immune-mediated mechanisms for stimulating wound healing in the ischemic myocardium by use of biomaterials designed for the controlled release of selected immunomodulatory cytokines. Colony-stimulating factor (CSF-1) and interleukin 4 (IL4) have been widely used to elicit human blood monocyte polarization into reparative macrophage phenotypes (Rovida et al., 2001; Boulakirba et al., 2018) and to modulate endothelial cell function (Bussolino et al., 1991). However, a potential involvement of CSF-1 and IL4 in atherosclerosis and other chronic inflammatory diseases has been identified (Smith et al., 1995; Qiao et al., 1997; von der Thusen et al., 2003; Shaposhnik et al., 2010), though the mechanisms by which these cytokines contribute to the development of these conditions remain unclear. In order to minimize risks of atherosclerotic activation of circulating CSF-1 and IL4 *in vivo*, a controlled and localized delivery of these factors after MI is necessary. Here we have designed an alginate-based biomaterial system for the release CSF-1 and IL4 to accelerate the polarization of blood monocytes into pro-healing macrophage phenotypes. Our hypothesis is that the activation of immune-mediated reparative mechanisms will promote wound healing and limit myocardial dysfunction after the infarct. We assess the ability of this new immunomodulatory treatment to revascularize ischemic wounds and to repair damaged tissues with clinically relevant predictive studies *in vitro* with use of human peripheral blood monocytes and *in vivo* with rodent models of ischemic skin flap and myocardial infarction.

MATERIALS AND METHODS

Isolation of Human Monocytes and Cell Culture

Peripheral blood was obtained from healthy donors (Centro Lavorazione e Validazione, Servizio di Immunoematologia e Medicina Trasfusionale, Fondazione I.R.C.C.S. Policlinico San Matteo, Pavia, Italy) according the following Italian Normative References: Decreto Ministero della Salute 2 novembre 2015 n.69 "Disposizioni relative ai requisiti di qualità e sicurezza del sangue e degli emocomponenti" and Accordo Stato-Regioni n.225/CSR 13 dicembre 2018 "Schema-tipo di convenzione per la cessione del sangue e dei suoi prodotti per uso di laboratorio e per la produzione di dispositivi medico-diagnostici *in vitro*." Written informed consent was obtained from all the participants enrolled in this study. Peripheral blood mononuclear cells (PBMC) were isolated from buffy coat by density gradient centrifugation using Histopaque®-1077 (1.077 g ml^{-1}; Sigma-Aldrich, St. Louis, MO, United States) as previously described (Kleiveland, 2015). Human CD14 + monocytes were then obtained by Monocyte Isolation Kit II (Miltenyi Biotec, Bergisch Gladbach, Germany) according to the manufacturer instructions. After isolation, CD14 + monocytes were counted by Trypan Blue assay (Sigma-Aldrich) and were plated in 24 well plates at a density of 1×10^5 cells/well. All cells were cultured in RPMI 1640 medium supplemented with 2 mM/L L-glutamine (Life Technologies, Frederick, MD), 10% heat inactivated FBS (Sigma-Aldrich), 100 U/ml penicillin (Life Technologies), and 100 mg/ml streptomycin (Life Technologies) at 37°C in a humidified incubator with 5% CO_2.

Production and Characterization of Alginate Hydrogels

Production of Alginate Hydrogels

For the production of unloaded alginate hydrogels, alginate (Sigma, 180947), D-(+)-gluconic acid δ-lactone (GDL, Sigma, G4750) and calcium carbonate (Fisher Scientific, S25220A and 10617581) were used as received. Alginate hydrogels were produced from aqueous alginate solutions (2–6% w/v) mixed with 10 mg/mL GDL. Calcium carbonate (2.5–40 mg/mL) was suspended with distilled water and sonicated at room temperature for 10 min. The calcium carbonate suspension was then added to the alginate – GDL solution to produce different hydrogel formulations, named AC2.5 (Alginate 1%, $CaCO_3$ 2.5 mg/mL), AC5 (Alginate 1%, $CaCO_3$ 5 mg/mL), and AC10 (Alginate 1%, $CaCO_3$ 10 mg/mL). The gelling mixture

was placed in 24 well plates (0.5 mL/well) and was left to gel at T = 37°C for 10–60 min. Gelling time was determined with the test-tube inversion assay, by tilting the plates containing the polymeric mixture every 2 min, until no flow was observed.

Swelling and Degradation Studies

Swelling and degradation studies were performed on hydrogel samples cut with a 6 mm biopsy punch and incubated in PBS at 37°C up to 14 days, by measuring wet and dry weight at each time point (t = 0, 1, 3, 7, and 14 days) to determine the% wet and dry weight variation (ΔW_w and ΔW_d), as previously described in Moreira et al. (2014).

Rheological Properties of Alginate Hydrogels

To evaluate the viscoelastic properties of alginate hydrogels, shear (0.01–100 s^{-1}) and frequency (10–300 rad/s) sweep tests were conducted on AC5 and AC10 samples at T = 23°C by use of a rheometer (TA Instruments) equipped with an 8 mm plate-plate geometry.

Evaluation of Alginate Hydrogel Cytotoxicity

AC5 and AC10 hydrogel samples were incubated in RPMI medium (Life Technologies) at 37°C, 5% CO_2 up to 10 days. At the end of the incubation period, the supernatant (containing the gel degradation products) was collected and added (undiluted or diluted 1:2 and 1:4 in complete culture medium) to isolated human CD14 + monocyte cultures, previously seeded at a density of 1×10^5 cells per well in 24-well plates. After 24 h, cell viability was assessed by the quantitative 3-[4,5-dimethylthiazol-2-yl]-2,5-diphenyl tetrazolium bromide (MTT) test (Sigma-Aldrich) as previously described (Gualandi et al., 2016).

Release Profiles of Bovine Serum Albumin (BSA) From Alginate Hydrogels

The release kinetics of alginate hydrogels were evaluated by loading the biomaterials with different amounts of a model protein, bovine serum albumin (BSA, molecular weight = 66 kDa; Sigma-Aldrich). The model protein was added to AC5 and AC10 gelling mixtures in the following concentrations: 0, 50, 100, and 150 μg/mL. After gelation, loaded and unloaded hydrogels were submersed in 1 mL of 1× PBS (pH 7.4) at 37°C. At selected time points (1–10 days) the incubation solution was completely collected and 1 mL of fresh PBS was added to maintain perfect sink conditions. The concentration of proteins in the supernatants was determined using the Bicinchoninic Protein Assay Kit (BCA assay, EuroClone S.p.A), according to the manufacturer protocol. Standard BSA curves were used to determine the protein concentrations in each sample.

Fluorescein isothiocyanate-labeled bovine serum albumin (FITC-BSA, Sigma-Aldrich) was immobilized in the hydrogels in order to evaluate the homogeneity of distribution of the protein by visual observation using a confocal laser scanning microscope (CLSM) model TCS SP8 (Leica Microsystems, Bensheim, Germany, Oil 40) at 24 h from loading.

Evaluation of the Immunomodulatory Effects of Colony- Stimulating Factor 1 and Interleukins 4/6/13 on Human Monocytes Isolated From Peripheral Blood

We have loaded AC10 hydrogels (0.5 mL final volume) with: (i) no cytokines (unloaded control); (ii) CSF-1 (150 ng/mL); (iii) CSF-1 (150 ng/mL) and IL4 (150 ng/mL, GenScript Corporation); and (iv) CSF-1 (150 ng/mL) with a combination of IL4, IL6, and IL13 (each cytokine at a concentration of 150 ng/mL, GenScript Corporation). Hydrogels were then maintained in monocyte culture medium for 10 days. Then, purified monocytes (1×10^5 cells seeded per well in 24-well) were incubated in the presence of the hydrogel extracts (1 mL) for 10 days. As control, human CD14 + monocytes were exposed for the same time to medium containing freshly prepared differentiation factors (20 ng/mL, alone or in combination), according to literature protocols (Zarif et al., 2016; **Supplementary Figure S2**).

Macrophage polarization toward pro-healing phenotypes was assessed after 10 days of culture by optical light microscopy (for morphology evaluation) and by immunofluorescence with specific antibodies for the expression of the haptoglobin–hemoglobin receptor CD163 and the mannose receptor CD206, strongly expressed on the reparative M2c and M2a macrophage subtypes, respectively (Yang et al., 2014), as described in the **Supplementary Material**. Quantification of CD163 or CD206 positive cells was determined by acquiring images with a confocal laser scanning microscope (TCS SP8, Leica Microsystems, Bensheim, Germany, Oil 40× and 63×), and processing them with ImageJ-Analyzer software (Schneider et al., 2012; van den Bosch et al., 2017). The number of CD163 + and CD206 + cells was expressed as total number of positive cells/total number of nuclei, analyzing five fields of view per sample.

Wound Healing Assessment in the Ischemic Skin Flap Model

The ischemic skin flap surgical procedure has been conducted according to the United States NIH Policy on Humane Care and Use of Laboratory Animals and the Brown University and Rhode Island Hospital Institutional Animal Care and Use Committee (IACUC protocol No. 1702000256). Male Sprague Dawley wild type rats, strain 001 (Charles Rivers), with an average weight of 310 ± 61 g, were sedated with 2.5–3% isoflurane, the skin of the back was shaved and four full-thickness excisional wounds were created with a 6 mm biopsy punch in the designated ischemic area. A bipedicled 4 cm × 6 cm skin flap was created, dissecting the panniculus carnosus muscle from the wound bed. A sterile 4 cm × 6 cm silicone sheet was inserted beneath the flap, to prevent perfusion of the flap from the underlying tissue. The flap incision was closed using surgical skin glue. A non-ischemic wound was created lateral to the bipedicled flap and used as non-ischemic control. Each animal received the following treatments in the four ischemic wounds: (i) no

treatment, (ii) unloaded AC10, and (iii) AC10 loaded with 2 μg CSF-1 and 2 μg IL4. Alginate hydrogels (d = 6 mm) were inserted in the ischemic wounds and maintained in the defect with two 4-0 nylon loop sutures. A transparent film dressing was applied to keep the wound environment clean. Rats recovered with saline and analgesic (Buprenorphine SR, 1 mg/kg). Digital images of the ischemic and non-ischemic wounds were acquired up to 21 days, after light sedation of the animals (1.5% isoflurane). Measurement of the epithelial gap was conducted using Fiji software. Wound tissues were harvested post-euthanasia making a square- shaped incision around the wound to include some healthy tissue. Samples were fixed in 4% paraformaldehyde (PFA) overnight and processed for subsequent paraffin embedding. Histological analysis was conducted with hematoxylin/eosin staining, RECA-1 and CD68 for phenotypical assessment of the cell population present in the ischemic wounds (staining protocols are described in detail in the **Supplementary Material**).

Injection of the Immunomodulatory Biomaterials in a Rodent Model of Infarcted Myocardium

All experiments were performed according to United States. NIH Policy on Humane Care and Use of Laboratory Animals and the Brown University and Rhode Island Hospital Institutional Animal Care and Use Committee (IACUC protocol No. 1702000256). Ischemia/reperfusion surgery was performed on Sprague Dawley male rats, strain 001 (Charles Rivers), 317 ± 37 g of weight. Animals were anesthetized with intraperitoneal injection of ketamine (80–100 mg/kg) and xylazine (5–10 mg/kg), were intubated and ventilated (1.8–2.5 mL/cycle, 65–90 cycles/min) with oxygen. After opening the chest cavity and exposing the heart, the left anterior descending coronary artery was ligated with a 7–0 polypropylene suture for 1 h, followed by reperfusion and immediate injection of the therapeutics. Three types of injections were performed: (i) injectable saline, (ii) unloaded AC10, and (iii) CSF-1 (2 μg)- and IL4 (2 μg)- loaded AC10. For each animal, three injections were performed in three different regions of the infarct (apical, mid anterior and mid anterolateral). Echocardiographic measurements performed at 4 days post MI allowed for evaluation of the left ventricular function. Animals presenting small infarcts, with fractional shortening above 45%, were excluded from this study. Echocardiography was performed (using GE Vivid 7 with a 10S 4–10 MHz transducer probe) under light inhaled isoflurane (1–2%) prior to the MI (baseline) and at 4 and 15 days post MI. Measurement of dimensional parameters (cavity dimensions and wall thickness) was conducted in M-mode, and fractional shortening and ejection fraction were calculated.

After euthanasia, hearts were harvested and post-fixed in 4% PFA over night at 4°C. Hearts were then cut by use of a coronal heart matrix to obtain 2 cm-thick cross-sectional slices and put in paraffin blocks subsequently cut in 5 μm-thick sections. Picrosirius red/fast green, cardiac troponin T (cTnT) and CD68 staining were performed to assess infarct area cardiomyocytes and macrophages density in the injured site Immunohistochemistry with CD68/CD206/DAPI and CD68/CD80/DAPI allowed to detect specific macrophages subtypes in the infarct and border zone (staining protocols are described in the **Supplementary Material**).

Infarct size was evaluated at 4 and 15 days post MI using Fiji software. Infarct area was measured in picrosirius red/fast green stained heart slices by manual segmentation of the red-stained collagenous scar tissue. The infarct area was then normalized to the left ventricle area. At least two slices were analyzed per each heart at the apical to mid-papillary level (s1–s3) and n = 3 hearts were analyzed per each group.

Statistical Analysis

Statistical analysis was carried out using GraphPad Prism 8.0 (GraphPad Inc., San Diego, CA, United States). Analysis was performed using one-way and two-ways analysis of variance (ANOVA), followed by Bonferroni or Tukey *post hoc* test (significance level of 0.05).

RESULTS

Alginate Hydrogels Are Suitable Soft and Biodegradable Biomaterials for Cytokine Delivery

Soft alginate hydrogels have been produced by internal gelation, using calcium carbonate and glucono-δ-lactone for lowering the pH of the gelling mixture, allowing slow dissociation of calcium ions and homogeneous gel formation. Varying the final concentration of alginate (in the range of 1-4% w/v) and $CaCO_3$ (in the range of 2.5–20 mg/mL), we were able to produce hydrogels characterized by different gelling time and rheological properties. Amongst the several formulations produced, alginate 1% - $CaCO_3$ 2.5 mg/mL (AC2.5), alginate 1% - $CaCO_3$ 5 mg/mL (AC5) and alginate 1% - $CaCO_3$ 10 mg/mL (AC10) exhibited a gelling time of 5–10 min at T = 37°C, ideal for the production of *in situ*-gelling injectable biomaterials (**Figure 1A**). Swelling/stability studies performed on AC2.5, AC5, and AC10 showed complete degradation of AC2.5 hydrogels in 1 day, while AC5 and AC10 formulations degraded in 14 days (**Figures 1B,C**). Rheological characterization of AC5 and AC10 hydrogels was performed within the linear viscoelastic region, determined with a strain sweep test ranging from 0.1 to 1%, at an oscillatory frequency of 10 rad/s. Storage (G′, Pa) and loss (G″, Pa) moduli, measured with a frequency sweep test at 0.5% strain, showed negligible differences between the AC5 and AC10 hydrogels (**Figure 1D**) and typical gel-like behavior, characterized by the predominance of the solid-like component (G′) over the viscous component (G″). Furthermore, AC5 and AC10 hydrogels exhibited a shear thinning behavior, manifested as a slight increase of shear stress (circles) and decrease of viscosity (triangles) at increasing shear rate at T = 23°C (**Figure 1E**). Comparing the results obtained in this work at T = 23°C with the results of other studies performed on alginate hydrogels at T = 37°C (Duan et al., 2017), we expect

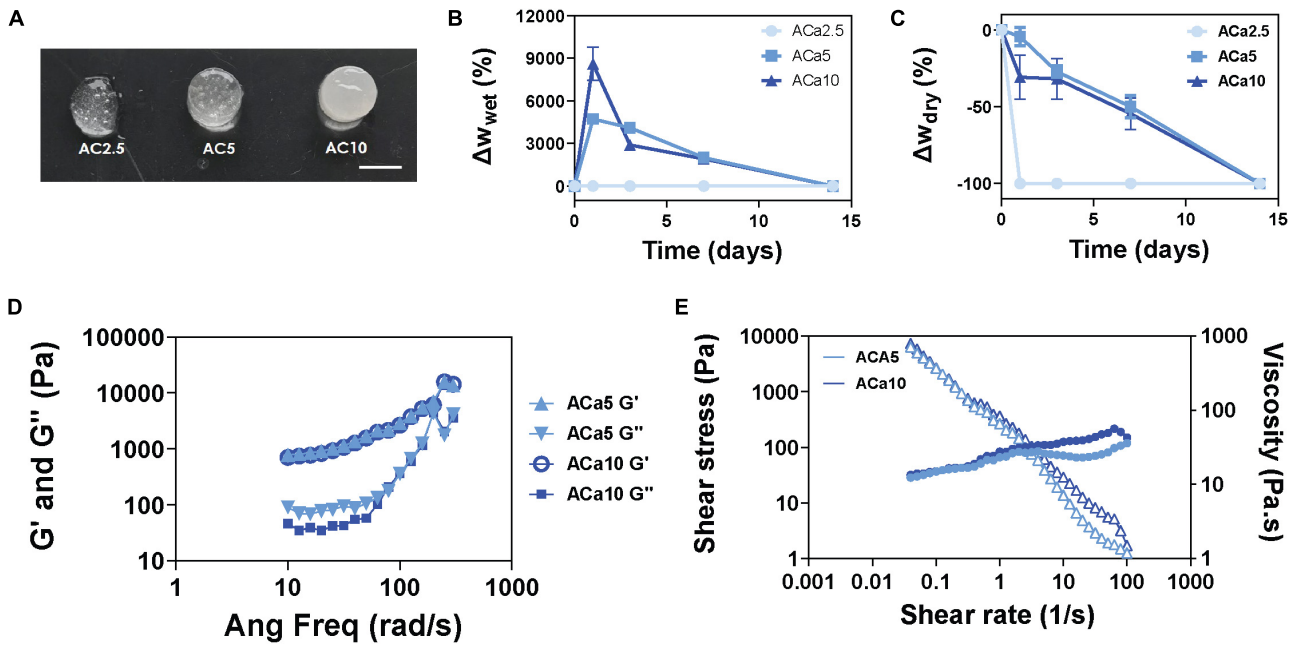

FIGURE 1 | Soft and biodegradable alginate hydrogels are produced by internal crosslinking with calcium carbonate. **(A)** Images of AC2.5, AC5, and AC10 hydrogels, scale bar = 5 mm. **(B)** Wet weight variation (swelling) of hydrogels compared to their initial weight at day 0. **(C)** Dry weight variation (mass loss) of hydrogels compared to the initial dry weight at day 0. **(D)** Rheological characterization of storage (G′) and loss (G″) moduli of AC5 and AC10 by frequency sweep test at 0.5% strain and T = 23°C and **(E)** shear rate dependence of shear stress (filled circles) and viscosity (open triangles) at T = 23°C.

no or modest decrease in the viscosity and elastic modulus at physiological temperature.

Cell viability test by the colorimetric MTT (3-(4,5-dimethylthiazol-2-yl)-2,5-diphenyltetrazolium bromide) assay, detecting cell viability and metabolic activity, showed that the degradation products of hydrogels did not induce toxic effects in human CD14 + monocytes cultures. Indeed, after 24 h of co-incubation with AC5 or AC10 extracts, the average cell viability was in the 90–94% range, with no statistical difference in cell viability ($p > 0.05$) between all tested samples and in comparison with cells cultured in degradation products free-RPMI medium.

Immobilization of a Model Protein in Alginate Hydrogels Enables Controlled and Localized Release

A model protein (bovine serum albumin, BSA) was immobilized at different concentrations (50–150 μg/mL) in AC5 and AC10 hydrogels to predict the release kinetics of the immunomodulatory cytokines. Images of the hydrogels acquired at the confocal microscope showed homogeneous dispersion of FITC-labeled BSA in the hydrogels (**Figures 2A,B**). The release profile of BSA from alginate hydrogels, measured with the BCA assay, a colorimetric assay for quantitation of protein release, showed a gradual release of the protein over a period of 5 days. No statistical differences were detected when comparing the release of increasing concentrations of BSA at each time point from AC5 and AC10 hydrogels (**Figures 2A,B**).

Colony- Stimulating Factor 1 and Interleukins 4, 6, and13 Released From Alginate Hydrogels Stimulate Polarization of Human Monocytes Isolated From Peripheral Blood

Based on evidence in the literature (Mia et al., 2014; Holloway, 2018), we have induced polarization of CD14 + human monocytes (purified from peripheral blood and characterized by flow cytometry analysis, **Supplementary Figure S1**) into pro-healing macrophage phenotypes (the so-called M2 macrophages) by adding 20 ng/mL CSF-1 for 6–13 days directly to the culture medium.

Addition of anti-inflammatory interleukins (IL4, 20 ng/mL or a combination of IL4/IL6/IL13, 20 ng/mL each) notably improved the yield of polarization of monocytes toward reparative macrophage phenotypes, as confirmed by the increasing expression of CD163 and CD206 markers, associated to the M2c and M2a reparative macrophage phenotypes (**Supplementary Figure S2**).

The bioactivity and efficacy of the immune-modulating cytokines released from AC10 hydrogels were investigated by evaluating morphology and the expression of pro-healing macrophage markers expressed by treated monocytes by optical light microscopy and immunohistochemistry, respectively (**Figure 3A**). As showed in **Figure 3B**, CSF-1 extracts from AC10 induced the differentiation of reparative macrophage phenotypes in 10 days, with similar effectiveness compared to the addition of fresh cytokines to the culture medium

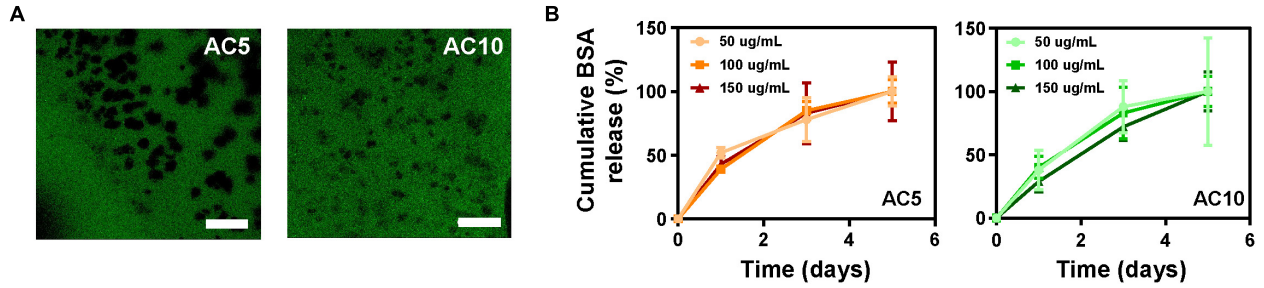

FIGURE 2 | BSA is released from AC5 and AC10 in 5 days. **(A)** Representative confocal laser scanning microscopy images of AC5 (left) and AC10 (right) hydrogels loaded with BSA-FITC protein acquired after 24 h in phosphate buffered saline (PBS). Scale bar: 100 μm. **(B)** Quantification of BSA content in PBS supernatant collected from hydrogels at different incubation times. Data are represented as cumulative percentage release relative to the initial loading dose ± SD (n = 3).

(**Supplementary Figure S2**A). Striking differences were noted among the different media eluting from hydrogels groups. The percentage of small and rounded cells, associated with pro-inflammatory macrophage subsets, was significantly higher in cultures of untreated monocytes and monocytes treated with CSF-1 alone, compared to the more elongated morphology observed for cells cultured with CSF-1 and ILs released from AC10 hydrogels. Indeed, the typical reparative heterogeneous population, composed of round macrophages (identified with white arrowheads in **Figure 3B**) and cells presenting cytoplasmic extensions with an elongated cell body (identified with red arrows in **Figure 3B**; Ploeger et al., 2013) was widely represented in presence of ILs. Antibodies against CD206 and CD163 were used to assess polarization of monocytes toward reparative phenotypes (Yang et al., 2014; Kumar et al., 2016). Similarly to what was observed with the morphological assessment, confocal imaging confirmed that the percentage of cells positive for M2 surface markers was significantly increased in the presence of medium containing the differentiation factors released from the hydrogels in comparison with the control, represented by untreated monocytes ($p < 0.05$, **Figures 3C,D**). Monocytes exposed to extracts of AC10 hydrogels loaded with combinations of CSF-1 and IL4 exhibited a slight but not statistically significant increase in the level of $CD163^+$ macrophages, compared to CSF-1 only ($p \geq 0.05$), and a marked increase of $CD206^+$ macrophage subtypes ($^{**}p < 0.01$) (**Figures 3C,D**). As expected, the addition of IL6 and IL13 cytokines induced both a strong CD163 and CD206 up-regulation at day 10 compared to the other test groups ($^{***}p < 0.0001$, **Figures 3C,D**). Overall, these data indicate that the immobilization and release of immunomodulatory cytokines from alginate hydrogels did not impair their biological activity, resulting in an efficient polarization of monocytes, comparable to the stimulation with fresh cytokines stock solutions added to the culture medium (**Supplementary Figure S2**).

Wound Healing in the Rat Ischemic Skin Flap Model Is Enhanced With Delivery of CSF-1 and IL4

To evaluate the reparative potential of the combination of CSF-1 and IL4 released from the biomaterials in ischemic tissues, we have adapted a predictive model of ischemic skin wounds created with a bipedicle skin flap (**Figure 4A**). With this model, a silicon membrane is placed beneath the flap as an inert barrier to inhibit vascularization of the skin, thus creating an ischemic site. Four wounds were created in the ischemic skin, and the alginate hydrogels releasing immunomodulatory cytokines were implanted. Evaluation of digital images and histological sections of the skin near the epithelial gap by hematoxylin/eosin staining allowed measurement of the kinetics of wound healing and hydrogel degradation, which was typically observed at 3–5 days post ischemia (**Figure 4B**). Phenotypic evaluation of the immune cell population was conducted by immunohistochemistry with CD68 (pan-macrophages marker) and CD206 (reparative macrophages marker) antibodies at 4 days post ischemia. Results show little or no differences among groups. The extensive co-localization of CD68 and CD206 markers, which can be associated with the presence of reparative macrophages subsets in the ischemic and non-ischemic wounds, indicates initiation of the healing process via a shifted macrophage polarization (**Figure 4C**). The limited presence of CD68 + CD80 + cells, associated with inflammatory macrophages phenotypes, at 4 days corroborates with the evidence of a rapid onset of the reparative process (**Supplementary Figure S3**).

A significant delay in wound healing was observed for the ischemic wounds compared to the non-ischemic controls, as shown in **Figure 4D** ($p < 0.05$ at days 7 and 14 for ischemic wounds that received no hydrogels or unloaded AC10 compared to non-ischemic control wounds). Importantly, accelerated healing trends were observed with delivery of CSF-1 and IL4 (2 μg each) from AC10 alginate hydrogels, compared to sham control and to wounds treated with unloaded alginate hydrogels (**Figures 4D,E**). Faster wound healing is obtained with the new therapeutic treatment compared to the unloaded controls (12% increase in the healed wound area at day 14). A chi-squared test performed on the fraction of healed wounds at 1, 7, 14, and 21 days (**Figure 4E**) showed statistical differences in the healing kinetics between cytokine-loaded AC10 hydrogels compared to the untreated ischemic wound ($p < 0.001$) and the unloaded AC10 hydrogels ($p < 0.05$).

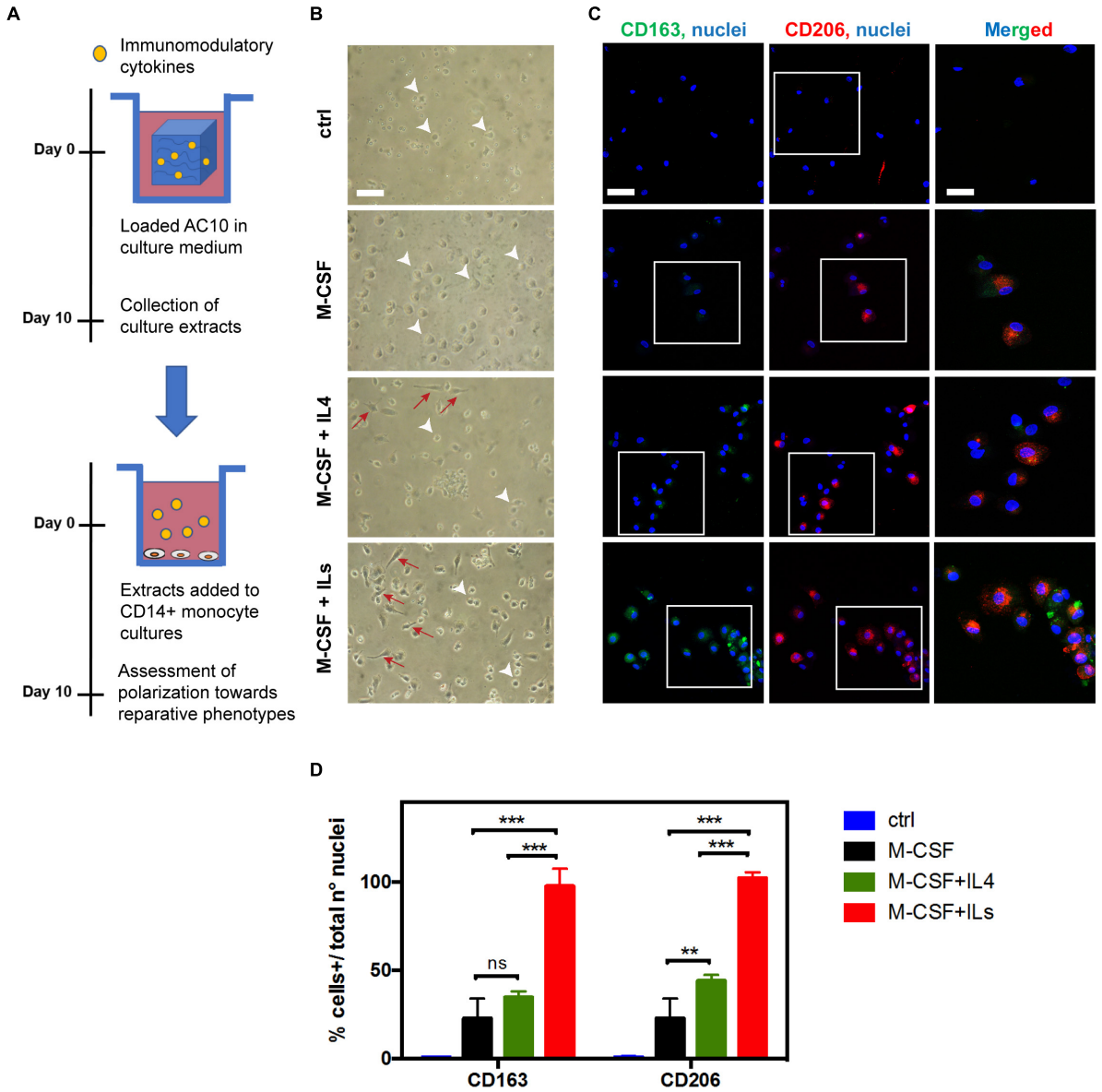

FIGURE 3 | Optimized combinations of immunomodulatory cytokines released from AC10 hydrogels promote monocytes polarization toward healing macrophage phenotypes. **(A)** Isolated human CD14 + monocytes were cultured for 10 days in the presence of medium containing cytokines obtained from solid hydrogels after 10 days of incubation. **(B)** Representative optical light microscopy showing inflammatory macrophages phenotypes characterized by the round morphology (white arrowheads) and anti-inflammatory macrophage subsets with elongated morphology (red arrows). Scale bar = 50 μm. **(C)** Confocal images obtained from the specified conditions. Expression of M2-macrophage markers, CD163 (green) and CD206 (red) was evaluated. Scale bar = 50 μm. Nuclei were counterstained with Hoechst 33342 (blue). Rectangles in panel **(C)** represent cells in magnified area, where merged CD163/CD206/nuclei signals are shown (Scale bar = 20 μm). **(D)** Number of CD163 + or CD206 + cells was expressed as total positive cell per total nuclei number per analyzed field (ns = $p > 0.05$, $^{**}p < 0.01$; $^{***}p < 0.001$, $n = 3$).

Injection of Immunomodulatory Biomaterials in the Infarcted Heart Induce Recovery of Cardiac Function at 15 Days Post Myocardial Infarction

Injectable formulations of AC10 hydrogels were introduced into the infarcted myocardium of wild type rats to evaluate their regenerative potential. Fully immunocompetent rats received MI by 60 min of ischemia then reperfusion, followed by intramyocardial injection of either (Wilkins et al., 2017) saline, (Benjamin et al., 2019) unloaded AC10, or (Shimokawa and Yasuda, 2008) AC10 loaded with CSF-1 and IL4 (2 μg each). Measurements of the infarct area on picrosirius red/fast green stained heart sections showed no difference in the size of the infarcts for the three groups at 4 and 15 days post MI; however, a significant increase in scar size from 4 to 15 days was

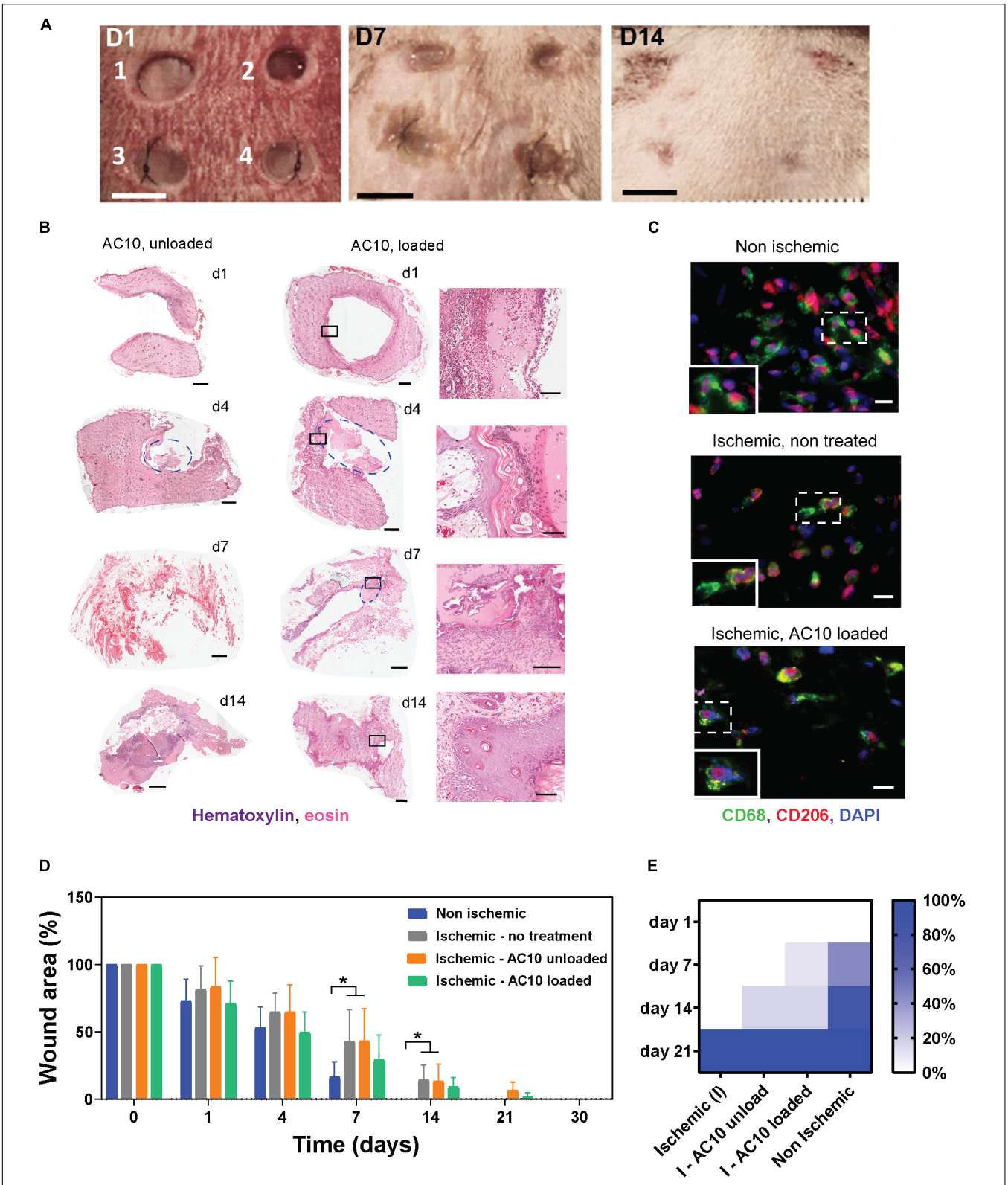

FIGURE 4 | The efficacy of the immunomodulatory biomaterials is tested in a predictive ischemic skin flap model. **(A)** Digital images of ischemic wounds at 0, 3, 7, and 14 days. Wounds received (1 and 2) no hydrogels, (3) unloaded alginate hydrogels, or (4) alginate hydrogels loaded with 2 μg CSF-1 and 2 μg IL4. Tissue necrosis is visible at day 14 in wounds 1 and 2. Scale bar = 5 mm. **(B)** Representative hematoxylin/eosin staining of wound tissues treated with AC10

(Continued)

FIGURE 4 | Continued
hydrogels unloaded or loaded with 2 μg CSF-1 and 2 μg IL4 at 1, 4, 7, and 14 days post ischemia (scale bar = 1 mm). Hydrogels are identified with a blue circle. Some of the hydrogels detached from the slides during the histological processing (for example, wound image at day 1). The black squares on the H&E staining of loaded AC10 hydrogels indicate the area represented at higher magnification on the right of each sample (scale bar = 200 μm. **(C)** Immune cells stained with CD68 (pan macrophage marker) and CD206 (reparative macrophage phenotypes) at the wound edges at 4 days post ischemia, scale bars = 20 μm. A 30 μm × 45 μm magnified area is shown in the bottom-left inset of each image. **(D)** Kinetics of wound closure for the four experimental conditions show increased wound healing in presence of cytokines. *N* = 4–9 wounds were analyzed at different time points for each group. **(E)** Fraction of healed wounds for the tested groups at different time points (I = ischemic, NI = non-ischemic). At 21 days, all wounds were completely healed.

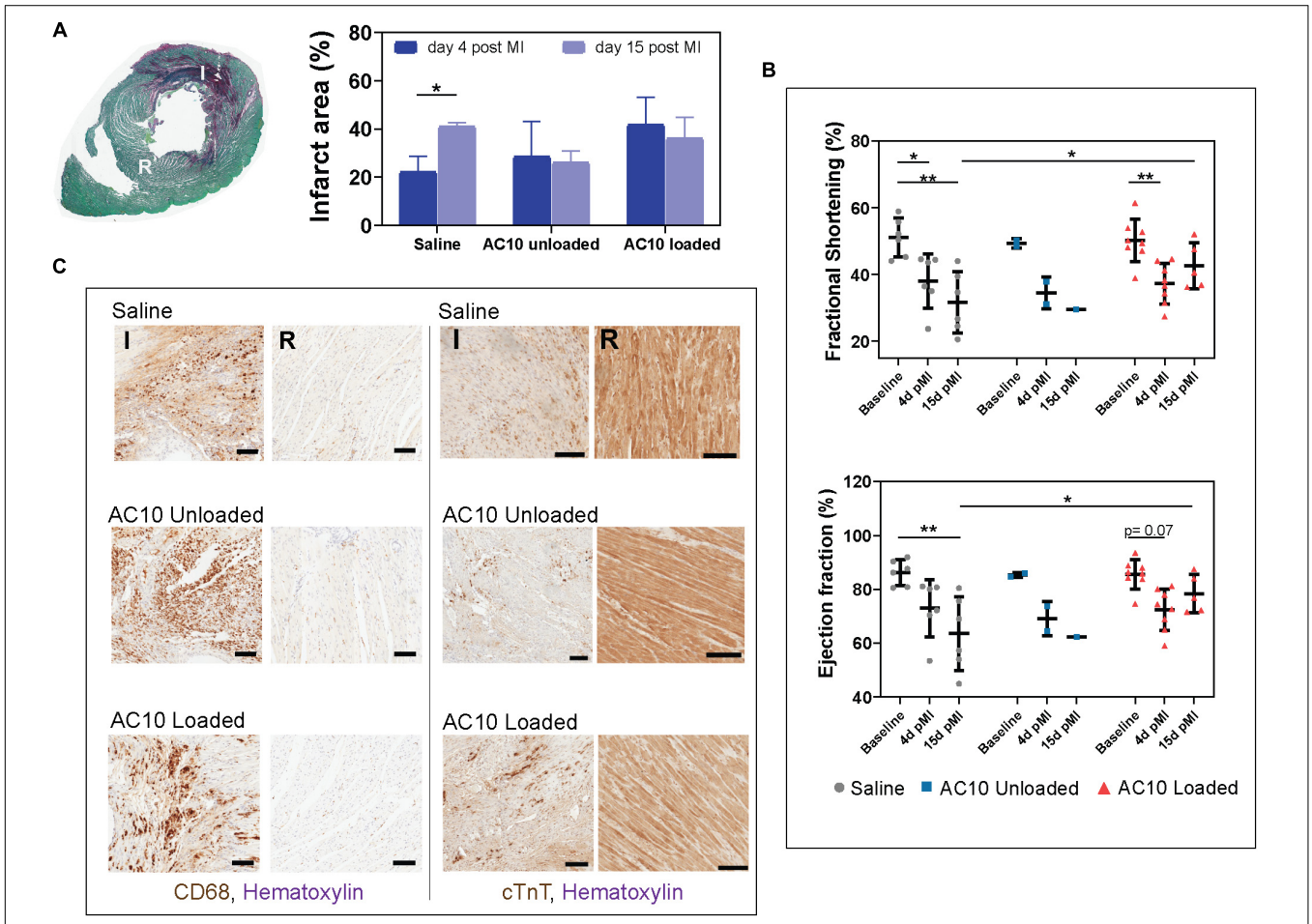

FIGURE 5 | Infarcted rat hearts receiving the immunomodulatory therapy show improvement in cardiac function and polarization of macrophages in the ischemic wound. **(A)** Cross section of a heart labeled with picrosirius red/fast green allow identification of the infarct area in red (I) and of the remote healthy tissue (R). Quantification of infarct area relative to the left ventricle area for all groups is shown on the right. Data are represented as mean ± standard deviation. *N* = 3 hearts were evaluated for all groups except AC10 unloaded- 15 days (*n* = 2) and AC10 loaded- 15 days (*n* = 10). **(B)** Cardiac function evaluated by fractional shortening (%) and ejection fraction (%) over 15 days. Each symbol represents the fractional shortening or ejection fraction of an individual rat. Data are expressed as mean ± standard deviation. **(C)** CD68 and cTnT staining for assessing macrophages and cardiomyocyte morphology in the infarct and remote area of the heart at day 15, scale bars = 100 μm.

visible for the group treated with saline injections (**Figure 5A**). Results from echocardiographic examination showed a decrease in cardiac function (measured as a 29.6 ± 1.0% decrease in fractional shortening and 18.3 ± 0.7% decrease in ejection fraction, averaging all groups) at 4 days post MI compared to the baseline (**Figure 5B**). A higher fractional shortening at day 15 between the group treated with the biomaterials loaded with the immunomodulatory cues versus sham treatment suggests the therapy improves functional outcomes (**Figure 5B**). Histological assessment with CD68, pan macrophage marker, and cardiac Troponin T (cTnT), cardiac marker, shows a broad presence of macrophages in the infarct area with few surviving cardiomyocytes (**Figure 5C**). The presence of inflammatory versus reparative macrophages was evaluated in the infarct area by use of CD68, CD206 (reparative macrophage phenotypes), and CD80 (inflammatory macrophages phenotypes). CD206

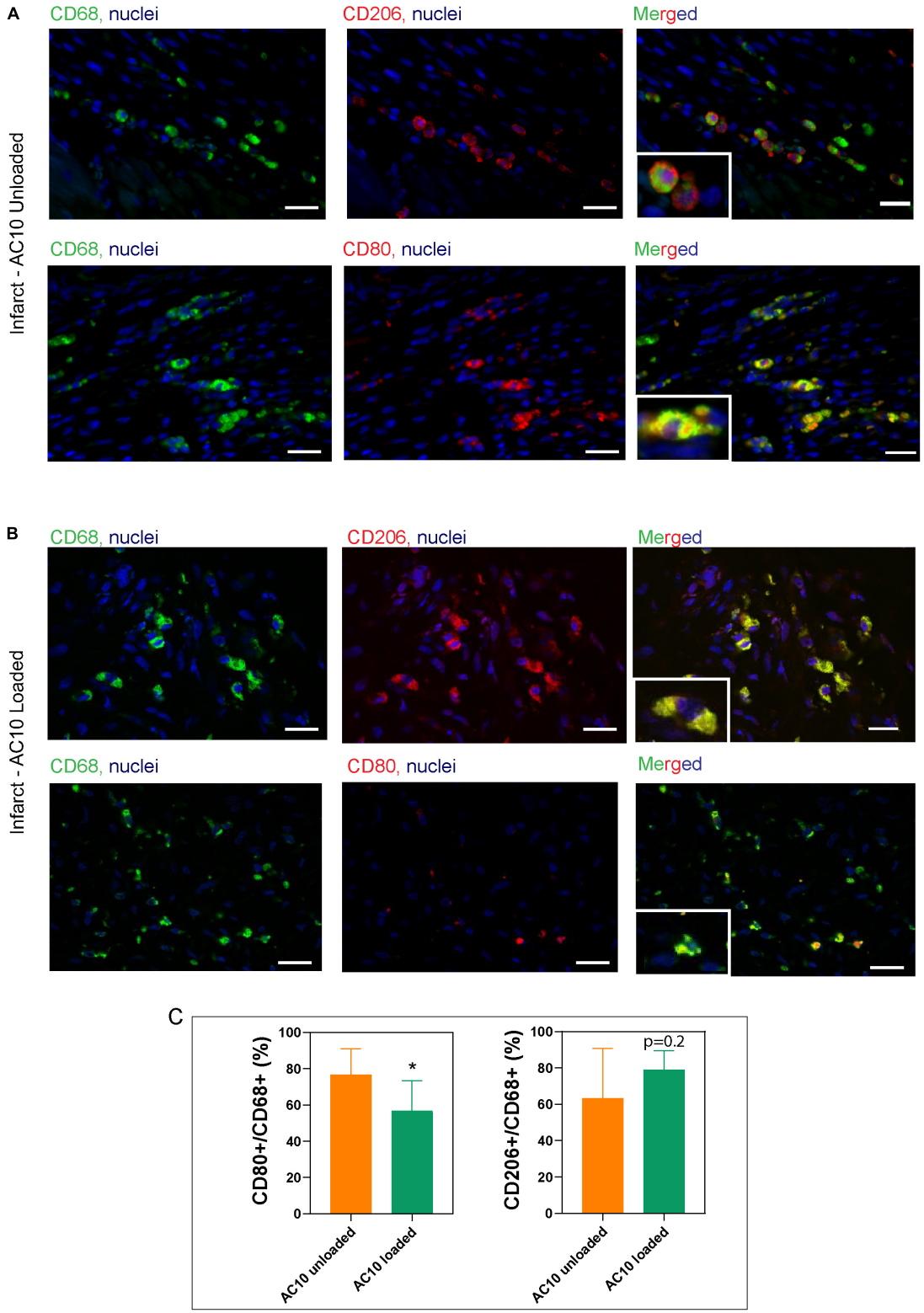

FIGURE 6 | Identification of macrophage subtypes in the infarct area shows the presence of reparative phenotypes in hearts treated with CSF-1 and IL4 loaded alginate hydrogels. Representative images of the infarct scar treated with unloaded AC10 hydrogels **(A)** or cytokine-loaded AC10 hydrogels **(B)** show macrophages

(Continued)

FIGURE 6 | Continued
stained with antibodies against CD68 (pan macrophage marker: left column), CD80 (inflammatory subsets: top row of A,B) and CD206 (reparative subsets: bottom row of A,B), scale bars = 20 μm. A 25 μm × 35 μm magnified area is shown in the bottom-left inset of each image. **(C)** Quantification for the macrophage phenotypes normalized to CD68 + cells was performed on $n = 198 \pm 47$ CD68 + cells per group (*$p < 0.05$).

expression is specific for the M2a macrophage sub-phenotype, that is known to be induced *in vitro* by IL-4 or IL-13 (Ma et al., 2018), and is therefore the marker selected for assessing the healing-type macrophages stimulated *in vivo* with our therapeutic. The significant decrease of CD80 positive macrophages in the infarct area of rat hearts receiving AC10 loaded hydrogels compared to the other treatment groups suggest possible transition away from inflammation and toward healing/repair (**Figure 6**). Presence of CD68 + CD206 + healing macrophages appears elevated in the infarct region of animals treated with either unloaded and cytokines-loaded injectable biomaterials, but with no statistical difference among groups, likely due to the high biological variability between animals.

DISCUSSION

In this study, we evaluate an innovative approach to address the need of an effective treatment for repairing damaged myocardium after an infarction, which uses biomaterials for the localized release of immunomodulatory cytokines. Previous works have explored immunomodulatory strategies for treating the infarcted myocardium, primarily by preventing excessive inflammation with anti-inflammatory or immunosuppressive agents targeting select pathways, initiators of inflammation (such as reactive oxygen species), inflammatory cytokines or immune cells, including B and T lymphocytes (Panahi et al., 2018). Here, we use CSF-1 and anti-inflammatory interleukins IL4, IL6, and IL13 to target monocytes and macrophages for initiating healing, repair and revascularization processes in the ischemic myocardium. In corroboration with results obtained *in vitro* in previous studies (Rovida et al., 2001; Mia et al., 2014; Boulakirba et al., 2018; Holloway, 2018), we were able to obtain a phenotypic switch of human blood monocytes toward pro-healing macrophage subtypes by treating cells with a combination of CSF-1 and IL4. Further, we have demonstrated that the efficacy of polarization increases with the use of a cocktail of anti-inflammatory interleukins, including IL6 and IL13 *in vitro*. Previous works in the literature show that CSF-1 is required for enhancing the final activation status of reparative macrophage phenotypes when cells are treated with a cocktail of anti-inflammatory cytokines (Mia et al., 2014; Zarif et al., 2016). Based on this evidence, we selected a combination of CSF-1 and IL4 for *in vivo* assessment as the most simple delivery system that elicits polarization of monocytes toward reparative macrophage sub-populations (**Figure 3**).

We used this acellular biomaterials system for the minimally invasive treatment and the localized delivery of "repair-instructive" cytokines in the setting of ischemic skin tissue and acute MI.

Soft alginate biomaterials are specifically designed (1) to gel at 37°C in 5–10 min, being optimal carriers for *in situ* gel formation; (2) to optimize timing and location of the treatment, tailoring their release to target the circulating monocytes and macrophages during the acute infarct phase (0–4 days) and prior to the formation of granulation tissue (4–14 days) (Ferrini et al., 2019); and (3) to rapidly biodegrade *in vivo* after releasing the therapeutics to avoid biomaterial-induced arrhythmias (Hernandez and Christman, 2017; **Figures 1**, **2**).

The efficacy of the developed immunomodulatory therapeutic has been evaluated *in vitro* (**Figure 3**) and in the ischemic skin flap model, a reliable model to study the effects of tissue ischemia on wound healing (**Figure 4**). This *in vivo* model recapitulates the pathology of ischemic wounds, with impaired vascularization and delayed wound healing (Schwarz et al., 1995; Gould et al., 2005; Trujillo et al., 2015; Patil et al., 2017), offering a convenient predictive model to optimize the immunomodulatory biomaterials prior to further testing in the infarcted myocardium. By measuring the epithelial gap (the distance between the wound margins) up to 21 days in ischemic and non-ischemic wounds, we demonstrate an accelerated healing of the ischemic wounds treated with the immunomodulatory biomaterials. Indeed, ischemic wound repair with CSF-1 and IL4 delivery was different from the non-treated ischemic wound and the unloaded control healing kinetics (**Figure 4E**). The promising healing trends obtained in this work with the delivery of immunomodulatory cytokines in ischemic rat skin wounds (**Figure 4**) show similar regenerative potential with the results of previous studies investigating topical applications or subcutaneous injections of exogenous pro-angiogenic growth factors, including vascular endothelial growth factor (VEGF) (Zhang et al., 2003), fibroblast growth factor (FGF) (Fayazzadeh et al., 2016) and platelet-derived growth factor (PDGF) (Chin et al., 2002). The beneficial effects of the immunomodulatory treatment observed in the skin flap model of ischemia provided the rationale for evaluating the immunomodulatory treatment in the MI, a more complex, non-healing wound generated by ischemia in the heart. We performed MI by ischemia/reperfusion injury, which is an established model to assess cardiac regeneration after MI (Lindsey et al., 2018). Compared to a permanent ligation procedure, the I/R model is more clinically-relevant, as it recapitulates reperfusion injury as observed in human patients, thus enabling a more appropriate study of the immune system response in an animal model due to the onset of inflammation (Chimenti et al., 2004).

Cardiomyocyte death following ischemia activates the innate immune response, and monocytes and inflammatory macrophages are rapidly recruited into the infarcted wound bed to remove dead cells and tissue debris. However, if a rapid polarization toward reparative macrophage phenotypes is not achieved within a few days, the heart progresses rapidly through

left ventricular remodeling, accompanied by deposition of collagenous scar and more severe functional decline, that can lead to heart failure (Ferrini et al., 2019).

Our therapeutic intervention aims to leverage the native immune cell population in the infarct during the acute inflammatory phase to alter the course of remodeling through pro-angiogenic processes. The soft alginate hydrogels produced in this study are designed as injectable carriers for the immunomodulatory cytokines and are not aimed at providing mechanical support to the infarcted area. The rheological properties of AC10 hydrogels are appropriate for intramyocardial injection via small needles (30G), and the viscoelastic behavior of AC10 hydrogels is comparable to that of other injectable biomaterials described in the literature (Oliveira et al., 2010; Munarin et al., 2014). Other acellular biomaterials have been injected in the myocardium with minimally invasive procedures for biomaterial-alone approaches or using biomaterials as carriers of growth factors, microribonucleic acids (miRNAs) or exosomes (Hernandez and Christman, 2017). However, to the best of our knowledge, this is the first study that reports the injection of biomaterials loaded with a cocktail of CSF-1 and IL4 as immunomodulatory cues for improving cardiac repair. Our study suggests that the cytokine-loaded hydrogels induce changes of the immune cell population in the infarct environment that reduces inflammatory phenotypes to tip the balance toward that results in improved heart function at 15 days post-MI. These results warrant further investigation of this injectable therapeutic system for advancing the healing process in the acute phase potentially via macrophage-driven revascularization that may reduce chronic ischemia for surviving cardiomyocytes and support subsequent long-term treatments of the infarct.

DATA AVAILABILITY STATEMENT

The datasets generated for this study are available on request to the corresponding author.

ETHICS STATEMENT

The animal study was reviewed and approved by Brown University and Rhode Island Hospital Institutional Animal Care and Use Committee (IACUC protocol No. 1702000256).

AUTHOR CONTRIBUTIONS

FM and KC developed the idea and edited the manuscript FM, KC, NB, and LV designed and directed the experiments and interpreted the data. FM and IR optimized the preparation of alginate hydrogels and performed rheological analysis and stability studies. NB performed *in vitro* experiments to assess polarization of monocytes and release kinetics from alginate hydrogels. GM contributed in monocytes isolation and characterization. CP, FM, and IR were involved with surgical procedures and post-operative animal care, histological preparations, and data analysis. FM supervised the work. NB, IR, and FM wrote the manuscript with critical inputs from all the authors.

FUNDING

This research has been supported by funds from the Rhode Island Foundation, Medical Research Grant Number: 006495 to FM, by INROAd funds from University of Pavia, Italy and by the Italian Ministry of Education, University and Research to the Department of Molecular Medicine of the University of Pavia under the initiative "Dipartimenti di Eccellenza (2018–2022)," by NIH R01HL135091 (to KC), and by discretionary funds from Brown University, School of Engineering to KC.

ACKNOWLEDGMENTS

The authors are grateful to Prof. Anubhav Tripathi (Brown University) for support with rheological assessment of alginate hydrogels, P. Vaghi (Centro Grandi Strumenti https://cgs.unipv.it/, University of Pavia, Pavia, Italy) for her technical assistance in confocal laser scanning microscopy and L. Freda for biological experiment support. The authors acknowledge Centro Lavorazione e Validazione, Servizio di Immunoematologia e Medicina Trasfusionale, Fondazione IRCCS Policlinico San Matteo, Pavia for peripheral blood samples.

SUPPLEMENTARY MATERIAL

The Supplementary Material for this article can be found online at: https://www.frontiersin.org/articles/10.3389/fbioe.2020.00292/full#supplementary-material

REFERENCES

Aurora, A. B., Porrello, E. R., Tan, W., Mahmoud, A. I., Hill, J. A., Bassel-Duby, R., et al. (2014). Macrophages are required for neonatal heart regeneration. *J. Clin. Invest.* 124, 1382–1392. doi: 10.1172/jci72181

Benjamin, E. J., Muntner, P., Alonso, A., Bittencourt, M. S., Callaway, C. W., Carson, A. P., et al. (2019). Heart disease and stroke statistics-2019 update: a report from the american heart association. *Circulation* 139, e56–e528.

Boulakirba, S., Pfeifer, A., Mhaidly, R., Obba, S., Goulard, M., Schmitt, T., et al. (2018). IL-34 and CSF-1 display an equivalent macrophage differentiation ability but a different polarization potential. *Sci. Rep.* 8:256.

Bussolino, F., Ziche, M., Wang, J. M., Alessi, D., Morbidelli, L., Cremona, O., et al. (1991). In vitro and in vivo activation of endothelial cells by colony-stimulating factors. *J. Clin. Invest.* 87, 986–995. doi: 10.1172/jci115107

Butoi, E., Gan, A. M., Tucureanu, M. M., Stan, D., Macarie, R. D., Constantinescu, C., et al. (2016). Cross-talk between macrophages and smooth muscle cells impairs collagen and metalloprotease synthesis and promotes angiogenesis. *Biochim. Biophys. Acta* 1863(7 Pt A), 1568–1578. doi: 10.1016/j.bbamcr.2016.04.001

Cattin, A. L., Burden, J. J., Van Emmenis, L., Mackenzie, F. E., Hoving, J. J., Garcia Calavia, N., et al. (2015). Macrophage-induced blood vessels guide schwann

cell-mediated regeneration of peripheral nerves. *Cell* 162, 1127–1139. doi: 10.1016/j.cell.2015.07.021

Chimenti, S., Carlo, E., Masson, S., Bai, A., and Latini, R. (2004). Myocardial infarction: animal models. *Methods Mol. Med.* 98, 217–226. doi: 10.1385/1-59259-771-8:217

Chin, G., Gowda, S., and Schultz, G. (2002). Evaluation of platelet-derived growth factor in a rat model of ischemic skin wound healing. *Wounds* 14, 199–203.

Duan, P., Kandemir, N., Wang, J., and Chen, J. (2017). Rheological characterization of alginate based hydrogels for tissue engineering. *MRS Adv.* 2, 1309–1314. doi: 10.1557/adv.2017.8

Dvir, T., Kedem, A., Ruvinov, E., Levy, O., Freeman, I., Landa, N., et al. (2009). Prevascularization of cardiac patch on the omentum improves its therapeutic outcome. *Proc. Natl. Acad. Sci. U.S.A.* 106, 14990–14995. doi: 10.1073/pnas.0812242106

Fayazzadeh, E., Yavarifar, H., Rafie, S. R., Motamed, S., Sotoudeh Anvari, M., and Boroumand, M. A. (2016). Fibroblast growth factor-1 vs. *Fibroblast Growth Factor*-2 in ischemic skin flap survival in a rat animal model. *World J. Plast. Surg.* 5, 274–279.

Ferrini, A., Stevens, M. M., Sattler, S., and Rosenthal, N. (2019). Toward regeneration of the heart: bioengineering strategies for immunomodulation. *Front. Cardiovasc. Med.* 6:26. doi: 10.3389/fcvm.2019.00026

Fleischer, S., Shapira, A., Feiner, R., and Dvir, T. (2017). Modular assembly of thick multifunctional cardiac patches. *Proc. Natl. Acad. Sci. U.S.A.* 114:1898. doi: 10.1073/pnas.1615728114

Frangogiannis, N. G. (2014). The inflammatory response in myocardial injury, repair, and remodelling. *Nat. Rev. Cardiol.* 11:255. doi: 10.1038/nrcardio.2014.28

Frangogiannis, N. G. (2018). Cell biological mechanisms in regulation of the post-infarction inflammatory response. *Curr. Opin. Physiol.* 1, 7–13. doi: 10.1016/j.cophys.2017.09.001

Frank, A., Bonney, M., Bonney, S., Weitzel, L., Koeppen, M., and Eckle, T. (2012). Myocardial ischemia reperfusion injury - from basic science to clinical bedside. *Semin. Cardiothor. Vasc. Anesth.* 16, 123–132. doi: 10.1177/1089253211436350

Godwin, J. W., Pinto, A. R., and Rosenthal, N. A. (2013). Macrophages are required for adult salamander limb regeneration. *Proc. Natl. Acad. Sci. U.S.A.* 110, 9415–9420. doi: 10.1073/pnas.1300290110

Gould, L. J., Leong, M., Sonstein, J., and Wilson, S. (2005). Optimization and validation of an ischemic wound model. *Wound Rep. Regen.* 13, 576–582. doi: 10.1111/j.1524-475x.2005.00080.x

Gualandi, C., Bloise, N., Mauro, N., Ferruti, P., Manfredi, A., Sampaolesi, M., et al. (2016). Poly-l-lactic acid nanofiber-polyamidoamine hydrogel composites: preparation, properties, and preliminary evaluation as scaffolds for human pluripotent stem cell culturing. *Macromol. Biosci.* 16, 1533–1544. doi: 10.1002/mabi.201600061

Hernandez, M. J., and Christman, K. L. (2017). Designing acellular injectable biomaterial therapeutics for treating myocardial infarction and peripheral artery disease. *JACC Basic Transl. Sci.* 2, 212–226. doi: 10.1016/j.jacbts.2016.11.008

Hesketh, M., Sahin, K. B., West, Z. E., and Murray, R. Z. (2017). Macrophage phenotypes regulate scar formation and chronic wound healing. *Intern. J. Mol. Sci.* 18:1545. doi: 10.3390/ijms18071545

Holloway, J. L. (2018). Harnessing the immune response to improve functional healing. *Sci. Transl. Med.* 10:eaav3889. doi: 10.1126/scitranslmed.aav3889

Kalucka, J., Bierhansl, L., Wielockx, B., Carmeliet, P., and Eelen, G. (2017). Interaction of endothelial cells with macrophages–linking molecular and metabolic signaling. *Pflügers Archiv. Eur. J. Physiol.* 469, 473–483. doi: 10.1007/s00424-017-1946-6

Kellar, R. S., Shepherd, B. R., Larson, D. F., Naughton, G. K., and Williams, S. K. (2005). Cardiac patch constructed from human fibroblasts attenuates reduction in cardiac function after acute infarct. *Tissue Eng.* 11, 1678–1687. doi: 10.1089/ten.2005.11.1678

Kleiveland, C. R. (2015). "Peripheral blood mononuclear cells," in *The Impact of Food Bioactives on Health: In Vitro And Ex Vivo Models*, eds K. Verhoeckx, P. Cotter, I. López-Expósito, C. Kleiveland, T. Lea, A. Mackie, et al. (Cham: Springer International Publishing), 161–167.

Kumar, M., Coburn, J., Kaplan, D. L., and Mandal, B. B. (2016). Immuno-informed 3D silk biomaterials for tailoring biological responses. *ACS Appl. Mater. Interf.* 8, 29310–29322. doi: 10.1021/acsami.6b09937

Lindsey, M. L., Bolli, R., Canty, J. M. Jr., Du, X. J., Frangogiannis, N. G., Frantz, S., et al. (2018). Guidelines for experimental models of myocardial ischemia and infarction. *Am. J. Physiol. Heart Circ. Physiol.* 314, H812–H838.

Ma, Y., Mouton, A. J., and Lindsey, M. L. (2018). Cardiac macrophage biology in the steady-state heart, the aging heart, and following myocardial infarction. *Transl. Res.* 191, 15–28. doi: 10.1016/j.trsl.2017.10.001

Mia, S., Warnecke, A., Zhang, X. M., Malmstrom, V., and Harris, R. A. (2014). An optimized protocol for human M2 macrophages using M-CSF and IL-4/IL-10/TGF-beta yields a dominant immunosuppressive phenotype. *Scand. J. Immunol.* 79, 305–314. doi: 10.1111/sji.12162

Moreira, H. R., Munarin, F., Gentilini, R., Visai, L., Granja, P. L., Tanzi, M. C., et al. (2014). Injectable pectin hydrogels produced by internal gelation: pH dependence of gelling and rheological properties. *Carbohyd. Polym.* 103, 339–347. doi: 10.1016/j.carbpol.2013.12.057

Mosser, D. M., and Edwards, J. P. (2008). Exploring the full spectrum of macrophage activation. *Nat. Rev. Immunol.* 8, 958–969. doi: 10.1038/nri2448

Munarin, F., Petrini, P., Barcellona, G., Roversi, T., Piazza, L., Visai, L., et al. (2014). Reactive hydroxyapatite fillers for pectin biocomposites. *Mater. Sci. Eng.* 45, 154–161. doi: 10.1016/j.msec.2014.09.003

Murray, P. J. (2017). Macrophage polarization. *Annu. Rev. Physiol.* 79, 541–566.

Oliveira, S. M., Almeida, I. F., Costa, P. C., Barrias, C. C., Ferreira, M. R. P., Bahia, M. F., et al. (2010). Characterization of polymeric solutions as injectable vehicles for hydroxyapatite microspheres. *AAPS Pharmsci. Tech.* 11, 852–858. doi: 10.1208/s12249-010-9447-3

Panahi, M., Papanikolaou, A., Torabi, A., Zhang, J. G., Khan, H., Vazir, A., et al. (2018). Immunomodulatory interventions in myocardial infarction and heart failure: a systematic review of clinical trials and meta-analysis of IL-1 inhibition. *Cardiovasc. Res.* 114, 1445–1461. doi: 10.1093/cvr/cvy145

Patil, P., Martin, J. R., Sarett, S. M., Pollins, A. C., Cardwell, N. L., Davidson, J. M., et al. (2017). Porcine ischemic wound-healing model for preclinical testing of degradable biomaterials. *Tissue Eng. Part C* 23, 754–762. doi: 10.1089/ten.tec.2017.0202

Ploeger, D. T., Hosper, N. A., Schipper, M., Koerts, J. A., de Rond, S., and Bank, R. A. (2013). Cell plasticity in wound healing: paracrine factors of M1/ M2 polarized macrophages influence the phenotypical state of dermal fibroblasts. *Cell Commun. Signal.* 11:29. doi: 10.1186/1478-811x-11-29

Qiao, J. H., Tripathi, J., Mishra, N. K., Cai, Y., Tripathi, S., Wang, X. P., et al. (1997). Role of macrophage colony-stimulating factor in atherosclerosis: studies of osteopetrotic mice. *Am. J. Pathol.* 150, 1687–1699.

Rovida, E., Paccagnini, A., Del Rosso, M., Peschon, J., and Dello Sbarba, P. (2001). TNF-α-Converting enzyme cleaves the macrophage colony-stimulating factor receptor in macrophages undergoing activation. *J. Immunol.* 166:1583. doi: 10.4049/jimmunol.166.3.1583

Schneider, C. A., Rasband, W. S., and Eliceiri, K. W. (2012). NIH Image to ImageJ: 25 years of image analysis. *Nat. Methods* 9, 671–675. doi: 10.1038/nmeth.2089

Schwarz, D. A., Lindblad, W. J., and Rees, R. S. (1995). Altered collagen metabolism and delayed healing in a novel model of ischemic wounds. *Wound Rep. Regen.* 3, 204–212. doi: 10.1046/j.1524-475x.1995.30212.x

Shaposhnik, Z., Wang, X., and Lusis, A. J. (2010). Arterial colony stimulating factor-1 influences atherosclerotic lesions by regulating monocyte migration and apoptosis. *J. Lipid Res.* 51, 1962–1970. doi: 10.1194/jlr.m005215

Shimokawa, H., and Yasuda, S. (2008). Myocardial ischemia: current concepts and future perspectives. *J. Cardiol.* 52, 67–78. doi: 10.1016/j.jjcc.2008.07.016

Sica, A., and Mantovani, A. (2012). Macrophage plasticity and polarization: in vivo veritas. *J. Clin. Invest.* 122, 787–795. doi: 10.1172/jci59643

Smith, J. D., Trogan, E., Ginsberg, M., Grigaux, C., Tian, J., and Miyata, M. (1995). Decreased atherosclerosis in mice deficient in both macrophage colony-stimulating factor (op) and apolipoprotein E. *Proc. Natl. Acad. Sci. U.S.A.* 92, 8264–8268. doi: 10.1073/pnas.92.18.8264

Swirski, F. K., and Nahrendorf, M. (2018). Cardioimmunology: the immune system in cardiac homeostasis and disease. *Nat. Rev. Immunol.* 18, 733–744. doi: 10.1038/s41577-018-0065-8

Trujillo, A. N., Kesl, S. L., Sherwood, J., Wu, M., and Gould, L. J. (2015). Demonstration of the rat ischemic skin wound model. *J. Vis. Exp.* 98:52637.

van den Bosch, T. P. P., Caliskan, K., Kraaij, M. D., Constantinescu, A. A., Manintveld, O. C., Leenen, P. J. M., et al. (2017). CD16+ monocytes and skewed macrophage polarization toward M2 type hallmark heart transplant acute cellular rejection. *Front. Immunol.* 8:346. doi: 10.3389/fimmu.2017.00346

von der Thusen, J. H., Kuiper, J., van Berkel, T., and Biessen, E. A. (2003). Interleukins in atherosclerosis: molecular pathways and therapeutic potential. *Pharmacol. Rev.* 55, 133–166. doi: 10.1124/pr.55.1.5

Wilkins, E., Wilson, L., Wickramasinghe, K., Bhatnagar, P., Leal, J., Luengo-Fernandez, R., et al. (2017). *European Cardiovascular Disease Statistics 2017*. Brussels: European Heart Network.

Yang, J., Zhang, L., Yu, C., Yang, X.-F., and Wang, H. (2014). Monocyte and macrophage differentiation: circulation inflammatory monocyte as biomarker for inflammatory diseases. *Biomark. Res.* 2:1. doi: 10.1186/2050-7771-2-1

Zarif, J. C., Hernandez, J. R., Verdone, J. E., Campbell, S. P., Drake, C. G., and Pienta, K. J. (2016). A phased strategy to differentiate human CD14+monocytes into classically and alternatively activated macrophages and dendritic cells. *Biotechniques* 61, 33–41.

Zhang, F., Lei, M. P., Oswald, T. M., Pang, Y., Blain, B., Cai, Z. W., et al. (2003). The effect of vascular endothelial growth factor on the healing of ischaemic skin wounds. *Br. J. Plast. Surg.* 56, 334–341. doi: 10.1016/s0007-1226(03)00175-9

Conflict of Interest: The authors declare that the research was conducted in the absence of any commercial or financial relationships that could be construed as a potential conflict of interest.

Copyright © 2020 Bloise, Rountree, Polucha, Montagna, Visai, Coulombe and Munarin. This is an open-access article distributed under the terms of the Creative Commons Attribution License (CC BY). The use, distribution or reproduction in other forums is permitted, provided the original author(s) and the copyright owner(s) are credited and that the original publication in this journal is cited, in accordance with accepted academic practice. No use, distribution or reproduction is permitted which does not comply with these terms.

frontiers in Bioengineering and Biotechnology

REVIEW
published: 24 April 2020
doi: 10.3389/fbioe.2020.00323

Combining Nanomaterials and Developmental Pathways to Design New Treatments for Cardiac Regeneration: The Pulsing Heart of Advanced Therapies

*Marco Cassani[1], Soraia Fernandes[1], Jan Vrbsky[1], Ece Ergir[1,2], Francesca Cavalieri[3,4] and Giancarlo Forte[1]**

[1] International Clinical Research Center, St Anne's University Hospital, Brno, Czechia, [2] Faculty of Technical Chemistry, Institute of Applied Synthetic Chemistry and Institute of Chemical Technologies and Analytics, Vienna University of Technology, Vienna, Austria, [3] School of Science, RMIT University, Melbourne, VIC, Australia, [4] Dipartimento di Scienze e Tecnologie Chimiche, Università di Roma "Tor Vergata", Via Della Ricerca Scientifica, Rome, Italy

OPEN ACCESS

Edited by:
Valeria Chiono,
Politecnico di Torino, Italy

Reviewed by:
Daniele Catalucci,
Institute for Genetic and Biomedical Research (IRGB), Italy
Susanna Sartori,
Politecnico di Torino, Italy
Jochen Salber,
Surgical Clinic, University Hospital Bochum GmbH, Germany

***Correspondence:**
Giancarlo Forte
giancarlo.forte@fnusa.cz

Specialty section:
This article was submitted to Biomaterials, a section of the journal Frontiers in Bioengineering and Biotechnology

Received: 21 October 2019
Accepted: 24 March 2020
Published: 24 April 2020

Citation:
Cassani M, Fernandes S, Vrbsky J, Ergir E, Cavalieri F and Forte G (2020) Combining Nanomaterials and Developmental Pathways to Design New Treatments for Cardiac Regeneration: The Pulsing Heart of Advanced Therapies. Front. Bioeng. Biotechnol. 8:323. doi: 10.3389/fbioe.2020.00323

The research for heart therapies is challenged by the limited intrinsic regenerative capacity of the adult heart. Moreover, it has been hampered by the poor results obtained by tissue engineering and regenerative medicine attempts at generating functional beating constructs able to integrate with the host tissue. For this reason, organ transplantation remains the elective treatment for end-stage heart failure, while novel strategies aiming to promote cardiac regeneration or repair lag behind. The recent discovery that adult cardiomyocytes can be ectopically induced to enter the cell cycle and proliferate by a combination of microRNAs and cardioprotective drugs, like anti-oxidant, anti-inflammatory, anti-coagulants and anti-platelets agents, fueled the quest for new strategies suited to foster cardiac repair. While proposing a revolutionary approach for heart regeneration, these studies raised serious issues regarding the efficient controlled delivery of the therapeutic cargo, as well as its timely removal or metabolic inactivation from the site of action. Especially, there is need for innovative treatment because of evidence of severe side effects caused by pleiotropic drugs. Biocompatible nanoparticles possess unique physico-chemical properties that have been extensively exploited for overcoming the limitations of standard medical therapies. Researchers have put great efforts into the optimization of the nanoparticles synthesis and functionalization, to control their interactions with the biological milieu and use as a viable alternative to traditional approaches. Nanoparticles can be used for diagnosis and deliver therapies in a personalized and targeted fashion. Regarding the treatment of cardiovascular diseases, nanoparticles-based strategies have provided very promising outcomes, in preclinical studies, during the last years. Efficient encapsulation of a large variety of cargos, specific release at the desired site and improvement of cardiac

function are some of the main achievements reached so far by nanoparticle-based treatments in animal models. This work offers an overview on the recent nanomedical applications for cardiac regeneration and highlights how the versatility of nanomaterials can be combined with the newest molecular biology discoveries to advance cardiac regeneration therapies.

Keywords: nanoparticles, cardiac regeneration, cardiomyopathy, targeted delivery, Hippo pathway, YAP

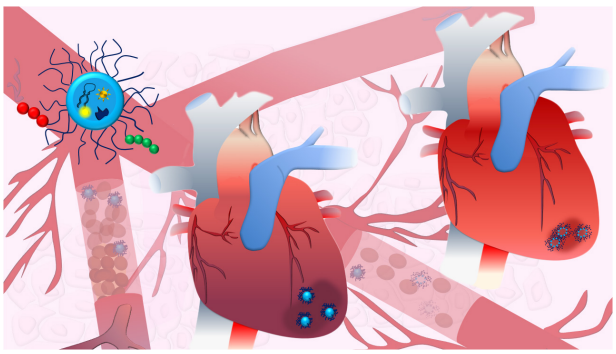

GRAPHICAL ABSTRACT | Learning from heart development and diseases to develop novel nano-therapeutics.

INTRODUCTION

For the last decades, cardiologists and researchers in the field have been fascinated by the idea of treating cardiomyopathies by inducing adult cardiomyocytes (CMs) to proliferate and generate new contractile force (Hashmi and Ahmad, 2019). The regenerative potential of mammalian heart is an age-dependent process and is already limited in newborns (Porrello et al., 2011b). After a few studies reported the limited potential of CMs to regenerate in human hearts during physiological aging and after injury (Bergmann et al., 2009; Senyo et al., 2013), a consensus was recently reached that their capacity is insufficient to restore heart function in case of injury (Eschenhagen et al., 2017). Also, cardiac muscle regenerative potential remains elusive due to the poor understanding of the biology of resident progenitor cells (Tzahor and Poss, 2017).

When damage occurs, rather than producing new functional muscle mass, the human heart is prone to protect its integrity by depositing a non-compliant scar, while inducing cardiomyocyte hypertrophy. Consequently, these two processes lead to the insurgence of arrhythmias and eventually to heart failure (HF). Therefore, overcoming this limitation would revolutionize the good clinical practice by finding a measure to counteract HF (Foglia and Poss, 2016).

To date, several clinical trials have been proposed to test cardiac repair stimulation in adults. However, no satisfactory outcomes were achieved (Banerjee et al., 2018), mainly due to either the poor understanding of resident cardiac progenitor (CPCs) biology in adult heart or by the lack of appropriate delivery tools (Smith et al., 2014; Vicinanza et al., 2017; Cianflone et al., 2018; Marino et al., 2019).

The proposed therapies entailed the transplantation of CPCs or the application of human induced pluripotent stem cells (hiPSCs), mainly delivered through cell injections (Bartunek et al., 2017; Butler et al., 2017), cell-matrix inoculation (Traverse et al., 2019; U.S. National Library of Medicine, 2019a), cell sheets (Miyagawa et al., 2017) and cell patches (Dolan et al., 2019). Despite the amount of work done in this direction, the lack of robust pre-clinical mechanistic studies remains the main hurdle for the failure of cardiac treatment (Menasché, 2018).

In this context, the design of nanoparticles (NPs) targeting the contractile component of the heart may offer interesting solutions to overcome the limitations of current therapeutics, by selective modulation of developmental pathways in cardiac cells. Currently, nanoparticles properties can be tuned and designed opportunely for different medical applications, thus offering the possibility for loading and delivering different kinds of cargos, according to the desired therapy. In this work, the current state-of-the-art of NP-based system for cardiac therapy and their therapeutic cargos such as microRNAs (miRNAs), cardioprotective drugs or growth factors is reported and critically discussed.

In conclusion, we point at Hippo pathway, a recently discovered intracellular axis being involved in fetal heart growth and cardiomyocyte proliferation (von Gise et al., 2012; Heallen et al., 2013), as a promising target for nanoparticle-based therapies.

THE BIOLOGY OF CARDIOMYOPATHIES

Heart failure is either determined by a primary cardiac event, such as in myocardial infarction (MI), or is chronically reached over a long time in non-ischemic cardiomyopathies (Tanai and Frantz, 2015). The treatment options for MI range from anti-inflammatory, anti-coagulants and analgesic drugs to angioplasty, coronary bypass or electronic implants, up to heart transplantation in the most severe cases (Lu et al., 2015). However, if the ischemic event persists for prolonged period, the damage to the heart muscle can be irreversible, and cardiac remodeling, achieved by myocardial fibrosis, results in impaired cardiac function (Briceno et al., 2016). Non-ischemic cardiomyopathies refer, instead, to muscle diseases affecting heart size, shape and structure, that eventually reduce the pumping function of the organ (Chan et al., 2018). They – in fact –

proceed to heart blood pump dysfunction, followed by the consequent remodeling of cardiac structures and eventually heart failure (Vikhorev and Vikhoreva, 2018). Based on structural and functional heart changes, several types of cardiomyopathies, having a non-ischemic basis, can be identified. Among them, hypertrophic (HCM), dilated (DCM), restrictive (RC), and arrhythmogenic right ventricular (ARVC) cardiomyopathies are inheritable, and caused by mutations in a single gene (Braunwald, 2017).

HCM is caused by single mutations on different specific genes encoding for proteins from the cardiac sarcomere and it is transmitted as a dominant trait (Alfares et al., 2015). Thus, direct relatives of affected people have 50% probability of acquiring the disease. Nevertheless, due to its incomplete penetrance at very young ages, diagnosis of the disease might be delayed till adulthood (Velzen et al., 2018). HCM is characterized by an inappropriate left ventricular hypertrophy (LVH) developed in the absence of pressure overload or infiltration, and, generally, it results in asymmetric septal hypertrophy, but any LVH pattern can be associated with the disease (Mazzarotto et al., 2019). Similarly, gene mutations can result in very distinct LVH patterns in terms of myocardial fibrosis and susceptibility to arrhythmias. Several genes that bear pathogenic mutations causing HCM have been identified. Among them, the combined cardiac myosin binding protein-C (MYBPC3) and b-myosin heavy chain (MYH7) account for up 50% of the clinically recognized HCM cases (Lopes et al., 2015). Histologically, HCM is defined by interstitial fibrosis, myocyte enlargement and microstructure disarray (**Figure 1**, middle panel).

DCM is the most common cardiomyopathy and a leading cause of heart failure, transplantation and death (Hershberger et al., 2013). It is caused by the pathological dilation of the left ventricle, followed by progressive contractile failure. It is histologically characterized by cardiomyocyte hypertrophy, loss of myofibrils, and interstitial fibrosis (**Figure 1**, right panel) (Cahill et al., 2013). DCM is a progressive disease that can originate from various factors (acquired or inherited) such as ischemia, infection, autoimmune disease, collagen vascular disease, toxins and drugs, nutritional deficiency, and genetic disease (Watkins et al., 2011; Schultheiss et al., 2019). Although patients with DCM may be initially asymptomatic, progressive heart failure or arrhythmia are often responsible for sudden death cases. DCM has a diverse array of familial or sporadic genetic causes, where mutations can be found in sarcomeric proteins and other structural protein genes (Burke et al., 2016). Mutations in the titin gene *(TTN)* are the most common causes of pathogenicity (∼25–27.6% of familial and 11.6–18% of sporadic cases) (Schafer et al., 2016). Other frequent mutations affect *MYH7* (Colegrave and Peckham, 2014), tropomyosin a1 chain *(TPM1)* (England et al., 2017), and the genes of cardiac troponins (*TNNT2)* (Hershberger et al., 2009).

ARVC is characterized by a progressive replacement of right ventricular myocardium by fibro-fatty tissue leading to ventricular arrhythmias and sudden cardiac death (Xu et al., 2017). Pathogenic mutations in 13 genes have been identified for patients with ARVC with genes encoding the cardiac desmosome accounting for more than 50% of the cases (Xu et al., 2017). The later include plakoglobin (JUP), plakophilin-2 (PKP2), desmoplakin (DSP), desmoglein-2 (DSG2), and desmocollin-2 (DSC2) (Xu et al., 2017).

Analogously to DCM, RC – the least common of the cardiomyopathies – may result from acquired or inherited predispositions. The most significant inherited mutations include *TNNT2*, troponin I (*TNNI3*), α-actin (*ACTC*), and *MYH7* (Muchtar et al., 2017). RC results in increased myocardial stiffness that ultimately leads to impaired ventricular filling (Muchtar et al., 2017). Usually RC is manifested from infiltrative processes, i.e., sarcoidosis, hemochromatosis and amyloidosis, for which tailored interventions and precise diagnosis are required to reveal the disease cause (Muchtar et al., 2017).

Other acquired disorders such as stress-induced and myocarditis cardiomyopathies have been identified. The first one is defined, according to the World Healt Organization (WHO) classification of cardiomyopathies, as an inflammatory disease often resulting from viral infections (Pollack et al., 2015). Clinically it is manifested by acute heart failure, ventricular arrythmias or cardiogenic shock, being associated with significant rates of morbidity and death (Pollack et al., 2015).

Stress or Takotsubo cardiomyopathy is a reversible disorder associated with transient left ventricular dysfunction and affects predominantly post-menopausal women (Nef et al., 2010). It mimics a myocardial infarction but in the absence of coronary artery occlusion and it is manifested by systolic apical ballooning (Dhulipala et al., 2018).

Currently available treatments for cardiomyopathies are mainly focused on the mitigation of the most severe symptoms instead of solving the pathology and in most cases the only resolutive intervention is the heart transplantation (U.S. Department of Health & Human Services).

Conversely, cardiac regeneration therapy looks for the complete remission of the disease to improve the patient's life quality, aiming to re-establish the lost heart functionality by stimulating the activity of cardiomyocytes.

NOVEL THERAPEUTIC APPROACHES TO TREAT CARDIOMYOPATHIES

Over the years, different kinds of therapies have been used to repair or regenerate the damaged heart. These include: (1) cell-based therapies (Behfar et al., 2014; Madonna et al., 2016); (2) direct reprogramming of resident cardiac fibroblasts into contractile cells (Fu et al., 2015; Engel and Ardehali, 2018); (3) endogenous cardiomyocyte proliferation induction *via* modulation of cardiomyocyte cell cycle regulators, e.g., the Hippo signaling pathway (Mohamed et al., 2018); (4) gene therapy *via* adeno associated viruses (AAVs) (Chamberlain et al., 2017). Since most of these approaches have been exploited when using nanoparticles for cardiac repair, we will briefly introduce them in the following paragraphs.

Cell-Based Therapies

Cell-based therapies envision the transplantation of cells to restore cardiac function. Implanted cells need to be able to

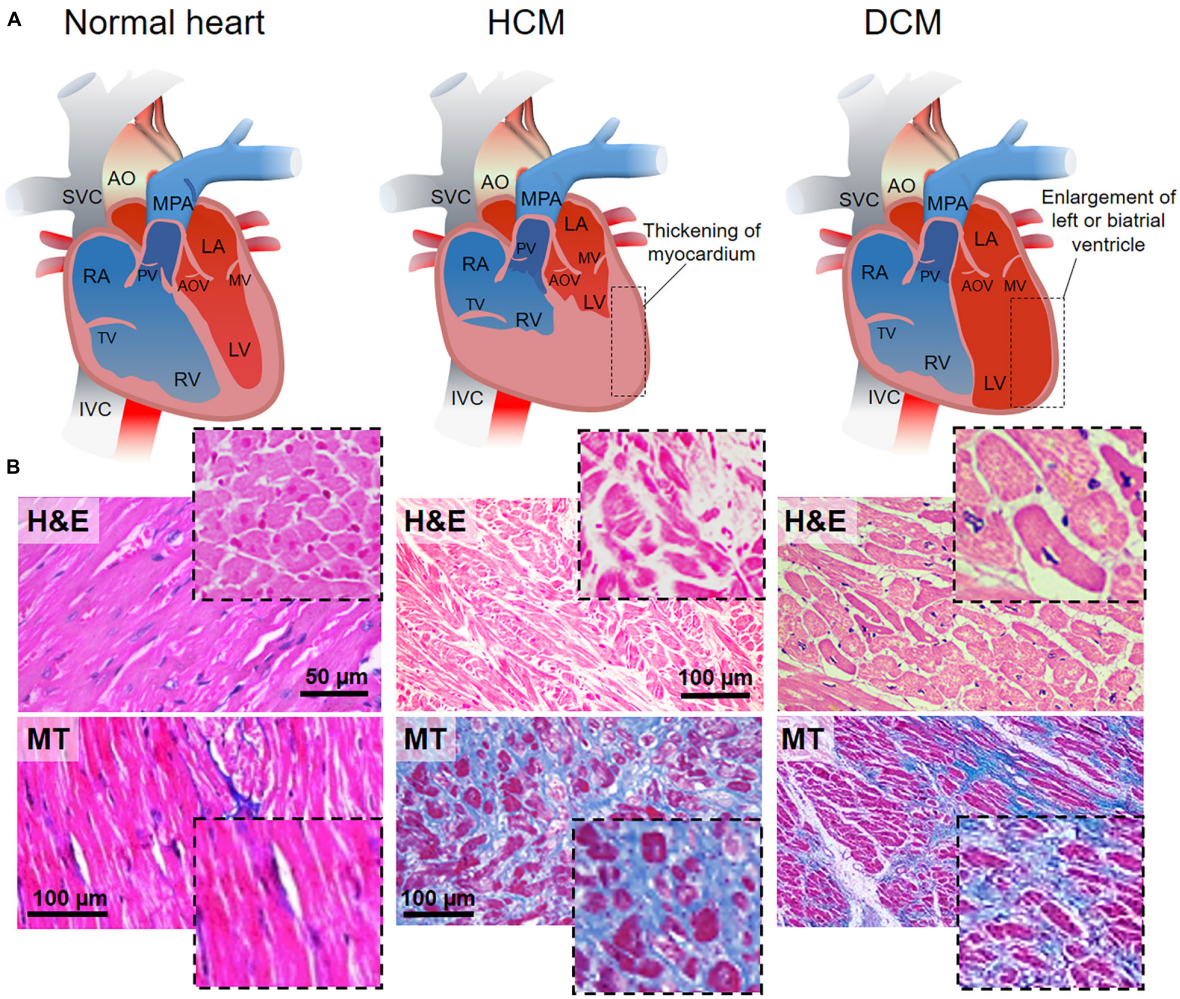

FIGURE 1 | HCM and DCM as the most common cardiomyopathies. **(A)** Schematic representations of the anatomy of normal (left), hypertrophic (hypertrophic cardiomyopathy, HCM, middle) and dilated (dilated cardiomyopathy, DCM, right) heart. HCM is characterized by left ventricle thickening, while DCM is defined by the dilation of the left ventricle. AO, aorta; SVC, superior vena cava; MPA, main pulmonary artery; RA, right atrium; RV, right ventricle; TV, tricuspid valve; PV, pulmonary valve; LA, left atrium; LV, left ventricle; MV, mitral valve; AOV, aortic valve; IVC, inferior vena cava. **(B)** Hematoxylin-eosin (H&E, top) staining in longitudinal and transversal (inset) sections of the cardiac muscle. Normal heart shows the organized and parallel alignment of cardiomyocytes (dashed black line) with preserved cell body and sarcomeric structures. Disorganized cellular structures are highlighted in HCM and DCM sections. Nuclei appear in violet, cytoplasm in pink. Masson's trichrome (MT, bottom) staining in longitudinal and transversal (inset) sections of cardiac muscle. The homogeneity, the continuity and organization of the healthy tissue (pink) is perturbed by the accumulation of fibrotic non-contractile tissue (blue) in HCM and DCM hearts. Missing scale bars were not provided in the original article. H&E healthy: Reprinted and adapted from Marian and Braunwald (2017) under the terms of the Creative Commons Attribution License. MT healthy: Reprinted and adapted from Wang et al. (2014) under the terms of the Creative Commons Attribution License. H&E HCM: Reprinted and adapted from Jain et al. (2017) under the terms of the Creative Commons Attribution License. MT HCM: Reprinted and adapted from: Guo et al. (2017) under the terms of the Creative Commons Attribution License. H&E DCM: Jain et al. (2017) under the terms of the Creative Commons Attribution License. MT DCM: Reprinted and adapted from: Mitrut et al. (2018) under the terms of the Creative Commons Attribution License.

engraft and differentiate into functional cardiomyocytes *in vivo* (Sanganalmath and Bolli, 2013). Several types of cells including skeletal myoblasts (Gavira et al., 2010), bone marrow-derived cells and mesenchymal stem cells (MSCs), cardiac progenitors and pluripotent stem cells [i.e., human embryonic (hESCs) and human induced pluripotent (hiPSCs) stem cells], have been proposed as suitable candidates for cardiac cell therapies (Psaltis et al., 2010; Müller et al., 2018). Despite the promising *in vitro* results and the beneficial short-term outcomes in *in vivo* tests, controversial evidence regarding long term side effects, like arrhythmias or possible tumor growth due to ineffective differentiation, together with inconsistencies in the reported cell engraftment rate and differentiation, have impaired the translation of such approaches into clinics (Rikhtegar et al., 2019). Nevertheless, different clinical trials featuring the delivery of cells, deemed to be beneficial to the heart, are currently undergoing. Most of these studies are based on the direct injection of different preparations of bone marrow-derived cells and are either in the recruitment phase – with estimated completion dates on May 2020 (NCT02032004) and March 2030 (NCT02503280) (Borow

et al., 2019; U.S. National Library of Medicine, 2019b, 2020a) – or with completion dates expected on June 2021 (NCT02438306), January 2023 (NCT02408432) and July 2023 (NCT02962661) (Raval et al., 2018; U.S. National Library of Medicine, 2019c,d). The outcomes of these clinical trials are likely to clarify the potentiality of cell-based therapy and mark the future direction for the application of this technique in cardiac regeneration.

Direct Reprogramming of Resident Cardiac Fibroblasts

Recently, the possibility that cardiomyocytes can be generated by direct cardiac reprogramming of non-contractile cells has gained momentum (Isomi et al., 2019). This approach consists in converting fully differentiated fibroblasts into cardiomyocytes. It combines the beneficial potential of increasing the contractile workforce of the heart with the reduction of the scar tissue formation (Ieda et al., 2010). The protocols currently in use utilize the forced expression of cardiac-specific transcription factors (e.g., GATA4, HAND2, MEF2C, TBX5) (Song et al., 2012) and relevant cardiac miRNAs to hijack the genetic program of non-contractile cells (Jayawardena et al., 2012). Several studies, both *in vitro* and *in vivo*, have reported the use of different combinations of transcription factors, miRNAs or chemical compounds to engineer mouse or human cardiac fibroblasts into cardiomyocyte-like cells, proving functional improvements in MI models (Nam et al., 2013; Wada et al., 2013; Cao et al., 2016). However, problems like inadequate reprogramming efficiency, uncertainty of the molecular mechanisms involved, and the heterogeneous population of induced cardiomyocyte-like cells still need to be addressed before the clinical application of this methodology can be foreseen (Engel and Ardehali, 2018). More details on the use of transcription factors used in cardiac repair have been reported in the literature (Hashimoto et al., 2018).

In the following paragraph, we will describe the role of miRNAs, growth factors and other cardioprotective drugs, in connection with their use as cargos in nanoparticle-driven cardiac regeneration.

Endogenous Cardiomyocytes Proliferation Induction

miRNA Regulation

Because of their regulatory role in cell fate, miRNAs are considered interesting molecular tools and new potent drugs for a number of diseases (Raso and Dirkx, 2017). miRNAs are small endogenous non-coding RNAs (∼23 nucleotides) that play gene-regulatory roles in plants and animals by directing the post-transcriptional repression of protein-coding mRNAs (Bartel, 2009). Over the last two decades, different cardiac miRNAs have been described. Here we refer to heart-specific microRNAs known together as myomiRs (myo = muscle + miR = microRNA), such as mir-128, miR-19a/19b, and other miRNAs with known effects on the heart. They were recently found to play a role in pivotal cell functions involved in cardiac regeneration, i.e., proliferation, reprogramming and differentiation (Huang et al., 2018; Gao et al., 2019).

Additionally, high throughput screening analysis recently performed by different laboratories identified a handful of miRNAs (**Table 1**) able to induce cardiomyocyte proliferation and stimulate cardiac regeneration in mice and rats (Giacca and Zacchigna, 2015). Following on these studies, miRNAs have also been found to be involved in the cardiac regulation of Hippo pathway, an evolutionarily conserved signaling pathway known for its role in proliferation and apoptosis control during organ development (Meng et al., 2016). This pathway and its impact on cardiac regeneration are described later in this review.

Growth Factors

Biologically active compounds (i.e., growth factors, cytokines) that act at different levels of regulatory processes can be exploited for cardiac repair. They can, for example, (1) activate resident progenitors to attract and differentiate them at the injury site, (2) induce cardiomyocyte dedifferentiation and proliferation, or (3) induce circulating progenitor cells to trigger neovascularization (Hastings et al., 2015). Unfortunately, growth factors and cytokine have usually pleiotropic effects and very short half-life *in vivo*.

A number of growth factors has been recently conjugated to nanoparticles for a controlled delivery at the heart (**Table 2**). Vascular endothelial growth factor (VEGF) and fibroblast growth factor (FGF) are among the most potent regulators of neo-vascularization and their efficacy has been tested in pre-clinical applications for improving cardiac function after heart failure (Unger et al., 2000; Simons et al., 2002; Henry et al., 2003). However, neither of them has been yet successfully used in clinical practice (U.S. National Library of Medicine, 2020c; Taimeh et al., 2013), due to their pleiotropic effects and limited half-life *in vivo* (Epstein et al., 2001; Henry et al., 2001).

Furthermore, insulin-like growth factor I (IGF-1) regulates contractility, metabolism, hypertrophy, autophagy, senescence, and apoptosis in the heart and its deficiency in humans and animal models has been associated with an elevated risk of cardiovascular disorders (Troncoso et al., 2014). More specifically, low levels of circulating IGF have been related to the development of heart diseases in patients diagnosed with ischemic heart (Juul et al., 2002). These evidences on the roles of IGF-1 explain the interest on developing new IGF-1-based treatments for heart repair.

Noteworthy, two drugs have been approved by food and drug administration (FDA) for the treatment of IGF1 deficiency: mecasermin (Increlex1) and mecasermin rinfabate (IPLEX1) (**Table 2**; Troncoso et al., 2014). Nevertheless, the safety of chronic systemic IGF-1 therapy is still open to debate due to the possibility of severe adverse effects such as cancer risk (Troncoso et al., 2014). In order to solve these problems, scientists have selectively overexpressed IGF-1 in the heart, revealing that IGF-1 in cardiomyocytes protects the heart from oxidative stress and promotes functional recovery after MI (Troncoso et al., 2014).

Despite the promising evidence supporting the use of growth factors for cardiac therapy, the development of delivery strategies

TABLE 1 | Cardiac function associated miRNAs with references to heart human orthologs.

MyomiRs gene family	Stem-loop sequence (human orthologs)	Mature sequence (human orthologs)	Heart linked function	Cardiac pathology associated function
mir-1	hsa-mir-1-1	hsa-miR-1-3p	Regulators of cardiac muscle growth and differentiation (Zhao et al., 2005, 2007; Liu et al., 2007, 2008; Callis et al., 2009; Sluijter et al., 2010).	Depletion induces myocyte hyperplasia (Zhao et al., 2007)
	hsa-mir-1-2	hsa-miR-1-3p		
mir-133	hsa-mir-133a	hsa-miR-133a-3p		Reduced in patients with hypertrophic cardiomyopathy (Carè et al., 2007)
mir-208	hsa-mir-208a hsa-mir-208b	hsa-miR-208a-3p hsa-miR-208b-3p		Possible cardio protective effect of miR-208 inhibition in heart failure patients (Kakimoto et al., 2016)
mir-499	hsa-mir-499a	hsa-miR-499a-5p		N.A.
mir-21	hsa-mir-21-5p	N.A.	Enhancement of fibroblast survival, interstitial fibrosis and consequent myocyte hypertrophy (Thum et al., 2008)	N.A.
mir-15	hsa-mir-15a	hsa-miR-15a-5p	Persistence of CM mitosis beyond the normal development window of cell cycle arrest and prolonged cellular proliferation of mouse CMs (Porrello et al., 2011a; Botting et al., 2012)	N.A.
	hsa	hsa		
	hsa	hsa		
	hsa	hsa		
mir-497	hsa-mir-497	hsa-miR-497-5p		
mir-126	hsa-mir-126	hsa-mir-126-5p hsa-mir-126-3p	Embryonic heart development (Fish et al., 2008)	N.A.
mir-128	hsa-mir-128-1	hsa-miR-128-1-5p	Regulator of cell cycle-related genes (Huang et al., 2018)	Deletion promotes cardiac regeneration in adults by activating CM proliferation (Huang et al., 2018)
mir-19	hsa-mir-19a hsa-mir-19b	hsa-miR-19a-5p hsa-miR-19b-1-5p	Cardiac protection-mediated expression induced in heart failure (Gao et al., 2019)	Enhancement of cardiomyocytes proliferation in response to cardiac injury (Gao et al., 2019)
mir-138	hsa-mir-138-1 hsa-mir-138-2	hsa-miR-138-5p hsa-miR-138-5p	Required to establish appropriate chamber-specific gene expression pattern, contributes to CM maturation in zebrafish (Morton et al., 2008)	N.A.
mir-143	hsa-mir-143	hsa-miR-143-3p	Chamber morphogenesis, heartbeat (Miyasaka et al., 2011)	N.A.
mir-195	hsa-mir-195	hsa-miR-195-5p	Ventricular hypertrophy-regulated miRNA (van Rooij et al., 2006)	N.A.
mir-218	hsa-mir-218-1	hsa-miR-218-5p	Heart patterning during embryonic development (Chiavacci et al., 2012)	N.A.
mir-302	hsa-mir-302a Has	hsa-miR-302a-3p hsa	Heart specific miRNA found in human tissue screening (Lee et al., 2008; Tian et al., 2015)	N.A.
	Has	hsa		
mir-367	hsa-mir-367	hsa-miR-367-5p hsa-miR-367-3p	Heart specific miRNA found in human tissue screening, contributes to proliferation of mouse cardiomyocyte (Tian et al., 2015)	N.A.
mir-486	hsa-mir-486-1	hsa-miR-486-5p	Embryonic heart development via PI3K/Akt signaling (Small et al., 2010)	N.A.

(Continued)

TABLE 1 | Continued

MyomiRs gene family	Stem-loop sequence (human orthologs)	Mature sequence (human orthologs)	Heart linked function	Cardiac pathology associated function
mir-25 (mir-92a family)	hsa-mir-25	hsa-miR-25-3p	N.A.	Inhibition improves cardiac contractility in the failing human heart by boosting intracellular calcium handling (Wahlquist et al., 2014)
				Inhibition of miR-25 in mouse reactivates Hand2 that is crucial for embryonic heart development (Dirkx et al., 2013)
	hsa-mir-92a	hsa-miR-92a-3p	N.A.	Reduces endothelial inflammation and promotes angiogenesis and functional recovery in ischemic myocardium (Bonauer et al., 2009; Loyer et al., 2014)
mir-34	hsa-mir-34a	hsa-miR-34a-5p	N.A.	Anti-apoptotic and telomere protective effect after MI in mice (Boon et al., 2013)
mir-199mir-590	hsa-mir-199a-1 hsa-mir-590	hsa-miR-199a-3p hsa-miR-590-5p hsa-miR-590-3p	N.A.	Upregulation in rodent heart upon myocardial infarction re-induces mitosis that helps to preserve cardiac function (Eulalio et al., 2012)

N.A., not assessed.

able to increase the biocompatibility, the circulation time and the release efficiency of these molecules at the injured site must be considered before foreseeing their clinical translation (Rebouças et al., 2016).

Selective Regulation of Hippo Pathway to Promote Adult Cardiomyocyte Proliferation

The Yes-associated protein one (YAP) is the core downstream effector of Hippo pathway. The role of Hippo signaling pathway will be discussed further in the present section. For a more detailed review in cellular mechanobiology, see the review from Martino et al. (2018). The activation of the Hippo pathway results in YAP phosphorylation at Ser127 by upstream LATS kinases (LATS1/2 in human) (Varelas, 2014), which further leads to cytoplasmic sequestration of YAP according to ubiquitin-mediated protein degradation. Conversely, repression of Hippo kinases induces YAP reactivation and accumulation in the nucleus (Boopathy and Hong, 2019) (content **Box 1**). In the adult organism, YAP is involved in numerous key biological processes where it acts either as repressor or activator in combination with context-specific transcription factors (**Figure 2A**). From the analysis of almost four hundred direct protein interactors of YAP, it is clear that many biological effects remain unexplored (thebiogrid.org, 2019). Among the most studied functions YAP exerts are stemness maintenance and tumorigenesis (Chen et al., 2019), cell mechanic control via focal adhesions (Nardone et al., 2017) and the regulation of organ size (Watt et al., 2015). The Hippo–YAP pathway regulates heart growth during prenatal life and is considered important for adult heart homeostasis (**Figure 2B**; Wang et al., 2018). Noteworthy, overexpression of YAP was proven to be sufficient for stimulating proliferation of post-natal rat cardiomyocytes (von Gise et al., 2012). In particular, inducible YAP overexpression in rat embryos and new-born individuals caused an increase in cardiomyocyte proliferation leading to hyperplasia and 20% gain in heart weight in 10 days. This happened due to the increase in cell number, whereas cell size remained unchanged.

Similarly, blocking the Hippo pathway upstream components MST1/2, LATS2 or SAV1 (WW45) enhanced cardiomyocytes proliferation during heart development (Heallen et al., 2013). Odashima et al. (2007) reported the occurrence of several "pro-regenerative" effects able to inhibit the development of heart failure after myocardial infarction in transgenic mice overexpressing MST1 dominant negative (resulting in downregulation of endogenous MST1 and subsequent YAP upregulation). These effects promoted the reduction of contractile cell apoptosis, intensification of proinflammatory cytokines, inhibition of cardiac dilation, and attenuation of cardiac dysfunction without inhibiting compensatory hypertrophy.

Although progresses in myocardial regeneration in Hippo-deficient heart was reported by Tao et al. (2016), restoration of overall cardiac function by tuning Hippo-pathway components seems to be a more complex task, which requires additional research and validation. In fact, Ikeda et al. (2019) described that long term activation of YAP facilitates the progression of heart failure, in response to pressure overload, in transgenic mice model lacking WW45 Hippo component. Despite homozygous knockout of WW45 (WW45cKO) in

TABLE 2 | Drugs and small molecules as cardioprotective agents in nanomedicine applications.

Molecule	class	Properties	Heart repair properties	Clinical trial	References
Simvastatin	Statin	Reduces LDL-C levels	Reduced cardiovascular morbidity and mortality in high risk patients	Heart failure	Heart Protection Study Collaborative and Group, 2002; Feringa et al., 2006; Cannon et al., 2015
VEGF	Growth factor	Promoting neovascularization	Enhanced angiogenesis	Ischemic heart disease and other cardiac conditions	Henry et al., 2001, 2003; U.S. National Library of Medicine, 2020c; Epstein et al., 2001; Taimeh et al., 2013
IGF-I	Growth factor	Regulates contractility, metabolism, hypertrophy, autophagy, senescence, and apoptosis in the heart.	IGF-1 in cardiomyocytes protects the heart from oxidative stress and promotes functional recovery after MI.	FDA approved drugs: Increlex1 and IPLEX1	Troncoso et al., 2014
AMO-1	Anti-miRNA oligonucleotide	Inhibition of miR-1	Reduce apoptosis of cardiomyocytes	N.A.	Xue et al., 2018
CoPP	Anti-oxidant	Suppresses the inflammatory activity of macrophages by induction of heme oxyenase-1 (HO-1) expression	Reduces adverse heart remodeling by controlling the inflammatory activity of macrophages	N.A.	Bulbake et al., 2017
SB431542	Inhibitor	TGFβ inhibitor	Reduces fibrosis, decreases hyperthrophy and improves cardiac function.	N.A.	Ferreira et al., 2018
CHIR99021	Inhibitor	GSK3 inhibitor	Upregulates Wnt signaling resulting in significant increase of mature cardiomyocyte proliferation.	N.A.	U.S. National Library of Medicine, 2020c
Berberine	Alkaloid	Anti-inflammatory, anti-microbial, anti-diharreal, anti-oxidative, vasorelaxant, cholesterol lowering	Reduces rate of MI	Study showed to improve survival of CHF patients when given oral or intraperitoneal	Zeng et al., 2003; Allijn et al., 2017

LDL-C, low density lipoprotein-C; CHF, congestive heart failure; Increlex1, mecasermin, a human recombinant IGF-1 analog; IPLEX1, mecasermin rinfabate, a binary protein complex of human recombinant IGF-1 and human recombinant IGBP-3; IGBP-3, insulin-like growth factor binding protein-3; HO-1, heme oxygenase-1; TGFβ, transforming growth factor β; GSK3, glycogen synthase kinase-3. N.A., not assessed.

BOX 1 | Hippo pathway overview.

Like every tissue of the human body, the heart tissue is subjected to either constant or temporary mechanical stimuli. The cell-extracellular matrix (ECM) interactions dynamically remodel the mechanical properties of the myocardium, and actively respond to extrinsic mechanical cues. **Hippo pathway** is a mechanosensitive signaling pathway transducing external mechanical stimuli into biochemical responses. The pathway functions as a negative regulator of the effectors YAP/TAZ, two paralog proteins acting as transcriptional co-activators. Here are the main components of Hippo pathway and their role in brief:

- YAP: Yes-associated protein. The effector of the pathway. It acts as a transcriptional co-activator (Boopathy and Hong, 2019);
- TAZ (WWTR1): WW domain-containing transcription regulator protein 1. Together with YAP, is the effector of the pathway. It acts as a transcriptional co-activator (Boopathy and Hong, 2019);
- LATS1/2: Large Tumor Suppressor Kinase 1. It is a serine/threonine protein kinase directly phosphorylating YAP/TAZ. The phosphorylation inhibits YAP/TAZ translocation to the nucleus (Tang et al., 2019);
- MOB1: MOB Kinase Activator 1A. It functions as a co-factor of LATS1/2 (Kulaberoglu et al., 2017);
- MST1/2 (STK3/4): Mammalian STE20-Like Protein Kinase 2. It acts upstream of LATS1/2 (Qin et al., 2013);
- SAV1 (WW45): Salvador Family WW Domain Containing Protein 1. It forms a heterodimer with MST1/2 (Bae et al., 2017);
- TAOK1: TAO kinase 1. It is a serine/threonine protein kinase acting upstream of MST1/2 (Plouffe et al., 2016);
- B-TrCP: Beta-Transducin Repeat Containing E3 Ubiquitin Protein Ligase (Fuchs et al., 2004);
- TEAD: transcription factor family forming an active transcriptional complex in association with YAP/TAZ (Boopathy and Hong, 2019).

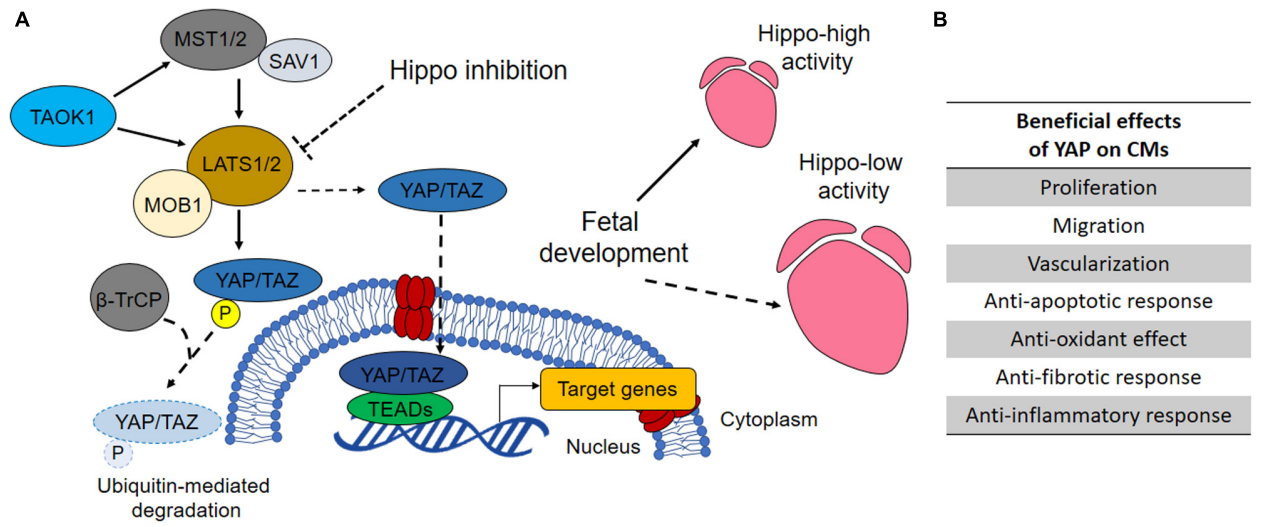

FIGURE 2 | The role of Hippo pathway in heart development and homeostasis. **(A)** When Hippo pathway is on, the mammalian MST1/2 (STE20-like protein kinase 1/2) and SAV1 (protein salvador homolog 1) complex activates LATS1/2 (large tumor suppressor homolog 1/2) that phosphorylates, in association with MOB1 (MOB kinase activator 1), YAP (Yes-associated protein 1) and TAZ (WW domain-containing transcription regulator protein 1), thus promoting their degradation. Conversely, when Hippo signaling is off, YAP and TAZ shuttle into the nucleus where they bind TEADs (TEA domain transcription factor family members) and regulate the transcription of genes involved in cell proliferation, survival and migration (Henry et al., 2001). By regulating the activity of YAP and consequently the proliferation of prenatal cardiomyocytes, Hippo pathway regulates heart size during development. YAP inhibitory kinase TAOK1 (TAO kinase 1) and E3 ubiquitin ligase β-TrCP (β-transducin repeats-containing protein) are involved in YAP degradation. Their silencing has been reported to increase YAP activity in cardiomyocytes (Torrini et al., 2019). **(B)** Increased YAP activity has been associated with several pro-regenerative effects in developed heart to prevent cardiac diseases or promoting restoration after MI, as indicated in the table (Watt et al., 2015).

mice exhibited greater cardiomyocytes cell cycle re-entry, adverse effects such as interstitial fibrosis, partial increase of infiltrating inflammatory cells and reduction in contractility were also observed.

Considering the very different effects Hippo pathway has on the contractile and structural components of the heart, pros and cons of targeting such a pathway in the whole organ need to be balanced. Also, the crosstalk with other regulatory pathways such as WNT/β-catenin signaling should be considered (Wang et al., 2018). In fact, β-catenin heterozygous mutation (the major effector of WNT pathway) in SAV1 KO mice was able to normalize the proliferation rate of ventricular cardiomyocytes and myocardial thickness, thus confirming the crucial role of WNT pathway in cardiac overgrowth induced by Hippo inactivation (Heallen et al., 2011).

Regarding cardiomyocyte homeostasis, the group of Mauro Giacca lately demonstrated that some miRNAs work in a network that preside over cardiomyocyte homeostasis by converging in the activation of nuclear translocation of YAP (Torrini et al., 2019). In particular, the authors proved that miR-199a-3p, miR-302d, miR-373, miR-590-3p, and miR-1825 can target the TAOK1 and β-TrCP (content **Box 1**), thus driving E3 ubiquitin ligase-mediated YAP degradation.

These results highlight the crucial role of Hippo pathway in cardiomyocyte homeostasis and the possible cardiac therapy horizons emerging from the regulation of YAP activity in the contractile figures of the heart.

Adeno-Associated Viruses (AAVs) for Targeted Gene Therapy

Another methodology proposed to treat the failing heart relies on the use of engineered viruses as vectors for transfection, given their natural ability to deliver nucleic acids into replicating host cells (Chen et al., 2017). In this direction, the intra-cardiac administration of miRNA-199a through adeno-associated viral vectors restored contractility and increased pig muscle mass by sustaining cardiomyocyte proliferation and de-differentiation (Gabisonia et al., 2019). Nevertheless, the long-term uncontrolled expression of the miRNA resulted in arrythmia events which led the animals to premature death, most likely due to the proliferation of poorly differentiated cardiac cells.

AAV technology is being used in clinics for several applications. A quick look at the website www.clinicaltrials.gov returns three clinical studies employing AAVs aiming to improving the function of the failing heart in patients with HF with reduced ejection fraction (HFrEF). The studies (CUPID and MYDICAR) relied on the intracoronary or the anterograde epicardial coronary artery infusion delivery of AAV1-encoding sarcoplasmic reticulum Ca^{2+}-ATPase (SERCA2a). Although encouraging, with favorable safety profile in terms of immunogenic responses and arrhythmias, the efficacy of the CUPID trial was not confirmed by the larger CUPID 2 study (Penny and Hammond, 2017).

As a general consideration, the use of AAVs still faces important limitations. In particular, several issues remain

unsolved, such as (1) long manufacturing processes and scalability; (2) strictly defined cDNA packaging capacity (∼5 kb) that dramatically limits the number of genes that can be carried; (3) the demanding screening of AAV variants suitable for the specific aim; (4) pre-existing immunological sensitivity along with the insurgence of immune response after repeated administrations (Chamberlain et al., 2017).

As an alternative to the use of AAVs, NPs, which can be "custom-made" by using different nano-constructs carrying therapeutic/regenerative drugs/miRNAs, have been proposed, thus opening the way to the application of nanomedicine in the cardiac regeneration field (Amezcua et al., 2016).

NANOPARTICLES DESIGN FOR CARDIAC REGENERATION

Generally, the term *nanomedicine* is applied to a number of innovative therapeutic approaches entailing the use of precisely bioengineered nanostructured materials (**Figure 3A**), with at least one dimension in the 1–100 nm range (Zhang et al., 2008). However, a broader definition is now accepted for structures above the 100 nm, such as sub-micrometer and nanostructured microparticles, which are commonly regarded as nanomaterials and used for nanomedical applications (Boverhof et al., 2015). Nanomedicine can be defined as the application of nanotechnology to medicine for diagnosis and therapy (Pelaz et al., 2017). It aims to minimize the side effects of therapeutic drugs while increasing their selective accumulation, thus enhancing the efficacy of the treatment in clinics (Davis et al., 2008). Conventional therapies are – in fact – often associated with tremendous side effects due to the intrinsic toxicity of the drugs, their broad spectrum of activity and the poor control over delivery (Jabir et al., 2012). Due to their tunable properties that potentially allow any kind of application, NPs can overwhelm the design limitations associated with AAVs described above. To date, various types of NPs have been loaded with miRNAs and drugs and used to vehiculate therapeutic agents *via* different administration routes, providing several advantages when compared to the standard therapies (**Figure 3B**). Remarkably, a major limitation in the therapeutic use of miRNAs is their fast clearance and rapid degradation in blood circulation and cellular cytoplasm mainly by ribonucleases, resulting in a short half-life (Sioud, 2005). Furthermore, these molecules cannot freely penetrate into the cell efficiently (Zhang et al., 2007). Extracellular miRNAs are physiologically carried inside the cell by membrane-derived vesicles, lipoprotein and ribonucleoprotein complexes (Boon and Vickers, 2013). Among these systems, exosomes are the main effectors of miRNA carriage and exosome miRNA-loaded release has been found to be involved in intercellular communications (Valadi et al., 2007). Therefore, the use of engineered miRNA nanocarriers represents a nature-inspired approach overcoming the previously described limitations. Several NP-based systems

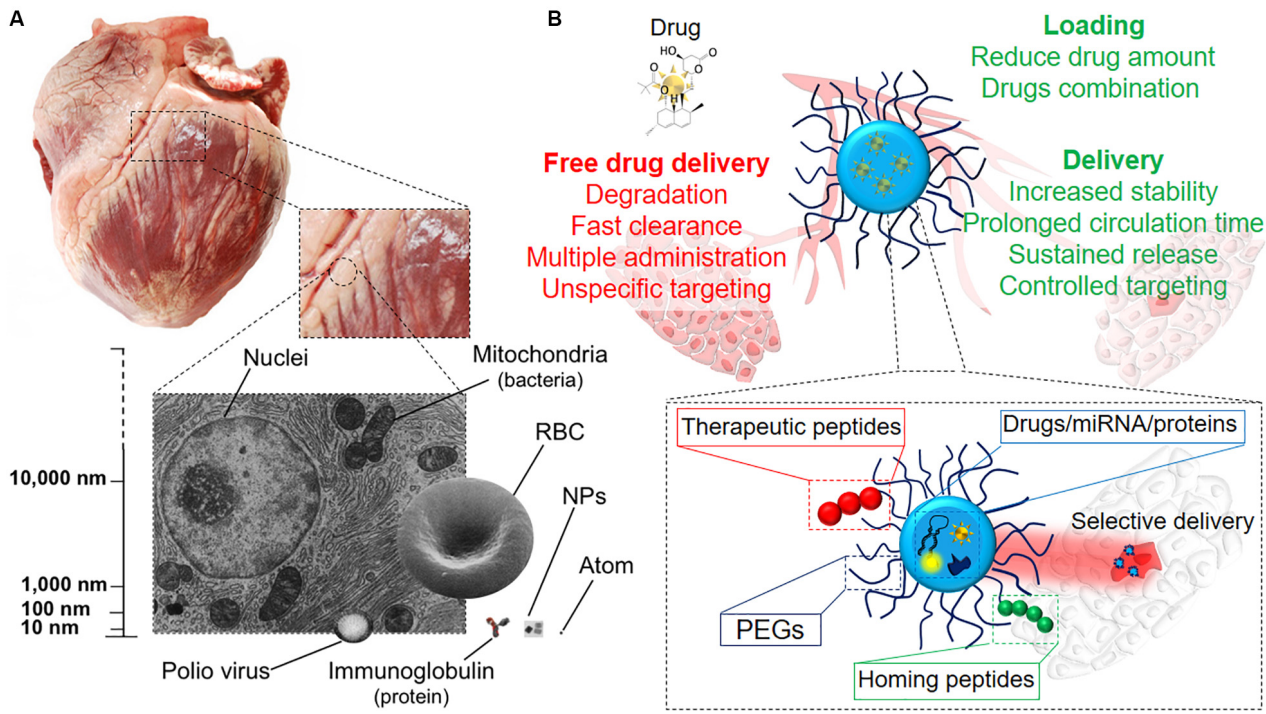

FIGURE 3 | Therapy at the nanoscale. **(A)** Representation of the nanosize, scaling down from the organ size (swine heart) to single cells and intracellular organelles, the latter being the group in which NPs are included. **(B)** Illustrative scheme of the different modalities of drug delivery. NPs as drug delivery systems have plenty of advantages if compared to systemic drug administration, such as targeted release and dosage reduction, thanks to the combination of several functional blocks within the same tool.

for miRNA delivery were so far developed, as recently reviewed in (Lee et al., 2019).

Along with the miRNA delivery, the use of bioengineered nanocarriers can enhance the circulation time, biodistribution and bioavailability of different drugs and proteins, as well as protecting them from degradation and inactivation (Patra et al., 2018). Indeed, many of the drugs currently available are lipophilic and their systemic administration is challenged by their scarce aqueous solubility, with consequent poor delivery and therapeutic efficiency (Kalepu and Nekkanti, 2015). Consequently, the encapsulation of these molecules inside amphiphilic systems may enhance their efficacy and promote their long lasting and sustained release at the desired site (Din et al., 2017).

Protein therapy offers higher specificity, greater activity, and less toxicity compared to standard drugs. However, the maintenance of their structural complexity and activity, which are crucial for achieving high therapeutic performances, can be challenged by (1) their enzymatic degradation/inactivation, (2) their short circulation half-lives and (3) their poor membrane permeability (Yu et al., 2016). Therefore, the use of nanoparticles may also protect therapeutic proteins from proteolysis while improving their delivery efficiency and sustaining their release at the target site (Zhao et al., 2016).

As a result, the use of nanotechnology to deliver cardioprotective drugs and assist the prolonged release of growth factors has arisen in the last years as a promising tool to restore compromised heart function, as it will be discussed below. Different administration routes, based on the physico-chemical properties of the drug/nanoparticle, on the predicted effect and desired target have been pursued for obtaining an optimal delivery of NPs to treat cardiomyopathies. Intravascular, including intra-cardiac (i.c.) and intravenous (i.v.) injection, and extravascular like inhalation (**Figure 4A**) are the most common administration routes used for this purpose. They all provide different advantages, and intrinsic disadvantages (**Figure 4B**; Dib et al., 2011; Yildirimer et al., 2011; Chenthamara et al., 2019), for the treatment of several pathological conditions, such as compromised vascularization, fibrosis and inflammation, while attempting to improve cardiac functionality (**Figure 4C**). However, despite the encouraging premises, the use of NP-based system for direct cardiac repair is still lagging at the preclinical stage.

In the next chapter we will provide an overview of the state-of-the-art in the field of nanomedicine for cardiac regeneration, and revise the main properties of the NPs – and their cargos – used to this aim (**Table 3**).

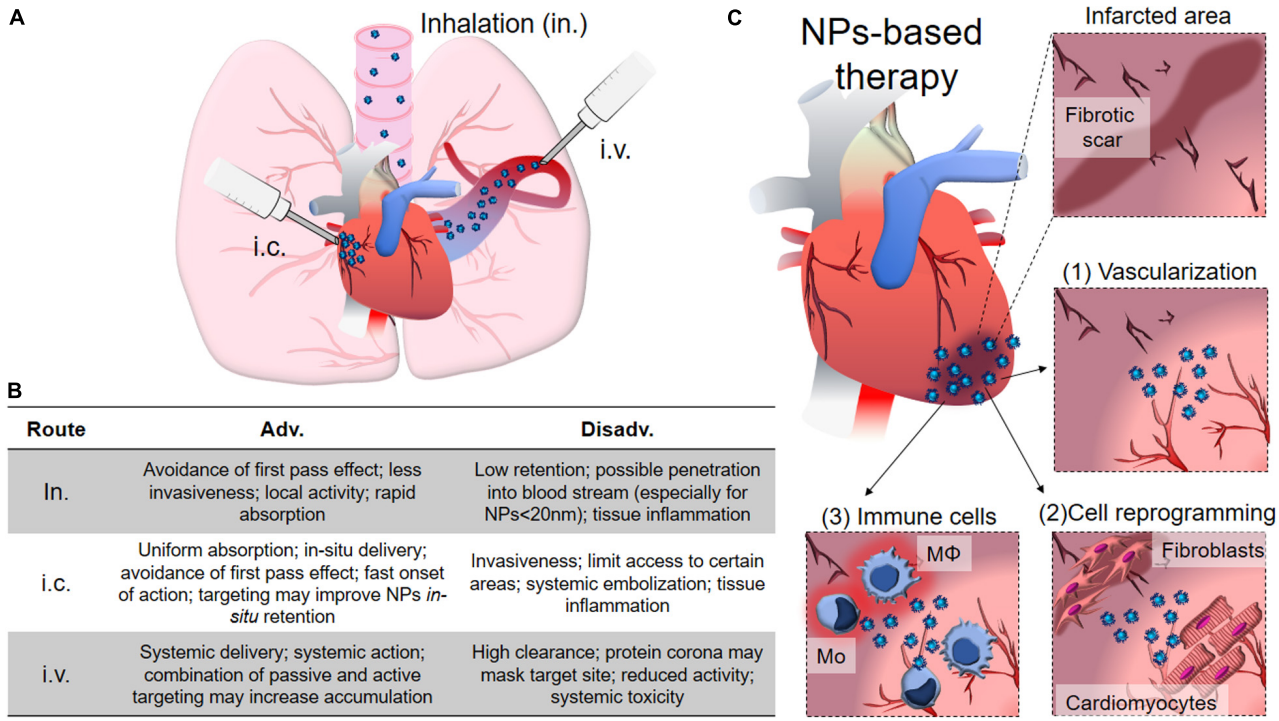

B

Route	Adv.	Disadv.
In.	Avoidance of first pass effect; less invasiveness; local activity; rapid absorption	Low retention; possible penetration into blood stream (especially for NPs<20nm); tissue inflammation
i.c.	Uniform absorption; in-situ delivery; avoidance of first pass effect; fast onset of action; targeting may improve NPs *in-situ* retention	Invasiveness; limit access to certain areas; systemic embolization; tissue inflammation
i.v.	Systemic delivery; systemic action; combination of passive and active targeting may increase accumulation	High clearance; protein corona may mask target site; reduced activity; systemic toxicity

FIGURE 4 | NPs for cardiac diseases. **(A)** The administration routes currently evaluated for delivery therapy at heart include inhalation (in.), intra-cardiac injection (i.c.) and intra-venous injection (i.v.). **(B)** Table showing advantages and disadvantages of the different administration routes. **(C)** The infarcted area typically shows loss of vessels and various degrees of fibrotic scar formation with limited contractility and functionality that dramatically compromise heart functions. NPs can be conceived to help restoring vascularization by promoting angiogenesis (1), locally transdifferentiating fibroblasts into CMs, resolving the fibrotic scar (2), and promoting the anti-inflammatory polarization of immune system cells, like macrophages (Mφ) and monocytes (Mo). The main text provides detailed discussion for each of the points here briefly described.

TABLE 3 | NPs for cardiac regeneration.

NPs type	Composition	Cargo	Hydrodynamic size and surface charge	Targeting moiety	Application	Stage of research	References
Polymeric	DSPE-PEG-NH_2, DSPE-PEG-Maleimide, PBFT	miR-199a	110 nm, ∼15–20 mV	TAT	Targeted miR-199a delivery for reducing scar size while maximizing muscle and vessel restoration and promote CMs proliferation.	*In vivo*: Rat MI model	Yang et al., 2019
	PEG-DGL	AMO-1	∼200 nm, ∼4 mV	AT1	Targeted delivery of miR-1 inhibitor (AMO-1) to attenuate cardiomyocytes apoptosis.	*In vivo*: C57BL/6 mice MI model	Xue et al., 2018
	HA-sulfate	miR-21	130 nm, -10 mV	N.A.	Delivery of miRNA-21 to cardiac macrophages after MI for inducing their modulation toward an anti-inflammatory, reparative state.	*In vivo*: C57BL/6 mice MI model	Bejerano et al., 2018
	PLGA	Simvastatin	∼160 nm, -4 mV (referred in a different work for similar NPs)	N.A.	Local recruitment of statin-PLGA-NPs-loaded AdSCs to the infarcted site and gradual release of the drug to improve neovascularization and cardiac regeneration.	*In vivo*: BALB/c nu/nu mice	Katsuki et al., 2014; Yokoyama et al., 2019
	PLGA	VEGF	113 nm, -55 mV	N.A.	Local release of reduced dosage of VEGF to favor angiogenesis and reduce risks associated with higher dosage therapy.	*In vivo*: NOD/SCID MI mice	Oduk et al., 2018
	AcDXSp	SB431542 CHIR99021	∼350 nm, ∼10 mV	ANP	pH-triggered delivery of combined poorly water-soluble small drug molecules for promoting cardiac regeneration.	*In vitro*: primary cardiac cells isolated from neonatal rats	Ferreira et al., 2018
	DSPE-PEG-Maleimide, PCPDTBT	N.A.	∼50 nm	CPP	Photoacustic imaging (PAI)	*In vivo*: NOD/SCID mice	Qin et al., 2018
Liposomes	HSPC, cholesterol, DSPE-PEG-OH, DSPE-PEG- Maleimide	VEGF	180 nm, N.A.	Anti-P-selectin	Targeted delivery of VEGF to the infarcted site to enhance vascularization.	*In vivo*: rat MI model	Scott et al., 2009
	DSPE-PEG-carboxy, HSPC, cholesterol	N.A.	142 nm, N.A.	AT1	Targeted delivery of NPs (48% accumulation in 24 h) to the left ventricle after MI.	*In vivo*: C57BL/6 mice MI model	Dvir et al., 2011
	PS, PC, cholesterol	N.A.	1.2 μm, -98 mV	PS	Apoptotic cell-like treatment for reducing inflammation at infarcted heart and promoting angiogenesis.	*In vivo*: Balb/c mice MI model	Harel-Adar et al., 2011

(Continued)

TABLE 3 | Continued

NPs type	Composition		Cargo	Hydrodynamic size and surface charge	Targeting moiety	Application	Stage of research	References
Liposomes	PMPs		CoPP	100 nm, -2.25 mV	N.A.	Promote biomimicked platelet like proteoliposomes interaction with monocytes, which serve as vehicle for enhanced liposome accumulation at the injured area for local release of therapeutic cargo.	*In vivo*: BALB/c mice	Cheng et al., 2016
	DPPC, DSPE-PEG-OH, cholesterol		Berberine	110 nm, N.A.	N.A.	EPR effect for liposome accumulation and local release of berberine after macrophage uptake, reducing inflammatory damage.	*In vivo*: C57BL/6 mice MI model	Allijn et al., 2017
Inorganic	**Core**	**Shell**						
	SiO_2	IRIS3-APTS	N.A.	50 nm, -25 mV	N.A.	Promoting hMSCs engraftment	*Ex vivo*: Wistar rat infarcted hearts	Popara et al., 2018
	$Ca_2(PO_4)_2$	Citrate	Hemagglutinin or mimetic peptide	~200 nm, ~31 mV	N.A.	Accumulation of nanoparticles at the myocardium via inhalation for local therapy aiming to restore heart contractility.	*In vivo*: Landrace pigs	Miragoli et al., 2018
	$Fe_{x-1}O_x/SiO_2$	SiO_2	N.A.	60 nm, N.A.	N.A.	Magnetic nanoparticles internalization on endothelial cells for their guidance to the ischemic heart resulting in improved remodeling and cardiac function.	*In vivo*: rat MI model	Zhang et al., 2019
	Fe_2O_3	DMSA, APTs, Glu	N.A.	10/35 nm, -43.1/28.9/-2.1 mV	N.A.	Cardioprotective activity *via* inhibition of intracellular ROS and decrease of peroxidation injury.	*In vivo*: Sprague-Dawley rats and Guinea pigs	Xiong et al., 2015
	Au	PEG-SH, OPSS-PEG-SVA	N.A.	80 nm, N.A.	CNA35	Myocardial scar detection with CT imaging	*In vivo*: Sprague-Dawley rat MI model	Kee and Danila, 2018

TAT, transactivator of transcription peptide; AT1, angiotensin II type 1 ligand; ANP, atrial natriuretic peptide; CPP, cell-penetrating peptide; AMO-1, Anti-miRNA-oligonucleotide; VEGF, vascular endothelial growth factor; TGFβ inhi, transforming growth factor β inhibitor; GSK3 inhi, glycogen synthase 3 inhibitor; DSPE-PEG, 1,2-distearoylphosphatidyl-ethanolamine-PEG; PBFT, poly(9,9-dioctylfluorene-alt-benzothiadiazole); PEG-DGL, pegylated dendrigraft poly-L-lysine; HA-sulfate, Hyaluronan sulfate; PLGA, Poly lactic-co-glycolic acid; AcDXSp, spermine-acetalated dextran; PCPDTBT, Poly [2, 6- (4,4-bis- (2- ethylhexyl) – 4H -cyclopenta [2,1-b;3,4-b'] dithiophene) –alt -4,7 (2,1,3 – benzothiadiazole)]; AT1, angiotensin II type 1 ligand; CoPP, cobalt protoporphyrin IX; D–PE-PEG, 1,2-distearoylphosphatidyl-ethanolamine-PEG; HSPC, L-α-phosphatidylcholine; PS, phosphatidyl serine; MPs, platelet membrane proteins; IRIS3-APTS, aminopropyltrietoxysilane derivative of IRIS3 cyanine; DMSA, dimercaptosuccinic acid: PEG-SH, PEG-thiol; OPSS-PEG-SVA, orthopyridyldisulfide-polyethylene glycol-succinimidyl valerate; CNA35, collagen binding adhesion protein 35. N.A, not assessed.

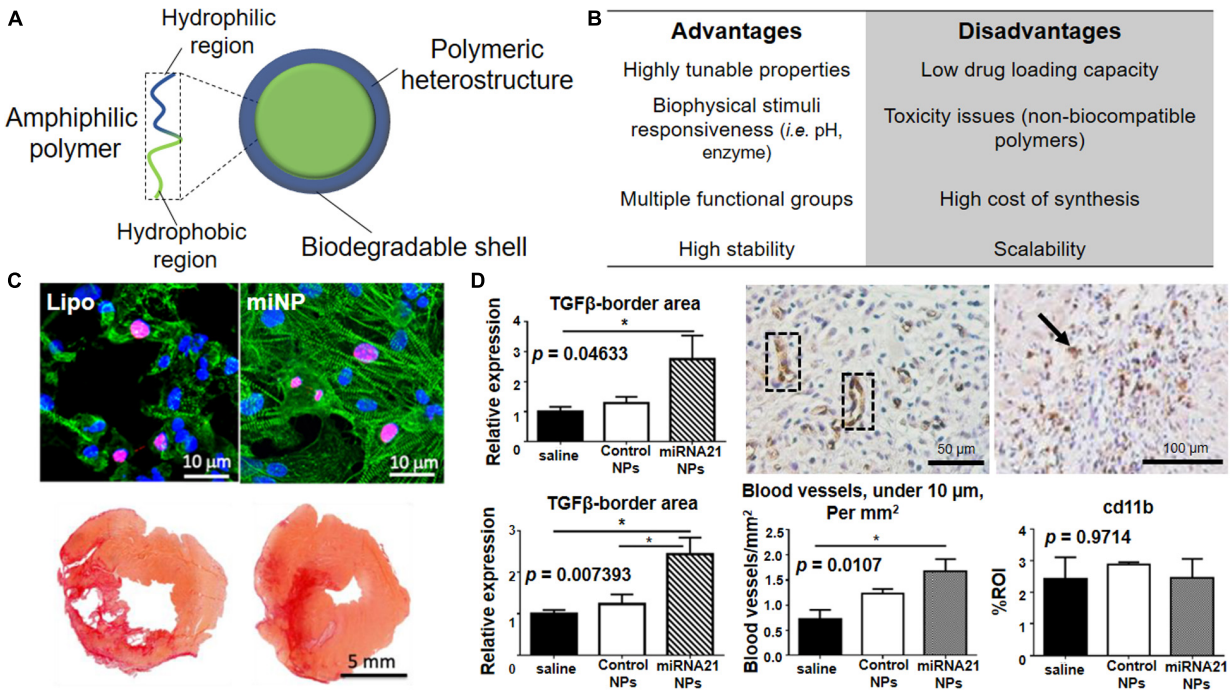

FIGURE 5 | Polymeric NPs for cardiac repair. **(A)** Schematic representation of polymeric NPs with overall composition and structure. The use of amphiphilic building block allows the formation of micelle-like structures in aqueous media. **(B)** Advantages and disadvantages associated with the use of polymeric nanoparticles in term of synthesis, long-term stability and clinical translation of the material. **(C) Top.** Polymeric nanoparticles carrying miRNAs (miNPs) are significantly less toxic for human embryonic stem cell-derived cardiomyocytes when compared to lipofectamine (lipo). Alpha-actinin (green) stains the contractile structure and Ki67 (red) accounts for the proliferation capacity. Nuclei are counterstained by DAPI (blue). **Bottom.** Picro Sirius Red *ex vivo* staining of heart transversal tissue sections showing a clear reduction of the scar size and fibrosis in left ventricle for the heart treated with miNPs (right) in comparison to the same particles carrying a scramble miRNA (left). **(D) Left.** miRNA-21 NPs myocardial infarction treatment causes increased levels of anti-inflammatory cytokine TGF-β both at infarction border zone (top) and in remote myocardium (bottom) when compared to saline-treated or control. **Center.** miRNA-21 NPs induce neovascularization in infarcted mouse myocardium, as shown by CD31 + blood vessels in cross-sections of the heart (dotted black box) and quantified in the graph by comparing it with saline and control NPs-treated groups $^*p < 0.05$. **Right**. Histological analysis shows the presence of macrophages in infarcted heart treated with miRNA-21 NPs, as shown by CD11b-positive cells positive cells (black arrow), but no macrophage accumulation as compared to saline and control NPs as shown in the graph. Reprinted from: **(C)** (Yang et al., 2019) with permission from American Chemical Society; **(D)** (Bejerano et al., 2018) with permission from American Chemical Society.

POLYMERIC NANOPARTICLES

Polymeric NPs have recently caught attention by virtue of their versatility and higher tunable properties, which make them extremely interesting tools for controlled drug encapsulation and release (**Figures 5A,B**). Indeed, their physico-chemical properties (i.e., surface charge, surface functionalities, hydrophobicity) can be finely tuned for accommodating nucleic acids, drugs and proteins to promote their efficient release inside the cells (Patil and Panyam, 2009; Fortuni et al., 2019). This large class of NP-based system include amphiphilic micelles, vesicles, dendrimers and polymersomes possessing unique structures and properties, which can be efficiently adjusted during synthesis for hosting different kind of cargos (Chandarana et al., 2018). Most of the designed polymeric NPs propose new synthetic copolymers able to combine different functionalities such as targeting and selective cargo delivery systems (El-Say and El-Sawy, 2017). Moreover, given the emerging use of miRNAs for cardiac regeneration, it is not surprising that many studies developed polymeric NPs as miRNA carriers, alone or in combination with targeting moieties or therapeutic drugs (see **Table 2**).

Recently, Yang and colleagues have reported the use of polymeric NPs composed by a combination of poly(9,9-dioctylfluorene-*alt*-benzothiadiazole) (PBFT) and 1,2-distearoylphosphatidyl-ethanolamine-PEG-amino (DSPE-PEG-NH_2), for the conjugation with miRNA molecules, or DSPE-PEG-maleimide for the binding of transactivator of transcription (TAT) peptide, in order to deliver therapeutic miRNA to the infarcted myocardium (**Figure 5C**) (Yang et al., 2019). The polymeric matrix provided by these miRNA NPs (miNPS) protects miR-199a against enzymatic degradation and facilitates the functionalization with TAT for improved cell uptake. *In vitro* experiments, performed by using hESCs-derived cardiac cells, revealed that the miNPs are less cytotoxic than commercially available lipocomplexes, while exhibiting comparable transfection efficiency, both in normoxia and hypoxia. Interestingly, miNPs were shown to selectively trigger the proliferation of both hESC-derived cardiomyocytes and endothelial cells, but not human cardiac fibroblasts (hCFs). This strategy was able to reduce scar size and maximize muscle and vessel restoration, giving good results *in vivo* when miNPs were injected into mice beating hearts in

combination with an injectable hydrogel. Indeed, cardiac function of the neo-vascularized myocardium was restored for over 3 months, indicating the long-term therapeutic effects of this treatment.

In another study the authors pursued targeted delivery of NPs carrying a miRNA inhibitor instead of a therapeutic miRNA. In detail, Xue et al. (2018) developed a pegylated dendrigraft poly-L-lysine (PEG-DGL) dendrimer functionalized with an early myocardium targeting peptide (AT1) and an antisense oligonucleotide able to inhibit miR-1 (AMO-1) (AT1-PEG-DGL-AMO-1). *In vivo* results showed that the nanovector was able to target the infarcted mouse heart within 30–60 min after a single i.v. injection and significantly reduced the infarcted area. The inhibition of miR-1 successfully attenuated cardiomyocytes apoptosis, thus reducing cell death and promoting cardiac repair.

Other than targeting directly cardiomyocytes, immune system cells can be programmed to enhance cardiac repair. The myocardium is – in fact – the site of massive immune cell infiltration during the acute phase of the infarction. In this context, co-assembled miR-21, Ca^{2+} and hyaluronan-sulfate NPs (HASCa^{2+}-miRNA) were used to target macrophages in the heart (**Figure 5D**) (Bejerano et al., 2018). After i.v. injection, NPs promoted the switch of macrophages from the pro-inflammatory to the reparative phenotype, thus promoting angiogenesis while reducing fibrosis and cell apoptosis. However, the poor understanding of the mechanism by which the interaction between NPs and macrophages occurs remains the major obstacle to the translation of this appealing procedure.

By using a different approach, Yokoyama et al. (2019) combined nanomaterials and stem cell therapy. The capacity of adipose-derived stem cell (ADSCs) for promoting neovascularization and inhibiting cell death after MI was exploited. The authors reported that simvastatin-conjugated PLGA NPs loaded *in vitro* on ADSCs induce spontaneous recovery of infarcted myocardium and increase vascularity. Indeed, statin-PLGA-NPs-loaded ADSCs were shown to be recruited to the ischemic myocardium to locally release the payload. This combined approach is bound to increase the cardiac regeneration potential of a very limited number of cells (10,000 cells per mouse), since the effect would be amplified by statin gradual release. This research work interestingly pointed out the therapeutic benefits emerging from the combination of NP-based and cell-based therapies for treating cardiac diseases.

Additionally, Oduk et al. (2018) described the use of PLGA NPs VEGF-loaded to restore the vascularization at the infarcted heart. The particles were able to continuously release VEGF for at least 31 days after injection in a mice model of MI, with improvements in cardiovascular system being still detected 4 weeks after the treatment. Noteworthy, the controlled release of the growth factor, due to the continuous biodegradation of PLGA matrix, effectively increased the delivery of VEGF at the target site, while reducing its systemic side effects.

In the context of cell reprogramming, spermine-modified acetylated dextran (AcDXSp) nanoparticles have been designed to encapsulate poorly water-soluble drugs (SB431542 – transforming growth factor β (TGFβ) inhibitor – and CHIR99021 – Glycogen synthase kinase-3 (GSK3) inhibitor) used to reprogram fibroblasts (Ferreira et al., 2018). These NPs were also tagged with a targeting peptide (atrial natriuretic peptide, ANP) specific for cardiac fibroblasts. The authors claimed the dual targeting and therapeutic effect might be exploited to circumvent the limitations of local injection. Nevertheless, *in vivo* experiments to prove this theory were not carried out so far.

Along with the efforts spent for developing therapeutic nanomaterials, NPs can also be designed as diagnostic tools allowing for superior performance in imaging cardiomyocytes in the failing heart or to monitor the progress of therapeutic protocols. Among the diagnostic techniques available at present, photoacoustic imaging (PAI) is a non-invasive diagnostic tool which provides high sensitivity and helps overcoming the limited depth penetration and spatial resolution of the conventional optical imaging (Wang and Hu, 2012). In order to increase the image contrast when using this technique, nanoparticles have been successfully employed as contrast agent material (Calcagno et al., 2019).

Qin et al. (2018) recently reported the use of NPs composed by a semiconductor polymeric contrast agent (PCPDTBT) encapsulated in a FDA approved lipid-based copolymer (DSPE-PEG-Maleimide). NPs functionalized with cell-penetrating peptide (CPP) were able to target and label hESCs-derived cardiomyocytes (hECS-CM). This labeling technique was suitable for cell detection using PAI both *ex vivo* and *in vivo*. In the latter case, the resolution obtained was as low as 2,000 injected cells, twenty-five times lower than what can be achieved with fluorescent imaging. Photoacoustic imaging was also successfully applied to monitor hECS-CMs transplantation in living mouse heart. Although being able to detect NPs-labeled cells, PAI sensitivity was lower for imaging the host myocardium, as recognized by the same authors. Nevertheless, this strategy holds great promises for monitoring cardiac regenerative processes and for live imaging of heart in the future. However, its application in monitoring cardiac disease and cardiac regeneration is still poorly investigated.

Despite the invaluable properties of polymeric NPs, their toxicity and biodegradability have to be carefully considered during their design. The use of non-biodegradable polymers has been associated with chronic toxicity and, as general warning, the long-term toxicity of these materials is still largely unknown (Banik et al., 2016). Consequently, the use of well-know and established biocompatible polymers is instead more likely to facilitate and improve the clinical translation of polymeric NPs (Ferrari et al., 2018).

LIPOSOMES

Another type of widely studied carrier for drug delivery/transfection applications is represented by liposomes (**Figures 6A,B**). Liposomes are artificial vesicles of phospholipids and cholesterol mixture, able to encapsulate drugs, proteins/peptides, and DNA (Akbarzadeh et al., 2013). Although they may face long-term stability issues in blood circulation, liposomes are extremely interesting for their cost-effective and

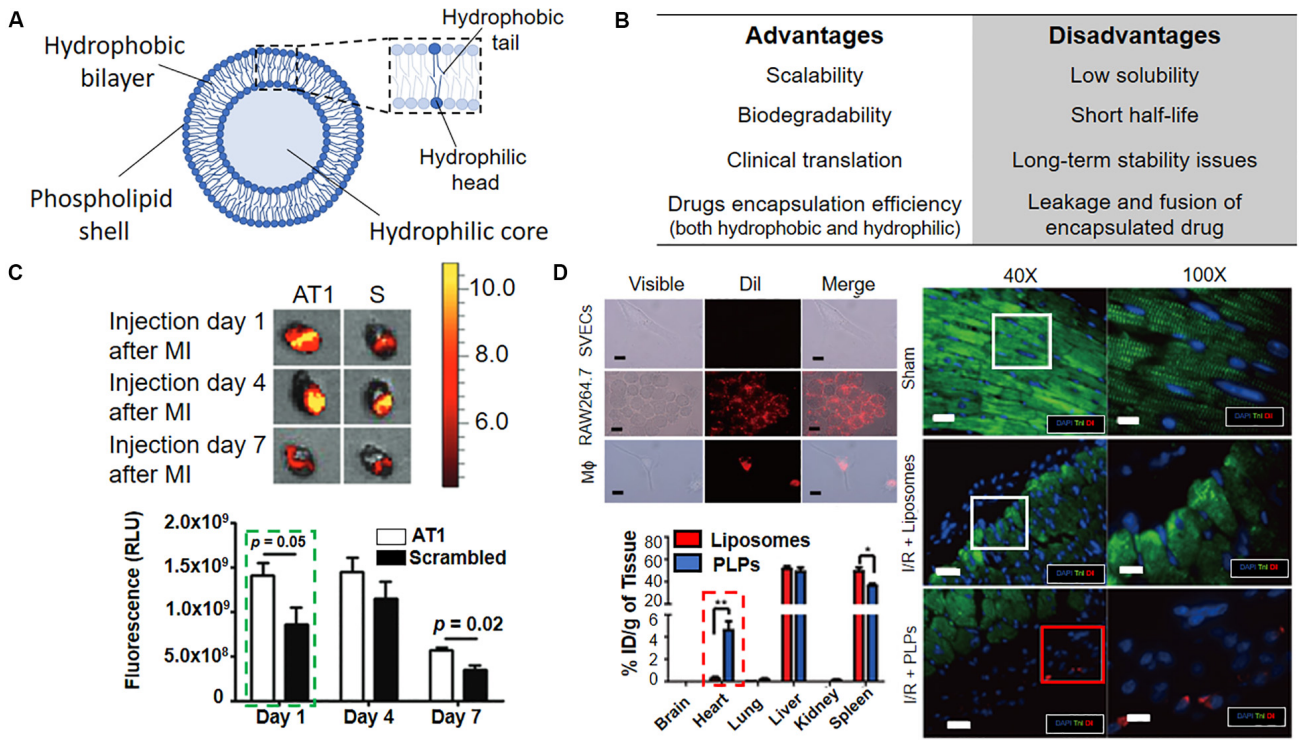

FIGURE 6 | Liposomes for active targeting of infarcted heart. **(A)** Schematic representation of liposomes with overall composition and structure. **(B)** Advantages and disadvantages associated with the use of liposomes. **(C) Top.** *In vivo* bioluminescence images of infarcted mouse hearts injected either with AT1 or scrambled (S) liposomes and analyzed at the indicated timepoints indicate AT1-liposomes preferential accumulation in the tissue (orange/red signal). The graph shows the quantification of the fluorescence due to AT1- and scramble-liposomes accumulation at the given timepoints. **(D) Top left.** Dil-labeled-Platelet-like proteoliposomes (PLPs) selectively interact with RAW264.7 monocytic cell line and macrophages (Mϕ) but not with SVECs endothelial cells, as indicated by the red signal. Scale bar 10 μm. Dil = 1,1′-Dioctadecyl-3,3,3′,3′-Tetramethylindocarbocyanine Perchlorate. **Bottom left.** Intravenously injected PLPs accumulate in the heart more efficiently than liposomes 72 h post-infarction $^{*}p < 0.05$, $^{**}p < 0.01$. **Right.** The persistence of Dil-labeled PLPs in the infarction area in a mouse model of ischemia/reperfusion (I/R + PLPs, red square) as compared to Dil-labeled liposomes (I/R + Liposomes, white square) and sham control. Troponin I (TnI, green), stains the heart muscle, Dil (red) injected liposomes, cell nuclei are counterstained with DAPI (blue), Scale bar were not reported in the original article. Reprinted and adapted from: **(C)** (Dvir et al., 2011) with permission from American Chemical Society; **(D)** (Cheng et al., 2016) with permission from Wiley.

scalable synthesis. These features have favored their clinical development (Doxil was the first FDA-approved nanodrug) as compared to other kinds of NPs (Sercombe et al., 2015). One of the first examples of liposomes applied to cardiomyopathy treatment was represented by anti-P-selectin-conjugated liposomes containing VEGF, as reported by Scott et al. (2009). The authors attempted to enhance neovascularization in a rat model of myocardial infarction. Targeted delivery through P-selectin antibody, overexpressed at the infarcted inflammatory site, promoted the selective and efficient delivery of VEGF, thus enhancing the fractional shortening and systolic function, with a 21% increase in anatomical vessels and 74% increase in perfused vessels in MI area. Conversely, systemic administration of VEGF resulted in no significant improvement in cardiac function.

In another study, PEGylated liposomes containing a targeting ligand against angiotensin II type 1 (AT1), a receptor which is widely expressed in infarcted heart were reported (**Figure 6C**; Dvir et al., 2011). *In vivo* experiments have confirmed particles accumulation in the left ventricle after MI (48% within 24 h post-i.v. injection), thus revealing a specific delivery at injured myocardium. No detail on the functional therapeutic cardiac regeneration potential of the nanovector was given, as the main rationale of the authors was to demonstrate the targeting efficiency of NPs at the heart after MI. Nevertheless, this study provides crucial information for understanding the accumulation of NP-based system at the diseased heart, as discussed below.

The use of liposomes for targeting the immune system cells, which regulates the inflammatory response at the infarcted heart, has also been studied. Targeting the immune system cells at the site of inflammation can be indeed an alternative and effective solution for increasing the targeting and delivery of NP-based therapy, due to the natural tendency of the innate components to recognize and internalize external materials administered in the body such as nanoparticles (Fadeel, 2019). The group of Cohen S. reported the use of phosphatidylserine (PS)-presenting liposomes, mimicking the anti-inflammatory effects of apoptotic cells (Harel-Adar et al., 2011). The uptake of PS-liposome induced the secretion by macrophages of high levels of anti-inflammatory cytokines (i.e., TGFβ and interleukin 10, IL-10) both *in vitro* and *in vivo*. The i.v. injection in a rat model of acute MI promoted angiogenesis, while preserving small scars and preventing ventricular dilatation and remodeling.

More recently, an alternative approach was presented by Cheng and collaborators (**Figure 6D**; Cheng et al., 2016). The authors developed biomimicking platelet-like proteoliposomes able to interact with monocytes. This methodology foresees the interaction between the immune system cells and platelet membrane proteins (PMPs) for promoting the accumulation of liposomes at the injured heart, where monocytes are recruited. Proteoliposomes were loaded with therapeutic cobalt protoporphyrin IX (CoPP), a compound able to suppress the inflammatory activity of macrophages and were "dragged" by the monocytes to the infarcted zone. This system showed promising results *in vivo* when compared to systemic administration of free CoPP. However, the randomization of the surface coating may jeopardize the reproducibility of this synthetic technique, as raw material, i.e., the PMPs derived from different samples or batches, could give different results in term of composition and biophysical features of the final particles. Moreover, the poor understanding of the interaction with monocytes, which can reduce the effective control over this mechanism, makes the clinical translation of proteolioposomes unlikely.

Furthermore, the group of Schiffelers have developed a liposomal carrier for berberine delivery, a natural product which is known for its anti-inflammatory, anti-oxidative and cardio-protective functions (Allijn et al., 2017). In its free form, berberine is poorly soluble in aqueous medium and have a short half-life time in circulation. The liposomes encapsulated with the dug tested *in vivo* in C57BL/6J mice showed to preserve the cardiac function by 64% at day 28 post-MI, in comparison to control liposomes and free drug. Liposomes administered I.V. targeted the inflammatory site and release the drug after macrophage uptake, reducing both inflammatory damage and systemic adverse effects. This study appears particularly promising because of the reproducible synthesis of the liposome formulation and for its effective targeting and long-term stability.

So far, liposomes have been the most tested NP-based system in clinical trials, encountering several cases of successful clinical translation, and many liposome formulations are currently available on the market for several therapies (Bulbake et al., 2017). However, their application in heart diseases therapy is still limited and needs further investigation.

INORGANIC NANOPARTICLES

Inorganic NPs are known for exhibiting appealing physical properties that can be potentially exploited for simultaneous diagnosis and therapy (i.e. theranostic) of several pathologies (**Figures 7A,B**; Giner-Casares et al., 2016). They are generally composed by an inorganic core surrounded by an organic/inorganic shell, which aim to increase the biocompatibility of the system and the interactions of the NP with the biological environment (Conde et al., 2014). Recently, Popara et al. (2018) showed that SiO_2-NPs passively interacted with human MSCs (hMSCs) mediating important molecular processes (**Figure 7C**; Popara et al., 2018). More specifically, the internalization of the SiO_2-NPs affected focal adhesions by promoting cell adhesive phenotype both *in vitro* and *ex vivo* upon injection in the infarcted rat heart. In addition, NPs internalization contributed to cell cross-talk between transplanted cells and the host, which is essential for an effective engraftment and tissue regeneration. However, the transient inhibition of lysosomal function by SiO2-NPs was reported, pointing out the need for a thorough evaluation of NPs long-term toxicity and possible side effects due to their sustained intracellular accumulation (Croissant et al., 2017).

Biodegradable inorganic particles have been also proposed to improve myocardial function after heart failure (Miragoli et al., 2018). Miragoli and co-workers demonstrated that biodegradable negatively charged calcium phosphate NPs (CaP-NPs) accumulated at the myocardium 60 min after inhalation in a mice model. The NPs functionalized with a non-penetrating mimetic peptide (NPs-MP) were shown to cross the alveolar-capillary barrier in the lung and translocate to the myocardium where the loaded peptide can be release for therapy. Despite the great potential, there are still some limitations to the use of such therapy. One above all, the mechanisms through which the NPs cross alveolar-capillary barrier are still unclear and unlikely to be accepted for clinical translation.

Interestingly, also the exploitation of hybrid materials, i.e., NPs composed by different inorganic core-shell structures, have been reported. Zhang et al. (2019) described the use of silica-coated magnetic nanoparticles for labeling endothelial progenitor cells (EPCs) for their magnetic guidance at the ischemic heart (**Figure 7D**), since EPCs are the most used cells for cell therapy after MI due to their mobilization, homing, and angiogenic effects (Zhang et al., 2019). In this study the authors showed the increased retention of EPCs at the infarcted border zone and the consequent attenuation of myocardial apoptosis associated to improved remodeling and cardiac function. Nevertheless, the evidenced improvements only lasted for a very limited term, claiming for the necessity of multiple administrations of the NP-cell system and possibly limiting the advantages obtainable with a NP-based therapy in comparison with other treatments.

Iron oxide nanoparticles have also been investigated as cardioprotective agents, as shown by Xiong et al. (2015). The authors demonstrated the potential of maghemite NPs for protecting the heart from ischemic damage both *in vivo* and *in vitro*. More specifically, Fe_2O_3 NPs coated with dimercaptosuccinic acid (DMSA) were demonstrated to efficiently inhibit calcium influx, which is responsible for the reactive oxygen species (ROS) production, therefore decreasing the peroxidation injury of membrane lipids. In addition, these NPs were able to increase the level of S-nitrosothiols and then to participate in nitric oxide (NO)-mediated protection against ischemia and reperfusion injury. However, the mechanisms which regulate the crosstalk between ROS, NO and calcium influx pathways and NPs remain unknown and possible long-term side effects of this activity has not been elucidated.

Diagnostic tools were also developed using inorganic nanoparticles. In particular, gold nanoparticles have been demonstrated to be promising tools for computed tomography (CT), an X-ray-based image diagnostic technique able to

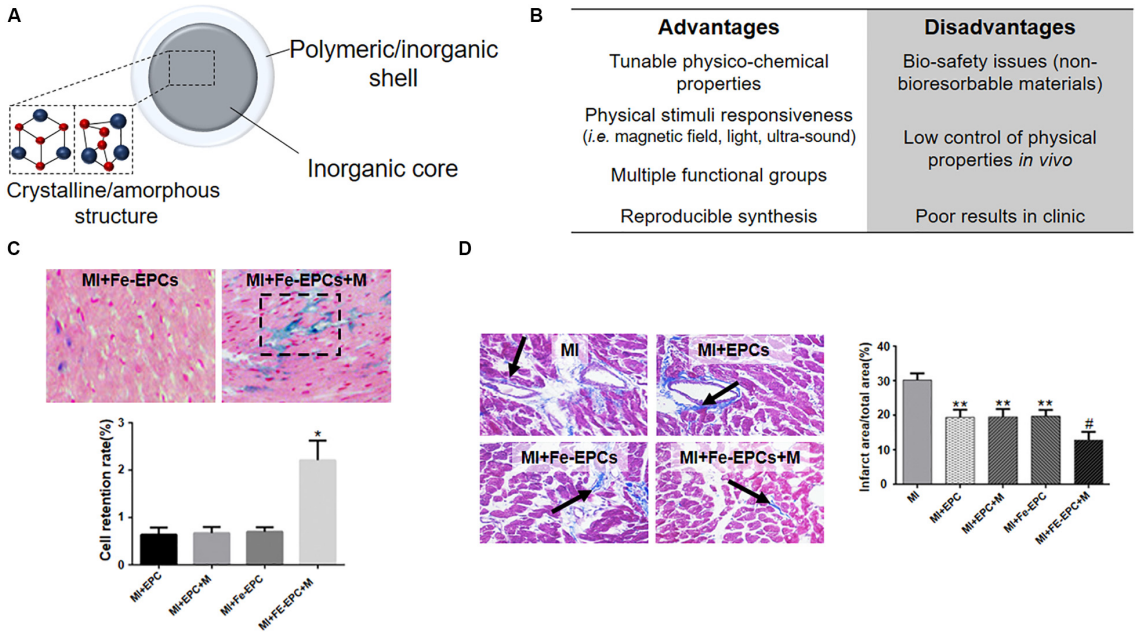

FIGURE 7 | Inorganic NPs for cardiac regeneration. **(A)** Schematic representation of inorganic NPs used for cardiac regeneration. **(B)** Table listing the advantages and disadvantages associated with the use of inorganic nanoparticles. **(C)** Representative hematoxylin/eosin (cell nuclei and cytoplasm) and Prussian blue (iron oxide nanoparticles) images of infarcted myocardium (MI) injected with endothelial progenitor cells loaded with iron oxide nanoparticles (Fe-EPCs) and exposed (+M) or not to external magnetic field. The graph quantifies the retention of EPCs and Fe-EPCs in the presence or not of magnetic field $^{*}p < 0.05$. **(D)** Representative Masson's trichrome staining of infarcted myocardium (MI) injected with endothelial progenitor cells loaded (Fe-EPCs) or not (EPCs) with iron oxide nanoparticles and exposed (+M) or not to external magnetic field. Blue color and black arrow identify the fibrotic area. The graph quantifies the infarction area as obtained by image analysis. $^{*}p < 0.05$ versus the control Sham operated group (not shown), $^{\#}p < 0.05$ versus the other group shown in the graph. Reprinted and adapted from: **(C,D)** (Zhang et al., 2019) with permission of Wiley.

exploit the differences in the absorption from different human tissues in order to produce images of body structures and tissues (Xi et al., 2012). In this context, Kee and Danila (2018) reported the use of gold nanoparticles coated with collagen-binding adhesion protein 35 (CNA35) for CT imaging of infarcted heart at molecular level. Thanks to their ability to target collagen I, abundant at myocardial scar, CNA35-Au NPs were able to enhance the signal from the infarcted site at 6 h after injection. Conversely, no detectable enhancement was noted when non-functionalized AuNPs was injected into rats with or without MI or CNA35-AuNPs in control rats without MI. These results highlighted the preferable use of gold nanoparticles as contrast agents compare to iodinated agents in terms of functionalization and blood circulation time, which ultimately could improve the *in vivo* targeting and detection of infarcted heart. However, some issues such as the relatively high amount of nanoparticles required and the inefficiency to enhance the contrast of the entire infarcted area may wane the application of Au NPs for CT-imaging, as stated by the same authors.

Currently, several clinical trials using inorganic nanoparticles are under investigation for applications in cardiovascular diseases (U.S. National Library of Medicine, 2020b). However, with regard to MI, only magnetic resonance imaging (MRI) applications were assessed, mainly *via* Ferumoxytol – a ultrasmall superparamagnetic iron oxide nanoparticles (USPION) formulation – and all of them were discontinued or did not provide acceptable outcomes (U.S. National Library of Medicine, 2013, 2014a,b). Indeed, as far as we know, the overall application of this kind of nanoparticles for MRI did not obtained the expected results and Ferumoxytol is now only used as iron replacement therapy for deficiency anemia in adult patient with chronic kidney diseases (Bobo et al., 2016).

Consequently, despite the long-dated use of inorganic nanoparticles in nanomedical applications, relatively few examples were reported for cardiac regeneration purposes and efficient clinical translation is still missing.

NANOMEDICINE IN CARDIAC REGENERATION: WHERE ARE WE HEADING TO?

Multi-therapies aiming to combine the regeneration potential of undifferentiated cells, the *in situ* reprogramming of cardiac fibroblasts and the simultaneous release of drugs appear promising, especially when fueled by the potential of cell-based therapies. Indeed, the use of different smart nanomaterials in combination with other technologies may lead to the development of advanced therapeutic strategies, which may strengthen the applicability of nanomedicine in the treatment of cardiac diseases.

As an example, hiPSC-derived cardiomyocytes (hiPSC-CMs) were recently combined with injectable nanostructured hydrogels loaded with erythropoietin (EPO), resulting in reduced cell death and increased remodeling post-MI (Chow et al., 2017). Also, injectable biomaterials have been used as stand-alone scaffolds for promoting endogenous repair or delivering therapeutics such as cells, growth factors or small molecules.

In this context, Nguyen et al. (2015) used matrix metalloproteinase (MMP)-responsive hydrogels that displayed the ability to be retained at the infarcted site upon enzymatically triggered bio-transformation, thus being potentially suitable for the sustained delivery of therapeutic molecules. Another recently developed strategy called *THEREPI* relies on the use of a biocompatible patch, which is placed epicardially at the border zone of the infarcted heart to achieve the sustained delivery of drugs, macromolecules and possibly cells for cardiac therapy (Whyte et al., 2018). Ideally, *THEREPI* can be efficiently used for the *in situ* administration of therapeutic nanoparticles, thus increasing their retention at the diseased site and improving cargo delivery.

In the case of ischemic cardiomyopathies, improved cargo delivery can be potentially obtained by relying on the enhanced permeability and retention effect (EPR). Similar to the blood vessels originated during tumor development, also those formed at the initial stages after MI are typically aberrant, marked by capillary sprouting, excessive vessels branching, abnormal levels of endothelial cell proliferation, distorted and enlarged vessels, resulting in weak and leaky vasculature (Paulis et al., 2012; Lundy et al., 2016). For those reasons, EPR phenomenon has been exploited for promoting the targeting of NPs at the diseased area, limiting their accumulation in healthy tissues (Golombek et al., 2018). However, while EPR occurring at tumor sites has shown poorly reproducible results, thus jeopardizing the applicability of NPs to cancer therapy (Danhier, 2016), the same phenomenon has been proven to be stable and reproducible following MI in the heart (Weis, 2008). Although mature fibrotic scar is known to be poorly vascularized (van der Meel et al., 2017) the exploitation of EPR phenomenon in the heart, soon after infarction, appears as a promising approach to be translated to the clinics in future for MI treatment (Kalyane et al., 2019).

Besides the pursue of innovative materials and strategies for enhancing therapeutics delivery, the investigation of new pathways involved in cardiac homeostasis is of utmost importance, due to the possibility to target their components for ultimately improving therapeutic outcomes, hence delaying or reversing cardiac dysfunction. In particular, the modulation of cardiac metabolism, gene expression, pharmacological therapy and miRNA-mediated regulatory network represent new and appealing opportunities for the treatment of cardiovascular diseases (Rochette et al., 2015).

In this direction, Hippo pathway has emerged as a possible switch in cardiomyocyte proliferation (Torrini et al., 2019), being tightly connected to the onset and progression of cardiomyopathies (Clippinger et al., 2019), as explained above. Its specific manipulation in the contractile figures of the heart may become a novel therapeutic option for treating cardiac diseases. Nevertheless, to the best of our knowledge, the only NP-based formulation for targeting YAP is at present represented by siRNA-lipid nanoparticles for silencing the protein expression in hepatocellular carcinoma cells and promote tumor regression (Fitamant et al., 2015). Therefore, research for developing NPs able to modulate the YAP activity in cardiomyocytes is at its infancy and may revolutionize the treatment of cardiac diseases and the applicability of NPs in the near future.

Furthermore, it is worth to highlight the potential held by gene editing in the restoration of cardiac function. The discovery that the clustered regularly interspaced short palindromic repeats (CRISPR)/CRISPR-associated (Cas) system could be used to introduce sequence-specific dsDNA cleavage in human cells has revolutionized the research worldwide (Jinek et al., 2012). CRISPR is involved in bacteria and archaea's adaptative immune system against viruses and their engineering for biological applications has enabled their application in different areas of investigations (Doudna and Charpentier, 2014). Nanomedicine-related sciences are of course included in this development and different systems have been engineered for carrying CRISPR/CAS9 machinery components and guide the genetic reprogramming inside the cells, based on lipid and inorganic nanoparticles (Lee et al., 2017; Liu et al., 2019). Therefore, although the exploitation of this technique in nanomedicine applied to cardiac regeneration can be attractive in the case of genetically-determined cardiomyopathies, technical challenges connected to its specificity must be considered. Indeed, while few studies have already shown that cardiomyocytes can be edited in the post-natal murine heart by CRISPR/Cas9 system components, the efficiency and safety of this strategy is still far from being characterized (Carroll and Olson, 2017). Moreover, the carriage of multiple components (Cas9 ribonucleoprotein, donor DNA and guide RNA) required for this therapy need complex nanoparticle-based systems, hardly scalable and possibly expensive.

Finally, in developing new therapies it is important to consider more practically physiological-like tissue models, not only for a more effective *in vitro* to *in vivo* transition of pharmacological studies, but also for disease modeling and studying the potential toxicity of nanomaterials. Traditional pre-clinical screenings are either made with monolayer cells on top of two dimensional (2D) and often rigid substrates, or in animal models which may not always reflect the human physiology precisely. Instead, a promising strategy to overcome these limitations involves utilizing organ-on-a-chip technologies, where recent microfluidic advances are combined with complex three-dimensional (3D) cell biology that provides organ-like physiology and pathophysiological cellular and tissue level responses (Ergir et al., 2018; Rothbauer et al., 2019).

CONCLUSION

Despite any progresses based on healthier life styles, cardiovascular diseases remain the major cause of death globally, according to the WHO (World Health Organization, 2019). Therefore, the development of new therapies to induce cardiac protection and repair are required to help reducing

undesirable drugs' side effects and ultimately improving the life quality of the patient.

In this scenario, material scientists need to exploit the physico-chemical properties of nanomaterials to develop suitable nanotools for smart delivery, targeting proteins and pathways involved in cardiomyocytes protection, differentiation and/or proliferation. Notwithstanding the great progresses made in the direction of a clearer comprehension of the nanoparticles behavior in biological environments, major challenges remain (Heath, 2015). The bioavailability, accumulation at the desired site and efficient release of the therapeutic cargo are just a small part of the challenges nanodrugs must face once administered to the body.

The poor understanding of the biological barriers, the misinterpretation of drug delivery concepts, the cost-effectiveness, manufacturing, scaling up, and regulatory issues have affected the clinical translation of nanomedicine so far, as well as its application for cardiac regeneration purposes (van der Meel et al., 2017).

Different NP-based systems were developed aiming to restore heart function. However, it is still difficult to deduct general guidelines describing the type of material, the class of drugs, the targeting strategies that may be more promising for the given purpose. The successes liposomes obtained in clinical outcomes and in different applications, make them suitable candidates for the treatment of cardiac diseases. However, it is undeniable that polymeric materials display higher tunable properties combined to superior capability of accommodating cargos.

Therefore, nanotechnologists, together with cell/molecular biologists and clinicians, have the duty of finding a common ground with pharmaceutical companies in order to bring potential therapeutic nanomedical devices for cardiac regeneration closer to their clinical translation.

AUTHOR CONTRIBUTIONS

MC proposed the subject and conceived the general structure of the review. MC and SF revised the existing literature regarding nanomedicine and the use of nanoparticles for cardiac regeneration. JV revised the literature on miRNAs involved in cardiac development and repair. EE revised the literature on cardiac diseases biology. MC and SF wrote the manuscript. FC and GF revised the text and contributed to the discussion and conclusion.

FUNDING

The work was supported by the European Regional Development Fund-Project MAGNET (No. CZ.02.1.01/0.0/0.0/15_003/0000492) and by the European Union Horizon 2020 Research and Innovation Programme under the Marie Skłodowska-Curie grant agreement no. 690901.

ACKNOWLEDGMENTS

We would like to thank Mrs. Romana Vlckova, Helena Durikova, Sabina Gomelska, Hana Zpevakova, Jana Vasickova, and Jana Bartonova for continuous support.

REFERENCES

Akbarzadeh, A., Rezaei-Sadabady, R., Davaran, S., Joo, S. W., Zarghami, N., Hanifehpour, Y., et al. (2013). Liposome: classification, preparation, and applications. *Nanoscale Res. Lett.* 8:102.

Alfares, A. A., Kelly, M. A., McDermott, G., Funke, B. H., Lebo, M. S., Baxter, S. B., et al. (2015). Results of clinical genetic testing of 2,912 probands with hypertrophic cardiomyopathy: expanded panels offer limited additional sensitivity. *Genet. Med.* 17:880. doi: 10.1038/gim.2014.205

Allijn, I. E., Czarny, B. M. S., Wang, X., Chong, S. Y., Weiler, M., da Silva, A. E., et al. (2017). Liposome encapsulated berberine treatment attenuates cardiac dysfunction after myocardial infarction. *J. Controll. Release* 247, 127–133. doi: 10.1016/j.jconrel.2016.12.042

Amezcua, R., Shirolkar, A., Fraze, C., and Stout, D. A. (2016). Nanomaterials for cardiac myocyte tissue engineering. *Nanomaterials (Basel)* 6:133. doi: 10.3390/nano6070133

Bae, S. J., Ni, L., Osinski, A., Tomchick, D. R., Brautigam, C. A., and Luo, X. (2017). SAV1 promotes Hippo kinase activation through antagonizing the PP2A phosphatase STRIPAK. *Elife* 6:e30278.

Banerjee, M. N., Bolli, R., and Hare, J. M. (2018). Clinical studies of cell therapy in cardiovascular medicine recent developments and future directions. *Circ. Res.* 123, 266–287. doi: 10.1161/circresaha.118.311217

Banik, B. L., Fattahi, P., and Brown, J. L. (2016). Polymeric nanoparticles: the future of nanomedicine. *Wiley Interdiscipl. Rev. Nanomed. Nanobiotechnol.* 8, 271–299. doi: 10.1002/wnan.1364

Bartel, D. P. (2009). MicroRNAs: target recognition and regulatory functions. *Cell* 136, 215–233. doi: 10.1016/j.cell.2009.01.002

Bartunek, J., Terzic, A., Davison, B. A., Filippatos, G. S., Radovanovic, S., Beleslin, B., et al. (2017). Cardiopoietic cell therapy for advanced ischaemic heart failure: results at 39 weeks of the prospective, randomized, double blind, sham-controlled CHART-1 clinical trial. *Eur. Heart J.* 38, 648–660.

Behfar, A., Crespo-Diaz, R., Terzic, A., and Gersh, B. J. (2014). Cell therapy for cardiac repair—lessons from clinical trials. *Nat. Rev. Cardiol.* 11, 232–246. doi: 10.1038/nrcardio.2014.9

Bejerano, T., Etzion, S., Elyagon, S., Etzion, Y., and Cohen, S. (2018). Nanoparticle delivery of miRNA-21 mimic to cardiac macrophages improves myocardial remodeling after myocardial infarction. *Nano Lett.* 18, 5885–5891. doi: 10.1021/acs.nanolett.8b02578

Bergmann, O., Bhardwaj, R. D., Bernard, S., Zdunek, S., Barnabé-Heider, F., Walsh, S., et al. (2009). Evidence for cardiomyocyte renewal in humans. *Science* 324, 98–102. doi: 10.1126/science.1164680

Bobo, D., Robinson, K. J., Islam, J., Thurecht, K. J., and Corrie, S. R. (2016). Nanoparticle-based medicines: a review of FDA-approved materials and clinical trials to date. *Pharm. Res.* 33, 2373–2387. doi: 10.1007/s11095-016-1958-5

Bonauer, A., Carmona, G., Iwasaki, M., Mione, M., Koyanagi, M., Fischer, A., et al. (2009). MicroRNA-92a controls angiogenesis and functional recovery of ischemic tissues in mice. *Science* 324, 1710–1713. doi: 10.1126/science.1174381

Boon, R. A., Iekushi, K., Lechner, S., Seeger, T., Fischer, A., Heydt, S., et al. (2013). MicroRNA-34a regulates cardiac ageing and function. *Nature* 495:107. doi: 10.1038/nature11919

Boon, R. A., and Vickers, K. C. (2013). Intercellular transport of microRNAs. *Arterioscler. Thrombos. Vasc. Biol.* 33, 186–192. doi: 10.1161/atvbaha.112.300139

Boopathy, G. T. K., and Hong, W. (2019). Role of hippo pathway-YAP/TAZ signaling in angiogenesis. *Front. Cell Dev. Biol.* 7:49. doi: 10.3389/fcell.2019.00049

Borow, K. M., Yaroshinsky, A., Greenberg, B., and Perin, E. C. (2019). Phase 3 DREAM-HF trial of mesenchymal precursor cells in chronic heart failure. *Circ. Res.* 125, 265–281. doi: 10.1161/circresaha.119.314951

Botting, K., Wang, K., Padhee, M., McMillen, I., Summers-Pearce, B., Rattanatray, L., et al. (2012). Early origins of heart disease: low birth weight and determinants of cardiomyocyte endowment. *Clin. Exp. Pharmacol. Physiol.* 39, 814–823. doi: 10.1111/j.1440-1681.2011.05649.x

Boverhof, D. R., Bramante, C. M., Butala, J. H., Clancy, S. F., Lafranconi, M., West, J., et al. (2015). Comparative assessment of nanomaterial definitions and safety evaluation considerations. *Regul. Toxicol. Pharmacol.* 73, 137–150. doi: 10.1016/j.yrtph.2015.06.001

Braunwald, E. (2017). Cardiomyopathies. *Circ. Res.* 121, 711–721.

Briceno, N., Schuster, A., Lumley, M., and Perera, D. (2016). Ischaemic cardiomyopathy: pathophysiology, assessment and the role of revascularisation. *Heart* 102, 397–406. doi: 10.1136/heartjnl-2015-308037

Bulbake, U., Doppalapudi, S., Kommineni, N., and Khan, W. (2017). Liposomal formulations in clinical use: an updated review. *Pharmaceutics* 9:12. doi: 10.3390/pharmaceutics9020012

Burke, M. A., Cook, S. A., Seidman, J. G., and Seidman, C. E. (2016). Clinical and mechanistic insights into the genetics of cardiomyopathy. *J. Am. Coll Cardiol.* 68, 2871–2886. doi: 10.1016/j.jacc.2016.08.079

Butler, J., Epstein, S. E., Greene, S. J., Quyyumi, A. A., Sikora, S., Kim, R. J., et al. (2017). Intravenous allogeneic mesenchymal stem cells for nonischemic cardiomyopathy safety and efficacy results of a phase II-A randomized trial. *Circ. Res.* 120, 332–340. doi: 10.1161/circresaha.116.309717

Cahill, T. J., Ashrafian, H., and Watkins, H. (2013). Genetic cardiomyopathies causing heart failure. *ESC Heart Fail* 113, 660–675. doi: 10.1161/circresaha.113.300282

Calcagno, V., Vecchione, R., Quagliariello, V., Marzola, P., Busato, A., Giustetto, P., et al. (2019). Oil core–PEG shell nanocarriers for in vivo MRI imaging. *Adv. Healthc. Mater.* 8:1801313. doi: 10.1002/adhm.201801313

Callis, T. E., Pandya, K., Seok, H. Y., Tang, R.-H., Tatsuguchi, M., Huang, Z.-P., et al. (2009). MicroRNA-208a is a regulator of cardiac hypertrophy and conduction in mice. *J. Clin. Investig.* 119, 2772–2786. doi: 10.1172/jci36154

Cannon, C. P., Blazing, M. A., Giugliano, R. P., McCagg, A., White, J. A., Theroux, P., et al. (2015). Ezetimibe added to statin therapy after acute coronary syndromes. *N. Engl. J. Med.* 372, 2387–2397.

Cao, N., Huang, Y., Zheng, J., Spencer, C. I., Zhang, Y., Fu, J.-D., et al. (2016). Conversion of human fibroblasts into functional cardiomyocytes by small molecules. *Science* 352, 1216–1220. doi: 10.1126/science.aaf1502

Carè, A., Catalucci, D., Felicetti, F., Bonci, D., Addario, A., Gallo, P., et al. (2007). MicroRNA-133 controls cardiac hypertrophy. *Nat. Med.* 13, 613–618.

Carroll, K. J., and Olson, E. N. (2017). Considerations for cardiac CRISPR. *Circ. Res.* 121, 1111–1112. doi: 10.1161/circresaha.117.311974

Chamberlain, K., Riyad, J. M., and Weber, T. (2017). Cardiac gene therapy with adeno-associated virus-based vectors. *Curr. Opin. Cardiol.* 32, 275–282.

Chan, K., Harper, A. R., Ashrafian, H., and Yavari, A. (2018). Cardiomyopathies. *Medicine* 46, 606–617.

Chandarana, M., Curtis, A., and Hoskins, C. J. A. N. (2018). The use of nanotechnology in cardiovascular disease. *Nanomedicine* 8, 1607–1619. doi: 10.1007/s13204-018-0856-z

Chen, C., Seeger, T., Termglinchan, V., and Karakikes, I. (2017). Recent advances in cardiac gene therapy strategies targeting advanced heart failure. *Continu. Cardiol. Educ.* 3, 163–169. doi: 10.1002/cce2.68

Chen, Y.-A., Lu, C.-Y., Cheng, T.-Y., Pan, S.-H., Chen, H.-F., and Chang, N.-S. (2019). WW domain-containing proteins YAP and TAZ in the hippo pathway as key regulators in stemness maintenance, tissue homeostasis, and tumorigenesis. *Front. Oncol.* 9:60. doi: 10.3389/fonc.2019.00060

Cheng, B., Toh, E. K. W., Chen, K.-H., Chang, Y.-C., Hu, C.-M. J., Wu, H.-C., et al. (2016). Biomimicking platelet–monocyte interactions as a novel targeting strategy for heart healing. *Adv. Healthc. Mater.* 5, 2686–2697. doi: 10.1002/adhm.201600724

Chenthamara, D., Subramaniam, S., Ramakrishnan, S. G., Krishnaswamy, S., Essa, M. M., Lin, F.-H., et al. (2019). Therapeutic efficacy of nanoparticles and routes of administration. *Biomater. Res.* 23:20.

Chiavacci, E., Dolfi, L., Verduci, L., Meghini, F., Gestri, G., Evangelista, A. M. M., et al. (2012). MicroRNA 218 mediates the effects of Tbx5a over-expression on zebrafish heart development. *PLoS ONE* 7:e50536. doi: 10.1371/journal.pone.0050536

Chow, A., Stuckey, D. J., Kidher, E., Rocco, M., Jabbour, R. J., Mansfield, C. A., et al. (2017). Human induced pluripotent stem cell-derived cardiomyocyte encapsulating bioactive hydrogels improve rat heart function post myocardial infarction. *Stem Cell Rep.* 9, 1415–1422. doi: 10.1016/j.stemcr.2017.09.003

Cianflone, E., Aquila, I., Scalise, M., Marotta, P., Torella, M., Nadal-Ginard, B., et al. (2018). Molecular basis of functional myogenic specification of Bona Fide multipotent adult cardiac stem cells. *Cell Cycle* 17, 927–946. doi: 10.1080/15384101.2018.1464852

Clippinger, S. R., Cloonan, P. E., Greenberg, L., Ernst, M., Stump, W. T., and Greenberg, M. J. (2019). Disrupted mechanobiology links the molecular and cellular phenotypes in familial dilated cardiomyopathy. *Proc. Natl. Acad. Sci. U.S.A.* 116, 17831–17840. doi: 10.1073/pnas.1910962116

Colegrave, M., and Peckham, M. (2014). Structural implications of β-cardiac myosin heavy chain mutations in human disease. *Anatom. Rec.* 297, 1670–1680. doi: 10.1002/ar.22973

Conde, J., Dias, J. T., Grazú, V., Moros, M., Baptista, P. V., and de la Fuente, J. M. (2014). Revisiting 30 years of biofunctionalization and surface chemistry of inorganic nanoparticles for nanomedicine. *Front. Chem.* 2:48. doi: 10.3389/fchem.2014.00048

Croissant, J. G., Fatieiev, Y., and Khashab, N. M. (2017). Degradability and clearance of silicon, organosilica, silsesquioxane, silica mixed oxide, and mesoporous silica nanoparticles. *Adv. Mater.* 29:1604634. doi: 10.1002/adma.201604634

Danhier, F. (2016). To exploit the tumor microenvironment: since the EPR effect fails in the clinic, what is the future of nanomedicine? *J. Controll. Release* 244, 108–121. doi: 10.1016/j.jconrel.2016.11.015

Davis, M. E., Chen, Z. G., and Shin, D. M. (2008). Nanoparticle therapeutics: an emerging treatment modality for cancer. *Nat. Rev. Drug Discov.* 7, 771–782. doi: 10.1038/nrd2614

Dhulipala, V., Bezwada, P., Gottimukkula, R., and Abboud, J. (2018). Stress-induced cardiomyopathy: as a diagnosis that is time sensitive and anticipative in certain individuals. *Case Rep. Cardiol.* 2018:4.

Dib, N., Khawaja, H., Varner, S., McCarthy, M., and Campbell, A. (2011). Cell therapy for cardiovascular disease: a comparison of methods of delivery. *J. Cardiovasc. Transl. Res.* 4, 177–181. doi: 10.1007/s12265-010-9253-z

Din, F. U., Aman, W., Ullah, I., Qureshi, O. S., Mustapha, O., Shafique, S., et al. (2017). Effective use of nanocarriers as drug delivery systems for the treatment of selected tumors. *Int. J. Nanomed.* 12, 7291–7309. doi: 10.2147/ijn.s146315

Dirkx, E., Gladka, M. M., Philippen, L. E., Armand, A.-S., Kinet, V., Leptidis, S., et al. (2013). Nfat and miR-25 cooperate to reactivate the transcription factor Hand2 in heart failure. *Nat. Cell Biol.* 15:1282. doi: 10.1038/ncb2866

Dolan, E. B., Hofmann, B., de Vaal, M. H., Bellavia, G., Straino, S., Kovarova, L., et al. (2019). A bioresorbable biomaterial carrier and passive stabilization device to improve heart function post-myocardial infarction. *Mater. Sci. Eng. C* 103, 109751. doi: 10.1016/j.msec.2019.109751

Doudna, J. A., and Charpentier, E. (2014). The new frontier of genome engineering with CRISPR-Cas9. *Science* 346:1258096. doi: 10.1126/science.1258096

Dvir, T., Bauer, M., Schroeder, A., Tsui, J. H., Anderson, D. G., Langer, R., et al. (2011). Nanoparticles targeting the infarcted heart. *Nano Lett.* 11, 4411–4414. doi: 10.1021/nl2025882

El-Say, K. M., and El-Sawy, H. S. (2017). Polymeric nanoparticles: promising platform for drug delivery. *Int. J. Pharm.* 528, 675–691. doi: 10.1016/j.ijpharm.2017.06.052

Engel, J. L., and Ardehali, R. (2018). Direct cardiac reprogramming: progress and promise. *Stem Cells Int.* 2018:10.

England, J., Granados-Riveron, J., Polo-Parada, L., Kuriakose, D., Moore, C., Brook, J. D., et al. (2017). Tropomyosin 1: multiple roles in the developing heart and in the formation of congenital heart defects. *J. Mol. Cell Cardiol.* 106, 1–13. doi: 10.1016/j.yjmcc.2017.03.006

Epstein, S. E., Kornowski, R., Fuchs, S., and Dvorak, H. F. (2001). Angiogenesis therapy: amidst the hype, the neglected potential for serious side effects. *Circulation* 104, 115–119. doi: 10.1161/01.cir.104.1.115

Ergir, E., Bachmann, B., Redl, H., Forte, G., and Ertl, P. (2018). Small Force, big impact: next generation organ-on-a-chip systems incorporating biomechanical cues. *Front. Physiol.* 9:1417. doi: 10.3389/fphys.2018.01417

Eschenhagen, T., Bolli, R., Braun, T., Field, L. J., Fleischmann, B. K., Frisén, J., et al. (2017). Cardiomyocyte regeneration. *Cells* 136, 680–686.

Eulalio, A., Mano, M., Ferro, M. D., Zentilin, L., Sinagra, G., Zacchigna, S., et al. (2012). Functional screening identifies miRNAs inducing cardiac regeneration. *Nature* 492:376. doi: 10.1038/nature11739

Fadeel, B. (2019). Hide and seek: nanomaterial interactions with the immune system. *Front. Immunol.* 10:133. doi: 10.3389/fimmu.2019.00133

Feringa, H. H. H., van Waning, V. H., Bax, J. J., Elhendy, A., Boersma, E., Schouten, O., et al. (2006). Cardioprotective medication is associated with improved survival in patients with peripheral arterial disease. *J. Am. College Cardiol.* 47, 1182–1187. doi: 10.1016/j.jacc.2005.09.074

Ferrari, R., Sponchioni, M., Morbidelli, M., and Moscatelli, D. (2018). Polymer nanoparticles for the intravenous delivery of anticancer drugs: the checkpoints on the road from the synthesis to clinical translation. *Nanoscale* 10, 22701–22719. doi: 10.1039/c8nr05933k

Ferreira, M. P. A., Talman, V., Torrieri, G., Liu, D., Marques, G., Moslova, K., et al. (2018). Dual-drug delivery using dextran-functionalized nanoparticles targeting cardiac fibroblasts for cellular reprogramming. *Adv. Funct. Mater.* 28:1705134. doi: 10.1002/adfm.201705134

Fish, J. E., Santoro, M. M., Morton, S. U., Yu, S., Yeh, R.-F., Wythe, J. D., et al. (2008). miR-126 regulates angiogenic signaling and vascular integrity. *Dev. Cell* 15, 272–284. doi: 10.1016/j.devcel.2008.07.008

Fitamant, J., Kottakis, F., Benhamouche, S., Tian, H. S., Chuvin, N., Parachoniak, C. A., et al. (2015). YAP inhibition restores hepatocyte differentiation in advanced HCC, leading to tumor regression. *Cell Rep.* 10, 1692–1707. doi: 10.1016/j.celrep.2015.02.027

Foglia, M. J., and Poss, K. D. (2016). Building and re-building the heart by cardiomyocyte proliferation. *Development* 143, 729–740. doi: 10.1242/dev.132910

Fortuni, B., Inose, T., Ricci, M., Fujita, Y., Van Zundert, I., Masuhara, A., et al. (2019). Polymeric engineering of nanoparticles for highly efficient multifunctional drug delivery systems. *Sci. Rep.* 9:2666.

Fu, Y., Huang, C., Xu, X., Gu, H., Ye, Y., Jiang, C., et al. (2015). Direct reprogramming of mouse fibroblasts into cardiomyocytes with chemical cocktails. *Cell Res.* 25, 1013–1024. doi: 10.1038/cr.2015.99

Fuchs, S. Y., Spiegelman, V. S., and Suresh Kumar, K. G. (2004). The many faces of β-TrCP E3 ubiquitin ligases: reflections in the magic mirror of cancer. *Oncogene* 23, 2028–2036. doi: 10.1038/sj.onc.1207389

Gabisonia, K., Prosdocimo, G., Aquaro, G. D., Carlucci, L., Zentilin, L., Secco, I., et al. (2019). MicroRNA therapy stimulates uncontrolled cardiac repair after myocardial infarction in pigs. *Nature* 569, 418–422. doi: 10.1038/s41586-019-1191-6

Gao, F., Kataoka, M., Liu, N., Liang, T., Huang, Z.-P., Gu, F., et al. (2019). Therapeutic role of miR-19a/19b in cardiac regeneration and protection from myocardial infarction. *Nat. Commun.* 10:1802.

Gavira, J. J., Nasarre, E., Abizanda, G., Perez-Ilzarbe, M., de Martino-Rodriguez, A., de Jalon, J. A. G., et al. (2010). Repeated implantation of skeletal myoblast in a swine model of chronic myocardial infarction. *Eur. Heart J.* 31, 1013–1021. doi: 10.1093/eurheartj/ehp342

Giacca, M., and Zacchigna, S. (2015). Harnsessing the microRNA pathway for cardiac regeneration. *J. Mol. Cell Cardiol.* 89, 68–74. doi: 10.1016/j.yjmcc.2015.09.017

Giner-Casares, J. J., Henriksen-Lacey, M., Coronado-Puchau, M., and Liz-Marzán, L. M. (2016). Inorganic nanoparticles for biomedicine: where materials scientists meet medical research. *Mater. Today* 19, 19–28. doi: 10.1016/j.mattod.2015.07.004

Golombek, S. K., May, J.-N., Theek, B., Appold, L., Drude, N., Kiessling, F., et al. (2018). Tumor targeting via EPR: strategies to enhance patient responses. *Adv. Drug Deliv. Rev.* 130, 17–38. doi: 10.1016/j.addr.2018.07.007

Guo, X., Fan, C., Tian, L., Liu, Y., Wang, H., Zhao, S., et al. (2017). The clinical features, outcomes and genetic characteristics of hypertrophic cardiomyopathy patients with severe right ventricular hypertrophy. *PLoS One.* 12:e0174118. doi: 10.1371/journal.pone.0174118

Harel-Adar, T., Mordechai, T. B., Amsalem, Y., Feinberg, M. S., Leor, J., and Cohen, S. (2011). Modulation of cardiac macrophages by phosphatidylserine-presenting liposomes improves infarct repair. *Proc. Natl. Acad. Sci. U.S.A.* 108, 1827–1832. doi: 10.1073/pnas.1015623108

Hashimoto, H., Olson, E. N., and Bassel-Duby, R. (2018). Therapeutic approaches for cardiac regeneration and repair. *Nat. Rev. Cardiol.* 15, 585–600. doi: 10.1038/s41569-018-0036-6

Hashmi, S., and Ahmad, H. R. (2019). Molecular switch model for cardiomyocyte proliferation. *Cell Regen. (Lond.)* 8, 12–20. doi: 10.1016/j.cr.2018.11.002

Hastings, C. L., Roche, E. T., Ruiz-Hernandez, E., Schenke-Layland, K., Walsh, C. J., and Duffy, G. P. (2015). Drug and cell delivery for cardiac regeneration. *Adv. Drug Deliv. Rev.* 84, 85–106. doi: 10.1016/j.addr.2014.08.006

Heallen, T., Morikawa, Y., Leach, J., Tao, G., Willerson, J. T., Johnson, R. L., et al. (2013). Hippo signaling impedes adult heart regeneration. *Development* 140, 4683–4690. doi: 10.1242/dev.102798

Heallen, T., Zhang, M., Wang, J., Bonilla-Claudio, M., Klysik, E., Johnson, R. L., et al. (2011). Hippo pathway inhibits wnt signaling to restrain cardiomyocyte proliferation and heart size. *Science* 332, 458–461. doi: 10.1126/science.1199010

Heart Protection Study Collaborative and Group. (2002). MRC/BHF heart protection study of cholesterol lowering with simvastatin in 20 536 high-risk individuals: a randomised placebocontrolled trial. *Lancet* 360, 7–22. doi: 10.1016/s0140-6736(02)09327-3

Heath, J. R. (2015). Nanotechnologies for biomedical science and translational medicine. *Proc. Natl. Acad. Sci. U.S.A.* 112, 14436–14443. doi: 10.1073/pnas.1515202112

Henry, T. D., Annex, B. H., McKendall, G. R., Azrin, M. A., Lopez, J. J., Giordano, F. J., et al. (2003). The VIVA trial. *Circulation* 107, 1359–1365.

Henry, T. D., Rocha-Singh, K., Isner, J. M., Kereiakes, D. J., Giordano, F. J., Simons, M., et al. (2001). Intracoronary administration of recombinant human vascular endothelial growth factor to patients with coronary artery disease. *Am. Heart J.* 142, 872–880. doi: 10.1067/mhj.2001.118471

Hershberger, R. E., Hedges, D. J., and Morales, A. (2013). Dilated cardiomyopathy: the complexity of a diverse genetic architecture. *Nat. Rev. Cardiol.* 10, 531–547. doi: 10.1038/nrcardio.2013.105

Hershberger, R. E., Pinto, J. R., Parks, S. B., Kushner, J. D., Li, D., Ludwigsen, S., et al. (2009). Clinical and functional characterization of TNNT2 mutations identified in patients with dilated cardiomyopathy. *Circulation* 2, 306–313. doi: 10.1161/circgenetics.108.846733

Huang, W., Feng, Y., Liang, J., Yu, H., Wang, C., Wang, B., et al. (2018). Loss of microRNA-128 promotes cardiomyocyte proliferation and heart regeneration. *Nat. Commun.* 9:700.

Ieda, M., Fu, J.-D., Delgado-Olguin, P., Vedantham, V., Hayashi, Y., Bruneau, B. G., et al. (2010). Direct reprogramming of fibroblasts into functional cardiomyocytes by defined factors. *Cell* 142, 375–386. doi: 10.1016/j.cell.2010.07.002

Ikeda, S., Mizushima, W., Sciarretta, S., Abdellatif, M., Zhai, P., Mukai, R., et al. (2019). Hippo deficiency leads to cardiac dysfunction accompanied by cardiomyocyte dedifferentiation during pressure overload. *Circ. Res.* 124, 292–305. doi: 10.1161/circresaha.118.314048

Isomi, M., Sadahiro, T., and Ieda, M. (2019). Progress and challenge of cardiac regeneration to treat heart failure. *J. Cardiol.* 73, 97–101. doi: 10.1016/j.jjcc.2018.10.002

Jabir, N. R., Tabrez, S., Ashraf, G. M., Shakil, S., Damanhouri, G. A., and Kamal, M. A. (2012). Nanotechnology-based approaches in anticancer research. *Int. J. Nanomed.* 7, 4391–4408.

Jain, P., Arava, S., Seth, S., Lalwani, S., and Ray, R. (2017). Histological and morphometric analysis of dilated cardiomyopathy with special reference to collagen IV expression. *Ind. J. Pathol. Microbiol.* 60, 481–486.

Jayawardena, T. M., Egemnazarov, B., Finch, E. A., Zhang, L., Payne, J. A., Pandya, K., et al. (2012). MicroRNA-mediated in vitro and in vivo direct reprogramming of cardiac fibroblasts to cardiomyocytes. *Circ. Res.* 110, 1465–1473. doi: 10.1161/circresaha.112.269035

Jinek, M., Chylinski, K., Fonfara, I., Hauer, M., Doudna, J. A., and Charpentier, E. (2012). A programmable dual-RNA–guided DNA endonuclease in adaptive bacterial immunity. *Science* 337, 816–821. doi: 10.1126/science.1225829

Juul, A., Scheike, T., Davidsen, M., Gyllenborg, J., and Jørgensen, T. (2002). Low serum insulin-like growth factor I is associated with increased risk of ischemic heart disease. *Circulation* 106, 939–944. doi: 10.1161/01.cir.0000027563.44593.cc

Kakimoto, Y., Tanaka, M., Kamiguchi, H., Hayashi, H., Ochiai, E., and Osawa, M. (2016). MicroRNA deep sequencing reveals chamber-specific miR-208 family

expression patterns in the human heart. *Int. J. Cardiol.* 211, 43–48. doi: 10.1016/j.ijcard.2016.02.145

Kalepu, S., and Nekkanti, V. (2015). Insoluble drug delivery strategies: review of recent advances and business prospects. *Acta Pharm. Sin. B* 5, 442–453. doi: 10.1016/j.apsb.2015.07.003

Kalyane, D., Raval, N., Maheshwari, R., Tambe, V., Kalia, K., and Tekade, R. K. (2019). Employment of enhanced permeability and retention effect (EPR): nanoparticle-based precision tools for targeting of therapeutic and diagnostic agent in cancer. *Mater. Sci. Eng. C* 98, 1252–1276. doi: 10.1016/j.msec.2019.01.066

Katsuki, S., Matoba, T., Nakashiro, S., Sato, K., Koga J-i, Nakano, K., et al. (2014). Nanoparticle-mediated delivery of pitavastatin inhibits atherosclerotic plaque destabilization/rupture in mice by regulating the recruitment of inflammatory monocytes. *Circulation* 129, 896–906. doi: 10.1161/circulationaha.113.002870

Kee, P. H., and Danila, D. (2018). CT imaging of myocardial scar burden with CNA35-conjugated gold nanoparticles. *Nanomedicine* 14, 1941–1947. doi: 10.1016/j.nano.2018.06.003

Kulaberoglu, Y., Lin, K., Holder, M., Gai, Z., Gomez, M., Assefa Shifa, B., et al. (2017). Stable MOB1 interaction with Hippo/MST is not essential for development and tissue growth control. *Nat. Commun.* 8:695.

Lee, E. J., Baek, M., Gusev, Y., Brackett, D. J., Nuovo, G. J., and Schmittgen, T. D. (2008). Systematic evaluation of microRNA processing patterns in tissues, cell lines, and tumors. *RNA* 14, 35–42. doi: 10.1261/rna.804508

Lee, K., Conboy, M., Park, H. M., Jiang, F., Kim, H. J., Dewitt, M. A., et al. (2017). Nanoparticle delivery of Cas9 ribonucleoprotein and donor DNA in vivo induces homology-directed DNA repair. *Nat. Biomed. Eng.* 1, 889–901. doi: 10.1038/s41551-017-0137-2

Lee, S. W. L., Paoletti, C., Campisi, M., Osaki, T., Adriani, G., Kamm, R. D., et al. (2019). MicroRNA delivery through nanoparticles. *J. Controll. Release* 313, 80–95. doi: 10.1016/j.jconrel.2019.10.007

Liu, J., Chang, J., Jiang, Y., Meng, X., Sun, T., Mao, L., et al. (2019). Fast and efficient CRISPR/Cas9 genome editing in vivo enabled by bioreducible lipid and messenger RNA nanoparticles. *Adv. Mater.* 31:1902575. doi: 10.1002/adma.201902575

Liu, N., Bezprozvannaya, S., Williams, A. H., Qi, X., Richardson, J. A., Bassel-Duby, R., et al. (2008). microRNA-133a regulates cardiomyocyte proliferation and suppresses smooth muscle gene expression in the heart. *Genes Dev.* 22, 3242–3254. doi: 10.1101/gad.1738708

Liu, N., Williams, A. H., Kim, Y., McAnally, J., Bezprozvannaya, S., Sutherland, L. B., et al. (2007). An intragenic MEF2-dependent enhancer directs muscle-specific expression of microRNAs 1 and 133. *Proc. Natl. Acad. Sci. U.S.A.* 104, 20844–20849. doi: 10.1073/pnas.0710558105

Lopes, L. R., Syrris, P., Guttmann, O. P., O'Mahony, C., Tang, H. C., Dalageorgou, C., et al. (2015). Novel genotype-phenotype associations demonstrated by high-throughput sequencing in patients with hypertrophic cardiomyopathy. *Heart* 101, 294–301. doi: 10.1136/heartjnl-2014-306387

Loyer, X., Potteaux, S., Vion, A.-C., Guérin, C. L., Boulkroun, S., Rautou, P.-E., et al. (2014). Inhibition of MicroRNA-92a prevents endothelial dysfunction and atherosclerosis in mice. *Circ. Res.* 114, 434–443. doi: 10.1161/circresaha.114.302213

Lu, L., Liu, M., Sun, R., Zheng, Y., and Zhang, P. J. C. B. (2015). Biophysics. *Myocardial Infarct.* 72, 865–867.

Lundy, D. J., Chen, K.-H., Toh, E. K. W., and Hsieh, P. C. H. (2016). Distribution of systemically administered nanoparticles reveals a size-dependent effect immediately following cardiac ischaemia-reperfusion injury. *Sci. Rep.* 6: 25613.

Madonna, R., Van Laake, L. W., Davidson, S. M., Engel, F. B., Hausenloy, D. J., Lecour, S., et al. (2016). Position paper of the european society of cardiology working group cellular biology of the heart: cell-based therapies for myocardial repair and regeneration in ischemic heart disease and heart failure. *Eur. Heart J.* 37, 1789–1798. doi: 10.1093/eurheartj/ehw113

Marian, A. J., and Braunwald, E. (2017). Hypertrophic cardiomyopathy: genetics, pathogenesis, clinical manifestations, diagnosis, and therapy. *Circ. Res.* 121, 749–770. doi: 10.1161/circresaha.117.311059

Marino, F., Scalise, M., Cianflone, E., Mancuso, T., Aquila, I., Agosti, V., et al. (2019). Role of c-kit in myocardial regeneration and aging. *Front. Endocrinol. (Lausanne)* 10:371. doi: 10.3389/fendo.2019.00371

Martino, F., Perestrelo, A. R., Vinarskɪ, V., Pagliari, S., and Forte, G. (2018). Cellular mechanotransduction: from tension to function. *Front. Physiol.* 9:824. doi: 10.3389/fphys.2018.00824

Mazzarotto, F., Girolami, F., Boschi, B., Barlocco, F., Tomberli, A., Baldini, K., et al. (2019). Defining the diagnostic effectiveness of genes for inclusion in panels: the experience of two decades of genetic testing for hypertrophic cardiomyopathy at a single center. *Genet. Med.* 21, 284–292. doi: 10.1038/s41436-018-0046-0

Menasché, P. (2018). Cell therapy trials for heart regeneration — lessons learned and future directions. *Nat. Rev. Cardiol.* 15, 659–671. doi: 10.1038/s41569-018-0013-0

Meng, Z., Moroishi, T., and Guan, K.-L. (2016). Mechanisms of hippo pathway regulation. *Genes Dev.* 30, 1–17. doi: 10.1101/gad.274027.115

Miragoli, M., Ceriotti, P., Iafisco, M., Vacchiano, M., Salvarani, N., Alogna, A., et al. (2018). Inhalation of peptide-loaded nanoparticles improves heart failure. *Sci. Transl. Med.* 10:eaan6205. doi: 10.1126/scitranslmed.aan6205

Mitrut, R., Stepan, A. E., and Pirici, D. (2018). Histopathological aspects of the myocardium in dilated cardiomyopathy. *Curr. Health Sci. J.* 44, 243–249. doi: 10.12865/CHSJ.44.03.07

Miyagawa, S., Domae, K., Yoshikawa, Y., Fukushima, S., Nakamura, T., Saito, A., et al. (2017). Phase I clinical trial of autologous stem cell-sheet transplantation therapy for treating cardiomyopathy. *J. Am. Heart Assoc.* 6:e003918.

Miyasaka, K. Y., Kida, Y. S., Banjo, T., Ueki, Y., Nagayama, K., Matsumoto, T., et al. (2011). Heartbeat regulates cardiogenesis by suppressing retinoic acid signaling via expression of miR-143. *Mech. Dev.* 128, 18–28. doi: 10.1016/j.mod.2010.09.002

Mohamed, T. M. A., Ang, Y. S., Radzinsky, E., Zhou, P., Huang, Y., Elfenbein, A., et al. (2018). Regulation of cell cycle to stimulate adult cardiomyocyte proliferation and cardiac regeneration. *Cell* 173, 104–116.

Morton, S. U., Scherz, P. J., Cordes, K. R., Ivey, K. N., Stainier, D. Y. R., and Srivastava, D. (2008). microRNA-138 modulates cardiac patterning during embryonic development. *Proc. Natl. Acad. Sci. U.S.A.* 105, 17830–17835. doi: 10.1073/pnas.0804673105

Muchtar, E., Blauwet, L. A., and Gertz, M. A. (2017). Restrictive cardiomyopathy: genetics, pathogenesis, clinical manifestations, diagnosis, and therapy. *Circ. Res.* 121, 819–837. doi: 10.1161/circresaha.117.310982

Müller, P., Lemcke, H., and David, R. (2018). Stem cell therapy in heart diseases – Cell types, mechanisms and improvement strategies. *Cell. Physiol. Biochem.* 48, 2607–2655. doi: 10.1159/000492704

Nam, Y.-J., Song, K., Luo, X., Daniel, E., Lambeth, K., West, K., et al. (2013). Reprogramming of human fibroblasts toward a cardiac fate. *Proc. Natl. Acad. Sci. U.S.A.* 110, 5588–5593. doi: 10.1073/pnas.1301019110

Nardone, G., Oliver-De, La Cruz, J., Vrbsky, J., Martini, C., Pribyl, J., et al. (2017). YAP regulates cell mechanics by controlling focal adhesion assembly. *Nat. Commun.* 8:15321.

Nef, H. M., Möllmann, H., Akashi, Y. J., and Hamm, C. W. (2010). Mechanisms of stress (Takotsubo) cardiomyopathy. *Nat. Rev. Cardiol.* 7, 187–193.

Nguyen, M. M., Carlini, A. S., Chien, M.-P., Sonnenberg, S., Luo, C., Braden, R. L., et al. (2015). Enzyme-responsive nanoparticles for targeted accumulation and prolonged retention in heart tissue after myocardial infarction. *Adv. Mater.* 27, 5547–5552. doi: 10.1002/adma.201502003

Odashima, M., Usui, S., Takagi, H., Hong, C., Liu, J., Yokota, M., et al. (2007). Inhibition of endogenous Mst1 prevents apoptosis and cardiac dysfunction without affecting cardiac hypertrophy after myocardial infarction. *Circ. Res.* 100, 1344–1352. doi: 10.1161/01.res.0000265846.23485.7a

Oduk, Y., Zhu, W., Kannappan, R., Zhao, M., Borovjagin, A. V., Oparil, S., et al. (2018). VEGF nanoparticles repair the heart after myocardial infarction. *Am. J. Physiol. Heart Circ. Physiol.* 314, H278–H284.

Patil, Y., and Panyam, J. (2009). Polymeric nanoparticles for siRNA delivery and gene silencing. *Int. J. Pharm.* 367, 195–203. doi: 10.1016/j.ijpharm.2008.09.039

Patra, J. K., Das, G., Fraceto, L. F., Campos, E. V. R., Rodriguez-Torres, MdP, et al. (2018). Nano based drug delivery systems: recent developments and future prospects. *J. Nanobiotechnol.* 16:71.

Paulis, L. E., Geelen, T., Kuhlmann, M. T., Coolen, B. F., Schäfers, M., Nicolay, K., et al. (2012). Distribution of lipid-based nanoparticles to infarcted myocardium with potential application for MRI-monitored drug delivery. *J. Controll. Release* 162, 276–285. doi: 10.1016/j.jconrel.2012.06.035

Pelaz, B., Alexiou, C., Alvarez-Puebla, R. A., Alves, F., Andrews, A. M., Ashraf, S., et al. (2017). Diverse applications of nanomedicine. *ACS Nano* 11, 2313–2381.

Penny, W. F., and Hammond, H. K. (2017). Randomized clinical trials of gene transfer for heart failure with reduced ejection fraction. *Hum. Gene Ther.* 28, 378–384. doi: 10.1089/hum.2016.166

Plouffe, S. W., Meng, Z., Lin, K. C., Lin, B., Hong, A. W., Chun, J. V., et al. (2016). Characterization of hippo pathway components by gene inactivation. *Mol. Cell* 64, 993–1008. doi: 10.1016/j.molcel.2016.10.034

Pollack, A., Kontorovich, A. R., Fuster, V., and Dec, G. W. (2015). Viral myocarditis—diagnosis, treatment options, and current controversies. *Nat. Rev. Cardiol.* 12, 670–680. doi: 10.1038/nrcardio.2015.108

Popara, J., Accomasso, L., Vitale, E., Gallina, C., Roggio, D., Iannuzzi, A., et al. (2018). Silica nanoparticles actively engage with mesenchymal stem cells in improving acute functional cardiac integration. *Nanomedicine* 13, 1121–1138. doi: 10.2217/nnm-2017-0309

Porrello, E. R., Johnson, B. A., Aurora, A. B., Simpson, E., Nam, Y.-J., Matkovich, S. J., et al. (2011a). miR-15 Family regulates postnatal mitotic arrest of cardiomyocytes. *Circ. Res.* 109, 670–679. doi: 10.1161/circresaha.111.248880

Porrello, E. R., Mahmoud, A. I., Simpson, E., Hill, J. A., Richardson, J. A., Olson, E. N., et al. (2011b). Transient regenerative potential of the neonatal mouse heart. *Science* 331, 1078–1080. doi: 10.1126/science.1200708

Psaltis, P. J., Carbone, A., Nelson, A. J., Lau, D. H., Jantzen, T., Manavis, J., et al. (2010). Reparative effects of allogeneic mesenchymal precursor cells delivered transendocardially in experimental nonischemic cardiomyopathy. *JACC* 3, 974–983. doi: 10.1016/j.jcin.2010.05.016

Qin, F., Tian, J., Zhou, D., and Chen, L. (2013). Mst1 and Mst2 kinases: regulations and diseases. *Cell Biosci.* 3:31. doi: 10.1186/2045-3701-3-31

Qin, X., Chen, H., Yang, H., Wu, H., Zhao, X., Wang, H., et al. (2018). Photoacoustic imaging of embryonic stem cell-derived cardiomyocytes in living hearts with ultrasensitive semiconducting polymer nanoparticles. *Adv. Funct. Mater.* 28:1704939. doi: 10.1002/adfm.201704939

Raso, A., and Dirkx, E. (2017). Cardiac regenerative medicine: at the crossroad of microRNA function and biotechnology. *Non-coding RNA Res.* 2, 27–37. doi: 10.1016/j.ncrna.2017.03.001

Raval, A. N., Cook, T. D., Duckers, H. J., Johnston, P. V., Traverse, J. H., Abraham, W. T., et al. (2018). The CardiAMP heart failure trial: a randomized controlled pivotal trial of high-dose autologous bone marrow mononuclear cells using the CardiAMP cell therapy system in patients with post–myocardial infarction heart failure: trial rationale and study design. *Am. Heart J.* 201, 141–148. doi: 10.1016/j.ahj.2018.03.016

Rebouças, JdS, Santos-Magalhães, N. S., and Formiga, F. R. (2016). Cardiac regeneration using growth factors: advances and challenges. *Arq. Bras. Cardiol.* 107, 271–275.

Rikhtegar, R., Pezeshkian, M., Dolati, S., Safaie, N., Afrasiabi Rad, A., Mahdipour, M., et al. (2019). Stem cells as therapy for heart disease: iPSCs, ESCs, CSCs, and skeletal myoblasts. *Biomed. Pharmacother.* 109, 304–313. doi: 10.1016/j.biopha.2018.10.065

Rochette, L., Zeller, M., Cottin, Y., and Vergely, C. (2015). Growth and differentiation factor 11 (GDF11): functions in the regulation of erythropoiesis and cardiac regeneration. *Pharmacol. Therapeut.* 156, 26–33. doi: 10.1016/j.pharmthera.2015.10.006

Rothbauer, M., Rosser, J. M., Zirath, H., and Ertl, P. (2019). Tomorrow today: organ-on-a-chip advances towards clinically relevant pharmaceutical and medical in vitro models. *Curr. Opin. Biotechnol.* 55, 81–86. doi: 10.1016/j.copbio.2018.08.009

Sanganalmath, S. K., and Bolli, R. (2013). Cell therapy for heart failure. *Curr. Cardiol. Rev.* 113, 810–834.

Schafer, S., de Marvao, A., Adami, E., Fiedler, L. R., Ng, B., Khin, E., et al. (2016). Titin-truncating variants affect heart function in disease cohorts and the general population. *Nat. Genet.* 49:46. doi: 10.1038/ng.3719

Schultheiss, H.-P., Fairweather, D., Caforio, A. L. P., Escher, F., Hershberger, R. E., Lipshultz, S. E., et al. (2019). Dilated cardiomyopathy. *Nat. Rev. Dis. Primers* 5:32.

Scott, R. C., Rosano, J. M., Ivanov, Z., Wang, B., Chong, P. L.-G., Issekutz, A. C., et al. (2009). Targeting VEGF-encapsulated immunoliposomes to MI heart improves vascularity and cardiac function. *FASEB J.* 23, 3361–3367. doi: 10.1096/fj.08-127373

Senyo, S. E., Steinhauser, M. L., Pizzimenti, C. L., Yang, V. K., Cai, L., Wang, M., et al. (2013). Mammalian heart renewal by pre-existing cardiomyocytes. *Nature* 493, 433–436. doi: 10.1038/nature11682

Sercombe, L., Veerati, T., Moheimani, F., Wu, S. Y., Sood, A. K., and Hua, S. (2015). Advances and challenges of liposome assisted drug delivery. *Front. Pharmacol.* 6:286. doi: 10.3389/fphar.2015.00286

Simons, M., Annex, B. H., Laham, R. J., Kleiman, N., Henry, T., Dauerman, H., et al. (2002). Pharmacological treatment of coronary artery disease with recombinant fibroblast growth factor-2. 105, 788–793. doi: 10.1161/hc0802.104407

Sioud, M. (2005). On the delivery of small interfering RNAs into mammalian cells. *Expert Opin. Drug Deliv.* 2, 639–651. doi: 10.1517/17425247.2.4.639

Sluijter, J. P. G., Mil, A. V., Vliet, P. V., and Metz, C. H. G., (2010). MicroRNA-1 and -499 regulate differentiation and proliferation in human-derived cardiomyocyte progenitor cells. *Arteriosclerosis Thrombosis Vasc. Biol.* 30, 859–868. doi: 10.1161/atvbaha.109.197434

Small, E. M., O'Rourke, J. R., Moresi, V., Sutherland, L. B., McAnally, J., Gerard, R. D., et al. (2010). Regulation of PI3-kinase/Akt signaling by muscle-enriched microRNA-486. *Proc. Natl. Acad. Sci. U.S.A.* 107, 4218–4223. doi: 10.1073/pnas.1000300107

Smith, A. J., Lewis, F. C., Aquila, I., Waring, C. D., Nocera, A., Agosti, V., et al. (2014). Isolation and characterization of resident endogenous c-Kit+ cardiac stem cells from the adult mouse and rat heart. *Nat. Protoc.* 9, 1662–1681. doi: 10.1038/nprot.2014.113

Song, K., Nam, Y.-J., Luo, X., Qi, X., Tan, W., Huang, G. N., et al. (2012). Heart repair by reprogramming non-myocytes with cardiac transcription factors. *Nature* 485, 599–604. doi: 10.1038/nature11139

Taimeh, Z., Loughran, J., Birks, E. J., and Bolli, R. (2013). Vascular endothelial growth factor in heart failure. *Nat. Rev. Cardiol.* 10, 519–530.

Tanai, E., and Frantz, S. (2015). Pathophysiology of heart failure. *Compr. Physiol.* 6, 187–214.

Tang, F., Gao, R., Jeevan-Raj, B., Wyss, C. B., Kalathur, R. K. R., Piscuoglio, S., et al. (2019). LATS1 but not LATS2 represses autophagy by a kinase-independent scaffold function. *Nat. Commun.* 10:5755.

Tao, G., Kahr, P. C., Morikawa, Y., Zhang, M., Rahmani, M., Heallen, T. R., et al. (2016). Pitx2 promotes heart repair by activating the antioxidant response after cardiac injury. *Nature* 534:119. doi: 10.1038/nature17959

thebiogrid.org. (2019). Available from: https://thebiogrid.org/115684.

Thum, T., Gross, C., Fiedler, J., Fischer, T., Kissler, S., Bussen, M., et al. (2008). MicroRNA-21 contributes to myocardial disease by stimulating MAP kinase signalling in fibroblasts. *Nature* 456, 980–984. doi: 10.1038/nature07511

Tian, Y., Liu, Y., Wang, T., Zhou, N., Kong, J., Chen, L., et al. (2015). A microRNA-Hippo pathway that promotes cardiomyocyte proliferation and cardiac regeneration in mice. *Sci. Transl. Med.* 7, ra38–ra38.

Torrini, C., Cubero, R. J., Dirkx, E., Braga, L., Ali, H., Prosdocimo, G., et al. (2019). Common regulatory pathways mediate activity of microRNAs inducing cardiomyocyte proliferation. *Cell Rep.* 27, 2759–2771.e5. doi: 10.1016/j.celrep.2019.05.005

Traverse, J. H., Henry, T. D., Dib, N., Patel, A. N., Pepine, C., Schaer, G. L., et al. (2019). First-in-man study of a cardiac extracellular matrix hydrogel in early and late myocardial infarction patients. *JACC* 4, 659–669. doi: 10.1016/j.jacbts.2019.07.012

Troncoso, R., Ibarra, C., Vicencio, J. M., Jaimovich, E., and Lavandero, S. (2014). New insights into IGF-1 signaling in the heart. *Trends Endocrinol. Metabol.* 25, 128–137. doi: 10.1016/j.tem.2013.12.002

Tzahor, E., and Poss, K. D. (2017). Cardiac regeneration strategies: staying young at heart. *Science* 356, 1035–1039. doi: 10.1126/science.aam5894

U.S. Department of Health & Human Services (2013). *Health Topic: Cardiomyopathy*. Available online at: https://www.nhlbi.nih.gov/health-topics/cardiomyopathy

U.S. National Library of Medicine (2013). *IRon Nanoparticle Enhanced MRI in the Assessment of Myocardial infarctioN (IRNMAN)*. Available online at: ClinicalTrials.govUNLom

U.S. National Library of Medicine (2014a). *Ferumoxytol for Magnetic Resonance Imaging of Myocardial Infarction*. Available online at: ClinicalTrials.govUNLom

U.S. National Library of Medicine (2014b). *Inflammatory Cell Trafficking After Myocardial Infarction*. Available online at: ClinicalTrials.govUNLom

U.S. National Library of Medicine (2019a). A Study of VentriGel in Post-MI Patient. Available online at: ClinicalTrials.govUNLom

U.S. National Library of Medicine (2019b). *The Transendocardial Autologous Cells (hMSC) or (hMSC) and (hCSC) in Ischemic Heart Failure Trial (TAC-HFT-II)*. Available online at: ClinicalTrials.gov UNLom

U.S. National Library of Medicine (2019c). *Bone Marrow Derived Mesenchymal Stem Cells in Improving Heart Function in Patients With Heart Failure Caused by Anthracyclines*. Available online at: ClinicalTrials.gov UNLom

U.S. National Library of Medicine (2019d). *CardiAMP*™ *Heart Failure Trial*. Available online at: ClinicalTrials.gov UNLoM

U.S. National Library of Medicine (2020a). *Efficacy and Safety of Allogeneic Mesenchymal Precursor Cells (Rexlemestrocel-L) for the Treatment of Heart Failure (DREAM HF-1)*. Available online at: ClinicalTrials.gov UNLom

U.S. National Library of Medicine (2020b). *Nanoparticles in Heart Diseases: Overview on the Existing Clinical Trials*. Available online at: https://clinicaltrials.gov/ct2/results?term=nanoparticles&cond=Heart+Diseases&draw=2&rank=7#rowId6. ClinicalTrials.govUNLoM

U.S. National Library of Medicine (2020c). *VEGF in Heart Diseases: Overview on the Existing Clinical Trials*. Available online at: https://clinicaltrials.gov/ct2/results?cond=heart&term=VEGF. ClinicalTrials.govUNLoM

Unger, E. F., Goncalves, L., Epstein, S. E., Chew, E. Y., Trapnell, C. B., Cannon, R. O. III, et al. (2000). Effects of a single intracoronary injection of basic fibroblast growth factor in stable angina pectoris. *Am. J. Cardiol.* 85, 1414–1419. doi: 10.1016/s0002-9149(00)00787-6

Valadi, H., Ekström, K., Bossios, A., Sjöstrand, M., Lee, J. J., and Lötvall, J. O. (2007). Exosome-mediated transfer of mRNAs and microRNAs is a novel mechanism of genetic exchange between cells. *Nat. Cell Biol.* 9, 654–659. doi: 10.1038/ncb1596

van der Meel, R., Lammers, T., and Hennink, W. E. (2017). Cancer nanomedicines: oversold or underappreciated? *Expert Opin. Drug Deliv.* 14, 1–5. doi: 10.1080/17425247.2017.1262346

van Rooij, E., Sutherland, L. B., Liu, N., Williams, A. H., McAnally, J., Gerard, R. D., et al. (2006). A signature pattern of stress-responsive microRNAs that can evoke cardiac hypertrophy and heart failure. *Proc. Natl. Acad. Sci. U.S.A.* 103, 18255–18260. doi: 10.1073/pnas.0608791103

Varelas, X. (2014). The Hippo pathway effectors TAZ and YAP in development, homeostasis and disease. *Development* 141, 1614–1626. doi: 10.1242/dev.102376

Velzen, HGv, Schinkel, A. F. L., Baart, S. J., Oldenburg, R. A., Frohn-Mulder, I. M. E., et al. (2018). Outcomes of contemporary family screening in hypertrophic cardiomyopathy. *Circulation* 11:e001896.

Vicinanza, C., Aquila, I., Scalise, M., Cristiano, F., Marino, F., Cianflone, E., et al. (2017). Adult cardiac stem cells are multipotent and robustly myogenic: c-kit expression is necessary but not sufficient for their identification. *Cell Death Differ.* 24, 2101–2116. doi: 10.1038/cdd.2017.130

Vikhorev, P. G., and Vikhoreva, N. N. (2018). Cardiomyopathies and related changes in contractility of human heart muscle. *Int. J. Mol. Sci.* 19:E2234.

von Gise, A., Lin, Z., Schlegelmilch, K., Honor, L. B., Pan, G. M., Buck, J. N., et al. (2012). YAP1, the nuclear target of Hippo signaling, stimulates heart growth through cardiomyocyte proliferation but not hypertrophy. *Proc. Natl. Acad. Sci. U.S.A.* 109, 2394–2399. doi: 10.1073/pnas.1116136109

Wada, R., Muraoka, N., Inagawa, K., Yamakawa, H., Miyamoto, K., Sadahiro, T., et al. (2013). Induction of human cardiomyocyte-like cells from fibroblasts by defined factors. *Proc. Natl. Acad. Sci. U.S.A.* 110, 12667–12672.

Wahlquist, C., Jeong, D., Rojas-Muñoz, A., Kho, C., Lee, A., Mitsuyama, S., et al. (2014). Inhibition of miR-25 improves cardiac contractility in the failing heart. *Nature* 508:531. doi: 10.1038/nature13073

Wang, H. P., Zhang, W. H., Wang, X. F., Zhu, J., Zheng, Y. Q., Xia, Q., et al. (2014). Exposure to AT1 receptor autoantibodies during pregnancy increases susceptibility of the maternal heart to postpartum ischemia-reperfusion injury in rats. *Int. J. Mol. Sci.* 15, 11495–11509. doi: 10.3390/ijms150711495

Wang, J., Liu, S., Heallen, T., and Martin, J. F. (2018). The Hippo pathway in the heart: pivotal roles in development, disease, and regeneration. *Nat. Rev. Cardiol.* 15, 672–684. doi: 10.1038/s41569-018-0063-3

Wang, L. V., and Hu, S. (2012). Photoacoustic tomography: in vivo imaging from organelles to organs. *Science* 335, 1458–1462. doi: 10.1126/science.1216210

Watkins, H., Ashrafian, H., and Redwood, C. (2011). Inherited cardiomyopathies. *Circ. J.* 364, 1643–1656.

Watt, K. I., Turner, B. J., Hagg, A., Zhang, X., Davey, J. R., Qian, H., et al. (2015). The Hippo pathway effector YAP is a critical regulator of skeletal muscle fibre size. *Nat. Commun.* 6:6048.

Weis, S. M. (2008). Vascular permeability in cardiovascular disease and cancer. *Curr. Opin. Hematol.* 15, 243–249. doi: 10.1097/moh.0b013e3282f97d86

Whyte, W., Roche, E. T., Varela, C. E., Mendez, K., Islam, S., O'Neill, H., et al. (2018). Sustained release of targeted cardiac therapy with a replenishable implanted epicardial reservoir. *Nat. Biomed. Eng.* 2, 416–428. doi: 10.1038/s41551-018-0247-5

World Health Organization (2019). *Cardiovascular Diseases (CVDs)*. Available online at: https://www.who.int/news-room/fact-sheets/detail/cardiovascular-diseases.

Xi, D., Dong, S., Meng, X., Lu, Q., Meng, L., and Ye, J. (2012). Gold nanoparticles as computerized tomography (CT) contrast agents. *RSC Adv.* 2, 12515–12524.

Xiong, F., Wang, H., Feng, Y., Li, Y., Hua, X., Pang, X., et al. (2015). Cardioprotective activity of iron oxide nanoparticles. *Sci. Rep.* 5: 8579.

Xu, Z., Zhu, W., Wang, C., Huang, L., Zhou, Q., Hu, J., et al. (2017). Genotype-phenotype relationship in patients with arrhythmogenic right ventricular cardiomyopathy caused by desmosomal gene mutations: a systematic review and meta-analysis. *Sci. Rep.* 7:41387.

Xue, X., Shi, X., Dong, H., You, S., Cao, H., Wang, K., et al. (2018). Delivery of microRNA-1 inhibitor by dendrimer-based nanovector: an early targeting therapy for myocardial infarction in mice. *Nanomedicine* 14, 619–631. doi: 10.1016/j.nano.2017.12.004

Yang, H., Qin, X., Wang, H., Zhao, X., Liu, Y., Wo, H.-T., et al. (2019). An in vivo miRNA delivery system for restoring infarcted myocardium. *ACS Nano* 13, 9880–9894. doi: 10.1021/acsnano.9b03343

Yildirimer, L., Thanh, N. T. K., Loizidou, M., and Seifalian, A. M. (2011). Toxicology and clinical potential of nanoparticles. *Nano Today* 6, 585–607. doi: 10.1016/j.nantod.2011.10.001

Yokoyama, R., Ii, M., Masuda, M., Tabata, Y., Hoshiga, M., Ishizaka, N., et al. (2019). Cardiac regeneration by statin-polymer nanoparticle-loaded adipose-derived stem cell therapy in myocardial infarction. *Stem Cells Transl. Med.* 8, 1055–1067. doi: 10.1002/sctm.18-0244

Yu, M., Wu, J., Shi, J., and Farokhzad, O. C. (2016). Nanotechnology for protein delivery: overview and perspectives. *J. Control. Release* 240, 24–37. doi: 10.1016/j.jconrel.2015.10.012

Zeng, X.-H., Zeng, X.-J., and Li, Y.-Y. (2003). Efficacy and safety of berberine for congestive heart failure secondary to ischemic or idiopathic dilated cardiomyopathy. *Am. J. Cardiol.* 92, 173–176. doi: 10.1016/s0002-9149(03)00533-2

Zhang, B.-F., Jiang, H., Chen, J., Hu, Q., Yang, S., and Liu, X.-P. (2019). Silica-coated magnetic nanoparticles labeled endothelial progenitor cells alleviate ischemic myocardial injury and improve long-term cardiac function with magnetic field guidance in rats with myocardial infarction. *J. Cell. Physiol.* 234, 18544–18559. doi: 10.1002/jcp.28492

Zhang, L., Gu, F., Chan, J., Wang, A., Langer, R., and Farokhzad, O. (2008). Nanoparticles in medicine: therapeutic applications and developments. *Clin. Pharmacol. Ther.* 83, 761–769. doi: 10.1038/sj.clpt.6100400

Zhang, S., Zhao, B., Jiang, H., Wang, B., and Ma, B. (2007). Cationic lipids and polymers mediated vectors for delivery of siRNA. *J. Controll. Release* 123, 1–10. doi: 10.1016/j.jconrel.2007.07.016

Zhao, H., Lin, Z. Y., Yildirimer, L., Dhinakar, A., Zhao, X., and Wu, J. (2016). Polymer-based nanoparticles for protein delivery: design, strategies and applications. *J. Mater. Chem. B* 4, 4060–4071. doi: 10.1039/c6tb00308g

Zhao, Y., Ransom, J. F., Li, A., Vedantham, V., von Drehle, M., Muth, A. N., et al. (2007). Dysregulation of cardiogenesis, cardiac conduction, and cell cycle in mice lacking miRNA-1-2. *Cell* 129, 303–317. doi: 10.1016/j.cell.2007.03.030

Zhao, Y., Samal, E., and Srivastava, D. (2005). Serum response factor regulates a muscle-specific microRNA that targets Hand2 during cardiogenesis. *Nature* 436, 214–220. doi: 10.1038/nature03817

Conflict of Interest: The authors declare that the research was conducted in the absence of any commercial or financial relationships that could be construed as a potential conflict of interest.

Copyright © 2020 Cassani, Fernandes, Vrbsky, Ergir, Cavalieri and Forte. This is an open-access article distributed under the terms of the Creative Commons Attribution License (CC BY). The use, distribution or reproduction in other forums is permitted, provided the original author(s) and the copyright owner(s) are credited and that the original publication in this journal is cited, in accordance with accepted academic practice. No use, distribution or reproduction is permitted which does not comply with these terms.

frontiers in Bioengineering and Biotechnology

REVIEW
published: 08 May 2020
doi: 10.3389/fbioe.2020.00414

Alginate Formulations: Current Developments in the Race for Hydrogel-Based Cardiac Regeneration

Giada Cattelan[1]†, Amparo Guerrero Gerbolés[1,2]*†, Ruben Foresti[2,3], Peter P. Pramstaller[1], Alessandra Rossini[1], Michele Miragoli[2,3] and Cristina Caffarra Malvezzi[2]**

[1] Institute for Biomedicine, Eurac Research, Affiliated Institute of the University of Lübeck, Bolzano, Italy, [2] Department of Medicine and Surgery, University of Parma, Parma, Italy, [3] CERT, Center of Excellence for Toxicological Research, University of Parma, Parma, Italy

OPEN ACCESS

Edited by:
Valeria Chiono,
Polytechnic University of Turin, Italy

Reviewed by:
Liliana Liverani,
University of Erlangen Nuremberg, Germany
Jochen Salber,
University Hospital Bochum GmbH, Germany

***Correspondence:**
Giada Cattelan
Giada.Cattelan@eurac.edu
Amparo Guerrero Gerbolés
amparo.guerrerogerboles@unipr.it
Cristina Caffarra Malvezzi
cristina.caffarra@unipr.it

† These authors have contributed equally to this work

Specialty section:
This article was submitted to Biomaterials, a section of the journal Frontiers in Bioengineering and Biotechnology

Received: 07 January 2020
Accepted: 14 April 2020
Published: 08 May 2020

Citation:
Cattelan G, Guerrero Gerbolés A, Foresti R, Pramstaller PP, Rossini A, Miragoli M and Caffarra Malvezzi C (2020) Alginate Formulations: Current Developments in the Race for Hydrogel-Based Cardiac Regeneration. Front. Bioeng. Biotechnol. 8:414. doi: 10.3389/fbioe.2020.00414

Cardiovascular diseases, including myocardial infarction (MI), represent the main worldwide cause of mortality and morbidity. In this scenario, to contrast the irreversible damages following MI, cardiac regeneration has emerged as a novel and promising solution for *in situ* cellular regeneration, preserving cell behavior and tissue cytoarchitecture. Among the huge variety of natural, synthetic, and hybrid compounds used for tissue regeneration, alginate emerged as a good candidate for cellular preservation and delivery, becoming one of the first biomaterial tested in pre-clinical research and clinical trials concerning cardiovascular diseases. Although promising results have been obtained, recellularization and revascularization of the infarcted area present still major limitations. Therefore, the demand is rising for alginate functionalization and its combination with molecules, factors, and drugs capable to boost the regenerative potential of the cardiac tissue. The focus of this review is to elucidate the promising properties of alginate and to highlight its benefits in clinical trials in relation to cardiac regeneration. The definition of hydrogels, the alginate characteristics, and recent biomedical applications are herewith described. Afterward, the review examines in depth the ongoing developments to refine the material relevance in cardiac recovery and regeneration after MI and presents current clinical trials based on alginate.

Keywords: alginate, hydrogels, biomaterials, heart failure, cardiac regeneration, clinical trials

Abbreviations: ADSCs, adipose derived stem cells; CMs, cardiomyocytes; CVDs, cardiovascular diseases; ECs, endothelial cells; ECM, extracellular matrix; EDD, end-diastolic dimension; EF, ejection fraction; ESD, end-systolic dimension; FDA, Food and Drugs Administration; G, 1,4 α-L-guluronic acid; GRAS, generally regarded as safe; hMSCs, human mesenchymal stem cells; LV, left ventricle; LVM, left ventricle mass; M, 1,4-linked β-D-mannuronic acid; MI, myocardial infarction; mPSCs, mouse pluripotent stem cells; MSCs, mesenchymal stem cells; NCD, non-communicable disease; PSCs, pluripotent stem cells; rMSCs, rat mesenchymal stem cells; VEGF, vascular endothelial growth factor; VSMCs, vascular smooth muscle cells.

INTRODUCTION

The incidence of cardiovascular diseases (CVDs) accounts for most of non-communicable disease (NCD) deaths annually[1] and has increased over the last few decades, primarily because of the expansion of the "modern" lifestyle in wealthy countries and the lengthening of life expectancy. However, despite improvements in its management, CVDs still remain the major cause of death worldwide claiming 17.9 million lives a year, with an estimated 31% of all deaths globally.

Among CVDs, myocardial infarction (MI) remains one of the leading cause of heart failure, which, in turns, represents the commonest driver for mortality and morbidity (Cahill and Kharbanda, 2017). At present, there is no definitive treatment for MI, although great effort has been made to find new therapies and permanent solutions (Mitter and Yancy, 2017). The available treatments for MI and consequent heart failure are drugs, medical electronic devices and, in the most severe cases, heart transplants (Ferrini et al., 2019). One of the main problems about infarcted heart is cardiomyocytes incapability of self-regeneration along with lack of treatments able to restore the lost parenchyma, thus the impossibility to reestablish normal pump function. Regenerative medicine, combining tissue engineering and drug delivery, aims to repair damaged or diseased tissues and organs, and plays an important role in restoring normal condition in the infarcted heart. Some evidence showed that once applied onto MI, three dimensional printed cardiac patches, and cardiac-tissue derived extracellular matrix (ECM) scaffolds seem to have the potential to improve cardiac functions, cardiac support, and tissue regeneration, improving angiogenesis and reducing the scar size (Kc et al., 2019; Yeung et al., 2019). The regenerative medicine approach can be cell-free (Domenech et al., 2016; McLaughlin et al., 2019), or cell-based, comprising stem cell therapy *via* injection or grafting into the infarcted area, e.g., resident stem cells (Forrester et al., 2003; Leor et al., 2007), myoblasts (Sekiya et al., 2009) or by reprogramming fibroblasts directly into cardiomyocytes (CMs) (Ieda et al., 2010). However, there are several intrinsic limitations in restoring a complete and functional heart: (i) cardiomyogenesis is very low and incapable to repair the damaged areas (Zacchigna and Giacca, 2014; Leitolis et al., 2019), and the infarcted area displays a hostile environment for cells due to high level of oxidative stress, poor nutrient supply, and it offers an open way for host immune system attack; (ii) the recovery of the cardiac tissue requires maturation and completeness in mechanical, electrical, and chemical function (Pena et al., 2018); (iii) the majority of stem cells used for therapeutic purposes in amending the infarcted heart are lost within 1 day after the injection without using any vehicle-matrix; (iv) the balance of cell-removal, ECM preservation, and recellularization is challenging due to the residual presence of detergent and endotoxin in the patch (Kc et al., 2019). Therefore it emerges the necessity of looking for appropriate biomaterials in a suitable form as cell preservation and delivery system (van den Akker et al., 2017; Weinberger et al., 2017; Zuppinger, 2019). Biomaterials should provide biological, mechanical, electrical, and chemical support for the myocardium and they should mimic its physiological and homeostatic conditions (Pena et al., 2018). Nowadays, the biomaterials that comprise cell-types and scaffold properties are evolving (Foresti et al., 2019), as well as the application strategies for these 3D artificial cardiac tissues. Recently, thanks to novel hydrogel formulations and 3D printing technology, it was possible to create *ad hoc* cardiac patches (scaffold) for myocardial repair (Chachques et al., 2020), drug or nanoparticles delivery (Bheri and Davis, 2019; Foresti et al., 2020b) or injectable hydrogel for mechanical stabilization of the repaired area (Seif-Naraghi et al., 2014; Kambe and Yamaoka, 2019).

Hydrogels are a network of polymers of different origin: natural, synthetic, or hybrid (a mix of natural and synthetic) (Ye et al., 2011), extensively described and detailed classified by Saludas et al. (2017) and Pena et al. (2018). Hydrogels have the capability to absorb water, maintain their shape, and dissolve in the body according to controlled kinetics Gauvin et al., 2012; Saludas et al., 2017). One of the principal qualities of the hydrogel is to be able to pass through a tiny syringe needle (27–30 G), turning from liquid state at room temperature to gel-state in the body at 37°C (Sepantafar et al., 2016; Ferrini et al., 2019; Milazzo et al., 2019).

Of note, hydrogels showed promising results in cardiac regeneration in both preclinical models (Saludas et al., 2017) and in some clinical trials as mechanical support in the infarcted heart (Tous et al., 2011). Hydrogels give a significant contribution to heart tissue regeneration being capable of simulating a temporary artificial ECM (Saygili et al., 2019) supporting cell infiltration, adhesion, proliferation, and differentiation (Hasan et al., 2015). The most widely used hydrogel (Lee and Mooney, 2012; Sun and Tan, 2013) is the natural biomaterial alginate, which, together with decellularized ECM [already extensively reviewed in Spinali's work, (Spinali and Schmuck, 2018)], represents the most promising material in cardiac regeneration. Degradable and bioactive microstructures of alginate-based hydrogel showed a great promise on the recovery of left ventricular function as well as the release of cardioactive substances (Hynes, 2009) in the target tissue.

ALGINATE

Sodium alginate is a natural polymer found in brown algae cell walls, including *Macrocystis pyrifera*, *Laminaria hyperborea*, *Ascophyllum nodosum* (Sachan et al., 2009) and in several bacteria strains (*Azotobacter*, *Pseudomonas*) (Remminghorst and Rehm, 2006). Alginate's hydrogels formed through physical crosslinking present highly tunable mechanical properties (Hecht and Srebnik, 2016), and thanks to its versatile and biological properties alginate is widely used in biomedical research Cheng et al., 2012; Ruvinov and Cohen, 2016; Saludas et al., 2017; Dhamecha et al., 2019). In this section, we intend to provide a brief insight into alginate characteristics.

[1]https://www.who.int/news-room/fact-sheets/detail/noncommunicable-diseases

Chemical Properties

Alginate is an anionic polysaccharide. It is a linear copolymer consisting of random sequences of 1,4-linked β-D-mannuronic acid (M) and 1,4 α-L-guluronic acid (G) residues (Hecht and Srebnik, 2016). Commercial alginate presents different ratios of M and G residues and block-length depending on its source; consequently, molecular weight (expressed as an average of all the molecules in the sample) is variable and changes in a range between 33,000 and 400,000 g/mol. Regarding polymer's solubility, it is important to underline that whereas alginic acid is insoluble in water and organic solvents, alginate monovalent salts and esters are water-soluble and form stable viscous solutions (Szekalska et al., 2016).

Physical Properties

Alginate physical properties strictly depend on its composition and concentration, which makes its characterization difficult, but allows for a wide range of customization according to the desired application (implantation, ECM mimic, etc.). An increase of polymer concentration in the solution coincides with an increase of gel stiffness, particularly when using high-molecular weight alginates that maintain long-range interactions within the gel (LeRoux et al., 1999). Nevertheless, increasing polymer concentration also implies an increased viscosity of the pre-gelled solution, which makes this strategy less feasible when cells or active ingredients need to be included (Kong et al., 2003). In order to modulate the stiffness without altering the viscosity, a possible strategy is the combination of high and low-MW alginates in specific ratios (Kong et al., 2002) or alternatively, the formation of polyelectrolyte complexes through the addition of cationic poly-(ethyleneimine) that increases the resistance to de-crosslinking (Kong and Mooney, 2003).

Another relevant criterion that determines alginate physical behavior is the crosslinking reaction. Many methods have been described for alginate crosslinking, including ionic crosslinking, covalent crosslinking, phase transition (thermal gelation), "click" reaction, free radical polymerization (Sun and Tan, 2013) and lowering the pH value below the pKa of alginate monomers using lactones, such as d-glucono-δ-lactone (Sachan et al., 2009). However, among these strategies, the most widespread is ionic crosslinking since allows instantaneous and almost temperature-independent solution/gel transition in relatively mild conditions, in presence of multivalent cations, physical crosslinking is instantaneous and almost temperature-independent.

Moreover, several studies revealed that, in presence of divalent ions, alginate solution/gel transition occurred under physiological conditions, such as the acidic environment of the body fluids (Fu et al., 2011). In particular, many of the technological applications of alginate rely on the gelation in presence of Ca^{2+} in a two-step process that leads to the formation of inter- and intra-chain bridging. Calcium ions interact with the acidic sites on the G residues leading to chain-chain association; following, the tightly linked dimers form weak interdimer associations mainly governed by electrostatic interactions among the dimers with higher Ca^{2+} concentration. This ion-chain interaction involves the formation of a cage-shape association of chain regions rich in G, implying that poly M-blocks and alternating MG blocks display lower selectivity toward Ca^{2+} (Fu et al., 2011; Hecht and Srebnik, 2016). Therefore, gelling properties depend not only on alginate molecular weight, but are also strongly associated with its structure and composition in terms of M-, G-, and MG-blocks (Sachan et al., 2009). High G-blocks content determines low shrinkage during gel formation and renders alginate stiffer, mechanically stable and more permeable due to larger pores' size (Martinsen et al., 1989), while high M-blocks content are required when alginate needs additional coating, such as enrichment of RGD sites to mediate cell adhesion (Kuo and Ma, 2001; Niekraszewicz and Niekraszewicz, 2009; Fu et al., 2011). Prevalence of MG-blocks, instead, give rise to alginate shrinkage and higher flexibility (Jorgensen et al., 2007; Szekalska et al., 2016).

Another relevant aspect to consider in the gelation process is the velocity of the reaction. Slow gelation provides uniform and ordered gel network structures with increased tensile properties and mechanical integrity (Kuo and Ma, 2001; Drury et al., 2004). One of the strategies to reduce the rate of gel forming process is the application of phosphate buffers (e.g., sodium hexametaphosphate); since the affinity of phosphate for calcium is higher compare to that of alginate, the presence of phosphate ions exert a chelating action and delay alginate gelation process (Dainty et al., 1986; Xu et al., 2007) alternatively, is possible to use calcium sulfate and calcium carbonate as Ca^{2+} sources: the lower solubility of these reagents prolongs gel formation. Lastly, another approach concerns the regulation of temperature: at lower temperatures, the reactivity of Ca^{2+} is reduced and allows the control of hydrogel formation (Augst et al., 2006; Zhao Y. et al., 2016).

Mechanical Properties

Alginate-based hydrogel mechanical properties strictly depend on the number and concentration of M and G residues (Augst et al., 2006). If G overcomes M, the hydrogel displays high mechanical stiffness. Therefore, by varying G and M content it is possible to change the elastic modulus. It was observed that elastic modulus homogeneity among 3D printing alginate-based scaffolds strictly depends on the gelation rate (Mahdi et al., 2016); slow processes result in greater homogenous scaffold (Kuo and Ma, 2001). Kaklamani et al. (2014) demonstrated how the gelation process can be modulated using divalent cations (Mg^{2+}, Ca^{2+}, and Sr^{2+}), resulting in a tight controlled Young modulus of elasticity as a function of cations and alginate concentration.

Recently, it was demonstrated that xylitol, mannitol, or peptides can modify the gelation process increasing strength and elasticity (Ochbaum et al., 2018). The swelling properties of alginate are also modulators of mechanical strength. Swelling degree is inversely dependent on gelation time (bt Ibrahim et al., 2019). Sodium alginate films immersed in $CaCl_2$ solution for 2 min denote a swelling degree of 51% compared to those immersed for 8 min (26%), suggesting that Ca^{2+} ions can penetrate into the film matrix and interact with sodium ions improving scaffold integrity and final geometry. In particular, in order to increase the volume of a given bio-based device it is necessary to increase the "surface-to-volume ratio" and

engineering the structure (Elviri et al., 2017; Foresti et al., 2019) by jellifying every single deposed layer (Campisi et al., 2018).

Finally, it becomes imperative to characterize the alginate mechanical properties in light with the method of fabrication (simple deposition/injection or scaffold manufacturing via 3D printer) (Ozbolat and Hospodiuk, 2016) and for the final use as a biomaterial (Ravnic et al., 2017).

Biological Properties

Alginate is regarded as biocompatible, non-immunogenic, and non-toxic material (Sachan et al., 2009). Alginate cross-linked gels are not degradable in mammalian digestive tract but the elution of the multivalent ions eventually leads to its dissolution; moreover, a physiological concentration of sodium ions has been proved to alter alginate's shear properties inducing a "softening effect" on the hydrogel's matrix (LeRoux et al., 1999). Alginate biocompatibility was confirmed *in vivo* after ocular (Lin et al., 2004), topical (Coskun et al., 2014), local (Veriter et al., 2010; Chang et al., 2012), and oral administration (Sosnik, 2014). Moreover, Food and Drug Administration has categorized several alginate salts (calcium, sodium, ammonium, and potassium) as well as propylene glycol alginate derivative as generally regarded as safe (GRAS) ingredients for oral administration[2] (Szekalska et al., 2016).

Besides being considered a safe polymer, alginate also presents some properties that enhance its attractiveness for biomedical applications, such as bio-adhesivity and antibacterial/-viral activity.

The presence of free carboxyl groups provides good mucoadhesive properties to alginate and allows its interaction with mucin by hydrogen and electrostatic bonding (Hecht and Srebnik, 2016; Szekalska et al., 2016). This property is strongly influenced by environmental factors such as pH, since only ionized carboxyl groups can interact with mucosal tissue. Moreover, different soluble formulations of alginate facilitate solvent penetration through its matrix, resulting in more viscous and cohesive gel structures that strengthen the mucoadhesive bonds; yet, an excessive hydration in physiological fluids might weaken mucoadhesiveness as a results of attenuation of the functional groups available for interactions (Taylor et al., 2005; Mythri et al., 2011; Haugstad et al., 2015). Ionized carboxyl groups also determine the reported antibacterial activity against a wide variety of species, including Pseudomonas, Escherichia, Proteus, and Acinetobacter (Khan et al., 2012; Pritchard et al., 2016), negatively charged alginate interacts with the outer bacterial cellular surface leading to its disruption (Yan et al., 2011; Benavides et al., 2012). Furthermore, the formation of a viscous layer around the bacterial cell prevents nutrient transport, decreases membrane function (Yan et al., 2011), and can exert chelation processes responsible for modulating the production of toxins, microbial growth and other crucial factors for microorganisms stability (Szekalska et al., 2016). Alginate antiviral activity relies on sulfated polysaccharides and alginic acid-containing fractions extracted from algae. The mechanism of action may be related to the strong anionic charge of sulfated alginate, capable of interacting with the positively charged host cell and, as a result, preventing virus contact with the host cell (Witvrouw and De Clercq, 1997; Sano, 1999; Meiyu et al., 2003). At present, antiviral efficacy has been reported against Flaviviridae, Togaviridae, Rhabdoviridae, and Herpesviridae viruses' families (Son et al., 2003; Lee et al., 2011; Wang et al., 2014; Ahmadi et al., 2015). Other relevant properties concern the modulation of several responses to pathology, from immunostimulation to anti-oxidant and anti-inflammatory activities. It has been reported that alginate with high M-block content is able to activate macrophages and monocytes leading to the secretion of cytokines and cytotoxic factors (Son et al., 2001). The anti-inflammatory cytokines secreted by monocytes, eventually lead to attenuate the production of nitric oxide, reactive oxygen species (ROS), prostaglandin E2, and cyclooxygenase COX-2, determining therefore alginate anti-oxidant effect (Rocha de Souza et al., 2007; Yamamoto et al., 2007; Maciel et al., 2013; Namvar et al., 2013). Calcium alginate displays hemostatic efficacy through platelets activation and thrombin generation (Hattori et al., 2010), and it has been reported to lower blood pressure as a results of calcium antagonist activity, especially toward voltage-operated calcium channels (Chaki et al., 2007; Terakado et al., 2012).

Alginate in Biomedical Research

Alginate due to its versatile and biologically properties such as biocompatibility, (possible) non-immunogenicity, chelating ability, water solubility, flexibility (it can be easily modified in any form) and low-cost, is widely used in biomedical research (Sun and Tan, 2013). In particular, alginate is used in protein/drug delivery systems, tissue regeneration, and wound healing (Miao et al., 2018). To date, there are several preclinical and clinical studies (see paragraph below) using alginate as a cargo system to control delivery bioactive agents, e.g., growth factors (Pawar and Edgar, 2012), cytokines (Lee and Mooney, 2012), doxorubicin (Paques et al., 2014), paclitaxel (Wu et al., 2014). Moreover, alginate is also used as an excipient in several drugs due to its gel forming, stabilizing and thickening properties, e.g., Gaviscon®, Bisodol®, Asilone (Miao et al., 2018). Regarding tissue regeneration, unless big steps have been done, there is still a considerable gap between research and clinical application of alginate in tissue regeneration. More studies should be performed in terms of improving alginate characterization, functionalization, biodegradability, and mechanical properties in order to facilitate tissue and organ regeneration. To date, several studies have been done implying use of alginate in cardiac regeneration (Rodness et al., 2016; Foresti et al., 2020a), skin regeneration (Yang et al., 2019), osteo and cartilage regeneration (Venkatesan et al., 2015; Calasans-Maia et al., 2019; Yang et al., 2019), and neural tissue regeneration (Homaeigohar et al., 2019). Due to its hydrophilicity, capability to adsorb wound exudate and maintaining a moist microenvironment alginate is suitable for wound dressing. Alginate dressings can be prepared by ionic crosslinking (with calcium, magnesium, etc.) to form a gel, or followed by processing to form freeze-dried porous sheets in form of foams, and fibrous dressings (Aderibigbe and Buyana, 2018).

[2] http://wayback.archive-it.org/7993/20171031063235/https://www.fda.gov/Food/IngredientsPackagingLabeling/GRAS/SCOGS/ucm260857.htm

At present, there are several alginate dressings commercially available including Algicell™, Fibracol™Plus, Hyalogran®, and Tromboguard®.

FUNCTIONALIZED ALGINATE

As mentioned in the introduction, the heart is a complex electromechanical organ. After MI, it occurs loss of CMs, lack of angiogenesis, and conductive connection disruption that brings to a malfunctioned heart. Lack of treatments to restore lost cardiomyocytes and cardiomyocytes incapability of self-regeneration brought scientists to think about regenerative medicine as a winner strategy to restore normal functionality of the infarcted heart. Alginate emerged as a promising natural polymer in cardiac regeneration, supporting heart vascularization, re-cellularization, and restoring electrical conductivity (**Figure 1**). In this section, it will be provided an overview of alginate's roles in restoring normal functionality of infarcted heart; the studies took into consideration are summarized in **Table 1**.

Alginate in Support of Heart Vascularization

A crucial hurdle in the recovery post MI is lack of angiogenesis that leads to the irreversible loss of cardiomyocytes in the first 2–4 h of the onset (Thygesen et al., 2007), thus contributing to the progression of maladaptive ventricular remodeling, including scar formation and ventricular dilatation, that can eventually lead to heart failure (French and Kramer, 2007). To address this deficiency in neovascularization both delivery of factors and/or cells have been explored. Specifically, most works are focused on delivering of mesenchymal stem cells (MSCs) and vascular endothelial growth factor (VEGF). Beneficial effects of MSCs on MI were already reported in literature (Gnecchi et al., 2008); their impact was mainly related to an hypoxia-dependent secretion of several cytokines, chemokines, and growth factors, that not only exert a cytoprotective effect on cardiomyocytes survival (Gnecchi et al., 2005), but lead also to an increase in collateral perfusion through paracrine stimulation of proliferation and migration of endothelial cells (ECs) and vascular smooth muscle cells (VSMCs) (Kinnaird et al., 2004). Marrow-derived stromal cells express genes encoding a broad spectrum of arteriogenic cytokines and promote *in vitro* and *in vivo* arteriogenesis through paracrine mechanisms (Nagaya et al., 2004). VEGF, instead, is the most powerful and well-characterized proangiogenic cytokine (Maharaj and D'Amore, 2007) associated with improvements in cardiac vascularization (Oduk et al., 2018). Unfortunately, delivery and retention of cells or growth factors to the damaged area remains critical. Moreover, VEGF delivering may lead to severe side effects, such as hypotension, limb edema, and retinopathy, growth of tumors and/or metastasis (Zietz et al., 1998; Baumgartner et al., 2000; Gasparini, 2000; Lee et al., 2000; Freedman and Isner, 2002; Henry et al., 2003). Given these considerations, it becomes clear why so much effort is put into defining an appropriate cell or molecules delivery system in order to help vascularization in the infarcted heart. In this scenario, several studies demonstrated alginate suitability as support material. Rodness et al. (2016) developed a VEGF-loaded patch made of compacted alginate microspheres, retained by a chitosan sheet. In order to combine alginate with the growth factor, the authors mixed recombinant VEGF with Na^+-alginate solution and produced microspheres using a water-in-oil-in-water double emulsion technique with pure olive oil and ddH_2O, and $CaCl_2$ crosslinking; microspheres were following compacted by centrifugation. From a certain point of view, this strategy seems to recall and overcome the approach of current clinical trials based on the mere injection of alginate in the ventricular wall. The rationale behind this approach relies on the highly tunable degradation of microspheres, that allows the controlled release of pro-angiogenic factors, and the restraint properties of a condensed microsphere patch reinforced with chitosan. After assessing the biological activity of VEGF-loaded patches *in vitro*, they were implanted on the epicardial surface of a MI-rat model. Both VEGF-loaded and control patches displayed similar functional outcomes in terms of fractional shortening, cell infiltration, wall thickness, scar area and length, to indicate that microsphere patch and chitosan sheet system may function as a ventricular restraint device that limits the extent of scar expansion post-MI. In addition, the team reported that VEGF-loaded patches maintained their biological activity *in vivo* up to 4 weeks after implantation, enhancing the spontaneous angiogenesis and vasculogenesis within the compacted alginate microspheres. An alternative approach to deliver VEGF to the infarcted area was proposed by Liu et al. (2017), who investigated the potential of MSCs as carriers of pro-angiogenetic factors. The team took advantage of MSCs natural tropism to the infarcted area (Lau and Wang, 2011) to deliver VEGF. They performed a layer-by-layer (LbL) self-assembly coating where alginate provided cohesion between two layers of gelatin embedded with VEGF. This tiny-film fabrication technique consisted in alternating steps of coating and washing, in which cells were progressively incubated with gelatin, alginate and gelatin. This strategy guarantees the maintenance of the metabolic activity of the encapsulated material and endows protection (Yang et al., 2011) without affecting cell viability, proliferation and differentiation (Li et al., 2015). Other interesting approaches to enhance vascularization involving cell delivery were successfully tested on muscle tissue, paving the way to possible transitions to the cardiac tissue. In the work of Nemati et al. (2017) HUVECs were encapsulated in a mixture of gelatin and alginate by the means of an electrostatic encapsulation method at high voltage rate (8kV) followed by extrusion through a 26G needle into a crosslinking solution of $CaCl_2$. The composition of the microcapsules allowed cell adhesion and migration through the porous structures; furthermore, the authors observed, *in vitro,* an increased production of NO combined with a high rate of cell survival and an increased tubulogenic activity of encapsulated HUVECs compared to control cells. The superior angiogenic capability of encapsulated HUVECs was also confirmed *in vivo* by injecting cell-laden microcapsules in the muscular tissue of an immune-compromised mouse model. Whereas the direct injection of HUVECs determined an extensive cell spread resulting in the failure of microvascular formation, encapsulated

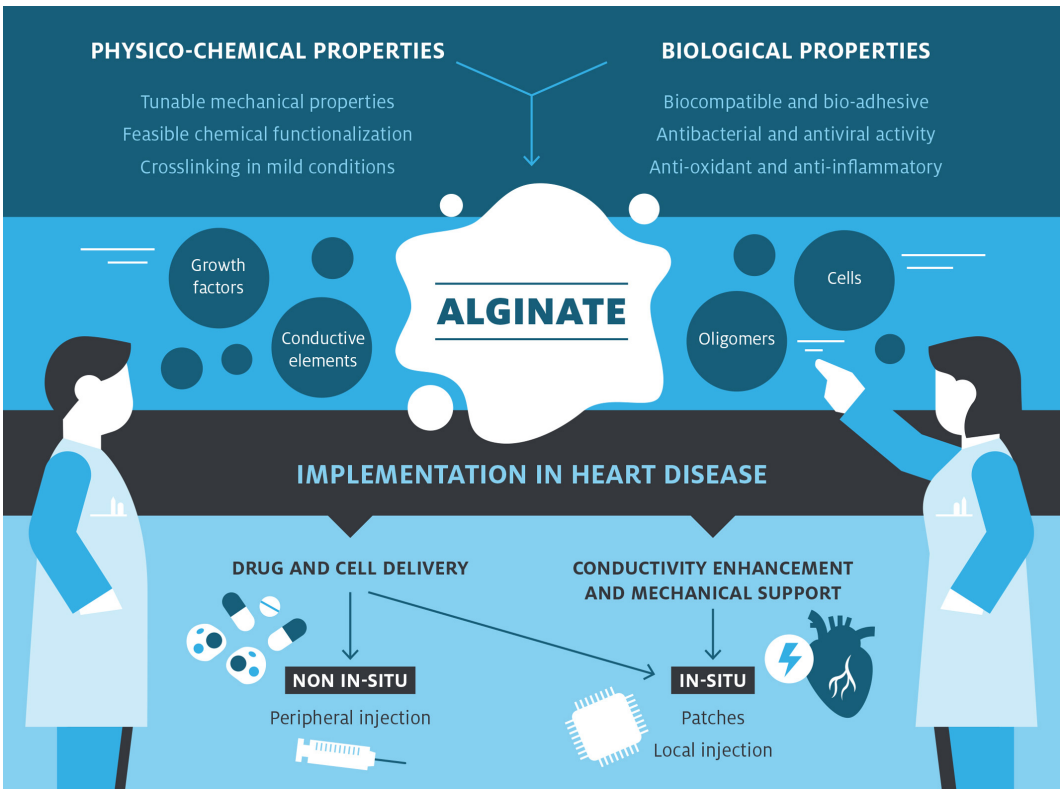

FIGURE 1 | Alginate-based devices development in cardiac treatment. Alginate displays some physico-chemical and biological advantageous characteristics that, combined together, render this biomaterial suitable for further modification. Possible modifications and implementations are: the inclusion of different cell types, bioactive molecules, functional oligomers, and conductive materials to provide further functionalities to the pristine material addressing the main issues in cardiac regeneration field. Thanks to its functionalization, alginate can be implied either as a delivery system or as a support material in cardiac regeneration choosing the most efficient way of administration, *in situ* or not.

cells promoted an increase of vascular density constituted of both large- and micro-size vascular structures with normal ECs alignment and epithelialization in the periphery. Bushkalova et al. (2019), instead, developed macroporous scaffolds made of alginate-chitosan polyelectrolyte complexes to deliver MSCs in soft tissues. This strategy exploits the association of alginate with a cationic polymer, chitosan, to form a polyelectrolyte complex of opposite charge that can be subsequently freeze-dried and crosslinked; in this way, chemically unaltered polymers preserve their initial biocompatibility while their rheological properties improve and adapt to the mechanical resistance of soft tissues. Instead of pursuing MSCs differentiation into a specific cell type within the scaffold, the main goal of this work was to ensure cells survival, retention, and paracrine activity in order to stimulate the vascularization. *In vitro* tests assessed cell viability and growth, besides an enhanced tendency to secrete FGF2. The most promising results concern the *in vivo* model, implantation in the pectoral muscle of healthy rats, where the team found a good engraftment of the scaffold in the target tissue within 28 days; the progressive degradation of the scaffold was followed by the increasing formation of small functional blood vessels and the reduction of the fibrous capsule. From these studies, it emerged the real possibility of treating MI through the combination of growth factors and a suitable cell source to promote angiogenesis. Undoubtedly, further work is needed to determine which cell source may be suitable in clinical applications, in order to avoid immune-response or off-target vascularization with consequent severe side effects (Epstein et al., 2001).

Alginate in Cell Delivery Systems

After supporting vascularization of the infarcted area, the second step is to repopulate the damaged area with cells. Mainly, two different cell populations can be implanted, stem cells that may form teratomas, or mature cardiomyocytes, which can cause an electromechanical mismatch within the heart (Chen et al., 2009; Liu et al., 2013). Recently, stem cell-based therapies emerged as possible candidates in treating MI. Unless many studies have been done, at present, only pluripotent stem cells (PCSc) have shown clear ability to differentiate into functional cardiomyocytes (Choe et al., 2019a). Furthermore, cells retention in the heart is very low (Sanganalmath and Bolli, 2013; Hirt et al., 2014); ischemic myocardium displays a hostile environment for cells due to high level of oxidative stress, poor nutrient supply and it offers an open way for host immune system attack. Alginate hydrogels, porous scaffolds,

TABLE 1 | Promising alginate-based systems in cardiac regeneration.

Material	Factors	Cell type	Model	Administration	Treatment timing	Monitoring time	Results	References
Alginate, gelatin	VEGF	rMSCs	Sprague-Dawley rats, left coronary artery block and reperfusion after 45′	VEGF-encapsuled rMSCs injection via tail vein	2 days after myocardial injury	6 weeks	Increased vascular density and perfusion rate in the border zone; restored indexes of ejection fraction and fractional shortening.	Liu et al., 2017
Alginate, gelatin		HUVECs	Immunocompromised Balb/c mice	Microcapsules injection in quadriceps muscle	3 days after cyclophosphamide injection	1 week	Increase of vascular density; endothelial cell alignment; peripheral epithelization.	Nemati et al., 2017
Alginate-chitosan PEC		MSCs	Lewis rats	Implantation of a macroporous scaffold in the pectoralis major muscle	12 h after scaffold hydration	1–4 weeks	Good engraftment and gradual scaffold degradation; functional blood vessels formation; reduction of the fibrous capsule.	Bushkalova et al., 2019
Alginate-chitosan micromatrix		mPSCs pre-differentiated into early cardiac lineage	C57BL6/J mice, permanent LAD ligation	Three injections in the periphery of infarcted tissue	5 min after myocardial injury	4 weeks	Increased cell retention, survival and migration into MI zone; improved ejection fraction, stroke volume, cardiac output and left ventricle end-systolic and end-diastolic volumes; reduced fibrosis ad hypertrophy.	Zhao S. et al., 2016
Alginate, chitosan	VEGF		Sprague-Dawley rats, permanent LAD ligation	Microspheres reinforced with chitosan net and applied on the LV epicardial surface	4 days after myocardial injury	4 weeks	Better fractional shortening; higher cell infiltration and vascular-like structures; increased scar thickness and decreased scar area and length.	Rodness et al., 2016
2-aminopyridine-5-thiocarboxamide, alginate-CHO, tetraaniline, gelatin		ADSCs	Sprague-Dawley rats, LAD ligation	Hydrogel injections adjacent to MI area	Immediately after myocardial injury	1–4 weeks	Good electroactivity *in vitro*; increased cell retention *in vivo*; improved ejection fraction; decreased fibrotic area and wall thinning; increased expression of VEGF and Ang-1.	Liang et al., 2019
Alginate, gold nanowires			Neonatal rat cardiomyocytes and fibroblasts	Cells were seeded onto the nanocomposite scaffold, and cultured for 3 days		3–8 days	Increased cell alignment; higher levels of proteins involved in contraction and electrical coupling; synchronous contraction and calcium transients in temporal sequence.	Dvir et al., 2011

or alginate cell sheets/patches were enrolled to improve cell retention, survival, and function in the ischemic heart. Despite the continuous effort in developing less invasive procedures, the evidence that alternative administration strategies, such as intracoronary injection, may lead to a compromised cell retention (Follin et al., 2018) drove most of the research toward *in situ* application of the developed devices. Partially oxidized alginate was used in preparing an ASDC-loaded conductive H2S-releasing hydrogel system able to improve performances of the infarcted zone in rats (Liang et al., 2019). Specifically, alginate was oxidized through sodium iodate, and tetraaniline (TA) and 2-aminopyridine-5-thiocarboxamide (APTC) were employed to synthetize the multifunctional co-polymer; while TA guaranteed conductive properties, APTC was responsible for inflammatory response inhibition and angiogenic stimuli. Moreover, in a recent *in vitro* study, alginate functionalized with RGD sequence was employed to assess encapsulated cells resistance to oxidative stress. The immobilization of the RGD peptide to sodium alginate was performed utilizing the aqueous carbodiimide chemistry (Shachar et al., 2011), thus the peptide was conjugated to alginate via an amide bond between its terminal amine and the carboxylate on alginate. The results showed that human mesenchymal stem cells (hMSCs) encapsulated in raw alginate or in alginate enriched with RGD have higher resistance to hydrogen peroxide-induced cell death (Choe et al., 2019b). Partially oxidized alginate was also employed in a recent work where PSCs pre-differentiated into the early cardiac lineage were encapsulated into an alginate-chitosan micromatrix (ACM); to create the so-call micromatrix the authors took advantage of the electrostatic interactions among the positively charged chitosan and the negative charges of cell membrane and alginate, by successively soaking cell aggregates in the saline solution of the polymers. These aggregates were injected into hearts of mice showing an increase in cardiac function and survival of animals after MI (Zhao S. et al., 2016). In addition to the previous challenges, another point needs to be addressed, timing of stem cells injection; it was showed that injection of SCs after 4–7 days from the MI improves cells survival but, at the same time, significant injury is accumulated in the ischemic heart (Suzuki et al., 2004; van den Akker et al., 2013). Unless many steps should be done, alginate cell-based therapy seems to be a promising way in the treatment of MI.

Alginate in Restoring Electrical Conductivity

The last aspect to be taken into consideration about restoring the infarcted area is electrical conductivity. Alteration of the normal cardiac conductive system, resulting in the interruption of connectivity between ion channels and connexins (Huang et al., 2017), is another evidence occurring after MI. CMs death and scar tissue formation play a pivotal role in the conductive connection disruption (Ongstad and Gourdie, 2016). The development of a conductive injectable hydrogel can help transmission of the electrical impulses and maintaining of a stable cardiac rhythm, restoring the normal interchange between the synchronous contractions and the relaxation time (Guo and Ma, 2018). On the contrary, injection of non-electroactive hydrogels, results in an electrically isolated system (Shin et al., 2013), impeding the transmission of electrical impulses to all the infarcted tissue and thus reducing the percentage of success of the regenerative process. Natural hydrogels represent convenient starting substrate to obtain electroactive biomaterials; in particular, thanks to high water level retention, good biocompatibility and their structural resemblance to ECM that enables the diffusion of small molecules (Shi et al., 2016). Moreover, hydrogels can be loaded with conductive components, e.g., nanoparticles (NPs) such as gold nanoparticles (AuNPs), carbon nanotubes (CNT), oligomers or conjugated with conductive polymers, such as polypyrrole (PPy), polythiophene, poly(3,4-ethylendioxythiophene (PEDOT), and Polyaniline (PANi) (Shi et al., 2013; Huang et al., 2017). The main ways to obtain conductive materials are, crosslinking between two or more different materials (Zhang et al., 2014), chemical oxidative *in situ* polymerization with an oxidant to start the reaction (Shi et al., 2012), electrochemical polymerization where hydrogels are used as conducting electrodes (Shi et al., 2014), and post-polymerization/coating by two subsequently hydrogel immersions, the first into monomer solution of conductive polymer and, the second, into an oxidant solution (Wu et al., 2015; Yang et al., 2016; Distler and Boccaccini, 2019; Jiang et al., 2019). Dvir et al. (2011) modified the conductive properties of alginate through a calcium crosslinking strategy incorporating gold nanowires (Alg–AuNW) obtaining a patch where they seeded neonatal rat cardiomyocytes and measured electrical conductivity. In particular, they demonstrated an increased electrical conductivity of the material itself and an increase of electrical conductivity of seeded rat cardiomyocytes. Furthermore, they showed an improvement in cell organization and contraction when the length of gold nanowires surpass the thickness of alginate's pores (Dvir et al., 2011). Kaklamani et al. (2014) demonstrated that alginate crosslinked with Ca^{2+} is more conductive than alginate crosslinked with Sr^{2+}; Sr^{2+} displays a larger ionic radius compare to Ca^{2+}, thus, it forms less ionic bridges with alginate hydrogel compared to Ca^{2+}. For instance, a higher ions level is associated with larger charge density of the hydrogel (Kaklamani et al., 2014). Alginate has also been used for neural differentiation. The conductive hydrogel composed with polypyrrole and alginate (PPy/Alg) has ten times more electrical conductance compared to solely alginate hydrogel (Yang et al., 2016; DeVolder et al., 2017; Ketabat et al., 2017; Ren et al., 2019). The hybrid polymer is obtained by chemically polymerizing PPy within ionically crosslinked alginate: pyrrole monomers are allowed to diffuse into alginate hydrogels before starting their polymerization with a chemical oxidant ($FeCl_3$); further stabilization is provided by the interactions among positively charged pyrrole oligomers and negatively charged alginate. PPy/Alg hydrogel promotes hMSC toward a neural differentiation, implying a possible use for neural tissue engineering (Yang et al., 2016). Interesting would be the evaluation of the same PPy/Alg hydrogel in the contest of cardiomyogenic maturity, or cardiovascular regeneration

therapy as well, since the conjugation of these two materials provide an enhanced electrical conductivity, extremely necessary for the cardiac regeneration.

Although great efforts have been put into developing a conductive alginate, suitable to restore normal electrical conductivity in infarcted heart, the way to reach this goal is still very far. In order to restore a normal electromechanical homeostasis within the myocardium the perfect material should be capable to transmit electrical impulses with a proper conduction velocity. Only recently, it emerged the importance to study also the conductivity of injectable hydrogels for cardiac regeneration. To conceive an ideal injectable alginate hydrogel several strategies of manufacture should be combined together. Only the implementation of alginate with cells, vascularization factors and conductive elements would give a "complete material" that can be used for cardiac therapy. The synergy of these three players, together, might be the most successful treatment in heart healing.

CLINICAL TRIALS IMPLICATING ALGINATE IN CARDIOVASCULAR DISEASES

Food and Drugs Administration (FDA) approved alginate as GRAS in food, pharma, and medicine (wound, bone) applications already in 1970 (Frey et al., 2014; Lee et al., 2015). To date, there are four clinical trials implying alginate in treating heart failure; three of them are completed and the forth one is still recruiting. Algisyl-LVR^{TM} is the most used and commercially available alginate hydrogel implied in sustaining the gradual remodeling of the ventricle in patients subjected to dilated left ventricle (LV), HF, and MI (Lee et al., 2013, 2015; Rao et al., 2016). Until now, two clinical trials have been reported implying Algisyl-LVR^{TM} in restoring infarcted myocardium. Algisyl-LVR^{TM} is conjugated with calcium and sodium (furnished respectively in an aqueous solution and insoluble particles in a 4.6% mannitol solution), reaching a final strength of 3–5 kPa (Lee et al., 2015). Algisyl-LVR is administered during a CABG procedure under general anesthesia. After the intramyocardial injection, it changes the status from liquid to gel remaining permanently in the human heart. Algisyl-LVR^{TM} showed no immune system reactions or rejections, and, thanks to the ability to reduce cardiac tension and cell stress, it enables the natural healing of the heart blocking the disease progression.

SYM-08-001

The first clinical trial (NCT00847964) was published in 2015, in which Algisyl-LVR^{TM} was administered to 11 patients with dilated cardiomyopathy underwent open-heart surgery with the aim of left ventricular wall augmentation. Only nine patients were able to complete the follow-up at day 8 and 3, 6, 12, 18, and 24 months later, showing promising results. Amelioration of LV size has been observed starting from the 3rd day after the injection procedure. At the last time point of the follow-up (24 months) no deaths occurred and the LV displayed a more ellipsoidal shape with a reduction in the LV end-systolic and LV end-diastolic dimension (LVESD–LVEDD) of respectively 9 and 12%. The ejection fraction (EF) improves of 28% over 24 months while the myofiber stress at the end-of-diastole/systole decreased for 35% over the same period. According to the New York Heart Association (NYHA) classification, the patients' life quality improved showing a change to a less critical category for almost all patients (II or III class) (Lee et al., 2015). Based on these results, Algisyl-LVR^{TM} has been considered feasible and safe for further clinical trials.

AUGMENT-HF and AUGMENT-HF II

The second clinical trial performed using Algisyl-LVR^{TM} was AUGMENT-HF (N: NCT01311791). The study was conducted in five different countries with a 1-year-follow-up, where Algisyl-LVR^{TM} was administered to 40 patients (plus 38 control patients for a total number of 78 subjects) aged between 18 and 79 years to modulate HF symptoms and improve heart functions (Anker et al., 2015). After 6 months from injections, the patients showed a progressive increase of the mean peak VO2 (the maximal quantity of O2 in blood that the heart is able to provide to muscles during a physical activity), while the six-minute walk test (6MWT) increased above 300 m threshold for the treated group but decreased in the control group. The 1-year-follow-up demonstrated further enhancement both in mean peak VO2 and in 6MWT in treated group compared to control group, where both conditions slightly worsen with time. These results are correlated with a return to the physical activity for the treated patients and the scaling up the NYHA functional class (I or II) (Mann et al., 2016). An increase in LVEF (16%) was observed after 12 months in the treated group, while LVEDD and left ventricle mass (LVM) resulted decreased for a total of 4 and 9%, respectively (none of the parameters are statistically significant but these findings are unexpected) (Mann et al., 2016). It is possible to deduce that the treatment for HF patients following the standard procedure with the additional Algisyl-LVR injections is a functional strategy to treat HF patients. This polymer lasts permanently in the heart bringing positive effects to the cardiac health (LV augmentation and reduction of LV stress) ameliorating the general mechanical support and life quality of all the treated subjects. To date another clinical trial is ongoing but not yet recruiting, AUGMENT-HF II (NCT03082508). It consists of evaluating the efficacy and safety of Algisyl in LV-augmentation and restoration in patients with dilated cardiomyopathy.

PRESERVATION-1

Frey et al. (2014) administered in the pivotal study NCT01226563 the so-called hydrogel IK-5001 (BioLineRx, Jerusalem, Israel) to 27 patients (aged between 18 and 75 years) trying to prevent or reverse left ventricular remodeling after a considerable MI (severe-acute) within 7 days from the attack. No control group is present in the study. IK-5001, an implantable bioabsorbable cardiac matrix (BCM) device, is made of 1% sodium alginate plus 0.3% calcium gluconate. IK-5001 hydrogel enters both in the heart and in the extracellular space. Subsequently, it crosslinks

TABLE 2 | Clinical trials using alginate as basic compound.

ID number	Trial name	Status	Years	Device	Condition or disease	Participants	Description
NCT00847964	SYM-08-001	Completed	February 2009–November 2012	Algisyl-LVR	Dilated cardiomyopathy	11	A pilot study to evaluate the safety and feasibility of Algisyl-LVR as a method of left ventricular restoration in patients with dilated cardiomyopathy undergoing open-heart surgery (Lee et al., 2015).
NCT01311791	AUGMENT-HF	Completed	August 2012–May 2016	Algisyl-LVR	Heart failure; dilated cardiomyopathy.	78	Randomized, controlled study to evaluate the safety and cardiovascular effects of Algisyl-LVR as a method of left ventricular augmentation in patients with dilated cardiomyopathy (Anker et al., 2015; Mann et al., 2016).
NCT03082508	AUGMENT -HFII	Not yet recruiting	Estimated August 2017–January 2024	Algisyl	Heart failure; dilated cardiomyopathy; heart failure with reduced ejection fraction.	Estimated 240	A pivotal trial to establish the efficacy and safety of Algisyl-LVR in patients with moderate to severe heart failure[1].
NCT01226563	PRESERVATION-1	Completed	April 2012–December 2015	IK-5001	Acute myocardial infarction; congestive heart failure; ST-elevation myocardial infarction.	303	A placebo controlled, multicenter, randomized double blind trial to evaluate the safety and effectiveness of IK-5001 for remodeling prevention of the ventricle and congestive heart failure after acute myocardial infarction (Frey et al., 2014; Rao et al., 2016).

[1] *https://clinicaltrials.gov/ct2/show/NCT03082508*

in a gel solution thanks to high ionized calcium concentration (characteristic of infarcted myocardium), creating a cardiac scaffold resembling ECM that is bioabsorbable by the tissue and is discarded by kidneys in 3–6 months after the injection (Rao et al., 2015, 2016). In parallel, in the animal model was shown that BCM reabsorption was followed and substituted by a network of capillaries, myofibroblasts and collagen fibrils (Sabbah et al., 2013; Ruvinov and Cohen, 2016). The subjects were controlled after 30, 90, and 180 days from the injections. No further myocardial damages, arrhythmias were observed (Frey et al., 2014). LV remodeling appeared mild recovered with a conservation of LV end-diastolic/end-systolic volume index (LVEDVI – LVESVI) and LVEF parameters. No adverse or serious events have been proven to be correlated with the injections; there was only one episode of syncope after 172 days of administration correlated with the treatment. The whole procedure was well tolerated by patients; in addition, the injections were performed under local anesthesia *via* percutaneous radial artery access and not undergoing an open-heart surgery under general anesthesia (Frey et al., 2014). This pilot study opened the window on a consecutive bigger clinical trial called PRESERVATION-1 (nr: NCT01226563) with the aim to prevent, after one severe MI, ventricle remodeling and heart failure congestion (congestive HF). Two hundred and one subjects were treated with IK-5001 and were compared with 102 healthy subjects. After 6 months, no significant results were obtained. LVEDVI and adverse events remained constant and similar between the two groups. No significant differences have been detected in the improvement of the 6MWT for the treated group; however, a positive and beneficial trend has been shown in the treated group. Severe adverse effects appear to be more frequent in treated subjects (5%) compared to control group (2.9%), on the contrary low rate of mortality and MI have been detected in the treated group compared to the control group. Given these results, neither impressive anatomical changes, nor progress of life quality has been demonstrated in MI subjects. It can be assumed that some results might be linked to the severe MI symptoms that affected some patients that, due to the severity of the damages, could not be treated (Rao et al., 2016).

So far, clinical trials demonstrated the feasibility and safety of treating MI with alginate. Nevertheless, is still necessary to identify the most suitable administration route to exert a therapeutic effect. Indeed, whereas the IK-5001 strategy has the appealing of providing a less-invasive administration, the lack of significant results and life-quality improvements in PRESERVATION-1 trial may indicate a poor specificity for the target area. The direct injection of Algisyl-LVR^{TM} prevents this issue but at the same time underlines the passive role of the biomaterial, whose therapeutic effects seems to rely on providing physical support to the weakened area. **Table 2** summarized the discussed clinical trials.

CONCLUSION

Cardiovascular diseases are the number one cause of death globally. In particular, acute MI, according to WHO, causes 7.3 million deaths worldwide. Despite great strides have been done in the last decade prognosis is still unfavorable, and the search to find new and innovative treatments to heal the infarcted heart is still open. Recently, cardiac regeneration emerged as a promising solution to restore injured heart. The heart is a complex, conductive, and electromechanical organ, thus the necessity to find a durable and conductive material to resist and persist in the "harsh infarcted heart environment." To date, there are no hydrogels able to mimic cardiac tissue. However, alginate, among all the biomaterials available, seems to be a good candidate for cardiac regeneration. On one hand alginate is a natural polymer, biodegradable, biocompatible, and already approved by FDA for human purposes; moreover, it can be easily modified, it is versatile, and it has affordable production costs. On the other hand, alginate contains many impurities and it is highly hydrophilic. Available results from clinical trials in patients showed that alginate only mildly ameliorates some cardiac parameters but seems to improve patient's quality of life. To be noted that, until now, all these trials have been focused on the injection of pristine alginate in the damaged area. Despite promising results, so far, no experimentation provided a decisive outcome. Although data from literature show encouraging results, improving vascularization and cell retention in the infarcted area, in a clinical context their potential is limited to temporary solutions and does not show deep ameliorates. To date, all clinical trials imply alginate as mechanical support of the infarcted area, thus the possible premature degradation of alginate inside the organism, in parallel with the incapability of the resident cardiomyocytes to regenerate the infarcted area and the failure in restoring a proper cardiac conductivity, could be the reasons of the partial outcome of the clinical trials. In order to overcome this issue could be useful to complete the stage of cellularization of the alginate matrix *in vitro* with cardiomyocytes; nevertheless, it is well known the difficulty of handling mature cardiomyocytes *in vitro* and the ethical limitations. Moreover, particular attention should be paid to electrical conductivity to prevent arrhythmias, both inserting an alginate matrix capable of substitute the infarcted area and transmit the electrical signal or guiding the cardiomyocytes within the scaffold avoiding spontaneous beating activity. Furthermore, it is necessary to know better the mechanisms underneath the remodeling occurring in the infarcted heart in order to establish when, where, and how much material to inject. So far, the use of alginate in cardiac regeneration seems to be promising, even though a deeper characterization is needed for the eventual translation to the clinical field.

AUTHOR CONTRIBUTIONS

GC, AG, AR, MM, and CC designed and wrote the manuscript. RF and PP read and commented the manuscript. GC, AG, and CC designed the study and edited the final manuscript with input from all authors.

FUNDING

This study was supported by the Department of Innovation and Research and University of the Autonomous Province of Bolzano/Bozen, by FIL_Miragoli-UNIPR_2018 to MM and by Fondazione Italiana per la Ricerca in Epatologia (F.I.R.E.) to CC.

ACKNOWLEDGMENTS

The authors thank the Department of Innovation, Research and University of the Autonomous Province of Bozen/Bolzano for covering the Open Access publication costs. The authors also thank Oscar Diodoro for the illustration.

REFERENCES

Aderibigbe, B. A., and Buyana, B. (2018). Alginate in wound dressings. *Pharmaceutics* 10:42. doi: 10.3390/pharmaceutics10020042

Ahmadi, A., Zorofchian Moghadamtousi, S., Abubakar, S., and Zandi, K. (2015). Antiviral potential of algae polysaccharides isolated from marine sources: a review. *Biomed. Res. Int.* 2015:825203. doi: 10.1155/2015/825203

Anker, S. D., Coats, A. J., Cristian, G., Dragomir, D., Pusineri, E., Piredda, M., et al. (2015). A prospective comparison of alginate-hydrogel with standard medical therapy to determine impact on functional capacity and clinical outcomes in patients with advanced heart failure (AUGMENT-HF trial). *Eur. Heart J.* 36, 2297–2309. doi: 10.1093/eurheartj/ehv259

Augst, A. D., Kong, H. J., and Mooney, D. J. (2006). Alginate hydrogels as biomaterials. *Macromol. Biosci.* 6, 623–633. doi: 10.1002/mabi.200600069

Baumgartner, I., Rauh, G., Pieczek, A., Wuensch, D., Magner, M., Kearney, M., et al. (2000). Lower-extremity edema associated with gene transfer of naked DNA encoding vascular endothelial growth factor. *Ann. Intern. Med.* 132, 880–884. doi: 10.7326/0003-4819-132-11-200006060-00005

Benavides, S., Villalobos-Carvajal, R., and Reyes, J. E. (2012). Physical, mechanical and antibacterial properties of alginate film: effect of the crosslinking degree and oregano essential oil concentration. *J. Food Eng.* 110, 232–239. doi: 10.1016/j.jfoodeng.2011.05.023

Bheri, S., and Davis, M. E. (2019). Nanoparticle–hydrogel system for post-myocardial infarction delivery of MicroRNA. *ACS Nano* 13, 9702–9706. doi: 10.1021/acsnano.9b05716

bt Ibrahim, S. F., Mohd Azam, N. A. N., and Mat Amin, K. A. (2019). Sodium alginate film: the effect of crosslinker on physical and mechanical properties. *IOP Conf. Ser. Mater. Sci. Eng.* 509:012063. doi: 10.1088/1757-899x/509/1/012063

Bushkalova, R., Farno, M., Tenailleau, C., Duployer, B., Cussac, D., Parini, A., et al. (2019). Alginate-chitosan PEC scaffolds: a useful tool for soft tissues cell therapy. *Int. J. Pharm.* 571:118692. doi: 10.1016/j.ijpharm.2019.118692

Cahill, T. J., and Kharbanda, R. K. (2017). Heart failure after myocardial infarction in the era of primary percutaneous coronary intervention: mechanisms, incidence and identification of patients at risk. *World J. Cardiol.* 9, 407–415. doi: 10.4330/wjc.v9.i5.407

Calasans-Maia, M. D., Barboza Junior, C. A. B., Soriano-Souza, C. A., Alves, A., Uzeda, M. J. P., Martinez-Zelaya, V. R., et al. (2019). Microspheres of alginate encapsulated minocycline-loaded nanocrystalline carbonated hydroxyapatite: therapeutic potential and effects on bone regeneration. *Int. J. Nanomedicine* 14, 4559–4571. doi: 10.2147/ijn.S201631

Campisi, M., Shin, Y., Osaki, T., Hajal, C., Chiono, V., and Kamm, R. D. (2018). 3D self-organized microvascular model of the human blood-brain barrier with endothelial cells, pericytes and astrocytes. *Biomaterials* 180, 117–129. doi: 10.1016/j.biomaterials.2018.07.014

Chachques, J. C., Lila, N., Soler-Botija, C., Martinez-Ramos, C., Valles, A., Autret, G., et al. (2020). Elastomeric cardiopatch scaffold for myocardial repair and ventricular support. *Eur. J. Cardiothorac. Surg.* 57, 545–555. doi: 10.1093/ejcts/ezz252

Chaki, T., Kajimoto, N., Ogawa, H., Baba, T., and Hiura, N. (2007). Metabolism and calcium antagonism of sodium alginate oligosaccharides. *Biosci. Biotechnol. Biochem.* 71, 1819–1825. doi: 10.1271/bbb.60620

Chang, A. A., Reuther, M. S., Briggs, K. K., Schumacher, B. L., Williams, G. M., Corr, M., et al. (2012). In vivo implantation of tissue-engineered human nasal septal neocartilage constructs: a pilot study. *Otolaryngol. Head Neck Surg.* 146, 46–52. doi: 10.1177/0194599811425141

Chen, H.-S. V., Kim, C., and Mercola, M. (2009). Electrophysiological challenges of cell-based myocardial repair. *Circulation* 120, 2496–2508. doi: 10.1161/CIRCULATIONAHA.107.751412

Cheng, K., Blusztajn, A., Shen, D., Li, T. S., Sun, B., Galang, G., et al. (2012). Functional performance of human cardiosphere-derived cells delivered in an in situ polymerizable hyaluronan-gelatin hydrogel. *Biomaterials* 33, 5317–5324. doi: 10.1016/j.biomaterials.2012.04.006

Choe, G., Kim, S.-W., Park, J., Park, J., Kim, S., Kim, Y. S., et al. (2019a). Anti-oxidant activity reinforced reduced graphene oxide/alginate microgels: mesenchymal stem cell encapsulation and regeneration of infarcted hearts. *Biomaterials* 225:119513. doi: 10.1016/j.biomaterials.2019.119513

Choe, G., Park, J., Jo, H., Kim, Y. S., Ahn, Y., and Lee, J. Y. (2019b). Studies on the effects of microencapsulated human mesenchymal stem cells in RGD-modified alginate on cardiomyocytes under oxidative stress conditions using in vitro biomimetic co-culture system. *Int. J. Biol. Macromol.* 123, 512–520. doi: 10.1016/j.ijbiomac.2018.11.115

Coskun, G., Karaca, E., Ozyurtlu, M., Ozbek, S., Yermezler, A., and Cavusoglu, I. (2014). Histological evaluation of wound healing performance of electrospun poly(vinyl alcohol)/sodium alginate as wound dressing in vivo. *Biomed. Mater. Eng.* 24, 1527–1536. doi: 10.3233/bme-130956

Dainty, A. L., Goulding, K. H., Robinson, P. K., Simpkins, I., and Trevan, M. D. (1986). Stability of alginate-immobilized algal cells. *Biotechnol. Bioeng.* 28, 210–216. doi: 10.1002/bit.260280210

DeVolder, R. J., Seo, Y., and Kong, H. (2017). Proangiogenic alginate-g-pyrrole hydrogel with decoupled control of mechanical rigidity and electrically conductivity. *Biomater. Res.* 21:24. doi: 10.1186/s40824-017-0110-x

Dhamecha, D., Movsas, R., Sano, U., and Menon, J. U. (2019). Applications of alginate microspheres in therapeutics delivery and cell culture: past, present and future. *Int. J. Pharm.* 569:118627. doi: 10.1016/j.ijpharm.2019.118627

Distler, T., and Boccaccini, A. R. (2019). 3D printing of electrically conductive hydrogels for tissue engineering and biosensors - A review. *Acta Biomater.* 101, 1–13. doi: 10.1016/j.actbio.2019.08.044

Domenech, M., Polo-Corrales, L., Ramirez-Vick, J. E., and Freytes, D. O. (2016). Tissue engineering strategies for myocardial regeneration: acellular versus cellular scaffolds? *Tissue Eng. B Rev.* 22, 438–458. doi: 10.1089/ten.TEB.2015.0523

Drury, J. L., Dennis, R. G., and Mooney, D. J. (2004). The tensile properties of alginate hydrogels. *Biomaterials* 25, 3187–3199. doi: 10.1016/j.biomaterials.2003.10.002

Dvir, T., Timko, B. P., Brigham, M. D., Naik, S. R., Karajanagi, S. S., Levy, O., et al. (2011). Nanowired three-dimensional cardiac patches. *Nat. Nanotechnol.* 6, 720–725. doi: 10.1038/nnano.2011.160

Elviri, L., Foresti, R., Bergonzi, C., Zimetti, F., Marchi, C., Bianchera, A., et al. (2017). Highly defined 3D printed chitosan scaffolds featuring improved cell growth. *Biomed. Mater.* 12:045009. doi: 10.1088/1748-605X/aa7692

Epstein, S. E., Fuchs, S., Zhou, Y. F., Baffour, R., and Kornowski, R. (2001). Therapeutic interventions for enhancing collateral development by administration of growth factors: basic principles, early results and potential hazards. *Cardiovasc. Res.* 49, 532–542. doi: 10.1016/s0008-6363(00)00217-0

Ferrini, A., Stevens, M. M., Sattler, S., and Rosenthal, N. (2019). Toward regeneration of the heart: bioengineering strategies for immunomodulation. *Front. Cardiovasc. Med.* 6:26. doi: 10.3389/fcvm.2019.00026

Follin, B., Ghotbi, A. A., Clemmensen, A. E., Bentsen, S., Juhl, M., Søndergaard, R. H., et al. (2018). Retention and functional effect of adipose-derived stromal cells administered in alginate hydrogel in a rat model of acute myocardial infarction. *Stem Cells Int.* 2018:7821461. doi: 10.1155/2018/7821461

Foresti, R., Rossi, S., Pinelli, S., Alinovi, R., Barozzi, M., Sciancalepore, C., et al. (2020a). Highly-defined bioprinting of long-term vascularized scaffolds with Bio-Trap: complex geometry functionalization and process parameters with computer aided tissue engineering. *Materialia* 9:100560. doi: 10.1016/j.mtla.2019.100560

Foresti, R., Rossi, S., Pinelli, S., Alinovi, R., Sciancalepore, C., Delmonte, N., et al. (2020b). In-vivo vascular application via ultra-fast bioprinting for future 5D personalised nanomedicine. *Sci. Rep.* 10:3205. doi: 10.1038/s41598-020-60196-y

Foresti, R., Rossi, S., and Selleri, S. (2019). "Bio composite materials: nano functionalization of 4D bio engineered scaffold," in *Proceedings of the 2019 IEEE International Conference on BioPhotonics*, Taipei, 1–2.

Forrester, J. S., Price, M. J., and Makkar, R. R. (2003). Stem cell repair of infarcted myocardium: an overview for clinicians. *Circulation* 108, 1139–1145. doi: 10.1161/01.CIR.0000085305.82019.65

Freedman, S. B., and Isner, J. M. (2002). Therapeutic angiogenesis for coronary artery disease. *Ann. Intern. Med.* 136, 54–71. doi: 10.7326/0003-4819-136-1-200201010-200201011

French, B. A., and Kramer, C. M. (2007). Mechanisms of post-infarct left ventricular remodeling. *Drug Discov. Today Dis. Mech.* 4, 185–196. doi: 10.1016/j.ddmec.2007.12.006

Frey, N., Linke, A., Suselbeck, T., Muller-Ehmsen, J., Vermeersch, P., Schoors, D., et al. (2014). Intracoronary delivery of injectable bioabsorbable scaffold (IK-5001) to treat left ventricular remodeling after ST-elevation myocardial infarction: a first-in-man study. *Circ. Cardiovasc. Interv.* 7, 806–812. doi: 10.1161/circinterventions.114.001478

Fu, S., Thacker, A., Sperger, D. M., Boni, R. L., Buckner, I. S., Velankar, S., et al. (2011). Relevance of rheological properties of sodium alginate in solution to calcium alginate gel properties. *AAPS Pharm. Sci. Tech.* 12, 453–460. doi: 10.1208/s12249-011-9587-0

Gasparini, G. (2000). Prognostic value of vascular endothelial growth factor in breast cancer. *Oncologist* 5(Suppl. 1), 37–44. doi: 10.1634/theoncologist.5-suppl_1-37

Gauvin, R., Parenteau-Bareil, R., Dokmeci, M. R., Merryman, W. D., and Khademhosseini, A. (2012). Hydrogels and microtechnologies for engineering the cellular microenvironment. *Wiley Interdiscip. Rev. Nanomed. Nanobiotechnol.* 4, 235–246. doi: 10.1002/wnan.171

Gnecchi, M., He, H., Liang, O. D., Melo, L. G., Morello, F., Mu, H., et al. (2005). Paracrine action accounts for marked protection of ischemic heart by Akt-modified mesenchymal stem cells. *Nat. Med.* 11, 367–368. doi: 10.1038/nm0405-367

Gnecchi, M., Zhang, Z., Ni, A., and Dzau, V. J. (2008). Paracrine mechanisms in adult stem cell signaling and therapy. *Circ. Res.* 103, 1204–1219. doi: 10.1161/circresaha.108.176826

Guo, B., and Ma, P. X. (2018). Conducting polymers for tissue engineering. *Biomacromolecules* 19, 1764–1782. doi: 10.1021/acs.biomac.8b00276

Hasan, A., Khattab, A., Islam, M. A., Hweij, K. A., Zeitouny, J., Waters, R., et al. (2015). Injectable hydrogels for cardiac tissue repair after myocardial infarction. *Adv. Sci.* 2:1500122. doi: 10.1002/advs.201500122

Hattori, H., Amano, Y., Nogami, Y., Takase, B., and Ishihara, M. (2010). Hemostasis for severe hemorrhage with photocrosslinkable chitosan hydrogel and calcium alginate. *Ann. Biomed. Eng.* 38, 3724–3732. doi: 10.1007/s10439-010-0121-124

Haugstad, K., Håti, A., Nordgard, C., Adl, P., Maurstad, G., Sletmoen, M., et al. (2015). Direct determination of chitosan–mucin interactions using a single-molecule strategy: comparison to alginate–mucin interactions. *Polymers* 7, 161–185. doi: 10.3390/polym7020161

Hecht, H., and Srebnik, S. (2016). Structural characterization of sodium alginate and calcium alginate. *Biomacromolecules* 17, 2160–2167. doi: 10.1021/acs.biomac.6b00378

Henry, T. D., Annex, B. H., McKendall, G. R., Azrin, M. A., Lopez, J. J., Giordano, F. J., et al. (2003). The VIVA trial: vascular endothelial growth factor in Ischemia for Vascular Angiogenesis. *Circulation* 107, 1359–1365. doi: 10.1161/01.cir.0000061911.47710.8a

Hirt, M. N., Hansen, A., and Eschenhagen, T. (2014). Cardiac tissue engineering: state of the art. *Circ. Res.* 114, 354–367. doi: 10.1161/circresaha.114.300522

Homaeigohar, S., Tsai, T. Y., Young, T. H., Yang, H. J., and Ji, Y. R. (2019). An electroactive alginate hydrogel nanocomposite reinforced by functionalized graphite nanofilaments for neural tissue engineering. *Carbohydr. Polym.* 224:115112. doi: 10.1016/j.carbpol.2019.115112

Huang, G., Li, F., Zhao, X., Ma, Y., Li, Y., Lin, M., et al. (2017). Functional and biomimetic materials for engineering of the three-dimensional cell microenvironment. *Chem. Rev.* 117, 12764–12850. doi: 10.1021/acs.chemrev.7b00094

Hynes, R. O. (2009). The extracellular matrix: not just pretty fibrils. *Science* 326, 1216–1219. doi: 10.1126/science.1176009

Ieda, M., Fu, J. D., Delgado-Olguin, P., Vedantham, V., Hayashi, Y., Bruneau, B. G., et al. (2010). Direct reprogramming of fibroblasts into functional cardiomyocytes by defined factors. *Cell* 142, 375–386. doi: 10.1016/j.cell.2010.07.002

Jiang, L., Wang, Y., Liu, Z., Ma, C., Yan, H., Xu, N., et al. (2019). Three-dimensional printing and injectable conductive hydrogels for tissue engineering application. *Tissue Eng. Part B Rev.* 25, 398–411. doi: 10.1089/ten.TEB.2019.0100

Jorgensen, T. E., Sletmoen, M., Draget, K. I., and Stokke, B. T. (2007). Influence of oligoguluronates on alginate gelation, kinetics, and polymer organization. *Biomacromolecules* 8, 2388–2397. doi: 10.1021/bm070208d

Kaklamani, G., Cheneler, D., Grover, L. M., Adams, M. J., and Bowen, J. (2014). Mechanical properties of alginate hydrogels manufactured using external gelation. *J. Mech. Behav. Biomed. Mater.* 36, 135–142. doi: 10.1016/j.jmbbm.2014.04.013

Kambe, Y., and Yamaoka, T. (2019). Biodegradation of injectable silk fibroin hydrogel prevents negative left ventricular remodeling after myocardial infarction. *Biomater. Sci.* 7, 4153–4165. doi: 10.1039/c9bm00556k

Kc, P., Hong, Y., and Zhang, G. (2019). Cardiac tissue-derived extracellular matrix scaffolds for myocardial repair: advantages and challenges. *Regen. Biomater.* 6, 185–199. doi: 10.1093/rb/rbz017

Ketabat, F., Karkhaneh, A., Mehdinavaz Aghdam, R., and Hossein Ahmadi Tafti, S. (2017). Injectable conductive collagen/alginate/polypyrrole hydrogels as a biocompatible system for biomedical applications. *J. Biomater. Sci. Polym. Ed.* 28, 794–805. doi: 10.1080/09205063.2017.1302314

Khan, S., Tondervik, A., Sletta, H., Klinkenberg, G., Emanuel, C., Onsoyen, E., et al. (2012). Overcoming drug resistance with alginate oligosaccharides able to potentiate the action of selected antibiotics. *Antimicrob. Agents Chemother.* 56, 5134–5141. doi: 10.1128/Aac.00525-512

Kinnaird, T., Stabile, E., Burnett, M. S., Lee, C. W., Barr, S., Fuchs, S., et al. (2004). Marrow-derived stromal cells express genes encoding a broad spectrum of arteriogenic cytokines and promote in vitro and in vivo arteriogenesis through paracrine mechanisms. *Circ. Res.* 94, 678–685. doi: 10.1161/01.Res.0000118601.37875.Ac

Kong, H.-J., Lee, K. Y., and Mooney, D. J. (2002). Decoupling the dependence of rheological/mechanical properties of hydrogels from solids concentration. *Polymer* 43, 6239–6246. doi: 10.1016/S0032-3861(02)00559-551

Kong, H. J., and Mooney, D. J. (2003). The effects of poly(ethyleneimine) (PEI) molecular weight on reinforcement of alginate hydrogels. *Cell Transplant.* 12, 779–785. doi: 10.3727/000000003108747253

Kong, H. J., Smith, M. K., and Mooney, D. J. (2003). Designing alginate hydrogels to maintain viability of immobilized cells. *Biomaterials* 24, 4023–4029. doi: 10.1016/s0142-9612(03)00295-293

Kuo, C. K., and Ma, P. X. (2001). Ionically crosslinked alginate hydrogels as scaffolds for tissue engineering: part 1. Structure, gelation rate and mechanical properties. *Biomaterials* 22, 511–521. doi: 10.1016/s0142-9612(00)00201-205

Lau, T. T., and Wang, D. A. (2011). Stromal cell-derived factor-1 (SDF-1): homing factor for engineered regenerative medicine. *Expert Opin. Biol. Ther.* 11, 189–197. doi: 10.1517/14712598.2011.546338

Lee, J.-B., Takeshita, A., Hayashi, K., and Hayashi, T. (2011). Structures and antiviral activities of polysaccharides from Sargassum trichophyllum. *Carbohydr. Polym.* 86, 995–999. doi: 10.1016/j.carbpol.2011.05.059

Lee, K. Y., and Mooney, D. J. (2012). Alginate: properties and biomedical applications. *Prog. Polym. Sci.* 37, 106–126. doi: 10.1016/j.progpolymsci.2011.06.003

Lee, L. C., Wall, S. T., Klepach, D., Ge, L., Zhang, Z., Lee, R. J., et al. (2013). Algisyl-LVR with coronary artery bypass grafting reduces left ventricular wall stress and improves function in the failing human heart. *Int. J. Cardiol.* 168, 2022–2028. doi: 10.1016/j.ijcard.2013.01.003

Lee, R. J., Hinson, A., Bauernschmitt, R., Matschke, K., Fang, Q., Mann, D. L., et al. (2015). The feasibility and safety of Algisyl-LVR as a method of left ventricular augmentation in patients with dilated cardiomyopathy: initial first in man clinical results. *Int. J. Cardiol.* 199, 18–24. doi: 10.1016/j.ijcard.2015.06.111

Lee, R. J., Springer, M. L., Blanco-Bose, W. E., Shaw, R., Ursell, P. C., and Blau, H. M. (2000). VEGF gene delivery to myocardium: deleterious effects of unregulated expression. *Circulation* 102, 898–901. doi: 10.1161/01.cir.102.8.898

Leitolis, A., Robert, A. W., Pereira, I. T., Correa, A., and Stimamiglio, M. A. (2019). Cardiomyogenesis modeling using pluripotent stem cells: the role of microenvironmental signaling. *Front. Cell Dev. Biol.* 7:164. doi: 10.3389/fcell.2019.00164

Leor, J., Gerecht, S., Cohen, S., Miller, L., Holbova, R., Ziskind, A., et al. (2007). Human embryonic stem cell transplantation to repair the infarcted myocardium. *Heart* 93, 1278–1284. doi: 10.1136/hrt.2006.093161

LeRoux, M. A., Guilak, F., and Setton, L. A. (1999). Compressive and shear properties of alginate gel: effects of sodium ions and alginate concentration. *J. Biomed. Mater. Res.* 47, 46–53. doi: 10.1002/(sici)1097-4636(199910)47:1<46::aid-jbm6<3.0.co;2-n

Li, W., Guan, T., Zhang, X., Wang, Z., Wang, M., Zhong, W., et al. (2015). The effect of layer-by-layer assembly coating on the proliferation and differentiation of neural stem cells. *ACS Appl. Mater. Interfaces* 7, 3018–3029. doi: 10.1021/am504456t

Liang, W., Chen, J., Li, L., Li, M., Wei, X., Tan, B., et al. (2019). Conductive hydrogen sulfide-releasing hydrogel encapsulating ADSCs for myocardial infarction treatment. *ACS Appl. Mater. Interfaces* 11, 14619–14629. doi: 10.1021/acsami.9b01886

Lin, H. R., Sung, K. C., and Vong, W. J. (2004). In situ gelling of alginate/pluronic solutions for ophthalmic delivery of pilocarpine. *Biomacromolecules* 5, 2358–2365. doi: 10.1021/bm0496965

Liu, G., Li, L., Huo, D., Li, Y., Wu, Y., Zeng, L., et al. (2017). A VEGF delivery system targeting MI improves angiogenesis and cardiac function based on the tropism of MSCs and layer-by-layer self-assembly. *Biomaterials* 127, 117–131. doi: 10.1016/j.biomaterials.2017.03.001

Liu, Y., Ye, X., Mao, L., Cheng, Z., Yao, X., Jia, X., et al. (2013). Transplantation of parthenogenetic embryonic stem cells ameliorates cardiac dysfunction and remodelling after myocardial infarction. *Cardiovasc. Res.* 97, 208–218. doi: 10.1093/cvr/cvs314

Maciel, D., Figueira, P., Xiao, S., Hu, D., Shi, X., Rodrigues, J., et al. (2013). Redox-responsive alginate nanogels with enhanced anticancer cytotoxicity. *Biomacromolecules* 14, 3140–3146. doi: 10.1021/bm400768m

Maharaj, A. S., and D'Amore, P. A. (2007). Roles for VEGF in the adult. *Microvasc. Res.* 74, 100–113. doi: 10.1016/j.mvr.2007.03.004

Mahdi, M. H., Diryak, R., Kontogiorgos, V., Morris, G. A., and Smith, A. M. (2016). In situ rheological measurements of the external gelation of alginate. *Food Hydrocolloids* 55, 77–80. doi: 10.1016/j.foodhyd.2015.11.002

Mann, D. L., Lee, R. J., Coats, A. J., Neagoe, G., Dragomir, D., Pusineri, E., et al. (2016). One-year follow-up results from AUGMENT-HF: a multicentre randomized controlled clinical trial of the efficacy of left ventricular augmentation with Algisyl in the treatment of heart failure. *Eur. J. Heart Fail.* 18, 314–325. doi: 10.1002/ejhf.449

Martinsen, A., Skjåk-Bræk, G., and Smidsrød, O. (1989). Alginate as immobilization material: I. Correlation between chemical and physical properties of alginate gel beads. *Biotechnol. Bioeng.* 33, 79–89. doi: 10.1002/bit.260330111

McLaughlin, S., McNeill, B., Podrebarac, J., Hosoyama, K., Sedlakova, V., Cron, G., et al. (2019). Injectable human recombinant collagen matrices limit adverse remodeling and improve cardiac function after myocardial infarction. *Nat. Commun.* 10:4866. doi: 10.1038/s41467-019-12748-12748

Meiyu, G., Fuchuan, L., Xianliang, X., Jing, L., Zuowei, Y., and Huashi, G. (2003). The potential molecular targets of marine sulfated polymannuroguluronate interfering with HIV-1 entry. Interaction between SPMG and HIV-1 rgp120 and CD4 molecule. *Antiviral Res.* 59, 127–135. doi: 10.1016/s0166-3542(03)00068-68

Miao, T., Wang, J., Zeng, Y., Liu, G., and Chen, X. (2018). Polysaccharide-based controlled release systems for therapeutics delivery and tissue engineering: from bench to bedside. *Adv. Sci.* 5:1700513. doi: 10.1002/advs.201700513

Milazzo, M., Contessi Negrini, N., Scialla, S., Marelli, B., Farè, S., Danti, S., et al. (2019). Additive manufacturing approaches for hydroxyapatite-reinforced composites. *Adv. Funct. Mater.* 29:1903055. doi: 10.1002/adfm.201903055

Mitter, S. S., and Yancy, C. W. (2017). Contemporary approaches to patients with heart failure. *Cardiol. Clin.* 35, 261–271. doi: 10.1016/j.ccl.2016.12.008

Mythri, G., Kavitha, K., Kumar, M. R., and Singh, S. D. (2011). Novel mucoadhesive polymers- A review. *J. Appl. Pharm. Sci.* 1, 37–42.

Nagaya, N., Fujii, T., Iwase, T., Ohgushi, H., Itoh, T., Uematsu, M., et al. (2004). Intravenous administration of mesenchymal stem cells improves cardiac function in rats with acute myocardial infarction through angiogenesis and myogenesis. *Am. J. Physiol. Heart Circ. Physiol.* 287, H2670–H2676. doi: 10.1152/ajpheart.01071.2003

Namvar, F., Mohamad, R., Baharara, J., Zafar-Balanejad, S., Fargahi, F., and Rahman, H. S. (2013). Antioxidant, antiproliferative, and antiangiogenesis effects of polyphenol-rich seaweed (*Sargassum muticum*). *Biomed. Res. Int.* 2013:604787. doi: 10.1155/2013/604787

Nemati, S., Rezabakhsh, A., Khoshfetrat, A. B., Nourazarian, A., Biray Avci, C., Goker Bagca, B., et al. (2017). Alginate-gelatin encapsulation of human endothelial cells promoted angiogenesis in in vivo and in vitro milieu. *Biotechnol. Bioeng.* 114, 2920–2930. doi: 10.1002/bit.26395

Niekraszewicz, B., and Niekraszewicz, A. (2009). "8 - The structure of alginate, chitin and chitosan fibres," in *Handbook of Textile Fibre Structure*, eds S. J. Eichhorn, J. W. S. Hearle, M. Jaffe, and T. Kikutani (Sawston: Woodhead Publishing), 266–304.

Ochbaum, G., Davidovich-Pinhas, M., and Bitton, R. (2018). Tuning the mechanical properties of alginate-peptide hydrogels. *Soft. Matter.* 14, 4364–4373. doi: 10.1039/c8sm00059j

Oduk, Y., Zhu, W., Kannappan, R., Zhao, M., Borovjagin, A. V., Oparil, S., et al. (2018). VEGF nanoparticles repair the heart after myocardial infarction. *Am. J. Physiol. Heart Circ. Physiol.* 314, H278–H284. doi: 10.1152/ajpheart.00471.2017

Ongstad, E. L., and Gourdie, R. G. (2016). Can heart function lost to disease be regenerated by therapeutic targeting of cardiac scar tissue? *Semin. Cell Dev. Biol.* 58, 41–54. doi: 10.1016/j.semcdb.2016.05.020

Ozbolat, I. T., and Hospodiuk, M. (2016). Current advances and future perspectives in extrusion-based bioprinting. *Biomaterials* 76, 321–343. doi: 10.1016/j.biomaterials.2015.10.076

Paques, J. P., van der Linden, E., van Rijn, C. J., and Sagis, L. M. (2014). Preparation methods of alginate nanoparticles. *Adv. Colloid Interface Sci.* 209, 163–171. doi: 10.1016/j.cis.2014.03.009

Pawar, S. N., and Edgar, K. J. (2012). Alginate derivatization: a review of chemistry, properties and applications. *Biomaterials* 33, 3279–3305. doi: 10.1016/j.biomaterials.2012.01.007

Pena, B., Laughter, M., Jett, S., Rowland, T. J., Taylor, M. R. G., Mestroni, L., et al. (2018). Injectable hydrogels for cardiac tissue engineering. *Macromol. Biosci.* 18:e1800079. doi: 10.1002/mabi.201800079

Pritchard, M. F., Powell, L. C., Menzies, G. E., Lewis, P. D., Hawkins, K., Wright, C., et al. (2016). A new class of safe oligosaccharide polymer therapy to modify the mucus barrier of chronic respiratory disease. *Mol. Pharm.* 13, 863–872. doi: 10.1021/acs.molpharmaceut.5b00794

Rao, S. V., Zeymer, U., Douglas, P. S., Al-Khalidi, H., Liu, J., Gibson, C. M., et al. (2015). A randomized, double-blind, placebo-controlled trial to evaluate the safety and effectiveness of intracoronary application of a novel bioabsorbable cardiac matrix for the prevention of ventricular remodeling after large ST-segment elevation myocardial infarction: rationale and design of the PRESERVATION I trial. *Am. Heart. J* 170, 929–937. doi: 10.1016/j.ahj.2015.08.017

Rao, S. V., Zeymer, U., Douglas, P. S., Al-Khalidi, H., White, J. A., Liu, J., et al. (2016). Bioabsorbable intracoronary matrix for prevention of ventricular remodeling after myocardial infarction. *J. Am. Coll. Cardiol.* 68, 715–723. doi: 10.1016/j.jacc.2016.05.053

Ravnic, D. J., Leberfinger, A. N., Koduru, S. V., Hospodiuk, M., Moncal, K. K., Datta, P., et al. (2017). Transplantation of bioprinted tissues and organs: technical and clinical challenges and future perspectives. *Ann. Surg.* 266, 48–58. doi: 10.1097/sla.0000000000002141

Remminghorst, U., and Rehm, B. H. A. (2006). Bacterial alginates: from biosynthesis to applications. *Biotechnol. Lett.* 28, 1701–1712. doi: 10.1007/s10529-006-9156-x

Ren, K., Cheng, Y., Huang, C., Chen, R., Wang, Z., and Wei, J. (2019). Self-healing conductive hydrogels based on alginate, gelatin and polypyrrole serve

as a repairable circuit and a mechanical sensor. *J. Mater. Chem. B* 7, 5704–5712. doi: 10.1039/c9tb01214a

Rocha de Souza, M. C., Marques, C. T., Guerra Dore, C. M., Ferreira da Silva, F. R., Oliveira Rocha, H. A., and Leite, E. L. (2007). Antioxidant activities of sulfated polysaccharides from brown and red seaweeds. *J. Appl. Phycol.* 19, 153–160. doi: 10.1007/s10811-006-9121-z

Rodness, J., Mihic, A., Miyagi, Y., Wu, J., Weisel, R. D., and Li, R.-K. (2016). VEGF-loaded microsphere patch for local protein delivery to the ischemic heart. *Acta Biomater.* 45, 169–181. doi: 10.1016/j.actbio.2016.09.009

Ruvinov, E., and Cohen, S. (2016). Alginate biomaterial for the treatment of myocardial infarction: progress, translational strategies, and clinical outlook: from ocean algae to patient bedside. *Adv. Drug Deliv. Rev* 96, 54–76. doi: 10.1016/j.addr.2015.04.021

Sabbah, H. N., Wang, M., Gupta, R. C., Rastogi, S., Ilsar, I., Sabbah, M. S., et al. (2013). Augmentation of left ventricular wall thickness with alginate hydrogel implants improves left ventricular function and prevents progressive remodeling in dogs with chronic heart failure. *JACC Heart Fail.* 1, 252–258. doi: 10.1016/j.jchf.2013.02.006

Sachan, N., Pushkar, S., Jha, A., and Bhattcharya, A. (2009). Sodium alginate: the wonder polymer for controlled drug delivery. *J. Pharmacy Res.* 2, 1191–1199.

Saludas, L., Pascual-Gil, S., Prosper, F., Garbayo, E., and Blanco-Prieto, M. (2017). Hydrogel based approaches for cardiac tissue engineering. *Int. J. Pharm.* 523, 454–475. doi: 10.1016/j.ijpharm.2016.10.061

Sanganalmath, S. K., and Bolli, R. (2013). Cell therapy for heart failure: a comprehensive overview of experimental and clinical studies, current challenges, and future directions. *Circ. Res.* 113, 810–834. doi: 10.1161/circresaha.113.300219

Sano, Y. (1999). Antiviral activity of alginate against infection by tobacco mosaic virus. *Carbohydr. Polym.* 38, 183–186. doi: 10.1016/S0144-8617(98)00119-112

Saygili, E., Dogan-Gurbuz, A. A., Yesil-Celiktas, O., and Draz, M. S. (2019). 3D bioprinting: a powerful tool to leverage tissue engineering and microbial systems. *Bioprinting* 18:e00071. doi: 10.1016/j.bprint.2019.e00071

Seif-Naraghi, S. B., Singelyn, J. M., Salvatore, M. A., Osborn, K. G., Wang, J. J., Sampat, U., et al. (2014). Safety and efficacy of an injectable extracellular matrix hydrogel for treating myocardial infarction. *Sci. Transl. Med.* 6::233er2. doi: 10.1126/scitranslmed.3005503

Sekiya, N., Matsumiya, G., Miyagawa, S., Saito, A., Shimizu, T., Okano, T., et al. (2009). Layered implantation of myoblast sheets attenuates adverse cardiac remodeling of the infarcted heart. *J. Thorac. Cardiovasc. Surg.* 138, 985–993. doi: 10.1016/j.jtcvs.2009.02.004

Sepantafar, M., Maheronnaghsh, R., Mohammadi, H., Rajabi-Zeleti, S., Annabi, N., Aghdami, N., et al. (2016). Stem cells and injectable hydrogels: synergistic therapeutics in myocardial repair. *Biotechnol. Adv.* 34, 362–379. doi: 10.1016/j.biotechadv.2016.03.003

Shachar, M., Tsur-Gang, O., Dvir, T., Leor, J., and Cohen, S. (2011). The effect of immobilized RGD peptide in alginate scaffolds on cardiac tissue engineering. *Acta Biomater.* 7, 152–162. doi: 10.1016/j.actbio.2010.07.034

Shi, Z., Gao, X., Ullah, M. W., Li, S., Wang, Q., and Yang, G. (2016). Electroconductive natural polymer-based hydrogels. *Biomaterials* 111, 40–54. doi: 10.1016/j.biomaterials.2016.09.020

Shi, Z., Li, Y., Chen, X., Han, H., and Yang, G. (2014). Double network bacterial cellulose hydrogel to build a biology-device interface. *Nanoscale* 6, 970–977. doi: 10.1039/c3nr05214a

Shi, Z., Phillips, G. O., and Yang, G. (2013). Nanocellulose electroconductive composites. *Nanoscale* 5, 3194–3201. doi: 10.1039/c3nr00408b

Shi, Z., Zang, S., Jiang, F., Huang, L., Lu, D., Ma, Y., et al. (2012). In situ nano-assembly of bacterial cellulose–polyaniline composites. *RSC Adv.* 2, 1040–1046. doi: 10.1039/C1RA00719J

Shin, S. R., Jung, S. M., Zalabany, M., Kim, K., Zorlutuna, P., Kim, S. B., et al. (2013). Carbon-nanotube-embedded hydrogel sheets for engineering cardiac constructs and bioactuators. *ACS Nano* 7, 2369–2380. doi: 10.1021/nn305559j

Son, E. H., Moon, E. Y., Rhee, D. K., and Pyo, S. (2001). Stimulation of various functions in murine peritoneal macrophages by high mannuronic acid-containing alginate (HMA) exposure *in vivo*. *Int. Immunopharmacol.* 1, 147–154. doi: 10.1016/s1567-5769(00)00012-16

Son, E. W., Rhee, D. K., and Pyo, S. (2003). Antiviral and tumoricidal activities of alginate-stimulated macrophages are mediated by different mechanisms. *Arch. Pharm. Res.* 26, 960–966. doi: 10.1007/bf02980206

Sosnik, A. (2014). Alginate particles as platform for drug delivery by the oral route: state-of-the-art. *ISRN Pharm.* 2014:926157. doi: 10.1155/2014/926157

Spinali, K. L., and Schmuck, E. G. (2018). Natural sources of extracellular matrix for cardiac repair. *Adv. Exp. Med. Biol.* 1098, 115–130. doi: 10.1007/978-3-319-97421-7_6

Sun, J., and Tan, H. (2013). Alginate-based biomaterials for regenerative medicine applications. *Materials* 6, 1285–1309. doi: 10.3390/ma6041285

Suzuki, K., Murtuza, B., Beauchamp, J. R., Brand, N. J., Barton, P. J., Varela-Carver, A., et al. (2004). Role of interleukin-1beta in acute inflammation and graft death after cell transplantation to the heart. *Circulation* 110(11 Suppl. 1), Ii219–Ii224. doi: 10.1161/01.Cir.0000138388.55416.06

Szekalska, M., Puciłowska, A., Szymańska, E., Winnicka, K., et al. (2016). Alginate: current use and future perspectives in pharmaceutical and biomedical applications. *Int. J. Polym. Sci.* 2016:17. doi: 10.1155/2016/7697031

Taylor, C., Pearson, J. P., Draget, K. I., Dettmar, P. W., and Smidsrød, O. (2005). Rheological characterisation of mixed gels of mucin and alginate. *Carbohydr. Polym.* 59, 189–195. doi: 10.1016/j.carbpol.2004.09.009

Terakado, S., Ueno, M., Tamura, Y., Toda, N., Yoshinaga, M., Otsuka, K., et al. (2012). Sodium alginate oligosaccharides attenuate hypertension and associated kidney damage in Dahl salt-sensitive rats fed a high-salt diet. *Clin. Exp. Hypertens.* 34, 99–106. doi: 10.3109/10641963.2011.618196

Thygesen, K., Alpert, J. S., and White, H. D. (2007). Universal definition of myocardial infarction. *Eur. Heart J.* 28, 2525–2538. doi: 10.1093/eurheartj/ehm355

Tous, E., Purcell, B., Ifkovits, J. L., and Burdick, J. A. (2011). Injectable acellular hydrogels for cardiac repair. *J. Cardiovasc. Transl. Res.* 4, 528–542. doi: 10.1007/s12265-011-9291-9291

van den Akker, F., Deddens, J. C., Doevendans, P. A., and Sluijter, J. P. (2013). Cardiac stem cell therapy to modulate inflammation upon myocardial infarction. *Biochim. Biophys. Acta* 1830, 2449–2458. doi: 10.1016/j.bbagen.2012.08.026

van den Akker, F., Feyen, D. A., van den Hoogen, P., van Laake, L. W., van Eeuwijk, E. C., Hoefer, I., et al. (2017). Intramyocardial stem cell injection: go(ne) with the flow. *Eur. Heart J.* 38, 184–186. doi: 10.1093/eurheartj/ehw056

Venkatesan, J., Bhatnagar, I., Manivasagan, P., Kang, K.-H., and Kim, S.-K. (2015). Alginate composites for bone tissue engineering: a review. *Int. J. Biol. Macromol.* 72, 269–281. doi: 10.1016/j.ijbiomac.2014.07.008

Veriter, S., Mergen, J., Goebbels, R. M., Aouassar, N., Gregoire, C., Jordan, B., et al. (2010). In vivo selection of biocompatible alginates for islet encapsulation and subcutaneous transplantation. *Tissue Eng. Part A* 16, 1503–1513. doi: 10.1089/ten.TEA.2009.0286

Wang, S. X., Zhang, X. S., Guan, H. S., and Wang, W. (2014). Potential anti-HPV and related cancer agents from marine resources: an overview. *Mar. Drugs* 12, 2019–2035. doi: 10.3390/md12042019

Weinberger, F., Mannhardt, I., and Eschenhagen, T. (2017). Engineering cardiac muscle tissue: a maturating field of research. *Circ. Res.* 120, 1487–1500. doi: 10.1161/CIRCRESAHA.117.310738

Witvrouw, M., and De Clercq, E. (1997). Sulfated polysaccharides extracted from sea algae as potential antiviral drugs. *Gen. Pharmacol.* 29, 497–511. doi: 10.1016/s0306-3623(96)00563-560

Wu, J. L., Wang, C. Q., Zhuo, R. X., and Cheng, S. X. (2014). Multi-drug delivery system based on alginate/calcium carbonate hybrid nanoparticles for combination chemotherapy. *Coll. Surf. B Biointerfaces* 123, 498–505. doi: 10.1016/j.colsurfb.2014.09.047

Wu, Y., Chen, Y. X., Yan, J., Yang, S., Dong, P., and Soman, P. (2015). Fabrication of conductive polyaniline hydrogel using porogen leaching and projection microstereolithography. *J. Mater. Chem. B* 3, 5352–5360. doi: 10.1039/C5TB00629E

Xu, Y., Zhan, C., Fan, L., Wang, L., and Zheng, H. (2007). Preparation of dual crosslinked alginate–chitosan blend gel beads and in vitro controlled release in oral site-specific drug delivery system. *Int. J. Pharm.* 336, 329–337. doi: 10.1016/j.ijpharm.2006.12.019

Yamamoto, Y., Kurachi, M., Yamaguchi, K., and Oda, T. (2007). Stimulation of multiple cytokine production in mice by alginate oligosaccharides following intraperitoneal administration. *Carbohydr. Res.* 342, 1133–1137. doi: 10.1016/j.carres.2007.02.015

Yan, G. L., Guo, Y. M., Yuan, J. M., Liu, D., and Zhang, B. K. (2011). Sodium alginate oligosaccharides from brown algae inhibit *Salmonella* enteritidis colonization in broiler chickens. *Poult. Sci.* 90, 1441–1448. doi: 10.3382/ps.2011-1364

Yang, S., Jang, L., Kim, S., Yang, J., Yang, K., Cho, S. W., et al. (2016). Polypyrrole/alginate hybrid hydrogels: electrically conductive and soft biomaterials for human mesenchymal stem cell culture and potential neural tissue engineering applications. *Macromol. Biosci.* 16, 1653–1661. doi: 10.1002/mabi.201600148

Yang, S. H., Kang, S. M., Lee, K. B., Chung, T. D., Lee, H., and Choi, I. S. (2011). Mussel-inspired encapsulation and functionalization of individual yeast cells. *J. Am. Chem. Soc.* 133, 2795–2797. doi: 10.1021/ja1100189

Yang, W., Xu, H., Lan, Y., Zhu, Q., Liu, Y., Huang, S., et al. (2019). Preparation and characterisation of a novel silk fibroin/hyaluronic acid/sodium alginate scaffold for skin repair. *Int. J. Biol. Macromol.* 130, 58–67. doi: 10.1016/j.ijbiomac.2019.02.120

Ye, Z., Zhou, Y., Cai, H., and Tan, W. (2011). Myocardial regeneration: roles of stem cells and hydrogels. *Adv. Drug Deliv. Rev* 63, 688–697. doi: 10.1016/j.addr.2011.02.007

Yeung, E., Fukunishi, T., Bai, Y., Bedja, D., Pitaktong, I., Mattson, G., et al. (2019). Cardiac regeneration using human-induced pluripotent stem cell-derived biomaterial-free 3D-bioprinted cardiac patch *in vivo*. *J. Tissue Eng. Regen. Med.* 13, 2031–2039. doi: 10.1002/term.2954

Zacchigna, S., and Giacca, M. (2014). Extra- and intracellular factors regulating cardiomyocyte proliferation in postnatal life. *Cardiovasc. Res.* 102, 312–320. doi: 10.1093/cvr/cvu057

Zhang, L., Li, Y., Li, L., Guo, B., and Ma, P. X. (2014). Non-cytotoxic conductive carboxymethyl-chitosan/aniline pentamer hydrogels. *React. Funct. Polym.* 82, 81–88. doi: 10.1016/j.reactfunctpolym.2014.06.003

Zhao, S., Xu, Z., Wang, H., Reese, B. E., Gushchina, L. V., Jiang, M., et al. (2016). Bioengineering of injectable encapsulated aggregates of pluripotent stem cells for therapy of myocardial infarction. *Nat. Commun.* 7:13306. doi: 10.1038/ncomms13306

Zhao, Y., Shen, W., Chen, Z., and Wu, T. (2016). Freeze-thaw induced gelation of alginates. *Carbohydr. Polym.* 148, 45–51. doi: 10.1016/j.carbpol.2016.04.047

Zietz, C., Rossle, M., Haas, C., Sendelhofert, A., Hirschmann, A., Sturzl, M., et al. (1998). MDM-2 oncoprotein overexpression, p53 gene mutation, and VEGF up-regulation in angiosarcomas. *Am. J. Pathol.* 153, 1425–1433. doi: 10.1016/s0002-9440(10)65729-x

Zuppinger, C. (2019). 3D cardiac cell culture: a critical review of current technologies and applications. *Front. Cardiovasc. Med.* 6:87. doi: 10.3389/fcvm.2019.00087

Conflict of Interest: The authors declare that the research was conducted in the absence of any commercial or financial relationships that could be construed as a potential conflict of interest.

Copyright © 2020 Cattelan, Guerrero Gerbolés, Foresti, Pramstaller, Rossini, Miragoli and Caffarra Malvezzi. This is an open-access article distributed under the terms of the Creative Commons Attribution License (CC BY). The use, distribution or reproduction in other forums is permitted, provided the original author(s) and the copyright owner(s) are credited and that the original publication in this journal is cited, in accordance with accepted academic practice. No use, distribution or reproduction is permitted which does not comply with these terms.

frontiers in Bioengineering and Biotechnology

REVIEW
published: 13 May 2020
doi: 10.3389/fbioe.2020.00447

Young at Heart: Combining Strategies to Rejuvenate Endogenous Mechanisms of Cardiac Repair

Edoardo Maghin[1,2†], Patrizia Garbati[3†], Rodolfo Quarto[3,4], Martina Piccoli[1†] and Sveva Bollini[3*†]*

[1] Tissue Engineering Laboratory, Fondazione Istituto di Ricerca Pediatrica Città della Speranza, Padua, Italy, [2] Department of Women's and Children Health, University of Padova, Padua, Italy, [3] Regenerative Medicine Laboratory, Department of Experimental Medicine, University of Genova, Genova, Italy, [4] UOC Cellular Oncology, IRCCS Ospedale Policlinico San Martino, Genova, Italy

OPEN ACCESS

Edited by:
Susanna Sartori,
Politecnico di Torino, Italy

Reviewed by:
Ziad Julier,
Australian Regenerative Medicine Institute (ARMI), Australia
Giovanni Vozzi,
University of Pisa, Italy
Anny Waloski Robert,
Oswaldo Cruz Institute, Oswaldo Cruz Foundation (Fiocruz), Brazil

***Correspondence:**
Martina Piccoli
m.piccoli@irpcds.org
Sveva Bollini
sveva.bollini@unige.it

[†] These authors have contributed equally to this work

Specialty section:
This article was submitted to Tissue Engineering and Regenerative Medicine, a section of the journal Frontiers in Bioengineering and Biotechnology

Received: 17 January 2020
Accepted: 17 April 2020
Published: 13 May 2020

Citation:
Maghin E, Garbati P, Quarto R, Piccoli M and Bollini S (2020) Young at Heart: Combining Strategies to Rejuvenate Endogenous Mechanisms of Cardiac Repair. Front. Bioeng. Biotechnol. 8:447. doi: 10.3389/fbioe.2020.00447

True cardiac regeneration of the injured heart has been broadly described in lower vertebrates by active replacement of lost cardiomyocytes to functionally and structurally restore the myocardial tissue. On the contrary, following severe injury (i.e., myocardial infarction) the adult mammalian heart is endowed with an impaired reparative response by means of meager wound healing program and detrimental remodeling, which can lead over time to cardiomyopathy and heart failure. Lately, a growing body of basic, translational and clinical studies have supported the therapeutic use of stem cells to provide myocardial regeneration, with the working hypothesis that stem cells delivered to the cardiac tissue could result into new cardiovascular cells to replenish the lost ones. Nevertheless, multiple independent evidences have demonstrated that injected stem cells are more likely to modulate the cardiac tissue via beneficial paracrine effects, which can enhance cardiac repair and reinstate the embryonic program and cell cycle activity of endogenous cardiac stromal cells and resident cardiomyocytes. Therefore, increasing interest has been addressed to the therapeutic profiling of the stem cell-derived *secretome* (namely the total of cell-secreted soluble factors), with specific attention to cell-released extracellular vesicles, including exosomes, carrying cardioprotective and regenerative RNA molecules. In addition, the use of cardiac decellularized extracellular matrix has been recently suggested as promising biomaterial to develop novel therapeutic strategies for myocardial repair, as either source of molecular cues for regeneration, biological scaffold for cardiac tissue engineering or biomaterial platform for the functional release of factors. In this review, we will specifically address the translational relevance of these two approaches with *ad hoc* interest in their feasibility to rejuvenate endogenous mechanisms of cardiac repair up to functional regeneration.

Keywords: paracrine, extracellular matrix, decellularization, cardiac repair, regeneration, extracellular vesicles, stem cell

DIVIDE AND CONQUER CARDIAC REPAIR AND TRUE HEART REGENERATION

Cardiovascular disorders significantly affect life expectancy; according to the World Health Organization (WHO), by 2030 about 23 million people annually will be severely affected by heart failure (Leone et al., 2015; Mozaffarian et al., 2015; Benjamin et al., 2018). Cardiac dysfunction may arise by significant loss of resident cardiomyocytes. Indeed, prolonged interruption of coronary blood circulation can cause myocardial infarction (MI) with consequent cardiomyocyte irreversible damage, leading to the development of fibrotic tissue that replaces the contractile myocardium. The injured heart can activate limited wound healing as life-saving mechanism to avoid cardiac rupture. This leads to maladaptive ventricle remodeling and compensatory cardiac hypertrophy leading to heart failure over time (Frantz et al., 2009). Despite significant improvements, interventional cardiology and prompt pharmacological treatments after MI cannot reverse cardiac damage, as they may only minimize cardiomyocyte death or delay heart failure onset (Ezekowitz et al., 2009). Thus, the most effective therapeutic approach is still represented by heart transplantation, with severe limitations due to donor organ availability and compatibility (Hsich, 2016). Since there is an unmet clinical need for current therapies to replenish loss of cardiomyocytes and vasculature, many efforts have been currently focusing on defining novel therapeutic strategies to implement myocardial repair and regeneration.

Notably, full regeneration of the injured heart is a well-established process in lower vertebrates, as opposite to the adult mammalian myocardium. The teleost fish has shown of functional cardiac reconstitution following injury, by means of replicating cardiomyocytes replacing a temporary scar within 1–3 months (Kikuchi et al., 2010; Han et al., 2019). Nevertheless, it has been recently reported that in adult humans *de novo* generation of cardiomyocytes can actually occur, although via very low self-renewal rate (ca. 0.5–1% per year), which is not therapeutically relevant *per se* (Bergmann et al., 2009; Senyo et al., 2013). Recent evidences that the neonatal rodent heart can still harbor significant cardiomyogenic potential has further driven the attention toward cardiomyocyte proliferation as *bona fide* regenerative mechanism. Within the first week of life, neonatal mice can almost entirely regenerate their heart after severe injury via renewal of surviving cardiomyocytes (Porrello et al., 2011, 2013; Mahmoud et al., 2014). After this short post-natal window, there is a clear transition from regeneration into scarring and fibrosis, as the typical molecular signature of the mature adult cardiac wound healing response (Aurora et al., 2014). Likewise, functional recovery of the myocardial tissue in a unique case of a human newborn undergoing severe MI by coronary artery occlusion has been recently reported; similarly to the neonatal rodent heart, the child showed rescue of cardiac function within weeks via putative cardiac regeneration (Haubner et al., 2016).

Evidences that the mammalian heart possesses some restorative potential have been supported by the identification of resident stromal mesenchymal cells, defined as cardiac progenitor cells (CPC). CPC were originally reported in 2003 when describing Lin^{-}c-kit^{+} cardiac stem cells acquiring phenotypic features of cardiomyocyte-like cells (Beltrami et al., 2003). Since then, different populations of endogenous CPC have been described, such as c-kit^{+}, Sca-1^{+}, cardiosphere-derived CPC and epicardium-derived progenitor cells (EPDC). All such stem-like cell populations can be isolated from discarded tissue obtained during heart surgery or endocardial biopsy according to different protocols, as extensively reviewed in Bollini et al. (2011b). While some CPC, like EPDC, may harbor some degree of vascular and cardiomyocyte plasticity during embryonic development (Zhou et al., 2008), generally speaking they become quiescent soon after birth, unless stimulated by injury (Lepilina et al., 2006; Limana et al., 2010; Huang et al., 2012). Initially, great excitement was addressed toward these cells as stem-like progenitors with cardiac-specific differentiation potential within the adult heart. Yet, multiple independent lines of investigation have recently questioned the cardiomyogenic and/or cardiovascular commitment of several adult CPC subpopulations (i.e., c-kit- and Sca-1-positive ones, Sultana et al., 2015; Kanisicak et al., 2017; Li et al., 2018; Tang et al., 2018; Zhang L. et al., 2018) with serious expression of concerns and retractions of several studies (Estes Mark, 2019). Despite the ongoing controversy on CPC cardiomyogenic conversion, CADUCEUS and ALLSTAR clinical trials based on autologous and allogeneic cardiosphere-derived cell therapy proved to be safe and resulted into some degree of improved viable heart mass and contractility in patients with MI and left ventricle dysfunction (Makkar et al., 2012; Chakravarty et al., 2017). Therefore, it seems reasonable that adult CPC may still contribute to improve heart function – although unlikely via direct differentiation- and represent a therapeutic target to optimize cardiac repair. Additionally, activation of resident CPC following injury showed to be much stronger and responsive in the neonatal mouse heart compared to the adult (Jesty et al., 2012).

Being loss of myocardial tissue the main limiting factor for heart function, preclinical research has been lately focused on two biological strategies to improve endogenous mechanisms of cardiac repair and regeneration: (*i)* preservation of viable myocardium during injury or disease and (*ii)* replacement of cardiomyocytes to restore structural and functional integrity of the damaged heart (Broughton et al., 2018). The first one is based on enhancing cardio-protection so to counteract pathological remodeling; this can be mainly achieved via prompt *in situ* inhibition of cardiomyocyte apoptosis and/or their premature senescence, by quenching prolonged inflammation, while supporting *de novo* local angiogenesis and (re)activating endogenous CPC (Prabhu and Frangogiannis, 2016; Spath et al., 2016; Huang and Frangogiannis, 2018; Li et al., 2019). The latter, which specifically targets myocardial renewal, truly represents the *sine qua non condition* to conquer true cardiac regeneration via restoration of active cardiomyocyte cell division (Cahill et al., 2017; Eschenhagen et al., 2017; Wang et al., 2017; Vujic et al., 2020). Indeed, increasing efforts have been lately dedicated to define putative therapeutic strategies to resurge myocardial renewal in the adult heart. Yet, it remains quite controversial to provide satisfactory and reliable validation of true cardiomyocyte

division by means of cytokinesis, over more limiting binucleation or polyploidy, as extensively reviewed in Leone et al. (2015) and Leone and Engel (2019). Moreover, microRNA therapy via viral vector has recently shown to successfully target cardiomyocyte de-differentiation and proliferation in a big preclinical animal model of MI, resulting in remarkable myocardial regeneration; nonetheless, *de novo* proliferating cardioblasts expressed an immature phenotype and caused lethal arrhythmia, indicating that their genetically induced constitutive stimulation may not be indicated, if timely control of such renewal mechanism cannot be provided (Gabisonia et al., 2019).

These evidences suggest that the mammalian heart can harbor some intrinsic regenerative capacity, based on reparative and renewal mechanisms; these are broadly active during embryonic development up to early neonatal stages. Such restorative program is transient, being lost after the first week of birth, suggesting a sort of "memory loss." Therefore, preclinical cardiovascular research has lately focused on alternative strategies to "rejuvenate" the forgotten endogenous potential of adult heart, including (a) the stimulation with stem/progenitor cell-derivatives and (b) the innovative use of cardiac decellularized extracellular matrix (dECM, **Figure 1**). In this review, we will provide an overview of these two possible experimental approaches to resurge intrinsic mechanisms of cardiac repair and myocardial renewal.

SAY IT RIGHT: AT THE HEART OF INTER-CELLULAR PARACRINE COMMUNICATION

Data from clinical and preclinical studies on stem cell-based therapy for cardiac disease have shown that cells transplanted into compromised myocardium are very unlikely to contribute to novel cardiovascular cells by means of differentiation (Murry et al., 2004; Noiseux et al., 2006; Langrzyk et al., 2018). Multiple independent analyses have also revealed that transplanted cells fail to engraft and survive in the long term (Freyman et al., 2006; Schachinger et al., 2008; Noort et al., 2010). Nonetheless, in most preclinical studies, they concurred to counteract worsening of cardiac function via beneficial paracrine effects acting on the local cardiac microenvironment, such as supporting resident cardiomyocyte survival and local angiogenesis, while modulating acute inflammation and limiting fibrosis (Gnecchi et al., 2006; Mirotsou et al., 2007, 2011). Indeed, there is common consent that different stem and progenitor cells secrete an extensive variety of trophic factors, as chemokines, cytokines, growth factors and extracellular matrix (ECM) molecules, which can influence and change the environment composition, thus modifying the neighboring cells behavior (Korf-Klingebiel et al., 2008; Baraniak and McDevitt, 2010; Hodgkinson et al., 2010; Albulescu et al., 2015). Such paracrine capacity may represent an appealing and useful tool for the development of innovative regenerative medicine strategies. As consequence, paracrine modulation of cardiac tissue by stem cell-secreted molecules has recently appeared as a promising tactic for boosting cardiac healing with rising attention toward the functional characterization of the stem/progenitor cell "secretome," as the growth factors, chemo-attractant molecules and extracellular vesicles (EVs) released by paracrine secretion (Hodgkinson et al., 2010). In this perspective, several studies have been reported proof-of-principle cardiac paracrine therapy, via the administration of different cell-conditioned media recapitulating the cardio-active beneficial effects of the secreting cells, including also the reinstatement of endogenous stromal cardiac progenitor embryonic potential and the restoration of cell cycle activity in resident cardiomyocytes (Hatzistergos et al., 2010; Nguyen et al., 2010; Bollini et al., 2011a; Timmers et al., 2011; Hynes et al., 2013; Yang et al., 2013; Danieli et al., 2015; Rao et al., 2015; Hodgkinson et al., 2016; Lazzarini et al., 2016; Balbi et al., 2019).

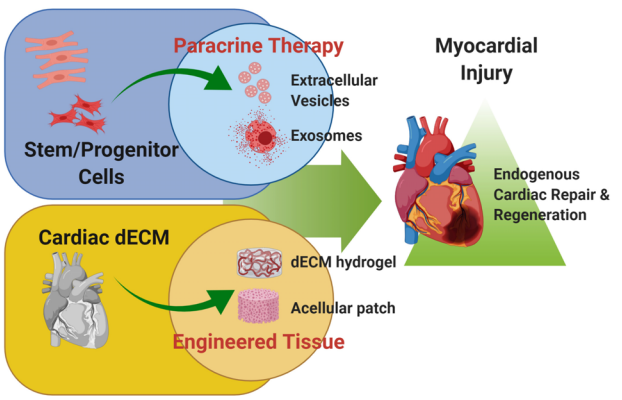

FIGURE 1 | Cardiac regenerative strategies. Schematic representation of the main experimental cardiac medicine approaches suggested to address myocardial injury and aiming at stimulating endogenous mechanisms of repair and myocardial restoration by means of stem cell-derived paracrine effectors and biomaterials. Schematic was made using BioRender (https://app.biorender.com).

From a translational point of view, the stem/progenitor cell secretome may represent an appealing ready-to-use *advanced therapy medicinal product* (ATMP) that could be manufactured via scale-up *in vitro* culture systems. Therefore it could offer the big advantage of being promptly accessible to cardiovascular patients, whenever needed; moreover, this strategy may overcome limits and concerns related to canonical cell therapy, including, for instance, donor cell engraftment, immune-compatibility and cost-effective, time-consuming procedures to provide an high amount of cells to be injected (Segers and Lee, 2008; Malliaras and Marban, 2011). Since paracrine therapy may represent a working tactic to resurge the neglected intrinsic potential of adult heart, the hunt is now on finding the most feasible stem cell source to be exploited for cardiac repair and regeneration. In such perspective, ease of isolation and proliferative potential, along with cardio-active secretory profile are strategic features for the ideal stem/progenitor cell candidate for paracrine therapy.

Different somatic stem cells have been investigated with studies mostly referring to mesenchymal stromal cells (MSC) as suitable source. MSC with relevant paracrine potential for cardiovascular disease have been described as isolated from either bone marrow or adipose tissue, which represent easily

accessible cell options. Likewise, fetal and perinatal MSC obtained from extra-embryonic annexes such as placenta tissue (Chen et al., 2015; Danieli et al., 2015; Van Linthout et al., 2017; Bier et al., 2018), umbilical cord (Corrao et al., 2013; Jin et al., 2013; Lim et al., 2018; Zhao et al., 2019) and amniotic fluid (Bollini et al., 2011a; Lazzarini et al., 2016; Balbi et al., 2019) have been reported as endowed with interesting paracrine potential in the cardiovascular field, as extensively reviewed in Bollini et al. (2018a). More recently, endogenous CPC have also been broadly investigated as exploitable options. While general consensus on adult CPC debatable differentiation capacity has not been reached, multiple studies confirmed their modulatory beneficial effects; these seems to be mediated by secreted soluble factors improving cardiac repair, as main functional mechanism of action (Barile et al., 2017a; Sharma et al., 2017; Broughton et al., 2018; Micheu et al., 2018; Pagano et al., 2018; Rafatian and Davis, 2018; Mardanpour et al., 2019). All such cell populations present different advantages and/or limitations, due to their properties. For instance, human adult somatic sources may be affected by low yield, invasive sampling, *in vitro* controversial self-renewal and phenotypic drifting due to donor age. On the other hand, more developmentally immature stromal cells offer a suitable alternative. These include progenitors that can be obtained from fetal and perinatal leftover samples of prenatal diagnosis (i.e., villi and amniotic fluid) or clinical waste material at birth (placenta membranes, amniotic fluid and umbilical cord tissue); specifically, they are endowed with remarkable proliferative potential along with ease of isolation, while avoiding ethical issues, as extensively reviewed in Bollini et al. (2018a,b). Interestingly, CPC have been broadly described to act as paracrine master regulators of cardiomyocyte proliferation during embryonic cardiac development by releasing mitogens targeting the underlying developing myocardium (Smith and Bader, 2007; Lavine and Ornitz, 2008). As well, they showed to underpin restorative responses within the injured heart of regenerative preclinical models (i.e., zebrafish and the mammalian neonatal heart), by locally instructing neighboring cardiovascular cells (Lepilina et al., 2006; Jesty et al., 2012; Simpson et al., 2012; Hesse et al., 2014; Wehman et al., 2017). Yet, despite such appealing paracrine profile, mammalian adult CPC become almost completely unresponsive after birth and need substantial stimulation to be reactivated following injury, thus making their isolation and further *in vitro* amplification challenging (Smart et al., 2011; Dube et al., 2017; Balbi et al., 2019).

Stem and Progenitor Cell-Extracellular Vesicles as Functional Messengers

Within the stem cell paracrine scenario, increasing attention has turned toward cell-secreted EVs, as functional biological conveyors of modulatory influence. EVs are phospholipid micro- and nano-vesicles that act as key mediators of inter-cellular communication affecting cellular functions. EVs are very heterogeneous and can be further sub-classified based on their size: from nano-scaled exosomes (ranging from 35 to 150-200nm) to medium-sized micro-vesicles (from 200 to 500nm) up to apoptotic bodies (>500 nm) (Thery et al., 2018). EVs carry a molecular cargo enriched with different bioactive factors (i.e., proteins, biolipids), as well as genetic information (more commonly non-coding RNA, such as microRNA, miRNA) (Teplitz, 1990).

EVs are secreted by different sources including cardiac, endothelial and inflammatory cells, advocating their relevant function in the cardiovascular system, especially within the damaged heart (Barile et al., 2014; Sluijter et al., 2018). Stem- and mesenchymal stromal cell-derived EVs have been shown to influence the immune system by modulating natural killer (NK) cells, dendritic cells (DC), monocytes/macrophages, microglia, T and B cells (Xie et al., 2020); indeed, MSC-derived EVs containing anti-inflammatory interleukin-10 (IL-10) and transforming growth factor beta 1 (TGF-β1) reduced the NK release of interferon gamma (INF-γ) and tumor necrosis factor alpha (TNF-α) release, thus alleviating the inflammatory response in a graft-versus-host disease model (Kordelas et al., 2014). Stem cell-derived EVs have also demonstrated to influence the skewing of macrophages toward a pro-resolving phenotype (Hyvarinen et al., 2018), as well as by reducing their *in vivo* infiltration along with quenching of severe inflammation following skeletal muscle tissue damage (Balbi et al., 2017; Lo Sicco et al., 2017). Moreover, human CPC-EVs delivered locally to the injured murine myocardium, either during the acute or chronic inflammatory phase, resulted in significant reduction of pro-inflammatory macrophages, neutrophils and circulating cytokines (Cambier et al., 2017; Harane et al., 2020). Of note, stem and progenitor cell-derived EVs have been broadly described as positively influencing physiological pathways involved in cardioprotective and tissue regeneration mechanisms (Baraniak and McDevitt, 2010). Both MSC- and CPC-derived EVs exerted cardio-active beneficial effects in preclinical animal models of myocardial injury, by more sustained influence – over their secreting parental cells - in enhancing reparative mechanisms (Shao et al., 2017) (**Figure 1**). Indeed, EVs delivered to the injured heart demonstrated to trigger relevant pro-survival effects as preserving more viable myocardial tissue, while decreasing fibrosis via the activation of specific signaling pathways, including those regulated by Wnt/β-catenin and AKT (Barile et al., 2014; Cui et al., 2017). Moreover, small EVs isolated from human fetal amniotic fluid progenitor cells have recently showed to protect the cardiac tissue in a rat preclinical model of ischemia/reperfusion injury when administered systematically; although they did not show clear cardioprotective or angiogenic effects *in vitro*, they expressed significant chemotactic influence on endothelial cell migration via phosphatidylinositol 3-kinase (PI3K) signaling (Takov et al., 2020). CPC-EVs have been reported to reprogram dermal fibroblast to express antifibrotic, antiapoptotic, and pro-angiogenic potential and prime them toward a cardioprotective profile when transplanted into a preclinical rodent model of MI (Tseliou et al., 2015). Interestingly, proteomic profiling of human CPC-EVs indicated in the pregnancy-associated plasma protein-A (PAPP-A) a molecular candidate for their cardioprotective potential; PAPP-A was demonstrated to instruct vesicle release of insulin-like growth factor-1 (IGF-1) via cleavage of IGF-binding protein-4 (IGFBP-4), resulting in AKT

and ERK1/2 phosphorylation in target cardiomyocytes, with marked pro-survival effect (Barile et al., 2018). The Notch pathway has also been indicated as potential mediator of MSC-EVs in exerting pro-angiogenic effects for the treatment of ischemia-related disease; EVs released by HIF-1α-overexpressing MSC were enriched with the Notch-ligand Jagged 1 and triggered angiogenetic responses on *in vitro* cultured endothelial cells (Gonzalez-King et al., 2017). Likewise, EVs secreted by Notch1-overexpressing cardiac stromal cells were highly cardioprotective and influenced resident cardiomyocyte cell cycle progression in a preclinical mouse MI model (Xuan et al., 2020).

A growing number of studies have also indicated a paracrine EV mechanism of action in the horizontal delivery of their RNA cargo to target cardiovascular cells. Y RNA fragment has been described as one of the most abundant RNA within cardiosphere-derived cells-EVs inducing a cardioprotective phenotype in target macrophage with secretion of anti-inflammatory IL-10 (Cambier et al., 2017). Similarly, several miRNAs have been associated with stem/progenitor-EV anti-apoptotic, proliferative and angiogenic effects, including – but not limited to - miR-210 and miR-146a (Barile et al., 2014, 2017b; Ibrahim et al., 2014; de Couto et al., 2017; Zhu et al., 2018; Milano et al., 2019). Stem cell-EVs, such as those isolated from immature amniotic fluid derived-MSC, also showed interesting "rejuvenating" effects, like *in situ* re-activation of endogenous CPC and the stimulation of resident cardiomyocytes progression within cell cycle stages after myocardial injury (Balbi et al., 2019). In particular, human amniotic fluid stem cell-EVs injected locally into the ischemic myocardium soon after MI, were able to trigger epicardium-derived progenitor cells to re-express the embryonic key gene *Wt1* as master regulator of their developmental juvenile potential (Smart et al., 2011; Bollini et al., 2014). The reactivated resident epicardial CPC did not show any sign of commitment toward either cardiomyogenic or cardiovascular lineages and disappeared after 4 weeks from treatment. Nonetheless, further *in vitro* investigation revealed that human epicardial CPC primed with human amniotic fluid stem cell-conditioned medium (containing EVs), produced a pro-angiogenic secretome driving tubulogenesis in HUVEC cells (Balbi et al., 2019). These results confirmed previous findings describing how severe myocardial injury can induce epicardial CPC proliferation, without differentiation into cardiomyocytes or endothelial cells, but with restoration of their paracrine activity on local *de novo* vascular network expansion (Zhou et al., 2011; Dube et al., 2017). In light of these evidences, endogenous CPC may represent an appealing therapeutic target for stem/progenitor cell-EVs for improving endogenous (paracrine) mechanisms of cardiac repair, as suggested by independent investigators (Alibhai et al., 2018).

Despite future paracrine therapy holds appealing potential for cardiovascular disease and heart failure, it may be challenged by some technical key aspects. Paracrine effects are limited in time *per se*, as swiftly impacting on the tissue micro-environment when released; hence, to significantly sustain reparative/regenerative mechanisms, multiple follow-up administration may be required. EVs isolated from human amniotic fluid-progenitors have shown to be effective in quenching skeletal muscle damage in a preclinical mouse model of muscle atrophy; yet, their beneficial effect was highest within 24 h from administration to then rapidly decrease within a week (Balbi et al., 2017). Interestingly, the same EVs, when delivered locally via intra-myocardial injection into a preclinical MI mouse model immediately after coronary ligation, were able to provide beneficial long-term effects in supporting cardiac function and counteracting pathological remodeling. This may suggest that, they may instruct resident cells to activate long-lasting responses, by promptly acting in the acute setting (Balbi et al., 2019).

Another relevant aspect to consider for the clinical translation of EV biology is the need for standard operative procedure for EV isolation to improve their yield and purity. Indeed, independent EVs preparations have shown different immunomodulatory potential (Kordelas et al., 2014). Likewise, reference guidelines for their *in vivo* administration and dosing are strictly required (Balbi et al., 2020; Yang et al., 2020). The International Society of Extracellular Vesicles (ISEV), has been addressing safety and regulatory requirements that must be considered for EV clinical application, as extensively reviewed in Thery et al. (2018). While an elegant study has recently described a CRISPR-Cas9-based readout system to investigate the regulatory mechanisms underlying EV-mediated RNA transfer between cells (de Jong et al., 2020), further investigation is still required to better elucidate EV targeting mechanism(s), along their pharmacokinetics and pharmacodynamics.

Considering these key aspects, it would be critical to take advantage of a controlled-release system to prolong the local administration of paracrine factors (such as EVs) within the injured myocardium. Systemic delivery of putative therapeutic paracrine factor(s), as the less invasive and more clinically compliant option, may be significantly restrained by the meager homing of the treatment to the cardiac tissue, as likely rapidly sequestered by off-target organs/tissues; thus, optimization of local administration would offer significant improvements.

DECELLULARIZED EXTRACELLULAR MATRIX IN CARDIAC REPAIR AND REGENERATION

In order to implement heart regenerative strategies, devices made from ECM and other biomaterials were recently developed as systems capable of delivery therapeutic factors. These ECM-derived scaffolds, gels, and protein suspensions, are able to both convey cells and factors, and to enhance survival and regeneration of the heart. Importantly, significant therapeutic benefits were obtained when these ECM-derived scaffolds were used stand-alone in post ischemic models (Sarig et al., 2016). These studies have expanded the field of cardiac regenerative medicine, including preclinical therapeutic use of biomaterials and different ECM-derived formulations as reviewed in Spinali and Schmuck (2018), Tang-Quan et al. (2018), Xing et al. (2019).

Initially, tissue ECM was considered a biologically inert space, able to provide only a physical support to the attached cells. However, it is now clear that ECM is a dynamic and complex network of fibrous and adhesive proteins, serving as reservoir of different bioactive peptides and growth factors.

Cell behavior is influenced by biochemical and biomechanical signaling present in the tissue microenvironment, including ECM, which is a dealer of cellular processes such as proliferation, differentiation, migration, and survival (Rao Pattabhi et al., 2014; Chen et al., 2018). In order to obtain ECM from a plethora of tissues and organs, decellularization protocols, by means of chemical/physical methods reaching the best compromise between the complete cell removal and the maintenance of the structural tissue proteins, are certainly the most used technique as reviewed in Gilbert et al. (2006), Song and Ott (2011), Keane et al. (2015), Taylor et al. (2017), Urciuolo and De Coppi (2018).

Within the cardiovascular scenario, a variety of naturally derived dECM sources have been investigated (with or without cells/factors) as cardiac patch or injected directly into the myocardium as hydrogel (Wainwright et al., 2010; Johnson et al., 2014). Since it was reported by the literature the importance of using tissue-specific derived biomaterials to obtain a precise and efficient organ regeneration, here we will specifically focused on heart-derived dECM.

Properties of Decellularized Cardiac Tissue

Application of decellularization technique in cardiac tissue engineering has rapidly progressed in the past 10 years. Ott et al. (2008) reported for the first time the development of decellularized rat whole heart perfusing different solutions through the coronary access. The so-treated decellularized heart preserved the complex ECM composition as well as deprived of genetic material (Ott et al., 2008). Following this pioneering research, several studies have reported that, after decellularization, cardiac dECM retains intact geometry and vascular network of native heart, which makes it a suitable physiological platform for producing engineered construct for cardiac repair (Song and Ott, 2011; Tapias and Ott, 2014; Taylor et al., 2014; Wang et al., 2014). For all tissues and organs of the body, and especially for those of musculoskeletal compartment, ECM structure, ultrastructure and composition are mandatory aspects to be considered before a therapeutic application. In the recent years, mechanical properties of biomaterial scaffolds have been recognized as important player in influencing tissue repair, especially in organs such as cardiac and skeletal muscles (Singelyn and Christman, 2011; Hasan et al., 2014; Piccoli et al., 2016). The preservation of structural and mechanical characteristics of dECM after *in vivo* implantation could allow improvement in the mechanisms of cardiac repair and regeneration. From one hand, dECM could provide the infarcted myocardium with incisive mechanical compensation. In fact, tissue mechanical properties are mainly determined by ECM. From the other hand, the structural, ultrastructural and mechanical characteristics of dECM could serve as physical messenger for the delivered cells or infiltrated host cells to augment cardiovascular differentiation and tissue regeneration. Together with the mechanical properties, preservation of biochemical cues within dECM could be desirable for cell attachment, proliferation and stem cell differentiation, both *in vivo* and *in vitro*, as demonstrated in many studies (Singelyn and Christman, 2010; Singelyn et al., 2012; Wang and Christman, 2016). Proteomic approaches evidenced the retention of ECM proteins after decellularization using human myocardium tissue (de Castro Bras et al., 2013; Johnson et al., 2016). Among all the major components, such as collagens, laminin, elastin and glycosaminoglycans, several studies have reported that cardiac dECM also holds the soluble growth factors after decellularization process (Methe et al., 2014; Ferng et al., 2017). Some of these peptides and cytokines within the decellularized myocardium tissue are involved in cardiac homeostasis and remodeling, angiogenesis, survival, proliferation, differentiation and cell recruitment in response to inflammation (Di Meglio et al., 2017). In particular, neonatal murine cardiac dECM obtained from 1-day-old pups has been shown to trigger *in vitro* turnover in unresponsive cardiomyocytes, as enriched with Agrin and Tgf - b1 which have been described acting like ECM-associated mitogens by inhibiting the Hippo effector Yap, via the dystrophin glycoprotein complex (Bassat et al., 2017; Eroglu and Chien, 2017). Differently from the mechanical cues, the component types and their amounts in the dECM are applicable for dECM patches as well as injectable dECM hydrogels.

Cardiac Extracellular Matrix-Derived Scaffolds and Hydrogels to Treat Cardiovascular Disease

Decellularized ECM-derived formulations, as alone or combined with cells/factors, have been described supporting cardiac repair in preclinical settings (Zisch et al., 2003; Seif-Naraghi et al., 2010; Sarig et al., 2016). One of the most remarkable obstacles in the classical cell-therapy vision is represented by the harsh cardiac environment following MI, which affects engraftment of transplanted cells and their capacity to *de novo* contribute to tissue repair. The fate of transplanted cells, in fact, is strongly affected by ischemic myocardium remodeling, including altered ECM anisotropy (Gupta et al., 1994; Carey et al., 2001). A promising therapeutic approach is represented by the inhibition of adverse post ischemic dilation to create a more suitable milieu that allows engrafted (or resident regenerating) cells to be functionally activated; myocardial or pericardial constructs are engineered to help preventing progression into heart failure and sustain cardiac function after acute myocardial impairment (Kameli et al., 2018; Zhang J. et al., 2018; Streeter and Davis, 2019).

Numerous experimental analyses confirmed that cardiac dECM may be considered an appealing source for the development of new myocardial repair strategies. First of all, thanks to the preservation of biomechanical properties, cardiac dECM patches could cope with the contraction/relaxation cycle of the heart, thus mechanically securing the infarcted area and counteracting fibrosis along with pathological remodeling (Carotenuto et al., 2019). Moreover, the important physical signals retained by the patches within their stiffness and texture are delivered to the resident cells while also sustaining diffusion of nutrients, and removal of pro-necrotic factors. It is important to stress, in fact, that stiffness and elastic modulus

of pathological hearts are different from the healthy tissue (Arani et al., 2017), and that this aspect heavily influences cellular behaviors. In addition, since dECM is biocompatible and degradable, serves as a temporary scaffold that enables cell engraftment directly into necrotic and infarcted regions, overcoming the benefits of synthetic materials commonly used in the clinic. Indeed, evidences have been reported on cardiac dECM patch being able to support host tissue-driven reconstruction of a full-thickness right ventricular outflow tract defect in a rat model, after 16 weeks of treatment (Wainwright et al., 2012).

Given that dECM patches and scaffolds are delivered epicardially by exposed−chest surgery, better methods to enhance the therapeutic efficacy and reduce invasiveness are desirable. In this scenario, injectable cardiac-based biomaterials may be very appealing as exploitable by minimally invasive approach, with *in vivo* similar efficacy in respect to cardiac dECM patches (Seif-Naraghi et al., 2010; Toeg et al., 2013). For example, decellularized pericardium produced as a milled matrix, was injected into the cardiac left ventricle of healthy rats, demonstrating to form a fibrous, porous scaffold *in vivo* (Seif-Naraghi et al., 2010). When injected as stand-alone formulations in small animal model of MI, this biomaterial contributed to preserve cardiac function. Interestingly, on the basis of neonatal rodent increased ability to regenerate after myocardial injury, a recent research work showed that neonatal rodent cardiac dECM counteracted ventricular remodeling in adult mice following MI, underlining once again the importance of tissue specificity and the strong relationship between regeneration and cardiac tissue age also when considering the ECM (Wang et al., 2019). While most of the mechanisms behind the effectiveness of these injectable dECM-derived biomaterials *in vivo* have yet to be comprehensively examined, it is clear that porous scaffolds facilitate cell homing and neovascularization in ischemic regions. Seif-Naraghi et al. (2011) demonstrated that the variability within human cardiac tissue samples obtained after protein composition, glycosaminoglycan content, *in vitro* degradation, *in vivo* gelation, and microstructure analyses of 7 different human specimens, does not prevent them from being processed into injectable scaffold. Moreover, all these samples displayed similar fibrous and porous texture and cell infiltration after *in vivo* injection, prompting a possible application to limit detrimental remodeling after MI (Seif-Naraghi et al., 2011).

Engineered Cardiac Extracellular Matrix-Derived Devices

dECM formulations as delivery platform for cardiovascular repair and regeneration are attracting growing attention. One of the most promising approach is the combination *in vitro* of natural scaffolds with patient-derived progenitor cells, in order to re-create tissue substitute before *in vivo* application. Healthy and responsive cells, in fact, are mandatory players in the regeneration game, especially when big portions of tissue are damaged. Their presence in the engineered scaffold before implantation results in tenability of the construct. In addition, cells increased their active bound and primed the dECM construct, according to their needs and behaviors (Chi Ting Au-Yeung et al., 2017). These interactions ensure an increased resistance of the engrafted construct and give also a good stabilization to the injured native tissue, rising the beneficial effect of this tissue engineering approach. Enhanced effects could be obtain with a multiple strategy, involving the injection of tissue specific cells, following the classical cell therapy approach, and a stromal cell-loaded patch, in which the engineered construct provides a microenvironment that stimulates vascular regeneration through prolonged secretion of paracrine factors and simultaneously ameliorates the engraftment of cells delivered locally and contributing to the rescue of cardiac function (Park et al., 2019).

At the same time, the use of natural derived hydrogels for the therapeutic administration of cells and factors has shown great efficacy and allowed a less invasive approach. On top of using bioactive dECM hydrogels as vehicle for the administration of putative cardiomyogenic precursors to optimize their retention and engraftment within the myocardial tissue (Bejleri et al., 2018; Bai et al., 2019; Kim et al., 2019), dECM scaffolds are becoming increasingly attractive as *in situ* releasing reservoir for secreted paracrine factors. In this scenario, loading of growth factors into biomaterial scaffolds increased their stability and activity. Data from a preclinical work indicate that delivery of a specific fragment of HGF in an ECM hydrogel supported neovascularization and limited ventricle dilation following MI (Zisch et al., 2003). The prolonged presence and the enhanced stability of the exogenous factor entrapped in the matrix material probably support and foster the native tissue response. In addition, the ECM hydrogel may also represent a working system to deliver cytokines to target cells similarly to endogenous factors physiologically requisitioned in the native cardiac ECM. This approach of secreted factors reservoir could be also obtained starting from *in vitro* cell culture material: human adipose dECM hydrogels as controlled-delivery system of factors secreted by adipose-derived stromal cells has been recently tested *in vitro* to demonstrate that different cell-derived paracrine factors could be delivered concurrently through a controlled-release approach on target cells in an *in vitro* wound healing model (van Dongen et al., 2019).

Likewise, dECM could be also envisaged as bioink for the precise and custom-made 3D-printing of bioactive scaffolds to deliver cells and/or their paracrine factors to the injured myocardium; indeed, 3D-printed bio-patches composed of cardiac ECM, human CPC, and gelatin methacrylate have been shown to be retained on rat hearts and mediated vascularization within 14 days from delivery. Notably, conditioned media from the bioengineered patches provided angiogenic effects, as detected by increased endothelial cell tube formation (Bejleri et al., 2018). Hence, by fostering cardio-active stem/precursor secretome potential via enhanced dECM delivery, we could define *ad hoc* paracrine cardiac therapy as future strategy (**Figure 1**). Furthermore, since dECM still maintains specific bioactive paracrine content *per se*, their EV profile is also gaining attention. Indeed, significant amount of EVs has been described to be released by cardiac ECM, namely ECM-EVs. Notably, ECM-EVs

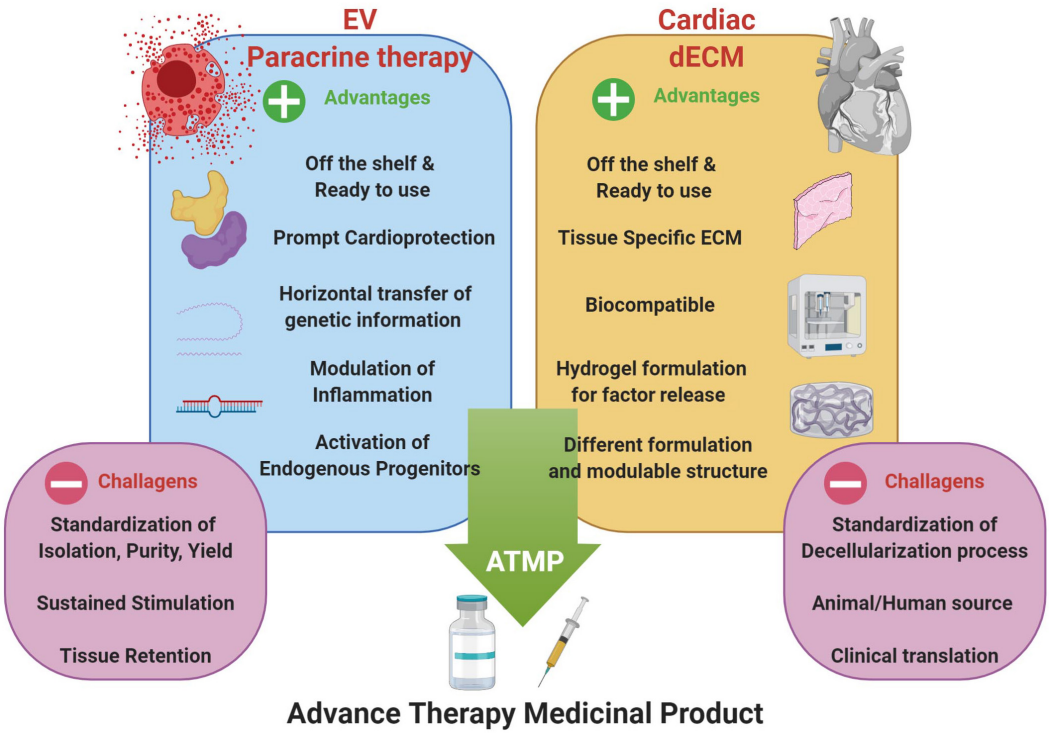

FIGURE 2 | Optimization of EV-based paracrine therapy with dECM technology. Cardiac regenerative strategy based on the synergistic combination of EV-based beneficial effects and cardiac dECM formulations for putative future paracrine therapy, as ready-to-use and off-shelf advanced therapy medicinal product (ATMP); indeed, such innovative approach may overcome some of the major limits of EV-based strategy, such as tissue retention, tissue specific tropism and sustained, controlled release. Schematic was drawn using BioRender (https://app.biorender.com).

showed to be enriched with the cardiomyogenic miR-199a-3p, promoting cell division in isolated neonatal cardiomyocytes, as well as supporting electrical activity (An et al., 2017).

Therefore, the combination of cell-based strategies, such as paracrine therapy via EV administration, with the functionalization of dECM formulations, may represent an innovative approach in cardiac regenerative medicine for the next future. The analysis of biopolymer/hydrogel formulations to deliver therapeutically relevant EVs is gaining increasing attention. Some critical aspects limiting the clinical translation of therapeutic use of EVs could be improved through the synergistic combination with hydrogel-based or injectable cardiac dECM formulations; these challenges include the need for sustained and controlled release of EVs within the cardiac tissue over time and their local delivery via compatible cardiac-specific formulations. To date, both xenogeneic and allogeneic dECM have been used in pre-clinical and clinical research with different results, but availability of donor tissues is often limited. From one hand, xenogeneic heart from big animals (e.g., porcine or bovine tissues) are easy to obtain, but may carry residual immunogenicity and may be contaminated with biological agents. On the other hand, human allogeneic tissues would be the ideal material to obtain dECM suitable for implantation or generation of hydrogel. Together with cadaver organ donation, human tissue Biobanks are important sources to augment organ availability (Porzionato et al., 2018), especially because the different formulations of cardiac dECM do not require all the stringent regulations necessary for the classic organ donation for transplant purposes. Moreover, general standard decellularization protocols should be set up before clinical application. Hence, in the next future, by exploiting EV biology with cardiac dECM technology we could envisage a possible novel ATMP (**Figure 2**). Currently, only a couple proof-of-principle studies have been performed on the functional encapsulation of EVs within dECM-derived hydrogels; porcine-derived dECM hydrogels have been tested as platform for sustained delivery of microRNAs and CPC-EVs to validate controlled release along with EV anti-apoptotic bioactivity *in vitro* (Hernandez et al., 2018). More recently, the feasibility of EV transport in hydrogels and a decellularized matrix has been demonstrated. Engineered biomaterials with specific matrix mechanical properties, as stress relaxation, showed to influence EV retention, while higher crosslinking density support their diffusion (Lenzini et al., 2020).

Future Perspectives: Translation Into the Clinical Scenario

When considering possible clinical translation of the most recent advances in cardiovascular research, there are relevant open questions that still need to be addressed. These include the optimal time point of intervention following injury/during

disease, and the most suitable strategy to pursue in terms of enhancement of cardiac repair over stimulation of endogenous regeneration, according to the cardiovascular patient's specific needs (i.e., acute MI or ischemic coronary disease versus chronic cardiomyopathy). In this scenario, innovative cardiac regenerative strategies, based on either paracrine or cell-therapy approaches, may be challenged by poor cardiac tropism of cells/factors injected systemically and may require local or intra-myocardial administration to enhance their effects. Novel bio-scaffold/hydrogel formulations can increase and enhance retention and release; yet they may depend on topical delivery, and thus being indicated as concomitant strategy during heart surgery or percutaneous coronary intervention/angioplasty. While not ideal for any kind of cardiovascular patient, they can still be therapeutically relevant for acute treatments, such as prompt intervention on patients experiencing MI. The functional combination of prompt EV modulatory effects with the tunable biological properties of dECM hydrogels may represent an ideal delivery platform to enhance intrinsic mechanisms of cardiac restoration. Another relevant cardiovascular scenario is then represented by congenital heart defects, which may affect up to ca. 35.000 newborns annually, significantly impacting on patient morbidity and mortality (Rossano et al., 2012). Palliative surgery with use of cardiac prosthetic devices is the elective options in these patients, although it does not offer a permanent solution, as follow-up interventions are required and may not be resolutive, with children ultimately developing heart failure. Moreover, constructs or supports have been often dispensed to the outer cardiac surface during open−chest surgery. Future efforts should provide less interfering systems based on implementing biomaterials as topical reservoir of bioactive factors, such as self-assembling tissue-specific hydrogels or other tunable and smart biomaterials. In this perspective, the use of cardiac dECM bio-printed platforms/bio-scaffolds to deliver cells/paracrine factors at the time of reconstructive surgery, could represent a synergic and implementing strategy, to provide endogenous repair and regeneration of the young cardiac tissue.

AUTHOR CONTRIBUTIONS

EM: manuscript writing, analytical discussion of decellularized extracellular matrix biology and applications, and figure design. PG: manuscript writing, critical discussion of stem cell paracrine biology. RQ: manuscript writing, contribution to critical discussion on cardiac repair. MP and SB: conception and design, manuscript writing and supervision. All authors reviewed the manuscript and approved it.

FUNDING

EM and MP are funded by Fondazione Istituto di Ricerca Pediatrica Città della Speranza. SB and PG are funded by the "Curiosity Driven" Starting Grant from University of Genova, Genova, Italy.

ACKNOWLEDGMENTS

This study contributes to the aims of the Horizon 2020 COST Action CA17116 SPRINT- *International Network for Translating Research on Perinatal Derivatives into Therapeutic Approaches*, in which SB is involved as partner.

REFERENCES

Albulescu, R., Tanase, C., Codrici, E., Popescu, D. I., Cretoiu, S. M., and Popescu, L. M. (2015). The secretome of myocardial telocytes modulates the activity of cardiac stem cells. *J. Cell. Mol. Med.* 19, 1783–1794. doi: 10.1111/jcmm.12624

Alibhai, F. J., Tobin, S. W., Yeganeh, A., Weisel, R. D., and Li, R. K. (2018). Emerging roles of extracellular vesicles in cardiac repair and rejuvenation. *Am. J. Physiol. Heart Circ. Physiol.* 315, H733–H744. doi: 10.1152/ajpheart.00100.2018

An, M., Kwon, K., Park, J., Ryu, D. R., Shin, J. A., Lee Kang, J., et al. (2017). Extracellular matrix-derived extracellular vesicles promote cardiomyocyte growth and electrical activity in engineered cardiac atria. *Biomaterials* 146, 49–59. doi: 10.1016/j.biomaterials.2017.09.001

Arani, A., Arunachalam, S. P., Chang, I. C. Y., Baffour, F., Rossman, P. J., Glaser, K. J., et al. (2017). Cardiac MR elastography for quantitative assessment of elevated myocardial stiffness in cardiac amyloidosis. *J. Magn. Reson. Imaging* 46, 1361–1367. doi: 10.1002/jmri.25678

Aurora, A. B., Porrello, E. R., Tan, W., Mahmoud, A. I., Hill, J. A., Bassel-Duby, R., et al. (2014). Macrophages are required for neonatal heart regeneration. *J. Clin. Invest.* 124, 1382–1392. doi: 10.1172/JCI72181

Bai, R., Tian, L., Li, Y., Zhang, J., Wei, Y., Jin, Z., et al. (2019). Combining ECM hydrogels of cardiac bioactivity with stem cells of high cardiomyogenic potential for myocardial repair. *Stem Cells Int.* 2019:6708435. doi: 10.1155/2019/6708435

Balbi, C., Costa, A., Barile, L., and Bollini, S. (2020). Message in a bottle: upgrading cardiac repair into rejuvenation. *Cells* 9:E724. doi: 10.3390/cells9030724

Balbi, C., Lodder, K., Costa, A., Moimas, S., Moccia, F., van Herwaarden, T., et al. (2019). Reactivating endogenous mechanisms of cardiac regeneration via paracrine boosting using the human amniotic fluid stem cell secretome. *Int. J. Cardiol.* 287, 87–95. doi: 10.1016/j.ijcard.2019.04.011

Balbi, C., Piccoli, M., Barile, L., Papait, A., Armirotti, A., Principi, E., et al. (2017). First characterization of human amniotic fluid stem cell extracellular vesicles as a powerful paracrine tool endowed with regenerative potential. *Stem Cells Transl. Med.* 6, 1340–1355. doi: 10.1002/sctm.16-0297

Baraniak, P. R., and McDevitt, T. C. (2010). Stem cell paracrine actions and tissue regeneration. *Regen. Med.* 5, 121–143. doi: 10.2217/rme.09.74

Barile, L., Cervio, E., Lionetti, V., Milano, G., Ciullo, A., Biemmi, V., et al. (2018). Cardioprotection by cardiac progenitor cell-secreted exosomes: role of pregnancy-associated plasma protein-A. *Cardiovasc. Res.* 114, 992–1005. doi: 10.1093/cvr/cvy055

Barile, L., Lionetti, V., Cervio, E., Matteucci, M., Gherghiceanu, M., Popescu, L. M., et al. (2014). Extracellular vesicles from human cardiac progenitor cells inhibit cardiomyocyte apoptosis and improve cardiac function after myocardial infarction. *Cardiovasc. Res.* 103, 530–541. doi: 10.1093/cvr/cvu167

Barile, L., Milano, G., and Vassalli, G. (2017a). Beneficial effects of exosomes secreted by cardiac-derived progenitor cells and other cell types in myocardial ischemia. *Stem Cell Investig.* 4:93. doi: 10.21037/sci.2017.11.06

Barile, L., Moccetti, T., Marban, E., and Vassalli, G. (2017b). Roles of exosomes in cardioprotection. *Eur. Heart J.* 38, 1372–1379. doi: 10.1093/eurheartj/ehw304

Bassat, E., Mutlak, Y. E., Genzelinakh, A., Shadrin, I. Y., Baruch Umansky, K., Yifa, O., et al. (2017). The extracellular matrix protein agrin promotes heart regeneration in mice. *Nature* 547, 179–184. doi: 10.1038/nature22978

Bejleri, D., Streeter, B. W., Nachlas, A. L. Y., Brown, M. E., Gaetani, R., Christman, K. L., et al. (2018). A bioprinted cardiac patch composed of cardiac-specific extracellular matrix and progenitor cells for heart repair. *Adv. Healthc Mater.* 7:e1800672. doi: 10.1002/adhm.201800672

Beltrami, A. P., Barlucchi, L., Torella, D., Baker, M., Limana, F., Chimenti, S., et al. (2003). Adult cardiac stem cells are multipotent and support myocardial regeneration. *Cell* 114, 763–776. doi: 10.1016/s0092-8674(03)00687-1

Benjamin, E. J., Virani, S. S., Callaway, C. W., Chamberlain, A. M., Chang, A. R., Cheng, S., et al. (2018). Heart disease and stroke statistics-2018 update: a report from the american heart association. *Circulation* 137, e67–e492. doi: 10.1161/CIR.0000000000000558

Bergmann, O., Bhardwaj, R. D., Bernard, S., Zdunek, S., Barnabe-Heider, F., Walsh, S., et al. (2009). Evidence for cardiomyocyte renewal in humans. *Science* 324, 98–102. doi: 10.1126/science.1164680

Bier, A., Berenstein, P., Kronfeld, N., Morgoulis, D., Ziv-Av, A., Goldstein, H., et al. (2018). Placenta-derived mesenchymal stromal cells and their exosomes exert therapeutic effects in Duchenne muscular dystrophy. *Biomaterials* 174, 67–78. doi: 10.1016/j.biomaterials.2018.04.055

Bollini, S., Cheung, K. K., Riegler, J., Dong, X., Smart, N., Ghionzoli, M., et al. (2011a). Amniotic fluid stem cells are cardioprotective following acute myocardial infarction. *Stem Cells Dev.* 20, 1985–1994. doi: 10.1089/scd.2010.0424

Bollini, S., Silini, A. R., Banerjee, A., Wolbank, S., Balbi, C., and Parolini, O. (2018a). Cardiac restoration stemming from the placenta tree: insights from fetal and perinatal cell biology. *Front. Physiol.* 9:385. doi: 10.3389/fphys.2018.00385

Bollini, S., Smart, N., and Riley, P. R. (2011b). Resident cardiac progenitor cells: at the heart of regeneration. *J. Mol. Cell. Cardiol.* 50, 296–303. doi: 10.1016/j.yjmcc.2010.07.006

Bollini, S., Smits, A. M., Balbi, C., Lazzarini, E., and Ameri, P. (2018b). Triggering endogenous cardiac repair and regeneration via extracellular vesicle-mediated communication. *Front. Physiol.* 9:1497. doi: 10.3389/fphys.2018.01497

Bollini, S., Vieira, J. M., Howard, S., Dube, K. N., Balmer, G. M., Smart, N., et al. (2014). Re-activated adult epicardial progenitor cells are a heterogeneous population molecularly distinct from their embryonic counterparts. *Stem Cells Dev.* 23, 1719–1730. doi: 10.1089/scd.2014.0019

Broughton, K. M., Wang, B. J., Firouzi, F., Khalafalla, F., Dimmeler, S., Fernandez-Aviles, F., et al. (2018). Mechanisms of cardiac repair and regeneration. *Circ. Res.* 122, 1151–1163. doi: 10.1161/CIRCRESAHA.117.312586

Cahill, T. J., Choudhury, R. P., and Riley, P. R. (2017). Heart regeneration and repair after myocardial infarction: translational opportunities for novel therapeutics. *Nat. Rev. Drug Discov.* 16, 699–717. doi: 10.1038/nrd.2017.106

Cambier, L., de Couto, G., Ibrahim, A., Echavez, A. K., Valle, J., Liu, W., et al. (2017). Y RNA fragment in extracellular vesicles confers cardioprotection via modulation of IL-10 expression and secretion. *EMBO Mol. Med.* 9, 337–352. doi: 10.15252/emmm.201606924

Carey, P. A., Turner, M., Fry, C. H., and Sheridan, D. J. (2001). Reduced anisotropy of action potential conduction in left ventricular hypertrophy. *J. Cardiovasc. Electrophysiol.* 12, 830–835. doi: 10.1046/j.1540-8167.2001.00830.x

Carotenuto, F., Teodori, L., Maccari, A. M., Delbono, L., Orlando, G., and Di Nardo, P. (2019). Turning regenerative technologies into treatment to repair myocardial injuries. *J. Cell. Mol. Med.* 24, 2704–2716. doi: 10.1111/jcmm.14630

Chakravarty, T., Makkar, R. R., Ascheim, D. D., Traverse, J. H., Schatz, R., DeMaria, A., et al. (2017). ALLogeneic heart stem cells to achieve myocardial regeneration (ALLSTAR) trial: rationale and design. *Cell Transplant.* 26, 205–214. doi: 10.3727/096368916X692933

Chen, H. J., Chen, C. H., Chang, M. Y., Tsai, D. C., Baum, E. Z., Hariri, R., et al. (2015). Human placenta-derived adherent cells improve cardiac performance in mice with chronic heart failure. *Stem Cells Transl. Med.* 4, 269–275. doi: 10.5966/sctm.2014-0135

Chen, H. Y., Pan, L., Yang, H. L., Xia, P., Yu, W. C., Tang, W. Q., et al. (2018). Integrin alpha5beta1 suppresses rBMSCs anoikis and promotes nitric oxide production. *Biomed. Pharmacother.* 99, 1–8. doi: 10.1016/j.biopha.2018.01.038

Chi Ting Au-Yeung, G., Sarig, U., Sarig, H., Bogireddi, H., Bronshtein, T., Baruch, L., et al. (2017). Restoring the biophysical properties of decellularized patches through recellularization. *Biomater. Sci.* 5, 1183–1194. doi: 10.1039/c7bm00208d

Corrao, S., La Rocca, G., Lo Iacono, M., Zummo, G., Gerbino, A., Farina, F., et al. (2013). New frontiers in regenerative medicine in cardiology: the potential of Wharton's jelly mesenchymal stem cells. *Curr. Stem Cell Res. Ther.* 8, 39–45. doi: 10.2174/1574888x11308010006

Cui, X., He, Z., Liang, Z., Chen, Z., Wang, H., and Zhang, J. (2017). Exosomes from adipose-derived mesenchymal stem cells protect the myocardium against ischemia/reperfusion injury through wnt/beta-catenin signaling pathway. *J. Cardiovasc. Pharmacol.* 70, 225–231. doi: 10.1097/FJC.0000000000000507

Danieli, P., Malpasso, G., Ciuffreda, M. C., Cervio, E., Calvillo, L., Copes, F., et al. (2015). Conditioned medium from human amniotic mesenchymal stromal cells limits infarct size and enhances angiogenesis. *Stem Cells Transl. Med.* 4, 448–458. doi: 10.5966/sctm.2014-0253

de Castro Bras, L. E., Ramirez, T. A., DeLeon-Pennell, K. Y., Chiao, Y. A., Ma, Y., Dai, Q., et al. (2013). Texas 3-step decellularization protocol: looking at the cardiac extracellular matrix. *J. Proteomics* 86, 43–52. doi: 10.1016/j.jprot.2013.05.004

de Couto, G., Gallet, R., Cambier, L., Jaghatspanyan, E., Makkar, N., Dawkins, J. F., et al. (2017). Exosomal microRNA transfer into macrophages mediates cellular postconditioning. *Circulation* 136, 200–214. doi: 10.1161/CIRCULATIONAHA.116.024590

de Jong, O. G., Murphy, D. E., Mager, I., Willms, E., Garcia-Guerra, A., Gitz-Francois, J. J., et al. (2020). A CRISPR-Cas9-based reporter system for single-cell detection of extracellular vesicle-mediated functional transfer of RNA. *Nat. Commun.* 11:1113. doi: 10.1038/s41467-020-14977-8

Di Meglio, F., Nurzynska, D., Romano, V., Miraglia, R., Belviso, I., Sacco, A. M., et al. (2017). Optimization of human myocardium decellularization method for the construction of implantable patches. *Tissue Eng. Part C Methods* 23, 525–539. doi: 10.1089/ten.TEC.2017.0267

Dube, K. N., Thomas, T. M., Munshaw, S., Rohling, M., Riley, P. R., and Smart, N. (2017). Recapitulation of developmental mechanisms to revascularize the ischemic heart. *JCI Insight* 2:96800. doi: 10.1172/jci.insight.96800

Eroglu, E., and Chien, K. R. (2017). Heart regeneration 4.0: matrix medicine. *Dev. Cell* 42, 7–8. doi: 10.1016/j.devcel.2017.06.017

Eschenhagen, T., Bolli, R., Braun, T., Field, L. J., Fleischmann, B. K., Frisen, J., et al. (2017). Cardiomyocyte regeneration: a consensus statement. *Circulation* 136, 680–686. doi: 10.1161/CIRCULATIONAHA.117.029343

Estes Mark, N. A. (2019). Expression of COncern. *Circ. Res.* 124, e4–e5. doi: 10.1161/RES.0000000000000241

Ezekowitz, J. A., Kaul, P., Bakal, J. A., Armstrong, P. W., Welsh, R. C., and McAlister, F. A. (2009). Declining in-hospital mortality and increasing heart failure incidence in elderly patients with first myocardial infarction. *J. Am. Coll. Cardiol.* 53, 13–20. doi: 10.1016/j.jacc.2008.08.067

Ferng, A. S., Connell, A. M., Marsh, K. M., Qu, N., Medina, A. O., Bajaj, N., et al. (2017). Acellular porcine heart matrices: whole organ decellularization with 3D-bioscaffold & vascular preservation. *J. Clin. Transl. Res.* 3, 260–270.

Frantz, S., Bauersachs, J., and Ertl, G. (2009). Post-infarct remodelling: contribution of wound healing and inflammation. *Cardiovasc. Res.* 81, 474–481. doi: 10.1093/cvr/cvn292

Freyman, T., Polin, G., Osman, H., Crary, J., Lu, M., Cheng, L., et al. (2006). A quantitative, randomized study evaluating three methods of mesenchymal stem cell delivery following myocardial infarction. *Eur. Heart J.* 27, 1114–1122. doi: 10.1093/eurheartj/ehi818

Gabisonia, K., Prosdocimo, G., Aquaro, G. D., Carlucci, L., Zentilin, L., Secco, I., et al. (2019). MicroRNA therapy stimulates uncontrolled cardiac repair after myocardial infarction in pigs. *Nature* 569, 418–422. doi: 10.1038/s41586-019-1191-6

Gilbert, T. W., Sellaro, T. L., and Badylak, S. F. (2006). Decellularization of tissues and organs. *Biomaterials* 27, 3675–3683. doi: 10.1016/j.biomaterials.2006.02.014

Gnecchi, M., He, H., Noiseux, N., Liang, O. D., Zhang, L., Morello, F., et al. (2006). Evidence supporting paracrine hypothesis for Akt-modified mesenchymal stem cell-mediated cardiac protection and functional improvement. *FASEB J.* 20, 661–669. doi: 10.1096/fj.05-5211com

Gonzalez-King, H., Garcia, N. A., Ontoria-Oviedo, I., Ciria, M., Montero, J. A., and Sepulveda, P. (2017). Hypoxia inducible factor-1alpha potentiates jagged 1-mediated angiogenesis by mesenchymal stem cell-derived exosomes. *Stem Cells* 35, 1747–1759. doi: 10.1002/stem.2618

Gupta, K. B., Ratcliffe, M. B., Fallert, M. A., Edmunds, L. H., Jr., and Bogen, D. K. (1994). Changes in passive mechanical stiffness of myocardial tissue with aneurysm formation. *Circulation* 89, 2315–2326. doi: 10.1161/01.cir.89.5.2315

Han, Y., Chen, A., Umansky, K. B., Oonk, K. A., Choi, W. Y., Dickson, A. L., et al. (2019). Vitamin D stimulates cardiomyocyte proliferation and controls organ size and regeneration in zebrafish. *Dev. Cell* 48, 853–863.e5. doi: 10.1016/j.devcel.2019.01.001

Harane, N. E., Correa, B. L., Gomez, I., Hocine, H. R., Vilar, J., Desgres, M., et al. (2020). Extracellular vesicles from human cardiovascular progenitors trigger a reparative immune response in infarcted Hearts. *Cardiovasc. Res.* cvaa028. doi: 10.1093/cvr/cvaa028 [Epub ahead of print].

Hasan, A., Ragaert, K., Swieszkowski, W., Selimovic, S., Paul, A., Camci-Unal, G., et al. (2014). Biomechanical properties of native and tissue engineered heart valve constructs. *J. Biomech.* 47, 1949–1963. doi: 10.1016/j.jbiomech.2013.09.023

Hatzistergos, K. E., Quevedo, H., Oskouei, B. N., Hu, Q., Feigenbaum, G. S., Margitich, I. S., et al. (2010). Bone marrow mesenchymal stem cells stimulate cardiac stem cell proliferation and differentiation. *Circ. Res.* 107, 913–922. doi: 10.1161/CIRCRESAHA.110.222703

Haubner, B. J., Schneider, J., Schweigmann, U., Schuetz, T., Dichtl, W., Velik-Salchner, C., et al. (2016). Functional recovery of a human neonatal heart after severe myocardial infarction. *Circ. Res.* 118, 216–221. doi: 10.1161/CIRCRESAHA.115.307017

Hernandez, M. J., Gaetani, R., Pieters, V. M., Ng, N. W., Chang, A. E., Martin, T. R., et al. (2018). Decellularized extracellular matrix hydrogels as a delivery platform for microRNA and extracellular vesicle therapeutics. *Adv. Ther.* 1:1800032. doi: 10.1002/adtp.201800032

Hesse, M., Fleischmann, B. K., and Kotlikoff, M. I. (2014). Concise review: the role of C-kit expressing cells in heart repair at the neonatal and adult stage. *Stem Cells* 32, 1701–1712. doi: 10.1002/stem.1696

Hodgkinson, C. P., Bareja, A., Gomez, J. A., and Dzau, V. J. (2016). Emerging concepts in paracrine mechanisms in regenerative cardiovascular medicine and biology. *Circ. Res.* 118, 95–107. doi: 10.1161/CIRCRESAHA.115.305373

Hodgkinson, C. P., Gomez, J. A., Mirotsou, M., and Dzau, V. J. (2010). Genetic engineering of mesenchymal stem cells and its application in human disease therapy. *Hum. Gene Ther.* 21, 1513–1526. doi: 10.1089/hum.2010.165

Hsich, E. M. (2016). Matching the market for heart transplantation. *Circ. Heart Fail.* 9:e002679. doi: 10.1161/CIRCHEARTFAILURE.115.002679

Huang, G. N., Thatcher, J. E., McAnally, J., Kong, Y., Qi, X., Tan, W., et al. (2012). C/EBP transcription factors mediate epicardial activation during heart development and injury. *Science* 338, 1599–1603. doi: 10.1126/science.1229765

Huang, S., and Frangogiannis, N. G. (2018). Anti-inflammatory therapies in myocardial infarction: failures, hopes and challenges. *Br. J. Pharmacol.* 175, 1377–1400. doi: 10.1111/bph.14155

Hynes, B., Kumar, A. H., O'Sullivan, J., Klein Buneker, C., Leblond, A. L., Weiss, S., et al. (2013). Potent endothelial progenitor cell-conditioned media-related anti-apoptotic, cardiotrophic, and pro-angiogenic effects post-myocardial infarction are mediated by insulin-like growth factor-1. *Eur. Heart J.* 34, 782–789. doi: 10.1093/eurheartj/ehr435

Hyvarinen, K., Holopainen, M., Skirdenko, V., Ruhanen, H., Lehenkari, P., Korhonen, M., et al. (2018). Mesenchymal stromal cells and their extracellular vesicles enhance the anti-inflammatory phenotype of regulatory macrophages by downregulating the production of interleukin (IL)-23 and IL-22. *Front. Immunol.* 9:771. doi: 10.3389/fimmu.2018.00771

Ibrahim, A. G., Cheng, K., and Marban, E. (2014). Exosomes as critical agents of cardiac regeneration triggered by cell therapy. *Stem Cell Rep.* 2, 606–619. doi: 10.1016/j.stemcr.2014.04.006

Jesty, S. A., Steffey, M. A., Lee, F. K., Breitbach, M., Hesse, M., Reining, S., et al. (2012). c-kit+ precursors support postinfarction myogenesis in the neonatal, but not adult, heart. *Proc. Natl. Acad. Sci. U.S.A.* 109, 13380–13385. doi: 10.1073/pnas.1208114109

Jin, H., Sanberg, P. R., and Henning, R. J. (2013). Human umbilical cord blood mononuclear cell-conditioned media inhibits hypoxic-induced apoptosis in human coronary artery endothelial cells and cardiac myocytes by activation of the survival protein Akt. *Cell Transplant.* 22, 1637–1650. doi: 10.3727/096368912X661427

Johnson, T. D., Dequach, J. A., Gaetani, R., Ungerleider, J., Elhag, D., Nigam, V., et al. (2014). Human versus porcine tissue sourcing for an injectable myocardial matrix hydrogel. *Biomater. Sci.* 2014:60283D. doi: 10.1039/C3BM60283D

Johnson, T. D., Hill, R. C., Dzieciatkowska, M., Nigam, V., Behfar, A., Christman, K. L., et al. (2016). Quantification of decellularized human myocardial matrix: a comparison of six patients. *Proteomics Clin. Appl.* 10, 75–83. doi: 10.1002/prca.201500048

Kameli, S. M., Khorramirouz, R., Eftekharzadeh, S., Fendereski, K., Daryabari, S. S., Tavangar, S. M., et al. (2018). Application of tissue-engineered pericardial patch in rat models of myocardial infarction. *J. Biomed. Mater. Res. A* 106, 2670–2678. doi: 10.1002/jbm.a.36464

Kanisicak, O., Vagnozzi, R. J., and Molkentin, J. D. (2017). Identity crisis for regenerative cardiac cKit(+) cells. *Circ. Res.* 121, 1130–1132. doi: 10.1161/CIRCRESAHA.117.311921

Keane, T. J., Swinehart, I. T., and Badylak, S. F. (2015). Methods of tissue decellularization used for preparation of biologic scaffolds and in vivo relevance. *Methods* 84, 25–34. doi: 10.1016/j.ymeth.2015.03.005

Kikuchi, K., Holdway, J. E., Werdich, A. A., Anderson, R. M., Fang, Y., Egnaczyk, G. F., et al. (2010). Primary contribution to zebrafish heart regeneration by gata4(+) cardiomyocytes. *Nature* 464, 601–605. doi: 10.1038/nature08804

Kim, I. G., Hwang, M. P., Park, J. S., Kim, S. H., Kim, J. H., Kang, H. J., et al. (2019). Stretchable ECM patch enhances stem cell delivery for post-MI cardiovascular repair. *Adv. Healthc Mater.* 8:1900593. doi: 10.1002/adhm.201900593

Kordelas, L., Rebmann, V., Ludwig, A. K., Radtke, S., Ruesing, J., Doeppner, T. R., et al. (2014). MSC-derived exosomes: a novel tool to treat therapy-refractory graft-versus-host disease. *Leukemia* 28, 970–973. doi: 10.1038/leu.2014.41

Korf-Klingebiel, M., Kempf, T., Sauer, T., Brinkmann, E., Fischer, P., Meyer, G. P., et al. (2008). Bone marrow cells are a rich source of growth factors and cytokines: implications for cell therapy trials after myocardial infarction. *Eur. Heart J.* 29, 2851–2858. doi: 10.1093/eurheartj/ehn456

Langrzyk, A., Nowak, W. N., Stepniewski, J., Jazwa, A., Florczyk-Soluch, U., Jozkowicz, A., et al. (2018). Critical view on mesenchymal stromal cells in regenerative medicine. *Antioxid. Redox Signal.* 29, 169–190. doi: 10.1089/ars.2017.7159

Lavine, K. J., and Ornitz, D. M. (2008). Fibroblast growth factors and Hedgehogs: at the heart of the epicardial signaling center. *Trends Genet.* 24, 33–40. doi: 10.1016/j.tig.2007.10.007

Lazzarini, E., Balbi, C., Altieri, P., Pfeffer, U., Gambini, E., Canepa, M., et al. (2016). The human amniotic fluid stem cell secretome effectively counteracts doxorubicin-induced cardiotoxicity. *Sci. Rep.* 6:29994. doi: 10.1038/srep29994

Lenzini, S., Bargi, R., Chung, G., and Shin, J. W. (2020). Matrix mechanics and water permeation regulate extracellular vesicle transport. *Nat. Nanotechnol.* 15, 217–223. doi: 10.1038/s41565-020-0636-2

Leone, M., and Engel, F. B. (2019). Advances in heart regeneration based on cardiomyocyte proliferation and regenerative potential of binucleated cardiomyocytes and polyploidization. *Clin. Sci.* 133, 1229–1253. doi: 10.1042/CS20180560

Leone, M., Magadum, A., and Engel, F. B. (2015). Cardiomyocyte proliferation in cardiac development and regeneration: a guide to methodologies and interpretations. *Am. J. Physiol. Heart Circ. Physiol.* 309, H1237–1250. doi: 10.1152/ajpheart.00559.2015

Lepilina, A., Coon, A. N., Kikuchi, K., Holdway, J. E., Roberts, R. W., Burns, C. G., et al. (2006). A dynamic epicardial injury response supports progenitor cell activity during zebrafish heart regeneration. *Cell* 127, 607–619. doi: 10.1016/j.cell.2006.08.052

Li, Y., He, L., Huang, X., Bhaloo, S. I., Zhao, H., Zhang, S., et al. (2018). Genetic lineage tracing of nonmyocyte population by dual recombinases. *Circulation* 138, 793–805. doi: 10.1161/CIRCULATIONAHA.118.034250

Li, Z., Solomonidis, E. G., Meloni, M., Taylor, R. S., Duffin, R., Dobie, R., et al. (2019). Single-cell transcriptome analyses reveal novel targets modulating cardiac neovascularization by resident endothelial cells following myocardial infarction. *Eur. Heart J.* 40, 2507–2520. doi: 10.1093/eurheartj/ehz305

Lim, M., Wang, W., Liang, L., Han, Z. B., Li, Z., Geng, J., et al. (2018). Intravenous injection of allogeneic umbilical cord-derived multipotent mesenchymal stromal cells reduces the infarct area and ameliorates cardiac function in a porcine model of acute myocardial infarction. *Stem Cell Res. Ther.* 9:129. doi: 10.1186/s13287-018-0888-z

Limana, F., Bertolami, C., Mangoni, A., Di Carlo, A., Avitabile, D., Mocini, D., et al. (2010). Myocardial infarction induces embryonic reprogramming of epicardial c-kit(+) cells: role of the pericardial fluid. *J. Mol. Cell. Cardiol.* 48, 609–618. doi: 10.1016/j.yjmcc.2009.11.008

Lo Sicco, C., Reverberi, D., Balbi, C., Ulivi, V., Principi, E., Pascucci, L., et al. (2017). Mesenchymal stem cell-derived extracellular vesicles as mediators of

anti-inflammatory effects: endorsement of macrophage polarization. *Stem Cells Transl. Med.* 6, 1018–1028. doi: 10.1002/sctm.16-0363

Mahmoud, A. I., Porrello, E. R., Kimura, W., Olson, E. N., and Sadek, H. A. (2014). Surgical models for cardiac regeneration in neonatal mice. *Nat. Protoc.* 9, 305–311. doi: 10.1038/nprot.2014.021

Makkar, R. R., Smith, R. R., Cheng, K., Malliaras, K., Thomson, L. E., Berman, D., et al. (2012). Intracoronary cardiosphere-derived cells for heart regeneration after myocardial infarction (CADUCEUS): a prospective, randomised phase 1 trial. *Lancet* 379, 895–904. doi: 10.1016/S0140-6736(12)60195-0

Malliaras, K., and Marban, E. (2011). Cardiac cell therapy: where we've been, where we are, and where we should be headed. *Br. Med. Bull.* 98, 161–185. doi: 10.1093/bmb/ldr018

Mardanpour, P., Nayernia, K., Khodayari, S., Khodayari, H., Molcanyi, M., and Hescheler, J. (2019). Application of stem cell technologies to regenerate injured myocardium and improve cardiac function. *Cell. Physiol. Biochem.* 53, 101–120. doi: 10.33594/000000124

Methe, K., Backdahl, H., Johansson, B. R., Nayakawde, N., Dellgren, G., and Sumitran-Holgersson, S. (2014). An alternative approach to decellularize whole porcine heart. *Biores. Open Access* 3, 327–338. doi: 10.1089/biores.2014.0046

Micheu, M. M., Scarlatescu, A. I., Scafa-Udriste, A., and Dorobantu, M. (2018). The winding road of cardiac regeneration-stem cell omics in the spotlight. *Cells* 7:255. doi: 10.3390/cells7120255

Milano, G., Biemmi, V., Lazzarini, E., Balbi, C., Ciullo, A., Bolis, S., et al. (2019). Intravenous administration of cardiac progenitor cell-derived exosomes protects against doxorubicin/trastuzumab-induced cardiac toxicity. *Cardiovasc. Res.* 116, 383–392. doi: 10.1093/cvr/cvz108

Mirotsou, M., Jayawardena, T. M., Schmeckpeper, J., Gnecchi, M., and Dzau, V. J. (2011). Paracrine mechanisms of stem cell reparative and regenerative actions in the heart. *J. Mol. Cell. Cardiol.* 50, 280–289. doi: 10.1016/j.yjmcc.2010.08.005

Mirotsou, M., Zhang, Z., Deb, A., Zhang, L., Gnecchi, M., Noiseux, N., et al. (2007). Secreted frizzled related protein 2 (Sfrp2) is the key Akt-mesenchymal stem cell-released paracrine factor mediating myocardial survival and repair. *Proc. Natl. Acad. Sci. U.S.A.* 104, 1643–1648. doi: 10.1073/pnas.0610024104

Mozaffarian, D., Benjamin, E. J., Go, A. S., Arnett, D. K., Blaha, M. J., Cushman, M., et al. (2015). Heart disease and stroke statistics–2015 update: a report from the American Heart Association. *Circulation* 131:e29–e322. doi: 10.1161/CIR.0000000000000152

Murry, C. E., Soonpaa, M. H., Reinecke, H., Nakajima, H., Nakajima, H. O., Rubart, M., et al. (2004). Haematopoietic stem cells do not transdifferentiate into cardiac myocytes in myocardial infarcts. *Nature* 428, 664–668. doi: 10.1038/nature02446

Nguyen, B. K., Maltais, S., Perrault, L. P., Tanguay, J. F., Tardif, J. C., Stevens, L. M., et al. (2010). Improved function and myocardial repair of infarcted heart by intracoronary injection of mesenchymal stem cell-derived growth factors. *J. Cardiovasc. Transl. Res.* 3, 547–558. doi: 10.1007/s12265-010-9171-0

Noiseux, N., Gnecchi, M., Lopez-Ilasaca, M., Zhang, L., Solomon, S. D., Deb, A., et al. (2006). Mesenchymal stem cells overexpressing Akt dramatically repair infarcted myocardium and improve cardiac function despite infrequent cellular fusion or differentiation. *Mol. Ther.* 14, 840–850. doi: 10.1016/j.ymthe.2006.05.016

Noort, W. A., Feye, D., Van Den Akker, F., Stecher, D., Chamuleau, S. A., Sluijter, J. P., et al. (2010). Mesenchymal stromal cells to treat cardiovascular disease: strategies to improve survival and therapeutic results. *Panminerva Med.* 52, 27–40.

Ott, H. C., Matthiesen, T. S., Goh, S. K., Black, L. D., Kren, S. M., Netoff, T. I., et al. (2008). Perfusion-decellularized matrix: using nature's platform to engineer a bioartificial heart. *Nat. Med.* 14, 213–221. doi: 10.1038/nm1684

Pagano, F., Picchio, V., Angelini, F., Iaccarino, A., Peruzzi, M., Cavarretta, E., et al. (2018). The biological mechanisms of action of cardiac progenitor cell therapy. *Curr. Cardiol. Rep.* 20:84. doi: 10.1007/s11886-018-1031-6

Park, S. J., Kim, R. Y., Park, B. W., Lee, S., Choi, S. W., Park, J. H., et al. (2019). Dual stem cell therapy synergistically improves cardiac function and vascular regeneration following myocardial infarction. *Nat. Commun.* 10:3123. doi: 10.1038/s41467-019-11091-2

Piccoli, M., Urbani, L., Alvarez-Fallas, M. E., Franzin, C., Dedja, A., Bertin, E., et al. (2016). Improvement of diaphragmatic performance through orthotopic application of decellularized extracellular matrix patch. *Biomaterials* 74, 245–255. doi: 10.1016/j.biomaterials.2015.10.005

Porrello, E. R., Mahmoud, A. I., Simpson, E., Hill, J. A., Richardson, J. A., Olson, E. N., et al. (2011). Transient regenerative potential of the neonatal mouse heart. *Science* 331, 1078–1080. doi: 10.1126/science.1200708

Porrello, E. R., Mahmoud, A. I., Simpson, E., Johnson, B. A., Grinsfelder, D., Canseco, D., et al. (2013). Regulation of neonatal and adult mammalian heart regeneration by the miR-15 family. *Proc. Natl. Acad. Sci. U.S.A.* 110, 187–192. doi: 10.1073/pnas.1208863110

Porzionato, A., Stocco, E., Barbon, S., Grandi, F., Macchi, V., and De Caro, R. (2018). Tissue-engineered grafts from human decellularized extracellular matrices: a systematic review and future perspectives. *Int. J. Mol. Sci.* 19:E4117. doi: 10.3390/ijms19124117

Prabhu, S. D., and Frangogiannis, N. G. (2016). The biological basis for cardiac repair after myocardial infarction: from inflammation to fibrosis. *Circ. Res.* 119, 91–112. doi: 10.1161/CIRCRESAHA.116.303577

Rafatian, G., and Davis, D. R. (2018). Concise review: heart-derived cell therapy 2.0: paracrine strategies to increase therapeutic repair of injured myocardium. *Stem Cells* 36, 1794–1803. doi: 10.1002/stem.2910

Rao, K. S., Aronshtam, A., McElory-Yaggy, K. L., Bakondi, B., VanBuren, P., Sobel, B. E., et al. (2015). Human epicardial cell-conditioned medium contains HGF/IgG complexes that phosphorylate RYK and protect against vascular injury. *Cardiovasc. Res.* 107, 277–286. doi: 10.1093/cvr/cvv168

Rao Pattabhi, S., Martinez, J. S., and Keller, T. C. 3rd. (2014). Decellularized ECM effects on human mesenchymal stem cell stemness and differentiation. *Differentiation* 88, 131–143. doi: 10.1016/j.diff.2014.12.005

Rossano, J. W., Kim, J. J., Decker, J. A., Price, J. F., Zafar, F., Graves, D. E., et al. (2012). Prevalence, morbidity, and mortality of heart failure-related hospitalizations in children in the United States: a population-based study. *J. Card. Fail.* 18, 459–470. doi: 10.1016/j.cardfail.2012.03.001

Sarig, U., Sarig, H., de-Berardinis, E., Chaw, S. Y., Nguyen, E. B., Ramanujam, V. S., et al. (2016). Natural myocardial ECM patch drives cardiac progenitor based restoration even after scarring. *Acta Biomater.* 44, 209–220. doi: 10.1016/j.actbio.2016.08.031

Schachinger, V., Aicher, A., Dobert, N., Rover, R., Diener, J., Fichtlscherer, S., et al. (2008). Pilot trial on determinants of progenitor cell recruitment to the infarcted human myocardium. *Circulation* 118, 1425–1432. doi: 10.1161/CIRCULATIONAHA.108.777102

Segers, V. F., and Lee, R. T. (2008). Stem-cell therapy for cardiac disease. *Nature* 451, 937–942. doi: 10.1038/nature06800

Seif-Naraghi, S. B., Horn, D., Schup-Magoffin, P. A., Madani, M. M., and Christman, K. L. (2011). Patient-to-patient variability in autologous pericardial matrix scaffolds for cardiac repair. *J. Cardiovasc. Transl. Res.* 4, 545–556. doi: 10.1007/s12265-011-9293-z

Seif-Naraghi, S. B., Salvatore, M. A., Schup-Magoffin, P. J., Hu, D. P., and Christman, K. L. (2010). Design and characterization of an injectable pericardial matrix gel: a potentially autologous scaffold for cardiac tissue engineering. *Tissue Eng. Part A* 16, 2017–2027. doi: 10.1089/ten.TEA.2009.0768

Senyo, S. E., Steinhauser, M. L., Pizzimenti, C. L., Yang, V. K., Cai, L., Wang, M., et al. (2013). Mammalian heart renewal by pre-existing cardiomyocytes. *Nature* 493, 433–436. doi: 10.1038/nature11682

Shao, L., Zhang, Y., Lan, B., Wang, J., Zhang, Z., Zhang, L., et al. (2017). MiRNA-sequence indicates that mesenchymal stem cells and exosomes have similar mechanism to enhance cardiac repair. *Biomed Res. Int.* 2017:4150705. doi: 10.1155/2017/4150705

Sharma, S., Mishra, R., Bigham, G. E., Wehman, B., Khan, M. M., Xu, H., et al. (2017). A deep proteome analysis identifies the complete secretome as the functional unit of human cardiac progenitor cells. *Circ. Res.* 120, 816–834. doi: 10.1161/CIRCRESAHA.116.309782

Simpson, D. L., Mishra, R., Sharma, S., Goh, S. K., Deshmukh, S., and Kaushal, S. (2012). A strong regenerative ability of cardiac stem cells derived from neonatal hearts. *Circulation* 126(11 Suppl 1), S46–S53. doi: 10.1161/CIRCULATIONAHA.111.084699

Singelyn, J. M., and Christman, K. L. (2010). Injectable materials for the treatment of myocardial infarction and heart failure: the promise of decellularized matrices. *J. Cardiovasc. Transl. Res.* 3, 478–486. doi: 10.1007/s12265-010-9202-x

Singelyn, J. M., and Christman, K. L. (2011). Modulation of material properties of a decellularized myocardial matrix scaffold. *Macromol. Biosci.* 11, 731–738. doi: 10.1002/mabi.201000423

Singelyn, J. M., Sundaramurthy, P., Johnson, T. D., Schup-Magoffin, P. J., Hu, D. P., Faulk, D. M., et al. (2012). Catheter-deliverable hydrogel derived from decellularized ventricular extracellular matrix increases endogenous cardiomyocytes and preserves cardiac function post-myocardial infarction. *J. Am. Coll. Cardiol.* 59, 751–763. doi: 10.1016/j.jacc.2011.10.888

Sluijter, J. P. G., Davidson, S. M., Boulanger, C. M., Buzas, E. I., de Kleijn, D. P. V., Engel, F. B., et al. (2018). Extracellular vesicles in diagnostics and therapy of the ischaemic heart: position paper from the working group on cellular biology of the heart of the European society of cardiology. *Cardiovasc. Res.* 114, 19–34. doi: 10.1093/cvr/cvx211

Smart, N., Bollini, S., Dube, K. N., Vieira, J. M., Zhou, B., Davidson, S., et al. (2011). De novo cardiomyocytes from within the activated adult heart after injury. *Nature* 474, 640–644. doi: 10.1038/nature10188

Smith, T. K., and Bader, D. M. (2007). Signals from both sides: control of cardiac development by the endocardium and epicardium. *Semin Cell Dev. Biol.* 18, 84–89. doi: 10.1016/j.semcdb.2006.12.013

Song, J.J., and Ott, H.C. (2011). Organ engineering based on decellularized matrix scaffolds. *Trends Mol. Med.* 17, 424–432. doi: 10.1016/j.molmed.2011.03.005

Spath, N. B., Mills, N. L., and Cruden, N. L. (2016). Novel cardioprotective and regenerative therapies in acute myocardial infarction: a review of recent and ongoing clinical trials. *Future Cardiol.* 12, 655–672. doi: 10.2217/fca-2016-0044

Spinali, K. L., and Schmuck, E. G. (2018). Natural sources of extracellular matrix for cardiac repair. *Adv. Exp. Med. Biol.* 1098, 115–130. doi: 10.1007/978-3-319-97421-7_6

Streeter, B. W., and Davis, M. E. (2019). Therapeutic cardiac patches for repairing the myocardium. *Adv. Exp. Med. Biol.* 1144, 1–24. doi: 10.1007/5584_2018_309

Sultana, N., Zhang, L., Yan, J., Chen, J., Cai, W., Razzaque, S., et al. (2015). Resident c-kit(+) cells in the heart are not cardiac stem cells. *Nat. Commun.* 6:8701. doi: 10.1038/ncomms9701

Takov, K., He, Z., Johnston, H. E., Timms, J. F., Guillot, P. V., Yellon, D. M., et al. (2020). Small extracellular vesicles secreted from human amniotic fluid mesenchymal stromal cells possess cardioprotective and promigratory potential. *Basic Res. Cardiol.* 115:26. doi: 10.1007/s00395-020-0785-3

Tang, J., Li, Y., Huang, X., He, L., Zhang, L., Wang, H., et al. (2018). Fate mapping of Sca1(+) cardiac progenitor cells in the adult mouse heart. *Circulation* 138, 2967–2969. doi: 10.1161/CIRCULATIONAHA.118.036210

Tang-Quan, K. R., Mehta, N. A., Sampaio, L. C., and Taylor, D. A. (2018). Whole cardiac tissue bioscaffolds. *Adv. Exp. Med. Biol.* 1098, 85–114. doi: 10.1007/978-3-319-97421-7_5

Tapias, L. F., and Ott, H. C. (2014). Decellularized scaffolds as a platform for bioengineered organs. *Curr. Opin. Organ. Transplant.* 19, 145–152. doi: 10.1097/MOT.0000000000000051

Taylor, D. A., Parikh, R. B., and Sampaio, L. C. (2017). Bioengineering hearts: simple yet complex. *Curr. Stem Cell Rep.* 3, 35–44. doi: 10.1007/s40778-017-0075-7

Taylor, D. A., Sampaio, L. C., and Gobin, A. (2014). Building new hearts: a review of trends in cardiac tissue engineering. *Am. J. Transplant.* 14, 2448–2459. doi: 10.1111/ajt.12939

Teplitz, L. (1990). Action stat! Hypertensive crisis. *Nursing* 20:33. doi: 10.1097/00152193-199004000-00011

Thery, C., Witwer, K. W., Aikawa, E., Alcaraz, M. J., Anderson, J. D., Andriantsitohaina, R., et al. (2018). Minimal information for studies of extracellular vesicles 2018 (MISEV2018): a position statement of the International Society for Extracellular Vesicles and update of the MISEV2014 guidelines. *J. Extracell. Vesicles* 7:1535750. doi: 10.1080/20013078.2018.1535750

Timmers, L., Lim, S. K., Hoefer, I. E., Arslan, F., Lai, R. C., van Oorschot, A. A., et al. (2011). Human mesenchymal stem cell-conditioned medium improves cardiac function following myocardial infarction. *Stem Cell Res.* 6, 206–214. doi: 10.1016/j.scr.2011.01.001

Toeg, H. D., Tiwari-Pandey, R., Seymour, R., Ahmadi, A., Crowe, S., Vulesevic, B., et al. (2013). Injectable small intestine submucosal extracellular matrix in an acute myocardial infarction model. *Ann. Thorac. Surg.* 96, 1686–1694. doi: 10.1016/j.athoracsur.2013.06.063

Tseliou, E., Fouad, J., Reich, H., Slipczuk, L., de Couto, G., Aminzadeh, M., et al. (2015). Fibroblasts rendered antifibrotic, antiapoptotic, and angiogenic by priming with cardiosphere-derived extracellular membrane vesicles. *J. Am. Coll. Cardiol.* 66, 599–611. doi: 10.1016/j.jacc.2015.05.068

Urciuolo, A., and De Coppi, P. (2018). Decellularized tissue for muscle regeneration. *Int. J. Mol. Sci.* 19:E2392. doi: 10.3390/ijms19082392

van Dongen, J. A., Getova, V., Brouwer, L. A., Liguori, G. R., Sharma, P. K., Stevens, H. P., et al. (2019). Adipose tissue-derived extracellular matrix hydrogels as a release platform for secreted paracrine factors. *J. Tissue Eng. Regen. Med.* 13, 973–985. doi: 10.1002/term.2843

Van Linthout, S., Hamdani, N., Miteva, K., Koschel, A., Muller, I., Pinzur, L., et al. (2017). Placenta-derived adherent stromal cells improve diabetes mellitus-associated left ventricular diastolic performance. *Stem Cells Transl. Med.* 6, 2135–2145. doi: 10.1002/sctm.17-0130

Vujic, A., Natarajan, N., and Lee, R. T. (2020). Molecular mechanisms of heart regeneration. *Semin Cell Dev. Biol.* 100, 20–28. doi: 10.1016/j.semcdb.2019.09.003

Wainwright, J. M., Czajka, C. A., Patel, U. B., Freytes, D. O., Tobita, K., Gilbert, T. W., et al. (2010). Preparation of cardiac extracellular matrix from an intact porcine heart. *Tissue Eng. Part C Methods* 16, 525–532. doi: 10.1089/ten.TEC.2009.0392

Wainwright, J. M., Hashizume, R., Fujimoto, K. L., Remlinger, N. T., Pesyna, C., Wagner, W. R., et al. (2012). Right ventricular outflow tract repair with a cardiac biologic scaffold. *Cells Tissues Organs* 195, 159–170. doi: 10.1159/000331400

Wang, B., Williams, L. N., de Jongh Curry, A. L., and Liao, J. (2014). Preparation of acellular myocardial scaffolds with well-preserved cardiomyocyte lacunae, and method for applying mechanical and electrical simulation to tissue construct. *Methods Mol. Biol.* 1181, 189–202. doi: 10.1007/978-1-4939-1047-2_17

Wang, R.M., and Christman, K.L. (2016). Decellularized myocardial matrix hydrogels: in basic research and preclinical studies. *Adv. Drug Deliv. Rev.* 96, 77–82. doi: 10.1016/j.addr.2015.06.002

Wang, W. E., Li, L., Xia, X., Fu, W., Liao, Q., Lan, C., et al. (2017). Dedifferentiation, proliferation, and redifferentiation of adult mammalian cardiomyocytes after ischemic injury. *Circulation* 136, 834–848. doi: 10.1161/CIRCULATIONAHA.116.024307

Wang, Z., Long, D. W., Huang, Y., Chen, W. C. W., Kim, K., and Wang, Y. (2019). Decellularized neonatal cardiac extracellular matrix prevents widespread ventricular remodeling in adult mammals after myocardial infarction. *Acta Biomater.* 87, 140–151. doi: 10.1016/j.actbio.2019.01.062

Wehman, B., Pietris, N., Bigham, G., Siddiqui, O., Mishra, R., Li, T., et al. (2017). Cardiac progenitor cells enhance neonatal right ventricular function after pulmonary artery banding. *Ann. Thorac. Surg.* 104, 2045–2053. doi: 10.1016/j.athoracsur.2017.04.058

Xie, M., Xiong, W., She, Z., Wen, Z., Abdirahman, A. S., Wan, W., et al. (2020). Immunoregulatory effects of stem cell-derived extracellular vesicles on immune cells. *Front. Immunol.* 11:13. doi: 10.3389/fimmu.2020.00013

Xing, H., Lee, H., Luo, L., and Kyriakides, T. R. (2019). Extracellular matrix-derived biomaterials in engineering cell function. *Biotechnol. Adv.* 2:107421. doi: 10.1016/j.biotechadv.2019.107421

Xuan, W., Khan, M., and Ashraf, M. (2020). Extracellular vesicles from notch activated cardiac mesenchymal stem cells promote myocyte proliferation and neovasculogenesis. *Front. Cell Dev. Biol.* 8:11. doi: 10.3389/fcell.2020.00011

Yang, D., Wang, W., Li, L., Peng, Y., Chen, P., Huang, H., et al. (2013). The relative contribution of paracine effect versus direct differentiation on adipose-derived stem cell transplantation mediated cardiac repair. *PLoS One* 8:e59020. doi: 10.1371/journal.pone.0059020

Yang, D., Zhang, W., Zhang, H., Zhang, F., Chen, L., Ma, L., et al. (2020). Progress, opportunity, and perspective on exosome isolation - efforts for efficient exosome-based theranostics. *Theranostics* 10, 3684–3707. doi: 10.7150/thno.41580

Zhang, J., Zhu, W., Radisic, M., and Vunjak-Novakovic, G. (2018). Can we engineer a human cardiac patch for therapy? *Circ. Res.* 123, 244–265. doi: 10.1161/CIRCRESAHA.118.311213

Zhang, L., Sultana, N., Yan, J., Yang, F., Chen, F., Chepurko, E., et al. (2018). Cardiac Sca-1(+) cells are not intrinsic stem cells for myocardial development, renewal, and repair. *Circulation* 138, 2919–2930. doi: 10.1161/CIRCULATIONAHA.118.035200

Zhao, L., Cheng, G., Choksi, K., Samanta, A., Girgis, M., Soder, R., et al. (2019). Transplantation of human umbilical cord blood-derived cellular fraction improves left ventricular function and remodeling after myocardial

ischemia/reperfusion. *Circ. Res.* 125, 759–772. doi: 10.1161/CIRCRESAHA.119.315216

Zhou, B., Honor, L. B., He, H., Ma, Q., Oh, J. H., Butterfield, C., et al. (2011). Adult mouse epicardium modulates myocardial injury by secreting paracrine factors. *J. Clin. Invest.*121, 1894–1904. doi: 10.1172/JCI45529

Zhou, B., Ma, Q., Rajagopal, S., Wu, S. M., Domian, I., Rivera-Feliciano, J., et al. (2008). Epicardial progenitors contribute to the cardiomyocyte lineage in the developing heart. *Nature* 454, 109–113. doi: 10.1038/nature07060

Zhu, J., Lu, K., Zhang, N., Zhao, Y., Ma, Q., Shen, J., et al. (2018). Myocardial reparative functions of exosomes from mesenchymal stem cells are enhanced by hypoxia treatment of the cells via transferring microRNA-210 in an nSMase2-dependent way. *Artif. Cells Nanomed. Biotechnol.* 46, 1659–1670. doi: 10.1080/21691401.2017.1388249

Zisch, A. H., Lutolf, M. P., and Hubbell, J. A. (2003). Biopolymeric delivery matrices for angiogenic growth factors. *Cardiovasc. Pathol.* 12, 295–310. doi: 10.1016/s1054-8807(03)00089-9

Conflict of Interest: The authors declare that the research was conducted in the absence of any commercial or financial relationships that could be construed as a potential conflict of interest.

Copyright © 2020 Maghin, Garbati, Quarto, Piccoli and Bollini. This is an open-access article distributed under the terms of the Creative Commons Attribution License (CC BY). The use, distribution or reproduction in other forums is permitted, provided the original author(s) and the copyright owner(s) are credited and that the original publication in this journal is cited, in accordance with accepted academic practice. No use, distribution or reproduction is permitted which does not comply with these terms.

frontiers in Bioengineering and Biotechnology

PERSPECTIVE
published: 26 May 2020
doi: 10.3389/fbioe.2020.00411

Blocking Extracellular Chaperones to Improve Cardiac Regeneration

*Laura Seclì[1], Matteo Sorge[1], Alessandro Morotti[2] and Mara Brancaccio[1]**

[1] Department of Molecular Biotechnology and Health Sciences, University of Turin, Turin, Italy, [2] Department of Clinical and Biological Sciences, University of Turin, Turin, Italy

Chronic or acute insults to the myocardium are responsible for the onset of cardiomyopathy and heart failure. Due to the poor regenerative ability of the human adult heart, the survival of cardiomyocytes is a prerequisite to support heart function. Chaperone proteins, by regulating sarcomeric protein folding, function, and turnover in the challenging environment of the beating heart, play a fundamental role in myocardial physiology. Nevertheless, a number of evidences indicate that, under stress conditions or during cell damage, myocardial cells release chaperone proteins that, from the extracellular milieu, play a detrimental function, by perpetuating inflammation and inducing cardiomyocyte apoptosis. Blocking the activity of extracellular chaperones has been proven to have beneficial effects on heart function in preclinical models of myocardial infarction and cardiomyopathy. The application of this approach in combination with tissue engineering strategies may represent a future innovation in cardiac regenerative medicine.

Keywords: extracellular chaperones, HSPs, Toll-like receptors, sterile inflammation, myocardial infarction, cardiomyopathy, heart failure

OPEN ACCESS

Edited by:
Ipsita Roy,
The University of Sheffield,
United Kingdom

Reviewed by:
Manuel Ahumada,
Universidad Mayor, Chile
Diego Cotella,
University of Eastern Piedmont, Italy

***Correspondence:**
Mara Brancaccio
mara.brancaccio@unito.it

Specialty section:
This article was submitted to Biomaterials, a section of the journal Frontiers in Bioengineering and Biotechnology

Received: *27 December 2019*
Accepted: *14 April 2020*
Published: *26 May 2020*

Citation:
Seclì L, Sorge M, Morotti A and Brancaccio M (2020) Blocking Extracellular Chaperones to Improve Cardiac Regeneration. Front. Bioeng. Biotechnol. 8:411. doi: 10.3389/fbioe.2020.00411

INTRACELLULAR CHAPERONES

Sarcomere efficiency is a priority to maintain cardiac function. The impressive sarcomere structure depends on the rigorous association of hundreds of proteins, held together by non-covalent bonds in the challenging context of continuous contractions and relaxations. Indeed, the rhythmic mechanical stretch of the beating heart is, *per se*, a source of protein unfolding and a number of pathological factors, such as pressure overload, metabolic challenges, oxidative stress, may tip the balance toward dysfunction. An efficient quality control mechanism is essential for sarcomere maintenance and dynamic adaptation to new physiological conditions (Willis et al., 2009). Further, unfolded protein degradation through the ubiquitin–proteasome pathway and autophagy (Ranek et al., 2018) is crucial in protecting cardiomyocytes from the accumulation of dangerous protein aggregates. Chaperone proteins are in charge of carrying out these essential tasks and monitoring the efficiency of the entire contractile system. Chaperones have been originally discovered as induced by hyperthermia, whereby the name of heat shock proteins (HSPs) has been attributed to a number of chaperones (Schlesinger, 1990). Later, it became clear that several chaperones are induced upon different types of stress stimuli, including oxidative stress, pathogen infection, mechanical stress, hypoxic conditions, and ischemia (Sbroggio et al., 2008; Tarone and Brancaccio, 2014; Sorge and Brancaccio, 2016; Penna et al., 2018). Chaperones are divided in different subfamilies depending on their structure, molecular weight and on their ability to hydrolyze ATP (Macario and Conway de Macario, 2005; Kampinga et al., 2009). In this review, we will

mention chaperones belonging to two subclasses: ATP-dependent chaperones and small heat shock proteins (sHSPs), lacking ATPase activity. The best known ATP-dependent chaperones are the heat shock proteins HSP90, HSP70, and HSP60 (numbers are indicative of their molecular weights). They bind to two classes of proteins: substrate proteins and co-chaperones. Chaperone binding allows substrate proteins, also called clients, to reach their functional conformation, to refold after denaturation and to be protected from degradation. Co-chaperones, instead, assist chaperones in their function, favoring client protein recognition and the transition toward the different structural states required for binding and release of clients. The family of sHSPs is characterized by the absence of ATPase activity, a lower molecular weight, the presence of a highly conserved α-crystallin domain, and their attitude to form oligomers (Carra et al., 2019; Haslbeck et al., 2019). Both ATP-dependent chaperones and sHSPs play a protective role in the myocardium thanks to their ability to cope with protein misfolding, to promote unfolded protein degradation and to support survival signaling in cardiomyocytes (Willis and Patterson, 2013; Tarone and Brancaccio, 2014).

EXTRACELLULAR CHAPERONES

Chaperones are conventionally considered intracellular proteins, prevalently located in the cytoplasm, in the endoplasmic reticulum, in mitochondria, and in the nucleus. In addition to their well-known roles inside the cells, some chaperones and co-chaperones have been found to be secreted in the extracellular milieu in response to cell stress, through an unconventional secretory pathway, and to exert different functions from the outside (Srivastava, 2002b; Calderwood, 2018; Pockley and Henderson, 2018). Among other activities, extracellular chaperones work as damage-associated molecular patterns (DAMPS). As for pathogen-associated molecular patterns (PAMPs), DAMPs are recognized by pattern-recognition receptors (PRRs), such as Toll-like receptors (TLRs), which, in turn, trigger inflammatory responses. In addition to chaperones, DAMPs include the high-mobility group box 1 (HMGB1), S100 family of proteins, RNA, mitochondrial DNA, uric acid, adenosine nucleotides, and others. These molecules may reach the outside by a regulated unconventional secretion induced by stress or may be released during cell damage. From the extracellular milieu, they bind to PRRs on different cell types, activate signaling pathways, and orchestrate cytokine production and immune cell recruitment (Asea et al., 2000; Asea, 2003; Bianchi, 2007). The release of DAMPs plays a role in different diseases in which the immune system is actively involved, including arthritis, multiple sclerosis, cancer, and cardiovascular diseases (Roh and Sohn, 2018). Nevertheless, the release of chaperones from stressed cells may represent an ancient and evolutionary conserved protection mechanism against pathogen infection (Srivastava, 2002a,b). Indeed, chaperones, by binding antigenic peptides and interacting with receptors on antigen-presenting cells, are crucial players in antigen internalization and processing, contributing to innate and adaptive immune responses. Stressful conditions and tissue necrosis, by mediating chaperone release, trigger a sterile inflammation that, besides clearing cellular debris, may extend organ damage and blunt reparative responses (Lai et al., 2019).

The myocardium is composed of different cell types, whereas cardiomyocytes and cardiac fibroblasts are the more represented, endothelial cells, vessel smooth muscle cells, and immune cells are also present in a relevant number. All these cell types express PRRs able to sense DAMPS and detect cardiac stress and damage. After myocardial infarction, the release of DAMPs from injured cardiomyocytes results primarily in the recruitment and activation of innate immune cells, causing endothelial damage and cardiomyocyte injury (Arslan et al., 2011). Accordingly, Toll-like receptor 2 (TLR2) and TLR4 null mice are protected from ischemia–reperfusion injury (Sakata et al., 2007; Arslan et al., 2010, 2011; Li et al., 2011). In addition, DAMPs promote fibroblast proliferation, extracellular matrix deposition, and secretion of metalloproteinases (MMPs) that may jeopardize the stability of the scar (Turner, 2016). Overall, TLR signaling in acute myocardial infarction has been convincingly associated to a maladaptive remodeling and with a decreased cardiac function (Shishido et al., 2003; Satoh et al., 2006b; Timmers et al., 2008; Turner, 2016).

HSP70

HSP70 is an ubiquitously expressed chaperone that, inside the cell, plays an essential role in mediating protein folding and exerts a protective activity against hypoxic and ischemic events (Hecker and McGarvey, 2011). Following different insults such as ischemia, hypoxia, and hemodynamic overload, HSP70 and its cognate protein HSC70 are upregulated in cardiomyocytes and secreted or passively released. Indeed, in mice subjected to abdominal aortic constriction, HSP70 accumulates on the cardiomyocyte plasma membranes and in the mouse serum in a time-dependent manner (Cai et al., 2010). Treatment of mice with doxorubicin, a chemotherapy drug known to cause cardiotoxicity, also induces HSP70 upregulation in the heart and its subsequent accumulation on cardiomyocyte membranes and mouse serum (Liu P. et al., 2019). Moreover, patients experiencing cardiac arrest (Jenei et al., 2013a), acute myocardial infarction (Dybdahl et al., 2005; Satoh et al., 2006a), or coronary artery bypass grafting with the use of cardiopulmonary bypass (Dybdahl et al., 2002) present a higher HSP70 level in the serum, compared to healthy subjects. In these patients, higher circulating levels of HSP70 correlate with increased serum levels of proinflammatory cytokines such as IL-1α, IL-6, TNF-α, IL-17, and TGF-β and myocardial necrosis markers, such as creatine kinase and cardiac troponin T, and are associated with an increased mortality during the follow-up period (Dybdahl et al., 2002, 2005; Satoh et al., 2006a; Jenei et al., 2013a,b). Primary isolated cardiomyocytes treated with recombinant HSP70 proteins show an increase in NF-κB activity, a decreased contractility and a raise in apoptotic death. Stimulation of the cardiac muscle cell line HL-1 with recombinant HSP70 promotes the expression of inflammatory markers downstream the p38 and the NF-κB signaling pathways. The activity of

the recombinant HSP70 was totally impaired in TLR2 null cardiomyocytes and in cardiomyocytes deficient for the TLR signal adaptor protein MyD88 (Mathur et al., 2011). Similarly, treatment of mouse cardiomyocytes with recombinant HSC70 induces the phosphorylation of p38; increases the expression of mRNA coding for TNF-α, IL-1β, and IL-6; and depresses cardiac contractility, in a TLR4-dependent manner (Zou et al., 2008; Ao et al., 2009). Overall, these data suggest that once secreted, HSP70 and HSC70 bind to TLR2 and TLR4 expressed on cardiomyocytes and induce the p38 MAPK and the NF-κB signaling pathways (**Figure 1**). Due to the high expression of TLRs on immune cells, it is not surprising that HSP70 and HSC70 possess a potent immunomodulatory role in the myocardium, regulating immune infiltration after stress stimuli. For instance, binding of a recombinant HSP70 to TLR4 on peritoneal-derived macrophages induces the production of TNF-α (**Figure 1**), which, in turn, stokes chronic inflammation in the myocardium. In patients with myocardial infarction, HSP70 serum levels are positively correlated with the number of TLR4-positive monocytes in the heart, which favor heart failure progression. The presence of HSP70 in patients' serum not only represents a reliable marker in heart failure (Jenei et al., 2013b), but may also be exploited as a target to treat cardiac pathologies. The functional antagonism of the extracellular HSP70 (eHSP70), using anti-HSP70 antibodies, significantly attenuates cardiac hypertrophy, fibrosis, and cardiomyocyte apoptosis induced by pressure overload. Moreover, the treatment with HSP70-neutralizing antibodies reduces pro-inflammatory M1 macrophage infiltration in the myocardium, blunting chronic inflammation (Cai et al., 2010; Liu P. et al., 2019). Injection of anti-HSP70 antibodies, after doxorubicin treatment in mice, significantly counteracts α-SMA and collagen-1 upregulation, two important markers of fibrosis in the myocardium, and reduces the production of IL-6, TFG-β, and IL-17A. At the same time, anti-HSP70 antibodies inhibit the expression of inducible NO synthase and cyclooxygenase 2, suggesting that the chronic inflammation in the hearts of doxorubicin-treated mice can be reversed by blocking eHSP70 activity (Liu P. et al., 2019). Similarly, treatment with anti-HSC70 antibodies in mice subjected to ischemia/reperfusion (I/R) improves post-ischemic cardiac functional recovery and reduces the expression of proinflammatory cytokines (IL-6, IL-1β, and TGF-β) (Zou et al., 2008), favoring cardiomyocyte survival. Neutralizing antibodies against TLR2 and TLR4 mimic the effect of HSP70/HSC70 blocking antibodies, preventing reduction in fractional shortening and increasing heart function (Mathur et al., 2011).

BAG3

Bcl-2-associated athanogene 3 (BAG3) plays crucial roles in cardiomyocytes by inhibiting apoptosis and promoting unfolded protein degradation through macroautophagy. Indeed, mutations in the BAG3 coding gene are associated with dilated cardiomyopathy (Liu L. et al., 2019). Besides this important intracellular role, BAG3 has been found secreted by the rat cardiomyoblast cell line H9c2 and by primary adult human cardiomyocytes in response to stress stimuli and it is detectable in the sera of heart failure patients (De Marco et al., 2013; Gandhi et al., 2015). The extracellular BAG3 triggers the PI3K/AKT/eNOS pathway in endothelial cells, causing nitric oxide release and vasorelaxation (Carrizzo et al., 2016). Of note, BAG3 secreted by cancer cells may activate macrophages and promote IL-6 production, suggesting that BAG3 may regulate inflammation also in the myocardial context (Rosati et al., 2015). Further studies are awaited to define the impact of the extracellular BAG3 on cardiac function after myocardial damage.

HSP90

HSP90 is an essential and ubiquitous chaperone that exerts multiple roles inside the cells, ranging from protein folding, buffering protein denaturation, and assisting signal transduction protein conformational changes (Schopf et al., 2017). HSP90 is secreted in response to different stress stimuli and, from the extracellular milieu, it is able to bind to several cellular receptors, among them TLR2 and 4, and to unleash intracellular signal transduction pathways (Calderwood et al., 2007). The role of the extracellular HSP90 (eHSP90) has been extensively studied in the cancer microenvironment, where it regulates metalloproteinase activity (Baker-Williams et al., 2019) and fibronectin matrix assembly (Chakraborty et al., 2020) and promotes cancer cell survival, migration, and invasion (Calderwood, 2018). In this context, eHSP90 can also recruit and activate stromal fibroblasts (Bohonowych et al., 2014; Tang et al., 2019). Garcia and colleagues described cardiac fibroblasts as a primary source of eHSP90 in the myocardium subjected to pressure overload. Cardiac fibroblasts are activated by myocardial damage or stress and are responsible for matrix deposition. eHSP90 has been found to interact with the transforming growth factor-β receptor I (TGFβRI) on the surface of cardiac fibroblasts, inducing TGF-β signaling and promoting collagen production and fibrosis. Indeed, mice null for the inducible HSP90α isoform show reduced collagen deposition and cardiac fibrosis in long-term pressure overload (Garcia et al., 2016; **Figure 1**).

HSP60

HSP60 is a chaperone protein located both in mitochondria and in the cytosol, responsible for the folding of mitochondrial-imported proteins (Singh et al., 1990; Brinker et al., 2001). In mitochondria, HSP60 monomers assemble in a double heptameric ring, associated with a co-chaperone, HSP10, that caps the inner cavity and regulates substrate processing (Xu et al., 1997). Instead, in the cytosol, HSP60 is present as a monomer or bound to specific interactors, as the pro-apoptotic protein Bax (Kirchhoff et al., 2002). Several studies demonstrated that the expression and distribution of HSP60 is altered in cardiac diseases (Novo et al., 2011). In a rat model of heart failure, HSP60 was found upregulated after ligation of the left anterior descending artery, together with proinflammatory cytokines, brain, and atrial natriuretic peptides (Lin et al., 2007). In isolated cardiac myocytes

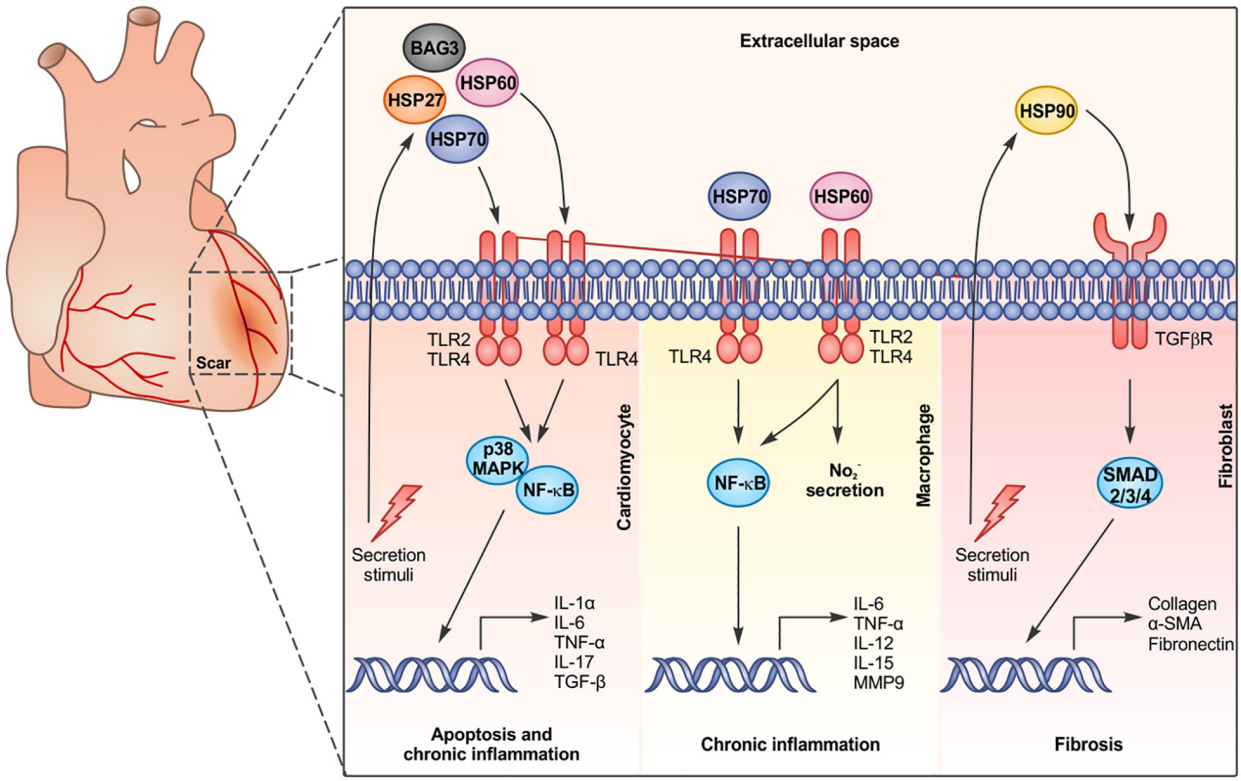

FIGURE 1 | Chaperone proteins are released by cardiac cells and bind to surface receptors on different cell types, activating specific signaling pathways and inducing apoptosis, chronic inflammation, and fibrosis.

subjected to ischemic insults, HSP60 translocates from the cytosol to plasma membrane lipid rafts and is secreted and released in exosomes (Gupta and Knowlton, 2002; Lin et al., 2007). HSP60 doubles in patients affected by ischemic disease, if compared with healthy controls (Knowlton et al., 1998), and its membrane translocation and release have been also demonstrated (Lin et al., 2007; Tian et al., 2013). Moreover, HSP60 circulating levels in patients with coronary artery disease and acute myocardial infarction correlate with the extent of the disease (Mandal et al., 2006; Novo et al., 2011).

The translocation of HSP60 to the plasma membrane and its secretion induce the release of Bax that can move to mitochondria and activate the apoptotic cascade (Gupta and Knowlton, 2002). In addition, HSP60 actively triggers apoptosis in cardiomyocytes from the extracellular compartment (Kim et al., 2009; Li et al., 2011). Indeed, in adult-rat cardiomyocytes or H9c2 cells, the extracellular HSP60 (eHSP60) binds to TLR4, but not TLR2, and promotes the expression of TNF-α, IL-6, and IL-1β (Kim et al., 2009; Tian et al., 2013; **Figure 1**). Pretreatment of cells with blocking antibodies against TLR4 or inhibitors for MyD88 significantly decreases cardiomyocyte apoptosis, while antibodies against TLR2 have no effect (Kim et al., 2009). Antibodies against TNF-α, but not against IL-1β, also block eHSP60-induced apoptosis (Kim et al., 2009). All these evidence suggest that extracellular eHSP60 specifically activates the TLR4-MyD88-NF-κB pathway, thus inducing TNF-α-mediated cardiomyocyte apoptosis. *In vivo* coronary artery ligation followed by reperfusion induces the activation of the interleukin receptor-associated kinase-1 (IRAK-1), a kinase critical for TLR signaling. The treatment of mice with anti-HSP60 antibodies, prior to the ligation, significantly attenuates IRAK-1 activation (Li et al., 2011). The absence of TLR4 or MyD88, but not TLR2, impairs IRAK-1 activation in response to I/R, confirming the specificity of eHSP60 in activating TLR4 signaling (Li et al., 2011). eHSP60 induces caspase-8-dependent apoptosis and the absence of TLR4, or the treatment of mice with anti-HSP60 antibodies, and attenuates I/R-induced cell death (Li et al., 2011).

In endothelial cells, HSP60 elicits the expression of E-selectin, ICAM-1, and VCAM-1, favoring the leukocyte trafficking within the vascular wall (Kol et al., 1999). In macrophages, it has been suggested that HSP60 binds to TLR2 and TLR4 and triggers an intracellular signal via MyD88 and TRAF6 (Vabulas et al., 2001), leading to the release of NO_2^-, the induction of TNF-α and IL-6 and the overexpression of IL-12 and IL-15 (Chen et al., 1999; Kol et al., 1999; **Figure 1**). HSP60 has also been found to localize in the atherosclerotic plaques, where it can provoke the production of TNF-α and MMP9 by macrophages (Kol et al., 1998). In addition, HSP60 can act as an autoantigen during chronic inflammation, as suggested by the presence of antibodies and T-cell responses to HSP60 in various inflammatory conditions (Nomoto and Yoshikai, 1991;

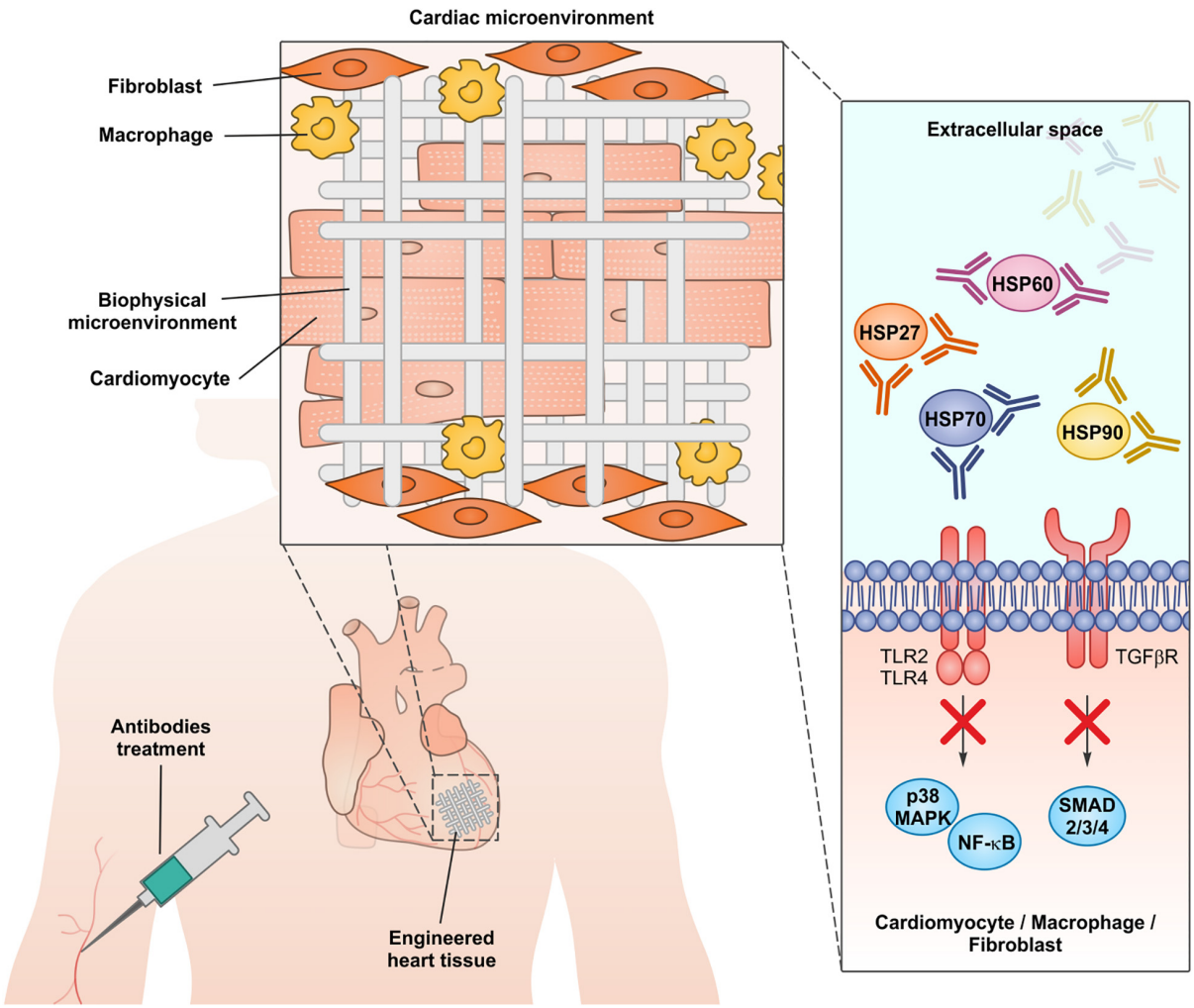

FIGURE 2 | The administration of neutralizing antibodies against extracellular chaperones, in conjunction with the implantation of engineered cardiac tissues, may represent a new approach to dampen myocardial inflammation and improve the engraftment.

Res et al., 1991), causing cardiac decline (Ohashi et al., 2000; Burian et al., 2001; Wysocki et al., 2002).

HSP27

HSP27 is a widely expressed chaperone protein belonging to the small HSP family, exerting a number of protective function in cardiomyocytes (Tarone and Brancaccio, 2014). Human and murine hearts release HSP27 in the circulation after myocardial infarction and I/R. Treatment of isolated mouse hearts with HSP27 recombinant proteins induces NF-κB activation and IL-6 production in the myocardium and causes a depression in cardiac function. Treatment with recombinant HSP27 activates an inflammatory response also in human and murine coronary vascular endothelial cells, promoting the overexpression of ICAM-1, MCP-1, IL-6, and IL-8 in a dose-dependent manner. All these effects are mediated by TLR2 and 4, since the treatment with HSP27 has no effect on cells derived from TLR2-null or TLR4-defective mice (**Figure 1**). Of note, neutralizing antibodies against HSP27 reduce myocardial NF-κB activity and IL-6 production and improve functional recovery after cardiac I/R (Jin et al., 2014).

CONCLUSION

All the evidence discussed above indicate that chaperones are actively secreted from stressed cells or released from damaged cells during chronic and acute cardiac insults or during clinical procedures like coronary artery bypass graft (Westaby, 1987; Levy and Kelly, 1993; Szerafin et al., 2008; Khan et al., 2014). Of note, the global inhibition of chaperone functions in heart using small molecules able to cross the plasma membrane would be seriously harmful, since chaperones are crucial in maintaining cardiomyocyte proteostasis and in sustaining heart function both in healthy conditions and during pathological insults (Willis et al., 2009; Willis and Patterson, 2013;

Tarone and Brancaccio, 2014; Sorge and Brancaccio, 2016; Penna et al., 2018). A number of therapeutic antibodies have already been approved for clinical applications and many are in late-stage trials mainly to treat cancer and autoimmune diseases. Antibodies may block the activity of extracellular proteins, without affecting the intracellular counterparts (Redman et al., 2015). Consistently, antibodies able to blunt the detrimental activity of extracellular chaperones have been used successfully in preclinical models of myocardial infarction and cardiomyopathy (Zou et al., 2008; Cai et al., 2010; Li et al., 2011; Jin et al., 2014; Liu P. et al., 2019). Research in developing engineered heart tissues to improve myocardial regeneration is an active field in regenerative medicine. The identification of suitable biocompatible materials to be colonized with functional cardiomyocytes is a promising strategy to heal an organ with a very poor regenerative potential as the human heart (Madonna et al., 2019). Nevertheless, human cardiomyocytes subjected to stress locally activate innate and adaptive immunity through chaperone release (Levy and Kelly, 1993; Veres et al., 2002; Wysocki et al., 2002; Mandal et al., 2006; Szerafin et al., 2008; Novo et al., 2011). This chronic sterile inflammation in the damaged myocardium may represent an issue in engineered tissue engraftment, by promoting apoptosis in colonizing cardiomyocytes and increasing the probability of rejection. We propose that the inhibition of extracellular chaperones during the implant of engineered heart tissues may represent a new advance in improving grafting and heart regeneration (**Figure 2**).

AUTHOR CONTRIBUTIONS

All authors wrote the manuscript and approved the contents for publication.

FUNDING

This work was supported by Italian Ministry of Education, University and Research (Progetto di Ricerca PRIN 2015), Compagnia di San Paolo/University of Torino (Progetti di ricerca di Ateneo 2016) to MB.

REFERENCES

Ao, L., Zou, N., Cleveland, J. C. Jr., Fullerton, D. A., and Meng, X. (2009). Myocardial TLR4 is a determinant of neutrophil infiltration after global myocardial ischemia: mediating KC and MCP-1 expression induced by extracellular HSC70. *Am. J. Physiol. Heart Circ. Physiol.* 297, H21–H28. doi: 10.1152/ajpheart.00292.2009

Arslan, F., De Kleijn, D. P., and Pasterkamp, G. (2011). Innate immune signaling in cardiac ischemia. *Nat. Rev. Cardiol.* 8, 292–300. doi: 10.1038/nrcardio.2011.38

Arslan, F., Smeets, M. B., O'neill, L. A., Keogh, B., Mcguirk, P., Timmers, L., et al. (2010). Myocardial ischemia/reperfusion injury is mediated by leukocytic toll-like receptor-2 and reduced by systemic administration of a novel anti-toll-like receptor-2 antibody. *Circulation* 121, 80–90. doi: 10.1161/CIRCULATIONAHA.109.880187

Asea, A. (2003). Chaperokine-induced signal transduction pathways. *Exerc. Immunol. Rev.* 9, 25–33.

Asea, A., Kraeft, S. K., Kurt-Jones, E. A., Stevenson, M. A., Chen, L. B., Finberg, R. W., et al. (2000). HSP70 stimulates cytokine production through a CD14-dependant pathway, demonstrating its dual role as a chaperone and cytokine. *Nat. Med.* 6, 435–442.

Baker-Williams, A. J., Hashmi, F., Budzynski, M. A., Woodford, M. R., Gleicher, S., Himanen, S. V., et al. (2019). Co-chaperones TIMP2 and AHA1 competitively regulate extracellular HSP90:client MMP2 activity and matrix proteolysis. *Cell Rep.* 28, 1894–1906.e6. doi: 10.1016/j.celrep.2019.07.045

Bianchi, M. E. (2007). DAMPs, PAMPs and alarmins: all we need to know about danger. *J. Leukoc. Biol.* 81, 1–5.

Bohonowych, J. E., Hance, M. W., Nolan, K. D., Defee, M., Parsons, C. H., and Isaacs, J. S. (2014). Extracellular Hsp90 mediates an NF-kappaB dependent inflammatory stromal program: implications for the prostate tumor microenvironment. *Prostate* 74, 395–407. doi: 10.1002/pros.22761

Brinker, A., Pfeifer, G., Kerner, M. J., Naylor, D. J., Hartl, F. U., and Hayer-Hartl, M. (2001). Dual function of protein confinement in chaperonin-assisted protein folding. *Cell* 107, 223–233.

Burian, K., Kis, Z., Virok, D., Endresz, V., Prohaszka, Z., Duba, J., et al. (2001). Independent and joint effects of antibodies to human heat-shock protein 60 and *Chlamydia pneumoniae* infection in the development of coronary atherosclerosis. *Circulation* 103, 1503–1508.

Cai, W. F., Zhang, X. W., Yan, H. M., Ma, Y. G., Wang, X. X., Yan, J., et al. (2010). Intracellular or extracellular heat shock protein 70 differentially regulates cardiac remodelling in pressure overload mice. *Cardiovasc. Res.* 88, 140–149. doi: 10.1093/cvr/cvq182

Calderwood, S. K. (2018). Heat shock proteins and cancer: intracellular chaperones or extracellular signalling ligands? *Philos. Trans. R. Soc. Lond. B Biol. Sci.* 373:20160524. doi: 10.1098/rstb.2016.0524

Calderwood, S. K., Theriault, J., Gray, P. J., and Gong, J. (2007). Cell surface receptors for molecular chaperones. *Methods* 43, 199–206.

Carra, S., Alberti, S., Benesch, J. L. P., Boelens, W., Buchner, J., Carver, J. A., et al. (2019). Small heat shock proteins: multifaceted proteins with important implications for life. *Cell Stress Chaperones* 24, 295–308. doi: 10.1007/s12192-019-00979-z

Carrizzo, A., Damato, A., Ambrosio, M., Falco, A., Rosati, A., Capunzo, M., et al. (2016). The prosurvival protein BAG3: a new participant in vascular homeostasis. *Cell Death Dis.* 7:e2431. doi: 10.1038/cddis.2016.321

Chakraborty, A., Boel, N. M., and Edkins, A. L. (2020). HSP90 interacts with the fibronectin N-terminal domains and increases matrix formation. *Cells* 9:272. doi: 10.3390/cells9020272

Chen, W., Syldath, U., Bellmann, K., Burkart, V., and Kolb, H. (1999). Human 60-kDa heat-shock protein: a danger signal to the innate immune system. *J. Immunol.* 162, 3212–3219.

De Marco, M., Falco, A., Basile, A., Rosati, A., Festa, M., D'avenia, M., et al. (2013). Detection of soluble BAG3 and anti-BAG3 antibodies in patients with chronic heart failure. *Cell Death Dis.* 4:e495.

Dybdahl, B., Slordahl, S. A., Waage, A., Kierulf, P., Espevik, T., and Sundan, A. (2005). Myocardial ischaemia and the inflammatory response: release of heat shock protein 70 after myocardial infarction. *Heart* 91, 299–304.

Dybdahl, B., Wahba, A., Lien, E., Flo, T. H., Waage, A., Qureshi, N., et al. (2002). Inflammatory response after open heart surgery: release of heat-shock protein 70 and signaling through toll-like receptor-4. *Circulation* 105, 685–690.

Gandhi, P. U., Gaggin, H. K., Belcher, A. M., Harisiades, J. E., Basile, A., Falco, A., et al. (2015). Analysis of BAG3 plasma concentrations in patients with acutely decompensated heart failure. *Clin. Chim. Acta* 445, 73–78. doi: 10.1016/j.cca.2015.02.048

Garcia, R., Merino, D., Gomez, J. M., Nistal, J. F., Hurle, M. A., Cortajarena, A. L., et al. (2016). Extracellular heat shock protein 90 binding to TGFbeta receptor I participates in TGFbeta-mediated collagen production in myocardial fibroblasts. *Cell. Signal.* 28, 1563–1579. doi: 10.1016/j.cellsig.2016.07.003

Gupta, S., and Knowlton, A. A. (2002). Cytosolic heat shock protein 60, hypoxia, and apoptosis. *Circulation* 106, 2727–2733.

Haslbeck, M., Weinkauf, S., and Buchner, J. (2019). Small heat shock proteins: simplicity meets complexity. *J. Biol. Chem.* 294, 2121–2132. doi: 10.1074/jbc.REV118.002809

Hecker, J. G., and McGarvey, M. (2011). Heat shock proteins as biomarkers for the rapid detection of brain and spinal cord ischemia: a review and comparison to other methods of detection in thoracic aneurysm repair. *Cell Stress Chaperones* 16, 119–131. doi: 10.1007/s12192-010-0224-8

Jenei, Z. M., Gombos, T., Forhecz, Z., Pozsonyi, Z., Karadi, I., Janoskuti, L., et al. (2013a). Elevated extracellular HSP70 (HSPA1A) level as an independent prognostic marker of mortality in patients with heart failure. *Cell Stress Chaperones* 18, 809–813. doi: 10.1007/s12192-013-0425-z

Jenei, Z. M., Szeplaki, G., Merkely, B., Karadi, I., Zima, E., and Prohaszka, Z. (2013b). Persistently elevated extracellular HSP70 (HSPA1A) level as an independent prognostic marker in post-cardiac-arrest patients. *Cell Stress Chaperones* 18, 447–454. doi: 10.1007/s12192-012-0399-2

Jin, C., Cleveland, J. C., Ao, L., Li, J., Zeng, Q., Fullerton, D. A., et al. (2014). Human myocardium releases heat shock protein 27 (HSP27) after global ischemia: the proinflammatory effect of extracellular HSP27 through toll-like receptor (TLR)-2 and TLR4. *Mol. Med.* 20, 280–289. doi: 10.2119/molmed.2014.00058

Kampinga, H. H., Hageman, J., Vos, M. J., Kubota, H., Tanguay, R. M., Bruford, E. A., et al. (2009). Guidelines for the nomenclature of the human heat shock proteins. *Cell Stress Chaperones* 14, 105–111. doi: 10.1007/s12192-008-0068-7

Khan, M. S., Islam, M. Y., Ahmed, M. U., Bawany, F. I., Khan, A., and Arshad, M. H. (2014). On pump coronary artery bypass graft surgery versus off pump coronary artery bypass graft surgery: a review. *Glob. J. Health Sci.* 6, 186–193. doi: 10.5539/gjhs.v6n3p186

Kim, S. C., Stice, J. P., Chen, L., Jung, J. S., Gupta, S., Wang, Y., et al. (2009). Extracellular heat shock protein 60, cardiac myocytes, and apoptosis. *Circ. Res.* 105, 1186–1195. doi: 10.1161/CIRCRESAHA.109.209643

Kirchhoff, S. R., Gupta, S., and Knowlton, A. A. (2002). Cytosolic heat shock protein 60, apoptosis, and myocardial injury. *Circulation* 105, 2899–2904.

Knowlton, A. A., Kapadia, S., Torre-Amione, G., Durand, J. B., Bies, R., Young, J., et al. (1998). Differential expression of heat shock proteins in normal and failing human hearts. *J. Mol. Cell Cardiol.* 30, 811–818.

Kol, A., Bourcier, T., Lichtman, A. H., and Libby, P. (1999). Chlamydial and human heat shock protein 60s activate human vascular endothelium, smooth muscle cells, and macrophages. *J. Clin. Invest.* 103, 571–577.

Kol, A., Sukhova, G. K., Lichtman, A. H., and Libby, P. (1998). Chlamydial heat shock protein 60 localizes in human atheroma and regulates macrophage tumor necrosis factor-alpha and matrix metalloproteinase expression. *Circulation* 98, 300–307.

Lai, S. L., Marin-Juez, R., and Stainier, D. Y. R. (2019). Immune responses in cardiac repair and regeneration: a comparative point of view. *Cell Mol. Life Sci.* 76, 1365–1380. doi: 10.1007/s00018-018-2995-5

Levy, J. H., and Kelly, A. B. (1993). Inflammation and cardiopulmonary bypass. *Can. J. Anaesth.* 40, 1009–1015.

Li, Y., Si, R., Feng, Y., Chen, H. H., Zou, L., Wang, E., et al. (2011). Myocardial ischemia activates an injurious innate immune signaling via cardiac heat shock protein 60 and Toll-like receptor 4. *J. Biol. Chem.* 286, 31308–31319. doi: 10.1074/jbc.M111.246124

Lin, L., Kim, S. C., Wang, Y., Gupta, S., Davis, B., Simon, S. I., et al. (2007). HSP60 in heart failure: abnormal distribution and role in cardiac myocyte apoptosis. *Am. J. Physiol. Heart Circ. Physiol.* 293, H2238–H2247.

Liu, L., Sun, K., Zhang, X., Tang, Y., and Xu, D. (2019). Advances in the role and mechanism of BAG3 in dilated cardiomyopathy. *Heart Fail. Rev.* doi: 10.1007/s10741-019-09899-7 [Epub ahead of print].

Liu, P., Bao, H. Y., Jin, C. C., Zhou, J. C., Hua, F., Li, K., et al. (2019). Targeting extracellular heat shock Protein 70 ameliorates doxorubicin-induced heart failure through resolution of toll-like receptor 2-mediated myocardial inflammation. *J. Am. Heart Assoc.* 8:e012338. doi: 10.1161/JAHA.119.012338

Macario, A. J., and Conway de Macario, E. (2005). Sick chaperones, cellular stress, and disease. *N. Engl. J. Med.* 353, 1489–1501.

Madonna, R., Van Laake, L. W., Botker, H. E., Davidson, S. M., De Caterina, R., Engel, F. B., et al. (2019). ESC working group on cellular biology of the heart: position paper for cardiovascular research: tissue engineering strategies combined with cell therapies for cardiac repair in ischaemic heart disease and heart failure. *Cardiovasc. Res.* 115, 488–500. doi: 10.1093/cvr/cvz010

Mandal, K., Afzal, A. R., Brecker, S. J., Poloniecki, J., Xu, Q., and Jahangiri, M. (2006). Association of serum soluble heat shock protein 60 with toll-like receptor 4 polymorphism and severity of coronary artery disease. *Heart* 92, 683–685.

Mathur, S., Walley, K. R., Wang, Y., Indrambarya, T., and Boyd, J. H. (2011). Extracellular heat shock protein 70 induces cardiomyocyte inflammation and contractile dysfunction via TLR2. *Circ. J.* 75, 2445–2452.

Nomoto, K., and Yoshikai, Y. (1991). Heat-shock proteins and immunopathology: regulatory role of heat-shock protein-specific T cells. *Springer Semin. Immunopathol.* 13, 63–80.

Novo, G., Cappello, F., Rizzo, M., Fazio, G., Zambuto, S., Tortorici, E., et al. (2011). Hsp60 and heme oxygenase-1 (Hsp32) in acute myocardial infarction. *Transl. Res.* 157, 285–292. doi: 10.1016/j.trsl.2011.01.003

Ohashi, K., Burkart, V., Flohe, S., and Kolb, H. (2000). Cutting edge: heat shock protein 60 is a putative endogenous ligand of the toll-like receptor-4 complex. *J. Immunol.* 164, 558–561.

Penna, C., Sorge, M., Femmino, S., Pagliaro, P., and Brancaccio, M. (2018). Redox aspects of chaperones in cardiac function. *Front. Physiol.* 9:216. doi: 10.3389/fphys.2018.00216

Pockley, A. G., and Henderson, B. (2018). Extracellular cell stress (heat shock) proteins-immune responses and disease: an overview. *Philos. Trans. R. Soc. Lond. B Biol. Sci.* 373:20160522. doi: 10.1098/rstb.2016.0522

Ranek, M. J., Stachowski, M. J., Kirk, J. A., and Willis, M. S. (2018). The role of heat shock proteins and co-chaperones in heart failure. *Philos. Trans. R. Soc. Lond. B Biol. Sci.* 373:20160530. doi: 10.1098/rstb.2016.0530

Redman, J. M., Hill, E. M., Aldeghaither, D., and Weiner, L. M. (2015). Mechanisms of action of therapeutic antibodies for cancer. *Mol. Immunol.* 67, 28–45. doi: 10.1016/j.molimm.2015.04.002

Res, P., Thole, J., and De Vries, R. (1991). Heat-shock proteins and autoimmunity in humans. *Springer Semin. Immunopathol.* 13, 81–98.

Roh, J. S., and Sohn, D. H. (2018). Damage-associated molecular patterns in inflammatory diseases. *Immune Netw.* 18:e27. doi: 10.4110/in.2018.18.e27

Rosati, A., Basile, A., D'auria, R., D'avenia, M., De Marco, M., Falco, A., et al. (2015). BAG3 promotes pancreatic ductal adenocarcinoma growth by activating stromal macrophages. *Nat. Commun.* 6:8695. doi: 10.1038/ncomms9695

Sakata, Y., Dong, J. W., Vallejo, J. G., Huang, C. H., Baker, J. S., Tracey, K. J., et al. (2007). Toll-like receptor 2 modulates left ventricular function following ischemia-reperfusion injury. *Am. J. Physiol. Heart Circ. Physiol.* 292, H503–H509.

Satoh, M., Shimoda, Y., Akatsu, T., Ishikawa, Y., Minami, Y., and Nakamura, M. (2006a). Elevated circulating levels of heat shock protein 70 are related to systemic inflammatory reaction through monocyte Toll signal in patients with heart failure after acute myocardial infarction. *Eur. J. Heart Fail.* 8, 810–815.

Satoh, M., Shimoda, Y., Maesawa, C., Akatsu, T., Ishikawa, Y., Minami, Y., et al. (2006b). Activated toll-like receptor 4 in monocytes is associated with heart failure after acute myocardial infarction. *Int. J. Cardiol.* 109, 226–234.

Sbroggio, M., Ferretti, R., Percivalle, E., Gutkowska, M., Zylicz, A., Michowski, W., et al. (2008). The mammalian CHORD-containing protein melusin is a stress response protein interacting with Hsp90 and Sgt1. *FEBS Lett.* 582, 1788–1794. doi: 10.1016/j.febslet.2008.04.058

Schlesinger, M. J. (1990). Heat shock proteins. *J. Biol. Chem.* 265, 12111–12114.

Schopf, F. H., Biebl, M. M., and Buchner, J. (2017). The HSP90 chaperone machinery. *Nat. Rev. Mol. Cell Biol.* 18, 345–360. doi: 10.1038/nrm.2017.20

Shishido, T., Nozaki, N., Yamaguchi, S., Shibata, Y., Nitobe, J., Miyamoto, T., et al. (2003). Toll-like receptor-2 modulates ventricular remodeling after myocardial infarction. *Circulation* 108, 2905–2910.

Singh, B., Patel, H. V., Ridley, R. G., Freeman, K. B., and Gupta, R. S. (1990). Mitochondrial import of the human chaperonin (HSP60) protein. *Biochem. Biophys. Res. Commun.* 169, 391–396.

Sorge, M., and Brancaccio, M. (2016). Melusin promotes a protective signal transduction cascade in stressed hearts. *Front. Mol. Biosci.* 3:53. doi: 10.3389/fmolb.2016.00053

Srivastava, P. (2002a). Interaction of heat shock proteins with peptides and antigen presenting cells: chaperoning of the innate and adaptive immune responses. *Annu. Rev. Immunol.* 20, 395–425.

Srivastava, P. (2002b). Roles of heat-shock proteins in innate and adaptive immunity. *Nat. Rev. Immunol.* 2, 185–194.

Szerafin, T., Hoetzenecker, K., Hacker, S., Horvath, A., Pollreisz, A., Arpad, P., et al. (2008). Heat shock proteins 27, 60, 70, 90alpha, and 20S proteasome in on-pump versus off-pump coronary artery bypass graft patients. *Ann. Thorac. Surg.* 85, 80–87.

Tang, X., Chang, C., Guo, J., Lincoln, V., Liang, C., Chen, M., et al. (2019). Tumour-secreted Hsp90alpha on external surface of exosomes mediates tumour - stromal cell communication via autocrine and paracrine mechanisms. *Sci. Rep.* 9:15108. doi: 10.1038/s41598-019-51704-w

Tarone, G., and Brancaccio, M. (2014). Keep your heart in shape: molecular chaperone networks for treating heart disease. *Cardiovasc. Res.* 102, 346–361. doi: 10.1093/cvr/cvu049

Tian, J., Guo, X., Liu, X. M., Liu, L., Weng, Q. F., Dong, S. J., et al. (2013). Extracellular HSP60 induces inflammation through activating and up-regulating TLRs in cardiomyocytes. *Cardiovasc. Res.* 98, 391–401. doi: 10.1093/cvr/cvt047

Timmers, L., Sluijter, J. P., Van Keulen, J. K., Hoefer, I. E., Nederhoff, M. G., Goumans, M. J., et al. (2008). Toll-like receptor 4 mediates maladaptive left ventricular remodeling and impairs cardiac function after myocardial infarction. *Circ. Res.* 102, 257–264.

Turner, N. A. (2016). Inflammatory and fibrotic responses of cardiac fibroblasts to myocardial damage associated molecular patterns (DAMPs). *J. Mol. Cell Cardiol.* 94, 189–200. doi: 10.1016/j.yjmcc.2015.11.002

Vabulas, R. M., Ahmad-Nejad, P., Da Costa, C., Miethke, T., Kirschning, C. J., Hacker, H., et al. (2001). Endocytosed HSP60s use toll-like receptor 2 (TLR2) and TLR4 to activate the toll/interleukin-1 receptor signaling pathway in innate immune cells. *J. Biol. Chem.* 276, 31332–31339.

Veres, A., Fust, G., Smieja, M., Mcqueen, M., Horvath, A., Yi, Q., et al. (2002). Relationship of anti-60 kDa heat shock protein and anti-cholesterol antibodies to cardiovascular events. *Circulation* 106, 2775–2780.

Westaby, S. (1987). Organ dysfunction after cardiopulmonary bypass. A systemic inflammatory reaction initiated by the extracorporeal circuit. *Intensive Care Med.* 13, 89–95.

Willis, M. S., and Patterson, C. (2013). Proteotoxicity and cardiac dysfunction–Alzheimer's disease of the heart? *N. Engl. J. Med.* 368, 455–464.

Willis, M. S., Schisler, J. C., Portbury, A. L., and Patterson, C. (2009). Build it up-Tear it down: protein quality control in the cardiac sarcomere. *Cardiovasc. Res.* 81, 439–448. doi: 10.1093/cvr/cvn289

Wysocki, J., Karawajczyk, B., Gorski, J., Korzeniowski, A., Mackiewicz, Z., Kupryszewski, G., et al. (2002). Human heat shock protein 60 (409-424) fragment is recognized by serum antibodies of patients with acute coronary syndromes. *Cardiovasc. Pathol.* 11, 238–243.

Xu, Z., Horwich, A. L., and Sigler, P. B. (1997). The crystal structure of the asymmetric GroEL-GroES-(ADP)7 chaperonin complex. *Nature* 388, 741–750.

Zou, N., Ao, L., Cleveland, J. C. Jr., Yang, X., Su, X., Cai, G. Y., et al. (2008). Critical role of extracellular heat shock cognate protein 70 in the myocardial inflammatory response and cardiac dysfunction after global ischemia-reperfusion. *Am. J. Physiol. Heart Circ. Physiol.* 294, H2805–H2813. doi: 10.1152/ajpheart.00299.2008

Conflict of Interest: The authors declare that the research was conducted in the absence of any commercial or financial relationships that could be construed as a potential conflict of interest.

Copyright © 2020 Seclì, Sorge, Morotti and Brancaccio. This is an open-access article distributed under the terms of the Creative Commons Attribution License (CC BY). The use, distribution or reproduction in other forums is permitted, provided the original author(s) and the copyright owner(s) are credited and that the original publication in this journal is cited, in accordance with accepted academic practice. No use, distribution or reproduction is permitted which does not comply with these terms.

frontiers in Bioengineering and Biotechnology

REVIEW
published: 27 May 2020
doi: 10.3389/fbioe.2020.00455

Toward Cardiac Regeneration: Combination of Pluripotent Stem Cell-Based Therapies and Bioengineering Strategies

Marta Mazzola[1] *and Elisa Di Pasquale*[1,2]*

[1] *Stem Cell Unit, Humanitas Clinical and Research Center – IRCCS, Rozzano, Italy,* [2] *Institute of Genetic and Biomedical Research (IRGB) – UOS of Milan, National Research Council (CNR), Milan, Italy*

OPEN ACCESS

Edited by:
Monica Boffito,
Politecnico di Torino, Italy

Reviewed by:
Felix B. Engel,
University Hospital Erlangen, Germany
Wuqiang Zhu,
Mayo Clinic in Arizona, United States
Sveva Bollini,
University of Genoa, Italy

***Correspondence:**
Elisa Di Pasquale
elisa.dipasquale@humanitasresearch.it;
elisadipa@gmail.com

Specialty section:
This article was submitted to Tissue Engineering and Regenerative Medicine, a section of the journal Frontiers in Bioengineering and Biotechnology

Received: *20 December 2019*
Accepted: *21 April 2020*
Published: *27 May 2020*

Citation:
Mazzola M and Di Pasquale E (2020) Toward Cardiac Regeneration: Combination of Pluripotent Stem Cell-Based Therapies and Bioengineering Strategies. Front. Bioeng. Biotechnol. 8:455. doi: 10.3389/fbioe.2020.00455

Cardiovascular diseases represent the major cause of morbidity and mortality worldwide. Multiple studies have been conducted so far in order to develop treatments able to prevent the progression of these pathologies. Despite progress made in the last decade, current therapies are still hampered by poor translation into actual clinical applications. The major drawback of such strategies is represented by the limited regenerative capacity of the cardiac tissue. Indeed, after an ischaemic insult, the formation of fibrotic scar takes place, interfering with mechanical and electrical functions of the heart. Hence, the ability of the heart to recover after ischaemic injury depends on several molecular and cellular pathways, and the imbalance between them results into adverse remodeling, culminating in heart failure. In this complex scenario, a new chapter of regenerative medicine has been opened over the past 20 years with the discovery of induced pluripotent stem cells (iPSCs). These cells share the same characteristic of embryonic stem cells (ESCs), but are generated from patient-specific somatic cells, overcoming the ethical limitations related to ESC use and providing an autologous source of human cells. Similarly to ESCs, iPSCs are able to efficiently differentiate into cardiomyocytes (CMs), and thus hold a real regenerative potential for future clinical applications. However, cell-based therapies are subjected to poor grafting and may cause adverse effects in the failing heart. Thus, over the last years, bioengineering technologies focused their attention on the improvement of both survival and functionality of iPSC-derived CMs. The combination of these two fields of study has burst the development of cell-based three-dimensional (3D) structures and organoids which mimic, more realistically, the *in vivo* cell behavior. Toward the same path, the possibility to directly induce conversion of fibroblasts into CMs has recently emerged as a promising area for *in situ* cardiac regeneration. In this review we provide an up-to-date overview of the latest advancements in the application of pluripotent stem cells and tissue-engineering for therapeutically relevant cardiac regenerative approaches, aiming to highlight outcomes, limitations and future perspectives for their clinical translation.

Keywords: cardiac regeneration, induced pluripotent stem cells (iPSCs), bioengineering, cell therapy, 3D-culture system, cardiomyocytes

INTRODUCTION

Cardiovascular diseases represent the major cause of morbidity and mortality worldwide, accounting for 31% of all deaths (Organization WH 2016). Myocardial infarction (MI) is associated with necrosis of the cardiac tissue due to the occlusion of the coronary arteries, a condition that irrevocably diminishes oxygen and nutrient delivery to the heart (Thygesen et al., 2007). While effective therapies, including surgical approaches, are currently used to treat numerous cardiac disorders, such as valvular or artery diseases, available therapeutic treatments for the damaged myocardium are still very limited and poorly effective. Furthermore, after an ischaemic insult, the formation of fibrotic scar takes place, interfering with mechanical and electrical functions of the cardiac tissue (Talman and Ruskoaho, 2016). Indeed, presence of fibrotic scar tissue leads to a reduction of the ejection fraction, due to the altered compliance of the cardiac chambers and to the increased stiffness of the myocardial matrix, thus impairing electrical properties of the heart and consequently the cardiac output (Kim P. et al., 2018). Currently, none of the commonly used therapies are able to remove such fibrotic scar, replacing the lost heart tissue with new functional cardiac cells. Thus, all these pathological conditions result into adverse remodeling of the cardiac muscle and ultimately lead to heart failure (HF), which is associated with poor prognosis in patients who survive a heart attack. The major drawback of all the potential therapeutic strategies for HF is represented by the limited regenerative capacity of the cardiac tissue. In fact, the regenerative potential of the adult human heart is extremely low, with a renewal rate of cardiomyocytes (CMs) of approximately 1% per year (Bergmann et al., 2009). Hence, the ideal approaches to restore the damaged myocardium are to either promote proliferation of resident CMs *in vivo* (Tian et al., 2015; Hashmi and Ahmad, 2019) or to directly provide new CMs for the replacement of necrotic tissue.

In this review, we will particularly focus on those cell replacement therapies based on the use of pluripotent stem cells (PSCs), either embryonic (ESCs – embryonic stem cells) or induced from somatic cells (iPSCs – induced pluripotent stem cells). Indeed, over the last 15 years, the discovery of iPSCs has opened a new chapter in the field of regenerative medicine for the treatment of degenerative disorders, including HF (Takahashi and Yamanaka, 2006). Similarly to ESCs, iPSCs possess the unique ability to differentiate into all cell types of the body, and therefore are emerging as a promising source of cells for regenerative medicine purposes. Furthermore, being generated from patients' somatic cells, iPSCs overcome the ethical limitations related to the use ESC derivatives and those related to immunological issues, providing an autologous source of human cells (Gonzales and Pedrazzini, 2009).

Pluripotent stem cell-based therapy has already demonstrated some beneficial effects, including the promotion of cell angiogenesis, increased vascularization, attenuation of cardiac cells apoptosis and the reduction of myocardial fibrosis (Gong et al., 2013; Sánchez et al., 2013; Sun et al., 2014; Traverse et al., 2014).

However, despite the initial enthusiasm generated this evidence, several issues have emerged over the years, limiting full application of PSCs to cell replacement-based therapeutic approaches for treatment of HF. Indeed, the low level of maturity of CMs generated from PSCs (PSC-CMs) and the related arrhythmogenic potential *in vivo*, together with the poor grafting of these cells into the heart after transplantation, are still major unsolved problems linked to the use of PSC-CMs for cell replacement therapy (Liu et al., 2018; Muller et al., 2018). Over the last years, research in the cardiovascular field has moved toward the implementation of bioengineering technologies to ameliorate both, survival and functionality of human CMs derived from iPSCs (iPSC-CMs). The combination between the bioengineering and stem cell biology fields has brought to light different technologies able to reproduce the three-dimensional (3D) environment of the heart, mimicking the real structure and function of cardiac tissue. In the same direction, the possibility to directly convert fibroblasts into CMs using microRNAs or small molecules, have recently emerged as a promising area for *in situ* cardiac regeneration.

This review aims to provide an updated overview on cell-based therapies and tissue-engineering, elucidating current applications and limitations, with a focus on future perspectives for their actual application in the clinics.

HISTORICAL VIEW ON PLURIPOTENT STEM CELLS: FROM DISCOVERY TO APPLICATION TO HUMAN DISEASES

There are two different types of pluripotent stem cells (PSCs): embryonic stem cells (ESCs) and induced pluripotent stem cells (iPSCs). ESCs were first isolated in 1981 (Evans and Kaufman, 1981; Martin, 1981) from the inner cell mass of a mouse blastocyst; more than a decade later, in 1998, Thomson et al. (1998) successfully derived ESC lines from humans. Both, mouse and human ESCs have shown the ability to spontaneously differentiate into various cell types when cultured in absence of the factors required to maintain pluripotency (i.e., LIF – leukemia inhibitory factor or bFGF – basic fibroblast growth factor). By using different protocols, researchers have been able to obtain several different cell types, including CMs and endothelial cells (ECs), and to demonstrate their potential therapeutic value *in vivo* in preclinical models of HF (Laflamme et al., 2007). However, use of ESCs for cell therapy applications in human is highly limited due to their potential immunogenicity and the ethical issues related to human embryo manipulation.

In 2006, the groundbreaking discovery of Takahashi and Yamanaka (2006) – the possibility to reprogram an adult somatic cell back to a pluripotent state – has given new hope to the regenerative medicine field, potentially allowing to overcome immunogenic and ethical limitations of ESCs to cell therapy. Reprogramming of somatic to pluripotent cells, namely induced pluripotent stem cells (iPSCs), has been first described in mouse fibroblasts by the retrovirus-mediated transduction of four transcription factors (c-Myc, Oct3/4, SOX2, and KLf4), now commonly referred as "pluripotency factors" (Takahashi

and Yamanaka, 2006). A year later, iPSCs were also obtained from human cells (Takahashi et al., 2007; Yu et al., 2007). iPSCs share their main features with ESCs, showing the ability of self-renewal and the capacity to differentiate into derivatives of the three germ layers. Indeed, genome-wide analyses revealed that, with few exceptions, human iPSCs and ESCs are mostly similar from the transcriptional and epigenetic point of view (Yu et al., 2007). However, on this regard, an advantage of human iPSCs over their embryonic counterpart resides in their genetic background, which is identical to the donor cell they are derived from **Figure 1**. Therefore, use of iPSCs promptly became the strategy of choice for studying human diseases *in vitro* (Park et al., 2008; Moretti et al., 2010; De Santis et al., 2017; Salvarani et al., 2019), and their application to drug screening (Yoshida and Yamanaka, 2010; Elitt et al., 2018; Farkhondeh et al., 2019) and toxicity testing is exponentially growing (Egashira et al., 2011; Luz and Tokar, 2018). Indeed, patient-specific lines have been developed in many laboratories worldwide and employed to investigate both functional and molecular phenotypes of a specific disease (Park et al., 2008; Moretti et al., 2010; Sun et al., 2012; Gu et al., 2017; Salvarani et al., 2019). Of note, iPSCs have been successfully differentiated into functional cardiovascular-relevant cells, including cardiomyocytes (Batalov and Feinberg, 2015), endothelial (Orlova et al., 2014), and smooth muscle cells (Xie et al., 2008), and thus have brought new hope to cure cardiac diseases, in particular in the field of cardiovascular regeneration. Additionally, recent advancements in genome-editing strategies by CRISPR/Cas9 technology have greatly expanded the potential of investigation of iPSC-based models, allowing the generation of isogenic iPSC lines, in which a desired gene mutation is either introduced or corrected, and the development of model systems that can be used for modulating endogenous genes expression and for genetic screening of genes function (Hockemeyer and Jaenisch, 2016).

However, the immature phenotype shown by cells differentiated from human PSCs still significantly limits their full applicability. Indeed, compared to adult human CMs, those derived from human PSCs display a fetal-like sarcomeric organization (i.e., absence of T-tubules and intercalated disks; shorter sarcomeres) and metabolism (i.e., less mitochondria; glycolysis-based energy production). Furthermore, hPSC-CMs exhibit distinct electrophysiological characteristics (diverse repertoire of ion channel densities and longer action potentials) and reduced force of contraction, due to an abnormal excitation-contraction coupling and calcium handling. In fact, in hPSC-CMs diverse components of calcium dynamic processes are missing, such as transverse tubules (T-tubules), invagination of the membrane in which channels and receptors key for impulse propagation and contraction are located (**Figure 2**). A comprehensive review on recent advances in the field of cardiomyocytes maturation and their implications for regenerative medicine is given by Karbassi et al. (2020).

In the context of tissue repair, this immature state may lead to lethal arrhythmia after hPSC-CMs transplantation (Chong and Murry, 2014). Thus, strategies aiming to differentiate these cells toward a more mature adult-like phenotype would significantly improve their therapeutic value (Yang et al., 2014; Scuderi and Butcher, 2017; Machiraju and Greenway, 2019; Karbassi et al., 2020). Many approaches have been proposed so far, spanning from the maintenance in culture for an extended period of time (Sartiani et al., 2007; Lundy et al., 2013), to the use of biochemical (i.e., growth factors and co-culture strategies) (Yoshida et al., 2018; Selvaraj et al., 2019) electrical stimuli (Nunes et al., 2013; Hirt et al., 2014) and mechanical load (Leychenko et al., 2011; Haggart et al., 2014); among them, those combining 3D culture and bioengineering methods have been the most effective (Tiburcy et al., 2017; Ronaldson-Bouchard et al., 2018; Ulmer et al., 2018).

CELLS-BASED THERAPY FOR MYOCARDIAL INFARCTION

The potential to repair cardiac tissue by cell grafting has attracted the attention of the field, due to the scarce capacity of CMs to proliferate and replace the damaged tissue. The dispute over the existence of cardiac progenitors in the adult heart is still unsolved; on the same trail, the ability of immature cardiac progenitor cells to engraft with pre-existing CMs *in vivo* has not been irrefutably determined (Witman and Sahara, 2018). Due to their unique capacity to produce functional CMs, both, ESCs and iPSCs, are among the most promising sources for cardiac regenerative medicine application. The first approach that employed CMs derived from PSCs for cell replacement, was simply based on the injection of the cells directly into the infarcted area of the myocardium. Since 2007, iPSC-CMs were employed in numerous studies for inducing cardiac regeneration after myocardial injury in diverse animal models, including rats, mice and pigs (Caspi et al., 2007; Laflamme et al., 2007; van Laake et al., 2007; Nelson et al., 2009; Ye et al., 2014; Liu et al., 2018). Zwi-Dantsis et al. (2013) used CMs differentiated from human iPSCs derived from patients with HF and demonstrated that, when transplanted in rats hearts, these cells were able to survive and to engraft. More recently, Rojas et al. (2017) developed a genetic-based protocol to maximize purity of CMs obtained from iPSCs differentiation, showing an improvement of the engraftment within the myocardium of mice that have been subjected to left anterior descendant (LAD) coronary artery ligation; in this study the authors also reported a contribution of the transplanted cells to the recovery of the left ventricular function. In another recent study, Zhu W. et al. (2018) investigated whether overexpressing the cell cycle activator cyclin D2 in human iPSC-CMs could improve the graft size through the induction of proliferation of the transplanted cells. The obtained results supported the authors' hypothesis, demonstrating that cell cycle progression induced by cyclin D2 overexpression was accompanied by a significant increase in heart repair.

Despite the encouraging results from these and other *in vivo* studies on the potential beneficial effects of iPSC-based cell therapy for HF, preclinical experiments in non-human primate models, using CMs derived from human iPSCs, have given controversial results (Chong et al., 2014; Zhu K. et al., 2018). Chong et al. (2014) showed that the injection of human ESC-CMs into failing myocardium of non-human primates

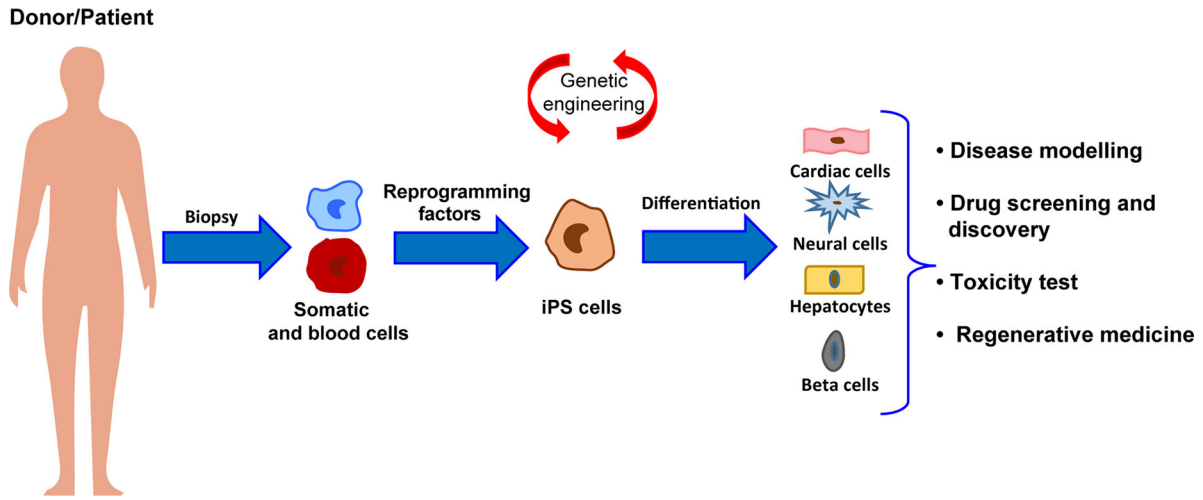

FIGURE 1 | Schematic representation of the workflow for iPSC generation and differentiation from patients somatic cells and major applications to human health.

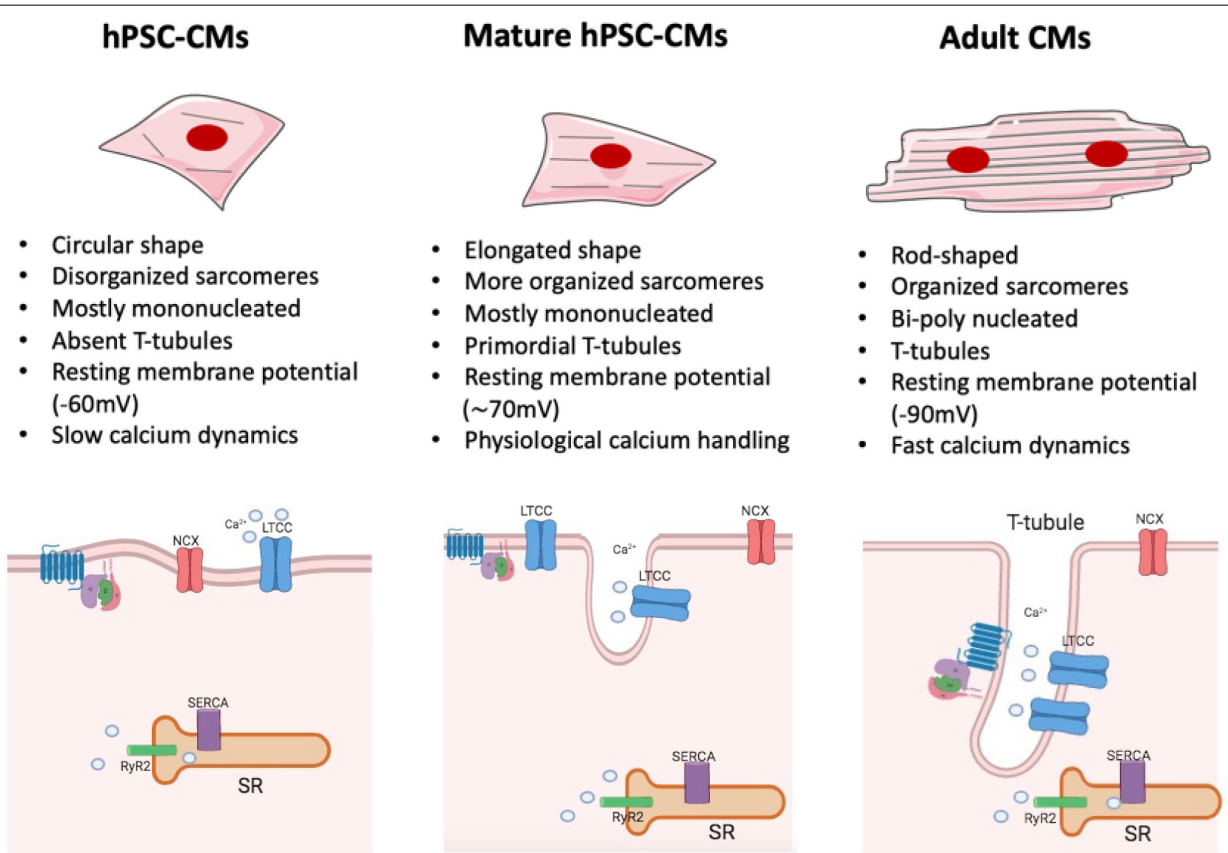

FIGURE 2 | Maturation features of hPSC-CMs. The figure shows a schematic representation of structural and functional features of hPSC-CMs **(left)**, mature hPSC-CMs **(central)**, and adult human CMs **(right)**. Some of the most relevant changes are listed (For a complete view, please refer to Karbassi et al., 2020). hiPSC-CMs **(left)** are mostly mononucleated, showing circular shape and a disorganized sarcomeres' structure compared to their adult counterpart **(right)**. The absence of T-tubules leads to the lack of organization of LTCC channel, which are not associated with the RyR complexes; such architecture generates slower calcium dynamics and abnormal excitation contraction coupling. Mature hiPSC-CMs **(center)** are still mostly mononucleated but start to exhibit some characteristic tipical of adult CMs: they show an elongated shape together with a more organized sarcomere structure and primordial T-tubule, which lead to physiological calcium handling. However, despite the increased level of maturation reached by mature hPSC-CMs, these cells still lack to achieve a complete functional maturation, as in the adult cardiac tissue. NCX, sodium–calcium exchanger; RYR2, ryanodine receptor 2; SR, sarcoplasmic/endoplasmic reticulum; LTCC, L-type calcium channel.

was able to promote heart regeneration; however, they also reported the concomitant occurrence of ectopic arrhythmic events, most likely elicited by the immature phenotype of the injected cells. Indeed, as already mentioned above, CMs differentiated from human PSCs differ significantly from their adult counterpart, while possessing structural, molecular, metabolic and functional characteristics comparable to CMs at the fetal stage. Indeed, human PSC-derived CMs possess a spontaneous contractile activity (probably the main reason behind their arrhythmogenicity) and show a poorly organized contractile machinery due to, among others, the reduced sarcomere length and their immature organization, the low expression of beta adrenergic receptors, ion channels and calcium binding proteins. Hence all of these factors together make the electrical and mechanical integration of these cells within the adult cardiac tissue extremely difficult, and significantly increase the potential incidence of arrhythmic events. As a matter of fact, in order to be effective, the newly injected CMs should rapidly achieve the functional features of the host cells, including all of the components of the excitation–contraction coupling machinery, such as gap junctions and transverse T-tubules, which are crucial for the proper functioning of the heart. On this regard, in the trial MAGIC, Menasche et al. (2008) evaluated the effect of transplantation of autologous skeletal myoblasts into the heart after myocardial infarction and found that these cells failed to improve cardiac function, most likely because of their poor coupling with the host myocardial cells.

Another important issue to be considered to properly evaluate the success of heart cell transplantation, is represented by the time-points at which functional measurements are carried out; indeed, the outcomes of these analyses may significantly differ depending on whether they are carried out early (i.e., 4 weeks) or at later stages (i.e., 12 weeks) post intervention (Laflamme et al., 2007; van Laake et al., 2008). In particular, using echocardiography or magnetic resonance imaging, van Laake et al. (2008) reported a significant increase of cardiac functionality at 4 weeks after cell injection. However, such functional improvements faded 12 weeks after MI, despite the initial engraftment, indicating the need to perform analyses at later endpoints. Another variable that may impact the efficacy of cell replacement therapy approaches lies in the number of transplanted cells: the definition of the ideal amount of cells to be transplanted in order to improve heart function and repair without induction of side effects is indeed a critical step, on which a common view is still missing. An additional obstacle to cell-based therapy is represented by the extremely low rate of stem cell retention, a condition that influences the engraftment into the host cardiac tissue (Lemcke et al., 2018; Park et al., 2019). Thus, researchers have started to abandon those approaches based on the injection of isolated cells, moving toward the development of strategies that may optimize coupling with the host. The first attempts in this direction regarded the use of cell-patches (formed by fibrin gel or collagen), that showed an improvement of cardiac function (Hamdi et al., 2009; Vallée et al., 2012; Wendel et al., 2015). Menasché et al. (2015) reported the first clinical application of cardiac patches made using human ESC-derived cardiac progenitor cells in a patient suffering from severe ischemic left ventricle dysfunction, demonstrating the possibility to use cells combined with a tissue-engineered construct for cardiac repair. In detail, ESC-derived cardiac progenitor cells were embedded into a fibrin scaffold, which was surgically delivered into the failing cardiac tissue of the patient suffering from severe heart failure. Although results from this study were encouraging, a greater number of clinical cases is mandatory in order to establish a standard and safe therapy applicable to a higher number of patients. Another approach, proposed by Park et al. (2019), showed a substantial increase in terms of cell retention using a patch loaded with a combination of human iPSC-CMs and mesenchymal stem cell in rat models of MI. The patch was generated using a bioink formed by a mixture containing hiPSC-CMs and porcine heart-derived decellularized extracellular matrix in presence of 0.02% (w/v) of vitamin B2, that was then printed in a disk-shaped polycaprolactone.

However, despite the fact that many different types of stem cells and derivatives have been proposed as valuable candidates for regeneration of the myocardium, a general consensus on which cell type should be considered the gold standard for cell replacement therapy of the heart, remains elusive. This issue mostly arises from the complex structure of the cardiac muscle, that is formed by different types of cells (mainly cardiomyocytes, fibroblasts and endothelial cells), all contributing to the proper functionality of the heart. By now, the majority of preclinical studies have been conducted in two-dimensional culture systems, a condition that does not take into account the multiple interactions occurring in a three-dimensional structure, like the heart: this is among the major issues still limiting the application of cell therapy approaches into the clinics. Thus, in the last years, many studies have directed their efforts to identify the optimal structural and environmental conditions for the development of a three-dimensional (3D) structure able to functionally resemble the cardiac tissue and suitable for heart transplantation. Thanks to the combination of bioengineering methods and the advances in the cardiovascular stem cell biology field, in particular in the protocols for generating CMs from PSCs, significant progress has been made in the development of 3D-cardiac tissue-like structures and their application to cardiac regeneration. The intent of this review is to provide an up-to-date overview of the available technologies and the recent advancements in the field, particularly in relation to their potential applicability for clinical purposes.

3D-CULTURE SYSTEMS AND CARDIAC REGENERATION

The function of each organ of the human body is determined by both cellular and non-cellular components. Ideally, a cell culture system that aims at reproducing an organ *in vitro* should be able to replicate the complex interactions occurring between extracellular environment, cells and specialized tissues within the organ itself, as well as their specific functions. In particular, the cardiac tissue is composed by contractile and non-contractile cells (i.e., cardiomyocytes, fibroblasts, and blood vessel cells), that

are organized as a complex 3D structure. The tightly regulated interaction among these diverse cell types plays a central role in the heart's function. Although 2D-cell cultures have been – and still are – widely used in cardiovascular research, 3D cell-based systems have the potential to add a layer of complexity and to generate cardiac-like structures which faithfully recapitulate cellular interactions as those *in vivo*. Furthermore, 3D systems may also integrate scaffolds and biomaterials, mimicking the properties of the extracellular matrix present in the human heart. Thus, in the last years, 3D cell cultures are emerging as a new tool for both drug discovery and regenerative medicine applications. Indeed, the increased knowledge in the cardiovascular biology field boosted the development of 3D cellular systems, that progressively and faithfully reproduce the morphological and functional features of cardiac tissue, overcoming the maturation-related limitations of 2D cultures. A growing number of studies have indeed demonstrated that hPSC-CMs differentiated in 3D systems acquire structural, metabolic and functional properties similar to their adult counterparts (Fong et al., 2016; Correia et al., 2018). On this regard, it is worth mentioning the recent study from Ronaldson-Bouchard et al. (2018) in which the authors were able to obtain a level of maturation unprecedently seen in human iPSC-CMs through the combination of a fibrin 3D-hydrogel and physical conditioning with increased intensity (stretch and auxotonic contractions). Overall, several types of 3D cellular models have been developed in the last decade for their application in the cardiovascular field. Based on the presence of a supporting scaffold or not, these models can be broadly divided in two groups: (i) spheroids and organoids, which are formed by self-assembly (scaffold-free) and are able to recapitulate native tissue structure and functionality without the use of any exogenous support, and (ii) engineered cardiac tissue constructs which instead combine the use of different exogenous scaffolds with living cells and eventually electro-mechanical signals.

Spheroids and Organoids

Spheroids and organoids both refer to 3D culture systems with a specialized architecture and cell organization that typically form through self-assembling processes. Currently, a precise and universal nomenclature that clearly distinguishes between these two models is still missing; thus, these terms are often used interchangeably.

Spheroids

Spheroids were first obtained in 1970 (Sutherland et al., 1971; Freedman et al., 2015; Takasato et al., 2015) to mimic the functional phenotype of human tumor cells and test their response to radiotherapy. Since then, several spheroid culture systems have been developed starting from different types of stem cells. This methodology presents several advantages with respect to the monolayer cell culture, particularly due to the spheroids' cell heterogeneity: these culture systems, in fact, include diverse cell-type populations that consume different kinds of nutrients and secrete distinct metabolites and soluble signals. One crucial point to consider in spheroid aggregation is their size, namely the number of cells per spheroid. In fact, if the number of cells is too high, it will result detrimental for cellular viability due to a reduction in the oxygen supply at the center of the spheroid (Tan et al., 2017). Tan et al. (2017) have recently described the use of human iPSC-CMs in the formation of cardiac spheroids; interestingly, the authors demonstrated that use of electrically conductive silicon nanowires (e-SiNWs) ameliorates self-assembly of the CMs during the spheroid aggregation process. Furthermore, the resulting construct displayed improved cardiac functionality, probably due to an increased cell maturation mediated by the electrical stimulus (Tan et al., 2017). Recently, Mattapally et al. (2018) also employed human iPSC-CMs to produce spheroids, demonstrating that such spheroids fused in culture, generating structures characterized by a uniform distribution of cells and electro-mechanical coupling. Relevantly, they also showed that such structures, embedded in a fibrin patch and transplanted *in vivo*, were able to engraft the infarcted area in a mouse model of myocardial infarction (MI), with an engraftment rate exceeding 25%, significantly improving cardiac function (Mattapally et al., 2018). Cardiac spheroids could also be generated by combining CMs with other cell types that typically compose the human heart, such as cardiac fibroblasts (CFs), attempting to recreate the heart microenvironment (Polonchuk et al., 2017; Hoang et al., 2018; Yan et al., 2019). On this regard, Choi and coworkers generated homotypic and heterotypic spheroid-derived cardiac microtissues, containing either CMs or CFs or both cell types together (Kim T. Y. et al., 2018). The authors evaluated the electrophysiological properties of these tissue-like microstructures, focusing their investigation on the role played by CFs in cardiac action potential propagation. Results emerged from this study support the hypothesis of a central role played by the "supporting" cells in mimicking heart environment, indicating CF sodium currents as key players in action potential conduction in CF/CM heterotypic spheroids. Importantly, this study also reported a delayed action potential propagation in spheroids composed by disproportioned distribution of CFs, as it occurs in the infarcted myocardium, further sustaining the role of CF engraftment in the arrhythmogenic defects associated MI and the utility of 3D hetero-cellular models for studying cardiac diseases and for the development of regenerative strategies. Altogether, these studies support the idea of using 3D structures made of iPSC-derived CMs and other cardiac cells as heart surrogates for cardiac repair.

Organoids

An organoid is defined as an organ-like tissue exhibiting multiple cell types that self-organize to form a structure not unlike the organ *in vivo* and functional (Lancaster and Knoblich, 2014). As already mentioned above, there is not a clear distinction between organoids and spheroids, and in the past, the two terms were often used as synonyms. However, even if sharing several features, such as self-assembly properties, multicellular composition and some functional cues, organoids and spheroids are characterized by few distinctive traits. In fact, while the latter are basically cell aggregates without a defined tissue-like structure, organoids typically exhibit a higher order of self-assembly and do show, at least in some cases, a distinctive tissue-like cellular architecture. Therefore, over the last few years,

the concept of organoids has changed and researchers usually refer to organoids to indicate a 3D tissue-like structure generated through self-assembly, while use of the term spheroid is limited to indicating a "premature" stage of what will then become an actual organoid.

The signaling pathways that control organoid formation and development were found to be the same as those occurring during the development of the organ itself. For this reason, growth factors and small molecules were used to manipulate different signaling pathways in order to increase cell survival, cell specification and organization of tissue-specific organoids. The first organoid was created in 2009 and was used to build intestinal tissue *in vitro*, through the establishment of a long-term culture system able to create the crypt–villus organization and physiology. The induction protocol relied on the use of a cocktail of small molecules required for the growth of the intestinal epithelium, such as Wnt proteins, epidermal growth factor and Noggin, which lead to sequential morphological changes and the formation of crypt domains (more than 40 per organoid) with a central lumen and an epithelium containing microvilli structures (Sato et al., 2009). Since then, many organoids have been developed to reproduce several organ-like structures including brain, lung and liver (Huch et al., 2013; Lancaster et al., 2013; Chen Y.-W. et al., 2017), so that in the recent years, the use of organoids has rapidly grown in several fields of medical research.

Despite these advances, very few studies have focused on the development of human cardiac organoids, and the obtained structures are still far from resembling the actual heart. This is mainly due to the structural and functional complexity of the heart, which is formed, in addition to CMs, by other cell types, such as CFs, vascular and immune cells, finely organized and embedded in the extracellular matrix to create its functional compartments. Thus, recapitulation of the 3D-multicellular structure and function of the developing myocardium through the use of human cardiac organoids remains a challenge. Given their multiple developmental potential, iPSCs represent a cell source of selection for the creation of cardiac organoids: manipulation of iPSCs is feasible and protocols are now available for specifically differentiating all the aforementioned heart-relevant cell types. It is indeed clear that to create a functional human cardiac organoid, the simultaneous presence of CMs, endothelial cells (ECs) and CFs is highly desirable. On this regard, Richards et al. (2017) have devised a developmental-driven scaffold-free fabrication strategy to assemble a functional vascularized cardiac organoid: their approach was inspired by the events that guide myocardial cell organization during heart development and was based on the self-assembly of human iPSC-CMs, -CFs and -ECs, that ultimately acquired a well-defined structure, exhibiting both biochemical and functional properties typical of the myocardium and being able to respond to drug treatments. Recently, Wimmer et al. (2019) also developed human organoids of blood vessels as models for studying diabetic vasculopathy. To this end, they induced PSCs (either iPSC or ESC) to commit toward a mesodermal lineage and then vascular specification using specific growth factors, that resulted in the generation of 3D blood vessel organoids possessing morphological and functional properties of the human microvasculature. Similarly, use of co-culture systems with iPSC-derived ECs, vascular cells and pericytes have been also employed by other researchers to recreate the vascular network (Kusuma et al., 2013; Orlova et al., 2014; Chan et al., 2015).

However, while the self-organization property of the organoids allows generation of a high level of tissue organization, one that cannot be reached by the current tissue engineering approaches with the only requirements of external cues and growth factors cocktails, this characteristic also represents the main weakness of this approach. In fact, the self-assembly process is not subjected to pre-defined extrinsic patterning instructions, but is instead a stochastic event, leading to heterogeneity in shape, size and cell composition (Brassard and Lutolf, 2019). In addition to this, the fabrication method limits the size of the organoids to the millimeter scale, thus resulting poorly applicable to regenerative medicine approaches. Recently, the generation of advanced engineered cardiac organoids that overcome some of the aforementioned limitations, such as sample heterogeneity, has been reported. This strategy, proposed by the James Hudson laboratory, implies the combination of bioengineering methods to the classical self-assembly protocol to obtain human cardiac organoids (hCOs) from PSC-CMs. More in detail, hCO constructs consisted of a mixture of differentiated PSC-CMs, collagen, sodium hydroxide and matrigel, which was then allowed to self-assemble on polydimethylsiloxane (PDMS) poles. The generated constructs were then used for investigating their regenerative capacity in response to injury (Eder et al., 2016) and for drug screening applications (Mills et al., 2019). However, although very advantageous for screening purposes, allowing to simultaneously evaluate multiple phenotypic parameters such as proliferation and side effects on cell functionality (i.e., contraction), this system is not ideal for developing cells for cell therapy. On this regard, conventional tissue engineering strategies are probably a more suitable option.

Engineered Cardiac Tissue Constructs

Tissue engineering is an emerging and multidisciplinary field which aims at developing functional tissue substitutes for medical purposes, mainly replacement of damaged tissues/organs or drug screening applications. Tissue engineering involves the combinatorial use of cells, materials, biochemical and/or physical factors and engineering methodologies, and has thus far been applied to a large variety of human tissues (Vacanti and Langer, 1999). The bio-engineered scaffolds serve as structural support for cell seeding, while the addition of biochemical/physical factors determines distinct cell phenotypes and metabolic properties of the originated tissue. Clinical applications of tissue engineering approaches are highly relevant for repair of bone (Jones et al., 2002; Sepulveda et al., 2002), cartilage (Cao et al., 1997; Risbud et al., 2001), and pancreatic tissue (Niknamasl et al., 2014). In addition to these, given the limited regenerative capacity of the heart, tissue engineering approaches are also ideal for cardiovascular regenerative medicine applications. The main goal is to create a cardiac graft which can be implanted and restore the functionality of the myocardium without major side effects. To this aim, tissue engineering intends to recreate the microenvironment of the cardiac tissue, in terms of cell

composition, stiffness, geometry, physical and electrical stimuli and, extracellular matrix.

The first engineered-based approaches simply implied the addition of cells to natural or synthetic biomaterials, that should mimic extracellular matrix providing mechanical support to the cells. Zimmermann et al. (2002) provided the first report on a 3D engineered heart tissue (EHT), developed using neonatal rat cardiac myocytes mixed with collagen I and matrix factors, added in a circular scaffold and subjected to phasic mechanical stretch. After that, many researchers applied similar methodologies using embryonic or neonatal/fetal rat cells embedded into polymer-based or extracellular matrix-like scaffolds, and showed the engraftment of these 3D-EHT constructs into rodent cardiac tissue (Li et al., 1999; Taylor, 2004; Ravichandran et al., 2013; Wendel et al., 2014). Many other cell types have been also used for generating 3D-EHT, that include adult and neonatal cardiomyocytes (Soonpaa et al., 1994; Li et al., 2000), bone marrow-derived stem cells (i.e., mesenchymal, endothelial, and hematopoietic stem/progenitor cells) (Janssens et al., 2006), cardiac stem cells (Barile et al., 2007), smooth muscle cells (Planat-Benard et al., 2004; Rehman et al., 2004), and skeletal myoblasts (Murry et al., 1996). In addition to these, in the last years, the use of CMs differentiated from PSCs exponentially increased, mainly because of their wide developmental potential and the rapid spread of iPSC technology in research laboratories worldwide. On this regard, Stevens et al. (2009) described, for the first time, a strategy to create macroscopic scaffold-free patches of human cardiac tissue exclusively composed of human CMs derived from ESCs. These patches showed synchronous calcium activity, which is indicative of proper electromechanical coupling. In addition, these patches were able to contract spontaneously and, by modulating the number of cells used for fabrication, it was also possible to tightly control the patch size. However, in order to generate constructs with an actual translational value, cardiac tissue engineering must take into account the native characteristics of the cardiac tissue. Indeed, the optimal engineered support should be formed by cardiac cell populations included into an extracellular matrix similar, in molecular composition, to that of the native tissue. Also, proper vascularization is key for long-term cell survival and function *in vivo*. Therefore, such complexity is not easy to achieve due to several limitations, mainly represented by the response of the host to biomaterials used to build the supports and the limited sources of suitable human cells.

The choice of the biomaterial is indeed key for developing effective cardiac regenerative strategies; biomaterials can indeed have different impacts on survival, proliferation and differentiation of a specific cell type, and allow specific scaffold anchoring to generate a functional tissue. Biomaterials used in tissue engineering can be either natural (e.g., collagen, alginate, fibrin, and natural ECM) or synthetic [e.g., poly(ethylene glycol), poly(ε-caprolactone), and poly(glycerol sebacate)]; both types of polymers may represent an optimal choice for fabrication of tissue-like cardiac structures and, depending on the specific application, have been alternatively employed to develop engineered constructs for cardiac regenerative purposes (Kai et al., 2014; Wendel et al., 2014).

Collagen is probably the most important "biomechanical" protein of the human body and it represents one of the most relevant natural polymers used in the field of cardiac regeneration. Indeed, due to its abundance in the ECM, collagen provides an optimal support for cell attachment and growth, and several studies in rodents have demonstrated positive effects of collagen-based scaffolds (Gaballa et al., 2006; Miyagi et al., 2011; Van Vlierberghe et al., 2011). Researchers have used collagen as a scaffold into the damaged myocardium, and found that this material was able to induce the formation of new vessels, resulting into a beneficial effect against cardiac remodeling (Shi et al., 2011). Masumoto et al. (2016) recently reported the generation of engineered cardiac tissue using collagen I, matrigel and human iPSC-derived cells. In detail, the authors generated a construct characterized by three cellular compositions – CMs, ECs and vascular mural cells, all derived from iPSCs – and showed a functional maturation of these cells, when assembled in this collagen-based tissue-engineered structure (Masumoto et al., 2016). Furthermore, they also demonstrated myocardial replacement after injection *in vivo*. However, despite the reported beneficial effects, collagen is a stiff material and this characteristic can impede its mechanical integration into the heart. To overcome this problem, several strategies have been proposed and demonstrated the ability to tune its mechanical properties; among these, Deng et al. (2010) showed that addition of chitosan is sufficient to increase the compression modulus of collagen fibrils (Geng et al., 2018). Indeed, the compression modulus of the collagen increases when combined with chitosan or elastin, whereas its tensile modulus is reduced, conferring greater stability to the heart and minimizing the ventricular wall dilatation (Fakoya et al., 2018). On this regard, it is worth mentioning the very recent work from Lee et al. (2019), who developed the FRESH methodology to 3D-bioprint collagen with improved mechanical properties, allowing the fabrication of cardiac components of different sizes.

Alginate is another natural material suitable for tissue engineering applications. It is an anionic polymer obtained from brown seaweed and it has been employed for numerous biomedical applications. In fact, alginate possess several characteristics – such as biocompatibility and low toxicity - that made it an ideal candidate for its medical use (Lee and Mooney, 2012). Alginate hydrogels can be produced by various cross-linking methods and the resulting structure is similar to the ECM, so that a positive effect on cardiac functionality has been reported with its injection in animal models after induction of MI, probably through a mechanism of reinforcement of the thickness of the scar (Landa et al., 2008). Despite these positive effects, the lack of integration between alginate and CMs is a major drawback of this biomaterial, limiting its full application for cardiac regeneration (Geng et al., 2018). However, a more recent study has reported the generation of a multi-cellular engineered construct containing alginate and iPSC-CMs (Maiullari et al., 2018). In this work, Maiullari et al. (2018) encapsulated iPSC-CMs into a hydrogel containing alginate and synthetic polyethylene glycol (PEG)-fibrinogen followed by custom bio-printing, and demonstrated an improved integration of this engineered support within the host tissue.

As for the collagen, the combined use of alginate with chitosan has shown beneficial effects in a rat model of MI, mitigating ventricular remodeling.

Another natural biomaterial with some applicability in regenerative therapy is fibrin, an insoluble protein formed from fibrinogen. Use of fibrin has been reported to improve cardiac function by reducing infarct size (Deng et al., 2015). However, fibrin poorly tolerates the mechanical stretch generated during the contraction of the cardiac muscle and, for this reason, is usually used in combination with other materials such as chitosan or collagen (Christman et al., 2004). Likewise, hyaluronic acid, a polysaccharide present in the ECM, is a good candidate for regenerative medicine applications and has been shown to be involved in angiogenesis and tissue repair. Indeed, hyaluronic acid has been largely utilized to develop scaffolds for tissue regeneration in different research areas and many clinical trials have already started to evaluate the regenerative power of hyaluronic acid-based materials for treatment of different kinds of tissue lesions as ulcers, osteo-articular and bone damages (Bonafè et al., 2014). With regards to the cardiac field, hyaluronic acid-based constructs have been used so far in pre-clinical models where they showed a positive effect on regeneration after MI (Yoon et al., 2009). In agreement with this, Abdalla et al. (2013) reported a recovery of rat heart functionality after injection of hyaluronic acid into the peri-infarct area in a sub-acute model of MI. However, this positive effect on regeneration was lost in a chronic model of MI, indicating that the injection timing of the therapeutic agents is also a major determinant to drive cardiac repair (Yoon et al., 2014).

The use of a decellularized extracellular matrix (dECM) directly isolated from tissues represents another option to build scaffolds for cardiac tissue engineering and has been applied in several conditions, from myocardial infarction to orthopedic injures (Shen et al., 2011; Perea-Gil et al., 2016; Hernandez et al., 2018; Hussey et al., 2018). dECM contains adhesion proteins, such as laminin or fibronectin, able to promote cell attachment, and retains biochemical cues and mechanical properties of the native tissue; these characteristics are critical for the subsequent recellularization of the scaffold. On this regard, it has been shown that porcine-derived myocardial dECM-based hydrogels are able to promote infiltration of cardiac progenitor and endothelial cells (Singelyn et al., 2012). In addition, Hernandez et al. (2018) used an analogous dECM-based system to deliver microRNA and extracellular vesicles. More recently, Tsui et al. (2019) proposed a new hybrid scaffold fabricated by combining porcine-derived dECM and reduced graphene oxide (rGO), demonstrating that it provides a valid microenvironment for both cellular and tissue development when used to create EHT constructs. The authors also showed that such dECM-rGO-based EHT structures improve cardiac contractility of hiPSC-CMs. Likewise, Goldfracht et al. (2019) demonstrated that hiPSC-CMs embedded into a chitosan-enhanced dECM hydrogel possess a more mature phenotype than their 2D-cultured counterparts and form EHT constructs with an anisotropic muscle structure, in which phenotypes of inherited forms of arrhythmias can be reproduced and drugs can be tested. In particular, in the context of dECM-based materials, the injectable forms have gained much interest in the field, due to their ease of delivery to the host tissue (Hernandez et al., 2020). The first clinical trial was recently reported, testing an injectable ECM-hydrogel derived from decellularized porcine myocardium, called VentriGel (Traverse et al., 2019). The results obtained so far in a cohort of post-MI patients with severe left ventricular dysfunction support the safety of the *trans*-endocardial injection of the hydrogel.

A valid option to the use of natural biomaterials is given by synthetic polymers. The major advantage of synthetic polymers lies in the possibility to synthetize materials with the optimal physico-chemical and mechanical properties resembling at best those of the tissue of interest; on the other hand, low biocompatibility and potential toxicity may represent a limitation and must be excluded prior to their application *in vivo*. With respect to the cardiovascular field, the most popular synthetic polymers are represented by poly(ethylene glycol), poly(ε-caprolactone), poly(propylene), poly(vinyl alcohol), poly(*N*-isopropylacrylamide), poly(glycerol sebacate), poly(ester urethane)s (Chen et al., 2010; Martins et al., 2014; Zhou et al., 2014; Moorthi et al., 2017; Denis et al., 2019). The authors can refer to the following reviews for additional details (Arnal-Pastor et al., 2013; Cui et al., 2016). In addition to these, several synthetic materials with electroconductive properties have been also developed to improve cardiac conduction and maintain the electrical integrity of the heart. Electroconductive materials used for this purpose include: nanoparticles (Zhu et al., 2017), nanowires (Wickham et al., 2016), carbon nanotubes (Shin et al., 2014; Roshanbinfar et al., 2018), and polymers (Kaur et al., 2015; Mohammadi et al., 2017). Electroconductive polymers, such as polyaniline (PANi) (Hsiao et al., 2013) and polypyrrole (PPy) (Wang et al., 2016) could be incorporated into 3D-printed scaffolds and have been used for developing engineered tissue constructs, also in the cardiac field. Among the others, PANi and PPy are widely used in the context of cardiac repair, due to their environmental stability and electrical properties (Razak et al., 2015). Different studies have shown that application of these polymers leads to an increase of connexin 43, the most abundant isoform of gap junctions in CMs, critical for impulse propagation within the heart (Nishizawa et al., 2007; Wang et al., 2016). However, insolubility of these polymers in water represent a major limitation for their full application (Wang et al., 2017). Indeed, they are preferentially used in "classical" cell-seeding approaches, in which cells are seeded onto a pre-fabricated scaffold, rather than being simultaneously encapsulated with cells into inks for 3D bioprinting.

A valid alternative option is represented by polythiophene polymers, that are biocompatible and highly soluble in water (Hempel et al., 2017; Sinha et al., 2017). In particular, poly(3,4-ethy lenedioxythiophene):polystyrene sulfonate (PEDOT:PSS) is a promising candidate, able to support mouse stem cell-derived CMs attachment (Jiang et al., 2017). Using these polymers, Roshanbinfar et al. (2018) developed an electroconductive bio-hybrid hydrogel, which is able to enhance maturation and physiological properties of engineered cardiac tissues. In detail, the authors incorporated PEDOT:PSS in a collagen–alginate hydrogel creating an electroconductive construct structurally similar to the native ECM. In addition, hiPSC-CMs seeded on

top of this polymer showed increased speed of contraction, high contraction amplitude, sarcomeric lengths more similar to adult CMs and synchronous rhythmic beating. More recently, the same research group developed a new construct able to mimic the native cardiac ECM in both structure and electrical activity (Roshanbinfar et al., 2020). For this purpose, they generated electrospun fiber mats using collagen, HA and PANi as synthetic polymer in different concentration. They used hiPSC-CMs to check the biocompatibility and the functionality of these supports, reporting an improved electrical coupling and contraction of the cells. Thus, within the last years, many biomaterials have emerged as good candidates for cardiac tissue engineering to fill the existing gap for their application to cardiac regeneration and treatment of MI. Notably, injectable materials, dECM and cardiac patches have been shown to be able to increase cell retention, improving cell survival and coupling with the host (Hastings et al., 2015; Cambria et al., 2017; Park et al., 2019). A summary of these biomaterials is provided in the **Table 1**, together with their *pro* and *cons*.

Another determinant factor to be considered when assembling an engineered tissue construct regards the scaffolds' assembly: many different methodologies have been developed to optimize their composition, structure and biocompatibility. Use of self-assembled monolayers (SAM) of different polymers by hydrogen bonds and hydrophobic or electrostatic interactions represents one of the proposed approaches to produce natural biomaterials (Mason and Shimanovich, 2018). This technique is particularly suitable to mimic the extracellular matrix (ECM) structure, which is important for cell adhesion and survival (Oh et al., 2003). Both synthetic and natural polymers may also be assembled in scaffolds by electrospinning, which is another, and widely used, methodology to produce nanofibers (Kitsara et al., 2017). Lastly, thermally induced phase-separation (TIPS) also represents a robust methodology for 3D scaffold production. This technique entails few crucial steps (polymer dissolution, a phase of separation, polymer gelation, extraction of the solvent from the gel and freezing after drying) that result in the production of a nanofibrous foam, very similar in size to the natural collagen present in the ECM (Nguyen et al., 2019). In this context, 3D-bioprinting is also emerging as another valuable technology to produce improved scaffolds that may include cells, matrices and bioactive molecules for cell growth. 3D-bioprinting refers to the generation of physical 3D platforms, made by deposition of materials with a progressive layered approach, which is regulated by custom digital designs (Ong et al., 2018). Bio-printed structures could be generated with different technologies, such as inkjet bioprinting, laser-assisted or micro-extrusion bioprinting; the choice among these strictly depends on the desired outcome (Murphy and Atala, 2014; Vukicevic et al., 2017). During the last decade, 3D-bioprinting has provided us with the possibility to create organized tissue-like structures, that contain living cells, including CMs (Gaetani et al., 2012). As a matter of fact, Gaetani et al. (2012) were able to generate a cardiac tissue *in vitro* by combining bioprinting techniques and human cardiac progenitor cells (hCPCs), demonstrating the applicability of bioprinting in this area of research. Specifically, they demonstrated that hCPCs can be printed in a scaffold containing alginate without affecting cell proliferation and viability; additionally they showed an improvement in the cardiac commitment of the "printed" cells, that exhibited a significant increase of the expression of both, early (i.e., Nkx2.5, GATA-4, and Mef2c) and late (i.e., cardiac troponin T - TnT) cardiac-specific markers (Gaetani et al., 2012). More recently, Noor et al. (2019) made an important step forward in the field by developing a 3D printing technique that employs patient-derived hydrogels as bioinks and iPSC-derived CMs and ECs: by specific combination of these acellular/cellular components, they reported the generation of thick and vascularized cardiac patches that match the immune-cellular properties of a specific patient. More in detail, the authors started from a biopsy of omental tissue from which they isolated cells and ECM: cells were employed to generate CMs and ECs through reprogramming and subsequent differentiation, while ECM was processed to a form a personalized hydrogel, used to blend the cell-specific bioink formulations. The cardiac patches described in this work are the result of the printing of these two distinct bioinks into superimposed layers, each containing parenchymal tissue (CMs) and blood vessel forming cells (ECs). In addition to vascularized cardiac patches, the technique was also applied to fabricate small-scale cellularized perfusable human hearts with a natural anatomical architecture and mechanical properties. Likewise, later in the same year, Lee et al. (2019) reported an improved methodology for collagen 3D-bioprinting, using freeform reversible embedding of suspended hydrogels (FRESH). Using this approach, the authors were able to engineer different components of the human heart, ranging from small capillaries, to the valves, and the whole organ (Lee et al., 2019). By finely tuning the collagen gelation process, it was possible to control the morphology and the size of the printed filaments, increasing the resolution power of the bioprinting process. Importantly, the authors showed that the cardiac components obtained using their improved FRESH-based 3D bioprinting accurately reproduce structural, mechanical, and biological properties of the native tissue.

However, regardless of the employed strategy, generation of tissue-like engineered structures suitable for regenerative medicine applications needs further considerations, specifically in relation to some aspects that may be critical for their efficacy and potential undesired effects *in vivo*. As already mentioned above, the choice of the biomaterial utilized for developing engineered cardiac constructs is one crucial aspect, since this material will constitute the support for the cells, and should guarantee the optimal conditions for their growth, differentiation and survival. Another important parameter to be considered is represented by the "structure" (or "shape") of the engineered supports, which provide the geometrical patterned for cell organization and for the establishment of cell-cell communication and 3D-microenvironment. Although there is no clear distinction between the different types of engineered-based constructs, based on their geometry and the methodology used for cell assembly, we can mainly identify cell sheets, cardiac patches and actual 3D-engineered cardiac tissue models.

TABLE 1 | Biomaterials used for cardiac tissue engineering.

Materials	Advantages	Disadvantages	References
Natural materials			
• Collagen	Biocompatibility, biodegradability and high cell proliferation rate	Stiffness makes difficult the integration within the heart	Shi et al., 2011; Masumoto et al., 2016; Geng et al., 2018
• Alginate	Biocompatibility and gelation capacity	Lack of integration with CMs	Landa et al., 2008; Geng et al., 2018; Maiullari et al., 2018
• Fibrin	Biocompatibility, high cell adhesion	Poor resistance to mechanical stretch	Christman et al., 2004; Deng et al., 2015
• Hyaluronic acid	Biocompatibility, high cell proliferation rate	Low mechanical properties	Abdalla et al., 2013; Bonafè et al., 2014
• Decellularized extracellular matrices (dECM)	Biocompatibility and promotion of cell attachment	Batch-to-batch variability	Singelyn et al., 2012; Hernandez et al., 2018; Spang and Christman, 2018; Goldfracht et al., 2019; Traverse et al., 2019; Tsui et al., 2019
Synthetic polymers			
• poly(ethylene glycol) poly(ε-caprolactone), poly(propylene) poly(vinyl alcohol), poly(*N*-isopropylacrylamide), poly(glycerol sebacate), poly(ester urethane)s	Possibility to customize material's properties	Low biocompatibility. Poor cell adhesion and proliferation.	Martins et al., 2014; Zhou et al., 2014; Moorthi et al., 2017
• Electroconductive polyaniline (PANi) and polypyrrole (PPy) polymers	Possibility to customize material's properties. Environmental stability and electrical properties	Low biocompatibility and insoluble in water	Hsiao et al., 2013; Razak et al., 2015; Wang et al., 2016
• Electroconductive Polythiophene polymers	Possibility to customize material's properties, soluble in water	Limited processability	Richardson-Burns et al., 2007; Kaur et al., 2015
• Electroconductive PEDOT:PSS polymers	Possibility to customize material's properties, support cell attachment, thermal, electrical and chemical stability	Limited processability, need to be combined with other supporting materials	Hempel et al., 2017; Jiang et al., 2017; Roshanbinfar et al., 2018, 2019

Cell Sheets and Cardiac Patches

One of the first examples of a tissue-like structure obtained through engineering-based methodologies is represented by cell sheets. Cell sheets are generated by detachment of monolayers of cells, grown at confluency, from the culture surface. Functional tissues can be then fabricated by layering the recovered cell sheets without the need of any scaffold or complicated manipulation. Cell sheets are also used to produce engineered cardiac patches containing aligned CMs. Compared to cell sheets, cardiac patches are thicker engineered supports, which recreate a functioning piece of "heart tissue" and can be used to replace the damaged area of a patient's heart, to maintain its contractile properties.

However, also in this case, it is difficult to establish a clear distinction between the two typologies of constructs. Compared to injection of isolated cells, CM-formed cell sheets showed enhanced cell vitality, heart-like electrical and histological properties with contractile ability *in vitro*; when transplanted *in vivo*, they were functional and electrically coupled with the recipient myocardium (Sawa et al., 2012).

In terms of technology, detachment of intact cell sheets from the culture surface may be achieved using different approaches. On this regard, Sawa et al. (2012) proposed a novel protocol based on poly(*N*-isopropylacrylamide) (PIPAAm), which is temperature-responsive polymer. Under normal culture conditions (37°C), the surface of the dishes is relatively hydrophobic and cells efficiently attach and proliferate. In turn, when temperature decreases to about 32°C (the polymer's lower critical solution temperature), the polymer becomes hydrophilic and a hydration layer forms between the surface of dishes and the cells, leading to their detachment from the culturing surface as an intact sheet, with no need of enzymatic treatments. Using the same approach, Masumoto et al. (2016) reported the use of cell sheets, formed by different cardiac cells generated through human iPSC differentiation *in vivo,* and demonstrated their ability to drive functional recovery after MI. More recently, Ishigami et al. (2018) demonstrated functional restoration of the failing myocardium also in a porcine model using human iPSC-derived cardiac sheets. In their work, the authors induced differentiation of iPSC into CMs, vascular cells and vascular mural cells and generated the cardiac sheets using 10 cm-sized temperature-responsive culture dishes. When transplanted *in vivo*, the generated cardiac sheets led to a significant reduction of the fibrotic area and an increase of the capillarity density in the border zone. However, the cell sheet layering methods still present some limitations mainly related to the number of cell layers that can be superimposed before incurring the decrease in oxygen and nutrients supply to the cells and thus leading to the necrosis of the transplanted patch after its implantation. On this regard, the recent work from Noor et al. (2019), already discussed above, gave a substantial contribution to the field, overcoming part of these limitations. By using 3D-printing techniques and iPSC-derived cardiac and endothelial cells encapsulated into tissue-derived hydrogels, they fabricated vascularized thick (2–7 mm) cardiac patches, that exhibit high cell viability and contractile activity. Future long-term *in vitro* studies and *in vivo* experiments will certainly establish the therapeutic potential of such cardiac constructs.

3D-Engineered Cardiac Tissue Models

Engineered cardiac tissue models have recently emerged as promising approaches to repair damaged cardiac tissue as well as suitable platforms for drug/toxicity testing and disease modeling (MacNeil, 2007). Through the use of the natural and/or synthetic biomaterials mentioned above, it is possible to generate implantable supports able to mimic the architecture and composition of the heart ECM, that are necessary to optimize cell growth, differentiation and survival *in vivo*. In fact, engineered cardiac tissue models are generated with the aim of recreating the heart environment, and to provide the proper electrical and mechanical support to the cell for their delivery into the heart. Eschenhagen et al. (1997) were the first to develop a method to culture chick cardiac CMs in 3D structures using a collagen matrix. The authors showed the possibility to measure the isometric force of contraction generated by CM-populated matrices, later referred as engineered heart tissue (EHT). In addition, this matrix was suitable for genetic manipulation, showing an efficient transduction rate to adenoviral-mediated gene transfer of the populating CMs. Zimmermann et al. (2000) reported the development of EHTs using rat CMs and 2 years later, they provided an improved version of this technique creating new EHT geometry (Zimmermann et al., 2002). Thus, such engineered cardiac tissues were first used to deliver CMs to the infarcted area after MI in preclinical animal models. In the first attempt, despite an initial improvement in cell survival, the engineered structures were unable to ameliorate cardiac function *in vivo* (Li et al., 1999). However, different results were subsequently obtained using cardiac engineered tissues with similar composition, that were instead associated to an increase in cell survival and ameliorated cardiac function (Leor et al., 2000; Akhyari et al., 2002; Eschenhagen et al., 2002; Kofidis et al., 2002). To give some examples, Eschenhagen et al. (2002) used collagen-based EHT to restore function of the damaged myocardium, demonstrating long-term survival and contraction of these structures *in vivo* (over 8 weeks after implantation). Similar results were obtained by Dar et al. (2002) using alginate-based scaffolds.

The improvement of protocols for differentiation of PSCs toward the cardiac lineage made the production of large amounts of human CMs feasible, bursting the development of human heart surrogates for disease modeling, drug testing and autologous cell therapy applications. On this regard, embedding CMs derived from PSCs into engineered structures has been shown to positively impact cell maturation to different extents, depending on the specific characteristics of the generated 3D-constructs. In fact, even if improved over time, use of both human iPSCs and ESCs still deals with an important issue of cell maturation following cardiac induction *in vitro*. One of the first evidence supporting the

maturation of CMs in 3D-engineered constructs is given by the study from Schaaf et al. (2011), who developed a EHT using CMs derived from human ESCs and showed that, when included into the fibrin-based 3D-constructs, despite an immature electrophysiological profile, these ESC-derived CMs displayed a more organized sarcomeric structure compared to those cultured in 2D under conventional conditions. In the same year, the group of Charles E. Murry also developed collagen-based bio-engineered human cardiac tissue constructs using CMs derived from both ESCs and iPSCs, demonstrating an improvement in their alignment and proliferation (Tulloch et al., 2011). They also found that these engineered constructs were able to engraft into the heart establishing connections with the host vasculature. Similarly, Mannhardt et al. (2016) investigated morphology and function of EHTs built using human iPSC-CMs, and tested their suitability for drug screening. In detail, these EHT constructs were anchored to two flexible silicone supports that generated a preload against which the EHTs perform auxotonic contractile work. This process led to the formation of muscle bundles in which CMs showed a better alignment and an improved sarcomeric organization. Thus, altogether these studies strongly indicate that EHT constructs are excellent supports for maturation of CMs derived from human PSCs, since they provide a physiological-like environment and stimuli to cells.

On this regard, the recent work from Ronaldson-Bouchard et al. (2018) gave a substantial contribution to the field. In their work, the authors showed that exposure of early-stage iPSC-CMs to myocardium-like mechanical forces and electrical stimuli at increasing intensity (from 2 to 6 Hz in 4 weeks) enables cells to reach unprecedent levels of maturation. In fact, the authors reported an upregulation of late-stage cardiac-specific markers, the length of the sarcomeres (up to 2.2 μm), the presence of intercalated disks and T-tubules, the high density of mitochondria, the switch to oxidative metabolism and the establishment of a more mature functional phenotype. Indeed, even if still inferior to the adult myocardium, the generated cardiac constructs showed more mature electrophysiological characteristics and calcium handling, increased conduction velocity, complete responsiveness to β-adrenergic stimulation and a positive force-frequency relationship (FFR), which is a stringent indicator of maturation never seen before in other EHT models (Ronaldson-Bouchard et al., 2018).

Overall, thanks to these improved characteristics, EHTs may be used as a model platform for the *in vitro* study of human cardiac functions, in terms of the force, pacemaking activity, contractile properties and electrophysiological parameters (Hansen et al., 2010; Mannhardt et al., 2016), in addition to representing a promising resource for future cardiac regenerative therapies. With respect to cardiac regeneration, preclinical studies conducted in a guinea pig model of MI showed an improvement of the left ventricle function after transplantation of iPSC-derived EHTs; in some cases these 3D-EHT constructs were also shown to be coupled to the host cardiac tissue (Weinberger et al., 2016). Recently, another study by the same research team, also assessed the issue of the increased risk of cardiac arrhythmia secondary to EHT implantation (Pecha et al., 2019). This analysis was performed through the implant of telemetric devices following EHT transplant and the monitoring of the electric activity of the heart for 28 days: results demonstrated that in this case, the incidence of ventricular arrhythmias was not affected by EHT transplant. However, other reports showed discordant results, demonstrating a link between transplantation of iPSC-derived CMs and induction of transient abnormal beating, potentially leading to malignant ventricular arrhythmia (Chong et al., 2014; Shiba et al., 2016). Furthermore, despite the encouraging results obtained from using cardiac-engineered tissues for cell transplantation *in vivo*, other studies reported a limited effect of cardiac patches, dampening the initial enthusiasm on their potential translation to the clinic in the short time. To give an example, in a recent study Sugiura et al. (2016) employed tissue-engineered biodegradable patches [made of polyglycolic acid poly(l-lactic-co-ε-caprolactone) copolymer] seeded with iPSC-CMs and tested their applicability *in vivo*. Their results showed that, at 4 weeks post-implantation, no iPSC-CMs remained in the patch (Sugiura et al., 2016), warning about the need of punctual experimentations that take into account all the potential variables (biomaterial, type of cells, degree of cardiac injury) before application of such tissue substitutes in patients. In this context, Park et al. (2019) recently demonstrated that iPSC-CMs and human mesenchymal stem cell-loaded patches are able to increase cardiac regeneration in a rat model of MI, improving cell retention and engraftment within the myocardium. The presence of human mesenchymal stem cells into the patch is likely providing a favorable microenvironment for vascular regeneration (Park et al., 2019). Very recently, similar work from the group of Charles E. Murry contributed to the field adding an additional layer of complexity to such tissue engineered constructs, and highlighting the importance of vascularization. Indeed, insufficient vascularization is one of the major problem of application of EHT for cardiovascular regeneration (Redd et al., 2019). In this work the authors combined stem cell methodologies and advanced tissue engineering to develop an engineered perfusable microvasculature system; specifically, they assembled ECs generated from ESCs into patterned micro-channels and a collagen matrix and demonstrated that, in these engineered constructs, ECs were able to form *de novo* vasculature through neo-angiogenesis and vascular remodeling processes. Furthermore, when transplanted *in vivo* in a rat model of MI, such perfusable microvascular graft integrated with the host coronary with a greater extent compared to non-perfusable constructs. Interestingly, when CMs were also embedded into the grafts, these were shown to support their survival after implantation, further supporting the importance of vascularization in the design of engineered cardiac tissue constructs for regenerative purposes. Altogether these studies showed that cardiac engineered constructs enhance intercellular organization and crosstalk of iPSC-CMs, improving their maturation *in vitro*, and ameliorate cardiac

performance after the transplantation *in vivo*, thus providing encouraging evidences for their future use to achieve cardiac regeneration in humans.

TRANSDIFFERENTIATION OF NON-CONTRACTILE CELLS: AN ALTERNATIVE APPROACH TO HEART REGENERATION

After myocardial infarction, the heart undergoes pathological remodeling, in order to preserve its function and the structural integrity of the cardiac muscle. During this process, necrotic cardiac tissue is replaced by non-CM components, mostly fibroblasts, that ultimately form fibrotic scar. The recent evidence that it is possible to directly induce the conversion of non-cardiomyocyte cells into CMs have emerged as a promising area to achieve *in situ* cardiac regeneration, by reducing the extent of the cardiac fibrotic scar (Talman and Ruskoaho, 2016). The first study dates back to 2010 and showed the direct reprogramming of postnatal cardiac or dermal murine fibroblasts into CM-like cells through the supply of a combination of three developmental transcription factors (i.e., Gata4, Mef2c, and Tbx5) (Ieda et al., 2010). In the same study, the authors showed the successful reprogramming into CMs when fibroblasts were transplanted *in vivo*. Subsequent studies further supported this evidence, showing the possibility to redirect the fate of cardiac fibroblasts (CFs) toward CMs *in vivo* through different strategies (Nam et al., 2013b; Doppler et al., 2015; Batty et al., 2016; Chen Y. et al., 2017).

Cardiac fibroblasts are abundantly represented in the adult cardiac tissue, where they play a crucial role both in physiological and pathological conditions: they are indeed crucial to maintain the normal cardiac function and are actively involved in cardiac remodeling leading to fibrosis and cardiac dysfunction (Batty et al., 2016). Local administration of the three cardiac transcription factors Gata4, Mef2c, and Tbx5 has been demonstrated to be sufficient to switch murine CFs toward a CM-like phenotype *in vivo*, and this was associated with a reduction of the infarct size and a modest mitigation of cardiac dysfunction after MI (Qian et al., 2012; Chen Y. et al., 2017). Along the same line, Fu et al. (2015) reported the induction of beating CMs from mouse CFs only by using a chemical cocktail, made of the GSK3β inhibitor CHIR99021, the inhibitor of the TGF-β type 1 receptor RepSox, Forskolin, valproic acid (VPA), the monoamine oxidase inhibitor Parnate, the analog of retinoic acid TTNPB, and the histone methylation inhibitor DZnep (3- deazaneplanocin A). These chemically induced cardiomyocyte-like cells (CiCMs) expressed CM-specific markers and exhibited evidence of sarcomeric organization (Fu et al., 2015).

Achievement of the simultaneous expression of all reprogramming factors in CFs is crucial for determining the efficiency of the reprogramming process. In fact, the reprogrammed fate is acquired within the first 48 h after *Gata4*, *Mef2c*, and *Tbx5* administration, and represents a critical step to be improved in order to overcome the extremely low efficiency initially reported for CF/CM transdifferentiation (Bektik and Fu, 2019; Stone et al., 2019; Zhang et al., 2019). On this regard, several methodologies have been developed in the recent years to enhance the efficiency of the "classical" transcription factor-based cardiac reprogramming protocol, including epigenetic modulation and treatments with inhibitors or cytokines (Nam et al., 2013a; Chen Y. et al., 2017). Addis et al. (2013) described an approach to optimize the direct conversion of fibroblast to CMs, using a reporter system in which the calcium indicator GCaMP was driven by the CM-specific Troponin T promoter. In addition to Gata4, Mef2c, and Tbx5, the authors also administered Hand2 and Nkx2.5, showing that this new transcription factor combination was 50-fold more efficient than the classical three cardiac transcription factor protocol and was able to induce CMs expressing specific markers and with robust calcium oscillation and spontaneous beating, which persisted after the subsequent inactivation of the reprogramming factors.

Based on this evidence, the possibility to achieve direct reprogramming of CFs into CMs *in vivo* holds great promise for restoring cardiac function. Diverse strategies have been already proposed, exhibiting a certain rate of success. Among the others, one interesting strategy for directing reprogramming of CFs into CMs relies on the use of microRNAs (miRNAs) (Jayawardena et al., 2012). Synthesized miRNA could be easily administered to cells of interest by lipid-based transfection, showing a low toxicity for the host (Elmén et al., 2008). Jayawardena et al. (2012) demonstrated that *in vitro* mouse fibroblasts could be directly reprogrammed to a cardiomyocyte-like phenotype using a specific cocktail of miRNAs (miRNAs 1, 133, 208, 499) and JAK inhibition. The "newly" generated CMs showed sarcomere organization and expressed cardiomyocyte-specific genes. At the functional level, the authors reported calcium transient and mechanical contraction (Jayawardena et al., 2012). Likewise, Muraoka et al. (2014) found that miR-133 is able to potentiate cardiac reprogramming by directly repressing Snai1 (master regulator epithelial-mesenchymal transition) and silencing the fibroblast signature. In the same way, Christoforou et al. (2017) described the transdifferentiation of human CFs toward CMs via the delivery of miRNAs miR-1 and miR-133a and the induction of the expression of Gata4, Tbx5, Mef2C, Myocd, and Nkx2.5. However, although the initial excitement on the potential use of direct cell reprogramming to achieve cardiac regeneration, the approach is still rather immature and not sufficiently tested for its translation into the clinic. Indeed, cardiac reprogramming efficiency is still very low (about 20% of cells expressing cardiac markers, corresponding to 1–2% of cells with recordable action potential and functional) and give rise to cardiac cells with an immature phenotype.

In addition to that, we should consider that cardiac reprogramming of human cells is more difficult – and therefore less efficient – compared to the murine counterpart. Wada et al. (2013) reported that the addition of Myocd and Mesp1 to three classical factors (Gata4, Mef2c, and Tbx5) could increase the switch of human cardiac and dermal fibroblasts into CMs. Similarly, Fu et al. (2013) reported that addition of *ESRRG* and

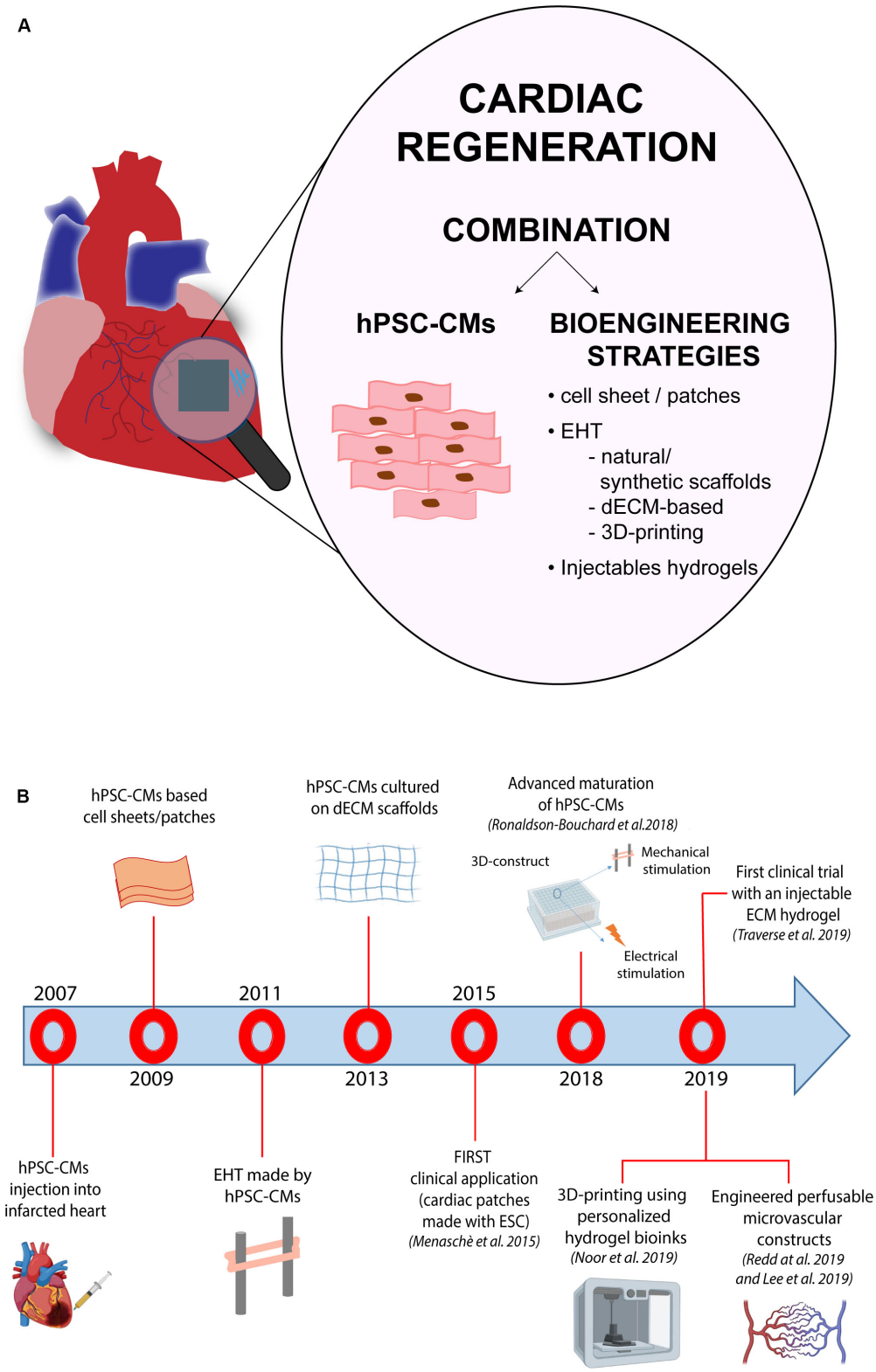

FIGURE 3 | hPSC-based bioengineering strategies for cardiac regeneration. The panel **(A)** shows a schematic representation of the different hPSC-based methodologies used for regenerative purposes in the cardiac field. The panel **(B)** provides a time line that summarizes the key milestones reached in the field, starting from the simple injection of hPSC-CMs into the heart to the development of tissue-like structures with enhanced hPSC-CM maturation, more complex perfusable and personalized constructs and injectable hydrogels.

TABLE 2 | Overview of iPSC-based 3D cell culture approaches.

Type	Bio-functional properties	Advantage	Disadvantage	References
Spheroids	Self-assembling multicellular aggregates.	Scaffold-free technology without the use of any exogenous support. Composition with different cell-type populations. Manipulation by pipetting and sedimentation. Size allows the miniaturized multi-well formats compatible with plate readers	Small size and heterogeneous composition of multicellular aggregates. No direct measurements of electrophysiological properties. Non-linear cell alignment. Number of cells: detrimental for the cellular viability.	Polonchuk et al., 2017; Tan et al., 2017; Correia et al., 2018; Hoang et al., 2018; Kim T. Y. et al., 2018; Mattapally et al., 2018; Yan et al., 2019
Organoids	Self-assembling organ-like tissue.	Composition with different cell-type populations. Mimics thicker tissues. High level of tissue organization. Size allows the miniaturized multi-well formats compatible with plate readers.	Stochastic events for self-assembly: heterogeneity in shape, size and cell composition. Size of multicellular aggregates. Number of cells: detrimental for the cellular viability.	Kusuma et al., 2013; Lancaster et al., 2013; Orlova et al., 2014; Chan et al., 2015; Eder et al., 2016; Chen Y.-W. et al., 2017; Richards et al., 2017; Mills et al., 2019; Wimmer et al., 2019
Cell sheet cardiac patches	Transplantable 3D-constructs.	Layering of CMs forming a tissue-like structure. Easy to produce and to manipulate. Precise control of cell sheet shape and structure.	Number of cell layers: possible decrease in oxygen and nutrients supply to cells; necrosis of the cells sheets after implantation.	Shimizu et al., 2006; Stevens et al., 2009; Gaetani et al., 2012; Vallée et al., 2012; Wendel et al., 2015; Masumoto et al., 2016; Ishigami et al., 2018; Noor et al., 2019; Park et al., 2019
Engineered cardiac tissue models	3D heart-like constructs with higher level of biological complexity.	Composition with different cell-type populations. Linear cells alignment. Improved maturation of hIPSC-CMs. Direct measurements of electrical activity of the cells.	Coupling with the host tissue. Vascularization. Biocompatibility of the materials.	Tulloch et al., 2011; Deng et al., 2015; Mannhardt et al., 2016; Masumoto et al., 2016; Sugiura et al., 2016; Weinberger et al., 2016; Hernandez et al., 2018; Maiullari et al., 2018; Ronaldson-Bouchard et al., 2018; Lee et al., 2019; Redd et al., 2019; Traverse et al., 2019; Tsui et al., 2019; Roshanbinfar et al., 2020

MESP1 genes was able to increase cardiac reprogramming from human cells, and to generate CMs showing sarcomere formation and cardiac-specific gene expression. Despite the low efficiency of the current protocols and the need of further studies to develop new and optimized direct reprogramming strategies, these reports are encouraging about the possibility to apply cardiac reprogramming to regenerative medicine in the future.

CONCLUSION AND FUTURE DIRECTIONS

Although different types of stem cells have been proposed as potential candidates for cardiac regenerative medicine, there is no consensus about which represents the best choice. Given the complexity of cardiac tissue, which is composed by diverse cell types, human PSCs – mostly iPSCs – are certainly among the most relevant sources. In particular, CMs differentiated from iPSC may represent a realistic option for the regeneration of the injured heart. During the last few decades, researchers have made substantial progress in generating iPSC-CMs which have led to a general better understanding the biology of these cells and, to the definition of highly efficient differentiation protocols. A significant number of different cell therapy strategies that employ iPSC-CMs have been proposed to restore cardiac function, ranging from injection of cells alone, to their combination with ECM-like biomaterials, and to more complicated engineered-based strategies, which aim to faithfully recreate the myocardium. The majority of these approaches have shown – at least to some extent – success in mimicking heart cells and improving cardiac function, providing new hope for the replacement of CMs after the irreversible loss of heart tissue occurring during myocardial infarction (**Figure 3**). Notably, as mentioned before, Menasché et al. (2015) reported the first clinical application of cardiac patches composed of human ESC-derived cardiac progenitor cells in a patient suffering from severe ischemic left ventricle dysfunction, demonstrating the possibility to use a engineered-based approaches for cardiac repair.

More recently, iPSC-based therapies are taking over ESCs, offering a solution that overcomes ethical issues related to the use of embryo-derived material and offering a source of autologous cells for transplantation. Few clinical studies using iPSC-derived cells have already started to treat patients suffering from different diseases, such as neovascular age-related macular degeneration and Parkinson disease (Barker et al., 2017; Mandai et al., 2017). Some progress in this regard is being made also in the cardiovascular field: in May 2018, Japan's government approved the transplantation of cardiac sheets made of CMs derived from human iPSCs to treat three patients suffering from heart disease (Cyranoski, 2018). Regardless of the questions arising with respect to this decision and whether or not it was too early to jump into clinics for iPSCs in the heart, results from this clinical trial (not available yet) will surely be crucial to set the stage for this kind of treatment in the cardiovascular field.

In this scenario, tissue engineering has emerged in the last years as a new field of research applied to cardiac tissue repair for developing improved strategies to treat cardiac dysfunctions after injury. Advantages of tissue-engineering based methodologies rely on the possibility to provide CMs with the biological environment mimicking that of the heart tissue: tissue engineering allows the creation of suitable three-dimensional matrices resembling the physico-chemical properties of the myocardium in which cells are maintained viable and functional, and therefore with a higher chance to positively act on cardiac regeneration (**Table 2**).

The progress made by tissue engineering technologies has been encouraging. Indeed, with currently available methodologies, it is feasible to create bio-supports able to incorporate the cells needed for the regeneration of cardiac tissue. However, besides the milestones reached thus far, significant improvements are still mandatory before we could consider their routine use in the clinical field for treatment of patients suffering from myocardial diseases. These improvements mainly regard scaffold production, through the careful analysis of biocompatibility and mechanical properties of the engineered constructs developed for the clinics. Also, further investigations on the interaction occurring between cells and the ECM and vascular integration with the host are highly desirable in order to further ameliorate tissue engineering-based supports, hopefully opening new doors for cardiac regeneration therapy via tissue engineering strategies. In this scenario, the possibility to directly convert fibroblast into CMs *in vivo* in the infarcted heart has emerged as potential option for cardiac regeneration. However, despite the promising results obtained by preclinical research, the approach is still rather immature for its clinical translation and further investigations are needed to develop effective and more efficient strategies to achieve cardiac regeneration *in vivo*.

AUTHOR CONTRIBUTIONS

MM performed the bibliographic search and wrote the manuscript. ED wrote and revised the manuscript and provided funding.

FUNDING

This research group was supported by the Italian Minister of Health (RF-2009-1504427), the Italian Ministry of Education, University and Research (2015583WMX) and by European Union's (Horizon 2020 Research and Innovation Programme under Grant Agreement No. 828984 and ERC-CoG-2017 -under the Grant Agreement No. 772168).

ACKNOWLEDGMENTS

We are grateful to Dr. Christina Pagiatakis (Humanitas Research Hospital) for language editing and proofreading.

REFERENCES

Abdalla, S., Makhoul, G., Duong, M., Chiu, R. C., and Cecere, R. (2013). Hyaluronic acid-based hydrogel induces neovascularization and improves cardiac function in a rat model of myocardial infarction. *Interact. Cardiovasc. Thorac. Surg.* 17, 767–772.

Addis, R. C., Ifkovits, J. L., Pinto, F., Kellam, L. D., Esteso, P., Rentschler, S., et al. (2013). Optimization of direct fibroblast reprogramming to cardiomyocytes using calcium activity as a functional measure of success. *J. Mol. Cell Cardiol.* 60, 97–106.

Akhyari, P., Fedak, P. W., Weisel, R. D., Lee, T.-Y. J., Verma, S., Mickle, D. A., et al. (2002). Mechanical stretch regimen enhances the formation of bioengineered autologous cardiac muscle grafts. *Circulation* 106, I–137–I–142.

Arnal-Pastor, M., Chachques, J., Pradas, M. M., and Vallés-Lluch, A. (2013). *Biomaterials for Cardiac tissue Engineering. Regenerative Medicine and Tissue Engineering*. London: Intechopen.

Barile, L., Chimenti, I., Gaetani, R., Forte, E., Miraldi, F., Frati, G., et al. (2007). Cardiac stem cells: isolation, expansion and experimental use for myocardial regeneration. *Nat. Rev. Cardiol.* 4(Suppl.1):S9.

Barker, R. A., Parmar, M., Studer, L., and Takahashi, J. (2017). Human trials of stem cell-derived dopamine neurons for Parkinson's disease: dawn of a new era. *Cell Stem Cell* 21, 569–573.

Batalov, I., and Feinberg, A. W. (2015). Differentiation of cardiomyocytes from human pluripotent stem cells using monolayer culture. *Biomark. Insights* 10(Suppl. 1), 71–76.

Batty, J. A., Lima, J. A. Jr., and Kunadian, V. (2016). Direct cellular reprogramming for cardiac repair and regeneration. *Eur. J. Heart Fail.* 18, 145–156.

Bektik, E., and Fu, J.-D. (2019). Ameliorating the fibrotic remodeling of the heart through direct cardiac reprogramming. *Cells* 8:679.

Bergmann, O., Bhardwaj, R. D., Bernard, S., Zdunek, S., Barnabé-Heider, F., Walsh, S., et al. (2009). Evidence for cardiomyocyte renewal in humans. *Science* 324, 98–102.

Bonafè, F., Govoni, M., Giordano, E., Caldarera, C. M., Guarnieri C., and Muscari C. (2014). Hyaluronan and cardiac regeneration. *J. Biomed. Sci.* 21:100. doi: 10.1186/s12929-014-0100-4

Brassard, J. A., and Lutolf, M. P. (2019). Engineering stem cell self-organization to build better organoids. *Cell Stem Cell* 24, 860–876.

Cambria, E., Pasqualini, F. S., Wolint, P., Günter, J., Steiger, J., Bopp, A., et al. (2017). Translational cardiac stem cell therapy: advancing from first-generation to next-generation cell types. *NPJ Regen. Med.* 2, 1–10.

Cao, Y., Vacanti, J. P., Paige, K. T., and Upton, J. (1997). Transplantation of Chondrocytes utilizing a polymer-cell construct to produce tissue-engineered cartilage in the. *Plast. Reconstr. Surg.* 100, 297–302.

Caspi, O., Huber, I., Kehat, I., Habib, M., Arbel, F., Gepstein, A., et al. (2007). Transplantation of human embryonic stem cell-derived cardiomyocytes improves myocardial performance in infarcted rat hearts. *J. Am. Coll Cardiol.* 50, 1884–1893.

Chan, X. Y., Black, R., Dickerman, K., Federico, J., Lévesque, M., Mumm, J., et al. (2015). Three-dimensional vascular network assembly from diabetic patient-derived induced pluripotent stem cells. *Arterioscler. Thromb. Vasc Biol.* 35, 2677–2685.

Chen, Q.-Z., Ishii, H., Thouas, G. A., Lyon, A. R., Wright, J. S., Blaker, J. J., et al. (2010). An elastomeric patch derived from poly (glycerol sebacate) for delivery of embryonic stem cells to the heart. *Biomaterials* 31, 3885–3893. doi: 10.1016/j.biomaterials.2010.01.108

Chen, Y., Yang, Z., Zhao, Z.-A., and Shen, Z. (2017). Direct reprogramming of fibroblasts into cardiomyocytes. *Stem Cell Res. Ther.* 8:118.

Chen, Y.-W., Huang, S. X., De Carvalho, A. L. R. T., Ho, S.-H., Islam, M. N., Volpi, S., et al. (2017). A three-dimensional model of human lung development and disease from pluripotent stem cells. *Nat. Cell Biol.* 19, 542–549.

Chong, J. J., and Murry, C. E. (2014). Cardiac regeneration using pluripotent stem cells—progression to large animal models. *Stem Cell Res.* 13, 654–665.

Chong, J. J., Yang, X., Don, C. W., Minami, E., Liu, Y.-W., Weyers, J. J., et al. (2014). Human embryonic-stem-cell-derived cardiomyocytes regenerate non-human primate hearts. *Nature* 510, 273–277.

Christman, K. L., Fok, H. H., Sievers, R. E., Fang, Q., and Lee, R. J. (2004). Fibrin glue alone and skeletal myoblasts in a fibrin scaffold preserve cardiac function after myocardial infarction. *Tissue Eng.* 10, 403–409.

Christoforou, N., Chakraborty, S., Kirkton, R. D., Adler, A. F., Addis, R. C., and Leong, K. W. (2017). Core transcription factors, MicroRNAs, and small molecules drive transdifferentiation of human fibroblasts towards the cardiac cell lineage. *Sci. Rep.* 7, 1–15.

Correia, C., Koshkin, A., Duarte, P., Hu, D., Carido, M., Sebastião, M. J., et al. (2018). 3D aggregate culture improves metabolic maturation of human pluripotent stem cell derived cardiomyocytes. *Biotechnol. Bioeng* 115, 630–644.

Cui, Z., Yang, B., and Li, R.-K. (2016). Application of biomaterials in cardiac repair and regeneration. *Engineering* 2, 141–148.

Cyranoski, D. (2018). 'Reprogrammed' stem cells approved to mend human hearts for the first time. *Nature* 557, 619–619. doi: 10.1038/d41586-018-05278-8

Dar, A., Shachar, M., Leor, J., and Cohen, S. (2002). Optimization of cardiac cell seeding and distribution in 3D porous alginate scaffolds. *Biotechnol. Bioeng* 80, 305–312.

De Santis, R., Santini, L., Colantoni, A., Peruzzi, G., de Turris, V., Alfano, V., et al. (2017). FUS mutant human motoneurons display altered transcriptome and microRNA pathways with implications for ALS pathogenesis. *Stem Cell Rep.* 9, 1450–1462.

Deng, B., Shen, L., Wu, Y., Shen, Y., Ding, X., Lu, S., et al. (2015). Delivery of alginate-chitosan hydrogel promotes endogenous repair and preserves cardiac function in rats with myocardial infarction. *J. Biomed. Mater. Res. Part A* 103, 907–918.

Deng, C., Zhang, P., Vulesevic, B., Kuraitis, D., Li, F., Yang, A. F., et al. (2010). A collagen–chitosan hydrogel for endothelial differentiation and angiogenesis. *Tissue Eng. Part A* 16, 3099–3109.

Denis, P., M. Wrzecionek, A. Gadomska-Gajadhur and P. Sajkiewicz (2019). Poly (Glycerol sebacate)-poly (L-Lactide) nonwovens. towards attractive electrospun material for tissue engineering. *Polymers* 11:2113. doi: 10.3390/polym11122113

Doppler, S. A., Deutsch, M.-A., Lange, R., and Krane, M. (2015). Direct reprogramming—the future of cardiac regeneration? *Int. J. Mol. Sci.* 16, 17368–17393.

Eder, A., Vollert, I., Hansen, A., and Eschenhagen, T. (2016). Human engineered heart tissue as a model system for drug testing. *Adv. Drug Deliv. Rev.* 96, 214–224.

Egashira, T., Yuasa, S., and Fukuda, K. (2011). Induced pluripotent stem cells in cardiovascular medicine. *Stem Cells Int.* 2011:348960.

Elitt, M. S., Barbar, L., and Tesar, P. J. (2018). Drug screening for human genetic diseases using iPSC models. *Hum. Mol. Genet.* 27, R89–R98.

Elmén, J., Lindow, M., Schütz, S., Lawrence, M., Petri, A., Obad, S., et al. (2008). LNA-mediated microRNA silencing in non-human primates. *Nature* 452, 896–899.

Eschenhagen, T., Didié, M., Münzel, F., Schubert, P., Schneiderbanger, K., and Zimmermann, W.-H. (2002). 3D engineered heart tissue for replacement therapy. *Basic Res. Cardiol.* 97, I146–I152.

Eschenhagen, T., Fink, C., Remmers, U., Scholz, H., Wattchow, J., Weil, J., et al. (1997). Three-dimensional reconstitution of embryonic cardiomyocytes in a collagen matrix: a new heart muscle model system. *FASEB J.* 11, 683–694.

Evans, M. J., and Kaufman, M. H. (1981). Establishment in culture of pluripotential cells from mouse embryos. *Nature* 292, 154–156.

Fakoya, A. O. J., Otohinoyi, D. A., and Yusuf, J. (2018). Current trends in biomaterial utilization for cardiopulmonary system regeneration. *Stem Cells Int.* 2018, 1–32.

Farkhondeh, A., Li, R., Gorshkov, K., Chen, K. G., Might, M., Rodems, S., et al. (2019). Induced pluripotent stem cells for neural drug discovery. *Drug Discov Today* 24, 992–999.

Fong, A. H., Romero-López, M., Heylman, C. M., Keating, M., Tran, D., Sobrino, A., et al. (2016). Three-dimensional adult cardiac extracellular matrix promotes maturation of human induced pluripotent stem cell-derived cardiomyocytes. *Tissue Eng. Part A* 22, 1016–1025.

Freedman, B. S., Brooks, C. R., Lam, A. Q., Fu, H., Morizane, R., Agrawal, V., et al. (2015). Modelling kidney disease with CRISPR-mutant kidney organoids derived from human pluripotent epiblast spheroids. *Nat. Commun.* 6:8715.

Fu, J.-D., Stone, N. R., Liu, L., Spencer, C. I., Qian, L., Hayashi, Y., et al. (2013). Direct reprogramming of human fibroblasts toward a cardiomyocyte-like state. *Stem Cell Rep.* 71, 235–247.

Fu, Y., Huang, C., Xu, X., Gu, H., Ye, Y., Jiang, C., et al. (2015). Direct reprogramming of mouse fibroblasts into cardiomyocytes with chemical cocktails. *Cell Res.* 25:1013.

Gaballa, M. A., Sunkomat, J. N., Thai, H., Morkin, E., Ewy, G., and Goldman, S. (2006). Grafting an acellular 3-dimensional collagen scaffold onto a non-transmural infarcted myocardium induces neo-angiogenesis and reduces cardiac remodeling. *J. Heart lung Trans.* 25, 946–954.

Gaetani, R., Doevendans, P. A., Metz, C. H., Alblas, J., Messina, E., Giacomello, A., et al. (2012). Cardiac tissue engineering using tissue printing technology and human cardiac progenitor cells. *Biomaterials* 33, 1782–1790.

Geng, X., Liu, B., Liu, J., Liu, D., Lu, Y., Sun, X., et al. (2018). Interfacial tissue engineering of heart regenerative medicine based on soft cell-porous scaffolds. *J. Thoracic Dis.* 10(Suppl. 20):S2333.

Goldfracht, Y., Efraim, I., Shinnawi, R., Kovalev, E., Huber, I., Gepstein, A., et al. (2019). Engineered heart tissue models from hiPSC-derived cardiomyocytes and cardiac ECM for disease modeling and drug testing applications. *Acta Biomate.* 92, 145–159.

Gong, M., Yu, B., Wang, Y.-G., and Xu, M. (2013). Bone marrow rejuvenation. An excellent potential therapy for age-related endothelial dysfunction. *Circ. J.* 77, 2886–2888.

Gonzales, C., and Pedrazzini, T. (2009). Progenitor cell therapy for heart disease. *Exp. Cell Res.* 315, 3077–3085.

Gu, M., Shao, N. Y., Sa, S., Li, D., Termglinchan, V., Ameen, M., et al. (2017). Patient-specific iPSC-derived endothelial cells uncover pathways that protect against pulmonary hypertension in BMPR2 mutation carriers. *Cell Stem Cell* 20, 490.e5–504.e5.

Haggart, C. R., Ames, E. G., Lee, J. K., and Holmes, J. W. (2014). Effects of stretch and shortening on gene expression in intact myocardium. *Physiol. Genomics* 46, 57–65.

Hamdi, H., Furuta, A., Bellamy, V., Bel, A., Puymirat, E., Peyrard, S., et al. (2009). Cell delivery: intramyocardial injections or epicardial deposition? A head-to-head comparison. *Ann. Thorac. Surg.* 87, 1196–1203.

Hansen, A., Eder, A., Bönstrup, M., Flato, M., Mewe, M., Schaaf, S., et al. (2010). Development of a drug screening platform based on engineered heart tissue. *Circ. Res.* 107, 35–44.

Hashmi, S., and Ahmad, H. R. (2019). Molecular switch model for cardiomyocyte proliferation. *Cell Regen.* 8, 12–20.

Hastings, C. L., Roche, E. T., Ruiz-Hernandez, E., Schenke-Layland, K., Walsh, C. J., and Duffy, G. P. (2015). Drug and cell delivery for cardiac regeneration. *Adv. Drug Deliv. Rev.* 84, 85–106.

Hempel, F., Law, J. K.-Y., Nguyen, T. C., Munief, W., Lu, X., Pachauri, V., et al. (2017). PEDOT: PSS organic electrochemical transistor arrays for extracellular electrophysiological sensing of cardiac cells. *Biosens. Bioelectron.* 93, 132–138.

Hernandez, M. J., Gaetani, R., Pieters, V. M., Ng, N. W., Chang, A. E., Martin, T. R., et al. (2018). Decellularized extracellular matrix hydrogels as a delivery platform for MicroRNA and extracellular vesicle therapeutics. *Adv. Ther.* 1:1800032.

Hernandez, M. J., Yakutis, G. E., Zelus, E. I., Hill, R. C., Dzieciatkowska, M., Hansen, K. C., et al. (2020). Manufacturing considerations for producing and assessing decellularized extracellular matrix hydrogels. *Methods* 171, 20–27.

Hirt, M. N., Boeddinghaus, J., Mitchell, A., Schaaf, S., Börnchen, C., Müller, C., et al. (2014). Functional improvement and maturation of rat and human engineered heart tissue by chronic electrical stimulation. *J. Mol. Cell Cardiol.* 74, 151–161.

Hoang, P., Wang, J., Conklin, B. R., Healy, K. E., and Ma, Z. (2018). Generation of spatial-patterned early-developing cardiac organoids using human pluripotent stem cells. *Nat. Protoc.* 13, 723–737.

Hockemeyer, D., and Jaenisch, R. (2016). Induced pluripotent stem cells meet genome editing. *Cell Stem Cell* 18, 573–586.

Hsiao, C.-W., Bai, M.-Y., Chang, Y., Chung, M.-F., Lee, T.-Y., Wu, C.-T., et al. (2013). Electrical coupling of isolated cardiomyocyte clusters grown on aligned conductive nanofibrous meshes for their synchronized beating. *Biomaterials* 34, 1063–1072.

Huch, M., Dorrell, C., Boj, S. F., van Es, J. H., Li, V. S., van de Wetering, M., et al. (2013). In vitro expansion of single Lgr5+ liver stem cells induced by Wnt-driven regeneration. *Nature* 494, 247–250.

Hussey, G. S., Dziki, J. L., and Badylak, S. F. (2018). Extracellular matrix-based materials for regenerative medicine. *Nat. Rev. Mater.* 3, 159–173.

Ieda, M., Fu, J.-D., Delgado-Olguin, P., Vedantham, V., Hayashi, Y., Bruneau, B. G., et al. (2010). Direct reprogramming of fibroblasts into functional cardiomyocytes by defined factors. *Cell* 142, 375–386.

Ishigami, M., Masumoto, H., Ikuno, T., Aoki, T., Kawatou, M., Minakata, K., et al. (2018). Human iPS cell-derived cardiac tissue sheets for functional restoration of infarcted porcine hearts. *PLoS One* 13:e0201650. doi: 10.1371/journal.pone.0201650

Janssens, S., Dubois, C., Bogaert, J., Theunissen, K., Deroose, C., Desmet, W., et al. (2006). Autologous bone marrow-derived stem-cell transfer in patients with ST-segment elevation myocardial infarction: double-blind, randomised controlled trial. *Lancet* 367, 113–121.

Jayawardena, T. M., Egemnazarov, B., Finch, E. A., Zhang, L., Payne, J. A., Pandya, K., et al. (2012). MicroRNA-mediated in vitro and in vivo direct reprogramming of cardiac fibroblasts to cardiomyocytes. *Circ. Res.* 110, 1465–1473.

Jiang, L., Gentile, C., Lauto, A., Cui, C., Song, Y., Romeo, T., et al. (2017). Versatile fabrication approach of conductive hydrogels via copolymerization with vinyl monomers. *ACS Appl. Mater. Interfaces* 9, 44124–44133. doi: 10.1021/acsami.7b15019

Jones, J. R., Sepulveda, P., and Hench, L. L. (2002). "The effect of temperature on the processing and properties of macroporous bioactive glass foams," in *Key Engineering Materials*, (Stafa-Zurich: Trans Tech Publication), 299–302.

Kai, D., Wang, Q.-L., Wang, H.-J., Prabhakaran, M. P., Zhang, Y., Tan, Y.-Z., et al. (2014). Stem cell-loaded nanofibrous patch promotes the regeneration of infarcted myocardium with functional improvement in rat model. *Acta Biomater.* 10, 2727–2738.

Karbassi, E., Fenix, A., Marchiano, S., Muraoka, N., Nakamura, K., Yang, X., et al. (2020). Cardiomyocyte maturation: advances in knowledge and implications for regenerative medicine. *Nat. Rev. Cardiol.* 1–19. doi: 10.1038/s41569-019-0331-x

Kaur, G., Adhikari, R., Cass, P., Bown, M., and Gunatillake, P. (2015). Electrically conductive polymers and composites for biomedical applications. *Rsc Adv.* 5, 37553–37567. doi: 10.1039/C5RA01851J

Kim, P., Chu, N., Davis, J., and Kim, D. H. (2018). Mechanoregulation of myofibroblast fate and cardiac fibrosis. *Adv. Biosyst.* 2:1700172.

Kim, T. Y., Kofron, C. M., King, M. E., Markes, A. R., Okundaye, A. O., Qu, Z., et al. (2018). Directed fusion of cardiac spheroids into larger heterocellular microtissues enables investigation of cardiac action potential propagation via cardiac fibroblasts. *PLoS One* 13:e0196714. doi: 10.1371/journal.pone.0196714

Kitsara, M., Agbulut, O., Kontziampasis, D., Chen, Y., and Menasché, P. (2017). Fibers for hearts: a critical review on electrospinning for cardiac tissue engineering. *Acta Biomater.* 48, 20–40.

Kofidis, T., Akhyari, P., Boublik, J., Theodorou, P., Martin, U., Ruhparwar, A., et al. (2002). In vitro engineering of heart muscle: artificial myocardial tissue. *J. Thoracic Cardiovasc. Surg.* 124, 63–69.

Kusuma, S., Shen, Y.-I., Hanjaya-Putra, D., Mali, P., Cheng, L., and Gerecht, S. (2013). Self-organized vascular networks from human pluripotent stem cells in a synthetic matrix. *Proc. Natl. Acad. Sci. U.S.A*110, 12601–12606.

Laflamme, M. A., Chen, K. Y., Naumova, A. V., Muskheli, V., Fugate, J. A., Dupras, S. K., et al. (2007). Cardiomyocytes derived from human embryonic stem cells in pro-survival factors enhance function of infarcted rat hearts. *Nat. Biotechnol.* 25, 1015–1024.

Lancaster, M. A., and Knoblich, J. A. (2014). Generation of cerebral organoids from human pluripotent stem cells. *Nat. Protoc.* 9:2329–2340.

Lancaster, M. A., Renner, M., Martin, C. A., Wenzel, D., Bicknell, L. S., Hurles, M. E., et al. (2013). Cerebral organoids model human brain development and microcephaly. *Nature* 501, 373–379.

Landa, N., Miller, L., Feinberg, M. S., Holbova, R., Shachar, M., Freeman, I., et al. (2008). Effect of injectable alginate implant on cardiac remodeling and function after recent and old infarcts in rat. *Circulation* 117, 1388–1396. doi: 10.1161/CIRCULATIONAHA.107.727420

Lee, A., Hudson, A., Shiwarski, D., Tashman, J., Hinton, T., Yerneni, S., et al. (2019). 3D bioprinting of collagen to rebuild components of the human heart. *Science* 365, 482–487.

Lee, K. Y., and Mooney, D. J. (2012). Alginate: properties and biomedical applications. *Prog. Polym. Sci.* 37, 106–126.

Lemcke, H., Voronina, N., Steinhoff, G., and David, R. (2018). Recent progress in stem cell modification for cardiac regeneration. *Stem Cells Int.* 2018:1909346.

Leor, J., Aboulafia-Etzion, S., Dar, A., Shapiro, L. I, Barbash, M., Battler, A., et al. (2000). Bioengineered cardiac grafts: a new approach to repair the infarcted myocardium? *Circulation* 102 (Suppl_3), III56–III61

Leychenko, A., Konorev, E., Jijiwa, M., and Matter, M. L. (2011). Stretch-induced hypertrophy activates NFkB-mediated VEGF secretion in adult cardiomyocytes. *PLoS One* 6:e29055. doi: 10.1371/journal.pone.0029055

Li, R.-K., Jia, Z.-Q., Weisel, R. D., Mickle, D. A., Choi, A., and Yau, T. M. (1999). Survival and function of bioengineered cardiac grafts. *Circulation* 100, (Suppl. 19):II63–II69.

Li, R.-K., Weisel, R. D., Mickle, D. A., Jia, Z.-Q., Kim, E.-J., Sakai, T., et al. (2000). Autologous porcine heart cell transplantation improved heart function after a myocardial infarction. *J. Thoracic Cardiovasc. Surg.* 119, 62–68.

Liu, Y.-W., Chen, B., Yang, X., Fugate, J. A., Kalucki, F. A., Futakuchi-Tsuchida, A., et al. (2018). Human embryonic stem cell–derived cardiomyocytes restore function in infarcted hearts of non-human primates. *Nat. Biotechnol.* 36, 597–605.

Lundy, S. D., Zhu, W.-Z., Regnier, M., and Laflamme, M. A. (2013). Structural and functional maturation of cardiomyocytes derived from human pluripotent stem cells. *Stem Cells Dev.* 22, 1991–2002.

Luz, A. L., and Tokar, E. J. (2018). Pluripotent stem cells in developmental toxicity testing: a review of methodological advances. *Toxicol. Sci.* 165, 31–39.

Machiraju, P., and Greenway, S. C. (2019). Current methods for the maturation of induced pluripotent stem cell-derived cardiomyocytes. *World J. Stem Cells* 11, 33–43.

MacNeil, S. (2007). Progress and opportunities for tissue-engineered skin. *Nature* 445, 874–880.

Maiullari, F., Costantini, M., Milan, M., Pace, V., Chirivì, M., Maiullari, S., et al. (2018). A multi-cellular 3D bioprinting approach for vascularized heart tissue engineering based on HUVECs and iPSC-derived cardiomyocytes. *Sci. Rep.* 8:13532.

Mandai, M., Watanabe, A., Kurimoto, Y., Hirami, Y., Morinaga, C., Daimon, T., et al. (2017). Autologous induced stem-cell–derived retinal cells for macular degeneration. *N. Engl. J. Med.* 376, 1038–1046.

Mannhardt, K., Breckwoldt, I., Letuffe-Brenière, D., Schaaf, S., Schulz, H., Neuber, C, et al. (2016). Human engineered heart tissue: analysis of contractile force. *Stem Cell Rep.* 7, 29–42.

Martin, G. R. (1981). Isolation of a pluripotent cell line from early mouse embryos cultured in medium conditioned by teratocarcinoma stem cells. *Proc. Natl. Acad. Sci. U.S.A.* 78, 7634–7638.

Martins, A. M., Eng, G., Caridade, S. G., Mano, J. O. F., Reis, R. L., and Vunjak-Novakovic, G. (2014). Electrically conductive chitosan/carbon scaffolds for cardiac tissue engineering. *Biomacromolecules* 15, 635–643.

Mason, T. O., and Shimanovich, U. (2018). Fibrous protein self-assembly in biomimetic materials. *Adv. Mater.* 30:e1706462.

Masumoto, H., Nakane, T., Tinney, J. P., Yuan, F., Ye, F., Kowalski, W. J., et al. (2016). The myocardial regenerative potential of three-dimensional engineered cardiac tissues composed of multiple human iPS cell-derived cardiovascular cell lineages. *Sci. Rep.* 6:29933.

Mattapally, S., Zhu, W., Fast, V. G., Gao, L., Worley, C., Kannappan, R., et al. (2018). Spheroids of cardiomyocytes derived from human-induced pluripotent stem cells improve recovery from myocardial injury in mice. *Ame. J. Physiol. -Heart Circ. Physiol.* 315, H327–H339.

Menasche, P., Alfieri, O., Janssens, S., McKenna, W., Reichenspurner, H., Trinquart, L., et al. (2008). The myoblast autologous grafting in ischemic cardiomyopathy (MAGIC) trial: first randomized placebo-controlled study of myoblast transplantation. *Circulation* 117, 1189–1200.

Menasché, P., Vanneaux, V., Hagège, A., Bel, A., Cholley, B., Cacciapuoti, I., et al. (2015). Human embryonic stem cell-derived cardiac progenitors for severe heart failure treatment: first clinical case report. *Eur. Heart J.* 36, 2011–2017.

Mills, R. J., Parker, B. L., Quaife-Ryan, G. A., Voges, H. K., Needham, E. J., Bornot, A., et al. (2019). Drug screening in human PSC-cardiac organoids identifies pro-proliferative compounds acting via the mevalonate pathway. *Cell Stem Cell* 24, 895–907. doi: 10.1016/j.stem.2019.03.009

Miyagi, Y., Chiu, L. L., Cimini, M., Weisel, R. D., Radisic, M., and Li, R.-K. (2011). Biodegradable collagen patch with covalently immobilized VEGF for myocardial repair. *Biomaterials* 32, 1280–1290.

Mohammadi , A. L., Massumi, M., Shamsara, M., Shabani, I., Amari, A., . Mossahebi , M., et al. (2017). Enhanced cardiac differentiation of human cardiovascular disease patient-specific induced pluripotent stem cells by applying unidirectional electrical pulses using aligned electroactive nanofibrous scaffolds. *ACS Appl. Mater. Interfaces* 9, 6849–6864.

Moorthi, A., Tyan, Y.-C., and Chung, T.-W. (2017). Surface-modified polymers for cardiac tissue engineering. *Biomater. Sci.* 5, 1976–1987.

Moretti, A., Bellin, M., Welling, A., Jung, C. B., Lam, J. T., Bott-Flugel, L., et al. (2010). Patient-specific induced pluripotent stem-cell models for long-QT syndrome. *N. Engl. J. Med.* 363, 1397–1409.

Muller, P., Lemcke, H., and David, R. (2018). Stem cell therapy in heart diseases - cell types, mechanisms and improvement strategies. *Cell Physiol. Biochem.* 48, 2607–2655.

Muraoka, N., Yamakawa, H., Miyamoto, K., Sadahiro, T., Umei, T., Isomi, M., et al. (2014). MiR-133 promotes cardiac reprogramming by directly repressing Snai1 and silencing fibroblast signatures. *EMBO J.* 33, 1565–1581.

Murphy, S. V., and Atala, A. (2014). 3D bioprinting of tissues and organs. *Nat. Biotechnol.* 32, 773–485.

Murry, C. E., Wiseman, R. W., Schwartz, S. M., and Hauschka, S. D. (1996). Skeletal myoblast transplantation for repair of myocardial necrosis. *J. Clin. Investiga.* 98, 2512–2523.

Nam, Y.-J., Song, K., Luo, X., Daniel, E., Lambeth, K., West, K., et al. (2013a). Reprogramming of human fibroblasts toward a cardiac fate. *Proc. NatL.Acad. Sci. U.S.A.*110, 5588–5593.

Nam, Y.-J., Song, K., and Olson, E. N. (2013b). Heart repair by cardiac reprogramming. *Nat. Med.* 19, 413–415.

Nelson, T. J., Martinez-Fernandez, A., Yamada, S., Perez-Terzic, C., Ikeda, Y., and Terzic, A. (2009). Repair of acute myocardial infarction by human stemness factors induced pluripotent stem cells. *Circulation* 120, 408–416.

Nguyen, A. H., Marsh, P., Schmiess-Heine, L., Burke, P. J., Lee, A., Lee, J., et al. (2019). Cardiac tissue engineering: state-of-the-art methods and outlook. *J. Biol. Eng.* 13:57.

Niknamasl, A., Ostad, S. N., Soleimani, M., Azami, M., Salmani, M. K., Lotfibakhshaiesh, N., et al. (2014). A new approach for pancreatic tissue engineering: human endometrial stem cells encapsulated in fibrin gel can differentiate to pancreatic islet beta-cell. *Cell Biol. Int.* 38, 1174–1182.

Nishizawa, M., Nozaki, H., Kaji, H., Kitazume, T., Kobayashi, N., Ishibashi, T., et al. (2007). Electrodeposition of anchored polypyrrole film on microelectrodes and stimulation of cultured cardiac myocytes. *Biomaterials* 28, 1480–1485.

Noor, N., Shapira, A., Edri, R., Gal, I., Wertheim, L., and Dvir, T. (2019). 3D printing of personalized thick and perfusable cardiac patches and hearts. *Adva. Sci.* 6:1900344.

Nunes, S. S., Miklas, J. W., Liu, J., Aschar-Sobbi, R., Xiao, Y., Zhang, B., et al. (2013). Biowire: a platform for maturation of human pluripotent stem cell–derived cardiomyocytes. *Nature methods* 10, 781–787.

Oh, H., Bradfute, S. B., Gallardo, T. D., Nakamura, T., Gaussin, V., Mishina, Y., et al. (2003). Cardiac progenitor cells from adult myocardium: homing, differentiation, and fusion after infarction. *Proc. NatL. Acad. Sci. U.S.A.*100, 12313–12318.

Ong, C. S., Nam, L., Ong, K., Krishnan, A., Huang, C. Y., Fukunishi, T., et al. (2018). 3D and 4D bioprinting of the myocardium: current approaches. Challenges, and Future Prospects. *Biomed. Res. Int.* 2018:6497242.

Orlova, V. V., Van Den Hil, F. E., Petrus-Reurer, S., Drabsch, Y., Ten Dijke, P., and Mummery, C. L. (2014). Generation, expansion and functional analysis of endothelial cells and pericytes derived from human pluripotent stem cells. *Nat. Protoc.* 9, 1514–1531.

Park, I. H., Zhao, R., West, J. A., Yabuuchi, A., Huo, H., Ince, T. A., et al. (2008). Reprogramming of human somatic cells to pluripotency with defined factors. *Nature* 451, 141–146.

Park, S.-J., Kim, R. Y., Park, B.-W., Lee, S., Choi, S. W., Park, J.-H., et al. (2019). Dual stem cell therapy synergistically improves cardiac function and vascular regeneration following myocardial infarction. *Nat. Commun.* 10, 1–12.

Pecha, S., Yorgan, K., Röhl, M., Geertz, B., Hansen, A., Weinberger, F., et al. (2019). Human iPS cell-derived engineered heart tissue does not affect ventricular arrhythmias in a guinea pig cryo-injury model. *Sci. Rep.* 9:9831.

Perea-Gil, C. I., Gálvez-Montón, S., Roura, A., Llucià-Valldeperas, C., Soler-Botija, A, et al. (2016). A cell-enriched engineered myocardial graft limits infarct size and improves cardiac function: pre-clinical study in the porcine myocardial infarction model. *JACC Basic Transl. Sci.* 1, 360–372.

Planat-Benard, V., Silvestre, J.-S., Cousin, B., André, M., Nibbelink, M., Tamarat, R., et al. (2004). Plasticity of human adipose lineage cells toward endothelial cells: physiological and therapeutic perspectives. *Circulation* 109, 656–663.

Polonchuk, L., Chabria, M., Badi, L., Hoflack, J.-C., Figtree, G., Davies, M. J., et al. (2017). Cardiac spheroids as promising in vitro models to study the human heart microenvironment. *Sci. Rep.* 7:7005.

Qian, L., Huang, Y., Spencer, C. I., Foley, A., Vedantham, V., Liu, L., et al. (2012). In vivo reprogramming of murine cardiac fibroblasts into induced cardiomyocytes. *Nature* 485, 593–598.

Ravichandran, R., Venugopal, J. R., Sundarrajan, S., Mukherjee, S., and Ramakrishna, S. (2013). Cardiogenic differentiation of mesenchymal stem cells on elastomeric poly (glycerol sebacate)/collagen core/shell fibers. *World J. Cardiol.* 5, 28–41.

Razak, A., Izwan, S. I, Wahab, F., Fadil, F., Dahli, F. N., Khudzari, M., et al. (2015). A review of electrospun conductive polyaniline based nanofiber composites and blends: processing features, applications, and future directions. *Adv. Mater. Scie. Engi.* 2015, 1–19.

Redd, M. A., Zeinstra, N., Qin, W., Wei, W., Martinson, A., Wang, Y., et al. (2019). Patterned human microvascular grafts enable rapid vascularization and increase perfusion in infarcted rat hearts. *Nat. Commun.* 10:584.

Rehman, J., Traktuev, D., Li, J., Merfeld-Clauss, S., Temm-Grove, C. J., Bovenkerk, J. E., et al. (2004). Secretion of angiogenic and antiapoptotic factors by human adipose stromal cells. *Circulation* 109, 1292–1298.

Richards, D. J., Coyle, R. C., Tan, Y., Jia, J., Wong, K., Toomer, K., et al. (2017). Inspiration from heart development: biomimetic development of functional human cardiac organoids. *Biomaterials* 142, 112–123.

Richardson-Burns, S. M., Hendricks, J. L., Foster, B., Povlich, L. K., Kim D.-H., and Martin D. C. (2007). Polymerization of the conducting polymer poly (3, 4-ethylenedioxythiophene)(PEDOT) around living neural cells. *Biomaterials* 28, 1539–1552. doi: 10.1016/j.biomaterials.2006.11.026

Risbud, M., Ringe, J., Bhonde, R., and Sittinger, M. (2001). In vitro expression of cartilage-specific markers by chondrocytes on a biocompatible hydrogel: implications for engineering cartilage tissue. *Cell Transplant.* 10, 755–763.

Rojas, S. V., Kensah, G., Rotaermel, A., Baraki, H., Kutschka, I., Zweigerdt, R., et al. (2017). Transplantation of purified iPSC-derived cardiomyocytes in myocardial infarction. *PLoS One* 12:e0173222. doi: 10.1371/journal.pone.0173222

Ronaldson-Bouchard, K., Ma, S. P., Yeager, K., Chen, T., Song, L., Sirabella, D., et al. (2018). Advanced maturation of human cardiac tissue grown from pluripotent stem cells. *Nature* 556, 239–243.

Roshanbinfar, K., Mohammadi, Z., Mesgar, A. S.-M., Dehghan, M. M., Oommen, O. P., Hilborn, J., et al. (2019). Carbon nanotube doped pericardial matrix derived electroconductive biohybrid hydrogel for cardiac tissue engineering. *Biomat. Sci.* 7, 3906–3917. doi: 10.1039/C9BM00434C

Roshanbinfar, K., Vogt, L., Greber, B., Diecke, S., Boccaccini, A. R., Scheibel, T., et al. (2018). Electroconductive biohybrid hydrogel for enhanced maturation and beating properties of engineered cardiac tissues. *Adv. Func. Mater.* 28:1803951.

Roshanbinfar, K., Vogt, L., Ruther, F., Roether, J. A., Boccaccini, A. R., and Engel, F. B. (2020). Nanofibrous composite with tailorable electrical and mechanical properties for cardiac tissue engineering. *Adv. Func. Mater.* 30:1908612. doi: 10.1002/adfm.201908612

Salvarani, N., Crasto, S., Miragoli, M., Bertero, A., Paulis, M., Kunderfranco, P., et al. (2019). The K219T-lamin mutation induces conduction defects through epigenetic inhibition of SCN5A in human cardiac laminopathy. *Nat. Commun.* 10:2267. doi: 10.1371/journal.pone.0173222

Sánchez, L. A., Guerrero-Beltrán, C. E., Cordero-Reyes, A. M., García-Rivas, G., and Torre-Amione, G. (2013). Use of stem cells in heart failure treatment: where we stand and where we are going. *Method.DeBakey Cardiovasc. J.* 9, 195–200.

Sartiani, L., Bettiol, E., Stillitano, F., Mugelli, A., Cerbai, E., and Jaconi, M. E. (2007). Developmental changes in cardiomyocytes differentiated from human embryonic stem cells: a molecular and electrophysiological approach. *Stem Cell*25, 1136–1144.

Sato, T., Vries, R. G., Snippert, H. J., Van De Wetering, M., Barker, N., Stange, D. E., et al. (2009). Single Lgr5 stem cells build crypt–villus structures in vitro without a mesenchymal niche. *Nature* 459, 262–265.

Sawa, Y., Miyagawa, S., Sakaguchi, T., Fujita, T., Matsuyama, A., Saito, A., et al. (2012). Tissue engineered myoblast sheets improved cardiac function sufficiently to discontinue LVAS in a patient with DCM: report of a case. *Surg. Today* 42, 181–184.

Schaaf, S., Shibamiya, A., Mewe, M., Eder, A., Stöhr, A., Hirt, M. N., et al. (2011). Human engineered heart tissue as a versatile tool in basic research and preclinical toxicology. *PLoS One* 6:e26397. doi: 10.1371/journal.pone.0026397

Scuderi, G. J., and Butcher, J. (2017). Naturally engineered maturation of cardiomyocytes. *Front. Cell Dev. Biol.* 5:50. doi: 10.3389/fcell.2017.00050

Selvaraj, S., Mondragon-Gonzalez, R., Xu, B., Magli, A., Kim, H., Lainé, J., et al. (2019). Screening identifies small molecules that enhance the maturation of human pluripotent stem cell-derived myotubes. *eLife* 8:e47970. doi: 10.7554/eLife.47970

Sepulveda, P., Jones, J. R., and Hench, L. L. (2002). Bioactive sol-gel foams for tissue repair. *J. Biomed. Mater. Res.* 59, 340–348.

Shen, D., Wang, X., Zhang, L., Zhao, X., Li, J., Cheng, K., et al. (2011). The amelioration of cardiac dysfunction after myocardial infarction by the injection of keratin biomaterials derived from human hair. *Biomaterials* 32, 9290–9299.

Shi, C., Li, Q., Zhao, Y., Chen, W., Chen, B., Xiao, Z., et al. (2011). Stem-cell-capturing collagen scaffold promotes cardiac tissue regeneration. *Biomaterials* 32, 2508–2515.

Shiba, Y., Gomibuchi, T., Seto, T., Wada, Y., Ichimura, H., Tanaka, Y., et al. (2016). Allogeneic transplantation of iPS cell-derived cardiomyocytes regenerates primate hearts. *Nature* 538, 388–391.

Shimizu, T., Sekine, H. Isoi, Y. Yamato, M. Kikuchi A. and Okano T. (2006). Long-term survival and growth of pulsatile myocardial tissue grafts engineered by the layering of cardiomyocyte sheets. *Tissue Eng.* 12, 499–507. doi: 10.1089/ten.2006.12.499

Shin, S. R., Aghaei-Ghareh-Bolagh, B., Gao, X., Nikkhah, M., Jung, S. M., Dolatshahi-Pirouz, A., et al. (2014). Layer-by-layer assembly of 3D tissue constructs with functionalized graphene. *Adv. Funct. Mater.* 24, 6136–6144.

Singelyn, J. M., Sundaramurthy, P., Johnson, T. D., Schup-Magoffin, P. J., Hu, D. P., Faulk, D. M., et al. (2012). Catheter-deliverable hydrogel derived from decellularized ventricular extracellular matrix increases endogenous cardiomyocytes and preserves cardiac function post-myocardial infarction. *J. Am. Coll. Cardiol.* 59, 751–763.

Sinha, S. K., Noh, Y., Reljin, N., Treich, G. M., Hajeb-Mohammadalipour, S., Guo, Y., et al. (2017). Screen-printed PEDOT: PSS electrodes on commercial finished textiles for electrocardiography. *ACS Appl. Mater. Interfaces* 9, 37524–37528.

Soonpaa, M. H., Koh, G. Y., Klug, M. G., and Field, L. J. (1994). Formation of nascent intercalated disks between grafted fetal cardiomyocytes and host myocardium. *Science* 264, 98–101.

Spang, M. T., and Christman, K. L. (2018). Extracellular matrix hydrogel therapies: *in vivo* applications and development. *Acta Biomater.* 68, 1–14. doi: 10.1016/j.actbio.2017.12.019

Stevens, K. R., Pabon, L., Muskheli, V., and Murry, C. E. (2009). Scaffold-free human cardiac tissue patch created from embryonic stem cells. *Tissue Eng. Part A* 15, 1211–1222.

Stone, N. R., Gifford, C. A., Thomas, R., Pratt, K. J., Samse-Knapp, K., Mohamed, T. M., et al. (2019). Context-specific transcription factor functions regulate epigenomic and transcriptional dynamics during cardiac reprogramming. *Cell Stem Cell* 25, 87.–102.

Sugiura, T., Hibino, N., Breuer, C. K., and Shinoka, T. (2016). Tissue-engineered cardiac patch seeded with human induced pluripotent stem cell derived cardiomyocytes promoted the regeneration of host cardiomyocytes in a rat model. *J. Cardiothor. Surg.* 11:163.

Sun, N., Yazawa, M., Liu, J., Han, L., Sanchez-Freire, V., Abilez, O. J., et al. (2012). Patient-specific induced pluripotent stem cells as a model for familial dilated cardiomyopathy. *Sci. Transl. Med.* 4:130ra147.

Sun, Q., Zhang, Z., and Sun, Z. (2014). The potential and challenges of using stem cells for cardiovascular repair and regeneration. *Genes Dis.* 1, 113–119.

Sutherland, R. M., McCredie, J. A., and Inch, W. R. (1971). Growth of multicell spheroids in tissue culture as a model of nodular carcinomas2. *J. Natl. Cancer Inst.* 46, 113–120.

Takahashi, K., Tanabe, K., Ohnuki, M., Narita, M., Ichisaka, T., Tomoda, K., et al. (2007). Induction of pluripotent stem cells from adult human fibroblasts by defined factors. *Cell* 131, 861–872.

Takahashi, K., and Yamanaka, S. (2006). Induction of pluripotent stem cells from mouse embryonic and adult fibroblast cultures by defined factors. *Cell* 126, 663–676.

Takasato, M., Er, P. X., Chiu, H. S., Maier, B., Baillie, G. J., Ferguson, C., et al. (2015). Kidney organoids from human iPS cells contain multiple lineages and model human nephrogenesis. *Nature* 526, 564–568.

Talman, V., and Ruskoaho, H. (2016). Cardiac fibrosis in myocardial infarction-from repair and remodeling to regeneration. *Cell Tissue Res.* 365, 563–581.

Tan, Y., Richards, D., Coyle, R. C., Yao, J., Xu, R., Gou, W., et al. (2017). Cell number per spheroid and electrical conductivity of nanowires influence the function of silicon nanowired human cardiac spheroids. *Acta Biomater.* 51, 495–504.

Taylor, D. A. (2004). Cell-based myocardial repair: how should we proceed? *Int. J. Cardiol.* 95, S8–S12.

Thomson, J. A., Itskovitz-Eldor, J., Shapiro, S. S., Waknitz, M. A., Swiergiel, J. J., Marshall, V. S., et al. (1998). Embryonic stem cell lines derived from human blastocysts. *Science* 282, 1145–1147.

Thygesen, K., Alpert, J. S., White, H. D., Jaffe, A. S., Apple, F. S., Galvani, M., et al. (2007). Universal definition of myocardial infarction. *Circulation* 116, 2634–2653.

Tian, Y., Liu, Y., Wang, T., Zhou, N., Kong, J., Chen, L., et al. (2015). A microRNA-Hippo pathway that promotes cardiomyocyte proliferation and cardiac regeneration in mice. *Sci. Transl. Med.* 7:279ra238.

Tiburcy, M., Hudson, J. E., Balfanz, P., Schlick, S., Meyer, T., Chang Liao, M.-L., et al. (2017). Defined engineered human myocardium with advanced maturation for applications in heart failure modeling and repair. *Circulation* 135, 1832–1847.

Traverse, J. H., Henry, T. D., Dib, N., Patel, A. N., Pepine, C., Schaer, G. L., et al. (2019). First-in-man study of a cardiac extracellular matrix hydrogel in early and late myocardial infarction patients. *Basic Transl. Sci.* 4, 659–669.

Traverse, J. H., Henry, T. D., Pepine, C. J., Willerson, J. T., and Ellis, S. G. (2014). One-year follow-up of intracoronary stem cell delivery on left ventricular function following ST-elevation myocardial infarction. *JAMA* 311, 301–302.

Tsui, J. H., Leonard, A., Camp, N. D., Long, J. T., Nawas, Z. Y., Chavanachat, R., et al. (2019). Functional maturation of human iPSC-based cardiac microphysiological systems with tunable electroconductive decellularized extracellular matrices. *bioRxiv* [preprint]. doi: 10.1101/786657

Tulloch, N. L., Muskheli, V., Razumova, M. V., Korte, F. S., Regnier, M., Hauch, K. D., et al. (2011). Growth of engineered human myocardium with mechanical loading and vascular coculture. *Circ. Res.* 109, 47–59.

Ulmer, B. M., Stoehr, A., Schulze, M. L., Patel, S., Gucek, M., Mannhardt, I., et al. (2018). Contractile work contributes to maturation of energy metabolism in hiPSC-derived cardiomyocytes. *Stem Cell Rep.* 10, 834–847.

Vacanti, J. P., and Langer, R. (1999). Tissue engineering: the design and fabrication of living replacement devices for surgical reconstruction and transplantation. *Lancet* 354, S32–S34.

Vallée, J.-P., Hauwel, M., Lepetit-Coiffé, M., Bei, W., Montet-Abou, K., Meda, P., et al. (2012). Embryonic stem cell-based cardiopatches improve cardiac function in infarcted rats. *Stem Cells Transl. Med.* 1, 248–260.

van Laake, L. W., Passier, R., Doevendans, P. A., and Mummery, C. L. (2008). Human embryonic stem cell-derived cardiomyocytes and cardiac repair in rodents. *Circ. Res.* 102, 1008–1010.

van Laake, L. W., Passier, R., Monshouwer-Kloots, J., Verkleij, A. J., Lips, D. J., Freund, C., et al. (2007). Human embryonic stem cell-derived cardiomyocytes survive and mature in the mouse heart and transiently improve function after myocardial infarction. *Stem Cell Res.* 1, 9–24.

Van Vlierberghe, S., Dubruel, P., and Schacht, E. (2011). Biopolymer-based hydrogels as scaffolds for tissue engineering applications: a review. *Biomacromolecules* 12, 1387–1408.

Vukicevic, M., Mosadegh, B., Min, J. K., and Little, S. H. (2017). Cardiac 3D printing and its future directions. *Cardiovas. Imaging* 10, 171–184.

Wada, R., Muraoka, N., Inagawa, K., Yamakawa, H., Miyamoto, K., Sadahiro, T., et al. (2013). Induction of human cardiomyocyte-like cells from fibroblasts by defined factors. *Proc. Natl. Acad. Sci. U.S.A.*110, 12667–12672.

Wang, L., Jiang, J., Hua, W., Darabi, A., Song, X., Song, C., et al. (2016). Mussel-inspired conductive cryogel as cardiac tissue patch to repair myocardial infarction by migration of conductive nanoparticles. *Adv. Func. Mater.* 26, 4293–4305.

Wang, L., Wu, Y., Hu, T., Guo, B., and Ma, P. X. (2017). Electrospun conductive nanofibrous scaffolds for engineering cardiac tissue and 3D bioactuators. *Acta Biomater.* 59, 68–81.

Weinberger, F., Breckwoldt, K., Pecha, S., Kelly, A., Geertz, B., Starbatty, J., et al. (2016). Cardiac repair in guinea pigs with human engineered heart tissue from induced pluripotent stem cells. *Sci. Transl. Med.* 8:363ra148.

Wendel, J. S., Ye, L., Tao, R., Zhang, J., Zhang, J., Kamp, T. J., et al. (2015). Functional effects of a tissue-engineered cardiac patch from human induced pluripotent stem cell-derived cardiomyocytes in a rat infarct model. *Stem Cells Transl. Med.* 4, 1324–1332.

Wendel, J. S., Ye, L., Zhang, P., Tranquillo, R. T., and Zhang, J. J. (2014). Functional consequences of a tissue-engineered myocardial patch for cardiac repair in a rat infarct model. *Tissue Eng. Part A* 20, 1325–1335.

Wickham, A., Vagin, M., Khalaf, H., Bertazzo, S., Hodder, P., Dånmark, S., et al. (2016). Electroactive biomimetic collagen-silver nanowire composite scaffolds. *Nanoscale* 8, 14146–14155.

Wimmer, R. A., Leopoldi, A., Aichinger, M., Wick, N., Hantusch, B., Novatchkova, M., et al. (2019). Human blood vessel organoids as a model of diabetic vasculopathy. *Nature* 565, 505–510.

Witman, N., and Sahara, M. (2018). Cardiac progenitor cells in basic biology and regenerative medicine. *Stem Cells Int.* 2018, 1–9.

Xie, C.-Q., Huang, H., Wei, S., Song, L.-S., Zhang, J., Ritchie, R. P., et al. (2008). A comparison of murine smooth muscle cells generated from embryonic versus induced pluripotent stem cells. *Stem Cells Dev.* 18, 741–748.

Yan, Y., Bejoy, J., Xia, J., Griffin, K., Guan, J., and Li, Y. (2019). Cell population balance of cardiovascular spheroids derived from human induced pluripotent stem cells. *Sci. Rep.* 9:1295.

Yang, X., Rodriguez, M., Pabon, L., Fischer, K. A., Reinecke, H., Regnier, M., et al. (2014). Tri-iodo-l-thyronine promotes the maturation of human cardiomyocytes-derived from induced pluripotent stem cells. *J. Mol. Cell Cardiol.* 72, 296–304.

Ye, L., Chang, Y. H., Xiong, Q., Zhang, P., Zhang, L., Somasundaram, P., et al. (2014). Cardiac repair in a porcine model of acute myocardial infarction with human induced pluripotent stem cell-derived cardiovascular cells. *Cell Stem Cell* 15, 750–761.

Yoon, S. J., Fang, Y. H., Lim, C. H., Kim, B. S., Son, H. S., Park, Y., et al. (2009). Regeneration of ischemic heart using hyaluronic acid-based injectable hydrogel. *J. Biomed. Mater. Res. Part B Appl. Biomater.* 91, 163–171.

Yoon, S. J., Hong, S., Fang, Y. H., Song, M., Son, K. H., Son, H. S., et al. (2014). Differential regeneration of myocardial infarction depending on the progression of disease and the composition of biomimetic hydrogel. *J. Biosci. Bioeng.* 118, 461–468. doi: 10.1016/j.jbiosc.2014.04.001

Yoshida, S., Miyagawa, S., Fukushima, S., Kawamura, T., Kashiyama, N., Ohashi, F., et al. (2018). Maturation of human induced pluripotent stem cell-derived cardiomyocytes by soluble factors from human mesenchymal stem cells. *Mol. Ther.* 26, 2681–2695.

Yoshida, Y., and Yamanaka, S. (2010). Recent stem cell advances: induced pluripotent stem cells for disease modeling and stem cell-based regeneration. *Circulation* 122, 80–87.

Yu, J., Vodyanik, M. A., Smuga-Otto, K., Antosiewicz-Bourget, J., Frane, J. L., Tian, S., et al. (2007). Induced pluripotent stem cell lines derived from human somatic cells. *Science* 318, 1917–1920.

Zhang, J., Tao, R., Campbell, K. F., Carvalho, J. L., Ruiz, E. C., Kim, G. C., et al. (2019). Functional cardiac fibroblasts derived from human pluripotent stem cells via second heart field progenitors. *Nat. Commun.* 10, 1–15.

Zhou, J., Chen, J., Sun, H., Qiu, X., Mou, Y., Liu, Z., et al. (2014). Engineering the heart: evaluation of conductive nanomaterials for improving implant integration and cardiac function. *Sci. Rep.* 4:3733. doi: 10.1038/srep03733

Zhu, K., Shin, S. R., van Kempen, T., Li, Y. C., Ponraj, V., Nasajpour, A., et al. (2017). Gold nanocomposite bioink for printing 3D cardiac constructs. *Adv. Func. Mater.* 27:1605352.

Zhu, K., Wu, Q., Ni, C., Zhang, P., Zhong, Z., Wu, Y., et al. (2018). Lack of remuscularization following transplantation of human embryonic stem cell-derived cardiovascular progenitor cells in infarcted nonhuman primates. *Circ. Res.* 122, 958–969.

Zhu, W., Zhao, M., Mattapally, S., Chen, S., and Zhang, J. (2018). CCND2 overexpression enhances the regenerative potency of human induced pluripotent stem cell–derived cardiomyocytes: remuscularization of injured ventricle. *Circ. Res.* 122, 88–96.

Zimmermann, W. H., Fink, C., Kralisch, D., Remmers, U., Weil, J., and Eschenhagen, T. (2000). Three-dimensional engineered heart tissue from neonatal rat cardiac myocytes. *Biotechnol. Bioeng.* 68, 106–114.

Zimmermann, W.-H., Schneiderbanger, K., Schubert, P., Didie, M., Munzel, F., Heubach, J., et al. (2002). Tissue engineering of a differentiated cardiac muscle construct. *Circ. Res.* 90, 223–230.

Zwi-Dantsis, L., Huber, I., Habib, M., Winterstern, A., Gepstein, A., Arbel, G, et al. (2013). Derivation and cardiomyocyte differentiation of induced pluripotent stem cells from heart failure patients. *Eur. Heart J.* 34, 1575–1586.

Conflict of Interest: The authors declare that the research was conducted in the absence of any commercial or financial relationships that could be construed as a potential conflict of interest.

Copyright © 2020 Mazzola and Di Pasquale. This is an open-access article distributed under the terms of the Creative Commons Attribution License (CC BY). The use, distribution or reproduction in other forums is permitted, provided the original author(s) and the copyright owner(s) are credited and that the original publication in this journal is cited, in accordance with accepted academic practice. No use, distribution or reproduction is permitted which does not comply with these terms.

frontiers in Bioengineering and Biotechnology

ORIGINAL RESEARCH
published: 29 May 2020
doi: 10.3389/fbioe.2020.00520

Molecular and Biomechanical Clues From Cardiac Tissue Decellularized Extracellular Matrix Drive Stromal Cell Plasticity

Gabriel Romero Liguori[1,2†], Tácia Tavares Aquinas Liguori[1,2†], Sérgio Rodrigues de Moraes[2], Viktor Sinkunas[2], Vincenzo Terlizzi[1], Joris A. van Dongen[1], Prashant K. Sharma[3], Luiz Felipe Pinho Moreira[2] and Martin Conrad Harmsen[1]*

[1] Department of Pathology and Medical Biology, University Medical Center Groningen, University of Groningen, Groningen, Netherlands, [2] Instituto do Coração (InCor), Hospital das Clinicas HCFMUSP, Faculdade de Medicina, Universidade de São Paulo, São Paulo, Brazil, [3] Department of Biomedical Engineering, University Medical Center Groningen, University of Groningen, Groningen, Netherlands

OPEN ACCESS

Edited by:
Valeria Chiono,
Polytechnic University of Turin, Italy

Reviewed by:
Ahmed El-Fiqi,
Dankook University, South Korea
Mohamed Ghorbel,
University of Bristol, United Kingdom

***Correspondence:**
Martin Conrad Harmsen
m.c.harmsen@umcg.nl

[†] These authors have contributed equally to this work

Specialty section:
This article was submitted to Biomaterials, a section of the journal Frontiers in Bioengineering and Biotechnology

Received: 20 October 2019
Accepted: 01 May 2020
Published: 29 May 2020

Citation:
Liguori GR, Liguori TTA, de Moraes SR, Sinkunas V, Terlizzi V, van Dongen JA, Sharma PK, Moreira LFP and Harmsen MC (2020) Molecular and Biomechanical Clues From Cardiac Tissue Decellularized Extracellular Matrix Drive Stromal Cell Plasticity. Front. Bioeng. Biotechnol. 8:520. doi: 10.3389/fbioe.2020.00520

Decellularized-organ-derived extracellular matrix (dECM) has been used for many years in tissue engineering and regenerative medicine. The manufacturing of hydrogels from dECM allows to make use of the pro-regenerative properties of the ECM and, simultaneously, to shape the material in any necessary way. The objective of the present project was to investigate differences between cardiovascular tissues (left ventricle, mitral valve, and aorta) with respect to generating dECM hydrogels and their interaction with cells in 2D and 3D. The left ventricle, mitral valve, and aorta of porcine hearts were decellularized using a series of detergent treatments (SDS, Triton-X 100 and deoxycholate). Mass spectrometry-based proteomics yielded the ECM proteins composition of the dECM. The dECM was digested with pepsin and resuspended in PBS (pH 7.4). Upon warming to 37°C, the suspension turns into a gel. Hydrogel stiffness was determined for samples with a dECM concentration of 20 mg/mL. Adipose tissue-derived stromal cells (ASC) and a combination of ASC with human pulmonary microvascular endothelial cells (HPMVEC) were cultured, respectively, on and in hydrogels to analyze cellular plasticity in 2D and vascular network formation in 3D. Differentiation of ASC was induced with 10 ng/mL of TGF-β1 and SM22α used as differentiation marker. 3D vascular network formation was evaluated with confocal microscopy after immunofluorescent staining of PECAM-1. In dECM, the most abundant protein was collagen VI for the left ventricle and mitral valve and elastin for the aorta. The stiffness of the hydrogel derived from the aorta (6,998 ± 895 Pa) was significantly higher than those derived from the left ventricle (3,384 ± 698 Pa) and the mitral valve (3,233 ± 323 Pa) (One-way ANOVA, $p = 0.0008$). Aorta-derived dECM hydrogel drove non-induced (without TGF-β1) differentiation, while hydrogels derived from the left ventricle and mitral valve inhibited TGF-β1-induced differentiation. All hydrogels supported vascular network formation within 7 days of culture, but ventricular dECM hydrogel demonstrated more

robust vascular networks, with thicker and longer vascular structures. All the three main cardiovascular tissues, myocardium, valves, and large arteries, could be used to fabricate hydrogels from dECM, and these showed an origin-dependent influence on ASC differentiation and vascular network formation.

Keywords: hydrogels, extracellular matrix proteins, tissue engineering, regenerative medicine, biocompatible materials, biomimetic materials, tissue scaffolds, tissue decellularization

INTRODUCTION

Decellularized organ-derived extracellular matrix (dECM) has been used for many years in tissue engineering and regenerative medicine (Conklin et al., 2002; Dahl et al., 2003; Schenke-Layland et al., 2003). Decellularization of the extracellular matrix can be achieved through different physical, chemical or biological processes, including freeze/thaw cycles, use of organic detergents, and mild treatment with proteolytic enzymes (Crapo et al., 2011; Hrebikova et al., 2015; Keane et al., 2015; Leonel et al., 2017; Kawecki et al., 2018). Commonly, different processes are combined or used sequentially, so as to decrease the damage caused by each of them to the extracellular matrix but, at the same time, to potentiate the decellularization protocol (Crapo et al., 2011; Kawecki et al., 2018). In dECM, both the structure and biochemical composition of the original tissue are largely retained which renders dECM a promising candidate for cell culture and tissue engineering (Hoshiba et al., 2010, 2016; Cigliano et al., 2012; Petersen et al., 2012; Poornejad et al., 2016). Also, regeneration-related processes such as recruitment of progenitor cells, induction of cell migration and proliferation, and M2 polarization of in macrophages appear to occur upon *in vivo* administration of dECM (Reing et al., 2009; Agrawal et al., 2011; Brown and Badylak, 2014; Dziki et al., 2017). In general, the large(r) macromolecules of ECM such as polysaccharides (glycosaminoglycans and proteoglycans) as well as constructive proteins (collagens, basement membrane proteins, and fibronectin to mention a few) remain after decellularization because of their size and their intermolecular crosslinks. Smaller ECM constituents such as growth factors, chemokines, and other small signaling molecules are largely washed out.

Originally, decellularization of whole organs was intended to reseed stem cells or parenchymal cells to recreate the organ. More recently, clinical interest shifted to use dECM, as powder or as hydrogel, for repair and regeneration purposes of organ damage more than as replacement therapy (Adam Young et al., 2011; Wolf et al., 2012; Mercuri et al., 2013; Fu et al., 2016; Ungerleider et al., 2016; Saldin et al., 2017). Hydrogels derived from dECM are tuneable with respect to biochemical parameters via loading with growth factors, stem cells while their physical parameters such as stiffness and viscoelasticity are tuneable too (Adam Young et al., 2011; DeQuach et al., 2012; Seif-Naraghi et al., 2012; Ungerleider et al., 2015; Wu et al., 2015). The use of 3D bioprinting, though in its infancy with dECM-derived hydrogels, enables to print predetermined shapes and geometries of factor and cell-loaded gels.

Traditionally, cardiovascular tissue engineering has focused on replacement tissue for coronary arteries, cardiac valves as well as left ventricular myocardium with no definitive success for any of these three (Singelyn et al., 2009, 2012; Seif-Naraghi et al., 2010, 2012; Duan et al., 2011; Johnson et al., 2011, 2014; O'Neill et al., 2013; Grover et al., 2014; Pok et al., 2014; Russo et al., 2015; Ungerleider et al., 2015, 2016; Kappler et al., 2016; Stoppel et al., 2016; Wassenaar et al., 2016a,b; Efraim et al., 2017; Fercana et al., 2017; Jang et al., 2017; Wang et al., 2017; Seo et al., 2018). Most of these efforts used collagen or single ECM molecule-based scaffolds besides a host of synthetic polymer materials. We reasoned that regeneration of damaged specific cardiac compartments (myocardium, valve, or arteries) would benefit from the use of dECM hydrogels derived from that same compartment. In other words, we hypothesized that dECM-derived hydrogels from myocardium, valves, and aorta would differ in biological and physical features.

METHODS

An illustrative overview of the methods used for the fabrication of dECM-derived hydrogels is presented in **Figure 1**. Detailed description is described below.

Extracellular Matrix Decellularization and Characterization

Decellularization Protocol

Porcine hearts (12-week old pigs) were bought from a local slaughterhouse (Kroon Vlees, Groningen, Netherlands) and dissected to separate the left myocardial tissue, the mitral valve, and the aorta. The tissues were washed at room temperature (RT) in phosphate buffer saline (PBS) and triturated in a commercial blender until pieces were smaller than 1 mm. Following a second wash in PBS, tissue material was sonicated for 1 min at 100% power, washed a third time and incubated in 0.05% trypsin (Gibco, Thermo Fisher Scientific, Waltham, USA) in PBS at 37°C for 3 h under constant shaking. After trypsin treatment, tissue material was washed again with PBS and frozen at −20°C overnight. After thawing, tissue material was incubated in demineralized water (dH_2O) for 3 h and then in saturated sodium chloride solution (NaCl, 6M) for another 3 h, both steps at 37°C while shaking continuously. This followed by a wash with 70% ethanol for 10 min and dH_2O for another 10 min. Afterwards, tissue material treated with 1% sodium dodecyl sulfate (SDS) (Sigma-Aldrich, St. Louis, USA) in water for 12 h, washed three times with dH_2O, incubated with 1% Triton X-100 (Sigma-Aldrich, St. Louis, USA) in water for 12 h, washed three times with dH_2O, incubated with 1% sodium deoxycholate (Sigma-Aldrich, St. Louis, USA) in water for 12 h and, again, washed three times with dH_2O, all steps while shaking

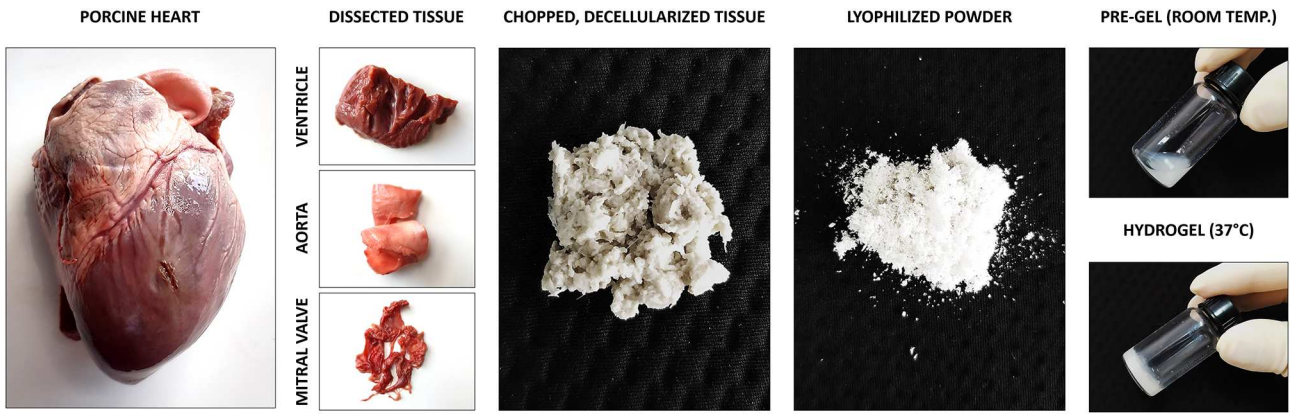

FIGURE 1 | Illustrative overview of the methods used to produce hydrogels derived from decellularized extracellular matrix.

continuously. After these detergent treatments, tissue material was incubated for 24 h with DNAse solution [30 μg/ml DNAse (Worthington Biochemical Corporation, Lakewood, USA), 1.3 mM $MgSO_4$, 2 mM $CaCl_2$] at 37°C and continuous shaking. After DNAse treatment, the decellularized tissue remainder i.e., extracellular matrix (dECM) was washed three times with dH_2O and stored at 4°C in 1% penicillin/streptomycin (#15140122, Gibco Invitrogen, Carlsbad, USA) in sterile PBS.

The dECM characterization was comprised of quantification of residual nuclei, genomic DNA, histochemical stainings (Hematoxylin/Eosin and Movat's Pentachrome), quantification of GAG contents and identification of proteins by mass spectrometry.

Residual Nuclei and DNA Quantification

For evaluating residual nuclei, native and dECM samples were stained with 4′,6-diamidino-2-phenylindole (DAPI) (4 μg/ml; #D9542-5MG, blue; Sigma-Aldrich, St. Louis, USA) and visualized with an Evos FL fluorescence microscope system (Thermo Fisher Scientific, Waltham, United States).

To isolate genomic DNA freeze-dried native and dECM samples ($n = 3$) were weighed and separated as samples of 10–15 mg in a 1.5 mL microfuge tube. Each sample was digested at 55°C in a solution containing 5 μL proteinase K (#3115828001, Roche, Basel, Switzerland), 50 μL 10% SDS, and 500 μL SE-buffer (75 mM NaCl; 25 mM EDTA; pH 8.0) overnight. Following the enzymatic digestion, 222 μL of 6 M NaCl and 777 μL chloroform were added and samples thoroughly shaken on a top-over-top rotator at room temperature (RT) for 1 h and centrifuged at 10,000 × g at 20°C for 10 min. After centrifugation, the upper layer was transferred to a new tube, and an equal volume of ice-cold isopropanol was added and gently mixed until DNA precipitated (if any). The DNA was collected by centrifugation at 10,000 × g at 4°C for 15 min. The DNA pellet was washed with 0.5 mL ice-cold 70% ethanol centrifuged at 10,000 × g at 4°C for 5 min. Upon removal of the supernatant, the pellet was left to air-dry in RT. The DNA was dissolved in 100 μL 10 mM Tris, 0.1 mM EDTA, pH 8.0 at 55°C and quantified with NanoDrop equipment (Thermo Scientific, Hemel Hempstead, United Kingdom).

Histochemical Analysis

For histochemical stainings, samples of native and dECM were fixed with 4% paraformaldehyde (PFA) in PBS for 1 h, washed with PBS twice, and embedded in paraffin. Five micrometer sections were mounted on glass microscope slides, deparaffinized, stained with Hematoxylin/Eosin (HE) or Movat's pentachrome stain, mounted with mounting medium and visualized with a light microscope (DM IL, Leica Microsystems, Wetzlar, Germany). All samples were stained simultaneously to rule out the influence of staining variations among groups.

GAG Quantification

The concentration of sulfated glycosaminoglycans (sGAG) was measured using the 1,9-dimethylmethylene blue (DMMB) assay, according to the protocol of Farndale et al. (1982). Briefly, dECM samples ($n = 3$) were weighed and separated as samples of 10–15 mg in a 1.5 mL microfuge tube. Each sample was digested at 55°C in a solution containing 5 μL proteinase K (#3115828001, Roche, Basel, Switzerland), 50 μL 10% SDS, and 500 μL SE-buffer (75 mM NaCl; 25 mM EDTA; pH 8.0) overnight. After digestion, DMMB staining solution (10:1 to the initial volume) was added to the samples and excitation was measured at 525 nm and 595 nm using a spectrophotometer. A titration curve of serially diluted chondroitin sulfate C (#C4384-250 mg, Sigma-Aldrich, St. Louis, USA) was used as control.

Mass Spectrometry

Samples ($n = 3$) of dECM from the three different types of cardiovascular tissue, resp. the left ventricle, mitral valve, and aorta, were submitted to mass spectrometry analyses to determine the protein composition in the decellularized tissue. Lyophilized dECM was milled to a fine powder and digested in pepsin (#P6887; >3,200 IU; Sigma-Aldrich, St. Louis, USA) solution. The digested solution was ultrafiltrated using

centrifugal filter units (Millipore, Billerica, USA) to remove undigested tissue debris. Liquid chromatography-tandem mass spectrometry (LC-MS/MS) analysis was performed using an integrated system composed of nano-LC (Tempo nano-LC system, MDS SCIEX, Ontario, Canada) and a Quadrupole-TOF MS/MS spectrometer (QStar Elite, Applied Biosystems, Foster City, USA) equipped with a nano-electrospray ionization source at an ion spray voltage of 2.3 keV. Solutions containing pepsin-digested protein fragments were injected into the nano-LC-MS/MS system and then separated on a Zorbax 300SB-C18 capillary column (Agilent Technologies, Palo Alto, USA). The loaded samples were eluted with a 2–35% gradient of solvent B for 30 min, then a 35–90% gradient for 10 min, followed by 90% solvent B for 5 min, and finally 5% solvent B for 15 min at a flow rate of 300 nL/min. Solvent A consisted of water/acetonitrile (98/2 [v/v]) and 0.1% formic acid, and solvent B consisted of water/acetonitrile (2/98 [v/v]) and 0.1% formic acid. Data acquisition and processing were performed with Analyst QS 2.0 software (Applied Biosystems, Foster City, United States). Generated MS/MS data were compared to the UniProtKB database for *Sus scrofa*.

dECM Hydrogels Fabrication and Characterization

dECM Gelation

For dECM gelation, the decellularized extracellular matrices of the three cardiovascular tissues were lyophilized and milled to a fine powder. The resulting dECM powder was digested with pepsin (#P6887; >3,200 IU; Sigma-Aldrich, St. Louis, USA) in hydrochloric acid solution (20 mg/mL dECM, 2 mg/mL pepsin, 0.01 M HCl) for 6 h at RT and constant stirring. After digestion, the solution pH was raised with sodium hydroxide (1/10 of solution volume, 0.1 M NaOH) and the electrolytes equilibrated with PBS (1/10 of solution volume, 10x PBS). The resulting solution was stored in liquid form (pre-gel) at 4°C or transformed into hydrogel by warming to 37°C for 1 h.

Scanning Electron Microscopy of dECM Hydrogels

Hydrogels derived from all the three different tissues were gelated and freeze-dried in a lyophilizer for 3 days. Samples were, then, analyzed with a tabletop scanning electron microscope (SEM, Hitachi TM3000, Hitachi High-Technologies, Japan). Images were acquired using 5 kV and 100X augmentation. The same settings were used for all the three specimens.

Biomechanical Properties of dECM Hydrogels

Hydrogels derived from the left ventricle, mitral valve, and aorta were subjected to compressive loading using a low load compression tester (LLCT), as described previously with minor modifications (Sharma et al., 2011; Peterson et al., 2013; Nibourg et al., 2015). Two hundred microliter of the hydrogel was placed inside polydimethylsiloxane (PDMS) donut-shaped support on top of a microscope glass slide, which were both placed on the load cell. First, gel thickness was measured by letting the stainless-steel plunger (diameter, 25 mm) drop down till it touched the glass surface; this position was recorded as the bottom of the gel. Then the gel was placed under the plunger and the top of the gel was determined, the difference in position between the top and bottom of the gel was taken as the thickness. Plunger dropped at a speed of 5 μm/s until it experienced a counterforce of 0.0981N and this was defined as touch. Next, the gel was deformed by 20% (strain = 0.2) i.e., to 80% of its original thickness within 1 s (strain rate of 0.2 s^{-1}) and the plunger was kept in this position for another 100 s. Gel stiffness was determined during the first second of experiment i.e., while the plunger was deforming the gel as the slope of the stress-strain curve. During the next 100 s the strain was kept constant (at 0.2) while the stress was observed to continuously decrease with time [$\sigma(t)$]. This stress relaxation at constant strain is proof that the gels are not elastic but viscoelasticity in nature. The viscoelastic properties were determined by dividing the decreasing stress with constant strain (0.2) to get $E(t)$ (=$((t)/0.2)$. A generalized Maxwell model was fit to $E(t)$ in the form of Equation (1).

$$E(t) = E_1 e^{\frac{-t}{\tau_1}} + E_2 e^{\frac{-t}{\tau_2}} + E_3 e^{\frac{-t}{\tau_3}} \ldots\ldots\ldots E_i e^{\frac{-t}{\tau_i}} \quad (1)$$

Each Maxwell element corresponds to one $E_i e^{\frac{-t}{\tau_i}}$ term in Equation (1) where i varies from 1 to n. A Maxwell element is characterized by its modulus i.e., E_i and relaxation time constant i.e., τ_i for which it remains active. Model fitting was performed with the Microsoft Excel 2016 Solver module, imposing positive values for physical relevance. Fitting started with one Maxwell element with an addition of a new element until the Chi-square (error function) kept on decreasing. Each element was assigned with a relative importance (RI_i) within each experiment on the basis of the value of its spring constant, E_i, and calculated using (Equation 2).

$$RI_i = 100.\frac{E_i}{(E_1 + E_2 + \ldots E_i)} \quad (2)$$

In order to average replicate measurements and compare different hydrogels based on their viscoelasticity, each Maxwell element was assigned to a relaxation time range. Four log scale-based relaxation time ranges were defined i.e., 0–1 s, 1–10 s, 10–100 s, and 100–1,000 s.

In vitro Influence of dECM Hydrogels on Mesenchymal and Endothelial Cells in 2D and 3D Cultures

Adipose Tissue-Derived Stromal Cell Culture and Differentiation on the dECM Hydrogels

Human ASC were isolated as described previously (Tuin et al., 2010). Briefly, human abdominal fat was obtained by liposuction, washed with phosphate-buffered saline (PBS) and digested enzymatically with 0.1% collagenase A (Roche Diagnostic, Mannheim, Germany) in PBS with 1% bovine serum albumin (BSA; Sigma-Aldrich, Boston, USA). The tissue was

shaken constantly at 37°C for 2 h. After this, the digested tissue was mixed with 1% PBS/BSA, filtered, centrifuged and the cell pellet was resuspended in Dulbecco's Modified Eagle's Medium (DMEM; #12-604F, Lonza, Basel, Switzerland) with 10% fetal bovine serum (FBS; #F0804, Sigma-Aldrich, Missouri, United States), 1% penicillin/streptomycin (#15140122, Gibco Invitrogen, Carlsbad, USA), and 1% L-glutamine (#17-605E, Lonza Biowhittaker, Verviers, Belgium). Cells were cultured at 37°C in a humidified incubator with 5% CO_2. The medium was refreshed every 2 days. Confluent cells were passed at a ratio of 1:3.

To assess the influence of hydrogel surfaces on the proliferation and differentiation of ASCs, wells of 24-well plates were covered with 200 μL of the pre-gel solutions from the three different ECM sources and allowed to gelate at 37°C for 1 h. ASC (P3 to 5) were seeded at 10,000 cells/cm^2 on the dECM hydrogels. Cells were cultured in Dulbecco's modified Eagle's medium (DMEM, Lonza, Verviers, Belgium) supplemented with 10% fetal bovine serum (FBS) (Thermo Scientific, Hemel Hempstead, United Kingdom), 1% L-glutamine (Lonza, Verviers, Belgium), and 1% penicillin/streptomycin (Gibco Invitrogen, Carlsbad, USA) at 37°C in a humidified incubator with 5% CO_2. As a control, ASC were seeded on tissue culture plastic in the same medium and at the same density. Seeded ASCs were stimulated with 10 μg/ml TGFβ-1 (PeproTech, London, United Kingdom) while non-stimulated cultures served as control. Stimulation was for 7 days and the medium was refreshed every 2 days.

Cells were washed with PBS and fixed with 2% paraformaldehyde in PBS for 30 min, washed with PBS twice, permeabilized with 0.5% Triton X-100 in PBS for 15 min and blocked with 1% BSA and 5% donkey serum solution in PBS for 15 min to avoid non-specific binding. Myogenic differentiation was assessed by staining with rabbit anti-SM22α primary antibody (1:800; Abcam, Cambridge, United Kingdom) for 2 h, washing with 0.05% Tween in PBS and detection with donkey anti-rabbit Alexa Fluor® 647 secondary antibody (1:800; red; Abcam, Cambridge, United Kingdom) for 1 h at room temperature. The cytoskeleton was stained by Phalloidin Alexa Fluor® 488 (1:400; green; ThermoFisher, Waltham, USA) and nuclei were stained with DAPI (4 μg/ml; #D9542-5MG, blue; Sigma-Aldrich, St. Louis, USA). SM22α expression was calculated by the normalized total cell fluorescence (CTCF) method as previously described (McCloy et al., 2014; Liguori et al., 2019), and plotted as the fold-change relative to the non-stimulated tissue culture plastic control. Briefly, the corrected total cell fluorescence (CTCF) is calculated as the integrated density (ID) subtracted of the product between the area covered by cells (A) and the mean fluorescence of background readings (B), i.e., CTCF = ID – (A × B).

Vascular Network Formation (VNF) in dECM Hydrogels

ASC and human pulmonary microvascular endothelial cells (HPMEC) were co-cultured inside the hydrogels to determine their 3D VNF potential. The HPMEC [HPMEC-ST1.6R (Krump-Konvalinkova et al., 2001), kind gift of dr. Unger, Johannes-Gutenberg University, Mainz, Germany] were seeded on gelatin-coated plates (1% gelatin solution in PBS) at a density of 35,000 cells/cm^2 and cultured until confluency in endothelial culture medium composed of RPMI-1640 basal medium (#BE04-558F, Lonza, Basel, Switzerland) with 10% heat-inactivated fetal bovine serum (FBS; #F0804, Sigma-Aldrich, Missouri, United States), 1% penicillin/streptomycin (#15140122, Gibco Invitrogen, Carlsbad, USA), 1% L-glutamine (#17-605E, Lonza Biowhittaker, Verviers, Belgium), 5 U/mL heparin (LEO Laboratories Limited, Ballerup, Denmark), and 50 g/mL bovine brain extract (BBE, in-house preparation). Cells were kept at 37°C with a minimum relative humidity of 95% and 5% CO_2.

For the determination of 3D VNF, ASC and HPMEC were seeded inside the three different pre-gels at a final density of 1×10^6 per mL, at an ASC:HMVEC ratio of 1:2. Pre-gels were prepared as described and adjusted to 1x DMEM by addition of 1/10th of the volume of 10x DMEM. After pre-gels were mixed with the cells, 200 μL of the suspension was pipetted inside wells of an 8-well Chamber Slide™ System (ibidi GmbH, Gräfelfing, Germany) and incubated at 37°C for 1 h. Upon gelation, 200 μL endothelial culture medium was added per well. Cells were cultured for 7 days and medium refreshed every 2 days.

After PBS washes, cell-loaded dECM hydrogels were fixed with 4% PFA in PBS for 1 h, washed with PBS twice, frozen in liquid nitrogen, cryosections (50 μm) were deposited on microscope slides. Samples were permeabilized with 0.5% Triton X-100 in PBS for 15 min and blocked with 1% BSA and 5% donkey serum solution in PBS for 15 min. To assess 3D VNF, samples were incubated overnight with rabbit anti-SM22α (1:400; #ab14106, Abcam, Cambridge, UK) for detection of ASC-derived pericytes (Hajmousa et al., 2018; Terlizzi et al., 2018) and mouse anti-human PECAM-1 (1:100, #M0823, Dako, Glostrup, Denmark) to detect endothelial cells, washed with 0.05% Tween in PBS and incubated with donkey anti-rabbit IgG (H+L) Alexa Fluor® 594 (1:400; #A-21207, Life Technologies, Carlsbad, United States) and donkey anti-mouse IgG (H+L) Alexa Fluor® 488 (1:400; #ab150105, Abcam, Cambridge, UK) at RT for 1 h. Nuclei were stained with DAPI (4 μg/ml; #D9542-5MG, Sigma-Aldrich, Missouri, United States). Confocal laser scanning microscope (TCS SP8, Leica Microsystems, Wetzlar, Germany) was used to acquire Z-stack images at 20x magnification. 3D vascular network formation was evaluated qualitatively in 3D reconstructed images post-processed using ImageJ 3D viewer plugin, and quantitatively by the fluorescence intensity of PECAM-1 labeling. In our experience, ASC do not express PECAM-1 when cultured in the endothelial culture medium, thus this marker solely visualized vascular-like structures in our system.

Statistical Analysis

All data were obtained from at least three independent experiments. Data are presented as the mean ± standard error

of the mean (SEM). Graphs and statistical analysis were done using GraphPad Prism (Version 6.01; GraphPad Software, Inc., La Jolla, United States). Differences between and among groups were analyzed by Student's *t*-test, One-way ANOVA with Sidak's multiple comparison test or Two-way ANOVA with Holm-Sidak multiple comparison test.

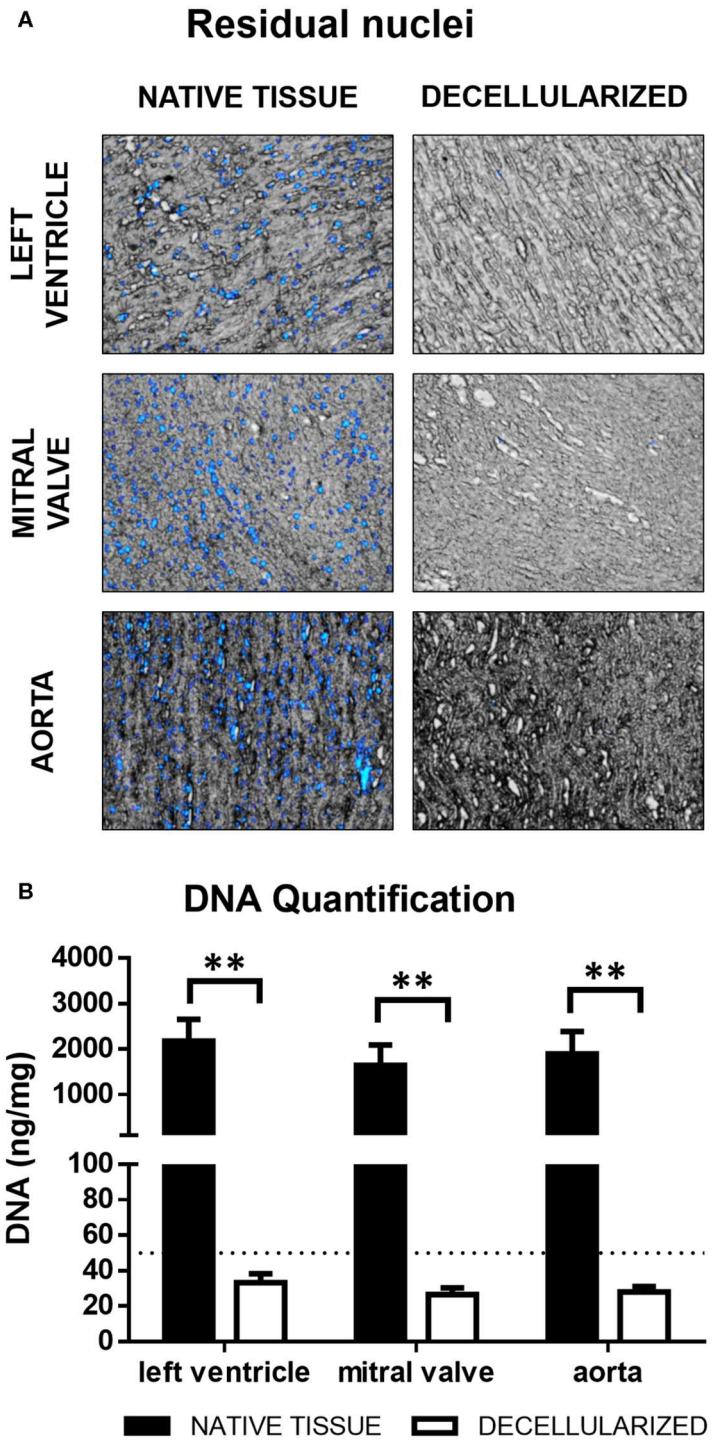

FIGURE 2 | (A) Residual nuclei. Fluorescence overlay on brightfield. **(B)** DNA quantification. $^{**}p < 0.01$. The dotted line represents the maximum accepted DNA concentration for decellularized tissues. Data derived from three independent experiments.

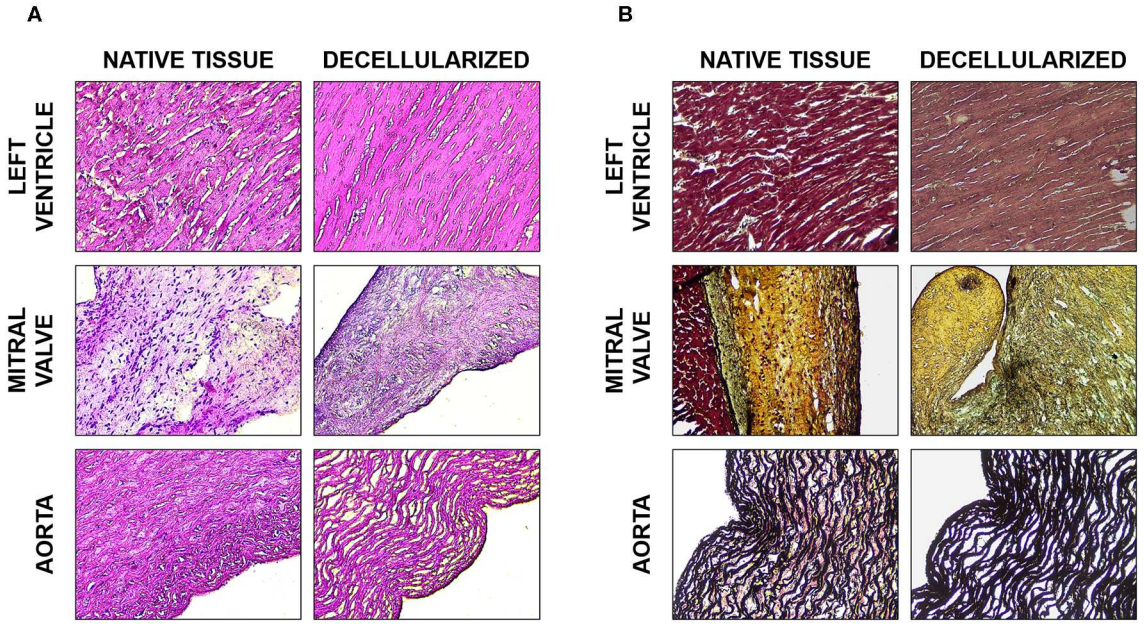

FIGURE 3 | Histological analysis. **(A)** H&E staining of the native and decellularized left ventricle, mitral valve, and aorta tissues. **(B)** Movat's pentachrome stain of the native and decellularized left ventricle, mitral valve, and aorta tissues; muscle in dark red, collagen and reticular fibers in yellow, nuclei and elastin fibers in black, GAGs in blue, and fibrin in bright red.

RESULTS

Decellularization of Cardiac Tissue Efficiently Removed Cellular Constituents and Maintained Extracellular Matrix Structure and Components

Porcine cardiac components i.e., left ventricle, mitral valves, and aorta were subjected to a rigorous decellularization procedure to generate cell-free extracellular matrix (dECM). The presence of remaining DNA in the decellularized ECM was assessed both by detection of nuclei with DAPI and by quantification of residual genomic DNA. For all three tissues, only rare disperse nuclei could be detected after decellularization (**Figure 2A**). The same finding was corroborated in Hematoxylin/Eosin-stained sections (**Figure 3A**) and Movat's Pentachrome stainings (**Figure 3B**). Genomic DNA quantification showed a near 99% reduction (**Figure 2B**, $n = 3$), in all three types of ECM compared to native tissue. The dECMs contained <50 ng/mg of DNA per dry weight, the standard maximal value for decellularized tissues (Crapo et al., 2011).

Hematoxylin/Eosin (**Figure 3A**) and Movat's pentachrome (**Figure 3B**) stained sections showed that the ECM organization was unaffected i.e., comparable to controls (native tissue, **Figure 3**). The original tissues, and consequently the dECM, presented diverse GAG content: mitral valves contained little more than 30 μg/mg of GAGs, aorta about 20 μg/mg and left ventricular myocardium about 15 μg/mg. The final percentage of GAGs content in the dECM was more than fifty percent of that present in the original tissue for all the three tissues (**Figure 4**).

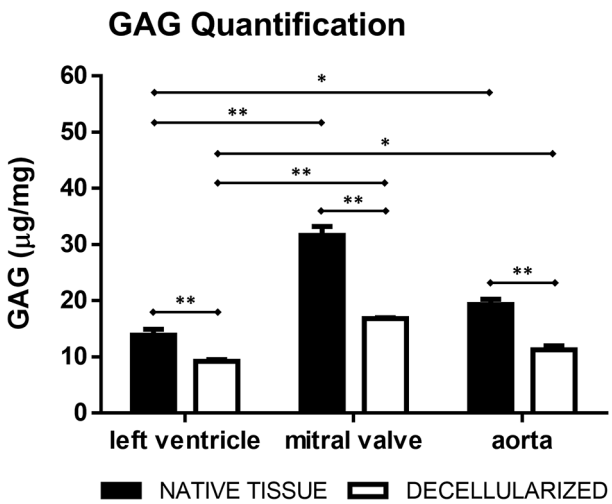

FIGURE 4 | GAG quantification in the native and decellularized left ventricle, mitral valve, and aorta tissues (μg/mg of dry weight). $^{*}p < 0.05$ and $^{**}p < 0.01$. Data derived from three independent experiments.

Decellularized Cardiovascular Tissues Differ in Protein Composition

The protein composition of the extracellular matrix from the three cardiovascular tissues (left ventricle, mitral valve, and aorta) was investigated with mass spectrometry. A total of 64 different ECM proteins was identified and their spectral percentage i.e.,

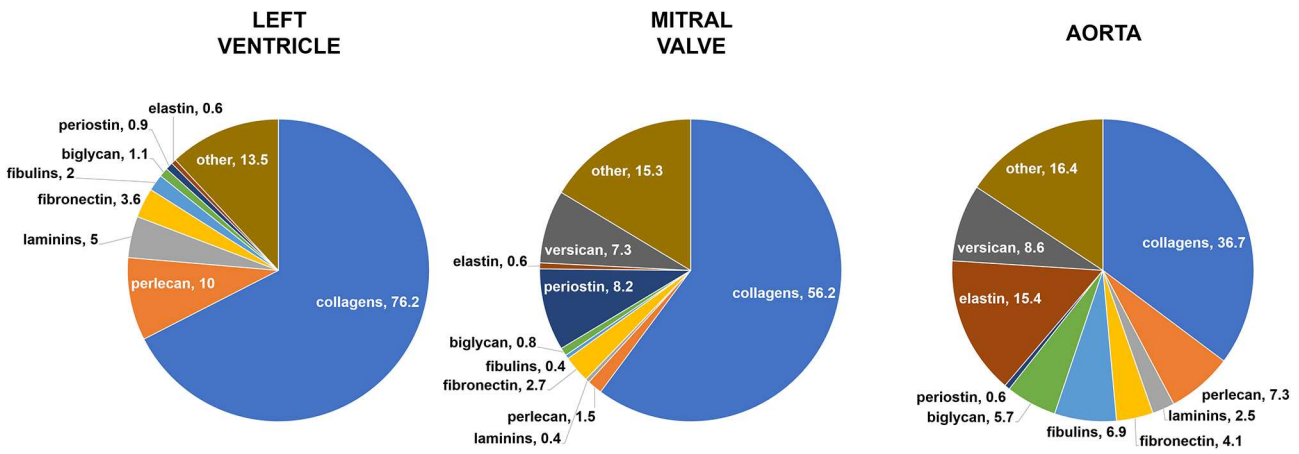

FIGURE 5 | Mass spectrometry analysis. Relative protein abundance (% of ECM spectra). The sum of the parts may be less than or greater than 100% because this graphical representation takes into account only the mean values, without standard deviations. Data derived from three independent experiments.

the proportional number of molecules of each ECM protein in the samples is given in **Table S1**. A summary of the results is in **Figure 5**.

The proteomics analyses ($n = 3$) showed that all three tissues contained collagens as their main ECM component, representing around 76% of left ventricle dECM, 56% of mitral valve dECM, and 37% of aortic dECM. The detailed distribution of the 64 proteins, including collagen types, is described in **Table S1**. When different types and isoforms of collagens were analyzed separately, it was demonstrated that ventricular ECM presented higher amounts of collagen III alpha-1 chain, collagen IV alpha-1 chain, collagen IV alpha-2 chain, and collagen VI alpha-2 chain when compared to both valvar and aortic ECM. A significant difference was also demonstrated for collagen VI alpha-3 chain, such as it was more expressed in the valvar ECM, corresponding to the main ECM protein in this tissue. Elastin, in turn, was found in expressive quantity in the aortic tissue (∼15%), but not in the other two cardiovascular ECM, in which it was found only in scanty amounts (<1%). Another fibrillar ECM protein found in mass spectrometry analysis was fibronectin, representing between 2.7 and 4.1% of all the ECM proteins for all the three tissues, without significant differences among them.

Laminins, a basement membrane constituent, were found in a less expressive, but still representative, amount. The ventricular ECM was the one presenting the higher quantity of laminins (5%), while the valvar ECM was the one presenting the less amount (0.4%), with an intermediate percentage for the aortic dECM (2.5%). The analysis of different isoforms of laminins showed significant differences for laminin subunit alpha-2 and for laminin subunit gamma-1, such as these isoforms were more expressed in the ventricle ECM than in the other cardiovascular tissues. Perlecan, another basement membrane constituent, was also found in a significant higher amount in ventricular (10%) and aortic (7.3%) ECM, when compared to the valvar (1.5%) ECM. Other main proteoglycans found in the three cardiovascular ECM were versican and biglycan. Versican was found in similar amounts in both the valvar (7.3%) and aortic (8.6%) ECM, but interestingly not found in the ventricular ECM. Finally, biglycan (a TGF-β co-receptor) was significantly more expressed in the aortic (5.7%) ECM than in the other two cardiovascular tissues, representing around 1% for the ventricle and mitral valve dECM.

Other ECM proteins found were fibulins, periostin, cartilage intermediate layer protein 2 (CILP-2), elastin microfibril interfacer 1 (EMILIN-1), latent-TGF-β-binding protein, and lysyl oxidase. Fibulins represented an important amount of the proteins found in cardiovascular ECM, particularly in the aortic tissue. The three types of fibulins found in mass spectrometry were fibulin-1, fibulin-2, and fibulin-5, such as the first two were found in lesser amount—and in similar distribution among the tissues—than the last. Fibulin-5, in turn, was expressed in a significantly higher amount in the aortic tissue (6.9%) when compared to both other cardiovascular ECM (<2% for both). Periostin was found in considerable amounts (8.2%) in the valvar ECM, but was almost non-existent in the other two ECM (<1%), although this difference did not reach statistical significance. CILP-2 was found in considerable quantity in the valvar tissue (3.7%), but not in ventricular or aortic ECM. EMILIN-1, a glycoprotein responsible for the interface between elastin and microfibrils, was only found in the aortic ECM, similarly to lysyl oxidase, an extracellular copper-dependent enzyme responsible for the cross-linking between collagen and elastin (and also between collagen fibers), which was found in greater amount in the aortic ECM (1.4%). Finally, latent-TGF-β-binding protein, which regulates TGF-β bioavailability, was also only found in the aortic ECM.

Hydrogels Derived From the Left Ventricle, Mitral Valve, and Aorta dECM Vary in Structural Morphology and Mechanical Properties

Scanning electron microscopy (SEM) demonstrated that the three hydrogels present considerably different structural

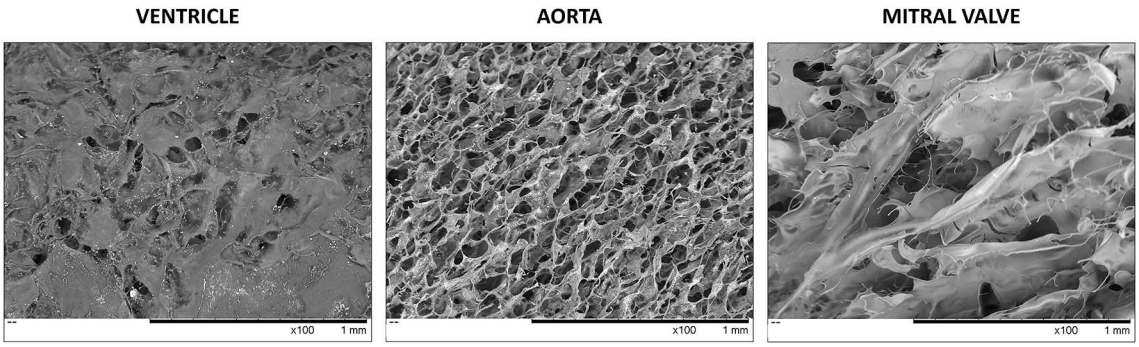

FIGURE 6 | Scanning electron microscopy of the left ventricular, mitral valve, and aortic dECM hydrogels.

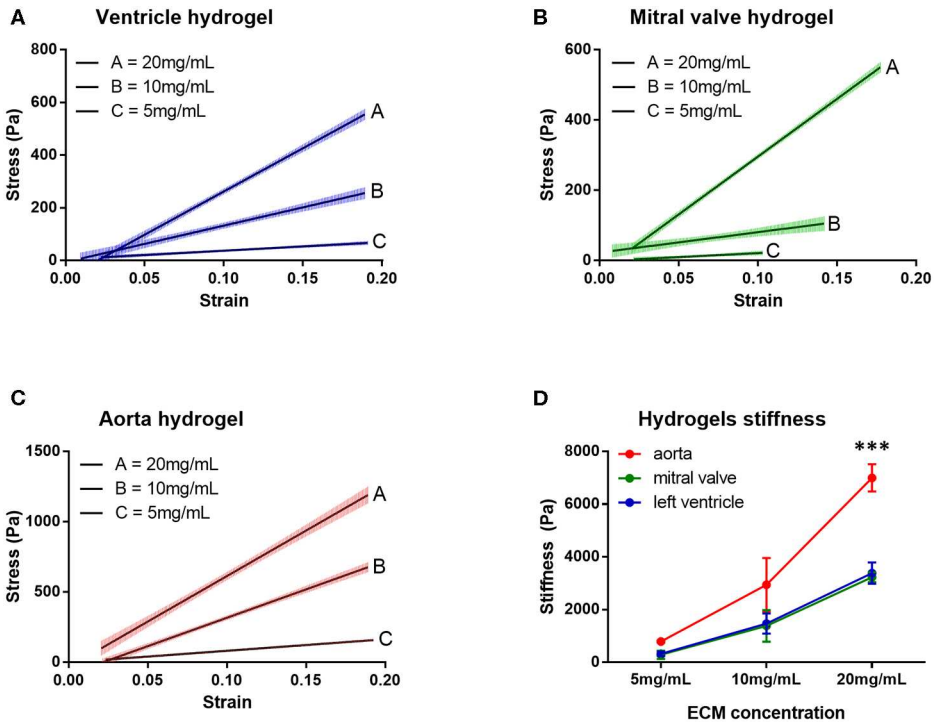

FIGURE 7 | Stress vs. strain curves measured at a strain rate of 0.2 s^{-1} for the three hydrogels at different concentrations: **(A)** ventricle hydrogel, **(B)** mitral valve hydrogel, and **(C)** aorta hydrogel. **(D)** Hydrogels stiffness of the three hydrogels in different concentrations. ***$p = 0.0001$. Data derived from three independent experiments.

morphology (**Figure 6**). The ventricle-derived hydrogel showed a pattern resembling a dense grouping of plate-like structures. Aorta-derived hydrogels, in turn, exhibited a network of honeycomb-like pores. Finally, mitral valve-derived hydrogels displayed another distinct pattern, with *millefeuille*-like sheets of extracellular matrix allocated in several very thin layers.

The stress vs. strain curves for the hydrogels derived from the three cardiovascular dECM were plotted for hydrogels with 5, 10, and 20 mg/mL dECM concentration and stiffness was calculated as the slope of the stress vs. strain curve (**Figure 7**, **Table 1**, $n = 3$). The stiffness increased, for all tissues, with the increase of ECM concentration (Two-way ANOVA, concentration factor, $p < 0.0001$). For 5 and 10 mg/mL ECM concentrations, no statistically significant differences were found among the hydrogels. For 20 mg/mL ECM concentration, however, hydrogels derived from aortic ECM proved to be significantly stiffer than both the ventricular and valvar hydrogels (Two-way ANOVA, hydrogel factor, $p = 0.0002$; Holm-Sidak multiple comparison test: left ventricle vs. aorta $p = 0.0001$, mitral valve vs. aorta $p = 0.0001$).

The stress relaxation over time was plotted and the generalized Maxwell model was fitted to the data. Each hydrogel was described according to their relaxation time constants (t), spring constants (E_i), and relative importance (**Figure 8**, **Table 1**, n

TABLE 1 | Mechanical properties of the three different hydrogels.

	Left ventricle				Mitral valve			Aorta		
STIFFNESS										
Concentration (mg/mL)	5	10	20		5	10	20	5	10	20
Stiffness (Pa)	325 ± 149	1473 ± 663	3384 ± 698		289 ± 222	1386 ± 1039	3233 ± 323	792 ± 75	2942 ± 1755	6998 ± 895
VISCOELASTICITY										
Element	E1	E2	E3	E4	E1	E2	E3	E1	E2	E3
T(s)	0.24 ± 0.02	1.96 ± 0.06	13.16 ± 0.49	198.50 ± 31.16	0.23 ± 0.02	2.56 ± 0.33	27.12 ± 11.70	0.26 ± 0.11	2.47 ± 1.13	25.22 ± 18.02
Ei	1169 ± 163	689 ± 140	508 ± 119	822 ± 202	1417 ± 222	567 ± 149	683 ± 142	4814 ± 995	1131 ± 608	671 ± 218
RI (%)	36.9 ± 2.6	21.5 ± 0.4	16.1 ± 1.1	25.5 ± 1.5	60.6 ± 12.1	23.5 ± 1.3	23.9 ± 5.5	74.9 ± 10.4	17.6 ± 8.9	11.2 ± 4.5

τ, relaxation time constant; E_i, spring constant; RI, relative importance.

= 3). The stress relaxation curves showed that left ventricular hydrogels started with a low stress value, but kept higher residual stress, while the aortic hydrogels started with a higher stress value and presented an important relaxation, reaching zero within the 100 s of follow-up. Mitral valve hydrogels, in turn, started with low stress values, relaxed quickly reaching zero within the 100 s. This indicates that ventricular hydrogel behaved more like viscoelastic solid, whereas the aorta and valvar hydrogel like a viscoelastic liquid.

Left ventricle hydrogel resolved in four Maxwell elements, while mitral valve and aortic hydrogels resolved in three Maxwell elements to fit to measured stress relaxation. For all the three hydrogels, the first Maxwell element presented the highest impact, representing around 37, 51, and 76% of the relaxation in, respectively, the ventricular, valvar, and aortic hydrogels. The relative importance of the second Maxwell element varied between 18 and 23% among the hydrogels, while these values were between 11 and 24% for the third Maxwell element. The fourth Maxwell element represented a significant relative importance for the ventricular hydrogels, of around 26%. The Maxwell elements, for all hydrogels, were defined according to their t values. The first Maxwell element showed different E_i and relative importance (RI_i) values among the hydrogels. E_i values were higher for the aortic hydrogel when compared to both the left ventricular and mitral valve hydrogels (One-way ANOVA, $p = 0.0005$; Holm-Sidak multiple comparison test: left ventricle vs. aorta $p = 0.0009$, mitral valve vs. aorta $p = 0.0009$). The first Maxwell element had a stronger impact in aortic hydrogels compared to left ventricle hydrogels, with the valvar hydrogels showing a relative importance value in between (One-way ANOVA, $p = 0.0087$; Holm-Sidak multiple comparison test: left ventricle vs. aorta $p = 0.0093$, left ventricle vs. mitral valve $p = 0.0492$). The E_i or RI_i of the second and the third Maxwell element did not differ.

Hydrogels Derived From the Left Ventricle, Mitral Valve, and Aorta dECM Differ in Bioactivity

After 7 days of culture, ASCs had formed confluent monolayers on tissue culture plastic (TCP), and on the left ventricle and aortic dECM hydrogels (**Figures 7A,B,D**). In these cases, the ASC had actin filaments throughout their cytoplasm. On mitral valve dECM hydrogel, ASCs had aggregated and formed long cytoplasmic protrusions (**Figure 9C**, arrows).

Our earlier research showed that TGF-β1 stimulation efficiently differentiates ASCs into smooth muscle cells (SMC). Seven days of TGF-β1 stimulation, on TCP indeed differentiated ASC in SM22α-expressing SMC (**Figure 10**, $n = 3$), while only few ASC normally expressed SM22α. In contrast, TGF-β1 stimulation of ASCs on left ventricular dECM hydrogels differentiated the cells when compared to non-induced ASC, but appeared to be blocked when compared to SMC differentiation in TCP, as evidenced by the reduced expression of SM22α (One-way ANOVA, $p = 0.0001$; Holm-Sidak multiple comparison test: TCP + TGF-β1 vs. left ventricle + TGF-β1 $p = 0.0108$). Similarly, on mitral valve dECM hydrogels, TGF-β1-induced SMC differentiation of ASCs was also blocked and SM22α expression was reduced when compared to cells induced in TCP (One-way ANOVA, $p = 0.0001$; Holm-Sidak multiple comparison test: TCP + TGF-β1 vs. mitral valve + TGF-β1 $p = 0.0400$). In contrast, non-induced ASC differentiated to SMC on aortic dECM hydrogels (One-way ANOVA, $p < 0.0001$; Holm-Sidak multiple comparison test: TCP vs. aorta $p < 0.0001$). The additional stimulation with TGF-β1 had no measurable influence.

Left Ventricular, Mitral Valve, and Aortic dEMC Hydrogels Differentially Influence VNF

Vascular network formation was evaluated in 3D by confocal microscopy in the three different hydrogels. After 7 days of co-culturing ASC and HPMEC (1:2) inside dECM hydrogels, VNF had occurred in the left ventricle, mitral valve and aortic hydrogels (**Figure 11**) albeit that the network morphologies differed. In left ventricle dECM hydrogels, vascular structures appeared to be both thicker and longer (**Figure 11**, red arrows) compared to both other hydrogels. In mitral valve and aortic dECM hydrogels, vascular structures were fewer and smaller (**Figure 11**). In all three gels, large aggregates of cells had formed as observed by nuclear staining with DAPI.

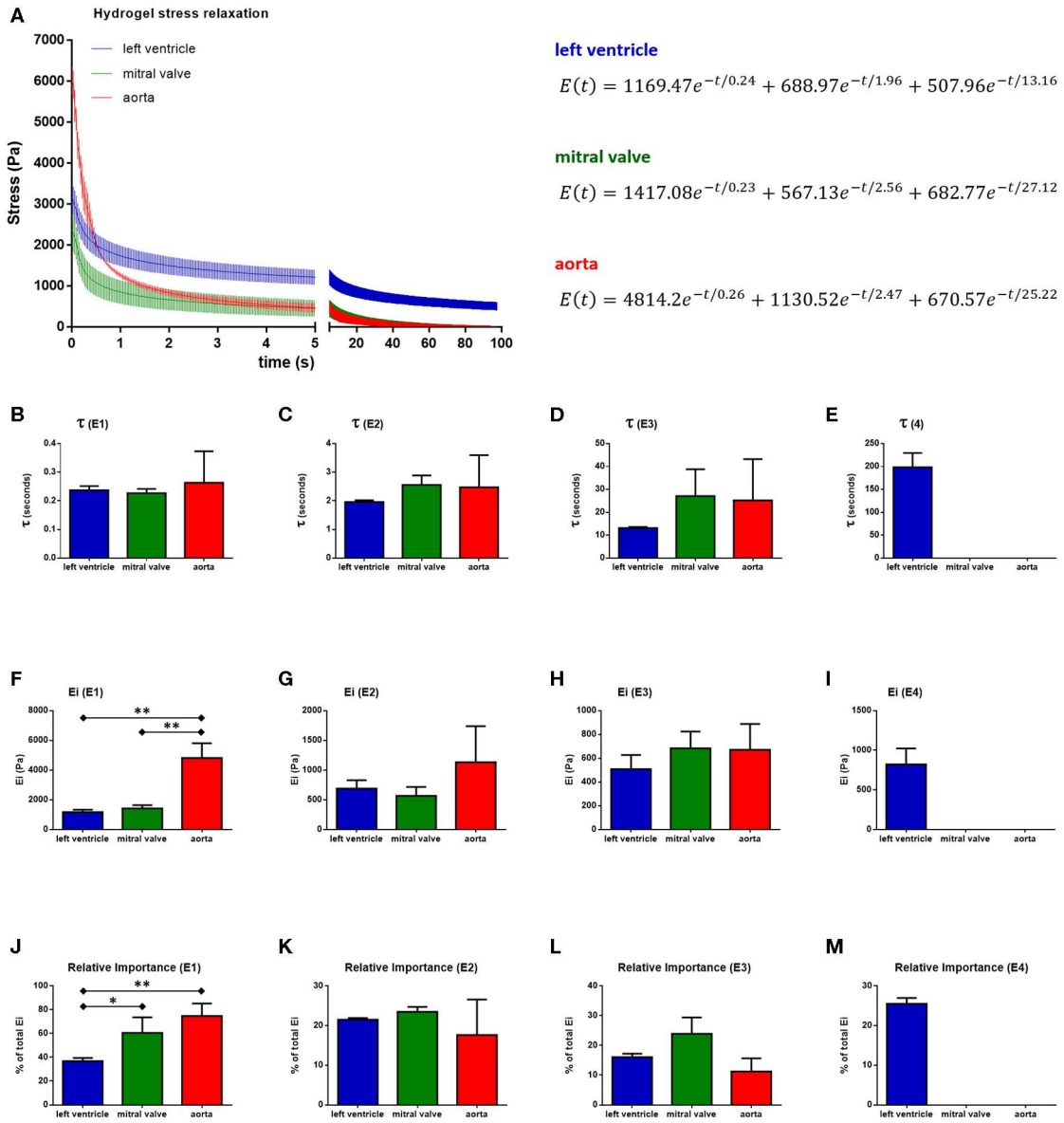

FIGURE 8 | Stress relaxation behavior of 20 mg/ml hydrogels and the average Maxwell model fitting output. **(A)** Hydrogels stress relaxation curves and their respective averaged Maxwell model equations. Relaxation time constants (t), spring constants (E_i), and relative importances (RI) are shown for the first **(B,F,J)**, second **(C,G,K)**, third **(D,H,L)**, and fourth **(E,I,M)** Maxwell elements. $^{*}p < 0.05$ and $^{**}p < 0.01$. Data derived from three independent experiments.

DISCUSSION

The main results of our investigations are that we optimized a procedure to reproducibly and reliably generate extracellular matrix hydrogels from decellularized, highly different cardiac components i.e., left ventricle, mitral valve, and aorta. We show that the left ventricle, mitral valve, and aorta dECM hydrogels differ in largely molecular composition, mechanical properties and bioactivity (**Table 2**). The major findings were that left ventricle dECM hydrogels (1) contained the highest content of basement membrane constituents; (2) had viscoelasticity comprising four Maxwell elements and around 3 kPa stiffness (20 mg/mL gel), (3) suppressed ASC differentiation, but (4) augmented VNF. Mitral valve dECM hydrogels, on the other hand, had (1) periostin as a major constituent; (2) a lower viscoelastic complexity (three elements) and also around 3 kPa stiffness (20 mg/mL gel); (3) suppressed ASC differentiation, and (4) had marginal VNF support. Finally, aortic dECM hydrogels differed from both others and (1) had the highest content of non-collagen constituents i.e., elastin, fibulins, and biglycan to mention a few; (2) a viscoelasticity of three elements with high stiffness, around 7 kPa (20 mg/mL gel); (3) caused non-induced ASC differentiation to SMC; and (4) marginally supported VNF.

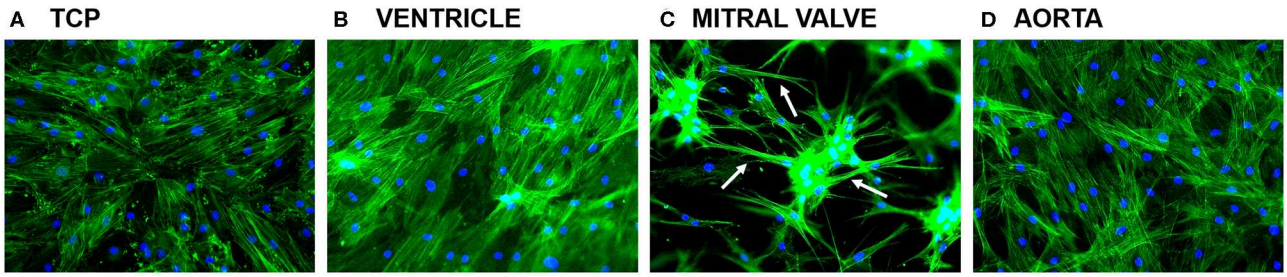

FIGURE 9 | ASC cultured for 7 days on top of tissue culture plastic (TCP), left ventricular, mitral valve, and aortic dECM hydrogels stained for phalloidin. **(A)** TCP, **(B)** ventricle, **(C)** mitral valve, and **(D)** aorta.

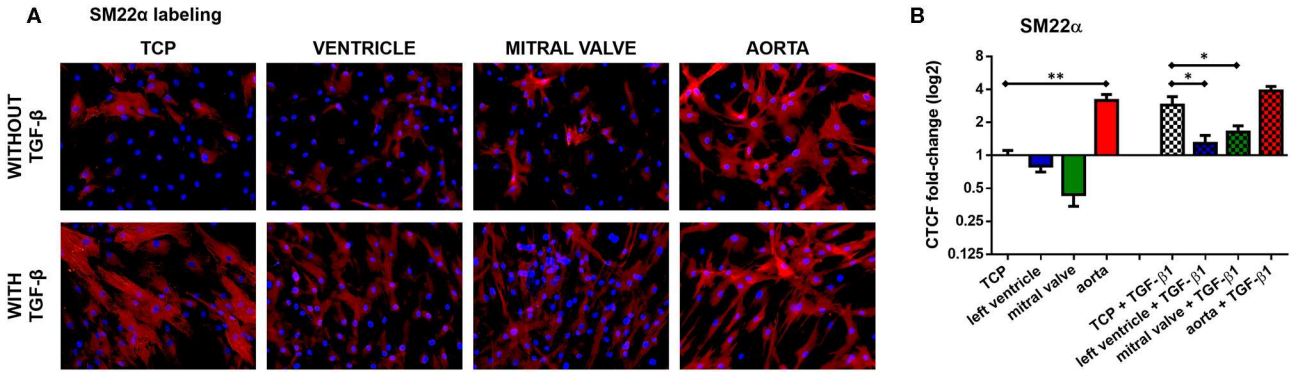

FIGURE 10 | ASC myogenic differentiation on the hydrogels (concentration: 20 mg/mL). **(A)** SM22α staining. **(B)** Quantification of SM22α expression. $^{*}p < 0.05$ and $^{**}p < 0.01$. Data derived from three independent experiments.

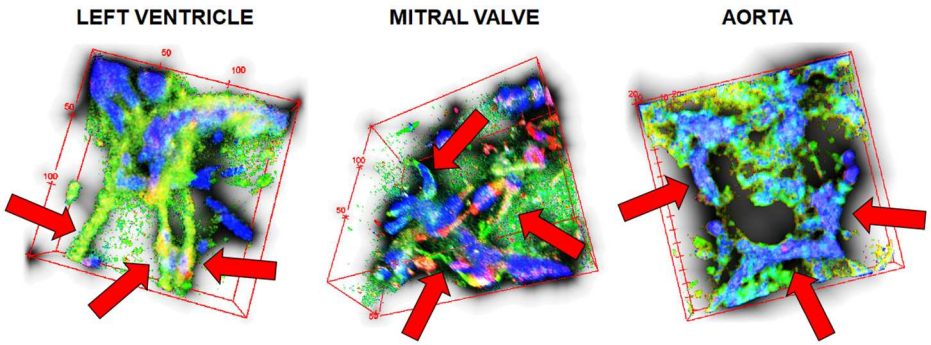

FIGURE 11 | 3D vascular networking formation in the three different dECMs hydrogels. Stacked 3D image reconstruction of 50 μm sections. Blue, nuclei; green, HPMEC; red, ASC. Red arrows point to the vessel-like structures within each micrograph.

These biochemical and biomechanical differences among the three different cardiovascular tissue-derived hydrogels correlates to the differences found in the physiological situation, i.e., the biochemical and biomechanical properties of the respective tissues. These differences, as shown in the present work, directly impact cell behavior and, thus, are of great relevance because they can be used to mimic the *in vivo* microenvironment during *in vitro* studies. In fact, the use of such tissue-specific microenvironments for tissue engineering has been proposed to reduce the use of animal models during drug development and pathophysiological studies, besides tissue-engineering for therapeutic purposes (Liguori et al., 2017).

Molecular Clues

In regard to the molecular clues, the first to be noted is the differences in GAG content. GAG are responsible for the binding of several growth factors that can stimulate cell response—such as fibroblast growth factors (FGF), hepatocyte growth factor (HGF)—chemokines as interleukins, enzymes (and their inhibitors), as well as several ECM proteins including fibronectin,

TABLE 2 | Molecular and biomechanical differences among ECM from different tissues and the respective biological response.

	Molecular differences	Biomechanical differences	Biological response
Left ventricle	↓ GAG ↑Collagen III alpha-1 chain ↑Collagen IV alpha-1 chain ↑Collagen IV alpha-2 chain ↑Collagen VI alpha-2 chain ↑Laminin subunit alpha-2 ↑Laminin subunit gamma-1 ↓Versican	↑Maxwell elements	1. Confluent monolayer cell growth 2. Inhibition of TGF-β1-induced myogenic differentiation 3. Substantial vascular network formation
Mitral valve	↑GAG ↑CILP-2 ↑Collagen VI alpha-3 chain ↓Perlecan		1. Clustered cell growth 2. Inhibition of TGF-β1-induced myogenic differentiation 3. Limited vascular network formation
Aorta	↑Biglycan ↑EMILIN-1 ↑Fibulin-5 ↑Latent TGF-β-binding protein 2 ↑Lysyl oxidase	↑Stiffness	1. Confluent monolayer cell growth 2. Non-induced myogenic differentiation 3. Limited vascular network formation

↑Greater expression/value than the other two dECM.
↓Lower expression/value than the other two dECM.

laminin, and type V collagen (Varki et al., 1999; Esko et al., 2017). Although in ventricular tissue the reduced GAG content followed the reduced content of the versican core protein, in valvar tissue GAG expression was increased compared to the other matrices besides the reduced content of the perlecan core protein. This shows that not only GAG content may vary among the matrices, but also the types of proteoglycans which are present in different tissues, which might influence how these GAGs interact with the cells. Previously, it was shown that extrinsic perlecan suppressed adipogenic and promoted osteogenic differentiation in bone marrow mesenchymal stem cells (Nakamura et al., 2014). Although the influence of perlecan on myogenic differentiation was never investigated, it is known that this proteoglycan binds the latent form of TGF-β, increasing the growth factor bioavailability (Chen et al., 2007; Sengle et al., 2011). Versican, in turn, facilitates chondrocyte differentiation *in vivo* by binding to TGF-β and fixating it to the ECM, thus, favoring TGF-β signaling pathways in the surrounding cells (Choocheep et al., 2010). *In vitro*, versican was shown to induce myogenic differentiation of fibroblasts by increasing active TGF-β signaling (Carthy et al., 2015).

The second difference in the molecular composition of the ECM refers to the increased presence of collagens type III, IV, and VI in the ventricular tissue when compared to the valvar and arterial matrices. The absence of type III collagen was shown to be responsible for the myofibroblast differentiation in a mice model, suggesting that this type of collagen plays an important role in maintaining the fibroblastic phenotype (Volk et al., 2011). Interestingly, collagen VI—which was increased in both the ventricular and valvar matrices—was shown to be responsible for cardiac fibroblast differentiation into myofibroblasts *in vitro* (Naugle et al., 2006). Paradoxically, collagen VI was also shown to enhance MSC expansion while maintaining the stem cell phenotype (Smeriglio et al., 2017). One of the reasons why collagen VI seems to be involved in cell fate might be related to the biophysical modulation of the environment—either in the native ECM or in a hydrogel—since it was shown that collagen VI is crucial for the biomechanical integrity of the pericellular matrix in MSC (Twomey et al., 2014) and also that soluble fragments of collagen VI can mediate stimulation of DNA synthesis via tyrosine phosphorylation of paxillin, FAK, and p130CAS—proteins that associate with focal adhesions—in the absence of classical growth factors (Rühl et al., 1999).

Laminin family was another group of proteins which was differentially expressed among the matrices. Ventricular ECM presented increased levels of laminin subunit alpha-2 and laminin subunit gamma-1 when compared to the other two ECM types. Laminins have been shown to suppress chondrogenic, but to induce osteogenic differentiation of mesenchymal stem cells, contributing to bone tissue development, through an ERK-dependent pathway (Klees et al., 2005, 2008; Hashimoto et al., 2006; Mittag et al., 2012). Other effects of laminins on mesenchymal stem cells related to ERK pathways are the differentiation into insulin-producing cells (Lin et al., 2010), and the promotion of neurite outgrowth (Mruthyunjaya et al., 2010). In regard to myogenic differentiation, laminin-2 has been suggested to induces smooth muscle myogenesis by down-regulation of RhoA, but no other studies investigated the effect of laminins on myogenic differentiation (Beqaj et al., 2002). Herein, we did not find the expected myogenic differentiation supposedly promoted by laminins, in fact, the opposite was demonstrated. This might be related to the fact that several other factors were acting on the ASC and the strength of laminin influence was not enough to exercise any effect. On the other hand, laminin was shown to promote 3D vascular network formation in collagen scaffolds by regulating VEGF uptake (Stamati et al., 2014), what corroborates our findings. We demonstrated that ventricular dECM-derived hydrogel, which present higher laminin content than the other two matrices, was also the one showing better 3D vascular network formation.

Mitral valve extracellular matrix showed increased protein expression of cartilage intermediate layer protein 2 (CILP-2), which was absent in both other tissues, although cartilage intermediate layer protein 1 (CILP-1) was present in both the ventricular and valvar matrices. This is an interesting finding that coincides with the behavior of the adipose stromal cells in regard to differentiation upon TGF-β1 stimulation. Cartilage intermediate layer protein is a large secreted glycoprotein and its CILP-1 form has been shown to block TGF-β1 activity through direct interaction with TGF-β1 and inhibition of TGF-β1

signaling (Seki et al., 2005; van Nieuwenhoven et al., 2017; Zhang et al., 2018). Although there are no studies in regard to the CILP-2 interaction with TGF-β1, it may probably present a similar behavior to CILP-1.

The aortic dECM hydrogels, in turn, showed a series of proteins significantly higher expressed compared to the two other matrices, all of them being proteins constituents of elastic fibers. One of them was biglycan, a proteoglycan that forms complexes with collagen and elastic fibers components and binds to TGF-β1 (Hildebrand et al., 1994; Reinboth et al., 2002). This, *per se*, might justify the contribution of the aortic matrix to the non-induced myogenic differentiation of ASC. In fact, the use of the word non-induced was preferred over spontaneous because it is known FBS-containing culture medium contains 1–2 ng/mL of TGF-β1 (Danielpour et al., 1989; Oida and Weiner, 2010). Thus, what might actually be in course is the binding of serum-derived TGF-β1 to the hydrogel and, consequently, its presentation to the cells in a higher concentration than that found in the culture medium. Another protein highly expressed in aortic ECM was elastin microfibril interfacer 1 (EMILIN-1), a protein responsible for the formation of the elastic fiber and for cell anchoring. EMILIN-1 has been shown to inhibit TGF-β signaling *in vivo* (Zanetti et al., 2004; Zacchigna et al., 2006), what could be understood as paradoxical to our findings. However, it was demonstrated that the mechanism of TGF-β signaling inhibition by EMILIN-1 occurs through the binding with the precursors of TGF-β (proTGF-β), not allowing it to be converted into mature TGF-β (Zacchigna et al., 2006). A third protein which was more abundantly present in the aortic matrix was fibulin-5. Fibulin-5 is an ECM protein crucial for elastogenesis and also able to promote elastic fiber organization (Hirai et al., 2007). The role of fibulin-5 is closely related to the fact this protein contains several Arg-Gly-Asp (RGD) motifs (Albig and Schiemann, 2005), besides also presenting calcium-binding EGF-like domains (Timpl et al., 2003). While the RGD motifs bind the integrins of cells, the calcium-binding EGF-like domains of fibulin-5 were shown to bind latent TGF-β-binding protein 2 (LTBP-2) (Hirai et al., 2007), another protein we found in significantly higher levels in the aortic matrix. The LTBP-2, in turn, plays an important role in TGF-β availability in the cell microenvironment by the binding latent form of TGF-β which is, then, cleaved by proteases into mature TGF-β (Robertson et al., 2015). Since ASC produce TGF-β (Rehman et al., 2004; Du et al., 2016), released in the latent form, LTBP-2 may increase TGF-β availability by binding the latent TGF-β in the ECM, not allowing it to be diluted in the medium and, then, also increasing the concentration of the growth factor available to the cells. Finally, the last protein found to be overexpressed in the aortic matrix, when compared to the ventricular and mitral matrices, was lysyl oxidase (LOX), an enzyme that initiates the crosslinking in collagen and elastin. LOX is known to both bind TGF-β (Atsawasuwan et al., 2008), but also to have its expression upregulated by the growth factor (Gacheru et al., 1997; Shanley et al., 1997).

Biomechanical Clues

Besides the different molecular clues given by the three different matrices, we also investigated the influence of their biomechanical properties, which differs for each matrix and may play a role in cell behavior. In summary, the two main findings in this regard were a significantly higher stiffness found in the hydrogels derived from aortic dECM and viscoelastic solid nature of hydrogels derived from ventricular dECM, which is also manifested as a higher number of Maxwell elements. Stiffness is known to influence cell behavior, including cell differentiation and microvascular network formation, being extensively discussed in literature (Engler et al., 2006; Even-Ram et al., 2006; Wells, 2008; Califano and Reinhart-King, 2009; Park et al., 2011; Schaap-Oziemlak et al., 2014; Ye et al., 2015; Mao et al., 2016). Viscoelasticity, on the other hand, is a combination of influencing factors much less debated. In general, authors treat their hydrogel materials as elastic when, in fact, they are viscoelastic due to large water content. This means that, besides elasticity, which is generally represented by stiffness, these materials present another important biomechanical property which is viscoelasticity, represented by stress relaxation.

Hydrogels with specific stiffnesses were previously shown to promote mesenchymal stem cells differentiation into smooth muscle cells under TGF-β induction, although non-induced differentiation was not described (Park et al., 2011). In fact, stiffnesses ranging between 8 and 17 kPa are considered to promote myogenic differentiation (Engler et al., 2006), which is very close to our findings for the hydrogels derived from aortic dECM (6.9 ± 0.8 kPa). This might be a contributing factor for the behavior of ASC cultured on aortic dECM hydrogels, particularly when taken together with the previously discussed biomolecular clues found in this matrix. Hydrogels constituted of pure collagen exhibit lower stiffness values in comparison to dECM hydrogels, ranging from 30 Pa for 3 mg/mL to 1.8 kPa for 20 mg/mL (Cross et al., 2010). This difference might be related to the combination of collagen fibers with other ECM proteins, such as elastin, present in dECM hydrogels, which importantly improve their elastic modulus. In regard to vascular network formation, literature is limited but it has been shown that soft substrates facilitate endothelial cell network assembly (Califano and Reinhart-King, 2008, 2009), which corroborates with our findings.

In regard to the stress relaxation, to the best of our knowledge there is no more than a handful of studies in literature describing the effects of stress relaxation on cell behavior, particularly regarding cell spreading (Cameron et al., 2011; McKinnon et al., 2013; Chaudhuri et al., 2015, 2016; Bauer et al., 2017; Charrier et al., 2018), proliferation (Cameron et al., 2011; Chaudhuri et al., 2016; Bauer et al., 2017), and differentiation (Cameron et al., 2011, 2014; Chaudhuri et al., 2016; Charrier et al., 2018). Unfortunately, the order of magnitude in stress relaxation varies among the studies, from $t_{1/2}$ (time until 50% relaxation) starting at 60 s (Chaudhuri et al., 2016) until $t_{1/2}$ of more than 30,000 min (Cameron et al., 2011). Chaudhuri et al. demonstrated that while osteogenic differentiation requires fast-relaxing hydrogels (optimal when $t_{1/2} = 60$ s), adipogenic differentiation requires slow-relaxing hydrogels (optimal when 50% relaxation $t_{1/2} = 2{,}300$ s) (Chaudhuri et al., 2016). Probably, myogenic differentiation would require a relaxation time between these two. Although Cameron *et al.* showed improved myogenic

differentiation in hydrogels presenting $t_{1/2} = 250$ min (15,000 s) when compared to hydrogels with even higher $t_{1/2}$ (up to over 30,000 min) (Cameron et al., 2011), they also showed that both adipogenic and osteogenic differentiation were increased in these hydrogels with lower $t_{1/2}$ values, what lead to questioning if the range of stress relaxation time used by the authors was not much above the ideal for cell culturing. The stress relaxation in our hydrogels, in contrast, was even faster than those reported by Chaudhuri et al., for all the three different matrices, with $t_{1/2}$ lower than 1 s.

Another difference between the studies was the stiffness of these hydrogels. Although both authors kept the stiffness constant within their experiments, Chaudhuri et al. used hydrogels with 9 and 17 kPa (Chaudhuri et al., 2016), while Cameron et al. used hydrogels of 4.7 kPa (Cameron et al., 2011). Thus, there is also the combinatory effect of stiffness and stress relaxation, which is the whole point of the viscoelasticity theory. In our study, for instance, stiffness was not controlled, so that hydrogels could present high values of stiffness while presenting low stress relaxation time (aorta), low values of stiffness with also low stress relaxation time (mitral valve), or low values of stiffness with high stress relaxation times (left ventricle). This points to the need for a more robust descriptive reference for viscoelasticity than only looking at stiffness and stress relaxation separately, which we believe to be the Maxwell elements. As previously mentioned, these elements allow the dissection of several main components exerting the resistive forces during and after strain.

In the present study, we showed that the hydrogels derived from ventricular dECM, which led to the inhibition of ASC differentiation but supported the growth of robust and interconnected vascular networks in 3D, presented an extra Maxwell element. To define what component is being represented by each Maxwell element is a difficult task in natural materials (Peterson et al., 2013), particularly because it is not possible to control the components present in these materials. It is, however, well accepted that the first element, which tends to present a *t*-value smaller than 1s, represents water and soluble small molecules (Bausch et al., 1999; Cense et al., 2006; Peterson et al., 2013). The second element, with a *t*-value between 1s and 10s, could represent glycosaminoglycans, small proteoglycans, and other small ECM proteins (e.g., biglycan, EMILIN-1, fibulin-5) and water bound to GAGs and other hygroscopic molecules, while the third, with a *t*-value between 10s and 100s, could be large extracellular matrix proteins (e.g., fibrillar collagens, versican, perlecan, laminin). Finally, the fourth Maxwell element, which was only present in the hydrogels derived from ventricular dECM, should then be related to some component either only present in the ventricular ECM or at least increased in this matrix when compared to the other two. Thus, considering the increased expression and the percentual protein content in the ventricular ECM (see **Table S1**), the fourth Maxwell element should be collagen IV.

Differently from fibrillar collagens (e.g., collagens type I, II, and III), collagen IV is network-forming collagen (Muiznieks and Keeley, 2013). It was previously shown that while crosslinked meshes of synthetic polymers increase the time required for stress relaxation, linear chains lead to faster stress relaxation (Chaudhuri et al., 2016; Charrier et al., 2018). This behavior found in synthetic polymers could also explain the findings of our study so that the crosslinked meshes of collagen IV are leading to the prolonged time necessary for stress relaxation. To date, no other study investigated the effect of viscoelasticity on cell differentiation or vascular network formation under the lens of Maxwell elements, so that the present work is the first to do so. Previous authors, however, hypothesized on how the viscosity i.e., stress relaxation may influence cell behavior. In our opinion, the next step is relating cell behavior to the strength and relaxation time constants of individual Maxwell elements, which are in turn related to the hydrogel composition. Briefly, while in elastic matrices the forces exerted by the cell on the matrix (and consequently by the matrix on the cell) are kept constant over time, in viscoelastic materials the matrix relaxes over time so that the forces are decreased and the matrix is remodeled (Chaudhuri et al., 2016). Faster relaxation i.e., faster matrix remodeling would lead to increased RGD-ligand clustering, cell shape change, proliferation, and differentiation stimuli (Chaudhuri et al., 2016).

LIMITATIONS

A limitation of the study is the use of CTCF, i.e., fluorescence intensity, to quantify the myogenic markers. Ideally, the quantification of the number of cells expressing the marker would be a preferable alternative. However, the fact that, as demonstrated in **Figure 9**, the mitral valve hydrogel tended to lead cells to form clusters, precludes running a cell to cell analysis.

CONCLUSION

The three main cardiovascular tissues (myocardium, valves, and vessels) can be used to fabricate hydrogels from dECM. Different tissues, however, can lead to different cell behavior, in regard to differentiation and vascular network formation, by combining different molecular and biomechanical clues. Our results motivate further studies on how hydrogels derived from different matrices (beyond cardiovascular tissue) can guide the behavior of different cell types.

DATA AVAILABILITY STATEMENT

The datasets generated for this study are available on request to the corresponding author.

AUTHOR CONTRIBUTIONS

GL and TL: conceptualization, data curation, formal analysis, investigation, methodology, writing—original draft, and writing—review and editing. SM, VS, VT, and JD: investigation. PS and LM: supervision, validation, and writing—review and editing. MH: conceptualization, funding acquisition, project administration, resources, supervision, validation, and writing-review and editing.

FUNDING

This study was financed in part by the Coordenação de Aperfeiçoamento de Pessoal de Nível Superior—Brasil (CAPES)—Finance Code 001.

SUPPLEMENTARY MATERIAL

The Supplementary Material for this article can be found online at: https://www.frontiersin.org/articles/10.3389/fbioe.2020.00520/full#supplementary-material

REFERENCES

Adam Young, D., Ibrahim, D. O., Hu, D., and Christman, K. L. (2011). Injectable hydrogel scaffold from decellularized human lipoaspirate. *Acta Biomater.* 7, 1040–1049. doi: 10.1016/j.actbio.2010.09.035

Agrawal, V., Tottey, S., Johnson, S. A., Freund, J. M., Siu, B. F., and Badylak, S. F. (2011). Recruitment of progenitor cells by an extracellular matrix cryptic peptide in a mouse model of digit amputation. *Tissue Eng. Part A* 17, 2435–2443. doi: 10.1089/ten.TEA.2011.0036

Albig, A. R., and Schiemann, W. P. (2005). Fibulin-5 function during tumorigenesis. *Future Oncol.* 1, 23–35. doi: 10.1517/14796694.1.1.23

Atsawasuwan, P., Mochida, Y., Katafuchi, M., Kaku, M., Fong, K. S. K., Csiszar, K., et al. (2008). Lysyl oxidase binds transforming growth factor-β and regulates its signaling via amine oxidase activity. *J. Biol. Chem.* 283, 34229–34240. doi: 10.1074/jbc.M803142200

Bauer, A., Gu, L., Kwee, B., Li, W. A., Dellacherie, M., Celiz, A. D., et al. (2017). Hydrogel substrate stress-relaxation regulates the spreading and proliferation of mouse myoblasts. *Acta Biomater.* 62, 82–90. doi: 10.1016/j.actbio.2017.08.041

Bausch, A. R., Möller, W., and Sackmann, E. (1999). Measurement of local viscoelasticity and forces in living cells by magnetic tweezers. *Biophys. J.* 76, 573–579. doi: 10.1016/S0006-3495(99)77225-5

Beqaj, S., Jakkaraju, S., Mattingly, R. R., Pan, D., and Schuger, L. (2002). High RhoA activity maintains the undifferentiated mesenchymal cell phenotype, whereas RhoA down-regulation by laminin-2 induces smooth muscle myogenesis. *J. Cell Biol.* 156, 893–903. doi: 10.1083/jcb.200107049

Brown, B. N., and Badylak, S. F. (2014). Extracellular matrix as an inductive scaffold for functional tissue reconstruction. *Transl. Res.* 163, 268–285. doi: 10.1016/j.trsl.2013.11.003

Califano, J. P., and Reinhart-King, C. A. (2008). A balance of substrate mechanics and matrix chemistry regulates endothelial cell network assembly. *Cell. Mol. Bioeng.* 1, 122–132. doi: 10.1007/s12195-008-0022-x

Califano, J. P., and Reinhart-King, C. A. (2009). The effects of substrate elasticity on endothelial cell network formation and traction force generation. *Conf. Proc. IEEE Eng. Med. Biol. Soc.* 2009, 3343–3345. doi: 10.1109/IEMBS.2009.5333194

Cameron, A. R., Frith, J. E., and Cooper-White, J. J. (2011). The influence of substrate creep on mesenchymal stem cell behaviour and phenotype. *Biomaterials* 32, 5979–5993. doi: 10.1016/j.biomaterials.2011.04.003

Cameron, A. R., Frith, J. E., Gomez, G. A., Yap, A. S., and Cooper-White, J. J. (2014). The effect of time-dependent deformation of viscoelastic hydrogels on myogenic induction and Rac1 activity in mesenchymal stem cells. *Biomaterials* 35, 1857–1868. doi: 10.1016/j.biomaterials.2013.11.023

Carthy, J. M., Meredith, A. J., Boroomand, S., Abraham, T., Luo, Z., Knight, D., et al. (2015). Versican V1 overexpression induces a myofibroblast-like phenotype in cultured fibroblasts. *PLoS ONE* 10:e0133056. doi: 10.1371/journal.pone.0133056

Cense, A. W., Peeters, E. A. G., Gottenbos, B., Baaijens, F. P. T., Nuijs, A. M., and van Dongen, M. E. H. (2006). Mechanical properties and failure of *Streptococcus mutans* biofilms, studied using a microindentation device. *J. Microbiol. Methods* 67, 463–472. doi: 10.1016/j.mimet.2006.04.023

Charrier, E. E., Pogoda, K., Wells, R. G., and Janmey, P. A. (2018). Control of cell morphology and differentiation by substrates with independently tunable elasticity and viscous dissipation. *Nat. Commun.* 9:449. doi: 10.1038/s41467-018-02906-9

Chaudhuri, O., Gu, L., Darnell, M., Klumpers, D., Bencherif, S. A., Weaver, J. C., et al. (2015). Substrate stress relaxation regulates cell spreading. *Nat. Commun.* 6:6364. doi: 10.1038/ncomms7365

Chaudhuri, O., Gu, L., Klumpers, D., Darnell, M., Bencherif, S. A., Weaver, J. C., et al. (2016). Hydrogels with tunable stress relaxation regulate stem cell fate and activity. *Nat. Mater.* 15, 326–334. doi: 10.1038/nmat4489

Chen, Q., Sivakumar, P., Barley, C., Peters, D. M., Gomes, R. R., Farach-Carson, M. C., et al. (2007). Potential role for heparan sulfate proteoglycans in regulation of transforming growth factor-beta (TGF-beta) by modulating assembly of latent TGF-beta-binding protein-1. *J. Biol. Chem.* 282, 26418–26430. doi: 10.1074/jbc.M703341200

Choocheep, K., Hatano, S., Takagi, H., Watanabe, H., Kimata, K., Kongtawelert, P., et al. (2010). Versican facilitates chondrocyte differentiation and regulates joint morphogenesis. *J. Biol. Chem.* 285, 21114–21125. doi: 10.1074/jbc.M109.096479

Cigliano, A., Gandaglia, A., Lepedda, A. J., Zinellu, E., Naso, F., Gastaldello, A., et al. (2012). Fine structure of glycosaminoglycans from fresh and decellularized porcine cardiac valves and pericardium. *Biochem. Res. Int.* 2012:979351. doi: 10.1155/2012/979351

Conklin, B. S., Richter, E. R., Kreutziger, K. L., Zhong, D.-S., and Chen, C. (2002). Development and evaluation of a novel decellularized vascular xenograft. *Med. Eng. Phys.* 24, 173–183. doi: 10.1016/s1350-4533(02)00010-3

Crapo, P. M., Gilbert, T. W., and Badylak, S. F. (2011). An overview of tissue and whole organ decellularization processes. *Biomaterials* 32, 3233–3243. doi: 10.1016/j.biomaterials.2011.01.057

Cross, V. L., Zheng, Y., Won Choi, N., Verbridge, S. S., Sutermaster, B. A., Bonassar, L. J., et al. (2010). Dense type I collagen matrices that support cellular remodeling and microfabrication for studies of tumor angiogenesis and vasculogenesis *in vitro*. *Biomaterials* 31, 8596–8607. doi: 10.1016/j.biomaterials.2010.07.072

Dahl, S. L. M., Koh, J., Prabhakar, V., and Niklason, L. E. (2003). Decellularized native and engineered arterial scaffolds for transplantation. *Cell Transplant.* 12, 659–666.

Danielpour, D., Kim, K. Y., Dart, L. L., Watanabe, S., Roberts, A. B., and Sporn, M. B. (1989). Sandwich enzyme-linked immunosorbent assays (SELISAs) quantitate and distinguish two forms of transforming growth factor-beta (TGF-beta 1 and TGF-beta 2) in complex biological fluids. *Growth Factors* 2, 61–71. doi: 10.3109/08977198909069082

DeQuach, J. A., Lin, J. E., Cam, C., Hu, D., Salvatore, M. A., Sheikh, F., et al. (2012). Injectable skeletal muscle matrix hydrogel promotes neovascularization and muscle cell infiltration in a hindlimb ischemia model. *Eur. Cell. Mater.* 23, 400–412. doi: 10.22203/ecm.v023a31

Du, W. J., Chi, Y., Yang, Z. X., Li, Z. J., Cui, J. J., Song, B. Q., et al. (2016). Heterogeneity of proangiogenic features in mesenchymal stem cells derived from bone marrow, adipose tissue, umbilical cord, and placenta. *Stem Cell Res. Ther.* 7:163. doi: 10.1186/s13287-016-0418-9

Duan, Y., Liu, Z., O'Neill, J., Wan, L. Q., Freytes, D. O., and Vunjak-Novakovic, G. (2011). Hybrid gel composed of native heart matrix and collagen induces cardiac differentiation of human embryonic stem cells without supplemental growth factors. *J. Cardiovasc. Transl. Res.* 4, 605–615. doi: 10.1007/s12265-011-9304-0

Dziki, J. L., Huleihel, L., Scarritt, M. E., and Badylak, S. F. (2017). Extracellular matrix bioscaffolds as immunomodulatory biomaterials. *Tissue Eng. Part A 23*, 1152–1159. doi: 10.1089/ten.TEA.2016.0538

Efraim, Y., Sarig, H., Cohen Anavy, N., Sarig, U., de Berardinis, E., Chaw, S.-Y., et al. (2017). Biohybrid cardiac ECM-based hydrogels improve long term cardiac function post myocardial infarction. Acta Biomater. 50, 220-233. doi: 10.1016/j.actbio.2016.12.015

Engler, A. J., Sen, S., Sweeney, H. L., and Discher, D. E. (2006). Matrix elasticity directs stem cell lineage specification. *Cell* 126, 677–689. doi: 10.1016/j.cell.2006.06.044

Esko, J. D. H., Prestegard, J., and Linhardt, R. J. (2017). "Proteins that bind sulfated glycosaminoglycans," in *Essentials of Glycobiology,* eds A. Varki, R. D. Cummings, J. D. Esko, P. Stanley, G. W. Hart, M. Aebi, A. G. Darvill, T. Kinoshita, N. H. Packer, J. H. Prestegard, R. L. Schnaar, and P. H. Seeberger (Cold Spring Harbor, NY: Cold Spring Harbor Laboratory Press).

Even-Ram, S., Artym, V., and Yamada, K. M. (2006). Matrix control of stem cell fate. *Cell* 126, 645–647. doi: 10.1016/j.cell.2006.08.008

Farndale, R. W., Sayers, C. A., and Barrett, A. J. (1982). A direct spectrophotometric microassay for sulfated glycosaminoglycans in cartilage cultures. *Connect. Tissue Res.* 9, 247–248. doi: 10.3109/03008208209160269

Fercana, G. R., Yerneni, S., Billaud, M., Hill, J. C., VanRyzin, P., Richards, T. D., et al. (2017). Perivascular extracellular matrix hydrogels mimic native matrix microarchitecture and promote angiogenesis via basic fibroblast growth factor. *Biomaterials.* 123, 142–154. doi: 10.1016/j.biomaterials.2017.01.037

Fu, Y., Fan, X., Tian, C., Luo, J., Zhang, Y., Deng, L., et al. (2016). Decellularization of porcine skeletal muscle extracellular matrix for the formulation of a matrix hydrogel: a preliminary study. *J. Cell. Mol. Med.* 20, 740–749. doi: 10.1111/jcmm.12776

Gacheru, S. N., Thomas, K. M., Murray, S. A., Csiszar, K., Smith-Mungo, L. I., and Kagan, H. M. (1997). Transcriptional and post-transcriptional control of lysyl oxidase expression in vascular smooth muscle cells: effects of TGF-beta 1 and serum deprivation. *J. Cell. Biochem.* 65, 395–407. doi: 10.1002/(sici)1097-4644(19970601)65:3<395::aid-jcb9>3.0.co;2-n

Grover, G. N., Rao, N., and Christman, K. L. (2014). Myocardial matrix-polyethylene glycol hybrid hydrogels for tissue engineering. *Nanotechnology.* 25:014011. doi: 10.1088/0957-4484/25/1/014011

Hajmousa, G., Przybyt, E., Pfister, F., Paredes-Juarez, G. A., Moganti, K., Busch, S., et al. (2018). Human adipose tissue-derived stromal cells act as functional pericytes in mice and suppress high-glucose-induced proinflammatory activation of bovine retinal endothelial cells. *Diabetologia* 61, 2371–2385. doi: 10.1007/s00125-018-4713-0

Hashimoto, J., Kariya, Y., and Miyazaki, K. (2006). Regulation of proliferation and chondrogenic differentiation of human mesenchymal stem cells by laminin-5 (laminin-332). *Stem Cells* 24, 2346–2354. doi: 10.1634/stemcells.2005-0605

Hildebrand, A., Romarís, M., Rasmussen, L. M., Heinegård, D., Twardzik, D. R., Border, W. A., et al. (1994). Interaction of the small interstitial proteoglycans biglycan, decorin and fibromodulin with transforming growth factor beta. *Biochem. J. 302(Pt 2),* 527–534. doi: 10.1042/bj3020527

Hirai, M., Horiguchi, M., Ohbayashi, T., Kita, T., Chien, K. R., and Nakamura, T. (2007). Latent TGF-β-binding protein 2 binds to DANCE/fibulin-5 and regulates elastic fiber assembly. *EMBO J.* 26, 3283–3295. doi: 10.1038/sj.emboj.7601768

Hoshiba, T., Chen, G., Endo, C., Maruyama, H., Wakui, M., Nemoto, E., et al. (2016). Decellularized extracellular matrix as an In Vitro model to study the comprehensive roles of the ECM in stem cell differentiation. *Stem Cells Int.* 2016:6397820. doi: 10.1155/2016/6397820

Hoshiba, T., Lu, H., Kawazoe, N., and Chen, G. (2010). Decellularized matrices for tissue engineering. *Expert Opin. Biol. Ther.* 10, 1717–1728. doi: 10.1517/14712598.2010.534079

Hrebikova, H., Diaz, D., and Mokry, J. (2015). Chemical decellularization: a promising approach for preparation of extracellular matrix. *Biomed. Pap. Med. Fac. Univ. Palacky Olomouc Czech. Repub.* 159, 12–17. doi: 10.5507/bp.2013.076

Jang, J., Park, H.-J., Kim, S.-W., Kim, H., Park, J. Y., Na, S. J., et al. (2017). 3D printed complex tissue construct using stem cell-laden decellularized extracellular matrix bioinks for cardiac repair. *Biomaterials.* 112, 264–274. doi: 10.1016/j.biomaterials.2016.10.026

Johnson, T. D., Braden, R. L., and Christman, K. L. (2014). Injectable ECM scaffolds for cardiac repair. *Methods Mol. Biol.* 1181, 109–120. doi: 10.1007/978-1-4939-1047-2_10

Johnson, T. D., Lin, S. Y., and Christman, K. L. (2011). Tailoring material properties of a nanofibrous extracellular matrix derived hydrogel. *Nanotechnology.* 22:494015. doi: 10.1088/0957-4484/22/49/494015

Kappler, B., Anic, P., Becker, M., Bader, A., Klose, K., Klein, O., et al. (2016). The cytoprotective capacity of processed human cardiac extracellular matrix. *J. Mater. Sci. Mater. Med.* 27:120. doi: 10.1007/s10856-016-5730-5

Kawecki, M., Łabuś, W., Klama-Baryla, A., Kitala, D., Kraut, M., Glik, J., et al. (2018). A review of decellurization methods caused by an urgent need for quality control of cell-free extracellular matrix' scaffolds and their role in regenerative medicine. *J. Biomed. Mater. Res. B Appl. Biomater.* 106, 909–923. doi: 10.1002/jbm.b.33865

Keane, T. J., Swinehart, I. T., and Badylak, S. F. (2015). Methods of tissue decellularization used for preparation of biologic scaffolds and in vivo relevance. *Methods.* 84, 25–34. doi: 10.1016/j.ymeth.2015.03.005

Klees, R. F., Salasznyk, R. M., Kingsley, K., Williams, W. A., Boskey, A., and Plopper, G. E. (2005). Laminin-5 induces osteogenic gene expression in human mesenchymal stem cells through an ERK-dependent pathway. *Mol. Biol. Cell* 16, 881–890. doi: 10.1091/mbc.e04-08-0695

Klees, R. F., Salasznyk, R. M., Ward, D. F., Crone, D. E., Williams, W. A., Harris, M. P., et al. (2008). Dissection of the osteogenic effects of laminin-332 utilizing specific LG domains: LG3 induces osteogenic differentiation, but not mineralization. *Exp. Cell Res.* 314, 763–773. doi: 10.1016/j.yexcr.2007.12.007

Krump-Konvalinkova, V., Bittinger, F., Unger, R. E., Peters, K., Lehr, H.-A., and James Kirkpatrick, C. (2001). Generation of human pulmonary microvascular endothelial cell lines. *Lab. Invest.* 81, 1717–1727. doi: 10.1038/labinvest.3780385

Leonel, L. C. P. C., Miranda, C. M. F. C., Coelho, T. M., Ferreira, G. A. S., Caãada, R. R., Miglino, M. A., et al. (2017). Decellularization of placentas: establishing a protocol. *Braz. J. Med. Biol. Res.* 51:e6382. doi: 10.1590/1414-431X20176382

Liguori, G. R., Jeronimus, B. F., de Aquinas Liguori, T. T., Moreira, L. F. P., and Harmsen, M. C. (2017). Ethical issues in the use of animal models for tissue engineering: reflections on legal aspects, moral theory, three Rs strategies, and harm-benefit analysis. *Tissue Eng. Part C Methods* 23, 850–862. doi: 10.1089/ten.tec.2017.0189

Liguori, G. R., Zhou, Q., Liguori, T. T. A., Barros, G. G., Kühn, P. T., Moreira, L. F. P., et al. (2019). Directional topography influences adipose mesenchymal stromal cell plasticity: prospects for tissue engineering and fibrosis. *Stem Cells Int.* 2019:5387850. doi: 10.1155/2019/5387850

Lin, H.-Y., Tsai, C.-C., Chen, L.-L., Chiou, S.-H., Wang, Y.-J., and Hung, S.-C. (2010). Fibronectin and laminin promote differentiation of human mesenchymal stem cells into insulin producing cells through activating Akt and ERK. *J. Biomed. Sci.* 17:56. doi: 10.1186/1423-0127-17-56

Mao, A. S., Shin, J.-W., and Mooney, D. J. (2016). Effects of substrate stiffness and cell-cell contact on mesenchymal stem cell differentiation. *Biomaterials* 98, 184–191. doi: 10.1016/j.biomaterials.2016.05.004

McCloy, R. A., Rogers, S., Caldon, C. E., Lorca, T., Castro, A., and Burgess, A. (2014). Partial inhibition of Cdk1 in G 2 phase overrides the SAC and decouples mitotic events. *Cell Cycle* 13, 1400–1412. doi: 10.4161/cc.28401

McKinnon, D. D., Domaille, D. W., Cha, J. N., and Anseth, K. S. (2013). Biophysically defined and cytocompatible covalently adaptable networks as viscoelastic 3D cell culture systems. *Adv. Mater.* 26, 865–872. doi: 10.1002/adma.201303680

Mercuri, J. J., Patnaik, S., Dion, G., Gill, S. S., Liao, J., and Simionescu, D. T. (2013). Regenerative potential of decellularized porcine nucleus pulposus hydrogel scaffolds: stem cell differentiation, matrix remodeling, and biocompatibility studies. *Tissue Eng. Part A* 19, 952–966. doi: 10.1089/ten.TEA.2012.0088

Mittag, F., Falkenberg, E.-M., Janczyk, A., Götze, M., Felka, T., Aicher, W. K., et al. (2012). Laminin-5 and type I collagen promote adhesion and osteogenic differentiation of animal serum-free expanded human mesenchymal stromal cells. *Orthop. Rev.* 4:e36. doi: 10.4081/or.2012.e36

Mruthyunjaya, S., Manchanda, R., Godbole, R., Pujari, R., Shiras, A., and Shastry, P. (2010). Laminin-1 induces neurite outgrowth in human mesenchymal stem cells in serum/differentiation factors-free conditions through activation of FAK-MEK/ERK signaling pathways. *Biochem. Biophys. Res. Commun.* 391, 43–48. doi: 10.1016/j.bbrc.2009.10.158

Muiznieks, L. D., and Keeley, F. W. (2013). Molecular assembly and mechanical properties of the extracellular matrix: a fibrous protein perspective. *Biochim. Biophys. Acta* 1832, 866–875. doi: 10.1016/j.bbadis.2012.11.022

Nakamura, R., Nakamura, F., and Fukunaga, S. (2014). Contrasting effect of perlecan on adipogenic and osteogenic differentiation of mesenchymal stem cells *in vitro*. *Anim. Sci. J.* 85, 262–270. doi: 10.1111/asj.12116

Naugle, J. E., Olson, E. R., Zhang, X., Mase, S. E., Pilati, C. F., Maron, M. B., et al. (2006). Type VI collagen induces cardiac myofibroblast differentiation: implications for postinfarction remodeling. *Am. J. Physiol. Heart Circ. Physiol.* 290, H323–H330. doi: 10.1152/ajpheart.00321.2005

Nibourg, L. M., Sharma, P. K., van Kooten, T. G., and Koopmans, S. A. (2015). Changes in lens stiffness due to capsular opacification in accommodative lens refilling. *Exp. Eye Res.* 134, 148–154. doi: 10.1016/j.exer.2015.02.015

Oida, T., and Weiner, H. L. (2010). Depletion of TGF-β from fetal bovine serum. *J. Immunol. Methods* 362, 195–198. doi: 10.1016/j.jim.2010.09.008

O'Neill, J. D., Freytes, D. O., Anandappa, A. J., Oliver, J. A., and Vunjak-Novakovic, G. V. (2013). The regulation of growth and metabolism of kidney stem cells with regional specificity using extracellular matrix derived from kidney. *Biomaterials.* 34, 9830–9841. doi: 10.1016/j.biomaterials.2013.09.022

Park, J. S., Chu, J. S., Tsou, A. D., Diop, R., Tang, Z., Wang, A., et al. (2011). The Effect of matrix stiffness on the differentiation of mesenchymal stem cells in response to TGF-β. *Biomaterials* 32, 3921-3930. doi: 10.1016/j.biomaterials.2011.02.019

Petersen, T. H., Calle, E. A., Colehour, M. B., and Niklason, L. E. (2012). Matrix composition and mechanics of decellularized lung scaffolds. *Cells Tissues Organs*. 195, 222–231. doi: 10.1159/000324896

Peterson, B. W., van der Mei, H. C., Sjollema, J., Busscher, H. J., and Sharma, P. K. (2013). A distinguishable role of eDNA in the viscoelastic relaxation of biofilms. *MBio* 4:e00497-13. doi: 10.1128/mBio.00497-13

Pok, S., Benavides, O. M., Hallal, P., and Jacot, J. G. (2014). Use of myocardial matrix in a chitosan-based full-thickness heart patch. *Tissue Eng. Part A* 20, 1877–1887. doi: 10.1089/ten.TEA.2013.0620

Poornejad, N., Schaumann, L. B., Buckmiller, E. M., Momtahan, N., Gassman, J. R., Ma, H. H., et al. (2016). The impact of decellularization agents on renal tissue extracellular matrix. *J. Biomater. Appl.* 31, 521–533. doi: 10.1177/0885328216656099

Rehman, J., Traktuev, D., Li, J., Merfeld-Clauss, S., Temm-Grove, C. J., Bovenkerk, J. E., et al. (2004). Secretion of angiogenic and antiapoptotic factors by human adipose stromal cells. *Circulation* 109, 1292–1298. doi: 10.1161/01.CIR.0000121425.42966.F1

Reinboth, B., Hanssen, E., Cleary, E. G., and Gibson, M. A. (2002). Molecular interactions of biglycan and decorin with elastic fiber components: biglycan forms a ternary complex with tropoelastin and microfibril-associated glycoprotein 1. *J. Biol. Chem.* 277, 3950–3957. doi: 10.1074/jbc.M109540200

Reing, J. E., Zhang, L., Myers-Irvin, J., Cordero, K. E., Freytes, D. O., Heber-Katz, E., et al. (2009). Degradation products of extracellular matrix affect cell migration and proliferation. *Tissue Eng. Part A* 15, 605–614. doi: 10.1089/ten.tea.2007.0425

Robertson, I. B., Horiguchi, M., Zilberberg, L., Dabovic, B., Hadjiolova, K., and Rifkin, D. B. (2015). Latent TGF-β-binding proteins. *Matrix Biol.* 47, 44–53. doi: 10.1016/j.matbio.2015.05.005

Rühl, M., Johannsen, M., Atkinson, J., Manski, D., Sahin, E., Somasundaram, R., et al. (1999). Soluble collagen VI induces tyrosine phosphorylation of paxillin and focal adhesion kinase and activates the MAP kinase erk2 in fibroblasts. *Exp. Cell Res.* 250, 548–557. doi: 10.1006/excr.1999.4540

Russo, V., Omidi, E., Samani, A., Hamilton, A., and Flynn, L. E. (2015). Porous, ventricular extracellular matrix-derived foams as a platform for cardiac cell culture. *Biores. Open Access* 4, 374–388. doi: 10.1089/biores.2015.0030

Saldin, L. T., Cramer, M. C., Velankar, S. S., White, L. J., and Badylak, S. F. (2017). Extracellular matrix hydrogels from decellularized tissues: structure and function. *Acta Biomater.* 49, 1–15. doi: 10.1016/j.actbio.2016.11.068

Schaap-Oziemlak, A. M., Kühn, P. T., van Kooten, T. G., and van Rijn, P. (2014). Biomaterial–stem cell interactions and their impact on stem cell response. *RSC Adv.* 4, 53307–53320. doi: 10.1039/C4RA07915A

Schenke-Layland, K., Vasilevski, O., Opitz, F., König, K., Riemann, I., Halbhuber, K. J., et al. (2003). Impact of decellularization of xenogeneic tissue on extracellular matrix integrity for tissue engineering of heart valves. *J. Struct. Biol.* 143, 201–208. doi: 10.1016/j.jsb.2003.08.002

Seif-Naraghi, S., Singelyn, J., Dequach, J., Schup-Magoffin, P., and Christman, K. (2010). Fabrication of biologically derived injectable materials for myocardial tissue engineering. *J. Vis. Exp.* 46:e2109 doi: 10.3791/2109

Seif-Naraghi, S. B., Horn, D., Schup-Magoffin, P. J., and Christman, K. L. (2012). Injectable extracellular matrix derived hydrogel provides a platform for enhanced retention and delivery of a heparin-binding growth factor. *Acta Biomater.* 8, 3695–3703. doi: 10.1016/j.actbio.2012.06.030

Seki, S., Kawaguchi, Y., Chiba, K., Mikami, Y., Kizawa, H., Oya, T., et al. (2005). A functional SNP in CILP, encoding cartilage intermediate layer protein, is associated with susceptibility to lumbar disc disease. *Nat. Genet.* 37, 607–612. doi: 10.1038/ng1557

Sengle, G., Ono, R. N., Sasaki, T., and Sakai, L. Y. (2011). Prodomains of transforming growth factor beta (TGFbeta) superfamily members specify different functions: extracellular matrix interactions and growth factor bioavailability. *J. Biol. Chem.* 286, 5087–5099. doi: 10.1074/jbc.M110.188615

Seo, Y., Jung, Y., and Kim, S. H. (2018). Decellularized heart ECM hydrogel using supercritical carbon dioxide for improved angiogenesis. *Acta Biomater.* 67, 270–281. doi: 10.1016/j.actbio.2017.11.046

Shanley, C. J., Gharaee-Kermani, M., Sarkar, R., Welling, T. H., Kriegel, A., Ford, J. W., et al. (1997). Transforming growth factor-beta 1 increases lysyl oxidase enzyme activity and mRNA in rat aortic smooth muscle cells. *J. Vasc. Surg.* 25, 446–452. doi: 10.1016/S0741-5214(97)70254-4

Sharma, P. K., Busscher, H. J., Terwee, T., Koopmans, S. A., and van Kooten, T. G. (2011). A comparative study on the viscoelastic properties of human and animal lenses. *Exp. Eye Res.* 93, 681–688. doi: 10.1016/j.exer.2011.08.009

Singelyn, J. M., DeQuach, J. A., Seif-Naraghi, S. B., Littlefield, R. B., Schup-Magoffin, P. J., and Christman, K. L. (2009). Naturally derived myocardial matrix as an injectable scaffold for cardiac tissue engineering. *Biomaterials.* 30, 5409–5416. doi: 10.1016/j.biomaterials.2009.06.045

Singelyn, J. M., Sundaramurthy, P., Johnson, T. D., Schup-Magoffin, P. J., Hu, D. P., Faulk, D. M., et al. (2012). Catheter-deliverable hydrogel derived from decellularized ventricular extracellular matrix increases endogenous cardiomyocytes and preserves cardiac function post-myocardial infarction. *J. Am. Coll. Cardiol.* 59, 751–763. doi: 10.1016/j.jacc.2011.10.888

Smeriglio, P., Lee, J., and Bhutani, N. (2017). Soluble Collagen VI treatment enhances mesenchymal stem cells expansion for engineering cartilage. *Bioeng. Transl. Med.* 2, 278–284. doi: 10.1002/btm2.10078

Stamati, K., Priestley, J. V., Mudera, V., and Cheema, U. (2014). Laminin promotes vascular network formation in 3D *in vitro* collagen scaffolds by regulating VEGF uptake. *Exp. Cell Res.* 327, 68–77. doi: 10.1016/j.yexcr.2014.05.012

Stoppel, W. L., Gao, A. E., Greaney, A. M., Partlow, B. P., Bretherton, R. C., Kaplan, D. L., et al. (2016). Elastic, silk-cardiac extracellular matrix hydrogels exhibit time-dependent stiffening that modulates cardiac fibroblast response. *J. Biomed. Mater. Res. A* 104, 3058–3072. doi: 10.1002/jbm.a.35850

Terlizzi, V., Kolibabka, M., Burgess, J. K., Hammes, H. P., and Harmsen, M. C. (2018). The pericytic phenotype of adipose tissue-derived stromal cells is promoted by NOTCH2. *Stem Cells* 36, 240–251. doi: 10.1002/stem.2726

Timpl, R., Sasaki, T., Kostka, G., and Chu, M.-L. (2003). Fibulins: a versatile family of extracellular matrix proteins. *Nat. Rev. Mol. Cell Biol.* 4, 479–489. doi: 10.1038/nrm1130

Tuin, A., Kluijtmans, S. G., Bouwstra, J. B., Harmsen, M. C., and Van Luyn, M. J. A. (2010). Recombinant gelatin microspheres: novel formulations for tissue repair? *Tissue Eng. Part A* 16, 1811–1821. doi: 10.1089/ten.tea.2009.0592

Twomey, J. D., Thakore, P. I., Hartman, D. A., Myers, E. G. H., and Hsieh, A. H. (2014). Roles of type VI collagen and decorin in human mesenchymal stem cell biophysics during chondrogenic differentiation. *Eur. Cell. Mater. 27, 237–50; discussion* 249–50. doi: 10.22203/eCM.v027a17

Ungerleider, J. L., Johnson, T. D., Hernandez, M. J., Elhag, D. I., Braden, R. L., Dzieciatkowska, M., et al. (2016). Extracellular matrix hydrogel promotes tissue remodeling, arteriogenesis, and perfusion in a rat hindlimb ischemia model. *JACC Basic Transl. Sci.* 1, 32–44. doi: 10.1016/j.jacbts.2016.01.009

Ungerleider, J. L., Johnson, T. D., Rao, N., and Christman, K. L. (2015). Fabrication and characterization of injectable hydrogels derived from decellularized skeletal and cardiac muscle. *Methods.* 84, 53–59. doi: 10.1016/j.ymeth.2015.03.024

van Nieuwenhoven, F. A., Munts, C., Op't Veld, R. C., González, A., Díez, J., Heymans, S., et al. (2017). Cartilage intermediate layer protein 1 (CILP1): a novel mediator of cardiac extracellular matrix remodelling. *Sci. Rep.* 7:16042. doi: 10.1038/s41598-017-16201-y

Varki, A., Cummings, R., Esko, J., Freeze, H., Hart, G., and Marth, J. (1999). "Chapter 29: glycosaminoglycan-binding proteins," in *Essentials of Glycobiology,* eds A. Varki, R. D. Cummings, J. D. Esko, P. Stanley, G. W. Hart, M. Aebi, A. G. Darvill, T. Kinoshita, N. H. Packer, J. H. Prestegard, R. L. Schnaar, and P. H. Seeberger (Cold Spring Harbor, NY: Cold Spring Harbor Laboratory Press).

Volk, S. W., Wang, Y., Mauldin, E. A., Liechty, K. W., and Adams, S. L. (2011). Diminished type III collagen promotes myofibroblast differentiation and increases scar deposition in cutaneous wound healing. *Cells Tissues Organs* 194, 25–37. doi: 10.1159/000322399

Wang, R. M., Johnson, T. D., He, J., Rong, Z., Wong, M., Nigam, V., et al. (2017). Humanized mouse model for assessing the human immune response to xenogeneic and allogeneic decellularized biomaterials. *Biomaterials.* 129, 98–110. doi: 10.1016/j.biomaterials.2017.03.016

Wassenaar, J. W., Braden, R. L., Osborn, K. G., and Christman, K. L. (2016a). Modulating in vivo degradation rate of injectable extracellular matrix hydrogels. *J. Mater. Chem. B* 4, 2794–2802. doi: 10.1039/C5TB02564H

Wassenaar, J. W., Gaetani, R., Garcia, J. J., Braden, R. L., Luo, C. G., Huang, D., et al. (2016b). Evidence for mechanisms underlying the functional benefits of a myocardial matrix hydrogel for post-mi treatment. *J. Am. Coll. Cardiol.* 67, 1074–1086. doi: 10.1016/j.jacc.2015.12.035

Wells, R. G. (2008). The role of matrix stiffness in regulating cell behavior. *Hepatology* 47, 1394–1400. doi: 10.1002/hep.22193

Wolf, M. T., Daly, K. A., Brennan-Pierce, E. P., Johnson, S. A., Carruthers, C. A., D'Amore, A., et al. (2012). A hydrogel derived from decellularized dermal extracellular matrix. *Biomaterials.* 33, 7028–7038. doi: 10.1016/j.biomaterials.2012.06.051

Wu, J., Ding, Q., Dutta, A., Wang, Y., Huang, Y.-H., Weng, H., et al. (2015). An injectable extracellular matrix derived hydrogel for meniscus repair and regeneration. *Acta Biomater.* 16, 49–59. doi: 10.1016/j.actbio.2015.01.027

Ye, K., Cao, L., Li, S., Yu, L., and Ding, J. (2015). Interplay of matrix stiffness and cell–cell contact in regulating differentiation of stem cells. *ACS Appl. Mater. Interf.* 8, 21903–21913. doi: 10.1021/acsami.5b09746

Zacchigna, L., Vecchione, C., Notte, A., Cordenonsi, M., Dupont, S., Maretto, S., et al. (2006). Emilin1 links TGF-beta maturation to blood pressure homeostasis. *Cell* 124, 929–942. doi: 10.1016/j.cell.2005.12.035

Zanetti, M., Braghetta, P., Sabatelli, P., Mura, I., Doliana, R., Colombatti, A., et al. (2004). EMILIN-1 deficiency induces elastogenesis and vascular cell defects. *Mol. Cell. Biol.* 24, 638–650. doi: 10.1128/MCB.24.2.638-650.2004

Zhang, C.-L., Zhao, Q., Liang, H., Qiao, X., Wang, J.-Y., Wu, D., et al. (2018). Cartilage intermediate layer protein-1 alleviates pressure overload-induced cardiac fibrosis via interfering TGF-β1 signaling. *J. Mol. Cell. Cardiol.* 116, 135–144. doi: 10.1016/j.yjmcc.2018.02.006

Conflict of Interest: The authors declare that the research was conducted in the absence of any commercial or financial relationships that could be construed as a potential conflict of interest.

Copyright © 2020 Liguori, Liguori, de Moraes, Sinkunas, Terlizzi, van Dongen, Sharma, Moreira and Harmsen. This is an open-access article distributed under the terms of the Creative Commons Attribution License (CC BY). The use, distribution or reproduction in other forums is permitted, provided the original author(s) and the copyright owner(s) are credited and that the original publication in this journal is cited, in accordance with accepted academic practice. No use, distribution or reproduction is permitted which does not comply with these terms.

frontiers in Bioengineering and Biotechnology

BRIEF RESEARCH REPORT
published: 05 June 2020
doi: 10.3389/fbioe.2020.00529

MicroRNA-Mediated Direct Reprogramming of Human Adult Fibroblasts Toward Cardiac Phenotype

*C. Paoletti[1], C. Divieto[2], G. Tarricone[1], F. Di Meglio[3], D. Nurzynska[3] and V. Chiono[1]**

[1] Department of Mechanical and Aerospace Engineering, Politecnico di Torino, Turin, Italy, [2] Istituto Nazionale di Ricerca Metrologica, Advanced Materials Metrology and Life Science, Turin, Italy, [3] Department of Public Health, University of Naples Federico II, Naples, Italy

Modulation of microRNA expression holds the promise to achieve direct reprogramming of fibroblasts into cardiomyocyte-like cells as a new strategy for myocardial regeneration after ischemic heart disease. Previous reports have shown that murine fibroblasts can be directly reprogrammed into induced cardiomyocytes (iCMs) by transient transfection with four microRNA mimics (miR-1, 133, 208, and 499, termed "miRcombo"). Hence, study on the effect of miRcombo transfection on adult human cardiac fibroblasts (AHCFs) deserves attention in the perspective of a future clinical translation of the approach. In this brief report, we studied for the first time whether miRcombo transient transfection of AHCFs by non-viral vectors might trigger direct reprogramming of AHCFs into cardiomyocyte-like cells. Initially, efficient miRNA delivery to cells was demonstrated through the use of a commercially available transfection agent (DharmaFECT1). Transient transfection of AHCFs with miRcombo was found to upregulate early cardiac transcription factors after 7 days post-transfection and cardiomyocyte specific marker cTnT after 15 days post-transfection, and to downregulate the expression of fibroblast markers at 15 days post-transfection. The percentage of cTnT-positive cells after 15 days from miRcombo transfection was ∼11%, as evaluated by flow cytometry. Furthermore, a relevant percentage of miRcombo-transfected AHCFs (∼38%) displayed spontaneous calcium transients at 30 days post-transfection. Results evidenced the role of miRcombo transfection on triggering the trans differentiation of AHCFs into iCMs. Although further investigations are needed to achieve iCM maturation, early findings from this study pave the way toward new advanced therapies for human cardiac regeneration.

Keywords: cardiac fibroblasts, direct reprogramming, cardiomyocytes, microRNAs, digital droplet PCR (ddPCR)

OPEN ACCESS

Edited by:
Paolo Madeddu,
University of Bristol, United Kingdom

Reviewed by:
Sveva Bollini,
University of Genoa, Italy
Paola Campagnolo,
University of Surrey, United Kingdom

***Correspondence:**
V. Chiono
valeria.chiono@polito.it

Specialty section:
This article was submitted to Tissue Engineering and Regenerative Medicine, a section of the journal Frontiers in Bioengineering and Biotechnology

Received: *21 August 2019*
Accepted: *04 May 2020*
Published: *05 June 2020*

Citation:
Paoletti C, Divieto C, Tarricone G, Di Meglio F, Nurzynska D and Chiono V (2020) MicroRNA-Mediated Direct Reprogramming of Human Adult Fibroblasts Toward Cardiac Phenotype. Front. Bioeng. Biotechnol. 8:529. doi: 10.3389/fbioe.2020.00529

INTRODUCTION

Myocardial infarction (MI) remains one of the leading causes of death globally. After MI, the injured area of the heart undergoes a deep tissue remodeling: cardiomyocytes (CMs) death, extracellular matrix (ECM) degradation and increased myocardial fibrosis dramatically impair cardiac function, leading to heart failure (van den Borne et al., 2010). The only available therapeutic

strategy against heart failure is heart transplantation. Hence, cardiac regeneration is still a major clinical challenge.

An ideal cardiac regenerative medicine strategy should replace lost CMs and recover myocardial contractility. Recently, efforts have been addressed at reducing the extent of cardiac fibrotic scar, as it reduces the contractile heart functionality (Talman and Ruskoaho, 2016). Direct reprogramming of fibroblasts into induced cardiomyocytes (iCMs) represents a new emerging strategy to convert cardiac fibrotic tissue into functional tissue (Bektik and Fu, 2019). Ieda et al. (2010) were the first to report direct reprogramming of mouse fibroblasts into beating iCMs through a simultaneous overexpression of GATA binding protein 4 (*GATA4*), Myocyte enhancer factor 2C (*MEF2C*), T-box 5 (*TBX5*) cardiac transcription factors (TFs) both *in vitro* and *in vivo*. Later, Song et al. (2012) added Heart and Neural Crest derivatives expressed 2 (*HAND2*) to the previous combination of cardiac TFs, increasing reprogramming efficiency of mouse fibroblasts *in vitro* and improving cardiac function of injured hearts *in vivo*. Since then, several other direct reprogramming strategies have been reported for mouse and human fibroblasts, generally based on gene therapy via viral overexpression of specific cardiac TFs (Chen et al., 2017).

Efforts are now addressed to develop a direct reprogramming method which is safe and free from ethical and technical concerns associated with genetic manipulation of cells. The use of microRNAs (miRNAs) may represent one valid strategy to induce direct reprogramming of human fibroblasts into iCMs, satisfying such requirements. miRNAs are short non-coding RNAs (of approximately 22 nucleotides) that regulate gene expression post-transcriptionally (He and Hannon, 2004). As cardiac tissue-specific miRNAs play pivotal role in cardiac development and functions, the regulation of their expression would aid in generating functional iCMs starting from human fibroblasts (Tian et al., 2017). Endogenous miRNAs can be easily overexpressed or downregulated through the administration of miRNA mimics or miRNA inhibitors, respectively (Peng et al., 2015). MiRNA mimics and inhibitors hold a great potential as therapeutic agents because of their cytoplasmic activity, relatively small size and ability to be administered systemically or locally by nanoparticle-based delivery systems, avoiding the use of viral vectors (Lee et al., 2019). Modulation of miRNAs for direct reprogramming was first proposed by Jayawardena et al. (2012), who demonstrated that a combination of four miRNA mimics (referred to as "miRcombo": miR-1, 133, 208 and 499) promotes the direct reprogramming of mouse fibroblasts into iCMs both *in vitro* and *in vivo*. The selected miRNAs are highly conserved in cardiac and skeletal tissue and have been found to regulate developmental and physiological processes in the heart (van Rooij et al., 2009; Xu et al., 2011). Furthermore, this specific set of microRNAs was found to be expressed in human embryonic stem cells-derived CMs, whereas their expression was nearly undetectable in fibroblasts (Kitchener et al., 2010).

Although the potentiality of miRcombo in reprogramming mouse fibroblasts into iCMs has been demonstrated (Jayawardena et al., 2012, 2015), the translation of miRcombo-mediated direct reprogramming from mouse to human cells is not straightforward and deserves further investigation. Indeed, human adult fibroblasts are intrinsically more resistant to direct reprogramming than mouse fibroblasts, as demonstrated by those direct reprogramming strategies, first developed on mouse fibroblasts, which failed on human fibroblasts or required substantial adjustments (Ieda et al., 2010; Nam et al., 2013).

In this brief research report, we sought to determine if miRcombo transient transfection of AHCFs was able to initiate the trans-differentiation process of AHCFs toward cardiomyocyte-like cells. After initial assessment of efficient miRNA delivery to AHCFs, cells were transfected with miRcombo, showing increased expression of cardiomyocyte markers and down-regulated expression of fibroblast markers after 7–15 days post-transfection. Moreover, miRcombo treated cells exhibited spontaneous calcium oscillation after 30 days from transfection.

Early findings presented in this brief research report pave the way toward future new advanced approaches for human cardiac regeneration, through *in situ* direct reprogramming of cardiac fibroblasts populating post-infarct scar into cardiomyocyte-like cells.

MATERIALS AND METHODS

Cell Culture

Normal human atrial cardiac fibroblasts (AHCFs) were purchased from Lonza (CC-2903; batch number: 0000662121; donor characteristics: male; 48 years old; passage number: 2) and maintained in culture using Fibroblasts Growth Medium-3 (Lonza, CC-4526) containing 10% fetal bovine serum (FBS), 1% insulin, 1% human basal fibroblast growth factor (hFGF-B) and 1% gentamicin. Cells were expanded until passage four and then used for experiments.

MiRNA Transient Transfection

AHCFs were plated either in six-well plates at 10×10^5 cells/well (for RNA isolation and flow cytometry experiments), or in 35 mm μ-dish (Ibidi) at 9×10^5 cells/well (for calcium transient analysis) in Dulbecco's Modified Eagle Medium (DMEM) High Glucose (Gibco) with 10% FBS (Sigma-Aldrich) and 1% glutamine (Sigma-Aldrich) 1 day before transfection.

To initially study miRNA internalization and mRNA target downregulation by AHCFs, cells were transfected using DharmaFECT1 (Dharmacon) with miR-1 (miR-1-3p, mirVana miRNA mimic, Life Technologies) or negmiR (Negative Control #1, mirVana miRNA Mimic, Life Technologies), at a final concentration of 25 nmol/L according to manufacturer's instructions, in DMEM High Glucose with 10% FBS and 1% L-glutamine. After 24 h, the medium was replaced with DMEM High Glucose with 15% FBS, 1% glutamine and 1% penicillin/streptomycin/ampicillin (Lonza). Culture was continued up to 48 h.

Then, AHCFs were transfected using DharmaFECT1 with miRcombo (miR-1-3p, miR-133a-3p, miR-208a-3p, and miR-499a-5p, mirVana miRNA mimic, Life Technologies) or negmiR (Negative Control #1, mirVana miRNA Mimic, Life Technologies), at a final concentration of 25 nmol/L according

to manufacturer's instructions, in DMEM High Glucose (Gibco) with 10% FBS and 1% glutamine. After 24 h, medium was replaced with DMEM High Glucose with 10% FBS, 1% glutamine and 1% penicillin/streptomycin/ampicillin (Lonza). Culture was continued up to 30 days.

RNA Isolation and Droplet Digital PCR

Total RNA was extracted using QIAzol Lysis Reagent (Qiagen) according to manufacturer's instructions. RNA concentration and quality were assessed using NanoQuant plate (Tecan Group Ltd). cDNA (200 ng) was obtained using High Capacity cDNA Reverse Transcription Kit (Applied Biosystems).

To study miR-1 uptake by cells, miRNA reverse-transcription PCR was performed using miRCURY LNA RT Kit (Qiagen) at 24 h (i.e., immediately after transfection) and 48 h (i.e., at 24 h from transfection) culture times. RNA samples were diluted to 5 ng/μl in nuclease-free water and the reaction was prepared following the manufacturer's instructions. Droplet digital PCR (ddPCR, Bio-Rad Laboratories) was performed to assess the expression of miR-1 (Hsa-miR-1-3p miRCURY LNA miRNA PCR Assay) using EvaGreen supermix (Bio-Rad Laboratories). Droplet generation was performed according to manufacturer's instructions. Thermal-cycling conditions were: 95°C for 5 min (1 cycle), 95°C for 30 s and 55°C for 1 min (40 cycles), 90°C for 5 min (1 cycle), and a 4°C infinite hold. PCR plate was loaded on Bio-Rad QX100 droplet reader for quantification of cDNA copies/μL. Analysis of the ddPCR data was performed by QuantaSoft analysis software (Bio-Rad Laboratories). No template control with water was included in each assay. Experiments were performed in triplicate and repeated three times.

Downregulation of *TWF-1* target after miR-1 transfection was analyzed at 24 h (i.e., immediately after transfection) and 48 h (i.e., at 24 h from transfection) culture times. The expression of *TWF-1* (ID assay: dHsaCPE5028122) was analyzed by ddPCR, using ddPCR supermix for probes without dUTP.

Similarly, after miRcombo or negmiR transfection, the expression of *GATA4* (ID assay: dHsaCPE5050488), *MEF2C* (ID assay: dHsaCPE5050696), *TBX5* (ID assay: dHsaCPE5048560), *HAND2* (ID assay: dHsaCPE5049426) and *NKX2.5* (ID assay: dHsaCPE5042098) was evaluated at 7 days post-transfection, while the expression of *TNNT2* (ID assay: dHsaCPE5052344), *TNNI3* (ID assay: dHsaCPE5050934), *VIM* (ID assay: dHsaCPE5032314), *DDR2* (ID assay: dHsaCPE5048156) and *FSP-1* (ID assay: dHsaCPE5042942) was assessed at 15 days post-transfection, using ddPCR supermix for probes without dUTP. Glyceraldehyde 3-phosphate dehydrogenase (*GAPDH*; ID assay: dHsaCPE5031597) was used as a housekeeping gene to perform quantitative normalization.

For *TWF-1* and cardiac markers analysis, droplet generation was performed according to manufacturer's instructions. Thermal-cycling conditions were 95°C for 10 min (1 cycle), 94°C for 30 s and 55°C for 30 s (40 cycles), 98°C for 10 min (1 cycle), and a 4°C infinite hold.

In all ddPCR experiments, PCR plate was loaded on Bio-Rad QX100 droplet reader for quantification of cDNA copies/μL. Analysis of the ddPCR data was performed by QuantaSoft analysis software (Bio-Rad Laboratories). No template control with H_2O was included in each assay. Experiments were performed in triplicate and repeated three times.

Results are reported as the concentration (cDNA copies/μL) of the gene of interest calculated on the concentration mean (cDNA copies/μL) of *GAPDH*.

Flow Cytometry

After transfection with miRcombo or negmiR, AHCFs were cultured for additional 15 days. Then, cells were trypsinized with 0.05% Trypsin/EDTA (Sigma Aldrich) and permeabilized with 0.5% v/v Tween 20 in phosphate buffered saline (PBS) for 5 min. Ice cold PBS with 10% FBS and 1% sodium azide (Sigma Aldrich) was used for washing between each step. Cells were incubated with Cardiac Troponin T primary antibody (cat #701620, Invitrogen) for 1 h at 4°C and Alexa Fluor 488-conjugated secondary antibody (ab150077, Abcam) for 1 h at 4°C in the dark. Cells were run on Guava EasyCyte (Merck) flow cytometer and data analysis was performed using GuavaSoft 3.2.

Measurements of Spontaneous Calcium Transients

Calcium transient was analyzed in AHCFs after 30 days post-transfection with miRcombo or negmiR. To record calcium transients, cells were loaded with 5μM of Fluo-4 AM (Invitrogen) in modified Tyrode's solution (140 mM NaCl, 5 mM KCl, 1.8 mM $CaCl_2$, 1 mM $MgCl_2$, 10 mM glucose and 10 mM Hepes) with 0.1% bovine serum albumin (BSA) at 37°C for 20 min while shielded from light. Cells were washed in modified Tyrode's solution at 37°C for 10 min. Calcium transient was recorded using Nikon Eclipse Ti2 spinning disk and NIS-Elements software (Nikon). At least 4 fields were observed for each sample. Data were analyzed using ImageJ software (NIH) and Ca^{2+} level was reported as F/F_0 ratio, where F is the intensity of fluorescence emission recorded for each cell, while F_0 is the background fluorescence.

Statistical Analysis

The results are shown as means ± standard error of the mean (SEM) of replicate experiments. Statistical analyses were performed with Student's *t*-test, with p-value reported as $^{*}p < 0.05$ considered statistically significant, $^{**}p < 0.01$ considered highly significant and $^{***}p < 0.0001$ very highly significant. All graphs were prepared using GraphPad software.

RESULTS

We initially studied the efficiency of DharmaFECT1 in delivering miRNAs to AHCFs, using miR-1 as a model miRNA, as compared to a non-targeting miRNA negative control (negmiR). DdPCR analysis of miR-1 transfected cells showed relative overexpression of miR-1, and knockdown of *TWF-1* target gene in AHCFs, at 24 and 48 h culture times (**Figures 1A,B**).

Then, the effect of miRcombo transient transfection on AHCFs trans-differentiation into iCMs was evaluated at different

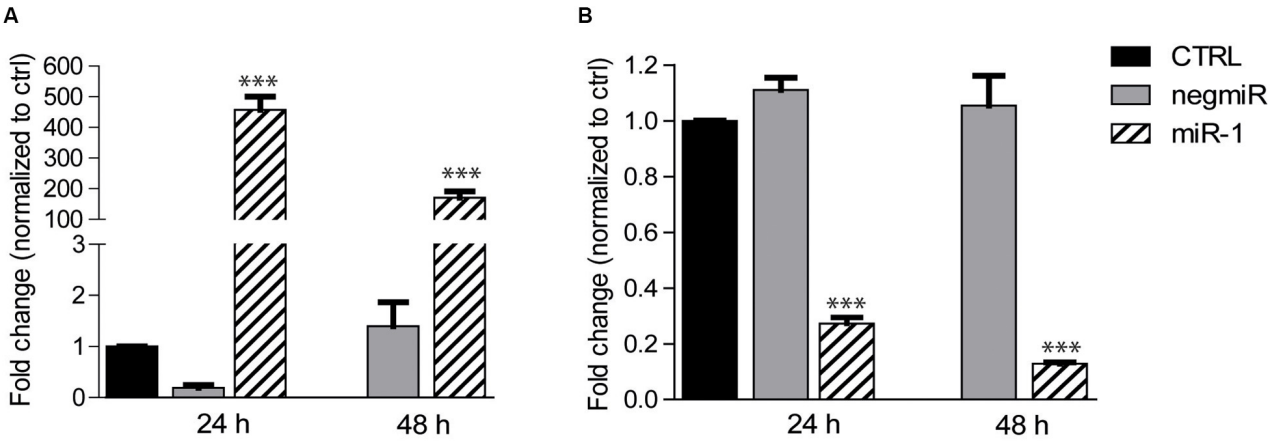

FIGURE 1 | DharmaFECT1 mediated delivery of miR-1 and *TWF-1* target downregulation in AHCFs. **(A)** Fold change of miR-1 expression (relative to untransfected control) in AHCFs transfected with negmiR or miR-1 using DharmaFECT1 at 24 h (i.e., immediately post-transfection) and 48 h (i.e., 24 h post-transfection) culture times, analyzed by ddPCR. Data are representative of three independent experiments. Stated *p*-value ***$p < 0{,}001$ is reported versus negmiR control. **(B)** Fold change of *TWF-1* mRNA target expression (relative to untransfected control) in AHCFs transfected with negmiR or miR-1 using DharmaFECT1 at 24 h (i.e., immediately post-transfection) and 48 h (i.e., 24 h post-transfection) culture times. Data are representative of three independent experiments. Stated *p*-value ***$p < 0{,}001$ is reported versus negmiR control. CTRL, untransfected control.

time points by different analyses depicted in **Figure 2A**. As a negative control, AHCFs were also transfected with negmiR.

DdPCR analysis showed that miRcombo transfected cells upregulated the expression of early cardiac transcription factors (TFs), with a significantly increased expression of *GATA4* ($p = 0.007$), *MEF2C* ($p = 0.0004$), *TBX5* ($p < 0.0001$) and *HAND2* ($p = 0.0001$) cardiac TFs, compared to negmiR transfected cells, 7 days after transfection (**Figures 2B–E**). Additionally, the expression of *NKX2.5* cardiac TF was increased in miRcombo transfected cells compared to controls, although not significantly (**Figure 2F**).

As a further step, the expression of mature cardiomyocyte markers was evaluated in miRcombo transfected AHCFs at 15 days after transfection. The expression of *TNNT2*, which encodes for cardiac troponin T (cTnT), was significantly increased in miRcombo-transfected cells compared to negmiR controls ($p = 0.0004$) (**Figure 3A**). Also, *TNNI3* expression was slightly increased in miRcombo transfected cells compared to controls, although non-significantly (**Figure 3B**).

The reprogramming efficiency of miRcombo-transfected cells was evaluated using flow cytometry. Notably, approximately 11% of fibroblasts were $cTnT^+$ after 15 days culture time from miRcombo transfection, whereas very low percentage of $cTnT^+$ cells (0.3%) was measured in negmiR transfected cells (**Figure 3C**).

Along with the upregulation of cardiomyocyte markers, ddPCR analysis showed that the expression of fibroblast markers, such as vimentin (*VIM*, $p = 0{,}0003$), discoidin domain receptor-2 (*DDR2*, $p = 0{,}0004$) and fibroblast specific protein-1 (*FSP-1/S100A4*, $p < 0{,}0001$) was significantly downregulated in miRcombo-transfected cells compared to controls after 15 days culture time from miRcombo transfection (**Figures 3D–F**).

Overall, the results suggested that, after 15 days from reprogramming induction, miRcombo-transfected cells started to display functional cardiomyocyte-specific markers along with a reduced fibroblast phenotype.

Finally, to determine whether miRcombo-transfected AHCFs exhibited functional cardiomyocyte properties after a long period of culture, we examined intracellular calcium oscillation at 30 days after transfection. Results showed that miRcombo transfection triggered calcium oscillation, lasting nearly 1 min, in ∼38% of total cells, while rare or no calcium oscillation was found in negmiR transfected control cells (**Figures 4A–C**).

In conclusion, results demonstrated that miRcombo-transfection triggered transdifferentiation of AHCFs into cardiomyocyte-like cells, also increasing functional cardiomyocyte properties compared to AHCFs transfected with negmiR.

DISCUSSION

Direct reprogramming of human cardiac fibroblasts into cardiomyocytes represents an attractive approach to revert cardiac fibrosis and recover heart function after MI (Chen et al., 2017), avoiding the need for cell-based therapies to replace cardiomyocytes (Hashimoto et al., 2018). Cardiac fibrotic scar is mainly composed by activated fibroblasts (myofibroblasts), while the target healthy cardiac tissue contains 20% cardiac fibroblasts and 35% cardiomyocytes (Gray et al., 2018). Ideally, through direct reprogramming, a suitable number of fibroblasts in the scar would be converted into cardiomyocytes to re-establish cell-cell connections and functionality of healthy cardiac tissue.

Since the first evidence of direct reprogramming of fibroblasts into cardiomyocytes in 2010 (Ieda et al., 2010), several efforts have been performed to directly reprogram fibroblasts into iCMs, using combinations of cardiac transcription factors (Song et al., 2012), microRNA mimics (Jayawardena et al., 2012),

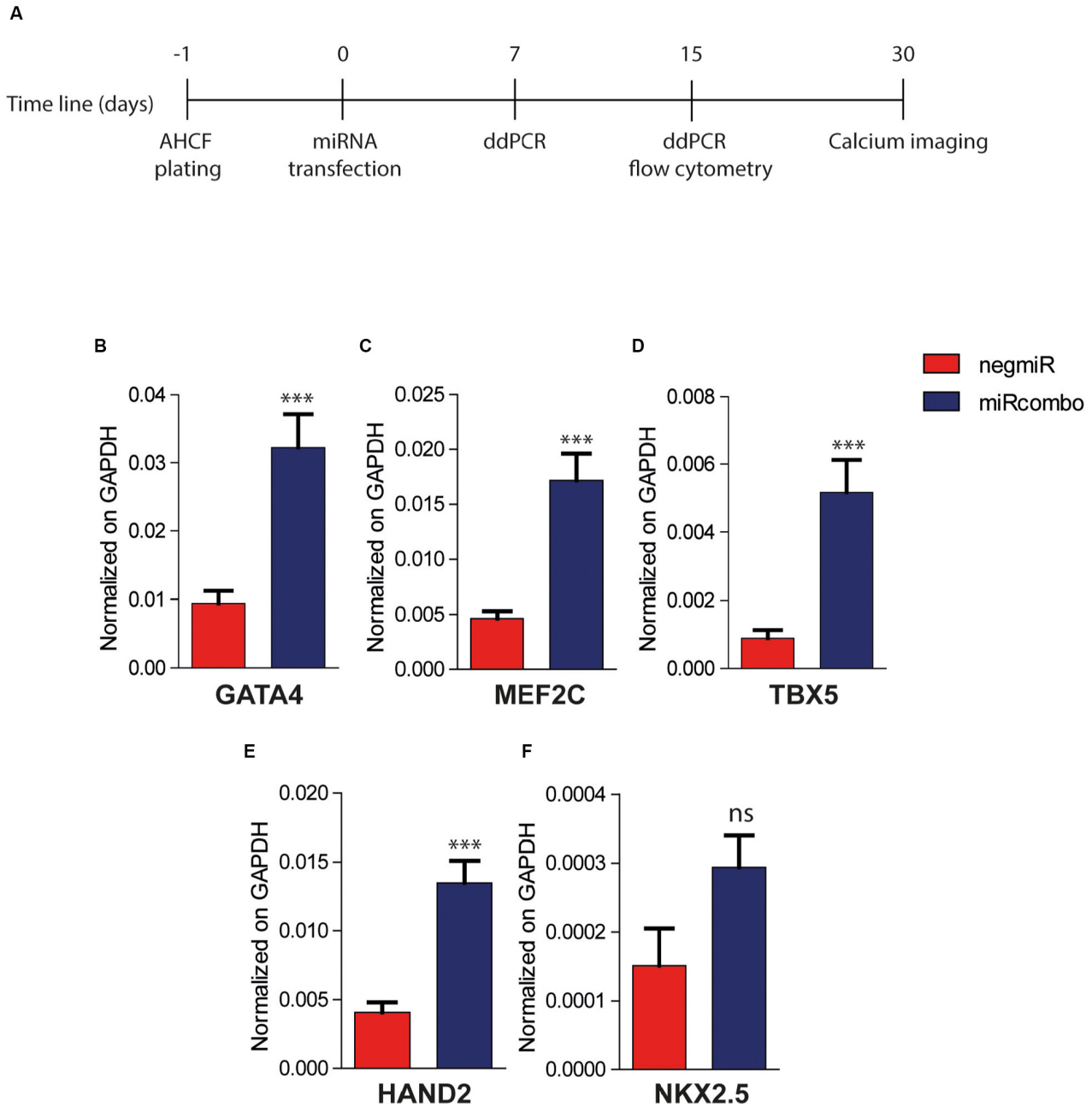

FIGURE 2 | MiRcombo-transfected AHCFs show increased cardiac transcription factor expression. **(A)** Representative scheme of experimental design. AHCFs were transfected with miRcombo or negative control (negmiR). The acquisition of cardiomyocyte-associated features was evaluated after 7 days (cardiac transcription factors), 15 days (cardiomyocyte and fibroblast markers) and 30 days (calcium transients). **(B–F)** Gene expression of cardiac transcription factors. The expression of *GATA4*, *MEF2C*, *TBX5*, *HAND2,* and *NKX2.5* was evaluated by ddPCR 7 days post transfection in AHCFs transfected with miRcombo (red) or negmiR (blue). Data are representative of three independent experiments, each performed in triplicate. Stated *P*-value is versus negmiR controls.

and small molecules (Fu et al., 2015). However, most direct reprogramming methods have been generally optimized on mouse cells, which does not assure their efficacy on AHCFs (Chen et al., 2017). Indeed, AHCFs are known to be more resistant to cellular reprogramming than murine fibroblasts due to epigenetic barriers that hinder phenotypic changes (Talkhabi et al., 2017).

Successful direct reprogramming of AHCFs into iCMs was achieved by inducing the expression of cardiac TFs and miRNAs, through retroviruses or inducible lentiviruses (Nam et al., 2013; Muraoka et al., 2014), which cause stable and heritable integration of a specific nucleic acid sequence into the target cell genome (Chen et al., 2017). As an example, Nam et al. (2013) directly reprogrammed

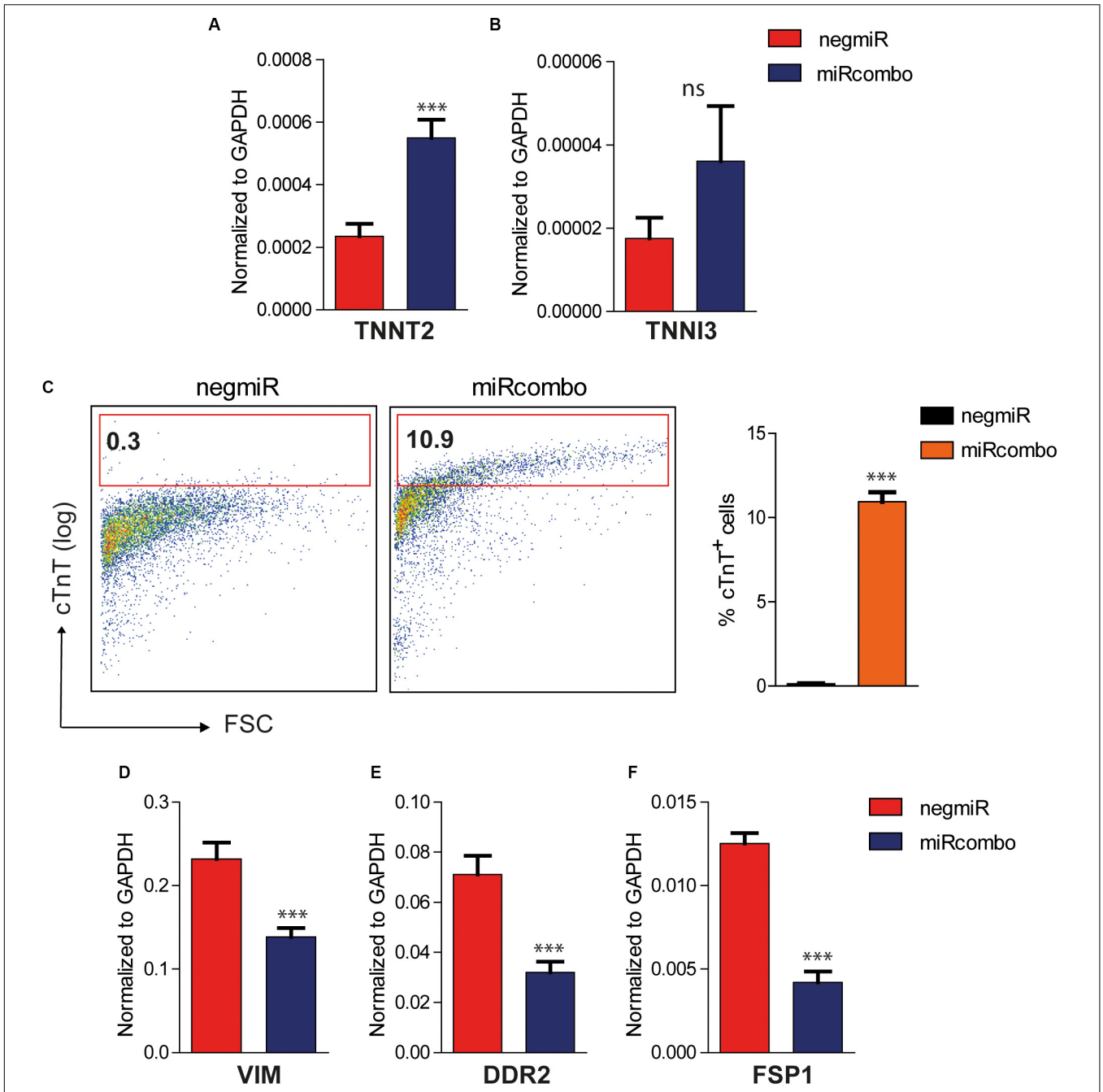

FIGURE 3 | Induction of cardiomyocyte markers in miRcombo-transfected AHCFs. **(A,B)** Gene expression of cardiomyocyte markers *TNNT2* and *TNNI3* in AHCFs transfected with miRcombo (red) or negmiR (blue) evaluated by ddPCR. Data are representative of three independent experiments, each performed in triplicate. **(C)** Representative flow plots (left panel) and percentage (right panel) of cTnT positive cells in AHCFs transfected with miRcombo (n = 3) and negmiR (n = 3) 15 days after transfection. **(D–F)** Gene expression of fibroblastic markers *VIM*, *DDR2*, and *FSP-1* in AHCFs transfected with miRcombo (red) or negmiR (blue) by ddPCR. Data are representative of three independent experiments, each performed in triplicate. Stated P-value is versus negmiR.

AHCFs into iCMs with an efficiency of ∼13% (measured by cTnT$^+$ cells at 2 weeks) by retroviral overexpression of miR-1, miR-133 and specific cardiac TFs. On the other hand, Muraoka et al. (2014) found out ∼20% of cTnT$^+$ cells after 1 week from simultaneous transfection of AHCFs with different TFs (by lentiviral vectors) and miR-133 (by Lipofectamine 2000), however, they used relatively young AHCFs (average age: 35 years old) and did not analyse cell functional properties. Overall, although effective, viral vectors suffer from potential risks which currently hinder an *in situ* clinical application (Labatut and Mattheolabakis, 2018).

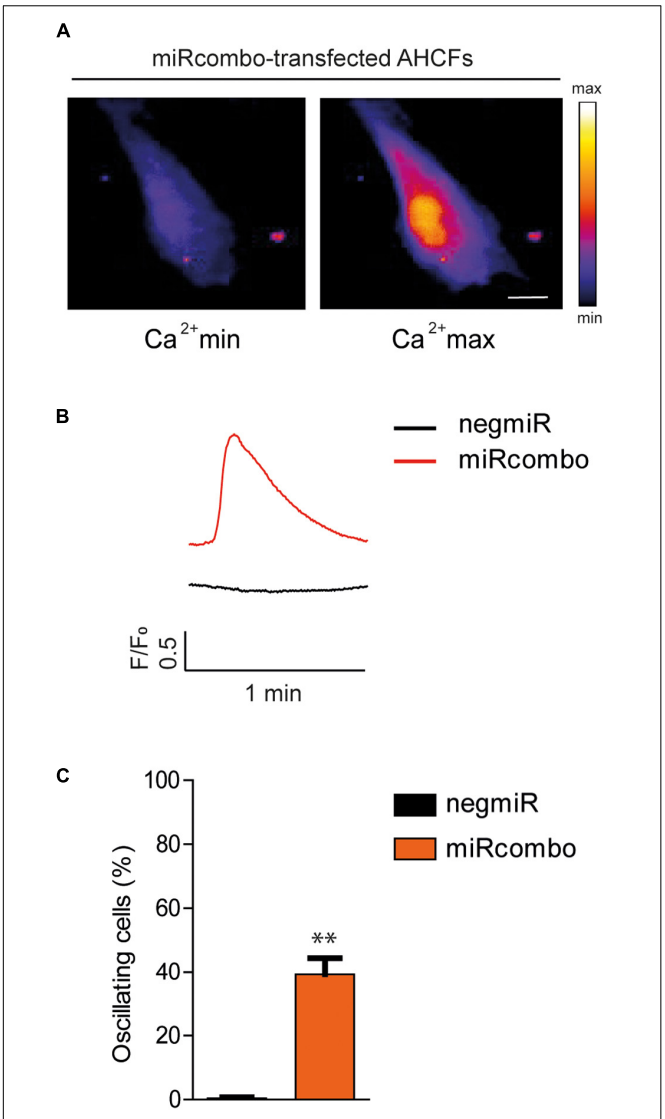

FIGURE 4 | miRcombo-transfected cells exhibit calcium transients. **(A,B)** Representative image, recorded with fluorescence microscopy **(A)** and trace **(B)** of Ca^{+2} oscillations in AHCFs transfected with miRcombo (n = 3) and negmiR (n = 3) after 30 days from transfection. Scale bar: 25 μm. **(C)** Bar graph reports the percentage of cells showing Ca^{+2} transients after 30 days from miRcombo and negmiR transfection. Stated P-value is versus negmiR.

MiRcombo, a combination of four miRNA mimics (miRs-1, 133, 208, and 499) has been previously demonstrated to successfully reprogram mouse neonatal fibroblasts into functional cardiomyocytes *in vitro,* and to regenerate cardiomyocytes *in vivo* after myocardial injury (Jayawardena et al., 2012, 2015). On the other hand, the effect of miRcombo transfection on human fibroblasts has never been tested. In the perspective of a future clinical application of miRcombo approach, preclinical studies should be carried out using human cells.

In this work, DharmaFECT1 was demonstrated to be an efficient agent for miRNA delivery to AHCFs (**Figures 1A,B**). Moreover, miR-1 delivery to AHCFs efficiently induced knockdown expression of *TWF-1* (miR-1 target in cardiac fibroblasts), which was maintained up to 48 h culture time.

Then, DharmaFECT1 was employed for transfection of AHCFs with miRcombo or negmiR, and cardiac gene and protein expression of transfected AHCFs was investigated at different time steps. After 7 days from transient transfection with miRcombo, AHCFs showed upregulation of early cardiac TF expression, such as *GATA4*, *MEF2C*, *TBX5*, *HAND2*, respect to negmiR transfected cells (**Figure 2**). Early cardiac TFs are known to work in synergy, guiding cardiac cell fate and contractile protein expression (Olson, 2006). Nuclear localization of cardiac TFs was found in chemically induced cardiomyocytes from mouse fibroblasts (Fu et al., 2015). In the future, immunostaining of cardiac TFs in miRcombo-transfected cells could help in understanding their correct location in cell nuclei, ensuring their function in inducing mature cardiomyocyte marker expression.

Then, the expression of functional and structural cardiomyocyte markers in AHCFs at longer time from transfection was evaluated. Particularly, gene expression of *TNNT2* was enhanced in miRcombo transfected AHCFs respect to negmiR transfected cells after 15 days from transfection (**Figure 3A**). These results were also confirmed by flow cytometry, showing a reprogramming efficiency – measured as percentage of $cTnT^{+}$ cells - of ∼11% (**Figure 3C**), which was indeed higher than the value reported for miRcombo-transfected neonatal murine cardiac fibroblasts (∼3%) (Li et al., 2016). On the other hand, the measured reprogramming efficiency was similar to values reported in previous investigations on direct reprogramming of AHCFs into iCMs (∼13% after 2 weeks reported by Nam et al., 2013).

Additionally, a reduced expression of fibroblastic markers (*VIM*, *DDR2* and *FSP-1*) was measured after 15 days of culture post-transfection (**Figures 3D–F**).

Notably, differently from previous studies on miRcombo transfection of mouse neonatal fibroblasts (Jayawardena et al., 2012; Dal-Pra et al., 2019), miRcombo-transfected AHCFs did not show sarcomeric organization after 15 days from miRcombo transfection, suggesting an immature phenotype (data not shown). On the other hand, previous studies reported early sarcomeric structure in AHCFs transfected with cardiac TFs and miRNAs, after at least 4–5 weeks from transfection (Nam et al., 2013; Muraoka et al., 2014). Compared to neonatal fibroblasts, AHCFs are more resistant to direct reprogramming, caused by their stable epigenetic program. For this reason, in the future, longer culture times and/or additional stimulating factors will be applied to transdifferentiate AHCFs into mature iCMs.

Upon maintaining miRcombo-transfected AHCFs in culture for 30 days, ∼38% of total cells exhibited spontaneous calcium oscillation, suggesting cardiomyocyte-like functionality (**Figures 4A–C**). This is a relevant result when compared to what reported by Nam et al. (2013) who found out a cell percentage of ∼15% exhibiting calcium transients induced by KCl stimulation, after 4 weeks from transfection. Although most of the previous studies on direct cardiac reprogramming

analyzed calcium transient through stimulation with high KCl concentration or caffeine (Fu et al., 2013; Nam et al., 2013), a few authors reported the analysis of spontaneous calcium oscillation of iCMs as in our case (Smith et al., 2013). In the future, induced calcium oscillation through KCl or caffeine stimulation will be analyzed to confirm cardiomyocyte-like functionality.

In conclusion, results demonstrated for the first time that miRcombo transfection was able to activate a phenotypic switch of AHCFs toward cardiomyocyte-like cells. Although other methods are under study to directly reprogram AHCFs into iCMs (Nam et al., 2013; Muraoka et al., 2014), the advantage of miRcombo-mediated approach derives from the possibility for non-viral transfection, overcoming the hurdles associated with viral vectors, such as high cost, difficulties in large scale production and potential mutagenesis and immunogenic behavior (Labatut and Mattheolabakis, 2018). Indeed, safety represents one key requirement for perspective application of direct reprogramming to humans. In the present study, the overexpression of defined cardiac developmental factors and mature markers was achieved by transient transfection with miRcombo through a commercially available lipidic transfection agent. AHCFs transfected with miRcombo were able to maintain the expression of specific cardiomyocyte markers at the tested time points (7 and 15 days). Future studies will be addressed to thoroughly study miRcombo-mediated direct reprogramming of AHCFs at longer times and under different microenvironmental stimulations, and to develop non-viral vectors for *in situ* transfection with miRcombo, paving the way toward a clinical translation of direct reprogramming strategies (Muraoka et al., 2014; Li et al., 2016; Paoletti et al., 2018).

CONCLUSION

This brief report provides a preliminary study showing that a combination of four microRNAs (miRcombo) is able to drive a significant change in human fibroblast phenotype, starting their trans-differentiation toward cardiomyocyte-like cells. Despite further investigations are required to confirm and to enhance the functional activity of iCMs, the present work demonstrates that miRcombo transfection is effective in directly reprogramming AHCFs into cardiomyocyte-like cells with potentialities for future clinical application.

DATA AVAILABILITY STATEMENT

The datasets generated for this study are available on request to the corresponding author.

AUTHOR CONTRIBUTIONS

CP designed the experimental part of the project, conducted experiments, and analyzed the data. CD supported CP in the *in vitro* culture experiments and trained CP in ddPCR analysis at INRIM biology lab. GT supported CP in ddPCR analysis for miR-1 overexpression and mRNA target downregulation. FD and DN supported CP in the *in vitro* culture experiments with adult human fibroblasts. VC supervised the work and acquired funding. The manuscript was written through main contributions by CP and VC and further help by all the authors. All authors have given approval to the final version of the manuscript.

FUNDING

The project has received funding from the European Research Council (ERC) under the European Union's Horizon 2020 Research and Innovation Programe (Grant Agreement No. 772168).

ACKNOWLEDGMENTS

The authors acknowledge support from the European Research Council (ERC) under the European Union's Horizon 2020 Research and Innovation Programe (Grant Agreement No. 772168), through BIORECAR ERC Consolidator project (www.biorecar.polito.it).

REFERENCES

Bektik, E., and Fu, J. (2019). Ameliorating the fibrotic remodeling of the heart through direct cardiac reprogramming. *Cells* 8:679. doi: 10.3390/cells8070679

Chen, Y., Yang, Z., Zhao, Z.-A., and Shen, Z. (2017). Direct reprogramming of fibroblasts into cardiomyocytes. *Stem Cell Res. Ther.* 8:118. doi: 10.1186/s13287-017-0569-3

Dal-Pra, S., Hodgkinson, C. P., and Dzau, V. J. (2019). Induced cardiomyocyte maturation: cardiac transcription factors are necessary but not sufficient. *PLoS One* 14:e0223842. doi: 10.1371/journal.pone.0223842

Fu, J. D., Stone, N. R., Liu, L., and Spencer, C. I (2013). Direct reprogramming of human fibroblasts toward a cardiomyocyte-like state. *Stem Cell Rep.* 1, 235–247. doi: 10.1016/j.stemcr.2013.07.005

Fu, Y., Huang, C., Xu, X., Gu, H., Ye, Y., Jiang, C., et al. (2015). Direct reprogramming of mouse fibroblasts into cardiomyocytes with chemical cocktails. *Cell Res.* 25, 1013–1024. doi: 10.1038/cr.2015.99

Gray, G., Toor, I., Castellan, R., Crisan, M., and Meloni, M. (2018). Resident cells of the myocardium: more than spectators in cardiac injury, repair and regeneration. *Curr. Opin. Physiol.* 1, 46–51. doi: 10.1016/J.COPHYS.2017.08.001

Hashimoto, H., Olson, E. N., and Bassel-Duby, R. (2018). Therapeutic approaches for cardiac regeneration and repair. *Nat. Rev. Cardiol.* 15, 585–600. doi: 10.1038/s41569-018-0036-6

He, L., and Hannon, G. J. (2004). MicroRNAs: small RNAs with a big role in gene regulation. *Nat. Rev. Genet.* 5, 522–531. doi: 10.1038/nrg1379

Ieda, M., Fu, J.-D., Delgado-Olguin, P., Vedantham, V., Hayashi, Y., Bruneau, B. G., et al. (2010). Direct reprogramming of fibroblasts into functional cardiomyocytes by defined factors. *Cell* 142, 375–386. doi: 10.1016/j.cell.2010.07.002

Jayawardena, T. M., Egemnazarov, B., Finch, E. A., Zhang, L., Payne, J. A., Pandya, K., et al. (2012). MicroRNA-mediated *in vitro* and *in vivo* direct reprogramming of cardiac fibroblasts to cardiomyocytes. *Circ. Res.* 110, 1465–1473. doi: 10.1161/CIRCRESAHA.112.269035

Jayawardena, T. M., Finch, E. A., Zhang, L., Zhang, H., Hodgkinson, C. P., Pratt, R. E., et al. (2015). MicroRNA induced cardiac reprogramming *in vivo*. *Circ. Res.* 116, 418–424. doi: 10.1161/CIRCRESAHA.116.304510

Kitchener, D. W., Shijun, H., Shivkumar, V., Ji-Dong, F., and Ning, S. (2010). Dynamic MicroRNA expression programs during cardiac differentiation of human embryonic stem cells role for miR-499. *Circ. Cardiovasc. Genet.* 3, 426–435. doi: 10.1161/CIRCGENETICS.109.934281

Labatut, A. E., and Mattheolabakis, G. (2018). Non-viral based miR delivery and recent developments. *Eur. J. Pharm. Biopharm.* 128, 82–90. doi: 10.1016/j.ejpb.2018.04.018

Lee, S. W. L., Paoletti, C., Campisi, M., Osaki, T., Adriani, G., Kamm, R. D., et al. (2019). MicroRNA delivery through nanoparticles. *J. Control. Release* 313, 80–95. doi: 10.1016/j.jconrel.2019.10.007

Li, Y., Dal-Pra, S., Mirotsou, M., Jayawardena, T. M., Hodgkinson, C. P., Bursac, N., et al. (2016). Tissue-engineered 3-dimensional (3D) microenvironment enhances the direct reprogramming of fibroblasts into cardiomyocytes by microRNAs. *Sci. Rep.* 6:38815. doi: 10.1038/srep38815

Muraoka, N., Yamakawa, H., Miyamoto, K., Sadahiro, T., Umei, T., Isomi, M., et al. (2014). MiR-133 promotes cardiac reprogramming by directly repressing Snai1 and silencing fibroblast signatures. *EMBO J.* 33, 1565–1581. doi: 10.15252/embj.201387605

Nam, Y.-J., Song, K., Luo, X., Daniel, E., Lambeth, K., West, K., et al. (2013). Reprogramming of human fibroblasts toward a cardiac fate. *Proc. Natl. Acad. Sci. U.S.A.* 110, 5588–5593. doi: 10.1073/pnas.1301019110

Olson, E. N. (2006). Gene regulatory networks in the evolution and development of the heart. *Science* 313, 1922–1927. doi: 10.1126/science.1132292

Paoletti, C., Divieto, C., and Chiono, V. (2018). Impact of biomaterials on differentiation and reprogramming approaches for the generation of functional cardiomyocytes. *Cells* 7:114. doi: 10.3390/cells7090114

Peng, B., Chen, Y., and Leong, K. W. (2015). MicroRNA delivery for regenerative medicine. *Adv. Drug Deliv. Rev.* 88, 108–122. doi: 10.1016/J.ADDR.2015.05.014

Smith, A. W., Hoyne, J. D., and Nguyen, P. K. (2013). Direct reprogramming of mouse fibroblasts to cardiomyocyte-like cells using Yamanaka factors on engineered poly(ethylene glycol) (PEG) hydrogels. *Biomaterials* 34, 6559–6571. doi: 10.1016/j.biomaterials.2013.05.050

Song, K., Nam, Y.-J., Luo, X., Qi, X., Tan, W., Huang, G. N., et al. (2012). Heart repair by reprogramming non-myocytes with cardiac transcription factors. *Nature* 485, 599–604. doi: 10.1038/nature11139

Talkhabi, M., Zonooz, E., and Baharvand, H. (2017). Boosters and barriers for direct cardiac reprogramming. *Life Sci.* 178, 70–86. doi: 10.1016/J.LFS.2017.04.013

Talman, V., and Ruskoaho, H. (2016). Cardiac fibrosis in myocardial infarction-from repair and remodeling to regeneration. *Cell Tissue Res.* 365, 563–581. doi: 10.1007/s00441-016-2431-9

Tian, J., An, X., and Niu, L. (2017). Role of microRNAs in cardiac development and disease. *Exp. Ther. Med.* 13, 3–8. doi: 10.3892/etm.2016.3932

van den Borne, S. W. M., Diez, J., Blankesteijn, W. M., Verjans, J., Hofstra, L., and Narula, J. (2010). Myocardial remodeling after infarction: the role of myofibroblasts. *Nat. Rev. Cardiol.* 7, 30–37. doi: 10.1038/nrcardio.2009.199

van Rooij, E., Quiat, D., Johnson, B. A., Sutherland, L. B., Qi, X., Richardson, J. A., et al. (2009). A family of microRNAs encoded by myosin genes governs myosin expression and muscle performance. *Dev. Cell* 17, 662–673. doi: 10.1016/j.devcel.2009.10.013

Xu, C., Lu, Y., Pan, Z., Chu, W., Luo, X., Lin, H., et al. (2011). The muscle-specific microRNAs miR-1 and miR-133 produce opposing effects on apoptosis by targeting HSP60, HSP70 and caspase-9 in cardiomyocytes. *J. Cell Sci.* 124, 3187. doi: 10.1242/jcs.098830

Conflict of Interest: The authors declare that the research was conducted in the absence of any commercial or financial relationships that could be construed as a potential conflict of interest.

Copyright © 2020 Paoletti, Divieto, Tarricone, Di Meglio, Nurzynska and Chiono. This is an open-access article distributed under the terms of the Creative Commons Attribution License (CC BY). The use, distribution or reproduction in other forums is permitted, provided the original author(s) and the copyright owner(s) are credited and that the original publication in this journal is cited, in accordance with accepted academic practice. No use, distribution or reproduction is permitted which does not comply with these terms.

frontiers in Bioengineering and Biotechnology

PERSPECTIVE
published: 16 June 2020
doi: 10.3389/fbioe.2020.00594

Agrin-Mediated Cardiac Regeneration: Some Open Questions

Maria Giulia Bigotti[1,2], Katie L. Skeffington[1], Ffion P. Jones[1], Massimo Caputo[1] and Andrea Brancaccio[2,3]**

[1] Bristol Heart Institute, Research Floor Level 7, Bristol Royal Infirmary, Bristol, United Kingdom, [2] School of Biochemistry, University of Bristol, Bristol, United Kingdom, [3] Institute of Chemical Sciences and Technologies "Giulio Natta" (SCITEC)—CNR, Rome, Italy

After cardiac injury, the mammalian adult heart has a very limited capacity to regenerate, due to the inability of fully differentiated cardiomyocytes (CMs) to efficiently proliferate. This has been directly linked to the extracellular matrix (ECM) surrounding and connecting cardiomyocytes, as its increasing rigidity during heart maturation has a crucial impact over the proliferative capacity of CMs. Very recent studies using mouse models have demonstrated how the ECM protein agrin might promote heart regeneration through CMs de-differentiation and proliferation. In maturing CMs, this proteoglycan would act as an inducer of a specific molecular pathway involving ECM receptor(s) within the transmembrane dystrophin-glycoprotein complex (DGC) as well as intracellular Yap, an effector of the Hippo pathway involved in the replication/regeneration program of CMs. According to the mechanism proposed, during mice heart development agrin gets progressively downregulated and ultimately replaced by other ECM proteins eventually leading to loss of proliferation/ regenerative capacity in mature CMs. Although the role played by the agrin-DGC-YAP axis during human heart development remains still largely to be defined, this scenario opens up fascinating and promising therapeutic avenues. Herein, we discuss the currently available relevant information on this system, with a view to explore how the fundamental understanding of the regenerative potential of this cellular program can be translated into therapeutic treatment of injured human hearts.

Keywords: heart regeneration, agrin, dystrophin-glycoprotein complex, dystroglycan, laminin, YAP, Hippo pathway, cardiomyocyte proliferation

OPEN ACCESS

Edited by:
Susanna Sartori, Politecnico di Torino, Italy

Reviewed by:
*Sayan Chakraborty, Institute of Molecular and Cell Biology (A*STAR), Singapore*
Yuka Morikawa, Texas Heart Institute, United States

****Correspondence:***
Maria Giulia Bigotti
g.bigotti@bristol.ac.uk
Andrea Brancaccio
andrea.brancaccio@cnr.it

Specialty section:
This article was submitted to Tissue Engineering and Regenerative Medicine, a section of the journal Frontiers in Bioengineering and Biotechnology

Received: *02 March 2020*
Accepted: *15 May 2020*
Published: *16 June 2020*

Citation:
Bigotti MG, Skeffington KL, Jones FP, Caputo M and Brancaccio A (2020) Agrin-Mediated Cardiac Regeneration: Some Open Questions. Front. Bioeng. Biotechnol. 8:594. doi: 10.3389/fbioe.2020.00594

INTRODUCTION

The repair of damaged hearts represents one of the most critical challenges in cardiovascular medicine, since mammalian cardiomyocytes (CMs) lose their proliferative potential very early in life, after which point hypertrophic processes become responsible for most of the remaining heart growth. Therefore, upon injury, CMs are replaced by fibrotic tissue, often with deleterious consequences. Recent advances in understanding the endogenous program(s) regulating the proliferation of cardiomyocytes at the molecular level [reviewed in Deshmukh et al. (2019), Heallen et al. (2019), Ali et al. (2020)] hold great promise for the development of new approaches to heart regeneration based on cell cycle re-activation. Unfortunately, a full characterization of the developmental pathway(s) of the mammalian heart and specifically of CMs, is hindered by an intrinsic difficulty in understanding the exact timing

and interchange of proliferation and differentiation events (Velayutham et al., 2019). Unlike certain fish and amphibian species (Zhang et al., 2013), mammalian CMs can follow a regenerative program only during a limited postnatal period. Due to important differences in the developmental milestones of specific mammalian species, the exact time frame of fetal/postnatal proliferative heart growth has however only been determined in few model systems. The best characterized of these is the mouse model, in which full proliferation of CMs lasts for only the first few days postnatally, possibly until postnatal day 2 (P2), with the regenerative program already shut down at P7, when CMs have stopped proliferating and switched to a hypertrophic program (Porrello et al., 2011; Notari et al., 2018). Some recent crucial findings in mice challenge in part the idea that this differentiation program cannot be somehow modulated, and proliferation re-activated (Bassat et al., 2017; Morikawa et al., 2017). Following previous work proving how the rigidity of the extracellular matrix (ECM) strongly influences heart development (Yahalom-Ronen et al., 2015), and specifically CMs maturation, Bassat et al. used a series of elegant experiments to identify the proteoglycan agrin as an ECM component that promotes cardiomyocyte proliferation. Interestingly, they found that this protein is involved in neonatal heart repair and is only enriched in the matrix in the very first postnatal days, while downregulated by the P7 stage. Crucially, administration of recombinant agrin to juvenile and adult infarct mouse models was sufficient to boost cardiac regeneration through reactivation of the CMs proliferative program.

Existing studies investigating the role of agrin in other biological organs and systems are invaluable for beginning to piece together the mechanisms of action of agrin in the heart. In recent years, agrin has been revealed to play an important role in cancer development. An increase in agrin has been demonstrated in cancerous cells, and studies using experimental models have shown that addition of agrin promotes cancer whilst agrin depletion slows tumor growth (Chakraborty et al., 2015, 2017; Lv et al., 2017; Rivera et al., 2018). It is now known that agrin forms a mechanotransductive link between the ECM and the transcriptional co-activators YAP (Yes associated protein) and TAZ (transcriptional activator with PDZ binding motif) [reviewed in Chakraborty and Hong (2018), Xiong and Mei (2017)]. YAP and TAZ activate the transcription of many pro-proliferative and anti-apoptopic genes and are themselves controlled by many upstream factors, including the Hippo signaling pathway which regulates growth via YAP phosphorylation, thus sequestering it in the cytosol and preventing its transcriptional activity (**Figure 1A**). Experiments using liver tumor cells suggest that the increase in ECM stiffness which is observed in at least some cancerous tissues results in increased levels of extracellular agrin (Chakraborty et al., 2017). Agrin binds to the cell via Lrp4 (low density lipoprotein receptor related protein 4), which in turn activates MuSK (muscle specific kinase 4). This results in activation of the FAK-ILK-PAK1 (Focal Adhesion Kinase—Integrin Linked Kinase—p21 Activated Kinase) signaling axis, resulting in inhibition of Hippo signaling and consequent nuclear localization of YAP/TAZ. YAP transcriptional activity itself is known to increase the ECM stiffness possibly due to enhanced agrin expression, and it has been suggested that a positive feedback loop thus exists between agrin levels (through ECM stiffness increase) and YAP transcriptional activity, in a functional mechanotransduction network that promotes uncontrolled proliferation (Calvo et al., 2013; Chakraborty and Hong, 2018) (**Figure 1A**). Similar signaling pathways exists in neuromuscular junctions, where agrin is responsible for recruiting acetylcholine receptors. Agrin secreted from nerve terminals activates YAP via Lrp4/MuSK signaling; this results in the aggregation of acetylcholine receptors on the postsynaptic muscle cells (Zhao et al., 2017; Chakraborty and Hong, 2018). Agrin has also been demonstrated to interact with dystroglycan (DG) at the neuromuscular junction; DG is a pivotal member of the large transmembrane complex connecting the ECM with the cytoskeleton [namely the dystrophin-glycoprotein complex (DGC)], which is necessary for stabilization of acetylcholine receptor clusters (Ervasti and Campbell, 1993; Jacobson et al., 2001). In line with these precedents, a role for agrin in similar pathways have been demonstrated to exist in the heart. Bassat et al. determined that agrin promotes heart regeneration by interacting with the DGC on the CMs cell surface, thus preventing its assembly into the stable adult form. Specifically, the interaction of agrin with the extracellular α-DG on CMs would influence the binding properties of the transmembrane/cytoplasmic β-subunit of DG, favoring its binding to dystrophin over that to YAP. Similarly to what described for cancer growth, YAP is known to be involved in heart growth through CM proliferation which, unlike in other tissues, is inhibited postnatally due to the activity of upstream kinases of the Hippo pathway (Von Gise et al., 2012; Xin et al., 2013). The view proposed by Bassat et al. was corroborated and complemented by equally important findings from the James Martin's laboratory which showed how, during heart maturation, YAP gets phosphorylated by the Hippo pathway and consequently establishes a stable interaction with the cytodomain of β-DG in the adult tissues (Morikawa et al., 2017). Such interaction would sequester YAP at the cell periphery, thus preventing it from exerting its proliferation-inducing activity in the nucleus. All this evidence has been put together to envisage a possible molecular mechanism linking the axis agrin-DGC-YAP to heart tissue proliferation, in which during development and very early after birth the interaction of agrin with α-DG would interfere with the proper assembly of β-DG into the DGC, ultimately preventing the tethering of YAP. During cardiac maturation, this arrangement would change since on one hand YAP would get actively phosphorylated by the Hippo signaling pathway, on the other agrin would be replaced by a different, yet unidentified, ECM component (see below), thus allowing for proper DGC assembly. These two events would lead to the locking of phospho YAP at the inner side of the cell surface through β-DG binding (**Figure 1B**). A series of evidences shows how, in this proposed mechanism, laminin represents a strong candidate to take over from agrin in the binding to the DGC axis during cardiac muscle development, at least at the later stages. It was in fact shown that embryonic stem cells carrying mutations in laminin 211, although differentiating normally *in vitro* into contracting myotubes, eventually undergo detachment and death

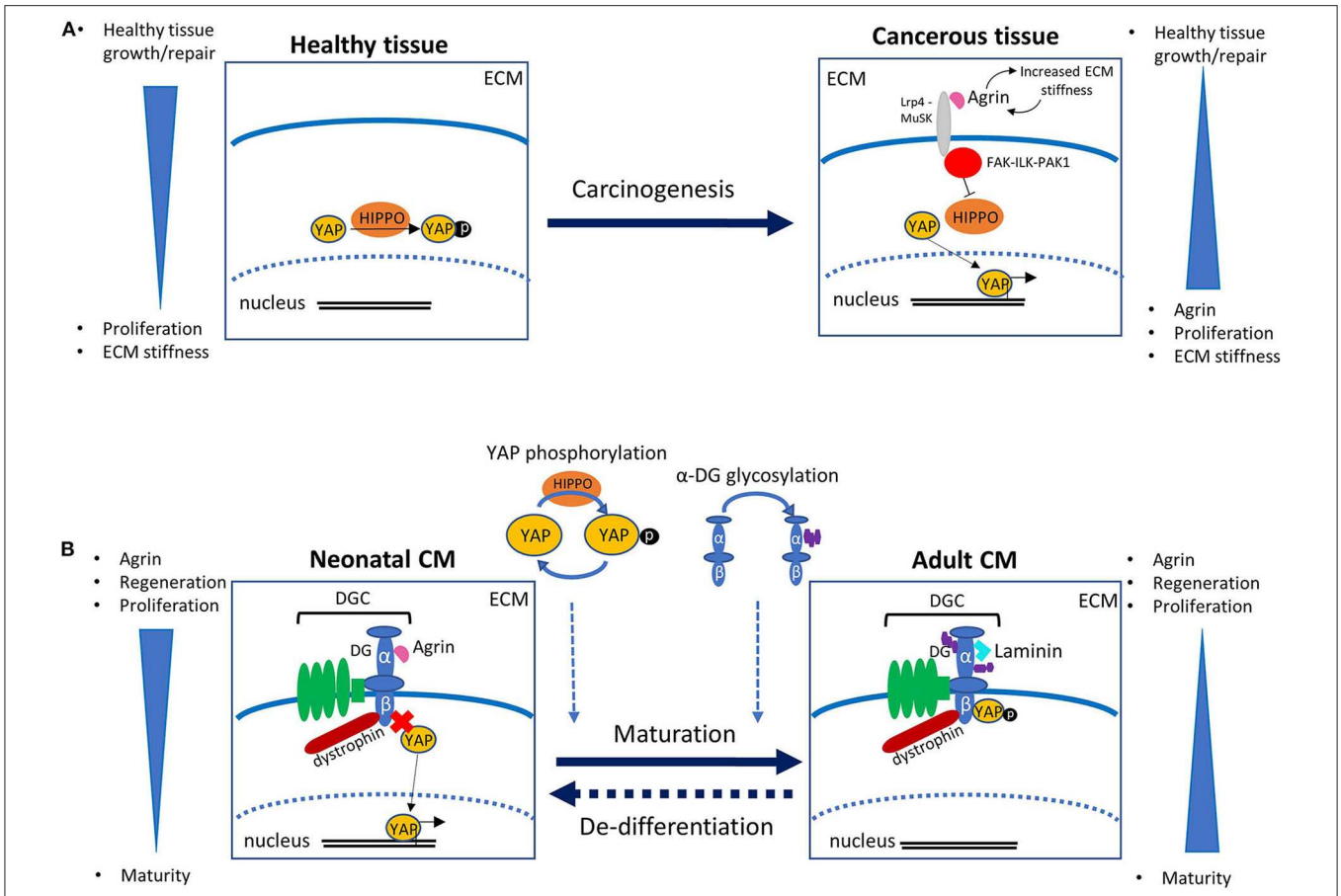

FIGURE 1 | (A) Role of agrin and YAP in carcinogenesis. In healthy tissue, the Hippo signaling pathway regulates transcription via phosphorylation of YAP, which results in its confinement out of the cell nucleus. In cancerous tissue an increase in ECM stiffness is associated with increased levels of extracellular agrin. Agrin binds to the receptor Lrp4, which activates MuSK, eventually promoting a signaling cascade involving the FAK-ILK-PAK1 axis. This results in the inhibition of the Hippo pathway that in turn leads to an increase in unphosphorylated YAP. The activity of YAP in the nucleus promotes not only cell-cycle and division but also a further increase in ECM stiffness, possibly following enhanced agrin expression, in a positive feedback mechanism that leads to uncontrolled proliferation. **(B)** Schematic of the role of agrin in mouse cardiomyocyte (CM) proliferation as proposed in Bassat et al. (2017). In neonates, binding of agrin to the α-subunit of dystroglycan (DG) interferes with its correct assembly within the dystrophin-glycoprotein complex (DGC), and ultimately prevents the β-subunit from binding the transcription factor YAP, whose activity in the nucleus promotes CM proliferation. With maturation, replacement of agrin with a different protein (probably laminin) of the extracellular matrix (ECM) allows for a stable assembly of the DGC, so that β-DG can bind and sequester phosphorylated YAP out of the nucleus, thus eventually hindering CM proliferation. The timing and mechanism of YAP phosphorylation, as well as of α-DG glycosylation, have to be determined yet, and might have a role in the molecular pathway. The dashed arrow between the two panels indicates the potential re-activation of CM proliferation induced by controlled delivery of exogenous agrin to injured cardiac tissue.

(Kuang et al., 1998). Together with the evidence that mutations or complete lack of laminin 211 are known to cause severe forms of congenital muscular dystrophy (CMD), these results stress the important role of laminin for adult skeletal muscle stabilization (Yurchenco et al., 2018) and cardiac muscle stability (Nguyen et al., 2019). Other laminins too (including laminin 511, 521, and 221) are known to play an important role for the differentiation of stem cells into cardiomyocytes (Wang et al., 2019; Yap et al., 2019; Chanthra et al., 2020). Recent evidence from studies in *Drosophila* suggests the possible involvement of β-DG in the Hippo signaling pathway as a mechano-receptor within muscle cells (Yatsenko et al., 2020), thus it is worth noting that the DG-Hippo pathway axis might have an evolutionarily conserved role in mediating muscle growth and regeneration. Although it is well-known that the composition of cardiac ECM, and thus its mechanosensing properties, play a fundamental role in heart development (Parker and Ingber, 2007; Garoffolo and Pesce, 2019), whether agrin regulates cardiac ECM stiffness, similarly to its role in hepatic cancer cells, is unknown. It will be certainly worth to investigate this point further, in order to understand whether, irrespective of the ECM receptors involved, agrin employs a similar strategy to stimulate proliferation of CMs and cancer cells.

A NEW HOPE FOR CARDIAC REGENERATION IN MAMMALS?

Aside from the fact that several aspects of the proposed mechanism remain unclear (see some of the points below), the

BOX 1 | Open questions on the cardiac regenerative role of the agrin-DG-Yap axis.

Open questions:

- How is the balance between agrin and laminin in binding to their receptor α-DG controlled/modulated?
- What is the impact of this agrin-dependent mechanism on CM proliferation during mouse heart growth?
- Does a similar pathway exist in human cardiac development?
- If so:
  1. What is the exact timeframe of the switch in humans?
  2. What is the contribution of the agrin-driven pathway to CM proliferation and to the overall development of human heart?
  3. Can we harness this pathway therapeutically to treat cardiac injury in humans without deleterious effects?

fundamental question arising is whether a similar mechanism is employed also by human heart. A pretty tricky question indeed, in the face of the complex and still elusive task of establishing a correlation between the developmental stages of different mammals that has to be added to the intrinsic challenge posed by development studies of the human heart. With a focus on the molecular aspects and on the therapeutic translational potential of agrin in human medicine, we have tried to highlight and discuss some of the open points (summarized in **Box 1**).

Role of ECM in Cardiac Regeneration: Agrin vs. Laminin, how Would Molecular Specificity Be Controlled?

The data collected by Bassat et al. (2017) using mouse models led them to propose that the regenerative program of CMs is directly linked to the levels of agrin in the ECM, which decrease over time to a minimum reached by P7 (likely earlier), when CMs have already switched to the hypertrophic program. Following this line of enquiry, the time window was revealed to be even shorter. Recent mouse experiments employing heart apical amputation as a tool to analyze possible regenerative pathways (Notari et al., 2018) established in fact that the timing at which CMs full proliferative program(s) can be triggered is even tighter than the postnatal period P1-P7 previously reported (Porrello et al., 2011, 2013). Indeed, a high degree of regeneration was observed only at P1, with the speed lowering considerably at P2–P3. This would suggest that the window available for fully inducing massive CM proliferation could be as short as 24 h after birth. Based on an overall transcriptomic analysis, the same study proposes that extracellular matrix proteins, rather than intracellularly acting cardiac fibers or transcription factors, are the most likely to influence this process by affecting/regulating the mechanical degree of stiffness. This would point to a predominantly "outside-inside" nature of the overall proliferation program, similarly to what has been shown in cancer cells, although the molecular mechanisms underlying it are yet to be elucidated.

The work of Bassat et al. clearly shows that the levels of agrin in mice are halved at P7, although how the protein changes between P1 and P7 is still unknown. As a matter of fact, the exact timing at which agrin ceases to have a measurable effect on the regeneration program remains to be debated. The only available data on the very first days after birth are those of Notari et al., and show how the expression levels of agrin (and its receptor dystroglycan) do not change between P1 and P2 [see Notari et al. (2018), Figure S5C]. With regard to the role of the agrin axis, there are two possible explanations for the lack of regenerative potential already observed at P2: (i) if it is laminin that replaces agrin during heart maturation, it could become over-expressed by P2 and therefore make a take-over on agrin because they display a similar affinity toward α-DG [see Sciandra et al. (2013)], (ii) post-P2, additional factors could intervene that favor the binding of laminin to α-DG over agrin. Notably, western blots reveal the presence of laminin already at P1 but a slight raise (∼1.3 times) of its levels at P2 (Notari et al., 2018), so not only could either hypothesis be correct, but the two mechanisms could coexist.

From the DGC receptor point of view, a specific molecular aspect that plays an important role in the binding to α-DG is the degree of glycosylation of α-DG itself. For example, in some dystroglycanopathies a significant reduction of α-DG glycosylation (hypoglycosylation) leads to a drop in laminin binding affinity, inducing severe muscular dystrophy phenotypes such as Walker-Warburg Syndrome or Muscle-Eye-Brain disease (Falsaperla et al., 2016; Brancaccio, 2019). It is known that cardiac α-DG is slightly less glycosylated than the skeletal muscle one (Brancaccio et al., 1995) and more glycosylated than brain α-DG (McDearmon et al., 2006). However, in chickens the affinity of cardiac α-DG to laminin-111 is still very high (Brancaccio et al., 1995), and agrin has only a slightly reduced affinity for brain DG relative to skeletal muscle, kidney, or lung (Gesemann et al., 1998). Overall, these data suggest that the effect of differential tissue glycosylation of α-DG on its interaction with both laminin and agrin might be small. Nonetheless, considering that the glycosylation shell of brain α-DG is similar to that of early embryonic α-DG (Leschziner et al., 2001), it may well be that agrin and laminin could display some minor although physiologically relevant differences in affinity toward α-DG tissue isoforms based on their differential degree of glycosylation at various stages of development. To the best of our knowledge no data on this are available in the literature, but if that was the case, it would be important to investigate with some direct protein analysis whether and when there is a transition from cardiac embryonic (less-glycosylated) to cardiac adult (more-glycosylated) α-DG in cardiac myocytes and fibers. From a translational point of view, such knowledge could guide the optimization of exogenous recombinant agrin that preferentially interacts with fully glycosylated α-DG over laminin in differentiated CMs, as to increase its regenerative potential upon administration to damaged hearts.

Although unlikely, a further scenario that should be considered is the possible presence of an additional "factor" that would be switched on after P2 to freeze/lock the system in a fashion in which agrin would not bind α-DG with the same affinity as before.

Agrin Exact Timing of Expression in the Human Heart

The regeneration potential of human cardiac muscular tissue is considered generally low, although a certain degree of cardiomyocyte renewal has been observed throughout life, with a peak reached at 10 years of age followed by a steady decrease throughout adulthood (Bergmann et al., 2015). The final number of CMs is reached already around 1 month after birth, but the exact timing (i.e., days or weeks) and molecular mechanisms by which the fully proliferative capacity of CMs would be substantially lost and replaced by a very low efficiency in cell division is unknown. No specific data have been collected so far on the transcription/expression levels of agrin or of other elements of the DGC within the first postnatal weeks, due to limitations imposed by obvious ethical concerns on the collection and use of human samples. Therefore, it is not known (i) how crucial is the role of agrin at different stages of human cardiac development and/or cardiomyocyte proliferation, (ii) whether exogenous agrin can exert on human hearts the same effect observed in mice. In this respect, some encouraging preliminary results have been obtained also in piglets, a model of MI more closely related to human cardiac physiology [see the preprint by Baehr et al. (2019)].

In order to fully grasp the possible therapeutic potential of agrin in heart regeneration, the levels of agrin in the human heart should be fully characterized as a function of time, from the embryonic to the childhood and through to the adult stage. This is undoubtedly a very challenging task, due to the limitations cited above that could, however, be at least partially overcome by analyzing (upon ethical approval and patient consent) peri-operative samples. Is agrin only expressed until early after birth, and then not expressed at all? In the light of what has been found in mice, it would be particularly important to collect data on the expression of agrin along all human developmental stages, which is a challenging task, mainly due to the intrinsic difficulties in collecting representative heart samples. Furthermore, is there a differential expression of agrin isoforms specific for each developmental stage? It seems likely that the A0B0 agrin isoform (the so-called muscle isoform, Gesemann et al., 1996) would be the most populated during development and neonatal growth, given that it has the largest affinity for α-DG, but this needs to be demonstrated yet. Ultimately, for a better therapeutic tailoring, it could be important to narrow down the expression profiles of other agrin splice isoforms in the human heart.

"Switching on" an Agrin-Driven Specific Regenerative Program?

Agrin knockout in mice results in death at birth, but no gross histological abnormalities have been recorded in cardiac tissues (Gautam et al., 1996; Burgess et al., 2000). Similar findings have been described for the only human case reported of an agrin-null variant leading to perinatal death, (Geremek et al., 2020). Such evidence strongly indicates that agrin is not essential for CM proliferation during embryogenesis. This means that the DGC could well be involved in the sequestration of phosphorylated YAP at the cytosolic side of sarcolemma but, although agrin can induce DGC disassembly when administered to postnatal heart, factors other than agrin (or complementary to it) could induce the DGC disassembly believed to be responsible for YAP release during development. What is certain is that administration of exogenous agrin promotes the activation of this specific CMs proliferation program in mouse and possibly in larger mammals, as proposed by Baehr et al. in a very recent preprint manuscript (Baehr et al., 2019) reporting the regenerative effect of intracoronary injection of agrin into porcine models of myocardial infarction.

To the best of our knowledge, there is a lack of evidence to show that in larger mammals the regeneration mechanism induced by agrin is an established and conserved genetic program rather than a "*una tantum*" effect induced upon administration of exogenous protein. Again, a thorough investigation to prove whether a similar agrin-induced mechanism is in place also in human cardiac tissues, whether during development or/and exogenously induced, is granted.

Translational Potential of Agrin for Heart Regeneration: Controlled Delivery of Agrin to the Damaged Tissues

From a translational point of view, a strategy based on an agrin-controlled proliferative program that can be triggered from outside CMs (i.e., within the ECM) should follow one of the basic principles of drug discovery and carefully consider the balance likely to exist between the beneficial and deleterious effects of an exogenous reactivation. In principle, any drug effective in raising the transcriptional levels of agrin could be appealing, but an estimate of the specific timing and dosage, as well of the most effective methods of administration, would be essential. If agrin is proven to be a competitor of laminin for binding to α-DG, important results could for example be obtained by reducing (temporarily) the expression of laminin. Another possibility would be to promote expression of a tailored agrin encompassing the α-DG binding site within the damaged tissues using retroviruses, that are commonly employed for delivering into cells nucleic acid sequences of interest to be integrated into the host cells genome. Indeed, a "mini-agrin" construct that binds to basement membranes as well as to α-DG has been already devised for use in skeletal muscle (Moll et al., 2001). Such construct is effective in attenuating the muscle pathology observed in a mouse model for congenital muscular dystrophy, through a mechanism that includes agrin-mediated stabilization of α-DG and the available laminin a5 chain. Retroviral strategies for a prolonged delivery of a series of therapeutic "mini-agrin" peptides (capable of binding both laminin and dystroglycan) have been recently proposed for the treatment of chronic pathologies such as congenital muscular dystrophies in available mouse model systems (Qiao et al., 2018; Yurchenco and McKee, 2019). In the case of agrin, "mini-agrin", or truncated agrin delivery to diseased cardiac tissue, complementary strategies should be in place to make the re-activation highly controlled, as a prolonged delivery of agrin could induce undesired hyperproliferative effects.

Both in mouse (Bassat et al., 2017) and porcine (Baehr et al., 2019) models of myocardial infarction (MI), recombinant agrin injected locally in the damaged heart seems to have an overall cardioprotective effect, with anti-inflammatory and angiogenic components to add to CM protection and (mild) proliferation induction. As the authors suggest, agrin could then enhance heart healing *via* a series of pleiotropic effects, but the hypothesis that agrin may act through a promiscuous rather than a specific mechanism bears important implications/repercussions when trying to envisage regenerative strategies. As an example, administration of agrin has been shown to stimulate the production of blood vessels in both murine and porcine MI (myocardial infarction) models (Baehr et al., 2019), which draws an analogy with the recently discovered role of agrin in recruiting endothelial cells within tumors and its ability to overall promote tumor angiogenesis (Njah et al., 2019). Specifically, agrin has been found to act in endothelial cells (ECs) by an ECM stiffness based mechanism similar to that described in tumor cells, although the mechanotransduction axis would not involve the activation of YAP/TAZ but rather the stabilization of VEGFR2 (Vascular Endothelial Growth Factor Receptor 2), a master regulator of ECs migration, proliferation and angiogenesis. Whether agrin acts following a similar pathway also in cardiac angiogenesis is unknown, but since the agrin isoforms produced within growing tumors by cancer cells and ECs have a similar angiogenic effect (Njah et al., 2019), it could be speculated that this specific agrin axis could be the same acting in cardiac ECs. Paradoxically, even when administered locally, agrin could thus have beneficial effects on certain heart cells/tissues, but at the same time be dangerous for the surrounding ones not directly involved in the damage and healing process, where it could induce hyperproliferation. Considering the role of agrin in tumorogenesis and angiogenesis and the evidences collected on MI models, caution should be exercised when trying to envisage cardiac regenerative strategies involving this proteoglycan. In this respect, another crucial point to also consider in order to further assess the potential benefit of using therapeutic agrin would be to verify whether this protein is stimulating the hyperproliferation of human cardiac fibroblasts, or the activity of other factors involved in fibrotic tissue formation.

Protein Therapy, Dosage, and Cost

The idea that an *in-situ* agrin-injection could potentially prevent or reduce the formation of scar tissue in the injured heart and stimulate the regrowth of healthy cardiac tissue is undoubtedly powerful. From an exquisitely biotechnological point of view, a full biochemical and structural characterization of the interaction of agrin with its partners primarily on CMs would be fundamental for the optimization of a series of parameters typically considered in drug discovery, such as (i) the solubility and stability of the employed recombinant protein, (ii) its capacity to trigger the regenerative program with high specificity, and thus (iii) the most effective dosage (with the least adverse effects), (iv) the final cost of treatments involving a recombinant system for the production of full-length agrin, or of the agrin C-terminal peptides that harbor the α-DG binding site. To note, as an alternative to local injection more physiological methods of administration could be employed. A promising example is offered by cardiac patches made of natural materials with specific biodegradable and biocompatible properties emulating closely the myocardial microenvironment (Albertario et al., 2019; McMahan et al., 2020), to be implanted upon corrective cardiac surgery. Such patches could be used as a matrix for storage and controlled release of agrin with different modalities. As an example, collagen scaffolds have been used to deliver vascular endothelial growth factor (VEGF) either by modifying the protein to include a collagen-binding domain or by seeding the scaffold with cells that have been genetically engineered to express VEGF, thereby extending the delivery time and promoting vascular growth in infarcted myocardial tissue [reviewed by Ye et al. (2013)]. The last frontier would be that of employing the very latest technologies that created an acellular cardiac patch composed of synthetic microparticles containing secreted cardiac regenerative factors embedded in a scaffold formed by decellularized myocardial ECM (Huang et al., 2020), to allow release of agrin in the absence of the complications associated with cellular components. However, it remains to be determined whether any of the above patches would allow for the necessary time-restricted controlled delivery of recombinant agrin to the damaged heart, and local injection might still be the preferential and more efficient mean of administration, as recently shown in pig models of MI (Baehr et al., 2019).

CONCLUSIONS

Agrin might represent a new player in the race to find innovative treatments for the cure of damaged hearts. Although the preliminary results obtained show great promise, it is still too early to foresee whether exogenous agrin-induced heart regeneration could become a realistic therapeutic avenue for injured human cardiac muscle. A thorough investigation at the molecular level into the proposed mechanism and a characterization of the role played by all factors involved will be pivotal to fully uncover the translational potential of this regenerative pathway.

AUTHOR CONTRIBUTIONS

MB and AB conceived the idea and wrote the first draft of the manuscript. KS and FJ prepared the illustration and box. KS, FJ, and MC reviewed and contributed to the various draft versions of the manuscript. All authors read and approved the final manuscript.

FUNDING

This work has been funded by grants from the Sir Jules Thorn Charitable Trust (MC) and the British Heart Foundation, grant no. CH/1/32804 (MB, FJ, and MC).

REFERENCES

Albertario, A., Swim, M. M., Ahmed, E. M., Iacobazzi, D., Yeong, M., Madeddu, P., et al. (2019). Successful reconstruction of the right ventricular cutflow tract by implantation of thymus stem cell engineered graft in growing swine. *JACC Basic Transl. Sci.* 4, 364–384. doi: 10.1016/j.jacbts.2019.02.001

Ali, H., Braga, L., and Giacca, M. (2020). Cardiac regeneration and remodelling of the cardiomyocyte cytoarchitecture. *FEBS J.* 287, 417–438. doi: 10.1111/febs.15146

Baehr, A., Umansky, K. B., Bassat, E., Klett, K., Jurisch, V., Bozoglu, T., et al. (2019). Agrin promotes coordinated therapeutic processes leading to improved cardiac repair in pigs. *bioRxiv [Preprint]*. 854372. doi: 10.1101/854372

Bassat, E., Mutlak, Y. E., Genzelinakh, A., Shadrin, I. Y., Baruch Umansky, K., Yifa, O., et al. (2017). The extracellular matrix protein agrin promotes heart regeneration in mice. *Nature* 547, 179–184. doi: 10.1038/nature22978

Bergmann, O., Zdunek, S., Felker, A., Salehpour, M., Alkass, K., Bernard, S., et al. (2015). Dynamics of cell generation and turnover in the human heart. *Cell* 161, 1566–1575. doi: 10.1016/j.cell.2015.05.026

Brancaccio, A. (2019). A molecular overview of the primary dystroglycanopathies. *J. Cell. Mol. Med.* 23, 3058–3062. doi: 10.1111/jcmm.14218

Brancaccio, A., Schulthess, T., Gesemann, M., and Engel, J. (1995). Electron microscopic evidence for a mucin-like region in chick muscle α-dystroglycan. *FEBS Lett.* 368, 139–142. doi: 10.1016/0014-5793(95)00628-m

Burgess, R. W., Skarnes, W. C., and Sanes, J. R. (2000). Agrin isoforms with distinct amino termini. *J. Cell Biol.* 151, 41–52. doi: 10.1083/jcb.151.1.41

Calvo, F., Ege, N., Grande-Garcia, A., Hooper, S., Jenkins, R. P., Chaudhry, S. I., et al. (2013). Mechanotransduction and YAP-dependent matrix remodelling is required for the generation and maintenance of cancer-associated fibroblasts. *Nat. Cell Biol.* 15, 637–646. doi: 10.1038/ncb2756

Chakraborty, S., and Hong, W. (2018). Linking extracellular matrix agrin to the hippo pathway in liver cancer and beyond. *Cancers* 10, 15–18. doi: 10.3390/cancers10020045

Chakraborty, S., Lakshmanan, M., Swa, H. L. F., Chen, J., Zhang, X., Ong, Y. S., et al. (2015). An oncogenic role of Agrin in regulating focal adhesion integrity in hepatocellular carcinoma. *Nat. Commun.* 6:6184. doi: 10.1038/ncomms7184

Chakraborty, S., Njah, K., Pobbati, A. V., Lim, Y. B., Raju, A., and Lakshmanan, M. (2017). Agrin as a mechanotransduction signal regulating YAP through the Hippo Pathway. *Cell Rep.* 18, 2464–2479. doi: 10.1016/j.celrep.2017.02.041

Chanthra, N., Abe, T., Miyamoto, M., Sekiguchi, K., Kwon, C., Hanazono, Y., et al. (2020). A novel fluorescent reporter system identifies laminin-511/521 as potent regulators of cardiomyocyte maturation. *Sci. Rep.* 10:4249. doi: 10.1038/s41598-020-61163-3

Deshmukh, V., Wang, J., and Martin, J. F. (2019). Leading progress in heart regeneration and repair. *Curr. Opin. Cell Biol.* 61, 79–85. doi: 10.1016/j.ceb.2019.07.005

Ervasti, J. M., and Campbell, K. P. (1993). A role for the dystrophin-glycoprotein complex as a transmembrane linker between laminin and actin. *J. Cell Biol.* 122, 809–823. doi: 10.1083/jcb.122.4.809

Falsaperla, R., Praticò, A. D., Ruggieri, M., Parano, E., Rizzo, R., Corsello, G., et al. (2016). Congenital muscular dystrophy: from muscle to brain. *Italian J. Pediatr.* 42:78. doi: 10.1186/s13052-016-0289-9

Garoffolo, G., and Pesce, M. (2019). Mechanotransduction in the cardiovascular system: from developmental origins to homeostasis and pathology. *Cells* 8:1607. doi: 10.3390/cells8121607

Gautam, M., Noakes, P. G., Moscoso, L., Rupp, F., Scheller, R. H., Merlie, J. P., et al. (1996). Defective neuromuscular synaptogenesis in agrin-deficient mutant mice. *Cell* 85, 525–535. doi: 10.1016/s0092-8674(00)81253-2

Geremek, M., Dudarewicz, L., Obersztyn, E., Paczkowska, M., Smyk, M., Sobecka, K., et al. (2020). Null variants in AGRN cause lethal fetal akinesia deformation sequence. *Clin. Genet.* 97, 634–638. doi: 10.1111/cge.13677

Gesemann, M., Brancaccio, A., Schumacher, B., and Ruegg, M. A. (1998). Agrin is a high-affinity binding protein of dystroglycan in non-muscle tissue. *J. Biol. Chem.* 273, 600–605. doi: 10.1074/jbc.273.1.600

Gesemann, M., Cavalli, V., Denzer, A. J., Brancaccio, A., Schumacher, B., and Ruegg, M. A. (1996). Alternative splicing of agrin alters its binding to heparin, dystroglycan, and the putative agrin receptor. *Neuron* 16, 755–767. doi: 10.1016/s0896-6273(00)80096-3

Heallen, T. R., Kadow, Z. A., Kim, J. H., Wang, J., and Martin, J. F. (2019). Stimulating cardiogenesis as a treatment for heart failure. *Circulation Res.* 124, 1647–1657. doi: 10.1161/circresaha.118.313573

Huang, K., Ozpinar, E. W., Su, T., Tang, J., Shen, D., Qiao, L., et al. (2020). An off-the-shelf artificial cardiac patch improves cardiac repair after myocardial infarction in rats and pigs. *Sci Transl Med.* 12:eaat9683. doi: 10.1126/scitranslmed.aat9683

Jacobson, C., Côt,é, P. D., Rossi, S. G., Rotundo, R. L., and Carbonetto, S. (2001). The dystroglycan complex is necessary for stabilization of acetylcholine receptor clusters at neuromuscular junctions and formation of the synaptic basement membrane. *J. Cell Biol.* 153, 435–450. doi: 10.1083/jcb.152.3.435

Kuang, W., Xu, H., Vachon, P. H., and Engvall, E. (1998). Disruption of the lama2 gene in embryonic stem cells: laminin alpha 2 is necessary for sustenance of mature muscle cells. *Exp. Cell Res.* 241, 117–125. doi: 10.1006/excr.1998.4025

Leschziner, A., Moukhles, H., Lindenbaum, M., Gee, S. H., Butterworth, J., Campbell, K. P., et al. (2001). Neural regulation of α-dystroglycan biosynthesis and glycosylation in skeletal muscle. *J. Neurochem.* 74, 70–80. doi: 10.1046/j.1471-4159.2000.0740070.x

Lv, X., Fang, C., Yin, R., Qiao, B., Shang, R., Wang, J., et al. (2017). Agrin para-secreted by PDGF-activated human hepatic stellate cells promotes hepatocarcinogenesis *in vitro* and *in vivo*. *Oncotarget* 8, 105340–105355. doi: 10.18632/oncotarget.22186

McDearmon, E. L., Combs, A. C., Sekiguchi, K., Fujiwara, H., and Ervasti, J. M. (2006). Brain α-dystroglycan displays unique glycoepitopes and preferential binding to laminin-10/11. *FEBS Lett.* 580, 3381–3385. doi: 10.1016/j.febslet.2006.05.010

McMahan, S., Taylor, A., Copeland, K. M., Pan, Z., Liao, J., and Hong, Y. (2020). Current advances in biodegradable synthetic polymer based cardiac patches. *J. Biomed. Mater. Res. A* 108, 972–983. doi: 10.1002/jbm.a.36874

Moll, J., Barzaghi, P., Lin, S., Bezakova, G., Lochmüller, H., Engvall, E., et al. (2001). An agrin minigene rescues dystrophic symptoms in a mouse model for congenital muscular dystrophy. *Nature* 413, 302–307. doi: 10.1038/35095054

Morikawa, Y., Heallen, T., Leach, J., Xiao, Y., and Martin, J. F. (2017). Dystrophin–glycoprotein complex sequesters Yap to inhibit cardiomyocyte proliferation. *Nature* 547, 227–231. doi: 10.1038/nature22979

Nguyen, Q., Lim, K. R. Q., and Yokota, T. (2019). Current understanding and treatment of cardiac and skeletal muscle pathology in laminin-α2 chain-deficient congenital muscular dystrophy. *Appl. Clin. Genet.* 12, 113–130. doi: 10.2147/TACG.S187481

Njah, K., Chakraborty, S., Qiu, B., Arumugam, S., Raju, A., Pobbati, A. V., et al. (2019). A role of agrin in maintaining the stability of vascular endothelial growth factor receptor-2 during tumor angiogenesis. *Cell Rep.* 28, 949–965.e7. doi: 10.1016/j.celrep.2019.06.036

Notari, M., Ventura-Rubio, A., Bedford-Guaus, S. J., Jorba, I., Mulero, L., Navajas, D., et al. (2018). The local microenvironment limits the regenerative potential of the mouse neonatal heart. *Sci. Advan.* 4:eaao5553. doi: 10.1126/sciadv.aao5553

Parker, K. K., and Ingber, D. E. (2007). Extracellular matrix, mechanotransduction and structural hierarchies in heart tissue engineering. *Philos. Trans. R Soc. Lond. B Biol. Sci.* 362, 1267–1279. doi: 10.1098/rstb.2007.2114

Porrello, E. R., Mahmoud, A. I., Simpson, E., Hill, J. A., Richardson, J. A., Olson, E. N., et al. (2011). Transient regenerative potential of the neonatal mouse heart. *Science* 331, 1078–1080. doi: 10.1126/science.1200708

Porrello, E. R., Mahmoud, A. I., Simpson, E., Johnson, B. A., Grinsfelder, D., Canseco, D., et al. (2013). Regulation of neonatal and adult mammalian heart regeneration by the miR-15 family. *Proc. Natl. Acad. Sci. U. S. A.* 110, 187–192. doi: 10.1073/pnas.1208863110

Qiao, C., Dai, Y., Nikolova, V. D., Jin, Q., Li, J., Xiao, B., et al. (2018). Amelioration of muscle and nerve pathology in LAMA2 muscular dystrophy by AAV9-mini-agrin. *Mol. Ther. Methods Clin. Dev.* 9, 47–56. doi: 10.1016/j.omtm.2018.01.005

Rivera, C., Zandonadi, F. S., Sánchez-Romero, C., Soares, C. D., Granato, D. C., González-Arriagada, W. A., et al. (2018). Agrin has a pathological role in the progression of oral cancer. *Br. J. Cancer* 118, 1628–1638. doi: 10.1038/s41416-018-0135-5

Sciandra, F., Bozzi, M., Bigotti, M. G., and Brancaccio, A. (2013). The multiple affinities of α-dystroglycan. *Curr. Protein Pept. Sci.* 14, 626–634. doi: 10.2174/1389203711209070644

Velayutham, N., Agnew, E. J., and Yutzey, K. E. (2019). Postnatal cardiac development and regenerative potential in large mammals. *Pediatr. Cardiol.* 40, 1345–1358. doi: 10.1007/s00246-019-02163-7

Von Gise, A., Lin, Z., Schlegelmilch, K., Honor, L. B., Pan, G. M., Buck, J. N., et al. (2012). YAP1, the nuclear target of Hippo signaling, stimulates heart growth through cardiomyocyte proliferation but not hypertrophy. *Proc. Natl. Acad. Sci. U. S. A.* 109, 2394–2399. doi: 10.1073/pnas.1116136109

Wang, D., Wang, Y., Liu, H., Tong, C., Ying, Q., Sachinidis, A., et al. (2019). Laminin promotes differentiation of rat embryonic stem cells into cardiomyocytes by activating the integrin/FAK/PI3K p85 pathway. *J. Cell. Mol. Med.* 23, 3629–3640. doi: 10.1111/jcmm.14264

Xin, M., Kim, Y., Sutherland, L. B., Murakami, M., Qi, X., McAnally, J., et al. (2013). Hippo pathway effector Yap promotes cardiac regeneration. *Proc. Natl. Acad. Sci. U. S. A.* 110, 13839–13844. doi: 10.1073/pnas.1313192110

Xiong, W.-C., and Mei, L. (2017). Agrin to YAP in cancer and neuromuscular junction. *Trends Cancer* 3, 247–248. doi: 10.1016/j.physbeh.2017.03.040

Yahalom-Ronen, Y., Rajchman, D., Sarig, R., Geiger, B., and Tzahor, E. (2015). Reduced matrix rigidity promotes neonatal cardiomyocyte dedifferentiation, proliferation and clonal expansion. *eLife* 4:e7455. doi: 10.7554/elife.07455

Yap, L., Tay, H. G., Nguyen, M. T. X., Tjin, M. S., and Tryggvason, K. (2019). Laminins in cellular differentiation. *Trends Cell Biol.* 29, 987–1000. doi: 10.1016/j.tcb.2019.10.001

Yatsenko, A. S., Kucherenko, M. M., Xie, Y., Aweida, D., Urlaub, H., Scheibe, R. J., et al. (2020). Profiling of the muscle-specific dystroglycan interactome reveals the role of Hippo signaling in muscular dystrophy and age-dependent muscle atrophy. *BMC Med.* 18:8. doi: 10.1186/s12916-019-1478-3

Ye, L., Zimmermann, W.-H., Garry, D. J., and Zhang, J. (2013). Patching the heart: cardiac repair from within and outside. *Circulation Res.* 113, 922–932. doi: 10.1161/CIRCRESAHA.113.300216

Yurchenco, P. D., and McKee, K. K. (2019). Linker protein repair of LAMA2 dystrophic neuromuscular basement membranes. *Front. Mol. Neurosci.* 12:305. doi: 10.3389/fnmol.2019.00305

Yurchenco, P. D., McKee, K. K., Reinhard, J. R., and Rüegg, M. A. (2018). Laminin-deficient muscular dystrophy: Molecular pathogenesis and structural repair strategies. *Matr. Biol.* 71–72, 174–187. doi: 10.1016/j.matbio.2017.11.009

Zhang, R., Han, P., Yang, H., Ouyang, K., Lee, D., Lin, Y.-F., et al. (2013). *In vivo* cardiac reprogramming contributes to zebrafish heart regeneration. *Nature* 498, 497–501. doi: 10.1038/nature12322

Zhao, K., Shen, C., Lu, Y., Huang, Z., Li, L., Rand, C. D., et al. (2017). Muscle yap is a regulator of neuromuscular junction formation and regeneration. *J. Neurosci.* 37, 3465–3477. doi: 10.1523/JNEUROSCI.2934-16.2017

Conflict of Interest: The authors declare that the research was conducted in the absence of any commercial or financial relationships that could be construed as a potential conflict of interest.

Copyright © 2020 Bigotti, Skeffington, Jones, Caputo and Brancaccio. This is an open-access article distributed under the terms of the Creative Commons Attribution License (CC BY). The use, distribution or reproduction in other forums is permitted, provided the original author(s) and the copyright owner(s) are credited and that the original publication in this journal is cited, in accordance with accepted academic practice. No use, distribution or reproduction is permitted which does not comply with these terms.

frontiers in Bioengineering and Biotechnology

ORIGINAL RESEARCH
published: 19 June 2020
doi: 10.3389/fbioe.2020.00535

DMD Pluripotent Stem Cell Derived Cardiac Cells Recapitulate *in vitro* Human Cardiac Pathophysiology

Sarka Jelinkova[1,2], Aleksandra Vilotic[1], Jan Pribyl[3], Franck Aimond[4], Anton Salykin[1], Ivana Acimovic[1], Martin Pesl[1,2,5], Guido Caluori[2,5], Simon Klimovic[6], Tomas Urban[1], Hana Dobrovolna[7], Vladimir Soska[7,8], Petr Skladal[5,6], Alain Lacampagne[4], Petr Dvorak[1,2], Albano C. Meli[1,4†] and Vladimir Rotrekl[1,2*†]*

[1] Department of Biology, Faculty of Medicine, Masaryk University, Brno, Czechia, [2] International Clinical Research Center ICRC, St. Anne's University Hospital Brno, Brno, Czechia, [3] CEITEC, Masaryk University, Brno, Czechia, [4] PhyMedExp, University of Montpellier, INSERM, CNRS, Montpellier, France, [5] First Department of Internal Medicine—Cardioangiology, Faculty of Medicine, Masaryk University, Brno, Czechia, [6] Department of Biochemistry, Faculty of Science, Masaryk University, Brno, Czechia, [7] Department of Clinical Biochemistry, St. Anne's University Hospital of Brno, Brno, Czechia, [8] Second Clinic of Internal Medicine, Masaryk University of Brno, Brno, Czechia

Duchenne muscular dystrophy (DMD) is a severe genetic disorder characterized by the lack of functional dystrophin. DMD is associated with progressive dilated cardiomyopathy, eventually leading to heart failure as the main cause of death in DMD patients. Although several molecular mechanisms leading to the DMD cardiomyocyte (DMD-CM) death were described, mostly in mouse model, no suitable human CM model was until recently available together with proper clarification of the DMD-CM phenotype and delay in cardiac symptoms manifestation. We obtained several independent dystrophin-deficient human pluripotent stem cell (hPSC) lines from DMD patients and CRISPR/Cas9-generated DMD gene mutation. We differentiated DMD-hPSC into cardiac cells (CC) creating a human DMD-CC disease model. We observed that mutation-carrying cells were less prone to differentiate into CCs. DMD-CCs demonstrated an enhanced cell death rate in time. Furthermore, ion channel expression was altered in terms of potassium (Kir2.1 overexpression) and calcium handling (dihydropyridine receptor overexpression). DMD-CCs exhibited increased time of calcium transient rising compared to aged-matched control, suggesting mishandling of calcium release. We observed mechanical impairment (hypocontractility), bradycardia, increased heart rate variability, and blunted β-adrenergic response connected with remodeling of β-adrenergic receptors expression in DMD-CCs. Overall, these results indicated that our DMD-CC models are functionally affected by dystrophin-deficiency associated and recapitulate functional defects and cardiac wasting observed in the disease. It offers an accurate tool to study human cardiomyopathy progression and test therapies *in vitro*.

Keywords: duchenne muscular dystrophy, DMD, human pluripotent stem cells, cardiomyocytes, intracellular calcium, excitation-contraction coupling, adrenergic response, cardiomyocyte death

OPEN ACCESS

Edited by:
Monica Boffito, Politecnico di Torino, Italy

Reviewed by:
Monica Mattioli-Belmonte, Marche Polytechnic University, Italy
Hannes Todt, Medical University of Vienna, Austria

***Correspondence:**
Albano C. Meli
albano.meli@inserm.fr
Vladimir Rotrekl
vrotrekl@med.muni.cz

† These authors have contributed equally to this work

Specialty section:
This article was submitted to Biomaterials, a section of the journal Frontiers in Bioengineering and Biotechnology

Received: *15 December 2019*
Accepted: *04 May 2020*
Published: *19 June 2020*

Citation:
Jelinkova S, Vilotic A, Pribyl J, Aimond F, Salykin A, Acimovic I, Pesl M, Caluori G, Klimovic S, Urban T, Dobrovolna H, Soska V, Skladal P, Lacampagne A, Dvorak P, Meli AC and Rotrekl V (2020) DMD Pluripotent Stem Cell Derived Cardiac Cells Recapitulate in vitro Human Cardiac Pathophysiology. Front. Bioeng. Biotechnol. 8:535. doi: 10.3389/fbioe.2020.00535

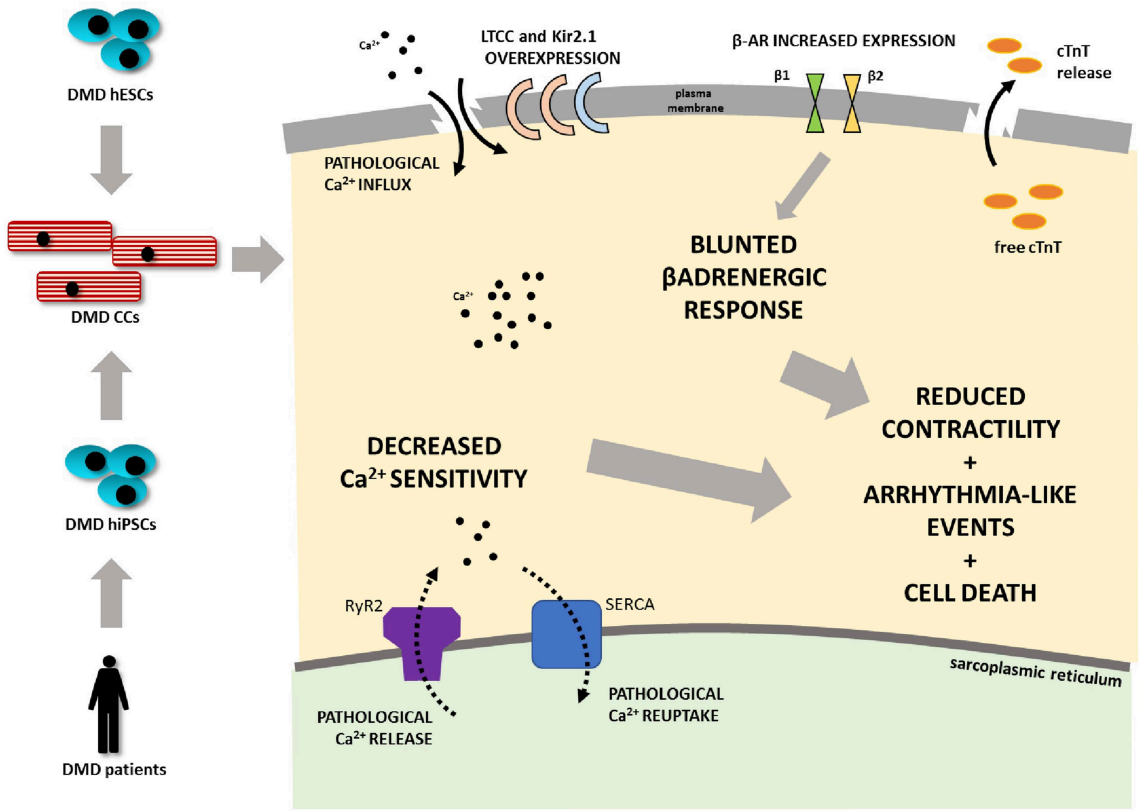

GRAPHICAL ABSTRACT | Duchenne muscular dystrophy (DMD) is associated with progressive dilated cardiomyopathy eventually leading to heart failure as the main cause of death in DMD patients. A human cardiomyocyte (CM) model was developed from several independent dystrophin-deficient human pluripotent stem cell (hPSC) lines from DMD patients and hESC line with deletion of DMD gene generated by CRISPR/Cas9 technology. DMD hPSC were differentiated into CMs. DMD mutation-carrying cells are less prone to differentiate into CMs. DMD CMs further demonstrate an enhanced cell death rate. Ion channel expression was altered in terms of potassium (Kir2.1 overexpression) and calcium handling (DHPR overexpression). DMD-CMs exhibited mishandling of calcium demonstrated by increased time of calcium release. Further mechanical impairment (hypocontractility), bradycardia, increased beat rate variability, and blunted β-adrenergic response connected with remodeling of β-adrenergic receptors' expression was found in DMD-CMs (LTCC L-type calcium channel, cTnT - cardiac troponin T, Kir2.1 - potassium channel).

Abbreviations: ACTC1, cardiac muscle alpha actin; AFM, atomic force microscopy; AP, action potential; APD, action potential duration; AR, adrenergic receptor; BMP4, bone morphogenic factor 4; CC, cardiac cell; cDMD, CRISPR/Cas9 generated DMD-hESC line; cl4, control hiPSC line; CM, cardiomyocyte; cTNT, cardiac troponin T; DAD, delayed after depolarization; DAPI, 4′,6-Diamidine-2′-phenylindole dihydrochloride; DCM, dilated cardiomyopathy; DHPR, dihydropyridine receptor; DMD, Duchenne muscular dystrophy; EB, embryonic body; ECC, excitation-contraction coupling; FGF2, fibroblast growth factor (basic, or 2); FKBP12. 6, calstabin 2; GJA1, connexin43; hESC, human embryonic stem cells; hiPSC, human induced pluripotent stem cells; hPSC, human pluripotent stem cells; IBI, inter-beat variability; ISO, isoproterenol; Kir2.1, Kir2.2, Kir2.3, potassium channels encoded by KCNJ2, KCNJ4, and KCNJ12 genes respectively; LTCC, L-type calcium channel; mdx; mdx:utr, muscular dystrophy on X chromosome, mouse model lacking dystrophin; utrophin and dystrophin lacking mouse model; mEF, mouse embryonic fibroblasts; METO, metoprolol; MYH6, myosin heavy chain α; MYH7, myosin heavy chain β; MYL2, myosin light chain 2; MYL7, myosin light chain 7; NKX2.5, NK homeobox 5; NOS, nitric oxide synthase, inducible (iNOS), neuronal (nNOS); qRT-PCR, quantitative real-time PCR; ROS, reactive oxygen species; RyR2, ryanodine receptor 2; SAC, stretch activated channels; SERCA (ATP2A), Sarcoplasmic/endoplasmic reticulum calcium ATPase 1; SR, sarcoplasmic reticulum; VEGF, vascular endothelial growth factor; WT, wild type control.

INTRODUCTION

Duchenne muscular dystrophy (DMD, prevalence 1/3,500–6,000 boys) is an X-linked genetic disorder which impairs striated muscles and results in severe disability and premature death in young men (Mah et al., 2014; Vry et al., 2016; Stehlíková et al., 2017). DMD is often associated with dilated cardiomyopathy (Manzur et al., 2008), which develops in affected patients during their teenage years. It is represented by a slowly progressing decline in diastolic function, systolic ejection fraction, and fractional shortening (Markham et al., 2006). Mechanical degeneration is associated with progressive cardiomyocyte (CM) wasting and spreading of fibrosis throughout the ventricular wall (Finsterer and Stöllberger, 2003; Panovský et al., 2019), which leads to intracardiac conduction disturbances, inducing atrial and life-threatening ventricular arrhythmias (Chenard et al., 1993; Himmrich et al., 2000). Gradual dilatation of the ventricle, thinning of the wall (Wagner et al., 2007), and consequent loss of contractility lead to repeated episodes of heart failure, which

recently became the most frequent mortality cause in DMD patients worldwide (Finsterer and Stöllberger, 2003; Fayssoil et al., 2010).

DMD is caused by mutations in the dystrophin gene (*DMD*), which can result in a total lack of functional dystrophin or presence of a truncated inactive form of the protein (Blake et al., 2002). Dystrophin plays a major role in the organization of dystrophin glycoprotein complex (Clarac et al., 2009) responsible for sarcolemmal adhesion to the basal lamina and intracellular pathway regulations. Whereas, skeletal muscle degeneration is extensively studied, the cellular mechanisms of the cardiac pathophysiology are still unclear. Available studies point out the role of oxidative stress and DMD-induced Ca^{2+} mismanagement (Williams and Allen, 2007; Jung et al., 2008; Caluori et al., 2019), with subsequent cytosolic imbalance and cell damage (Gerke et al., 2005).

In DMD (muscular dystrophy on X chromosome, *mdx)* mice, we have shown that dystrophin deficiency caused post-translational remodeling of the cardiac ryanodine receptor (RyR2) macromolecular complex, due to S-nitrosylation and Calstabin2 (FKBP12.6) depletion, which leads to intracellular diastolic Ca^{2+} leak and ventricular arrhythmias (Fauconnier et al., 2010).

Intracellular Ca^{2+} leak from the sarcoplasmic reticulum (SR) was also associated with deregulation of stretch-activated channels (SAC) though reactive oxygen species (ROS)-mediated hyperactivity (Jung et al., 2008).

Further studies in animal models showed misregulation of other ion channels such as voltage-gated Nav1.5 and L-type calcium channel (LTCC) hyperactivation (Koenig et al., 2011), as well as upregulation of inflammation-related induced nitric oxide synthase (iNOS) (Fauconnier et al., 2010; Peterson et al., 2018). Such observations remain to be validated in human DMD. Furthermore, to this day, there are only limited studies of human DMD cardiac cell (CC) models, describing some of the discrepancies eventually leading to DMD-CM damage (Eisen et al., 2019; Pioner et al., 2020). In the present study, we thus focused, for the first time, on evaluating the impact of dystrophin-deficiency on some molecular properties of the excitation-contraction coupling (ECC) and flight-or-fight response in some patient-specific DMD human pluripotent stem cell-derived cardiac cells (DMD-hPSC-CCs) as well as in CRISPR/Cas9 engineered hPSC-CCs (summarized in **Graphical abstract**).

MATERIALS AND METHODS

A wide selection of methods was used for analysis of the model starting from generation of the hPSC lines to analysis of 3D contracting clusters and dissociated CCs; thus, the methodological approach has been summarized in **Figure 1**.

Cell Lines, Cultivation, Reprogramming, and hPSC Differentiation Into Cardiomyocytes via Embryoid Bodies

Patient-specific DMD human induced pluripotent stem cell (hiPSC) lines (DMD02 and DMD03) and CRISPR/Cas9 dystrophin-deficient human embryonic stem cell (hESC) line (cDMD) were used (described in Jelinkova et al., 2019a,b). The fibroblasts of two DMD patients were derived from skin/muscle (for DMD02/DMD03, respectively) biopsies. Informed consents approved by Ethics Committee (Faculty of Medicine, Masaryk University) were signed by parents of the patients beforehand and the investigation conformed to the principles outlined in the Declaration of Helsinki.

Control human embryonic stem cell (hESC) line CCTL14 (serving as isogenic control for cDMD) as well as CCTL12 hESC line (further referred to as WT hESC) derived in Masaryk University, Brno, and previously characterized (International Stem Cell Initiative et al., 2007), were used. hiPSC control line UEFhfiPS1.4 (Qu et al., 2013) and cl.4 obtained from Majlinda Lako (NewCastle, UK) (further called WT-hiPSC) were used for comparison with DMD-hiPSC to reduce the effect of reprogramming on the CC phenotype.

All human pluripotent stem cell (hPSC) lines were routinely maintained on feeder layer of mitotically inactivated mouse embryonic fibroblasts (mEF) as previously described (Dvorak et al., 2005; Krutá et al., 2014; Jelinkova et al., 2019a).

Cardiac differentiation and eventual subsequent dissociation of hPSC-CCs were performed for confocal fluorescent intracellular Ca^{2+} measurements, patch-clamp, atomic force microscopy (AFM), and immunocytochemistry as previously described (Pesl et al., 2014) with minor modifications. Briefly, grown colonies were cut into pieces with a pipette tip and clumps were transferred into differentiating embryonic body (EB) medium (86% KnockOut Dulbecco modified eagle medium, 10% fetal bovine serum, 1% L-glutamine, 1% penicillin/streptomycin, 1% nonessential amino acids, 0,1mM 2-mercaptoethanol) with 10 ng/ml bone morphogenic protein 4 (BMP4, R&D) and 10 μg/ml ascorbic acid (Sigma Aldrich) where they formed EBs. After 2 days, the medium was changed into EB medium with 5 ng/ml basic fibroblast growth factor (FGF2, Peprotech), 10 ng/ml BMP4, 6 ng/ml Activin A (R&D) and 10 μg/ml ascorbic acid (Sigma Aldrich) and incubated for 4 days. The next 3 days consisted of EB medium supplemented with 10 ng/ml vascular endothelial growth factor (VEGF, R&D), 10 μM IWR1 (Sigma Aldrich), and 10 μg/ml ascorbic acid. The EBs were further cultivated in EB medium with 10 μg/ml ascorbic acid, 10 ng/ml VEGF, and 5 ng/ml FGF2 for 12 days with medium changed every 4 days, and then with EB medium with 10 μg/ml ascorbic acid until further analysis. The differentiation procedure was performed for 13 days in hypoxic conditions (5% oxygen). Then, the EBs were moved into normoxic conditions (20% oxygen) for further cultivation.

Immunodetection

Immunocytological analyses utilized [antibody specific against N-terminal (1:50 ICC/1:50-1:300 WB, Cat# NCL-DYSB, Leica Biosystems), and antibody specific against C-terminal (1:100 ICC/1:1000 WB, Abcam, Cat# ab15277)], for cardiac markers cardiac troponin T (cTnT; SantaCruz, Cat# sc-8121, 1:200) α-actinin (SigmaAldrich, Cat# A7180, 1:500) L-type channel (LTCC, dihydropyridine receptor DHPR alpha 2 subunit/CACNA2D1 antibody abcam, Cat# ab2864, 1:200),

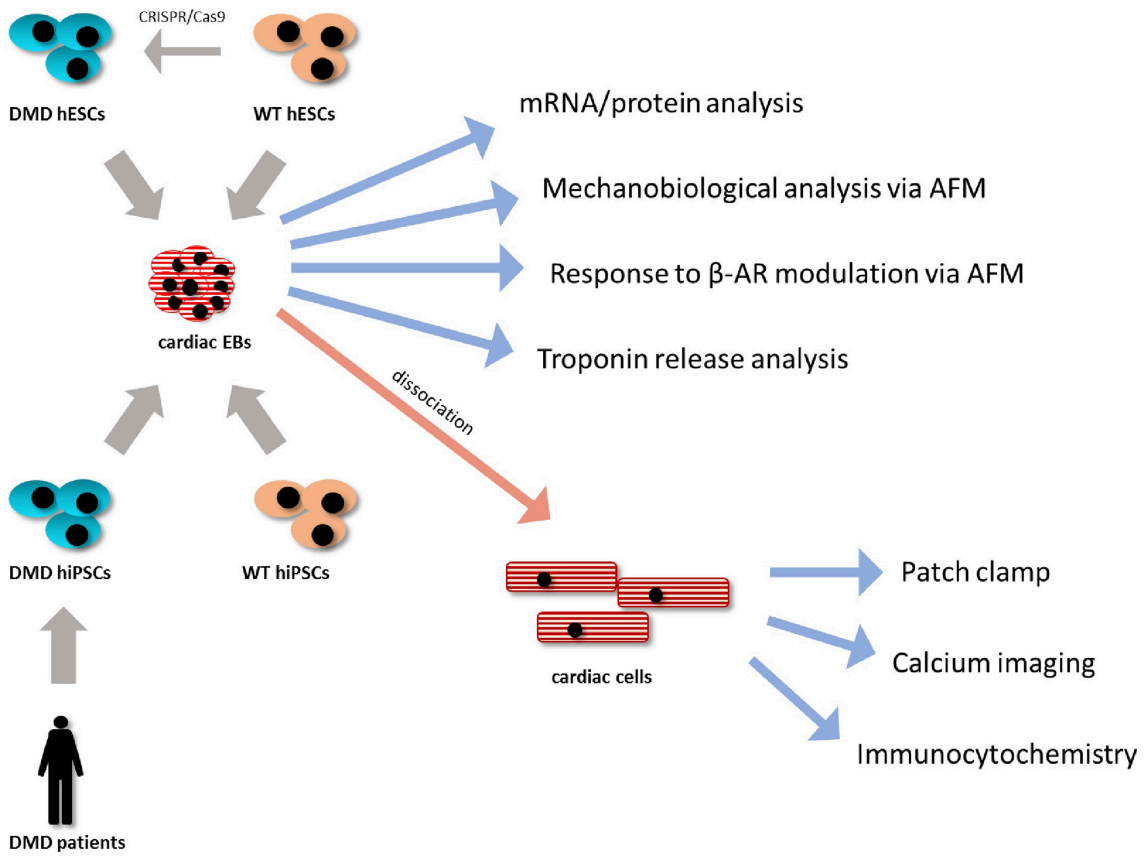

FIGURE 1 | Methodological approach. DMD-hiPSC lines from two Duchenne muscular dystrophy (DMD) patients were generated and analyzed compared to WT-hiPSC lines. DMD-hESC line was generated using CRISPR/Cas9 technology by targetted deletion of the DMD gene from a healthy WT hESC line serving as isogenic control. All hPSC lines were differentiated using 3D cell aggregates (embryonic bodies, EBs). These EBs were then used for molecular and mechanobiological analysis methods or were enzymatically dissociated into isolated cardiac cells, which were further analyzed using single cell specific analysis as protein localization and ion fluxes analyses.

assays were performed as described previously (Krutá et al., 2013). For cTnT and α-actinin, cells were fixed using 4% paraformaldehyde at room temperature for 10-15 min. Cells for dystrophin labeling were fixed with 2% paraformaldehyde for 10 min at room temperature, then with ice cold methanol for 5 min, and incubated with pre-extraction buffer (25 mM HEPES, 50 mM NaCl, 1 mM EDTA, 3 mM MgCl2, 200 mM sucrose, 0.5% Triton X-100) before continuing to blocking steps.

The cells were permeabilized and blocked with blocking solution 1 (1% bovine serum albumin, BSA, 0.2% Triton X-100 in phosphate buffer saline, PBS, 15 min on ice) and blocking solution 2 (1% BSA, 1% NaN3, 0.05% Tween 20 in PBS, 60 min on ice). Primary antibodies were diluted in PBS/Tween (0.05%) and incubated overnight at 4°C. Samples were extensively washed with PBS/Tween (0.05%) and incubated with appropriate fluorescent secondary antibody for 1 h at room temperature. For nuclear counterstain, 4′,6-Diamidine-2′-phenylindole dihydrochloride (DAPI) was used. All fluorescent and confocal microscopy experiments were performed using Confocal LSM700 microscope and processed using Zen software (both Carl Zeiss, Oberkochen, Germany).

For dystrophin immunoblots, protein samples from cell lysates were run in 4–12% gradient polyacrylamide gel for 70 min/170V/400mA, blotted at 100 V/300 mA for 2 h, and labeled with antibody against dystrophin protein. After dystrophin detection, the membrane was incubated with antibody against lamin B as loading control (1:1000, Santa Cruz, sc6217). Adrenergic receptors (AR) were analyzed using β1 specific (Thermo Fisher, PA5-28808, 1:500) and β2 specific (abcam, ab137494, 1:500) antibody. Human heart atrial tissue was obtained as procedural surplus material, available during bicaval orthotopic heart transplantation from donor organs and was used as positive control as previously described (Pesl et al., 2020).

Quantitative Real-Time PCR

Cardiac EBs 30–50 days old and human heart samples (obtained as surplus material from donor hearts during cardiac transplantations) were lysed using RNA Blue reagent (Top-Bio, Prague, Czech Republic) according to the manufacturer's instructions, and the total mRNA was isolated using the RNeasy Micro Kit (Qiagen, Hilden, Germany). RNA concentration and purity were determined using NanoDrop (NanoDrop

technologies, Wilmington, DE, USA). cDNA was synthesized by Moloney Mouse Leukemia Virus (M-MLV) reverse transcriptase (Invitrogen, Carlsbad, CA, USA) at 37°C for 1 h followed by 5 min at 85°C. For quantitative real-time PCR (qRT-PCR), LightCycler® 480 SYBR Green Master kit (Roche, Basel, Switzerland) was used according to manufacturer's instructions, and PCR was performed, with annealing temperature 60°C and 55 cycles on LightCycler LC480 Instrument (Roche). The PCR primers (Generi-Biotech, Hradec Kralove, Czech Republic) are shown in **Supplementary Table 1**.

Measurements of Intracellular Cytosolic Ca^{2+} Variations by Fluorescent Confocal Microscopy

The contracting EBs were dissociated to single CCs by incubation in Ca^{2+}-free solution [120 mM NaCl, 5.4 mM KCl, 5 mM $MgSO_4$, 5 mM sodium pyruvate, 20 mM glucose, 20 mM taurine, 10 mM HEPES (all Sigma Aldrich), pH6.9] at room temperature and enzymatically treated with 0.8 mg/ml type II collagenase (Gibco) and 0.037 mg/ml type XIV proteinase (Sigma Aldrich) in the same solution for 3 min at 37°C. The clusters were then incubated in dissociating solution (85 mM KCl, 30 mM K_2HPO_4, 5 mM $MgSO_4$, 1 mM EGTA, 5 mM sodium pyruvate, 5 mM creatine, 20 mM taurine, 20 mM glucose, 2 mM disodium pyruvate, pH = 7.4) for 20 min at 37°C and plated on gelatin coated 35 mm glass bottom culture dishes (MatTek) in EB medium until the next day. On the day of measurements, cells were incubated in a Tyrode's solution (140 mM NaCl, 5 mM HEPES, 4 mM KCl, 1 mM $MgCl_2$, 1.8 mM $CaCl_2$, 10 mM glucose, pH 7.4) with 3 μM Fluo4-AM (Invitrogen, Carlsbad, CA, USA) for 20 min at room temperature. After the incubation with Fluo4-AM, the solution was replaced with the fresh Tyrode's solution and the cells were placed on the stage of an inverted microscope. Ca^{2+} images in line-scan mode were recorded with a laser scanning confocal microscope Zeiss LSM Exciter (Carl Zeiss), with 40x water immersion objective, in x–y mode, 1 image/0.495 s. Electrical pacing was set up with frequency 0.5, 1 Hz (20 V, 0.5 ms duration and 1 ms delay). The kinetic properties of intracellular Ca^{2+} variations including Ca^{2+} transients and diastolic events were analyzed by in-house developed PeakInspector software (https://asalykin.github.io/PeakInspector/) as previously described (Acimovic et al., 2018).

Electrophysiological Recordings Through Patch-Clamp

Electrophysiological recordings were obtained using whole-cell patch-clamp technique on an Axopatch 200B (Axon Instruments, Foster City, CA) at room temperature (22–24°C). The recording pipettes contained: 120 mM KCl, 8 mM EGTA, 10 mM HEPES, 6.8 mM $MgCl_2$, 3 mM $CaCl_2$, 4 mM $ATPNa_2$, 0.4 mM $GTPNa_2$ (pH 7.2). The bath solution contained: 130 mmol/L NaCl, 4 mM/L KCl, 1.8 mM/L $MgCl_2$, 1.8 mM/L $CaCl_2$, 10 mM/L HEPES, 11 mM/L glucose (pH 7.4). Action potentials (APs) were measured in the current-clamp configuration in response to brief (1–2 ms) depolarizing current injections at 1 Hz. The resting membrane potential, the amplitude and duration (APDs) at 20, 50, and 90% repolarization of the APs were measured (respectively indicated as APD_{20}, APD_{50}, and APD_{90}). 7 DMD-hPSC-derived CCs (DMD-CCs) and 18 WT-hPSC-derived CCs (WT-CCs) were analyzed. Cells arrhythmogenicity was tested using application of successive 10 s runs in the current clamp configuration defined by 5 brief (1 ms) depolarizing current injections at 2 Hz followed by a resting period. Data were analyzed using the Clampfit 10.0 (Axon Instruments) software.

Atomic Force Microscopy Measurements

Atomic force microscope (JPK NanoWizard 3, JPK, Berlin, Germany), combined with an inverted light microscope (IX-81S1F-3, Olympus, Tokyo, Japan), was used to obtain mechanocardiograms of beating EBs as previously described (Pesl et al., 2014; Caluori et al., 2019; Pribyl et al., 2019). Drug response tests were performed after initial equilibration in Tyrode's solution, followed by addition of 70 μM metoprolol, 10 min of stabilization time, and then 10 min of measurement. Isoproterenol (1 μM) was subsequently added into the solution, and mechanocardiograms were measured after 20 min of stabilization. The mechanical properties of beating EBs were expressed as force of contraction in nN as previously described (Pesl et al., 2014); however, the values were relativized for final comparison.

Free Troponin Analysis

The EBs were formed and cardiac induction was initiated as described above. On day 18, individual EBs homogenous in size and shape were separated onto 12 well plate coated with gelatin and 1ml of proper induction medium was added. From day 21 to 51 with frequency of 4 days, medium sample was collected, spun, and the supernatant frozen in −20°C until all samples were harvested. The samples were then analyzed for free troponin T concentration using two epitopes based immunochemical system Cobas e602 (Basel, Switzerland) specifically high sensitive short turnaround time (STAT) kit Elecsys Tropo T hs STAT 100 (Roche diagnostics, Basel, Switzerland; Hess et al., 2008) according to the manufacturer's instructions.

Statistical Analysis

Statistical evaluation was carried out in GraphPad Prism 8.3 software (GraphPad Software, Inc., La Jolla, CA, USA). Available normality tests were performed for the obtained data, and Student's two-tailed *t*-test or ANOVA was used to assess statistically significant differences on normally distributed group pairs. Where normality tests failed, non-parametric tests were used. Individual statistical test used was specified in individual figure legends.

RESULTS

DMD-CCs Do Not Express Full-Length Dystrophin Protein

Three previously described patient-specific DMD-hiPSC and one CRISPR/Cas9-mediated DMD-hESC lines (Jelinkova et al., 2019a,b) were differentiated into CMs (Pesl et al., 2014). WT hESC [hESC CCTL12 (hPSCreg name MUNIe005-A, passages

15–61) and CCTL14 (hPSCreg name MUNIe007-A, passages 15–63) derived in Masaryk University, Brno, and characterized previously (International Stem Cell Initiative et al., 2007)] and WT-hiPSC [cl.4 (passages 43–84) obtained from Dr. Majlinda Lako (Newcastle University, UK) (Armstrong et al., 2010) and hfiPSC (passages 20–52) (Qu et al., 2013)] were used as controls. The obtained DMD-CCs were evaluated for dystrophin presence. The strategy for antibody detection is illustrated in **Figure 2A**. Dystrophin expression was evaluated using immunocytology with specific antibodies against high molecular weight isoform of dystrophin (antibody specific to N-terminus detecting the full-length 427 kDa isoform, **Figure 2B**, left panel), as well as shorter isoforms (antibody specific to C-terminus, which is present in various lower molecular weight dystrophin isoforms, **Figure 2B**, right panel). Dystrophin expression was observed with both antibodies in WT-CCs as membranous signal of the antibody (**Supplementary Figure 2**). No membranous/cytoplasmic protein signal was detected in any DMD-CCs (**Figure 2B**). Nuclear signal of dystrophin was detected by C-ter antibody (which can detect shorter dystrophin isoforms, most likely the Dp71 isoform), and no cytoplasmic/membranous signal was observed in CCs derived from either DMD-hPSC lines. Furthermore, western blot analysis with N-ter and C-ter antibodies showed expression of some shorter dystrophin isoforms (Dp140, Dp116, and Dp71) in the DMD cell lines, but none in the full high molecular band (Dp427) (**Figure 2C**, full membranes in **Supplementary Figure 2**).

Dystrophin Deficiency Leads to Cardiac Differentiation With Lower Yield of Spontaneously Beating EBs

Next, we aimed at characterizing the impact of dystrophin deficiency on the cardiac differentiation of hPSCs through the EB-based method as previously published (Pesl et al., 2014). We compared the yield of beating EBs upon differentiation of all DMD and WT-hPSC lines. First of all, we used the spontaneous beat in 3D EB clusters as a criterion to evaluate the cardiac differentiation success. The differentiation efficacy represented by the fraction of spontaneously beating EBs (detected at day 29 after cardiac differentiation start) was decreased in DMD-EBs compared to WT-EBs (**Figure 3A**, statistical evaluation in **Supplementary Table 2**). At the cellular level, the beating EBs from all tested cell lines contained CCs (**Figure 3B**) with striated pattern of cardiac troponin T (cTnT) and α-actinin. The differentiation efficacy was also measured in age-matched groups of DMD- and WT-EBs aged 25–29 days by qRT-PCR of well-known cardiac markers [*NKX2.5* ($p = 0.42$), myosin heavy chain α (*MYH6*, $p = 0.71$), myosin heavy chain β (*MYH7*, $p = 0.82$), myosin light chain 2 (*MYL2*, $p = 0.17$), myosin light chain 7 (*MYL7*, $p = 0.42$), ryanodine receptor 2 (*RYR2*, $p = 0.61$), cardiac muscle alpha actin (*ACTC1*, $p = 0.78$), connexin43 (*GJA1*, $p = 0.36$)], showing no significant difference in relative mRNA expression. However, a tendency for lower yield of most of the markers in the obtained DMD clusters was observed, with the exception for *MYH7* and *GJA1* (**Figure 3C**). Inward rectifier potassium channels Kir2.1, Kir2.2, and Kir2.3 were also tested (*KCNJ2*, *KCNJ4*, and *KCNJ12*, respectively) with significant increase in Kir2.1 expression ($p = 0.004$); SERCA (*ATP2A*) shows no difference in mRNA expression.

DMD-CCs Display Altered Electrophysiological Properties

Next, we tested whether dystrophin deficiency alters the cardiac electrophysiological properties and arrhythmogenicity of single hPSC-derived CCs. Action potential (AP) properties (resting membrane potential (RP), amplitude, and duration (APD) in DMD- (26–46 days old) and WT-CCs (36–41 days old) were recorded using the patch clamp technique. Age matching of the CCss was not possible in this instance due to technical reasons as only a limited number of CCs were analyzed. Both DMD- and WT-CCs mostly exhibited triangular-shaped APs with various APD90 durations ranging from 20 to 380 ms (**Figures 4A,B**) similarly to WT with measured APD90 ranging from 20 to 520 ms. More occasionally, plateau-shaped APs with longer (>300 ms) APD90 durations were observed (**Figures 4A,B**, **Supplementary Figure 7**). No significant difference was observed in RP, amplitude, and durations between DMD- ($n = 7$) and WT-CCs ($n = 18$) APs (**Figure 4B**). Occurrence of fast pacing induced delayed afterdepolarization (DAD) events was observed and quantified. No difference ($p = 0.25$) between DMD-CCs (50%; 1.2 ± 0.3 events/10 s, $n = 7$) and WT-CCs (35%; 1.9 ± 0.4 events/10 s, $n = 18$) in the occurrence of DAD was observed (**Figure 4C**).

DMD-CCs Exhibit Abnormal Intracellular Ca^{2+} Handling

Intracellular SR Ca^{2+} handling has been shown to be affected in several DMD models, in particular through RyR2 mediated Ca^{2+} leak (Andersson and Marks, 2010; Fauconnier et al., 2010; Andersson et al., 2012). Using confocal fluorescent microscopy as we previously showed in hPSC-CCs (Pesl et al., 2014; Acimovic et al., 2018), we investigated the enzymatically dissociated single cell Ca^{2+} handling in DMD and WT-CCs matched between 40 and 50 days after differentiation. We chose this age as a safe timepoint to interpret the eventual differences as prevalently caused by the DMD mutation: it is in fact reported that calcium machinery in hPSC-CCs reaches a "stationary state" between 21 and 30 days after induction (Hwang et al., 2015). We acquired intracellular Ca^{2+} transients in resting state and under physiological pacing conditions (0.5 and 1 Hz). We analyzed spontaneous frequency of calcium transients, together with their time parameters, and occurrence of secondary small diastolic calcium events possibly triggering increased automaticity.

A lower frequency was observed in the major Ca^{2+} transients in DMD- compared to WT-CCs in resting conditions (1.262 ± 1.608 Hz vs. 2.416 ± 3.441 Hz respectively, $p < 0.0001$). Ca^{2+} transient dynamics resulted altered in DMD single CCs: either in resting or in paced conditions, the time to peak, dependent on the SR Ca^{2+} release properties, was significantly elongated in dystrophin deficient cells ($p < 0.0001$, **Figure 5A**). Ca^{2+} transient

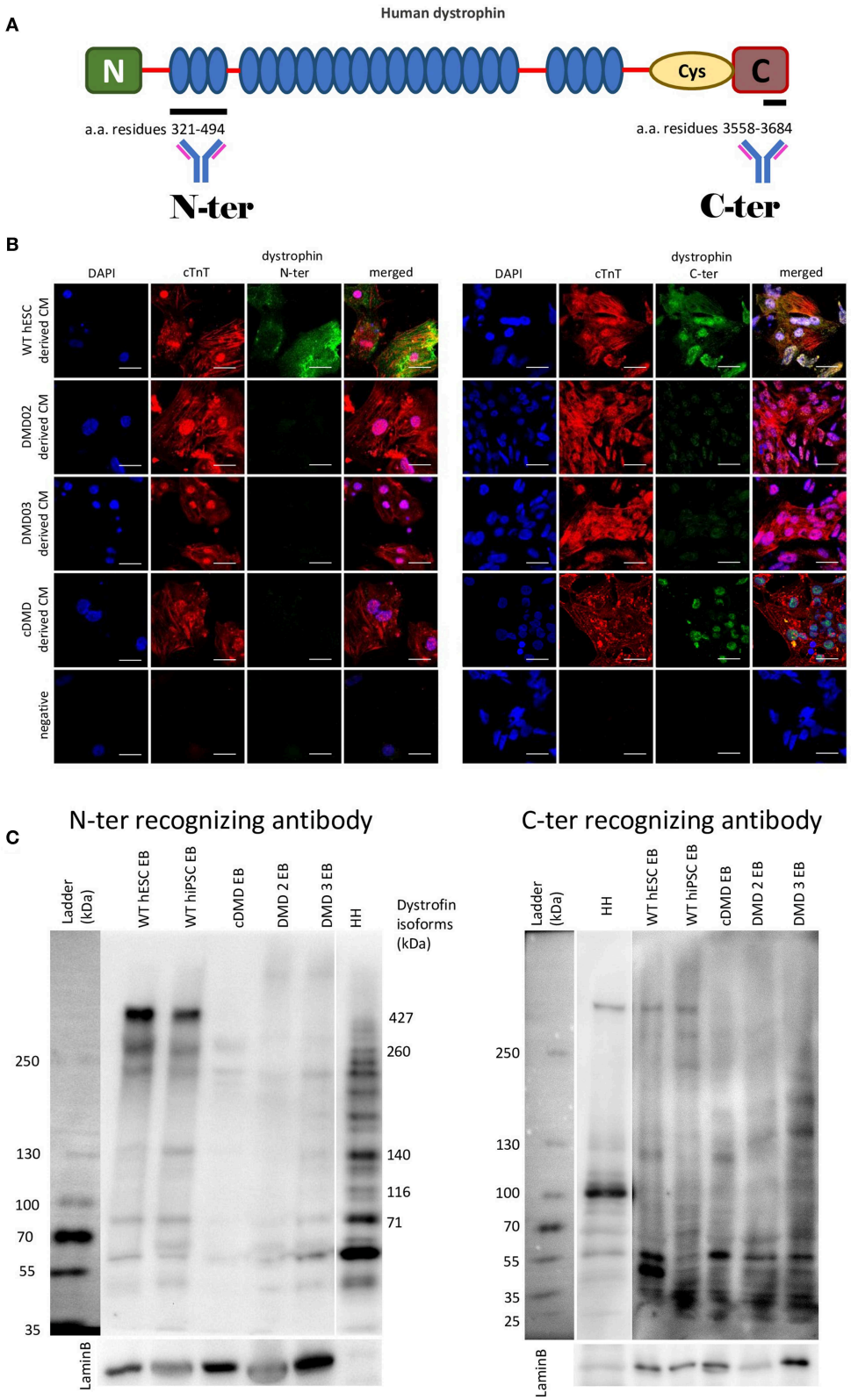

FIGURE 2 | DMD-hPSC differentiate into cardiac cells (CCs), which do not express dystrophin. **(A)** Antibodies against dystrophin N-terminal (N) aminoacid (a.a.) residues 321–494 and C-terminal aminoacid residues 3558–3684 were used. **(B)** hPSC derived CCs were analyzed for presence of dystrophin (in green). WT hESC

(Continued)

FIGURE 2 | derived CCs dissociated from spontaneously beating EBs presenting with positive signal for cardiac troponin T (red) showed positive signal for dystrophin labeled by N-terminus specific antibody as well as by C-terminus specific antibody. None of the DMD-hPSC lines (DMD02, DMD03, and cDMD) derived CCs showed any signal for dystrophin. DAPI was used for nuclear counterstain. Ruler represents 50 μm. **(C)** The differentiated EBs were lyzed and western blot analysis was performed to identify the individual isoforms expressed. Both used WT-hPSC derived EBs show expression of various dystrophin isoforms including Dp427, Dp260, Dp140, and Dp71. The CRISPR/Cas9 generated cDMD-EBs show no expression of either isoform, while only shorter isoforms were identified in patient DMD-hiPSC-EBs with promoters downstream of the patient's mutations. Human heart tissue (HH) was used as positive control. LaminB was used as loading control.

decay time, expression of the features of calcium reuptake, was increased in DMD in resting state (+59.24 ms average increase, $p = 0.013$, **Figure 5B**); this prolongation was non-significant in pacing conditions. Transient duration, which determines the contraction cycle and possible Ca^{2+}-induced arrhythmogenicity, was also elongated in DMD-CCs (**Figure 5C**; 63.53 ms in resting state, $p = 0.002$, and 71.51 ms under 0.5 Hz pacing, $p = 0.025$). These data suggest that the lack of dystrophin affects DMD-CCs during spontaneous and triggered SR Ca^{2+} release, affecting overall calcium dynamic.

We then observed and quantified the occurrence of secondary small-amplitude Ca^{2+} release events occurring after a main transient during diastole (relaxation and baseline, **Figure 5D**) and found significantly increased frequency of these events in DMD-CCs ($p = 0.0172$, **Figure 5E**).

Aberrant L-Type Voltage-Dependent Ca^{2+} Channel Expression in DMD-CCs

To further understand how dystrophin deficiency affects Ca^{2+} homeostasis and ECC in DMD-CCs, we verified the expression pattern of LTCCs using dihydropyridine receptor (DHPR) α2 subunit/CACNA2D1 antibody. At the protein level, DHPR α2 subunit expression was increased in patient-specific DMD-CCs (DMD02 and 03, **Figure 5F**). No difference was observed on the mRNA level of the CACNA1C (encoding Cav1.2) or CACNA1D (encoding Cav1.3) between the WT and DMD groups (**Figure 5G**). We then tested the cellular localization of the L-type channels using DHPR immunostaining. In line with previous protein analysis, DMD-CCs (detected by cTnT labeling) showed stronger signal of the LTCC, and no other difference was detected (**Figure 5H**).

DMD-EBs Display Hypocontractility, Bradycardia, and Higher Heart Rate Variability

DMD-associated dilated cardiomyopathies is characterized by thinner left ventricle, reduced cardiac output, and hypo-contractility of the heart (Hajjar et al., 1993; Bondue et al., 2018; Amedro et al., 2019). We thus tested whether DMD-CCs contained in 3D cardiac clusters (EBs) exhibit weaker contractile properties by measuring the contraction force and beat rate by AFM as we previously published (Pesl et al., 2014, 2016; Acimovic et al., 2018). We observed weaker spontaneous contraction force in DMD-EBs (**Figure 6A**, $p < 0.0001$) while they exhibited similar overall beat rate compared to WT-EBs (**Figure 6B**, $p = 0.139$; for separate data of each line, see **Supplementary Figure 6**). We noticed a peculiar variability in the inter-beat interval (IBI, **Figure 6C**, $p = 0.0039$) (examples of AFM curves are shown in **Supplementary Figure 6A**) across the different samples. While WT-EBs showed consistent IBI with few exceptions, DMD-EBs showed high heterogeneity (**Figure 6C**, **Supplementary Figures 5B–D**). We observed not only different variability in recorded IBI but also prevalence in shorter IBI in WT-EBs compared to DMD-EBs (1 ± 1.0 s, and 0.96 ± 0.35 s for WT-hESC- and hiPSC-EBs respectively, 2.4 ± 1,6 s for DMD02-EBs, 2.1 ± 1.2 s for DMD03-EBs and 1.9 ± 1.2 s for cDMD-EBs, *p*-values in **Supplementary Table 3**) (**Figures 6D–G**).

Moreover, DMD-EBs displayed more dispersed IBI scatter plot and histogram than WT-EBs (**Figures 6H,I**). Using representative Poincaré plots, a quantitative measure of the evolvement in time of the IBI, we found more scattered inter-contraction pattern in DMD-EBs compared to WT-EBs (**Figures 6J,K**) showing a higher beat rate variability.

Loss of Dystrophin Leads to β-Adrenergic Remodeling and Cardiomyocyte Wasting

Dystrophin-deficient mouse CMs have been shown to display aberrant response to β-AR stimulation (Li et al., 2014). Thus, we evaluated the β-adrenergic response in DMD-EBs to investigate the effect of stress. We monitored the mechanobiological properties of the contracting clusters upon a selective β1-AR inhibitor (metoprolol, METO) followed by a non-selective β-AR activator (isoproterenol, ISO). In presence of METO, the WT-hPSC-EBs exhibited a significant decrease in contraction force ($p = 0.0042$ for WT hESC, $p = 0.0156$ for WT-hiPSC) and beat rate ($p = 0.0051$ for WT hESC, **Figures 7A,B**). DMD-hiPSC-EBs showed no response in beat rate nor contraction force to modulation by ISO nor METO. cDMD-EBs showed a response in contraction force to METO application similarly to its isogenic control ($p = 0.0003$ for contraction force and $p = 0.103$ for beat rate). WT-EBs responded to subsequent β-adrenergic stimulation by ISO application (partially competing with METO) through marginally significant increase in relative contraction force ($p = 0.0596$ for WT hESC, $p = 0.03$ for WT hiPSC, **Figure 7A**), DMD-EBs did not show statistically significant responses to ISO nor METO. cDMD-hESC line, however, responded similarly to its isogenic WT control in contraction force increase (with significant change in response to modulation, $p = 0.0039$). The pharmacokinetic answer to ISO has been additionally tested by exclusion of METO response using division of Tyrode and ISO value still showing response in WT-EBs ($p = 0.0021$) with no significant change in DMD-EBs ($p = 0.1309$) (as shown in **Supplementary Figure 4C**).

These mechanobiological data suggest that the DMD-EBs exhibit much weaker response to stress conditions in presence of β-AR modulation. Thus, we compared the expression of the β1, β2, and β3 AR at the protein level between DMD- and

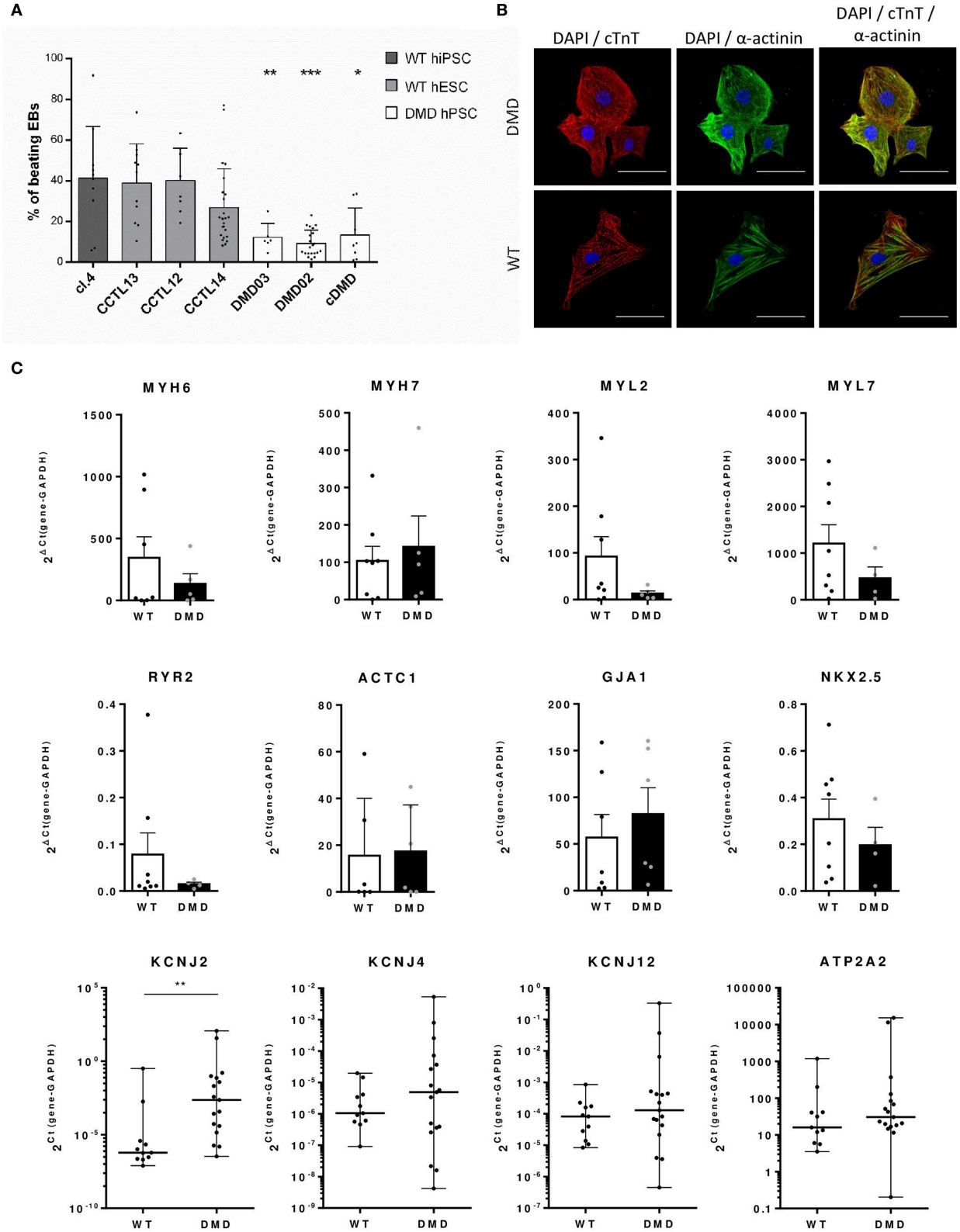

FIGURE 3 | Differentiation efficacy is lower in DMD-hPSC lines. **(A)** All DMD-hPSC and WT-hPSC lines were differentiated into spontaneously contracting EBs containing cardiomyocytes and cardiac cells. The ratio of these spontaneously contracting clusters was evaluated and compared to wild-type (WT) controls ($n = 36$

(Continued)

FIGURE 3 | for CCTL14 EBs, $n = 8$ for CCTL12 EBs, $n = 13$ for CCTL13, $n = 12$ for cl.4 EBs, $n = 25$ for DMD02 EBs, $n = 6$ for DMD03 EBs, $n = 19$ for cDMD-EBs). Lesser yields of beating EBs were identified in all DMD-hPSC lines. Statistical difference was calculated by one-way ANOVA and multiple comparison with Dunn's test. Significance (*$p < 0.05$, **$p < 0.01$, ***$p < 0.01$) is visualized as asterisks for the lowest values; for individual p-values, see **Supplementary Table 1**. **(B)** EBs were dissociated and cells labeled for cardiac markers α-actinin (in green) and cardiac troponin T (cTnT, in red) (DAPI is labeling the nuclei). WT and DMD-CCs presented similar level of typical striated pattern of sarcomeres. Line represents 50 μm. **(C)** Differentiation efficacy was evaluated by rt qPCR on mRNA levels of cardiac markers showing only non-significant differences in expression of various markers (MYH6, $n = 7$ for WT and $n = 5$ for DMD; MYL2, $n = 8$ for WT and $n = 4$ for DMD; MYL7, $n = 8$ for WT and $n = 4$ for DMD; RYR2, $n = 8$ for WT and $n = 4$ for DMD; ACTC1 $n = 6$ for WT and $n = 5$ for DMD; NKX2.5, $n = 8$ for WT and $n = 4$ for DMD, ATP2A2, $n = 11$ for WT and $n = 17$ for DMD) and non-significant increase in MYH7 ($n = 8$ for WT and $n = 5$ for DMD) and GJA1 ($n = 7$ for WT and $n = 6$ for DMD). Potassium channels were analyzed using Kir2.x isoforms mRNA expression (KCNJ2 – Kir2.1, KCNJ4 – Kir2.2 and KCNJ12 – Kir2.3, for all $n = 11$ for WT and $n = 17$ for DMD). Statistical significance on pooled DMD and pooled WT data sets was calculated using Mann–Whitney test; exact value for each is represented by • in each graph.

WT-EBs. While DMD-EBs derived from patient hiPSC showed increased β1 ($p = 0.0103$) and β2 AR expression ($p = 0.0162$) compared to isogenic WT-EBs, cDMD-EBs show similar or lower expression of both (**Figures 7C–E**). β3 expression was analyzed by quantitative rt qPCR showing no significant differences in between WT- and DMD-EBs (**Supplementary Figure 4D**).

A pathological overexpression of β-AR together with the blunted drug response and hypocontractility above described lead us to ask whether our derived CCs are already undergoing complex changes leading to their death, with consequential depletion and mechanical function deterioration in our 3D model. Thus, CC death was quantified, over time after differentiation, via cTnT concentration in the culture medium, originating from the dying CCs in the EBs. DMD lines showed from day 35 a significantly increased free cTnT level in their medium, compared to WT samples (**Figure 7F**, statistical evaluation in **Supplementary Table 4**). Interestingly, the DMD-EB kept beating even late after cardiac induction, even over the observed increased CM death (**Supplementary Video 1**).

DISCUSSION

Dilated cardiomyopathy, ultimately leading to heart failure, is the most common outcome in patients with dystrophin mutations (Kamdar and Garry, 2016; Papa et al., 2017), and it develops in DMD patients due to muscle wasting, but remains mostly unexplained in its dynamics. The DMD (*mdx)* mouse model has critical limitations since it develops only mild symptoms of heart failure with slow progression and unaffected lifespan compared to control mice (Carnwath and Shotton, 1987; Coulton et al., 1988; Shirokova and Niggli, 2013). In the present study, we provided a detailed description of patient-specific hiPSC-CCs and CRISPR/Cas9 engineered hESC-CCs. DMD-CC exhibited several molecular and functional abnormalities including an altered Ca^{2+} handling, irregular bradycardic beating, hypocontractility, and remodeling processes such as βAR alteration and CMs wasting. Our evidences on the alteration of ECC are in agreement with symptoms described in DMD patients.

Our results showed that dystrophin deficiency leads to lower efficacy in differentiating hPSCs into CCs. Interestingly, DMD-CCs exhibited a similar relative expression of known cardiac markers, and with trending increased Connexin 43 expression, similarly observed in *mdx* and *mdx:utr* CMs as a remodeling mechanism following functional dystrophin absence, with potential fatal arrhythmias in presence of β adrenergic stimulation (Patrick Gonzalez et al., 2015). Lower differentiation efficacy can point to cell fate errors: these can result from increased DNA damage caused by deregulated NOS activity (Jelinkova et al., 2019a). This process can lead to loss of stemness both at the commitment and self-renewal level (Rossi et al., 2007; Inomata et al., 2009). DNA damage can also affect multipotent stem cells division, rendering muscular differentiation ineffective (Dumont et al., 2015). Dystrophin loss was recently associated, in advanced CM *in vitro* models, with delayed contractile machinery formation, suggesting a mutation-derived impairment even at the latest stage of CM development (Pioner et al., 2020).

Then, we inquired whether and to what extent the mutation affected the single cell and EB ECC. We measured the electrophysiological properties and found similar AP features between DMD- and WT-CCs. While most of the recorded AP displayed atrial-like AP properties, our results suggested that dystrophin deficiency does not alter the electrophysiological properties of the derived hPSC-CCs. The AP durations we obtained indicate mixed population of various type of excitable cells from ventricular-like CMs (APD90 $\geq$ 300 ms), through atrial- and nodal-like CMs (APD90 $\geq$ 160 ms) and undefined/immature cardiomyocyte-like cells (APD90 $<$ 100 ms) similarly to what others previously found (He et al., 2003; Zhu et al., 2016). Nevertheless, a significant increase of Kir2.1 mRNA expression level point to a possible alteration of APD, which results in reduced effective refractory period during diastole *in vivo*. Furthermore, regarding the voltage-gated ion channels expression, DMD-CCs exhibited increased expression of DHPRα subunit of L-type Ca^{2+} channels but no difference in Cav1.2 and Cav1.3 isoform expression. L-type Ca^{2+} channels presenting gain-of-function mechanism was reported in dystrophic hearts (Koenig et al., 2014). In a recently published work (Eisen et al., 2019), it was shown that prolongation of APD in DMD-CMs was caused by increased $I_{Ca,L}$ density, which can be matched to prolonged diastole in DMD patients (Panovský et al., 2019). APD alterations, both at the potassium and calcium current levels, can lead to ventricular tachycardia (Choi et al., 2002; McNally et al., 2015), or premature ventricular beats, possibly degenerating into Torsades-de-Pointes ventricular fibrillations (Weiss et al., 2010).

Correlated with the mentioned calcium channels alterations, we measured the intracellular Ca^{2+} transients on dissociated CCs and observed a reduced spontaneous firing in DMD-CCs, with a significantly higher occurrence of small Ca^{2+} events in diastolic phase. For Ca^{2+} dynamics, DMD-CCs presented

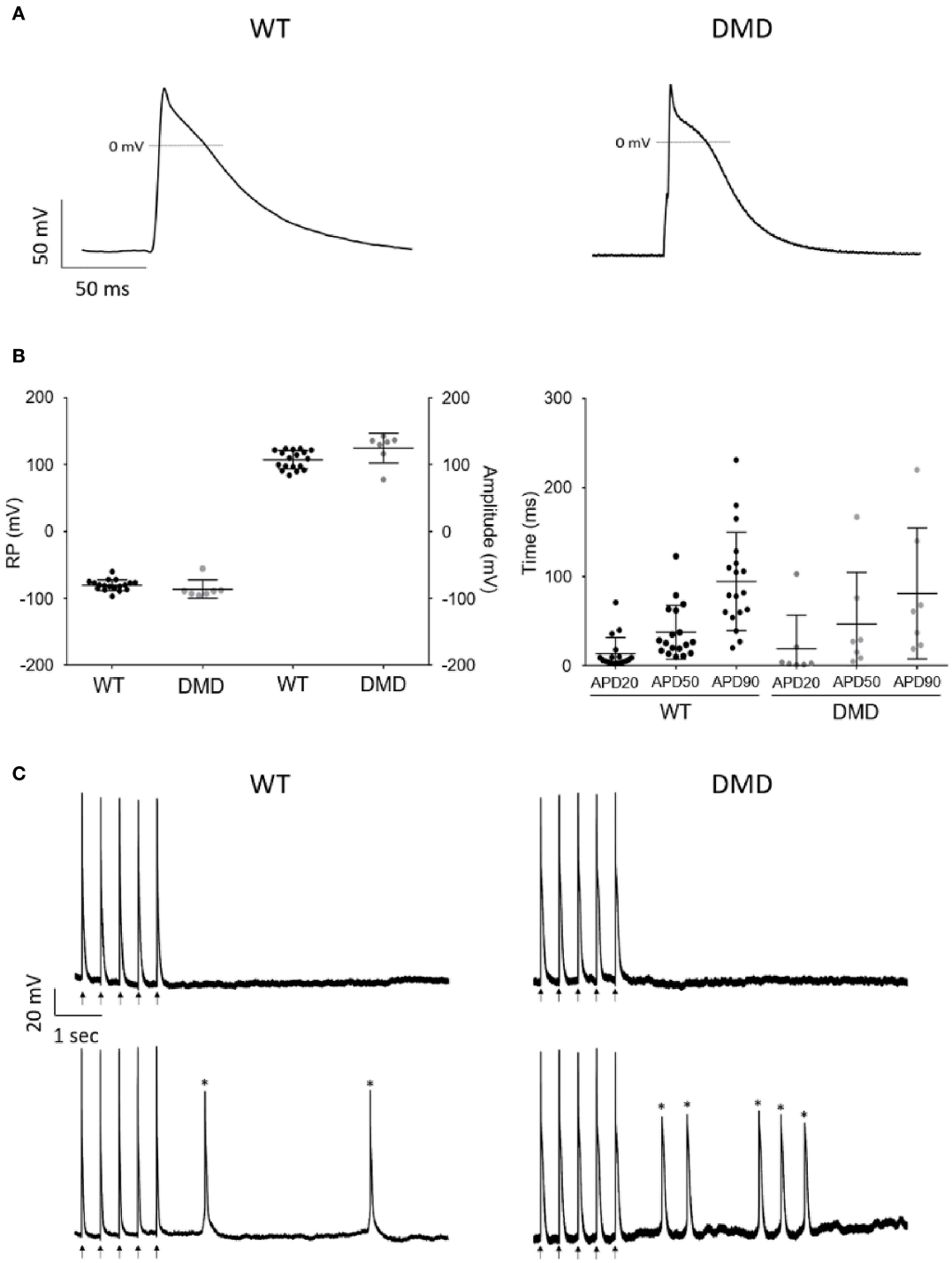

FIGURE 4 | AP recordings showed no difference in WT and DMD-CCs. **(A)** Representative AP recordings obtained from WT and DMD-hiPSC derived CCs, under current clamp configuration. **(B)** Scatter plot of RP (mV) and amplitude (mV) (left) and APD 20, 50, and 90 durations (right) of WT ($n = 18$) and DMD ($n = 7$) hPSC-CCs are represented. No significant difference was observed among these parameters between WT and DMD-hPSC-CCs. Exact n value for each is represented by • in each graph. Mean ± SEM are represented. **(C)** Representative arrhythmic events recorded in WT-CCs (left) and DMD-CCs (right). Upper panels show representative recordings of non-arrhythmogenic cells from WT-CCs and DMD-CCs and bottom panels show representative recordings of arrhythmogenic cells showing extra events, such as DAD (Asterisks).

FIGURE 5 | The dynamics of Ca^{2+} release and re-pumping is affected by dystrophin deficiency. Release of Ca^{2+} transients was measured using Fluo4 dyes in enzymatically dissociated DMD (91 cells and $n = 278$ transients were analyzed for resting conditions; 20 cells and $n = 83$ transients were analyzed for low frequency

(Continued)

FIGURE 5 | paced at 0.5 Hz) and WT-CCs (30 cells and $n = 262$ transients were analyzed for resting conditions; 15 cells and $n = 128$ transients were analyzed for low frequency paced at 0.5 Hz) in the age 40–50 days of differentiation. **(A)** Time to peak, **(B)** decay time, and **(C)** contraction duration time were analyzed for the main Ca^{2+} transients. The DMD-CMs showed significantly higher Ca^{2+} amplitude and longer time to release and repump/extrude the Ca^{2+} back into the SR/out of the cell in comparison to WT. The exact values are plotted in the graphs; red line represents the median. Significance (*$p < 0.05$) is visualized as asterisks as calculated by Mann–Whitney one-sided test (*$p < 0.05$, **$p < 0.01$, ****$p < 0.0001$). The Ca^{2+} leakage is demonstrated by Ca^{2+} events of low-amplitude (arrows) among the main Ca^{2+} transients [**D**—the obtained data from microscope with line scanning (upper bar) and transferred into peak graph by PeakInspector (lower bar) with and without electrical pacing of 0.5 Hz]. The occurrence of these small events is increased in DMD-CCs transients **(E)** as analyzed by Mann–Whitney test ($n = 54$ and $n = 35$ analyzed cells, for DMD and WT, respectively). **(F)** L-type channel (DHPR subunit) expression was characterized, showing non-significant increase in protein expression in DMD-hiPSC compared to WT-EBs as calculated by one-way ANOVA ($n = 4$, $n = 4$, $n = 4$ and $n = 8$ for WT hESC, WT-hiPSC, cDMD, and DMD-hiPSC-EBs). HH was used as positive control, HFF (human foreskin fibroblasts) as non-CM cell sample. **(G)** CaV isoform's (CACNA1C and CACNA1D) mRNA expression of LTCC subunits were analyzed using rt qPCR showing no difference between the groups. The values were calculated for CMs using ACTC for normalization. At least three biological repetitions were used for the analysis with exact value for each represented by • in the graph. Statistical difference was calculated using one-way ANOVA. **(H)** ICC analysis showed stronger signal for LTCC (in red) in DMD-hiPSC CCs recognized by cTnT labeling (in green). Line represents 50 μm.

prolonged rising time under resting and paced conditions with high variability. The Ca^{2+} transient decay time mean was significantly longer in resting conditions for DMD-CCs, even if this difference was abolished during pacing. This led to a measured prolonged duration of the transients, except under the 1 Hz physiological pacing.

Altered Ca^{2+} transients dynamics correlate with cellular alteration of ECC, as previously shown in our work and others (Sato et al., 2007; Caluori et al., 2019; Pioner et al., 2020). In particular, longer rising time might be correlated to a state of calcium overload, derived from sarcolemmal tears (Danialou et al., 2001) and SR leakage by remodeling of RyR2 by S-nitrosylation (Fauconnier et al., 2010; Oda et al., 2015) or loss of the closed-state stabilizer calstabin2 (Fauconnier et al., 2010). RyR2 misregulation can explain also that the presence of small Ca^{2+} amplitude events by random firing is a state of overload. Prolonged cytosolic Ca^{2+}, as expressed by increased duration of the transients, can contribute to arrhythmic events via inverse Na^{+}-Ca^{2+}-exchange activation (Voigt et al., 2012) and electromechanical dissociation. However, it should be noted that young DMD boys rarely exhibit arrhythmias (Villa Chet et al., 2015). We performed patch-clamp experiments and observed no difference in the number of arrhythmic events in WT- and DMD-CCs. In our previous work, we have shown how DMD-EBs are insensitive to positive chronotropic effect of high extracellular Ca^{2+} concentration, most likely due to low diffusion gradients in case of constant cytosolic overload (Caluori et al., 2019). Nevertheless, WT-EBs tolerated high levels of extracellular Ca^{2+} by modulating their contractile activity, while DMD-EBs presented an increased and erratic electromechanical coupling delay, together with an increased calcium reuptake time. In accordance with the presented evidences, we have previously shown how DMD-EBs are less sensitive to Verapamil L-type channels inhibition.

From the single cell electrochemical experiments, and previous results in the DMD-EB electromechanical alterations, we focused on the study of 3D mechanical behavior and its modulation. EBs showed that the overall spontaneous beat rate of WT and DMD groups did not differ at rest. However, we identified an increased heart rate variability though IBI analysis and its time-dependent correlation, similarly to Eisen et al.'s observations (Eisen et al., 2019), which also showed high heterogeneity in beat rate variability in dissociated DMD-hiPSC-CCs. Heart rate variability via L-type inactivation can be increased and even become pro-arrhythmogenic in case of spontaneous SR leakage (Johnson et al., 2013), a condition proven in the case of DMD models. The measured contraction force in DMD-EBs was significantly lowered compared to WT-EBs, as previously shown in single cell models (Pioner et al., 2020) and correlated to the ejection fraction decrease in reported patient's hearts (Corrado et al., 2002; Villa Chet et al., 2015; Panovský et al., 2019). Both lower contraction force and arrhythmic events occur in DMD patient's heart from a very young age and before dilated cardiomyopathy onset. In fact, 25% of pediatric DMD patients under 10 years old already showed decreased ejection fraction and have developed sinus tachycardia (Sadek et al., 2017). Overall, our model presents functional alterations of an early-stage cardiac manifestation of DMD.

For the first time, we further evaluated the ECC modulation abilities by pharmacological response in DMD-CCs through the β-AR response. We found an impaired response in DMD-EBs through lack of contraction force and beat rate modulation similarly to *mdx* hearts (Meyers et al., 2019). Our data showed visible changes in contraction force and beat rate in WT-EBs in the presence of isoproterenol (non-selective β adrenergic agonist) or metoprolol (β1 receptor inhibitor) but no change of both parameters in DMD-EBs. Surprisingly, the CRISPR/Cas9-induced cDMD-EBs reacted to β adrenergic modulation similarly to WT-EBs. The response might involve an unknown compensatory mechanism proper of the engineered line. As further confirmation, cDMD-CCs presented similar levels of β-AR with respect to its isogenic hESC-derived WT-CCs. In contrast, patient-specific DMD-EBs showed an increased expression in β1 and β2 receptors compared to WT-EBs. It has been previously shown that *mdx* CMs present lowered density of β1-AR (Li et al., 2014) with blunted β-adrenergic signaling pathway (Lu and Hoey, 2000; Li et al., 2014). Here, patient-specific DMD-CCs showed increased protein expression level of both, still with blunted response to adrenergic modulation.

That is also similar to non-DMD heart failure, where β1 overexpression is quite common (Engelhardt et al., 1999); trying to compensate for the weak contractility of the organ and the overactivation of the receptors then leads to receptor dysfunction in signaling, thus their insensitivity (Bristow et al., 1982; Rengo et al., 2009; de Lucia et al., 2018). The impaired contraction

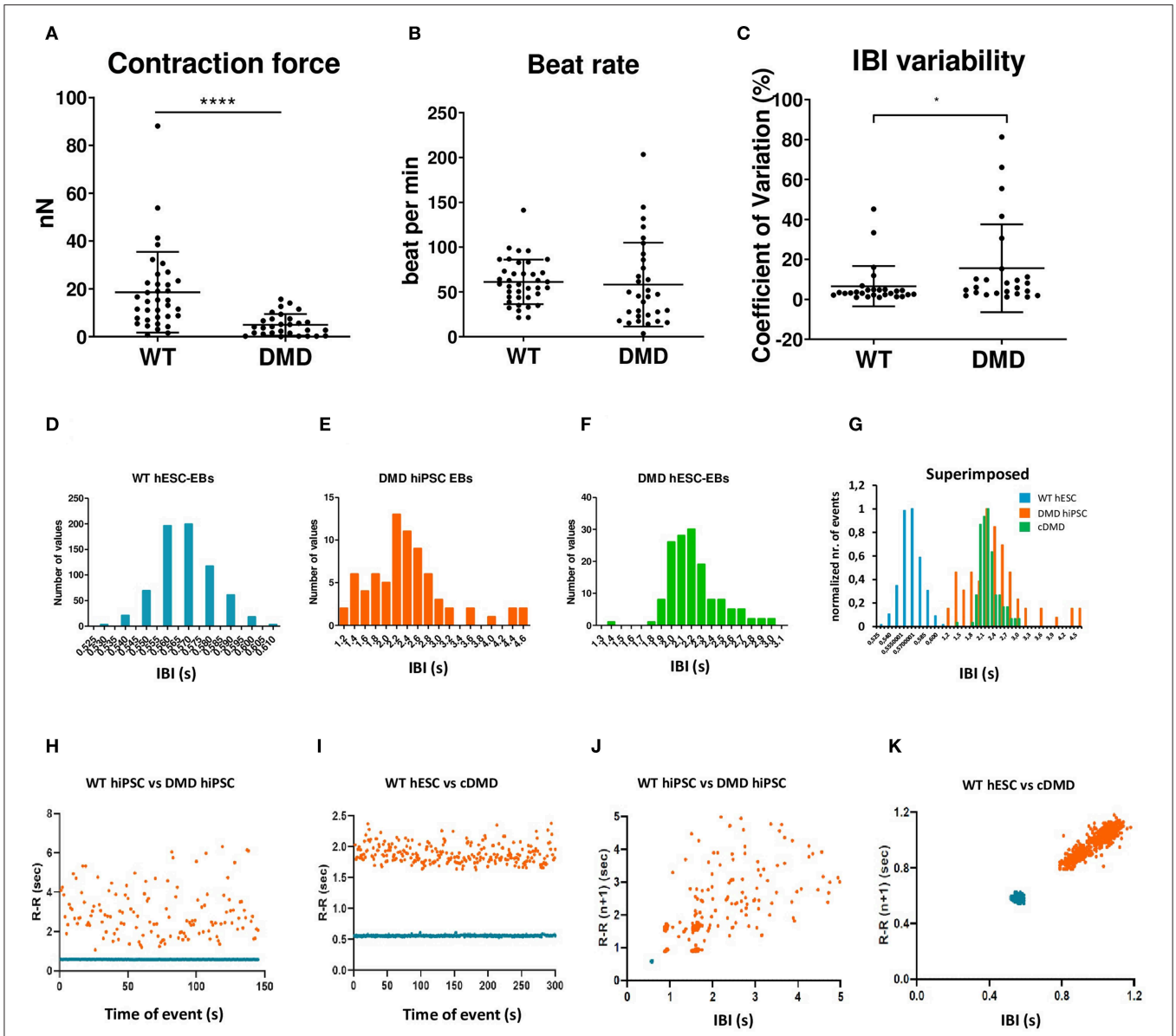

FIGURE 6 | The spontaneously contracting EBs lacking dystrophin showed weaker contraction force and signs of arrhythmias. The EBs were analyzed by AFM-based methods. **(A,B)** Contraction force is decreased in DMD-hPSC derived EBs ($n = 36$ for WT, $n = 29$ for DMD-EBs), beat rate is not affected by DMD mutation ($n = 38$ for WT, $n = 31$ for DMD-EBs). The statistical difference was calculated by Mann-Whitney test (*$p < 0.05$, ****$p < 0.0001$). At least five biological repetitions were used in each differentiated line; exact value for each is represented by • in each graph. Beat rate variability was identified in DMD-EBs. Graph shows coefficient of variation analysis **(C)** of pooled control and DMD groups. The data were cleaned of outliers by ROUT test ($q = 1\%$), and normality was tested by available tests showing non-normal distribution. Statistical difference was calculated using Mann–Whitney test. Representative IBI histograms of control (**D**, $n = 712$ peaks of the representative EB analyzed), DMD-hiPSC (**E**, $n = 76$ peaks of the representative EB analyzed), and DMD-hESC (**F**, $n = 165$ peaks of the representative EB analyzed) EBs and superimposed example of all three groups with normalized values **(G)**. Superimposed representative inter-beat-interval (IBI) scatter plots of control hiPSC with DMD-hiPSC-EBs ($n = 145$ time points for each EB) **(H)** and control hESC with DMD-hESC-EBs ($n = 334$ time points for each EB) **(I)**. Superimposed Poincaré plots of control hiPSC with DMD-hiPSC-EBs (**J**, same representative EBs as in **H**) and control hESC with DMD-hESC-EBs (**K**, same representative EBs as in **I**).

force observed in DMD-EBs can also be caused by β3 inhibitory function (Skeberdis, 2004). β3 normally acts as β-adrenergic break, but has been also shown to temper with mechanical properties of skeletal muscle together with nNOS expression increase leading to elevated ROS production (Puzzo et al., 2016). However, our results indicated that β3 expression was unchanged in DMD-CCs although we cannot exclude difference in β3 cellular distribution. The use of β-AR modulators has been shown to be challenging in management of cardiomyopathy in DMD patients due to severe hypotension events (McNally et al., 2015). Investigations using β blockers in DMD cardiomyopathy have turned up mixed results, with some studies demonstrating a

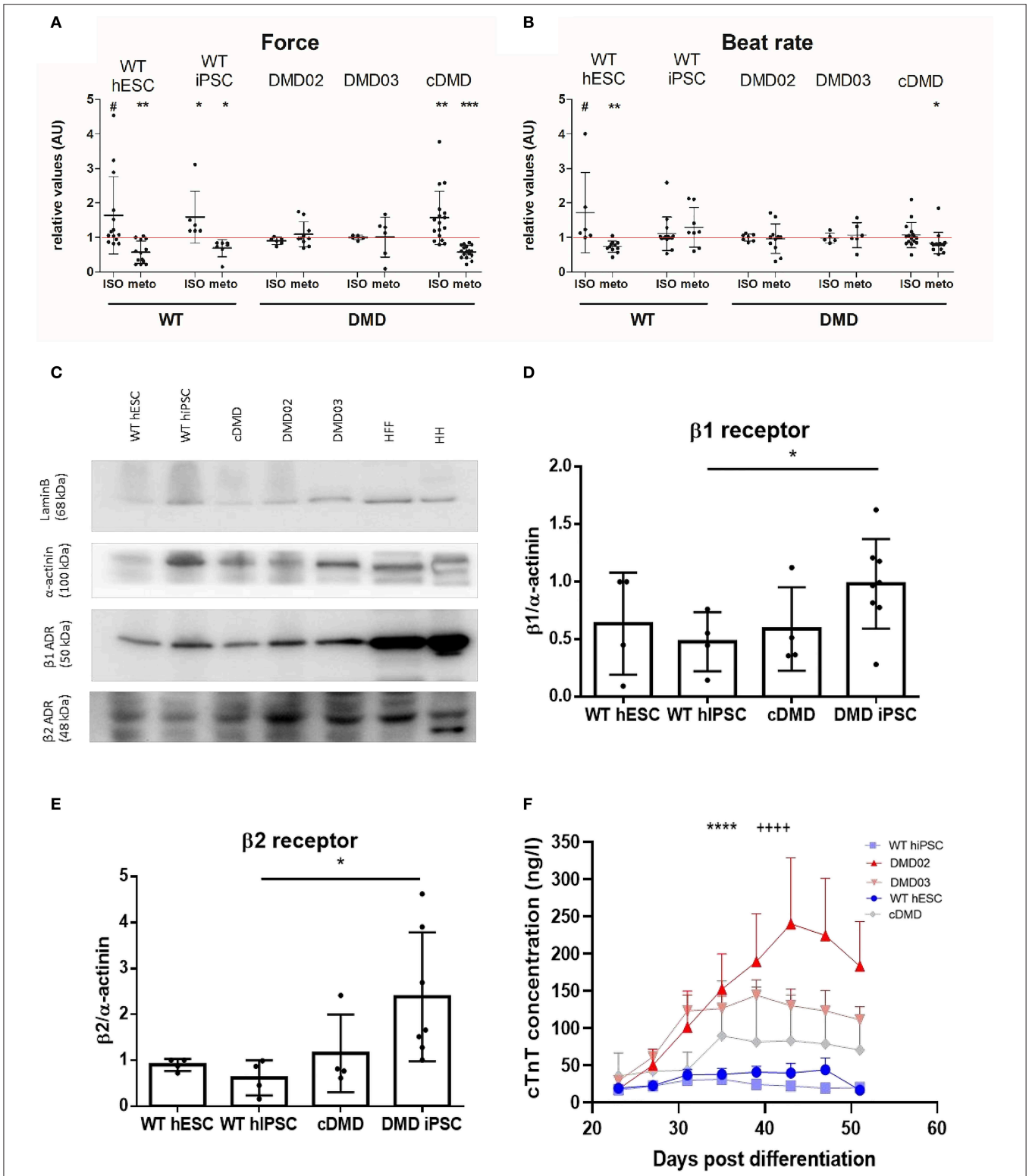

FIGURE 7 | DMD-CCs show remodeled β-adrenergic response and increased death. The contraction force and beat rate were measured using an AFM-based method and tested for β adrenergic response with isoproterenol (ISO, activator) and metoprolol (METO, inhibitor) **(A)**. WT-CMs show increase in contraction force (n = ISO/METO: n = 14/13 for WT hESC, n = 6/7 for WT-hiPSC-EBs, n = 6/10 for DMD02 EBs, n = 5/6 for DMD03 EBs, n = 17/17 for cDMD-EBs, exact value for each is represented by • in each graph) and **(B)** beat rate (n = ISO/METO: n = 6/11 for WT hESC, n = 14/8 for WT-hiPSC-EBs, n = 7/11 for DMD02 EBs, n = 5/6 for DMD03 EBs, n = 15/15 for cDMD-EBs, exact value for each is represented by • in each graph) after ISO treatment and decrease in both parameters under METO

(Continued)

FIGURE 7 | treatment. The DMD-hiPSC-EBs remained unresponsive to any of these stimulations. cDMD derived EBs show similar response in contraction force to its isogenic WT control. The red line represents the ratio of 1 for better orientation in change. Significance calculated by Wilcoxon test (*$p < 0.05$, **$p < 0.01$, ***$p < 0.01$, #$p < 0.1$) is visualized as asterisks. **(C–E)** Western blot analysis of β receptors shows higher expression of β1 in DMD-hiPSC derived EBs compared to WT-EBs; cDMD line shows similar expression to its isogenic WT control (calculates as β1 signal/actinin signal). β2 receptor showed increased levels in DMD-hiPSC-EBs. Human heart (HH) sample was used as positive control, human foreskin fibroblasts (HFF) as CM negative sample. Lamin B was used as loading control. Exact value for each is represented by • in each graph. Statistical difference was calculated by Mann-Whitney test for both β1 and β2 receptor expression. **(F)** CM death in the EBs was evaluated using free troponin level analysis in the medium. All DMD-EBs show significantly increased free cTnT levels compared to WT-EBs. Statistical difference was calculated using two-way ANOVA with uncorrected Fisher's post hoc test. ****$p < 0.0001$ according to cell line factor (WT vs. DMD) and $++++p < 0.0001$ according to day of differentiation factor.

clear benefit while others showed little effect of β-AR blockade on outcomes signaling lack of response to the modulation (Kajimoto et al., 2006; Matsumura et al., 2010; Viollet et al., 2012). The β-AR responsiveness might as well be linked to the type of mutation of the *DMD* gene, which might explain why one of our models lacked dystrophin expression yet was responsive to adrenergic modulation. Nevertheless, the beat rate and contraction force response to adrenergic modulation in patient-specific DMD-EBs suggested that the human DMD phenotype is accompanied by altered density of the β-AR on the sarcolemma and less sensitive β-AR pathway. The latter can involve a hampered lusitropic effect, resulting in a hypocontractile Ca^{2+}-saturated sarcomere (Culligan et al., 2002; Asp et al., 2013).

As a further original contribution, we finally investigated whether ECC alterations and regulatory pathways remodeling were associated in the dish with CCs wasting. Serum concentration of cTnT is a routinely used marker of CMs death, especially for acute myocardial infarction, although with high sensitivity assays it is also a prognostic marker of non-ischemic cardiac diseases (Park et al., 2017). We have indeed observed how even *in vitro* early stage models of DMD undergo progressive CMs injury, with detected levels of free cTnT up to 10 times the one of age-matched control lines. Dystrophin mutations, with severe symptomatology like in Duchenne's or milder like in Becker's, are all characterized with progressive cardiac symptoms stemming from loss of CMs, remodeling of the cardiac tissue with substitutive fibrosis, and ventricular dilation leading to heart failure accompanied by non-CM cell population depletion (Pesl et al., 2020). CM death can be indirectly caused by high levels of cytosolic Ca^{2+}, reportedly present in DMD through several mechanisms, which increases proteolysis and triggers mitochondrial dysfunctions with consequent ATP exhaustion (Meyers and Townsend, 2019; Tsurumi et al., 2019). Despite the fact that troponin levels measured by immunoassay methods in the media cannot define the mechanisms of cardiomyocyte injury, nor prove if the cell remains viable after such injury or became apoptotic, our findings confirmed that clinical assays can be used together with our model to follow subclinical stages of DMD cardiac involvement. Remarkably, this progressive CCs death is not correlated with loss of contractility. Pioner at al. demonstrated how up to 100 days of cultivation DMD models preserved their contractile function assuming a hypertrophic phenotype (Pioner et al., 2020). A similar mechanism could explain the similar evidence we observed in our 3D model, where CM depletion might be compensated by surviving CM hypertrophy. This evidence opens further uses of our presented model to study progressive cellular adaptation at different stages of the diseases.

LIMITATIONS OF THE STUDY

The reported study presents several limitations. The electrophysiological analysis via patch clamp lacks a proper age matching; therefore, the highly variable parameters might have masked mutation-related changes. Furthermore, no channel-specific study was performed to make a causative link between the presented channels overexpression to the calcium handling and contractile alterations observed. We did not directly characterize the age effect on calcium handling and contractility on hPSC-CC. However, we have relied on existent information on the topic to exclude a significant contribution of incomplete maturation to the reported differences.

CONCLUSIONS

The purpose of this work was to model some key cardiac molecular properties in DMD cardiomyopathy using DMD patient-specific and engineered CRISPR/Cas9 isogenic hPSC derived cardiac cells. Our results indicated that our DMD models in the dish are functionally affected by dystrophin deficiency and recapitulate functional defects and cardiac wasting observed in the disease. This work contributes to determine cardiac defects in DMD patients. It offers an accurate tool to study human cardiomyopathy progression and test therapies in the dish.

DATA AVAILABILITY STATEMENT

The datasets generated for this study are available on request to the corresponding author.

ETHICS STATEMENT

The fibroblasts of two DMD patients were derived from skin/muscle biopsies with the patients informed consent and St. Anne's University Hospital (Brno, Czech Republic) Ethics Committee approval under the number 37/2011. Written informed consent to participate in this study was provided by the patient/participants legal guardian.

AUTHOR CONTRIBUTIONS

All the authors have contributed to the manuscript writing and corrections and were included substantially in the project preparation, conception, and evaluation. SJ has differentiated the cardiomyocytes, ran ICC, PCR, and western blot analyses, evaluated obtained data and interpreted them, prepared the figures, and wrote the draft of the manuscript. AV was included in the experimental design, differentiated cardiomyocytes and performed Ca^{2+} imaging and ICC staining, and helped interpret the data. JP performed the AFM measurements and initial evaluation of the data. FA performed the electrophysiological measurements and interpreted them. MP performed AFM measurement of the EBs. GC participated in AFM measurements and interpretation of the results. AS performed AFM and Ca^{2+} imaging data analysis. IA performed Ca^{2+} imaging of the WT cells and helped interpret the data. VS and HD performed cTnT assays. SK evaluated AFM data. TU performed dystrophin western blot. PS, AL, PD, AM, and VR supervised the project, interpreted the obtained results, and corrected the manuscript. AM and VR were responsible for the experimental design of the project, coordination, and supervision in equal matter.

FUNDING

This work was supported by the Ministry of Education, Youth, and Sports of the Czech Republic (7AMB13FR011, No. CZ.02.1.01/0.0/0.0/16_013/0001776, No. CZ.02.1.01/0.0/0.0/16_019/0000868), CIISB research infrastructure LM2018127 and supported by funds from the Faculty of Medicine MU to junior researchers SJ and MP. This work was also supported by grants of the European Regional Development Fund (CIISB4HEALTH No. CZ.02.1.01/0.0/0.0/16_013/0001776), South Moravian Centre for International Mobility (SoMoPro No. 2SGA2744), and the European Society of Cardiology (ESC; R12042FF). The French Muscular Dystrophy Association (AFM; project 16073, MNM2 2012, and 20225), the Fondation pour la Recherche Médicale (FRM; SPF20130526710), the PHC Barrande (Duchenstem No. 28379TE), the Institut National pour la Santé et la Recherche Médicale (INSERM) also supported this work.

SUPPLEMENTARY MATERIAL

The Supplementary Material for this article can be found online at: https://www.frontiersin.org/articles/10.3389/fbioe.2020.00535/full#supplementary-material

REFERENCES

Acimovic, I., Refaat, M. M., Moreau, A., Salykin, A., Reiken, S., Sleiman, Y., et al. (2018). Post-translational modifications and diastolic calcium leak associated to the novel RyR2-D3638A mutation lead to CPVT in patient-specific hiPSC-derived cardiomyocytes. *J. Clin. Med.* 7:423. doi: 10.3390/jcm7110423

Amedro, P., Vincenti, M., De La Villeon, G., Lavastre, K., Barrea, C., Guillaumont, S., et al. (2019). Speckle-tracking echocardiography in children with duchenne muscular dystrophy: a prospective multicenter controlled cross-sectional study. *J. Am. Soc. Echocardiogr.* 32, 412–422. doi: 10.1016/j.echo.2018.10.017

Andersson, D. C., and Marks, A. R. (2010). Fixing ryanodine receptor Ca leak - a novel therapeutic strategy for contractile failure in heart and skeletal muscle. *Drug Discov. Today Dis. Mech.* 7, e151–e157. doi: 10.1016/j.ddmec.2010.09.009

Andersson, D. C., Meli, A. C., Reiken, S., Betzenhauser, M. J., Umanskaya, A., Shiomi, T., et al. (2012). Leaky ryanodine receptors in β-sarcoglycan deficient mice: a potential common defect in muscular dystrophy. *Skelet. Muscle* 2:9. doi: 10.1186/2044-5040-2-9

Armstrong, L., Tilgner, K., Saretzki, G., Atkinson, S. P., Stojkovic, M., Moreno, R., et al. (2010). Human induced pluripotent stem cell lines show stress defense mechanisms and mitochondrial regulation similar to those of human embryonic stem cells. *Stem Cells* 28, 661–673. doi: 10.1002/stem.307

Asp, M. L., Martindale, J. J., Heinis, F. I., Wang, W., and Metzger, J. M. (2013). Calcium mishandling in diastolic dysfunction: mechanisms and potential therapies. *Biochim. Biophys. Acta* 1833, 895–900. doi: 10.1016/j.bbamcr.2012.09.007

Blake, D. J., Weir, A., Newey, S. E., and Davies, K. E. (2002). Function and genetics of dystrophin and dystrophin-related proteins in muscle. *Physiol. Rev.* 82, 291–329. doi: 10.1152/physrev.00028.2001

Bondue, A., Arbustini, E., Bianco, A., Ciccarelli, M., Dawson, D., De Rosa, M., et al. (2018). Complex roads from genotype to phenotype in dilated cardiomyopathy: scientific update from the working group of myocardial function of the european society of cardiology. *Cardiovasc. Res.* 114, 1287–1303. doi: 10.1093/cvr/cvy122

Bristow, M. R., Ginsburg, R., Minobe, W., Cubicciotti, R. S., Sageman, W. S., Lurie, K., et al. (1982). Decreased catecholamine sensitivity and beta-adrenergic-receptor density in failing human hearts. *N. Engl. J. Med.* 307, 205–211. doi: 10.1056/NEJM198207223070401

Caluori, G., Pribyl, J., Pesl, M., Jelinkova, S., Rotrekl, V., Skladal, P., et al. (2019). Non-invasive electromechanical cell-based biosensors for improved investigation of 3D cardiac models. *Biosens. Bioelectron.* 124–125, 129–135. doi: 10.1016/j.bios.2018.10.021

Carnwath, J. W., and Shotton, D. M. (1987). Muscular dystrophy in the mdx mouse: histopathology of the soleus and extensor digitorum longus muscles. *J. Neurol. Sci.* 80, 39–54. doi: 10.1016/0022-510X(87)90219-X

Chenard, A. A., Becane, H. M., Tertrain, F., de Kermadec, J. M., and Weiss, Y. A. (1993). Ventricular arrhythmia in duchenne muscular dystrophy: prevalence, significance and prognosis. *Neuromuscul. Disord.* 3, 201–206. doi: 10.1016/0960-8966(93)90060-W

Choi, B.-R., Burton, F., and Salama, G. (2002). Cytosolic Ca^{2+} triggers early afterdepolarizations and torsade de pointes in rabbit hearts with type 2 long QT syndrome. *J. Physiol.* 543, 615–631. doi: 10.1113/jphysiol.2002.024570

Clarac, F., Massion, J., and Smith, A. M. (2009). Duchenne, charcot and babinski, three neurologists of la salpetrière hospital, and their contribution to concepts of the central organization of motor synergy. *J. Physiol. Paris* 103, 361–376. doi: 10.1016/j.jphysparis.2009.09.001

Corrado, G., Lissoni, A., Beretta, S., Terenghi, L., Tadeo, G., Foglia-Manzillo, G., et al. (2002). Prognostic value of electrocardiograms, ventricular late potentials, ventricular arrhythmias, and left ventricular systolic dysfunction in patients with Duchenne muscular dystrophy. *Am. J. Cardiol.* 89, 838–841. doi: 10.1016/S0002-9149(02)02195-1

Coulton, G. R., Morgan, J. E., Partridge, T. A., and Sloper, J. C. (1988). The mdx mouse skeletal muscle myopathy: I. A histological, morphometric and biochemical investigation. *Neuropathol. Appl. Neurobiol.* 14, 53–70. doi: 10.1111/j.1365-2990.1988.tb00866.x

Culligan, K., Banville, N., Dowling, P., and Ohlendieck, K. (2002). Drastic reduction of calsequestrin-like proteins and impaired calcium binding in dystrophic mdx muscle. *J. Appl. Physiol.* 92, 435–445. doi: 10.1152/japplphysiol.00903.2001

Danialou, G., Comtois, A. S., Dudley, R., Karpati, G., Vincent, G., Des Rosiers, C., et al. (2001). Dystrophin-deficient cardiomyocytes are abnormally vulnerable

to mechanical stress-induced contractile failure and injury. *FASEB J.* 15, 1655–1657. doi: 10.1096/fj.01-0030fje

de Lucia, C., Eguchi, A., and Koch, W. J. (2018). New insights in cardiac β-adrenergic signaling during heart failure and aging. *Front. Pharmacol.* 9:904. doi: 10.3389/fphar.2018.00904

Dumont, N. A., Wang, Y. X., von Maltzahn, J., Pasut, A., Bentzinger, C. F., Brun, C. E., et al. (2015). Dystrophin expression in muscle stem cells regulates their polarity and asymmetric division. *Nat. Med.* 21, 1455–1463. doi: 10.1038/nm.3990

Dvorak, P., Dvorakova, D., Koskova, S., Vodinska, M., Najvirtova, M., Krekac, D., et al. (2005). Expression and potential role of fibroblast growth factor 2 and its receptors in human embryonic stem cells. *Stem Cells* 23, 1200–1211. doi: 10.1634/stemcells.2004-0303

Eisen, B., Ben Jehuda, R., Cuttitta, A. J., Mekies, L. N., Shemer, Y., Baskin, P., et al. (2019). Electrophysiological abnormalities in induced pluripotent stem cell-derived cardiomyocytes generated from duchenne muscular dystrophy patients. *J. Cell. Mol. Med.* 23, 2125–2135. doi: 10.1111/jcmm.14124

Engelhardt, S., Hein, L., Wiesmann, F., and Lohse, M. J. (1999). Progressive hypertrophy and heart failure in beta1-adrenergic receptor transgenic mice. *Proc. Natl. Acad. Sci. U.S.A.* 96, 7059–7064. doi: 10.1073/pnas.96.12.7059

Fauconnier, J., Thireau, J., Reiken, S., Cassan, C., Richard, S., Matecki, S., et al. (2010). Leaky RyR2 trigger ventricular arrhythmias in duchenne muscular dystrophy. *Proc. Natl. Acad. Sci. U.S.A.* 107, 1559–1564. doi: 10.1073/pnas.0908540107

Fayssoil, A., Nardi, O., Orlikowski, D., and Annane, D. (2010). Cardiomyopathy in duchenne muscular dystrophy: pathogenesis and therapeutics. *Heart Fail Rev.* 15, 103–107. doi: 10.1007/s10741-009-9156-8

Finsterer, J., and Stöllberger, C. (2003). The heart in human dystrophinopathies. *Cardiology* 99, 1–19. doi: 10.1159/000068446

Gerke, V., Creutz, C. E., and Moss, S. E. (2005). Annexins: linking Ca^{2+} signalling to membrane dynamics. *Nat. Rev. Mol. Cell Biol.* 6, 449–461. doi: 10.1038/nrm1661

Hajjar, R. J., Liao, R., Young, J. B., Fuleihan, F., Glass, M. G., and Gwathmey, J. K. (1993). Pathophysiological and biochemical characterisation of an avian model of dilated cardiomyopathy: comparison to findings in human dilated cardiomyopathy. *Cardiovasc. Res.* 27, 2212–2221. doi: 10.1093/cvr/27.12.2212

He, J.-Q., Ma, Y., Lee, Y., Thomson, J. A., and Kamp, T. J. (2003). Human embryonic stem cells develop into multiple types of cardiac myocytes: action potential characterization. *Circ. Res.* 93, 32–39. doi: 10.1161/01.RES.0000080317.92718.99

Hess, G. P. D., Horsch, A. D., and Zdunek, D. D. (2008). *Means and Methods for Optimization of Diagnostic and Therapeutic Approaches in Chronic Artery Disease Based on the Detection of Troponin T and NT-proBNP*. Available online at: https://patents.google.com/patent/EP1925943A1/en/en22 (accessed December 14, 2019).

Himmrich, E., Popov, S., Liebrich, A., Rosocha, S., Zellerhoff, C., Nowak, B., et al. (2000). [Hidden intracardiac conduction disturbances and their spontaneous course in patients with progressive muscular dystrophy]. *Z Kardiol.* 89, 592–598. doi: 10.1007/s003920070208

Hwang, H. S., Kryshtal, D. O., Feaster, T. K., Sánchez-Freire, V., Zhang, J., Kamp, T. J., et al. (2015). Comparable calcium handling of human iPSC-derived cardiomyocytes generated by multiple laboratories. *J. Mol. Cell. Cardiol.* 85, 79–88. doi: 10.1016/j.yjmcc.2015.05.003

Inomata, K., Aoto, T., Binh, N. T., Okamoto, N., Tanimura, S., Wakayama, T., et al. (2009). Genotoxic stress abrogates renewal of melanocyte stem cells by triggering their differentiation. *Cell* 137, 1088–1099. doi: 10.1016/j.cell.2009.03.037

International Stem Cell Initiative, Adewumi, O., Aflatoonian, B., Ahrlund-Richter, L., Amit, M., Andrews, P. W., et al. (2007). Characterization of human embryonic stem cell lines by the international stem cell initiative. *Nat. Biotechnol.* 25, 803–816. doi: 10.1038/nbt1318

Jelinkova, S., Fojtik, P., Kohutova, A., Vilotic, A., Marková, L., Pesl, M., et al. (2019a). Dystrophin deficiency leads to genomic instability in human pluripotent stem cells via NO synthase-induced oxidative stress. *Cells* 8:53. doi: 10.3390/cells8010053

Jelinkova, S., Markova, L., Pesl, M., Valáškova, I., Makaturová, E., Jurikova, L., et al. (2019b). Generation of two duchenne muscular dystrophy patient-specific induced pluripotent stem cell lines DMD02 and DMD03 (MUNIi001-A and MUNIi003-A). *Stem Cell Res.* 40:101562. doi: 10.1016/j.scr.2019.101562

Johnson, D. M., Heijman, J., Bode, E. F., Greensmith, D. J., van der Linde, H., Abi-Gerges, N., et al. (2013). Diastolic spontaneous calcium release from the sarcoplasmic reticulum increases beat-to-beat variability of repolarization in canine ventricular myocytes after β-adrenergic stimulation. *Circ. Res.* 112, 246–256. doi: 10.1161/CIRCRESAHA.112.275735

Jung, C., Martins, A. S., Niggli, E., and Shirokova, N. (2008). Dystrophic cardiomyopathy: amplification of cellular damage by Ca^{2+} signalling and reactive oxygen species-generating pathways. *Cardiovasc. Res.* 77, 766–773. doi: 10.1093/cvr/cvm089

Kajimoto, H., Ishigaki, K., Okumura, K., Tomimatsu, H., Nakazawa, M., Saito, K., et al. (2006). Beta-blocker therapy for cardiac dysfunction in patients with muscular dystrophy. *Circ. J.* 70, 991–994. doi: 10.1253/circj.70.991

Kamdar, F., and Garry, D. J. (2016). Dystrophin-deficient cardiomyopathy. *J. Am. Coll. Cardiol.* 67, 2533–2546. doi: 10.1016/j.jacc.2016.02.081

Koenig, X., Dysek, S., Kimbacher, S., Mike, A. K., Cervenka, R., Lukacs, P., et al. (2011). Voltage-gated ion channel dysfunction precedes cardiomyopathy development in the dystrophic heart. *PLoS ONE* 6:e20300. doi: 10.1371/journal.pone.0020300

Koenig, X., Rubi, L., Obermair, G. J., Cervenka, R., Dang, X. B., Lukacs, P., et al. (2014). Enhanced currents through L-type calcium channels in cardiomyocytes disturb the electrophysiology of the dystrophic heart. *Am. J. Physiol. Heart Circ. Physiol.* 306, H564–H573. doi: 10.1152/ajpheart.00441.2013

Krutá, M., Bálek, L., Hejnová, R., Dobšáková, Z., Eiselleová, L., Matulka, K., et al. (2013). Decrease in abundance of apurinic/apyrimidinic endonuclease causes failure of base excision repair in culture-adapted human embryonic stem cells. *Stem Cells* 31, 693–702. doi: 10.1002/stem.1312

Krutá, M., Šeneklová, M., Raška, J., Salykin, A., Zerzánková, L., Pešl, M., et al. (2014). Mutation frequency dynamics in HPRT locus in culture-adapted human embryonic stem cells and induced pluripotent stem cells correspond to their differentiated counterparts. *Stem Cells Dev.* 23, 2443–2454. doi: 10.1089/scd.2013.0611

Li, Y., Zhang, S., Zhang, X., Li, J., Ai, X., Zhang, L., et al. (2014). Blunted cardiac beta-adrenergic response as an early indication of cardiac dysfunction in duchenne muscular dystrophy. *Cardiovasc. Res.* 103, 60–71. doi: 10.1093/cvr/cvu119

Lu, S., and Hoey, A. (2000). Changes in function of cardiac receptors mediating the effects of the autonomic nervous system in the muscular dystrophy (MDX) mouse. *J. Mol. Cell. Cardiol.* 32, 143–152. doi: 10.1006/jmcc.1999.1063

Mah, J. K., Korngut, L., Dykeman, J., Day, L., Pringsheim, T., and Jette, N. (2014). A systematic review and meta-analysis on the epidemiology of duchenne and becker muscular dystrophy. *Neuromuscul. Disord.* 24, 482–491. doi: 10.1016/j.nmd.2014.03.008

Manzur, A. Y., Kinali, M., and Muntoni, F. (2008). Update on the management of duchenne muscular dystrophy. *Arch. Dis. Child.* 93, 986–990. doi: 10.1136/adc.2007.118141

Markham, L. W., Michelfelder, E. C., Border, W. L., Khoury, P. R., Spicer, R. L., Wong, B. L., et al. (2006). Abnormalities of diastolic function precede dilated cardiomyopathy associated with Duchenne muscular dystrophy. *J. Am. Soc. Echocardiogr.* 19, 865–871. doi: 10.1016/j.echo.2006.02.003

Matsumura, T., Tamura, T., Kuru, S., Kikuchi, Y., and Kawai, M. (2010). Carvedilol can prevent cardiac events in duchenne muscular dystrophy. *Intern. Med.* 49, 1357–1363. doi: 10.2169/internalmedicine.49.3259

McNally, E. M., Kaltman, J. R., Benson, D. W., Canter, C. E., Cripe, L. H., Duan, D., et al. (2015). Contemporary cardiac issues in duchenne muscular dystrophy. *Circulation* 131, 1590–1598. doi: 10.1161/CIRCULATIONAHA.114.015151

Meyers, T. A., Heitzman, J. A., Krebsbach, A. M., Aufdembrink, L. M., Hughes, R., Bartolomucci, A., et al. (2019). Acute AT1R blockade prevents isoproterenol-induced injury in mdx hearts. *J. Mol. Cell. Cardiol.* 128, 51–61. doi: 10.1016/j.yjmcc.2019.01.013

Meyers, T. A., and Townsend, D. (2019). Cardiac pathophysiology and the future of cardiac therapies in duchenne muscular dystrophy. *Int. J. Mol. Sci.* 20:4098. doi: 10.3390/ijms20174098

Oda, T., Yang, Y., Uchinoumi, H., Thomas, D. D., Chen-Izu, Y., Kato, T., et al. (2015). Oxidation of ryanodine receptor (RyR) and calmodulin enhance Ca release and pathologically alter, RyR structure and calmodulin affinity. *J. Mol. Cell. Cardiol.* 85, 240–248. doi: 10.1016/j.yjmcc.2015.06.009

Panovský, R., Pešl, M., Holeček, T., Máchal, J., Feitová, V., Mrázová, L., et al. (2019). Cardiac profile of the czech population of duchenne muscular dystrophy patients: a cardiovascular magnetic resonance study with T1 mapping. *Orphanet J. Rare Dis.* 14:10. doi: 10.1186/s13023-018-0986-0

Papa, A. A., D'Ambrosio, P., Petillo, R., Palladino, A., and Politano, L. (2017). Heart transplantation in patients with dystrophinopathic cardiomyopathy: review of the literature and personal series. *Intractable Rare Dis Res.* 6, 95–101. doi: 10.5582/irdr.2017.01024

Park, K. C., Gaze, D. C., Collinson, P. O., and Marber, M. S. (2017). Cardiac troponins: from myocardial infarction to chronic disease. *Cardiovasc. Res.* 113, 1708–1718. doi: 10.1093/cvr/cvx183

Patrick Gonzalez, J., Ramachandran, J., Xie, L.-H., Contreras, J. E., and Fraidenraich, D. (2015). Selective connexin43 inhibition prevents isoproterenol-induced arrhythmias and lethality in muscular dystrophy mice. *Sci. Rep.* 5:13490. doi: 10.1038/srep13490

Pesl, M., Acimovic, I., Pribyl, J., Hezova, R., Vilotic, A., Fauconnier, J., et al. (2014). Forced aggregation and defined factors allow highly uniform-sized embryoid bodies and functional cardiomyocytes from human embryonic and induced pluripotent stem cells. *Heart Vessels* 29, 834–846. doi: 10.1007/s00380-013-0436-9

Pesl, M., Jelinkova, S., Caluori, G., Holicka, M., Krejci, J., Nemec, P., et al. (2020). Cardiovascular progenitor cells and tissue plasticity are reduced in a myocardium affected by Becker muscular dystrophy. *Orphanet J. Rare Dis.* 15:65. doi: 10.1186/s13023-019-1257-4

Pesl, M., Pribyl, J., Acimovic, I., Vilotic, A., Jelinkova, S., Salykin, A., et al. (2016). Atomic force microscopy combined with human pluripotent stem cell derived cardiomyocytes for biomechanical sensing. *Biosens. Bioelectron.* 85, 751–757. doi: 10.1016/j.bios.2016.05.073

Peterson, J. M., Wang, D. J., Shettigar, V., Roof, S. R., Canan, B. D., Bakkar, N., et al. (2018). NF-κB inhibition rescues cardiac function by remodeling calcium genes in a duchenne muscular dystrophy model. *Nat. Commun.* 9:3431. doi: 10.1038/s41467-018-05910-1

Pioner, J. M., Guan, X., Klaiman, J. M., Racca, A. W., Pabon, L., Muskheli, V., et al. (2020). Absence of full-length dystrophin impairs normal maturation and contraction of cardiomyocytes derived from human-induced pluripotent stem cells. *Cardiovasc. Res.* 116, 368–382.

Pribyl, J., Pešl, M., Caluori, G., Acimovic, I., Jelinkova, S., Dvorak, P., et al. (2019). Biomechanical characterization of human pluripotent stem cell-derived cardiomyocytes by use of atomic force microscopy. *Methods Mol. Biol.* 1886, 343–353. doi: 10.1007/978-1-4939-8894-5_20

Puzzo, D., Raiteri, R., Castaldo, C., Capasso, R., Pagano, E., Tedesco, M., et al. (2016). CL316,243, a β3-adrenergic receptor agonist, induces muscle hypertrophy and increased strength. *Sci. Rep.* 5:37504. doi: 10.1038/srep37504

Qu, C., Puttonen, K. A., Lindeberg, H., Ruponen, M., Hovatta, O., Koistinaho, J., et al. (2013). Chondrogenic differentiation of human pluripotent stem cells in chondrocyte co-culture. *Int. J. Biochem. Cell Biol.* 45, 1802–1812. doi: 10.1016/j.biocel.2013.05.029

Rengo, G., Lymperopoulos, A., and Koch, W. J. (2009). Future g protein-coupled receptor targets for treatment of heart failure. *Curr. Treat. Options Cardiovasc. Med.* 11, 328–338. doi: 10.1007/s11936-009-0033-5

Rossi, D. J., Bryder, D., Seita, J., Nussenzweig, A., Hoeijmakers, J., and Weissman, I. L. (2007). Deficiencies in DNA damage repair limit the function of haematopoietic stem cells with age. *Nature* 447, 725–729. doi: 10.1038/nature05862

Sadek, A. A., Mahmoud, S. M., El-Aal, M. A., Allam, A. A., and El-Halim, W. I. A. (2017). Evaluation of cardiac functions in children with duchenne muscular dystrophy: a prospective case-control study. *Electron. Physician.* 9, 5732–5739. doi: 10.19082/5732

Sato, H., Shiraishi, I., Takamatsu, T., and Hamaoka, K. (2007). Detection of TUNEL-positive cardiomyocytes and c-kit-positive progenitor cells in children with congenital heart disease. *J. Mol. Cell. Cardiol.* 43, 254–261. doi: 10.1016/j.yjmcc.2007.05.011

Shirokova, N., and Niggli, E. (2013). Cardiac phenotype of duchenne muscular dystrophy: insights from cellular studies. *J. Mol. Cell. Cardiol.* 58, 217–224. doi: 10.1016/j.yjmcc.2012.12.009

Skeberdis, V. A. (2004). Structure and function of beta3-adrenergic receptors. *Medicina (Kaunas).* 40, 407–413.

Stehlíková, K., Skálová, D., Zídková, J., Haberlová, J., Vohánka, S., Mazanec, R., et al. (2017). Muscular dystrophies and myopathies: the spectrum of mutated genes in the czech republic. *Clin. Genet.* 91, 463–469. doi: 10.1111/cge.12839

Tsurumi, F., Baba, S., Yoshinaga, D., Umeda, K., Hirata, T., Takita, J., et al. (2019). The intracellular Ca^{2+} concentration is elevated in cardiomyocytes differentiated from hiPSCs derived from a duchenne muscular dystrophy patient. *PLoS ONE* 14:e0213768. doi: 10.1371/journal.pone.0213768

Villa Chet, R., Czosek Richard, J., Ahmed, H., Khoury Philip, R., Anderson Jeffrey, B., Knilans Timothy, K., et al. (2015). Ambulatory monitoring and arrhythmic outcomes in pediatric and adolescent patients with duchenne muscular dystrophy. *J. Am. Heart Assoc.* 5:e002620. doi: 10.1161/JAHA.115.002620

Viollet, L., Thrush, P. T., Flanigan, K. M., Mendell, J. R., and Allen, H. D. (2012). Effects of angiotensin-converting enzyme inhibitors and/or beta blockers on the cardiomyopathy in duchenne muscular dystrophy. *Am. J. Cardiol.* 110, 98–102. doi: 10.1016/j.amjcard.2012.02.064

Voigt, N., Li, N., Wang, Q., Wang, W., Trafford, A. W., Abu-Taha, I., et al. (2012). Enhanced sarcoplasmic reticulum Ca^{2+}-leak and increased Na+-Ca2+-exchanger function underlie delayed afterdepolarizations in patients with chronic atrial fibrillation. *Circulation* 125, 2059–2070. doi: 10.1161/CIRCULATIONAHA.111.067306

Vry, J., Gramsch, K., Rodger, S., Thompson, R., Steffensen, B. F., Rahbek, J., et al. (2016). European cross-sectional survey of current care practices for duchenne muscular dystrophy reveals regional and age-dependent differences. *J. Neuromuscul. Dis.* 3, 517–527. doi: 10.3233/JND-160185

Wagner, K. R., Lechtzin, N., and Judge, D. P. (2007). Current treatment of adult duchenne muscular dystrophy. *Biochim. Biophys. Acta* 1772, 229–237. doi: 10.1016/j.bbadis.2006.06.009

Weiss, J. N., Garfinkel, A., Karagueuzian, H. S., Chen, P.-S., and Qu, Z. (2010). Early afterdepolarizations and cardiac arrhythmias. *Heart Rhythm.* 7, 1891–1899. doi: 10.1016/j.hrthm.2010.09.017

Williams, I. A., and Allen, D. G. (2007). Intracellular calcium handling in ventricular myocytes from mdx mice. *Am. J. Physiol. Heart Circ. Physiol.* 292, H846–H855. doi: 10.1152/ajpheart.00688.2006

Zhu, R., Millrod, M. A., Zambidis, E. T., and Tung, L. (2016). Variability of action potentials within and among cardiac cell clusters derived from human embryonic stem cells. *Sci. Rep.* 6:18544. doi: 10.1038/srep18544

Conflict of Interest: The authors declare that the research was conducted in the absence of any commercial or financial relationships that could be construed as a potential conflict of interest.

Copyright © 2020 Jelinkova, Vilotic, Pribyl, Aimond, Salykin, Acimovic, Pesl, Caluori, Klimovic, Urban, Dobrovolna, Soska, Skladal, Lacampagne, Dvorak, Meli and Rotrekl. This is an open-access article distributed under the terms of the Creative Commons Attribution License (CC BY). The use, distribution or reproduction in other forums is permitted, provided the original author(s) and the copyright owner(s) are credited and that the original publication in this journal is cited, in accordance with accepted academic practice. No use, distribution or reproduction is permitted which does not comply with these terms.

frontiers in Bioengineering and Biotechnology

REVIEW
published: 30 June 2020
doi: 10.3389/fbioe.2020.00657

Elastin-Based Materials: Promising Candidates for Cardiac Tissue Regeneration

Israel Gonzalez de Torre, Matilde Alonso and Jose-Carlos Rodriguez-Cabello*

BIOFORGE, CIBER-BBN, Edificio LUCIA, University of Valladolid, Valladolid, Spain

Stroke and cardiovascular episodes are still some of the most common diseases worldwide, causing millions of deaths and costing billions of Euros to healthcare systems. The use of new biomaterials with enhanced biological and physical properties has opened the door to new approaches in cardiovascular applications. Elastin-based materials are biomaterials with some of the most promising properties. Indeed, these biomaterials have started to yield good results in cardiovascular and angiogenesis applications. In this review, we explore the latest trends in elastin-derived materials for cardiac regeneration and the different possibilities that are being explored by researchers to regenerate an infarcted muscle and restore its normal function. Elastin-based materials can be processed in different manners to create injectable systems or hydrogel scaffolds that can be applied by simple injection or as patches to cover the damaged area and regenerate it. Such materials have been applied to directly regenerate the damaged cardiac muscle and to create complex structures, such as heart valves or new bio-stents that could help to restore the normal function of the heart or to minimize damage after a stroke. We will discuss the possibilities that elastin-based materials offer in cardiac tissue engineering, either alone or in combination with other biomaterials, in order to illustrate the wide range of options that are being explored. Moreover, although tremendous advances have been achieved with such elastin-based materials, there is still room for new approaches that could trigger advances in cardiac tissue regeneration.

Keywords: elastin-like, cardiovascular, cardiac patch, heart valve, vascular graft, angiogenesis

OPEN ACCESS

Edited by:
Valeria Chiono,
Polytechnic University of Turin, Italy

Reviewed by:
Piyush Koria,
University of South Florida,
United States
Laurent Duca,
Université de Reims
Champagne-Ardenne, France

****Correspondence:***
Israel Gonzalez de Torre
igonzalez@bioforge.uva.es

Specialty section:
This article was submitted to Biomaterials, a section of the journal Frontiers in Bioengineering and Biotechnology

Received: *04 March 2020*
Accepted: *27 May 2020*
Published: *30 June 2020*

Citation:
Gonzalez de Torre I, Alonso M and Rodriguez-Cabello J-C (2020) Elastin-Based Materials: Promising Candidates for Cardiac Tissue Regeneration. Front. Bioeng. Biotechnol. 8:657. doi: 10.3389/fbioe.2020.00657

INTRODUCTION

Cardiovascular diseases (CVDs), which are a group of illnesses that directly affect the heart and its normal function, including valve failure, stroke, aneurism of coronary vessels and other heart diseases, are the leading cause of death in the United States and Europe. Indeed, in the period 2014–2015, the annual direct and indirect cost of CVDs in the United States was an estimated 351.2 billion dollars, including 213.8 billion in expenditures and 137.4 billion in lost future productivity attributed to premature CVD and stroke mortality (Benjamin et al., 2019).

The use of new biomaterials with enhanced biological and physical properties has opened the door to new approaches in cardiovascular applications. Biomaterials, as defined by Williams (1999), have been used for many different purposes in the field of regenerative medicine, especially as artificial extracellular matrixes, vehicles for cell delivery and controlled delivery systems for bioactive molecules. It could be thought that a special tissue, such as cardiac muscle may require biomaterials with special characteristics, although basically they should present biocompatibility,

adequate mechanical strength, bioresorption or biodegradation, adequate internal morphology and cell-friendly fabrication (Ruvinov et al., 2014; Salerno and Netti, 2014), as is also the case for biomaterials used in other biomedical applications.

Elastin, which is an elastomeric, insoluble and fibrous protein, is one of the principal components of the extracellular matrix (ECM) and is mainly found in those tissues in which high deformations are required. Indeed, elastin can undergo hundreds of millions of cycles with no memory effect while maintaining its original behavior. In the cardiovascular field, it is of paramount importance in blood vessels, heart valves and other cardiac tissues (Powell et al., 1992; Scott and Vesely, 1995; Vesely, 1997; Huang et al., 2018). Elastin is necessary from a mechanical point of view and is also involved in many cell-signaling processes (Almine et al., 2010a, 2012). It is formed by the crosslinking of tropoelastin, its soluble precursor, in a process known as elastogenesis, which has been excellently described elsewhere (Hinek and Rabinovitch, 1994; Brown-Augsburger et al., 1995, 1996; Daamen et al., 2007; Almine et al., 2010b; Vindin et al., 2019). As such, tropoelastin itself (either natural or recombinantly produced) has been widely studied and applied in tissue engineering (Clarke et al., 2006; Mithieux et al., 2009; Wise and Weiss, 2009; Annabi et al., 2017). Unfortunately, once elastin has been degraded or disrupted, it is not easy to repair, at least without markedly affecting the natural alignment and arrangement of the undamaged tissue (Rodríguez-Cabello et al., 2018b). Moreover, its turnover is very low in healthy adults, with elastogenesis primarily occurring during the late fetal and early neonatal periods (Uitto and Larjava, 1991). As such, elastogenesis, which is a complicated process that has already been described elsewhere (Indik et al., 1989; Brown-Augsburger et al., 1997), decreases with age (Vrhovski and Weiss, 1998; Miriam et al., 2013), and is difficult to achieve under *in vitro* conditions (Flanagan et al., 2009; Syedain et al., 2011; Driessen-Mol et al., 2014; Moreira et al., 2016). Given this lack of elastogenesis in adults and the crucial importance of elastin in cardiac tissues, some researchers have focused their efforts on the use of elastin-based biomaterials, or at least those based on the repetition of the amino acid sequence valine-proline-glycine-valine-glycine (VPGVG) that codes for the elasticity of the elastin molecule according to Urry's model (Urry, 2006). These five amino acids form a β-turn, with proline-glycine at the angle of the turn and a $4 \rightarrow 1$ hydrogen bond connecting the keto group of the first valine to the amino group of the fourth valine along the sequence. A helical arrangement is produced by repetition of these β-turns to form a so-called β-spiral in which the β-turns act as spacers between the turns of the spirals. Valine-glycine sequences allow large-amplitude, low-frequency vibrations. Reductions in the amplitude of these vibrations cause a marked decrease in the entropy of the segment, thus providing the driving force for a return to the relaxed state, which drives the elastic behavior of the protein (Tamburro et al., 1990, 1992, 2003).

Among these biomaterials, elastin-like polypeptides (ELPs) or elastin-like recombinamers (ELRs), depending on whether they are synthesized (Rodriguez-Cabello et al., 2017) by traditional chemical synthesis or by recombinant techniques, respectively, have been shown to be promising biocompatible candidates for use in tissue-engineering applications (Ibáñez-Fonseca et al., 2018). ELRs are based on the repetition of the five amino acids that confer the elastic properties to the elastin molecule, namely VPGVG, in which the V at the fourth position can be substituted by any amino acid except proline (Rodríguez-Cabello et al., 2018a). The use of recombinant techniques employing iterative-recursive methods ensures a high control over the amino acid sequence that forms the ELR and a very high monodispertsity, which is one of the principal problems of traditional chemical synthesis (Won and Barron, 2002; Chilkoti et al., 2006). This control allows the possibility to tailor ELRs with specific mechanical properties and include specific biofunctionalities for the target application or tissue (**Figure 1**).

ELRs exhibit a thermoresponsive behavior in aqueous solvents, which means that above a certain temperature, known as the transition temperature (T_t) (Urry et al., 1992; Urry, 1997), they undergo a self-assembly process directed by electrostatic interactions that trigger a change in the conformation of the protein. This change consists of the exclusion of water, thus resulting in loss of the clathrate-like extended structure of the ELRs that leads to a viscoelastic state in which the governing structure is a β-spiral containing three units of the basic pentamer VPGVG, which form a type II β-turn per turn of the spiral, as mentioned. Previously. This change in conformation is accompanied by a shortening in the length of the ELR and release of a certain quantity of energy (Urry, 1993). The temperature (Tt) that defines this change is determined mainly by the amino acid sequence, the polarity of the amino acid present in the fourth position and the molecular mass of the ELR molecule (Urry, 1993).

Although one very optimistic goal in this field, at least currently, is to create a completely functional heart using tissue engineering, significant efforts are being dedicated to the three main sections into which this field can be subdivided, namely cardiac muscle, vasculature and heart valves (Zandonella, 2003; Sacks et al., 2009). In this review, we will focus on the latest results arising from the application of elastin-like materials in these three main areas.

CARDIAC MUSCLE REGENERATION AND ANGIOGENESIS

It is very important to understand the special characteristics of cardiac tissue. This muscle is mainly formed by cardiomyocytes, a kind of hypertrophied muscle cell, which are perfectly aligned and electrically synchronized with the surrounding cells. As they are permanently beating, a constantly high intake of nutrients and oxygen is required to meet their metabolic needs. These nutrients and oxygen are supplied by a dense and very well-organized vascular network, in which smooth muscle cells and endothelial cells are the main cell sources that form and maintain the vascular network (Eng et al., 2016).

Acute myocardial infraction (AMI) has traditionally been defined as a decrease or suspension of blood flow to a portion of the cardiac muscle leading to necrosis. It usually results as a

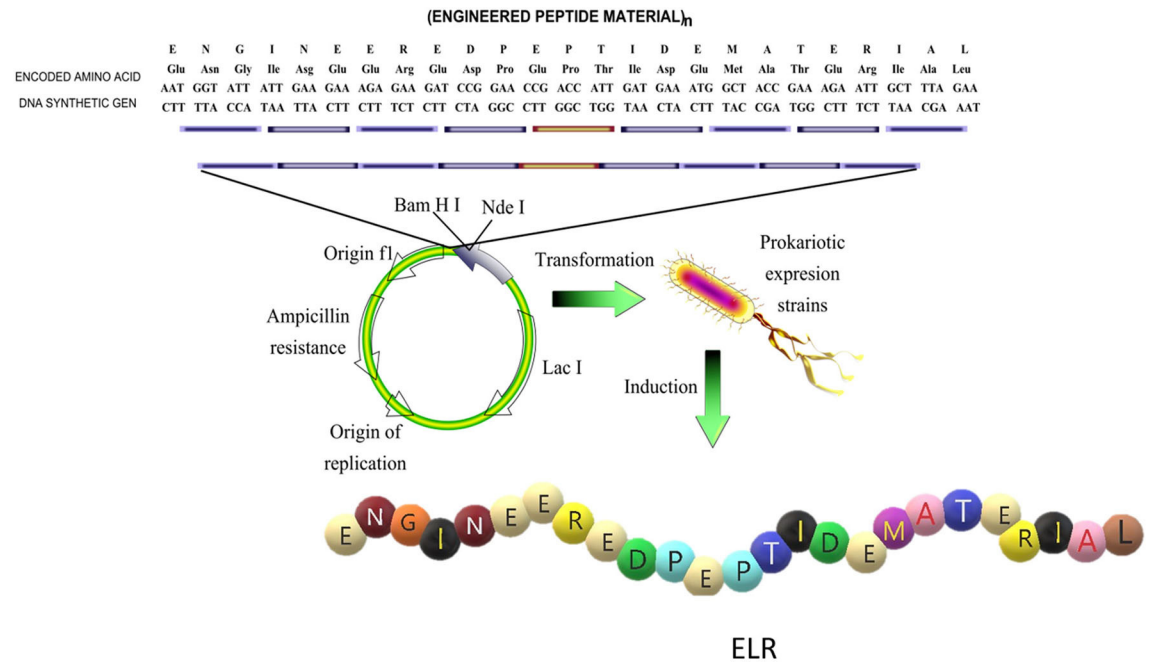

FIGURE 1 | Schematic representation of the design of the sequence and production of an elastin like recombinamer (ELR). Reproduced with permission from Rodríguez-Cabello et al. (2018b).

consequence of a blood clot in an epicardial artery that supplies nutrients and oxygen to that region. However, the definition of this kind of event has been changed recently—not all cases now unavoidably involve a blood clot—to a discrepancy between the amount of oxygen that the cardiac muscle requires and the supply that it effectively receives. This discrepancy may lead to myocardial damage, usually in the left ventricle (Saleh and Ambrose, 2018). As in any other muscle tissue, the subsequent ischemia produces a necrotic wound and a reduction in the ability of the affected region to perform its normal function. Therefore, in the case of cardiac muscle, this reduction could compromise the pumping capacity of the entire organ. From a histological point of view, slight changes can be appreciated after the MI. In the first 12 h, hypereosinophilic changes to the myocyte sarcoplasm are present before neutrophilic infiltrates. Subsequently, coagulative necrosis begins and progresses over the next 3 days, resulting in loss of myocyte nuclei and neutrophilic infiltration. Myocyte fragmentation and early phagocytosis occur during the first week. After that time, granulation tissue evolves to form a denser region of collagen which, over the following few weeks, will produce a poorly populated scar tissue with dense and compact collagen. All these events, accompanied by wall thinning and ventricular dilation, impede the normal functioning of the affected region (Pasotti et al., 2006; Ruvinov et al., 2008; Seliktar and Shapira-Schweitzer, 2010). As can be seen, the steps after MI follow a similar path to the wound-healing process (Stroncek and Reichert, 2008) until the final scar is formed, although they are aggravated by what is defined as "infarct extension." This "infarct extension" is characterized by a remodeling of the ECM in both the directly damaged region and in the viable borders and beyond, reaching the remote region of the ventricle. The limitations arising due to the wound healing process in the affected region are importance as regards rehabilitation of the lost functionality in the affected region, and the limited ability of adult cardiomyocytes terminally differentiated after a myocardial infarction to regenerate clearly affects the regeneration of the affected region (Huang et al., 2018). To overcome this low regeneration ability of adult cardiomyocytes, numerous research groups have attempted to create cardiac patches and injectable systems.

Scaffolds used in cardiac tissue engineering have to provide both an adequate environment to promote cell growth and an integrative system that allows perfect conjunction with the surrounding tissues which, ideally, should be replaced by a perfectly functional natural tissue. Regardless of whether an acellular or cellular approach is used, such scaffolds (injected or preformed) have to provide support to create the vascular network needed to supply the nutrients and oxygen needed by the new cells that will populate them. This vascular network can be pre-formed *in vitro* or induced *in vivo* but, in both cases, has to be integrated and well-connected to the pre-existing natural vasculature from undamaged regions. As such, this is one of the key issues that biomaterial scientists have to overcome when creating engineered tissues that can survive in the long-term. Indeed, the lack of appropriate vascular integration is one of the key problems of some approaches for the creation of cardiac patches (Ruvinov et al., 2008; Zhang et al., 2018).

In light of the above, biomaterials for cardiac patches must be biocompatible and must provide the correct mechanical stiffness, matrix density, and viscoelasticity to induce angiogenesis together with the appropriate biological clues (Crosby and Zoldan, 2019). In this regard, ELR/ELP-based scaffolds can be created with tunable mechanical properties that can be adjusted on-demand, depending on the final application, simply by varying the final concentration and/or amino acid composition of the polypeptides. Scaffolds based on elastin-like materials with stiffnesses ranging from a few hundred to some tens of thousands of Pascals have been described in the literature (González De Torre et al., 2014; Gonzalez De Torre et al., 2016; De Torre et al., 2015; Cipriani et al., 2018), thus highlighting the mechanical versatility of this type of biomaterials. Moreover, although mechanical and physical features are critical for tissue-engineering applications, the micro-topography of elastin-derived materials has a crucial impact on the alignment and fate of cardiac cells. Thus, micropatterned tropoelastin-based hydrogels have been shown to promote CM attachment, spreading and elongation. These micropatterned scaffolds also maintained the phenotype and contractile properties of the CMs, and can be electrically stimulated to induce or control the beating of the CMs seeded on them (Annabi et al., 2013).

Elastin-derived materials have proved to be suitable biomaterials for the creation of scaffolds that can trigger angiogenesis. Thus, Robinet et al. have shown that peptides containing the sequence VGVAPG (found in tropoelastin and elastin-like materials) can trigger the angiogenic phenotype of ECs from the micro- and macrovasculatrue (Robinet et al., 2005). This was corroborated by Reddel et al., who showed that exposed elastin sequences are able to increase the levels of matrix metalloproteinases (MMP-2), which contribute to the digestion of connective tissue growth factor (CTGF) and, together with transforming growth factor (TGF-β1), increase the amount of free vascular endothelial growth factor (VEGF) (Reddel et al., 2013), both of which are closely related to angiogenesis. An option to increase the angiogenic potential of the ELRs is to fuse them with this grow factor (VEGF). the Three VEGF genes, namely VEGF-1, VEGF-2 or VEGF-C and VEGF-3 or VEGF-B, VEGF-D, VEGF-E, have been identified in humans (Seandel et al., 2001; Vale et al., 2001). Although located in different chromosomes, all these genes share similar features and behaviors but have different actions in endothelial cells (ECs), affecting different endothelial-specific fms-like tyrosine kinases (VEGFR-1, VEGFR-2, VEGFR-3) and therefore producing different effects in ECs. For instance, VEGFR-1 is related to the assembly of ECs into tubes to yield functional vessels (Seandel et al., 2001), VEGFR-2 is involved in EC proliferation and migration (Shalaby et al., 1995; Carmeliet and Collen, 1997), while VEGFR-3 is more closely related to the lymphatic system (Jeltsch et al., 1997). VEGF can be incorporated into elastin-like scaffolds to provide a pro-angiogenic environment to increase the inherent angiogenic potential of the elastin-derived materials (Flora et al., 2019a) (**Figure 2**). Moreover, in some studies not related with the regeneration of the cardiac muscle but very related with vascular diseases, as for instance renovascular disease, this combination of ELR-VEGF have been tested in order to increase its angiogenic potential. Both, *in vitro*, and more importantly, *in vivo* experiments showed that this biomaterial was able to stimulate the cells related with vessel formation to produce tubular structures. Accumulations of ELRs-VEGF in stenotic kidneys triggered the newly formation of micro-vessels in the cortical and medullar area of the kidneys. ELRs-VEGF did not alter the potency of VEGF alone but this combination increased the half-life with respect to free VEGF resulting in a more effective at recovering the renal function (Chade et al., 2016). However, despite the evident angiogenic potential resulting from the incorporation of VEGFs into scaffolds for tissue-engineering applications (Testa et al., 2008), some studies have pointed out that the use of growth factors has some intrinsic drawbacks, such as low stability and, subsequently, a loss of bioactivity, as well as the possibility of immunogenicity (Lee et al., 2011). To overcome these possible disadvantages, synthetic peptides known as QK peptides, based on the 17–25 alpha region of $VEGF_{165}$ that binds to the main VEGF receptors, such as VEGFR-1 and VEGFR-2, have been designed (D'Andrea et al., 2005). This QK peptide has shown excellent stability while maintaining its helical structure and bioactivity (Diana et al., 2008; Leslie-Barbick et al., 2011). QK peptides have been incorporated into ELRs in order to enhance their angiogenetic ability with the aim of obtaining better integration of the tissue-engineered scaffold into the natural surrounding tissue. An initial *in vitro* study showed that QK peptides anchored to the backbone of ELP-based hydrogels could enhance the adhesion and proliferation of HUVECs in 2D systems and could stimulate more sprouting in 3D environments (Cai et al., 2014). In a similar study, Flora et al. demonstrated that tethering QK to ELRs provided a proangiogenic environment in a similar manner to VEGF and that this ELR-QK combination enhanced the formation of new functional capillaries *in vivo*. This new microvasculature is essential for the survival of the cells colonizing the tissue-engineered scaffold, thus suggesting that this approach could be of great interest in a wide-range of cardiovascular applications that require the spatial-temporal control of growth factors (Flora et al., 2019a). Under the light of the previous lines, the inclusion of GFs into ELR based hydrogels for cardiac regeneration or even fused with the ELR molecules could be an interesting option. However, the use of free GFs entrapped on ELR based hydrogels could have some limitations, as for instance low effective time before their (GFs) degradation. Other key factor to be considered is the dose and how to obtain the optimal concentration from a GF loaded hydrogel. Such spatial-temporal control is still a great challenge even though many strategies have been followed (Martino et al., 2014, 2015). In the case of GFs fused to ELRs, the latency of the GF is clearly increased, as previously mentioned. Moreover, it has to be considered when designing a scaffold based on ELRs fused with GFs, that an increase on the half-life of the GF could be reflected in a lowering of the dose to avoid overdose issues.

In addition to the intrinsic benefits of elastin-derived materials, their tunable mechanical properties and the possibility of tethering pro-angiogenic factors, the option of incorporating

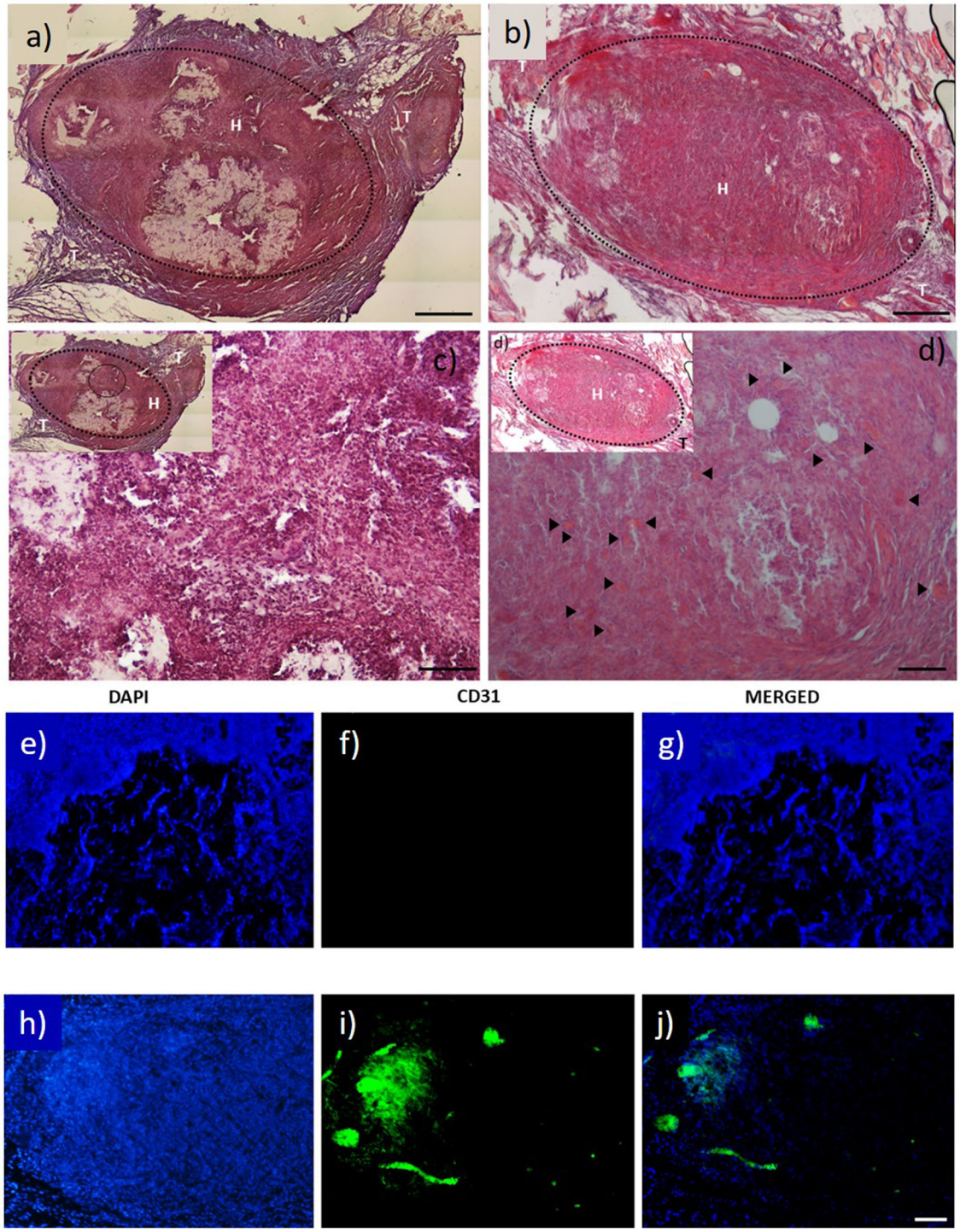

FIGURE 2 | H&E staining images of: **(a)** ELR factor-free hydrogel; and **(b)** ELR-QK hydrogel; **(c,d)** magnification 20× of image and **(b)**, respectively. Black arrows indicate the presence of newly formed capillaries. Scale bar **(a–d)** images 100 μm. **(e–j)** CD31 immunofluorescent staining images: **(e–g)** factor free ELR hydrogel (ELR), **(h–j)** ELR-QK hydrogel. DAPI: nucleus staining **(e,h)**. CD31: expression of CD31 protein **(f,i)**. MERGED: merged channels (DAPI + CD31) **(g,j)**. Scale bar: 50 μm. Reproduced with permission from Flora et al. (2019a).

selected bioactivities into the backbone of ELRs is essential to meet the precise requirements of specific applications. In this case, cardiac tissue requires a highly vascularized environment, therefore a precise combination of bioactive sequences that could trigger a specific response of endothelial cells compared with other cell types is of great interest. In this

regard, Flora et al. have demonstrated that a correct choice of bioactivities (RGD and REDV, Arg-Gly-Asp, and Arg-Glu-Asp-Val, respectively), and the right proportion between them, could induce the selective adhesion of endothelial cells from a co-culture with human foreskin fibroblast (HFF-1) and human umbilical vein endothelial cells (HUVECs). Although the choice of a highly selective bioactive sequence for endothelial cells, such as REDV (Massia and Hubbell, 1992; Heilshorn et al., 2003), may not be sufficient in terms of adhesion and proliferation, in conjugation with other bioactive sequences this adhesion and proliferation can be enhanced without losing selectivity (Flora et al., 2018). In addition, the correct selection of bioactivities in terms of cell adhesion and proliferation properties is important. Thus, an appropriate degradation rate is paramount to synchronize the degradation rate of the scaffold and the regeneration rate of the damaged tissue. In this regard, a combination of protease-sensitive bioactive sequences that could harmonize the colonization rate of the cells and the degradation rate of the scaffold, or a cell-demanding degradable scaffold, could be the key to achieving complete and efficient regeneration with adequate vascularization (Trappmann et al., 2017).

Some successful attempts to introduce protease-sensitive sequences into elastin-like materials in order to modulate vascularization of tissue-engineered scaffolds *in vivo* have been performed. Thus, Staulbi et al. created a scaffold based on two different ELRs that combined cell-adhesion sequences, such as RGDs (general cell-adhesion sequence) and REDV (EC-specific cell-adhesion sequence) with an elastase-sensitive sequence, such as Val-Gly-Val-Ala-Pro-Gly (VGVAPG). A non-biofunctionalized ELR was used as control. These ELRs were chemically modified to bear chemically reactive groups that were used to create hydrogels under different conditions. The study aimed to evaluate the contribution of the gel structure and biofunctionalization on control of the angiogenic potential of this kind of material for use in cardiovascular applications. Stromal vascular fraction cells (SVF), a heterogeneous mixture of cells in which mesenchymal and endothelial/mural progenitor cells are the key cell types, were used in this study. To investigate the angiogenic potential of these scaffolds, several pro- and anti-angiogenic factors secreted by the SVF were evaluated *in vitro*. Scaffolds containing RGD, REDV, and VGVAPG sequences were prone to inducing cells to produce pro-angiogenic factors, such as monocyte chemoattractant protein-1 (MCP-1), insulin growth factor binding protein-2 (IGFBP-2), heparin-binding epidermal growth factor (HB-EGF), VEGF, interleukin-1b (IL-1b), and urokinase-type plasminogen activator (uPA). In contrast, with non-functionalized scaffolds, anti-angiogenic factors, such as insulin growth factor binding protein-3 (IGFBP-3), prolactin, angiostatin, or vasohibin, were mainly secreted by cells. Moreover, functionalized scaffolds showed higher endothelial cell infiltration than their non-functionalized counterparts. These findings were in agreement with those found in *in vivo* experiments, which showed a higher cell infiltration and better integration of the scaffold in functionalized scaffolds (Staubli et al., 2017) (**Figure 3**). As such, it can be concluded from this study that angiogenesis and host integration of these kinds of ELR-based scaffolds can be controlled by modulating the functionalization of the hydrogel alone, which may prove to be an excellent tool in cardiac tissue regeneration.

Other protease-sensitive sequences have been tested in ELRs to induce controlled biodegradability of the scaffolds and promote directed and guided cell infiltration. These sequences, namely YAVTG**DRIR**SASPASSA and YAVTG**GTAR**SASPASSA (DRIR and GTAR, respectively), were based on the previously mentioned urokinase plasminogen activator (uPA) (Straky and Heilshorn, 2009). These two sequences were combined with the previously mentioned general cell-adhesion sequence RGD to create two different kinds of scaffold, namely one with a slow degradation rate containing the DRIR sequence and one with a fast degradation rate containing the GTAR sequence. *In vitro* experiments showed that the different degradation rates depended on the bioactive sequence selected. However, the appearance of new functional vascular vessels within the regenerated region is more relevant from a cardiac tissue-engineering point of view as this allows the creation of a quickly colonizable scaffold. This finding suggests that such a fast degradability induces a fast colonization that is supported by the creation of new functional vasculature (Flora et al., 2019b), which could be crucial for a rapid and functional regeneration of the damaged cardiac tissue.

VASCULAR GRAFTS (VGs)

The mismatch between the oxygen requirements of cardiac tissue and the amount that effectively reaches it is often caused by a failure in the blood supply due to the blockage or rupture of a blood vessel that must provide this oxygen. The first attempts at blood vessel substitution date back to the 1950s (Blakemore et al., 1952; Blakemore and Voorhees, 1954; De Bakey et al., 1958). However, in those days, the two main approaches for replacing damaged blood vessels, which are currently still the most widely used in surgical procedures, involved the use of an autologous (Brescia et al., 1966) or a synthetic graft (De Bakey et al., 1958). It is commonly accepted that the use of autologous vessels as grafts for bypass procedures is the best option even though limitations related to the availability of suitable autologous grafts could represent a problem. On some occasions, surgeons have to choose the synthetic route. However, this can lead to issues related to the small diameter of synthetic conduits, which have a particular propensity to re-stenosis and thrombus formation. Given these limitations, the field of vascular grafts is still relatively underdeveloped and new materials, concepts and approaches are being developed by materials and tissue engineering scientists in their search for the optimal conduit that fulfills all the requirements of this demanding application. Among the different options being studied, the use of tissue-engineered vascular grafts (TEVGs) is one of the most promising approaches to achieve the desired goal of a fully functional vascular vessel with a performance and biological properties similar to native ones. The leading principle in the field of tissue engineering for the creation of TEVGs is biomimicry. It is well-known that nature

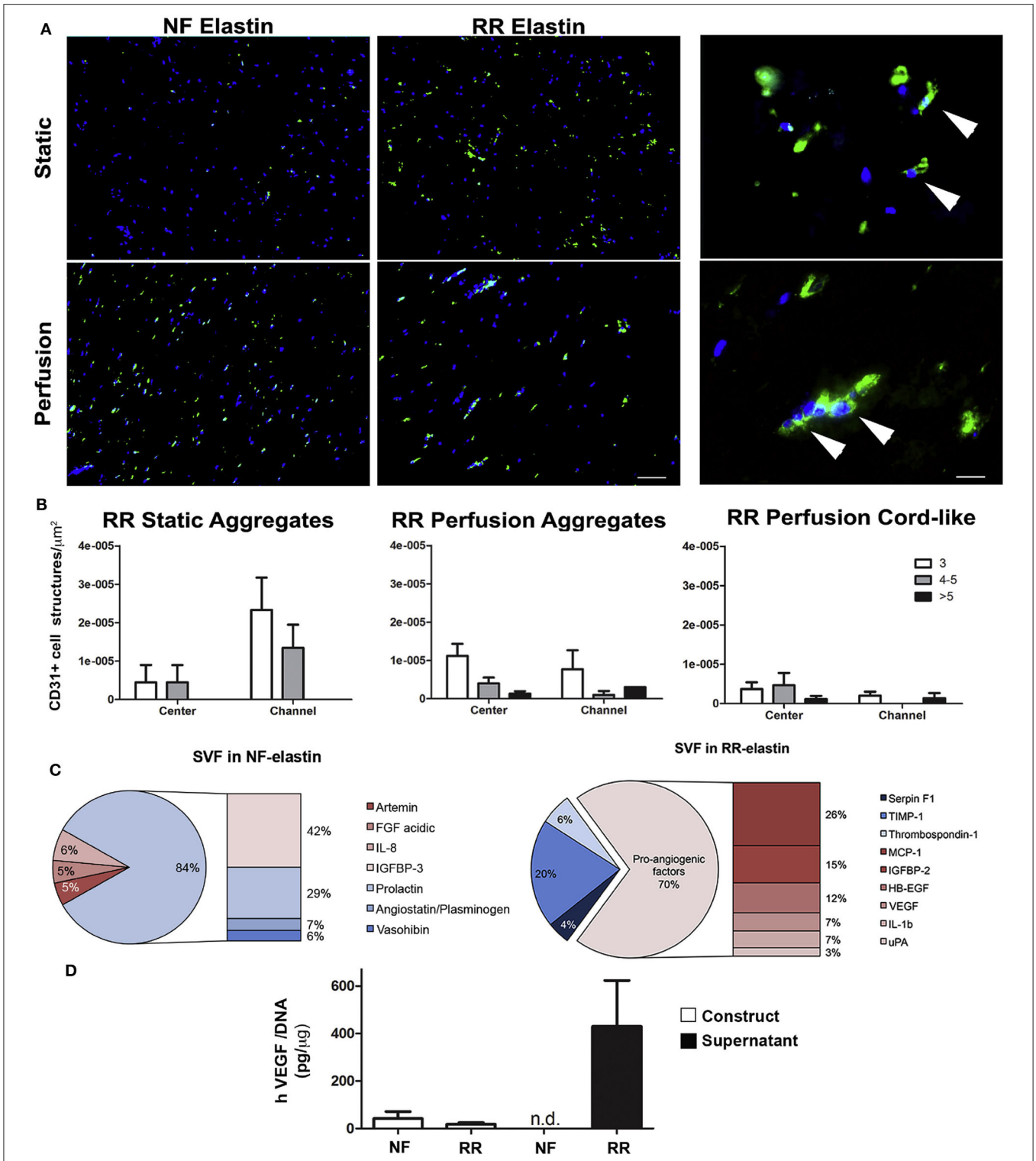

FIGURE 3 | *In vitro* angiogenic potential of SVF cell-based ELR constructs. **(A)** Immunofluorescence staining for CD31 (green) of constructs generated by SVF cells in either non-functionalized (NF) or functionalized with REDV-RGD (RR-ELR) in static or perfusion-based culture at low (left) and high (right) magnifications. Nuclei were stained with DAPI (blue). High magnifications were provided only for the RR-ELR condition to distinguish between the formation of cell aggregates and cord-like structures. White arrowheads indicate the specific staining for endothelial cells. Scale bars = 100 and 20 mm, for low and high magnification, respectively. **(B)** Quantification of CD31$^+$ cell aggregates formed in static or perfusion culture and cord-like structures in perfusion in areas proximal (channel) or distal (center) to the

(Continued)

FIGURE 3 | perfusion channels. Both aggregates and cord-like structures were distinguished by the number of endothelial cells included in them (3, 4, or 5, more than 5). **(C)** Pie graph representing all the upregulated factors in NF (left) or RR- (right) ELR constructs generated in perfusion culture, divided into pro- and anti-angiogenic factors. **(D)** Quantification of VEGF released by and entrapped in constructs generated in NF or RR-ELR in dynamic condition. Number of donors = 2 (duplicate samples for each donor) **(B–D)**. Reproduced with permission from Staubli et al. (2017).

has served as the inspiration to recreate different structures, tools and devices (airplanes, helicopters, submarines, etc.). The same biomimicry, or imitation of nature, forms the basis for the generation of TEVGs. These TEVGs are intended to be more than mere tubes or conduits to channel blood without leaking as they must avoid immune rejection after implantation and should trigger the formation of autologous tissue that finally replaces the artificial implanted structure, thus forming a completely functional vessel. Basically, they have to accomplish a series of requirements or attributes, as discussed by Benrashid et al. in a nice review of TEVGs (Benrashid et al., 2016):

- Low risk of infectious complication
- Lack of an immune response
- Long-term patency
- Controlled degradation
- Suture integrity
- Suturability
- Ability to be remodeled by cells as a functional tissue
- Responsive to physiological stimuli
- Antithrombotic
- Internal structure that allows for cell migration/seeding
- Durability and mechanical strength
- Cost effectiveness
- Ready availability for use

The first TEVG was reported in 1986 and had a structure based on a multilayer collagen tube and a combination of endothelial and smooth muscle cells (SMCs) (Weinberg and Bell, 1986). Since this first approach, several other TEVGs have been created by varying the base biomaterial and/or cell type and source (Kannan et al., 2005; Buttafoco et al., 2006b; L'Heureux et al., 2006, 2007; Wang et al., 2007; Allen et al., 2014; Wystrychowski et al., 2014).

There are several fabrication techniques to obtain prosthetic VGs. Although it is not intended in this review to explore depply the different fabricating technologies to obtain prosthetic VGs (Wang et al., 2019). It is particularly interesting a novel method developed by Wang et al. in which sacrificial ice scaffolds are created by 3D printing and coated with different materials (tropoelastin alone or mixed with PCL or PDMS, and pure silk or silk/PMDS mixtures) to finally obtain scaffolds with the desired architecture after melting the inner ice core (Hiob et al., 2017).

Many synthetic plastic-based VGs have been designed and tested. Although all of these systems have different mechanical and biological properties, none of them are extensively used as substitutes for blood vessels in clinical practice (Liu et al., 2018). As such, we will not analyze them in this review as our focus here is on approaches that involve the presence of elastin or elastin-derived materials.

Elastin, which is one of the main components of the extracellular matrix in blood vessels, provides long-range deformability and resilience to these vessels, thus allowing a perfect adaptation and performance of the vessel to physiological demands. Elastin is a very stable molecule that rarely undergoes remodeling and exhibits high resistance to the action of degrading enzymes, with only elastase and metalloproteinases (MMPs) having some activity against this resistant molecule (Fornieri et al., 1992; Kielty et al., 2002; Chuang et al., 2009). Since elastogenesis is a process that rarely occurs *in vitro* (Hinderer et al., 2015), some approaches for generating TEVGs have focused their efforts on the use of elastin-derived materials to create these artificial blood vessels. One of the first such approaches involved decellularize and the removal of collagen from porcine arteries. The resulting structure, which mainly comprised the remaining elastin, was further stabilized by the use of penta-galloyl glucose (PGG). The stabilized constructs showed adequate mechanical properties and allowed cell repopulation of the scaffolds. *In vivo* experiments indicated a low calcification of the grafts (Chuang et al., 2009). This pathway, based on decellularized tissue scaffolds, has been widely studied, mainly starting from porcine tissues (Roy et al., 2005; Tillman et al., 2012; Syedain et al., 2014; Koobatian et al., 2016). Although all of them confirmed the feasibility of using TEVGs from decellularized animal vessels and their stable geometry, low thrombogenicity, and durable wall structure under *in vitro* and *in vivo* conditions none of them are being used clinically.

A second approach for obtaining tissue-engineered blood vessels (TEBVs) with some quantity of elastin in their structure involves the use of fibroblasts to create cell sheets that are subsequently rolled to obtain tubular constructs. These constructs are then dehydrated and decellularized to give a cylindrical structure comprising the extracellular matrix produced by the fibroblast. This acellular tubular substrate has two functions, namely as a barrier to avoid cell migration toward the lumen and as a substrate for endothelial cell seeding in order to obtain a complete endothelial layer covering the lumen of the tubular scaffold and mimicking the natural structure of blood vessels. This approach was developed by L'Heureux et al. (2006), who obtained TEBVs with two different internal diameters (4.5 and 1.5 mm) and a wall thickness of between 0.2 and 0.45 mm. These TEBVs showed good mechanical properties and performance and were found to integrate perfectly with the host vessel, at an anastomosis level, in *in vivo* experiments in primates. Unfortunately, the time required to create one of these TEBVs (more than 7 months) is too long to allow them to be used in emergency situations, such as stroke or aneurism.

Buijtenhuijs et al. prepared tubular constructs from a dilute acetic acid suspension of collagen I and elastin. These tubular constructs were tested *in vitro* by seeding smooth muscle cells, which were able to proliferate and colonize the scaffolds

(Buijtenhuijs et al., 2004; Buttafoco et al., 2006a; Engbers-Buijtenhuijs et al., 2006). Similarly, combinations of different types of collagen and elastin cross-linked with glutaraldehyde scaffolds have been tested by several authors (van Wachem et al., 1994; Stitzel et al., 2006), although the presence of organic chemicals compromises the biocompatibility of the resulting scaffolds (Daamen et al., 2007). Electrospinning has been explored to process mixtures of collagen and elastin using poly(ethylene) oxide and NaCl as co-reagents. *In vitro* tests showed the proliferation of smooth muscle cells on these tubular scaffolds (Huang et al., 2001; Buttafoco et al., 2006b). Following on from the use of electrospinning, McKenna et al. developed a tubular vascular scaffold by dissolving recombinant tropoelastin in 1,1,1,3,3,3-hexafluoro-2-propanol and cross-linking with diusccinimidyl suberate. The resulting vascular scaffolds could be precisely designed in terms of length and diameter and exhibited adequate mechanical properties similar to those of native elastin, thus meaning that the use of organic solvents did not produce significant changes in the conformation of the recombinant tropoelastin. However, the presence of these organic compounds has to be controlled and limited to low values in order to avoid cytotoxic effects (McKenna et al., 2012).

Tropoelastin has been used as both a structural biomaterial for constructing VGs, as discussed above, and as an anti thrombogenic coating for VGs created from other materials. Thus, Sugiura et al. developed a bioresorbable VG made from a non-woven poly (glycolic acid) (PGA) fiber mesh coated with a copolymer sealant solution of poly(L-lac tic-co-e-caprolactone) (PLCL) and reinforced by electrospinning poly(L-lactic acid) (PLA) nano-fiber onto the outer side of the PLCL scaffold. This scaffold was functionalized with a monolayer of physisorbed tropoelastin molecules. These VGs were implanted in the infra-renal aortic position in mice and were shown to be able to control the proliferation of vascular SMCs, thereby reducing intimal hyperplasia. However, these authors pointed out that more acute thrombosis was found in the tropoelastin-treated group and that this could be attributed to occasional tropoelastin aggregation increasing the roughness of the luminal surface (Sugiura et al., 2017). On the contrary, some studies point that tropoelastin coated scaffolds inhibit intimal hyperplasia enhancing attachment and proliferation of endothelial cells and substantial reduction in platelet attachment (Wise et al., 2011; Kondyurina et al., 2017; Sugiura et al., 2017). Tropoelastin can be used to create electrospun vascular grafts and it seems that although tropoelastin retains its structural integrity mimicking the ECM and supporting cell growth, pure tropoelastin scaffolds lack of the sufficient tensile strength to be used as scaffolds for VGs (Wise et al., 2011; Hiob et al., 2017).

ELRs (or ELPs, depending their recombinant or chemical origin; Rodriguez-Cabello et al., 2017) are another large family of elastin-based materials that have been used to create VGs. In 2010, for example, Caves et al. published a study in which the procedure for manufacturing VGs from elastin-like proteins reinforced with collagen microfibers was described. This study showed how differences in fiber orientation, spacing and fraction affected the final physical and mechanical properties (burst pressure, compliance and suture retention) of the ELP-based VGs (Caves et al., 2010). ELRs alone have been used as biomaterials for electrospinning with the aim of forming an elastic and resistant mesh that can be used for tissue-engineering applications (Fernández-Colino et al., 2018; González de Torre et al., 2018) and, more specifically, for cardiovascular applications (Putzu et al., 2016, 2019). González de Torre et al. were the first to synthesize stable electrospun ELR fibers without the need for any additional crosslinking step after the electrospinning process. The scaffolds obtained showed a maximum percentage strain of 247.5 ± 36.08%, with a mean Young's modulus of 1.73 ± 0.95 MPa and excellent cytocompatibility in *in vitro* experiments. Similarly, Putzu et al. created tubular scaffolds from electrospun ELRs using a rotating mandrel as collector. The engineered VGs were formed by an inner layer mainly comprising ELRs containing REDV sequences (tetrapeptide specifically recognized by the integrin α4β1 present in endothelial cells) in order to selectively recruit endothelial precursor cells. The outer layers mainly comprised ERLs containing the general cell adhesion sequence RGD to induce the attachment of structural cells that could colonize the external part of the scaffold. The tubular scaffolds were cross-linked with 0.1% genipin/acetone solutions and subsequenty rinsed with PBS in order to eliminate any organic residues that could have cytotoxic effects (Putzu et al., 2016). In order to avoid the use of potentially cytotoxic crosslinking agents, the same group tried to electrospin a Silk-ELR copolymer containing amino acid sequences from silk (GAGAGS) and from elastin (VPGVG). This latter sequence was intended to provide elasticity and biocompatibility, while the silk sequence spontaneously self-assembled into β-sheets stabilized by hydrogen bonding. This combination was used to cover stents and catheter balloons to create fibrous scaffolds.

Recently, Fernandez-Colino et al. developed a small caliber multicomponent vascular substitute based on a combination of three components, namely a textile reinforcement, a macroporous ELR-based scaffold and an external layer of electrospun PCL. These multicomponent vascular grafts exhibited good mechanical properties in terms of burst pressure (up to 2,000 mmHg) and suture retention force (higher than 2.1 ± 1.4 N) while allowing an efficient transmission of pulsatile flow. The compliance of the grafts can be tuned by varying the thickness of the PLC layer. *In vitro*, these vascular substitutes promote the formation of an endothelial cell layer, which should increase the hemocompatibility of the grafts (Fernández-Colino et al., 2019) (**Figure 4**).

In 2015, Gonzalez de Torre et al. developed a system for hiding bare metal stents (BMS) from the immune system by embedding them in ELR-based hydrogels. The idea involved designing an endovascular device with high mechanical stability and physiological hemocompatibility that could act as a physical barrier for the atherosclerotic plaque. These devices were created by placing a BMS in an appropriate tubular mold and producing a chemically cross-linked hydrogel containing the stent by injecting a mixture of two different solutions containing complementary reacting ELRs. ELRs with different bioactivities (RGD, REDV and ELRs lacking any bioactive sequence) were used in order to evaluate the thrombogenicity and endothelization capacity of the finale ELR-biostents. The

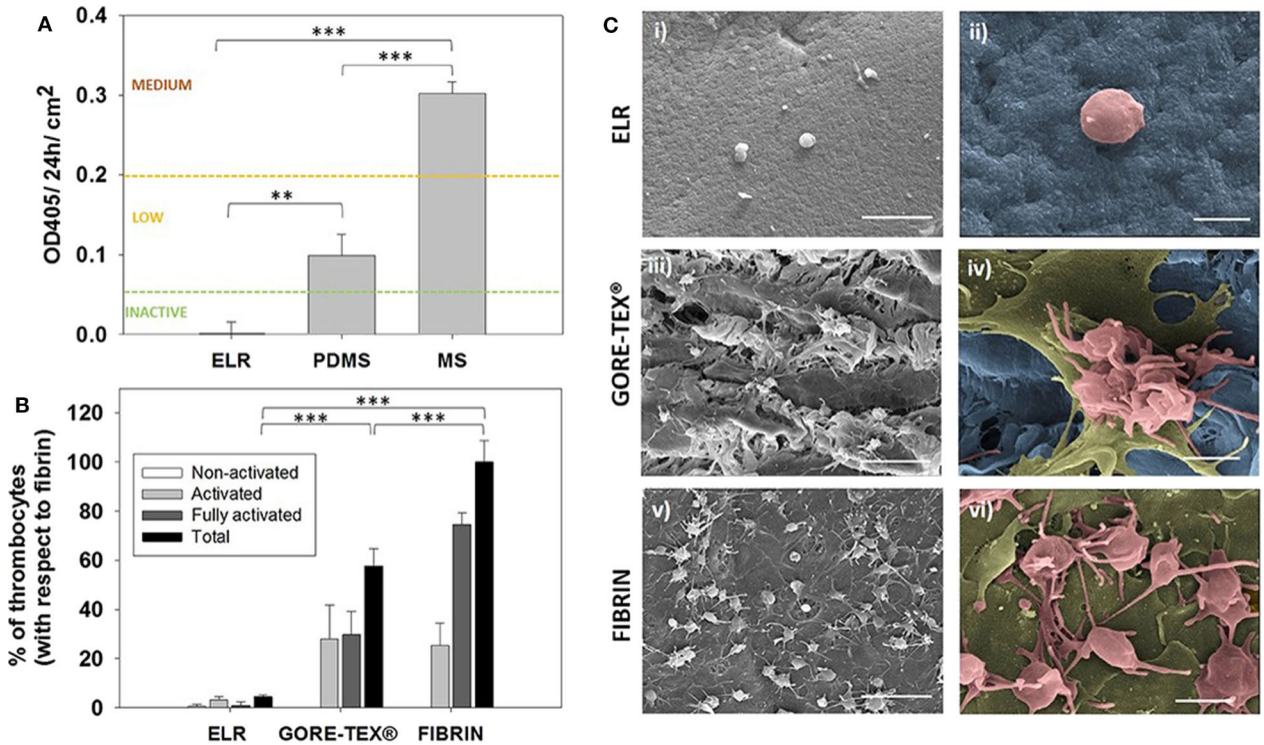

FIGURE 4 | Hemocompatibility assessment. **(A)** Hemocompatibility of ELR-gels assessed using the C5 complement convertase activity. Control materials used for comparison: medical steel (MS) and polydimethylsiloxane (PDMS). **(B)** Evaluation of adhered platelets based on SEM images. Results are plotted as the mean of three different experiments ± standard deviation. **(C)** SEM images of (i,ii) ELR hydrogel, (iii,iv) GORE-TEX®, and (v,vi) fibrin-gel after 1 h in contact with platelet rich plasma. Activated and fully activated platelets were covering fibrin and GORE-TEX® surfaces, while ELR surfaces presented minimal platelet adhesion. In the images ii, iv, and vi, the ELR and GORE-TEX® scaffolds were colored in blue, the platelets with a spread morphology in gold and the more rounded platelets in salmon. Scale bars: (i,iii,v): 10 μm; (ii,iv,vi) 2 μm. Reproduced with permission from Fernández-Colino et al. (2018). $^{**}p < 0.01$, $^{***}p < 0.001$.

lowest platelet adhesion and lowest endothelial cell recruiting capacity were obtained using ELRs lacking a bioactive sequence. ELR-biostents containing REDV and RGD sequences showed a very low platelet adhesion and a good ability to trigger the formation of a continuous endothelial cell layer on the lumen of the ELR-biostent (De Torre et al., 2015).

Fernandez-Colino et al. have continued the approach of covering stents with ELRs. In 2019, this group published a study in which they developed a coronary stent covered with ELRs using a clickable layer-by-layer (LbL) technique. These coated coronary stents were tested *in vitro* under simulated implantation conditions, demonstrating an excellent elastic performance of the ELR-based coating. Moreover, these devices proved to be mechanically stable under high-flow conditions *in vitro*. From a biological point of view, only minimal platelet adhesion/activation was observed after *in vitro* blood exposure in a Chandler loop. Human endothelial progenitor cells were able to form a continuous and confluent endothelial layer over the ELR membrane covering the coronary stent (**Figure 5**).

These latter two approaches based on covering BMS with ELRs seem to be promising alternatives for reducing the risk of re-stenosis and thrombosis after stent implantation and should be tested *in vivo* to confirm the potential non-inflammatory nature of the ELR-covered stents.

HEART VALVES

In the previous few pages we have reviewed the state-of-the-art as regards the tissue engineering approaches that are being explored by scientists for cardiac muscle and the vascular network that supplies it with nutrients and oxygen. However, the heart has another internal structure, namely heart valves (aortic and mitral valves), that is frequently affected by genetic malformations, stenosis or simply failure. Aortic stenosis (AS) is the most common type of aortic valve disease (AVD), with a prevalence of around 0.5% in the general population and 5% among people aged over 75 years. AS is a severe condition that reduces life expectancy to <10 years if untreated, with half of patients dying within only 2–3 years. Calcification of the aortic valve is characterized by fibro-calcific remodeling of the valve leaflets, which lose elasticity and mobility and leads, in severe cases, to blood obstruction. Currently available drugs are not effective at stopping or reverting the process of native aortic valve degeneration (Lindman et al., 2016; Baumgartner et al., 2017; Musumeci et al., 2018). As such, existing solutions are based on surgical repair, reconstruction and replacement. Since introduction of the first artificial aortic valve by Hufnagel et al. (1954), the field of prosthetic heart valves has experienced a continuous evolution, with improvement of the design and

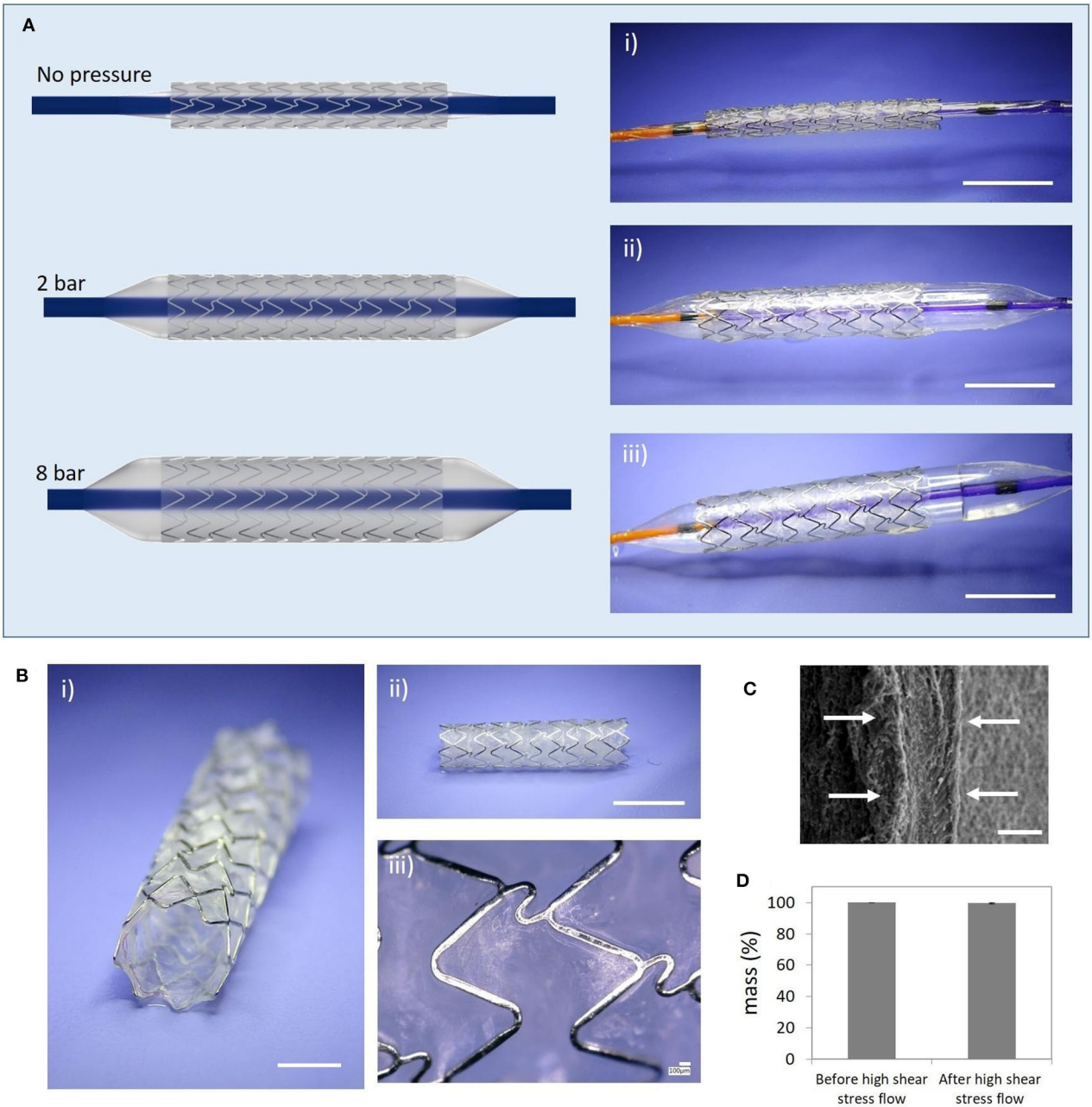

FIGURE 5 | Simulated *in vitro* ELR-covered stent delivery procedure and mechanical stability. **(A)** Balloon-expansion of the ELR-covered stent; (i) initial state before starting the expansion (stent diameter: 1.8 mm); (ii) intermediate state (balloon pressure 2 bar); (iii) final state (balloon pressure: 8 bar; stent diameter: 3.4 mm); **(B)** Deployed ELR-covered stent; (i) semi-frontal image; (ii) lateral image; (iii) detailed view of the ELR membrane; **(C)** SEM image showing the thickness of the layer (white arrows, ~30 μm); **(D)** Assessment of the dry-weight of the covered stent before and after high shear stress flow. Scale bars: **(A)** (i–iii) 5 mm; **(B)** (i) 2 mm, (ii) 5 mm, (iii) 100 μm; **(C)** 20 μm. Reproduced with permission from Fernández-Colino et al. (2019).

performance of both mechanical and biological and tissue-engineered heart valves. However, both kinds of prosthetic heart valve (mechanical and biological) have important drawbacks. Thus, although mechanical valves made from different materials (stainless steel, pyrolitic carbon, or ceramic) and with different architectures (caged-ball, monoleaflet, and bileaflet) were the most common type of implanted prosthesis for many years, the need for lifelong oral anticoagulation medication to prevent thrombus formation swiftly highlighted the need for biological prostheses (Arsalan and Walther, 2016; Søndergaard et al., 2018). Currently, some 87% of aortic valves that require replacement are substituted by bioprostheses, which are mainly obtained from

porcine and bovine tissue (Beckmann et al., 2015). As in the case of vascular grafts, one of the first approaches for obtaining bioscaffolds for the creation of heart valve bioprostheses was to decellularize natural heart valves from human donors or from animals (Tedder et al., 2009). The latter are the most widely used due to the high availability of these tissues compared with those from human donors. Similarly, several physical, chemical and biological techniques can be used to obtain acellular scaffolds (Crapo et al., 2011). Bioprostheses are hemodynamically superior to mechanical valves, and amongst biological valves, bovine ones seem to have better hemodynamic performance than porcine valves, thereby reducing the structural valve deterioration (SVD) that usually appears at around 10 years post-implantation (Fries et al., 2000; Lehmann et al., 2007, 2011; Yap et al., 2013). As noted above, although bioprostheses have some advantages with respect to mechanical valves, they are not exempt from problems. In addition to SVD, which is mainly caused by calcification in the commissural and basal areas of the cusps, tearing of the leaflets, calcific degeneration, endocarditis, pannus (abnormal thickening of the valve tissue, mainly in the cusps) and thrombus are the main complications after implantation of a bioprosthesis (Musumeci et al., 2018). The two leading acellular TEHVs available on the market, namely Cryolife's SynerGraft® and AutoTissue GmbH's Matrix P plus N™, both exhibit high variability as regards the results post-implantation and can provoke strong inflammatory responses, conduit failure, pseudoaneurysms, and allograft dissection, with the need for graft replacement, and a pulmonary artery pressure similar to native valves in healthy subjects (Simon et al., 2003; Brown et al., 2011; Perri et al., 2012; Voges et al., 2013). All these factors mean that these artificial valves do not match the behavior and durability of their natural counterparts, with a new valve replacement being necessary 10–15 years after the first prosthetic valve implantation (Yacoub and Takkenberg, 2005) (**Figure 6**).

A completely different approach involves building a new valve by combining a degradable biomaterial with cells to create a living implant. This tissue-engineering approach is currently being studied by several research groups to obtain functional heart valves that can undergo cell remodeling *in situ* and even grow (in the case of pediatric patients). The base concept of heart valve tissue engineering (HVTE) relies on degradable artificial heart valve shaped scaffolds that are able to evolve into viable living tissues with growth potential following a "normal" inflammatory response. This inflammatory response should start just after implantation of the scaffold and colonization by immune cells recruited from the blood stream, followed by the arrival of macrophages, lymphocytes, and progenitor cells from surrounding tissues, attracted by the cytokines secreted by the immune cells (Bouten et al., 2018). Finally, the scaffolds should be remodeled or even completely degraded by the cells while new endogenous extracellular matrix is produced, replacing the scaffold structure and producing a completely functional living heart valve.

Many biopolymers have been explored as biomaterials for TEHVs. These biopolymers can be classified into two main families: synthetic biopolymers and biological protein-based polymers. Synthetic biopolymers, such as PGA, PLA, PCL, and poly(4-hydroxybutyrate) (P4HB), offer the possibility to be tailored to provide precise control over the mechanical and chemical properties and degradation rate (Filová et al., 2009; Pérez et al., 2013). Some limitations of these synthetic biomaterials include their initial stiffness and rigidity, which could lead to stenosis of the implant. Inappropriate degradation rates (faster or slower than needed) can lead to structural incompetency or chronic inflammation, which produces fibrosis, respectively (Sodian et al., 2000; Ghanbari et al., 2009). Biomaterials based on biological polymers, mainly proteins, such as collagen and fibrin, have been extensively used to design and create TEHVs. Collagen is the most abundant component of the fibrosa layer of natural aortic valves and fibrinogen—a fibrin precursor—can be obtained from the patient's own blood and used to generate autologous, molded fibrin heart valves.

The mechanical properties of collagen-based TEHVs were explored by Shy et al. in a study in which a mixture of solubilized collagen and neonatal rat aortic smooth muscle cells (NRASMC) was used to create mitral heart valves and their chordae. Constructs were stimulated in a specially designed bioreactor and the failure stress values (200 kPa) recorded and compared with non-stimulated samples (100 kPa). Biological parameters, such as the collagen and DNA content of the samples pointed to an increase in extracellular matrix deposition in stimulated samples (Shi et al., 2005). In a similar study, Chen et al. examined the impact of the composition of the collagen-based scaffolds used for TEHVs by evaluating the microstructure and, biological and mechanical properties of scaffolds made from mixtures of collagen, elastin and gycosaminoglycans. Depending on the composition, the tensile, compressive, and bending moduliranged from 39.8 ± 8.8, 10.2 ± 1.6, and 25.4 ± 5.1 kPa to 344.6 ± 42.6, 28.3 ± 4.6, and 78.3 ± 9.7 kPa, respectively. The cytocompatibility of the scaffolds was evaluated by culturing cardiosphere-derived cells (CDCs), which are able to differentiate into cells of the three cardiac lineages and are derived from the endogenous stem cell population in adults. These cells showed good cell proliferation on the collagen-based scaffolds (Chen, 2012).

The research groups of Tranquillo and Jockenhoevel have focused their efforts on designing and producing fibrin-based heart valves, using different approaches to obtain TEHVs that mimic the behavior of their natural counterparts (Jockenhoevel et al., 2001; Weber et al., 2014; Reimer et al., 2017). These TEHVs are based on a tubular leaflet design that can eventually incorporate a textile reinforcement to increase the mechanical properties of the fibrin gels used as biomaterials. These approaches comprise the use of several types of cell sources, such as ovine dermal fibroblasts, vascular cells isolated from ovine umbilical arteries or human vascular cells, amongst others. The resulting fibrin-based TEHVs exhibited similar mechanical properties, with a modulus about 4 MPa and performances similar to the native versions (Moreira et al., 2016; Reimer et al., 2017). Although fibrin-based TEHVs showed excellent hemodynamic performance *in vitro* and *in vivo* (Reimer et al., 2015), most of them exhibited shrinkage of the leaflets, which produces regurgitation and leads to their failure (Flanagan et al., 2009; Gottlieb et al., 2010; Syedain et al., 2011; Driessen-Mol

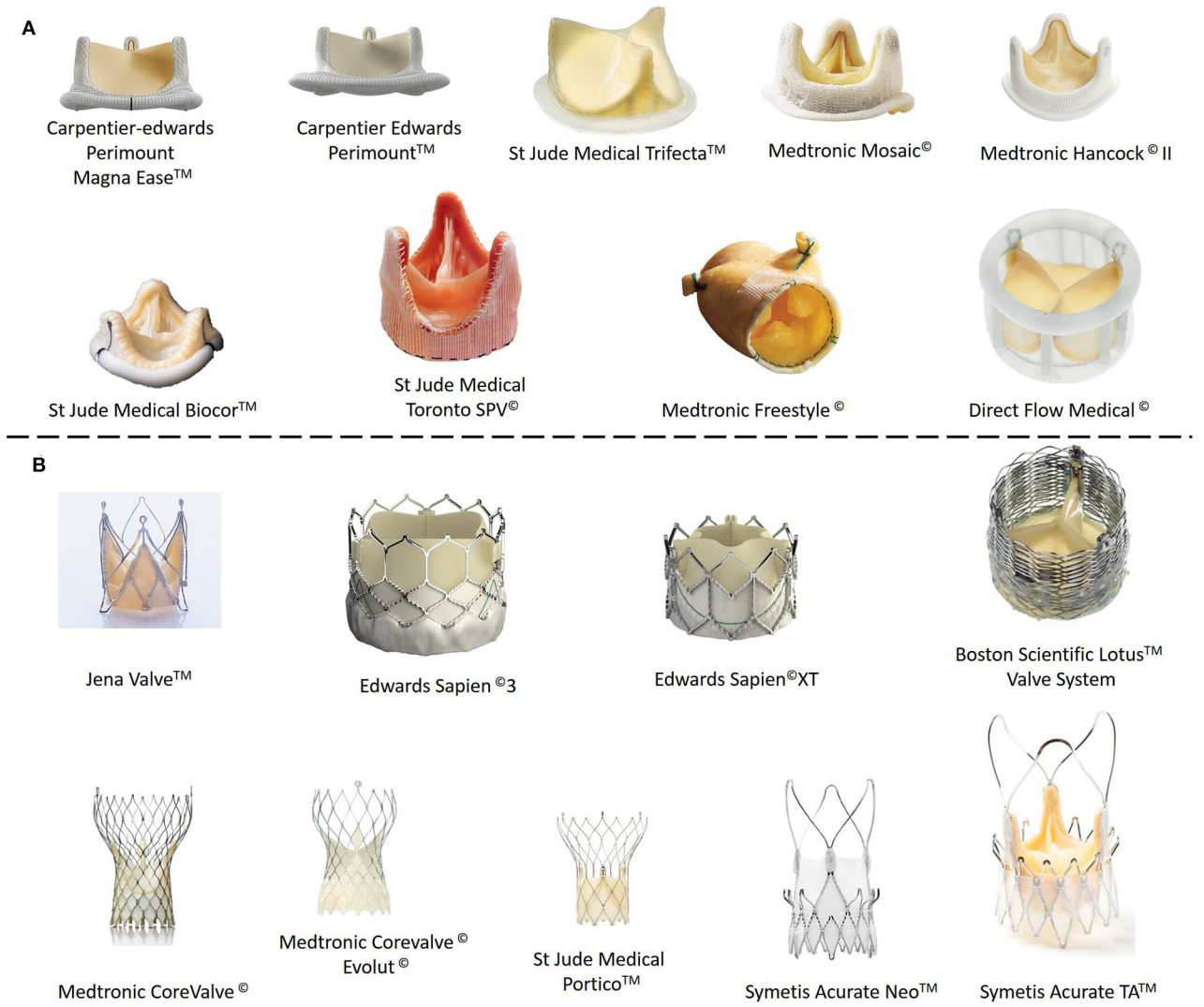

FIGURE 6 | Commercial biological (ovine or porcine tissue) heart valve prostheses. **(A)** Stentless prostheses. **(B)** Heart valve prostheses with stent support.

et al., 2014; Reimer et al., 2017). One of the main causes of this shortening of the leaflets is the very low production of elastin required to provide elasticity in the leaflets in order to complete coaptation of the leaflet and closure of the valve and avoid undesirable regurgitation events. Moreover, this low elastin production and high extracellular matrix secretion, mainly collagen, by the cells colonizing the scaffolds produces a stiffening of the leaflets, thus enhancing their shrinkage and leading to a non-functional TEHV. These findings suggest that the role of elastin in the proper performance of heart valves is crucial. The aortic valve cusp is a three-layered structure (fibrosa, ventricularis, and spongiosa) with different proportions of collagen and elastin but with an average of about 13% elastin in healthy adults. During diastolic loading, the cusps extend with a strain of more than 50%, then recoil elastically. As collagen is not a highly elastic protein, this elastic behavior must be due to the presence of elastin. Taking into account this low percentage of elastin and its high importance in the elasticity of the leaflets, it is clear that the arrangement of the elastin fibers and their interaction with collagen must play a paramount role. Scott and Vesely suggested an interaction between collagen and elastin that could explain the mechanical behavior of the leaflets in aortic valves. This mechanism proposes that elastin may act as a return spring by establishing connections between different collagen fibers or between different regions of the same collagen fiber. Once the collagen fibers are stretched, they take up a great proportion of the load. The elastin in the aortic valve then restores the geometry of the collagen fiber to its original conformation between successive loading cycles and, consequently, is essential for proper functioning of the valve (Scott and Vesely, 1995). This close interaction between collagen and elastin is reflected in the mechanical properties exhibited by heart valves (Vesely, 1997). The authors conclude by introducing the idea that any biomaterial intended to emulate

the micromechanisms of heart valves should take into account the close relationship between collagen and elastin.

To the best of our knowledge, there is no approach to building THEVs based exclusively on elastin or elastin-like biomaterials. Taking into account the findings regarding the composition of natural valves and the approaches based on collagen or fibrin mentioned above, it seems that the path to functional TEHVs is likely to involve the use of hybrid materials that combine the mechanical and biological properties of their individual components. In this sense, hybrid ELR-fibrin gels have been created and characterized mechanically and biologically. These ELR-FGs showed better mechanical properties than the pure fibrin gels used to create TEHVs as they combine the elastic properties of ELRs with the well-known cell-affinity of fibrin gels. Moreover, these ELR-FGs served as excellent materials to fabricate semilunar heart valves that could be colonized by ovine umbilical smooth muscle cells (OUSMCs). These cells were able to create their own extracellular matrix, forming collagen I and III as well as alpha-smooth muscle actin with some degree of alignment in TEHVs cultured *in vitro* for 21 days (Gonzalez De Torre et al., 2016). Following this hybrid ELR-FG based approach, Webber et al. developed TEHVs using a multi-step injection molding system, thus paving the way to the creation of TEHVs with a heterogeneous composition from a cell and scaffold material point of view. This system was intended to create TEHVs with different compositions for the walls and leaflets of the engineered valves without the need for suturing or gluing the different materials, thus ensuring that the leaflets are firmly attached to the wall of the TEHV. The functionality and integrity of the engineered valves were tested *in vitro*, with and without cells and with continuous stimulation for 2 weeks. Using this multi-step molding technique, different cell lines were embedded in different regions of the TEHVs and proliferated separately, generating their own ECM, which means that both the material arrangement and cell composition can be controlled and precisely placed in the desired region of the TEHV (**Figure 7**).

CONCLUSION AND FUTURE PERSPECTIVES

In light of the above, it can be deduced that elastin is a crucial component of the extracellular matrix in cardiovascular tissues, although it is not the major component in terms of dry weight. Despite its paramount role in cardiac tissues, biomaterials based on elastin or elastin-derived materials have mostly been used to create artificial vascular grafts. Elastin-derived materials have been processed, either alone or mixed with others, in several ways, including electrospinning and molding, to obtain artificial tubular constructs that can act as blood vessel substitutes. These different approaches have shown that elastin-derived biomaterials are non-thrombogenic and cell-friendly materials that are close to reaching preclinical and clinical stages after promising *in vivo* results. However, and although the research in ELRs started some decades ago, it can be seen that most of the studies and works in cardiovascular regeneration summarized in this review are from the last 5–10 years, a boom period in which we still are, and which is a short time for reaching preclinical or clinical trials.

Scaffolds for cardiac muscle regeneration is the second area of cardiovascular tissue engineering in which elastin-based materials have been applied. Recently, ELR-based scaffolds have started to gain importance as they can induce the rapid angiogenesis needed for cardiac muscle regeneration thanks to the introduction of angiogenic and specific protease sensitiveness. However, only a limited number of examples in which elastin-based scaffolds are used directly as cardiac patches can be found in the literature, and only a few of these have been applied *in vivo*.

Heart valves are the third big area explored in this review as regards cardiovascular tissue regeneration. As has been discussed, elastin plays a crucial role in the proper functioning of HVs and a lack therefore is possibly the main reason for shortening of the leaflets in TEHVs. Despite its obvious importance in this kind of structure, very few approaches have used biomaterials based on elastin or elastin-like materials.

It is worth pointing out that, under our knowledge, no clinical trials have been done with ELRs-based scaffolds for cardiac tissue regeneration although some preclinical test (Ibáñez-Fonseca et al., 2018) and patent based on ELRs have been registered (EP3124495A1; US9328154B2; WO/2010/092224; WO/2012/168532 and others). There are several reasons that could explain this fact but all of them fall under the speculation. The first one is the novelty of these biomaterials. It is important to understand that ELRs have gained importance in the last two decades, attending to the number of references that can be found in literature, and this is a short time for a biomaterial to reach clinical trials. The tailored design of these molecules is a double-edged sword, in one side it has enormous potential and benefits as for instance to design and precisely incorporate the desired bioactive sequences in the backbone of the polymer. However, in the other side, the possibility to create a huge variety of ELRs lead to another big challenge from the regulatory point of view. Many of the ELRs are more than mere polymeric materials without any bioactive property by themselves. They are more than scaffolds that offer support and mechanical properties; they can be designed to develop an active role during the regeneration process. This complexity in their design and functionality is transferred to regulatory aspects; actually, it is not easy to elucidate if these ELRs based materials should be classified as drugs, medical devices or even as advanced therapy medical products (if they are used with cells embedded).

Many improvements have been achieved in the field of tissue engineering for cardiovascular applications, including improvements in our understanding of the macro- and micromechanical performance of these tissues, improvements in the cell-ECM interaction and cell function, improvements in new biomaterials, improvements in processing technology, and *in vitro* experiments. However, unfortunately, these improvements are yet to produce a completely functional bioscaffold that could be implanted into patients and could mean actual regeneration of the damaged tissue. As such, there is still room for further improvements in the cardiovascular field, especially as regards

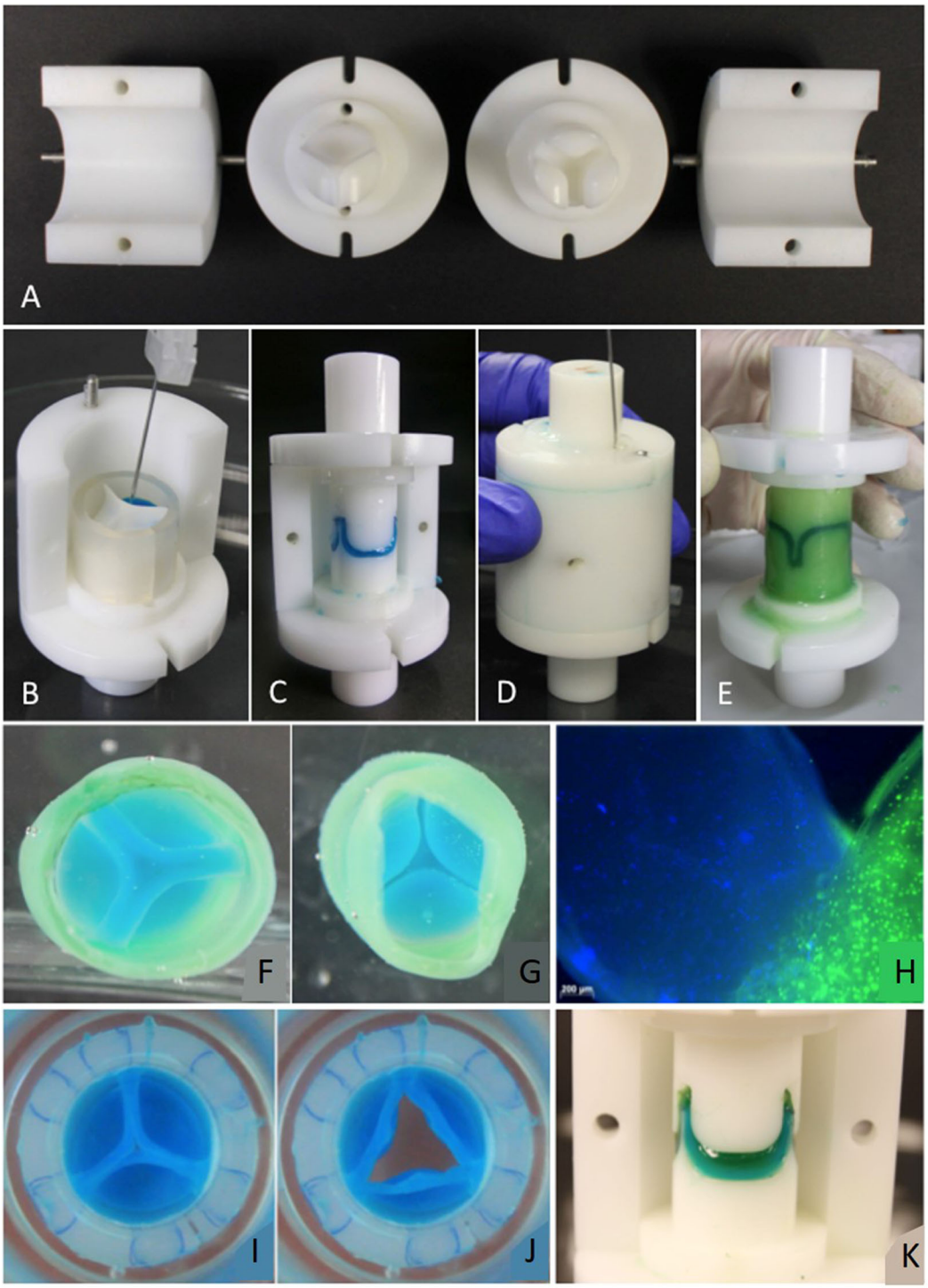

FIGURE 7 | (A) Mold parts: Ventricular and vascular stamp and shells. Molding procedure (Valve molded with colored fibrin gel to prove feasibility of molding design): **(B)** The components of the leaflets are inserted in the mold. **(C)** The leaflets are molded by placing the vascular stamp on top. Afterwards, the silicone ring is removed. **(D)** The components for the wall are inserted into the mold with a needle. **(E)** For demolding, the shells and then the stamps are removed carefully. **(F)** View from "vascular" side. **(G)** View from "ventricular" side. **(H)** Commissure area of a TEHV molded with live stained cells. The nuclei in the leaflet are stained blue with Hoechst 33258, the cytoplasm of cells in the valvular wall green with Calcein AM. **(I,J)** TEHV with leaflets made of an ELR-fibrin hybrid gel and the wall made of fibrin. **(K)** Leaflets made of two layers of fibrin (first layer blue, second layer green). Reproduced from Weber et al. (2014).

biomaterials, in which elastin-derived materials should become more important and attract the attention of research groups focused on cardiovascular tissue engineering.

AUTHOR CONTRIBUTIONS

IG has written the review. J-CR-C and MA have helped in reviewing the manuscript.

FUNDING

The authors were grateful for the funding from the Spanish Government (MAT2016-78903-R), Junta de Castilla y León (VA317P18), Interreg V A España Portugal POCTEP (0624_2IQBIONEURO_6_E), and Centro en Red de Medicina Regenerativa y Terapia Celular de Castilla y León.

REFERENCES

Allen, R. A., Wu, W., Yao, M., Dutta, D., Duan, X., Bachman, T. N., et al. (2014). Nerve regeneration and elastin formation within poly(glycerol sebacate)-based synthetic arterial grafts one-year post-implantation in a rat model. *Biomaterials* 35, 165–173. doi: 10.1016/j.biomaterials.2013.09.081

Almine, J. F., Bax, D. V., and Mithieux, S. M. (2010b). Elastin-based materials. *Chem. Soc. Rev.* 39, 3371–3379.

Almine, J. F., Bax, D. V., Mithieux, S. M., Nivison-Smith, L., Rnjak, J., Waterhouse, A., et al. (2010a). Elastin-based materials. *Chem. Soc. Rev.* 39:3371. doi: 10.1039/b919452p

Almine, J. F., Wise, S. G., and Weiss, A. S. (2012). Elastin signaling in wound repair. *Birth Defects Res. Part C Embryo Today Rev.* 96, 248–257. doi: 10.1002/bdrc.21016

Annabi, N., Tsang, K., Mithieux, S. M., Nikkhah, M., Ameri, A., Khademhosseini, A., et al. (2013). Highly elastic micropatterned hydrogel for engineering functional cardiac tissue. *Adv. Funct. Mater.* 23, 1–18. doi: 10.1002/adfm.201300570

Annabi, N., Zhang, Y.-N., Assmann, A., Sani, E. S., Cheng, G., Lassaletta, A. D., et al. (2017). Engineering a highly elastic human protein–based sealant for surgical applications. *Sci. Transl. Med.* 9:eaai7466. doi: 10.1126/scitranslmed.aai7466

Arsalan, M., and Walther, T. (2016). Durability of prostheses for transcatheter aortic valve implantation. *Nat. Rev. Cardiol.* 13, 360–367. doi: 10.1038/nrcardio.2016.43

Baumgartner, H., Falk, V., Bax, J. J., De Bonis, M., Hamm, C., Holm, P. J., et al. (2017). 2017 ESC/EACTS guidelines for the management of valvular heart disease. *Eur. Heart J.* 38, 2739–2786. doi: 10.1093/eurheartj/ehx391

Beckmann, A., Funkat, A. K., Lewandowski, J., Frie, M., Ernst, M., Hekmat, K., et al. (2015). Cardiac surgery in Germany during 2014: a report on behalf of the German society for thoracic and cardiovascular surgery. *Thorac. Cardiovasc. Surg.* 63, 258–269. doi: 10.1055/s-0034-1383430

Benjamin, E. J., Paul Muntner, C., Chair Alvaro Alonso, V., Marcio Bittencourt, F. S., Clifton Callaway, M. W., April Carson, F. P., et al. (2019). Heart disease and stroke statistics-−2019 update subcommittee. *Circulation* 139, 56–528. doi: 10.1161/CIR.0000000000000659

Benrashid, E., McCoy, C. C., Youngwirth, L. M., Kim, J., Manson, R. J., Otto, J. C., et al. (2016). Tissue engineered vascular grafts: origins, development, and current strategies for clinical application. *Methods* 99, 13–19. doi: 10.1016/j.ymeth.2015.07.014

Blakemore, A. H., Jaretzki, A., and Voorhees, A. B. (1952). The use of tubes constructed from vinyon "N" cloth in bridging arterial defects. *Ann. Surg.* 135, 332–336. doi: 10.1097/00000658-195203000-00006

Blakemore, A. H., and Voorhees, A. B. (1954). The use of tubes constructed from vinyon N cloth in bridging arterial defects; experimental and clinical. *Ann. Surg.* 140, 324–334. doi: 10.1097/00000658-195409000-00008

Bouten, C. V. C., Smits, A. I. P. M., and Baaijens, F. P. T. (2018). Can We Grow Valves Inside the Heart? perspective on material-based *in situ* heart valve tissue engineering. *Front. Cardiovasc. Med.* 5:54. doi: 10.3389/fcvm.2018.00054

Brescia, M. J., Cimino, J. E., Appel, K., and Hurwich, B. J. (1966). Chronic hemodialysis using venipuncture and a surgically created arteriovenous fistula. *N. Engl. J. Med.* 275, 1089–1092. doi: 10.1056/NEJM196611172752002

Brown, J. W., Ruzmetov, M., Eltayeb, O., Rodefeld, M. D., and Turrentine, M. W. (2011). Performance of synerGraft decellularized pulmonary homograft in patients undergoing a Ross procedure. *Ann. Thorac. Surg.* 91, 416–422. doi: 10.1016/j.athoracsur.2010.10.069

Brown-Augsburger, P., Broekelmann, T., Rosenbloom, J., and Mecham, R. P. (1996). Functional domains on elastin and microfibril-associated glycoprotein involved in elastic fibre assembly. *Biochem. J.* 318(Pt 1), 149–155. doi: 10.1042/bj.3180149

Brown-Augsburger, P., Broekelmann, T., Rosenbloom, J., and Mecham, R. P. (1997). Functional domains on elastin and microfibril-associated glycoprotein involved in elastic fibre assembly. *Biochem. J.* 323(Pt 1), 149–155. doi: 10.1042/bj3230863u

Brown-Augsburger, P., Tisdale, C., Broekelmann, T., Sloan, C., and Mecham, R. P. (1995). Identification of an elastin cross-linking domain that joins three peptide chains possible role in nucleated assembly. *J. Biol. Chem.* 270, 17778–17783. doi: 10.1074/jbc.270.30.17778

Buijtenhuijs, P., Buttafoco, L., Poot, A. A., Daamen, W. F., van Kuppevelt, T. H., Dijkstra, P. J., et al. (2004). Tissue engineering of blood vessels: characterization of smooth-muscle cells for culturing on collagen-and-elastin-based scaffolds. *Biotechnol. Appl. Biochem.* 39:141. doi: 10.1042/BA20030105

Buttafoco, L., Engbers-Buijtenhuijs, P., Poot, A. A., Dijkstra, P. J., Vermes, I., and Feijen, J. (2006a). Physical characterization of vascular grafts cultured in a bioreactor. *Biomaterials* 27, 2380–2389. doi: 10.1016/j.biomaterials.2005.10.017

Buttafoco, L., Kolkman, N. G., Engbers-Buijtenhuijs, P., Poot, A. A., Dijkstra, P. J., Vermes, I., et al. (2006b). Electrospinning of collagen and elastin for tissue engineering applications. *Biomaterials* 27, 724–734. doi: 10.1016/j.biomaterials.2005.06.024

Cai, L., Dinh, C. B., and Heilshorn, S. C. (2014). One-pot synthesis of elastin-like polypeptide hydrogels with grafted VEGF-mimetic peptides. *Biomater. Sci.* 2, 757–765. doi: 10.1039/C3BM60293A

Carmeliet, P., and Collen, D. (1997). Molecular analysis of blood vessel formation and disease. *Am. J. Physiol. Hear. Circ. Physiol.* 273, H2091–H2104. doi: 10.1152/ajpheart.1997.273.5.H2091

Caves, J. M., Kumar, V. A., Martinez, A. W., Kim, J., Ripberger, C. M., Haller, C. A., et al. (2010). The use of microfiber composites of elastin-like protein matrix reinforced with synthetic collagen in the design of vascular grafts. *Biomaterials* 31, 7175–7182. doi: 10.1016/j.biomaterials.2010.05.014

Chade, A. R., Tullos, N. A., Harvey, T. W., Mahdi, F., and Bidwell, G. L. (2016). Renal therapeutic angiogenesis using a bioengineered polymer-stabilized vascular endothelial growth factor construct. *J. Am. Soc. Nephrol.* 27, 1741–1752. doi: 10.1681/ASN.2015040346

Chen, Q. (2012). Collagen-based scaffolds for potential application of heart valve tissue engineering. *J. Tissue Sci. Eng.* S11, 1–6. doi: 10.4172/2157-7552.S11-003

Chilkoti, A., Christensen, T., and MacKay, J. A. (2006). Stimulus responsive elastin biopolymers: applications in medicine and biotechnology. *Curr. Opin. Chem. Biol.* 10, 652–657. doi: 10.1016/j.cbpa.2006.10.010

Chuang, T. H., Stabler, C., Simionescu, A., and Simionescu, D. T. (2009). Polyphenol-stabilized tubular elastin scaffolds for tissue engineered vascular grafts. *Tissue Eng. A* 15, 2837–2851. doi: 10.1089/ten.tea.2008.0394

Cipriani, F., Krüger, M., Gonzalez de Torre, I., Quintanilla Sierra, L., Alonso Rodrigo, M., Kock, L., et al. (2018). Cartilage regeneration in preannealed silk elastin-like co-recombinamers injectable hydrogel embedded with mature chondrocytes in an *ex vivo* culture platform. *Biomacromolecules* 19, 4333–4347. doi: 10.1021/acs.biomac.8b01211

Clarke, A. W., Arnspang, E. C., Mithieux, S. M., Korkmaz, E., Braet, F., and Weiss, A. S. (2006). Tropoelastin massively associates during coacervation to form quantized protein spheres. *Biochemistry*. 45, 9989–9996. doi: 10.1021/bi0610092

Crapo, P. M., Gilbert, T. W., and Badylak, S. F. (2011). An overview of tissue and whole organ decellularization processes. *Biomaterials* 32, 3233–3243. doi: 10.1016/j.biomaterials.2011.01.057

Crosby, C. O., and Zoldan, J. (2019). Mimicking the physical cues of the ECM in angiogenic biomaterials. *Regen. Biomater*. 6, 61–73. doi: 10.1093/rb/rbz003

Daamen, W. F., Veerkamp, J. H., van Hest, J. C. M., and van Kuppevelt, T. H. (2007). Elastin as a biomaterial for tissue engineering. *Biomaterials* 28, 4378–4398. doi: 10.1016/j.biomaterials.2007.06.025

D'Andrea, L. D., Iaccarino, G., Fattorusso, R., Sorriento, D., Carannante, C., Capasso, D., et al. (2005). Targeting angiogenesis: structural characterization and biological properties of a *de novo* engineered VEGF mimicking peptide. *Proc. Natl. Acad. Sci. U.S.A*. 102, 14215–14220. doi: 10.1073/pnas.0505047102

De Bakey, M. E., Cooley, D. A., Crawford, E. S., and Morris, G. C. (1958). Clinical application of a new flexible knitted dacron arterial substitute. *Am. Surg*. 24, 862–869. doi: 10.1001/archsurg.1958.01290040061008

De Torre, I. G., Wolf, F., Santos, M., Rongen, L., Alonso, M., Jockenhoevel, S., et al. (2015). Elastin-like recombinamer-covered stents: towards a fully biocompatible and non-thrombogenic device for cardiovascular diseases. *Acta Biomater*. 12, 146–155. doi: 10.1016/j.actbio.2014.10.029

Diana, D., Ziaco, B., Colombo, G., Scarabelli, G., Romanelli, A., Pedone, C., et al. (2008). Structural determinants of the unusual helix stability of a de novo engineered vascular endothelial growth factor (VEGF) mimicking peptide. *Chem. A Eur. J*. 14, 4164–4166. doi: 10.1002/chem.200800180

Driessen-Mol, A., Emmert, M. Y., Dijkman, P. E., Frese, L., Sanders, B., Weber, B., et al. (2014). Transcatheter implantation of homologous "Off-the-Shelf" tissue-engineered heart valves with self-repair capacity: long-term functionality and rapid *in vivo* remodeling in sheep. *J. Am. Coll. Cardiol*. 63, 1320–1329. doi: 10.1016/j.jacc.2013.09.082

Eng, G., Lee, B. W., Radisic, M., and Vunjak-Novakovic, G. (2016). "Cardiac tissue engineering," in *Tissue Engineering for Artificial Organs: Regenerative Medicine, Smart Diagnostics and Personalized Medicine*, eds R. Lanza, R. Langer, and J. Vacanti (San Diego, CA: Elsevier), 413–443. doi: 10.1002/9783527689934.ch13

Engbers-Buijtenhuijs, P., Buttafoco, L., Poot, A. A., Dijkstra, P. J., De Vos, R. A. I., Sterk, L. M. T., et al. (2006). Biological characterisation of vascular grafts cultured in a bioreactor. *Biomaterials*. 27, 2390–2397. doi: 10.1016/j.biomaterials.2005.10.016

Fernández-Colino, A., Wolf, F., Rütten, S., Rodríguez-Cabello, J. C., Jockenhoevel, S., and Mela, P. (2018). Combining catalyst-free click chemistry with coaxial electrospinning to obtain long-term, water-stable, bioactive elastin-like fibers for tissue engineering applications. *Macromol. Biosci*. 18, 1–7. doi: 10.1002/mabi.201800147

Fernández-Colino, A., Wolf, F., Rütten, S., Schmitz-Rode, T., Rodriguez-Cabello, J. C., Jockenhoevel, S., et al. (2019). Small caliber compliant vascular grafts based on elastin-like recombinamers for *in situ* tissue engineering. *Front. Bioeng. Biotechnol*. 7:340. doi: 10.3389/fbioe.2019.00340

Filová, E., Straka, F., Mirejovský, T., Mašín, J., and Bačáková, L. (2009). Tissue-engineered heart valves. *Physiol. Res.*

Flanagan, T. C., Sachweh, J. S., Frese, J., Schnoring, H., Gronloh, N., Koch, S., et al. (2009). *In vivo* remodeling and structural characterization of fibrin-based tissue-engineered heart valves in the adult sheep model. *Tissue Eng. A* 15, 2965–2976. doi: 10.1089/ten.tea.2009.0018

Flora, T., de Torre, I. G., Alonso, M., and Rodríguez-Cabello, J. C. (2019a). Tethering QK peptide to enhance angiogenesis in elastin-like recombinamer (ELR) hydrogels. *J. Mater. Sci. Mater. Med*. 30:30. doi: 10.1007/s10856-019-6232-z

Flora, T., de Torre, I. G., Quintanilla, L., Alonso, M., and Rodríguez-Cabello, J. C. (2018). Spatial control and cell adhesion selectivity on model gold surfaces grafted with elastin-like recombinamers. *Eur. Polym. J*. 106, 19–29. doi: 10.1016/j.eurpolymj.2018.06.026

Flora, T., González De Torre, I., Alonso, M., and Rodríguez-Cabello, J. C. (2019b). Use of proteolytic sequences with different cleavage kinetics as a way to generate hydrogels with preprogrammed cell-infiltration patterns imparted over their given 3D spatial structure. *Biofabrication* 11:035008. doi: 10.1088/1758-5090/ab10a5

Fornieri, C., Quaglino, D., and Mori, G. (1992). Role of the extracellular matrix in age-related modifications of the rat aorta–ultrastmctural, morphometric, and enzymatic evaluations. *Arterioscler. Thromb. Vasc. Biol*. 12, 1008–1016. doi: 10.1161/01.ATV.12.9.1008

Fries, R., Wendler, O., Schieffer, H., and Schäfers, H. J. (2000). Comparative rest and exercise hemodynamics of 23-mm stentless versus 23-mm stented aortic bioprostheses. *Ann. Thorac. Surg*. 69, 817–822. doi: 10.1016/S0003-4975(99)01409-5

Ghanbari, H., Viatge, H., Kidane, A. G., Burriesci, G., Tavakoli, M., and Seifalian, A. M. (2009). Polymeric heart valves: new materials, emerging hopes. *Trends Biotechnol*. 27, 359–367. doi: 10.1016/j.tibtech.2009.03.002

González de Torre, I., Ibáñez-Fonseca, A., Quintanilla, L., Alonso, M., and Rodríguez-Cabello, J. C. (2018). Random and oriented electrospun fibers based on a multicomponent, *in situ* clickable elastin-like recombinamer system for dermal tissue engineering. *Acta Biomater*. 72, 137–149. doi: 10.1016/j.actbio.2018.03.027

González De Torre, I., Santos, M., Quintanilla, L., Testera, A., Alonso, M., and Rodríguez Cabello, J. C. (2014). Elastin-like recombinamer catalyst-free click gels: characterization of poroelastic and intrinsic viscoelastic properties. *Acta Biomater*. 10, 2495–2505. doi: 10.1016/j.actbio.2014.02.006

Gonzalez De Torre, I., Weber, M., Quintanilla, L., Alonso, M., Jockenhoevel, S., Rodríguez Cabello, J. C., et al. (2016). Hybrid elastin-like recombinamer-fibrin gels: physical characterization and: *in vitro* evaluation for cardiovascular tissue engineering applications. *Biomater. Sci*. 4, 1361–1370. doi: 10.1039/C6BM00300A

Gottlieb, D., Kunal, T., Emani, S., Aikawa, E., Brown, D. W., Powell, A. J., et al. (2010). *In vivo* monitoring of function of autologous engineered pulmonary valve. *J. Thorac. Cardiovasc. Surg*. 139, 723–731. doi: 10.1016/j.jtcvs.2009.11.006

Heilshorn, S. C., DiZio, K. A., Welsh, E. R., and Tirrell, D. A. (2003). Endothelial cell adhesion to the fibronectin CS5 domain in artificial extracellular matrix proteins. *Biomaterials* 24, 4245–4252. doi: 10.1016/S0142-9612(03)00294-1

Hinderer, S., Shen, N., Ringuette, L. J., Hansmann, J., Reinhardt, D. P., Brucker, S. Y., et al. (2015). *In vitro* elastogenesis: instructing human vascular smooth muscle cells to generate an elastic fiber-containing extracellular matrix scaffold. *Biomed. Mater*. 10:034102. doi: 10.1088/1748-6041/10/3/034102

Hinek, A., and Rabinovitch, M. (1994). 67-kD elastin-binding protein is a protective "companion" of extracellular insoluble elastin and intracellular tropoelastin. *J. Cell Biol*. 126, 563–574. doi: 10.1083/jcb.126.2.563

Hiob, M. A., She, S., Muiznieks, L. D., and Weiss, A. S. (2017). Biomaterials and modifications in the development of small-diameter vascular grafts. *ACS Biomater. Sci. Eng*. 3, 712–723. doi: 10.1021/acsbiomaterials.6b00220

Huang, L., Nagapudi, K., Apkarian, P. R., and Chaikof, E. L. (2001). Engineered collagen–PEO nanofibers and fabrics. *J. Biomater. Sci. Polym. Ed*. 12, 979–993. doi: 10.1163/156856201753252516

Huang, S., Yang, Y., Yang, Q., Zhao, Q., and Ye, X. (2018). Engineered circulatory scaffolds for building cardiac tissue. *J. Thorac. Dis*. 10:S2312. doi: 10.21037/jtd.2017.12.92

Hufnagel, C. A., Harvey, W. P., Rabil, P. J., and Mcdermott, T. F. (1954). Surgical correction of aortic insufficiency. *Surgery* 35, 673–83.

Ibáñez-Fonseca, A., Ramos, T. L., González de Torre, I., Sánchez-Abarca, L. I., Muntión, S., Arias, F. J., et al. (2018). Biocompatibility of two model elastin-like recombinamer-based hydrogels formed through physical or chemical cross-linking for various applications in tissue engineering and regenerative medicine. *J. Tissue Eng. Regen. Med*. 12, e1450–e1460. doi: 10.1002/term.2562

Indik, Z., Yeh, H., Ornstein-Goldstein, N., Kucich, U., Abrams, W., Rosenbloom, J. C., et al. (1989). Structure of the elastin gene and alternative splicing of elastin mRNA: implications for human disease. *Am. J. Med. Genet*. 34, 81–90. doi: 10.1002/ajmg.1320340115

Jeltsch, M., Kaipainen, A., Joukov, V., Meng, X., Lakso, M., Rauvala, H., et al. (1997). Hyperplasia of lymphatic vessels in VEGF-C transgenic mice. *Science* 276, 1423–1425. doi: 10.1126/science.276.5317.1423

Jockenhoevel, S., Chalabi, K., Sachweh, J. S., Groesdonk, H. V., Demircan, L., Grossmann, M., et al. (2001). Tissue engineering: complete autologous valve conduit–a new moulding technique. *Thorac. Cardiovasc. Surg.* 49, 287–290. doi: 10.1055/s-2001-17807

Kannan, R. Y., Salacinski, H. J., Butler, P. E., Hamilton, G., and Seifalian, A. M. (2005). Current status of prosthetic bypass grafts: a review. *J. Biomed. Mater. Res. B Appl. Biomater*. 74, 570–581. doi: 10.1002/jbm.b.30247

Kielty, C. M., Sherratt, M. J., and Shuttleworth, C. A. (2002). Elastic fibres. *J. Cell Sci.* 115, 2817–2828. Available online at: https://jcs.biologists.org/content/joces/115/14/2817.full.pdf

Kondyurina, I., Wise, S. G., Y., Ngo, A. K., Filipe, E. C., Kondyurin, A., et al. (2017). Plasma mediated protein immobilisation enhances the vascular compatibility of polyurethane with tissue matched mechanical properties. *Biomed. Mater* 12:045002. doi: 10.1088/1748-605X/aa6eb6

Koobatian, M. T., Row, S., Smith, R. J., Koenigsknecht, C., Andreadis, S. T., and Swartz, D. D. (2016). Successful endothelialization and remodeling of a cell-free small-diameter arterial graft in a large animal model. *Biomaterials* 76, 344–358. doi: 10.1016/j.biomaterials.2015.10.020

Lee, K., Silva, E. A., and Mooney, D. J. (2011). Growth factor delivery-based tissue engineering: General approaches and a review of recent developments. *J. R. Soc. Interface* 8, 153–170. doi: 10.1098/rsif.2010.0223

Lehmann, S., Walther, T., Kempfert, J., Leontjev, S., Rastan, A., Falk, V., et al. (2007). Stentless versus conventional xenograft aortic valve replacement: midterm results of a prospectively randomized trial. *Ann. Thorac. Surg.* 84, 467–472. doi: 10.1016/j.athoracsur.2007.02.017

Lehmann, S., Walther, T., Kempfert, J., Leontyev, S., Bakhtiary, F., Rastan, A., et al. (2011). Ten-year follow up after prospectively randomized evaluation of stentless versus conventional xenograft aortic valve replacement. *J. Heart Valve Dis*. 20, 681–687. doi: 10.1055/s-0030-1268970

Leslie-Barbick, J. E., Saik, J. E., Gould, D. J., Dickinson, M. E., and West, J. L. (2011). The promotion of microvasculature formation in poly(ethylene glycol) diacrylate hydrogels by an immobilized VEGF-mimetic peptide. *Biomaterials* 32, 5782–5789. doi: 10.1016/j.biomaterials.2011.04.060

L'Heureux, N., Dusserre, N., Konig, G., Victor, B., Keire, P., Wight, T. N., et al. (2006). Human tissue-engineered blood vessels for adult arterial revascularization. *Nat. Med.* 12, 361–365. doi: 10.1038/nm1364

L'Heureux, N., McAllister, T. N., and De La Fuente, L. M. (2007). Tissue-engineered blood vessel for adult arterial revascularization [10]. *N. Engl. J. Med*. 357, 1451–1453. doi: 10.1056/NEJMc071536

Lindman, B. R., Clavel, M.-A., Mathieu, P., Iung, B., Lancellotti, P., Otto, C. M., et al. (2016). Calcific aortic stenosis. *Nat. Rev. Dis. Prim*. 2:16006. doi: 10.1038/nrdp.2016.6

Liu, R. H., Ong, C. S., Fukunishi, T., Ong, K., and Hibino, N. (2018). Review of vascular graft studies in large animal models. *Tissue Eng. B Rev*. 24, 133–143. doi: 10.1089/ten.teb.2017.0350

Martino, M. M., Briquez, P. S., Guc, E., Tortelli, F., Kilarski, W. W., Metzger, S., et al. (2014). Growth factors engineered for super-affinity to the extracellular matrix enhance tissue healing. *Science* 343, 885–888. doi: 10.1126/science.1247663

Martino, M. M., Brkic, S., Bovo, E., Burger, M., Schaefer, D. J., Wolff, T., et al. (2015). Extracellular matrix and growth factor engineering for controlled angiogenesis in regenerative medicine. *Front. Bioeng. Biotechnol.* 3:45. doi: 10.3389/fbioe.2015.00045

Massia, S. P., and Hubbell, J. A. (1992). Vascular endothelial cell adhesion and spreading promoted by the peptide REDV of the IIICS region of plasma fibronectin is mediated by integrin α4β1. *J. Biol. Chem.* 267, 14019–14026.

McKenna, K. A., Hinds, M. T., Sarao, R. C., Wu, P. C., Maslen, C. L., Glanville, R. W., et al. (2012). Mechanical property characterization of electrospun recombinant human tropoelastin for vascular graft biomaterials. *Acta Biomater*. 8, 225–233. doi: 10.1016/j.actbio.2011.08.001

Miriam, V., Daniel, A., Carvajal, B., Alexander, H., Laetitia, S., Dieter, P., Reinhardt, Ali, N., et al. (2013). Elastogenesis at the onset of human cardiac valve development. *Development* 140, 2345–2353. doi: 10.1242/dev.093500

Mithieux, S. M., Tu, Y., Korkmaz, E., Braet, F., and Weiss, A. S. (2009). *In situ* polymerization of tropoelastin in the absence of chemical cross-linking. *Biomaterials* 30, 431–435. doi: 10.1016/j.biomaterials.2008.10.018

Moreira, R., Neusser, C., Kruse, M., Mulderrig, S., Wolf, F., Spillner, J., et al. (2016). Tissue-engineered fibrin-based heart valve with bio-inspired textile reinforcement. *Adv. Healthc. Mater*. 5, 2113–2121. doi: 10.1002/adhm.201600300

Musumeci, L., Jacques, N., Hego, A., Nchimi, A., Lancellotti, P., and Oury, C. (2018). Prosthetic Aortic valves: challenges and solutions. *Front. Cardiovasc. Med*. 5:14. doi: 10.3389/fcvm.2018.00046

Pasotti, M., Prati, F., and Arbustini, E. (2006). The pathology of myocardial infarction in the pre- and post-interventional era. *Heart* 1552–1556. doi: 10.1136/hrt.2005.086934

Pérez, R. A., Won, J. E., Knowles, J. C., and Kim, H. W. (2013). Naturally and synthetic smart composite biomaterials for tissue regeneration. *Adv. Drug Deliv. Rev*. 65, 471–496. doi: 10.1016/j.addr.2012.03.009

Perri, G., Polito, A., Esposito, C., Albanese, S. B., Francalanci, P., Pongiglione, G., et al. (2012). Early and late failure of tissue-engineered pulmonary valve conduits used for right ventricular outflow tract reconstruction in patients with congenital heart disease. *Eur. J. Cardiothorac. Surg.* 41, 1320–1325. doi: 10.1093/ejcts/ezr221

Powell, J. T., Vine, N., and Crossman, M. (1992). On the accumulation of d-aspartate in elastin and other proteins of the ageing aorta. *Atherosclerosis* 97, 201–208. doi: 10.1016/0021-9150(92)90132-Z

Putzu, M., Causa, F., Nele, V., de Torre, I. G., Rodriguez-Cabello, J. C., and Netti, P. A. (2016). Elastin-like-recombinamers multilayered nanofibrous scaffolds for cardiovascular applications. *Biofabrication* 8:045009. doi: 10.1088/1758-5090/8/4/045009

Putzu, M., Causa, F., Parente, M., González de Torre, I., Rodriguez-Cabello, J. C., and Netti, P. A. (2019). Silk-ELR co-recombinamer covered stents obtained by electrospinning. *Regen. Biomater*. 6, 21–28. doi: 10.1093/rb/rby022

Reddel, C. J., Cultrone, D., Rnjak-Kovacina, J., Weiss, A. S., and Burgess, J. K. (2013). Tropoelastin modulates TGF-β1-induced expression of VEGF and CTGF in airway smooth muscle cells. *Matrix Biol*. 32, 407–413. doi: 10.1016/j.matbio.2013.04.003

Reimer, J., Syedain, Z., Haynie, B., Lahti, M., Berry, J., and Tranquillo, R. (2017). Implantation of a tissue-engineered tubular heart valve in growing lambs. *Ann. Biomed. Eng*. 45, 439–451. doi: 10.1007/s10439-016-1605-7

Reimer, J. M., Syedain, Z. H., Haynie, B. H. T., and Tranquillo, R. T. (2015). Pediatric tubular pulmonary heart valve from decellularized engineered tissue tubes. *Biomaterials* 62, 88–94. doi: 10.1016/j.biomaterials.2015.05.009

Robinet, A., Fahem, A., Cauchard, J. H., Huet, E., Vincent, L., Lorimier, S., et al. (2005). Elastin-derived peptides enhance angiogenesis by promoting endothelial cell migration and tubulogenesis through upregulation of MT1-MMP. *J. Cell Sci*. 118, 343–356. doi: 10.1242/jcs.01613

Rodriguez-Cabello, J. C., Ibáñez Fonseca, A., Alonso, M., Poocza, L., Cipriani, F., and González de Torre, I. (2017). "Elastin-like polymers: properties, synthesis, and applications," in *Encyclopedia of Polymer Science and Technology*, ed K. Matyjaszewski (Hoboken, NJ: John Wiley & Sons, Inc.), 1–36.

Rodríguez-Cabello, J. C., González de Torre, I., Ibañez-Fonseca, A., and Alonso, M. (2018b). Bioactive scaffolds based on elastin-like materials for wound healing. *Adv. Drug Deliv. Rev*. 129, 118–133. doi: 10.1016/j.addr.2018.03.003

Rodríguez-Cabello, J. C., de Torre, I. G., Acosta, S., Salinas, S., and Herrero, M. (2018a). "Elastin-like proteins: molecular design for self-assembling," in *Self-assembling Biomaterials*, eds H. S. Azevedo and R. M. P. da Silvaand (Cambridge, MA: Elsevier), 49–78.

Roy, S., Silacci, P., and Stergiopulos, N. (2005). Biomechanical proprieties of decellularized porcine common carotid arteries. *Am. J. Physiol. Hear. Circ. Physiol*. 289, H1567–H1576. doi: 10.1152/ajpheart.00564.2004

Ruvinov, E., Dvir, T., Leor, J., and Cohen, S. (2008). Myocardial repair: from salvage to tissue reconstruction. *Expert Rev. Cardiovasc. Ther*. 6, 669–686. doi: 10.1586/14779072.6.5.669

Ruvinov, E., Shandalov, Y., Levenberg, S., and Cohen, S. (2014). *Principles of Cardiovascular Tissue Engineering. 2nd Edn.* Cambridge, MA: Elsevier Inc.

Sacks, M. S., Schoen, F. J., and Mayer, J. E. (2009). Bioengineering challenges for heart valve tissue engineering. *Annu. Rev. Biomed. Eng.* 11, 289–313. doi: 10.1146/annurev-bioeng-061008-124903

Saleh, M., and Ambrose, J. A. (2018). Understanding myocardial infarction. *F1000Res.* 7:F1000 Faculty Rev-1378. doi: 10.12688/f1000research.15096.1

Salerno, A., and Netti, P. A. (2014). Introduction to biomedical foams. *Woodh. Publish. Limit.* 2014, 3–39. doi: 10.1533/9780857097033.1.3

Scott, M., and Vesely, I. (1995). Aortic valve cusp microstructure: the role of elastin. *Ann. Thorac. Surg*. 60, S391–S394. doi: 10.1016/0003-4975(95)00263-K

Seandel, M., Noack-Kunnmann, K., Zhu, D., Aimes, R. T., and Quigley, J. P. (2001). Growth factor-induced angiogenesis *in vivo* requires specific cleavage of fibrillar type I collagen. *Blood* 97, 2323–2332. doi: 10.1182/blood.V97.8.2323

Seliktar, D., and Shapira-Schweitzer, K. (2010). *Biomaterials and Devices for the Circulatory System*, (Cambridge).

Shalaby, F., Janet, R., Yamaguchi, T. P., Gertsenstein, M., Wu, X. F., Breitman, M. L., et al. (1995). Failure of blood-island formation and vasculogenesis in Flk-1-deficient mice. *Nature* 376, 62–66. doi: 10.1038/376062a0

Shi, Y., Iyer, R., Soundararajan, A., Dobkin, D., and Vesely, I. (2005). Collagen-based tissue engineering as applied to heart valves. *Conf. Proc. IEEE Eng. Med. Biol. Soc.* 2005, 4912–4915. doi: 10.1109/IEMBS.2005.1615574

Simon, P., Kasimir, M. T., Seebacher, G., Weigel, G., Ullrich, R., Salzer-Muhar, U., et al. (2003). Early failure of the tissue engineered porcine heart valve SYNERGRAFTTM in pediatric patients. *Eur. J. Cardiothorac. Surg.* 23, 1002–1006. doi: 10.1016/S1010-7940(03)00094-0

Sodian, R., Hoerstrup, S. P., Sperling, J. S., Daebritz, S., Martin, D. P., Moran, A. M., et al. (2000). Early *in vivo* experience with tissue-engineered trileaflet heart valves. *Circulation* 102, III22–III29. doi: 10.1161/01.CIR.102.suppl_3.III-22

Søndergaard, L., Saraste, A., Christersson, C., and Vahanian, A. (2018). The year in cardiology 2017: valvular heart disease. *Eur. Heart J*. 39, 650–657. doi: 10.1093/eurheartj/ehx772

Staubli, S. M., Cerino, G., Gonzalez De Torre, I., Alonso, M., Oertli, D., Eckstein, F., et al. (2017). Control of angiogenesis and host response by modulating the cell adhesion properties of an elastin-like recombinamer-based hydrogel. *Biomaterials* 135, 30–41. doi: 10.1016/j.biomaterials.2017.04.047

Stitzel, J., Liu, J., Lee, S. J., Komura, M., Berry, J., Soker, S., et al. (2006). Controlled fabrication of a biological vascular substitute. *Biomaterials* 27, 1088–1094. doi: 10.1016/j.biomaterials.2005.07.048

Straky, K. S., and Heilshorn, S. C. (2009). Dynamic, 3D-pattern formation within enzyme-responsive hydrogels. *Adv. Mater*. 21, 4148–4152. doi: 10.1002/adma.200990152

Stroncek, J. D., and Reichert, W. M. (2008). "Overview of wound healing in different tissue types," in *Indwelling Neural Implants: Strategies for Contending With the in vivo Environment*, ed W. M. Reichert (Boca Raton, FL: CRC Press; Taylor & FrancisTaylor & Francis Group, LLC), 3–38.

Sugiura, T., Agarwal, R., Tara, S., Yi, T., Lee, Y. U., Breuer, C. K., et al. (2017). Tropoelastin inhibits intimal hyperplasia of mouse bioresorbable arterial vascular grafts. *Acta Biomater*. 52, 74–80. doi: 10.1016/j.actbio.2016.12.044

Syedain, Z. H., Lahti, M. T., Johnson, S. L., Robinson, P. S., Ruth, G. R., Bianco, R. W., et al. (2011). Implantation of a tissue-engineered heart valve from human fibroblasts exhibiting short term function in the sheep pulmonary artery. *Cardiovasc. Eng. Technol*. 2, 101–112. doi: 10.1007/s13239-011-0039-5

Syedain, Z. H., Meier, L. A., Lahti, M. T., Johnson, S. L., and Tranquillo, R. T. (2014). Implantation of completely biological engineered grafts following decellularization into the sheep femoral artery. *Tissue Eng. A* 20, 1726–1734. doi: 10.1089/ten.tea.2013.0550

Tamburro, A. M., Bochicchio, B., and Pepe, A. (2003). Dissection of human tropoelastin: exon-by-exon chemical synthesis and related conformational studies. *Biochemistry* 42, 13347–13362. doi: 10.1021/bi034837t

Tamburro, A. M., Guantieri, V., and Gordini, D. D. (1992). Synthesis and structural studies of a pentapeptide sequence of elastin. poly (Val-Gly-Gly-Leu-Gly). *J. Biomol. Struct. Dyn*. 10, 441–454. doi: 10.1080/07391102.1992.10508661

Tamburro, A. M., Guantieri, V., Pandolfo, L., and Scopa, A. (1990). Synthetic fragments and analogues of elastin. II. Conformational studies. *Biopolymers* 29, 855–870. doi: 10.1002/bip.360290419

Tedder, M. E., Liao, J., Weed, B., Stabler, C., Zhang, H., Simionescu, A., et al. (2009). Stabilized collagen scaffolds for heart valve tissue engineering. *Tissue Eng. A* 15, 1257–1268. doi: 10.1089/ten.tea.2008.0263

Testa, U., Pannitteri, G., and Condorelli, G. L. (2008). Vascular endothelial growth factors in cardiovascular medicine. *J. Cardiovasc. Med*. 9, 1190–1221. doi: 10.2459/JCM.0b013e3283117d37

Tillman, B. W., Yazdani, S. K., Neff, L. P., Corriere, M. A., Christ, G. J., Soker, S., et al. (2012). Bioengineered vascular access maintains structural integrity in response to arteriovenous flow and repeated needle puncture. *J. Vasc. Surg*. 56, 783–793. doi: 10.1016/j.jvs.2012.02.030

Trappmann, B., Baker, B. M., Polacheck, W. J., Choi, C. K., Burdick, J. A., and Chen, C. S. (2017). Matrix degradability controls multicellularity of 3D cell migration. *Nat. Commun*. 8:371. doi: 10.1038/s41467-017-00418-6

Uitto, V.-J., and Larjava, H. (1991). Extracellular matrix molecules and their receptors: an overview with special emphasis on periodontal tissues. *Crit. Rev. Oral Biol. Med*. 2, 323–354. doi: 10.1177/10454411910020030301

Urry, D. (1997). Physical chemistry of biological free energy transduction as demonstrated by elastic protein-based polymers. *J. Phys. Chem. B* 101, 11007–11028. doi: 10.1021/jp972167t

Urry, D. W. (1993). Molecular machines–how motion and other functions of living organisms can result from reversible chemical-changes. *Angew. Chemie Int. Ed. Eng*. 32, 819–841. doi: 10.1002/anie.199308191

Urry, D. W., Gowda, D. C., Parker, T. M., Luan, C. H., Reid, M. C., Harris, C. M., et al. (1992). Hydrophobicity scale for proteins based on inverse temperature transitions. *Biopolymers* 32, 1243–1250. doi: 10.1002/bip.360320913

Urry, D. W. (2006). *What Sustains Life? Consilient Mechanisms for Protein-Based Machines and Materials*. Berlin; Heidelberg: Springer.

Vale, P. R., Losordo, D. W., Symes, J. F., and Isner, J. M. (2001). Growth factors for therapeutic angiogenesis in cardiovascular diseases. *Rev. Esp. Cardiol*. 54, 1210–1224. doi: 10.1016/S0300-8932(01)76480-9

van Wachem, P. B., van Luyn, M. J., Olde Damink, L. H., Dijkstra, P. J., Feijen, J., and Nieuwenhuis, P. (1994). Biocompatibility and tissue regenerating capacity of crosslinked dermal sheep collagen. *J. Biomed. Mater. Res*. 28, 353–363. doi: 10.1002/jbm.820280310

Vesely, I. (1997). The role of elastin in aortic valve mechanics. *J. Biomech*. 31, 115–123. doi: 10.1016/S0021-9290(97)00122-X

Vindin, H., Mithieux, S. M., and Weiss, A. S. (2019). Elastin architecture. *Matrix Biol*. 84, 4–16. doi: 10.1016/j.matbio.2019.07.005

Voges, I., Bräsen, J. H., Entenmann, A., Scheid, M., Scheewe, J., Fischer, G., et al. (2013). Adverse results of a decellularized tissue-engineered pulmonary valve in humans assessed with magnetic resonance imaging. *Eur. J. Cardiothorac. Surg*. 44, e272–e279. doi: 10.1093/ejcts/ezt328

Vrhovski, B., and Weiss, A. S. (1998). Biochemistry of tropoelastin. *Eur. J. Biochem*. 258, 1–18. doi: 10.1046/j.1432-1327.1998.2580001.x

Wang, X., Lin, P., Yao, Q., and Chen, C. (2007). Development of small-diameter vascular grafts. *World J. Surg*. 682–689. doi: 10.1007/s00268-006-0731-z

Wang, Z., Mithieux, S. M., and Weiss, A. S. (2019). Fabrication techniques for vascular and vascularized tissue engineering. *Adv. Healthc. Mater*. 8:1900742. doi: 10.1002/adhm.201900742

Weber, M., Heta, E., Moreira, R., Gesche, V. N., Schermer, T., Frese, J., et al. (2014). Tissue-engineered fibrin-based heart valve with a tubular leaflet design. *Tissue Eng. C Methods* 20, 265–275. doi: 10.1089/ten.tec.2013.0258

Weinberg, C. B., and Bell, E. (1986). A blood vessel model constructed from collagen and cultured vascular cells. *Science* 231, 397–400. doi: 10.1126/science.2934816

Williams, D. (1999). *The Williams Dictionary of Biomaterials*. Liverpool University Press, 342–342. doi: 10.5949/UPO9781846314438

Wise, S. G., Byrom, M. J., Waterhouse, A., Bannon, P. G., Ng, M. K. C., and Weiss, A. S. (2011). A multilayered synthetic human elastin/polycaprolactone hybrid vascular graft with tailored mechanical properties. *Acta Biomater*. 7, 295–303. doi: 10.1016/j.actbio.2010.07.022

Wise, S. G., and Weiss, A. S. (2009). Tropoelastin. *Int. J. Biochem. Cell Biol*. 41, 494–497. doi: 10.1016/j.biocel.2008.03.017

Won, J. I., and Barron, A. E. (2002). A new cloning method for the preparation of long repetitive polypeptides without a sequence requirement. *Macromolecules* 35, 8281–8287. doi: 10.1021/ma020892i

Wystrychowski, W., McAllister, T. N., Zagalski, K., Dusserre, N., Cierpka, L., and L'Heureux, N. (2014). First human use of an allogeneic tissue-engineered vascular graft for hemodialysis access. *J. Vasc. Surg*. 60, 1353–1357. doi: 10.1016/j.jvs.2013.08.018

Yacoub, M. H., and Takkenberg, J. J. M. (2005). Will heart valve tissue engineering change the world? *Nat. Clin. Pract. Cardiovasc. Med*. 2, 60–61. doi: 10.1038/ncpcardio0112

Yap, K. H., Murphy, R., Devbhandari, M., and Venkateswaran, R. (2013). Aortic valve replacement: Is porcine or bovine valve better? *Interact. Cardiovasc. Thorac. Surg*. 16, 361–373. doi: 10.1093/icvts/ivs447

Zandonella, C. (2003). The beat goes on. *Nature* 421, 884–886. doi: 10.1038/421884a

Zhang, J., Zhu, W., Radisic, M., and Vunjak-Novakovic, G. (2018). Can we engineer a human cardiac patch for therapy? *Circ. Res*. 123, 244–265. doi: 10.1161/CIRCRESAHA.118.311213

Conflict of Interest: The authors declare that the research was conducted in the absence of any commercial or financial relationships that could be construed as a potential conflict of interest.

Copyright © 2020 Gonzalez de Torre, Alonso and Rodriguez-Cabello. This is an open-access article distributed under the terms of the Creative Commons Attribution License (CC BY). The use, distribution or reproduction in other forums is permitted, provided the original author(s) and the copyright owner(s) are credited and that the original publication in this journal is cited, in accordance with accepted academic practice. No use, distribution or reproduction is permitted which does not comply with these terms.

frontiers in Bioengineering and Biotechnology

ORIGINAL RESEARCH
published: 14 July 2020
doi: 10.3389/fbioe.2020.00733

Bioreactor Platform for Biomimetic Culture and *in situ* Monitoring of the Mechanical Response of *in vitro* Engineered Models of Cardiac Tissue

Diana Massai[1,2†], Giuseppe Pisani[1,3,4†], Giuseppe Isu[1,3,4], Andres Rodriguez Ruiz[1], Giulia Cerino[3,4], Renato Galluzzi[5], Alessia Pisanu[3,4], Andrea Tonoli[5], Cristina Bignardi[1,2], Alberto L. Audenino[1,2], Anna Marsano[3,4†] and Umberto Morbiducci[1,2†]*

[1] PolitoBIOMed Lab, , Department of Mechanical and Aerospace Engineering, Politecnico di Torino, Turin, Italy, [2] Interuniversity Center for the Promotion of the 3Rs Principles in Teaching and Research, Turin, Italy, [3] Department of Surgery, University Hospital of Basel, Basel, Switzerland, [4] Department of Biomedicine, University of Basel, Basel, Switzerland, [5] Department of Mechanical and Aerospace Engineering, Politecnico di Torino, Turin, Italy

OPEN ACCESS

Edited by:
Paolo Madeddu,
University of Bristol, United Kingdom

Reviewed by:
Bojana Obradovic,
University of Belgrade, Serbia
Arghya Paul,
The University of Western Ontario, Canada

***Correspondence:**
Diana Massai
diana.massai@polito.it

† These authors have contributed equally to this work

Specialty section:
This article was submitted to Tissue Engineering and Regenerative Medicine, a section of the journal Frontiers in Bioengineering and Biotechnology

Received: 07 January 2020
Accepted: 10 June 2020
Published: 14 July 2020

Citation:
Massai D, Pisani G, Isu G, Rodriguez Ruiz A, Cerino G, Galluzzi R, Pisanu A, Tonoli A, Bignardi C, Audenino AL, Marsano A and Morbiducci U (2020) Bioreactor Platform for Biomimetic Culture and in situ Monitoring of the Mechanical Response of in vitro Engineered Models of Cardiac Tissue. Front. Bioeng. Biotechnol. 8:733. doi: 10.3389/fbioe.2020.00733

In the past two decades, relevant advances have been made in the generation of engineered cardiac constructs to be used as functional *in vitro* models for cardiac research or drug testing, and with the ultimate but still challenging goal of repairing the damaged myocardium. To support cardiac tissue generation and maturation *in vitro*, the application of biomimetic physical stimuli within dedicated bioreactors is crucial. In particular, cardiac-like mechanical stimulation has been demonstrated to promote development and maturation of cardiac tissue models. Here, we developed an automated bioreactor platform for tunable cyclic stretch and *in situ* monitoring of the mechanical response of *in vitro* engineered cardiac tissues. To demonstrate the bioreactor platform performance and to investigate the effects of cyclic stretch on construct maturation and contractility, we developed 3D annular cardiac tissue models based on neonatal rat cardiac cells embedded in fibrin hydrogel. The constructs were statically pre-cultured for 5 days and then exposed to 4 days of uniaxial cyclic stretch (sinusoidal waveform, 10% strain, 1 Hz) within the bioreactor. Explanatory biological tests showed that cyclic stretch promoted cardiomyocyte alignment, maintenance, and maturation, with enhanced expression of typical mature cardiac markers compared to static controls. Moreover, *in situ* monitoring showed increasing passive force of the constructs along the dynamic culture. Finally, only the stretched constructs were responsive to external electrical pacing with synchronous and regular contractile activity, further confirming that cyclic stretching was instrumental for their functional maturation. This study shows that the proposed bioreactor platform is a reliable device for cyclic stretch culture and *in situ* monitoring of the passive mechanical response of the cultured constructs. The innovative feature of acquiring passive force measurements *in situ* and along the culture allows monitoring the construct maturation trend without interrupting the culture, making the proposed device a powerful tool for *in vitro* investigation and ultimately production of functional engineered cardiac constructs.

Keywords: bioreactor, mechanical stimulation, *in situ* monitoring, engineered cardiac tissues, cardiac tissue maturation, cardiac tissue engineering

INTRODUCTION

The native myocardium is a complex tissue composed of an anisotropic network of elongated, tightly interconnected cardiomyocytes (CMs) and cardiac fibroblasts (FBs) embedded in a collagen-rich extracellular matrix (ECM) with a dense supporting vasculature. Defined pacemaker cells and electrically coupled CMs are responsible for the coordinated and cyclic wringing contraction of the heart. Myocardial infarction can cause irreversible damage to the myocardium; indeed, its inability to regenerate together with consequent cardiac fibrosis and irreversible ventricular remodeling can significantly impair heart function over time (Murtha et al., 2017). In the past two decades, relevant advances have been made in the development of three-dimensional (3D) engineered cardiac tissues (ECTs) aimed to recapitulate the structural and functional properties of the native myocardium (Eschenhagen and Zimmermann, 2005; Ye et al., 2013; Zimmermann, 2013; Hirt et al., 2014b; Ogle et al., 2016; Fujita and Zimmermann, 2017; Weinberger et al., 2017). Although these approaches still did not attain complete functionality and immunosafety suitable for clinical translation, ECTs are widely used as *in vitro* models for basic cardiac research (Engelmayr et al., 2008; Tiburcy et al., 2011), for drug screening (El-Armouche et al., 2007; Hansen et al., 2010; Schaaf et al., 2011; Vunjak-Novakovic et al., 2014; Mannhardt et al., 2016; Marsano et al., 2016), and for investigating cardiac disease (de Lange et al., 2011; Hirt et al., 2012; Occhetta et al., 2018; Chen and Vunjak-Novakovic, 2019; Mytsyk et al., 2019), with the ultimate but still challenging goal to act as functional substitutes for replacement of damaged myocardium (Zimmermann and Eschenhagen, 2003; Zimmermann et al., 2006; Lesman et al., 2010; Menasché et al., 2015; Riegler et al., 2015; Weinberger et al., 2016; Miyagawa et al., 2017; Tiburcy et al., 2017; Frati et al., 2019; Belviso et al., 2020).

Successful strategies for the *in vitro* generation of functional ECTs require a synergistic combination of appropriate cells, scaffolds, and cardiac-like biochemical and biophysical signals (Bilodeau and Mantovani, 2006; Vunjak-Novakovic et al., 2010). In particular, it has been demonstrated that providing biomimetic mechanical stimulation within dedicated bioreactors promotes growth, maturation, and contractile function of ECTs together with the development of a myocardium-like anisotropic architecture (Massai et al., 2013; Liaw and Zimmermann, 2016; Parsa et al., 2016; Stoppel et al., 2016). In several studies, phasic mechanical stretch (isotonic load) was delivered to ECTs for mimicking the cyclic diastolic filling of the ventricles, leading to morphological and phenotypic changes, referred to as hypertrophy, accompanied by improved cell proliferation, organized matrix formation, and enhanced contractile performance (Fink et al., 2000; Akhyari et al., 2002; Zimmermann et al., 2002; Naito et al., 2006; Birla et al., 2007; Tulloch et al., 2011; Salazar et al., 2015). However, due to the absence of *in situ* monitoring, in these approaches ECTs were transferred to dedicated measurement devices to characterize their mechanical response. This made force measurements mainly used as end-point analyses, without a continuous characterization of the stage-specific maturation of the constructs. In parallel works, ECTs were suspended between load-adjustable mounts or flexible posts for mimicking the native auxotonic contractions against the hydrostatic pressure of the circulation (Zimmermann, 2013; Hirt et al., 2014a; Liaw and Zimmermann, 2016). Under auxotonic load, ECTs progressively induced the deflection of the posts by gradually adapting and increasing their contraction force, with consequent structural and functional tissue maturation (Zimmermann et al., 2006; Hansen et al., 2010; Schaaf et al., 2011; Boudou et al., 2012; Mannhardt et al., 2016; Tiburcy et al., 2017). This approach enabled culturing miniaturized ECTs in modular platforms designed for simultaneous individual control of culture environment and for automatic video-optical evaluation of contractile activity, crucial features in the perspective of automated high-throughput analyses for drug screening (Hansen et al., 2010; Schaaf et al., 2011; Mannhardt et al., 2016). Despite these advantages, auxotonic load requires long culture periods for tissue adaptation. Furthermore, flexible posts do not allow to either control the mechanical load imposed to the ECTs or adapt the load to the construct maturation stage, so that muscle training or pathological stimulation regimes cannot be applied (Liaw and Zimmermann, 2016).

In order to overcome these limitations and being inspired by the challenge to adapt the mechanical conditioning to the actual maturation stage of the cultured constructs, we developed an automated bioreactor platform for tunable cyclic stretch culture and *in situ* non-destructive monitoring of the passive mechanical response of the cultured ECTs (Pisani, 2016). To demonstrate the bioreactor platform performance and to investigate the impact that cyclic stretch has on maturation and contractility of engineered models of cardiac tissue, we produced 3D annular constructs based on neonatal rat CMs and FBs embedded in fibrin hydrogel (Bian et al., 2009; Black et al., 2009; Hansen et al., 2010). The hydrogel technique was adopted since it allows to define the ECT shape by using customized casting molds and to support cell spreading and connections throughout the constructs (Hirt et al., 2014b). Fibrin hydrogel was selected since it is easy to pour, tunable in stiffness, and FDA-approved (Jockenhoevel et al., 2001). Fibrin-based ECTs were subjected to controlled cyclic stretch within the proposed bioreactor platform, and their mechanical response was *in situ* monitored along the culture. The effect of cyclic stretch conditioning was analyzed in terms of cell organization, cardiac marker expression, collagen content, mechanical properties, and electrical functionality.

MATERIALS AND METHODS

Bioreactor Platform Design and Working Principle

Design Requirements

Specific requirements guided the design phase. The bioreactor platform should provide tunable uniaxial cyclic stretch in the range of physiological and pathological stimuli experienced by human cardiac tissue *in vivo* (strain = 5–100%, frequency = 1–4 Hz; Kuznetsova et al., 2008). Furthermore, the device should enable *in situ* monitoring of the passive mechanical response

of the cultured constructs, using non-destructive methods. Modularity and customization requirements came from the need to guarantee versatility of the device, intended to be used with multiple and different constructs and for several cell/tissue applications. For Good Laboratory Practice (GLP) compliance, the bioreactor platform should be easy to use and to clean with standard tools and techniques commonly available in a cell biology laboratory, and the culture chamber components should be cytocompatible and autoclavable. In addition, the bioreactor platform should have an overall size suitable to be assembled under laminar flow hood and placed on a standard incubator shelf (40 cm × 30 cm × 40 cm).

Design, Components, and Working Principle

In order to accomplish all the abovementioned requirements, the proposed bioreactor platform consists of (1) a culture unit, for housing the constructs; (2) a monitoring unit, for *in situ* monitoring of culture environment and construct mechanical response; (3) a stimulation unit, for providing tunable uniaxial cyclic stretch; and (4) a control unit, for controlling the stimulation, acquiring and recording the sensor signals, and guaranteeing communications from and to the user (**Figure 1A**). In detail, the culture unit is composed of a polycarbonate culture chamber (140 mm × 80 mm × 75 mm with a priming volume of ∼100 ml, **Figure 1B**), in which interchangeable polyoxymethylene (POM) sample holders, designed for ring- or patch-shaped constructs (**Supplementary Figure 1**), can be mounted (**Figure 1C**). One sample holder is coupled to an AISI 316L stainless-steel through-shaft, externally connected to the motor, while the other sample holder is fixed and mounted on an AISI 316L stainless-steel through-shaft, externally connected to a load cell. This setup allows connection of the ECTs to the motor on one side and the force sensor on the other, while silicone bellows (J-Flex rubber, United Kingdom) fitted on the internal side of both through-shafts assure watertightness and sterility maintenance of the culture chamber. The polycarbonate lid, screwed on the vessel and sealed by a silicone O-ring, can accommodate up to four immersed sensors and is equipped with one medium sampling/replacement port and one air filter. A central optical access allows for the visual inspection of the constructs during culture (**Figure 1D**). The monitoring unit can include pH (InLab Ultra-Micro sensor, Mettler Toledo, Switzerland) and dissolved oxygen (MI-730 Micro-Oxygen Electrode, Microelectrodes Inc., United States) sensors inserted in the lid and a load cell with a 10-N full scale (XFTC300, Measurement Specialties TE Connectivity, United States) connected to the fixed holder through-shaft for *in situ* non-destructive monitoring of the mechanical response of the constructs (**Figure 1D**). The stimulation unit is based on a linear voice coil motor (GVCM-051-064-01, Moticont, United States), which is connected by a through-shaft to one sample holder and provides sinusoidal uniaxial cyclic stretch with strain values in the range of 5–100% for constructs of 2–15-mm length, with a stimulation frequency range of 1–6 Hz. A contactless linear position transducer (ONP1-A, Gefran, IT) is located under the motor to measure its displacement. An aluminum/POM chassis houses the culture chamber, the monitoring unit, and the stimulation unit (**Figure 1B**) to be placed within a standard cell culture incubator (37°C, 5% CO_2, and 90% humidity). The control unit is composed of a laptop, with a purpose-built software, and hardware components contained in a customized control box. In detail, the CompactRIO-9075 real-time controller (National Instruments, United States) was selected to drive the monitoring and control of the bioreactor. The motor is controlled by a feedback-loop strategy based on the position transducer and a drive motion module (NI 9505 Full H-Bridge, National Instruments, United States). A numerical lumped-element model (MATLAB & Simulink, MathWorks, United States) of the control loop of the motor was developed and supported the tuning of the stimulation unit control (see details in **Supplementary Material**). A signal conditioner (ARD154, Measurement Specialties TE Connectivity, United States) amplifies the signal of the load cell and increases measurement resolution, improving the signal-to-noise ratio. The analog signals collected from the position transducer, the sensors, and the load cell are processed and digitalized by the NI 9219 acquisition module (National Instruments, United States). Finally, a user-friendly software interface, developed using the LabView® graphical system design platform (National Instruments, United States), allows the user to set the mechanical stimulation parameters (displacement mode, displacement value, frequency), to be guided during the sensor calibration protocols, and to monitor and save the data collected from the monitoring unit (**Supplementary Figure 2**). The bioreactor components were designed using the commercial computer-aided design (CAD) software SolidWorks (Dassault Systemes, France). Working prototypes of the sample holders were 3D printed (Stratasys uPrint SE Plus, Stratasys, United States) to test their functionality and ease of use. The final bioreactor components were manufactured by computer-controlled milling and drilling. Cytocompatible and autoclavable materials were selected for all components in contact with medium or constructs.

Bioreactor Testing

Preliminary tests on the whole bioreactor platform were performed for assessing ease of assembling, watertightness, functionality, and reliability. The 3D-printed prototypes of the sample holders were tested in-house in terms of coupling with the culture chamber components, and their holding performance was verified using silicone samples. Concerning the monitoring unit, calibration protocols were defined for both the sensors and the load cell, which was then characterized (see details in **Supplementary Material**). Ease of use, functionality, and reliability of the bioreactor were preliminarily tested in a cell culture laboratory. Laboratory operators assembled the bioreactor under hood, filled it with culture medium, placed it in incubator, and ran explanatory cyclic stimulation tests (10% strain, 1 Hz frequency) without constructs for 1–2 weeks.

ECT Preparation and Culture

Annular silicone molds (external diameter = 16 mm, internal diameter = 10 mm, height = 3 mm, with a volume of approximately 400 μL) were manufactured for ECT casting.

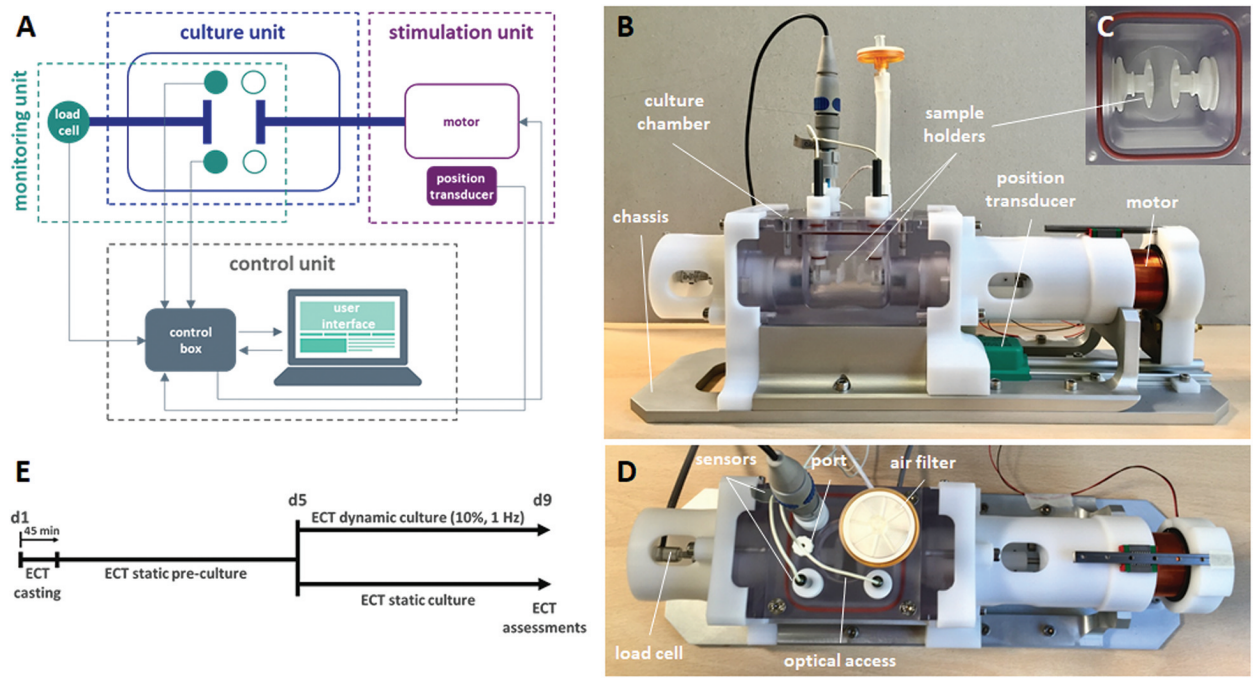

FIGURE 1 | Bioreactor platform and experimental plan. **(A)** Scheme of the connections among the bioreactor units: culture, stimulation, monitoring, and control units. **(B)** Lateral view of the bioreactor platform showing the chassis, the culture chamber, the sample holders, the position transducer, and the motor. **(C)** Top view of the sample holders within the culture chamber. **(D)** Top view of the bioreactor platform showing the load cell and, on the culture chamber lid, the sensors, the medium sampling/replacement port, the air filter, and the optical access. **(E)** Experimental plan of the ECT culture, showing the static pre-culture time up to day 5 (d5) and the following culture in either dynamic or static condition up to day 9 (d9).

In each mold, a solution of 10 μL of thrombin (2.5 U/mL final, or 0.1 U/mL thrombin solution per mg fibrinogen, Sigma-Aldrich, United States) (Hansen et al., 2010; Morgan and Black, 2014), 23 μL of aprotinin (3000 KIU/mL, Sigma-Aldrich, United States) (Centola et al., 2013), and 116 μL of $CaCl_2$ (40 mM, Sigma-Aldrich, United States) (Cholewinski et al., 2009) was injected. In parallel, freshly isolated neonatal rat cardiac cells (circa 80% CMs and 20% FBs) were isolated as previously described from 2–3-day-old Sprague Dawley rat hearts (Radisic et al., 2008), according to the Swiss Federal guidelines for animal welfare, and all procedures were approved by the Veterinary Office of the Canton Basel (Basel, Switzerland). Cardiac cells were suspended at a density of 18×10^6 cells/mL (Vunjak-Novakovic et al., 2010) in 150 μL of high-glucose (4.5 g/L) Dulbecco's Modified Eagle Medium (DMEM, Gibco, United States) supplemented with 1% fetal bovine serum (FBS, HyClone, United States), 1% penicillin/streptomycin (Sigma-Aldrich, United States), 1% L-glutamine (Sigma-Aldrich, United States), and 1% HEPES (Sigma-Aldrich, United States) and mixed with 100 μL of fibrinogen (25 mg/mL, Sigma-Aldrich, United States). Fibrin hydrogels were obtained by pouring the cell-fibrinogen solution within each mold already containing the thrombin solution. After 45 min in incubator at 37°C for complete hydrogel polymerization, the annular ECTs were removed from the molds, placed into a 6-well plate with 4-mL/well culture medium, and pre-cultured in incubator at 37°C and 5% CO_2 for 5 days under static conditions (Zimmermann et al., 2000). Thereafter, ECTs were transferred into the bioreactor culture chamber and subjected to unidirectional cyclic stretch (sinusoidal waveform, 10% strain, 1 Hz) for an additional 4 days. As control experiment, ECTs were cultured statically for the entire duration of 9 days (**Figure 1E**). The culture medium, changed twice a week, consisted of low-glucose (1 g/L) DMEM, supplemented with 10% FBS, 1% penicillin/streptomycin, 1% L-glutamine, and 1% HEPES. At day 3, tranexamic acid (tAMCA, Sigma-Aldrich, United States) at a concentration of 160 g/mL was added to each well to delay fibrin hydrogel degradation (Cholewinski et al., 2009).

ECT Assessments

Histology and Immunofluorescence Staining and CM Orientation Analysis

Cell distribution and tissue development and organization were evaluated by hematoxylin and eosin (H&E, Biosystems, Switzerland) staining on sample slices. Each construct was cut into two halves, and each part was fixed for 1 h in 1.5% paraformaldehyde (Sigma-Aldrich, United States), followed by an overnight treatment with 30% sucrose solution (Sigma-Aldrich, United States). Only the straight parts of the constructs (aligned to the stretch) were embedded in optimal cutting temperature compound (OCT, CellPath, United Kingdom) and successively cut in the longitudinal (parallel to the stretch)

direction. Sections of 12 μm in thickness were cut in the cryostat by a microtome (Microm International GmbH, Germany) and stained with H&E according to standard protocols. Images were acquired with the Olympus BX63 microscope (Olympus, Japan). The most relevant cardiac markers, such as sarcomeric α-actinin, cardiac troponin I (cTnI), and connexin 43 (Cx43), were investigated by immunofluorescence analysis. The presence of cardiac FBs and cell proliferation were assessed by using anti-Vimentin and anti-ki67 antibodies, respectively. In detail, sections were incubated for 1 h in 0.3% Triton X-100 (Sigma-Aldrich, United States) and 2% normal goat/donkey serum (Sigma-Aldrich, United States) in PBS and successively for 1 h with the following primary antibodies: mouse monoclonal anti-sarcomeric α-actinin (Abcam, United Kingdom) at 1:400; mouse monoclonal anti-cardiac troponin I (Abcam, United Kingdom) at 1:100; rabbit polyclonal anti-Connexin 43 (Millipore, United States) at 1:100; goat polyclonal anti-Vimentin (Abcam, United Kingdom) at 1:100; and rabbit polyclonal anti-Ki67 (Abcam, United Kingdom) at 1:100. Sections were then incubated in the dark for 1 h with fluorescently labeled Alexa 488 and Alexa 647 anti-mouse and anti-rabbit antibodies (Invitrogen, United States) or Alexa 488, Alexa 546, and Alexa 647 anti-mouse, anti-rabbit, and anti-goat secondary antibodies (Invitrogen, United States) at 1:200. Nuclei were stained using 4′,6-diamidino-2-phenylindole (DAPI, Invitrogen, United States) at 1:50 for 1 h. Antibodies were diluted in 0.3% Triton X-100 and 2% normal goat/donkey serum in PBS. Images were taken by using an LSM-710 confocal microscope (ZEISS, Switzerland). The immunofluorescence staining images of statically (n = 3 biological samples) and dynamically (n = 4 biological samples) cultured ECTs collected at day 9 were then analyzed for quantifying the CM orientation. In detail, for each experimental group at least 5 immunofluorescence staining images of 3–5 constructs (from at least two independent experiments) were acquired using a 20X objective lens with the Olympus BX63 microscope (Olympus, Japan) and were analyzed using ImageJ software (NIH, United States). Cardiomyocyte orientation was quantified by calculating the angle between the primary axis of each troponin-positive cell and the x-axis of the image, corresponding to the direction of stimulation and considering the CMs aligned when the angle ranged angle ranged from 0° to 45° or from 135° to 180°. A two-way ANOVA statistical test was performed ($p < 0.05$). All data were represented as mean ± standard deviation.

DNA and Collagen Quantifications

To assess the amount of cells, DNA was quantified by CyQUANT® Cell Proliferation Assay (Invitrogen, United States). Statically cultured constructs and straight parts of the dynamically cultured constructs were weighed and digested overnight at 57°C in 500 μL of proteinase K solution (1 mg/mL proteinase K, 50 mM TRIS, 1 mM EDTA, 1 mM iodoacetamide, and 10 mg/mL pepstatin-A; Sigma-Aldrich, United States) in double-distilled water or potassium phosphate buffer (Sadr et al., 2012). Working solutions were prepared according to the manufacturer's protocols. Fluorescence was measured by a SpectraMax Gemini XS Microplate Spectrofluorometer (Molecular Devices, United States), with excitation and emission wavelengths equal to 485 and 583 nm, respectively. Each sample was measured in triplicate. The quantification of the ECT collagen content was carried out by hydroxyproline assay. After digestion in proteinase K (the same used for DNA quantification), samples were mixed with 12 M HCl, hydrolyzed at 120°C for 24 h, and then dried (Cigan et al., 2013). Subsequently, samples were mixed with 50 μL buffered chloramine T reagent (63.5 mg of chloramine T dissolved in 1 mL water, and then diluted with 1.5 mL n-propanol and 2.5 mL acetate–citrate buffer (pH 6); made fresh daily) and incubated for 20 min at room temperature. Further, 50 μL of dimethylaminobenzaldehyde (DMAB) solution mixed with perchloric acid were added (0.45 DMAB in 2 mL n-propanol and 1 mL perchloric acid 20%). The mass ratio of hydroxyproline to collagen was assumed equal to 1:10. The mixture was heated at 60°C for 20 min and cooled, and the absorbance determined at 550 nm. The hydroxyproline concentration was determined from a standard curve (stock solution of hydroxyproline: 1 mg/mL) (Hofman et al., 2011). The total amount of collagen was also normalized by the corresponding wet weight (ww) of the sample.

Mechanical Characterization

During the cyclic stretch culture, the bioreactor load cell was used at day 5 (start of the bioreactor culture) and day 9 (end of the bioreactor culture) for *in situ* measurement of the ECT mechanical response. The constructs were then collected from the bioreactor and hooked within a standard tensile testing machine (MicroBionix system, MTS Systems Corporation, United States), using a 2-N load cell. For both the bioreactor and the testing machine force measurements, (1) ECTs were pre-tensioned at an initial load of 0.02 N; (2) using a digital caliper, the initial length L_0 between the two hooks was measured and the cross-sectional areas A_1 and A_2 of the two straight parts of the constructs were estimated; and (3) a series of 10 cycles (0–10% strain based on L_0, 1 Hz) was performed. Force measurements were converted in engineering stress σ, defined as

$$\sigma = \frac{F}{(A_1 + A_2)}$$

where F is the recorded force.

Stress *vs.* time curves generated from bioreactor and testing machine measurements at days 5 and 9 were compared in terms of peak-to-peak stress amplitude. The stiffness of the constructs, measured in terms of linear elastic modulus (E), was calculated from the testing machine data as the slope of the engineering stress–strain curves at increasing physiologic levels of strain (from 0 up to 30%). Moreover, imposing a ramp rate of 5 mm/min, ECTs were stretched until failure to assess the ultimate tensile strength (UTS, i.e., the maximum stress that the constructs can withstand before failure).

Electrical Functionality

ECT spontaneous beating and contractile activity upon external electrical pacing were monitored at days 5 and 9. A bright-field microscope IX81 (Olympus, Japan) at 2X/4X magnification was used, and images of specimen were captured. In detail,

to evaluate the response to external pacing under controlled temperature of 37°C, each construct was placed within a Petri dish, filled with 5 mL of medium, in between two carbon rod electrodes connected to a custom-built electrical stimulator (Tandon et al., 2009). Electrical pacing (rectangular pulses, 2-ms duration) was applied at a rate of 1 Hz starting with a 1-V/cm electric field amplitude. The excitation threshold (ET), defined as the minimum electric field amplitude at which constructs are observed to beat synchronously, and the maximum capture rate (MCR), defined as the maximum pacing frequency for synchronous contraction using an electric field amplitude of two times the ET, were determined (Radisic et al., 2004). With the adopted microscope magnification levels, it was not possible to record the image of the entire construct while pacing. To overcome this limitation, different randomly sampled regions of the constructs (from 3 to 4, depending on the specimen) were image-recorded and analyzed. Once the image acquisition system was focused on the region of interest, the electric field amplitude was increased by single steps of 0.5 V/cm until the ET was reached. The MCR was determined imposing the electric field amplitude set at two times the ET and increasing the stimulation frequency by steps of 0.1 Hz, until the paced contractions became irregular or desisted at all. To assess the regularity and the frequency of contraction under external pacing, a video analysis of the constructs was performed using a customized image-processing algorithm. Each stimulation sequence was image-recorded [frames per second (fps) set in the range 20–40], and image frames were analyzed with ImageJ 1.47 software (NIH, United States). To assess the capability of the ECTs to follow synchronously the imposed pacing, the center of mass of the image-recorded construct portion was identified and its displacement with respect to its position in a reference frame was calculated and tracked (see details in **Supplementary Material**).

Statistical Analysis

Statistical analysis was performed with GraphPad Prism software (GraphPad Software, Inc., United States). All data are presented as mean ± standard deviation. The one-way ANOVA multiple-comparison test was used to compare two different groups. In the figures, statistical significance is denoted as * for p-value ≤ 0.05, ** for p-value ≤ 0.01, *** for p-value ≤ 0.001, and **** for p-value ≤ 0.0001.

RESULTS

Bioreactor Testing

Preliminary tests confirmed the bioreactor platform performance in terms of ease of assembling, watertightness, functionality, and reliability. In detail, the coupling and assembling/disassembling procedures of the mechanical components did not present any critical warnings, and the correct alignment of the culture unit, stimulation unit, and monitoring unit components was verified. Once assembled, the structural and electrical functionality of the bioreactor units was tested using the control unit user interface. In particular, the stimulation unit was tested in terms of accuracy and reliability, showing regular frequency and small oscillations in peak amplitude with no detectable drift from the imposed working parameters, while characterization tests confirmed the functionality of the load cell (see details in **Supplementary Material**). Thereafter, the bioreactor platform was preliminarily tested in a cell culture laboratory. The assembling procedure under laminar flow hood was easy and fast. Explanatory cyclic stimulation tests run for 1–2 weeks in incubator confirmed watertightness and sterility maintenance of the culture chamber.

ECT Assessments

Remodeling, Histology, and Collagen/DNA Content

The initial size of the ECTs was reproducible, but ECT shrinking was observed along the culture. In particular, the cross section of the constructs changed from an initial square shape with an estimated area equal to 5.2 ± 1.1 mm^2 at day 1 to a circular shape with an estimated area equal to 4.0 ± 0.4 mm^2 at day 5, and equal to 1.5 ± 0.7 mm^2 and 0.9 ± 0.2 mm^2 for static and dynamic culture at day 9, respectively (**Figure 2**). Representative images of the constructs stained for H&E at day 1 revealed that cells were homogeneously distributed within ECTs (**Figure 3A**). Concerning cell morphology, cells encapsulated within the fibrin hydrogel appeared round-shaped at day 1, and after 5 days of static pre-culture no appreciable differences in cell distribution and shape were observed (**Figure 3B**). At day 9, ECTs cultured under static conditions presented mostly round-shaped cells, sparsely distributed (**Figure 3C**). Differently, an increased cell density at the borders (at 50–200 μm from the edge) was observed in dynamically cultured ECTs, with the majority of the cells presenting an elongated morphology aligned with the construct edge, corresponding to the imposed stretch direction (**Figure 3D**). The amount of DNA was similar in the ECTs after 1 and 5 days; however, following 4 additional days, either in static or dynamic conditions the amount of DNA was reduced (**Figure 3E**). Construct remodeling and reorganization was investigated also by quantifying collagen deposition (**Supplementary Figure 3**) and collagen content per wet weight (**Figure 3F**). During static pre-culture (from day 1 to day 5), collagen content per ww did not significantly vary, while at day 9 it significantly increased (**Figure 3F**). This variation of the collagen content per ww along culture time is consistent with the observed remodeling of the constructs (**Figure 2**).

Cardiac Marker Immunofluorescence

Cardiomyocyte organization and maturation within the ECTs were assessed quantifying the cardiac marker α-sarcomeric actinin and the mature cardiac markers cTnI and Cx43. In particular, ECTs cultured in static conditions presented isolated and non-interconnected CMs both at day 5 (**Supplementary Figure 4**) and at day 9, with few cTnI-positive structures and absence of Cx43 gap junctions at day 9 (**Figures 4A,B**). In dynamically cultured ECTs, at day 9 most of the CMs close to the edges presented elongated and organized sarcomere units, positive for cTnI, typical of mature differentiation stage and Cx43 gap-junctional proteins (**Figures 4C,D**). In addition, the presence of striated α-sarcomeric actinin-positive structures was observed within ECTs cultured in dynamic conditions, where elongated cells exhibited the typical features of mature cardiac contractile

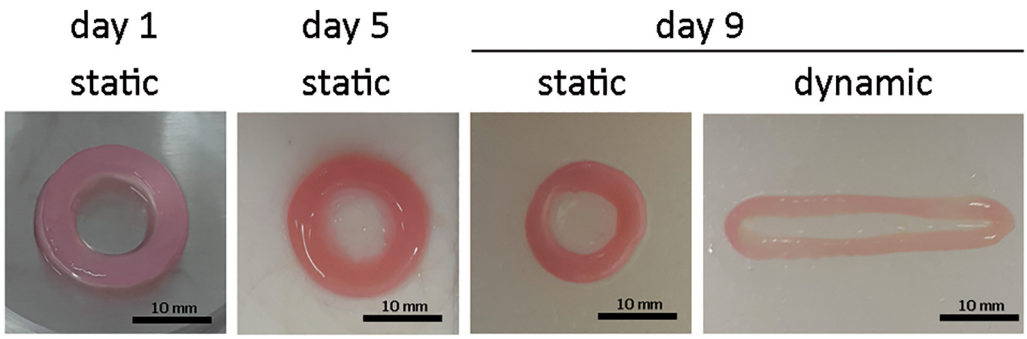

FIGURE 2 | ECT shape remodeling. Representative macroscopic pictures showing the top view of an explanatory ECT at the beginning (day 1) and at day 5 of the culture, and following either static or dynamic culture (day 9). Scale bar = 10 mm.

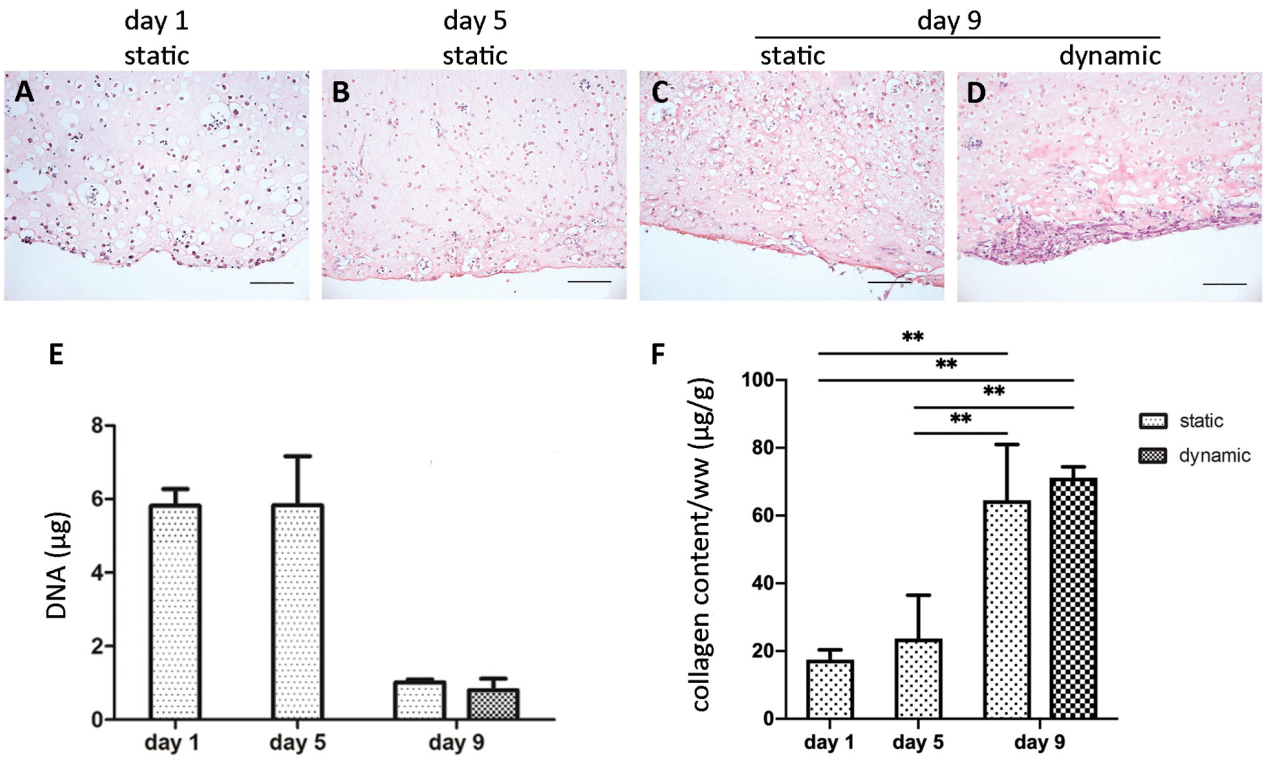

FIGURE 3 | ECT cell distribution and DNA and collagen content. Representative H&E staining showing cell distribution within an explanatory ECT at the beginning (day 1) of the culture **(A)**, at day 5 **(B)**, and following either static **(C)** or dynamic **(D)** culture at day 9. Scale bar = 100 µm. Graphs showing the DNA amount **(E)** and the collagen content normalized by ww **(F)** for ECTs at the beginning (day 1) of the culture, at day 5, and following either static or dynamic culture (day 9). For all groups $n = 3$, $^{**}p \leq 0.01$.

units (**Figures 4G,H**). Such features were not detected in statically cultured ECTs, characterized by round-shaped cell morphology (**Figures 4E,F**). As concerns CM orientation, **Figure 4I** shows that in stretched ECTs almost 60% of CMs were aligned with the mechanical stimulation direction, while in statically cultured ECTs no significant differences were found. Cardiac FBs positive for DAPI and Vimentin, and negative for α-actinin, were observed in ECTs cultured under both dynamic and static conditions (**Figures 4E–H**). Notably, stretch stimulation promoted a significantly higher percentage of proliferating cardiac FBs (20% *vs.* 10% for dynamic culture and static control, respectively—**Figure 4J**), corresponding to Vim^+ and $Ki67^+$ cells. Furthermore, dynamic culture sustained the maintenance of the CM subpopulation, which resulted to be 1.2 times more than cardiac FBs, whereas in statically cultured ECTs cardiac FBs were two times higher in number than CMs (**Figure 4K**).

Mechanical Characterization

The mechanical response of ECTs undergoing cyclic stretch within the bioreactor was *in situ* measured at day 5 and at

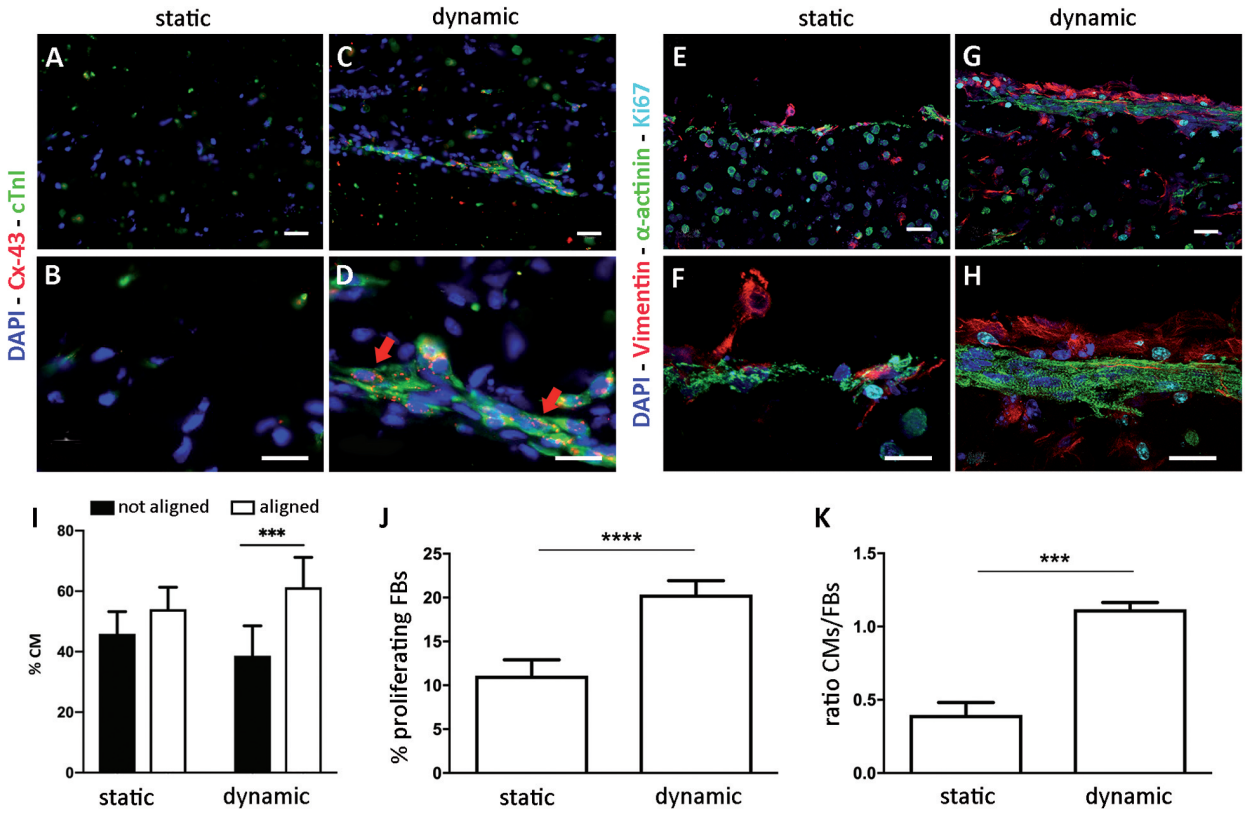

FIGURE 4 | ECT biological characterization. Representative immunofluorescence images of statically **(A,B,E,F)** and dynamically **(C,D,G,H)** cultured ECTs at low (**A,C,E,G**, scale bar = 30 μm) and high (**B**,**D**,**F**,**H**, scale bar = 10 μm) magnification, stained for cardiac markers connexin-43 (Cx-43, red), Troponin I (cTnI, green), and α-sarcomeric actinin (α-actinin, green); for FB marker Vimentin (red); and for proliferating marker Ki67 (cyan). Nuclei are stained with DAPI (blue). **(I)** Graph showing the percentage of CMs aligned and not aligned with the direction of the mechanical stimulation, for statically (n = 3) and dynamically (n = 4) cultured ECTs. **(J)** Graph showing the percentage of proliferating FBs in statically and dynamically cultured ECTs at day 9. **(K)** Graph showing the ratio of CMs and FBs in statically and dynamically cultured ECTs at day 9. For all groups, n = 3, ***$p \leq 0.001$; ****$p \leq 0.0001$.

day 9, showing marked differences (**Figure 5A**). In detail, at day 9 ECTs exhibited a 2-fold increase in the root mean square (RMS) force magnitude and approximately a 4-fold increase in the peak-to-peak force amplitude in comparison with day 5 (n = 3, **Figure 5B**). For the sake of completeness, **Supplementary Figure 5** shows an example of ECT passive forces measured *in situ* by the bioreactor load cell over 5 days of dynamic culture in a preliminary experiment. In accordance with data shown in **Figure 5A**, the magnitude of the measured forces increased along the culture (**Supplementary Figure 5**). As a check of consistency, stress *vs.* time curves obtained at days 5 and 9 from the bioreactor *in situ* monitoring and from the standard testing machine revealed comparable peak-to-peak stress amplitudes, thus confirming the reliability of the *in situ* monitoring setup (**Figures 5C,D**).

Freshly casted ECTs, statically cultured ECTs, and dynamically cultured ECTs collected immediately after bioreactor force monitoring were then mechanically characterized by using the standard testing machine (**Figures 6A,B**): (1) freshly casted ECTs and statically pre-cultured ECTs at day 5 presented a similar mechanical behavior in terms of linear elastic modulus (E = 34.4 ± 5.4 kPa and E = 31.7 ± 3.1 kPa, respectively), with no significant difference in terms of ultimate tensile strength (UTS = 60.5 ± 17.6 kPa and UTS = 42.9 ± 8.4 kPa, respectively), while (2) a statistically significant increase of the linear elastic modulus and ultimate tensile strength was observed at day 9 for ECTs cultured in both static (E = 87.5 ± 9.2 kPa, UTS = 107.0 ± 21.3 kPa) and dynamic (E = 117.3 ± 13.0 kPa, UTS = 95.6 ± 15.3 kPa) conditions. In particular, dynamically cultured ECTs exhibited an almost 4-fold increase of the linear elastic modulus compared with statically pre-cultured ECTs at day 5 and a 1.3-fold increase with respect to statically cultured ECTs at day 9 (**Figure 6A**).

Electrical Functionality

After 5 days of static pre-culture, ECTs did not spontaneously beat. When electrically paced starting with 1 V/cm electric field amplitude (rectangular pulses, 2 ms duration, 1 Hz), they reached the excitation threshold at 7.2 ± 3.3 V/cm (**Figure 7A**), even though from the analysis of contractility an irregular, not synchronous beating over time emerged (**Figure 7B**). Although the pacing frequency was increased,

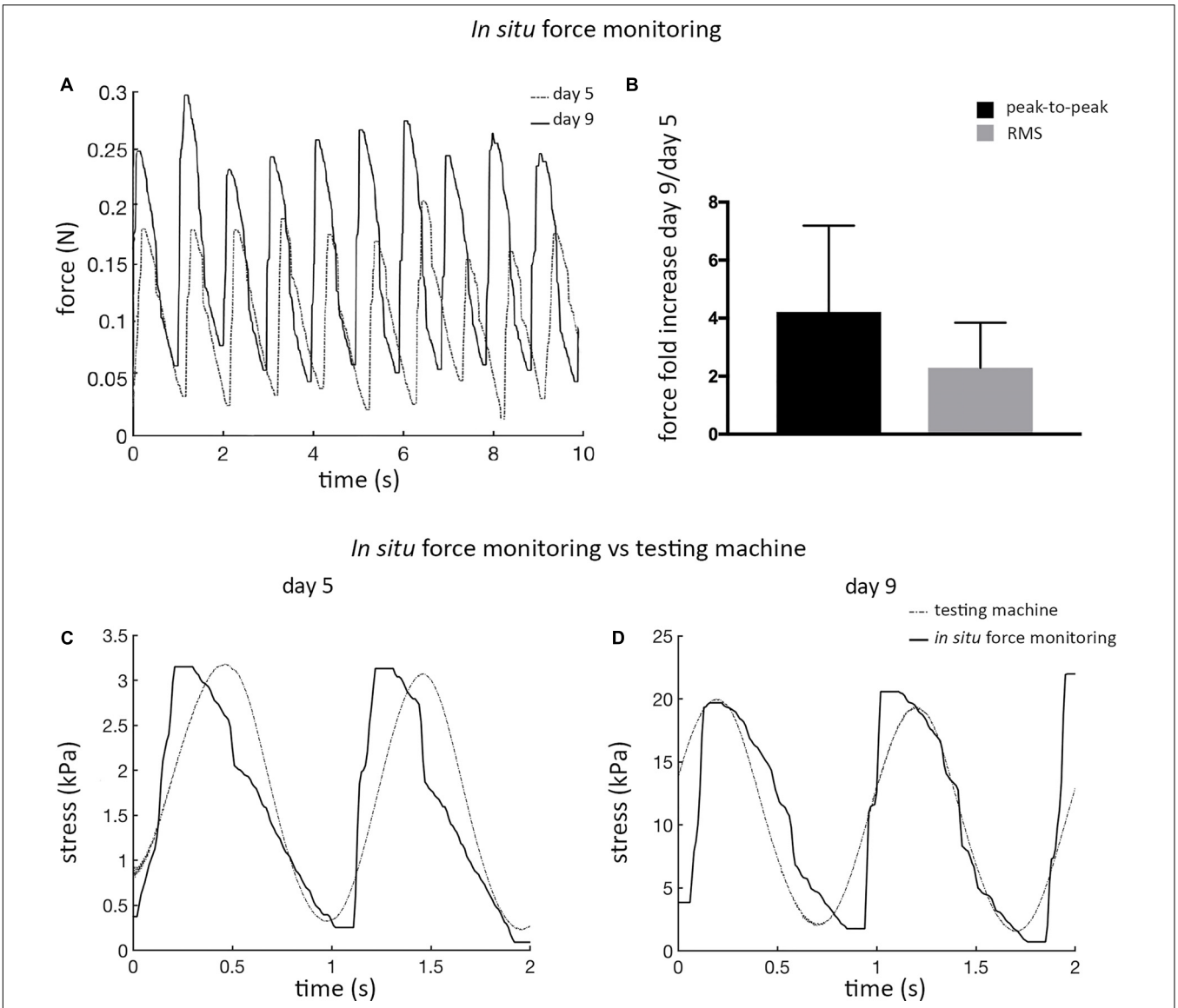

FIGURE 5 | ECT *in situ* bioreactor force monitoring. **(A)** Real-time force curves measured *in situ* by the bioreactor load cell at day 5 and at day 9 for an explanatory ECT undergoing cyclic stretch. **(B)** Graph showing the increase in the peak-to-peak force amplitude and in the root mean square (RMS) force magnitude at day 9 in comparison to day 5, respectively ($n = 3$). Comparison of the stress *vs.* time curves obtained at days 5 **(C)** and 9 **(D)** from the bioreactor load cell (solid line) and from the standard testing machine (dotted line) data.

it was not possible to determine the MCR of statically pre-cultured ECTs (**Figure 7C**). At day 9, any spontaneous beating was observed neither in dynamically cultured ECTs nor in static controls. Exposed to electrical pacing at increasing electric field amplitude (rectangular pulses, 2 ms duration, 1 Hz), the control group did not respond to the stimulation, while dynamically cultured ECTs reached the ET at 3.6 ± 0.8 V/cm (**Figure 7A**), with a regular, synchronous contractile activity over time (**Figure 7D** and **Supplementary Video 1**). Furthermore, imposing an electric field value 2-fold the ET and increasing the pacing frequency, dynamically cultured ECTs exhibited a MCR equal to 5.2 ± 1.46 Hz (**Figure 7C**). Finally, the contractile response of dynamically cultured ECTs exposed to increasing pacing frequencies (1.5–5 Hz) is presented in **Figure 7E**, where the capability of cyclically stretched ECTs to tune the beating rate accordingly to the imposed pacing frequency variation can be appreciated.

DISCUSSION

Biomechanics is a key player in governing and regulating myocardium development, homeostasis, and pathophysiology (Duscher et al., 2014; Voorhees and Han, 2015). During embryo development, CM contraction and blood flow exist within the primitive heart tube and influence the chamber

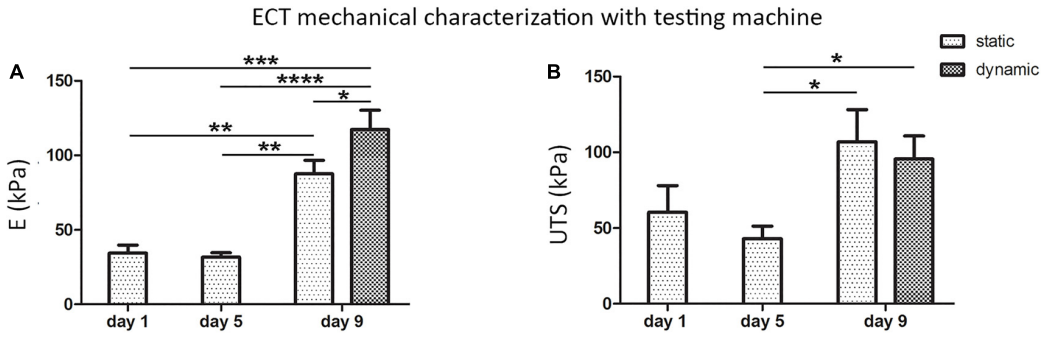

FIGURE 6 | ECT mechanical characterization. Linear elastic modulus (E) values **(A)** and ultimate tensile strength (UTS) values **(B)** of freshly casted ECTs (day 1), ECTs at day 5, and statically and dynamically cultured ECTs at day 9 collected immediately after *in situ* force monitoring and measured using a standard testing machine. For all groups, $n \geq 3$, $^{*}p \leq 0.05$; $^{**}p \leq 0.01$; $^{***}p \leq 0.001$; $^{****}p \leq 0.0001$.

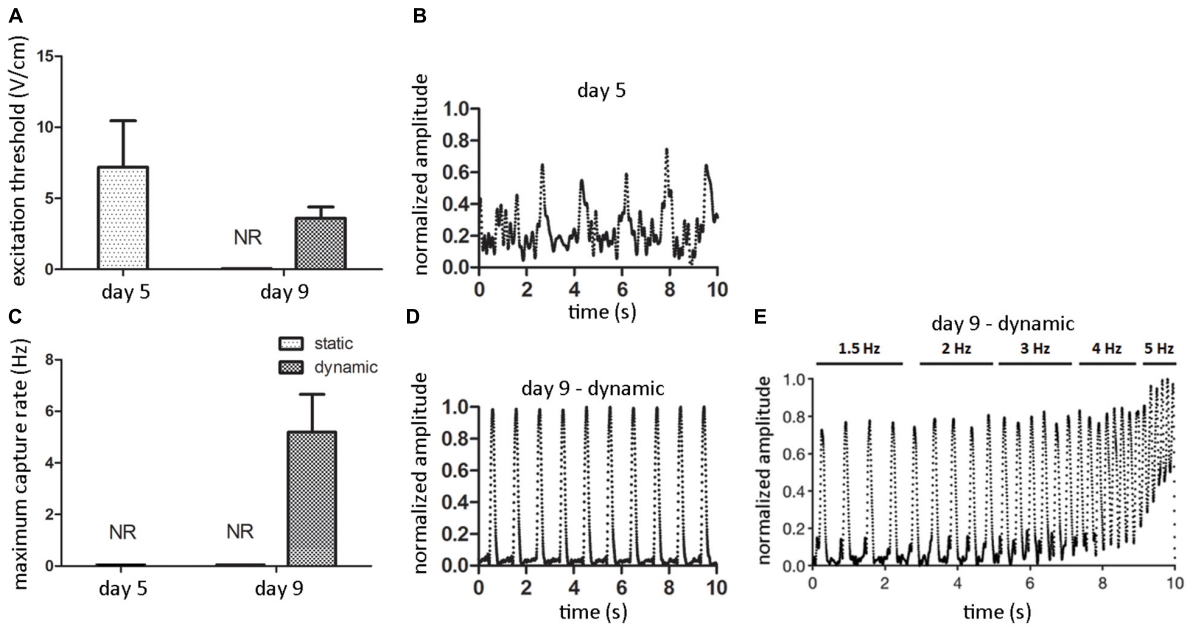

FIGURE 7 | ECT electrical functionality. Graphs showing the excitation threshold (ET, **A**) and the maximum capture rate (MCR, **C**) of ECTs at day 5 and following static and dynamic culture at day 9 (NR = not responding to external electrical pacing, $n = 3$). Explanatory reconstructions from video-recorded images of the contraction amplitude waveforms (normalized to the maximum peak value) of ECTs exposed to electrical pacing at day 5 **(B)** and following dynamic culture at day 9 **(D)**. **(E)** Explanatory reconstruction of the contraction amplitude waveform of day 9-dynamic cultured ECT exposed to electrical pacing at increasing frequency.

curvature formation (Auman et al., 2007). Throughout neonatal development, myocardial stiffness increases together with an increase in heart contractility (Hopkins et al., 1973; Rodriguez et al., 2011). In cardiac disease development, alterations in cardiac function can be due to long-term changes in loading conditions, and in turn alterations in functionality and response of CMs and FBs can alter the mechanical properties of the heart with consequent maladaptive cardiac remodeling (McCain and Parker, 2011; Duscher et al., 2014; van Putten et al., 2016; Pesce and Santoro, 2017; Saucerman et al., 2019). As recently thoroughly investigated, cardiac cells are extremely sensitive to mechanical stimuli and react by activating defined mechanotransduction pathways, i.e., converting mechanical forces into biochemical signals that can lead to phenotypic changes (Lammerding et al., 2004; Sheehy et al., 2012; Lyon et al., 2015; Chimenti et al., 2017). For this reason, mechanical cues are paramount *in vivo* for the development of structurally and physiologically mature CMs and play a continuous, crucial regulatory role in cardiac growth and maintenance (Zhu et al., 2014). Moreover, *in vivo* physical forces are tightly regulated, or deregulated, not only in space but also in time (Valon et al., 2017). Thus, to promote *in vitro* a physiological-like maturation of cardiac tissue models, the provision of biomimetic physical conditioning with tunable intensity over time (Ronaldson-Bouchard et al., 2019), properly adapted to the actual maturation stage of the cultured constructs, is crucial.

Inspired by these arguments, we developed a bioreactor platform for biomimetic dynamic culture of cardiac tissue models and *in situ* non-destructive monitoring of their mechanical response. The rationale behind the design of the proposed bioreactor platform was to develop a unique, reliable, and versatile culture device able (1) to deliver tunable native-like or pathological-like cyclic stretch for the maturation of 3D cardiac tissue models or the development of diseased cardiac tissue models and (2) to *in situ* measure their passive mechanical response along the culture in a non-destructive manner, in the future perspective of continuously adapting the load to the actual maturation stage of the cultured constructs. In terms of mechanical stimulation, the adopted engineering and technological solutions led to the implementation of a displacement-controlled strategy allowing a wide range of well-defined physiological/pathological-like stretching and frequencies. In particular, the use of a linear voice coil motor enabled high displacement amplitude and frequency. Moreover, the adopted feedback-loop control strategy guaranteed high-fidelity tracking of the motor reference position with consequent high-displacement resolution even in case of variations of the environmental conditions (e.g., temperature, humidity, and pressure), which could induce unexpected friction. Further preliminary tests, carried out in a cell culture laboratory running explanatory stimulation tests without constructs, proved the bioreactor watertightness and sterility maintenance and confirmed that the bioreactor is an easy-to-use platform.

Proof-of-concept experiments were then performed on specifically developed fibrin-based annular ECTs, tested under static and dynamic conditions. These experiments had the dual aim of (1) testing the bioreactor performance in terms of cyclic stretching and *in situ* monitoring of the mechanical response of cardiac tissue models and (2) investigating the effect of cyclic mechanical stimulation on cardiac tissue organization, maturation, mechanical properties, and electrical functionality. In detail, ECTs were prepared, pre-cultured for 5 days in static conditions, and successively transferred into the bioreactor culture chamber to be cyclically stretched (sinusoidal waveform, 10% strain at 1 Hz) for an additional 4 days. In parallel, corresponding static control experiments were carried out. At the end of the culture, dynamically cultured ECTs presented increased cell density and elongated cells at the borders, parallel to the stretch direction (**Figure 3D**). This was confirmed by immunofluorescence analyses, which revealed a network of cTnI/sarcomeric α-actinin-positive CMs longitudinally oriented along the longitudinal cross section of the constructs (**Figure 4I**) and prevalently localized on lateral edges, expressing Cx43 electrical gap junctional proteins, all typical features of mature cardiac contractile units (**Figures 4C,D**).

Although the total amount of DNA decreased in both culture conditions at day 9 compared to day 5 (**Figure 3E**) and FBs proliferated more in dynamic than in static culture (**Figure 4J**), the number of CMs was still superior to FBs following stretching (**Figure 4K**), most likely due to a better CM survival under dynamic conditions. On the contrary, statically cultured ECTs presented round-shaped, isolated, non-interconnected CMs, with low or even lacking expression of mature cardiac markers (**Figures 4A,B**). Under static culture, although FBs proliferated less (**Figure 4J**), the final FB number was two times higher than the CM number (**Figure 4K**), possibly linked to the apoptosis of several CMs following prolonged static conditions. Mechanical stimulation might indeed have promoted the further maturation of CMs and the exchange of nutrients, oxygen, and waste products, which in static conditions was limited to the diffusion process.

Concerning ECT maturation in terms of matrix remodeling/generation and mechanical properties, the total amount of collagen did not vary significantly along the culture (**Supplementary Figure 3**), although it has to be considered that this information refers to the total amount of proteins and it does not take into account the fiber types, morphology, and organization, while the collagen content per ww increased with the time in culture (**Figure 3F**), consistently with the construct remodeling (**Figure 2**). *In situ* monitoring allowed measuring the ECT passive force response to cyclic stretch, showing a force increase in terms of both RMS force magnitude and peak-to-peak amplitude along the culture (**Figures 5A,B**). Moreover, stretched constructs presented increased mechanical properties (E and UTS) over culture time (**Figures 6A,B**). Since the total collagen content remained constant, it can be argued that the observed differences in mechanical properties are related to the remodeling of the constructs.

Finally, ECTs were tested in terms of electrical functionality by investigating their regularity and frequency of contraction under external electrical pacing. ECTs did not spontaneously beat, neither at the end of the pre-static culture (day 5) nor at day 9. When electrically paced, only stretched ECTs presented a decreasing ET and an increasing MCR over time (**Figures 7A,C**), and at day 9 they regularly and synchronously beat following the external pacing (**Figure 7D**), while statically cultured constructs did not respond. This observation is further evidence of the instrumental role of cyclic stretch in promoting the functional coupling and the development of adult-like CMs in cultured ECTs, able to respond synchronously to increasing pacing frequency (**Figure 7E**). Although our preliminary biological results are not representative of cardiac tissue models exhibiting uniform and complete cardiac cell maturation, with this study we confirmed the developmental effect of cyclic stretch on ECT organization and maturation, in accordance with previous studies (Liaw and Zimmermann, 2016; Parsa et al., 2016; Stoppel et al., 2016). Time in culture under mechanical stimulation longer than 4 days should be able to provide a more uniform maturation and organization of CMs.

The reliability of the bioreactor platform was thus verified both for the engineering design and for the feasibility of dynamically culturing 3D ECTs. Moreover, the comparison of the stress *vs.* time curves obtained using the bioreactor load cell and the testing machine (**Figures 5C,D**) confirmed the reliability of the *in situ* monitoring setup for non-destructive measurement of passive mechanical response of the constructs to cyclic stretch.

In the past, a plethora of studies used dynamic culture devices developed to expose ECTs to cardiac-like isotonic load by using actuators (Fink et al., 2000; Zimmermann et al., 2002; Naito et al., 2006; Birla et al., 2007; Tulloch et al., 2011; Salazar et al., 2015).

However, the mechanical response of the cultured ECTs was not monitored along the culture in any of these studies, where the constructs were mechanically characterized only at the end of the culture by using, e.g., testing machines or organ baths, thus providing only end-point measurements. On the other hand, in other studies flexible posts were adopted to stimulate ECTs by auxotonic load (Zimmermann et al., 2006; Hansen et al., 2010; Schaaf et al., 2011; Boudou et al., 2012; Mannhardt et al., 2016). This made possible the implementation of automated methods for the evaluation of the contractile activity of the constructs along the culture but required long-term culture periods and led to ECTs characterized by structural and functional properties typical of postnatal myocardium. To our knowledge, only Kensah et al. (2011) combined cyclic stretch and *in situ* monitoring of mechanical behavior within a bioreactor, using a device designed for dynamically culturing and real-time measuring the contraction force of spontaneously beating miniaturized ECTs, based on a matrix of collagen and Matrigel.

Differently, our bioreactor platform was designed to stretch and *in situ* measure along the culture the passive mechanical response of macroscopic constructs, which can be of different shape and composition. By comparing the force measurements acquired along the culture, related to the mechanical properties of the constructs as shown, our device allows to monitor the construct maturation trend without interrupting the culture. This enables reducing the number of time-point analyses and thus of replicate samples. Furthermore, this bioreactor platform could be exploited for continuously adapting the stimulation to the actual development of the constructs. In principle, by equipping the platform with an additional feedback-loop control between the *in situ* force monitoring and the motor, this approach would enable the biomimetic adaptation of the mechanical load to the developmental stage of the cultured ECTs. Moreover, the integration of a compact digital camera and an autofocus lens for macro photography located perpendicularly to the bioreactor optical access would allow acquiring real-time images of the constructs during dynamic culture. This feature could be exploited for automatically *in situ* measuring the ECT geometry, ultimately providing real-time mechanical characterization of the constructs in terms of stress–strain curves.

In terms of versatility, in the future the proposed platform will be equipped with an electrical stimulation unit to provide individual, alternate, and/or combined mechanical and electrical stimulations to mimic the complex biophysical cardiac environment present *in vivo*. Furthermore, enabling a wide range of displacements and stimulation frequencies, this bioreactor could be used for several applications in different research fields, such as skeletal muscle or tendon/ligament tissue engineering or for disease modeling imposing pathological physical conditioning. In conclusion, the proposed bioreactor platform represents a powerful tool for *in vitro* investigation and ultimately production of functional engineered constructs.

DATA AVAILABILITY STATEMENT

The raw data supporting the conclusions of this article will be made available by the authors, without undue reservation, to any qualified researcher.

ETHICS STATEMENT

The animal study was reviewed and approved by the Veterinary Office of the Canton Basel (Basel, Switzerland), according to the Swiss Federal guidelines for animal welfare.

AUTHOR CONTRIBUTIONS

DM, GP, AM, and UM conceived the study. GP and DM conceived the bioreactor platform design. AR, GP, and RG developed the control unit and the control software. AT and RG selected the motor. GP, GI, DM, CB, AA, and UM conceived and designed the in-house experiments. GP and AM conceived the biological experiments. GP and GC performed the biological experiments and assessments. GP, GI, AP, and AM analyzed the biological data. DM and GP reviewed the state of the art. GI and DM prepared the figures. AM and UM contributed to the writing of the manuscript. DM, GI, and GP wrote the manuscript. All the authors contributed to the article and approved the submitted version.

FUNDING

This work was partially supported by the European Union FP7-NMP Programme (BIOSCENT, grant 214539), by the Italian Ministry of Economic Development and the Italian Trade Commission (Agreement MISE-ICE-CRUI 2010, PROBING, grant 232), and by the Italian Ministry of Education, University and Research [PRIN 2012, BEAT3DHEART, grant 20123E8FH4; NOP for Research and Competitiveness 2007–2013, IRMI (CTN01_00177_888744)].

SUPPLEMENTARY MATERIAL

The Supplementary Material for this article can be found online at: https://www.frontiersin.org/articles/10.3389/fbioe.2020.00733/full#supplementary-material

REFERENCES

Akhyari, P., Fedak, P. W., Weisel, R. D., Lee, T. Y., Verma, S., Mickle, D. A., et al. (2002). Mechanical stretch regimen enhances the formation of bioengineered autologous cardiac muscle grafts. *Circulation* 106(12 Suppl. 1), I137–I142.

Auman, H. J., Coleman, H., Riley, H. E., Olale, F., Tsai, H. J., and Yelon, D. (2007). Functional modulation of cardiac form through regionally confined cell shape changes. *PLoS Biol.* 5:e53. doi: 10.1371/journal.pbio.0050053

Belviso, I., Romano, V., Sacco, A. M., Ricci, G., Massai, D., Cammarota, M., et al. (2020). Decellularized human dermal matrix as a biological scaffold for cardiac

repair and regeneration. *Front. Bioeng. Biotechnol.* 8:229. doi: 10.3389/fbioe.2020.00229

Bian, W., Liau, B., Badie, N., and Bursac, N. (2009). Mesoscopic hydrogel molding to control the 3D geometry of bioartificial muscle tissues. *Nat. Protoc.* 4, 1522–1534. doi: 10.1038/nprot.2009.155

Bilodeau, K., and Mantovani, D. (2006). Bioreactors for tissue engineering: focus on mechanical constraints. A comparative review. *Tissue Eng.* 12, 2367–2383. doi: 10.1089/ten.2006.12.2367

Birla, R. K., Huang, Y. C., and Dennis, R. G. (2007). Development of a novel bioreactor for the mechanical loading of tissue-engineered heart muscle. *Tissue Eng.* 13, 2239–2248. doi: 10.1089/ten.2006.0359

Black, L. D. III, Meyers, J. D., Weinbaum, J. S., Shvelidze, Y. A., and Tranquillo, R. T. (2009). Cell-induced alignment augments twitch force in fibrin gel-based engineered myocardium via gap junction modification. *Tissue Eng. Part A* 15, 3099–3108. doi: 10.1089/ten.TEA.2008.0502

Boudou, T., Legant, W. R., Mu, A., Borochin, M. A., Thavandiran, N., Radisic, M., et al. (2012). A microfabricated platform to measure and manipulate the mechanics of engineered cardiac microtissues. *Tissue Eng. Part A* 18, 910–919. doi: 10.1089/ten.tea.2011.0341

Centola, M., Abbruzzese, F., Scotti, C., Barbero, A., Vadalà, G., Denaro, V., et al. (2013). Scaffold-based delivery of a clinically relevant anti-angiogenic drug promotes the formation of in vivo stable cartilage. *Tissue Eng. Part A* 19, 1960–1971. doi: 10.1089/ten.TEA.2012.0455

Chen, T., and Vunjak-Novakovic, G. (2019). Human tissue-engineered model of myocardial ischemia-reperfusion injury. *Tissue Eng. Part A* 25, 711–724. doi: 10.1089/ten.TEA.2018.0212

Chimenti, I., Massai, D., Morbiducci, U., Beltrami, A. P., Pesce, M., and Messina, E. (2017). Stem cell spheroids and ex vivo niche modeling: rationalization and scaling-up. *J. Cardiovas. Transl. Res.* 10, 150–166. doi: 10.1007/s12265-017-9741-5

Cholewinski, E., Dietrich, M., Flanagan, T. C., Schmitz-Rode, T., and Jockenhoevel, S. (2009). Tranexamic acid–an alternative to aprotinin in fibrin-based cardiovascular tissue engineering. *Tissue Eng. Part A* 15, 3645–3653. doi: 10.1089/ten.tea.2009.0235

Cigan, A. D., Nims, R. J., Albro, M. B., Esau, J. D., Dreyer, M. P., Vunjak-Novakovic, G., et al. (2013). Insulin, ascorbate, and glucose have a much greater influence than transferrin and selenous acid on the in vitro growth of engineered cartilage in chondrogenic media. *Tissue Eng. Part A* 19, 1941–1948. doi: 10.1089/ten.TEA.2012.0596

de Lange, W. J., Hegge, L. F., Grimes, A. C., Tong, C. W., Brost, T. M., Moss, R. L., et al. (2011). Neonatal mouse-derived engineered cardiac tissue: a novel model system for studying genetic heart disease. *Circ. Res.* 109, 8–19. doi: 10.1161/CIRCRESAHA.111.242354

Duscher, D., Maan, Z. N., Wong, V. W., Rennert, R. C., Januszyk, M., Rodrigues, M., et al. (2014). Mechanotransduction and fibrosis. *J. Biomech.* 47, 1997–2005. doi: 10.1016/j.jbiomech.2014.03.031

El-Armouche, A., Singh, J., Naito, H., Wittköpper, K., Didié, M., Laatsch, A., et al. (2007). Adenovirus-delivered short hairpin RNA targeting PKCalpha improves contractile function in reconstituted heart tissue. *J. Mol. Cell. Cardiol.* 43, 371–376. doi: 10.1016/j.yjmcc.2007.05.021

Engelmayr, G. C. Jr., Cheng, M., Bettinger, C. J., Borenstein, J. T., Langer, R., and Freed, L. E. (2008). Accordion-like honeycombs for tissue engineering of cardiac anisotropy. *Nat. Mater.* 7, 1003–1010. doi: 10.1038/nmat2316

Eschenhagen, T., and Zimmermann, W. H. (2005). Engineering myocardial tissue. *Circ. Res.* 9, 1220–1231.

Fink, C., Ergün, S., Kralisch, D., Remmers, U., Weil, J., and Eschenhagen, T. (2000). Chronic stretch of engineered heart tissue induces hypertrophy and functional improvement. *FASEB J.* 14, 669–679. doi: 10.1096/fasebj.14.5.669

Frati, C., Graiani, G., Barbani, N., Madeddu, D., Falco, A., Quaini, F., et al. (2019). Reinforced alginate/gelatin sponges functionalized by avidin/biotin-binding strategy: a novel cardiac patch. *J. Biomater. Appl.* 34, 975–987. doi: 10.1177/0885328219886029

Fujita, B., and Zimmermann, W. H. (2017). Myocardial tissue engineering for regenerative applications. *Curr. Cardiol. Rep.* 19:78. doi: 10.1007/s11886-017-0892-4

Hansen, A., Eder, A., Bönstrup, M., Flato, M., Mewe, M., Schaaf, S., et al. (2010). Development of a drug screening platform based on engineered heart tissue. *Circ. Res.* 107, 35–44. doi: 10.1161/CIRCRESAHA.109.211458

Hirt, M. N., Boeddinghaus, J., Mitchell, A., Schaaf, S., Börnchen, C., Müller, C., et al. (2014a). Functional improvement and maturation of rat and human engineered heart tissue by chronic electrical stimulation. *J. Mol. Cell. Cardiol.* 74, 151–161. doi: 10.1016/j.yjmcc.2014.05.009

Hirt, M. N., Hansen, A., and Eschenhagen, T. (2014b). Cardiac tissue engineering: state of the art. *Circ. Res.* 114, 354–367. doi: 10.1161/CIRCRESAHA.114.300522

Hirt, M. N., Sörensen, N. A., Bartholdt, L. M., Boeddinghaus, J., Schaaf, S., Eder, A., et al. (2012). Increased afterload induces pathological cardiac hypertrophy: a new in vitro model. *Basic Res. Cardiol.* 107:307. doi: 10.1007/s00395-012-0307-z

Hofman, K., Hall, B., Cleaver, H., and Marshall, S. (2011). High-throughput quantification of hydroxyproline for determination of collagen. *Anal. Biochem.* 417, 289–291. doi: 10.1016/j.ab.2011.06.019

Hopkins, S. F. Jr., McCutcheon, E. P., and Wekstein, D. R. (1973). Postnatal changes in rat ventricular function. *Circ. Res.* 32, 685–691. doi: 10.1161/01.res.32.6.685

Jockenhoevel, S., Zund, G., Hoerstrup, S. P., Chalabi, K., Sachweh, J. S., Demircan, L., et al. (2001). Fibrin gel – advantages of a new scaffold in cardiovascular tissue engineering. *Eur. J. Cardio Thoracic Surg.* 19, 424–430. doi: 10.1016/s1010-7940(01)00624-8

Kensah, G., Gruh, I., Viering, J., Schumann, H., Dahlmann, J., Meyer, H., et al. (2011). A novel miniaturized multimodal bioreactor for continuous in situ assessment of bioartificial cardiac tissue during stimulation and maturation. *Tissue Eng. Part C Methods* 17, 463–473. doi: 10.1089/ten.TEC.2010.0405

Kuznetsova, T., Herbots, L., Richart, T., D'hooge, J., Thijs, L., Fagard, R. H., et al. (2008). Left ventricular strain and strain rate in a general population. *Eur. Heart J.* 29, 2014–2023. doi: 10.1093/eurheartj/ehn280

Lammerding, J., Kamm, R. D., and Lee, R. T. (2004). Mechanotransduction in cardiac myocytes. *Ann. N. Y. Acad. Sci.* 1015, 53–70. doi: 10.1196/annals.1302.005

Lesman, A., Habib, M., Caspi, O., Gepstein, A., Arbel, G., Levenberg, S., et al. (2010). Transplantation of a tissue-engineered human vascularized cardiac muscle. *Tissue Eng. Part A* 16, 115–125. doi: 10.1089/ten.TEA.2009.0130

Liaw, N. Y., and Zimmermann, W. H. (2016). Mechanical stimulation in the engineering of heart muscle. *Adv. Drug Deliv. Rev.* 96, 156–160. doi: 10.1016/j.addr.2015.09.001

Lyon, R. C., Zanella, F., Omens, J. H., and Sheikh, F. (2015). Mechanotransduction in cardiac hypertrophy and failure. *Circ. Res.* 116, 1462–1476. doi: 10.1161/CIRCRESAHA.116.304937

Mannhardt, I., Breckwoldt, K., Letuffe-Brenière, D., Schaaf, S., Schulz, H., Neuber, C., et al. (2016). Human engineered heart tissue: analysis of contractile force. *Stem Cell Rep.* 7, 29–42. doi: 10.1016/j.stemcr.2016.04.011

Marsano, A., Conficconi, C., Lemme, M., Occhetta, P., Gaudiello, E., Votta, E., et al. (2016). Beating heart on a chip: a novel microfluidic platform to generate functional 3D cardiac microtissues. *Lab Chip* 16, 599–610. doi: 10.1039/c5lc01356a

Massai, D., Cerino, G., Gallo, D., Pennella, F., Deriu, M. A., Rodriguez, A., et al. (2013). Bioreactors as engineering support to treat cardiac muscle and vascular disease. *J. Healthc. Eng.* 4, 329–370. doi: 10.1260/2040-2295.4.3.329

McCain, M. L., and Parker, K. K. (2011). Mechanotransduction: the role of mechanical stress, myocyte shape, and cytoskeletal architecture on cardiac function. *Pflugers Arch. Eur. J. Physiol.* 462, 89–104. doi: 10.1007/s00424-011-0951-4

Menasché, P., Vanneaux, V., Hagège, A., Bel, A., Cholley, B., Cacciapuoti, I., et al. (2015). Human embryonic stem cell-derived cardiac progenitors for severe heart failure treatment: first clinical case report. *Eur. Heart J.* 36, 2011–2017. doi: 10.1093/eurheartj/ehv189

Miyagawa, S., Domae, K., Yoshikawa, Y., Fukushima, S., Nakamura, T., Saito, A., et al. (2017). Phase I clinical trial of autologous stem cell-sheet transplantation therapy for treating cardiomyopathy. *J. Am. Heart Assoc.* 6:e003918. doi: 10.1161/JAHA.116.003918

Morgan, K. Y., and Black, L. D. III (2014). Creation of a bioreactor for the application of variable amplitude mechanical stimulation of fibrin gel-based engineered cardiac tissue. *Methods Mol. Biol.* 1181, 177–187. doi: 10.1007/978-1-4939-1047-2_16

Murtha, L. A., Schuliga, M. J., Mabotuwana, N. S., Hardy, S. A., Waters, D. W., Burgess, J. K., et al. (2017). The processes and mechanisms of cardiac and pulmonary fibrosis. *Front. Physiol.* 8:777. doi: 10.3389/fphys.2017.00777

Mytsyk, M., Isu, G., Cerino, G., Grapow, M., Eckstein, F. S., and Marsano, A. (2019). Paracrine potential of adipose stromal vascular fraction cells to recover hypoxia-induced loss of cardiomyocyte function. *Biotechnol. Bioeng.* 116, 132–142. doi: 10.1002/bit.26824

Naito, H., Melnychenko, I., Didié, M., Schneiderbanger, K., Schubert, P., Rosenkranz, S., et al. (2006). Optimizing engineered heart tissue for therapeutic applications as surrogate heart muscle. *Circulation* 114(Suppl.), I72–I78. doi: 10.1161/CIRCULATIONAHA.105.001560

Occhetta, P., Isu, G., Lemme, M., Conficconi, C., Oertle, P., Räz, C., et al. (2018). A three-dimensional in vitro dynamic micro-tissue model of cardiac scar formation. *Integr. Biol.* 10, 174–183. doi: 10.1039/c7ib00199a

Ogle, B. M., Bursac, N., Domian, I., Huang, N. F., Menasché, P., Murry, C. E., et al. (2016). Distilling complexity to advance cardiac tissue engineering. *Sci. Transl. Med.* 8:42s13. doi: 10.1126/scitranslmed.aad2304

Parsa, H., Ronaldson, K., and Vunjak-Novakovic, G. (2016). Bioengineering methods for myocardial regeneration. *Adv. Drug Deliv. Rev.* 96, 195–202. doi: 10.1016/j.addr.2015.06.012

Pesce, M., and Santoro, R. (2017). Feeling the right force: how to contextualize the cell mechanical behavior in physiologic turnover and pathologic evolution of the cardiovascular system. *Pharmacol. Ther.* 171, 75–82. doi: 10.1016/j.pharmthera.2016.08.002

Pisani, G. (2016). *Training-to-Beat Bioreactor for Investigating Engineered Cardiac Tissues: Design, Development & Validation*. Dissertation, Politecnico di Torino, Torino.

Radisic, M., Marsano, A., Maidhof, R., Wang, Y., and Vunjak-Novakovic, G. (2008). Cardiac tissue engineering using perfusion bioreactor systems. *Nat. Protoc.* 3, 719–738. doi: 10.1038/nprot.2008.40

Radisic, M., Park, H., Shing, H., Consi, T., Schoen, F. J., Langer, R., et al. (2004). Functional assembly of engineered myocardium by electrical stimulation of cardiac myocytes cultured on scaffolds. *Proc. Nal. Acad. Sci. U.S.A.* 101, 18129–18134. doi: 10.1073/pnas.0407817101

Riegler, J., Tiburcy, M., Ebert, A., Tzatzalos, E., Raaz, U., Abilez, O. J., et al. (2015). Human engineered heart muscles engraft and survive long term in a rodent myocardial infarction model. *Circ. Res.* 117, 720–730. doi: 10.1161/CIRCRESAHA.115.306985

Rodriguez, A. G., Han, S. J., Regnier, M., and Sniadecki, N. J. (2011). Substrate stiffness increases twitch power of neonatal cardiomyocytes in correlation with changes in myofibril structure and intracellular calcium. *Biophys. J.* 101, 2455–2464. doi: 10.1016/j.bpj.2011.09.057

Ronaldson-Bouchard, K., Yeager, K., Teles, D., Chen, T., Ma, S., Song, L., et al. (2019). Engineering of human cardiac muscle electromechanically matured to an adult-like phenotype. *Nat. Protoc.* 14, 2781–2817. doi: 10.1038/s41596-019-0189-8

Sadr, N., Pippenger, B. E., Scherberich, A., Wendt, D., Mantero, S., Martin, I., et al. (2012). Enhancing the biological performance of synthetic polymeric materials by decoration with engineered, decellularized extracellular matrix. *Biomaterials* 33, 5085–5093. doi: 10.1016/j.biomaterials.2012.03.082

Salazar, B. H., Cashion, A. T., Dennis, R. G., and Birla, R. K. (2015). Development of a cyclic strain bioreactor for mechanical enhancement and assessment of bioengineered myocardial constructs. *Cardiovasc. Eng. Technol.* 6, 533–545. doi: 10.1007/s13239-015-0236-8

Saucerman, J. J., Tan, P. M., Buchholz, K. S., McCulloch, A. D., and Omens, J. H. (2019). Mechanical regulation of gene expression in cardiac myocytes and fibroblasts. *Nat. Revi. . Cardiol.* 16, 361–378. doi: 10.1038/s41569-019-0155-8

Schaaf, S., Shibamiya, A., Mewe, M., Eder, A., Stöhr, A., Hirt, M. N., et al. (2011). Human engineered heart tissue as a versatile tool in basic research and preclinical toxicology. *PLoS One* 6:e26397. doi: 10.1371/journal.pone.0026397

Sheehy, S. P., Grosberg, A., and Parker, K. K. (2012). The contribution of cellular mechanotransduction to cardiomyocyte form and function. *Biomech. Model. Mechanobiol.* 11, 1227–1239. doi: 10.1007/s10237-012-0419-2

Stoppel, W. L., Kaplan, D. L., and Black, L. D. III (2016). Electrical and mechanical stimulation of cardiac cells and tissue constructs. *Adv. Drug Deliv. Rev.* 96, 135–155. doi: 10.1016/j.addr.2015.07.009

Tandon, N., Cannizzaro, C., Chao, P. H., Maidhof, R., Marsano, A., Au, H. T., et al. (2009). Electrical stimulation systems for cardiac tissue engineering. *Nat. Protoc.* 4, 155–173. doi: 10.1038/nprot.2008.183

Tiburcy, M., Didié, M., Boy, O., Christalla, P., Döker, S., Naito, H., et al. (2011). Terminal differentiation, advanced organotypic maturation, and modeling of hypertrophic growth in engineered heart tissue. *Circ. Res.* 109, 1105–1114. doi: 10.1161/CIRCRESAHA.111.251843

Tiburcy, M., Hudson, J. E., Balfanz, P., Schlick, S., Meyer, T., Chang Liao, M. L., et al. (2017). Defined engineered human myocardium with advanced maturation for applications in heart failure modeling and repair. *Circulation* 135, 1832–1847. doi: 10.1161/CIRCULATIONAHA.116.024145

Tulloch, N. L., Muskheli, V., Razumova, M. V., Korte, F. S., Regnier, M., Hauch, K. D., et al. (2011). Growth of engineered human myocardium with mechanical loading and vascular coculture. *Circ. Res.* 109, 47–59. doi: 10.1161/CIRCRESAHA.110.237206

Valon, L., Marín-Llauradó, A., Wyatt, T., Charras, G., and Trepat, X. (2017). Optogenetic control of cellular forces and mechanotransduction. *Nat. Commun.* 8:14396. doi: 10.1038/ncomms14396

van Putten, S., Shafieyan, Y., and Hinz, B. (2016). Mechanical control of cardiac myofibroblasts. *J. Mol. Cell. Cardiol.* 93, 133–142. doi: 10.1016/j.yjmcc.2015.11.025

Voorhees, A. P., and Han, H. C. (2015). Biomechanics of cardiac function. *Compr. Physiol.* 5, 1623–1644. doi: 10.1002/cphy.c140070

Vunjak-Novakovic, G., Eschenhagen, T., and Mummery, C. (2014). Myocardial tissue engineering: in vitro models. *Cold Spring Harbor Perspect. Med.* 4:a014076. doi: 10.1101/cshperspect.a014076

Vunjak-Novakovic, G., Tandon, N., Godier, A., Maidhof, R., Marsano, A., Martens, T. P., et al. (2010). Challenges in cardiac tissue engineering. *Tissue Eng. Part B Rev.* 16, 169–187. doi: 10.1089/ten.TEB.2009.0352

Weinberger, F., Breckwoldt, K., Pecha, S., Kelly, A., Geertz, B., Starbatty, J., et al. (2016). Cardiac repair in guinea pigs with human engineered heart tissue from induced pluripotent stem cells. *Sci. Transl. Med.* 8:363ra148. doi: 10.1126/scitranslmed.aaf8781

Weinberger, F., Mannhardt, I., and Eschenhagen, T. (2017). engineering cardiac muscle tissue: a maturating field of research. *Circ. Res.* 120, 1487–1500. doi: 10.1161/CIRCRESAHA.117.310738

Ye, L., Zimmermann, W. H., Garry, D. J., and Zhang, J. (2013). Patching the heart: cardiac repair from within and outside. *Circ. Res.* 113, 922–932. doi: 10.1161/CIRCRESAHA.113.300216

Zhu, R., Blazeski, A., Poon, E., Costa, K. D., Tung, L., and Boheler, K. R. (2014). Physical developmental cues for the maturation of human pluripotent stem cell-derived cardiomyocytes. *Stem Cell Res. Ther.* 5:117. doi: 10.1186/scrt507

Zimmermann, W. H. (2013). Biomechanical regulation of in vitro cardiogenesis for tissue-engineered heart repair. *Stem Cell Res. Ther.* 4:137. doi: 10.1186/scrt348

Zimmermann, W. H., and Eschenhagen, T. (2003). Cardiac tissue engineering for replacement therapy. *Heart Fail. Rev.* 8, 259–269. doi: 10.1023/a:1024725818835

Zimmermann, W. H., Fink, C., Kralisch, D., Remmers, U., Weil, J., and Eschenhagen, T. (2000). Three-dimensional engineered heart tissue from neonatal rat cardiac myocytes. *Biotechnol. Bioeng.* 68, 106–114. doi: 10.1002/(sici)1097-0290(20000405)68:1<106::aid-bit13>3.0.co;2-3

Zimmermann, W. H., Melnychenko, I., Wasmeier, G., Didié, M., Naito, H., Nixdorff, U., et al. (2006). Engineered heart tissue grafts improve systolic and diastolic function in infarcted rat hearts. *Nat. Med.* 12, 452–458. doi: 10.1038/nm1394

Zimmermann, W. H., Schneiderbanger, K., Schubert, P., Didié, M., Münzel, F., Heubach, J. F., et al. (2002). Tissue engineering of a differentiated cardiac muscle construct. *Circ. Res.* 90, 223–230. doi: 10.1161/hh0202.103644

Conflict of Interest: The authors declare that the research was conducted in the absence of any commercial or financial relationships that could be construed as a potential conflict of interest.

Copyright © 2020 Massai, Pisani, Isu, Rodriguez Ruiz, Cerino, Galluzzi, Pisanu, Tonoli, Bignardi, Audenino, Marsano and Morbiducci. This is an open-access article distributed under the terms of the Creative Commons Attribution License (CC BY). The use, distribution or reproduction in other forums is permitted, provided the original author(s) and the copyright owner(s) are credited and that the original publication in this journal is cited, in accordance with accepted academic practice. No use, distribution or reproduction is permitted which does not comply with these terms.

frontiers in Bioengineering and Biotechnology

REVIEW
published: 11 August 2020
doi: 10.3389/fbioe.2020.00955

Cells, Materials, and Fabrication Processes for Cardiac Tissue Engineering

*Pilar Montero[1†], María Flandes-Iparraguirre[1†], Saioa Musquiz[1,2], María Pérez Araluce[1,3], Daniel Plano[3,4], Carmen Sanmartín[3,4], Gorka Orive[2,4,5,6], Juan José Gavira[4,7], Felipe Prosper[1,4,8] and Manuel M. Mazo[1,4,8]**

[1] Regenerative Medicine Program, Cima Universidad de Navarra, Foundation for Applied Medical Research, Pamplona, Spain, [2] NanoBioCel Group, Laboratory of Pharmaceutics, School of Pharmacy, University of the Basque Country – UPV/EHU, Vitoria-Gasteiz, Spain, [3] Department of Pharmaceutical Technology and Chemistry, University of Navarra, Pamplona, Spain, [4] IdiSNA, Navarra Institute for Health Research, Pamplona, Spain, [5] University Institute for Regenerative Medicine and Oral Implantology – UIRMI (UPV/EHU – Fundación Eduardo Anitua), Vitoria-Gasteiz, Spain, [6] Singapore Eye Research Institute, Singapore, Singapore, [7] Cardiology Department, Clínica Universidad de Navarra, Pamplona, Spain, [8] Hematology and Cell Therapy Area, Clínica Universidad de Navarra, Pamplona, Spain

OPEN ACCESS

Edited by:
Susanna Sartori,
Politecnico di Torino, Italy

Reviewed by:
Karina Nakayama,
Oregon Health and Science University, United States
Diana Massai,
Politecnico di Torino, Italy

***Correspondence:**
Manuel M. Mazo
mmazoveg@unav.es

[†] These authors have contributed equally to this work

Specialty section:
This article was submitted to Tissue Engineering and Regenerative Medicine, a section of the journal Frontiers in Bioengineering and Biotechnology

Received: 10 April 2020
Accepted: 23 July 2020
Published: 11 August 2020

Citation:
Montero P, Flandes-Iparraguirre M, Musquiz S, Pérez Araluce M, Plano D, Sanmartín C, Orive G, Gavira JJ, Prosper F and Mazo MM (2020) Cells, Materials, and Fabrication Processes for Cardiac Tissue Engineering. Front. Bioeng. Biotechnol. 8:955. doi: 10.3389/fbioe.2020.00955

Cardiovascular disease is the number one killer worldwide, with myocardial infarction (MI) responsible for approximately 1 in 6 deaths. The lack of endogenous regenerative capacity, added to the deleterious remodelling programme set into motion by myocardial necrosis, turns MI into a progressively debilitating disease, which current pharmacological therapy cannot halt. The advent of Regenerative Therapies over 2 decades ago kick-started a whole new scientific field whose aim was to prevent or even reverse the pathological processes of MI. As a highly dynamic organ, the heart displays a tight association between 3D structure and function, with the non-cellular components, mainly the cardiac extracellular matrix (ECM), playing both fundamental active and passive roles. Tissue engineering aims to reproduce this tissue architecture and function in order to fabricate replicas able to mimic or even substitute damaged organs. Recent advances in cell reprogramming and refinement of methods for additive manufacturing have played a critical role in the development of clinically relevant engineered cardiovascular tissues. This review focuses on the generation of human cardiac tissues for therapy, paying special attention to human pluripotent stem cells and their derivatives. We provide a perspective on progress in regenerative medicine from the early stages of cell therapy to the present day, as well as an overview of cellular processes, materials and fabrication strategies currently under investigation. Finally, we summarise current clinical applications and reflect on the most urgent needs and gaps to be filled for efficient translation to the clinical arena.

Keywords: cardiac tissue engineering, human pluripotent stem cells, material properties, cell differentiation, fabrication strategies

A PERSPECTIVE ON CARDIAC DISEASE AND REGENERATIVE MEDICINE

Organ transplantation is one of the greatest medical achievements of the 20th century. However, its applicability is hampered by donor shortage, life-long immunosuppression and its success rates are linked to the experience of the surgical team. It requires a well-coordinated national effort, which is sometimes hindered by ethical issues (Prabhu, 2019). The search for novel ways to approach organ repair inspired the field of regenerative medicine, with Stem Cell Therapy as one of the most representative examples. Since this began, stem cells have been discovered even in low turnover adult tissues, such as the central nervous system (Doetsch et al., 1999), the lung, (Rock et al., 2009; Barkauskas et al., 2013) or the heart, (Beltrami et al., 2003) and have been widely assayed in animal models of disease, quickly reaching clinical trials. This swift progression in general met with rapid failure, but on the bright side, it also enabled specialists to gain immense insights into their mechanisms and ways of action.

Nothing exemplifies this journey better than the cardiac field. Cardiovascular diseases are well recognised as the leading cause of death worldwide, accounting for almost 1 in 2 deaths in Europe and causing 3.9 million deaths per year (Townsend et al., 2016). Ischemic heart disease (IHD) is one shade on this spectrum. It is generally caused by the clotting of a coronary vessel, which in turn leads to the death of a portion of the myocardium and the subsequent functional impairment of the organ. Being mostly non-regenerative, the heart is chronically impaired (Eschenhagen et al., 2017). A real epidemic, IHD is the leading single cause of death globally, responsible for over 15 million deaths in 2016, ranking first in high- and lower-middle-income countries, and third in low-income countries (World Health Organization [WHO], 2018). As per 2015, over 22 million EU citizens were living with the disease, with approximately 3 million new cases yearly. IHD imposes an enormous burden on society as affected patients must be cared for by health systems, requiring lifelong highly specialised medical attention and multimedication. It also jeopardises the structure of the workforce and puts significant pressure on families. In terms of economic cost, the total burden of IHD for EU economies is estimated at €59 billion/year. Of these, €19 billion is directly related to healthcare costs, while €20 billion is linked to productivity losses and the remaining €20 billion to the cost of indirect care. Estimations sketch out a grim future. In the United States, heart attacks are projected to contribute more than $818 billion to annual healthcare costs and lost productivity by 2030, (Nowbar et al., 2019) while in the South Asia region, direct medical costs for CVD are estimated to reach US $16.6 billion in 2021 (Walker et al., 2018). Organ transplant cannot match this overwhelming demand and become a widespread therapeutic option (Stehlik et al., 2011).

It was hoped that cell therapy would provide new means to regenerate the scarred myocardium. Remarkable discoveries encouraged rapid progression towards clinical trials, with the first one launched in record time (Behfar et al., 2014). After the BOOST and REPAIR-AMI trials reported significant benefits in cardiac function, (Wollert et al., 2004; Schächinger et al., 2006) hundreds of patients were recruited often in individual efforts mostly based on local experience. This led to the first voicing of concerns. The primary initial objective, improvement of cardiac function, failed to be met in many cases. Although statistically significant benefits in cardiac function were sometimes found, their magnitude was not as great as had been expected (reviewed in Gyöngyösi et al., 2016; Menasché, 2018). This reversal of fortunes coincided also with a remarkable twist in our understanding of what basic science and animal models conveyed: no true regeneration of the myocardium was achieved by adult stem cells. The underlying effects were mostly due to the paracrine secretion of beneficial molecules (Hodgkinson et al., 2016). Although this general perspective is valid for most adult stem cells, use of their embryonic counterpart, although boosted by their capacity to give rise to new tissue once transplanted, was still marred by some common issues such as lack of proper engraftment, and crucially by safety concerns as teratoma formation and need for immune suppression, as well as ethical issues.

Did stem cell regenerative medicine approaches fail? They obviously did not achieve the initial aims, but looking back, those can no doubt be branded as overambitious (Pagano et al., 2019). It did succeed in gathering a whole new compendium of knowledge, which has led to renewed and better efforts in the regenerative direction and, importantly, has built a worldwide network of excellence encompassing not only different nationalities, but also very diverse scientific disciplines. One of the greatest and perhaps now evident realisations in the field is the notion that cells are not alone in a tissue, and that the extracellular matrix (ECM) has a predominant role, not only as a passive architectural element, but crucially as a signal transducer and determinant of functionality (Majkut et al., 2013; Crowder et al., 2016; Kumar et al., 2017). Specifically in the myocardium, the ECM is highly dynamic, changing during development and disease. This latter change is bidirectional, as disease induces pathological ECM deposition but an abnormal matrix is able to produce malfunction (Frangogiannis, 2019). In consequence, it is now recognised that a cell-based cardiac regeneration without an adequate ECM is not viable. Generating new myocardium thus requires the participation of the most promising cells, with a surrounding matrix able to replicate the conditions of the native tissue and the proper 3D architecture. This is precisely one of the main directions of cardiac Tissue Engineering.

Cardiac Tissue Engineering (cTE) is a highly interdisciplinary scientific discipline, aiming at reproducing as accurately as possible the function and biology of cardiac muscle, during development or maturity, health or disease. Although its first objective was focused on meeting the needs of cardiac regenerative Medicine, as knowledge and experience on how the ECM influences cardiac cell biology increased and the fabrication capacities widened, its scope has greatly expanded into areas such as disease modelling, drug testing and personalised medicine amongst others (Feric et al., 2019; Noor et al., 2019; Mastikhina et al., 2020). This review aims at presenting the reader with an overview of the specific characteristics of the myocardium that determine the needs regenerative cTE has to meet, as well as providing a non-exhaustive revision of what the field has

delivered to attain this end, with a focus on human myocardium and human pluripotent stem cells.

THE HEART

The mammalian heart is an incredible organ. Its main role is to provide a continuous unidirectional supply of blood to the organism. This comes at a stringent metabolic cost, consuming the equivalent of 6 kg of ATP per day, with a complete renewal of its ATP pool every 10 seconds. Most of this energy is obtained through the oxidation of fatty acids in adulthood, though cardiac metabolism is dependent on glucose during embryonic stages, being able to employ lactate as a metabolic substrate (Neejy, 1974). Correct function is achieved through a specialised organ architecture, dividing the heart into 4 chambers: atria, which are smaller in size and muscular mass, receive blood and push it out into the ventricles, which in turn pump either towards the lungs or the body. In consequence, the left ventricle is larger and has a thicker muscular wall than its right counterpart. Chambers, inlets and outlets are separated by valves impeding back flow. The heart is the first organ to function, around day 8 in mice and the 4th gestational week in humans (Brand, 2003). It pumps continuously throughout life, efficiently ejecting blood through an exquisite 3D structure, (Buckberg, 2002) established by a complex set of embryonic movements, cellular growth and incorporation (Günthel et al., 2018). Disruption of this structure is seen in disease and can be in itself the cause of organ malfunction: cardiac congenital defects and malformation are a main cause of perinatal death, (Bressan et al., 2013) but also give rise to many cardiomyopathies (McKenna et al., 2017).

Cardiac Embryonic Development: A Brief Overview

The formation of the mammalian four-chambered heart encompasses a series of tightly coordinated morphological, cellular and molecular events (reviewed in Vincent and Buckingham, 2010; Meilhac et al., 2014; Ruiz-Villalba et al., 2016). Different pools of cardiac and extracardiac progenitors are involved, including the mesoderm-derived First, Second and Third Heart Fields (FHF, SHF and THF respectively) and the Cardiac Neural Crest Cells (CNCCs). Cells of the FHF contribute primarily to the left ventricle (LV) but there is also a small contribution to the atria; SHF will form the right ventricle (RV), outflow tract (OFT), atria and part of inflow tract (IFT); (Buckingham et al., 2005). THF cells contribute to the sinus node, some regions in the caval myocardium, and the Pro-Epicardial Organ (PEO) (Mommersteeg et al., 2010; Bressan et al., 2013). CNCCs arise from the dorsal neural tube, contribute to the parasympathetic innervation of the heart, valves and play a pivotal role in OFT patterning and optimal septation (Keyte et al., 2014).

Early precardiac progenitors from the lateral mesoderm have been mapped into the mid-anterior region of the primitive streak, characterised by the presence of both anterior Nodal/Activin and posterior bone morphogenetic protein (BMP) signalling at low levels, (Zhang et al., 2008; Vallier et al., 2009; Yamauchi et al., 2010; Yu et al., 2011) promoting the emergence of cardiogenic mesodermal MIXL1 + KDR + cells. As a result of these signalling gradients set in gastrulation, multipotent cardiovascular progenitor (M) expressing the cardiac master regulator MESP1 move in an anterior-lateral direction, forming a horseshoe-like region termed the cardiac crescent or FHF (Bondue et al., 2008; Chan S. S. K. et al., 2013). At a molecular level, MESP1 induces the expression of the minimal core of the essential cardiogenic transcription factors including ISL1, TBX5, NKX2.5, and GATA4, in combination with the chromatin remodeller SMARCD3 (BAF60C), which further drive cardiomyogenesis (Vincent and Buckingham, 2010; Meilhac et al., 2014; Meilhac and Buckingham, 2018). The cardiac crescent fuses at the midline, forming the linear heart tube, which consists of an interior layer of endocardial cells and an exterior layer of myocardial cells separated by an acellular, ECM-rich space, the cardiac jelly. Located central and dorsal to the FHF, SHF cells remain in contact with the pharyngeal endoderm and in a proliferative state as undifferentiated ISL1 + MEF2C + cells. As development proceeds, SHF cells are added to the poles of the heart tube, with the tube looping to position the different regions into place. Chambers balloon out as a result of the differential proliferation rates of CMs (Jong et al., 1997; Christoffels et al., 2004). As already mentioned, THF cells (TBX18 + NKX2.5-) contribute to the sinus node, caval myocardial cells and the PEO. PEO-cells give rise to the epicardium, and some cells of this layer undergo epithelial-to-mesenchymal transition to form epicardial derived cells (EPDC), which will differentiate into vascular cells (including the coronaries) as well as interstitial fibroblasts and valvular cells, being essential for compaction (Pérez-Pomares et al., 2002; Weeke-Klimp et al., 2010; Katz et al., 2012). Lastly, CNCCs originate by delamination from the neuroectoderm, (Hildreth et al., 2008) initially contributing to smooth muscle cells and CMs, (Mjaatvedt et al., 2001) and making a significant contribution to the innervation of the organ and to the OFT (Hildreth et al., 2008; Sizarov et al., 2012). We refer the reader to **Table 1** for a full description of the mentioned gene abbreviations.

Post-birth Cardiac Development: Foetal CMs vs. Adult CMs

Aside from the formation of the mammalian heart, CMs continue to develop postnatally (Guo and Pu, 2020). Embryonic CMs can beat spontaneously, express sarcomeric proteins and ion channels, and exhibit action potentials and calcium transients which are significantly distinctive from their adult counterpart (Vincent and Buckingham, 2010; Meilhac et al., 2014). Human and rodent embryonic CMs are around 30-40 fold less in size and feature an irregular shape, in comparison with adult CMs (Yang et al., 2014). These are characterised by an ultrastructural organisation with a large mitochondrial volume and specific mitochondria positioning between myofibrils. Sarcomeres in postnatal CMs are long and well-aligned, in contrast to shorter and disarrayed ones found in foetal CM. At a metabolic level, embryonic CMs rely on glycolysis, whereas adult myocytes preferentially consume fatty acids, a much more efficient energy source. Myofibrillar protein isoform undergoes switching, being

TABLE 1 | Full description of genes names.

Abbreviation	Description
MIXL1	Mix Paired-Like Homeobox
KDR	Kinase Insert Domain Receptor
MESP1	Mesoderm Posterior BHLH Transcription Factor 1
ISL1	Islet-1 LIM Homeobox
TBX5	T-Box Transcription Factor 5
NKX2.5	NK2 homeobox 5
GATA4	GATA Binding Protein 4
SMARCD3	SWI/SNF Related, Matrix Associated, Actin Dependent Regulator Of Chromatin, Subfamily D, Member 3
BX18	T-Box Transcription Factor 18

myosin heavy chain 7 (MYH7), myosin light chain 2 ventricular isoform (MLC2v), cardiac troponin I3 (TNNI3) and a shorter and stiffer Titin isoform, preferentially expressed in adult CMs, in contrast to myosin heavy chain 6 (MYH6), myosin light chain 2 atrial isoform (MLC2a), and slow skeletal-type troponin I1 (TNNI1) on foetal CMs (Bedada et al., 2014). All these differences directly correlate with contractile capacity, with adult CMs able to generate more force than embryonic ones (Vincent and Buckingham, 2010; Meilhac et al., 2014; Tan and Ye, 2018). For example, strips of adult rat myocardium have been reported to produce a peak twitch tension of 56.4 ± 44 mN/mm2, (Hasenfuss et al., 1991) whereas collagen constructs with neonatal rat CMs generated 0.4-0.8 mN/mm2 (Zimmermann et al., 2002). The same difference in magnitude is believed to exist for human cells, as comparisons with primary foetal human CMs are rare (Yang et al., 2014).

The cardiac action potential and associated channels and currents also distinguishes adult and foetal CMs. In immature CMs, the expression of channels involved in repolarisation, including potassium transient outward channels, L-type calcium currents and the rectifying K + current (encoded mainly by KCNJ2), is lower than in adult cells resulting in a less negative resting membrane potential (−50mv ∼ −60 mv in embryonic CMs) compared to normal (–85mv ∼ –90 mv in adult CMs) (Zhang et al., 2009). Also, the pacemaker current I_f is present in embryonic CMs but does not occur in adult myocytes (Sartiani et al., 2007). The distribution of the gap junction protein connexin 43 (Cx43) also plays an important role in regulating electrical activity. While Cx43 concentrates at the intercalated disc of adult CMs, it is circumferentially distributed in immature CMs, which is not optimal for longitudinal electrical propagation (Vreeker et al., 2014; Jiang et al., 2018). Adult CMs have a well-developed sarcoplasmic reticulum (SR) with a high level of SR-specific proteins like ryanodine receptor 2 (RYR2) and sarcoplasmic/endoplasmic reticulum Ca2 + ATPase 2a (SERCA2), (Ivashchenko et al., 2013) which, coupled with the presence of transverse tubules (t-tubules), leads to a highly coordinated Ca-induced-Ca-release and hence faster Ca transient kinetics and amplitude when compared to foetal CMs (Louch et al., 2015). Finally, where embryonic CMs are diploid, adult CMs present different degrees of polyploidy, achieved through DNA-synthesis without karyokinesis (Adler and Costabel, 1975; Herget et al., 1997). Understanding how an embryonic CM evolves into a mature cell is already proving fundamental in human cTE. As the bioartificial tissues developed so far resemble more their foetal counterpart, this insight is being incorporated into the effort of driving engineered tissues towards an adult-like functionality (Karbassi et al., 2020).

Heart Characteristics: What We Aim to Engineer

Generating human myocardial surrogates in the laboratory requires knowing what the natural composition and properties of the organ are. The following paragraphs provide an overview of what nature has achieved, specifically, what the main cellular and extracellular components of the heart are, how they are arranged in space, and importantly, what this means regarding the resulting material properties (**Figure 1**).

Cellular Composition

As already explained, most cells forming the structure of the heart are of mesodermal origin: CMs, vascular (endothelial and smooth muscle) cells and fibroblasts. Others reside in the tissue but are formed elsewhere, as immune cells, which play a significant role in organ surveillance and disease. Deciphering the cellular composition of the heart has been a very controversial subject, be it in rodents or humans (Zhou and Pu, 2016). Histology can determine that CMs are the largest fraction by volume. However, numbers vary, with reports of murine myocytes being the largest population by number [56/27/7 for CMs/fibroblasts/endothelial cells respectively (Banerjee et al., 2007)] and others attributing greater numbers to endothelial cells [43.6% vs 31% of CMs (Pinto et al., 2016)]. Human proportions are similarly contradictory, with some publications showing non-CM/endothelial cells are the most abundant (Bergmann et al., 2015) and others endothelial cells (Anversa et al., 1978). Furthermore, several studies have reported varying cell proportions throughout the anatomical regions of the organ (Sussman et al., 2002; Gaudesius et al., 2003; Camelliti et al., 2004, 2005; Kohl, 2004; Baudino et al., 2006). Things become more complicated if we take into account the age of the individual, as some claim the final number of myocytes is reached by one month, remaining constant over the lifetime of the individual (Bergmann et al., 2015) whereas others have reported a 3.4-fold increase in CM number between 1 and 20 years of age (Mollova et al., 2013). Other cell type numbers change dynamically over time, with a reported 6.5-fold increase in endothelial cells and an 8.2-fold increase for mesenchymal cells (including fibroblasts) during heart growth. Interactions between these cells are multidirectional and exert great influence over crucial aspects of cardiac biology. Both endothelial cells and fibroblasts are key for tissue function and homeostasis. Aside from delivering oxygen and nutrients to the metabolically demanding CMs, the endothelium is fundamental for tissue hypertrophy and post-disease remodelling, (Holopainen et al., 2015) and maturation, (Giacomelli et al., 2020) displaying a strong paracrine influence (reviewed in Leucker and Jones, 2014). Fibroblasts also affect organ function and cell maturity, (Woodall et al., 2016; Wang Y. et al., 2020) whilst other cell

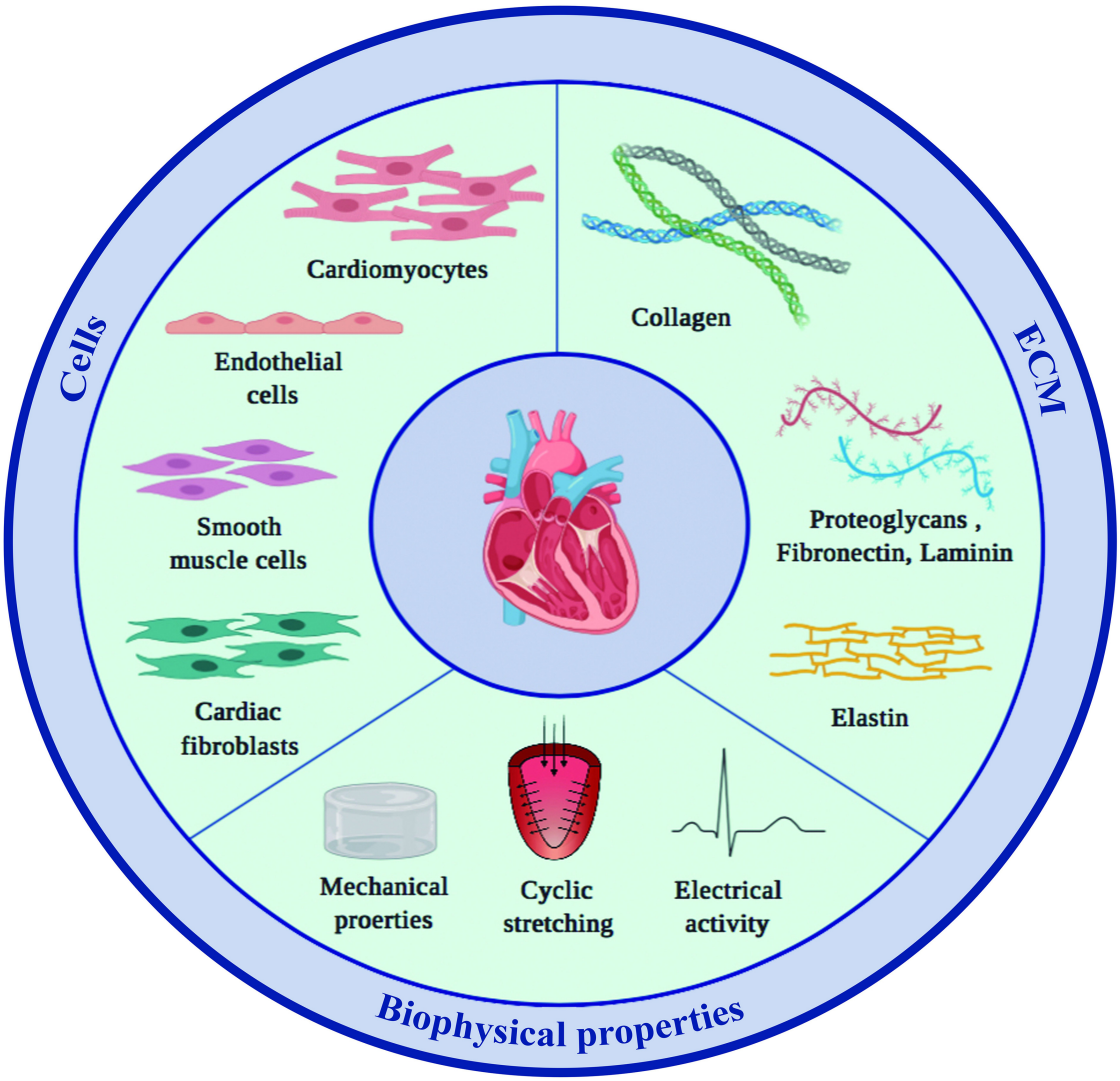

FIGURE 1 | Main components of the mammalian heart. The two main constituents of the myocardium, cardiac cells and the surrounding ECM, both contribute to and modulate the specific material properties of the tissue.

types, such as immune cells, have been reported to display direct and significant interactions with CMs, as is the case with the electrical coupling of macrophages with atrioventricular node cells (Hulsmans et al., 2017). All in all, the general consensus supported by unambiguous histological evidence is that CMs are the largest fraction by volume, each nurtured by a median of 3 capillaries, where fibroblasts constantly keep the ECM through a degradation-deposition equilibrium. This brings us to our next player: the cardiac ECM.

ECM Composition

The cardiac cell types discussed above are arranged within a glycoprotein matrix which supports and provides them with a structure. Moreover, the cardiac ECM also has an active role in transmitting contraction and avoiding hyper-stretching of CMs. Its principal component is collagen, which accounts for 2–5% of the total weight of the heart, mainly types I (89%) and III (11%). Collagen type IV is present in the basement membranes, and collagen type V is located in the pericellular space (Weber, 1989; Eghbali and Weber, 1990; Sommer et al., 2015a). The collagen matrix has classically been categorised depending on which elements it tethers together into endomysium (binds adjoining CMs), perimysium (aggregates myocytes into myofibrils) and epimysium (present at the epicardial and endocardial surfaces). Cardiac fibroblasts have been identified as the main cell type responsible for secreting and remodelling the collagen matrix, although CMs seem to contribute to collagen type IV deposition (Eghbali et al., 1988). Apart from the structural function, the collagen network makes an important contribution to the whole myocardial tensile properties (Fomovsky et al., 2010).

Another key element of the cardiac extracellular matrix is elastic fibres. These are composites, made of an elastin core

surrounded by a myriad of microfibrils. They provide elastic properties, by stretching upon mechanical demand and going back to their original length once the load is removed. Hence the importance of elastic fibres in tissues which have to accommodate their structure, such as skin, arteries or lungs or the heart. However, although elastic fibres are paramount for the heart's elasticity, other factors are known to have an influence upon it, namely the proportion of muscle bundles to fibrotic tissue, and the density of collagen crosslinking (Forrest and Jackson, 1971; Parmley et al., 1973). In fact, elastic fibres are found in most cases close to the collagenous network and in intimate association with it (Sato et al., 1983). Of note, mature elastic fibres show slight architectural differences depending on the tissue (Kielty et al., 2002). As aforementioned, elastin forms the core of elastic fibres. Unlike most matrix proteins, which undergo a constant/continuous deposition and turnover, in healthy conditions elastin is synthesised only until adolescence (Dubick et al., 1981; Burnett et al., 1982; Davidson et al., 1982; Myers et al., 1985; Sephel et al., 1987; Parks et al., 1988; Pollock et al., 1990; Ritz-Timme et al., 2003). Other fundamental components of the cardiac matrix include, to a lesser extent, laminin, fibronectin, proteoglycans and glycoproteins (Fan et al., 2012). Laminin molecules are part of the basement membrane and are thus in close contact with the cell, playing an active role in modulating cell behaviour, including migration, differentiation and phenotype stabilisation (Yap et al., 2019). Fibronectin, besides promoting cell attachment, acts as an ECM organiser and is involved in collagen deposition (Valiente-Alandi et al., 2018). However, all components are crucial for tissue integrity and function.

Many, if not all, cardiovascular diseases have repercussions for the cardiac ECM. The reverse is also true. For instance, infarction studies in pigs show that the collagenous network starts to become disarranged after just 20 min of coronary occlusion, whilst elastin begins to disappear after 40 min, and both components appear detached from the basement membrane after 120 min. The balance of collagens I and III has been widely studied, revealing a significant increase in type III collagen after myocardial infarction (MI) (Sato et al., 1983). Dilated cardiomyopathies, in which the shape of the cardiac cavity is abnormal, are at least partly related to aberrant collagen remodelling, with less thick collagen and thinner fibres, which results in weaker tensile properties, more muscle slippage and wall thinning (Weber et al., 1988; Weber, 1989). Ventricular hypertrophy consists of the thickening of the ventricular wall associated with some conditions like hypertension, and it is found together with overexpression of collagen in the form of interstitial fibrosis (Eghbali and Weber, 1990).

Cardiac Architecture

In most tissues, structure and function are closely intertwined, and the heart is no exception. However, certain aspects of this relationship are still under debate. The overall manner in which the heart contracts and pumps blood is known, as is the arrangement of the tissue microstructure. The gap lies in providing a theory that explains how the different architectural elements interact to produce the global behaviour. For example, there is an ongoing debate about whether the myocardium forms a single myocardial band, (Buckberg et al., 2015a,b) or the so-called myocardial mesh model is more accurate (MacIver et al., 2018a,b). The controversy has two aspects. On the one hand, there is no consensus on whether the basic functional unit is the CM, or groupings of this into bundles (groups of CMs), sheetlets (groups of bundles), sheets (groups of sheetlets) or even laminae (groups of sheets). On the other hand, although imaging techniques allow us to visualise phenomena across the whole myocardium, it is not feasible to ascertain the distinct contribution of the individual functional units to producing the global outcome. According to Buckberg et al., the CM can undergo six functional events: shortening, lengthening, narrowing, widening, twisting and uncoiling (Buckberg et al., 2015a, 2018). There are an estimated 2.5-10 billion cells (Bergmann et al., 2015) in the heart, each of them performing one or more of these six actions in the same or a different direction, and all we are able to see is the macroscopic effect: a torsion-contraction movement of the organ. Still under controversy, there are at least 7 proposed models to accurately describe cardiac architecture, (Gilbert et al., 2007) which is widely recognised to have a profound effect, whether at a mechanical (LeGrice et al., 1995; Zócalo et al., 2008) or electrical (Roberts et al., 1979; Taccardi et al., 2008) level. During disease, myocardial architecture is severely disarranged, leading to inefficient contraction (Roberts et al., 1987; Wickline et al., 1992). It is expected that the application of advanced technology like diffusion tensor MRI (DT-MRI), which can obtain highly detailed information on fibre architecture, will soon shed light on this debate (Scollan et al., 1998; Poveda et al., 2013).

At a simpler histological level, CMs (and CM bundles/sheetlets) are arranged in different orientations depending on their location in the organ, which in turn determines the direction of the stress produced. Myocytes are always in intimate contact with capillaries, which no doubt stems from the high metabolic demand of an ever-working muscular tissue: capillaries are located within 20 μm of CMs. Each CM is surrounded by a basement membrane containing laminin and collagen type IV, amongst others, and embedded in a highly structured ECM where collagen type I, as already discussed, is the main component (**Figure 2**). CMs connect to each other mainly by intercalated disks at their ends, but also through side branches, coupled to at least 2 CMs on the long axis and 1 laterally (Spach and Heidlage, 1995). Intercalated disks contain gap junctions, allowing fast current flow between neighbouring cells (Klabunde, 2012). As mentioned above, both individual CMs and groupings of these are surrounded by enveloping collagen. Fibroblasts do not participate in the electrical syncytium formed by the CMs, but rather lie in the interstitial space.

Cardiac Biophysical Properties

When attempting to engineer a tissue, it is essential to carefully recapitulate not only the cellular-extracellular components and their architecture, but also the resulting biophysical properties. These must reliably mimic those of their natural counterpart. In the heart, material properties are very complex: not only are they direction-dependent, but they also vary within the

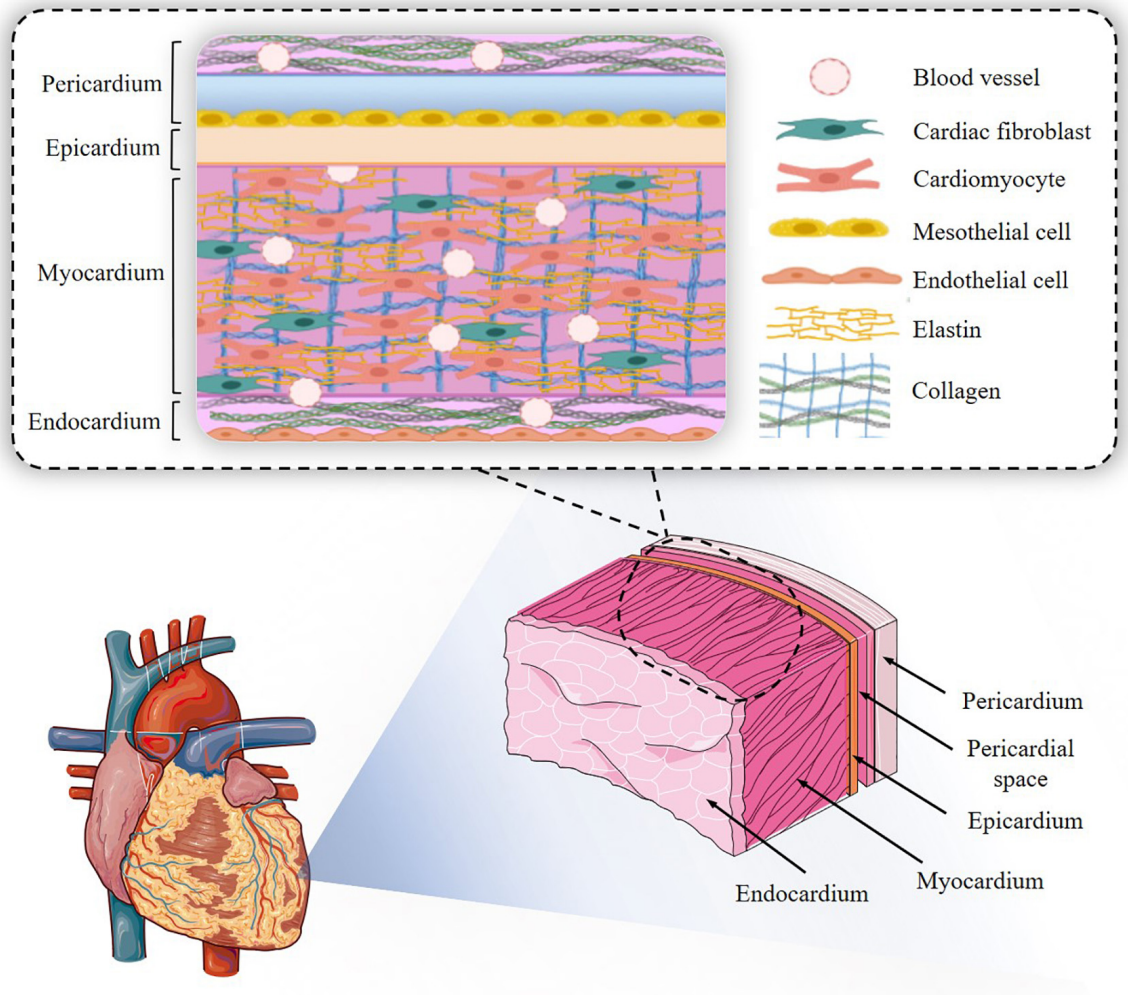

FIGURE 2 | Cardiac structure. The endocardial-to-pericardial structure is outlined, with the main cellular and extracellular components.

anatomical regions and the stage of the cardiac cycle. As an example, the literature reports variations in stiffness between the beginning and the end of diastole higher than an order of magnitude. For human LV, the reported values are 10-20 kPa at the beginning of the diastole, and 200-500 kPa at the end (Chen et al., 2008). Contraction itself results in a significant stiffening: from 0.5 to > 10 kPa. This magnitude is species-dependent, with a reported 3-fold increase in mouse, (Jacot et al., 2010) 2-fold in rat, (Prakash et al., 1999) and over 20 times in zebrafish (Krieg et al., 2008). Development also leads to a stiffening in the tissue, which arises from a relatively soft mesodermal layer (Krieg et al., 2008). Disease severely stiffens the organ, mostly due to the excessive deposition of collagen (scar for MI, interstitial in hypertension or other conditions), with values of over 50-100 kPa (Engler et al., 2008). Stiffness itself has a fundamental influence on how efficient CM contraction is, with CMs on softer- or stiffer-than-normal substrates doing little work or overstraining themselves, respectively (Engler et al., 2008). Reports on cardiac mechanical properties are extremely variable. This stems from a mix-up of animal vs human, fresh vs fixed, and healthy vs diseased data. In general, it is now accepted that most of the heart's passive mechanical properties are due to the collagen in the matrix, (Sommer et al., 2015a) but at short sarcomere lengths the protein titin is the predominant contributor (Nguyen-Truong and Wang, 2018). Quoting Sommer et al., 'results suggest that the passive human LV myocardium under quasi-static and dynamic multiaxial loadings is a non-linear, anisotropic (orthotropic), viscoelastic and history-dependent soft biological material undergoing large deformations' (Sommer et al., 2015b). Or in simpler words: it is very complex and with multiple contributions from cellular/extracellular components. Added to this, scales differ, depending whether the tissue is macroscopically characterised using biaxial mechanical tests, (Sommer et al., 2015b) or whether isolated CMs are probed at a cell-relevant scale with Atomic Force Microscopy (AFM) (Andreu et al., 2014). Furthermore, some conflicting results have been reported, from reports showing force production from CMs to be increased with increasing stiffness, (Bhana et al., 2010) to stiffness having

no influence at all (Jacot et al., 2008). In fact and as explained by Domian et al. (2017), it might even be the case that the material properties of cardiac tissue are not the main actor in the myocardial scenario, but this role is rather played by chamber pressure. More experimental and theoretical work needs to be done in this area before we reach a definitive conclusion.

Adding another layer of complexity, the heart has constant, potent and highly relevant electrical activity. Sparking at a small and specialised region called the sinoatrial node, the electrical wave travels through the auricles, reaching the atrioventricular node where it is delayed (allowing for the filling of the ventricles), and then spreads apex-to-base through the ventricles in a coordinated manner. All this process is controlled by a singular CM type, termed pacemaker cell, displaying disarrayed sarcomeres and low work generation capacity, but able to autonomously start the cardiac action potential. Ultimately, the action potential results in the entry of Ca^{+2} ions into the CM, releasing the sarcoplasmic stores of Ca^{+2} and freeing myosin of the inhibitory action of troponin I. CMs are also electrically connected through connexins, which form bridges between the cytoplasm of adjacent myocytes, effectively making the myocardium an electrical syncytium. However, it is an anisotropic one, with faster propagation in the direction of the fibres as opposed to the transverse direction (Chung et al., 2007). Conduction velocity is the speed with which the cardiac impulse travels from one point in the tissue to another. In adulthood, it lies in the range of 0.3-1 m/s, but developmental stage and disease will affect it (Yang et al., 2014). Achieving a similar value in any cardiac engineered tissue is paramount, given the fact that a mismatch between conduction velocities may give rise to potentially fatal electrical abnormalities such as arrhythmias (Kadota et al., 2013; Zhang et al., 2018). It is interesting that one of the foci in cTE is towards providing material-based electronic conductivity, although cardiac cells do not function by transmitting electrons but ions.

As mentioned already, both the mechanical and electrical properties exert a strong influence upon myocardial biology and function, in both health and disease. For example, increased fibrosis due to pathological conditions like MI or hypertension significantly stiffens cardiac muscle and affects CM contraction (Sessions and Engler, 2016). Ventricle loading induces CM elongation which, as explained by the Frank-Starling law, renders higher stroke with increase diastolic filling (Solaro, 2007). The coordinated conduction of the depolarisation wave throughout the organ, including the atrioventricular delay and the apex-to-base transmission, all contribute to optimal functionality and must be taken into account when engineering a human myocardium.

ENGINEERING CARDIAC TISSUE: THE BUILDING BLOCKS

cTE aims to generate tissue surrogates, either micro or macro, for various purposes, from developmental biology, (Young and Engler, 2011) to therapy (Miyagawa et al., 2018). In the following paragraphs, we will outline the main cells and materials, as well as the different fabrication technologies assayed in the field and the procedures for their maturation. **Table 2** summarises some of the most relevant engineered myocardium examples, with a focus on human cardiac tissue.

Cells

The capacity to obtain human cardiac cell phenotypes in the laboratory began with the derivation of human embryonic stem cells (hESC) by Thomson and colleagues in 1998, (Thomson et al., 1998) which was soon followed by the first protocols for differentiation towards CMs (Mummery et al., 2003; Kattman et al., 2006). In 2006, thanks to the breakthrough of the reprogramming technology (Takahashi and Yamanaka, 2006; Yu et al., 2007) it became possible to relieve the field of some of its most notorious encumbrances, including the ethical ones. Both, hESCs and human induced pluripotent stem cells (hiPSC) fall within the wider category of human pluripotent stem cells (hPSC). Current methods, including scaling up protocols, (Serra et al., 2011) have paved the way for their widespread use. In general direct, efficient and reproducible hPSCs differentiation methods try to recapitulate embryonic development, from the induction of cardiac mesoderm, to CM, endothelial cells (ECs), cardiac fibroblast (CFs) or smooth muscle cells (SMCs) *in vitro* specification and maturation (**Figure 3**) (Burridge et al., 2015).

According to the culture format employed, derivation of CMs, CFs, ECs and pericytes/SMCs from hPSCs can be categorised into 3 main approaches: (i) inductive co-culture with visceral endodermal-like cells, (ii) suspension aggregates such as three dimensional (3D) embryoid bodies (EBs) and (iii) two-dimensional (2D) cell monolayer differentiation (Mummery et al., 2003; Kattman et al., 2006; Laflamme et al., 2007; Moretti et al., 2010). Early reports showed that co-culturing hPSCs with the mouse endodermal cell line END2 was able to induce beating foci (MacIver et al., 2018a). The low efficiency of this method, as well as the need for xenogenic co-culture, precluded its widespread application. EBs are formed by culturing dissociated hPSC in non-adherent plastic dishes and partially recapitulate the 3D structure and interactions of a developing embryo. hESC-EBs differentiate to derivatives of the three primary germ layers, resulting in spontaneously contracting outgrowths of human CM (Kehat et al., 2001). Based on EB differentiation protocols, CM from a variety of hESC and hiPSC lines have been generated, usually with a purity of $< 10\%$ (Zhang et al., 2009). ECs can also be isolated from spontaneously differentiating EBs, at a similarly low yield ($\approx$2%) (Levenberg et al., 2002). In both cases, early reports explored the addition of cardiac mesoderm-inducing growth factors, including FGF2, VEGF BMP4, Activin A, Wnt agonists (WNT3A) or antagonists (DKK1), amongst others (Yuasa et al., 2005; Kattman et al., 2006, 2011; Yang et al., 2008; Tran et al., 2009; James et al., 2010). In general, however, EB-based differentiations have lost ground to more advanced and defined procedures, as the former are generally inefficient and render a mixture of cardiac cells with other non-cardiac phenotypes, requiring additional purification.

Monolayer-based differentiation is nowadays the most usually applied method. Cytokine-based protocols were developed first (Taccardi et al., 2008). These have been progressively modified

TABLE 2 | Summary of materials, cells and methods employed to engineer cardiac tissues, their biomimicry and resulting outcome.

REF	Materials		Fabrication	Cellular mimicry				Material mimicry			Maturation		Benefit of the selected approach?			
	Hydrogel	Fibres		CM	EC	SMC	CF	Mech.	Elect.	Align	Mech	Elec	vs.	Gene exp.	Structure	Function
Godier-Furnémont et al., 2015	Col I	–	Mould casting		Rat neonatal			Yes	No	No	+	+	NM	nd	+	+
Hirt et al., 2014	Fibrin	.	Mould casting		Rat neonatal			Yes	No	No	+	+	EHT	+	+	+
Jackman et al., 2018	FGN	–	Mould casting		Rat neonatal			Yes	No	No	+	–	NM	+	+	+
Amdursky et al., 2018	Albumin	–	Mould casting		Rat neonatal			Yes	No	No	–	–	2D	+	+	–
Nunes et al., 2013	Col I	–	Mould casting	hPSC				+	–	–	–	+	NM	+	+	+
Ruan et al., 2016	Col I	–	Mould casting	hPSC				+	–	–	+	+	EHT	+	+	+
Tiburcy et al., 2017	Col I	–	Mould casting	hPSC			FK	+	–	–	+	–	2D	nd	+	+
Valls-Margarit et al., 2019	Col I + ELN	–	Mould casting	hPSC			FK	+	–	–	+	+	2D	nd	+	+
Zhang et al., 2013	Fibrin	–	Mould casting	hPSC				nd	–	–	–	–	2D	+	+	+
Hirt et al., 2014	Fibrin	.	Mould casting	hPSC				+	–	–	+	+	EHT	+	+	+
Weinberger et al., 2016	Fibrin	–	Mould casting	hPSC	hPSC			+	–	–	+	–	NM	nd	–	–
Ulmer et al., 2018	Fibrin	–	Mould casting	hPSC				+	–	–	+	–	2D	–	+	nd
Ronaldson-Bouchard et al., 2018	Fibrin	–	Mould casting	hPSC			DF	+	–	–	+	+	2D	+	nd	nd
Jackman et al., 2016	FGN	–	Mould casting	hPSC				+	–	–	+	–	NM	nd	+	+
Shadrin et al., 2017	FGN	–	Mould casting	hPSC	hPSC	hPSC		+	–	–	+	–	NM	+	–	+
Dattola et al., 2019	PVA*	–	Foaming + FD	hPSC				+	–	–	–	–	2D	nd	–	nd
Han et al., 2016	–	PCL	SE	hPSC				–	–	+	–	–	2D	+	+	–
Joanne et al., 2016	–	Col I	SE	hPSC				+	–	–	–	–	NM	nd	+	+
Sireesha et al., 2015	–	POCS–FGN	SE	hCM				+	–	–	–	–	2D	nd	+	nd
Khan et al., 2015	–	PLGA	SE	hPSC				–	–	+	–	–	2D	–	+	–
Roshanbinfar et al., 2020	–	Col I/HA/PANi	SE	hPSC				+	+	–	–	–	EHT	nd	+	+
Macqueen et al., 2018	–	PCL/Gelat	Pull spinning	hPSC				+	–	+	–	–	2D	nd	+	+
Castilho et al., 2018	Col I	PCL	MEW	hPSC				–	–	–	–	–	2D	+	+	nd
Vaithilingam et al., 2019	PETra + MWCNT		3DP–SLA	hPSC				No	+	+	–	–	2D	nd	+	nd
Lee et al., 2019	Col I	–	3DbioP	hPSC			CF	+	–	–	–	–	NM	nd	+	–
Maiullari et al., 2018	FGN/PEG	–	3DbioP	hPSC	HUVEC			nd	–	–	–	–	EHT	nd	+	nd
Noor et al., 2019	dECM	–	3DbioP	hPSC	hPSC			+	–	–	–	–	NM	nd	+	+
Arai et al., 2018	–	–	3DbioP	hPSC	HUVEC		DF	nd	–	–	–	–	EHT	nd	+	nd

*REF, Reference; CM, Cardiomyocyte; EC, Endothelial cell; SMC, Smooth muscle cell; CF, Cardiac fibroblast; Mech, mechanical; Elec, electrical; Gene exp., Gene expression; Col I, collagen type I; FGN, Fibrinogen; hPSC, human pluripotent stem cell; FK, Foreskin fibroblast; DF, Dermal fibroblast; PVA, poly-vinil-alcohol; FD, Freeze-drying; *, foam; SE, Solution electrospinning; POCS, poly[1,8-octanediol-co-(citric acid)-co-(sebacic acid)]; hCM, primary human CM; PLGA, polylactide-co-glycolide; PCL, polycaprolactone; Gelat, Gelatin; PETrA, pentaerythritol triacrylate; MWCNT, Multi-walled carbon nanotubes; 3DP,3D Printing; SLA, Stereolithography; PEG, polyethylene glycol; ALG, Alginate; 3DbioP, 3D bioprinting; nd, not described; dECM, decellularised extracellular matrix; ELN, elastin; HA, Hyaluronic acid; PANi, polyaniline; NM, native myocardium; EHT, engineered heart tissue.*

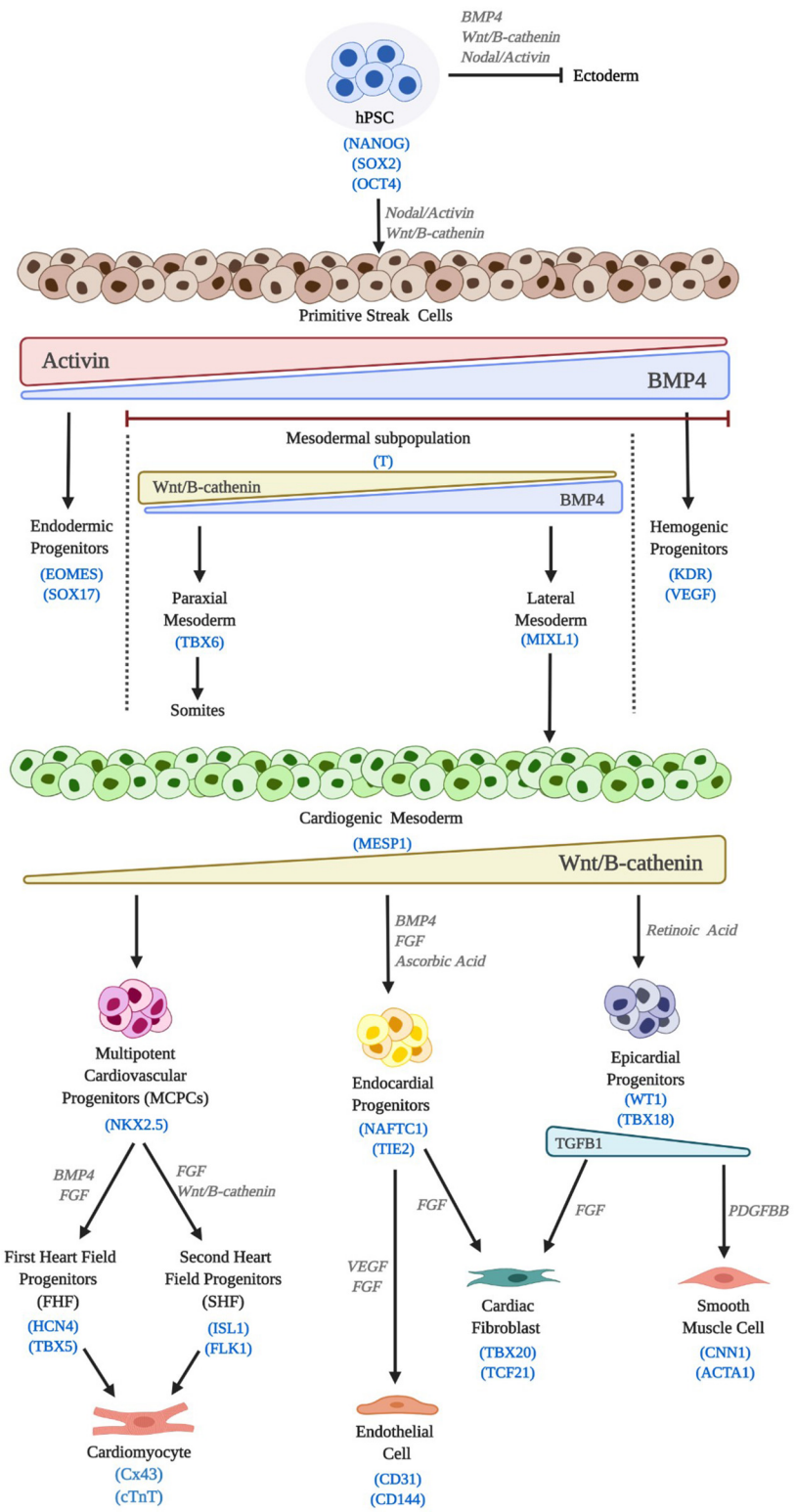

FIGURE 3 | Cardiac differentiation of hPSC. hPSC differentiation *in vitro* mimics embryonic development. Induction signals, main molecular pathways and lineage markers are outlined.

by the discovery of Wnt signals playing a biphasic role in cardiac differentiation *in vivo*, (Marvin et al., 2001; Ueno et al., 2007) with early signals directing hPSCs towards cardiac fate, whilst later inhibition of those signals is a prerequisite for CM specification. Almost 10 years ago, this concept was incorporated into the CM differentiation from hPSCs, (Lian et al., 2012) paving the way for the grounding of a chemically defined procedure (Burridge et al., 2014). Based on small molecules rather than cytokines, and thus less costly, this protocol is now widely applied, providing highly pure yields of hPSC-derived CMs when in combination with a metabolic-based selection (Tohyama et al., 2013). This means that complicated and inefficient EB-forming procedures or expensive and time-consuming immune-selection protocols have now been discarded (Burridge et al., 2007; Hattori et al., 2010; Elliott et al., 2011; Uosaki et al., 2011). However, even this latest protocol still requires a degree of set up to avoid inconsistent efficiencies amongst cell lines and experimental repeats, mostly related to different patterns of endogenous early canonical Wnt expression (Paige et al., 2010). In general, CMs obtained from these protocols consist of a mixture of pacemaker, atrial and ventricular myocytes, though some researchers consider that this is open to question, as hPSC-CMs are immature and intrinsically plastic (Du et al., 2015).

The derivation of other cardiac phenotypes has been also achieved, with a variety of protocols now available. Palpant et al. reported the generation of CMs, cardiac- or hemogenic-derived ECs as well as blood cells by finely dosing BMP4 and Activin A in order to pattern hPSC towards different mesodermal fates (Palpant et al., 2017). Others have employed a mixture of small molecules and cytokines to derive vascular cells from hPSCs in monolayer culture with high efficiency (Orlova et al., 2014; Patsch et al., 2015). Global gene transcription analysis has demonstrated low variability between ECs differentiated via cytokine-based methods from multiple lines of hPSCs (White et al., 2013). CFs, have been increasingly recognised as major players in cardiac development and homeostasis, having a similarly significant effect upon the capacity to build cardiac tissues in the lab. Recently, two independent groups have reported the generation of hPSC-derived CFs, giving also proof of their capacity to affect hPSC-CM function (Zhang H. et al., 2019; Zhang J. et al., 2019). Epicardial cells have similarly been derived, (Witty et al., 2014) demonstrating their ability to increase the therapeutic capacity of hPSC-CMs *in vivo* (Bargehr et al., 2019). Finally, sinoatrial node pacemaker CMs have been obtained from hPSC, and their capacity to pace tissues *in vivo* has been reported (Protze et al., 2017). Other approaches to the differentiation of cardiac lineages include the generation of CVPs, (Blin et al., 2010; Birket et al., 2015; Zhang Y. et al., 2016) or direct reprogramming strategies, (Mohamed et al., 2017) but they have rarely been explored in cTE.

Materials

In parallel to the way differentiation of hPSC mimics the natural embryonic development, the current view is that the more a material replicates the properties of cardiac tissue, the higher the chances of success. Development over the last 15 years has yielded a wide portfolio of materials and biomaterials. Classifications are numerous, be it by origin (natural, synthetic or hybrid), crosslinking (chemical vs physical), size (macro, micro or nano), polymerisation mechanism (enzymatic, light-triggered or pH-responsive) or whether they are or not reinforced with other structures like fibres. For specific insight into these classifications, we direct the reader towards some of the excellent latest papers (Peña et al., 2018; Liu et al., 2019; Xu et al., 2019). One of the most relevant classifications is, however, on the physical consistency of the applied material, where we can differentiate (i) injectable materials and hydrogels, (ii) solid or fibrous scaffolds and (iii) composite systems.

Hydrogels are probably the most widely explored type of material in cTE. Collagen, being the main component of the cardiac ECM, has been widely employed (see the following sections). It can be readily isolated from animal or even human tissues in sufficient quantities, extracted and solubilised, although it requires acidic pH for this. Therefore, a careful control over pH is needed for optimal polymerisation and embedded cell survival. Gelatin, being denatured/digested collagen, has also been intensely explored and the basis for the generation of some of the most applied semi-synthetic materials, such as gelatin methacryloyl (GelMA)(Yue et al., 2015) and several biorthogonal derivatives (Koshy et al., 2016; Bertlein et al., 2017). Alginate, a sugar-based natural hydrogel obtained from algae, (Orive et al., 2006) has been employed due to their tailorable mechanical properties and simple polymerisation, mediated by cations such as Ca or Mg, albeit lacking biological binding motifs. Silk and its derivatives have also been processed into hydrogels, (Holland et al., 2019) and modified to incorporate electrically active particles (Barreiro et al., 2019) or photocrosslinkable chemical groups (Cui et al., 2020). Allergic and anti-inflammatory side reactions have been reported with some silk derivatives, so care should be taken when incorporating them into an engineered tissue. Amongst natural hydrogels, decellularised ECM (dECM) has attracted significant interest since the breakthrough discovery of the process, as applied to the building of tissues (Ott et al., 2008; Belviso et al., 2020). In principle, dECM retains all components of the ECM of origin, thus creating a more complex and biomimetic environment. Garreta et al. obtained human dECM slices on which they cultured hPSC-CMs. The human CMs demonstrated enhanced conduction velocity and gene expression of related genes (SERCA, KCNJ2, CACNA1C or SCN5A amongst others) (Garreta et al., 2016). The group of Lior Gepstein employed dECM-chitosan mixtures in combination with hiPSC-CMs. The resulting engineered myocardium displayed enhanced maturity as compared with cells cultured in 2D, showing tissue-like drug responses. Their work also provided proof-of-concept of the capacity of this system to model human cardiac diseases (Long QT syndrome) and arrhythmias (Goldfracht et al., 2019). On the synthetic side, polyethylene glycol (PEG) and its several modifications have been extensively studied in the TE field (Iyer et al., 2009).

Most of the materials so far outlined in this section can be processed into fibres employing strategies explained in the next section. Thermoplastics have also been applied to cTE, mostly as fibrous scaffolds. Examples include poly-ε-caprolactone (PCL), (Woodruff and Hutmacher, 2010) or elastomers like poly (glycerol-sebacate) (PGS) (Kharaziha et al., 2013). Conductive

polymers have only recently began to be applied to the field, though some of the most remarkable examples have not incorporated the use of cells and would therefore not qualify as engineered tissues (Mawad et al., 2016; Kapnisi et al., 2018). Finally, given the low mechanical properties displayed by most hydrogels, composite fibre-reinforced materials are also being developed, (Bas et al., 2015) with some examples explained in the following section.

Maturation Stimuli

Cells derived from hPSC are immature (see Karbassi et al., 2020 for a review). Although not the direct focus of this work, neonatal myocytes, which are another cell source commonly employed, also suffer from this drawback. cTE has long been aware of this limitation and has applied three main stimuli, namely physical, mechanical and electrical, and combinations thereof Parsa et al. (2016) and Stoppel et al. (2016). Perfusion is able to improve engineered tissues' properties, as it will boost nutrient access and renewal, as has been shown for neonatal cells (Radisic et al., 2004b) as well as hiPSC-cardiac derivatives (Valls-Margarit et al., 2019). Materials' physical properties (e.g., stiffness) are able to induce maturation features in these CMs, or at least preserve primary CMs from dedifferentiation (Amdursky et al., 2018). In general, most hydrogels are able to replicate the right myocardial-like properties. For example, Feaster and colleagues found that plating hiPSC-CMs on thick Matrigel induced a certain degree of molecular and functional maturation, in comparison to thin, diluted hydrogel coating, which essentially transmits the rigidity of the underlying plastic (Feaster et al., 2015). Herron et al. employed soft (albeit supra-cardiac) substrates and compared them with glass in their capacity to influence hiPSC-CMs, with a significant effect on maturation, showing improvement in the expression of Na and K channels, as well as on the degree of binucleation, cell cycle exit and hypertrophy (Herron et al., 2016). Although not purely based on engineered tissues, they and others give proof of the crucial role stiffness plays in cardiac maturation.

Mechanical stimulation has a leading role in cardiac development and aging (Happe and Engler, 2016; Sessions and Engler, 2016). It can be isometric, isotonic or auxotonic (Liaw and Zimmermann, 2016). In isometric stimulation, the construct is preloaded and must exert force against a static load. In isotonic stimulation, a device will cyclically exert active elongation on the engineered tissue. Finally, auxotonic stimulation occurs when the myocardial tissue has to contract against a resilient load. In principle, the auxotonic mode confers a more physiological stimulation, although all three are reported to deliver maturation upon engineered myocardium (Godier-Furnémont et al., 2015; Lux et al., 2016; Ruan et al., 2016; Ulmer et al., 2018). Although the exact mechanisms by which mechanical stimulation matures the cardiac engineered tissue are not known in depth, it is presumed that they will operate by the same ones occurring during cardiac development or physiologic hypertrophy (Nakamura and Sadoshima, 2018). After all, being a striated muscle, the myocardium can undergo hypertrophy if exercised (Kim et al., 2008).

As an electro-sensitive organ, the heart can be stimulated by electrical pulses, which can help maintain its function *ex vivo* (Watson et al., 2019). Electrical stimulation is known to have a relevant effect on hPSC-CM differentiation and maturation. Over 20 years ago, Sauer et al. established a relationship between this stimulation and mouse ESC differentiation to CM (EB method). They showed the effect was at least partly mediated by reactive oxygen species (ROS) generation and NF-κB, and could be replicated by ROS from H_2O_2 incubation (Sauer et al., 1999). Serena et al. analysed the effects of the type of electrode and stimulation length on CM differentiation via the EB method from hESC, finding a role for ROS, though the effect on the efficiency of differentiation was not determined (Serena et al., 2009). Hernández et al. employed brief (5 min) electrical stimulation, of hiPSC-EBs, finding an increase in the percentage of cardiac differentiation (% of beating EBs) after 14 days (Hernández et al., 2016). However, the use of the EB method complicates findings, as the effect could also be mediated by other cell types within the EB. Electrical stimulation has also been shown to enhance hPSC-CM maturation at the gene expression and functional levels (Ca transients), as well as promoting the ventricular phenotype (Chan Y. C. et al., 2013). Reasoning that exogenous electrical stimulation would act as an artificial pacemaker, Richards and coworkers evaluated the implementation of electrically conductive silicon nanowires in hiPSC-derived cardiac spheroids, showing that it was able to improve CM-to-CM communication (measured by staining for Connexin 43 and N-cadherin) and structural quality, though some of these quantifications might nowadays be regarded as debatable (Richards et al., 2016). The cTE field has implemented electrical stimulation to cardiac constructs with success. The group of Gordana Vunjak-Novakovic pioneered work in this area, showing the enhanced of contraction (synchronicity) and structure (alignment, ultrastructure) on neonatal rat CMs seeded on Ultrafoam collagen sponges and Matrigel (Radisic et al., 2004a). The group developed stimulation protocols as well as bioreactors, (Tandon et al., 2008, 2009; Massai et al., 2013) which have influenced the whole field. The group of Milica Rasidic built hPSC-based cardiac tissues by embedding hPSC-dissociated EBs in collagen type I and Matrigel. After electrical stimulation, they showed an increased myofibril ultrastructural organisation and improved function (conduction velocity and Ca handling properties) as compared to non-stimulated controls (Nunes et al., 2013).

Finally, some remarkable advances have been made when combining electrical and mechanical stimulation. Ruan et al. generated collagen-based cardiac engineered tissues containing hPSC-CMs, which were subjected to electromechanical stimulation and compared to static stretch or no stimulus. Results showed a positive Frank-Starling effect (increased force production with increased preload), a less negative force-frequency relationship (increased force production with increased pacing frequency) and maximum stress generation for the electromechanical stimulation group, which was correlated with increased expression of RYR2 and SERCA2, thus supporting the use of combined stimulation for enhanced maturation (Ruan et al., 2016). The group of Dr. Zimmermann employed auxotonic stimulation delivered through stretchers in combination with electrical pacing at 0, 2, 4, or 6 Hz

(Godier-Furnémont et al., 2015). Results on tissues generated with collagen and neonatal rat cells showed that the 4 Hz regime was able to generate tissues with a physiological and positive force-frequency and enhanced functionality. Also, the presence of T-tubules was demonstrated. Finally, the group of Prof Vunjak-Novakovic generated hiPSC-CM-based collagen tissues on flexible stretchers (auxotonic mechanical stimulation) and supplied no stimulation (control), 2 Hz and 0.33 Hz/day progressive increase over 2 weeks ('intensity training'). Their results demonstrated the effectiveness of this strategy, as shown by a physiological sarcomere length, increased density of mitochondria, T-tubules, a more mature metabolism and functional improvements at the level of Ca cycling and a positive force-frequency relationship (Ronaldson-Bouchard et al., 2018).

Fabrication Strategies

Materials confer cTE with significant options, not only due to the available range, but also through the application of different fabrication modalities, which can deliver different properties out of the same starting material. For example, collagen can be mould-casted, (Godier-Furnémont et al., 2015) extruded, (Araña et al., 2014) or bioprinted, (Lee et al., 2019) and the resulting properties will vary widely, with casted and bioprinted collagen having a stiffness in the range of kPa, whilst the extruded film will be significantly stiffer (MPa). In addition, structure will also differ. 3D printing and bioprinting have no doubt revolutionised our capacity to engineer cardiac tissues, however, other technologies can provide relevant features. The following paragraphs outline some of the most employed strategies, classified depending on their capacity to produce a controlled architecture (**Table 3**).

Techniques With No True Architecture Control

Mould casting

Probably the simplest and most widely employed fabrication mode, requires the generation of a mould of the desired shape, and is the fabrication technique of choice in many biomedical-based laboratories, where other methods could not be implemented due to lack of expertise or specific equipment. It does not provide much control over the resulting architecture, but can be combined with others, like porogen leaching, to add specifically selected features to the resulting tissue. The first reports on engineered cardiac tissues by Thomas Eschenhagen and coworkers in the late 1990s were developed by mould-casting a mixture of chick embryonic CMs embedded in a collagen solution. This was allowed to gel between two Velcro-coated glass tubes. The resulting tissues, later termed engineered heart tissues (EHTs), could be cultured *in vitro* and maintained over several days, responded to electrical stimulation, displayed a positive Frank-Starling relationship, were sensitive to levels of extracellular calcium, and could be modified with viral vectors (Eschenhagen et al., 1997; Zimmermann et al., 2000).

Since then, the technology has evolved enormously. It was expanded to neonatal rat cells, (Zimmermann et al., 2002) and refined, with the possibility of fabricating more complex and thicker EHTs, which functioned synchronously (Zimmermann et al., 2006). These stacked EHTs also showed promise as a therapy when transplanted in a rat model of infarction. EHTs have been employed by the groups of Eschenhagen and Zimmermann, either fibrin- or collagen type I-based, to study the effect of chronic stretch on CM hyperthrophy, (Fink et al., 2000) as a disease model of hypertrophic cardiomyopathy, (Stöhr et al., 2013) or to analyze the effect of electrical stimulation (Hirt et al., 2014). EHT technology has greatly benefited from the implementation of hPSC-derived cells, as the findings, models and application have gained greater impact, be it as a drug testing platform (Eder et al., 2016), an *in vitro* tool to study cardiac stimulation, (Godier-Furnémont et al., 2015) or as a potential myocardial regenerative therapeutic (Weinberger et al., 2016; Tiburcy et al., 2017). The Bursac group has also employed mould casting of rat and human (hiPSC-derived) cells to engineer cardiac tissues and explore different strategies to mature them *in vitro* (Jackman et al., 2016). They applied this strategy to fabricate tissues up to human scale, though thickness was limited by nutrient and oxygen diffusion. When assayed in a rat model of disease, their cardiopatches retained integrity after 3 weeks, showing extensive vascularisation by host-derived vessels and maintaining electrical activity, although they did not functionally integrate with the endogenous myocardium (Shadrin et al., 2017). The team of Milica Radisic employed PDMS moulds to form engineered cardiac tissues around a surgical suture, composed of hPSC-derived cardiac cells, collagen type I and 10% Matrigel (Nunes et al., 2013). By employing electrical stimulation, through carbon rods immersed in the culture medium, they were able to drive the hPSC-CMs towards a more mature phenotype and functionality. This system was later applied also to drug testing (Feric et al., 2019). Finally, one of the most advanced pieces of evidence for hPSC-CM maturation *in vitro* was provided by the group of Gordana Vunjak-Novakovic, as explained in the previous section (Ronaldson-Bouchard et al., 2018). They employed a 3:1 mixture of hPSC-CMs and dermal fibroblasts embedded in a fibrin matrix, cast into wells where flexible PDMS posts were also included. These conferred pre-tension on the generated engineered myocardium, thus adding physiological-like auxotonic stimulation (Mannhardt et al., 2019). A set of custom-made carbon electrodes delivered electrical stimulation. The resulting bioartifical myocardium displayed adult-like gene expression profiles, ultrastructural features such as M-bands and T-tubules, as well as oxidative metabolism and mature functionality. In summary, although mould casting cannot generate fine features, it is one of the most widely applied and highly evolved methods to obtain human mature cardiac tissue, and the one closest to translation.

Macro-to-micro pore-forming strategies

Cryogelation, based on freeze drying, is a common preservation strategy that is also applied to TE. The pre-crosslinked material is subjected to freeze-thawing cycles, which induces ice crystal formation. These crystals act as porogens, to be removed when pressure is decreased and the solvent sublimated. In general, pores are well inter-connected, as demonstrated early on by O'Brien and colleagues for collagen-glycosaminoglycans scaffolds (O'Brien et al., 2004). In addition, varying conditions make it possible to modulate material properties, as shown by

TABLE 3 | Summary of fabrication methods, advantages and disadvantages.

		Fabrication technique	Advantages	Disadvantages
No true architecture control	Mould casting	Mould casting (Janik and Marzec, 2015)	– Simplicity and cost – High cell survival – Range of compatible materials – Mechanical properties – Scale up feasible	– Lowest architectural control – Limited thickness
	Pore-forming	Solvent Casting, Particle Leaching, Cryogelation (Janik and Marzec, 2015)	– Control of pore size – No specialised equipment – Cost	– Use of organic solvents – Limited scaffold thickness – Mechanical properties – Time consuming leaching – Limited pore architecture
	Electrically produced	SE (Liang et al., 2007)	– Nanometer features – Range of compatible materials – Scaling up feasible	– Use of organic solvents – Limited scaffold thickness – Usually produces high stiffness substrates
	Textile-based	Weaving, Braiding, Knitting (Akbari et al., 2016)	– Simple – Scaling up feasible	– Specialised equipment (cost) – Not widespread – Limited porosity
True architecture control	Build & seed	SLA (Melchels et al., 2010)	– High architectural control – Self-supporting process	– Only photosensitive polymers – Remove supporting materials – Use of UV light – Toxicity of photoinitiator – Specialised equipment (cost)
		SLS (Mazzoli, 2013)	– No solvents required – High architectural control – Self-supporting process – Range of compatible materials	– High temperature – Materials in powder form – Rough surface – Specialised equipment (cost)
		MEW (Brown et al., 2011)	– No solvents required – Control over porosity, pore size and fibre diameter – High architectural control	– Limited thickness – Range of available material – Specialised equipment (cost)
		FDM (Moroni et al., 2006)	– No solvents required – Speed of printing – Good reproducibility	– Restricted to materials with good melt viscosity properties – High temperature – Filament required – Limited resolution
	Bioprinting	LGDW, LIFT, BioLP (Koch et al., 2010; Gaebel et al., 2011; Hu et al., 2017)	– Range of cells/biomaterials – Single cell resolution – Precise cell printing	– Low cell viability – Limited 3D structure – Time consuming
		3DbioP (Zhang et al., 2015)	– Range of cells/biomaterials – High cell viability – Process at room temperature	– Weak structural support – Specialised equipment – Multimaterial printing expensive (multinozzle)

SE, Solution electrospinning; LGDW, Laser-guided direct writing; LIFT, Laser Induced Forward Transfer, BioLP, Bio-laser Printing; 3DbioP, 3D bioprinting; SLA, Stereolithography; SLS, Selective laser sintering; MEW, Melt Electrospinning Writing; FDM, Fused deposition modelling.

Kim et al. (2015). In combination with gas foaming, Dattola et al. fabricated a poly(vinyl) alcohol scaffold with pores within the size of CMs, and Young's Modulus similar to that of the native cardiac ECM. These substrates are able to support the growth and cardiac differentiation of hiPSC, albeit at apparently low rates as demonstrated by the immunostaining for cardiac proteins (Dattola et al., 2019).

Gas foaming has also been extensively applied to TE, though its use within the cardiac field is not extensive. This technique relies on the formation of bubbles, either by adding exogenous agents such as sodium bicarbonate or through the inclusion of enzymatic-driven reaction in the fabrication process (Mooney et al., 1996). As the solution polymerises, these bubbles are trapped inside. In consequence, the choice of foaming agent is crucial for the later survival of cells. Although relatively simple to implement, this technique provides no control over the degree of interconnection between the formed pores or their directionality.

Porogen templating is based on the inclusion of salt crystals in the pre-polymer solution. Similar to freeze drying, these crystals will act as templates, creating an empty space (pore) when the particles are leached out, in most cases by dissolving in aqueous solution, weak bases or heating, (Thomson et al., 1995) with sodium chloride being one of the most frequently employed porogens. On the down side, limitations are related to

low architectural control and suboptimal processing of porogens, which might compromise biocompatibility as well as mechanical properties. Salt leaching has not been as widely employed in cTE as in other areas. Ganji et al. used table salt as a simple yet efficient way to generate defined pores in polyurethane-based scaffolds where gold nanotubes and nanowires were incorporated, thus combining 3-dimensionality with the additional benefit of electrical conductivity (Ganji et al., 2016). Biocompatibility tested with H9c2 rat cardiomyoblasts showed a positive effect on cell growth, though no hPSC-derived cells were tested. Other examples have employed porogen templating for the fabrication of porous polysaccharide-based vascular scaffolds and engineered heart valves (Lavergne et al., 2012; Masoumi et al., 2014).

Thermally induced phase separation is based on the use of temperature to induce the de-mixing of a homogeneous polymer solution. The controlled change in temperature prompts the formation of a polymer-rich and a polymer-poor phase, which can be used to obtain an interconnected porous structure (Nam and Park, 1999). Vozzi et al. synthesised the elastomer polyesterurethane, and used thermal phase separation to create a porous and biocompatible structure, which they functionalised with fibronectin by NHS-EDC chemistry. Although material properties were off the cardiac optimal range (in the order of > 0.25 MPa), neonatal rat cardiac cells attached and grew on the scaffolds, with specific modulation of gene expression. However, no use of human cells was reported (Vozzi et al., 2018).

Electrically produced

Solution electrospinning (SE), on the other hand, was one of the first and most employed fabrication modalities in the field. In this technique, a polymer solution is subjected to a relatively high electric field while it travels towards a collector plate. This electric field causes the polymeric jet to whip, producing very thin fibres of even sub-micron size, that can be collected randomly or in an aligned fashion. For a review see Sensini and Cristofolini (2018). In general, most SE applications produce low thickness mats of (semi-)randomly arranged fibres of different materials, though use of appliances such as a rotating mandrel can increase alignment (Han et al., 2016). Although relying on the use of potentially toxic solvents, SE has the advantage of being open to a wide range of materials, both natural and synthetic (Kitsara et al., 2017).

The concurrent use of SE with hPSC-derived cardiac cells has not been widely explored but some remarkable examples can be found. The group of Onnik Agbulut tested different crosslinking times of a clinical-grade collagen electrospun scaffold for the most suitable conditions for hiPSC-CM culture. The resulting mats had fibres of 0.6-2.2 μm, with pores in the range of 2-3 μm. After no deleterious effects were found after mat implantation in animals, the mats were seeded with hiPSC-CMs (10^6 per scaffold), and produced a significant benefit when transplanted in a dilated cardiomyopathy model. Importantly, scaffolds were compliant enough to allow the generation of macroscopic contractions by the hiPSC-CMs (Joanne et al., 2016). Sireesha et al. used a combination of the elastomer poly[1,8-octanediol-co-(citric acid)-co-(sebacic acid)] and fibrinogen to produce scaffolds with a sub-micron fibre diameter, whose mechanical properties laid on the upper end of cardiac elasticity (hundreds of kPa) and which showed good biocompatibility with human CMs. However, no further tests in animal models were performed (Sireesha et al., 2015). Khan and co-workers electrospun polylactide-co-glycolide (PLGA) as 50 μm-thick aligned nanofibrous scaffolds, seeded with hiPSC-CM, and compared the outcome versus conventional tissue culture plastic surfaces. Results showed the scaffolds were able to align the CMs, as well as inducing changes at the level of functionality (Ca transients) and gene expression, though the high stiffness of the mats (1-2 orders of magnitude above the cardiac tissue) could have a negative impact (Khan et al., 2015). On the other side of the coin, Han et al. assayed the capacity of aligned electrospun mats made of PCL coated with matrigel to induce hiPSC-CM maturation, showing a limited effect at the functional level, but with some differences in gene expression (Han et al., 2016).

Aside from employing different materials or combinations of natural and synthetic polymers, SE offers increased possibilities by modifying the properties of the resulting engineered tissue by combination with nanoparticles or other fabrication technologies. For example, the group of Tal Dvir built on his previous work on the electrospinning of albumin (Fleischer et al., 2014) to increase the anisotropy of the fabricated engineered tissue. To do this, they employed a double strategy: they used laser patterning to create micro-holes and unidirectional grooves, in order to increase mass transport and cell alignment respectively, and they stacked several layers of patterned mats, inspired by the anisotropy found across the ventricular wall. In this fashion, they also modulated the mechanical properties of the layers, getting closer to human myocardial values. They did not, however, test the stiffness of the resulting stacked construct, nor populate it with human cells, using rat neonatal cardiac cells instead (Fleischer et al., 2017). The group of Ali Khademhosseini used poly(glycerol sebacate):gelatin (PG) solution where gelatin-methacryloyl (GelMA)-coated carbon nanotubes had been incorporated to electrospun aligned nanofibrous mats with improved electrical properties, though at the cost of increased stiffness (Kharaziha et al., 2014). This is similar to their previous work with GelMA-embedded carbon nanotubes, (Shin et al., 2013) with a significant effect on gene expression, structure and functionality, but again no human cells were employed. Walker et al. employed bio-ionic liquids to modulate the electrical properties and adhesion strength of electrospun GelMA scaffolds, assaying their *in vitro* and *in vivo* regenerative potential, though no tissue was constructed (Walker et al., 2019). Again, mechanical properties were affected. Recently, the group of Felix Engel used SE to generate fibres combining the conductive polymer polyaniline (PANi) with collagen/hyaluronic acid, producing mats of suitable mechanical and electrical properties. Scaffolds supported the attachment of hiPSC-CMs, which displayed typical striations and contractions. Substrates incorporating PANi induced a faster beating rate on hiPSC-CMs, though this was not further explored (Roshanbinfar et al., 2020). All in all, SE is a very versatile fabrication technique, and this is also increased by the possibility of combining it with other materials and technologies. However, it faces limitations related to the thickness

and dimensions of the final construct, as well as long-range alignment capacity.

Textile-based fabrication

Historically speaking, weaving is one of the oldest fabrication techniques and many (bio)materials can be processed by knitting, weaving or braiding, (Akbari et al., 2016) giving rise to new architectures and importantly, mechanical properties unattainable for individual fibres. Curiously, these have not been mainstream in the cTE field, with few studies combining these fabrication methods with hPSC-derived cells. Though their work cannot fully be categorised as textile-based, the lab of Kevin K. Parker employed pull spinning to generate nanofibrous scaffolds composed of PCL/Gelatin over an ellipsoidal mandrel, mimicking the shape of an idealised ventricle. After additional coating with the ECM protein fibronectin, they seeded either neonatal cardiac rat cells or hiPSC-CMs, generating scale-models of the heart with striking functional properties (Macqueen et al., 2018).

Techniques With True Architecture Control

Additive manufacturing, also known as 3D printing, is one of the technological revolutions of this century. It is based on the building of a volumetric object from a computer aided design (CAD), often in a layer-by-layer basis. Broadly speaking, we can distinguish between bioprinting, where cells are also printed, from the build & seed strategies, where the scaffold is first printed and the cells incorporated in a subsequent step, either as a standalone element or embedded in a hydrogel matrix. In any case, the degree of control over the resulting structure is orders of magnitude above what is achievable with the above-mentioned technologies, with the exception of filament dimensions, with SE being able to go into sub-micron diameter, albeit at the expense of thickness and architecture.

3D Build and Seed

In this category we have gathered those additive manufacturing technologies that do not allow the concurrent printing of materials and cells, be it because they employ high temperature, damaging lasers, toxic solvents or for other reasons. This section includes selective laser sintering (SLS), consisting of iteratively spreading layers of powdered materials and fusing it together to achieve the programmed shape, (Duan et al., 2010) stereolithography, where a bath with photosensitive resin is selectively cured layer by layer with a UV laser or similar power source, (Gauvin et al., 2012) or fused deposition modelling (FDM), by which the printed polymer is melted and deposited in layers in order to acquire the desired 3D architecture (Moroni et al., 2006). All these technologies have in common the need to first generate the architecture and in a second step add the biologicals, with the only exception of laser-curable materials in SLS. Although these technologies are in increased demand for the building of prosthetics, personalised solid implants or educational/surgery planning models, (Giannopoulos et al., 2016) their application to cTE is not widespread, especially in light of the increasing importance of bioprinting techniques (next section).

A special note however must be dedicated to Melt Electrowriting (MEW), a highly specialised additive manufacturing technology (Brown et al., 2011). It works on the same basis as SE, where a high voltage is applied between a syringe tip and a grounded collector. In this case however, the polymer is not dissolved, but melted. The superior stability of the jet allows a highly controlled deposition of fibres, which solidify in-flight or shortly upon collection. These, although bigger in diameter than those from SE, are at least an order of magnitude below what is usually attainable with 3D printing or bioprinting (tens of μm in diameter). The polymer of choice must be melted within the capacities of the printer, which limits the range of the available polymers. Another significant limitation is the achievable 3-dimensionality, which is usually below the mm-range. The groups of Paul Dalton and Dietmar Hutmacher have spearheaded its use (Bas et al., 2015, 2017; Hochleitner et al., 2018) and have developed methods to increase the thickness of the MEW scaffolds to almost one cm, but again these are far from mainstream (Wunner et al., 2018). The groups of Jos Malda and Joost Sluijter have been the first ones to apply MEW to cTE. In their first approach, they MEW-printed the hydroxyl-functionalised polyester, (poly(hydroxymethylglycolide-co-ε-caprolactone) in orthogonal patterns, and seeded them with human cardiac progenitor cells (CPC) embedded in a collagen type I hydrogel. CPCs survived well, with the scaffolds producing a significant alignment (Castilho et al., 2017). In a further optimisation of the system, Castilho et al. fabricated hexagonally patterned MEW scaffolds with superior compliance, and seeded them with hiPSC-CMs. Their results showed the superior biaxial mechanical properties of the hexagonal designs, and their significant, positive effect on cell alignment and gene expression. Moreover, these scaffolds could be transplanted in a large animal (pig) after passing through a catheter-like tube, paving the way for their future percutaneous transplantation (Castilho et al., 2018). Finally, an auxetic patch, that is, featuring a negative Poisson ratio, was recently fabricated with MEW, and the conductive polymer polypyrrole *in situ* polymerised on it, with electroconductive properties close to those of the human myocardium (Olvera et al., 2020).

Bioprinting

The capacity to print human tissues on-demand has roused the expectations of scientists, clinicians and patients alike, with a range of modalities available. Laser-assisted bioprinting (LAB) for example, features several methodologies. Laser-induced forward transfer of material/ink (LIFT)(Koch et al., 2010) allows printing with a single-cell resolution at high densities (up to 10^8 cells/ml) (Gaebel et al., 2011). However, it requires selected materials to gel relatively fast, which in practice restricts the range of available materials, and can be technically challenging. 2 photon polymerisation is a type of LAB with high spatial resolution (as low as 70 nm) without the need for support structures (Hu et al., 2017). Vaithilingam et al. employed this technique to fabricate electroactive 3D architectures by incorporation of multi-walled carbon nanotubes (CNTs). The mechanical properties were however highly deviated from what has been described for human cardiac tissue (GPa range). hiPSC-CMs were able to

survive and, after the application of electrical stimulation, a significant effect on sarcomere length was found (Vaithilingam et al., 2019). There are other printing technologies based on LAB, such as Biological Laser Printing and Laser Guided Direct Writing, (Odde and Renn, 2000; Barron et al., 2004) but no reports on these include hiPSC-derived cardiac cells.

Extrusion-based bioprinting is probably the best-known bioprinting method: a bioink containing both cells and the biomaterial is extruded through a nozzle onto a motorised collector. The coordination between the gelation of the bioink and its deposition permits the generation of thick tissues. A range of nozzles, including pneumatic, screw- or plunger-based, as well as inks, is available. However, the material properties of the latter are fundamental, as shear stress generated upon printing highly impacts cell viability (Jungst et al., 2016). Some strategies, like *in situ* crosslinking of the bioink immediately prior to its deposition, (Ouyang et al., 2017) are being developed to overcome these and other limitations. Extrusion-based bioprinting has been extensively researched in the cTE field. Jang et al. employed a multi-nozzle printer to generate tissues with 2 decellularised cardiac ECM-based bioinks reinforced with a thermoplastic (PCL) backbone. One of the bioinks contained human CPCs (c-kit-positive), and the other mesenchymal stem cells (MSC) and pro-angiogenic factors (VEGF). The application of this patch in a rat model of disease demonstrated a rapid vascularisation as well as a significant benefit at the functional and histological levels. However, no new contractile tissue was formed (Jang et al., 2017). Zhang and coworkers employed a more advanced strategy, where they used coaxial printing to pattern human umbilical vein endothelial cells (HUVECs) in a ink containing alginate, GelMA and the UV-curable photoinitiator Irgacure. The mixture was quickly crosslinked by $CaCl_2$ from the outer sheath, and further gelled by exposure to UV light (for alginate and GelMA respectively) (Zhang Y. S. et al., 2016). HUVECs migrated to the outer border of the printed structures, forming 3D vessel-like structures over a period of 15 days, after which neonatal rat CMs were added to complete the tissue. Izadifar et al. explored varying the electrical properties of the generated tissues by incorporating alginate-coated carbon nanotubes (CNT) to methacrylated collagen. The system displayed as expected enhanced electrical properties, once more at the expense of becoming stiffer, though within acceptable values, and was able to support the growth of human coronary artery endothelial cells. No CMs were employed (Izadifar et al., 2018). Maiullari and coworkers applied a different version of extrusion printing termed microfluidic printing, to generate vascularised engineered tissues combining HUVECs and hiPSC-CMs (Maiullari et al., 2018). The bioartificial myocardium was fabricated with a bioink combining alginate for a rapid crosslinking, and polyethylene glycol (PEG) monoacrylate-fibrinogen, for UV-curing and cell adhesion. These tissues were tested *in vivo*, were the presence of vascular cells was able to promote integration with the recipient vascular system. Zhu et al. formulated a bioink with capacity to electrically influence neonatal rat CMs by incorporating gold nanorods in GelMA. Thick constructs were generated, although cell viability was below 80% in most cases. This is extremely relevant if we take into account that CMs are non-proliferative cells, so no re-growth is likely to occur (Zhu et al., 2017).

Freeform embedding of suspended hydrogels (FRESH) is one of most exciting 3D bioprinting methods (Hinton et al., 2015). Here, the biomaterial ink or bioink of choice is printed within the support of another hydrogel serving as a temporary support. Noor and co-workers developed a personalised hydrogel ink from human decellularised omental tissue, which could be printed into complex structures using FRESH. They used it in combination with hiPSC which they differentiated within the matrix into beating, perfused cardiac mini-tissues (Noor et al., 2019). Lastly, the Feinberg group used FRESH to accurately (20 μm resolution) 3D print different components of the human heart with collagen, including a model of the left ventricle on the scale of the neonatal organ, incorporating hESC-CMs (Lee et al., 2019). These engineered tissues displayed synchronised functional activity.

Finally, some the applications build tissues without the use of biomaterials. This includes the additive manufacturing with spheroids, as demonstrated by Arai et al., where they combined commercially available hPSC-CMs with HUVECs and dermal fibroblasts to generate the spheroids, organised in a tubular 3D structure with a bioprinter (Arai et al., 2018). However, the authors used a needle array to provide initial transient support for their structures, which in the end played the role of a scaffolding material. Recently, Ayan et al. reported a novel strategy, termed aspiration-assisted bioprinting, relying on the aspiration of 3D spheroids and their precise deposition in 3D. This could also be combined with FRESH, but no use of hiPSC-derived cardiac cells was reported (Ayan et al., 2020).

CLINICAL TRANSLATION OF hPSC-BASED cTE STRATEGIES

Survival post-cardiac ischemia has raised with advances in the cardiology and cardiovascular surgery areas, as well as through the development of new drugs in the last decades. This includes the application of reperfusion by percutaneous coronary intervention, anticoagulants and antithrombotics, amongst others. Though cTE has potential to address different cardiac conditions, its main activity has been directed towards the loss of viable myocardium by supplying new one, engineered in the lab.

In stark contrast to the short time elapsing between the first reports on regenerative medicine with adult stem cells and their first in-human application (reviewed in Banerjee et al., 2018) cTE with hPSCs has scarcely reached the clinical arena. Be it because both scientists and clinicians have learnt from past experiences or because translation presents additional complications, (Desgres and Menasché, 2019; Ghaemi et al., 2019; Ke and Murphy, 2019) clinical application is yet to become a reality. The technology faces challenges in the area of regulation, where reprogrammed cells under GMP-conditions are not widely derived, in logistics, with the size of engineered tissues in most instances requiring open chest surgery, and in economic terms. However, progress is being made. Tiburcy et al., created an engineered human myocardium with advanced structural and functional maturation by combining

hPSC-derived cells with collagen type I (Tiburcy et al., 2017). Their work, standing on the shoulders of decade-long progress, (Zimmermann et al., 2002, 2006) demonstrated the building of human-scale relevant tissues (3.5 × 3.4 cm, containing 40 million CMs) under defined conditions and their pre-clinical safety assessment in rats, though no large animal testing was performed. The group of Prof Bursac applied dynamic culture conditions to improve the maturation of a patch formed from hiPSC-derived cardiac cells in a fibrin matrix. Although they achieved human adult-like electrical properties (e.g., conduction velocity) and formed large grafts when transplanted into rodents, the use of matrigel in the forming mixture precludes further translation (Shadrin et al., 2017; Jackman et al., 2018). In addition, myocytes were mostly randomly arrayed, which added to the low thickness of the grafts precludes any efficient and substantial force generation, and therefore makes providing contractile support to diseased hearts difficult.

Menasche et al. performed the first clinical case of an hPSC-based patch in 2015, transplanting a 20 cm^2 fibrin-based tissue. This patch contained 4 million hESC-derived Isl^+ $SSEA1^+$ CPCs and was implanted epicardially in a 68-year-old patient with advanced heart failure. Concomitant to the implantation of the patch, a coronary artery bypass was also performed. After 3 months, the patient had better symptoms, and there was improved evidence in the echocardiogram too (form akinetic to moderately hypokinetic). Moreover, no adverse effect was observed (Menasché et al., 2015). This was part of the first clinical trial carried out with six patients suffering from advanced IHD (NCT02057900), called ESCORT. The aim of the trial was to demonstrate the safety of the patch at 1 year. All patients improved symptomatically, with four showing an increased systolic motion. One died early in the post-operative period from treatment-unrelated comorbidities and another after in 22 months due to heart failure (Menasché et al., 2018).

Japan has made huge efforts to spearhead research in the hiPSC field, and has one of the most streamlined regulatory frameworks (see Cyranoski, 2019 for a comment). It has recently started the first clinical trial of hiPSC-CM transplant in ischemic heart dysfunction. The study will deliver 100 million hiPSC-CMs in the form of a cell sheet of 4 × 5 × 0.1 cm (Kawamura et al., 2017). The aim of the study is to evaluate efficacy and safety of the treatment in a total of 10 patients (Cyranoski, 2018).

Overall, clinical applications of hPSC-based cardiac engineered tissues, though scarce, are starting to emerge. However, the scientific and logistic/economic concerns mentioned above need addressing further before any of these technologies reach the clinical arena.

CONCLUSION AND OUTLOOK

The capacity to fabricate human myocardium in the laboratory is no longer restricted to science fiction. Recent breakthroughs such as cell reprogramming and 3D (bio)printing have shifted the question from 'Can we do it?' to 'How do we want to do it?'. However, lessons from its predecessor in the area of regenerative medicine should teach us the value of caution. Crucial questions remain, some of which include the following:

-*What are the most suitable components for building an engineered myocardium?* Of course, this absolutely depends on the application/pathology we are targeting. If the objective is to reconstruct the post-disease myocardium, especially in cases when muscular mass has been loss (as IHD), this will require new CMs, alongside new vessels and support cells. Although not supplying new CMs might still be beneficial, it will not regenerate the tissue to pre-disease levels. So far, only hPSCs can produce the required cells in sufficiently large amounts, and whether it is better to use fully differentiated cells or progenitors is still an open question. Regarding the ECM-mimics, the current state can seem confusing. All reported (bio)material formulations seem to provide a benefit (**Table 2**). It is plausible that the most important factor is for the material to recapitulate the mechanical environment of cardiac tissue long enough for delivered cells to build their own structure. Also, although collagen type I has repeatedly been positioned as being the main component of the cardiac ECM, this does not account for all its mechanical capacities, nor it is as abundant as the levels supplemented in engineered tissues. Probably, cost and translation capacity will have much to say here. Lastly, regarding the fabrication mode, though 3D bioprinting has captivated both scientists and the wider public, its actual ability to deliver tissues able to withstand the mechanical forces in play in the human myocardium is far from optimal in most cases. Fibre reinforcement might be a solution to this, but remains to be fully tested in a human scale. In addition, recent technical developments such as 4D printing or cyborganics will certainly widen the scope of possibilities at hand (Tamay et al., 2019; Orive et al., 2020).

– *How is translation going to happen?* The hurdles are significant, (Desgres and Menasché, 2019; Ghaemi et al., 2019) not only due to the use of genetically modified cells (hiPSCs), exogenous materials and complex equipment, but also because in order to attain sufficient functional capacity, it is likely that some lengthy period of *in vitro* electromechanical maturation must be implemented. Also, no standard equipment currently exists to apply this to a human-scale tissue. In this area, it is crucial that biomedical researchers work alongside lawmakers. Cell therapy mostly relied on an autologous application of a non-cultured material, which smoothened its approval. Tissue engineering applications based on hiPSC products are highly promising but are impeded by stringent regulations. Japan has spearheaded hiPSC translation as a national flagship (Azuma and Yamanaka, 2016). Although some consider this too loose, it is clear that unless scientists provide a clear direction and get themselves involved in depth in the regulatory process, advances will be limited.

– *Will costs be sensible?* hiPSC culture and differentiation are expensive. Additive manufacturing is expensive. GMP-grade materials are expensive. hiPSC line derivation costs between €4000-8000 depending on the provider, multi-nozzle 3D bioprinters are usually budgeted above €30000, and some medical-grade materials as human collagen type I are prohibitive

(> €200 per 100 μg). Highly trained personnel costs need to be added on top of this, as well as the cost of hiPSC expansion and differentiation. The cost of a heart transplant in the United States is above $150000 (including 120-day medical care), with Left Ventricular Assist Devices (LVADs), employed for patients with end stage heart failure as a bridge to transplant (and now trialled as destination therapy) are estimated to cost even more (see Miller et al., 2013 for a concise review). If economic issues are not addressed from day one, we run the risk of ending up with a highly effective therapy only that very few people can pay for. Large-scale production of hiPSC-derived cells has been demonstrated and will no doubt help decrease costs (Abecasis et al., 2017; Halloin et al., 2019; Buikema et al., 2020). Strategies to induce hiPSC-CM division would significantly improve the economics.

– *Will the new therapy be safe?* hPSCs have been marred by concerns related to persistence of pluripotent cells after differentiation and the subsequent risk of teratoma formation. But also, the new tissue must conform to the host's electrical activity. Again, lessons from Cell Therapy call for caution (Menasché et al., 2008). Advanced genomics and other analysis tools not available 10 years ago will significantly enhance the safety analysis and help researchers and clinicians along the way (Wang Z. et al., 2020).

– *Are the aims achievable?* The objective of cTE is to generate new human myocardium whose properties and functionality are similar to its natural counterpart, but that might not be achievable within a sensible timeframe. Human cardiac maturation advances significantly after birth but continues throughout the first decades of life. Current advanced methods for maturation, like those based on electromechanical stimulation, do not achieve anything even close to adult properties. However, it is plausible that only a minimal maturity is needed in order to avoid lethal arrhythmias, as hPSC-CMs are reported to undergo maturation after transplantation in the heart (Kadota et al., 2017).

– *What is the state of non-therapeutic applications?* Though the aim of cTE within regenerative medicine is directed towards treatment, bioartificial human myocardium is becoming increasingly relevant with respect to other applications such as disease modelling and drug testing (Vunjak-Novakovic et al., 2014; Sharma et al., 2020), where the scale of the fabricated tissues is not an issue. In drug testing, the CiPA initiative has already pointed to the relevance of hiPSC-CMs, (Millard et al., 2018) especially given cardiac side effects are one of the main reasons for drug withdrawal, and there is no primary source of human CMs available (Laverty et al., 2011). Current efforts have already proven the capacity of cTE-based systems to better recapitulate physiological human drug response [reviewed in Kadota et al. (2017) and Millard et al. (2018), or to generate chamber-specific microtissues (Zhao et al., 2019)]. Translation towards industrial and clinical testing is envisioned to be more straightforward and immediate.

As can be seen, the challenges ahead are not minor. However, humankind has never been closer to achieving success in tissue fabrication. Whole functional heart generation in the laboratory, though frequently dreamt of, is still not achievable, as severe physiological and technical roadblocks remain in place. Challenges include ensuring adequate vascularisation, electromechanical coupling over long distances, atrioventricular delay, autonomous nervous system innervation or designing materials both biocompatible but capable of supporting the strong mechanics of a whole heart, amongst others. At this extraordinary moment, it is crucial for scientists, clinicians, and lay people to stay focused and deliver.

AUTHOR CONTRIBUTIONS

PM, MF-I, SM, and MP revised the literature, wrote the initial draft of the manuscript and figures. DP and JG revised the text and generated the tables. CS, GO, and FP supervised the development and revised the text. MM wrote the final revised version. All authors contributed to the article and approved the submitted version.

FUNDING

This work was supported by funds from the ISCIII Red TERCEL RETIC RD16/0011/0005, PI 19/01350, ERANET II (Nanoreheart) and Gobierno de Navarra Departamento de Salud GNª8/2019, co-funded by FEDER funds, MINECO (Program RETOS Cardiomesh RTC-2016-4911-1), Gobierno de Navarra 0011-1383-2019-000006 and 0011-1383-2018-000011, and European Union's H2020 Program under grant agreement No. 874827 (BRAV∃).

ACKNOWLEDGMENTS

The authors acknowledge Medical Arts and BioRender (registered user) for the building of the figures in the manuscript.

REFERENCES

Abecasis, B., Aguiar, T., Arnault, É, Costa, R., Gomes-Alves, P., Aspegren, A., et al. (2017). Expansion of 3D human induced pluripotent stem cell aggregates in bioreactors: bioprocess intensification and scaling-up approaches. *J. Biotechnol.* 246, 81–93. doi: 10.1016/j.jbiotec.2017.01.004

Adler, C. P., and Costabel, U. (1975). Cell number in human heart in atrophy, hypertrophy, and under the influence of cytostatics. *Recent Adv. Stud. Card. Struct. Metab.* 6, 343–355.

Akbari, M., Tamayol, A., Bagherifard, S., Serex, L., Mostafalu, P., Faramarzi, N., et al. (2016). Textile technologies and tissue engineering: a path toward organ weaving. *Adv. Healthc. Mater.* 5, 751–766. doi: 10.1002/adhm.201500517

Amdursky, N., Mazo, M. M., Thomas, M. R., Humphrey, E. J., Puetzer, J. L., St-Pierre, J. P., et al. (2018). Elastic serum-albumin based hydrogels: mechanism of formation and application in cardiac tissue engineering. *J. Mater. Chem. B* 6, 5604–5612. doi: 10.1039/c8tb01014e

Andreu, I., Luque, T., Sancho, A., Pelacho, B., Iglesias-García, O., Melo, E., et al. (2014). Heterogeneous micromechanical properties of the extracellular matrix

in healthy and infarcted hearts. *Acta Biomater.* 10, 3235–3242. doi: 10.1016/j.actbio.2014.03.034

Anversa, P., Loud, A. V., Giacomelli, F., and Wiener, J. (1978). Absolute morphometric study of myocardial hypertrophy in experimental hypertension. II. Ultrastructure of myocytes and interstitium. *Lab. Investig.* 38, 597–609.

Arai, K., Murata, D., Verissimo, A. R., Mukae, Y., Itoh, M., Nakamura, A., et al. (2018). Fabrication of scaffold-free tubular cardiac constructs using a Bio-3D printer. *PLoS ONE* 13:e0209162. doi: 10.1371/journal.pone.0209162

Araña, M., Gavira, J. J., Peña, E., González, A., Abizanda, G., Cilla, M., et al. (2014). Epicardial delivery of collagen patches with adipose-derived stem cells in rat and minipig models of chronic myocardial infarction. *Biomaterials* 35, 143–151. doi: 10.1016/j.biomaterials.2013.09.083

Ayan, B., Heo, D. N., Zhang, Z., Dey, M., Povilianskas, A., Drapaca, C., et al. (2020). Aspiration-assisted bioprinting for precise positioning of biologics. *Sci. Adv.* 6:eaaw5111. doi: 10.1126/sciadv.aaw5111

Azuma, K., and Yamanaka, S. (2016). Recent policies that support clinical application of induced pluripotent stem cell-based regenerative therapies. *Regen. Ther.* 4, 36–47. doi: 10.1016/j.reth.2016.01.009

Banerjee,. I., Fuseler, J. W., Price, R. L., Borg, T. K., and Baudino, T. A. (2007). Determination of cell types and numbers during cardiac development in the neonatal and adult rat and mouse. *Am. J. Physiol. – Hear Circ. Physiol.* 293, 1883–1891

Banerjee, M. N., Bolli, R., and Hare, J. M. (2018). Clinical studies of cell therapy in cardiovascular medicine recent developments and future directions. *Circ. Res.* 123, 266–287. doi: 10.1161/circresaha.118.311217

Bargehr, J., Ong, L. P., Colzani, M., Davaapil, H., Hofsteen, P., Bhandari, S., et al. (2019). Epicardial cells derived from human embryonic stem cells augment cardiomyocyte-driven heart regeneration. *Nat. Biotechnol.* 37, 895–906. doi: 10.1038/s41587-019-0197-9

Barkauskas, C. E., Noble, P. W., Brigid, L. M., Barkauskas, C. E., Cronce, M. J., Rackley, C. R., et al. (2013). Type 2 alveolar cells are stem cells in adult lung. *J. Clin. Invest.* 123, 3025–3036.

Barreiro, D. L., Martín-Moldes, Z., Yeo, J., Shen, S., Hawker, M. J., Martin-Martinez, F. J., et al. (2019). Conductive silk-based composites using biobased carbon materials. *Adv. Mater.* 31:e1904720.

Barron, J., Wu, P., Ladouceur, H. D., and Ringeisen, B. R. (2004). Biological laser printing: a novel technique for creating heterogeneous 3-dimensional cell patterns. *Biomed. Microdevices* 6, 139–147. doi: 10.1023/b:bmmd.0000031751.67267.9f

Bas, O., D'Angella, D., Baldwin, J. G., Castro, N. J., Wunner, F. M., Saidy, N. T., et al. (2017). An integrated design, material, and fabrication platform for engineering biomechanically and biologically functional soft tissues. *ACS Appl. Mater. Interfaces.* 9, 29430–29437. doi: 10.1021/acsami.7b08617

Bas, O., De-Juan-Pardo, E. M., Chhaya, M. P., Wunner, F. M., Jeon, J. E., Klein, T. J., et al. (2015). Enhancing structural integrity of hydrogels by using highly organised melt electrospun fibre constructs. *Eur. Polym. J.* 72, 451–463. doi: 10.1016/j.eurpolymj.2015.07.034

Baudino, T. A., Carver, W., Giles, W., and Borg, T. K. (2006). Cardiac fibroblasts: friend or foe? *Am. J. Physiol. – Hear Circ. Physiol.* 291, H1015–H1026.

Bedada, F. B., Chan, S. S. K., Metzger, S. K., Zhang, L., Zhang, J., Garry, D. J., et al. (2014). Acquisition of a quantitative, stoichiometrically conserved ratiometric marker of maturation status in stem cell-derived cardiac myocytes. *Stem Cell Rep.* 3, 594–605. doi: 10.1016/j.stemcr.2014.07.012

Behfar, A., Crespo-Diaz, R., Terzic, A., and Gersh, B. J. (2014). Cell therapy for cardiac repair-lessons from clinical trials. *Nat. Rev. Cardiol.* 11, 232–246. doi: 10.1038/nrcardio.2014.9

Beltrami, A. P., Barlucchi, L., Torella, D., Baker, M., Limana, F., Chimenti, S., et al. (2003). Adult cardiac stem cells are multipotent and support myocardial regeneration. *Cell* 114, 763–776. doi: 10.1016/s0092-8674(03)00687-1

Belviso, I., Romano, V., Sacco, A. M., Ricci, G., Massai, D., Cammarota, M., et al. (2020). Decellularized human dermal matrix as a biological scaffold for cardiac repair and regeneration. *Front. Bioeng. Biotechnol.* 8:229. doi: 10.3389/fbioe.2020.00229

Bergmann, O., Zdunek, S., Felker, A., Salehpour, M., Alkass, K., Bernard, S., et al. (2015). Dynamics of cell generation and turnover in the human heart. *Cell* 161, 1566–1575. doi: 10.1016/j.cell.2015.05.026

Bertlein, S., Brown, G., Lim, K. S., Jungst, T., Boeck, T., Blunk, T., et al. (2017). Thiol-ene clickable gelatin: a platform bioink for multiple 3D biofabrication technologies. *Adv. Mater.* 29:1703404.

Bhana, B., Iyer, R. K., Chen, W. L. K., Zhao, R., Sider, K. L., Likhitpanichkul, M., et al. (2010). Influence of substrate stiffness on the phenotype of heart cells. *Biotechnol. Bioeng.* 105, 1148–1160.

Birket, M. J., Ribeiro, M. C., Verkerk, A. O., Ward, D., Leitoguinho, A. R., Den Hartogh, S. C., et al. (2015). Expansion and patterning of cardiovascular progenitors derived from human pluripotent stem cells. *Nat. Biotechnol.* 33, 970–979. doi: 10.1038/nbt.3271

Blin, G., Nury, D., Stefanovic, S., Neri, T., Guillevic, O., Brinon, B., et al. (2010). A purified population of multipotent cardiovascular progenitors derived from primate pluripotent stem cells engrafts in postmyocardial infarcted nonhuman primates. *J. Clin. Invest.* 120, 1125–1139. doi: 10.1172/jci40120

Bondue, A., Lapouge, G., Paulissen, C., Semeraro, C., Iacovino, M., Kyba, M., et al. (2008). Mesp1 acts as a master regulator of multipotent cardiovascular progenitor specification. *Cell Stem Cell* 3, 69–84. doi: 10.1016/j.stem.2008.06.009

Brand, T. (2003). Heart development: molecular insights into cardiac specification and early morphogenesis. *Dev. Biol.* 258, 1–19. doi: 10.1016/s0012-1606(03)00112-x

Bressan, M., Liu, G., and Mikawa, T. (2013). Early mesodermal cues assign avian cardiac pacemaker fate potential in a tertiary heart field. *Science(80-)* 340, 744–748. doi: 10.1126/science.1232877

Brown, T. D., Dalton, P. D., and Hutmacher, D. W. (2011). Direct writing by way of melt electrospinning. *Adv. Mater.* 23, 5651–5657. doi: 10.1002/adma.201103482

Buckberg, G., Nanda, N., Nguyen, C., and Kocica, M. (2018). What is the heart? Anatomy, function, pathophysiology, and misconceptions. *J. Cardiovasc Dev. Dis.* 5:33. doi: 10.3390/jcdd5020033

Buckberg, G. D. (2002). Basic science review: the helix and the heart. *J. Thorac. Cardiovasc. Surg.* 124, 863–883. doi: 10.1067/mtc.2002.122439

Buckberg, G. D., Hoffman, J. I. E., Cecil Coghlan, H., and Nanda, N. C. (2015a). Ventricular structure-function relations in health and disease: part I. The normal heart. *Eur. J. Cardio-thoracic Surg.* 47, 587–601. doi: 10.1093/ejcts/ezu278

Buckberg, G. D., Hoffman, J. I. E., Coghlan, H. C., and Nanda, N. C. (2015b). Ventricular structure-function relations in health and disease: part II. Clinical considerations. *Eur. J. Cardio-thoracic. Surg.* 47, 778–787. doi: 10.1093/ejcts/ezu279

Buckingham, M., Meilhac, S., and Zaffran, S. (2005). Building the mammalian heart from two sources of myocardial cells. *Nat. Rev. Genet.* 6, 826–835. doi: 10.1038/nrg1710

Buikema, J. W., Lee, S., Goodyer, W. R., Maas, R. G., Chirikian, O., Li, G., et al. (2020). Wnt activation and reduced cell-cell contact synergistically induce massive expansion of functional human iPSC-derived cardiomyocytes. *Cell Stem Cell* 27, 50.e5–63.e5.

Burnett, W., Finnigan-Bunick, A., Yoon, K., and Rosenbloom, J. (1982). Analysis of elastin gene expression in the developing chick aorta using cloned elastin cDNA. *J. Biol. Chem.* 257, 1569–1572.

Burridge, P. W., Anderson, D., Priddle, H., Barbadillo Muñoz, M. D., Chamberlain, S., Allegrucci, C., et al. (2007). Improved human embryonic stem cell embryoid body homogeneity and cardiomyocyte differentiation from a novel V-96 plate aggregation system highlights interline variability. *Stem Cells* 25, 929–938. doi: 10.1634/stemcells.2006-0598

Burridge, P. W., Matsa, E., Shukla, P., Lin, Z. C., Churko, J. M., Ebert, A. D., et al. (2014). Chemically defned generation of human cardiomyocytes. *Nat. Methods* 11, 855–860. doi: 10.1038/nmeth.2999

Burridge, P. W., Sharma, A., and Wu, J. C. (2015). Genetic and epigenetic regulation of human cardiac reprogramming and differentiation in regenerative medicine. *Annu. Rev. Genet.* 49, 461–484. doi: 10.1146/annurev-genet-112414-054911

Camelliti, P., Borg, T. K., and Kohl, P. (2005). Structural and functional characterisation of cardiac fibroblasts. *Cardiovasc. Res.* 65, 40–51. doi: 10.1016/j.cardiores.2004.08.020

Camelliti, P., Green, C. R., LeGrice, I., and Kohl, P. (2004). Fibroblast network in rabbit sinoatrial node: structural and functional identification of homogeneous and heterogeneous cell coupling. *Circ. Res.* 94, 828–835. doi: 10.1161/01.res.0000122382.19400.14

Castilho, M., Feyen, D., Flandes-Iparraguirre, M., Hochleitner, G., Groll, J., Doevendans, P. A. F., et al. (2017). Melt electrospinning writing of poly-hydroxymethylglycolide-co-ε-caprolactone-based scaffolds for cardiac tissue engineering. *Adv. Healthc. Mater.* 6:1700311.

Castilho, M., van Mil, A., Maher, M., Metz, C., Hochleitner, G., Groll, J., et al. (2018). Melt electrowriting allows tailored microstructural and mechanical design of scaffolds to advance functional human myocardial tissue formation. *Adv. Funct. Mater.* 28:1803151. doi: 10.1002/adfm.201803151

Chan, S. S. K., Shi, X., Toyama, A., Arpke, R. W., Dandapat, A., Iacovino, M., et al. (2013). Mesp1 patterns mesoderm into cardiac, hematopoietic, or skeletal myogenic progenitors in a context-dependent manner. *Cell Stem Cell* 12, 587–601. doi: 10.1016/j.stem.2013.03.004

Chan, Y. C., Ting, S., Lee, Y. K., Ng, K. M., Zhang, J., Chen, Z., et al. (2013). Electrical stimulation promotes maturation of cardiomyocytes derived from human embryonic stem cells. *J. Cardiovasc. Transl. Res.* 6, 989–999. doi: 10.1007/s12265-013-9510-z

Chen, Q. Z., Bismarck, A., Hansen, U., Junaid, S., Tran, M. Q., Harding, S. E., et al. (2008). Characterisation of a soft elastomer poly(glycerol sebacate) designed to match the mechanical properties of myocardial tissue. *Biomaterials* 29, 47–57. doi: 10.1016/j.biomaterials.2007.09.010

Christoffels, V. M., Burch, J. B. E., and Moorman, A. F. M. (2004). Architectural plan for the heart: early patterning and delineation of the chambers and the nodes. *Trends Cardiovasc. Med.* 14, 301–307. doi: 10.1016/j.tcm.2004.09.002

Chung, C. Y., Bien, H., and Entcheva, E. (2007). The role of cardiac tissue alignment in modulating electrical function. *J. Cardiovasc. Electrophysiol.* 18, 1323–1329. doi: 10.1111/j.1540-8167.2007.00959.x

Crowder, S. W., Leonardo, V., Whittaker, T., Papathanasiou, P., and Stevens, M. M. (2016). Material cues as potent regulators of epigenetics and stem cell function. *Cell Stem Cell* 18, 39–52. doi: 10.1016/j.stem.2015.12.012

Cui, X., Soliman, B. G., Alcala-Orozco, C. R., Li, J., Vis, M. A. M., Santos, M., et al. (2020). Rapid photocrosslinking of silk hydrogels with high cell density and enhanced shape fidelity. *Adv. Healthc. Mater.* 9:e1901667.

Cyranoski, D. (2018). "Reprogrammed" stem cells approved to mend human hearts for the first time. *Nature* 557, 619–620. doi: 10.1038/d41586-018-05278-8

Cyranoski, D. (2019). The potent effects of Japan's stem-cell policies. *Nature* 573, 482–485. doi: 10.1038/d41586-019-02847-3

Dattola, E., Parrotta, E. I., Scalise, S., Perozziello, G., Limongi, T., Candeloro, P., et al. (2019). Development of 3D PVA scaffolds for cardiac tissue engineering and cell screening applications. *RSC Adv.* 9, 4246–4257. doi: 10.1039/c8ra08187e

Davidson, J. M., Smith, K., Shibahara, S., Tolstoshev, P., and Crystal, R. G. (1982). Regulation of elastin synthesis in developing sheep nuchal ligament by elastin mRNA levels. *J. Biol. Chem.* 257, 747–754.

Desgres, M., and Menasché, P. (2019). Clinical translation of pluripotent stem cell therapies: challenges and considerations. *Cell Stem Cell* 25, 594–606. doi: 10.1016/j.stem.2019.10.001

Doetsch, F., Caille, I., Lim, D. A., Garcı, J. M., and Alvarez-buylla, A. (1999). Subventricular zone astrocytes are neural stem cells in the adult mammalian brain. *Cell* 97, 703–716. doi: 10.1016/s0092-8674(00)80783-7

Domian, I. J., Yu, H., and Mittal, N. (2017). On materials for cardiac tissue engineering. *Adv. Healthc. Mater.* 6:1600768.

Du, D. T. M., Hellen, N., Kane, C., and Terracciano, C. M. N. (2015). Action potential morphology of human induced pluripotent stem cell-derived cardiomyocytes does not predict cardiac chamber specificity and is dependent on cell density. *Biophys. J.* 108, 1–4. doi: 10.1016/j.bpj.2014.11.008

Duan, B., Wang, M., Zhou, W. Y., Cheung, W. L., Li, Z. Y., and Lu, W. W. (2010). Three-dimensional nanocomposite scaffolds fabricated via selective laser sintering for bone tissue engineering. *Acta Biomater.* 6, 4495–4505. doi: 10.1016/j.actbio.2010.06.024

Dubick, M. A., Rucker, R. B., Cross, C. E., and Last, J. A. (1981). Elastin metabolism in rodent lung. *BBA – Gen. Subj.* 672, 303–306. doi: 10.1016/0304-4165(81)90297-x

Eder, A., Vollert, I., Hansen, A., and Eschenhagen, T. (2016). Human engineered heart tissue as a model system for drug testing. *Adv. Drug Deliv. Rev.* 96, 214–224. doi: 10.1016/j.addr.2015.05.010

Eghbali, M., Czaja, M. J., Zeydel, M., Weiner, F. R., Zern, M. A., Seifter, S., et al. (1988). Collagen chain mRNAs in isolated heart cells from young and adult rats. *J. Mol. Cell. Cardiol.* 20, 267–276. doi: 10.1016/s0022-2828(88)80059-2

Eghbali, M., and Weber, K. T. (1990). Collagen and the myocardium: fibrillar structure, biosynthesis and degradation in relation to hypertrophy and its regression. *Mol. Cell. Biochem.* 96, 1–14.

Elliott, D. A., Braam, S. R., Koutsis, K., Ng, E. S., Jenny, R., Lagerqvist, E. L., et al. (2011). NKX2-5eGFP/w hESCs for isolation of human cardiac progenitors and cardiomyocytes. *Nat. Methods* 8, 1037–1040. doi: 10.1038/nmeth.1740

Engler, A. J., Carag-Krieger, C., Johnson, C. P., Raab, M., Tang, H. Y., Speicher, D. W., et al. (2008). Embryonic cardiomyocytes beat best on a matrix with heart-like elasticity: scar-like rigidity inhibits beating. *J. Cell Sci.* 121, 3794–3802. doi: 10.1242/jcs.029678

Eschenhagen, T., Bolli, R., Braun, T., Field, L. J., Fleischmann, B. K., Frisén, J., et al. (2017). Cardiomyocyte regeneration: a consensus statement. *Circulation* 136, 680–686. doi: 10.1161/circulationaha.117.029343

Eschenhagen, T., Fink, C., Remmers, U., Scholz, H., Wattchow, J., Weil, J., et al. (1997). Three-dimensional reconstitution of embryonic cardiomyocytes in a collagen matrix: a new heart muscle model system. *FASEB J.* 11, 683–694. doi: 10.1096/fasebj.11.8.9240969

Fan, D., Takawale, A., Lee, J., and Kassiri, Z. (2012). Cardiac fibroblasts, fibrosis and extracellular matrix remodeling in heart disease. *Fibrogenes Tissue Repair.* 5, 1–13.

Feaster, T. K., Cadar, A. G., Wang, L., Williams, C. H., Chun, Y. W., Hempel, J. E., et al. (2015). Matrigel mattress: a method for the generation of single contracting human-induced pluripotent stem cell-derived cardiomyocytes. *Circ Res.* 117, 995–1000. doi: 10.1161/circresaha.115.307580

Feric, N. T., Pallotta, I., Singh, R., Bogdanowicz, D. R., Gustilo, M. M., Chaudhary, K. W., et al. (2019). Engineered cardiac tissues generated in the biowire II: a platform for human-based drug discovery. *Toxicol. Sci.* 172, 89–97. doi: 10.1093/toxsci/kfz168

Fink, C., Ergün, S., Kralisch, D., Remmers, U., Weil, J., and Eschenhagen, T. (2000). Chronic stretch of engineered heart tissue induces hypertrophy and functional improvement. *FASEB J.* 14, 669–679. doi: 10.1096/fasebj.14.5.669

Fleischer, S., Shapira, A., Feiner, R., and Dvir, T. (2017). Modular assembly of thick multifunctional cardiac patches. *Proc. Natl. Acad. Sci. U.S.A.* 114, 1898–1903. doi: 10.1073/pnas.1615728114

Fleischer, S., Shapira, A., Regev, O., Nseir, N., Zussman, E., and Dvir, T. (2014). Albumin fiber scaffolds for engineering functional cardiac tissues. *Biotechnol. Bioeng.* 111, 1246–1257. doi: 10.1002/bit.25185

Fomovsky, G. M., Thomopoulos, S., and Holmes, J. W. (2010). Contribution of extracellular matrix to the mechanical properties of the heart. *J. Mol. Cell Cardiol.* 48, 490–496. doi: 10.1016/j.yjmcc.2009.08.003

Forrest, L., and Jackson, D. (1971). Intermolecular cross-linking of collagen in human and guinea pig scar tissue. *Biochim. Biophys. Acta Protein Struct.* 229, 681–689. doi: 10.1016/0005-2795(71)90284-4

Frangogiannis, N. G. (2019). The extracellular matrix in ischemic and nonischemic heart failure. *Circ Res.* 125, 117–146. doi: 10.1161/circresaha.119.311148

Gaebel, R., Ma, N., Liu, J., Guan, J., Koch, L., Klopsch, C., et al. (2011). Patterning human stem cells and endothelial cells with laser printing for cardiac regeneration. *Biomaterials* 32, 9218–9230. doi: 10.1016/j.biomaterials.2011.08.071

Ganji, Y., Li, Q., Quabius, E. S., Böttner, M., Selhuber-Unkel, C., and Kasra, M. (2016). Cardiomyocyte behavior on biodegradable polyurethane/gold nanocomposite scaffolds under electrical stimulation. *Mater. Sci. Eng. C* 59, 10–18. doi: 10.1016/j.msec.2015.09.074

Garreta, E., de Oñate, L., Fernández-Santos, M. E., Oria, R., Tarantino, C., Climent, A. M., et al. (2016). Myocardial commitment from human pluripotent stem cells: rapid production of human heart grafts. *Biomaterials* 1, 64–78. doi: 10.1016/j.biomaterials.2016.04.003

Gaudesius, G., Miragoli, M., Thomas, S. P., and Rohr, S. (2003). Coupling of cardiac electrical activity over extended distances by fibroblasts of cardiac origin. *Circ Res.* 93, 421–428. doi: 10.1161/01.res.0000089258.40661.0c

Gauvin, R., Chen, Y. C., Lee, J. W., Soman, P., Zorlutuna, P., Nichol, J. W., et al. (2012). Microfabrication of complex porous tissue engineering scaffolds using 3D projection stereolithography. *Biomaterials* 33, 3824–3834. doi: 10.1016/j.biomaterials.2012.01.048

Ghaemi, R. V., Siang, L. C., and Yadav, V. G. (2019). Improving the rate of translation of tissue engineering products. *Adv. Healthc. Mater.* 8:e1900538.

Giacomelli, E., Meraviglia, V., Campostrini, G., Cochrane, A., Cao, X., van Helden, R. W. J., et al. (2020). Human-iPSC-derived cardiac stromal cells

enhance maturation in 3D cardiac microtissues and reveal non-cardiomyocyte contributions to heart disease. *Cell Stem Cell* 26, 862.e11–879.e11.

Giannopoulos, A. A., Mitsouras, D., Yoo, S. J., Liu, P. P., Chatzizisis, Y. S., and Rybicki, F. J. (2016). Applications of 3D printing in cardiovascular diseases. *Nat. Rev. Cardiol.* 13, 701–718.

Gilbert, S. H., Benson, A. P., Li, P., and Holden, A. V. (2007). Regional localisation of left ventricular sheet structure: integration with current models of cardiac fibre, sheet and band structure. *Eur. J. Cardio-Thoracic. Surg.* 32, 231–249. doi: 10.1016/j.ejcts.2007.03.032

Godier-Furnémont, A. F. G., Tiburcy, M., Wagner, E., Dewenter, M., Lämmle, S., El-Armouche, A., et al. (2015). Physiologic force-frequency response in engineered heart muscle by electromechanical stimulation. *Biomaterials* 1, 82–91. doi: 10.1016/j.biomaterials.2015.03.055

Goldfracht, I., Efraim, Y., Shinnawi, R., Kovalev, E., Huber, I., Gepstein, A., et al. (2019). Engineered heart tissue models from hiPSC-derived cardiomyocytes and cardiac ECM for disease modeling and drug testing applications. *Acta Biomater.* 92, 145–159. doi: 10.1016/j.actbio.2019.05.016

Günthel, M., Barnett, P., and Christoffels, V. M. (2018). Development, proliferation, and growth of the mammalian heart. *Mol. Ther.* 26, 1599–1609. doi: 10.1016/j.ymthe.2018.05.022

Guo, Y., and Pu, W. T. (2020). Cardiomyocyte maturation: new phase in development. *Circ. Res.* 126, 1086–1106. doi: 10.1161/circresaha.119.315862

Gyöngyösi, M., Wojakowski, W., Navarese, E. P., and Moye, L. (2016). Meta-analyses of human cell-based cardiac regeneration therapies: controversies in meta-analyses results on cardiac cell-based regenerative studies. *Circ. Res.* 118, 1254–1263. doi: 10.1161/circresaha.115.307347

Halloin, C., Coffee, M., Manstein, F., and Zweigerdt, R. (2019). Production of cardiomyocytes from human pluripotent stem cells by bioreactor technologies. *Methods Mol. Biol.* 1994, 55–70. doi: 10.1007/978-1-4939-9477-9_5

Han, J., Wu, Q., Xia, Y., Wagner, M. B., and Xu, C. (2016). Cell alignment induced by anisotropic electrospun fibrous scaffolds alone has limited effect on cardiomyocyte maturation. *Stem Cell Res.* 16, 740–750. doi: 10.1016/j.scr.2016.04.014

Happe, C. L., and Engler, A. J. (2016). Mechanical forces reshape differentiation cues that guide cardiomyogenesis. *Circ. Res.* 118, 296–310. doi: 10.1161/circresaha.115.305139

Hasenfuss, G., Mulieri, L. A., Blanchard, E. M., Holubarsch, C., Leavitt, B. J., Ittleman, F., et al. (1991). Energetics of isometric force development in control and volume-overload human myocardium, Comparison with animal species. *Circ Res.* 68, 836–846. doi: 10.1161/01.res.68.3.836

Hattori, F., Chen, H., Yamashita, H., Tohyama, S., Satoh, Y.-S., Yuasa, S., et al. (2010). Nongenetic method for purifying stem cell-derived cardiomyocytes. *Nat. Methods* 7, 61–66. doi: 10.1038/nmeth.1403

Herget, G. W., Neuburger, M., Plagwitz, R., and Adler, C. P. (1997). DNA content, ploidy level and number of nuclei in the human heart after myocardial infarction. *Cardiovasc. Res.* 36, 45–51. doi: 10.1016/s0008-6363(97)00140-5

Hernández, D., Millard, R., Sivakumaran, P., Wong, R. C. B., Crombie, D. E., Hewitt, A. W., et al. (2016). Electrical stimulation promotes cardiac differentiation of human induced pluripotent stem cells. *Stem Cells Int.* 2016, 1718041.

Herron, T. J., Da Rocha, A. M., Campbell, K. F., Ponce-Balbuena, D., Willis, B. C., Guerrero-Serna, G., et al. (2016). Extracellular matrix-mediated maturation of human pluripotent stem cell-derived cardiac monolayer structure and electrophysiological function. *Circ. Arrhythmia Electrophysiol.* 9, 1–12.

Hildreth, V., Webb, S., Bradshaw, L., Brown, N. A., Anderson, R. H., and Henderson, D. J. (2008). Cells migrating from the neural crest contribute to the innervation of the venous pole of the heart. *J. Anat.* 212, 1–11.

Hinton, T. J., Jallerat, Q., Palchesko, R. N., Park, J. H., Grodzicki, M. S., Shue, H. J., et al. (2015). Three-dimensional printing of complex biological structures by freeform reversible embedding of suspended hydrogels. *Sci. Adv.* 1:e1500758. doi: 10.1126/sciadv.1500758

Hirt, M. N., Boeddinghaus, J., Mitchell, A., Schaaf, S., Börnchen, C., Müller, C., et al. (2014). Functional improvement and maturation of rat and human engineered heart tissue by chronic electrical stimulation. *J. Mol. Cell Cardiol.* 74, 151–161. doi: 10.1016/j.yjmcc.2014.05.009

Hochleitner, G., Fürsattel, E., Giesa, R., Groll, J., Schmidt, H.-W., and Dalton, P. D. (2018). Melt electrowriting of thermoplastic elastomers. *Macromol. Rapid Commun.* 39:e1800055.

Hodgkinson, C. P., Bareja, A., Gomez, J. A., and Dzau, V. J. (2016). Emerging concepts in paracrine mechanisms in regenerative cardiovascular medicine and biology. *Circ Res.* 118, 95–107. doi: 10.1161/circresaha.115.305373

Holland, C., Numata, K., Rnjak-Kovacina, J., and Seib, F. P. (2019). The biomedical use of silk: past, present, future. *Adv. Healthc. Mater.* 8:e1800465.

Holopainen, T., Räsänen, M., Anisimov, A., Tuomainen, T., Zheng, W., Tvorogov, D., et al. (2015). Endothelial Bmx tyrosine kinase activity is essential for myocardial hypertrophy and remodeling. *Proc. Natl. Acad. Sci. U.S.A.* 112, 13063–13068. doi: 10.1073/pnas.1517810112

Hu, Q., Sun, X. Z., Parmenter, C. D. J., Fay, M. W., Smith, E. F., Rance, G. A., et al. (2017). Additive manufacture of complex 3D Au-containing nanocomposites by simultaneous two-photon polymerisation and photoreduction. *Sci. Rep.* 7, 1–9.

Hulsmans, M., Clauss, S., Xiao, L., Aguirre, A. D., King, K. R., Hanley, A., et al. (2017). Macrophages facilitate electrical conduction in the heart. *Cell* 169, 510.e20–522.e20.

Ivashchenko, C. Y., Pipes, G. C., Lozinskaya, I. M., Lin, Z., Xiaoping, X., Needle, S., et al. (2013). Human-induced pluripotent stem cell-derived cardiomyocytes exhibit temporal changes in phenotype. *Am. J. Physiol. – Hear Circ. Physiol.* 305, H913–H922.

Iyer, R. K., Chiu, L. L. Y., and Radisic, M. (2009). Microfabricated poly(ethylene glycol) templates enable rapid screening of triculture conditions for cardiac tissue engineering. *J. Biomed. Mater. Res. – Part A* 89, 616–631. doi: 10.1002/jbm.a.32014

Izadifar, M., Chapman, D., Babyn, P., Chen, X., and Kelly, M. E. (2018). UV-assisted 3D bioprinting of nanoreinforced hybrid cardiac patch for myocardial tissue engineering. *Tissue Eng. Part C Methods* 24, 74–88. doi: 10.1089/ten.tec.2017.0346

Jackman, C. P., Carlson, A. L., and Bursac, N. (2016). Dynamic culture yields engineered myocardium with near-adult functional output. *Biomaterials* 1, 66–79. doi: 10.1016/j.biomaterials.2016.09.024

Jackman, C. P., Ganapathi, A. M., Asfour, H., Qian, Y., Allen, B. W., Li, Y., et al. (2018). Engineered cardiac tissue patch maintains structural and electrical properties after epicardial implantation. *Biomaterials* 1, 48–58. doi: 10.1016/j.biomaterials.2018.01.002

Jacot, J. G., Martin, J. C., and Hunt, D. L. (2010). Mechanobiology of cardiomyocyte development. *J. Biomech.* 43, 93–98. doi: 10.1016/j.jbiomech.2009.09.014

Jacot, J. G., McCulloch, A. D., and Omens, J. H. (2008). Substrate stiffness affects the functional maturation of neonatal rat ventricular myocytes. *Biophys J.* 1, 3479–3487. doi: 10.1529/biophysj.107.124545

James, D., Nam, H., Seandel, M., Nolan, D., Janovitz, T., Tomishima, M., et al. (2010). Expansion and maintenance of human embryonic stem cell–derived endothelial cells by TGFb inhibition is Id1 dependent. *Nat. Biotechnol.* 28, 161–167.

Jang, J., Park, H. J., Kim, S. W., Kim, H., Park, J. Y., Na, S. J., et al. (2017). 3D printed complex tissue construct using stem cell-laden decellularized extracellular matrix bioinks for cardiac repair. *Biomaterials* 112, 264–274. doi: 10.1016/j.biomaterials.2016.10.026

Janik, H., and Marzec, M. (2015). A review: fabrication of porous polyurethane scaffolds. *Mater. Sci. Eng. C* 48, 586–591. doi: 10.1016/j.msec.2014.12.037

Jiang, Y., Park, P., Hong, S. M., and Ban, K. (2018). Maturation of cardiomyocytes derived from human pluripotent stem cells: current strategies and limitations. *Mol. Cells* 41, 613–621.

Joanne, P., Kitsara, M., Boitard, S. E., Naemetalla, H., Vanneaux, V., Pernot, M., et al. (2016). Nanofibrous clinical-grade collagen scaffolds seeded with human cardiomyocytes induces cardiac remodeling in dilated cardiomyopathy. *Biomaterials* 80, 157–168. doi: 10.1016/j.biomaterials.2015.11.035

Jong, F. D., Virágh, S., and Moorman, A. F. M. (1997). Cardiac development: a morphologically integrated molecular approach. *Compar. Toxicol.* 7, 131–146. doi: 10.1017/s1047951100009379

Jungst, T., Smolan, W., Schacht, K., Scheibel, T., and Groll, J. (2016). Strategies and molecular design criteria for 3D printable hydrogels. *Chem. Rev.* 116, 1496–1539. doi: 10.1021/acs.chemrev.5b00303

Kadota, S., Minami, I., Morone, N., Heuser, J. E., Agladze, K., and Nakatsuji, N. (2013). Development of a reentrant arrhythmia model in human pluripotent stem cell-derived cardiac cell sheets. *Eur. Heart J.* 34, 1147–1156. doi: 10.1093/eurheartj/ehs418

Kadota, S., Pabon, L., Reinecke, H., and Murry, C. E. (2017). In vivo maturation of human induced pluripotent stem cell-derived cardiomyocytes in neonatal and adult rat hearts. *Stem Cell Rep.* 8, 278–289. doi: 10.1016/j.stemcr.2016.10.009

Kapnisi, M., Mansfield, C., Marijon, C., Guex, A. G., Perbellini, F., Bardi, I., et al. (2018). Auxetic cardiac patches with tunable mechanical and conductive properties toward treating myocardial infarction. *Adv. Funct Mater.* 28:1800618. doi: 10.1002/adfm.201800618

Karbassi, E., Fenix, A., Marchiano, S., Muraoka, N., Nakamura, K., Yang, X., et al. (2020). Cardiomyocyte maturation: advances in knowledge and implications for regenerative medicine. *Nat. Rev. Cardiol.* 17, 341–359. doi: 10.1038/s41569-019-0331-x

Kattman, S. J., Huber, T. L., and Keller, G. M. M. (2006). Multipotent Flk-1+ cardiovascular progenitor cells give rise to the cardiomyocyte, endothelial, and vascular smooth muscle lineages. *Dev. Cell* 11, 723–732. doi: 10.1016/j.devcel.2006.10.002

Kattman, S. J., Witty, A. D., Gagliardi, M., Dubois, N. C., Niapour, M., Hotta, A., et al. (2011). Stage-specific optimization of activin/nodal and BMP signaling promotes cardiac differentiation of mouse and human pluripotent stem cell lines. *Cell Stem Cell* 8, 228–240. doi: 10.1016/j.stem.2010.12.008

Katz, T. C., Singh, M. K., Degenhardt, K., Rivera-Feliciano, J., Johnson, R. L., Epstein, J. A., et al. (2012). Distinct compartments of the proepicardial organ give rise to coronary vascular endothelial cells. *Dev. Cell* 22, 639–650. doi: 10.1016/j.devcel.2012.01.012

Kawamura, M., Miyagawa, S., Fukushima, S., Saito, A., Miki, K., Funakoshi, S., et al. (2017). Enhanced therapeutic effects of human iPS cell derived-cardiomyocyte by combined cell-sheets with omental flap technique in porcine ischemic cardiomyopathy model. *Sci. Rep.* 7:8824.

Ke, D., and Murphy, S. V. (2019). Current challenges of bioprinted tissues towards clinical translation. *Tissue Eng. Part B Rev.* 25, 1–13. doi: 10.1089/ten.teb.2018.0132

Kehat, I., Kenyagin-Karsenti, D., Snir, M., Segev, H., Amit, M., Gepstein, A., et al. (2001). Human embryonic stem cells can differentiate into myocytes with structural and functional properties of cardiomyocytes. *J. Clin. Invest.* 108, 407–414. doi: 10.1172/jci200112131

Keyte, A. L., Alonzo-Johnsen, M., and Hutson, M. R. (2014). Evolutionary and developmental origins of the cardiac neural crest: building a divided outflow tract. *Birth Defects Res. Part C – Embryo Today Rev.* 102, 309–323. doi: 10.1002/bdrc.21076

Khan, M., Xu, Y., Hua, S., Johnson, J., Belevych, A., Janssen, P. M. L., et al. (2015). Evaluation of changes in morphology and function of human induced pluripotent stem cell derived cardiomyocytes (hiPSC-CMs) cultured on an aligned-nanofiber cardiac patch. *PLoS ONE* 10:e0126338. doi: 10.1371/journal.pone.0126338

Kharaziha, M., Nikkhah, M., Shin, S. R., Annabi, N., Masoumi, N., Gaharwar, A. K., et al. (2013). PGS:Gelatin nanofibrous scaffolds with tunable mechanical and structural properties for engineering cardiac tissues. *Biomaterials* 34, 6355–6366. doi: 10.1016/j.biomaterials.2013.04.045

Kharaziha, M., Shin, S. R., Nikkhah, M., Topkaya, S. N., Masoumi, N., Annabi, N., et al. (2014). Tough and flexible CNT-polymeric hybrid scaffolds for engineering cardiac constructs. *Biomaterials* 35, 7346–7354. doi: 10.1016/j.biomaterials.2014.05.014

Kielty, C. M., Shuttleworth, M. J., Sherratt, and Adrian, C. (2002). Elastic fibres. *J. Cell Sci.* 115, 2817–2828.

Kim, J., Wende, A. R., Sena, S., Theobald, H. A., Soto, J., Sloan, C., et al. (2008). Insulin-like growth factor I receptor signaling is required for exercise-induced cardiac hypertrophy. *Mol. Endocrinol.* 22, 2532–2543.

Kim, T. H., An, D. B., Oh, S. H., Kang, M. K., Song, H. H., and Lee, J. H. (2015). Creating stiffness gradient polyvinyl alcohol hydrogel using a simple gradual freezing-thawing method to investigate stem cell differentiation behaviors. *Biomaterials* 40, 51–60. doi: 10.1016/j.biomaterials.2014.11.017

Kitsara, M., Agbulut, O., Kontziampasis, D., Chen, Y., and Menasché, P. (2017). Fibers for hearts: a critical review on electrospinning for cardiac tissue engineering. *Acta Biomater.* 48, 20–40. doi: 10.1016/j.actbio.2016.11.014

Klabunde, R. (2012). "Cellular structure and function," in *Cardiovascular Physiology Concepts*, 2nd Edn, ed. C. Taylor (Philadelphia, PA: Lippincott Williams & Wilkins), 41–58.

Koch, L., Kuhn, S., Sorg, H., Gruene, M., Schlie, S., Gaebel, R., et al. (2010). Laser printing of skin cells and human stem cells. *Tissue Eng. Part C Methods* 16, 847–854. doi: 10.1089/ten.tec.2009.0397

Kohl, P. (2004). Cardiac cellular heterogeneity and remodelling. *Cardiovasc. Res.* 64, 195–197. doi: 10.1016/j.cardiores.2004.08.011

Koshy, S. T., Desai, R. M., Joly, P., Li, J., Bagrodia, R. K., Lewin, S. A., et al. (2016). Click-crosslinked injectable gelatin hydrogels. *Adv. Healthc. Mater.* 5, 541–547. doi: 10.1002/adhm.201500757

Krieg, M., Arboleda-Estudillo, Y., Puech, P. H., Käfer, J., Graner, F., Müller, D. J., et al. (2008). Tensile forces govern germ-layer organization in zebrafish. *Nat. Cell Biol.* 10, 429–436. doi: 10.1038/ncb1705

Kumar, A., Placone, J. K., and Engler, A. J. (2017). Understanding the extracellular forces that determine cell fate and maintenance. *Development* 144, 4261–4270. doi: 10.1242/dev.158469

Laflamme, M. A., Chen, K. Y., Naumova, A. V., Muskheli, V., Fugate, J. A., Dupras, S. K., et al. (2007). Cardiomyocytes derived from human embryonic stem cells in pro-survival factors enhance function of infarcted rat hearts. *Nat. Biotechnol.* 25, 1015–1024. doi: 10.1038/nbt1327

Lavergne, M., Derkaoui, M., Delmau, C., Letourneur, D., Uzan, G., and Le Visage, C. (2012). Porous polysaccharide-based scaffolds for human endothelial progenitor cells. *Macromol. Biosci.* 12, 901–910. doi: 10.1002/mabi.201100431

Laverty, H. G., Benson, C., Cartwright, E. J., Cross, M. J., Garland, C., Hammond, T., et al. (2011). How can we improve our understanding of cardiovascular safety liabilities to develop safer medicines? *Br. J. Pharmacol.* 163, 675–693. doi: 10.1111/j.1476-5381.2011.01255.x

Lee, A., Hudson, A. R., Shiwarski, D. J., Tashman, J. W., Hinton, T. J., Yerneni, S., et al. (2019). 3D bioprinting of collagen to rebuild components of the human heart. *Science (80-)* 365, 482–487. doi: 10.1126/science.aav9051

LeGrice, I. J., Takayama, Y., and Covell, J. W. (1995). Transverse shear along myocardial cleavage planes provides a mechanism for normal systolic wall thickening. *Circ. Res.* 77, 182–193. doi: 10.1161/01.res.77.1.182

Leucker, T. M., and Jones, S. P. (2014). Endothelial dysfunction as a nexus for endothelial cell-cardiomyocyte miscommunication. *Front. Physiol.* 5:328. doi: 10.3389/fphys.2014.00328

Levenberg, S., Golub, J. S., Amit, M., Itskovitz-Eldor, J., and Langer, R. (2002). Endothelial cells derived from human embryonic stem cells. *Proc. Natl. Acad. Sci. U.S.A.* 99, 4391–4396.

Lian, X., Hsiao, C., Wilson, G., Zhu, K., Hazeltine, L. B., Azarin, S. M., et al. (2012). Robust cardiomyocyte differentiation from human pluripotent stem cells via temporal modulation of canonical Wnt signaling. *Proc. Natl. Acad. Sci. U.S.A.* 109, E1848–E1857.

Liang, D., Hsiao, B. S., and Chu, B. (2007). Functional electrospun nanofibrous scaffolds for biomedical applications. *Adv. Drug Deliv. Rev.* 59, 1392–1412. doi: 10.1016/j.addr.2007.04.021

Liaw, N. Y., and Zimmermann, W. H. (2016). Mechanical stimulation in the engineering of heart muscle. *Adv. Drug Deliv. Rev.* 96, 156–160. doi: 10.1016/j.addr.2015.09.001

Liu, H., Wang, Y., Cui, K., Guo, Y., Zhang, X., and Qin, J. (2019). Advances in hydrogels in organoids and organs-on-a-chip. *Adv Mater.* 31:e1902042.

Louch, W. E., Koivumäki, J. T., and Tavi, P. (2015). Calcium signalling in developing cardiomyocytes: implications for model systems and disease. *J. Physiol.* 593, 1047–1063. doi: 10.1113/jphysiol.2014.274712

Lux, M., Andrée, B., Horvath, T., Nosko, A., Manikowski, D., Hilfiker-Kleiner, D., et al. (2016). In vitro maturation of large-scale cardiac patches based on a perfusable starter matrix by cyclic mechanical stimulation. *Acta Biomater.* 30, 177–187. doi: 10.1016/j.actbio.2015.11.006

MacIver, D. H., Partridge, J. B., Agger, P., Stephenson, R. S., Boukens, B. J. D., Omann, C., et al. (2018a). The end of the unique myocardial band: part II. Clinical and functional considerations. *Eur. J. Cardio-thoracic Surg.* 53, 120–128. doi: 10.1093/ejcts/ezx335

MacIver, D. H., Stephenson, R. S., Jensen, B., Agger, P., Sánchez-Quintana, D., Jarvis, J. C., et al. (2018b). The end of the unique myocardial band: part I. Anatomical considerations. *Eur. J. Cardio-Thoracic. Surg.* 53, 112–119. doi: 10.1093/ejcts/ezx290

Macqueen, L. A., Sheehy, S. P., Chantre, C. O., Zimmerman, J. F., Pasqualini, F. S., Liu, X., et al. (2018). A tissue-engineered scale model of the heart ventricle. *Nat. Biomed. Eng.* 2, 930–941. doi: 10.1038/s41551-018-0271-5

Maiullari, F., Costantini, M., Milan, M., Pace, V., Chirivì, M., Maiullari, S., et al. (2018). A multi-cellular 3D bioprinting approach for vascularized heart tissue engineering based on HUVECs and iPSC-derived cardiomyocytes. *Sci. Rep.* 8, 1–15.

Majkut, S., Idema, T., Swift, J., Krieger, C., Liu, A., and Discher, D. E. (2013). Heart-specific stiffening in early embryos parallels matrix and myosin expression to optimize beating. *Curr. Biol.* 23, 2434–2439. doi: 10.1016/j.cub.2013.10.057

Mannhardt, I., Warncke, C., Trieu, H. K., Müller, J., and Eschenhagen, T. (2019). Piezo-bending actuators for isometric or auxotonic contraction analysis of engineered heart tissue. *J. Tissue Eng. Regen Med.* 13, 3–11. doi: 10.1002/term.2755

Marvin, M. J., Di Rocco, G., Gardiner, A., Bush, S. M., and Lassar, A. B. (2001). Inhibition of Wnt activity induces heart formation from posterior mesoderm. *Genes Dev.* 15, 316–327. doi: 10.1101/gad.855501

Masoumi, N., Annabi, N., Assmann, A., Larson, B. L., Hjortnaes, J., Alemdar, N., et al. (2014). Tri-layered elastomeric scaffolds for engineering heart valve leaflets. *Biomaterials* 35, 7774–7785. doi: 10.1016/j.biomaterials.2014.04.039

Massai, D., Cerino, G., Gallo, D., Pennella, F., Deriu, M. A., Rodriguez, A., et al. (2013). Bioreactors as engineering support to treat cardiac muscle and vascular disease. *J. Healthc. Eng.* 4, 329–370. doi: 10.1260/2040-2295.4.3.329

Mastikhina, O., Moon, B. U., Williams, K., Hatkar, R., Gustafson, D., Mourad, O., et al. (2020). Human cardiac fibrosis-on-a-chip model recapitulates disease hallmarks and can serve as a platform for drug testing. *Biomaterials* 233:119741. doi: 10.1016/j.biomaterials.2019.119741

Mawad, D., Mansfield, C., Lauto, A., Perbellini, F., Nelson, G. W., Tonkin, J., et al. (2016). A conducting polymer with enhanced electronic stability applied in cardiac models. *Sci. Adv.* 2:e1601007. doi: 10.1126/sciadv.1601007

Mazzoli, A. (2013). Selective laser sintering in biomedical engineering. *Med. Biol. Eng. Comput.* 51, 245–256. doi: 10.1007/s11517-012-1001-x

McKenna, W. J., Maron, B. J., and Thiene, G. (2017). Classification, epidemiology, and global burden of cardiomyopathies. *Circ. Res.* 121, 722–730. doi: 10.1161/circresaha.117.309711

Meilhac, S. M., and Buckingham, M. E. (2018). The deployment of cell lineages that form the mammalian heart. *Nat. Rev. Cardiol.* 15, 705–724. doi: 10.1038/s41569-018-0086-9

Meilhac, S. M., Lescroart, F., Blanpain, C. D., and Buckingham, M. E. (2014). Cardiac cell lineages that form the heart. *Cold Spring. Harb. Perspect. Med.* 4:a013888. doi: 10.1101/cshperspect.a013888

Melchels, F. P. W., Feijen, J., and Grijpma, D. W. (2010). A review on stereolithography and its applications in biomedical engineering. *Biomaterials* 31, 6121–6130. doi: 10.1016/j.biomaterials.2010.04.050

Menasché, P. (2018). Cell therapy trials for heart regeneration – Lessons learned and future directions. *Nat. Rev. Cardiol.* 15, 659–671. doi: 10.1038/s41569-018-0013-0

Menasché, P., Alfieri, O., Janssens, S., McKenna, W., Reichenspurner, H., Trinquart, L., et al. (2008). The myoblast autologous grafting in ischemic cardiomyopathy (MAGIC) trial: first randomized placebo-controlled study of myoblast transplantation. *Circulation* 117, 1189–1200. doi: 10.1161/circulationaha.107.734103

Menasché, P., Vanneaux, V., Hagège, A., Bel, A., Cholley, B., Cacciapuoti, I., et al. (2015). Human embryonic stem cell-derived cardiac progenitors for severe heart failure treatment: first clinical case report. *Eur. Heart J.* 36, 2011–2017. doi: 10.1093/eurheartj/ehv189

Menasché, P., Vanneaux, V., Hagège, A., Bel, A., Cholley, B., Parouchev, A., et al. (2018). Transplantation of human embryonic stem cell–derived cardiovascular progenitors for severe ischemic left ventricular dysfunction. *J. Am. Coll Cardiol.* 71, 429–438. doi: 10.1016/j.jacc.2017.11.047

Millard, D., Dang, Q., Shi, H., Zhang, X., Strock, C., Kraushaar, U., et al. (2018). Cross-site reliability of human induced pluripotent stem cell-derived cardiomyocyte based safety assays using microelectrode arrays: results from a blinded cipa pilot study. *Toxicol. Sci.* 164, 550–562. doi: 10.1093/toxsci/kfy110

Miller, L. W., Guglin, M., and Rogers, J. (2013). Cost of ventricular assist devices can we afford the progress? *Circulation* 127, 743–748. doi: 10.1161/circulationaha.112.139824

Miyagawa, S., Domae, K., Kainuma, S., Matsuura, R., Yoshioka, D., Hata, H., et al. (2018). Long-term outcome of a dilated cardiomyopathy patient after mitral valve surgery combined with tissue-engineered myoblast sheets—report of a case. *Surg. Case Rep.* 4, 1–5.

Mjaatvedt, C. H., Nakaoka, T., Moreno-Rodriguez, R., Norris, R. A., Kern, M. J., Eisenberg, C. A., et al. (2001). The outflow tract of the heart is recruited from a novel heart-forming field. *Dev. Biol.* 238, 97–109. doi: 10.1006/dbio.2001.0409

Mohamed, T. M. A., Stone, N. R., Berry, E. C., Radzinsky, E., Huang, Y., Pratt, K., et al. (2017). Chemical enhancement of in vitro and in vivo direct cardiac reprogramming. *Circulation* 135, 978–995. doi: 10.1161/circulationaha.116.024692

Mollova, M., Bersell, K., Walsh, S., Savla, J., Das, L. T., Park, S. Y., et al. (2013). Cardiomyocyte proliferation contributes to heart growth in young humans. *Proc. Natl. Acad. Sci. U.S.A.* 110, 1446–1451. doi: 10.1073/pnas.1214608110

Mommersteeg, M. T. M., Domínguez, J. N., Wiese, C., Norden, J., De Gier-De Vries, C., Burch, J. B. E., et al. (2010). The sinus venosus progenitors separate and diversify from the first and second heart fields early in development. *Cardiovasc. Res.* 87, 92–101. doi: 10.1093/cvr/cvq033

Mooney, D. J., Baldwin, D. F., Suh, N. P., Vacanti, J. P., and Langer, R. (1996). Novel approach to fabricate porous sponges of poly(D,L-lactic-co-glycolic acid) without the use of organic solvents. *Biomaterials* 17, 1417–1422. doi: 10.1016/0142-9612(96)87284-x

Moretti, A., Bellin, M., Welling, A., Jung, C. B., Lam, J. T., Bott-Flügel, L., et al. (2010). Patient-specific induced pluripotent stem-cell models for long-QT syndrome. *New. Engl. J. Med.* 363, 1397–1409.

Moroni, L., De Wijn, J. R., and Van Blitterswijk, C. A. (2006). 3D fiber-deposited scaffolds for tissue engineering: influence of pores geometry and architecture on dynamic mechanical properties. *Biomaterials* 27, 974–985. doi: 10.1016/j.biomaterials.2005.07.023

Mummery, C., Ward-van Oostwaard, D., Doevendans, P., Spijker, R., Van den Brink, S., Hassink, R., et al. (2003). Differentiation of human embryonic stem cells to cardiomyocytes: role of coculture with visceral endoderm-like cells. *Circulation* 107, 2733–2740. doi: 10.1161/01.cir.0000068356.38592.68

Myers, B., Dubick, M. A., Keen, C. L., and Rucker, R. B. (1985). Elastin synthesis during perinatal lung development in the rat. *Exp. Lung Res.* 8, 227–241. doi: 10.3109/01902148509087806

Nakamura, M., and Sadoshima, J. (2018). Mechanisms of physiological and pathological cardiac hypertrophy. *Nat. Rev. Cardiol.* 15, 387–407. doi: 10.1038/s41569-018-0007-y

Nam, Y. S., and Park, T. G. (1999). Porous biodegradable polymeric scaffolds prepared by thermally induced phase separation. *J. Biomed. Mater. Res.* 47, 8–17. doi: 10.1002/(sici)1097-4636(199910)47:1<8::aid-jbm2>3.0.co;2-l

Neejy, J. R. (1974). Relationship between carbohydrate and lipid metabolism and the energy balance of heart muscle. *Annu. Rev. Physiol.* 36, 413–459. doi: 10.1146/annurev.ph.36.030174.002213

Nguyen-Truong, M., and Wang, Z. (2018). Biomechanical properties and mechanobiology of cardiac ECM. *Adv. Exp. Med. Biol.* 1098, 1–19. doi: 10.1007/978-3-319-97421-7_1

Noor, N., Shapira, A., Edri, R., Gal, I., Wertheim, L., and Dvir, T. (2019). 3D Printing of personalized thick and perfusable cardiac patches and hearts. *Adv. Sci.* 6:1900344. doi: 10.1002/advs.201900344

Nowbar, A. N., Gitto, M., Howard, J. P., Francis, D. P., and Al-Lamee, R. (2019). Mortality from ischemic heart disease: analysis of data from the world health organization and coronary artery disease risk factors from NCD risk factor collaboration. *Circ. Cardiovasc. Qual. Outcomes* 12, 1–11.

Nunes, S. S., Miklas, J. W., Liu, J., Aschar-Sobbi, R., Xiao, Y., Zhang, B., et al. (2013). Biowire: a platform for maturation of human pluripotent stem cell-derived cardiomyocytes. *Nat. Methods* 10, 781–787.

O'Brien, F. J., Harley, B. A., Yannas, I. V., and Gibson, L. (2004). Influence of freezing rate on pore structure in freeze-dried collagen-GAG scaffolds. *Biomaterials* 25, 1077–1086. doi: 10.1016/s0142-9612(03)00630-6

Odde, D. J., and Renn, M. J. (2000). Laser-guided direct writing of living cells. *Biotechnol. Bioeng.* 67, 312–318. doi: 10.1002/(sici)1097-0290(20000205)67:3<312::aid-bit7>3.0.co;2-f

Olvera, D., Molina, M., Hendy, G., and Monaghan, M. (2020). Electroconductive melt electrowritten patches matching the mechanical anisotropy of human myocardium . *Adv. Funct. Mater.* 1909880.

Orive, G., Taebnia, N., and Dolatshahi-Pirouz, A. (2020). A new era for cyborg science is emerging: the promise of cyborganic beings. *Adv. Healthc. Mater.* 9:e1901023.

Orive, G., Tam, S. K., Pedraz, J. L., and Hallé, J. P. (2006). Biocompatibility of alginate-poly-l-lysine microcapsules for cell therapy. *Biomaterials* 27, 3691–3700. doi: 10.1016/j.biomaterials.2006.02.048

Orlova, V. V., Van Den Hil, F. E., Petrus-Reurer, S., Drabsch, Y., Ten Dijke, P., and Mummery, C. L. (2014). Generation, expansion and functional analysis of endothelial cells and pericytes derived from human pluripotent stem cells. *Nat. Protoc.* 9, 1514–1531. doi: 10.1038/nprot.2014.102

Ott, H. C., Matthiesen, T. S., Goh, S. K., Black, L. D., Kren, S. M., Netoff, T. I., et al. (2008). Perfusion-decellularized matrix: using nature's platform to engineer a bioartificial heart. *Nat. Med.* 14, 213–221. doi: 10.1038/nm1684

Ouyang, L., Highley, C. B., Sun, W., and Burdick, J. A. (2017). A generalizable strategy for the 3D bioprinting of hydrogels from nonviscous photo-crosslinkable inks. *Adv. Mater.* 29:1604983.

Pagano, F., Picchio, V., Chimenti, I., Sordano, A., De Falco, E., Peruzzi, M., et al. (2019). On the road to regeneration: "tools" and "routes" towards efficient cardiac cell therapy for ischemic cardiomyopathy. *Curr. Cardiol. Rep.* 21:133.

Paige, S. L., Osugi, T., Afanasiev, O. K., Pabon, L., Reinecke, H., and Murry, C. E. (2010). Endogenous wnt/β-Catenin signaling is required for cardiac differentiation in human embryonic stem cells. *PLoS ONE* 5:e11134. doi: 10.1371/journal.pone.0011134

Palpant, N. J., Pabon, L., Friedman, C. E., Roberts, M., Hadland, B., Zaunbrecher, R. J., et al. (2017). Generating high-purity cardiac and endothelial derivatives from patterned mesoderm using human pluripotent stem cells. *Nat. Protoc.* 12, 15–31. doi: 10.1038/nprot.2016.153

Parks, W. C., Secrist, H., Wu, L. C., and Mecham, R. P. (1988). Developmental regulation of tropoelastin isoforms. *J. Biol. Chem.* 263, 4416–4423.

Parmley, W. W., Chuck, L., Kivowitz, C., Matloff, J. M., and Swan, H. J. C. (1973). In vitro length-tension relations of human ventricular aneurysms: relation of stiffness to mechanical disadvantage. *Am. J. Cardiol.* 32, 889–894. doi: 10.1016/s0002-9149(73)80153-5

Parsa, H., Ronaldson, K., and Vunjak-Novakovic, G. (2016). Bioengineering methods for myocardial regeneration. *Adv. Drug Deliv. Rev.* 96, 195–202. doi: 10.1016/j.addr.2015.06.012

Patsch, C., Challet-Meylan, L., Thoma, E. C., Urich, E., Heckel, T., O'Sullivan, J. F., et al. (2015). Generation of vascular endothelial and smooth muscle cells from human pluripotent stem cells. *Nat. Cell Biol.* 17, 994–1003.

Peña, B., Laughter, M., Jett, S., Rowland, T. J., Taylor, M. R. G., Mestroni, L., et al. (2018). Injectable hydrogels for cardiac tissue engineering. *Macromol. Biosci.* 18, 1–22.

Pérez-Pomares, J. M., Phelps, A., Sedmerova, M., Carmona, R., González-Iriarte, M., Muoz-Chápuli, R., et al. (2002). Experimental studies on the spatiotemporal expression of WT1 and RALDH2 in the embryonic avian heart: a model for the regulation of myocardial and valvuloseptal development by epicardially derived cells (EPDCs). *Dev. Biol.* 247, 307–326. doi: 10.1006/dbio.2002.0706

Pinto, A. R., Ilinykh, A., Ivey, M. J., Kuwabara, J. T., D'antoni, M. L., Debuque, R., et al. (2016). Revisiting cardiac cellular composition. *Circ. Res.* 118, 400–409. doi: 10.1161/circresaha.115.307778

Pollock, J., Baule, V. J., Rich, C. B., Ginsburg, C. D., Curtiss, S. W., and Foster, J. A. (1990). Chick tropoelastin isoforms. From the gene to the extracellular matrix. *J. Biol. Chem.* 265, 3697–3702.

Poveda, F., Gil, D., Martí, E., Andaluz, A., Ballester, M., and Carreras, F. (2013). Helical structure of the cardiac ventricular anatomy assessed by diffusion tensor magnetic resonance imaging with multiresolution tractography. *Rev. Española Cardiol. (English Ed.)* 66, 782–790. doi: 10.1016/j.rec.2013.04.021

Prabhu, P. K. (2019). Is presumed consent an ethically acceptable way of obtaining organs for transplant? *J. Intensive Care Soc.* 20, 92–97. doi: 10.1177/1751143718777171

Prakash, Y. S., Cody, M. J., Housmans, P. R., Hannon, J. D., and Sieck, G. C. (1999). Comparison of cross-bridge cycling kinetics in neonatal vs. adult rat ventricular muscle. *J. Muscle Res. Cell Motil.* 20, 717–723.

Protze, S. I., Liu, J., Nussinovitch, U., Ohana, L., Backx, P. H., Gepstein, L., et al. (2017). Sinoatrial node cardiomyocytes derived from human pluripotent cells function as a biological pacemaker. *Nat. Biotechnol.* 35, 56–68. doi: 10.1038/nbt.3745

Radisic, M., Park, H., Shing, H., Consi, T., Schoen, F. J., Langer, R., et al. (2004a). Functional assembly of engineered myocardium by electrical stimulation of cardiac myocytes cultured on scaffolds. *Proc. Natl. Acad. Sci. U.S.A.* 101, 18129–18134. doi: 10.1073/pnas.0407817101

Radisic, M., Yang, L., Boublik, J., Cohen, R. J., Langer, R., Freed, L. E., et al. (2004b). Medium perfusion enables engineering of compact and contractile cardiac tissue. *Am. J. Physiol. – Hear Circ. Physiol.* 286, 507–516.

Richards, D. J., Tan, Y., Coyle, R., Li, Y., Xu, R., Yeung, N., et al. (2016). Nanowires and electrical stimulation synergistically improve functions of hiPSC cardiac spheroids. *Nano Lett.* 16, 4670–4678. doi: 10.1021/acs.nanolett.6b02093

Ritz-Timme, S., Laumeier, I., and Collins, M. J. (2003). Aspartic acid racemization: evidence for marked longevity of elastin in human skin. *Br. J. Dermatol.* 149, 951–959. doi: 10.1111/j.1365-2133.2003.05618.x

Roberts, D. E., Hersh, L. T., and Scher, A. M. (1979). Influence of cardiac fiber orientation on wavefront voltage, conduction velocity, and tissue resistivity in the dog. *Circ Res.* 44, 701–712. doi: 10.1161/01.res.44.5.701

Roberts, W. C., Siegel, R. J., and McManus, B. M. (1987). Idiopathic dilated cardiomyopathy: analysis of 152 necropsy patients. *Am. J. Cardiol.* 60, 1340–1355. doi: 10.1016/0002-9149(87)90618-7

Rock, J. R., Onaitis, M. W., Rawlins, E. L., Lu, Y., Clark, C. P., Xue, Y., et al. (2009). Basal cells as stem cells of the mouse trachea and human airway epithelium. *Proc. Natl. Acad. Sci. U.S.A.* 106, 12771–12775. doi: 10.1073/pnas.0906850106

Ronaldson-Bouchard, K., Ma, S. P., Yeager, K., Chen, T., Song, L. J., Sirabella, D., et al. (2018). Advanced maturation of human cardiac tissue grown from pluripotent stem cells. *Nature* 1, 239–243. doi: 10.1038/s41586-018-0016-3

Roshanbinfar, K., Vogt, L., Ruther, F., Roether, J. A., Boccaccini, A. R., and Engel, F. B. (2020). Nanofibrous composite with tailorable electrical and mechanical properties for cardiac tissue engineering. *Adv. Funct. Mater.* 30:1908612.

Ruan, J. L., Tulloch, N. L., Razumova, M. V., Saiget, M., Muskheli, V., Pabon, L., et al. (2016). Mechanical stress conditioning and electrical stimulation promote contractility and force maturation of induced pluripotent stem cell-derived human cardiac tissue. *Circulation* 134, 1557–1567. doi: 10.1161/circulationaha.114.014998

Ruiz-Villalba, A., Hoppler, S., and van den Hoff, M. J. B. (2016). Wnt signaling in the heart fields: variations on a common theme. *Dev. Dyn.* 245, 294–306. doi: 10.1002/dvdy.24372

Sartiani, L., Bettiol, E., Stillitano, F., Mugelli, A., Cerbai, E., and Jaconi, M. E. (2007). Developmental changes in cardiomyocytes differentiated from human embryonic stem cells: a molecular and electrophysiological approach. *Stem Cells* 25, 1136–1144. doi: 10.1634/stemcells.2006-0466

Sato, S., Ashraf, M., Millard, R. W., Fujiwara, H., and Schwartz, A. (1983). Connective tissue changes in early ischemia of porcine myocardium: an ultrastructural study. *J. Mol. Cell Cardiol.* 15, 261–275. doi: 10.1016/0022-2828(83)90281-x

Sauer, H., Rahimi, G., Hescheler, J., and Wartenberg, M. (1999). Effects of electrical fields on cardiomyocyte differentiation of embryonic stem cells. *J. Cell Biochem.* 75, 710–723. doi: 10.1002/(sici)1097-4644(19991215)75:4<710::aid-jcb16>3.0.co;2-z

Schächinger, V., Erbs, S., Elsässer, A., Haberbosch, W., Hambrecht, R., Hölschermann, H., et al. (2006). Intracoronary bone marrow-derived progenitor cells in acute myocardial infarction. *N. Engl. J. Med.* 355, 1210–1221.

Scollan, D. F., Holmes, A., Winslow, R., and Forder, J. (1998). Histological validation of myocardial microstructure obtained from diffusion tensor magnetic resonance imaging. *Am. J. Physiol. – Hear Circ Physiol.* 275, 2308–2318.

Sensini, A., and Cristofolini, L. (2018). Biofabrication of electrospun scaffolds for the regeneration of tendons and ligaments. *Materials (Basel)* 11, 1–43.

Sephel, G. C., Buckley, A., and Davidson, J. M. (1987). Developmental initiation of elastin gene expression by human fetal skin fibroblasts. *J. Invest. Dermatol.* 88, 732–735. doi: 10.1111/1523-1747.ep12470403

Serena, E., Figallo, E., Tandon, N., Cannizzaro, C., Gerecht, S., Elvassore, N., et al. (2009). Electrical stimulation of human embryonic stem cells: cardiac differentiation and the generation of reactive oxygen species. *Exp. Cell Res.* 315, 3611–3619. doi: 10.1016/j.yexcr.2009.08.015

Serra, M., Correia, C., Malpique, R., Brito, C., Jensen, J., Bjorquist, P., et al. (2011). Microencapsulation technology: a powerful tool for integrating expansion and cryopreservation of human embryonic stem cells. *PLoS One* 6:e23212. doi: 10.1371/journal.pone.0023212

Sessions, A. O., and Engler, A. J. (2016). Mechanical regulation of cardiac aging in model systems. *Circ Res.* 118, 1553–1562. doi: 10.1161/circresaha.116.307472

Shadrin, I. Y., Allen, B. W., Qian, Y., Jackman, C. P., Carlson, A. L., Juhas, M. E., et al. (2017). Cardiopatch platform enables maturation and scale-up of human pluripotent stem cell-derived engineered heart tissues. *Nat. Commun.* 8:1825.

Sharma, A., Sances, S., Workman, M. J., and Svendsen, C. N. (2020). Multi-lineage human iPSC-derived platforms for disease modeling and drug discovery. *Cell Stem Cell* 26, 309–329. doi: 10.1016/j.stem.2020.02.011

Shin, S. R., Jung, S. M., Zalabany, M., Kim, K., Zorlutuna, P., Kim, S. B., et al. (2013). Carbon-nanotube-embedded hydrogel sheets for engineering cardiac constructs and bioactuators. *ACS Nano* 7, 2369–2380. doi: 10.1021/nn305559j

Sireesha, M., Jagadeesh Babu, V., and Ramakrishna, S. (2015). Biocompatible and biodegradable elastomer/fibrinogen composite electrospun scaffolds for cardiac tissue regeneration. *RSC Adv.* 5, 103308–103314. doi: 10.1039/c5ra20322h

Sizarov, A., Lamers, W. H., Mohun, T. J., Brown, N. A., Anderson, R. H., and Moorman, A. F. M. (2012). Three-dimensional and molecular analysis of the arterial pole of the developing human heart. *J. Anat.* 220, 336–349. doi: 10.1111/j.1469-7580.2012.01474.x

Solaro, R. J. (2007). Mechanisms of the frank-starling law of the heart: the beat goes on. *Biophys. J.* 93, 4095–4096. doi: 10.1529/biophysj.107.117200

Sommer, G., Haspinger, D. C., Andrä, M., Sacherer, M., Viertler, C., Regitnig, P., et al. (2015a). Quantification of shear deformations and corresponding stresses in the biaxially tested human myocardium. *Ann. Biomed. Eng.* 43, 2334–2348. doi: 10.1007/s10439-015-1281-z

Sommer, G., Schriefl, A. J., Andrä, M., Sacherer, M., Viertler, C., Wolinski, H., et al. (2015b). Biomechanical properties and microstructure of human ventricular myocardium. *Acta Biomater.* 24, 172–192. doi: 10.1016/j.actbio.2015.06.031

Spach, M. S., and Heidlage, J. F. (1995). The stochastic nature of cardiac propagation at a microscopic level. Electrical description of myocardial architecture and its application to conduction. *Circ Res.* 76, 366–380. doi: 10.1161/01.res.76.3.366

Stehlik, J., Edwards, L. B., Kucheryavaya, A. Y., Benden, C., Christie, J. D., Dobbels, F., et al. (2011). The registry of the international society for heart and lung transplantation: twenty-eighth adult heart transplant report-2011. *J. Hear Lung Transplant.* 30, 1078–1094. doi: 10.1016/j.healun.2011.08.003

Stöhr, A., Friedrich, F. W., Flenner, F., Geertz, B., Eder, A., Schaaf, S., et al. (2013). Contractile abnormalities and altered drug response in engineered heart tissue from Mybpc3-targeted knock-in mice. *J. Mol. Cell Cardiol.* 63, 189–198. doi: 10.1016/j.yjmcc.2013.07.011

Stoppel, W. L., Kaplan, D. L., and Black, L. D. (2016). Electrical and mechanical stimulation of cardiac cells and tissue constructs. *Adv. Drug Deliv. Rev.* 96, 135–155. doi: 10.1016/j.addr.2015.07.009

Sussman, M. A., McCulloch, A., and Borg, T. K. (2002). Dance band on the Titanic: biomechanical signaling in cardiac hypertrophy. *Circ. Res.* 91, 888–898. doi: 10.1161/01.res.0000041680.43270.f8

Taccardi, B., Punske, B. B., Macchi, E., MacLeod, R. S., and Ershler, P. R. (2008). Epicardial and intramural excitation during ventricular pacing: effect of myocardial structure. *Am. J. Physiol. – Hear Circ Physiol.* 294, 1753–1766.

Takahashi, K., and Yamanaka, S. (2006). Induction of pluripotent stem cells from mouse embryonic and adult fibroblast cultures by defined factors. *Cell* 126, 663–676. doi: 10.1016/j.cell.2006.07.024

Tamay, D. G., Usal, T. D., Alagoz, A. S., Yucel, D., Hasirci, N., and Hasirci, V. (2019). 3D and 4D printing of polymers for tissue engineering applications. *Front. Bioeng. Biotechnol.* 7:164. doi: 10.3389/fbioe.2019.00164

Tan, S. H., and Ye, L. (2018). Maturation of pluripotent stemcell-derived cardiomyocytes: a critical step for drug development and cell therapy. *J. Cardiovasc. Transl. Res.* 11, 375–392. doi: 10.1007/s12265-018-9801-5

Tandon, N., Cannizzaro, C., Chao, P. P.-H. G., Maidhof, R., Marsano, A., Au, H. T. H., et al. (2009). Electrical stimulation systems for cardiac tissue engineering. *Nat. Protoc.* 4, 155–173.

Tandon, N., Marsano, A., Cannizzaro, C., Voldman, J., and Vunjak-Novakovic, G. (2008). Design of electrical stimulation bioreactors for cardiac tissue engineering. *Conf. Proc. IEEE Eng. Med. Biol. Soc.* 2008, 3594–3597.

Thomson, J. A., Itskovitz-eldor, J., Shapiro, S. S., Michelle, A., Swiergiel, J. J., Marshall, V. S., et al. (1998). Embryonic stem cell lines derived from human blastocysts. *Science (80-)* 282, 1145–1147. doi: 10.1126/science.282.5391.1145

Thomson, R. C., Yaszemski, M. J., Powers, J. M., and Mikos, A. G. (1995). Fabrication of biodegradable polymer scaffolds to engineer trabecular bone. *J. Biomater. Sci. Polym. Ed.* 7, 23–38. doi: 10.1163/156856295x00805

Tiburcy, M., Hudson, J. E., Balfanz, P., Schlick, S., Meyer, T., Liao, M. L. C., et al. (2017). Defined engineered human myocardium with advanced maturation for applications in heart failure modeling and repair. *Circulation* 9, 1832–1847. doi: 10.1161/circulationaha.116.024145

Tohyama, S., Hattori, F., Sano, M., Hishiki, T., Nagahata, Y., Matsuura, T., et al. (2013). Distinct metabolic flow enables large-scale purification of mouse and human pluripotent stem cell-derived cardiomyocytes. *Cell Stem Cell* 12, 127–137. doi: 10.1016/j.stem.2012.09.013

Townsend, N., Wilson, L., Bhatnagar, P., Wickramasinghe, K., Rayner, M., and Nichols, M. (2016). Cardiovascular disease in Europe: epidemiological update 2016. *Eur. Heart J.* 37, 3232–3245. doi: 10.1093/eurheartj/ehw334

Tran, T. H., Wang, X., Browne, C., Zhang, Y., Schinke, M., Izumo, S., et al. (2009). Wnt3a-induced mesoderm formation and cardiomyogenesis in human embryonic stem cells. *Stem Cells* 27, 1869–1878. doi: 10.1002/stem.95

Ueno, S., Weidinger, G., Osugi, T., Kohn, A. D., Golob, J. L., Pabon, L., et al. (2007). Biphasic role for Wnt/β-catenin signaling in cardiac specification in zebrafish and embryonic stem cells. *Proc. Natl. Acad. Sci. U.S.A.* 104, 9685–9690. doi: 10.1073/pnas.0702859104

Ulmer, B. M., Stoehr, A., Schulze, M. L., Patel, S., Gucek, M., Mannhardt, I., et al. (2018). Contractile work contributes to maturation of energy metabolism in hiPSC-derived cardiomyocytes. *Stem Cell Rep.* 10, 834–847. doi: 10.1016/j.stemcr.2018.01.039

Uosaki, H., Fukushima, H., Takeuchi, A., Matsuoka, S., Nakatsuji, N., Yamanaka, S., et al. (2011). Efficient and scalable purification of cardiomyocytes from human embryonic and induced pluripotent stem cells by VCAM1 surface expression. *PLoS ONE* 6:e23657. doi: 10.1371/journal.pone.0023657

Vaithilingam, J., Sanjuan-Alberte, P., Campora, S., Rance, G. A., Jiang, L., Thorpe, J., et al. (2019). Multifunctional bioinstructive 3D architectures to modulate cellular behavior. *Adv. Funct. Mater.* 29:1902016.

Valiente-Alandi, I., Potter, S. J., Salvador, A. M., Schafer, A. E., Schips, T., Carrillo-Salinas, F., et al. (2018). Inhibiting fibronectin attenuates fibrosis and improves cardiac function in a model of heart failure. *Circulation* 138, 1236–1252. doi: 10.1161/circulationaha.118.034609

Vallier, L., Mendjan, S., Brown, S., Ching, Z., Teo, A., Smithers, L. E., et al. (2009). Activin/Nodal signalling maintains pluripotency by controlling Nanog expression. *Development* 136, 1339–1349. doi: 10.1242/dev.033951

Valls-Margarit, M., Iglesias-García, O., Di Guglielmo, C., Sarlabous, L., Tadevosyan, K., Paoli, R., et al. (2019). Engineered macroscale cardiac constructs elicit human myocardial tissue-like functionality. *Stem Cell Rep.* 9, 207–220. doi: 10.1016/j.stemcr.2019.05.024

Vincent, S. D., and Buckingham, M. E. (2010). How to make a heart. The origin and regulation of cardiac progenitor cells. *Curr. Top. Dev. Biol.* 90, 1–41.

Vozzi, F., Lograng, F., Cabiati, M., Cicione, C., Boffito, M., Carmagnola, I., et al. (2018). Biomimetic engineering of the cardiac tissue through processing, functionalization, and biological characterization of polyester urethanes. *Biomed. Mater.* 13:055006. doi: 10.1088/1748-605x/aaca5b

Vreeker, A., Van Stuijvenberg, L., Hund, T. J., Mohler, P. J., Nikkels, P. G. J., and Van Veen, T. A. B. (2014). Assembly of the cardiac intercalated disk during preand postnatal development of the human heart. *PLoS ONE* 9:e94722. doi: 10.1371/journal.pone.0094722

Vunjak-Novakovic, G., Eschenhagen, T., and Mummery, C. (2014). Myocardial tissue engineering: in vitro models. *Cold Spring Harb. Perspect. Med.* 4, 1–16.

Walker, B. W., Lara, R. P., Yu, C. H., Sani, E. S., Kimball, W., Joyce, S., et al. (2019). Engineering a naturally-derived adhesive and conductive cardiopatch. *Biomaterials* 1, 89–101. doi: 10.1016/j.biomaterials.2019.03.015

Walker, I. F., Garbe, F., Wright, J., Newell, I., Athiraman, N., Khan, N., et al. (2018). *The Economic Costs of Cardiovascular Disease, Diabetes Mellitus, and Associated Complications in South Asia: A Systematic Review*. Available online at: http://eprints.whiterose.ac.uk/118785/ (accessed June 16, 2020).

Wang, Y., Yao, F., Wang, L., Li, Z., Ren, Z., Li, D., et al. (2020). Single-cell analysis of murine fibroblasts identifies neonatal to adult switching that regulates cardiomyocyte maturation. *Nat. Commun.* 11:2585.

Wang, Z., Gagliardi, M., Mohamadi, R. M., Ahmed, S. U., Labib, M., Zhang, L., et al. (2020). Ultrasensitive and rapid quantification of rare tumorigenic stem cells in hPSC-derived cardiomyocyte populations. *Sci. Adv.* 6, 1–12.

Watson, S. A., Duff, J., Bardi, I., Zabielska, M., Atanur, S. S., Jabbour, R. J., et al. (2019). Biomimetic electromechanical stimulation to maintain adult myocardial slices in vitro. *Nat. Commun.* 10:2168.

Weber, K. T. (1989). Cardiac interstitium in health and disease: the fibrillar collagen network. *J. Am. Coll. Cardiol.* 13, 1637–1652. doi: 10.1016/0735-1097(89)90360-4

Weber, K. T., Pick, R., Janicki, J. S., Gadodia, G., and Lakier, J. B. (1988). Inadequate collagen tethers in dilated cardiopathy. *Am. Heart J.* 116, 1641–1646. doi: 10.1016/0002-8703(88)90763-6

Weeke-Klimp, A., Bax, N. A. M., Bellu, A. R., Winter, E. M., Vrolijk, J., Plantinga, J., et al. (2010). Epicardium-derived cells enhance proliferation, cellular maturation and alignment of cardiomyocytes. *J. Mol. Cell Cardiol.* 49, 606–616. doi: 10.1016/j.yjmcc.2010.07.007

Weinberger, F., Breckwoldt, K., Pecha, S., Kelly, A., Geertz, B., Starbatty, J., et al. (2016). Cardiac repair in Guinea pigs with human engineered heart tissue from induced pluripotent stem cells. *Sci. Transl. Med.* 8:363ra148. doi: 10.1126/scitranslmed.aaf8781

White, M. P., Rufaihah, A. J., Liu, L., Ghebremariam, Y. T., Ivey, K. N., Cooke, J. P., et al. (2013). Limited gene expression variation in human embryonic stem cell and induced pluripotent stem cell-derived endothelial cells. *Stem Cells* 31, 92–103. doi: 10.1002/stem.1267

Wickline, S. A., Verdonk, Wong, A. K., Shepard, R. K., and Miller, J. G. (1992). Structural remodeling of human myocardial tissue after infarction, quantification with ultrasonic backscatter. *Circulation* 85, 259–268. doi: 10.1161/01.cir.85.1.259

Witty, A. D., Mihic, A., Tam, R. Y., Fisher, S. A., Mikryukov, A., Shoichet, M. S., et al. (2014). Generation of the epicardial lineage from human pluripotent stem cells. *Nat. Biotechnol.* 32, 1026–1035.

Wollert, K. C., Meyer, G. P., Lotz, J., Ringes-Lichtenberg, S., Lippolt, P., and Breidenbach, C. (2004). Randomised controlled trial of intracoroanry autologous bone marrow cell transfer after myocardial infarction. *Lancet* 2004, 141–148. doi: 10.1016/s0140-6736(04)16626-9

Woodall, M. C., Woodall, B. P., Gao, E., Yuan, A., and Koch, W. J. (2016). Cardiac fibroblast GRK2 deletion enhances contractility and remodeling following ischemia/reperfusion injury. *Circ. Res.* 119, 1116–1127. doi: 10.1161/circresaha.116.309538

Woodruff, M. A., and Hutmacher, D. W. (2010). The return of a forgotten polymer – Polycaprolactone in the 21st century. *Prog. Polym. Sci.* 35, 1217–1256. doi: 10.1016/j.progpolymsci.2010.04.002

World Health Organization [WHO] (2018). *Global Health Estimates 2016: Deaths by Cause, Age, Sex, by Country and by Region, 2000–2016*. Genoa: World Health Organization [WHO].

Wunner, F. M., Wille, M. L., Noonan, T. G., Bas, O., Dalton, P. D., De-Juan-Pardo, E. M., et al. (2018). Melt electrospinning writing of highly ordered large volume scaffold architectures. *Adv. Mater.* 30, 1–6.

Xu, C., Dai, G., and Hong, Y. (2019). Recent advances in high-strength and elastic hydrogels for 3D printing in biomedical applications. *Acta Biomater.* 95, 50–59. doi: 10.1016/j.actbio.2019.05.032

Yamauchi, K., Sumi, T., Minami, I., Otsuji, T. G., Kawase, E., Nakatsuji, N., et al. (2010). Cardiomyocytes develop from anterior primitive streak cells induced by β-catenin activation and the blockage of BMP signaling in hESCs. *Genes Cells* 15, 1216–1227. doi: 10.1111/j.1365-2443.2010.01455.x

Yang, L., Soonpaa, M. H., Adler, Roepke, T. K., Kattman, S. J., Kennedy, M., et al. (2008). Human cardiovascular progenitor cells develop from a KDR+ embryonic-stem-cell-derived population. *Nature* 453, 524–528. doi: 10.1038/nature06894

Yang, X., Pabon, L., and Murry, C. E. (2014). Engineering adolescence: maturation of human pluripotent stem cell-derived cardiomyocytes. *Circ. Res* 114, 511–523. doi: 10.1161/circresaha.114.300558

Yap, L., Wang, J. W., Moreno-Moral, A., Chong, L. Y., Sun, Y., Harmston, N., et al. (2019). In vivo generation of post-infarct human cardiac muscle by laminin-promoted cardiovascular progenitors. *Cell Rep.* 26, 3231.e9–3245.e9.

Young, J. L., and Engler, A. J. (2011). Hydrogels with time-dependent material properties enhance cardiomyocyte differentiation in vitro. *Biomaterials* 32, 1002–1009. doi: 10.1016/j.biomaterials.2010.10.020

Yu, J., Vodyanik, M. A., Smuga-Otto, K., Antosiewicz-Bourget, J., Frane, J. L., Tian, S., et al. (2007). Induced pluripotent stem cell lines derived from human somatic cells. *Science (80-)* 318, 1917–1920.

Yu, P., Pan, G., Yu, J., and Thomson, J. A. (2011). FGF2 sustains NANOG and switches the outcome of BMP4-induced human embryonic stem cell differentiation. *Cell Stem Cell* 8, 326–334. doi: 10.1016/j.stem.2011.01.001

Yuasa, S., Itabashi, Y., Koshimizu, U., Tanaka, T., Sugimura, K., Kinoshita, M., et al. (2005). Transient inhibition of BMP signaling by Noggin induces cardiomyocyte differentiation of mouse embryonic stem cells. *Nat. Biotechnol.* 23, 607–611. doi: 10.1038/nbt1093

Yue, K., Trujillo-de Santiago, G., Alvarez, M. M., Tamayol, A., Annabi, N., and Khademhosseini, A. (2015). Synthesis, properties, and biomedical applications of gelatin methacryloyl (GelMA) hydrogels. *Biomaterials* 73, 254–271.

Zhang, D., Shadrin, I. Y., Lam, J., Xian, H. Q., Snodgrass, H. R., and Bursac, N. (2013). Tissue-engineered cardiac patch for advanced functional maturation of human ESC-derived cardiomyocytes. *Biomaterials* 34, 5813–5820. doi: 10.1016/j.biomaterials.2013.04.026

Zhang, H., Tian, L., Shen, M., Tu, C., Wu, H., Gu, M., et al. (2019). Generation of quiescent cardiac fibroblasts from human induced pluripotent stem cells for in vitro modeling of cardiac fibrosis. *Circ. Res.* 125, 552–566. doi: 10.1161/circresaha.119.315491

Zhang, J., Tao, R., Campbell, K. F., Carvalho, J. L., Ruiz, E. C., Kim, G. C., et al. (2019). Functional cardiac fibroblasts derived from human pluripotent stem cells via second heart field progenitors. *Nat. Commun.* 10:2238.

Zhang, J., Wilson, G. F., Soerens, A. G., Koonce, C. H., Yu, J., Palecek, S. P., et al. (2009). Functional cardiomyocytes derived from human induced pluripotent stem cells. *Circ. Res.* 104, 30–41.

Zhang, J., Zhu, W., Radisic, M., and Vunjak-Novakovic, G. (2018). Can we engineer a human cardiac patch for therapy? *Circ. Res.* 123, 244–265. doi: 10.1161/circresaha.118.311213

Zhang, L. G., Fisher, J., and Leong, K. (2015). *3D Bioprinting and Nanotechnology in Tissue Engineering and Regenerative Medicine*, 1st Edn. Cambridge: Academic Press, 60–68.

Zhang, P., Li, J., Tan, Z., Wang, C., Liu, T., Chen, L., et al. (2008). Short-term BMP-4 treatment initiates mesoderm induction in human embryonic stem cells. *Blood* 111, 1933–1941. doi: 10.1182/blood-2007-02-074120

Zhang, Y., Cao, N., Huang, Y., Spencer, C. I., Fu, J. D., Yu, C., et al. (2016). Expandable cardiovascular progenitor cells reprogrammed from fibroblasts. *Cell Stem Cell* 18, 368–381. doi: 10.1016/j.stem.2016.02.001

Zhang, Y. S., Arneri, A., Bersini, S., Shin, S. R., Zhu, K., Goli-Malekabadi, Z., et al. (2016). Bioprinting 3D microfibrous scaffolds for engineering endothelialized myocardium and heart-on-a-chip. *Biomaterials* 110, 45–59. doi: 10.1016/j.biomaterials.2016.09.003

Zhao, Y., Rafatian, N., Feric, N. T., Cox, B. J., Aschar-Sobbi, R., Wang, E. Y., et al. (2019). A platform for generation of chamber-specific cardiac tissues and disease modeling. *Cell* 176, 913.e18–927.e18.

Zhou, P., and Pu, W. T. (2016). Recounting cardiac cellular composition. *Circ. Res.* 118, 368–370. doi: 10.1161/circresaha.116.308139

Zhu, K., Shin, S. R., van Kempen, T., Li, Y. C., Ponraj, V., Nasajpour, A., et al. (2017). Gold nanocomposite bioink for printing 3D cardiac constructs. *Adv. Funct. Mater.* 27:1605352. doi: 10.1002/adfm.201605352

Zimmermann, W. H., Fink, C., Kralisch, D., Remmers, U., Weil, J., and Eschenhagen, T. (2000). Three-dimensional engineered heart tissue from neonatal rat cardiac myocytes. *Biotechnol. Bioeng.* 68, 106–114. doi: 10.1002/(sici)1097-0290(20000405)68:1<106::aid-bit13>3.0.co;2-3

Zimmermann, W. H., Melnychenko, I., Wasmeier, G., Didié, M., Naito, H., Nixdorff, U., et al. (2006). Engineered heart tissue grafts improve systolic and diastolic function in infarcted rat hearts. *Nat. Med.* 12, 452–458. doi: 10.1038/nm1394

Zimmermann, W. H., Schneiderbanger, K., Schubert, P., Didié, M., Münzel, F., Heubach, J. F., et al. (2002). Tissue engineering of a differentiated cardiac muscle construct. *Circ. Res.* 90, 223–230. doi: 10.1161/hh0202.103644

Zócalo, Y., Guevara, E., Bia, D., Giacche, E., Pessana, F., Peidro, R., et al. (2008). A reduction in the magnitude and velocity of left ventricular torsion may be associated with increased left ventricular efficiency: evaluation by speckle-tracking echocardiography. *Rev. española Cardiol.* 61, 705–713.

Conflict of Interest: The authors declare that the research was conducted in the absence of any commercial or financial relationships that could be construed as a potential conflict of interest.

Copyright © 2020 Montero, Flandes-Iparraguirre, Musquiz, Pérez Araluce, Plano, Sanmartín, Orive, Gavira, Prosper and Mazo. This is an open-access article distributed under the terms of the Creative Commons Attribution License (CC BY). The use, distribution or reproduction in other forums is permitted, provided the original author(s) and the copyright owner(s) are credited and that the original publication in this journal is cited, in accordance with accepted academic practice. No use, distribution or reproduction is permitted which does not comply with these terms.

frontiers in Bioengineering and Biotechnology

ORIGINAL RESEARCH
published: 13 August 2020
doi: 10.3389/fbioe.2020.00991

Cytocompatibility Evaluation of a Novel Series of PEG-Functionalized Lactide-Caprolactone Copolymer Biomaterials for Cardiovascular Applications

Sandra Pacharra[1†], Seán McMahon[2†], Patrick Duffy[2], Pooja Basnett[3], Wenfa Yu[4], Sabine Seisel[5], Ulrik Stervbo[6], Nina Babel[6], Ipsita Roy[7], Richard Viebahn[8], Wenxin Wang[9] and Jochen Salber[1,8]*

[1] Salber Laboratory, Centre for Clinical Research, Department of Experimental Surgery, Ruhr-Universität Bochum, Bochum, Germany, [2] Laboratory A, Synergy Centre, Ashland Specialties Ireland Ltd., Dublin, Ireland, [3] School of Life Sciences, College of Liberal Arts and Sciences, University of Westminster, London, United Kingdom, [4] Rosenhahn Group, Faculty of Chemistry and Biochemistry, Analytical Chemistry – Biointerfaces, Ruhr-Universität Bochum, Bochum, Germany, [5] Faculty of Chemistry and Biochemistry, Analytical Chemistry – Center for Electrochemical Sciences, Ruhr-Universität Bochum, Bochum, Germany, [6] Centre for Translational Medicine, Medical Department I, Marien Hospital Herne, University Hospital of the Ruhr-University Bochum, Herne, Germany, [7] Roy Group, Kroto Innovation Centre, Department of Materials Science and Engineering, University of Sheffield, Sheffield, United Kingdom, [8] Department of Surgery, Universitätsklinikum Knappschaftskrankenhaus Bochum GmbH, Bochum, Germany, [9] The Charles Institute of Dermatology, School of Medicine and Medical Science, University College Dublin, Dublin, Ireland

OPEN ACCESS

Edited by:
Francesca Boccafoschi, Università degli Studi del Piemonte Orientale, Italy

Reviewed by:
Piergiorgio Gentile, Newcastle University, United Kingdom
Shun Duan, Beijing University of Chemical Technology, China

***Correspondence:**
Jochen Salber
jochen.salber@ruhr-uni-bochum.de; jochen.salber@hotmail.com

† These authors have contributed equally to this work and share first authorship

Specialty section:
This article was submitted to Biomaterials, a section of the journal Frontiers in Bioengineering and Biotechnology

Received: *21 April 2020*
Accepted: *29 July 2020*
Published: *13 August 2020*

Citation:
Pacharra S, McMahon S, Duffy P, Basnett P, Yu W, Seisel S, Stervbo U, Babel N, Roy I, Viebahn R, Wang W and Salber J (2020) Cytocompatibility Evaluation of a Novel Series of PEG-Functionalized Lactide-Caprolactone Copolymer Biomaterials for Cardiovascular Applications. Front. Bioeng. Biotechnol. 8:991. doi: 10.3389/fbioe.2020.00991

Although the use of bioresorbable materials in stent production is thought to improve long-term safety compared to their durable counterparts, a recent FDA report on the 2-year follow-up of the first FDA-approved bioresorbable vascular stent showed an increased occurrence of major adverse cardiac events and thrombosis in comparison to the metallic control. In order to overcome the issues of first generation bioresorbable polymers, a series of polyethylene glycol-functionalized poly-L-lactide-co-ε-caprolactone copolymers with varying lactide-to-caprolactone content is developed using a novel one-step PEG-functionalization and copolymerization strategy. This approach represents a new facile way toward surface enhancement for cellular interaction, which is shown by screening these materials regarding their cyto- and hemocompatibility in terms of cytotoxicity, hemolysis, platelet adhesion, leucocyte activation and endothelial cell adhesion. By varying the lactide-to-caprolactone polymer composition, it is possible to gradually affect endothelial and platelet adhesion which allows fine-tuning of the biological response based on polymer chemistry. All polymers developed were non-cytotoxic, had acceptable leucocyte activation levels and presented non-hemolytic (<2% hemolysis rate) behavior except for PLCL-PEG 55:45 which presented hemolysis rate of 2.5% ± 0.5. Water contact angles were reduced in the polymers containing PEG functionalization (PLLA-PEG: 69.8° ± 2.3, PCL-PEG: 61.2° ± 7.5) versus those without (PLLA: 79.5° ± 3.2, PCL: 76.4° ± 10.2) while the materials PCL-PEG550, PLCL-PEG550 90:10 and PLCL-PEG550 70:30 demonstrated

best endothelial cell adhesion. PLLA-PEG550 and PLCL-PEG550 70:30 presented as best candidates for cardiovascular implant use from a cytocompatibility perspective across the spectrum of testing completed. Altogether, these polymers are excellent innovative materials suited for an application in stent manufacture due to the ease in translation of this one-step synthesis strategy to device production and their excellent *in vitro* cyto- and hemocompatibility.

Keywords: poly-L-lactide, poly-ε-caprolactone, polyethylene glycol, bioresorbable, cytocompatibility

INTRODUCTION

Stents are used in percutaneous coronary intervention to restore blood flow in patients with coronary artery disease (CAD) which is characterized by the occlusion of a coronary artery due to plaque formation (Garg and Serruys, 2010; Li et al., 2010). Researchers are dedicated to the development of new biocompatible materials for use in stent devices, that on the one hand provide enough strength for vessel support during constrictive re-modeling while also allowing for good cyto- and hemocompatibility (Van Oeveren et al., 1999; Williams, 2008; Huang et al., 2014; Zhang et al., 2014; Blok et al., 2016). Complications still arise from stent placement, the main issues being in-stent restenosis and stent thrombosis resulting from inadequate mechanical properties or poor biocompatibility (Zhang et al., 2014). Drug Eluting Stents (DES) were successful in reducing the rate of in-stent restenosis (Khan et al., 2012), however, the requirement of longer dual antiplatelet therapy (DAPT) to prevent stent thrombosis means that they are not suitable for all patients. In addition, complications have arisen relating to DES with reported cases of late thrombosis, hypersensitivity and delayed healing (Al-Dehneh et al., 2010). A major disadvantage of BMS and DES stent devices is the permanence of the scaffold associated with adverse events including stent jailing, side vessel obstruction, impairment of vessel geometries and the need for long term anti-coagulant therapy (Waksman, 2006; Meraj et al., 2015).

Fully absorbable stent technologies are the freshest development in this sector and introduce a new paradigm in CAD treatment (Tenekecioglu et al., 2016). Scaffold resorption after vessel repair is thought to offer several advantages including a reduced risk of late stent thrombosis, facilitation of repeat treatments, restoration of vasomotion and freedom from side branch obstruction (Ormiston and Serruys, 2009). Realization has been hampered by material performance inferiority in comparison to permanent metallic counterparts. Two-year follow–up on patients treated with the Abbott ABSORB BVS stent showed an 11% rate of major adverse cardiac events (e.g., cardiac death, heart attack, additional procedures) in comparison to a 7.9% rate for patients treated with the metallic XIENCE drug eluting stent. Furthermore, an increased rate of thrombus formation was observed with the BVS compared to the XIENCE stent (1.9% in BVS versus 0.8% in XIENCE) (Maisel, 2017). The current state of the art absorbable polymer stent technologies (including ABSORB) rely on the polymer poly–L–lactide (PLLA) (Gupta et al., 2007; Iqbal et al., 2013; Verheye et al., 2014), which displays a relatively high elastic modulus with a low elongation at break. PLLA's high crystallinity and glass transition temperature (T_g of 60°C) result in relatively brittle behavior in medical application (Fernández et al., 2012). Furthermore, polymers used in bioresorbable stent (BRS) technologies thus far have presented considerably lower ultimate tensile strengths (UTS) with respect to gold standard metals. Thus, the application is hampered by fracture risks, strut thickness limitations, recoil, deployment limitations and limited expansion among a host of new challenges arising with degradable devices including degradation profile, biocompatibility of by-products, shelf-life concerns, and reduction in mechanical strength as degradation proceeds (Khamis et al., 2014; Collet et al., 2016; Foin et al., 2016; McMahon et al., 2018).

Copolymers offer a potential solution to address many of the homo-polymer performance limitations in absorbable stent devices without significantly compromising relevant material properties that make PLLA such a useful candidate. Copolymerizing of lactide with small amounts of ε-caprolactone (Fernández et al., 2012) yielded a reduced T_g and crystallinity, thus improving the elongation at break and presenting a valuable performance tuning opportunity (Ugartemendia et al., 2015). In addition, polyethylene glycol functionalization offers potential to tailor the surface properties in terms of hydrophilicity and therefore control cellular adhesion and responses. PEG grafting techniques are typically multi-step approaches (Kingshott and Griesser, 1999; Lieb et al., 2003; Shin et al., 2009; Vasilev et al., 2010; Melchiorri et al., 2013) which are difficult to translate to the complex architectural design of stents post fabrication. Furthermore, there are significant challenges in stabilizing PEG grafts through the processes of crimping, sterilization, storage and expansion of a stent. With polymer-based stents, there is a new opportunity to solve these issues via incorporation of PEG in the raw materials chemical structure adding significant application potential and by-passing complex grafting procedures (Kim et al., 2011; McMahon et al., 2016). Short PEG end chains (Mw 550 Daltons) were carefully selected to ensure bioresorption of this PLCL solution is not compromised since low molar mass PEG may be eliminated from the body safely (Jeong et al., 2004; Webster et al., 2007).

Combining the two strategies (PEG copolymerization with PLCL copolymers) we have systematically created polymer series that allows refined control over a wider degree of material performance which will become an important biomedical device strategy in future. These polymers have been synthesized using a proprietary approach yielding a cleaner polymer lacking

solvent residues therefore inherently reducing the risk of adverse inflammatory effects on the patient and removing the risk of solvent residue interactions with active pharmaceutical ingredients or therapy (Barnes and Harris, 2008).

Here, we present the results of *in vitro* biocompatibility assessment of these new chemically defined lactide/caprolactone/PEG copolymers using a panel of five cell-based tests. While *in vitro* biocompatibility evaluation of medical devices is described by a series of standards collectively under the ISO 10993 set, it does not include available assays that may be more relevant to a cardiovascular application. Therefore, we selected a panel of five *in vitro* tests to easily screen and thoroughly evaluate the cyto- and hemocompatibility of the new materials. On the one hand, we performed the tests required by ISO 10993-5 standard comprising material toxicity testing according to the multiplex assay format and hemolysis testing (ISO 10993-4) (Beuth Publishing, 2009, 2017). In addition, we analyzed the materials' thrombogenic and inflammation inducing properties. Since ECs maintain a non-thrombogenic blood-tissue interface, regulate thrombosis, thrombolysis, vascular tone and blood flow in their basal state they are considered the ideal non-thrombogenic and non-inflammatory surface (Galley and Webster, 2004). We analyzed EC adhesion to the materials to assess their usefulness in facilitating fast and complete reendothelialization. Platelet adhesion and morphology was used to analyze thrombus formation risk and a leucocyte activation assay based on PMN elastase release was used to test for inflammatory induction. Together, these tests allowed a more in-depth view on all relevant properties of a cardiovascular device material which ideally should be non-toxic, non-hemolytic, non-thrombogenic, non-inflammatory and facilitate EC adhesion.

RESULTS

Polymers

Synthesis

PEG-functionalized PLCL polymers of varying composition (lactide to caprolactone of 90:10, 80:20, 70:30 and 55:45, see **Figure 1** for synthesis scheme and **Supplementary Table S1** for a list of all polymers used in this study) were synthesized using a proprietary polymerization approach. Molecular weight analysis by gel permeation chromatography (GPC) showed that all polymers presented medium to high relative molecular weights and relatively low polydispersity (PDi range of 1.5–2.4, see **Table 1**).

The molecular weights were large enough to exceed a critical value for entanglement formation thus allowing comparison across the series. Relative fractions of lactide to caprolactone were confirmed by ^{1}H-NMR to lie within an acceptable $\pm$ 2 molar fraction of the target molar ratios while polymer purity with respect to monomer residues was $\geq$98% for lactide monomer conversion and $\geq$96% for caprolactone monomer conversion (see **Table 1**). Furthermore, presence of PEG was confirmed by the appearance of a peak at a chemical shift of 3.65 ppm in all PEG-functionalized polymers.

Surface Properties of Polymer Films

For the analysis of *in vitro* biocompatibility films of PEG-functionalized polymers and non-functionalized controls were prepared and their surface properties examined via water contact angle (WCA) measurement, FTIR-ATR and SEM (see **Table 2** for a summary on all film surface results).

Water contact angle analyses were conducted in order to get a first impression on film surface characteristics, especially hydrophilicity (see **Supplementary Figure S2**). Films of the controls PLLA and PCL exhibited contact angles of 80 $\pm$ 3° and 76 $\pm$ 10°, respectively while incorporation of PEG resulted in a significant reduction of contact angles for the PLLA-PEG550 and PCL-PEG550 films to 70 $\pm$ 2° and 61 $\pm$ 8°, respectively. Contact angles of the PLCL-PEG series films were lower than non-PEGylated controls while a slight but significant increase was observed with increasing caprolactone content from PLCL-PEG550 90:10 and 80:20 to 70:30 and 55:45.

Polymer film surfaces were analyzed by FTIR-ATR measurement (**Figure 2**) which clearly proved the presence of lactide and/or caprolactone in the films. The most prominent indicator of PCL presence was the band at 2945 cm^{-1} (asymmetrical stretching of CH_2, see details on PCL-specific signals in **Supplementary Table S3**) while in case of PLLA a distinctive signal pattern was observed in the range from 1250 to 1000 cm^{-1} (particularly the symmetrical stretching mode C-CH_3 at 1045 cm^{-1}, see details on PLA-specific signals in **Supplementary Table S4**) (Schrader, 1995; Oliveira et al., 2013). Using these signals presence of polylactide could be shown in PLLA, PLLA-PEG550 and all candidates of the PLCL-PEG series while caprolactone presence was observed in PCL, PCL-PEG and the PLCL-PEG series. Here, the normalized signal intensities of the caprolactone specific 2945 cm^{-1} signal actually increased with increasing content of caprolactone in the polymer, while the main PLLA signal decreased. The stretching vibration of the carbonyl group was observed as a prominent peak at 1756 cm^{-1} for PLA containing polymers and at 1723 cm^{-1} for PCL. In the mixed polymers, the band at 1723 cm^{-1} for PCL could only be observed as a shoulder. A shift to lower wavelength also is indicative of increased crystallinity which is the case in PCL and PCL-PEG550. Also, in the two polymers with higher caprolactone content (PLCL-PEG70:30 and 55:45) the shoulder to lower wavelength indicates crystallinity which was more pronounced in PLCL-PEG550 55:45. Presence of PEG could not be shown using this method since PEG signals are overlapping with PLA and PCL signals (see details on PEG-specific signals in **Supplementary Table S5**).

SEM revealed a good surface quality for all polymer films as shown in **Figure 3**. In all cases, the films were flat and well-formed without presence of air bubbles or holes, whereas these polymers presented differences in terms of surface morphology and topography. Since all film casting was conducted using the same approach, changes in surface morphology can be accredited to the variance in polymer physical properties. In case of PLLA-PEG550, we observed a very smooth surface with no irregularity in terms of surface structuring. PLCL-PEG550 90:10, PLCL-PEG550 80:20, and PLCL-PEG550 70:30 were similar in surface quality showing mild deviation from the flat surface observed

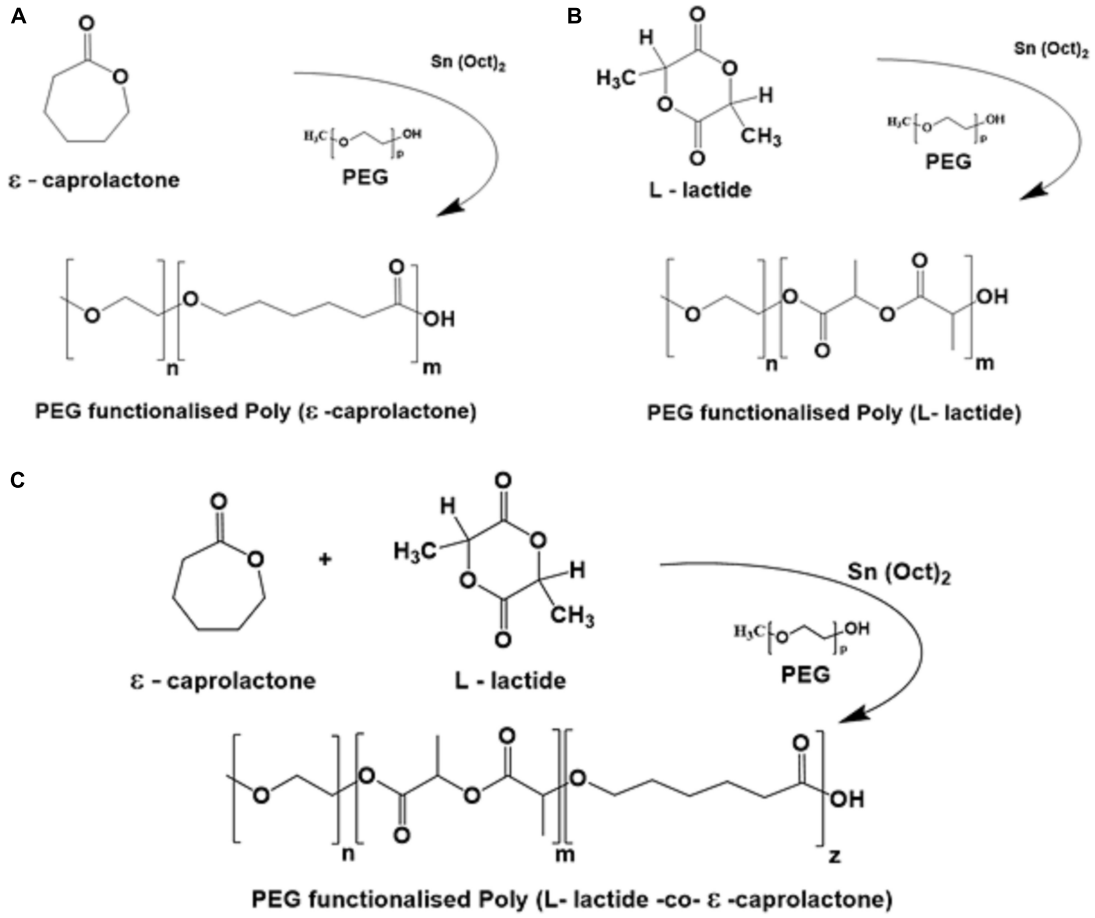

FIGURE 1 | Structural overview on each reaction for the synthesized PEG functionalized materials **(A)** PCL-PEG, **(B)** PLLA-PEG, and **(C)** PLCL-PEG.

TABLE 1 | Results summary of GPC and ^{1}H-NMR analyses of synthetic polymers.

Material	M_n /kDa	M_w /kDa	PDi[a)]	LA	CL	PLA	PCL	PEG
PLLA	374.2	584.6	1.52	0.99	–	1.0	–	–
PLLA-PEG550	236.6	347.8	1.47	0.98	–	1.0	–	+
PCL	61.6	115.0	1.87	–	0.99	–	1.0	–
PCL-PEG550	77.8	175.4	2.26	–	0.99	–	1.0	+
PLCL-PEG550 90:10	116.7	279.8	2.40	0.99	0.99	0.88	0.12	+
PLCL-PEG550 80:20	91.0	164.5	1.81	0.99	0.98	0.80	0.20	+
PLCL-PEG550 70:30	101.3	177.3	1.75	0.99	0.96	0.68	0.32	+
PLCL-PEG550 55:45	83.4	139.8	1.68	0.99	0.99	0.56	0.44	+

Polymer number average molecular weight (M_n) and weight average molecular weight (M_w) were determined by GPC while polymer monomer purity (lactide: LA and caprolactone: CL), copolymer molar fractions (polylactide: PLA and polycaprolactone: PCL) and presence of PEG were confirmed by ^{1}H-NMR. [a)]Polydispersity index = M_w/M_n; The values for M_n and M_w resulted from individual determinations.

in PLLA-PEG550 although PLCL-PEG550 90:10 exhibited a slightly roughened surface. All of these polymers had large lactide fractions leading to relatively similar film formation and surface behavior. Whereas the PLCL-PEG 55:45 material yielded films that presented a more ordered surface morphology with slight elevations created in the form of rising ridges of approximately 1 μm diameter. This can be accredited to the highly elastomeric behavior of this polymer allowing it the flexibility to form these ridges (Fernández et al., 2012). PCL showed a very ordered surface morphology with obvious surface patterns of crystalline areas. PCL-PEG550 was the most crystalline, where the film surface presented spherulite structures.

In vitro Cell Compatibility

Films of PLCL-PEG copolymers were evaluated using a panel of different *in vitro* methods – according to ISO 10993 and

TABLE 2 | Summary of film surface properties.

Material	Contact angle[a)]	PLA[b)]	PCL[b)]	Crystalline[b)]	SEM[c)]
PLLA	79.5° ± 3.2	+	−	No	−
PLLA-PEG550	69.8° ± 2.3	+	−	No	Flat and smooth
PCL	76.4° ± 10.2	−	+	Yes	Spherulitic structure
PCL-PEG550	61.2° ± 7.5	−	+	Yes	Spherulitic structure
PLCL-PEG550 90:10	65.5° ± 4.1	+	+	No	Flat but roughened
PLCL-PEG550 80:20	67.2° ± 3.1	+	+	No	Alternating smooth and roughened areas
PLCL-PEG550 70:30	75.5° ± 2.0	+	+	Yes	Flat and smooth
PLCL-PEG550 55:45	72.3° ± 6.1	+	+	Yes	Homogeneous ridged structure

*Water contact angles, presence of polylactide(PLA) and polycaprolactone (PCL) as determined by FTIR, FTIR evidence of crystalline surface and SEM appearance are presented. [a)]see **Supplementary Figure S2**; [b)]see **Figure 2** for FTIR graphs and **Supplementary Tables S3–S5** for FTIR peak summary; [c)]see **Figure 3** for SEM micrographs.*

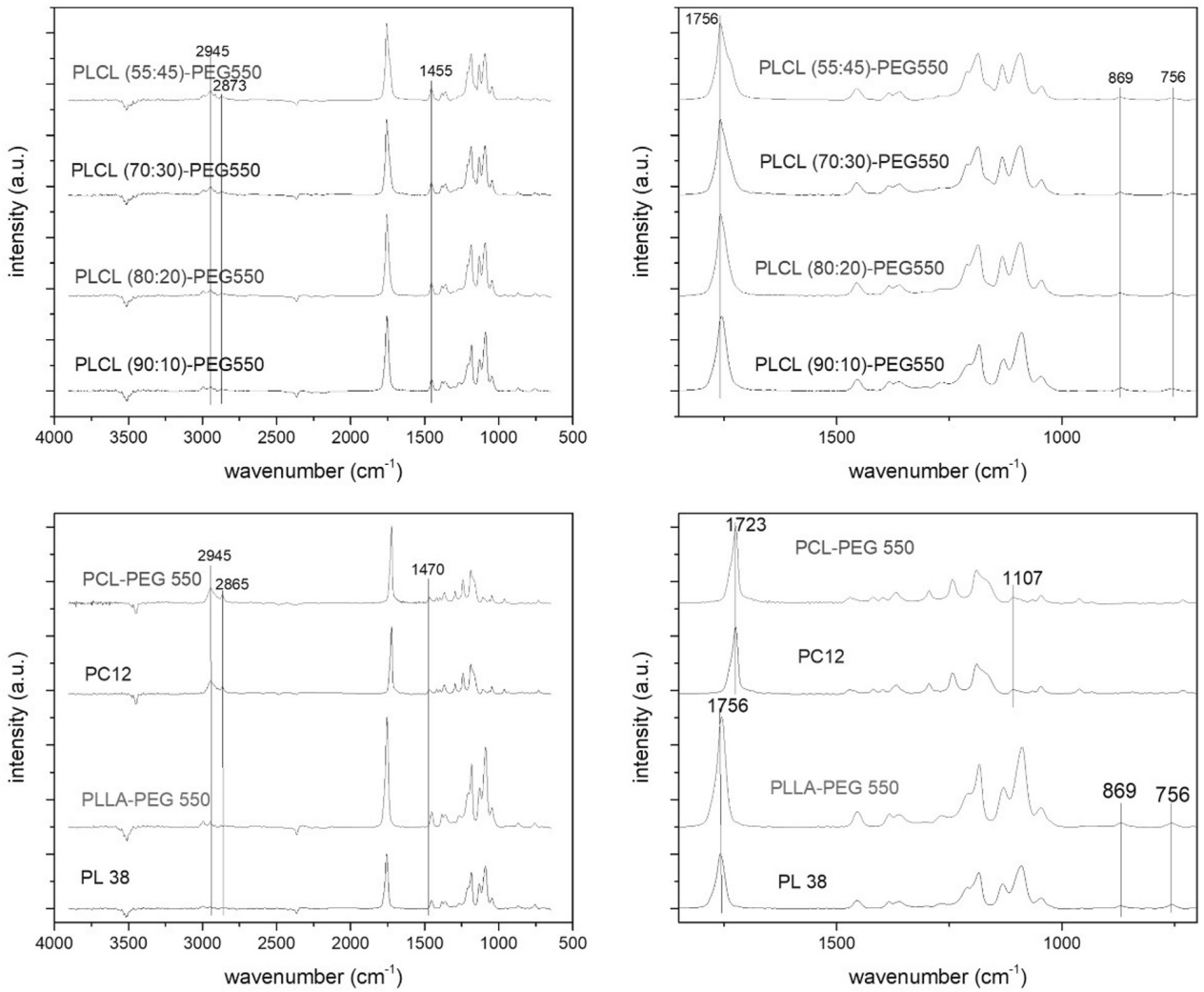

FIGURE 2 | FTIR-ATR spectra of PCL (PC12) and PCL-PEG550, PLLA (PL38) and PLLA-PEG550 and the PLCL-PEG550 series. The figures show overview spectra **(left side)** and zoom-in spectra **(right side)** of the 650 – 1800 cm^{-1} wavenumber region.

beyond. Here, we were specifically interested in the effect the new materials had on cells present at a stent implantation site (especially different types of blood cells and endothelial cells).

Toxicity Testing With L929

First of all, we tested if the materials caused any adverse reactions in a standard cell line as suggested in ISO 10993-5 (Beuth

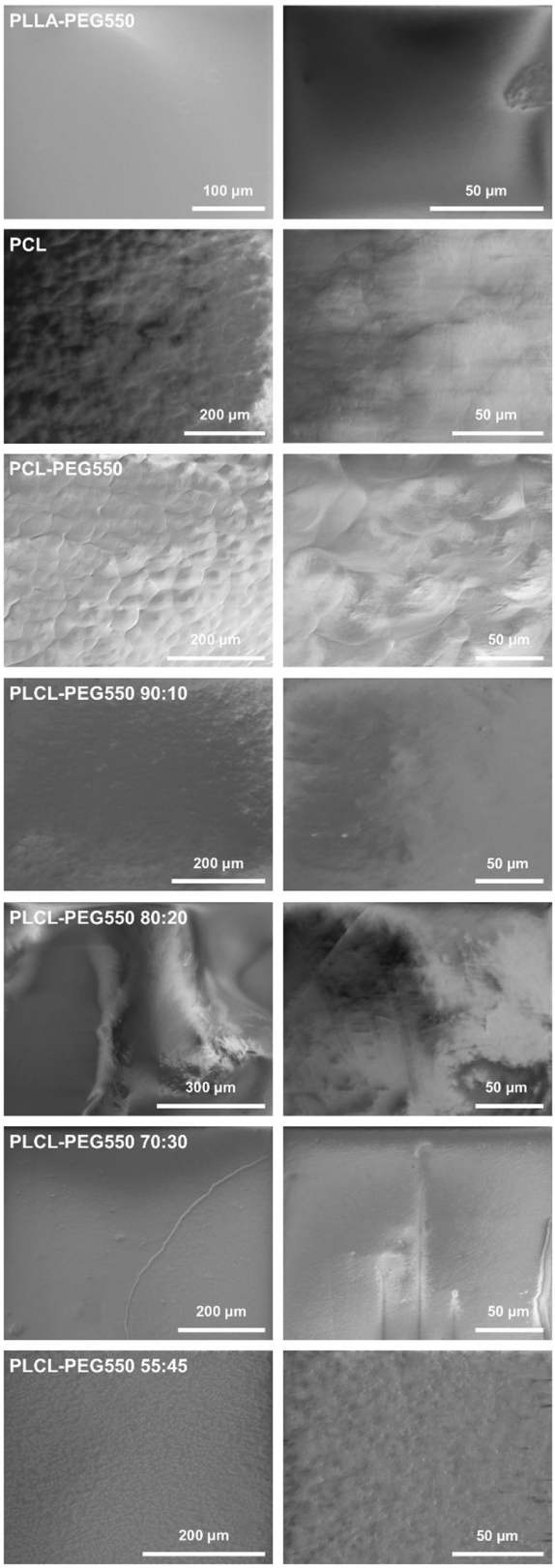

FIGURE 3 | Representative SEM pictures of material films in different magnifications.

Publishing, 2009). Since finally, cardiovascular implants will be in direct contact with the vessel wall we chose a direct contact multiplex assay format which allowed parallel determination of the amount of attached cells ("Viability"), the amount of dead cells ("Toxicity") and the amount of cells undergoing apoptosis ("Apoptosis"). Cell attachment and proliferation on materials ("Viability") was the same or only slightly reduced on film samples compared to the ideal surface of tissue culture-treated polystyrene (TCPS) (**Figure 4**). Since in addition, no material toxicity was observed all presented polymer films can be rated as non-cytotoxic. Also, none of the lactide/caprolactone materials led to significantly increased apoptosis induction compared to TCPS control.

Hemolysis

Hemolysis testing is required for the evaluation of biomaterials intended for stent devices according to ISO 10993-4 (Beuth Publishing, 2017). It is a sensitive indicator of the destructive degree of a material to erythrocytes. Among the tested biomaterials only PLCL-PEG 55:45 showed an elevated hemolysis rate of 2.5% $\pm$ 0.5 (**Figure 5**). All other materials showed rates smaller than 2%. However, the increase in hemolysis on the surface of the material PLCL-PEG550 55:45 compared to the other materials and in relation to the threshold value of 2% was significant after Bonferroni correction (for criteria see review by Van Oeveren, 2013).

Platelet Adhesion and Morphology

Platelet adhesion together with morphology of adhered platelets is a common indicator to evaluate hemocompatibility of newly developed biomaterials more precisely their thrombus formation potential. Based on their shape, adhered platelets can be classified into five categories (**Supplementary Table S6**), whereby only category V platelets might also form aggregates and are indicative of material thrombogenicity (Ko et al., 1993).

In our study clear differences in platelet adhesion onto the various materials were observed as can be seen in the representative micrographs in **Figure 6**. While most materials showed low platelet adhesion and spreading, PCL control, PCL-PEG550 and PLCL-PEG550 90:10 exhibited high platelet adhesion rate accompanied by spreading to a fully spread (category V) state and formation of aggregates which indicates potential thrombogenicity of these materials. Among these, the PCL control showed most adhesion with the formation of a complete carpet of spread platelets and the presence of many aggregate buds. Onto PCL-PEG550 and PLCL-PEG550 90:10 platelet adhesion occurred in a grouped order with free spaces in between. PLLA exhibited slightly more adhered platelets than PLLA-PEG550.

Leucocyte Activation

PMN elastase expression levels are an indicator for leucocyte activation since inflammatory stimulation of neutrophils – the most abundant leucocytes – results in the rapid release of high amounts of this proteolytic enzyme (Alam et al., 2012). Here, we analyzed PMN elastase release after 1 h of incubation between

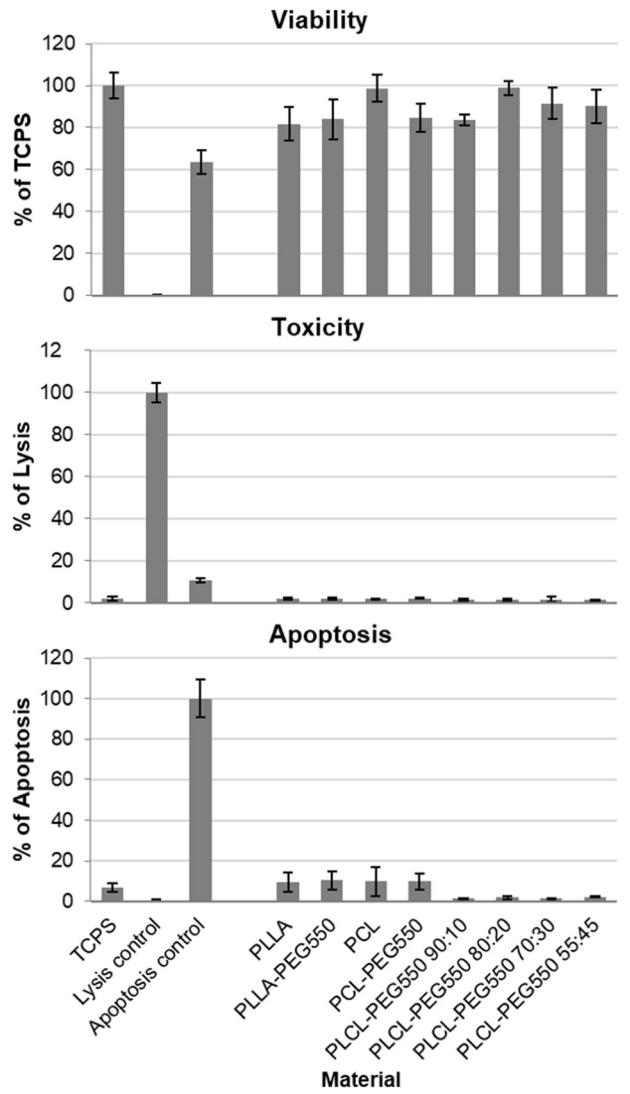

FIGURE 4 | Lactide/caprolactone film cytocompatibility was analyzed in multiplex format using L929 cell line. L929 cells were seeded directly onto material disks and grown for 24 h. Cell viability of attached cells was measured using CellTiter-Blue assay and results are depicted in % compared to TCPS. Cytotoxicity was analyzed using CytoTox-ONE assay, whereby lysed cells were used as positive control (100% of cell lysis) and apoptosis induction was determined using ApoONE assay, by using staurosporine induced cells as positive control (100% of apoptosis). Measurements were carried out in quadruplicate.

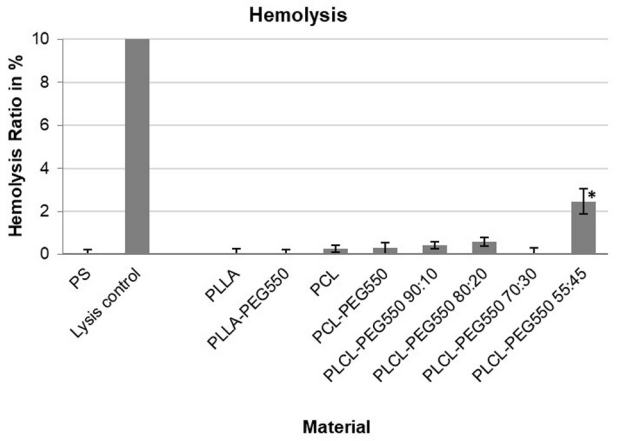

FIGURE 5 | Hemolysis ratios of the tested biomaterials after 1 h of incubation with diluted whole blood at 37°C. Hemolysis of the empty well (PS) was set to 0 while lysis control equals 100%. PLCL-PEG550 55:45 exhibited significantly increased hemolysis with $*p < 0.006$ after Bonferroni correction.

whole blood and material films (**Figure 7**). Most of the presented materials showed no significant increase in leucocyte activity. The PMN elastase value for PLCL-PEG550 90:10 was increased on average, but did not turn out to be significant compared to the control. In contrast, the value for material type PLCL-PEG550 55:45 showed a significant increase.

Endothelial Cell Adhesion

Since re-endothelialization is thought to greatly improve anti-thrombotic and anti-restenotic properties of a surface we analyzed each material's potential to facilitate endothelial cell adhesion using primary human cardiac microvascular endothelial cells (HCMECs). Representative micrographs of attached HCMECs 24 h after seeding onto the different materials and stained using live/dead staining are depicted in **Figure 8** and average cell numbers are given in **Figure 9**. Although cells on PEGylated lactide/caprolactone films were viable indicating again that the materials are non-toxic, big differences in number of attached cells and cell morphology were observed. From the described materials PCL-PEG550 and PLCL-PEG550 90:10 showed highest cell adhesion accompanied by a high grade of spreading. While on PCL-PEG550 ECs appeared in ordered groups cell adhesion in case of PLCL-PEG550 90:10 the ECs seemed more evenly distributed. Although even more endothelial cells were able to attach onto PLCL-PEG550 70:30, cells had a rounder shape and cluster formation was observed. Among the tested samples PLLA-PEG550 and PLCL-PEG550 55:45 exhibited lowest cell numbers and nearly no spreading was seen.

DISCUSSION

PLCL-PEG Copolymerization Strategy Resulted in Highly Accurate Composition

Copolymerizing lactide with caprolactone and incorporating a polyethylene glycol end chain has been successfully achieved. The intended molar ratios of lactide to caprolactone (100:0, 90:10, 80:20, 70:30, 55:45, 0:100) were achieved with high accuracy to an industrial standard and within ±2 moles of the target molar fractions (**Table 1**). The presence of PEG (M_n = 550 Da) was confirmed using ^{1}H-NMR while all synthesized polymers presented low polydispersity indexes and outstanding control. Furthermore, copolymers were synthesized with high molecular weights (M_w = 128 – 348 kDa) which remains

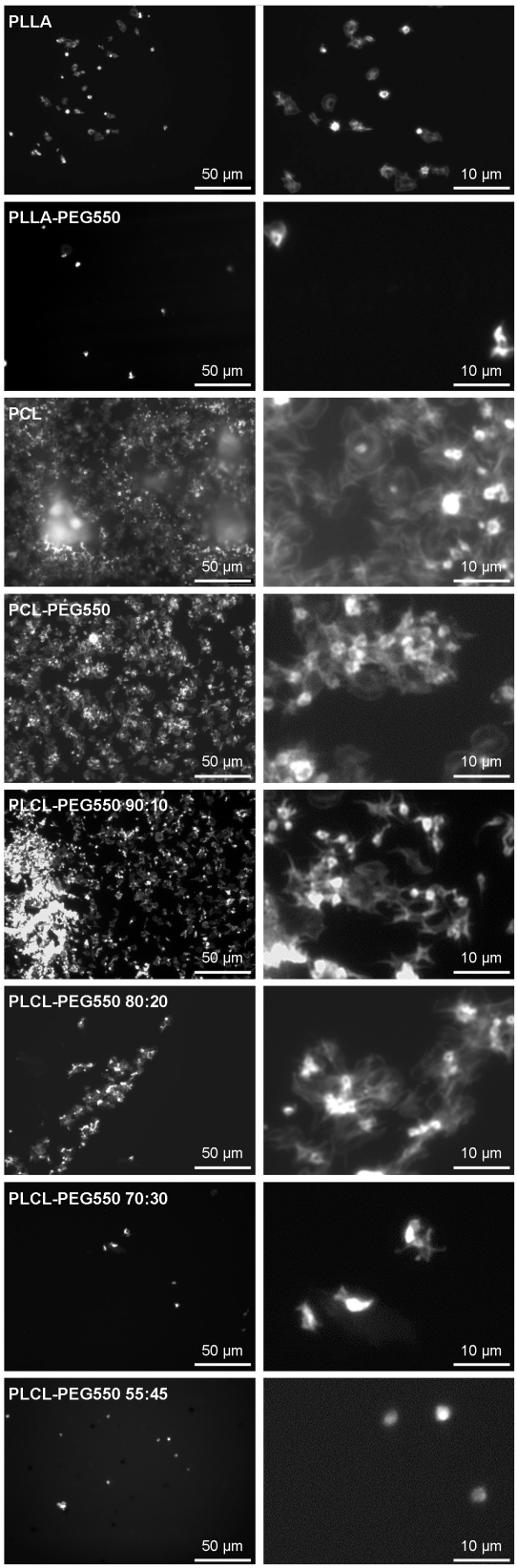

FIGURE 6 | Continued

FIGURE 6 | Representative micrographs of platelet adhesion onto the lactide/caprolactone polymer films. Platelet-rich plasma was incubated for 1 h on film samples and adherent platelets were visualized using *F*-actin staining. Micrographs of 500x magnification give an overview (scale bar corresponds to 50 µm) while micrographs of 2500x magnification show platelet morphology in more detail (scale bar corresponds to 10 µm).

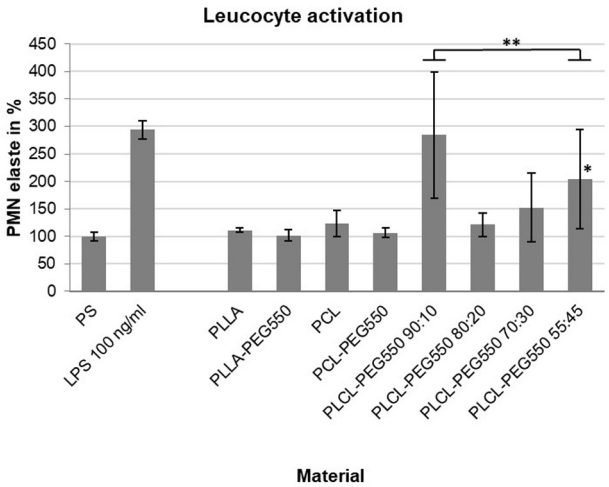

FIGURE 7 | Leucocyte activation during a 1 h blood/biomaterial interaction was analyzed using PMN elastase ELISA assay. The baseline PMN elastase expression in non-activated blood in an empty PS well was set to 100%. An exemplary induction of leucocyte activation was achieved by the addition of bacterial lipopolysaccharides (LPS). Measurements were carried out in quadruplicate, $*p \leq 0.05$; $**p \leq 0.01$.

challenging with conventional polymerization procedures (Auras et al., 2004; Lasprilla et al., 2012). Polymerization reported herein is even more impressive considering that these polymers were produced entirely in the absence of toxic organic solvents yielding cleaner biomaterials that elicit lowered inflammatory response.

Film Surface Characteristics

Using WCA measurements, FTIR-ATR and SEM imaging we confirmed the high quality of our film preparation and analyzed the surface characteristics in more detail (see **Table 2** for summary). While all films were flat without the presence of air bubbles and holes, differences in their surface morphologies and topographies were observed. Surface texturing was observed in PCL and PCL-PEG550 in form of spherulite crystallization as seen in SEM images (**Figure 3**) which was also confirmed by the presence of a typical band shift of the carbonyl peak in FTIR (**Figure 2**). This surface inhomogeneity also explains the higher variance in contact angle measurements. PLCL-PEG550 55:45 was shown to exhibit high grade of crystallinity which was represented in SEM in the formation of ridged structures and in FTIR by the existence of a lower wavelength shoulder of the carbonyl peak. These changing surface properties relate to the solvent casting process and material behavior. Since all films were

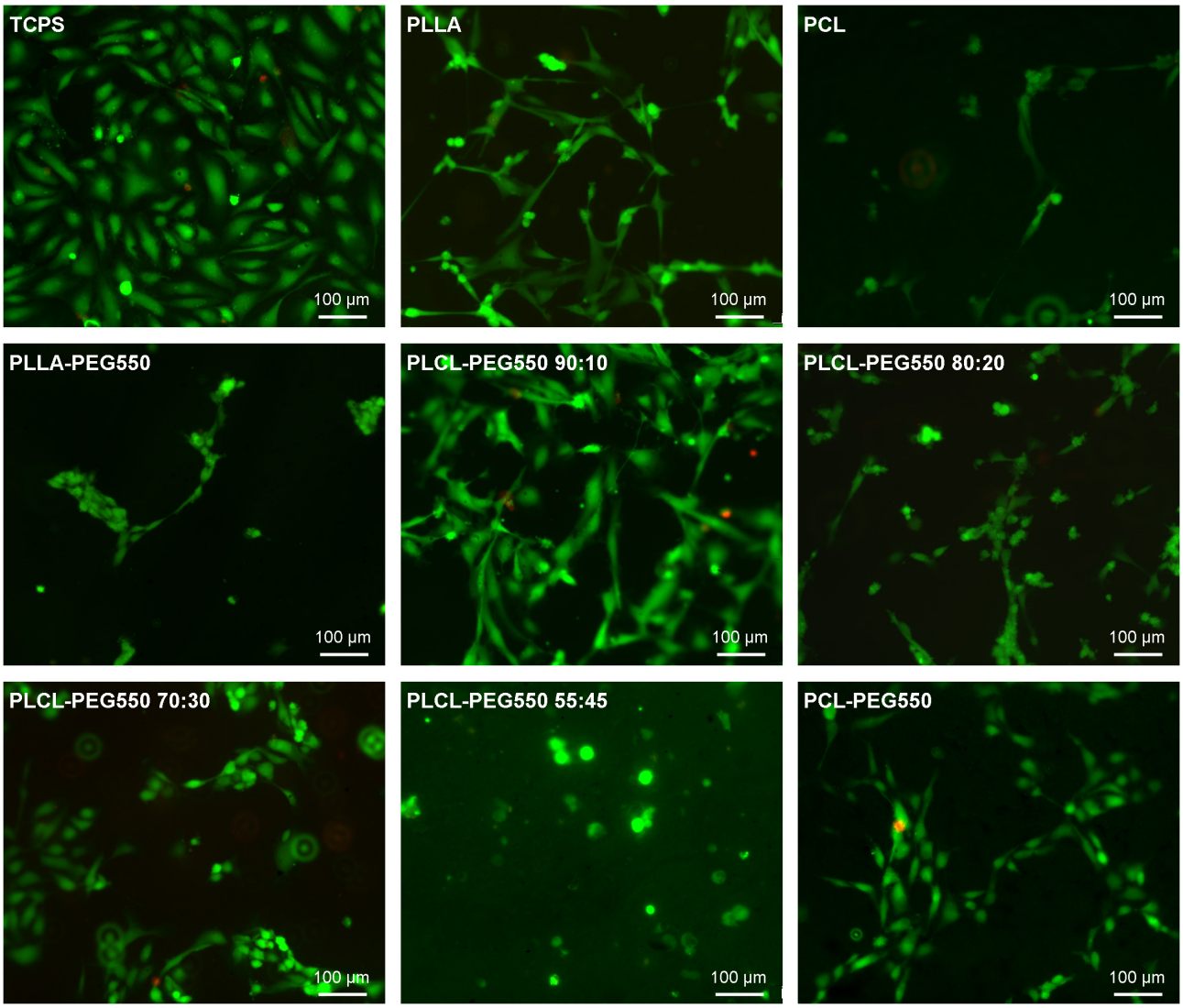

FIGURE 8 | Representative micrographs of adherent endothelial cells on the different lactide/caprolactone materials stained with Live/Dead staining. The cells were seeded directly onto material films, incubated for 24 h and stained (green: cytoplasm of viable cells, red: nuclei of cells with damaged cell membrane). Bar corresponds to 100 µm.

cast using the same method, we believe that material behavior leads to the formation of a slightly varied surface quality. No clear trend was observed in the other PEG-modified films: While PLLA-PEG550 and PLCL-PEG550 70:30 exhibited smooth surfaces PLCL-PEG550 90:10 showed slight surface roughness and PLCL-PEG550 80:20 consisted of smooth areas and more roughened areas.

All PEG-containing materials showed lower water contact angles than the controls – although to different degrees – indicating that PEG addition increased hydrophilicity. This also proves that PEG groups were present at the surfaces of all sample films whereby hydrophilicity was highest in PCL-PEG550, PLCL-PEG550 90:10 and 80:20. The values for PEG functionalized PLCL films were significantly lower than values reported in the literature for non-PEGylated lactide-caprolactone polymers owing to the incorporation of PEG in the polymer structure (Lim et al., 2008; Inthanon et al., 2016).

In vitro Biocompatibility

Copolymerization Method Has No Negative Effect on Cells

General cytocompatibility testing as required by ISO 10993-5 (Beuth Publishing, 2009) was conducted in direct contact format – seeding the L929 cells directly onto film samples – because the materials are intended as cardiovascular materials that will directly be colonized *in vivo*. With L929 cell line no significant differences in number of viable adherent cells were observed among all tested materials. Thus, together with the results of absolutely no toxicity, we concluded that the

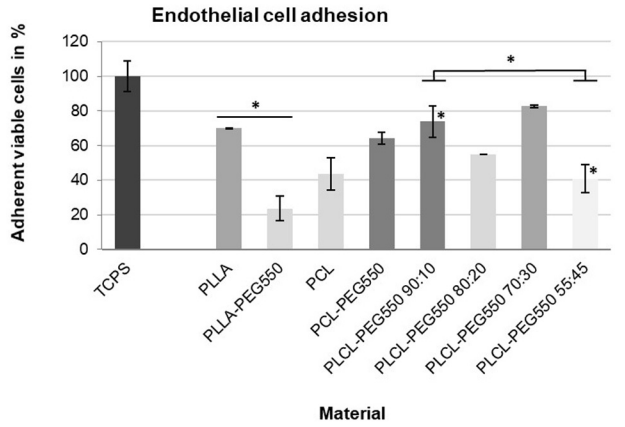

FIGURE 9 | Number of viable endothelial cells attached to material disks. The cells were seeded directly onto material films, incubated for 24 h and counted after Live/Dead staining. At least 10 microscopic images were counted per material. Bar shade indicates cell morphology (from dark gray = good spreading, normal morphology to light gray = mostly non-spread); $*p \leq 0.01$.

presented copolymerization strategy generated completely non-toxic materials. In addition, no other adverse effects as measured by apoptotic induction were observed.

Hemolysis on the one hand is a measure of blood toxicity (Beuth Publishing, 2017) for example originating from residual solvent in the polymer. On the other hand, specific material surface structures might cause blood cell rupture. Here, we found that PLCL-PEG copolymers were non-toxic to blood erythrocytes although possibly topography related slightly elevated hemolysis was observed in case of PLCL-PEG550 55:45. As seen in SEM, this material exhibited a high degree of surface irregularity in the form of ridges of approximately 1 μm diameter that seem to be able to lacerate red blood cells. PEG incorporation was shown to prevent hemolysis in a hemolytic material (Wang et al., 2010) but the ridges presented by PLCL-PEG550 55:45 seem to be too sharp so that the presence of PEG was partially overcompensated by the topographic effect. Surface patterning is a well-known and important tool that can be used to enhance biocompatibility of these materials for medical applications while here we can also see the potential for adverse impact that an uncontrolled surface may have (Pacharra et al., 2019).

Cell Adhesion and Activation Can Be Fine-Tuned by Polymer Composition

In addition to mandatory testing required for every material intended for implant use, we wanted to obtain more information regarding a possible use of these materials as cardiovascular implants. Since stents and vascular grafts will be in contact to the vessel wall and the blood, we chose three additional direct contact assays to analyze thrombogenic and inflammatory properties, and endothelialization.

Platelet adhesion, as an indicator of possible material thrombogenicity, in general could be reduced by the presence of PEG chains on the films compared to controls without PEG – although the extent depended on the polymer type. It has already been shown that the presence of PEG on the surface of a material leads to the formation of more inert surfaces with reduced cell adhesion capabilities for various materials (Chuang and Masters, 2009; Noel et al., 2015) while Chen et al. (2011) found that the degree of adhesion reduction might vary depending on the type of PEG. In case of PCL-PEG550 substantial platelet adhesion and spreading but less aggregation was observed than on un-PEGylated PCL. From film characterization via SEM, we know that these polymer surfaces presented ordered spherulitic structures which may have caused an enhanced affinity for platelet adhesion. In addition, the high platelet adhesion on both PCL and PCL-PEG550 might be due to the partial presence of negatively charged carboxyl groups at the film surface as was already described for carboxyl presenting surfaces (Sperling et al., 2009). In contrast, the very smooth and uncharged surface of PLLA and PLLA-PEG550 offered little attachment points for platelets while the presence of PEG further reduced platelet adhesion and spreading. This indicates that PEG chains were presented to the solid/liquid interface of this material. In case of the PLCL-PEG550 series the observed differences in platelet adhesion and spreading originated in the different morphologies. As the caprolactone content increased in the copolymer samples PLCL-PEG550 90:10 to 55:45, we observed that the platelet adhesion and spreading decreased. In all samples the content of caprolactone was low, not enough to create a negatively charged surface similar to that of the pure PCL-PEG550 which furthered platelet adhesion.

Overall, the lactide/caprolactone materials did not lead to substantial leucocyte activation as tested on the basis of PMN elastase release from neutrophils in human whole blood. In contrast, PLCL-PEG550 55:45 showed a significant increase in PMN elastase levels. In the case of PLCL-PEG550 55:45, the effect of surface irregularities, which has already been described in hemolysis, may come into play again and seems to be responsible for the slightly increased hemolysis activity. So far, the mechanism of neutrophil activation by a material surface is not clearly understood but surface chemistry and topography have been shown to influence neutrophil behavior (Tan et al., 2000; Patel et al., 2006). Thus, PLCL-PEG550 55:45 might lead to partial activation of neutrophils because of its roughened or ridged surface structures, respectively.

Since rapid and complete endothelialization is thought to greatly improve cardiovascular implant biocompatibility we also tested endothelial cell adhesion using primary human cardiac microvascular endothelial cells (HCMECs) – a cell type actually present in the coronary vasculature. We found that EC adhesion and spreading gradually increased with increasing lactide content and decreasing crystallinity as did platelet adhesion and spreading. This suggests that PEG presentation is strongly affected by polymer chain orientation and alignment. In PLCL-PEG550 90:10 it seemed that PEG was not accumulated at the film surface possibly due to the random polymer orientation of this amorphous material allowing cell adhesion. In contrast, PEG chains seemed to be evenly enriched at the surface of the highly crystalline PLCL-PEG550 55:45 resulting in a cell-repellent more inert surface. Thus, the presented copolymerization of lactide/caprolactone/PEG allows gradual

tuning of cell adhesion properties. On the smoother materials with a better presentation of PEG chains to the interface (e.g., PLLA-PEG550) cell adhesion of endothelial cells and platelets was much lower.

In vivo, a fast and complete endothelialization might greatly influence the hemocompatibility of materials. On the one hand, the presence of an endothelial cell layer can cover the foreign surface from direct contact with blood cells and thereby hinder blood cell activation. In addition, healthy endothelial cells can actively prevent thrombus formation and inflammatory responses (de Mel et al., 2008; Ren et al., 2015). Therefore, PCL-PEG550, PLCL-PEG550 90:10, and PLCL-PEG550 70:30, which showed good endothelial cell coverage, might be promising candidates for cardiovascular implant production. This will be studied in more detail in the future by more advanced *in vitro* testing (for example in a bioreactor under flow conditions) or in animal experiments.

EXPERIMENTAL SECTION

Materials

All customized polymer formulations (PLLA-PEG550, PLCL9010-PEG550, PLCL8020-PEG550, PLCL7030-PEG550, PLCL5545-PEG550, PCL-PEG550) were supplied by Ashland Specialties Ireland Ltd. (Dublin, Ireland). PL38 and PC12 with inherent viscosity of 3.8 and 1.2 dl/g respectively were used as controls and supplied from Purac (Gorinchem, Netherlands). Chloroform ($CHCL_3$ and $CDCL_3$) were supplied from Sigma Aldrich and used for all film casting, GPC and NMR testing.

Polymer Synthesis

PEG-functionalized PCL, PLLA and PLCL of varied composition were synthesized by Ashland Specialties Ireland Ltd. Briefly, these polymers were achieved through the Ring-Opening Polymerization (ROP) of the monomers L-lactide and ε-caprolactone using the catalyst stannous octoate initiated by the hydroxyl terminal group of the relevant initiation molecule (polyethylene glycol methyl ether). This resulted in polymers consisting of long chains of PLLA, PCL or PLCL connected to a singular PEG end group. In each polymerization reaction, pre-determined amounts of monomer, initiator and catalyst were added to the autoclave and were then heated to the reaction conditions. This reaction achieved good reaction control in terms of target molar mass, monomer conversion and a relatively low polydispersity polymer. A structural overview on each reaction is presented in **Figure 1** and a summary of all materials used in this study is given in **Supplementary Table S1**.

Characterization of Polymer Composition

Gel permeation chromatography (GPC) measurements were performed using an Agilent triple detector system which was calibrated with polystyrene standards at a concentration of 10 mg/ml. Chloroform ($CHCL_3$) was used as mobile phase with a flow rate of 1.0 ml/min. Weight average molecular weight (M_w), number average molecular weight (M_n) and polydispersity (PDi) data were collected using refractive index peak height in the range of <10 mV. For each polymer 3–7 mg powder was dissolved in 2 ml chloroform and filtered [0.2 μm pore size, 13 mm diameter, Millipore SLFG013NL, Fluropore PTFE (F) membrane]. An Agilent Technologies column (PLgel, 5 μm MIXED-C, 300 × 7.5 mm) was used for GPC analysis.

Proton nuclear magnetic resonance spectroscopy (^{1}H-NMR) was utilized for identification of the polymer, confirmation of the polymer purity in terms of monomer conversion, molar ratio of relevant copolymer units and to confirm the presence of PEG in the chemical structure. A 300 MHz Bruker NMR machine was used to obtain the spectra which were analyzed and processed using MestReC software package. Deuterated chloroform ($CDCl_3$) was used to dissolve the polymer which was then filtered using a Milnex (0.2 μm) into NMR sample tubes. Lactide methyl presented a signal centered around 5.16 ppm and caprolactone on 4.02 ppm while PEG presence was identified at a chemical shift of 3.65 ppm (Wu et al., 2010). These signals were taken as reference points for the determination of the polymer composition given in **Table 2**. From the ^{1}H-NMR we observed the polymer conversion based on the CH_3 and CH peaks for respective polymers and monomers introduced.

Polymer Film Preparation

Film casting was achieved by dissolving 0.5 g of polymer in 15 ml of chloroform. Each solution was dissolved until transparency and poured into a glass petri dish of dimensions 60 mm × 15 mm. Chloroform was evaporated overnight resulting in thin uniform films which were peeled from the glass surface once solvents had evaporated entirely.

Analysis of Film Surface Properties

Water contact angle was measured to analyze the wettability of the film samples. This study was carried out using KSV Cam 200 optical goniometer (Helsinki, Finland). Hundred μl of deionized water was dropped on the surface of the films using a micro-syringe. Images were captured with a frame interval of 1 s. KSV Cam software was used to analyze the images. This was done at Eastman Dental Institute, University College London, United Kingdom. For each material, the contact angles of three independent samples were measured with at least 10 measurements per sample.

Fourier transform infrared (FTIR) spectroscopy was performed as attenuated total reflectance (ATR) measurement. Spectral manipulations were performed by spectroscopy software OPUS provided by Bruker.

The ATR measurements were performed by a Tensor 27 FTIR spectrometer from Bruker, equipped with a VariGATRTM ATR accessory, with a resolution of 4 cm^{-1}, for each sample using 50 scans. The spectra were acquired by a liquid N_2 cooled mercury cadmium telluride (MCT) detector, in the range of 4000–600 cm^{-1}.

Scanning electron microscopy (SEM) images were obtained using a Quanta 3D FEG scanning electron microscope (FEI). Samples were cut from the central part of the produced films and were fixed on a commercial aluminum stub with conductive

carbon tape (Plano), in a way that a part of the film sample was overlapping and no contact to the stub or carbon tape occurred. This part of the sample has always been analyzed. The optimum in image quality was obtained with an acceleration voltage of 2 kV, a spot size of 4.5 and a working distance of around 10 mm. Under these conditions no or a minimum of degradation of the sample during imaging was observed.

Toxicity Testing With L929 (Multiplex Assay)

The mouse fibroblast cell line L929 was obtained from DSMZ (Leibniz-Institut DSMZ - Deutsche Sammlung von Mikroorganismen und Zellkulturen GmbH) and handled according to their manual. Briefly, L929 cells were grown in RPMI 1640 medium (PAN Biotech, Aidenbach, Germany) supplemented with 10% FBS (PAN Biotech) and a penicillin/streptomycin mixture (Thermo Fisher Scientific, Dreieich, Germany) in an incubator (37°C, 5% CO_2). For subculturing cells were detached using 0.25% Trypsin solution (Thermo Fisher Scientific).

This multiplexed assay was adapted from Neuss et al. (2008). From each polymer film disks of 6 mm diameter were generated by punching. Disinfection was achieved by incubation in 70% ethanol followed by washing with sterile water and equilibration in medium. Material disks of 6 mm in diameter were placed into the wells of a 96 well polystyrene(PS) plate and fixed with Teflon rings. Tissue culture-treated polystyrene (TCPS, Nunc) plates were used as controls for ideal cell growth. L929 cells ($2{\cdot}10^4$ cells per well) were seeded on top of the disks and grown for 24 h under standard cell culture conditions. Blank values were obtained from wells without material disks and cells. As a positive control for cytotoxicity cells grown on TCPS were lysed prior to assaying. As a positive control for apoptosis 100 nM staurosporine (Santa Cruz Biotechnology, Heidelberg, Germany) was added to cells grown on TCPS 6 h after seeding. Each sample was analyzed in quadruplicate.

After 24 h of incubation the cell culture supernatants were transferred into black 96 well plates and subjected to cytotoxicity analysis using the CytoTox-ONE™ Homogeneous Membrane Integrity Assay (Promega, Mannheim, Germany) following the manufacturer's protocol. After equilibration to ambient temperature assay reagent was added to each well in a 1:1 ratio and incubated for 10 min. The reaction was stopped by addition of Stop Solution and the fluorescence monitored (excitation: 560 nm, emission: 590 nm).

Directly after supernatant removal for cytotoxicity analysis cell viability was analyzed using the CellTiter-Blue® Cell Viability Assay (Promega) following the manufacturer's protocol. After addition of the reagent/medium mixture plates were incubated for 2 h at 37°C, 5% CO_2. Cell culture supernatant was transferred to black 96 well plates and fluorescence monitored (excitation: 560 nm, emission: 590 nm).

Directly after supernatant removal for viability measurement cells were subjected to apoptosis analysis using the Apo-ONE® Homogeneous Caspase-3/7 Assay (Promega) following the manufacturer's protocol. After addition of the reagent/medium mixture plates were incubated for 2 h at ambient temperature. The supernatant was transferred to black 96 well plates, incubated for further 18 h and the fluorescence monitored (excitation: 485 nm, emission: 527 nm).

Blood Collection

Fresh human whole blood was obtained from healthy adult volunteers (no medication (e.g., aspirin) in the previous 2 weeks) by venipuncture into either *S*-Monovette 9 ml LH (Sarstedt, Nümbrecht, Germany). Blood was collected at the Centre for Translational Medicine, Medical Department I, University Hospital of the Ruhr-University Bochum, Herne, Germany according to appropriate legal and ethical guidelines. The participants provided written informed consent to participate in this study. The study was reviewed and approved by the Ethics Committee of the Medical Faculty of the Ruhr-University Bochum, Gesundheitscampus 33, D-44801 Bochum. The registration number of the study is 16-5649.

Hemolysis

Hemolysis testing was done based on the protocol by Wang et al. (2013) with slight modifications. Lithium heparin (LH) blood was diluted 4:5 in 0.9% (w/v) sodium chloride (NaCl) solution. Material disks of 14 mm diameter were placed into the wells of a PS 24 well plate (Nunc, Fisher Scientific, Schwerte, Germany) and fixed using silicone rings. After washing with 0.9% NaCl solution the disks were incubated for 30 min at 37°C with 980 µl NaCl solution. As negative control the bare PS was used and as positive control of complete red blood cell lysis 980 µl of distilled water was added instead of 0.9% NaCl. To each well 20 µl of pre-diluted blood was added, mixed and incubated for 60 min at 37°C with slow shaking. After centrifugation at 700 × *g* for 10 min 200 µl of supernatant were transferred to a 96 well plate and the absorbance was measured at 542 nm using 691 nm as reference wavelength. Measurements were done in quadruplicate. The hemolysis ratio (HR, in %) was calculated as follows $HR = (A - C_{neg}) / (C_{pos} - C_{neg})$ x 100%, where A is the absorbance of the sample, C_{neg} is the absorbance of the negative control and C_{pos} is the absorbance of the positive control.

Platelet Adhesion and Morphology

Platelet-rich plasma (PRP) was isolated from LH blood according to the description from Parnham and Wetzig (Parnham and Wetzig, 1993). Briefly, whole blood was centrifuged at 250 × *g* for 10 min and the supernatant (=PRP) was recovered.

Material disks of 14 mm diameter were placed into the wells of a 24 PS well plate and fixed using silicone rings. After washing with 0.9% NaCl solution three times the disks were incubated at 37°C for 1 h with 500 µl of PRP. Adhered platelets were visualized using F-actin staining. Briefly, disks were washed three times with PBS (PAN-Biotech), fixed with 4% formaldehyde (Life Technologies, Darmstadt, Germany) in PBS, permeabilized with 0.4% Triton X-100 in PBS and blocked using 2% BSA in PBS. After staining with PromoFluor 546 phalloidin (PromoKine) the disks were mounted using Fluoroshield with PPD. Fluorescence

microscopy was done with the IX 51 microscope (Olympus, Hamburg, Germany). At least 2 independent samples were visualized per material and at least 5 images of different areas per sample were recorded.

Leucocyte Activation

Material disks of 14 mm diameter were placed into the wells of a PS 24 well plate, fixed using silicone rings and disinfected in 70% ethanol. After washing with 0.9% NaCl solution the disks were incubated at 37°C for 1 h with 500 μl of LH blood. 100 ng/ml lipopolysaccharides (LPS) from *E. coli* (Sigma-Aldrich, Schnelldorf, Germany) were used as positive control. From each sample, the plasma was isolated by centrifugation at 1400 × g for 15 min.

Leucocyte activation of these plasma samples was then assessed based on expression analysis of polymorphonuclear neutrophil (PMN) elastase using the PMN elastase ELISA (Demeditec, Kiel, Germany) according to the manufacturer's protocol. Measurements were carried out in quadruplicate. The concentration of PMN elastase was determined from absorbance measurements by using the 4-parameter algorithm.

Endothelial Cell Adhesion

The primary human cardiac microvascular endothelial cells (HCMEC) were obtained from PromoCell (Heidelberg, Germany) and cultured according to the manufacturer's protocol in endothelial cell growth medium MV. Medium was changed every 2–3 days while subculturing was performed at 70–90% confluence using the detach kit from PromoCell.

The polymer films disks of 14 mm diameter were generated by punching. Disinfection was achieved by incubation in 70% ethanol followed by washing with sterile water and equilibration in medium. Material disks were placed into the wells of a 24 well PS plate and fixed with Teflon rings. Cell-culture treated polystyrene (TCPS) plates were used as controls for ideal cell growth. Cells were seeded on top of the disks ($5{\cdot}10^4$ cells per disk) and grown for 24 h under standard cell culture conditions. Staining was done using the Live/Dead Cell Staining Kit II (PromoKine, Heidelberg, Germany) followed by fluorescence microscopy using the IX 51 microscope. At least 2 independent samples were visualized per material and at least 5 images of different areas per sample were recorded and counted.

Statistical Analysis

Values are given as mean together with the standard deviation (number of replicates is given in each experimental section). Statistical significance was determined using independent sample *t*-tests. The Bonferroni method was used to adjust for multiple comparisons (Noble, 2009).

CONCLUSION

A logical series of new copolymers have been synthesized for application in a fully resorbable cardiovascular medical device consisting of a bulk polymer of lactide and caprolactone in systematic fractions and a polyethylene glycol end functional group. Poly-(L-lactide-co-ε-caprolactone) with lactide: caprolactone contents of 100:0, 90:10, 80:20, 70:30, 55:45, 0:100 have been successfully synthesized and evaluated. Polymer chemical properties were well controlled with respect to molar fractions, polymer purity, molar mass, PEG presence and polydispersity. Excellent control over material chemistry yielded a systematic spectrum of materials with tailored copolymer fractions and thereby allowed us to make comparisons between subsets of chemical compositions and to draw relevant conclusions.

Biological evaluation of material films revealed that all polymers were non-toxic, non-apoptotic and did not induce significant hemolysis while only the polymer PLCL 55:45-PEG550 induced a mild hemolytic and leucocyte (PMN elastase) response. This work indicated again that polymer chemistry is only one angle while surface morphology had a significant role to plan. From a hemocompatibility perspective, PLLA-PEG550 and PLCL-PEG550 70:30 (non-toxic, non-hemolytic, non-inflammatory and non-thrombogenic) presented the best candidates for use in cardiovascular implants while from a endothelialization perspective, PCL-PEG550, PLCL-PEG550 90:10, and PLCL-PEG550 70:30 showed best endothelial cell adhesion. In light of the overall application target, it might actually be more important in the *in vivo* situation to execute this improved endothelial cell adhesion over platelet repelling properties since a fully endothelialised surface is considered to offer ideal hemocompatibility.

DATA AVAILABILITY STATEMENT

All datasets generated for this study are included in the article/**Supplementary Material**.

ETHICS STATEMENT

The studies involving human participants were reviewed and approved by the Ethics Committee of the Medical Faculty of the Ruhr-University Bochum, Gesundheitscampus 33, D-44801 Bochum. The patients/participants provided their written informed consent to participate in this study.

AUTHOR CONTRIBUTIONS

PD supported the polymer synthesis and characterisation. PB carried out the WCA measurements. WY performed the FTIR-ATR analysis of copolymers and controls. SS executed all SEM experiments and supported the image interpretation. US and NB were responsible for the acquisition of the donors, their education, the proper blood collection, and the immediate transport of the fresh blood samples to the laboratory. IR was involved in WCA analytics and critical proofreading. RV carried out a critical proofreading as well. WW was responsible for the concept of copolymer synthesis and functionalization and supervised SM and PD. JS was responsible for the overall

design of this research work, supervised particularly SP and was involved in all biological work of this manuscript. All the authors contributed to the article and approved the submitted version.

FUNDING

This work was supported by the European Community's Seventh Framework Programme under grant agreement number 604251 (ReBioStent) and the Irish Research Council (Grant Number EBPPG/2014/70).

SUPPLEMENTARY MATERIAL

The Supplementary Material for this article can be found online at: https://www.frontiersin.org/articles/10.3389/fbioe.2020.00991/full#supplementary-material

REFERENCES

Alam, S. R., Newby, D. E., and Henriksen, P. A. (2012). Role of the endogenous elastase inhibitor, elafin, in cardiovascular injury: from epithelium to endothelium. *Biochem. Pharmaco.* 83, 695–704. doi: 10.1016/j.bcp.2011.11.003

Al-Dehneh, A., Virk, H., Alkhouri, Y., Hamdan, A., and Bikkina, M. (2010). Drug-eluting stent thrombosis 1659 days after stent deployment: case report and literature review. *Texas Heart Inst. J.* 37, 343–346. s

Auras, R., Harte, B., and Selke, S. (2004). An overview of polylactides as packaging materials. *Macromol. Biosci.* 4, 835–864. doi: 10.1002/mabi.200400043

Barnes, S. J., and Harris, L. P. (2008). *Tissue Engineering: Roles, Materials, and Applications*. New York, NY: Nova Science Publishers, 5.

Beuth Publishing (2009). "International organization for standardization, ISO 10993-5," in *Biological Evaluation of Medical Devices - Part 5: Tests for in Vitro Cytotoxicity*, (Berlin: Beuth Publishing DIN), doi: 10.31030/1499596

Beuth Publishing (2017). "International organization for standardization, ISO 10993-4," in *Biological Evaluation of Medical Devices - Part 4: Selection of Tests for Interactions With Blood*, (Berlin: Beuth Publishing DIN), doi: 10.31030/2597308

Blok, S. L. J., Engels, G. E., and Van Oeveren, W. (2016). In vitro hemocompatibility testing: the importance of fresh blood. *Biointerphases* 11, 29802–29801. doi: 10.1116/1.4941850

Chen, J., Cao, J., Wang, J., Maitz, M. F., Guo, L., Zhao, Y., et al. (2011). Biofunctionalization of titanium with PEG and anti-CD34 for hemocompatibility and stimulated endothelialization. *J. Colloid Interface Sci.* 368, 636–647. doi: 10.1016/j.jcis.2011.11.039

Chuang, T.-W., and Masters, K. S. (2009). Regulation of polyurethane hemocompatibility and endothelialization by tethered hyaluronic acid oligosaccharides. *Biomaterials* 30, 5341–5351. doi: 10.1016/j.biomaterials.2009.06.029

Collet, C., De Winter, R. J., Onuma, Y., and Serruys, P. W. (2016). The Absorb bioresorbable vascular scaffold for the treatment of coronary artery disease. *Expert Opin. Drug Deli.* 13, 1489–1499. doi: 10.1080/17425247.2016.1227788

de Mel, A., Jell, G., Stevens, M. M., and Seifalian, A. M. (2008). Biofunctionalization of biomaterials for accelerated in situ endothelialization: a review. *Biomacromolecules* 9, 2969–2979. doi: 10.1021/bm800681k

Fernández, J., Etxeberria, A., and Sarasua, J.-R. (2012). Synthesis, structure and properties of poly(L-lactide-co-ε-caprolactone) statistical copolymers. *J. Mech. Behav. Biomed. Mater.* 9, 100–112. doi: 10.1016/j.jmbbm.2012.01.003

Foin, N., Lee, R., Mattesini, A., Caiazzo, G., Fabris, E., Kilic, D., et al. (2016). Bioabsorbable vascular scaffold overexpansion: insights from in vitro post-expansion experiments. *EuroIntervention* 11, 1389–1399. doi: 10.4244/EIJY15M07_02

Galley, H.-F., and Webster, N. R. (2004). Physiology of the endothelium. *Br. J. Anaesthesia* 93, 105–113. doi: 10.1093/bja/aeh163

Garg, S., and Serruys, P. W. (2010). Coronary Stents – Current status. *J. Am. Coll. Cardiol.* 56(Suppl.), S1–S42.

Gupta, B., Revagade, N., and Hilborn, J. (2007). Poly(lactic acid) fiber: an overview. *Prog. Polym. Sci.* 32, 455–482. doi: 10.1016/j.progpolymsci.2007.01.005

Huang, Y., Ng, H. C. A., Ng, X. W., and Subbu, V. (2014). Drug-eluting biostable and erodible stents. *J. Control. Release* 193, 188–201. doi: 10.1016/j.jconrel.2014.05.011

Inthanon, K., Daranarong, D., Techaikool, P., Punyodom, W., Khaniyao, V., Bernstein, A. M., et al. (2016). Biocompatibility assessment of PLCL-sericin copolymer membranes using Wharton's Jelly mesenchymal stem cells. *Stem Cells Internat.* 2016, 1–16. doi: 10.1155/2016/5309484

Iqbal, J., Gunn, J., and Serruys, P. W. (2013). Coronary stents: historical development, current status and future directions. *Br. Med. Bull.* 106, 193–211. doi: 10.1093/bmb/ldt009

Jeong, S. I., Kim, B.-S., Kang, S. W., Kwon, J. H., Lee, Y. M., Kim, S. H., et al. (2004). In vivo biocompatibilty and degradation behavior of elastic poly(l-lactide-co-ε-caprolactone) scaffolds. *Biomaterials* 25, 5939–5946. doi: 10.1016/j.biomaterials.2004.01.057

Khamis, H., Shokry, K., Ramzy, A., and Samir, A. (2014). Bioresorbable vascular scaffold (ABSORB BVS);first report in egyptian patients with 6 month angiographic/IVUS follow up. *Egyptian Heart J.* 66, 227–232. doi: 10.1016/j.ehj.2013.09.005

Khan, W., Farah, S., and Domb, A. J. (2012). Drug eluting stents: developments and current status. *J. Control. Release* 161, 703–712. doi: 10.1016/j.jconrel.2012.02.010

Kim, J. H., Noh, H., Kang, J. H., Lee, B. S., Choi, J., Park, K., et al. (2011). Characteristics of PLLA films blended with PEG block copolymers as additives for biodegradable polymer stents. *Biomed. Eng. Lett.* 1, 42–48. doi: 10.1007/s13534-011-0004-0

Kingshott, P., and Griesser, H. J. (1999). Surfaces that resist bioadhesion. *Cur. Opin. Solid State Mater. Sci.* 4, 403–412. doi: 10.1016/s1359-0286(99)00018-2

Ko, T.-M., Jui-Che, L., and Cooper, S. L. (1993). Surface characterization and platelet adhesion studies of plasma-sulphonated polyethylene. *Biomaterials* 14, 657–664. doi: 10.1016/0142-9612(93)90064-9

Lasprilla, A. J. R., Martinez, G. A. R., Lunelli, B. H., Jardini, A. L., and Filho, R. M. (2012). Poly-lactic acid synthesis for application in biomedical devices - a review. *Biotechnol. Adv.* 30, 321–328. doi: 10.1016/j.biotechadv.2011.06.019

Li, A. Y., Law, K. B., Phillips, K. R. B., Nwachukwu, H., Butany, J., and Gotlieb, A. I. (2010). Pathology of cardiovascular interventions and surgery. *Diagn. Histopathol.* 16, 17–30.

Lieb, E., Tessmar, J., Hacker, M., Fischbach, C., Rose, D., Blunk, T., et al. (2003). Poly(D,L-lactic acid)-poly(ethylene glycol)-monomethyl ether diblock copolymers control adhesion and osteoblastic differentiation of marrow stromal cells. *Tissue Eng.* 9, 71–84. doi: 10.1089/107632703762687555

Lim, J. I., Yu, B., and Lee, Y. K. (2008). Fabrication of collagen hybridized elastic PLCL for tissue engineering. *Biotech. Lett.* 30, 2085–2090. doi: 10.1007/s10529-008-9808-0

Maisel, W. (2017). FDA Investigating Increased Rate of Major Adverse Cardiac Events Observed in Patients Receiving Abbott Vascular's Absorb GT1 Bioresorbable Vascular Scaffold (BVS). Available online at: https://www.fda.gov/MedicalDevices/Safety/LetterstoHealthCareProviders/ucm546808.htm (accessed February 16, 2018).

McMahon, S., Bertollo, N., O' Cearbhaill, E. D., Salber, J., Pierucci, L., Duffy, P., et al. (2018). Bio-resorbable polymer stents: a review of material progress and prospects. *Prog. Polym .Sci.* 83, 79–96. doi: 10.1016/j.progpolymsci.2018.05.002

McMahon, S., Kennedy, R., Duffy, P., Vasquez, J. M., Wall, J. G., Tai, H., et al. (2016). Poly(ethylene glycol)-based hyperbranched polymer from RAFT and Its application as a silver-sulfadiazine-loaded antibacterial hydrogel in wound care. *ACS Appl. Mater. Interfaces* 8, 26648–26656. doi: 10.1021/acsami.6b11371

Melchiorri, A. J., Hibino, N., and Fisher, J. P. (2013). Strategies and techniques to enhance the in situ endothelialization of small-diameter biodegradable

polymeric vascular grafts. *Tissue Eng. Part B Rev.* 19, 292–307. doi: 10.1089/ten.TEB.2012.0577

Meraj, P. M., Jauhar, R., and Singh, A. (2015). Bare metal stents versus drug eluting stents: where do we stand in 2015? *Curr. Treat. Opt. Cardiovasc. Med.* 17, 39–49. doi: 10.1007/s11936-015-0393-y

Neuss, S., Apel, C., Buttler, P., Denecke, B., Dhanasingh, A., Ding, X., et al. (2008). Assessment of stem cell/biomaterial combinations for stem cell-based tissue engineering. *Biomaterials* 29, 302–313. doi: 10.1016/j.biomaterials.2007.09.022

Noble, W. S. (2009). How does multiple testing correction work? *Nat. Biotechnol.* 27, 1135–1137. doi: 10.1038/nbt1209-1135

Noel, S., Hachem, A., Merhi, Y., and De Crescenzo, G. (2015). Development of a polyester coating combining antithrombogenic and cell adhesive properties: influence of sequence and surface density of adhesion peptides. *Biomacromolecules* 16, 1682–1694. doi: 10.1021/acs.biomac.5b00219

Oliveira, J. E., Mattoso, L. H. C., Orts, W. J., and Medeiros, E. S. (2013). Structural and morphological characterization of micro and nanofibers produced by electrospinning and solution blow spinning: a comparative study. *Adva. Mater. Sci. Eng.* 2013, 1–14. doi: 10.1155/2013/409572

Ormiston, J. A., and Serruys, P. W. (2009). Bioabsorbable coronary stents. *Circ. Cardiovasc. Interv.* 2, 255–260. doi: 10.1161/circinterventions.109.859173

Pacharra, S., Ortiz, R., McMahon, S., Wang, W., Viebahn, R., Salber, J., et al. (2019). Surface patterning of a novel PEG-functionalized poly-l-lactide polymer to improve its biocompatibility: applications to bioresorbable vascular stents. *J. Biomed. Mater. Res. B Appl. Biomater.* 107, 624–634. doi: 10.1002/jbm.b.34155

Parnham, M. J., and Wetzig, H. (1993). Toxicity screening of liposomes. *Chem. Phys. Lipids* 64, 263–274. doi: 10.1016/0009-3084(93)90070-j

Patel, J. D., Krupka, T., and Anderson, J. M. (2006). iNOS-mediated generation of reactive oxygen and nitrogen species by biomaterial-adherent neutrophils. *J. Biomed. Mater Res. Part A* 80, 381–390. doi: 10.1002/jbm.a.30907

Ren, X., Feng, Y., Guo, J., Wang, H., Li, Q., Yang, J., et al. (2015). Surface modification and endothelialization of biomaterials as potential scaffolds for vascular tissue engineering applications. *Chem. Soc. Rev.* 44, 5680–5742. doi: 10.1039/c4cs00483c

Schrader, B. (1995). *Infrared and Raman Spectroscopy: Methods and Applications*. Weinheim: Wiley-VCH Verlag GmbH.

Shin, H.-S., Park, K., Kim, J. H., Kim, J.-J., Han, D. K., Moon, M.-W., et al. (2009). Biocompatible PEG Grafting on DLC-coated nitinol alloy for vascular stents. *J. Bioact. Comp. Polym.* 24, 316–328. doi: 10.1177/0883911509104273

Sperling, C., Fischer, M., Maitz, M. F., and Werner, C. (2009). Blood coagulation on biomaterials requires the combination of distinct activation processes. *Biomaterials* 30, 4447–4456. doi: 10.1016/j.biomaterials.2009.05.044

Tan, J., Shen, H., Carter, K. L., and Saltzman, W. M. (2000). Controlling human polymorphonuclear leukocytes motility using microfabrication technology. *J. Biomed. Mater. Res.* 51, 694–702. doi: 10.1002/1097-4636(20000915)51:4<694::aid-jbm18>3.0.co;2-n

Tenekecioglu, E., Farooq, V., Bourantas, C. V., Silva, R. C., Onuma, Y., Yilmaz, M., et al. (2016). Bioresorbable scaffolds: a new paradigm in percutaneous coronary intervention. *BMC Cardiovasc. Dis.* 16:38. doi: 10.1186/s12872-016-0207-5

Ugartemendia, J. M., Munoz, M. E., Santamaria, A., and Sarasua, J. R. (2015). Supramolecular structure, phase behaviorand thermo-rheological properties of a poly(L-lactide-co-ε-caprolactone) statistical copolymer. *J. Mech. Behav. Biomed. Mater.* 48, 153–163. doi: 10.1016/j.jmbbm.2015.04.007

Van Oeveren, W. (2013). Obstacles in haemocompatibility testing. *Scientifica* 2013, 1–14. doi: 10.1155/2013/392584

Van Oeveren, W., Schoen, P., Maijers, C. A., Monnink, S. H., and Van Boven, A. J. (1999). Hemocompatibility of stents. *Prog. Biomed. Res.* 4, 17–22.

Vasilev, K., Poh, Z., Kant, K., Chan, J., Michelmore, A., and Losic, D. (2010). Tailoring the surface functionalities of titania nanotube arrays. *Biomaterials* 31, 532–540. doi: 10.1016/j.biomaterials.2009.09.074

Verheye, S., Ormiston, J. A., Stewart, J., Webster, M., Sanidas, E., Costa, R., et al. (2014). A next-generation bioresorbable coronary scaffold system: from bench to first clinical evaluation: 6- and 12-month clinical and multimodality imaging results. *JACC Cardiovasc. Interv.* 7, 89–99. doi: 10.1016/j.jcin.2013.07.007

Waksman, R. (2006). Biodegradable stents: they do their job and disappear. *J. Invasive Cardiol.*18, 70–74.

Wang, J., He, Y., Maitz, M. F., Collins, B., Xiong, K., Guo, L., et al. (2013). A surface-eroding poly(1,3-trimethylene carbonate) coating for fully biodegradable magnesium-based stent applications: toward better biofunction, biodegradation and biocompatibility. *Acta Biomate.* 9, 8678–8689. doi: 10.1016/j.actbio.2013.02.041

Wang, W., Xiong, W., Zhu, Y., Xu, H., and Yang, X. (2010). Protective effect of PEGylation against poly(amidoamine) dendrimer-induced hemolysis of human red blood cells. *J. Biomed. Mater. Res. B Appl. Biomater.* 93, 59–64. doi: 10.1002/jbm.b.31558

Webster, R., Didier, E., Harris, P., Siegel, N., Stadler, J., Tilbury, L., et al. (2007). PEGylated proteins: evaluation of their safety in the absence of definitive metabolism studies. *Drug Metab. Disposit.* 35, 9–16. doi: 10.1124/dmd.106.012419

Williams, D. F. (2008). On the mechanisms of biocompatibility. *Biomaterials* 29, 2941–2953. doi: 10.1016/j.biomaterials.2008.04.023

Wu, Y., Wang, W., Chen, Y., Huang, K., Shuai, X., Chen, Q., et al. (2010). The investigation of polymer-siRNA nanoparticle for gene therapy of gastric cancer in vitro. *Int. J. Nanomed.* 5, 129–136. doi: 10.2147/IJN.S8503

Zhang, K., Liu, T., Li, J.-A., Chen, J.-Y., Wang, J., and Huang, N. (2014). Surface modification of implanted cardiovascular metal stents: from antithrombosis and antirestenosis to endothelialization. *J. Biomed. Mater. Res. Part A* 102, 588–609. doi: 10.1002/jbm.a.34714

Conflict of Interest: SM and PD were employed by the company Ashland Specialties Ireland.

The remaining authors declare that the research was conducted in the absence of any commercial or financial relationships that could be construed as a potential conflict of interest.

Copyright © 2020 Pacharra, McMahon, Duffy, Basnett, Yu, Seisel, Stervbo, Babel, Roy, Viebahn, Wang and Salber. This is an open-access article distributed under the terms of the Creative Commons Attribution License (CC BY). The use, distribution or reproduction in other forums is permitted, provided the original author(s) and the copyright owner(s) are credited and that the original publication in this journal is cited, in accordance with accepted academic practice. No use, distribution or reproduction is permitted which does not comply with these terms.

frontiers in Bioengineering and Biotechnology

REVIEW
published: 09 December 2020
doi: 10.3389/fbioe.2020.529244

Biomaterials in Valvular Heart Diseases

Bita Taghizadeh[1], Laleh Ghavami[2], Hossein Derakhshankhah[3], Ehsan Zangene[4], Mahdieh Razmi[5], Mehdi Jaymand[6], Payam Zarrintaj[7], Nosratollah Zarghami[1], Mahmoud Reza Jaafari[8,9], Matin Moallem Shahri[10], Adrineh Moghaddasian[11], Lobat Tayebi[12] and Zhila Izadi[3,13]**

[1] Department of Medical Biotechnology, School of Advanced Medical Sciences, Tabriz University of Medical Sciences, Tabriz, Iran, [2] Laboratory of Biophysics and Molecular Biology, Department of Biophysics, Institute of Biochemistry and Biophysics, University of Tehran, Tehran, Iran, [3] Pharmaceutical Sciences Research Center, Health Institute, Kermanshah University of Medical Sciences, Kermanshah, Iran, [4] Department of Bioinformatics, Institute of Biochemistry and Biophysics, University of Tehran, Tehran, Iran, [5] Department of Biochemistry, Institute of Biochemistry and Biophysics, University of Tehran, Tehran, Iran, [6] Nano Drug Delivery Research Center, Health Technology Institute, Kermanshah University of Medical Sciences, Kermanshah, Iran, [7] Polymer Engineering Department, Faculty of Engineering, Urmia University, Urmia, Iran, [8] Biotechnology Research Center, Pharmaceutical Technology Institute, Mashhad University of Medical Sciences, Mashhad, Iran, [9] Department of Pharmaceutical Nanotechnology, School of Pharmacy, Mashhad University of Medical Sciences, Mashhad, Iran, [10] Cardiology Department, Taleghani Trauma Center, Mashhad University of Medical Sciences, Mashhad, Iran, [11] School of Medicine, Mashhad University of Medical Sciences, Mashhad, Iran, [12] Marquette University School of Dentistry, Milwaukee, WI, United States, [13] Department of Regenerative Medicine, Cell Science Research Center, Academic Center for Education, Culture and Research (ACECR), Royan Institute for Stem Cell Biology and Technology, Tehran, Iran

OPEN ACCESS

Edited by:
Susanna Sartori,
Politecnico di Torino, Italy

Reviewed by:
Xing Zhang,
Chinese Academy of Sciences, China
Anna Guarino,
Monzino Cardiology Center (IRCCS), Italy

***Correspondence:**
Lobat Tayebi
lobat.tayebi@marquette.edu
Zhila Izadi
izadi_zh@razi.tums.ac.ir;
izadi.zhila@yahoo.com

Specialty section:
This article was submitted to Tissue Engineering and Regenerative Medicine, a section of the journal Frontiers in Bioengineering and Biotechnology

Received: 23 January 2020
Accepted: 16 November 2020
Published: 09 December 2020

Citation:
Taghizadeh B, Ghavami L, Derakhshankhah H, Zangene E, Razmi M, Jaymand M, Zarrintaj P, Zarghami N, Jaafari MR, Moallem Shahri M, Moghaddasian A, Tayebi L and Izadi Z (2020) Biomaterials in Valvular Heart Diseases. Front. Bioeng. Biotechnol. 8:529244. doi: 10.3389/fbioe.2020.529244

Valvular heart disease (VHD) occurs as the result of valvular malfunction, which can greatly reduce patient's quality of life and if left untreated may lead to death. Different treatment regiments are available for management of this defect, which can be helpful in reducing the symptoms. The global commitment to reduce VHD-related mortality rates has enhanced the need for new therapeutic approaches. During the past decade, development of innovative pharmacological and surgical approaches have dramatically improved the quality of life for VHD patients, yet the search for low cost, more effective, and less invasive approaches is ongoing. The gold standard approach for VHD management is to replace or repair the injured valvular tissue with natural or synthetic biomaterials. Application of these biomaterials for cardiac valve regeneration and repair holds a great promise for treatment of this type of heart disease. The focus of the present review is the current use of different types of biomaterials in treatment of valvular heart diseases.

Keywords: valvular heart diseases, heart valve replacement, cardiac valve regeneration, tissue-engineered heart valves, biomaterials

INTRODUCTION

According to the American Heart Association's 2019 report, cardiovascular diseases remain a major source of mortality and disease-related cost burden in the United States and worldwide (Benjamin et al., 2019). Some of the major heart and circulatory diseases include valvular heart disease (VHD), coronary heart disease, aortic disease, myocardial infarction, cardiac myopathy, and heart failure. All these conditions involve physical damage to the heart resulting in functional loss.

In particular, VHD occurs as the result of valvular malfunction. Left untreated, valvular diseases can lead to stroke, heart failure and death due to sudden cardiac arrest (SCA). Different treatment regimens are available for management of VHD, including medications and lifestyle changes, as well as surgical and interventional procedures. Although most of these treatments can be helpful in reducing the symptoms, the gold standard approach is to repair or replace the injured valve tissue in order to restore full cardiac function. On the other hand, some impaired cardiac valves cannot be repaired (in 70% of cases) and need to be replaced by biomaterials (Yacoub and Cohn, 2004). Although cardiac regeneration ability immediately after birth has been indicated in humans, adult valvular tissues lack self-regeneration capacity following injuries, which can eventually lead to heart failure and death (Rabkin-Aikawa et al., 2005; Uygur and Lee, 2016). Various surgical valve repair and replacement procedures are available in order to avoid these fatal consequences.

As life expectancy and access to screening methods has improved across the world, the number of VHD cases has increased considerably in the past few years. Many people with valvular defects have no symptoms and in most cases, this condition remains constant throughout the person's life. However, for other people, VHD slowly progresses and the symptoms become worse. Estimations suggest that the prevalence of VHD may increase up to 122% by the end of 2056, creating a significant socio-economic impact on the society (D'arcy et al., 2016). Currently, mitral regurgitation and aortic stenosis are the most common types of VHDs worldwide (Nkomo et al., 2006).

In the last decade, along with the tremendous growth in biomaterials applications, there have been numerous successful implementation of biomaterials in the replacement and repair of body tissues, including cardiac valves. Biomaterials are simply defined as materials that either would interact with body's tissues for medical purposes, as implanted medical devices or used to support, augment or replace injured tissues and/or organs or as drug carriers. The main characteristics of a biomaterial substance include bio-functionality, biocompatibility, bioactivity, sterilizability and bio-inertia.

Various synthetic and natural biomaterials have been used for replacement and repair of damaged valvular tissues (Ratner, 2013). These biomaterials must be blood compatible and be able to interact with the physiological environment of cells or tissues in which they are being implanted. The most important parameters of a biomaterial that need to be assessed prior to implantation are physical properties, mechanical strength, geometry as well as friction, flow and wear resistance. Except the aforementioned materials, other types of biomaterials have also been studied and used for this purposes. In the present review, we will discuss the most commonly used biomaterials in treatment of heart valve diseases.

VALVE HEART DISEASES (VHD)

Heart valve diseases are among the most common CVDs in the world, affecting nearly 2.5% of the US population (Brinkley and Gelfand, 2013). Potential risk factors related to VHD includes genetics, age, male gender, hypertension, hyperlipidemia, smoking, diabetes, and adrenal insufficiency, as well as rheumatic disease and infectious endocarditis. Despite challenges in identifying the underlying genetic basis of familial VHDs, mainly due to genetic and phenotypic heterogeneity of the disease, incomplete penetrance, and genetic modifiers, recent studies using genome-wide linkage analysis and transcriptomics approaches, transgenic animals, and microRNAs have been able to demonstrate genetic mechanisms of common VHDs, including bicuspid aortic valve (BAV) and mitral valve prolapse (MVP). Identifying these genetic cues can significantly improve treatment strategies for VHD patients and their at-risk family members (Lahaye et al., 2014; Helgadottir et al., 2018; Nagy et al., 2019; Chen et al., 2020).

There are two main classes of VHD—valvular stenosis and valvular insufficiency. Valvular stenosis occurs because of the stiffening and reduced elasticity of valve leaflets, which can lead to narrowing of the valve opening and subsequently, reduction of blood flow. Valvular insufficiency or regurgitation occurs as the result of incomplete closure of valve leaflets, leading to leakage or regurgitant flow development (Topilsky, 2018; Crousillat and Wood, 2019).

According to American Heart Association (AHA)/American College of Cardiology (ACC) guidelines, VHD progression can be categorized according to disease stage as follow (Nishimura et al., 2014):

Stage A: Patients who have the risk factors for development of VHD.
Stage B: Asymptomatic patients with progressive VHD (mild to moderate severity).
Stage C: Asymptomatic patients with severe VHD with either normal right or left ventricular systolic function (Stage C_1) or decompensated ventricular function (Stage C_2).
Stage D: Symptomatic patients with severe VHD.

VHD diagnosis might be challenging since patients may be asymptomatic or VHD might be accompanied by possible comorbidities. In this regard, precise patient evaluation in terms of family history and risk factors as well as careful physical examination (including intra- and extra-cardiac conditions and comorbidities) are mandatory.

VHD conditions can be congenital or acquired and may involve any of the four valves of the heart, however, when the aortic and mitral valves are involved, patient's condition is often more serious. Age is another determining risk factor in VHD, in a way that the risk of VHD increases from less than 1% in people in the age of 18–44, to more than 13% in people over 75 years old (Brinkley and Gelfand, 2013).

Since the heart valve tissue cannot regenerate spontaneously, replacement (with biological or mechanical heart valves), repair (via reconstructive surgery) or interventional catheterization are the current treatment options for management of VHD. Abnormal valves that are not repairable are replaced with bio-prosthetic (i.e., biological) or mechanical (prosthetic) valves

(Borer et al., 2004). Extensive research has been conducted on the design and development of biomaterials used in heart valves, with the aim of achieving the closest replica to natural human heart valves.

Generally, cardiac valve biomaterials should be biocompatible with good hemodynamics, high mechanical stability and resistance to degradation and calcification. Despite recent advances in valvular replacement, mechanical and bio-prosthetic heart valves, both share the disadvantage of remodeling and growth following implantation, which is considered a major limitation in their application—especially in children with congenital valve disorders, since the transplanted heart valve should be able to simultaneously grow along with the patient's heart. Tissue-engineered heart valves (TEHVs) are possible substitutes for bio-prosthetic and mechanical valves, with the ability of remodeling and acquiring patient's normal valve structure.

BIOMECHANICS OF HEART VALVES

Understanding the mechanical properties of natural heart valves is essential for successful design and fabrication of prosthetic valves so they can more closely resemble native valve's structure and function. Cardiac tissue is composed of different cell types including cardiomyocytes, fibroblasts, endothelial, and smooth muscle cells. Fibroblasts are the most frequent cell types in the myocardium, which are responsible for the extracellular matrix (ECM) components deposition (Mackenna et al., 2000). Cardiac valve tissue is a mechanically active and a complex system of different cell types and their interactions with the components of ECM. The main valvular cell types are valvular interstitial cells (VICs) and valvular endothelial cells (VECs), which are responsible for synthesizing and maintaining the ECM, as well as maintaining the heart valve's hemostasis, structure and integrity (Taylor et al., 2003). Cardiac ECM is a complex network of proteins involved in strength and elasticity—including collagen, elastin, fibronectin, glycosaminoglycans (GAGs), glycoproteins (GPs), and proteoglycans (PGs)—with collagen being the most common protein in the heart valve tissue (Schoen, 1997; Brand et al., 2006; Rienks et al., 2014). Excellent biomechanical features of heart valves is the result of close interactions between VECs and VICs, as well as their interactions with ECM, in response to biological and mechanical stimuli. In cellular level, VECs are the first valvular components on the leaflet's surface that are exposed to hemodynamic shear stress of the blood flow. The biomechanical stimuli induced by shear forces result in gene expression alterations in these cells (Butcher et al., 2006). Valvular ECM functions as an organizing matrix for cellular support, which transmits biomechanical stimuli to the VICs, inducing subsequent VIC's phenotypical changes as well as ECM remodeling (Rabkin-Aikawa et al., 2004). According to a study by El-Hamamsy and colleagues, the interactions between VICs and VECs seem to unify different components of valve tissue and brings mechanical integrity to the valve (El-Hamamsy et al., 2009).

Four cardiac valves provide unidirectional forward blood flow during each cardiac cycle. Two types of cardiac valves exist: semilunar valves (including pulmonary and aortic valves) with three identical leaflets or cusps and sigmoid or atrioventricular valves (including mitral and tricuspid valves). The sigmoid valves have a more complex structure compared to semilunar valves due to their asymmetrical geometry and unequal leaflet size (Sacks et al., 2009).

All the four heart valves lie on the basal plane of the heart, made from dense collagen fibers, which help maintain their constant position relative to the movements of other parts of the heart. While the mitral and tricuspid valves are responsible for regulating the blood inflow to the heart, the aortic and pulmonary valves control the blood flow from the left and right ventricles into the aorta and pulmonary artery, respectively (Hasan et al., 2014).

Each valvular leaflet is made of three different layers including fibrosa, spongiosa, and the ventricularis with their distinct ECM composition. All these layers are composed of VICs with their surrounding ECM, covered with VECs. Fibrosa is the main load bearing and the thickest layer of the valve leaflet, which is made of type I collagen fibers that can endure high tensile forces. Ventricularis is made of dense collagen and radially aligned elastin fibers and is responsible for reducing the radial strain during valve opening and maximum forward blood flow. The spongiosa layer provides lubrication during leaflet bending and pressurization and is composed of collagen fibers, hydrated PGs, and GAGs. Hydrated PGs and GAGs are also involved in oxygen and nutrient elements diffusion through the valve tissue, as well as growth factor sequestration and controlled release (Latif et al., 2005; Sacks et al., 2009; Li et al., 2019).

Heart valves undergo 30 million heart cycles a year, while operating under high dynamic and mechanical forces (fluid shear stress, hydrodynamics, flexural, and tensile forces) (Sacks et al., 2009; Butcher et al., 2011). These forces are induced and controlled by surrounding hemodynamic environment of the heart and are inflicted periodically; valve opening (flexural force), blood flow through the valve (shear stress and hemodynamic pressure), valve closure (flexural force) and prevention of blood back-flow (tensile forces). The trans-valvular pressure on each heart valve under physiological conditions is as follows: tricuspid valve = 25 mmHg, mitral valve = 120 mmHg, pulmonary valve = 10 mmHg, and aortic valve = 80 mmHg. The ability of heart valves to endure such mechanical forces throughout a person's lifetime is due to their constant remodeling and adjusting their ECM.

Natural valve leaflets represent a dynamic biological material with a heterogeneous anisotropic structure and complex mechanical behavior. They present the optimum structure and geometry, which minimizes the shear stress resistance while maximizing the blood flow. Some of the most important features of heart valves include dynamic motion, complex surface geometry, anisotropic deformation, thin leaflets, and remodeling (Guyton and Hall, 1996; Sacks et al., 2006, 2009; Loerakker et al., 2013). The precise combination of all these multi-modal features ensure heart valve's functionality throughout a person's entire lifetime. Altogether, biomechanical valvular

features are among determining factors that should be considered in biomaterial selection, as well as the design and engineering of bio-prosthetic or mechanical heart valves. According to CDC, 61% of VHD-related deaths are due to aortic valve diseases. Since aortic valve involvement leads to serious health complications, biomechanical behavior of healthy and abnormal aortic valve is particularly discussed in the following section.

The common aortic valve is a tricuspid valve responsible for maintaining the unidirectional blood flow from the left ventricle into the aorta. The leaflets does not have uniform thickness, their thickness increases toward free cusps margins (Ho, 2009). Similar to other heart valves, each aortic leaflet is composed of three layers (fibrosa, spongiosa, and ventricularis). Aortic valve stenosis is the most common aortic valve disease, which is caused by thickening and calcification of the cusps (Rajamannan et al., 2011). The peak velocity of the blood flow through aortic valve during each cardiac systole is approximately 1.35 m/s (Balachandran et al., 2011). When aortic leaflets become calcified, the blood flow velocity and the hemodynamic pressure on the aortic valve increases due to increased cusps thickness (velocity may exceed 4 m/s), which eventually leads to progression of valvular stenosis. The aortic valve also endures shear stress during cardiac systole (when blood flow passes the leaflets) and during diastole (when the blood pools into the sinuses). Valve closure induces flexural stress during diastole. As mentioned previously, biomechanical stimuli induce phenotypic and gene expression profile changes in valvular cells. Different hemodynamic forces are inflicted on the aortic and ventricular sides of the aortic valve during each cardiac cycle, which requires different mechanical features on each side of the cusps. The ventricular surface of aortic cusps are exposed to unidirectional shear stress while the aortic side is exposed to oscillatory shear stress (Sacks and Liao, 2019). This leads to side-dependent VEC biology, which means that VECs on different sides of the aortic leaflets have distinct phenotype and gene expression profiles. Based on previous reports, calcified aortic valve disease (CAVD) initiates from the aortic side of the leaflets while the spongiosa and ventricularis layers remain disease-protected (Yip and Simmons, 2011). Majority of patients suffering from aortic stenosis are presented with concomitant aortic regurgitation as well (Honda et al., 2012). Aortic regurgitation in these patients mainly occurs due to the loss of stretch in calcified cusps during diastole (Balachandran et al., 2011). A bicuspid aortic valve (BAV) with only two cusps instead of three is present in 1–2% of the population due to a congenital abnormality (Mordi and Tzemos, 2012). The normal aortic valve has circular ring whereas BAV has oval-shaped ring geometry. Oval geometry of BAV leads to high-frequency unsteady shear force on the cusps leading to early calcification and valve failure (Yap et al., 2012). Calcified valves in BAV, have reduced effective orifice area, which is associated with increased transvalvular pressure and subsequent elevated mechanical strain on the cusps (Chien et al., 2016). Major complications associated with BAV include aortopathy (thoracic aorta dilation) and aorta coarctation, both of which lead to early stenosis and valve failure. Due to severe complications associated with BAV, the ultimate treatment option for these patients is surgical. Surgical management of BAV patients is similar to those with tricuspid aortic valve disease.

APPLICATION OF BIOMATERIALS IN HEART VALVES

Prosthetic Heart Valves (PHVs)

PHVs or mechanical heart valves fabricated from synthetic materials (**Table 1**) have lifetime durability. However, patients

TABLE 1 | Commonly used natural and synthetic biomaterials in heart valve replacement and repair.

Mechanical Heart valves	Biomaterials (Natural and Synthetic)	References
	Polypropylene	Detmer et al., 1972; Gentle and Juden, 1984; Thornton et al., 1997
	Polyurethane urea	Jayabalan et al., 2000; Thomas et al., 2001; Thomas and Jayabalan, 2009
	Polyurethane (PU)	Mackay et al., 1996; Bernacca et al., 1997a,b, 2002b; Wheatley et al., 2000
	Polyvinyl alcohol (PVA)	Tadavarthy et al., 1975; Wan et al., 2002; Jiang et al., 2004; Millon and Wan, 2006
	Silicone	Carmen and Kahn, 1968; Carmen and Mutha, 1972; Cuddihy et al., 1976; Parfeev et al., 1983; Smith and Black, 1984
	Titanium	Mitamura et al., 1989; Jones et al., 2000; Aagaard, 2004; Leng et al., 2006; Guldner et al., 2011
	Pyrolytic carbon	Björk, 1972; Schoen et al., 1982; Goodman et al., 1996; Ritchie, 1996; Ely et al., 1998; Litzler et al., 2007
	Polyether urethane (PEU)	Boretos et al., 1975; Bernacca et al., 1995, 1997a; Wheatley et al., 2000
	Polycarbonate urethane (PCU)	Daebritz et al., 2004; Sachweh and Daebritz, 2006; Clauser et al., 2014
	Polyethylene glycol (PEG)	Paul et al., 1998; Ota et al., 2007; Ouyang et al., 2008; Zhou et al., 2013; Tseng et al., 2014; Zhang et al., 2015
Biological Heart valves	Gelatin	Tayama et al., 2000; Wong et al., 2010; Duan et al., 2013; Laila Roudsari et al., 2014; Yue et al., 2015
	Fibrin	Ye et al., 2000; Lieshout et al., 2006; Flanagan et al., 2007; Robinson and Tranquillo, 2009; Weber et al., 2014
	Collagen	Taylor et al., 2002; Flanagan et al., 2006; Tedder et al., 2008, 2010; Chen et al., 2013
	Elastin	Lu et al., 2004; Tedder et al., 2008; Chen et al., 2013; González De Torre et al., 2016

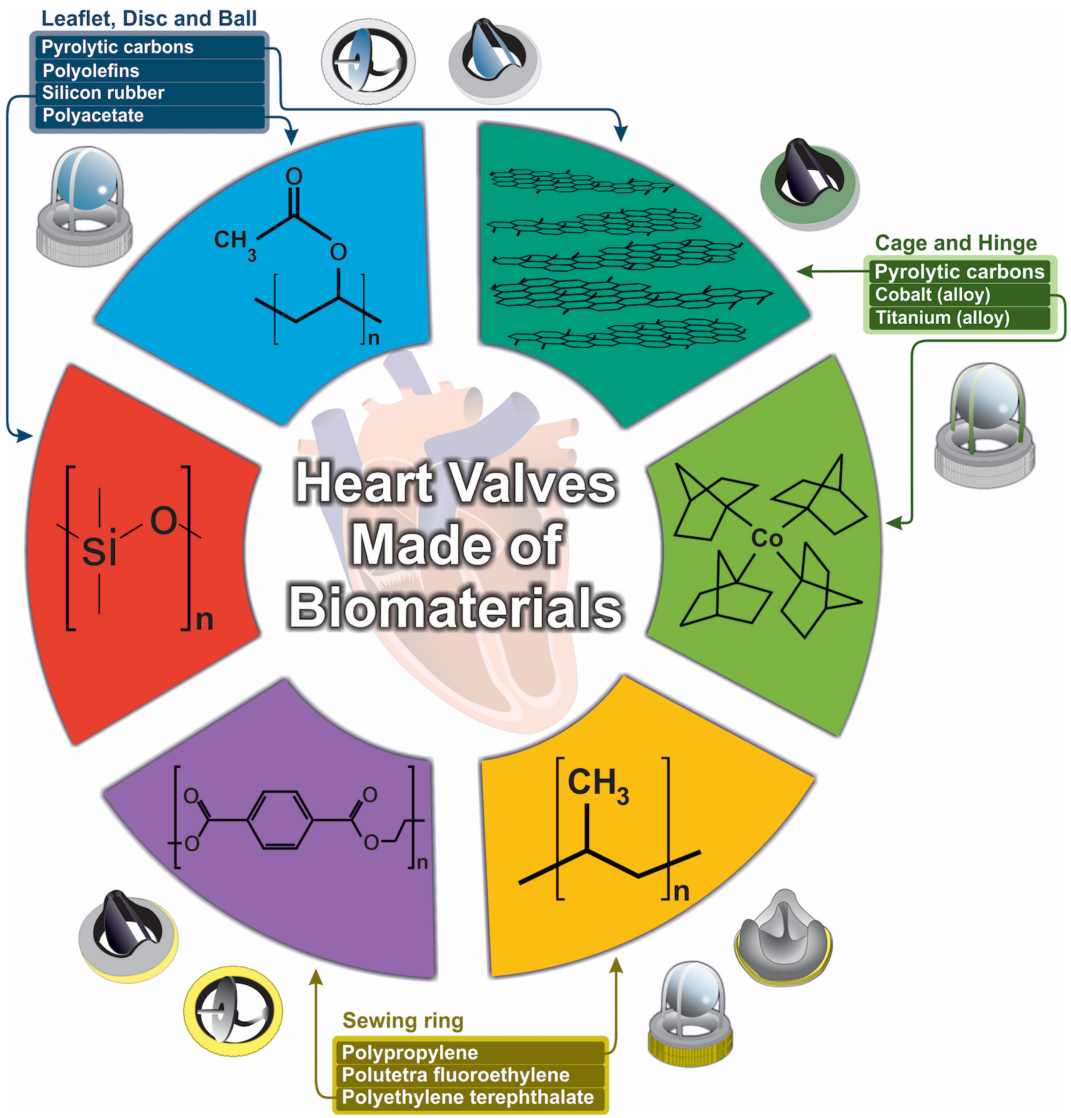

FIGURE 1 | Design and development of biomaterials used in heart valves.

who have received PHV transplants require lifetime consumption of anticoagulation medications, which can increase the chance of thromboembolism and hemorrhage (Russo et al., 2008; Chiang et al., 2014; Glaser et al., 2016). Synthetic materials are more advantageous compared to natural biomaterials, as their properties—such as degree of porosity, pore size, and 3D structure as well as mechanical strength and degradation time—can be controlled through the synthesis process (Kim and Mooney, 1998). However, issues related to their biocompatibility and subsequent inflammation, thrombosis or thromboembolism can cause limitations in their application. Moreover, prosthetic valve endocarditis (PVE) may also occur following prosthetic valve transplant, which may lead to surgical removal of the prosthesis (Wilson et al., 1982). Toxicity of synthetic materials, especially in the case of biodegradable materials, should also be considered.

Fatigue and wear stress are two other major problems associated with valve prostheses failure (Klepetko et al., 1989). Generally, biomaterial's fatigue is the result of body's immune response to generated wear debris. This is why fatigue fracture and wear resistance of biomaterials should be addressed in PHV applications (Teoh, 2000). On the other hand, transvalvular pressure (following valve closure), is considered the heaviest burden on mechanical valves and can cause impact- and friction-wear stress (Legg et al., 2012). Since the first introduction of prosthetic heart valves, various models have been developed, each one made from different biomaterials and with specific geometry as well as mechanical and hemodynamic characteristics (**Figure 1**).

The main types of PHVs include ball in cage, tilting disc and bileaflet valves. The first successful prosthetic heart valve implantation (ball in cage valve, **Figure 1**), dates back to 1960s

by Dr. Hufnagel. The Hufnagel valve consisted of an occluder ball, fabricated from methyl methacrylate (Plexiglas), restrained by a metal cage attached to a sewing ring, which was placed in the descending thoracic aorta instead of the heart itself. Plexiglas was later replaced by a silicone-coated hollow nylon poppet to reduce valve noise (Butany et al., 2002). The Starr-Edwards (SE) valve, which consisted of a methacrylate cage and a silicone elastomer rubber-ball, showed first promising results, since it had smaller size and could be placed inside the heart itself. Due to various complications associated with ball in cage valve (including aortic necrosis, pannus formation, paravalvular or paraprosthetic leakage, thrombosis, and infection), its production was discontinued in 2007. Most of these complications were related to non-optimal hemodynamic characteristics of these valves, including relatively large size of the occluder ball, which could damage blood cells in the passing blood flow. However, there has been an interesting case of a patient who had mitral stenosis and received SE valve transplant in 1974, with no major complications until 44 years after SE valve implantation (Hirji et al., 2018). Despite its disadvantages, the caged ball valve represented a new beginning in the area of biomaterials application in VHD management. Following the introduction of cardiopulmonary bypass technique in the early 1960's, the next generation of PHVs were developed. Tilting disc (or mono-leaflet) valves are composed of a circular occluding disc attached to metal struts. This type of prosthetic valve allows more natural blood flow and less blood cell damage during blood passage through the valve, which results in lower occurrence of thromboembolism compared to the ball in cage valves (Raj, 2005). The tilting disc opens in an angle range of 60–80°, which provides two orifice areas with different sizes (Pibarot and Dumesnil, 2009). The first tilting disc valve was fabricated from Derlin polymer and introduced in the late 1960's. The Derlin polymer was replaced by pyrolytic carbon (pyrolyte) in the later designs, since water absorption by the Derlin polymer resulted in valve disfiguration (Bjork, 1981). The thromboresistant feature of pyrolytic carbon further improved functionality of the tilting disc valves (Raj, 2005). However, one of the major complications associated with this type of mechanical heart valves is struts fracture due to fatigue.

Bileaflet valves consist of two semilunar leaflets attached to a rigid ring with the opening angle of 75–90°, resulting in three orifices with different sizes. Blood flow through these two leaflets, resembles natural heart valves, making bileaflet valves superior to other prosthetic valves (Raj, 2005). Today, bileaflet valves has become the most widely implanted valves due to their improved hemodynamic characteristics. Pyrolyte is the most commonly used biomaterial for production of the inner orifice and the leaflets of this type of prosthetic valve. However, despite its improved hemodynamics, presence of backflow is considered an important shortcoming.

Nowadays, commonly used materials in PHVs include elastomers (mainly polyurethanes and silicones) (Parfeev et al., 1983), titanium (Phillips, 2001; Zhou et al., 2015), pyrolytic carbon (Cao, 1996; Ely et al., 1998; Phillips, 2001) and metal alloys (Akins, 1979; Buchanan, 2005; **Table 1**).

Elastomers (so called "rubbers") are commonly used in the biomedical field, mainly due to their ability to sustain deformation under stress conditions without being ruptured and resuming their original state upon removal of the stress. Elastomeric materials exist as natural and synthetic (including silicones and polyurethanes) forms (Yoda, 1998). Polyurethanes (PUs) have been the subject of extensive research in fabrication of PHVs (Braunwald et al., 1960). PUs are a large family of synthetic elastomers with diverse compositions and properties, which makes them one of the most biocompatible materials that currently exist. Despite these advantages, PU's stability and susceptibility to biodegradation and calcification (leading to prosthesis premature failure), remains the major challenge in their application. Toxicity of biodegradation products of PUs is a concerning problem as well, since some of these products have been shown to be carcinogenic (Schoental, 1968; Cardy, 1979). The most commonly used PUs in valve prostheses include polyester urethane, polyether urethane (PEU) and polycarbonate urethane (Zdrahala and Zdrahala, 1999). A mechanical performance study by Bernacca et al. revealed that calcification in heart valves made of PEU was lower than the biological valves under the same conditions. Since PEU leaflets have lower thickness compared to bio-prosthetic valve leaflets, they are more susceptible to accumulation of calcified debris, which can be simply detached and released into the bloodstream. On the other hand, PEU valves have shown durability problems, as they have failed after 7.5 years following implantation (Bernacca et al., 1995, 1997a; Mackay et al., 1996). Further studies on the performance of PEU valves compared to urea-containing polyetherurethaneurea (PEUE) valves showed higher resistance and durability (up to 10 years) of PEUE compared to PEU valves (Bernacca et al., 1997a).

Surface modification is a useful strategy for manipulation of PU's resistance to biodegradation, thrombogenesis and calcification. Alves et al. (2014) used 2 hydroxyethylmethacrylate (HEMA) with UV or argon plasma treatment for surface modification of Elastollan® (a thermoplastic PU) and were able to improve surface hydrophilicity up to 30%, as well as enhanced antibacterial activity and hemocompatibility.

Bernacca et al. used heparin, taurine, 3-aminopropyltriethoxysilane and polyethylene oxide (PEO) to modify PEU and PEUE heart valves and to improved their fatigue resistance and durability (Bernacca and Wheatley, 1998). Many similar studies have reported the application of different materials to modify PU's surfaces including sulfonated poly (ethylene oxide) (PEO) (Han et al., 2006) and poly (ethylene glycol) methacrylate (PEGMA) (Qiu et al., 1996). In one study by Stachelek et al. (2006) endothelial seeding of PU heart valve leaflets was accomplished by cholesterol modification of PU's surface, promoting the resistance of the PU valve to thrombosis.

Flexibility of PU heart valves is obtained by using low modulus materials, however, low modulus PUs show poor durability due to high strain accumulation (Bernacca et al., 2002a). Since the first silicone rubbers used in PHVs fabrication tended to absorb lipids resulting in valve deterioration, they were later replaced by metal alloys. The strength, durability, and biocompatibility of metals have made titanium and stainless steel among the most common

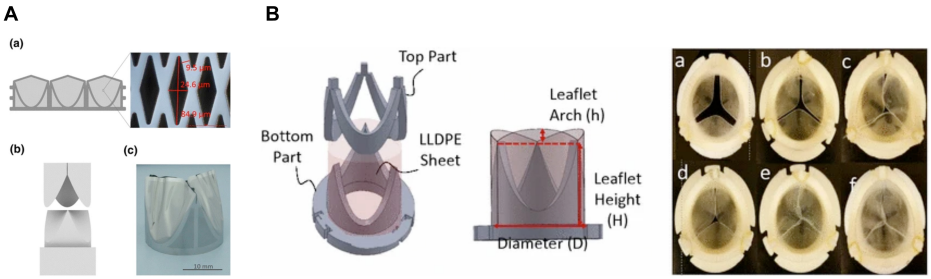

FIGURE 2 | (A) Schematic micro-structured Nickle-Titanium (NiTi) thin film as a matrix scaffold for tissue engineered hybrid heart valves. (a) Formation of 3D valve leaflets by a steel mold. (b) Fabricated NiTi film valve leaflets. Reprinted with permission from Loger et al. (2016). Copyright (2016), Springer Nature. **(B)** Leaflets and stents assembly for fabricating heart valves (left), Top view of each six HVs with different arch profiles. Reprinted with permission from Yousefi et al. (2017). Copyright (2017), Springer Nature.

materials in PHVs fabrication (Van Putte et al., 2012; Loger et al., 2016; **Figure 2A**).

Pyrolytic carbon's excellent features including its strength, clot forming prevention, and wear resistance as well as tissue- and blood-compatibility, make it an interesting biomaterial for fabricating PHVs (Bokros, 1989; Karp and Sand, 1993). Low-temperature isotropic (LTI) pyrolytic carbon is the most commonly used form of pyrolytic carbon in commercially available PHVs.

Blood-flow hemodynamics near the heart valve as well as the interactions of blood cells and platelets with valvular structures are among the most important determining factors for prosthetic valve's success or failure. Since thrombosis and thromboembolism, are two major complications associated with PHVs, novel mechanical valves with improved hemodynamic characteristics are needed to be developed. The blood flow mechanics of each prosthetic heart valve design, will determine PHV's performance. For example, in the ball in cage model, presence of a low-velocity recirculating blood flow with high shear stress downstream of the cage's apex, which extends throughout the forward blood flow, has been identified. The turbulent shear stress in this region is high enough to activate platelets and trap them inside the recirculating blood flow, which in turn promotes platelet-platelet contacts and leads to thrombose formation at the apex region (Chandran et al., 1985; Wurzinger et al., 1985). As for the tilting-disc PHVs, two blood flows with different velocities emerge from the large and small orifices. Mixing of these two flow jets leads to generation of a major recirculating turbulent blood flow with high shear stress in the sinus region (Chandran et al., 1983). As mentioned before, presence of such turbulent flows promote platelet activation and blood cell damage. In bileaflet valves, turbulent blood flow with high shear stress generates due to high velocity gradient between the flow jets emerging from lateral and central orifices (Chandran et al., 2012). In addition to mentioned turbulent flows, blood leakage and regurgitating flow generation during valve closure, is also common in PHVs, in the locations of the gaps between the leaflets and at disk peripheries or in the hinge region. These regurgitating blood flows can enhance blood cell damage. Trileaflet valve's hemodynamics closely resemble the native trileaflet aortic valve. However, incomplete closure of the leaflets during valve closure phase may lead to regurgitation (Leo et al., 2005, 2006).

In an interesting study by Yousefi et al. (2017), effect of leaflet's geometry on PHV's performance and hemodynamic features is investigated. They studied two geometric parameters including stent profile and leaflet arch length in six valve models (**Figure 2B**). They used different height to diameter rations (0.6, 0.7, and 0.88) and three arch heights to stent diameter ratios (0, 0.081, and 0.116) in their model designs. They found out that higher stent profile and presence of arches, reduce regurgitating flow generation, peak systole downstream velocity, subsequent shear stress and prevents loss of energy due to earlier reattachment of the forward blood flow (Yousefi et al., 2017).

In a recent breakthrough, Hofferberth, and colleagues at the Harvard University introduced a geometrically adaptable bileaflet valve for children with congenital VHD, who need valve replacement. As mentioned earlier, currently the outcome of valve replacement in young children is not promising, since the patient will continually outgrow the replaced valve and need a new one. Since all the available prosthetic valves have fixed sizes and lack remodeling ability, developing novel PHVs with growth-accommodating ability is of particular importance. This group of researchers developed a biomimetic balloon-expandable PHV with adjustable size inspired from native human venous valves. They studied the performance and functionality of this new prosthetic valve via *in vivo* experiments in juvenile and adult ships, and used computational simulations to assess its stress-strain profile under physiological conditions. Three main geometrical factors were considered in the design of their prototypes including leaflet's geometry, leaflets attachment and valve expansion geometries. A key parameter in geometrical consideration of their concept design was to fix the length of leaflet attachment, so that upon radial expansion, the valve's height reduces. As a result, the valve shortens upon increasing the opening diameter, which fulfills valve coaptation without the need to increase leaflet's surface. Expandable polytetrafluoroethylene (ePTFE) was used to fabricate the leaflets of the prototype, which were sewed to a stent made from stainless steel (**Figure 3**). *In vitro* experiments are performed in pediatric-specific hemodynamic conditions. In addition, they conducted computational modeling to study

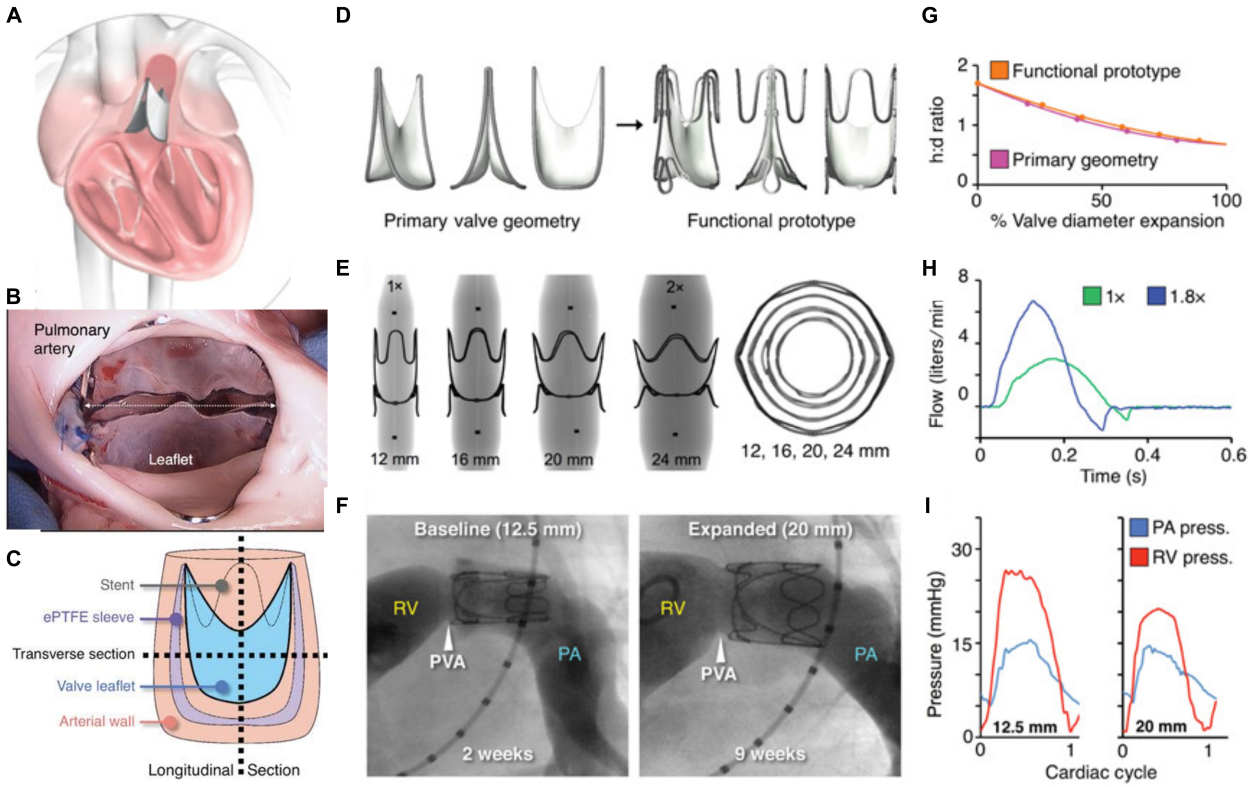

FIGURE 3 | Expandable polytetrafluoroethylene (ePTFE) was used to fabricate the leaflets of the prototype, which were sewed to a stent made from stainless steel. **(A)** An arterial valve based on ePTFE located in the heart. **(B)** Photograph of implanted valve's outflow surface. **(C)** The method of device sectioning after performing plastic embedding. **(D–F)** Valve expansion geometry for the primary valve geometry, X-ray images of laser-cut stainless steel functional valve prototypes being expanded via serial balloon dilation and representative right ventricular angiograms in a lamb. **(G–I)** Valve expansion geometry for the primary valve geometry and functional prototype, *in vitro* flow loop testing of functional prototype at two polar expansion states, and representative right ventricular and pulmonary artery pressures recorded at two states of valve expansion. Reprinted with permission from Hofferberth et al. (2020). Copyright (2020), American Association for the advancement of Science.

the stress-strain profile of the prototypes under physiological condition. Their results validated valve performance and durability. The adjustable dimensions of this valve allows it to be implanted at any age. Although, they used ePTFE for fabricating valve leaflets, the authors conclude that more research is needed to confirm that ePTFE is the ideal biomaterial for this purpose (Hofferberth et al., 2020).

Material selection is of great importance in designing the heart valves, since the biocompatibility and durability of the fabricated valves directly relates to the material's performance in biological conditions. Selected polymers should possess proper affinity for endothelial cells attachment as well (**Table 2**; Kidane et al., 2009; Zarrintaj et al., 2018). Surface topology and chemical/physical features—including stiffness and hydrophilicity/hydrophobicity—determine the polymer's biological response in the body's physiological environment. As mentioned above, surface modification is a favorable technique to improve the surface interactions with biological milieu without deteriorating the bulk features. For example, plasma treatment, peptide conjugation, and cholesterol modifications have been shown to improve cellular attachment and activity. Such modifications can also enhance the endothelialization process, which is essential for reducing the immune responses and enhancing blood compatibility (**Table 3**).

Bio-Prosthetic Heart Valves (BPHVs)

Unlike PHVs, bio-prosthetic heart valves (or tissue valves), which are made partly or entirely from biological materials (derived from humans or animals), show good hemodynamic characteristics without necessary lifetime anticoagulation treatments. Natural biomaterials in BPHVs generally consist of ECM components or decellularized tissues such as arterial wall, pericardium, heart valve or small intestinal sub-mucosa (Schmidt and Baier, 2000; Hodde, 2002).

BPHVs can be classified as autografts (harvested from, and implanted into the same person), homografts or allografts (human heart valves removed post mortem), and xenografts. The Ross procedure (Switch procedure) is the autograft replacement of faulty aortic valve with patient's own pulmonary valve. The pulmonary valve is then replaced with a homograft cadaveric pulmonary valve. This procedure was first introduced in 1967 and has been performed on young patients and children since (Ross, 1967). This durable BPHV will grow simultaneously with the patient's heart, however, the procedure is complex and

TABLE 2 | Different types of polymeric valves.

Polymer	Properties	Disadvantage(s)	Performance	References
PU	Good viscoelasticity	Rapid hydrolysis	Calcium deposition and biodegradation hinders its performance	Simmons et al., 2004
PEU	Resistance to hydrolysis	Susceptibility to oxidation		Christenson et al., 2004
PCU	Resistance to oxidation and hydrolysis	Susceptibility to calcification		Tang et al., 2001
PTFE	Good hemodynamics	Possible occurrence of thromboembolism, low resistance and high calcification and stiffening	Major complications	Nistal et al., 1990
Silicone	Good flexibility and biocompatibility	Low durability, distorted and thickened leaflets, tearing, thrombosis formation	Structural failure and impaired hemodynamic performance	Kiraly et al., 1982
PVA	Proper mechanical features	Not appropriate for dip-casting	Low elasticity	Jiang et al., 2004
PS-PIB-PS	High resistance to hydrolysis and oxidation	Platelet activation and thrombogenicity	Proper bio-stability	Gallocher et al., 2006
PDMS–PHMO PU	Proper mechanical properties; proper resistance to calcification and oxidation	Difficult processing	Proper bio-stability	Dabagh et al., 2005
POSS–PCU Nanocomposite	Proper resistance to oxidation, hydrolysis and calcification; high biocompatibility; anti-thrombogenicity		High bio-stability	Kannan et al., 2005

PU, Polyurethane; PEU, polyether urethane; PCU, polycarbonate-urethane; PTEE, polytetrafluoroethylene; PVA, polyvinyl alcohol; PS-PIB-PS, poly (styrene–b–isobutylene–b–styrene); PDMS–PHMO PU, poly (dimethylsiloxane)/poly (hexamethylene oxide)-based polyurethane; POSS–PCU, polyhedral oligomeric silsesquioxane poly (carbonate-urea) urethane.

TABLE 3 | Modifications of polymeric valves.

Modification	Advantages	Comments	References
HEBP-bounded PU	Enhances resistivity to calcification	HEBP is used as an anti-calcification agents	Lamba, 2017
Cholesterol-modified PU	Improves endothelial cell adhesion	Enhances self-endothelialization by increasing cell affinity, decreases thrombosis formation and enzymatic degradation	Bergmeister et al., 2015
Fiber-reinforced SIBS	Ameliorates hemocompatibility	Improves mechanical features, stability and hemocompatibility	Hossainy et al., 2015
RGD incorporation	Promotes endothelial cell adhesion	Improves cell adhesion and endothelialization and hemocompatibility	Danilucci et al., 2019
PIII	Adjusts surface hydrophobicity	Enhances biocompatibility, weakens foreign body response	Chudinov et al., 2019
Nanotopographic surface	Enhances cellular activity	Might improve cell adhesion, growth, proliferation and differentiation	Zarrintaj et al., 2017
Incorporation of nanomaterials	Enhances mechanical features and durability	Nanoparticles can improve biocompatibility, resistance to calcification and stability	Nilforoushzadeh et al., 2018

HEBP, 2-hydroxyethane bisphosphonic acid; PU, polyurethane; SIBS, Styrene Isoprene Butadiene; RGD, a tripeptide containing arginine, glycine and aspartic acid; PIII, Plasma immersion ion implantation.

careful and proper young adult patient selection is necessary (Schaff, 2016). The growing shortage of available cardiac valves for transplantation has turned xenograft valves into valuable alternatives. Xenograft valves provide an unlimited source of valves prosthesis with different sizes, shapes, and anatomical configurations. Pericardial and porcine valves, made of cow's pericardium and porcine aortic valve, respectively, are the most common types of xenograft BPHVs. The first successful xenograft valve transplant into a human was performed in 1965 (Binet et al., 1965). However, early attempts were accompanied with high rate of valve failure (nearly 60% failure in 1 year following the transplant), mainly due to host's acute immune responses to xenograft tissue (Carpentier et al., 1969).

Different steps have been taken in order to increase xenograft valve's stability and biocompatibility including; soluble protein removal by washing or electrolysis, sodium periodate denaturation of structural glycoproteins and mucopolysaccharides, neutralization by ethylene glycol and

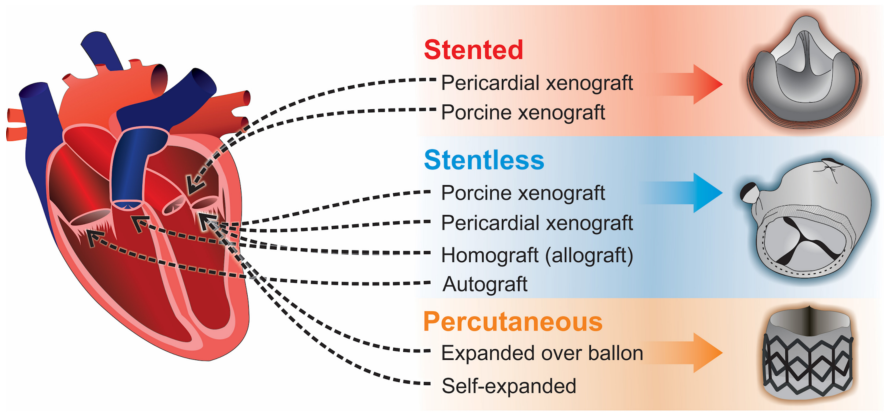

FIGURE 4 | Three types of bioprosthetic valve replacements: stented, stentless, and percutaneous.

finally, glutaraldehyde treatment for cross-linking the remaining free amino groups of amino acids. Glutaraldehyde treatment is the most effective step in preserving and reducing the antigenicity of xenograft tissues (Manji et al., 2015). Despite increased functionality, biocompatibility, and mechanical strength of xenograft valves following glutaraldehyde fixation, occurrence of structural valvular deterioration (SVD) is still another major drawback (Manji et al., 2015). SVD is the result of host's immune response to glutaraldehyde-treated tissue and subsequent calcification leading to valvular stenosis or regurgitation and eventual failure (Carpentier, 1989; Schoen and Levy, 2005; Manji et al., 2006). The rate of SVD occurrence is age dependent and is significantly higher in younger patients, mainly due to their robust immune system activity (Siddiqui et al., 2009) and accelerated rate of calcium metabolism (Simionescu, 2004). Nevertheless, glutaraldehyde-fixed BPHVs have limited durability of up to 15–20 years (Simionescu, 2004). Manufacturers have used different combinations of calcification-preventive agents in order to reduce SVD occurrence, including sodium dodecyl sulfate (SDS), α-amino oleic acid, toluidine blue by Medtronic (Minneapolis, MN, United States), ethanol by Epic (St. Jude Medical, Minneapolis, MN, United States) and ethanol with Tween-80 by Edwards Lifesciences Corporation, Santa Ana, CA, United States) (Simionescu, 2004).

Glutaraldehyde toxicity toward residual cells in xenograft valves is also associated with SVD, since dead resident cells cannot be removed from the tissue. These cells are not able to maintain calcium hemostasis and can initiate calcium nucleation leading to eventual SVD (Schoen and Levy, 2005).

Another issue that greatly affects BPHV's durability is the expression of different antigenic epitopes (including α-Gal) in xenograft valves. The α-Gal epitope is not presented in the human body but it is preserved in non-primate mammals. However, the anti-Gal antibody constitutes 1% of immunoglobulins in the human body and is responsible for anti-gal reactivity and early rejection of xenograft BPHVs (Huai et al., 2016). Glutaraldehyde's efficiency in inactivating or masking these epitopes is essential for successful BPHV preparation for clinical applications (Konakci et al., 2005). Naso et al. (2013) performed a quantitative evaluation of the number of α-Gal epitopes on seven commercially available glutaraldehyde-treated models of BPHVs. According to their results, the Epic valve was the only tested model that had completely masked α-Gal epitopes (Naso et al., 2013). They also suggested that α-Gal ELISA test can be applied as a quality control step for commercially available BPHVs. Decellularized tissues have also been prepared to minimize the possibility of immune rejection to xenograft valves. Decellularization mainly preserves ECM components to serve as a supporting scaffold in the process of damaged tissue repair (Byrne and Mcgregor, 2012). Decellularized tissues (such as decellularized aorta) brings major advantages including regeneration ability, ideal functional properties and biocompatibility (Wu et al., 2015).

More recently, the use of genetically modified animals expressing low levels of α-Gal epitopes have attracted researcher's attention (Zeyland et al., 2014; Hryhorowicz et al., 2017). In this regard, Rahmani et al. (2019) have recently introduced a novel glutaraldehyde-fixed porcine pericardial BPHV obtained from transgenic pigs which showed excellent *in vitro* durability.

Three types of BPHV replacements exist: stented, stentless, and percutaneous (**Figure 4**). Stented BPHVs are generally made from glutaraldehyde-treated bovine pericardium or porcine aortic valve tissue sutured on a stent (polymeric or metal). Until early 2000s, bovine pericardium or porcine aortic valve tissue were the only options for fabrication of BPHVs. At that time, percutaneous transcatheter aortic valve implantation (TAVI) using equine pericardium as the biomaterial of valve leaflets, was introduced (Cribier et al., 2002). The first stented BPHV was developed in 1970s from glutaraldehyde-fixed bovine pericardium sewed on a flexible stent for obtaining a synchronous opening of the leaflets (Bartek et al., 1974). However, early SVD due to leaflet tearing within the stent was observed. Later BPHVs utilized thinner and more flexible stents in order to reduce valvular stress, allowing implantation of larger BPHVs. Patient-prosthesis mismatch (PPM) (due to small valvular effective orifice area) as well as stent-induced turbulent flow through the valve are important issues of current clinical practice. PPM puts patients at higher risks of postoperative mortality. Different modifications

in stent architecture were proposed in order to overcome these problem, which eventually lead to development of stentless BPHVs in 1988 (David et al., 1988). Stentless BPHVs are made of porcine and bovine tissues without being sewed to a stent. They provide larger orifice area and reduced dimensions, both of which significantly affecting PPM. However, while the implantation of stented BPHVs is easier, especially through the small aortic root, surgical implantation of stentless valves is more difficult and time-consuming. In a recent study by Schaefer and colleagues, superior hemodynamic characteristics of stentless aortic valves in comparison to a stented aortic valve was confirmed, however, the rate of SVD occurrence and subsequent endocarditis was higher in patients who received stentless valves (Schaefer et al., 2018).

Percutaneous or trans-catheter valve replacement is the most advanced alternative approach to open heart surgery for patients with high risk of complications. Transcatheter endovascular delivery of BPHVs requires the BPHV to be crimped, which reduces its dimensions to up to 3-fold without rupturing the leaflets. Throughout these years, different issues have been reported that can potentially limit the application of percutaneous valves including paravalvular leakage, vascular, and neurological complications as well as complete atrioventricular blockage. The development of first percutaneous valve dates back to 1965, which was an umbrella-shaped valve placed on a catheter that was implanted into a dog (Andersen, 2009). An early percutaneous heart valve model was fabricated with a construct of folded wires to accommodate the valve. The prepared construct was then folded into a balloon shaped dilation catheter (Andersen et al., 1992). The next designed percutaneous valve was based on the ball and cage model (Pavcnik et al., 1992). After that, a platinum-iridium balloon-based stent was introduced by Boudjemline and Bonhoeffer (2002). Professor Alain Cribier performed the first percutaneous valve implantation in a human in 2002 (Cribier et al., 2002). Cribier valve was made of equine pericardium with a frame made of stainless steel. Introduction of a polyethylene terephthalate fabric cover to this percutaneous valve lead to development of the first Edwards SAPIEN valve model.

Based on a study published in 2009, aortic valve stent devices fabricated from stainless steel, cobalt chromium, nickel and titanium for percutaneous implantation, were characterized and evaluated by finite element analysis technique to assess the effect of biomaterial properties on stent performance under high blood pressure conditions. Their results indicated that titanium had the greatest impact on device performance, with maximum displacement and minimum stress levels (Kumar and Mathew, 2009).

Prosthetic vs. Bio-Prosthetic Heart Valve Replacement

Current guidelines recommend using of MHVs for younger patients (<50 years of age) and BPHVs in patients over 70 years of age, and either type of these prosthetic valves can be used for patients in the range of 50–70 years old (Nishimura et al., 2017). The choice of valvular prosthesis is often made by evaluating the risk of re-operation and hemorrhage. In a recent study, Goldstone and colleagues evaluated the long-term post-operational complications including stroke, hemorrhage and mortality rate, in patients with severe valvular disease who underwent MHV or BPHV replacement, between 1996 and 2013 (Goldstone et al., 2017). According to their results, the risk of re-operation and mortality rate of patients who received MHVs was lower than those who received BPHVs. However, MHVs were associated with higher risk of hemorrhage and stroke. Similar results have been reported by Glaser et al. showing higher rate of long-term survival in patients who received MHVs than those who received BPHVs (Glaser et al., 2016). Other than that, several studies have reported higher risk of re-operation in patients aged 50–69 with BPHVs (Hammermeister et al., 2000; Oxenham et al., 2003; Chiang et al., 2014) which is mainly due to SVD and valve failure. Since valvular deterioration leading to re-operation limits the durability of BPHVs, this prosthesis is more suitable for older patients. Children will outgrow MHVs due to absent remodeling and will need re-operation. Younger patients can benefit more from BPHVs or TEHVs. Despite limited durability of BPHVs, application of these valve has increased compared to MHVs in older patients over the past few years, especially since the introduction of percutaneous transcatheter valve replacement. This approach is an excellent alternative for high-risk patients with similar safety outcomes as those of open-heart surgery (Makkar et al., 2020).

Children and young adults are not good candidates for mechanical heart valve replacement since they are at risk of complications due to long-term consumption of anti-coagulation medications and lack of implanted valve remodeling. On the other hand, they cannot fully benefit from advantages of BPHVs as well, due to early occurrence of SVD. Taken together, these patients are in need of suitable valvular prosthesis and extensive research in this area seems mandatory. α-Gal-free porcine pericardium obtained from transgenic pigs seems to be a promising biomaterial for increasing the durability of BPHVs, especially in younger patients. It should be noted that α-Gal is not the only antigenic epitope that can trigger immune responses in the recipient patients and evaluation of other xenogeneic antigenic epitopes might be essential for quality control assessment of BPHVs.

Tissue-Engineered Heart Valves (TEHVs)

The ideal approach in valve replacement is to provide a viable valve capable of self-regeneration and growth, with greater life span and better biocompatibility. Tissue engineering, which is the use of biomaterials and engineering in combination with cells, offers a new generation of cardiac valves aiming to overcome the shortcomings of existing biological and mechanical heart valves (Rippel et al., 2012). To achieve this goal, different natural and synthetic biomaterials are investigated for fabrication of tissue-engineered heart valves (TEHV).

Two strategies for fabricating TEHVs include: *in vitro* and *in situ* valve heart tissue engineering (**Figure 5**). The *in vitro* approach is based on the *ex vivo* formation of TEHV, which includes harvesting of autologous cells from the patient, cell seeding on a 3D scaffold, *in vitro* tissue generation and finally, implantation of the generated tissue into the same patient.

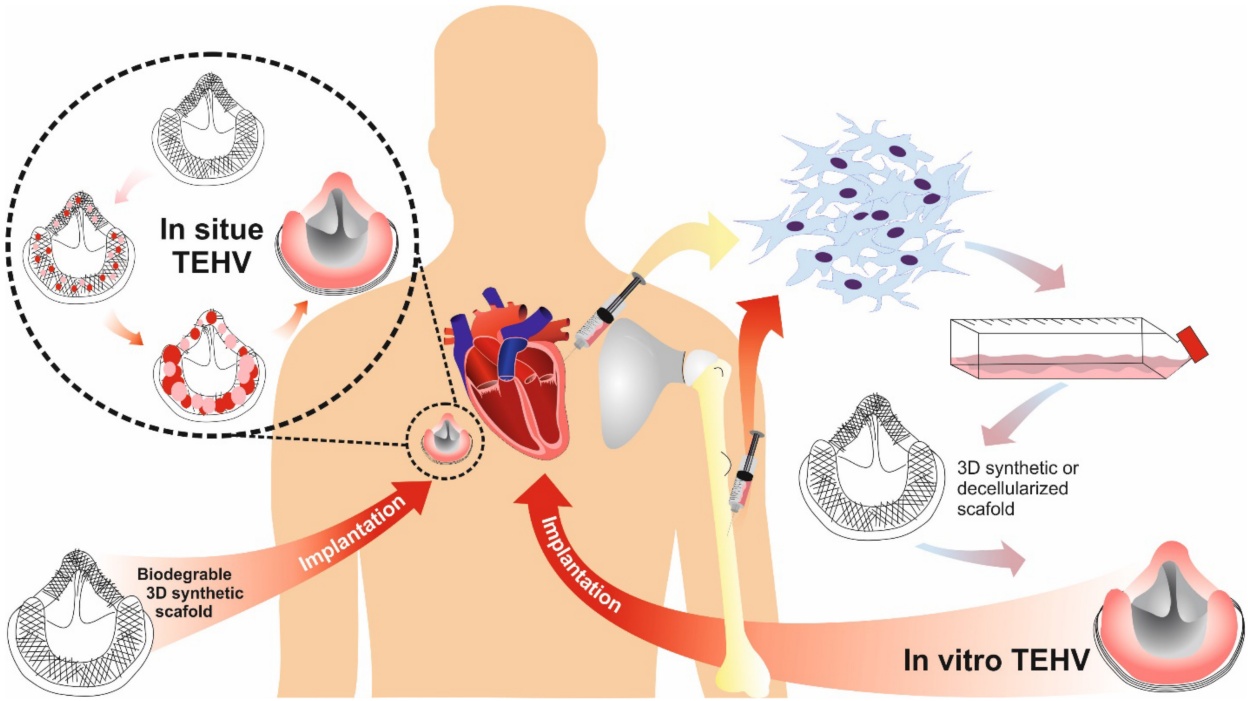

FIGURE 5 | TEHV approaches comparison: *in situ* vs. *in vitro*.

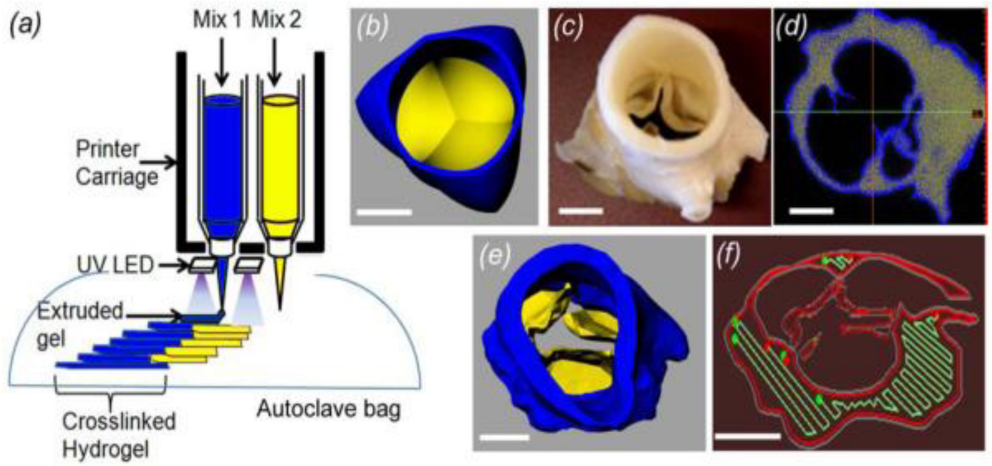

FIGURE 6 | An engineered heterogeneous valve scaffold with poly-ethylene glycol-diacrylate (PEG-DA) hydrogels/alginate, supplemented with porcine aortic valve interstitial cells (PAVIC) by 3D-printing/photocrosslinking technique **(a)** 3D Printer setup of heterogeneous valve scaffolds. **(b–f)** Axisymmetric valve STL file of valve, micro-CT scan of aortic valve, the leaflet and root regions, the printable STL geometries of the threshold regions and the printing software sliced the geometries into layers and generated extrusion paths for each layer. Reprinted with permission from Hockaday et al. (2012). Copyright (2012), IOP science Publishing Ltd.

Hockaday et al. (2012) introduced an engineered heterogeneous valve scaffold made from poly-ethylene-glycol-diacrylate (PEG-DA) hydrogel and alginate, supplemented with porcine aortic valve interstitial cells (PAVIC), fabricated by 3D-printing/photo-crosslinking technique (**Figure 6**). Their results demonstrated that this 3D scaffold supports cell engraftment and provides acceptable dynamics and mechanical heterogeneity (Hockaday et al., 2012). The *in situ* approach, on the other hand, involves using biological or polymeric heart valve scaffolds, which are seeded with patient's autologous cells and upon implantation undergo subsequent cell attraction and tissue remodeling (Weber et al., 2012).

As mentioned earlier, endothelial and interstitial cells are responsible for forming and maintaining valvular integrity (Brody and Pandit, 2007). Since VECs show anti-thrombogenic properties, they are being used for surface cell lining, while VICs

produce ECM components (Hoerstrup et al., 2000). Currently, patient-derived endothelial and interstitial cells are the main cell sources for TEHVs fabrication. The cell isolation process involves sacrificing healthy donor vascular tissues, while the isolated cell's function could also be affected by risk factors including diabetes or atherosclerosis (De Vriese et al., 2000). To avoid these complications, stem cells from different sources are available, including non-hematopoietic bone marrow-derived stem cells (mesenchymal and mononuclear stem cells) (Hoerstrup et al., 2002; Sutherland et al., 2005; Schmidt et al., 2010; Weber et al., 2011), blood-derived endothelial progenitor cells (Schmidt et al., 2010), mesenchymal stem cells derived from adipose tissue (Colazzo et al., 2010), amniotic fluid (Schmidt et al., 2007), chorionic villi (Schmidt et al., 2006a) and the umbilical cord (Schmidt et al., 2006b; Sodian et al., 2010).

The scaffold provides a 3D structure for cellular attachment and tissue growth. Structural characteristics of the scaffold (including pore size, surface biochemistry and topology, biocompatibility and biodegradation as well as mechanical strength) can pre-determine TEHV's performance (Nie et al., 2014). In general, two types of scaffolds exist for fabrication of TEHVs including decellularized ECM and synthetic biomaterials. Decellularized scaffolds are the most promising choices for TEHV fabrication, which can have allogeneic and xenogeneic sources or be tissue-engineered with intact ECM. Shortage of decellularized allogeneic valves limits their availability. In this regard, decellularized xenogeneic valves are the best alternatives. In hybrid scaffolds, an inorganic mesh with high mechanical resistance is exposed to valvular tissues. Loger et al. designed a 3D Nickle-Titanium (NiTi) hybrid scaffold for engineering thin, durable, and efficient valve leaflets for transcatheter implantation. Their fabrication process involved magnetron sputtering, lithography, wet etching, and a final step for shape setting the scaffold. The scaffold was exposed to cardiac smooth muscle cells. The performance of fabricated leaflets was studied under pulsatile condition *in vitro* and was compared to a porcine valve as a reference. Their results showed higher effective opening area, lower systolic transvalvular pressure due to increased cardiac output and low flow resistance. They suggest further design optimization with increased duration of cell seeding process as well as addition of cardiac fibroblasts and VECs could improve the durability of their NiTi thin film leaflets (Loger et al., 2016; **Figure 2A**).

Different techniques used for decellularization can be classified as physical, chemical (or enzymatic) or the combination of both. Each technique consists of the following steps: cell lysis and removal, genetic material removal (for lowering the immunogenicity) and preserving the composition and structure of the ECM (Gilpin and Yang, 2017). Chemical decellularization is usually performed by using surfactants (SDS and TritonX-100, Tween 20, TnBP, CHAPS), acids, bases, and enzymes (pancreatin and trypsin) (Nie et al., 2014). Despite their wide application, toxicity of these chemical agents, as well as damage to the structural proteins of the EMC are concerning. Physical techniques including freeze-thaw, ultrasonication, high hydrodynamic pressure (HHP) and supercritical carbon dioxide (CO_2) treatment are alternative approaches. Due to specific advantages and disadvantages of each technique, combinatorial treatments may be performed in order to achieve the best results. For example, physical approaches are more successful in maintaining intact ECM, while they are unable to eliminate tissue's immunogenicity. Chemical approaches on the other hand are not ideal for removing cellular debris. Combining these two approaches can yield an intact ECM with no debris. Ramm and colleagues in 2019 studied decellularized porcine pulmonary heart valves (dpPHVs), implanted in sheep. They used nine different techniques for generation of these dpPHVs. They evaluated the amount of residual SDS as well as DNA, GAGs and hydroxyproline content of dpPHVs and observed that addition of trypsin to Triton X-100 in the decellularization process results in efficient removal of cellular debris, while preserving the ECM. Trypsin- and Triton X-100-treated pdPHV's performance was comparable to allogeneic decellularized valves. For DNA and N-linked glycans removal, they observed that the combination of PNGase F and DNase I with Triton X-100 and SDS improved the efficacy. However, the combination of trypsin and Triton X-100 resulted in lowest immunogenicity (Ramm et al., 2020). Among different chemical agents used for decellularization, SDS is more common, since it can almost completely remove caridac valve cells, while preserving the ECM. However, possible toxicity of these decellularized scaffolds due to leakage of the remained SDS within the valve's tissue is a matter of concern. It is reported that following several washing steps, even when small SDS concentrations are used (0.01%), SDS is still present in the tissue (Naso and Gandaglia, 2018). Another limitation in the application of SDS is insoluble elastin degradation following SDS exposure, which negatively affects ECM's tensile strength (Jordan et al., 1974).

The issue of decellularized valve's immunogenicity should also be addressed. Hyperacute, acute and chronic rejection may occur following xenogeneic decellularized tissue implantation due to presence of xenoantigens. The process of decellularization can increase tissue's immunogenicity, itself. For example, cardiovascular ECM is reach in hyaluronan (HA) polymers (Ding et al., 2019). Anti-inflammatory actions of HA provides cellular protection via inhibiting phagocytosis by macrophages, neutrophils and monocytes (Delmage et al., 1986). Despite their protective role, HA fragments (which are produced via HA filaments degradation by released proteases during the first step of decellularization), can be pro-inflammatory and lead to acute rejection of the implanted valve (Naso and Gandaglia, 2018). One of the most effective strategies for lowering decellularized tissue's immunogenicity is targeted antigen removal of well-known xenoantigens (for example; targeted removal of α-gal by α-galactosidases) (Nam et al., 2012). Unknown xenogeneic antigens removal is performed through solubilization-based techniques. This strategy is based on the fact that all tissue components need to be solubilized in order to be removed from the ECM. The solubilization-based approaches do not require identification of specific graft's antigens and are based on the xenoantigen's solubility in a common antigen removal buffer (Wong and Griffiths, 2014). Another issue regarding the safety of decellularized cardiac valves is complete removal of cell debris. Although decellularized tissue is considered the

most suitable substrate for fabrication of TEHVs, in terms of 3D structure, composition, and function, its limited availability and the risk of possible immunogenicity restrict its application (Schenke-Layland et al., 2003).

Natural polymesr including collagen, elastin (Chen et al., 2013), polyhydroxyalkanoates (PHA) (Sodian et al., 2000), polyethylene glycol (PEG) (Zhang et al., 2015), PEG-poly lactic acid (PEG-PLA) (Hinderer et al., 2014), and poly glycerol sebacate (PGS)-Polycaprolactone (PCL) (Masoumi et al., 2014), can be used as alternatives for decellularized scaffolds. One of the main challenges of long-term application of polymer-based 3D scaffolds is calcification or tearing. Several strategies have been used to prevent calcification, including local administration of bisphosphonates (Levy et al., 1985; Golomb et al., 1986, 1987), bisphosphonate-bound PUs (Alferiev et al., 2001) and ethanol pre-treatment of glutaraldehyde cross-linked bio-prosthetic heart valves (Vyavahare et al., 1997).

Ozaki et al. (2011) introduced a novel aortic valve repair procedure using glutaraldehyde-treated autologous pericardium, which could be an alternative for aortic valve replacement in older patients who are candidate for aortic valve replacement. As mentioned earlier, bioprosthetic valve transplantation is the preferred option for older patients, and valve repair is not routinely performed in these cases. Since the performance of biological valves is far from ideal, repairing patient's own aortic valve becomes an interesting alternative. In Ozaki procedure, patient's pericardium is harvested and treated with glutaraldehyde prior to be trimmed based on the measured value of the distance between each commissures. Treatment with glutaraldehyde can increase pericardium's resistance and maintain tissue's intrinsic elasticity. Trimmed glutaraldehyde-treated autologous pericardium is sewed into the native aortic valve's annulus and root, following removal of the diseased valve leaflets. The Ozaki procedure is applicable to different types of aortic valve diseases and can be performed by using bovine or patient's own pericardium (Ozaki et al., 2011). Although this procedure was primarily developed for treatment of aortic valve diseases in older patients, it has now become an attractive strategy for children with congenital valve disease since the new valve leaflets can expand along with patient's heart growth.

Once the scaffold is ready and seeded, the new construct is placed inside a bioreactor in order to get adapted to the physiological biochemical and mechanical conditions. This process prepares the TEHV for implantation into the patient's body. Bioreactors may also be used to study cellular functionality, cell-cell and cell-ECM interactions as well as cellular responses to physiological conditions of the valve prior to implantation. Various bioreactor designs have been developed for this purpose including cell-stretching bioreactors (Engelmayr et al., 2008; Syedain and Tranquillo, 2009), dynamic flexure bioreactors (Engelmayr et al., 2003), and flow bioreactors (Jockenhoevel et al., 2002; Ramaswamy et al., 2014). In addition, different commercial models of bioreactors are also available. By studying cellular and ECM responses to the physiological conditions of the target valve's environment in the human heart prior to TEHV implantation, a wealth of information would be obtained, which could be very useful in choosing the proper cell types and biomaterials.

FUTURE CHALLENGES AND DIRECTIONS

Despite numerous attempts over the past decades in the area of design and development of biomaterial-based cardiac valves, this task remains extremely challenging. This is partly due to the difficulty of replicating biomechanical features of native heart valves, since cardiac valves are not merely passive systems and undergo constant on-demand adjustment and remodeling. One of the main purposes of studying valve biomechanics is to understand the mechanisms by which the biomechanical forces are transmitted to valvular cells and the ECM. This can be achieved by using mathematical modeling and computer simulations. The level of complexity of valvular micro and macrostructure should be considered in material selection for prosthetic heart valves. In this regard, more research toward better understanding of valvular biomechanics via accurate simulations and mathematical modeling can lead to significant advancements in the performance of designed valves. This task requires a thorough understanding of the biomechanics of healthy and diseased valvular tissue, and with help of state-of-the-art techniques (such as nanotechnology), biomaterials with adjustable characteristics can be obtained.

Both medical professionals and researchers strive to provide durable hemocompatible, anticoagulant-independent and thrombus-free heart valves with the ability of remodeling. While these attempts are not far from becoming the standard routine in clinical practice, novel biomaterials with adjustable properties and mechanized industrial processing techniques are currently under research, since biomaterial's properties, cost and availability are among the most important determining factors in material selection for biomaterial-based valve prosthesis.

Biomaterials have shown great potential in management of CVD. Biocompatibility and biodegradation rates of most common biomaterials have been widely studied by various research groups. The optimum biomaterial-based heart valve should possess combined advantages of MHVs and BPHVs. It seems that the future of biomaterials-based CVD management is headed toward TEHVs. However, the optimum combination of cells and biomaterials for promotion of tissue regeneration is yet to be identified.

Another concern that needs to be addressed, is minimizing the immunogenicity of applied biomaterials or tissue constructs, as they may trigger immune responses which have negative impact on their efficacy and performance.

Despite these challenges, research in the field of biomaterials and tissue engineering for CVD treatment has achieved significant progress. However, the gold standard approach would provide the ability of using biomaterial scaffolds in combination with suitable cell types with good functionality, biocompatibility, and durability, with the aim of providing partial or whole heart regenerational capacity. Achieving this goal will ultimately eliminate the need for heart transplant in patients with heart

failure, manage disease states in which irreversible functional loss has occurred and result in improved patient's quality of life.

AUTHOR CONTRIBUTIONS

ZI, LT, and HD performed the main conceptual ideas and proof outline. BT, HD, and LG wrote the manuscript with support MR, MJ, and PZ. NZ, MJ, MM, and ZI designed the figures. LT supervised the manuscript and final approval of the version to be published. All authors contributed to the article and approved the submitted version.

FUNDING

This research has been financially supported by Kermanshah University of Medical Sciences (KUMS).

REFERENCES

Aagaard, J. (2004). The carbomedics aortic heart valve prosthesis: a review. *J. Cardiovasc. Surg.* 45, 531–534.

Akins, R. J. (1979). Nickel-Titanium Alloy, Heart Valve. Prosthetic device couplings, 4233690A.

Alferiev, I., Vyavahare, N., Song, C., Connolly, J., Hinson, J. T., Lu, Z., et al. (2001). Bisphosphonate derivatized polyurethanes resist calcification. *Biomaterials* 22, 2683–2693. doi: 10.1016/S0142-9612(01)00010-2

Alves, P., Cardoso, R., Correia, T. R., Antunes, B. P., Correia, I. J., and Ferreira, P. (2014). Surface modification of polyurethane films by plasma and ultraviolet light to improve haemocompatibility for artificial heart valves. *Colloids Surf. B Biointerfaces* 113, 25–32. doi: 10.1016/j.colsurfb.2013.08.039

Andersen, H. R. (2009). History of percutaneous aortic valve prosthesis. *Herz* 34, 343–346. doi: 10.1007/s00059-009-3251-4

Andersen, H. R., Knudsen, L. L., and Hasenkam, J. M. (1992). Transluminal implantation of artificial heart valves. Description of a new expandable aortic valve and initial results with implantation by catheter technique in closed chest pigs. *Eur. Heart J.* 13, 704–708. doi: 10.1093/oxfordjournals.eurheartj.a060238

Balachandran, K., Sucosky, P., and Yoganathan, A. P. (2011). Hemodynamics and mechanobiology of aortic valve inflammation and calcification. *Int. J. Inflam.* 2011:263870. doi: 10.4061/2011/263870

Bartek, I. T., Holden, M. P., and Ionescu, M. I. (1974). Frame-mounted tissue heart valves: technique of construction. *Thorax* 29, 51–55. doi: 10.1136/thx.29.1.51

Benjamin, E. J., Muntner, P., Alonso, A., Bittencourt, M. S., Callaway, C. W., Carson, A. P., et al. (2019). Heart disease and stroke statistics-2019 update: a report from the american heart association. *Circulation* 139:e0056-8. doi: 10.1161/CIR.0000000000000659

Bergmeister, H., Seyidova, N., Schreiber, C., Strobl, M., Grasl, C., Walter, I., et al. (2015). Biodegradable, thermoplastic polyurethane grafts for small diameter vascular replacements. *Acta Biomater.* 11, 104–113. doi: 10.1016/j.actbio.2014.09.003

Bernacca, G., Mackay, T., Wilkinson, R., and Wheatley, D. (1995). Calcification and fatigue failure in a polyurethane heart valve. *Biomaterials* 16, 279–285. doi: 10.1016/0142-9612(95)93255-C

Bernacca, G. M., Mackay, T. G., Gulbransen, M. J., Donn, A. W., and Wheatley, D. J. (1997a). Polyurethane heart valve durability: effects of leaflet thickness and material. *Int. J. Artif. Organs* 20, 327–331. doi: 10.1177/039139889702000606

Bernacca, G. M., Mackay, T. G., Wilkinson, R., and Wheatley, D. J. (1997b). Polyurethane heart valves: fatigue failure, classification, and polyurethane structure. *J. Biomed. Mater. Res.* 34, 371-379 doi: 10.1002/(SICI)1097-4636(19970305)34:3<371::AID-JBM12>3.0.CO;2-J

Bernacca, G. M., O'connor, B., Williams, D. F., and Wheatley, D. J. (2002a). Hydrodynamic function of polyurethane prosthetic heart valves: influences of Young's modulus and leaflet thickness. *Biomaterials* 23, 45–50. doi: 10.1016/S0142-9612(01)00077-1

Bernacca, G. M., Straub, I., and Wheatley, D. J. (2002b). Mechanical and morphological study of biostable polyurethane heart valve leaflets explanted from sheep. *J. Biomed. Mater. Res. Part A* 61, 138–145. doi: 10.1002/jbm.10149

Bernacca, G. M., and Wheatley, D. J. (1998). Surface modification of polyurethane heart valves: effects on fatigue life and calcification. *Int. J. Artif. Organs* 21, 814–819. doi: 10.1177/039139889802101202

Binet, J. P., Carpentier, A., Langlois, J., Duran, C., and Colvez, P. (1965). [Implantation of heterogenic valves in the treatment of aortic cardiopathies]. *C.R Acad. Hebd. Seances Acad. Sci. D* 261, 5733–5734.

Björk, V. O. (1972). The pyrolytic carbon occluder for the Björk-Shiley tilting disc valve prosthesis. *Scand. J. Thorac. Cardiovasc. Surg.* 6, 109–113. doi: 10.3109/14017437209134787

Bjork, V. O. (1981). Advantages and long term results of the Bjork-Shiley valve. *Verh. Dtsch. Ges. Inn. Med.* 87, 1365–1367.

Bokros, J. C. (1989). Carbon in prosthetic heart valves. *Ann. Thorac. Surg.* 48, S49-S50. doi: 10.1016/0003-4975(89)90635-8

Borer, J. S., Isom, O. W., and Diseases, C. U. H. G. I. V. H. (2004). *Pathophysiology, Evaluation and Management of Valvular Heart Diseases*. Basel: Karger. doi: 10.1159/isbn.978-3-318-01063-3

Boretos, J. W., Pierce, W. S., Baier, R. E., Leroy, A. F., and Donachy, H. J. (1975). Surface and bulk characteristics of a polyether urethane for artificial hearts. *J. Biomed. Mater. Res. Part A* 9, 327–340. doi: 10.1002/jbm.820090308

Boudjemline, Y., and Bonhoeffer, P. (2002). Percutaneous implantation of a valve in the descending aorta in lambs. *Eur. Heart J.* 23, 1045–1049. doi: 10.1053/euhj.2001.3076

Brand, N. J., Roy, A., Hoare, G., Chester, A., and Yacoub, M. H. (2006). Cultured interstitial cells from human heart valves express both specific skeletal muscle and non-muscle markers. *Int. J. Biochem. Cell Biol.* 38, 30–42. doi: 10.1016/j.biocel.2005.06.018

Braunwald, N. S., Cooper, T., and Morrow, A. G. (1960). Complete replacement of the mitral valve. Successful clinical application of a flexible polyurethane prosthesis. *J. Thorac. Cardiovasc. Surg.* 40, 1–11. doi: 10.1016/S0022-5223(19)32638-8

Brinkley, D. M., and Gelfand, E. V. (2013). Valvular heart disease: classic teaching and emerging paradigms. *Am. J. Med.* 126, 1035–1042. doi: 10.1016/j.amjmed.2013.05.022

Brody, S., and Pandit, A. (2007). Approaches to heart valve tissue engineering scaffold design. *J. Biomed. Mater. Res. B Appl. Biomater.* 83, 16–43. doi: 10.1002/jbm.b.30763

Buchanan, E. S. (2005). Prosthetic heart valve with slit stent. Google Patents.

Butany, J., Ahluwalia, M. S., Fayet, C., Munroe, C., Blit, P., and Ahn, C. (2002). Hufnagel valve: the first prosthetic mechanical valve. *Cardiovasc. Pathol.* 11, 351–353. doi: 10.1016/S1054-8807(02)00132-1

Butcher, J. T., Mahler, G. J., and Hockaday, L. A. (2011). Aortic valve disease and treatment: the need for naturally engineered solutions. *Adv. Drug Deliv. Rev.* 63, 242–268. doi: 10.1016/j.addr.2011.01.008

Butcher, J. T., Tressel, S., Johnson, T., Turner, D., Sorescu, G., Jo, H., et al. (2006). Transcriptional profiles of valvular and vascular endothelial cells reveal phenotypic differences: influence of shear stress. *Arterioscler. Thromb. Vasc. Biol.* 26, 69–77. doi: 10.1161/01.ATV.0000196624.70507.0d

Byrne, G. W., and Mcgregor, C. G. (2012). Cardiac xenotransplantation: progress and challenges. *Curr. Opin. Organ Transpl.* 17, 148–154. doi: 10.1097/MOT.0b013e3283509120

Cao, H. (1996). Mechanical performance of pyrolytic carbon in prosthetic heart valve applications. *J. Heart Valve Dis.* 5(Suppl. 1), S32-S49.

Cardy, R. H. (1979). Carcinogenicity and chronic toxicity of 2,4-toluenediamine in F344 rats. *J. Natl. Cancer Inst.* 62, 1107–1116.

Carmen, R., and Kahn, P. (1968). In vitro testing of silicone rubber heart-valve poppets for lipid absorption. *J. Biomed. Mater. Res.* 2, 457-464. doi: 10.1002/jbm.820020406

Carmen, R., and Mutha, S. C. (1972). Lipid absorption by silicone heart valve poppets—in-vivo and in-vitro results. *J. Biomed. Mater. Res.* 6, 327–346. doi: 10.1002/jbm.820060504

Carpentier, A. (1989). From valvular xenograft to valvular bioprosthesis: 1965-1970. *Ann. Thorac. Surg.* 48, S73-S74. doi: 10.1016/0003-4975(89)90646-2

Carpentier, A., Lemaigre, G., Robert, L., Carpentier, S., and Dubost, C. (1969). Biological factors affecting long-term results of valvular heterografts. *J. Thorac. Cardiovasc. Surg.* 58, 467–483. doi: 10.1016/S0022-5223(19)42561-0

Chandran, K. B., Cabell, G. N., Khalighi, B., and Chen, C. J. (1983). Laser anemometry measurements of pulsatile flow past aortic valve prostheses. *J. Biomech.* 16, 865–873. doi: 10.1016/0021-9290(83)90011-8

Chandran, K. B., Khalighi, B., and Chen, C. J. (1985). Experimental study of physiological pulsatile flow past valve prostheses in a model of human aorta–I. *Caged ball valves*. *J. Biomech.* 18, 763–772. doi: 10.1016/0021-9290(85)90051-X

Chandran, K. B., Rittgers, S. E., and Yoganathan, A. P. (2012). *Biofluid Mechanics: the Human Circulation*. Boca Raton, FL: CRC press. doi: 10.1201/b11709

Chen, H.-X., Li, M.-Y., Jiang, Y.-Y., Hou, H.-T., Wang, J., Liu, X.-C., et al. (2020). Role of the PPAR pathway in atrial fibrillation associated with heart valve disease: transcriptomics and proteomics in human atrial tissue. *Signal Trans. Target. Ther.* 5:4. doi: 10.1038/s41392-019-0093-2

Chen, Q., Bruyneel, A., Carr, C., and Czernuszka, J. (2013). Bio-mechanical properties of novel Bi-layer collagen-Elastin scaffolds for heart valve tissue engineering. *Proc. Eng.* 59, 247–254. doi: 10.1016/j.proeng.2013.05.118

Chiang, Y. P., Chikwe, J., Moskowitz, A. J., Itagaki, S., Adams, D. H., and Egorova, N. N. (2014). Survival and long-term outcomes following bioprosthetic vs mechanical aortic valve replacement in patients aged 50 to 69 years. *JAMA* 312, 1323–1329. doi: 10.1001/jama.2014.12679

Chien, S., Engler, A. J., and Wang, P. Y. (2016). *Molecular and Cellular Mechanobiology*. New York, NY: Springer. doi: 10.1007/978-1-4939-5617-3

Christenson, E. M., Anderson, J. M., and Hiltner, A. (2004). Oxidative mechanisms of poly (carbonate urethane) and poly (ether urethane) biodegradation: in vivo and in vitro correlations. *J. Biomed. Mater. Res. Part A* 70, 245–255. doi: 10.1002/jbm.a.30067

Chudinov, V., Kondyurina, I., Terpugov, V., and Kondyurin, A. (2019). Weakened foreign body response to medical polyureaurethane treated by plasma immersion ion implantation. *Nucl. Instr. Methods Phys. Res. Sec. B* 440, 163–174. doi: 10.1016/j.nimb.2018.12.026

Clauser, J., Gester, K., Roggenkamp, J., Mager, I., Maas, J., Jansen, S. V., et al. (2014). Micro-structuring of polycarbonate-urethane surfaces in order to reduce platelet activation and adhesion. *J. Biomater. Sci. Polym. Ed.* 25, 504–518. doi: 10.1080/09205063.2013.879561

Colazzo, F., Chester, A. H., Taylor, P. M., and Yacoub, M. H. (2010). Induction of mesenchymal to endothelial transformation of adipose-derived stem cells. *J. Heart Valve Dis.* 19, 736–744.

Cribier, A., Eltchaninoff, H., Bash, A., Borenstein, N., Tron, C., Bauer, F., et al. (2002). Percutaneous transcatheter implantation of an aortic valve prosthesis for calcific aortic stenosis: first human case description. *Circulation* 106, 3006–3008. doi: 10.1161/01.CIR.0000047200.36165.B8

Crousillat, D. R., and Wood, M. J. (2019). Valvular heart disease and heart failure in women. *Heart Fail. Clin.* 15, 77–85. doi: 10.1016/j.hfc.2018.08.008

Cuddihy, E.F., Moacanin, J., Roschke, E.J., and Harrison, E.C. (1976). In vivo degradation of silicone rubber poppets in prosthetic heart valves. *J. Biomed. Mater. Res.* 10, 471-481. doi: 10.1002/jbm.820100314

Dabagh, M., Abdekhodaie, M., and Khorasani, M. (2005). Effects of polydimethylsiloxane grafting on the calcification, physical properties, and biocompatibility of polyurethane in a heart valve. *J. Appl. Polym. Sci.* 98, 758–766. doi: 10.1002/app.22132

Daebritz, S. H., Fausten, B., Hermanns, B., Franke, A., Schroeder, J., Groetzner, J., et al. (2004). New flexible polymeric heart valve prostheses for the mitral and aortic positions. *Heart Surg. Forum* 7, E525-E532. doi: 10.1532/HSF98.20041083

Danilucci, T. M., Santos, P. K., Pachane, B. C., Pisani, G. F., Lino, R. L., Casali, B. C., et al. (2019). Recombinant RGD-disintegrin Dis Ba-01 blocks integrin α v β 3 and impairs VEGF signaling in endothelial cells. *Cell Commun. Signal.* 17:27. doi: 10.1186/s12964-019-0339-1

D'arcy, J. L., Coffey, S., Loudon, M. A., Kennedy, A., Pearson-Stuttard, J., Birks, J., et al. (2016). Large-scale community echocardiographic screening reveals a major burden of undiagnosed valvular heart disease in older people: the OxVALVE Population Cohort Study. *Eur. Heart J.* 37, 3515–3522. doi: 10.1093/eurheartj/ehw229

David, T. E., Ropchan, G. C., and Butany, J. W. (1988). Aortic valve replacement with stentless porcine bioprostheses. *J. Cardiac. Surg.* 3, 501–505. doi: 10.1111/j.1540-8191.1988.tb00444.x

De Vriese, A. S., Verbeuren, T. J., Van De Voorde, J., Lameire, N. H., and Vanhoutte, P. M. (2000). Endothelial dysfunction in diabetes. *Br. J. Pharmacol.* 130, 963–974. doi: 10.1038/sj.bjp.0703393

Delmage, J. M., Powars, D. R., Jaynes, P. K., and Allerton, S. E. (1986). The selective suppression of immunogenicity by hyaluronic acid. *Ann. Clin. Lab. Sci.* 16, 303–310.

Detmer, D. E., Mcintosh, C. L., Boretos, J. W., and Braunwald, N. S. (1972). Polypropylene poppets for low-profile prosthetic heart valves. *Ann. Thorac. Surg.* 13, 122–127. doi: 10.1016/S0003-4975(10)64824-2

Ding, H.-Y., Xie, Y.-N., Dong, Q., Kimata, K., Nishida, Y., Ishiguro, N., et al. (2019). Roles of hyaluronan in cardiovascular and nervous system disorders. *J. Zhejiang Univ. Sci. B* 20, 428–436. doi: 10.1631/jzus.B1900155

Duan, B., Hockaday, L. A., Kang, K. H., and Butcher, J. T. (2013). 3D bioprinting of heterogeneous aortic valve conduits with alginate/gelatin hydrogels. *J. Biomed. Mater. Res. A* 101, 1255–1264. doi: 10.1002/jbm.a.34420

El-Hamamsy, I., Balachandran, K., Yacoub, M. H., Stevens, L. M., Sarathchandra, P., Taylor, P. M., et al. (2009). Endothelium-dependent regulation of the mechanical properties of aortic valve cusps. *J. Am. Coll. Cardiol.* 53, 1448–1455. doi: 10.1016/j.jacc.2008.11.056

Ely, J. L., Emken, M. R., Accuntius, J. A., Wilde, D. S., Haubold, A. D., More, R. B., et al. (1998). Pure pyrolytic carbon: preparation and properties of a new material, On-X carbon for mechanical heart valve prostheses. *J. Heart Valve Dis.* 7, 626–632.

Engelmayr, G. C., Jr., Hildebrand, D. K., Sutherland, F. W., Mayer, J. E., Jr., et al. (2003). A novel bioreactor for the dynamic flexural stimulation of tissue engineered heart valve biomaterials. *Biomaterials* 24, 2523–2532. doi: 10.1016/S0142-9612(03)00051-6

Engelmayr, G. C., Jr., Soletti, L., Vigmostad, S. C., Budilarto, S. G., Federspiel, W. J., et al. (2008). A novel flex-stretch-flow bioreactor for the study of engineered heart valve tissue mechanobiology. *Ann. Biomed. Eng.* 36, 700–712. doi: 10.1007/s10439-008-9447-6

Flanagan, T. C., Cornelissen, C., Koch, S., Tschoeke, B., Sachweh, J. S., Schmitz-Rode, T., et al. (2007). The in vitro development of autologous fibrin-based tissue-engineered heart valves through optimised dynamic conditioning. *Biomaterials* 28, 3388–3397. doi: 10.1016/j.biomaterials.2007.04.012

Flanagan, T. C., Wilkins, B., Black, A., Jockenhoevel, S., Smith, T. J., and Pandit, A. S. (2006). A collagen-glycosaminoglycan co-culture model for heart valve tissue engineering applications. *Biomaterials* 27, 2233–2246. doi: 10.1016/j.biomaterials.2005.10.031

Gallocher, S. L., Aguirre, A. F., Kasyanov, V., Pinchuk, L., and Schoephoerster, R. T. (2006). A novel polymer for potential use in a trileaflet heart valve. *J. Biomed. Mater. Res. Part B* 79, 325–334. doi: 10.1002/jbm.b.30546

Gentle, C. R., and Juden, H. (1984). Wear tests on polypropylene for use in prosthetic heart valves. *Tribol. Int.* 17, 151–154. doi: 10.1016/0301-679X(84)90007-0

Gilpin, A., and Yang, Y. (2017). Decellularization strategies for regenerative medicine: from processing techniques to applications. *Biomed. Res. Int.* 2017:9831534. doi: 10.1155/2017/9831534

Glaser, N., Jackson, V., Holzmann, M. J., Franco-Cereceda, A., and Sartipy, U. (2016). Aortic valve replacement with mechanical vs. biological prostheses in patients aged 50-69 years. *Eur. Heart J.* 37, 2658–2667. doi: 10.1093/eurheartj/ehv580

Goldstone, A. B., Chiu, P., Baiocchi, M., Lingala, B., Patrick, W. L., Fischbein, M. P., et al. (2017). Mechanical or biologic prostheses for aortic-valve and mitral-valve replacement. *New Engl. J. Med.* 377, 1847–1857. doi: 10.1056/NEJMoa1613792

Golomb, G., Dixon, M., Smith, M. S., Schoen, F. J., and Levy, R. J. (1987). Controlled-release drug delivery of diphosphonates to inhibit bioprosthetic heart valve calcification: release rate modulation with silicone matrices via drug solubility and membrane coating. *J. Pharm. Sci.* 76, 271–276. doi: 10.1002/jps.2600760402

Golomb, G., Langer, R., Schoen, F. J., Smith, M. S., Yong Mi, C., and Levy, R. J. (1986). Controlled release of diphosphonate to inhibit bioprosthetic heart valve calcification: dose-response and mechanistic studies. *J. Control. Rel.* 4, 181–194. doi: 10.1016/0168-3659(86)90002-7

González De Torre I, M.R., Alonso M, Jockenhoevel S, Rodríguez Cabello J and Mela P (2016). EA-valve: development of a tissue-engineered elastin-based heart valve prosthesis. *Front. Bioeng. Biotechnol.* 4:1035. doi: 10.3389/conf.FBIOE.2016.01.01035

Goodman, S. L., Tweden, K. S., and Albrecht, R. M. (1996). Platelet interaction with pyrolytic carbon heart-valve leaflets. *J. Biomed. Mater. Res.* 32, 249–258. doi: 10.1002/(SICI)1097-4636(199610)32:2<249::AID-JBM15>3.0.CO;2-E

Guldner, N. W., Zimmermann, H., and Sievers, H. H. (2011). *Nano-Coating with Titanium of Glutaraldehyde-Fixed Heart Valve Prostheses Enables a Reduced Immune Response and a Self-Seeding Within Circulation*. Rijeka: INTECH Open Access Publisher. doi: 10.1055/s-0030-1269349

Guyton, A. C., and Hall, J. E. (1996). *Textbook of Medical Physiology*. Philadelphia, PA: W.B. Saunders.

Hammermeister, K., Sethi, G. K., Henderson, W. G., Grover, F. L., Oprian, C., and Rahimtoola, S. H. (2000). Outcomes 15 years after valve replacement with a mechanical versus a bioprosthetic valve: final report of the Veterans Affairs randomized trial. *J. Am. Coll. Cardiol.* 36, 1152–1158. doi: 10.1016/S0735-1097(00)00834-2

Han, D.K., Park, K., Park, K.D., Ahn, K.D., and Kim, Y.H. (2006). In vivo biocompatibility of sulfonated PEO-grafted polyurethanes for polymer heart valve and vascular graft. *Artif Organs* 30, 955-959. doi: 10.1111/j.1525-1594.2006.00327.x

Hasan, A., Ragaert, K., Swieszkowski, W., Selimovic, S., Paul, A., Camci-Unal, G., et al. (2014). Biomechanical properties of native and tissue engineered heart valve constructs. *J. Biomech.* 47, 1949–1963. doi: 10.1016/j.jbiomech.2013.09.023

Helgadottir, A., Thorleifsson, G., Gretarsdottir, S., Stefansson, O. A., Tragante, V., Thorolfsdottir, R. B., et al. (2018). Genome-wide analysis yields new loci associating with aortic valve stenosis. *Nat. Commun.* 9:987. doi: 10.1038/s41467-018-03252-6

Hinderer, S., Seifert, J., Votteler, M., Shen, N., Rheinlaender, J., Schaffer, T. E., et al. (2014). Engineering of a bio-functionalized hybrid off-the-shelf heart valve. *Biomaterials* 35, 2130–2139. doi: 10.1016/j.biomaterials.2013.10.080

Hirji, S. A., Kaneko, T., and Aranki, S. (2018). The revolution and evolution of mechanical valves: the ball has left the cage. *J. Thorac. Cardiovasc. Surg.* 155, e149-e150. doi: 10.1016/j.jtcvs.2018.01.009

Ho, S. Y. (2009). Structure and anatomy of the aortic root. *Eur. J. Echocardiogr.* 10, i3-i10. doi: 10.1093/ejechocard/jen243

Hockaday, L., Kang, K., Colangelo, N., Cheung, P., Duan, B., Malone, E., et al. (2012). Rapid 3D printing of anatomically accurate and mechanically heterogeneous aortic valve hydrogel scaffolds. *Biofabrication* 4:035005. doi: 10.1088/1758-5082/4/3/035005

Hodde, J. (2002). Naturally occurring scaffolds for soft tissue repair and regeneration. *Tissue Eng.* 8, 295–308. doi: 10.1089/107632702753725058

Hoerstrup, S. P., Kadner, A., Melnitchouk, S., Trojan, A., Eid, K., Tracy, J., et al. (2002). Tissue engineering of functional trileaflet heart valves from human marrow stromal cells. *Circulation* 106, I143-I150.

Hoerstrup, S. P., Sodian, R., Daebritz, S., Wang, J., Bacha, E. A., Martin, D. P., et al. (2000). Functional living trileaflet heart valves grown in vitro. *Circulation* 102, III44-III49. doi: 10.1161/01.CIR.102.suppl_3.III-44

Hofferberth, S. C., Saeed, M. Y., Tomholt, L., Fernandes, M. C., Payne, C. J., Price, K., et al. (2020). A geometrically adaptable heart valve replacement. *Sci. Transl. Med.* 12:eaay4006. doi: 10.1126/scitranslmed.aay4006

Honda, S., Kitai, T., Okada, Y., Tani, T., Kim, K., Kaji, S., et al. (2012). Impact of aortic regurgitation on the prognosisof severe aortic stenosis. *Heart* 98, 1591–1594. doi: 10.1136/heartjnl-2012-302089

Hossainy, S. F., Tang, Y., and Kleiner, L. W. (2015). *Depot Stent Comprising An Elastin-Based Copolymer*. U.S. Patent No US-9078958-B2. Washington, DC: U.S. Patent and Trademark Office.

Hryhorowicz, M., Zeyland, J., Slomski, R., and Lipinski, D. (2017). Genetically modified pigs as organ donors for xenotransplantation. *Mol. Biotechnol.* 59, 435–444. doi: 10.1007/s12033-017-0024-9

Huai, G., Qi, P., Yang, H., and Wang, Y. (2016). Characteristics of alpha-Gal epitope, anti-Gal antibody, alpha1,3 galactosyltransferase and its clinical exploitation (Review). *Int. J. Mol. Med.* 37, 11–20. doi: 10.3892/ijmm.2015.2397

Jayabalan, M., Lizymol, P. P., and Thomas, V. (2000). Synthesis of hydrolytically stable low elastic modulus polyurethane-urea for biomedical applications. *Polym. Int.* 49, 88–92. doi: 10.1002/(SICI)1097-0126(200001)49:1<88::AID-PI298>3.0.CO;2-7

Jiang, H., Campbell, G., Boughner, D., Wan, W.-K., and Quantz, M. (2004). Design and manufacture of a polyvinyl alcohol (PVA) cryogel tri-leaflet heart valve prosthesis. *Medical Eng. Phys.* 26, 269–277. doi: 10.1016/j.medengphy.2003.10.007

Jockenhoevel, S., Zund, G., Hoerstrup, S. P., Schnell, A., and Turina, M. (2002). Cardiovascular tissue engineering: a new laminar flow chamber for in vitro improvement of mechanical tissue properties. *ASAIO J.* 48, 8–11. doi: 10.1097/00002480-200201000-00003

Jones, M. I., Mccoll, I. R., Grant, D. M., Parker, K. G., and Parker, T. L. (2000). Protein adsorption and platelet attachment and activation, on TiN, TiC, and DLC coatings on titanium for cardiovascular applications. *J. Biomed. Mater. Res.* 52, 413–421. doi: 10.1002/1097-4636(200011)52:2<413::AID-JBM23>3.0.CO;2-U

Jordan, R. E., Hewitt, N., Lewis, W., Kagan, H., and Franzblau, C. (1974). Regulation of elastase-catalyzed hydrolysis of insoluble elastin by synthetic and naturally occurring hydrophobic ligands. *Biochemistry* 13, 3497–3503. doi: 10.1021/bi00714a013

Kannan, R. Y., Salacinski, H. J., Butler, P. E., and Seifalian, A. M. (2005). Polyhedral oligomeric silsesquioxane nanocomposites: the next generation material for biomedical applications. *Accounts Chem. Res.* 38, 879–884. doi: 10.1021/ar050055b

Karp, R. B., and Sand, M. E. (1993). Mechanical prostheses: old and new. *Cardiovasc. Clin.* 23, 235–253.

Kidane, A. G., Burriesci, G., Cornejo, P., Dooley, A., Sarkar, S., Bonhoeffer, P., et al. (2009). Current developments and future prospects for heart valve replacement therapy. *J. Biomed. Mater. Res. Part B* 88, 290–303. doi: 10.1002/jbm.b.31151

Kim, B. S., and Mooney, D. J. (1998). Development of biocompatible synthetic extracellular matrices for tissue engineering. *Trends Biotechnol.* 16, 224–230. doi: 10.1016/S0167-7799(98)01191-3

Kiraly, R., Yozu, R., Hillegass, D., Harasaki, H., Murabayashi, S., Snow, J., et al. (1982). Hexsyn trileaflet valve: application to temporary blood pumps. *Artif. Organs* 6, 190–197. doi: 10.1111/j.1525-1594.1982.tb04082.x

Klepetko, W., Moritz, A., Mlczoch, J., Schurawitzki, H., Domanig, E., and Wolner, E. (1989). Leaflet fracture in Edwards-Duromedics bileaflet valves. *J. Thorac. Cardiovasc. Surg.* 97, 90–94. doi: 10.1016/S0022-5223(19)35130-X

Konakci, K. Z., Bohle, B., Blumer, R., Hoetzenecker, W., Roth, G., Moser, B., et al. (2005). Alpha-Gal on bioprostheses: xenograft immune response in cardiac surgery. *Eur. J. Clin. Invest* 35, 17–23. doi: 10.1111/j.1365-2362.2005.01441.x

Kumar, G. V., and Mathew, L. (2009). Biomaterial optimization in a percutaneous aortic valve stent using finite element analysis. *Cardiovasc. Revasc. Med.* 10, 247–251. doi: 10.1016/j.carrev.2008.12.003

Lahaye, S., Lincoln, J., and Garg, V. (2014). Genetics of valvular heart disease. *Curr. Cardiol. Rep.* 16:487. doi: 10.1007/s11886-014-0487-2

Laila Roudsari, C. A., Tara, D., Shelley, F., Cane, H., Kenneth, L., and Evelyn, P. (2014). Gelatin-coated resorbable polymer mesh as a novel scaffold for aortic heart valve tissue engineering. *Int. Public Health Forum* 1, 39–45.

Lamba, N. K. (2017). *Polyurethanes in Biomedical Applications*. Abingdon: Routledge. doi: 10.1201/9780203742785

Latif, N., Sarathchandra, P., Taylor, P. M., Antoniw, J., and Yacoub, M. H. (2005). Localization and pattern of expression of extracellular matrix components in human heart valves. *J. Heart Valve Dis.* 14, 218–227.

Legg, M., Mathews, E., and Pelzer, R. (2012). The design and development of a stented tissue mitral and aortic heart valve replacement for human implantation. *Cardiovasc. J. Afr.* 23, 126–130. doi: 10.5830/CVJA-2010-065

Leng, Y., Chen, J., Yang, P., Wang, J., Zhao, A., Wan, G., et al. (2006). The microstructure and mechanical properties of TiN and TiO 2/TiN duplex films synthesized by plasma immersion ion implantation and deposition on artificial heart valve. *Surf. Coat. Technol.* 201, 1012–1016. doi: 10.1016/j.surfcoat.2006.01.024

Leo, H. L., Dasi, L. P., Carberry, J., Simon, H. A., and Yoganathan, A. P. (2006). Fluid dynamic assessment of three polymeric heart valves using particle image velocimetry. *Ann. Biomed. Eng.* 34, 936–952. doi: 10.1007/s10439-006-9117-5

Leo, H. L., Simon, H., Carberry, J., Lee, S. C., and Yoganathan, A. P. (2005). A comparison of flow field structures of two tri-leaflet polymeric heart valves. *Ann. Biomed. Eng.* 33, 429–443. doi: 10.1007/s10439-005-2498-z

Levy, R. J., Wolfrum, J., Schoen, F. J., Hawley, M. A., Lund, S. A., and Langer, R. (1985). Inhibition of calcification of bioprosthetic heart valves by local controlled-release diphosphonate. *Science* 228, 190–192. doi: 10.1126/science.3919445

Li, R. L., Russ, J., Paschalides, C., Ferrari, G., Waisman, H., Kysar, J. W., et al. (2019). Mechanical considerations for polymeric heart valve development: biomechanics, materials, design and manufacturing. *Biomaterials* 225:119493. doi: 10.1016/j.biomaterials.2019.119493

Lieshout, M. V., Peters, G., Rutten, M., and Baaijens, F. (2006). A knitted, fibrin-covered polycaprolactone scaffold for tissue engineering of the aortic valve. *Tissue Eng.* 12, 481–487. doi: 10.1089/ten.2006.12.481

Litzler, P.-Y., Benard, L., Barbier-Frebourg, N., Vilain, S., Jouenne, T., Beucher, E., et al. (2007). Biofilm formation on pyrolytic carbon heart valves: influence of surface free energy, roughness, and bacterial species. *J. Thorac. Cardiovasc. Surg.* 134, 1025–1032. doi: 10.1016/j.jtcvs.2007.06.013

Loerakker, S., Argento, G., Oomens, C. W., and Baaijens, F. P. (2013). Effects of valve geometry and tissue anisotropy on the radial stretch and coaptation area of tissue-engineered heart valves. *J. Biomech.* 46, 1792–1800. doi: 10.1016/j.jbiomech.2013.05.015

Loger, K., Engel, A., Haupt, J., De Miranda, R. L., Lutter, G., and Quandt, E. (2016). Microstructured nickel-titanium thin film leaflets for hybrid tissue engineered heart valves fabricated by magnetron sputter deposition. *Cardiovasc. Eng. Technol.* 7, 69-77. doi: 10.1007/s13239-015-0254-6

Lu, Q., Ganesan, K., Simionescu, D. T., and Vyavahare, N. R. (2004). Novel porous aortic elastin and collagen scaffolds for tissue engineering. *Biomaterials* 25, 5227–5237. doi: 10.1016/j.biomaterials.2003.12.019

Mackay, T. G., Wheatley, D. J., Bernacca, G. M., Fisher, A. C., and Hindle, C. S. (1996). New polyurethane heart valve prosthesis: design, manufacture and evaluation. *Biomaterials* 17, 1857–1863. doi: 10.1016/0142-9612(95)00242-1

Mackenna, D., Summerour, S. R., and Villarreal, F. J. (2000). Role of mechanical factors in modulating cardiac fibroblast function and extracellular matrix synthesis. *Cardiovasc. Res.* 46, 257–263. doi: 10.1016/S0008-6363(00)00030-4

Makkar, R. R., Thourani, V. H., Mack, M. J., Kodali, S. K., Kapadia, S., Webb, J. G., et al. (2020). Five-year outcomes of transcatheter or surgical aortic-valve replacement. *New Engl. J. Med.* 382, 799–809. doi: 10.1056/NEJMoa1910555

Manji, R. A., Lee, W., and Cooper, D. K. C. (2015). Xenograft bioprosthetic heart valves: Past, present and future. *Int. J. Surg.* 23, 280–284. doi: 10.1016/j.ijsu.2015.07.009

Manji, R. A., Zhu, L. F., Nijjar, N. K., Rayner, D. C., Korbutt, G. S., Churchill, T. A., et al. (2006). Glutaraldehyde-fixed bioprosthetic heart valve conduits calcify and fail from xenograft rejection. *Circulation* 114, 318–327. doi: 10.1161/CIRCULATIONAHA.105.549311

Masoumi, N., Annabi, N., Assmann, A., Larson, B. L., Hjortnaes, J., Alemdar, N., et al. (2014). Tri-layered elastomeric scaffolds for engineering heart valve leaflets. *Biomaterials* 35, 7774–7785. doi: 10.1016/j.biomaterials.2014.04.039

Millon, L. E., and Wan, W. K. (2006). The polyvinyl alcohol–bacterial cellulose system as a new nanocomposite for biomedical applications. *J. Biomed. Mater. Res. Part B* 79B, 245–253. doi: 10.1002/jbm.b.30535

Mitamura, Y., Hosooka, K., Matsumoto, T., Otaki, K., Sakai, K., Tanabe, T., et al. (1989). Development of a ceramic heart valve. *J. Biomater. Appl.* 4, 33–55. doi: 10.1177/088532828900400103

Mordi, I., and Tzemos, N. (2012). Bicuspid aortic valve disease: a comprehensive review. *Cardiol Res Pract* 2012:196037. doi: 10.1155/2012/196037

Nagy, O., Barath, S., and Ujfalusi, A. (2019). The role of microRNAs in congenital heart disease. *EJIFCC* 30, 165–178.

Nam, J., Choi, S. Y., Sung, S. C., Lim, H. G., Park, S. S., Kim, S. H., et al. (2012). Changes of the structural and biomechanical properties of the bovine pericardium after the removal of alpha-gal epitopes by decellularization and alpha-galactosidase treatment. *Korean J. Thorac. Cardiovasc. Surg.* 45, 380–389. doi: 10.5090/kjtcs.2012.45.6.380

Naso, F., and Gandaglia, A. (2018). Different approaches to heart valve decellularization: a comprehensive overview of the past 30 years. *Xenotransplantation* 25. doi: 10.1111/xen.12354

Naso, F., Gandaglia, A., Bottio, T., Tarzia, V., Nottle, M. B., D'apice, A. J., et al. (2013). First quantification of alpha-Gal epitope in current glutaraldehyde-fixed heart valve bioprostheses. *Xenotransplantation* 20, 252–261. doi: 10.1111/xen.12044

Nie, B. E., Hu, S. D., and Zhou, J. L. (2014). Construction of three-dimensional scaffold for tissue engineered heart valves. *Adv. Mater. Res.* 873, 627–634. doi: 10.4028/www.scientific.net/AMR.873.627

Nilforoushzadeh, M. A., Zare, M., Zarrintaj, P., Alizadeh, E., Taghiabadi, E., Heidari-Kharaji, M., et al. (2018). Engineering the niche for hair regeneration–a critical review. *Nanomedicine* 15, 70-85. doi: 10.1016/j.nano.2018.08.012

Nishimura, R. A., Otto, C. M., Bonow, R. O., Carabello, B. A., Erwin, J. P., 3rd, Fleisher, L. A., et al. (2017). 2017 AHA/ACC Focused Update of the 2014 AHA/ACC guideline for the management of patients with valvular heart disease: a report of the american college of cardiology/american heart association task force on clinical practice guidelines. *J. Am. Coll. Cardiol.* 70, 252–289. doi: 10.1016/j.jacc.2017.03.011

Nishimura, R. A., Otto, C. M., Bonow, R. O., Carabello, B. A., Erwin, J. P., Guyton, R. A., et al. (2014). 2014 AHA/ACC guideline for the management of patients with valvular heart disease: executive summary. *Circulation* 129, 2440–2492. doi: 10.1161/CIR.0000000000000029

Nistal, F., Garcia-Martinez, V., Arbe, E., Fernandez, D., Artinano, E., Mazorra, F., et al. (1990). In vivo experimental assessment of polytetrafluoroethylene trileaflet heart valve prosthesis. *J. Thorac. Cardiovasc. Surg.* 99, 1074-1081. doi: 10.1016/S0022-5223(20)31464-1

Nkomo, V. T., Gardin, J. M., Skelton, T. N., Gottdiener, J. S., Scott, C. G., and Enriquez-Sarano, M. (2006). Burden of valvular heart diseases: a population-based study. *Lancet* 368, 1005–1011. doi: 10.1016/S0140-6736(06)69208-8

Ota, T., Taketani, S., Iwai, S., Miyagawa, S., Furuta, M., Hara, M., et al. (2007). Novel method of decellularization of porcine valves using polyethylene glycol and gamma irradiation. *Ann. Thorac. Surg.* 83, 1501–1507. doi: 10.1016/j.athoracsur.2006.11.083

Ouyang, H., Zhang, J., Liu, Y., Li, Q., Peng, Y., Kang, X., et al. (2008). Research on application of modified polyethylene glycol hydrogels in the construction of tissue engineered heart valve. *Chin. J. Surg.* 46, 1723–1726.

Oxenham, H., Bloomfield, P., Wheatley, D. J., Lee, R. J., Cunningham, J., Prescott, R. J., et al. (2003). Twenty year comparison of a Bjork-Shiley mechanical heart valve with porcine bioprostheses. *Heart* 89, 715–721. doi: 10.1136/heart.89.7.715

Ozaki, S., Kawase, I., Yamashita, H., Uchida, S., Nozawa, Y., Matsuyama, T., et al. (2011). Aortic valve reconstruction using self-developed aortic valve plasty system in aortic valve disease. *Interact. Cardiovascu. Thorac. Surg.* 12, 550–553. doi: 10.1510/icvts.2010.253682

Parfeev, V. M., Grushetskii, I. V., and Smurova, E. V. (1983). Mechanical properties of elastomers for artificial leaflet heart valves. *Mech. Comp. Mater.* 19, 92–99. doi: 10.1007/BF00604034

Paul, W., Vasudev, S. C., and Sharma, C. P. (1998). Polyethylene glycol (PEG) modified bovine pericardiuim as a biomaterial: a comparative study on immunogenicity. *J. Biomater. Appl.* 13, 158–165. doi: 10.1177/088532829801300205

Pavcnik, D., Wright, K. C., and Wallace, S. (1992). Development and initial experimental evaluation of a prosthetic aortic valve for transcatheter placement. *Work Prog. Radiol.* 183, 151–154. doi: 10.1148/radiology.183.1.1549662

Phillips, S. J. (2001). Thrombogenic influence of biomaterials in patients with the Omni series heart valve: pyrolytic carbon versus titanium. *ASAIO J.* 47, 429–431. doi: 10.1097/00002480-200109000-00002

Pibarot, P., and Dumesnil, J. G. (2009). Prosthetic heart valves. *Circulation* 119, 1034–1048. doi: 10.1161/CIRCULATIONAHA.108.778886

Qiu, Y. X., Klee, D., Plüster, W., Severich, B., and Höcker, H. (1996). Surface modification of polyurethane by plasma-induced graft polymerization of poly(ethylene glycol) methacrylate. *J. Appl. Polym. Sci.* 61, 2373–2382. doi: 10.1002/(SICI)1097-4628(19960926)61:13<2373::AID-APP17>3.0.CO;2-5

Rabkin-Aikawa, E., Farber, M., Aikawa, M., and Schoen, F. J. (2004). Dynamic and reversible changes of interstitial cell phenotype during remodeling of cardiac valves. *J. Heart Valve Dis.* 13, 841–847.

Rabkin-Aikawa, E., Mayer Jr, J.E., and Schoen, F.J. (2005). "Heart Valve Regeneration," in *Regenerative Medicine II: Clinical and Preclinical Applications*, ed. I.V. Yannas. (Berlin: Springer), 141-179. doi: 10.1007/b100003

Rahmani, B., Mcgregor, C., Byrne, G., and Burriesci, G. (2019). A durable porcine pericardial surgical bioprosthetic heart valve: a proof of concept. *J. Cardiovasc. Transl. Res.* 12, 331–337. doi: 10.1007/s12265-019-09868-3

Raj, B. (2005). *Frontiers in Materials Science*. Cambridge: Universities Press.

Rajamannan, N. M., Evans, F. J., Aikawa, E., Grande-Allen, K. J., Demer, L. L., Heistad, D. D., et al. (2011). Calcific aortic valve disease: not simply a degenerative process: A review and agenda for research from the National Heart and Lung and Blood Institute Aortic Stenosis Working Group. *Execut. Summary*124, 1783–1791. doi: 10.1161/CIRCULATIONAHA.110.006767

Ramaswamy, S., Boronyak, S. M., Le, T., Holmes, A., Sotiropoulos, F., and Sacks, M. S. (2014). A novel bioreactor for mechanobiological studies of engineered heart valve tissue formation under pulmonary arterial physiological flow conditions. *J. Biomech. Eng.* 136:121009. doi: 10.1115/1.4028815

Ramm, R., Goecke, T., Theodoridis, K., Hoeffler, K., Sarikouch, S., Findeisen, K., et al. (2020). Decellularization combined with enzymatic removal of N-linked glycans and residual DNA reduces inflammatory response and improves performance of porcine xenogeneic pulmonary heart valves in an ovine in vivo model. *Xenotransplantation* 27:e12571. doi: 10.1111/xen.12571

Ratner, B. D. (2013). *Biomaterials Science: An Introduction to Materials in Medicine*. Boston, CA: Elsevier.

Rienks, M., Papageorgiou, A.-P., Frangogiannis, N. G., and Heymans, S. (2014). Myocardial extracellular matrix. *Circ. Res.* 114, 872–888. doi: 10.1161/CIRCRESAHA.114.302533

Rippel, R. A., Ghanbari, H., and Seifalian, A. M. (2012). Tissue-engineered heart valve: future of cardiac surgery. *World J. Surg.* 36, 1581–1591. doi: 10.1007/s00268-012-1535-y

Ritchie, R. O. (1996). Fatigue and fracture of pyrolytic carbon: a damage-tolerant approach to structural integrity and life prediction in "Ceramic" heart valve prostheses. *J. Heart Valve Dis.* 5, S9-S31.

Robinson, P. S., and Tranquillo, R. T. (2009). Planar biaxial behavior of fibrin-based tissue-engineered heart valve leaflets. *Tissue Eng. Part A* 15, 2763–2772. doi: 10.1089/ten.tea.2008.0426

Ross, D. N. (1967). Replacement of aortic and mitral valves with a pulmonary autograft. *Lancet* 2, 956–958. doi: 10.1016/S0140-6736(67)90794-5

Russo, A., Grigioni, F., Avierinos, J. F., Freeman, W. K., Suri, R., Michelena, H., et al. (2008). Thromboembolic complications after surgical correction of mitral regurgitation incidence, predictors, and clinical implications. *J. Am. Coll. Cardiol.* 51, 1203–1211. doi: 10.1016/j.jacc.2007.10.058

Sachweh, J. S., and Daebritz, S. H. (2006). Novel "biomechanical" polymeric valve prostheses with special design for aortic and mitral position: a future option for pediatric patients? *ASAIO J.* 52, 575–580.

Sacks, M. S., David Merryman, W., and Schmidt, D. E. (2009). On the biomechanics of heart valve function. *J. Biomech.* 42, 1804–1824. doi: 10.1016/j.jbiomech.2009.05.015

Sacks, M. S., and Liao, J. (2019). *Advances in Heart Valve Biomechanics: Valvular Physiology, Mechanobiology, and Bioengineering*. New York, NY: Springer International Publishing. doi: 10.1007/978-3-030-01993-8

Sacks, M.S., Enomoto, Y., Graybill, J.R., Merryman, W.D., Zeeshan, A., Yoganathan, A.P., et al. (2006). In-vivo dynamic deformation of the mitral valve anterior leaflet. *Ann. Thorac. Surg.* 82, 1369-1377. doi: 10.1016/j.athoracsur.2006.03.117

Schaefer, A., Dickow, J., Schoen, G., Westhofen, S., Kloss, L., Al-Saydali, T., et al. (2018). Stentless vs. stented bioprosthesis for aortic valve replacement: a case matched comparison of long-term follow-up and subgroup analysis of patients with native valve endocarditis. *PLoS One* 13:e0191171. doi: 10.1371/journal.pone.0191171

Schaff, H. V. (2016). Ross procedure for aortic valve replacement in young adults. *Circulation* 134, 586–588. doi: 10.1161/CIRCULATIONAHA.116.024305

Schenke-Layland, K., Opitz, F., Gross, M., Doring, C., Halbhuber, K. J., Schirrmeister, F., et al. (2003). Complete dynamic repopulation of decellularized heart valves by application of defined physical signals-an in vitro study. *Cardiovasc. Res.* 60, 497–509. doi: 10.1016/j.cardiores.2003.09.002

Schmidt, C. E., and Baier, J. M. (2000). Acellular vascular tissues: natural biomaterials for tissue repair and tissue engineering. *Biomaterials* 21, 2215–2231. doi: 10.1016/S0142-9612(00)00148-4

Schmidt, D., Achermann, J., Odermatt, B., Breymann, C., Mol, A., Genoni, M., et al. (2007). Prenatally fabricated autologous human living heart valves based on amniotic fluid derived progenitor cells as single cell source. *Circulation* 116, I64-I70. doi: 10.1161/CIRCULATIONAHA.106.681494

Schmidt, D., Dijkman, P. E., Driessen-Mol, A., Stenger, R., Mariani, C., Puolakka, A., et al. (2010). Minimally-invasive implantation of living tissue engineered heart valves: a comprehensive approach from autologous vascular cells to stem cells. *J. Am. Coll. Cardiol.* 56, 510–520. doi: 10.1016/j.jacc.2010.04.024

Schmidt, D., Mol, A., Breymann, C., Achermann, J., Odermatt, B., Gossi, M., et al. (2006a). Living autologous heart valves engineered from human prenatally harvested progenitors. *Circulation* 114, I125-I131. doi: 10.1161/CIRCULATIONAHA.105.001040

Schmidt, D., Mol, A., Odermatt, B., Neuenschwander, S., Breymann, C., Gossi, M., et al. (2006b). Engineering of biologically active living heart valve leaflets using human umbilical cord-derived progenitor cells. *Tissue Eng.* 12, 3223–3232. doi: 10.1089/ten.2006.12.3223

Schoen, F. J. (1997). Aortic valve structure-function correlations: role of elastic fibers no longer a stretch of the imagination. *J. Heart Valve Dis.* 6, 1–6.

Schoen, F. J., and Levy, R. J. (2005). Calcification of tissue heart valve substitutes: progress toward understanding and prevention. *Ann. Thorac Surg.* 79, 1072–1080. doi: 10.1016/j.athoracsur.2004.06.033

Schoen, F. J., Titus, J. L., and Lawrie, G. M. (1982). Durability of pyrolytic carbon-containing heart valve prostheses. *J. Biomed. Mater. Res. Part A* 16, 559–570. doi: 10.1002/jbm.820160504

Schoental, R. (1968). Carcinogenic and chronic effects of 4,4′-diaminodiphenylmethane, an epoxyresin hardener. *Nature* 219, 1162–1163. doi: 10.1038/2191162a0

Siddiqui, R. F., Abraham, J. R., and Butany, J. (2009). Bioprosthetic heart valves: modes of failure. *Histopathology* 55, 135–144. doi: 10.1111/j.1365-2559.2008.03190.x

Simionescu, D. T. (2004). Prevention of calcification in bioprosthetic heart valves: challenges and perspectives. *Exp. Opin. Biol. Ther.* 4, 1971–1985. doi: 10.1517/14712598.4.12.1971

Simmons, A., Hyvarinen, J., Odell, R. A., Martin, D. J., Gunatillake, P. A., Noble, K. R., et al. (2004). Long-term in vivo biostability of poly (dimethylsiloxane)/poly (hexamethylene oxide) mixed macrodiol-based polyurethane elastomers. *Biomaterials* 25, 4887–4900. doi: 10.1016/j.biomaterials.2004.01.004

Smith, K., and Black, K. (1984). Characterization of the treated surfaces of silicon alloyed pyrolytic carbon and SiC. *J. Vacuum Sci. Technol.A* 2, 744–747. doi: 10.1116/1.572562

Sodian, R., Hoerstrup, S. P., Sperling, J. S., Daebritz, S. H., Martin, D. P., Schoen, F. J., et al. (2000). Tissue engineering of heart valves: in vitro experiences. *Ann. Thorac. Surg.* 70, 140–144. doi: 10.1016/S0003-4975(00)01255-8

Sodian, R., Schaefermeier, P., Abegg-Zips, S., Kuebler, W. M., Shakibaei, M., Daebritz, S., et al. (2010). Use of human umbilical cord blood-derived progenitor cells for tissue-engineered heart valves. *Ann. Thorac. Surg.* 89, 819–828. doi: 10.1016/j.athoracsur.2009.11.058

Stachelek, S. J., Alferiev, I., Connolly, J. M., Sacks, M., Hebbel, R. P., Bianco, R., et al. (2006). Cholesterol-modified polyurethane valve cusps demonstrate blood outgrowth endothelial cell adhesion post-seeding in vitro and in vivo. *Ann. Thorac. Surg.* 81, 47–55. doi: 10.1016/j.athoracsur.2005.07.061

Sutherland, F. W., Perry, T. E., Yu, Y., Sherwood, M. C., Rabkin, E., Masuda, Y., et al. (2005). From stem cells to viable autologous semilunar heart valve. *Circulation* 111, 2783–2791. doi: 10.1161/CIRCULATIONAHA.104.498378

Syedain, Z. H., and Tranquillo, R. T. (2009). Controlled cyclic stretch bioreactor for tissue-engineered heart valves. *Biomaterials* 30, 4078–4084. doi: 10.1016/j.biomaterials.2009.04.027

Tadavarthy, S. M., Moller, J. H., and Amplatz, K. (1975). Polyvinyl alcohol (ivalon)—a new embolic material. *Am. J. Roentgenol.* 125, 609–616. doi: 10.2214/ajr.125.3.609

Tang, Y., Labow, R., and Santerre, J. (2001). Enzyme-induced biodegradation of polycarbonate-polyurethanes: dependence on hard-segment chemistry. *J. Biomed. Mater. Res.* 57, 597–611. doi: 10.1002/1097-4636(20011215)57:4<597::AID-JBM1207>3.0.CO;2-T

Tayama, E., Akashi, H., Ishihara, K., Hayashida, N., Akasu, K., Kosuga, T., et al. (2000). Early results with the Carbo-seal composite valve conduit for aortic root replacement: comparison with the St. *Jude Medical/Hemashield composite graft*. *J. Artif. Organs* 3, 120–125. doi: 10.1007/BF02479978

Taylor, P. M., Allen, S. P., Dreger, S. A., and Yacoub, M. H. (2002). Human cardiac valve interstitial cells in collagen sponge: a biological three-dimensional matrix for tissue engineering. *J. Heart Valve Dis.* 11, 298-306.

Taylor, P. M., Batten, P., Brand, N. J., Thomas, P. S., and Yacoub, M. H. (2003). The cardiac valve interstitial cell. *Int. J. Biochem. Cell Biol.* 35, 113–118. doi: 10.1016/S1357-2725(02)00100-0

Tedder, M. E., Liao, J., Weed, B., Stabler, C., Zhang, H., Simionescu, A., et al. (2008). Stabilized collagen scaffolds for heart valve tissue engineering. *Tissue Eng. Part A* 15, 1257–1268. doi: 10.1089/ten.tea.2008.0263

Tedder, M. E., Simionescu, A., Chen, J., Liao, J., and Simionescu, D. T. (2010). Assembly and testing of stem cell-seeded layered collagen constructs for heart valve tissue engineering. *Tissue Eng. Part A* 17, 25–36. doi: 10.1089/ten.tea.2010.0138

Teoh, S. H. (2000). Fatigue of biomaterials: a review. *Int. J. Fatigue* 22, 825–837. doi: 10.1016/S0142-1123(00)00052-9

Thomas, V., and Jayabalan, M. (2009). A new generation of high flex life polyurethane urea for polymer heart valve–studies on in vivo biocompatibility and biodurability. *J. Biomed. Mater. Res. A* 89, 192–205. doi: 10.1002/jbm.a.31937

Thomas, V., Kumari, T.V., and Jayabalan, M. (2001). In vitro studies on the effect of physical cross-linking on the biological performance of aliphatic poly(urethane urea) for blood contact applications. *Biomacromolecules* 2, 588-596. doi: 10.1021/bm010044f

Thornton, M. A., Howard, I. C., and Patterson, E. A. (1997). Three-dimensional stress analysis of polypropylene leaflets for prosthetic heart valves. *Med. Eng. Phys.* 19, 588–597. doi: 10.1016/S1350-4533(96)00042-2

Topilsky, Y. (2018). Tricuspid valve regurgitation: epidemiology and pathophysiology. *Min. Cardioangiol.* 66, 673–679. doi: 10.23736/S0026-4725.18.04670-4

Tseng, H., Puperi, D. S., Kim, E. J., Ayoub, S., Shah, J. V., Cuchiara, M. L., et al. (2014). Anisotropic poly(ethylene glycol)/polycaprolactone hydrogel-fiber composites for heart valve tissue engineering. *Tissue Eng. Part A* 20, 2634–2645. doi: 10.1089/ten.tea.2013.0397

Uygur, A., and Lee, R. T. (2016). Mechanisms of cardiac regeneration. *Dev. Cell* 36, 362–374. doi: 10.1016/j.devcel.2016.01.018

Van Putte, B. P., Ozturk, S., Siddiqi, S., Schepens, M. A., Heijmen, R. H., and Morshuis, W. J. (2012). Early and late outcome after aortic root replacement with a mechanical valve prosthesis in a series of 528 patients. *Ann. Thorac. Surg.* 93, 503–509. doi: 10.1016/j.athoracsur.2011.07.089

Vyavahare, N., Hirsch, D., Lerner, E., Baskin, J. Z., Schoen, F. J., Bianco, R., et al. (1997). Prevention of bioprosthetic heart valve calcification by ethanol preincubation. *Efficacy and mechanisms*. *Circulation* 95, 479–488. doi: 10.1161/01.CIR.95.2.479

Wan, W. K., Campbell, G., Zhang, Z. F., Hui, A. J., and Boughner, D. R. (2002). Optimizing the tensile properties of polyvinyl alcohol hydrogel for the construction of a bioprosthetic heart valve stent. *J. Biomed. Mater. Res.* 63, 854–861. doi: 10.1002/jbm.10333

Weber, B., Emmert, M. Y., and Hoerstrup, S. P. (2012). Stem cells for heart valve regeneration. *Swiss Med Wkly* 142:w13622. doi: 10.4414/smw.2012.13622

Weber, B., Scherman, J., Emmert, M. Y., Gruenenfelder, J., Verbeek, R., Bracher, M., et al. (2011). Injectable living marrow stromal cell-based autologous tissue engineered heart valves: first experiences with a one-step intervention in primates. *Eur. Heart J.* 32, 2830–2840. doi: 10.1093/eurheartj/ehr059

Weber, M., Heta, E., Moreira, R., Gesche, V. N., Schermer, T., Frese, J., et al. (2014). Tissue-engineered fibrin-based heart valve with a tubular leaflet design. *Tissue Eng. Part C Methods* 20, 265–275. doi: 10.1089/ten.tec.2013.0258

Wheatley, D. J., Raco, L., Bernacca, G. M., Sim, I., Belcher, P. R., and Boyd, J. S. (2000). Polyurethane: material for the next generation of heart valve prostheses? *Eur. J. Cardio Thorac. Surg.* 17, 440–448. doi: 10.1016/S1010-7940(00)00381-X

Wilson, W. R., Laird, N., Moo-Young, G., Soeldner, J. S., Kavesh, D. A., and Macmeel, J. W. (1982). The relationship of idiopathic sudden hearing loss to diabetes mellitus. *Laryngoscope* 92, 155–160. doi: 10.1002/lary.1982.92.2.155

Wong, C., Shital, P., Chen, R., Owida, A., and Morsi, Y. (2010). Biomimetic electrospun gelatin–chitosan polyurethane for heart valve leaflets. *J. Mech. Med. Biol.* 10, 563–576. doi: 10.1142/S0219519410003551

Wong, M. L., and Griffiths, L. G. (2014). Immunogenicity in xenogeneic scaffold generation: antigen removal vs. *decellularization*. *Acta Biomater.* 10, 1806–1816. doi: 10.1016/j.actbio.2014.01.028

Wu, P. L., Nakamura, N., Kimura, T., Nam, K., Fujisato, T., Funamoto, S., et al. (2015). Decellularized porcine aortic intima-media as a potential cardiovascular biomaterial. *Interact. Cardiovasc. Thorac. Surg.* 21, 189–194. doi: 10.1093/icvts/ivv113

Wurzinger, L. J., Opitz, R., Wolf, M., and Schmid-Schonbein, H. (1985). "Shear induced platelet activation"—a critical reappraisal. *Biorheology* 22, 399–413. doi: 10.3233/BIR-1985-22504

Yacoub, M. H., and Cohn, L. H. (2004). Novel approaches to cardiac valve repair: from structure to function: Part I. *Circulation* 109, 942–950. doi: 10.1161/01.CIR.0000115633.19829.5E

Yap, C. H., Saikrishnan, N., Tamilselvan, G., Vasilyev, N., and Yoganathan, A. P. (2012). The congenital bicuspid aortic valve can experience high-frequency unsteady shear stresses on its leaflet surface. *Am. J. Physiol. Heart Circ. Physiol.* 303, H721-H731. doi: 10.1152/ajpheart.00829.2011

Ye, Q., Zünd, G., Benedikt, P., Jockenhoevel, S., Hoerstrup, S. P., Sakyama, S., et al. (2000). Fibrin gel as a three dimensional matrix in cardiovascular tissue engineering. *Eur. J. Cardio Thorac. Surg.* 17, 587–591. doi: 10.1016/S1010-7940(00)00373-0

Yip, C. Y., and Simmons, C. A. (2011). The aortic valve microenvironment and its role in calcific aortic valve disease. *Cardiovasc. Pathol.* 20, 177–182. doi: 10.1016/j.carpath.2010.12.001

Yoda, R. (1998). Elastomers for biomedical applications. *J. Biomater. Sci. Polym. Ed.* 9, 561–626. doi: 10.1163/156856298X00046

Yousefi, A., Bark, D. L., and Dasi, L. P. (2017). Effect of arched leaflets and stent profile on the hemodynamics of tri-leaflet flexible polymeric heart valves. *Ann. Biomed. Eng.* 45, 464–475. doi: 10.1007/s10439-016-1674-7

Yue, K., Trujillo-De Santiago, G., Alvarez, M. M., Tamayol, A., Annabi, N., and Khademhosseini, A. (2015). Synthesis, properties, and biomedical applications of gelatin methacryloyl (GelMA) hydrogels. *Biomaterials* 73, 254–271. doi: 10.1016/j.biomaterials.2015.08.045

Zarrintaj, P., Bakhshandeh, B., Rezaeian, I., Heshmatian, B., and Ganjali, M. R. (2017). A novel electroactive agarose-aniline pentamer platform as a potential candidate for neural tissue engineering. *Sci. Rep.* 7:17187. doi: 10.1038/s41598-017-17486-9

Zarrintaj, P., Saeb, M. R., Ramakrishna, S., and Mozafari, M. (2018). Biomaterials selection for neuroprosthetics. *Curr. Opin. Biomed. Eng.* 6, 99-109. doi: 10.1016/j.cobme.2018.05.003

Zdrahala, R. J., and Zdrahala, I. J. (1999). Biomedical applications of polyurethanes: a review of past promises, present realities, and a vibrant future. *J. Biomater. Appl.* 14, 67–90. doi: 10.1177/088532829901400104

Zeyland, J., Woźniak, A., Gawrońska, B., Juzwa, W., Jura, J., Nowak, A., et al. (2014). Double transgenic pigs with combined expression of human α1,2-Fucosyltransferase and α-galactosidase designed to avoid hyperacute xenograft rejection. *Arch. Immunol. Ther. Exp.* 62, 411–422. doi: 10.1007/s00005-014-0280-3

Zhang, X., Xu, B., Puperi, D. S., Yonezawa, A. L., Wu, Y., Tseng, H., et al. (2015). Integrating valve-inspired design features into poly(ethylene glycol) hydrogel scaffolds for heart valve tissue engineering. *Acta Biomater.* 14, 11–21. doi: 10.1016/j.actbio.2014.11.042

Zhou, F., Cui, Y., Wu, L., Sun, H., and Huang, N. (2015). Preparation of Ti-O film deposited on the surface of a new type of artificial mechanical heart valve. *Sheng Wu Yi Xue Gong Cheng Xue Za Zhi* 32, 430–433.

Zhou, J., Hu, S., Ding, J., Xu, J., Shi, J., and Dong, N. (2013). Tissue engineering of heart valves: PEGylation of decellularized porcine aortic valve as a scaffold for in vitro recellularization. *Biomed. Eng. Online* 12:87. doi: 10.1186/1475-925X-12-87

Conflict of Interest: The authors declare that the research was conducted in the absence of any commercial or financial relationships that could be construed as a potential conflict of interest.

Copyright © 2020 Taghizadeh, Ghavami, Derakhshankhah, Zangene, Razmi, Jaymand, Zarrintaj, Zarghami, Jaafari, Moallem Shahri, Moghaddasian, Tayebi and Izadi. This is an open-access article distributed under the terms of the Creative Commons Attribution License (CC BY). The use, distribution or reproduction in other forums is permitted, provided the original author(s) and the copyright owner(s) are credited and that the original publication in this journal is cited, in accordance with accepted academic practice. No use, distribution or reproduction is permitted which does not comply with these terms.

Advantages of publishing in Frontiers

OPEN ACCESS
Articles are free to read for greatest visibility and readership

FAST PUBLICATION
Around 90 days from submission to decision

HIGH QUALITY PEER-REVIEW
Rigorous, collaborative, and constructive peer-review

TRANSPARENT PEER-REVIEW
Editors and reviewers acknowledged by name on published articles

Frontiers
Avenue du Tribunal-Fédéral 34
1005 Lausanne | Switzerland

Visit us: www.frontiersin.org
Contact us: frontiersin.org/about/contact

REPRODUCIBILITY OF RESEARCH
Support open data and methods to enhance research reproducibility

DIGITAL PUBLISHING
Articles designed for optimal readership across devices

FOLLOW US
@frontiersin

IMPACT METRICS
Advanced article metrics track visibility across digital media

EXTENSIVE PROMOTION
Marketing and promotion of impactful research

LOOP RESEARCH NETWORK
Our network increases your article's readership